ATTACHMENT A

Technical Memorandum 10111.0

1901 Camino Vida Roble, Suite 105 • Carlsbad, California • 92008
Phone: (760) 730-0701 FAX: (415) 457-1638 e-mail: ConorK@stetsonengineers.com

TO:	IWV Groundwater Authority	DATE:	October 7, 2022
		ADDENDUM DATE:	January 10, 2023
FROM:	Stetson Engineers, Inc.	JOB NO:	2652-63

RE: Phase I Investigation for Recharge Sites

CONTENTS

1.0. INTRODUCTION 1
1.1 LITERATURE REVIEW AND PREVIOUS STUDIES 3
1.1.1 Krieger and Stewart (1989, 1996) and IWVWD (2005) 3
1.1.2 Krieger and Stewart; Cato Geoscience, 2008 5
1.1.3 BSK Associates, 2011 5
1.1.4 Provost & Pritchard, 2015 6
1.1.5 Los Angeles Department of Water and Power (LA DWP), 2018 6
1.2 RULES AND REGULATIONS RELATED TO RECHARGE OF RECYCLED WATER RECHARGE 7
1.2.1 DDW Groundwater Replenishment Regulation 7
1.2.2 Pathogenic Microorganism Control 7
1.2.3 Underground Retention Time 8
1.2.4 Response Retention Time (RRT) 8
1.2.5 Recycled Water Contribution 9
1.2.6 Hydrogeologic Assessment 9
1.3 ENVIRONMENTAL PERMITTING AND OTHER REGULATORY CONSIDERATIONS 9
1.4 CASE STUDIES 10
1.4.1 Projects in Lahontan Region 6 10
1.4.2 Projects in Colorado River Region 7 11

2.0. PHYSICAL DATA, LAND OWNERSHIP, AND SITE SELECTION 13
2.1 LAND OWNERSHIP AND PHYSICAL DATA SETS 13
2.1.1 Land Ownership 13
2.1.2 Soils 13
2.1.3 Surface Slope 13
2.2 HYDROGEOLOGY 17
2.2.1 Water Quality 18
2.3 SITE SELECTION 22

3.0. FACILITY AND ENGINEERING REQUIREMENTS 23
3.1 IPR OPTION 1 FACILITIES 23
3.2 IMPORTED WATER RECHARGE OPTION 2 FACILITIES 27
3.3 EVAPORATIVE WATER LOSSES 28

4.0. SUMMARY AND RECOMMENDATIONS 30
4.1 FIELD INVESTIGATION RECOMMENDATIONS 32
4.1.1 Hydrogeologic Investigation 32
4.1.2 Pilot Testing 35

5.0. BIBLIOGRAPHY 36

TABLES

TABLE 1-1 SUMMARY OF PREVIOUS INFILTRATION AND SUPPORTING INVESTIGATIONS 4
TABLE 3-1 COSTS FOR IPR OF RECYCLED WATER (OPTION 1) 27
TABLE 3-2 COSTS FOR IMPORTED WATER RECHARGE (OPTION 2) 28
TABLE 3-3 ESTIMATED EVAPORATION FROM INFILTRATION PONDS 29

FIGURES

FIGURE 1-1 PROJECT LOCATION 2
FIGURE 2-1 LAND OWNERSHIP 14
FIGURE 2-2 SOILS 15
FIGURE 2-3 SLOPE 16
FIGURE 2-4 GEOLOGIC MAP OF EL PASO SUBBASIN 19
FIGURE 2-5 GEOLOGIC CROSS-SECTION AND DEPTH TO WATER 20
FIGURE 2-6 EL PASO BASIN GROUNDWATER LEVELS 21
FIGURE 3-1 SITE 1 FACILITIES LAYOUT 24
FIGURE 3-2 SITE 2 FACILITIES LAYOUT 25
FIGURE 3-3 SITE 3 FACILITIES LAYOUT 26
FIGURE 4-1 PREFERRED MAR SITE 34

ATTACHMENTS

Attachment A Excerpt from Ramboll Hydrogeologic Conceptual Framework

Attachment B Hydrogrpahs in the El Paso Subbasin

Attachment C Detailed Engineering Costs for Sites 1, 2, and 3

Addendum No. 1

Findings of the Technical Advisory Committee

on January 6, 2023

IWVGA Staff presented the findings of the Phase I Investigation for Recharge Sites to IWVGA's Technical Advisory Committee (TAC) at January 6, 2022 TAC meeting. Based on information presented in the investigation, including the presence of extensive interbedded clay and sand lenses, extensive cementing present in the finer alluvial materials in the basin, and inconclusive results from the IWVWD's previous percolation test, and the significant cost to conduct addition work to further investigate the feasibility of percolation through surface spreading, the TAC members concluded that surface spreading is not currently viable in the Basin due to significant uncertainty as to where and how the water recharged through spreading will percolate into the aquifers that are used for pumping.

1.0. INTRODUCTION

The purpose of this Phase I Reconnaissance Infiltration Investigation of Potential Recharge Basins is to develop study sites for further investigation as part of a three-phase study. Phase II will present a feasibility-level study of the most probable site; Phase III will develop a pre-design level study based on the results of pilot testing. A reconnaissance-level investigation addresses the purpose of the study, description of the study area, relevant data, and cost estimates, but typically does not include the collection of new data. The Phase I report will provide recommendations for future field work and the collection of new data required to assess the feasibility of specific sites in Phase II.

The purpose of this investigation is to characterize the existing conditions based on previously published studies and potential groundwater recharge rates based on available soils, geologic, and hydrogeologic datasets. The boundary of the study area includes south-central portion of the Indian Wells Valley groundwater basin, including the Cities of Ridgecrest and Inyokern, as well as the El Paso Subbasin (Figure 1-1). Sources of water used for recharge include both reclaimed wastewater and imported water sources.

In addition to the physical characteristics that control infiltration rates, the water quality and available quantity, if known, of reclaimed and imported source waters will be described. Applicable Regional Water Quality Control Board (RWQCB) and Department of Drinking Water (DDW) regulations regarding Groundwater Recharge and Recovery Projects (GRRP) will be described to identify possible constraints. Additionally, case studies of other GRRP or Indirect Potable Reuse (IPR) projects in RWQCB Colorado River Basin Region 7 of California will also be described to provide other examples in the area.

The results of the Phase I Reconnaissance Investigation will be presented in a Technical Memorandum (TM) format that describes physical, environmental, and legal benefits and constraints associated with likely recharge locations. Reconnaissance-level capital and Operation and Maintenance (O&M) costs will be estimated for each alternative. Recommended sites for further investigation under the Phase II Feasibility Investigation will be provided.

1.0. INTRODUCTION

The purpose of this Phase I Reconnaissance Infiltration Investigation of Potential Recharge Basins is to develop study sites for further investigation as part of a three-phase study. Phase II will present a feasibility-level study of the most probable site; Phase III will develop a pre-design level study based on the results of pilot testing. A reconnaissance-level investigation addresses the purpose of the study, description of the study area, relevant data, and cost estimates, but typically does not include the collection of new data. The Phase I report will provide recommendations for future field work and the collection of new data required to assess the feasibility of specific sites in Phase II.

The purpose of this investigation is to characterize the existing conditions based on previously published studies and potential groundwater recharge rates based on available soils, geologic, and hydrogeologic datasets. The boundary of the study area includes south-central portion of the Indian Wells Valley groundwater basin, including the Cities of Ridgecrest and Inyokern, as well as the El Paso Subbasin (Figure 1-1). Sources of water used for recharge include both reclaimed wastewater and imported water sources.

In addition to the physical characteristics that control infiltration rates, the water quality and available quantity, if known, of reclaimed and imported source waters will be described. Applicable Regional Water Quality Control Board (RWQCB) and Department of Drinking Water (DDW) regulations regarding Groundwater Recharge and Recovery Projects (GRRP) will be described to identify possible constraints. Additionally, case studies of other GRRP or Indirect Potable Reuse (IPR) projects in RWQCB Colorado River Basin Region 7 of California will also be described to provide other examples in the area.

The results of the Phase I Reconnaissance Investigation will be presented in a Technical Memorandum (TM) format that describes physical, environmental, and legal benefits and constraints associated with likely recharge locations. Reconnaissance-level capital and Operation and Maintenance (O&M) costs will be estimated for each alternative. Recommended sites for further investigation under the Phase II Feasibility Investigation will be provided.

FIGURE 1-1 PROJECT LOCATION

1.1 Literature Review and Previous Studies

Previous studies determined that soil infiltration rates vary widely near the City of Ridgecrest and the El Paso Subbasin, ranging from as low as 0.23 inches per day up to 24 inches per day. In general, the recharge sites closest to the valley floor and the City of Ridgecrest are characterized by the smallest infiltration rates, while the greatest recharge rates occur higher in the basin off the valley floor. A summary of the results from each of the studies is provided in table format (Table 1-1) and discussed below in the following sections.

1.1.1 Krieger and Stewart (1989, 1996) and IWVWD (2005)

A series of reports prepared by the Indian Wells Valley Water District developed the foundation for investigation into groundwater banking in the Indian Wells Valley. The first of these reports, *Southwest Well Field Test and Monitoring Wells Construction and Development*, September 1989, (Krieger and Stewart, 1989) documented the development of a test well and three monitoring wells located approximately three miles south of Inyokern. Identified as the "Southwest Well Field", the purpose of the 1989 report was to construct and complete the test and monitoring wells and perform aquifer tests in this section of the IWV Basin.

Results from the drilling and geologic investigation indicated a general coarsening upwards of depositional material that support the conclusion that the Southwest Well Field was at one time a large lake within a chain of Pleistocene lakes. These lakes supported the deposition of silty sand and clay along nearshore shelves and basins. The 1989 Krieger and Stewart report concludes by suggesting the formation samples from the wells indicate a general trend of coarser sediments emplaced on finer sediments.

The second report developed by the IWVWD, *Results of the 1996 Southwest Well Field Aquifer Test Program*, (Krieger and Stewart, 1996) documented the results of aquifer testing in the Southwest Well Field. The primary purpose of said testing was to establish the feasibility of developing groundwater resources in the southwest region[1] The results from the investigation found that the Southwest Well Field was a favorable area to develop production wells based on the area characterized by an unconfined to semi-confined aquifer with significant saturated thickness, excellent water quality, and good recharge rates. Issues of concern identified during the investigation was potential low permeability layer at depth, vertical structure (i.e., faults), and encrustation or other factors that result in very low well efficiency.

[1] Krieger and Stewart, 1996, page 1.

TABLE 1-1 SUMMARY OF PREVIOUS INFILTRATION AND SUPPORTING INVESTIGATIONS

Author	Year	Study Area	Focus	Results
Krieger and Stewart	1989	3 mi. South of Inyokern Southwest Well Field	Well Installation	Test and Monitoring Wells completed
Converse Consultants Southwest, Inc	1991	City of Ridgecrest	Sewage Disposal	2.7 – 6.6 inches/day infiltration rate
Krieger and Stewart	1996	3 mi. South of Inyokern Southwest Well Field	Aquifer Test	Unconfined to semi-confined aquifer
IWVWD	2005	3 mi. South of Inyokern Southwest Well Field	Recharge Study	12 to 24 inches/day Infiltration rate.
Krieger and Stewart; Cato Geoscience	2008	Sierras/El Paso	Recharge Site Selection	El Paso Subbasin preferable recharge area
BSK & Assoc	2011	City of Ridgecrest	Soils Investigation	1.1 to 2.2 inches/day infiltration rate
Provost & Pritchard	2015	City of Ridgecrest	WWTP Facility Review	0.23 inches/day infiltration rate
LA DWP	2018	El Paso Subbasin	Recharge Study	Average 20 inches/day infiltration rate (1.7 ft/d)

The third report developed by the IWVWD, *Southwest Well Field Recharge Feasibility Study*, November 2005 (IWVWD, 2005) investigated whether water could be percolated into the ground in the Southwest Well Field. During the investigation, 527 acre-feet of water was recharged into two different ponds over a period of 6 ½ months from October 2003 through April 2004. There was no recorded rise in groundwater level elevations in nearby monitoring wells, leaving the report to suggest further study would be required to identify where the water went. Although the data and results from the feasibility study were not favorable, there were no conclusions from the IWVWD 2005 report regarding the feasibility of a groundwater bank in the Southwest Well Field. The IWVWD 2005 report concludes that recharge water had not reached the saturation zone and that the distance from the surface to the saturation zone is greater than most percolation projects.

1.1.2 Krieger and Stewart; Cato Geoscience, 2008

The IWVWD prepared a reconnaissance-level assessment to identify up to five potential groundwater banking sites within the Indian Wells Valley the Ground Water Banking Site Selection Report, Geologic and Engineering Considerations, September 2008 (Krieger and Stewart; Cato, 2008). A total of eight potential banking sites were evaluated as part of the study that relied on existing geology, soils, and other physical data sets to assess site suitability for developing a groundwater banking program. In general, the report found that the Lower (east of Hwy 14) and Upper (west of Hwy 14) El Paso area ranked the best largely due to geologic and hydrologic criteria. The least preferable areas for developing a groundwater banking program were the Lower (east of Hwy 14) and Upper (west of Hwy 14) Sierra area, located immediately north of Inyokern.

1.1.3 BSK Associates, 2011

BSK Associates developed the 2011 Draft Preliminary Soil Investigation Report Ridgecrest Wastewater Treatment Plan, Ridgecrest California (BSK, 2011) for Provost & Pritchard Engineering Group. The purpose of the report was to characterize the subsurface conditions in the areas of future percolation pond locations. Twenty-two borings drilled up to 50.5 feet below the ground surface and six percolation tests were performed as part of the investigation. The area of investigation was between Bowman Road and Ridgecrest Boulevard in the vicinity of the old wastewater treatment facility. The results indicated that the infiltration rates ranged from 1.1 inches per day to 2.2 inches per day. The recommendation from the report was that the percolation ponds at the site of the Ridgecrest Wastewater Treatment Plan was not recommended due to low infiltration rates.

1.1.4 Provost & Pritchard, 2015

Provost & Pritchard developed the 2015 Review Draft Wastewater Treatment Facility Plan, City of Ridgecrest, California (Provost & Pritchard, 2015) for the City of Ridgecrest (City). Although the focus of the report was for the development of a wastewater plan for the City, the report addressed previous infiltrations studies. In summary, the report found that infiltration rates identified in both the 1991 Converse Study and 2011 BSK Study were higher than those determined from a water balance method. The recommendation from the 2015 Provost & Pritchard report was to use a percolation rate of 0.23 inches per day.

The 2015 Provost & Pritchard report addressed sodic soils that are characterized by a high sodium adsorption ratio (SAR). The report suggests that sodic soils cause low permeability and sealing or clogging of permeability rates over time. While there are methods for mitigating the issue related to reduced permeability over time, the SAR of soils associated with future infiltration ponds should be characterized.

1.1.5 Los Angeles Department of Water and Power (LA DWP), 2018

LA DWP prepared a July 2018 Technical Memorandum regarding Evaluation of the Feasibility of Storage of Excess Los Angeles Aqueduct Water South of Owens Valley in the Antelope Valley and Indian Wells Valley Groundwater Basins (LA DWP, 2018). Withing the northeast portion of the El Paso Subbasin, the report focused on 3,512 acres (5.5 square miles) of parcels currently owned by LA DWP. The report estimates that infiltration rates may be as high as 2.5 feet per day (averagely 1.7 feet per day) and that the El Paso Subbasin is favorable for recharge and recovery facilities.

The 2018 LA DWP report suggests that within the El Paso Subbasin, the average depth to groundwater is 208 feet over an area of 49,537 acres. Based on a target water level of 50 feet below ground surface (bgs) and a specific yield of 0.15, the total storage available in the El Paso Subbasin for groundwater banking is 1,174,027 acre-feet. Based on LA DWP's 3,512 acres of currently owned land, the total storage available is 158,000 acre-feet. Additional information regarding the quality of water in the aqueduct and El Paso Subbasin can be found in the 2018 LA DWP report.

1.2 Rules and Regulations Related to Recharge of Recycled Water Recharge

Title 22 of the California Code of Regulations addresses water recycling criteria for surface spreading recharge projects. Application of recycled water for IPR under a GRRP is regulated by the State Water Resources Control Board's Division of Drinking Water (DDW) and the Regional Water Quality Control Board (RWQCB). DDW addresses Direct and Indirect Potable Reuse (Chapter 7.3) in the California Statutes Related to Recycled Water & the State Board's Division of Drinking Water released on January 13, 2017. Regulations related to recycled water applications for GRRPs are addressed in their July 16, 2015, document under Article 5.1. The San Diego RWQCB regulates the discharge of recycled water through the establishment of Water Discharge Requirements for groundwater quality and monitoring practices.

1.2.1 DDW Groundwater Replenishment Regulation

DDW issued Regulations Related to Recycled Water on July 16, 2015, to address how a GRRP may utilize recycled water. Article 5.1 of the regulations specifically addresses Indirect Potable Reuse projects that rely on surface application of recycled water. The California Statutes related to recycled water & the State Board's Division of Drinking Water (July 13, 2017) define "Indirect Potable Reuse for Groundwater Recharge" as follows:

> *"Indirect potable reuse for groundwater recharge" means the planned use of recycled water for replenishment of a groundwater basin or an aquifer that has been designated as a source of water supply for a public water system, as defined in Section 116275 of the Health and Safety Code.*
>
> §13561(a) DDW Recycled Water-Related Statutes

IPR includes an "environmental buffer" between the wastewater treatment plan and the potable water supply. Sections of the Recycled Water Regulations related to recycled water that control the design of the project include pathogenic microorganism control, underground retention time, recycled water contribution (RWC), and response retention time (RRT).

1.2.2 Pathogenic Microorganism Control

A project sponsor shall design and operate a GRRP such that recycled wastewater used as recharge receives treatment that achieves at least 12-log enteric virus reduction, 10-log

Cryptosporidium (*Crypto*) reduction, and 10-log *Giardia* cyst reduction. A GRRP that relies on (1) filtered wastewater, (2) disinfected tertiary recycled water, and (3) demonstrates at least six months retention underground will be credited with this 12-10-10 LRV. Alternatively, if a six-month retention time cannot be demonstrated, the project should employ at least three (3) separate treatment process, each of which can provide a maximum of a 6-log reduction in viruses, *Crypto,* and *Giardia*. In addition, for each pathogen, at least three processes must provide a minimum of a 1-log reduction. For each month of retention time underground, the project can be credited with a 1-log virus reduction.

1.2.3 Underground Retention Time

Underground retention time in the aquifer serves two purposes: (1) provide time to respond to potential system failures; and (2) allow for reduction of microbial and chemical contaminants. For the purpose of siting a GRRP location during project planning, underground retention time can be determined using either analytical modeling, numerical modeling, or a tracer study. If numerical modeling is employed to estimate underground retention time, then the project will be credited with only half the underground residence time as shown by the model. For example, if the modeling shows 4 months of underground retention time, then the project will be credited for only 2 months. If a tracer study utilizing an added tracer is performed to determine underground retention time, then the project will be credited for the same time as shown by the tracer study.

1.2.4 Response Retention Time (RRT)

The recycled wastewater applied by a GRRP must be retained underground for a period of time necessary to allow a project sponsor sufficient response time to identify treatment failures and implement appropriate corrective actions. During planning, the RRT is determined based on the method used to establish underground retention time. If numerical groundwater modeling is used for establishing underground retention time, the project sponsor will be credited with 0.5 months RRT for each month of underground retention; if a tracer study is performed utilizing an added tracer, then the RRT will be the same as the underground retention time determined by the tracer study.

1.2.5 Recycled Water Contribution

The initial RWC of a GRRP shall not exceed 20% based on the total volume of recycled wastewater and credited diluent water for the preceding 120 months. A GRRP may increase the RWC if the RWC does not exceed 0.5 mg/L divided by the maximum total organic carbon (TOC) concentration of the recycled water before application. Hence, if the TOC concentration is 1 mg/L, then the RWC cannot be greater than 0.5 mg/L divided by 1 mg/L or 50%.

1.2.6 Hydrogeologic Assessment

A hydrogeologic assessment from the project sponsor is required by the Engineering Report (*§ 60323*), and must include the following

(1) Qualifications of individual preparing assessment

(2) General description of the geologic and hydrogeologic setting of groundwater basins that will potentially be affected by the GRRP

(3) Stratigraphic description of aquifers that will potentially be affected by the GRRP including composition, extent, and physical properties

(4) Description of seasonal impacts to potentially affected aquifers (based on 4 rounds of consecutive monitoring)

(5) Existing hydrogeology and anticipated hydrogeology as a result of the GRRP

(6) Maps showing quarterly groundwater elevation contours, vector flow directions and hydraulic gradients

1.3 Environmental Permitting and Other Regulatory Considerations

Depending on the scope and location of the final Managed Aquifer Recharge (MAR) projects in the IWV Basin, permitting and/or consultation with the SWRCB, RWQCB, Department of Drinking Water (DDW), California Department of Wildlife, the Army Corps of Engineers (ACOE), and the U.S. Fish and Wildlife Service will be required. Depending on use of federal or state lands, National Environmental Policy Act (NEPA) and/or California Environmental Quality Act (CEQA) compliance will be required. Additional consideration of the Basin's Salt and Nutrient Management Plan and other planning documents should be addressed in the final planning process. Permitting for infiltration testing will require

environmental review and right-of-way agreements for pilot testing and investigations performed on federal and/or state land, which require NEPA/CEQA compliance.

1.4 Case Studies

In support of the Indian Wells Valley (IWV) Infiltration Study, a case study on Indirect Potable Reuse (IPR) projects in the Lahontan and Colorado River Regions was conducted. Currently, no IPR projects have been permitted in the Lahontan Region, however Palmdale Water District is working towards permitting of the Palmdale Regional Recharge and Recovery Project. The Colorado River Region has one permitted project, the Yucca Valley Wastewater Reclamation Plant. These projects were reviewed to gain insight into project permitting, general requirements associated with groundwater replenishment, and issues that may be faced during project development.

1.4.1 Projects in Lahontan Region 6

Littlerock Creek Groundwater Recharge and Recovery Project

The Littlerock Creek Groundwater Recharge Recovery Project is a project lead by the Palmdale Water District (PWD). Although this project has not been permitted by the California Regional Water Quality Control Board (CRWQB), Lahontan Region, the PWD has taken significant steps in the permitting process.

The Recharge and Recovery Project was originally planned as a groundwater replenishment project where tertiary treated, nitrogen reduced wastewater effluent was to be mixed with State Water Project water and percolated to the Lancaster subbasin aquifer. The project was to occur in two phases. Phase 1 was set to provide 14,125 acre-feet per year (AFY) over the first 22 years, followed by Phase 2, which was set to provide 24,250 AFY (with a max design potential of 30,000 AFY) through 2067.

From 2015 to 2018, the CRWQB, Lahontan Region held meetings where updates on the Recharge and Recovery Project were discussed. In November 2015, the Recharge and Recovery Project Draft Environmental Impact Report was rejected due to an inadequate evaluation of impacts to groundwater quality for the project's duration. The Division of Drinking Water (DDW) met with PWD in September 2018 to verify the status of a soil column study demonstrating aquifer treatment. Jay Cass, the Senior Water Resources Control Engineer of the

Lahontan Water Board, provided follow-up information on the status of PWD's Recharge and Recovery Project.

As of June 2021, the PWD submitted a draft Title 22 Engineering Report, and was in the process of completing further studies associated with DDW comments. A recent phone conversation with Scott Rogers (Engineering Manager at PWD) revealed PWD received a negative outcome in testing where recharge capacity of the planned percolation area was half of what was expected and needed. As a result, the project has transitioned from surface spreading of wastewater effluent to injection exclusively. This project is currently awaiting budgetary approval.

1.4.2 Projects in Colorado River Region 7

Yucca Valley Wastewater Reclamation Plant

The Yucca Valley Wastewater Reclamation Plant is an IPR project lead by the High Desert Water District (HDWD) located in the Town of Yucca Valley. The project consists of two parts: 1) establishment of a sewer service to parts of the Town of Yucca Valley; and 2) construction of a Wastewater Reclamation Plant (WRP), discharge spreading areas, and the first phase of a wastewater collection system. The WRP is to consist of two 40-acre parcels that contain an influent pump station, headworks, a membrane bioreactor, UV disinfection unit, a facility to handle solids, storage, and dewatering, four recharge basins for disposal of effluent, and an odor control system. The initial design capacity of the WRP is 1.0 million gallons per day (mgd), with the final design capacity reaching 1.6 mgd.

As the lead agency, the HDWD prepared a Mitigated Negative Declaration (MND) as required by the California Environmental Quality Act (CEQA) and implementing Guidelines. Following a 30-day public commenting period, the MND was approved in October 2009. In 2013, two addendums were added to the MND. Addendum No. 1 (March 2013) was added to guarantee the Phase 1 project area was adequately served. This addendum includes addition of sewer laterals from the main line to septic tanks, as well as installation of additional or alternate sewage lines. Addendum No. 2 (November 2013) altered the treatment technology of the WRP, converting the original oxidation ditch to a membrane bioreactor. This addendum also revised the initial WRP capacity from 2.0 mgd to 1.0 mgd and the final buildout capacity from 6.0 mgd to 2.9 mgd.

In May 2015, the Town of Yucca Valley approved funding for the WRP. This was followed by the CRWQB, Colorado River Region adopting Order R7-2015-0043 for the WRP in September 2015. Since 2015, the scope of this project has morphed and evolved due to budgetary concerns, and the order will have to be re-written to fit the new project scope.

2.0. PHYSICAL DATA, LAND OWNERSHIP, AND SITE SELECTION

The purpose of this section is to present and describe existing datasets that provide a basis for selecting site(s) to perform infiltration studies. These data include soils, topography, geology, and land ownership. These data are combined with recommendations and results from previous studies that were described in Section 1 of this Technical Memorandum. The results of analyzing existing datasets and previous studies results in the focus of this investigation being limited to the El Paso Basin. Areas outside the El Paso Basin were eliminated from further investigation due to results from previous studies that identified constraints due to infiltration rates, depth to groundwater, land use and other factors.

2.1 Land Ownership and Physical Data Sets

2.1.1 Land Ownership

Most of the land in the El Paso Subbasin is owned by the BLM with minority holding by private entities and LA DWP (Figure 2-1). The LA DWP parcels total 3,512 acres and are located at the mouth of Freeman Wash (LADWP, 2018).

2.1.2 Soils

The predominant soil in the El Paso Subbasin is described as the Dove Canyon-Koehn Association with 2 to 8 percent slopes (Figure 2-2) The Dove Canyon-Koehn association consists of well drained sandy loam that formed in material weathered mainly from granitic alluvium (NRCS, 2021). The typical profile in the upper 79 inches is loamy sand (0-2 inches) overlying coarse sandy loam and gravelly sand and loam (2 to 79 inches). The capacity of the most limiting layer to transmit water is classified as moderately high to high with rates that vary from 0.71 to 5.67 inches per hour in the upper 79 inches. The well-drained nature of this soil suggests that most of the valley floor is potentially feasible for recharge operation. The current NRCS soil coverage does not include areas east of Highway 14, that are known to contain similar soils (see LA DWP, 2018).

2.1.3 Surface Slope

Digital Elevation Model (DEM) 10-meter data provided by USGS (2021) was used to determine slopes in the El Paso Subbasin (Figure 2-3). Steeper slopes are located along the base of alluvial fans and tributary drainages along the base of the Sierra Nevada Mountains, while gentler slopes of less than 5% are predominant throughout the valley floor. This surface slope analysis is consistent with the description of soils in the El Paso Subbasin.

FIGURE 2-1 LAND OWNERSHIP

FIGURE 2-2 SOILS

FIGURE 2-3 SLOPE

2.2 Hydrogeology

The El Paso Subbasin comprises the southwestern-most extent of the IWV groundwater basin. It is bounded to the west and southeast by the Sierra Nevada range and the El Paso Mountains, respectively. Two fault zones are located within the El Paso Subbasin: the Sierra Nevada Frontal Fault and the Freeman Fault. The Sierra Nevada Frontal Fault is located along the eastern edge of the Sierra Nevada range. The Freeman Fault is a concealed northwest-trending fault at the northeast opening of the basin that divides the El Paso Subbasin from the main IWV groundwater basin (LADWP, 2018). It has been inferred that the Freeman Fault acts as a barrier to groundwater flow between the El Paso Subbasin and the IWV main basin (IWVGA, 2021; LADWP, 2018; Garner et al, 2017; Kunkel & Chase, 1969).

Tertiary or older rocks outcrop in the Sierra Nevada to the west and the El Paso Mountains to the southeast. Granitic rocks, biotite hornblende, hornblende diorite and gabbro compose the rocks of the Sierra Nevada, while basalt composes the rocks of the El Paso Mountains (LADWP, 2018). The floor of the El Paso Subbasin is dominated by alluvium (older and younger), fanglomerate, and fluvial fill along the major washes (LADWP, 2018 and TTEMI, 2003). The Little Dixie Wash is the predominant northeast-trending wash with two tributaries that feed into it, Freeman Wash and Sage Wash. In 1991, the U.S. Bureau of Reclamation drilled 2 wells (USBR-01 and USBR-02). From those borehole cuttings, they determined that there is at least 1,800 feet of alluvial fan deposition and the bottom of the formation is identified as the Ricardo Formation (LADWP, 2018; TTEMI, 2003; USBR, 1993). A geologic map of the area is shown in Figure 2-4.

Geologic cross section A-A' through the El Paso Subbasin is shown in Figure 2-5. The cross section passes through 3 wells (27S/38E-31, AB303-05, and 27S/38E-1), and data from 10 additional wells was projected onto the cross section. Land surface elevations on this cross section begin at approximately 3,330 feet above mean sea level (ft, amsl) and decrease northward toward the main basin to approximately 2,500 ft, amsl. In general, the upper 600 feet of the stratigraphic column in the El Paso Subbasin consists of Pleistocene unconsolidated sands and gravels deposited from adjacent alluvial fans. Clays and lake-bed deposits are present at depths of around 250 feet bgs in wells 27S/38E-31 and -30 at the southern end of the cross section A-A'. These low permeability layers do not appear to be continuous or extensive in the center and northern part of the El Paso Subbasin north of Freeman Wash. Review of the Ramboll

Hydrogeologic Conceptual Framework[2] model show similar sequences and thicknesses of coarse-grained material overlying finer grained deposits (Ramboll, 2019)

Depth to groundwater is least along the east side of the El Paso Subbasin and increases along its margins as ground surface rises at a faster rate than the groundwater table. Measured depth to groundwater levels in these wells range from 184 ft bgs in well USBR-1 to 505 ft bgs in well 27S/38E-08R1. Generally, groundwater levels south of the Freeman Fault may be expected to range from 200 to 400 feet bgs, depending on location; while depth to groundwater is least on the east of Highway 14 compared to depths on the west side of the highway. The Ramboll Hydrogeologic Conceptual Framework[3] model shows depth to groundwater ranging from 50 meters to 100 meters (165 feet to 330 feet) in the vicinity of Freeman Wash (Ramboll, 2019).

The Kern County Water Agency (KCWA) has been measuring spring and fall depth to groundwater since 1989, however, the earliest measurement collected by KCWA in the El Paso Subbasin was in 1991. KCWA currently measures depth to groundwater at 12 monitoring wells in the El Paso Subbasin. Depth to water levels vary across the subbasin from approximately 200 ft bgs in the southern part of the basin to over 400 ft bgs in the areas between Highway 14 and the Freeman Fault. Hydrographs showing both groundwater elevations and depth to water levels for these wells can be found in Appendix B.

KCWA also produces groundwater elevation contours for the IWV groundwater basin Sustainable Groundwater Management Act Annual Report. Fall 2019 groundwater level contours for the El Paso Subbasin are shown in Figure 2-6. Groundwater level contours indicate that flow occurs from the El Paso Subbasin toward the IWV main basin. These groundwater elevation contours steepen as they approach the Freeman Fault.

2.2.1 Water Quality

Water quality of both the source water (i.e., recycled or imported water) and the groundwater at the recharge site must be addressed to determine whether impacts will occur and whether they can be mitigated. The source water's reaction with sodic soils should be assessed to determine when impermeable layers may be created and whether they can be mitigated through water conditioning. Finally, general chemistry, metals, gross alpha, and other constituents in the El Paso Subbasin groundwater should be assessed for consistency with state primary and secondary drinking water standards.

[2] See Appendix A, page 61.
[3] Ibid, page 62.

FIGURE 2-4 GEOLOGIC MAP OF EL PASO SUBBASIN

FIGURE 2-5 GEOLOGIC CROSS-SECTION AND DEPTH TO WATER

FIGURE 2-6 EL PASO BASIN GROUNDWATER LEVELS

2.3 Site Selection

This investigation has been focused on the El Paso Subbasin based on results from previous studies (Chapter 1). Areas that were excluded from investigation included: (1) Naval Air Station China Lake; (2) The City of Ridgecrest; (3) Southwest Well Field near Inyokern; and (4) Sierra drainages north of Inyokern. These areas were eliminated from investigation due to restricted land use, low infiltration rates, and hydrogeologic restrictions. Previous reports supporting wastewater planning in the City of Ridgecrest identified percolation rates as little as 0.23 inches per day, which are believed to be characteristic of the lowest portions of the IWV Basin valley floor. No further investigation was warranted at the Southwest Well Field, in the areas south of Inyokern, due to depth to groundwater, potential low permeability horizontal layers, and fault boundaries. Finally, the areas north of Inyokern, along the eastern flank of the Sierra Nevada Mountains. were eliminated from further investigation due to land use issues, groundwater development, and depth to groundwater (Stewart and Krieger; Cato, 2008).

The available land ownership, soils, surface slope, and hydrogeology data may be used to assess the potential locations for future infiltration sites. The central and southern portions of the El Paso Subbasin, including the area in the vicinity of the Freeman Canyon and Little Dixie Washes, provide preferable locations for groundwater recharge and recovery operations. While these areas of the El Paso Subbasin provide relatively shallow depths to groundwater and potentially high surface infiltration rates, specific subsurface geology varies from one location to another. As discussed in greater detail at the end of this Technical Memorandum, a drilling and coring program will be required to assess the lithology at each site to determine if horizontal low permeability layers (i.e., caliche or other hardpan) exist or have the potential to develop based on soils and anticipated recharge water quality.

Based on previously published reports and the data presented in this Technical Memorandum, three site locations have been chosen to perform engineering and cost analysis. These three sites represent typical locations where either reclaimed water recharge (i.e., Indirect Potable Reuse) or recharge of imported water (i.e., aqueduct or adjacent basin) surface infiltration could occur. These sites have been chosen to provide a range of costs and estimated loss of water that could be expected to occur over the life of a project. The final location and size of a recharge and recovery facility would be based pilot infiltration testing and feasibility analysis.

3.0. FACILITY AND ENGINEERING REQUIREMENTS

Three sites were selected to assess required facilities and costs associated with conveying either recycled water or imported water to the El Paso Subbasin for groundwater banking. Site 1 is located immediately north of the of Freeman Canyon Wash and represents the shortest distance from the existing Wastewater Treatment Facility to a potential recharge site. Site 3 is the southernmost location in the El Paso Subbasin, downstream of Bird Spring Canyon, and would be closest to either the aqueduct or an imported water source from a southern basin, but farthest from a recycled water source. Site 2 is located in between Sites 1 and 3, downstream from Sage Canyon, and represents a half-way point in terms of proximity to recycled or imported water.

Two options have been developed for each of the three sites. Option 1 is the IPR option that reflects 2,095 AFY of recycled water recharge and recovery via surface spreading. Option 2 is the imported water recharge options that is based on recharging up to a maximum of 10,000 AFY and recovering an annual average of 5,000 AFY. Average annual recovery is less than maximum delivery due to long-term variability in supply.

3.1 IPR Option 1 Facilities

Option 1 facilities include a 12-inch pipeline and appropriate pump station to deliver water from the City's Wastewater Treatment Plant to each of the three recharge sites (Figures 3-1, 3-2, and 3-3). Based on an infiltration rate of 1.7 feet per day (20.4 inches per day) and the delivery of 2,095 AFY, approximately 3.4 acres are required for infiltration. An additional 50% recharge area has been added to provide operational flexibility for managing the recharge rates, resulting in a total required recharge area of 5.1 acres. Sites 2 and 3 include recovery wells, a manifold between wells, and a 12-inch pipeline from the manifold to the intersection of highways 395 and 14 in Inyokern. Site 1 does not include the cost for recovery wells, a manifold, or a return pipeline due to the proximity of existing production wells. Recovery of recycled water will occur from existing wells.

The estimated capital cost of IPR Option 1 Facilities is $32.1 million, $79.9 million, and $92.7 million at Sites 1, 2, and 3, respectively (Table 3-1). The estimated capital costs represent the minimum investment to deliver and recharge recycled water from the Ridgecrest Wastewater Treatment Plant to each of the three sites for eventual deliver of an equivalent amount to Inyokern. Annual Operation and Maintenance costs, which includes power and repair, are $1.2 million, $2,1 million, and $2.4 million at Sites 1, 2, and 3, respectively.

FIGURE 3-1 SITE 1 FACILITIES LAYOUT

FIGURE 3-2 SITE 2 FACILITIES LAYOUT

FIGURE 3-3 SITE 3 FACILITIES LAYOUT

TABLE 3-1 COSTS FOR IPR OF RECYCLED WATER (OPTION 1)
($ Million)

Facility	Site 1	Site 2	Site 3
Recycled Water Pipeline	$28.0	$44.3	$51.1
Pump Station	3.6	4.0	4.0
Levee and Berm[1]	0.5	0.4	0.3
Groundwater Wells	n/a	3.2	3.2
Potable Water Pipeline	n/a	28.0	34.1
Total	$32.1	$79.9	$92.7
Annual O&M	$1.2	$2.1	$2.4

Note(s): (1) Levee and Berm includes land acquisition costs
Potable Water Pipeline terminates in Inyokern.
See Attachment C for detailed costs.

3.2 Imported Water Recharge Option 2 Facilities

Imported Water Recharge Option 2 facilities only include recharge ponds, collection wells, and return flow pipeline to Inyokern. No allowance has been made for the cost to deliver 10,000 AFY of imported water to each of the sites. Based on an infiltration rate of 1.7 feet per day (20.4 inches per day) and the delivery of 10,000 AFY, approximately 16.2 acres of recharge ponds are required for infiltration. An additional 50% recharge area has been added to provide operational flexibility for managing the recharge rates, resulting in a total required recharge area of 24.3 acres. Sites 2, and 3 include recovery wells, a manifold between wells, and a 24-inch pipeline from the manifold to the intersection of highways 395 and 14 in Inyokern. Site 1 has been excluded from this option due to poor hydrogeologic conditions for recharge and recovery of imported water. The estimated capital cost of Import Water Recharge Facilities is $41.7 million and $48.8 million for Option 2 at Sites 2 and 3, respectively (Table 3-2). Annual Operation and Maintenance costs, which includes power and repair, are $0.9 million and $1.0 million at Sites 2 and 3, respectively. The estimated capital and O&M costs represent the minimum investment to recharge and recover imported water to Sites 1 and 2 for eventual delivery of an equivalent amount to Inyokern.

TABLE 3-2 COSTS FOR IMPORTED WATER RECHARGE (OPTION 2)
($ Million)

Facility	Site 1	Site 2	Site 3
Imported Water Pipeline	n/a	n/a	n/a
Pump Station	n/a	n/a	n/a
Levee and Berm[1]	n/a	0.8	0.8
Groundwater Wells		6.4	6.4
Potable Water Pipeline		33.5	41.6
Total	n/a	$40.7	$48.8
Annual O&M	n/a	$0.9	$1.0

Note(s): (1) Levee and Berm includes land acquisition costs
Potable Water Pipeline terminates in Inyokern.
See Attachment C for detailed costs.

3.3 Evaporative Water Losses

Water loss from recharge ponds located within the IWV Basin will vary depending on the infiltration rate and required surface area of the recharge pond. Higher infiltration rates will require smaller recharge ponds and result in higher efficiencies and less evaporative losses. Similarly, wind can also impact evaporation rates by reducing both humidity and vapor pressure above a water body, resulting in additional evaporative losses. Both high wind and high daytime temperatures and related solar radiation will adversely impact water loss from recharge ponds in the IWV Basin.

Actual evaporation data from the 2003/2004 Recharge Study (IWVWD, 2005) was compared to 2020/2021 ETo data for the Ridgecrest Station #257. During the October through April months, the ETo data were higher than that which was recorded at during the recharge study. Although the discrepancy may be explained by the different years that represented by the data, they show a similar and expected trend of higher evaporation rates in the fall and spring months and less during the winter months. The evaporation from an open water body varies based on time of year, depth, area, temperature, topography, and vegetation surrounding the

water (Brown). Based on these factors, monthly evaporation can range from ETo to 1.4 times ETo. In order to estimate evaporation from infiltration ponds, ETo for Ridgecrest was multiplied by a factor of 1.2 as shown in the last column of Table 3-3. The recommended annual evaporation rate of 90.1 inches (7.5 feet) represents a conservative estimate greater than that recorded during the 2003/2004 Recharge Study by IWVWD.

TABLE 3-3 ESTIMATED EVAPORATION FROM INFILTRATION PONDS
(inches)

Month	ETo	2003/2004 Pilot Study	Recommended Evaporation Rate
Oct	4.7	9.8	5.7
Nov	3.0	2.7	3.6
Dec	2.0	2.1	2.4
Jan	2.5	1.5	3.0
Feb	3.4	2.7	4.1
Mar	5.6	3.7	6.8
Apr	8.0	8.2	9.6
May	9.4	*9.9*	11.3
Jun	10.0	*10.4*	11.9
Jul	9.8	*10.3*	11.8
Aug	9.4	*9.9*	11.3
Sep	7.2	*7.5*	8.6
Total	75.1	78.8	90.1

Notes: ETo is reported CIMS data for 2020-2021.
2003/2004 Pilot Study values estimated for May through Sept.

Total evaporative losses from either the IPR Recharge Project (Option 1) or the Imported Water Recharge Project (Option 2) are estimated to be 25 AFY and 122 AFY, respectively. Both these losses equate to approximately 1.2% of the delivered 2,095 AFY and 10,000 AFY under Options 1 and 2. The annual loss due to evaporation may be quantified in operation and maintenance costs associated with the final project.

4.0. SUMMARY AND RECOMMENDATIONS

The purpose of this reconnaissance-level investigation was to identify potential groundwater recharge sites in the IWV Basin for further investigation and collection of new data. Previous studies investigated soils, hydrogeology, infiltration rates, and other factors affecting groundwater recharge using surface application methods. This investigation relied on existing data and previous studies' results to identify specific locations that would be suitable for detailed field investigation and potential recharge pond pilot testing.

In general, the IWV Basin's valley floor is characterized by low infiltration rates due to the presence of fine-grained low-permeability materials. Because of the presence of these materials, this investigation focused on areas outside of the valley floor along the base of the Sierra Nevada Mountains. Detailed review of the previous studies eliminated areas north of Inyokern due to the depth to groundwater, fault barriers, existing production wells, and the availability of land. Areas on the east and southeast side of the IWV Basin were eliminated from further investigation due to land ownership and distance from production wells and sources of imported water. Therefore, this investigation focused on areas within the El Paso Subbasin where recharge and recovery operations would be physically supported by available land, hydrogeology, and surface conditions.

A large portion of the El Paso Subbasin is managed by the BLM, not including 3,512 acres owned by LA DWP and other privately owned parcels. The floor of the El Paso Subbasin is characterized by slopes of less than 5% and range in elevation from 2,500 feet msl to more than 3,330 feet msl. The soils are predominantly characterized by well drained sandy loam that formed in material weathered mainly from granitic alluvium. The upper 80 inches of the soil column is predominantly composed of coarse sandy loam and gravelly sand and loam (2 inches to 79 inches). Estimated infiltration rates in the El Paso Subbasin averaged 1.7 feet per day and ranged from 0.2 to 2.5 feet per day (LADWP, 2018).

Geologic borehole information shows thick sequences of lakebed or fine-grained material at depths greater than 250 feet in the southernmost portion of the El Paso Subbasin and thicker sequences of coarser gained material to the north. The coarse-grained sand and gravelly fanglomerate sequences located in the center and northern portions of the El Paso Subbasin are suitable for groundwater storage and recovery. Based on available borehole information, there are no known near surface continuous clay or low permeable layers that would restrict groundwater recharge. The depth to groundwater is least along the east side of the El Paso Subbasin and increases along its western margins as ground surface rises at a faster rate than the

groundwater table. Generally, groundwater levels south of the Freeman Fault may be expected to range from 200 to 400 feet bgs.

Three site locations were investigated to estimate capital costs for delivering and recharging either recycled or imported water to the IWV Basin. The engineering analysis was based on delivering either 2,095 AFY of recycled water (Option 1) or up to a maximum of 10,000 AFY of imported water (Option 2). Similarly, the engineering analysis was based on recovering all of the recycled water, but only 50%[4] (5,000 AFY) of recharged imported water. Of the three sites investigated, only Sites 2 and 3 included the use of new recovery wells and a conveyance pipeline to deliver up to 5,000 AFY of water to Inyokern. Site 1 relied on existing production wells to manage groundwater storage and recovery of recycled water only since this site was not analyzed for imported water recharge (Option 2). The capital costs for Option 1 recharge of recycled water, not including pre-treatment requirements, ranged from $32.1 million to $92.7 million, while the capital cost for Option 2 recharge of imported water ranged from $40.7 million to $48.8 million.

Annual O&M costs were also investigated for each of the options at the three sites. O&M costs were greatest for Option 1 due to power costs and booster station maintenance for facilities associated with delivering recycled water from the WWTP to the recharge facilities. The O&M costs for Option 1, Sites 1, 2, and 3 were $1.2 million, $2.1 million, and $2.4 million respectively. The equivalent per acre-foot costs, not including capital costs, for the same sites based on 2,095 acre-feet delivered are $560, $1,020, and $1,130, respectively. The O&M costs for Option 2, Sites 2 and 3 were $0.9 million and $1.0 million, respectively. The equivalent per acre-foot costs, not including capital costs, for the same sites based on 5,000 AFY recovered and delivered to Inyokern, are $190 and $200, respectively.

Evaporative losses from a MAR project in the El Paso Subbasin are estimated to be about 1.2%, which equates to about 25 AFY for Option 1 and 122 AFY for Option 2. The evaporative losses were based on actual October through April data collected during the recharge pilot study at the Southwest Wellfield (IWVWD, 2005) and adjusted for year-around losses. Water supply losses due to evaporation should be accounted for in annual operation and maintenance costs estimated as part of project feasibility.

[4] The recharge ponds are sized for a maximum delivery year of 10,000 AFY, while recovery was assumed to average 5,000 AFY due to long-term variability in supply subject to availability.

Site 2 provides the most likely areas to develop a MAR project based on land ownership, hydrogeology, and surface infiltration rates. Site 1 may be suitable for IPR of recycled water to supplement groundwater storage, but depth to water and the proximity to the Sierra Nevada boundary fault makes it less desirable for recovering imported recharge water. Site 3 is also less preferable due to its distance from the wastewater treatment plant (Option 1) and the regional groundwater level occurring at the top of the clay layer at a depth of approximately 250 feet bgs. Therefore, Site 2 represents the best area for developing a MAR project based on surface conditions, thick sequences of coarse-grained aquifer material, depth to groundwater, and available land.

4.1 Field Investigation Recommendations

Future field investigations required to assess suitability for a MAR should include geophysical, hydrogeologic, and operational pilot studies. A high-definition seismic survey is recommended to identify whether continuous clays or fine-grained material are present between the surface and the top of the groundwater. The hydrogeologic investigation is intended to identify soil infiltration rates, lithology, aquifer properties, and groundwater conditions related to both the recharge and recovery of groundwater. The hydrogeologic investigation will assess both the movement of water through the aquifer as well as potential water quality concerns. The pilot recharge study is intended to demonstrate the feasibility of operating a MAR based on the results from the hydrogeologic investigation.

4.1.1 Geophysical Investigation

High-resolution seismic techniques may be employed to identify horizontal and vertical anisotropies using shear wave reflection methods that employ three component geophones. The geophysical investigation study area should extend from the recharge basin to the recovery wells to map potential low permeability confining layers not identified in existing well logs. Results from this type of investigation may be used to relocate the infiltration basin or determine if other recharge techniques would be more suitable. Based on the results of this investigation, downhole seismic techniques could be employed during the Hydrogeologic Investigation.

4.1.2 Hydrogeologic Investigation

The hydrogeologic investigation includes the construction and development of monitoring and test wells to assess the aquifer properties in the vicinity of the proposed MAR project. The success of a proposed MAR project relies on both the ability to recharge water as

well as to recover water added to basin storage. Therefore, core samples and soil analysis of the near surface layers will be performed to assess whether low permeability layers (i.e., hardpan, clays, fine-grained sediments) exists. Additionally, water quality samples will be collected to determine whether sodic soils exist and if the potential exists for low-permeability layers to be created over time.

Project proponents should work with the BLM to assess the potential for developing a right of way or land exchange for up to 30 acres of land in the vicinity of Site 2. Land will be required for a minimum of 24 acres of recharge ponds, eight production wells, electrical facilities, pipelines, and appurtenant facilities. The location of the proposed MAR project could be on either side of the Highway 14 in the vicinity of Armistead, outside of existing LADWP owned lands (Figure 4-1). Following initial determination of a proposed site, the following investigation should be performed.

- Construct up to three (3) two-inch monitoring wells to 600 feet.
- Construct one (1) 8-inch test well to 800 feet bgs.
- Perform down-hole geophysical logging
- Perform Soil and Water Quality Sampling
- Perform an aquifer test
- Perform surface soil infiltration tests
- Trenching in select locations

FIGURE 4-1 PREFERRED MAR SITE

4.1.3 Pilot Testing

Following geophysical and hydrogeologic investigations, approximately five acres of land could be acquired to construct two one-acre infiltration basins (to allow cycling of ponds during operation), with site piping, control valves, and instrumentation and monitoring equipment. Monitoring and production wells constructed as part of the hydrogeologic investigation should be used to monitor changes in groundwater levels and flow directions. Flow meters, sampling equipment, climatic recording instruments (precipitation and evaporation), and down-hole data loggers for the test well and monitoring wells. The pilot test should be performed for a minimum of one year or until groundwater mounding is observed.

5.0. BIBLIOGRAPHY

Brown, Paul W., AZMET Evapotranspiration Estimates: A Tool for Improving Water Management of Turfgrass. Located at: https://cals.arizona.edu/azmet/et1.htm

BSK Associates, 2011. Draft Preliminary Soil Investigation Report, Ridgecrest Wastewater Treatment Plan, Ridgecrest, California. Prepared for Provost & Pritchard Engineering Group, January 7, 2011.

Conserve Consultants Southwest, Inc., 1991. Preliminary Slow Rate Infiltration Study Inactive Sewage Treatment Facility, Ridgecrest, California. Prepared for the City of Ridgecrest, April 12, 1991.

Garner, C., Bacon, S., Pohll, G., and Chapman, J., 2017. *Technical memorandum: Indian Wells Valley Groundwater Model Update.* Prepared by Desert Research Institute. November 17, 2017.

IWVGA, 2021. GSP Annual Report Water Year 2020. April, 2021.

Indian Wells Valley Water District, 2005. Southwest Well Field Recharge Feasibility Study. Prepared by IWVWD, November 2005.

Krieger & Stewart, Inc., 1996. Results of the 1996 Southwest Well Field Aquifer Test Program. Prepared for Indian Wells Valley Water District, document not dated.

Krieger & Stewart, Inc., 1989. Southwest Well Field Test and Monitoring Wells Construction and Development. Prepared for Indian Wells Valley Water District, September 1989.

Krieger & Stewart, Inc. and Cato Geoscience Inc., 2008. Ground Water Banking Site Selection Report, Geologic and Engineering Considerations. Prepared for Indian Wells Valley Water District, September 2008.

Kunkel, Fred and G.H. Chase, 1969. *Geology and Ground Water in Indian Wells Valley, California.* USGS Open-File Report 69-329. Prepared in cooperation with the Naval Weapons Center, China Lake, California.

LADWP, 2018. *Draft TM-2: Detailed Hydrogeologic Review of Antelope Valley and Indian Wells Valley Groundwater Basins.* Task Order 013. July 2018.

Provost & Pritchard Consulting Group, 2015. Wastewater Treatment Plant Facility Plan, City of Ridgecrest, CA, Review Draft. Prepared for the City of Ridgecrest, October 2015.

Ramboll, 2019. Hydrogeologic Conceptual Framework, Indian Wells Valley. Prepared for Indian Wells Valley Water District and the Brackish Groundwater Resources Study Group. Final Report, June 2019.

SWRCB, 2021 Statutory Water Rights Law, 2021. C.C.R WAT §§13560. -13569. State Water Resources Control Board. January 2021.

SWRCB, 2018. Regulation Related to Recycled Water. Title 22 Code of Regulations §§60320.100-60320.130. State Water Resources Control Board, Division of Drinking Water. October 2018.

SWRCB, Regulation Related to Recycled Water, 2018. Title 22 Code of Regulations §60323. State Water Resources Control Board, Division of Drinking Water. October 2018.

RWQCB, Lahontan Region, 2016. *Palmdale Draft Environmental Impact Report.* Executive Officer's Report. February 2016.

RWQCB, Colorado River Basin Region, 2015. *Waste Discharge Requirements for Hi-Desert Water District, Owner/Operator Yucca Valley Wastewater Reclamation Plant, Yucca Valley-San Bernardino County.* Adopted by the CRWQCB, Colorado River Basin Region on September 17, 2015.

RWQCB, Lahontan Region, 2015. *Littlerock Creek Groundwater Recharge and Recovery Project.* Executive Officer's Report. April 2015.

TTEMI, 2003. *Groundwater Management in the Indian Wells Valley Basin, Ridgecrest, California.* AB 303 Grant State of California Water Resources Department. June 2003.

USBR, 1993. *Indian Wells Valley Groundwater Project: USBR Technical Report Volume II*. A cooperative effort among the BOR, IWVWD, North American Chemical Company, and NAWS. December 1993. Prepared by USBR Lower Colorado Region.

U.S. Geological Survey, 2019. USGS 1 arc-second n36w118 1 x 1 degree: U.S. Geological Survey.

Attachment A

Excerpt from Ramboll Hydrogeologic Conceptual Framework

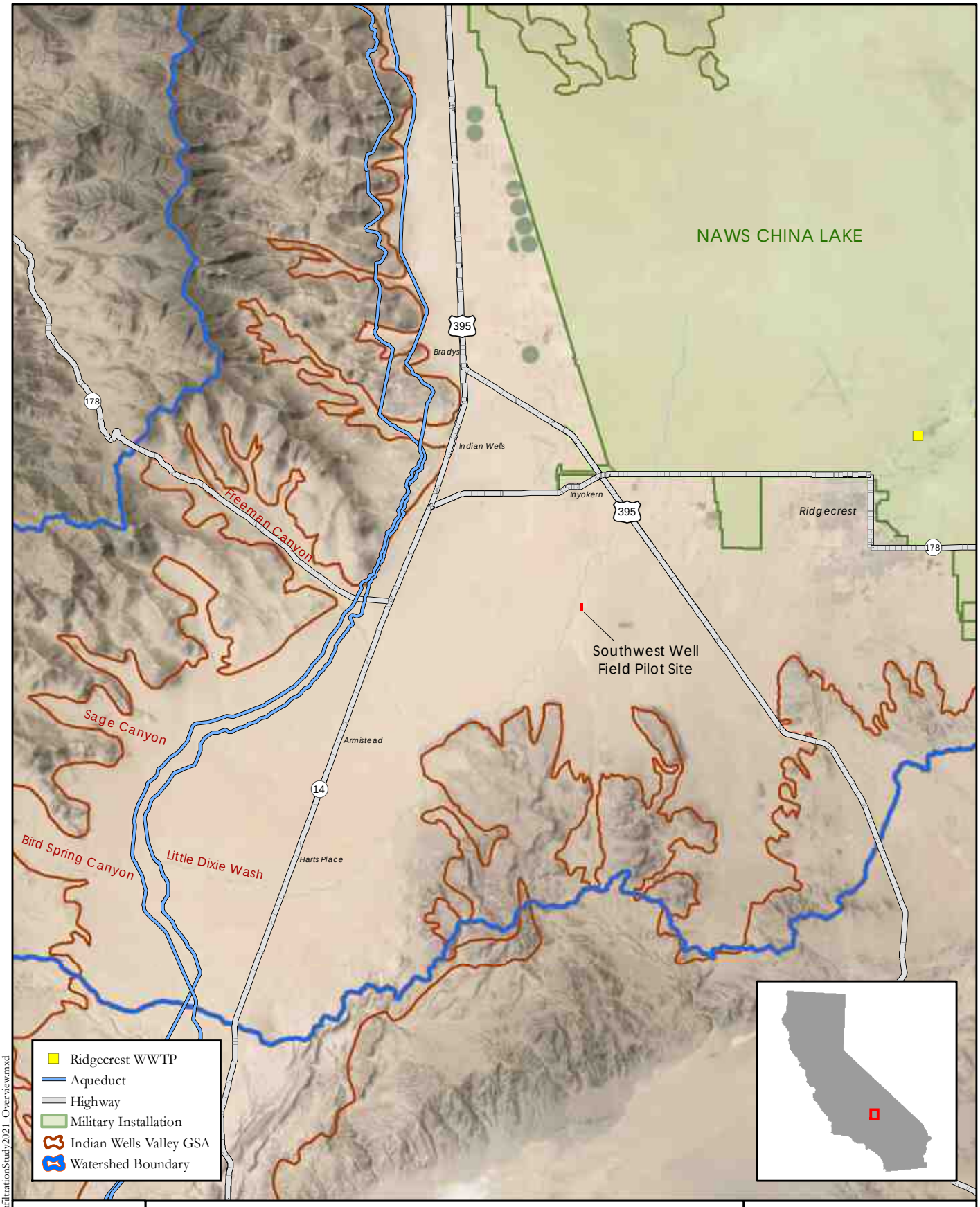
Attachment B

El Paso Subbasin Hydrographs

Attachment C

Detailed Engineering Costs for Sites 1, 2, and 3

FIGURE 1-1



STETSON ENGINEERS INC.

PROJECT OVERVIEW
INFILTRATION STUDY
INDIAN WELLS VALLEY, CA

N

0 2 4

Miles

Document Path: J:\jn2652\InfiltrationStudy2021_Overview.mxd

1.1 Literature Review and Previous Studies

Previous studies determined that soil infiltration rates vary widely near the City of Ridgecrest and the El Paso Subbasin, ranging from as low as 0.23 inches per day up to 24 inches per day. In general, the recharge sites closest to the valley floor and the City of Ridgecrest are characterized by the smallest infiltration rates, while the greatest recharge rates occur higher in the basin off the valley floor. A summary of the results from each of the studies is provided in table format (Table 1-1) and discussed below in the following sections.

1.1.1 Krieger and Stewart (1989, 1996) and IWVWD (2005)

A series of reports prepared by the Indian Wells Valley Water District developed the foundation for investigation into groundwater banking in the Indian Wells Valley. The first of these reports, *Southwest Well Field Test and Monitoring Wells Construction and Development*, September 1989, (Krieger and Stewart, 1989) documented the development of a test well and three monitoring wells located approximately three miles south of Inyokern. Identified as the "Southwest Well Field", the purpose of the 1989 report was to construct and complete the test and monitoring wells and perform aquifer tests in this section of the IWV Basin.

Results from the drilling and geologic investigation indicated a general coarsening upwards of depositional material that support the conclusion that the Southwest Well Field was at one time a large lake within a chain of Pleistocene lakes. These lakes supported the deposition of silty sand and clay along nearshore shelves and basins. The 1989 Krieger and Stewart report concludes by suggesting the formation samples from the wells indicate a general trend of coarser sediments emplaced on finer sediments.

The second report developed by the IWVWD, *Results of the 1996 Southwest Well Field Aquifer Test Program*, (Krieger and Stewart, 1996) documented the results of aquifer testing in the Southwest Well Field. The primary purpose of said testing was to establish the feasibility of developing groundwater resources in the southwest region[1] The results from the investigation found that the Southwest Well Field was a favorable area to develop production wells based on the area characterized by an unconfined to semi-confined aquifer with significant saturated thickness, excellent water quality, and good recharge rates. Issues of concern identified during the investigation was potential low permeability layer at depth, vertical structure (i.e., faults), and encrustation or other factors that result in very low well efficiency.

[1] Krieger and Stewart, 1996, page 1.

TABLE 1-1 SUMMARY OF PREVIOUS INFILTRATION AND SUPPORTING INVESTIGATIONS

Author	Year	Study Area	Focus	Results
Krieger and Stewart	1989	3 mi. South of Inyokern Southwest Well Field	Well Installation	Test and Monitoring Wells completed
Converse Consultants Southwest, Inc	1991	City of Ridgecrest	Sewage Disposal	2.7 – 6.6 inches/day infiltration rate
Krieger and Stewart	1996	3 mi. South of Inyokern Southwest Well Field	Aquifer Test	Unconfined to semi-confined aquifer
IWVWD	2005	3 mi. South of Inyokern Southwest Well Field	Recharge Study	12 to 24 inches/day Infiltration rate.
Krieger and Stewart; Cato Geoscience	2008	Sierras/El Paso	Recharge Site Selection	El Paso Subbasin preferable recharge area
BSK & Assoc	2011	City of Ridgecrest	Soils Investigation	1.1 to 2.2 inches/day infiltration rate
Provost & Pritchard	2015	City of Ridgecrest	WWTP Facility Review	0.23 inches/day infiltration rate
LA DWP	2018	El Paso Subbasin	Recharge Study	Average 20 inches/day infiltration rate (1.7 ft/d)

The third report developed by the IWVWD, *Southwest Well Field Recharge Feasibility Study*, November 2005 (IWVWD, 2005) investigated whether water could be percolated into the ground in the Southwest Well Field. During the investigation, 527 acre-feet of water was recharged into two different ponds over a period of 6 ½ months from October 2003 through April 2004. There was no recorded rise in groundwater level elevations in nearby monitoring wells, leaving the report to suggest further study would be required to identify where the water went. Although the data and results from the feasibility study were not favorable, there were no conclusions from the IWVWD 2005 report regarding the feasibility of a groundwater bank in the Southwest Well Field. The IWVWD 2005 report concludes that recharge water had not reached the saturation zone and that the distance from the surface to the saturation zone is greater than most percolation projects.

1.1.2 Krieger and Stewart; Cato Geoscience, 2008

The IWVWD prepared a reconnaissance-level assessment to identify up to five potential groundwater banking sites within the Indian Wells Valley the Ground Water Banking Site Selection Report, Geologic and Engineering Considerations, September 2008 (Krieger and Stewart; Cato, 2008). A total of eight potential banking sites were evaluated as part of the study that relied on existing geology, soils, and other physical data sets to assess site suitability for developing a groundwater banking program. In general, the report found that the Lower (east of Hwy 14) and Upper (west of Hwy 14) El Paso area ranked the best largely due to geologic and hydrologic criteria. The least preferable areas for developing a groundwater banking program were the Lower (east of Hwy 14) and Upper (west of Hwy 14) Sierra area, located immediately north of Inyokern.

1.1.3 BSK Associates, 2011

BSK Associates developed the 2011 Draft Preliminary Soil Investigation Report Ridgecrest Wastewater Treatment Plan, Ridgecrest California (BSK, 2011) for Provost & Pritchard Engineering Group. The purpose of the report was to characterize the subsurface conditions in the areas of future percolation pond locations. Twenty-two borings drilled up to 50.5 feet below the ground surface and six percolation tests were performed as part of the investigation. The area of investigation was between Bowman Road and Ridgecrest Boulevard in the vicinity of the old wastewater treatment facility. The results indicated that the infiltration rates ranged from 1.1 inches per day to 2.2 inches per day. The recommendation from the report was that the percolation ponds at the site of the Ridgecrest Wastewater Treatment Plan was not recommended due to low infiltration rates.

1.1.4 Provost & Pritchard, 2015

Provost & Pritchard developed the 2015 Review Draft Wastewater Treatment Facility Plan, City of Ridgecrest, California (Provost & Pritchard, 2015) for the City of Ridgecrest (City). Although the focus of the report was for the development of a wastewater plan for the City, the report addressed previous infiltrations studies. In summary, the report found that infiltration rates identified in both the 1991 Converse Study and 2011 BSK Study were higher than those determined from a water balance method. The recommendation from the 2015 Provost & Pritchard report was to use a percolation rate of 0.23 inches per day.

The 2015 Provost & Pritchard report addressed sodic soils that are characterized by a high sodium adsorption ratio (SAR). The report suggests that sodic soils cause low permeability and sealing or clogging of permeability rates over time. While there are methods for mitigating the issue related to reduced permeability over time, the SAR of soils associated with future infiltration ponds should be characterized.

1.1.5 Los Angeles Department of Water and Power (LA DWP), 2018

LA DWP prepared a July 2018 Technical Memorandum regarding Evaluation of the Feasibility of Storage of Excess Los Angeles Aqueduct Water South of Owens Valley in the Antelope Valley and Indian Wells Valley Groundwater Basins (LA DWP, 2018). Withing the northeast portion of the El Paso Subbasin, the report focused on 3,512 acres (5.5 square miles) of parcels currently owned by LA DWP. The report estimates that infiltration rates may be as high as 2.5 feet per day (averagely 1.7 feet per day) and that the El Paso Subbasin is favorable for recharge and recovery facilities.

The 2018 LA DWP report suggests that within the El Paso Subbasin, the average depth to groundwater is 208 feet over an area of 49,537 acres. Based on a target water level of 50 feet below ground surface (bgs) and a specific yield of 0.15, the total storage available in the El Paso Subbasin for groundwater banking is 1,174,027 acre-feet. Based on LA DWP's 3,512 acres of currently owned land, the total storage available is 158,000 acre-feet. Additional information regarding the quality of water in the aqueduct and El Paso Subbasin can be found in the 2018 LA DWP report.

1.2 Rules and Regulations Related to Recharge of Recycled Water Recharge

Title 22 of the California Code of Regulations addresses water recycling criteria for surface spreading recharge projects. Application of recycled water for IPR under a GRRP is regulated by the State Water Resources Control Board's Division of Drinking Water (DDW) and the Regional Water Quality Control Board (RWQCB). DDW addresses Direct and Indirect Potable Reuse (Chapter 7.3) in the California Statutes Related to Recycled Water & the State Board's Division of Drinking Water released on January 13, 2017. Regulations related to recycled water applications for GRRPs are addressed in their July 16, 2015, document under Article 5.1. The San Diego RWQCB regulates the discharge of recycled water through the establishment of Water Discharge Requirements for groundwater quality and monitoring practices.

1.2.1 DDW Groundwater Replenishment Regulation

DDW issued Regulations Related to Recycled Water on July 16, 2015, to address how a GRRP may utilize recycled water. Article 5.1 of the regulations specifically addresses Indirect Potable Reuse projects that rely on surface application of recycled water. The California Statutes related to recycled water & the State Board's Division of Drinking Water (July 13, 2017) define "Indirect Potable Reuse for Groundwater Recharge" as follows:

> *"Indirect potable reuse for groundwater recharge" means the planned use of recycled water for replenishment of a groundwater basin or an aquifer that has been designated as a source of water supply for a public water system, as defined in Section 116275 of the Health and Safety Code.*
>
> §13561(a) DDW Recycled Water-Related Statutes

IPR includes an "environmental buffer" between the wastewater treatment plan and the potable water supply. Sections of the Recycled Water Regulations related to recycled water that control the design of the project include pathogenic microorganism control, underground retention time, recycled water contribution (RWC), and response retention time (RRT).

1.2.2 Pathogenic Microorganism Control

A project sponsor shall design and operate a GRRP such that recycled wastewater used as recharge receives treatment that achieves at least 12-log enteric virus reduction, 10-log

Cryptosporidium (*Crypto*) reduction, and 10-log *Giardia* cyst reduction. A GRRP that relies on (1) filtered wastewater, (2) disinfected tertiary recycled water, and (3) demonstrates at least six months retention underground will be credited with this 12-10-10 LRV. Alternatively, if a six-month retention time cannot be demonstrated, the project should employ at least three (3) separate treatment process, each of which can provide a maximum of a 6-log reduction in viruses, *Crypto,* and *Giardia*. In addition, for each pathogen, at least three processes must provide a minimum of a 1-log reduction. For each month of retention time underground, the project can be credited with a 1-log virus reduction.

1.2.3 Underground Retention Time

Underground retention time in the aquifer serves two purposes: (1) provide time to respond to potential system failures; and (2) allow for reduction of microbial and chemical contaminants. For the purpose of siting a GRRP location during project planning, underground retention time can be determined using either analytical modeling, numerical modeling, or a tracer study. If numerical modeling is employed to estimate underground retention time, then the project will be credited with only half the underground residence time as shown by the model. For example, if the modeling shows 4 months of underground retention time, then the project will be credited for only 2 months. If a tracer study utilizing an added tracer is performed to determine underground retention time, then the project will be credited for the same time as shown by the tracer study.

1.2.4 Response Retention Time (RRT)

The recycled wastewater applied by a GRRP must be retained underground for a period of time necessary to allow a project sponsor sufficient response time to identify treatment failures and implement appropriate corrective actions. During planning, the RRT is determined based on the method used to establish underground retention time. If numerical groundwater modeling is used for establishing underground retention time, the project sponsor will be credited with 0.5 months RRT for each month of underground retention; if a tracer study is performed utilizing an added tracer, then the RRT will be the same as the underground retention time determined by the tracer study.

1.2.5 Recycled Water Contribution

The initial RWC of a GRRP shall not exceed 20% based on the total volume of recycled wastewater and credited diluent water for the preceding 120 months. A GRRP may increase the RWC if the RWC does not exceed 0.5 mg/L divided by the maximum total organic carbon (TOC) concentration of the recycled water before application. Hence, if the TOC concentration is 1 mg/L, then the RWC cannot be greater than 0.5 mg/L divided by 1 mg/L or 50%.

1.2.6 Hydrogeologic Assessment

A hydrogeologic assessment from the project sponsor is required by the Engineering Report (*§ 60323*), and must include the following

(1) Qualifications of individual preparing assessment

(2) General description of the geologic and hydrogeologic setting of groundwater basins that will potentially be affected by the GRRP

(3) Stratigraphic description of aquifers that will potentially be affected by the GRRP including composition, extent, and physical properties

(4) Description of seasonal impacts to potentially affected aquifers (based on 4 rounds of consecutive monitoring)

(5) Existing hydrogeology and anticipated hydrogeology as a result of the GRRP

(6) Maps showing quarterly groundwater elevation contours, vector flow directions and hydraulic gradients

1.3 Environmental Permitting and Other Regulatory Considerations

Depending on the scope and location of the final Managed Aquifer Recharge (MAR) projects in the IWV Basin, permitting and/or consultation with the SWRCB, RWQCB, Department of Drinking Water (DDW), California Department of Wildlife, the Army Corps of Engineers (ACOE), and the U.S. Fish and Wildlife Service will be required. Depending on use of federal or state lands, National Environmental Policy Act (NEPA) and/or California Environmental Quality Act (CEQA) compliance will be required. Additional consideration of the Basin's Salt and Nutrient Management Plan and other planning documents should be addressed in the final planning process. Permitting for infiltration testing will require

environmental review and right-of-way agreements for pilot testing and investigations performed on federal and/or state land, which require NEPA/CEQA compliance.

1.4 Case Studies

In support of the Indian Wells Valley (IWV) Infiltration Study, a case study on Indirect Potable Reuse (IPR) projects in the Lahontan and Colorado River Regions was conducted. Currently, no IPR projects have been permitted in the Lahontan Region, however Palmdale Water District is working towards permitting of the Palmdale Regional Recharge and Recovery Project. The Colorado River Region has one permitted project, the Yucca Valley Wastewater Reclamation Plant. These projects were reviewed to gain insight into project permitting, general requirements associated with groundwater replenishment, and issues that may be faced during project development.

1.4.1 Projects in Lahontan Region 6

Littlerock Creek Groundwater Recharge and Recovery Project

The Littlerock Creek Groundwater Recharge Recovery Project is a project lead by the Palmdale Water District (PWD). Although this project has not been permitted by the California Regional Water Quality Control Board (CRWQB), Lahontan Region, the PWD has taken significant steps in the permitting process.

The Recharge and Recovery Project was originally planned as a groundwater replenishment project where tertiary treated, nitrogen reduced wastewater effluent was to be mixed with State Water Project water and percolated to the Lancaster subbasin aquifer. The project was to occur in two phases. Phase 1 was set to provide 14,125 acre-feet per year (AFY) over the first 22 years, followed by Phase 2, which was set to provide 24,250 AFY (with a max design potential of 30,000 AFY) through 2067.

From 2015 to 2018, the CRWQB, Lahontan Region held meetings where updates on the Recharge and Recovery Project were discussed. In November 2015, the Recharge and Recovery Project Draft Environmental Impact Report was rejected due to an inadequate evaluation of impacts to groundwater quality for the project's duration. The Division of Drinking Water (DDW) met with PWD in September 2018 to verify the status of a soil column study demonstrating aquifer treatment. Jay Cass, the Senior Water Resources Control Engineer of the

Lahontan Water Board, provided follow-up information on the status of PWD's Recharge and Recovery Project.

As of June 2021, the PWD submitted a draft Title 22 Engineering Report, and was in the process of completing further studies associated with DDW comments. A recent phone conversation with Scott Rogers (Engineering Manager at PWD) revealed PWD received a negative outcome in testing where recharge capacity of the planned percolation area was half of what was expected and needed. As a result, the project has transitioned from surface spreading of wastewater effluent to injection exclusively. This project is currently awaiting budgetary approval.

1.4.2 Projects in Colorado River Region 7

Yucca Valley Wastewater Reclamation Plant

The Yucca Valley Wastewater Reclamation Plant is an IPR project lead by the High Desert Water District (HDWD) located in the Town of Yucca Valley. The project consists of two parts: 1) establishment of a sewer service to parts of the Town of Yucca Valley; and 2) construction of a Wastewater Reclamation Plant (WRP), discharge spreading areas, and the first phase of a wastewater collection system. The WRP is to consist of two 40-acre parcels that contain an influent pump station, headworks, a membrane bioreactor, UV disinfection unit, a facility to handle solids, storage, and dewatering, four recharge basins for disposal of effluent, and an odor control system. The initial design capacity of the WRP is 1.0 million gallons per day (mgd), with the final design capacity reaching 1.6 mgd.

As the lead agency, the HDWD prepared a Mitigated Negative Declaration (MND) as required by the California Environmental Quality Act (CEQA) and implementing Guidelines. Following a 30-day public commenting period, the MND was approved in October 2009. In 2013, two addendums were added to the MND. Addendum No. 1 (March 2013) was added to guarantee the Phase 1 project area was adequately served. This addendum includes addition of sewer laterals from the main line to septic tanks, as well as installation of additional or alternate sewage lines. Addendum No. 2 (November 2013) altered the treatment technology of the WRP, converting the original oxidation ditch to a membrane bioreactor. This addendum also revised the initial WRP capacity from 2.0 mgd to 1.0 mgd and the final buildout capacity from 6.0 mgd to 2.9 mgd.

In May 2015, the Town of Yucca Valley approved funding for the WRP. This was followed by the CRWQB, Colorado River Region adopting Order R7-2015-0043 for the WRP in September 2015. Since 2015, the scope of this project has morphed and evolved due to budgetary concerns, and the order will have to be re-written to fit the new project scope.

2.0. PHYSICAL DATA, LAND OWNERSHIP, AND SITE SELECTION

The purpose of this section is to present and describe existing datasets that provide a basis for selecting site(s) to perform infiltration studies. These data include soils, topography, geology, and land ownership. These data are combined with recommendations and results from previous studies that were described in Section 1 of this Technical Memorandum. The results of analyzing existing datasets and previous studies results in the focus of this investigation being limited to the El Paso Basin. Areas outside the El Paso Basin were eliminated from further investigation due to results from previous studies that identified constraints due to infiltration rates, depth to groundwater, land use and other factors.

2.1 Land Ownership and Physical Data Sets

2.1.1 Land Ownership

Most of the land in the El Paso Subbasin is owned by the BLM with minority holding by private entities and LA DWP (Figure 2-1). The LA DWP parcels total 3,512 acres and are located at the mouth of Freeman Wash (LADWP, 2018).

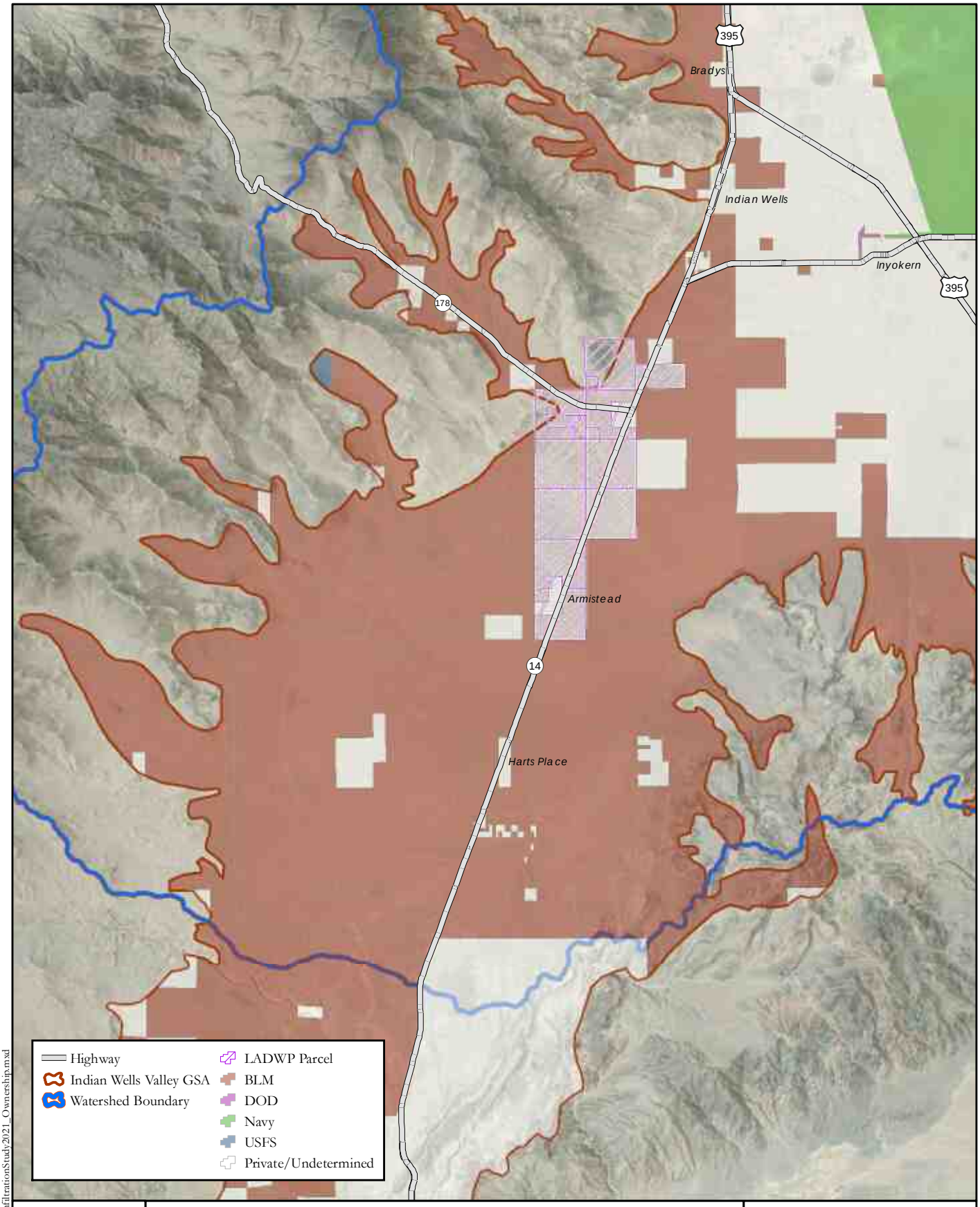
2.1.2 Soils

The predominant soil in the El Paso Subbasin is described as the Dove Canyon-Koehn Association with 2 to 8 percent slopes (Figure 2-2) The Dove Canyon-Koehn association consists of well drained sandy loam that formed in material weathered mainly from granitic alluvium (NRCS, 2021). The typical profile in the upper 79 inches is loamy sand (0-2 inches) overlying coarse sandy loam and gravelly sand and loam (2 to 79 inches). The capacity of the most limiting layer to transmit water is classified as moderately high to high with rates that vary from 0.71 to 5.67 inches per hour in the upper 79 inches. The well-drained nature of this soil suggests that most of the valley floor is potentially feasible for recharge operation. The current NRCS soil coverage does not include areas east of Highway 14, that are known to contain similar soils (see LA DWP, 2018).

2.1.3 Surface Slope

Digital Elevation Model (DEM) 10-meter data provided by USGS (2021) was used to determine slopes in the El Paso Subbasin (Figure 2-3). Steeper slopes are located along the base of alluvial fans and tributary drainages along the base of the Sierra Nevada Mountains, while gentler slopes of less than 5% are predominant throughout the valley floor. This surface slope analysis is consistent with the description of soils in the El Paso Subbasin.

FIGURE 2-1



STETSON ENGINEERS INC.

LAND OWNERSHIP
INFILTRATION STUDY
INDIAN WELLS VALLEY, CA

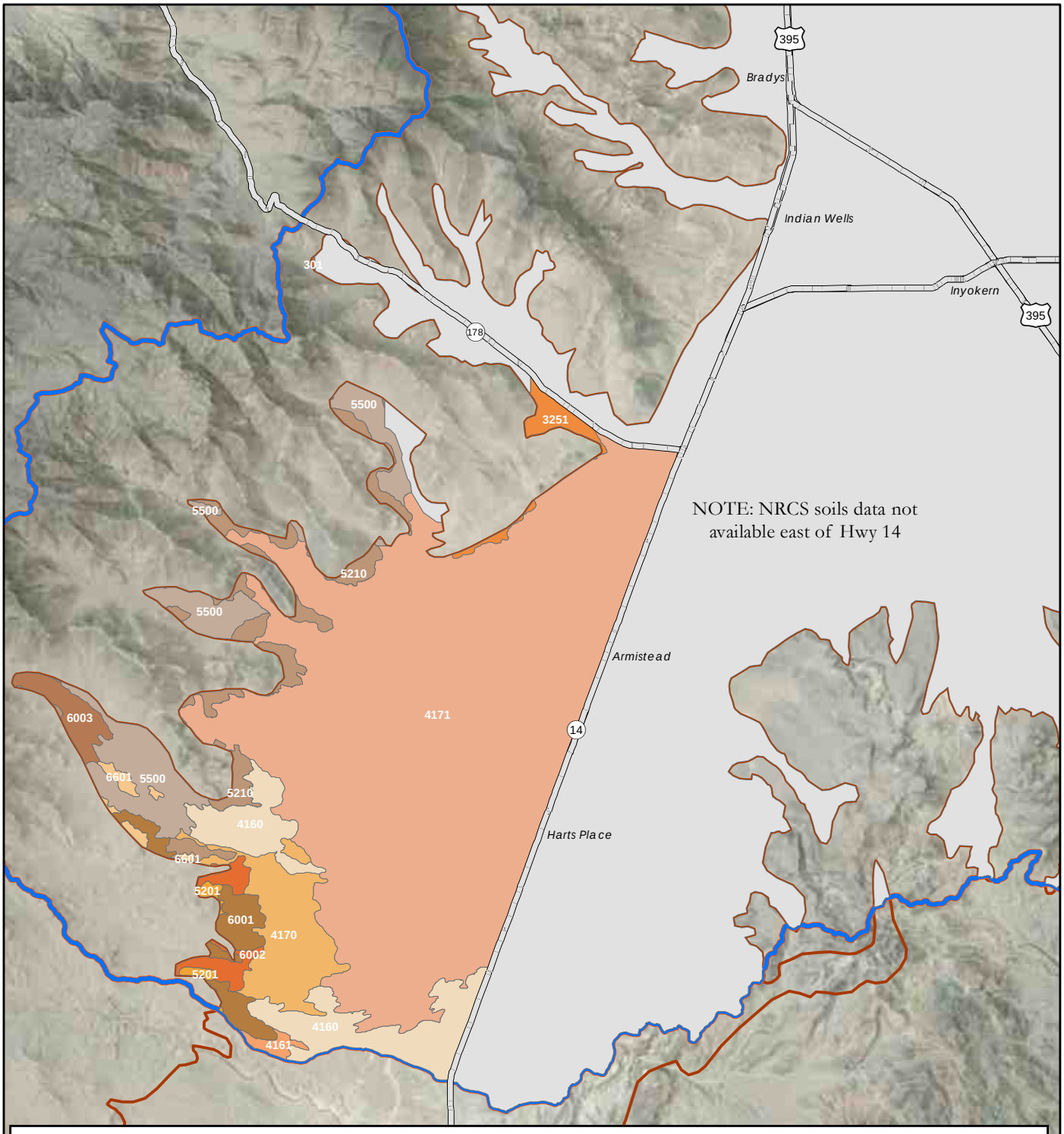
Source: BLM (Surface Management Agency v10)

N

0 1.5 3

Miles

Document Path: J:\jn2652\InfiltrationStudy2021_Ownership.mxd



Highway
Indian Wells Valley GSA
Watershed Boundary

NRCS Soils
- 301~Xerofluvents-Xerorthents association, sloping
- 3251~Jawbone association, 8 to 50 percent slopes
- 4160~Dovecanyon-Cutterbank association, 4 to 50 percent slopes
- 4161~Dovecanyon loamy sand, 2 to 8 percent slopes
- 4170~Dovecanyon association, 2 to 8 percent slopes
- 4171~Dovecanyon-Koehn association, 2 to 8 percent slopes
- 5201~Wingap-Pinyonpeak association, 8 to 30 percent slopes
- 5210~Grandora-Pinyonpeak association, 8 to 60 percent slopes
- 5500~Birdcanyon coarse sand, 4 to 15 percent slopes
- 6001~Goldpeak-Pinyonpeak-Wingap complex, 2 to 30 percent slopes
- 6002~Goldpeak gravelly loamy sand, 2 to 8 percent slopes
- 6003~Goldpeak-Pinyonpeak association, 2 to 30 percent slopes
- 6601~Pinyonpeak-Wingap-Rock outcrop association, 8 to 30 percent slopes
- NOTCOM~No Digital Data Available

STETSON ENGINEERS INC.

SOILS
INFILTRATION STUDY
INDIAN WELLS VALLEY, CA

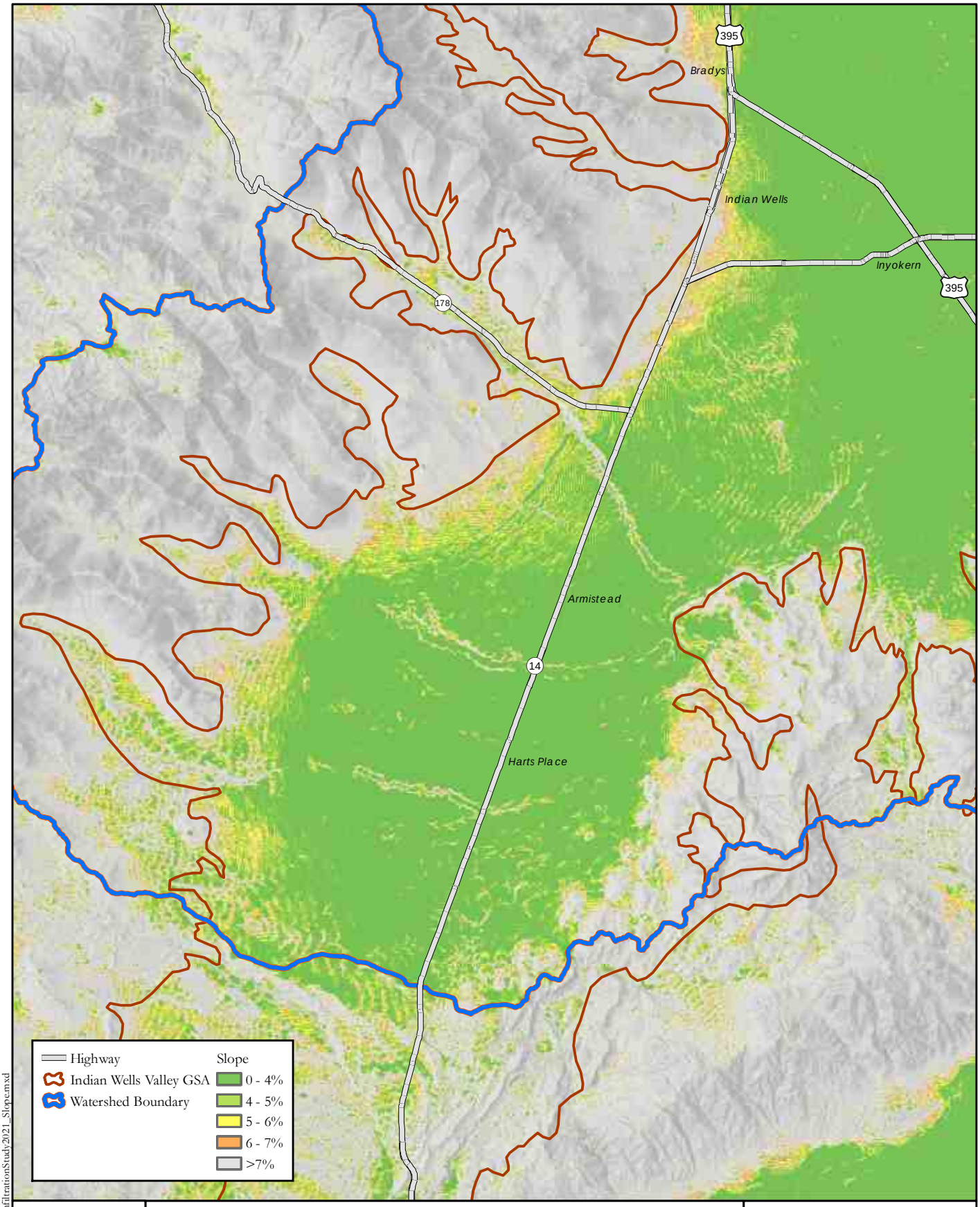
Source: NRCS Soils (2021)

N

0 1.5 3
Miles

Document Path: J:\jn2652\InfiltrationStudy2021_Soils.mxd

FIGURE 2-3



STETSON ENGINEERS INC.

SLOPE
INFILTRATION STUDY
INDIAN WELLS VALLEY, CA

N

0 1.5 3

Miles

Document Path: J:\jn2652\InfiltrationStudy2021_Slope.mxd

2.2 Hydrogeology

The El Paso Subbasin comprises the southwestern-most extent of the IWV groundwater basin. It is bounded to the west and southeast by the Sierra Nevada range and the El Paso Mountains, respectively. Two fault zones are located within the El Paso Subbasin: the Sierra Nevada Frontal Fault and the Freeman Fault. The Sierra Nevada Frontal Fault is located along the eastern edge of the Sierra Nevada range. The Freeman Fault is a concealed northwest-trending fault at the northeast opening of the basin that divides the El Paso Subbasin from the main IWV groundwater basin (LADWP, 2018). It has been inferred that the Freeman Fault acts as a barrier to groundwater flow between the El Paso Subbasin and the IWV main basin (IWVGA, 2021; LADWP, 2018; Garner et al, 2017; Kunkel & Chase, 1969).

Tertiary or older rocks outcrop in the Sierra Nevada to the west and the El Paso Mountains to the southeast. Granitic rocks, biotite hornblende, hornblende diorite and gabbro compose the rocks of the Sierra Nevada, while basalt composes the rocks of the El Paso Mountains (LADWP, 2018). The floor of the El Paso Subbasin is dominated by alluvium (older and younger), fanglomerate, and fluvial fill along the major washes (LADWP, 2018 and TTEMI, 2003). The Little Dixie Wash is the predominant northeast-trending wash with two tributaries that feed into it, Freeman Wash and Sage Wash. In 1991, the U.S. Bureau of Reclamation drilled 2 wells (USBR-01 and USBR-02). From those borehole cuttings, they determined that there is at least 1,800 feet of alluvial fan deposition and the bottom of the formation is identified as the Ricardo Formation (LADWP, 2018; TTEMI, 2003; USBR, 1993). A geologic map of the area is shown in Figure 2-4.

Geologic cross section A-A' through the El Paso Subbasin is shown in Figure 2-5. The cross section passes through 3 wells (27S/38E-31, AB303-05, and 27S/38E-1), and data from 10 additional wells was projected onto the cross section. Land surface elevations on this cross section begin at approximately 3,330 feet above mean sea level (ft, amsl) and decrease northward toward the main basin to approximately 2,500 ft, amsl. In general, the upper 600 feet of the stratigraphic column in the El Paso Subbasin consists of Pleistocene unconsolidated sands and gravels deposited from adjacent alluvial fans. Clays and lake-bed deposits are present at depths of around 250 feet bgs in wells 27S/38E-31 and -30 at the southern end of the cross section A-A'. These low permeability layers do not appear to be continuous or extensive in the center and northern part of the El Paso Subbasin north of Freeman Wash. Review of the Ramboll

Hydrogeologic Conceptual Framework[2] model show similar sequences and thicknesses of coarse-grained material overlying finer grained deposits (Ramboll, 2019)

Depth to groundwater is least along the east side of the El Paso Subbasin and increases along its margins as ground surface rises at a faster rate than the groundwater table. Measured depth to groundwater levels in these wells range from 184 ft bgs in well USBR-1 to 505 ft bgs in well 27S/38E-08R1. Generally, groundwater levels south of the Freeman Fault may be expected to range from 200 to 400 feet bgs, depending on location; while depth to groundwater is least on the east of Highway 14 compared to depths on the west side of the highway. The Ramboll Hydrogeologic Conceptual Framework[3] model shows depth to groundwater ranging from 50 meters to 100 meters (165 feet to 330 feet) in the vicinity of Freeman Wash (Ramboll, 2019).

The Kern County Water Agency (KCWA) has been measuring spring and fall depth to groundwater since 1989, however, the earliest measurement collected by KCWA in the El Paso Subbasin was in 1991. KCWA currently measures depth to groundwater at 12 monitoring wells in the El Paso Subbasin. Depth to water levels vary across the subbasin from approximately 200 ft bgs in the southern part of the basin to over 400 ft bgs in the areas between Highway 14 and the Freeman Fault. Hydrographs showing both groundwater elevations and depth to water levels for these wells can be found in Appendix B.

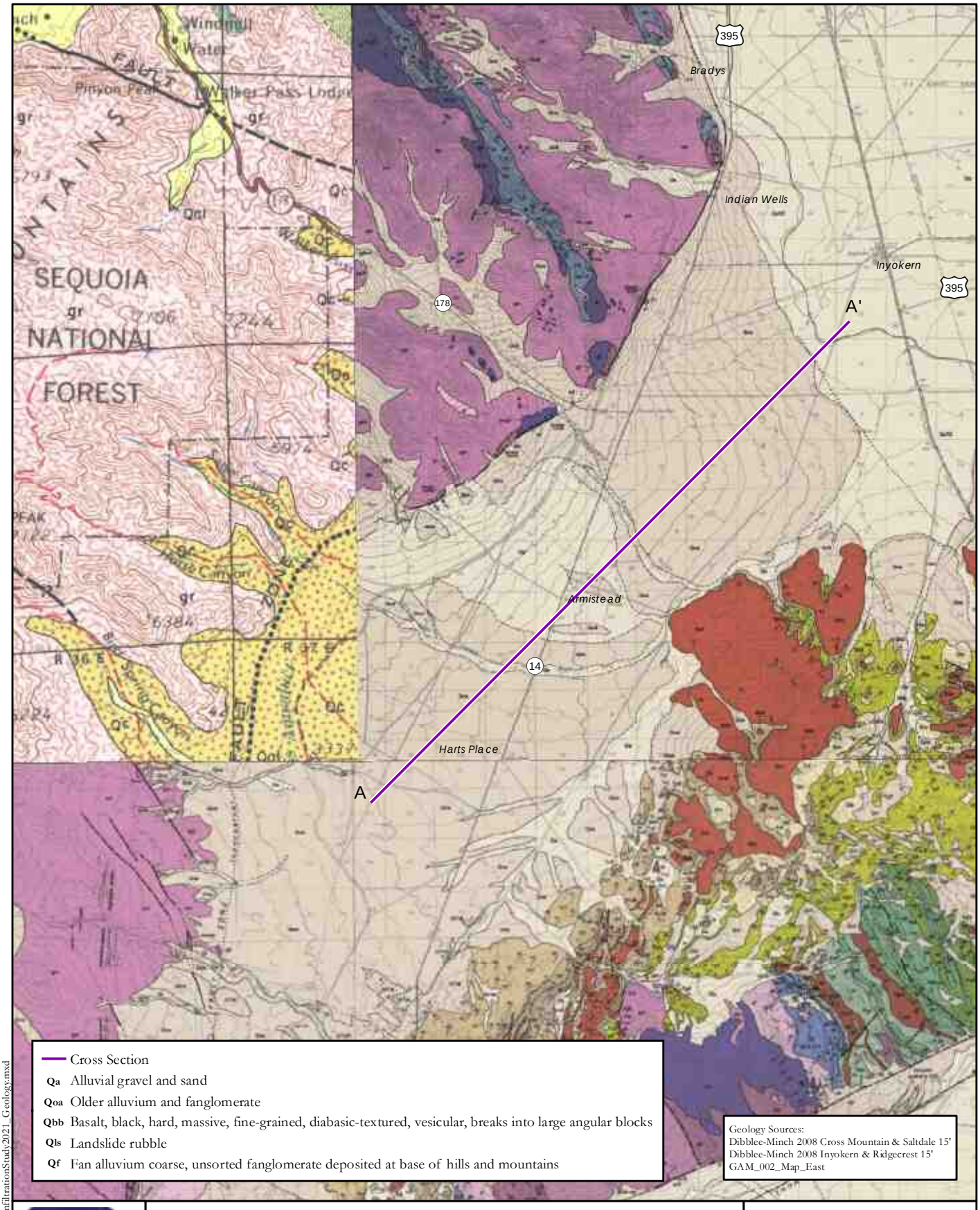
KCWA also produces groundwater elevation contours for the IWV groundwater basin Sustainable Groundwater Management Act Annual Report. Fall 2019 groundwater level contours for the El Paso Subbasin are shown in Figure 2-6. Groundwater level contours indicate that flow occurs from the El Paso Subbasin toward the IWV main basin. These groundwater elevation contours steepen as they approach the Freeman Fault.

2.2.1 Water Quality

Water quality of both the source water (i.e., recycled or imported water) and the groundwater at the recharge site must be addressed to determine whether impacts will occur and whether they can be mitigated. The source water's reaction with sodic soils should be assessed to determine when impermeable layers may be created and whether they can be mitigated through water conditioning. Finally, general chemistry, metals, gross alpha, and other constituents in the El Paso Subbasin groundwater should be assessed for consistency with state primary and secondary drinking water standards.

[2] See Appendix A, page 61.
[3] Ibid, page 62.

FIGURE 2-4



STETSON ENGINEERS INC.

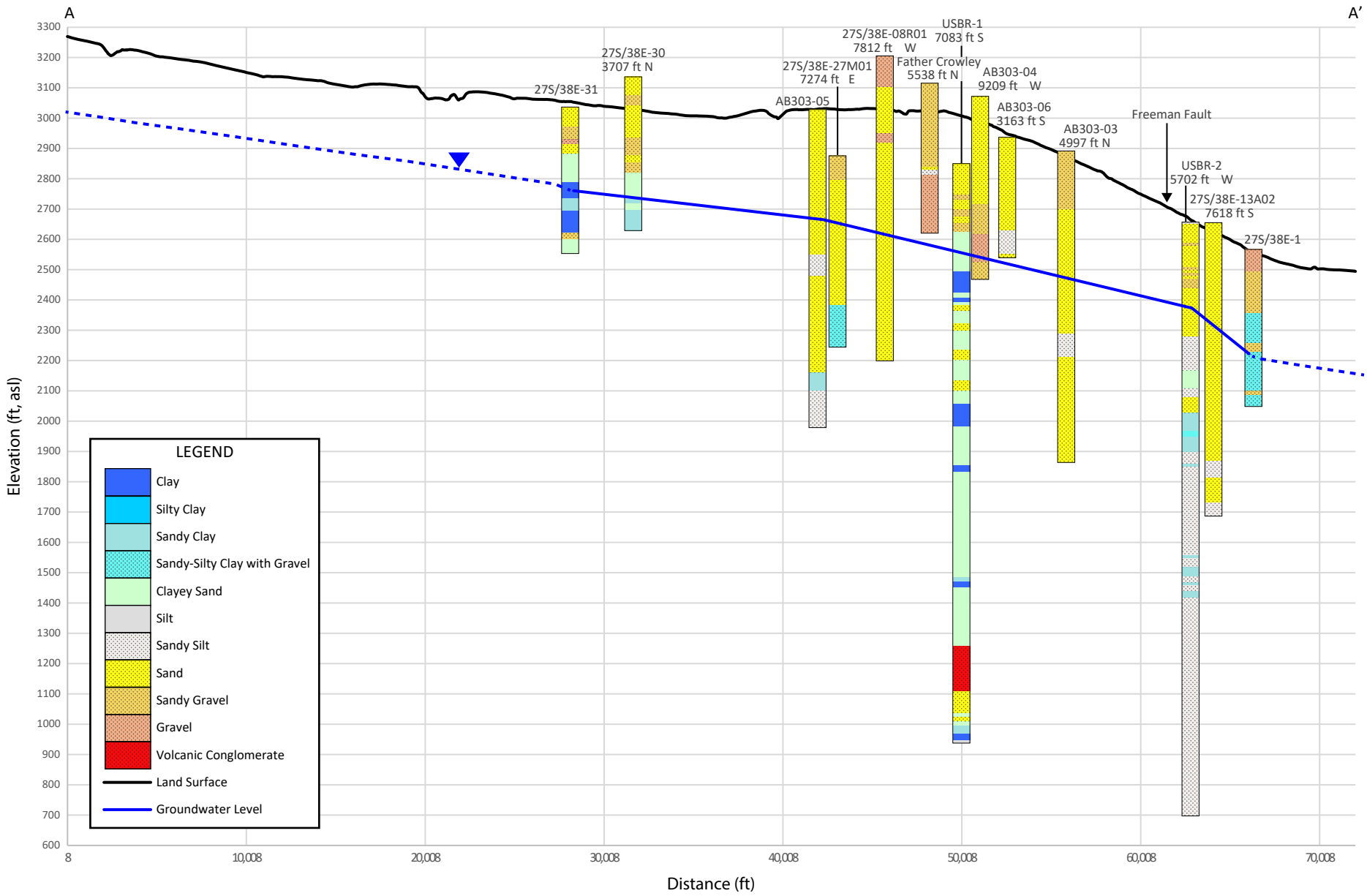
SURFACE GEOLOGY
INFILTRATION STUDY
INDIAN WELLS VALLEY, CA

N

0 1.5 3

Miles

Document Path: J:\jn2652\InfiltrationStudy2021_Geology.mxd



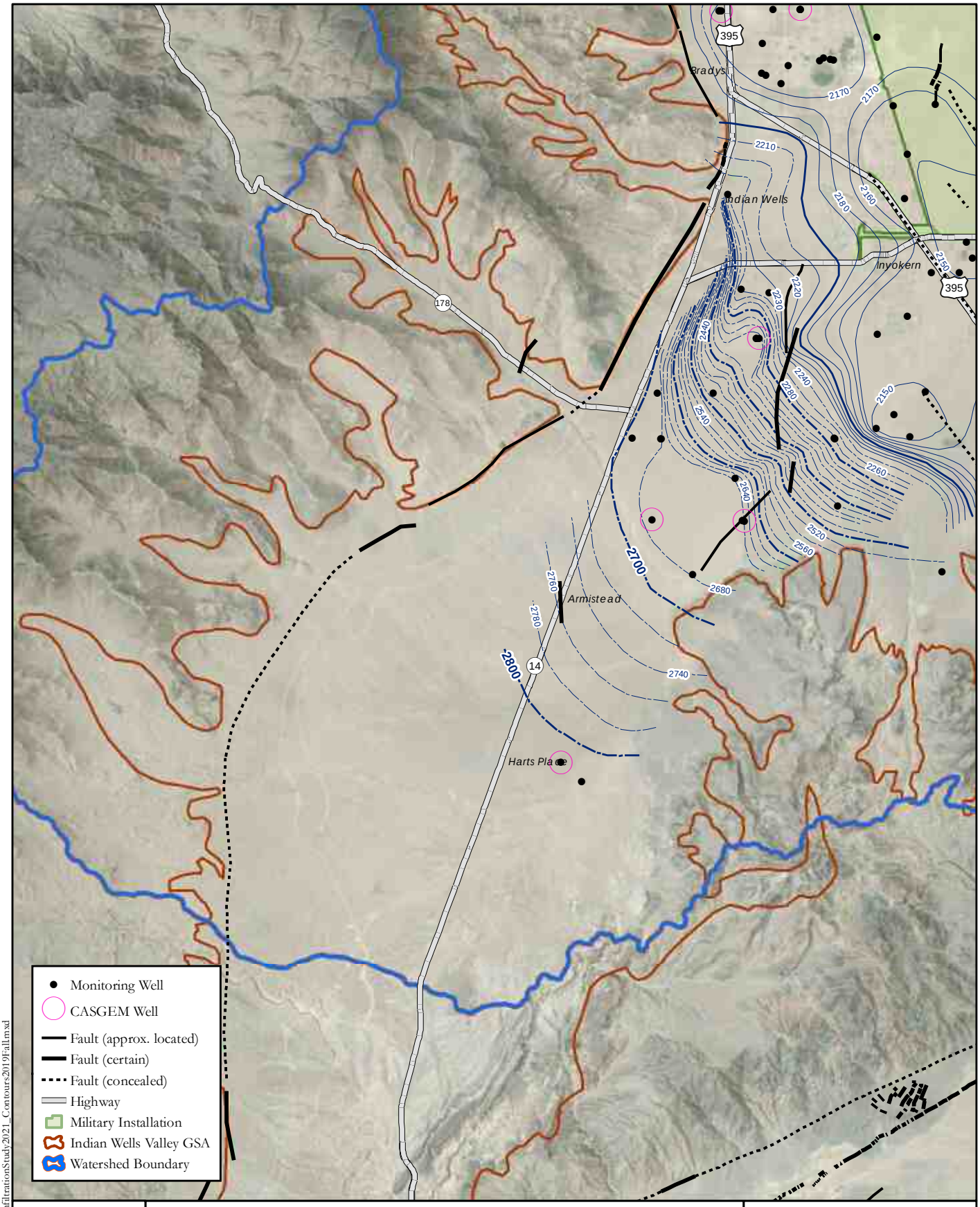
STETSON ENGINEERS INC.

Geologic Cross Section A-A'
Infiltration Study
Indian Wells Valley, CA

Note 1: well log information from IWV Data Management System (DMS), 2021 and LADWP, 2018.
Note 2: Dashed line indicates inferred water level.

FIGURE 2-5

FIGURE 2-6



Document Path: J:\jn2652\InfiltrationStudy2021_Contours2019Fall.mxd

STETSON ENGINEERS INC.

FALL 2019
GROUNDWATER ELEVATION CONTOURS
INDIAN WELLS VALLEY
DRAFT 10/6/2021

Source: California Geological Survey fault activity GIS database (2021)

N

0 1.5 3

Miles

2.3 Site Selection

This investigation has been focused on the El Paso Subbasin based on results from previous studies (Chapter 1). Areas that were excluded from investigation included: (1) Naval Air Station China Lake; (2) The City of Ridgecrest; (3) Southwest Well Field near Inyokern; and (4) Sierra drainages north of Inyokern. These areas were eliminated from investigation due to restricted land use, low infiltration rates, and hydrogeologic restrictions. Previous reports supporting wastewater planning in the City of Ridgecrest identified percolation rates as little as 0.23 inches per day, which are believed to be characteristic of the lowest portions of the IWV Basin valley floor. No further investigation was warranted at the Southwest Well Field, in the areas south of Inyokern, due to depth to groundwater, potential low permeability horizontal layers, and fault boundaries. Finally, the areas north of Inyokern, along the eastern flank of the Sierra Nevada Mountains. were eliminated from further investigation due to land use issues, groundwater development, and depth to groundwater (Stewart and Krieger; Cato, 2008).

The available land ownership, soils, surface slope, and hydrogeology data may be used to assess the potential locations for future infiltration sites. The central and southern portions of the El Paso Subbasin, including the area in the vicinity of the Freeman Canyon and Little Dixie Washes, provide preferable locations for groundwater recharge and recovery operations. While these areas of the El Paso Subbasin provide relatively shallow depths to groundwater and potentially high surface infiltration rates, specific subsurface geology varies from one location to another. As discussed in greater detail at the end of this Technical Memorandum, a drilling and coring program will be required to assess the lithology at each site to determine if horizontal low permeability layers (i.e., caliche or other hardpan) exist or have the potential to develop based on soils and anticipated recharge water quality.

Based on previously published reports and the data presented in this Technical Memorandum, three site locations have been chosen to perform engineering and cost analysis. These three sites represent typical locations where either reclaimed water recharge (i.e., Indirect Potable Reuse) or recharge of imported water (i.e., aqueduct or adjacent basin) surface infiltration could occur. These sites have been chosen to provide a range of costs and estimated loss of water that could be expected to occur over the life of a project. The final location and size of a recharge and recovery facility would be based pilot infiltration testing and feasibility analysis.

3.0. FACILITY AND ENGINEERING REQUIREMENTS

Three sites were selected to assess required facilities and costs associated with conveying either recycled water or imported water to the El Paso Subbasin for groundwater banking. Site 1 is located immediately north of the of Freeman Canyon Wash and represents the shortest distance from the existing Wastewater Treatment Facility to a potential recharge site. Site 3 is the southernmost location in the El Paso Subbasin, downstream of Bird Spring Canyon, and would be closest to either the aqueduct or an imported water source from a southern basin, but farthest from a recycled water source. Site 2 is located in between Sites 1 and 3, downstream from Sage Canyon, and represents a half-way point in terms of proximity to recycled or imported water.

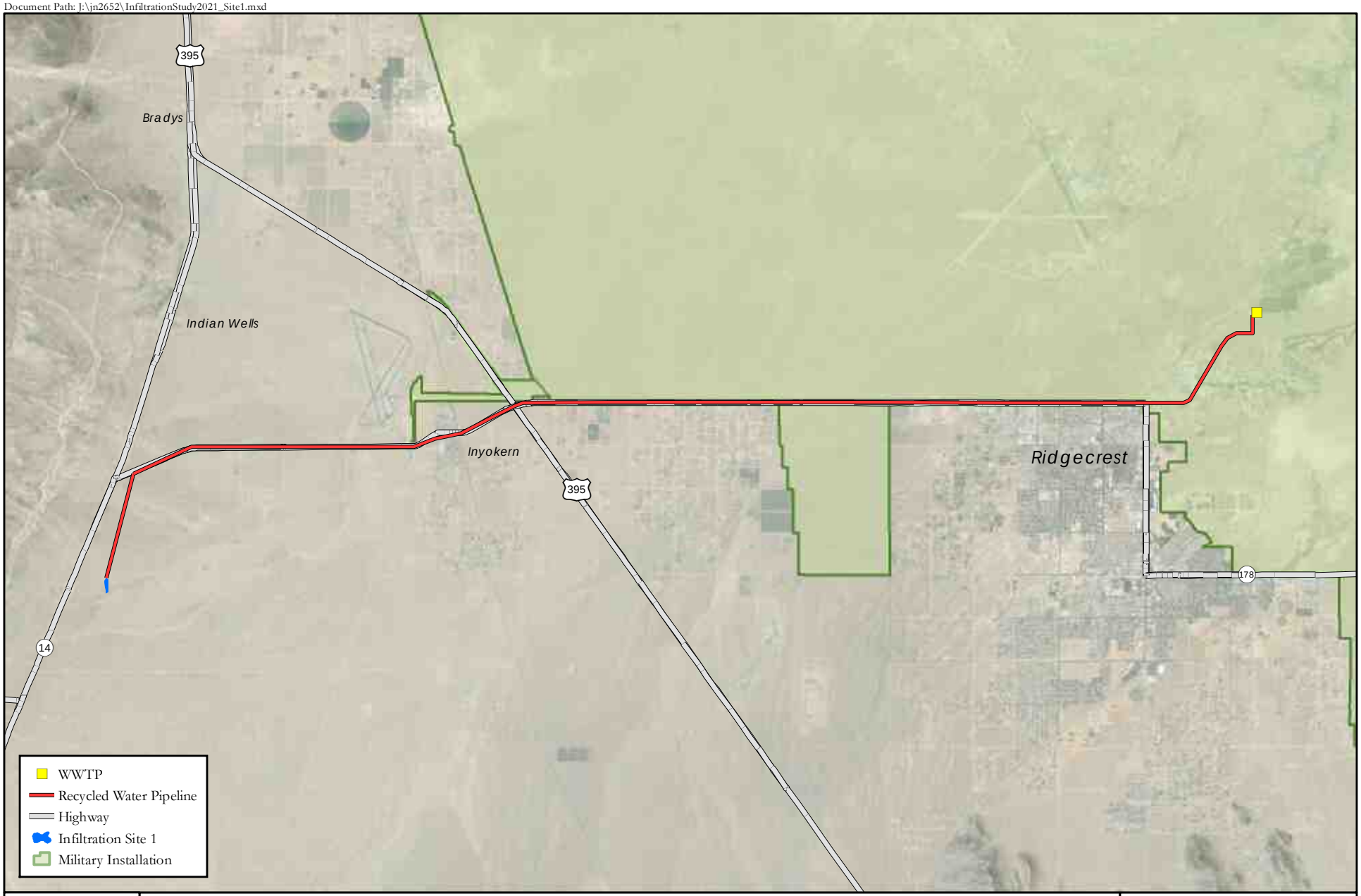
Two options have been developed for each of the three sites. Option 1 is the IPR option that reflects 2,095 AFY of recycled water recharge and recovery via surface spreading. Option 2 is the imported water recharge options that is based on recharging up to a maximum of 10,000 AFY and recovering an annual average of 5,000 AFY. Average annual recovery is less than maximum delivery due to long-term variability in supply.

3.1 IPR Option 1 Facilities

Option 1 facilities include a 12-inch pipeline and appropriate pump station to deliver water from the City's Wastewater Treatment Plant to each of the three recharge sites (Figures 3-1, 3-2, and 3-3). Based on an infiltration rate of 1.7 feet per day (20.4 inches per day) and the delivery of 2,095 AFY, approximately 3.4 acres are required for infiltration. An additional 50% recharge area has been added to provide operational flexibility for managing the recharge rates, resulting in a total required recharge area of 5.1 acres. Sites 2 and 3 include recovery wells, a manifold between wells, and a 12-inch pipeline from the manifold to the intersection of highways 395 and 14 in Inyokern. Site 1 does not include the cost for recovery wells, a manifold, or a return pipeline due to the proximity of existing production wells. Recovery of recycled water will occur from existing wells.

The estimated capital cost of IPR Option 1 Facilities is $32.1 million, $79.9 million, and $92.7 million at Sites 1, 2, and 3, respectively (Table 3-1). The estimated capital costs represent the minimum investment to deliver and recharge recycled water from the Ridgecrest Wastewater Treatment Plant to each of the three sites for eventual deliver of an equivalent amount to Inyokern. Annual Operation and Maintenance costs, which includes power and repair, are $1.2 million, $2,1 million, and $2.4 million at Sites 1, 2, and 3, respectively.

Document Path: J:\jn2652\InfiltrationStudy2021_Site1.mxd



STETSON ENGINEERS INC.

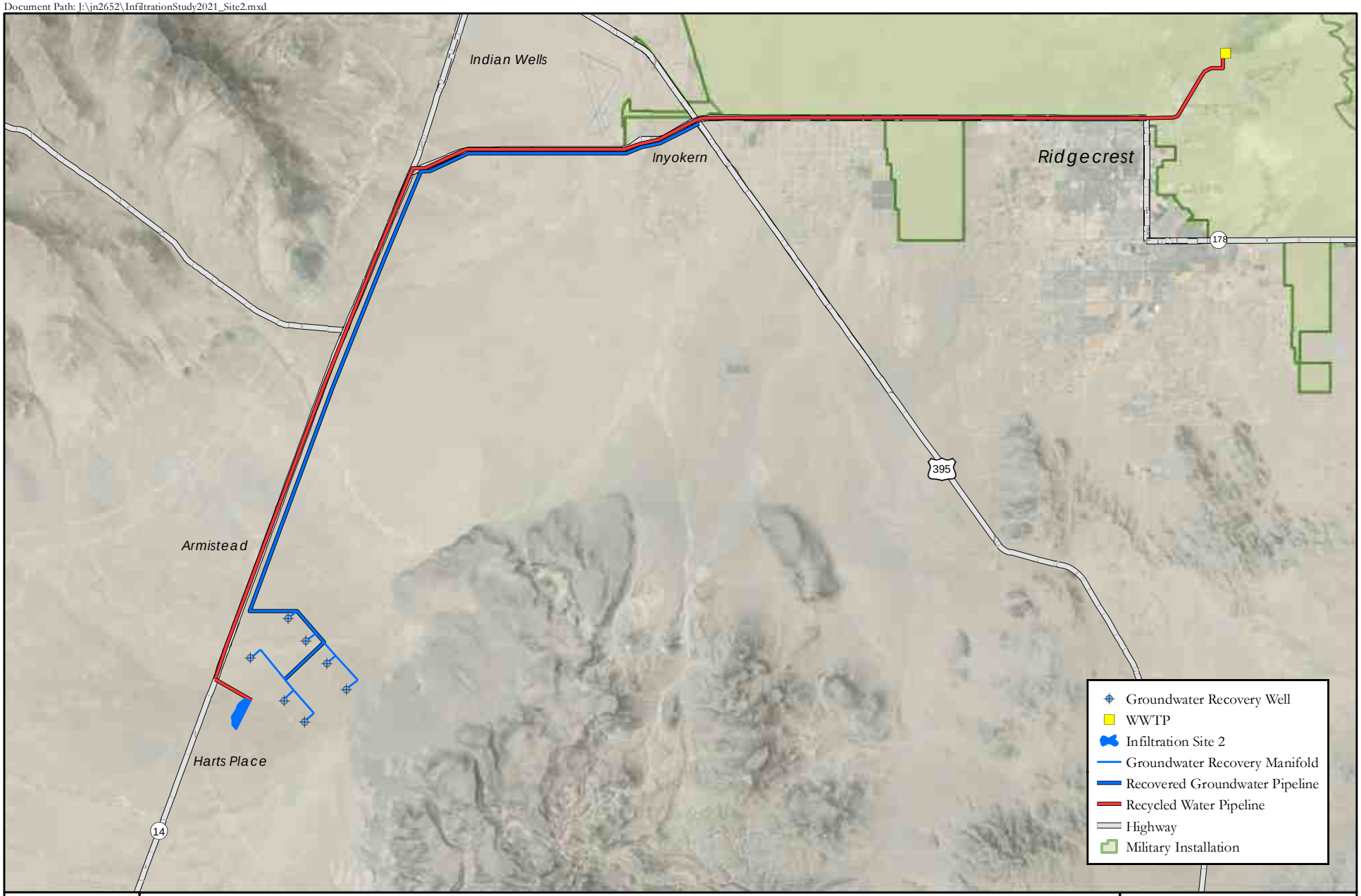
SITE 1
OPTION 1 IPR FACILITIES
INDIAN WELLS VALLEY, CA

N

0 1 2
Miles

FIGURE 3-1

Document Path: J:\jn2652\InfiltrationStudy2021_Site2.mxd



STETSON ENGINEERS INC.

SITE 2
OPTION 1 IPR FACILITIES
OPTION 2 IMPORT RECHARGE FACILITIES
INDIAN WELLS VALLEY, CA

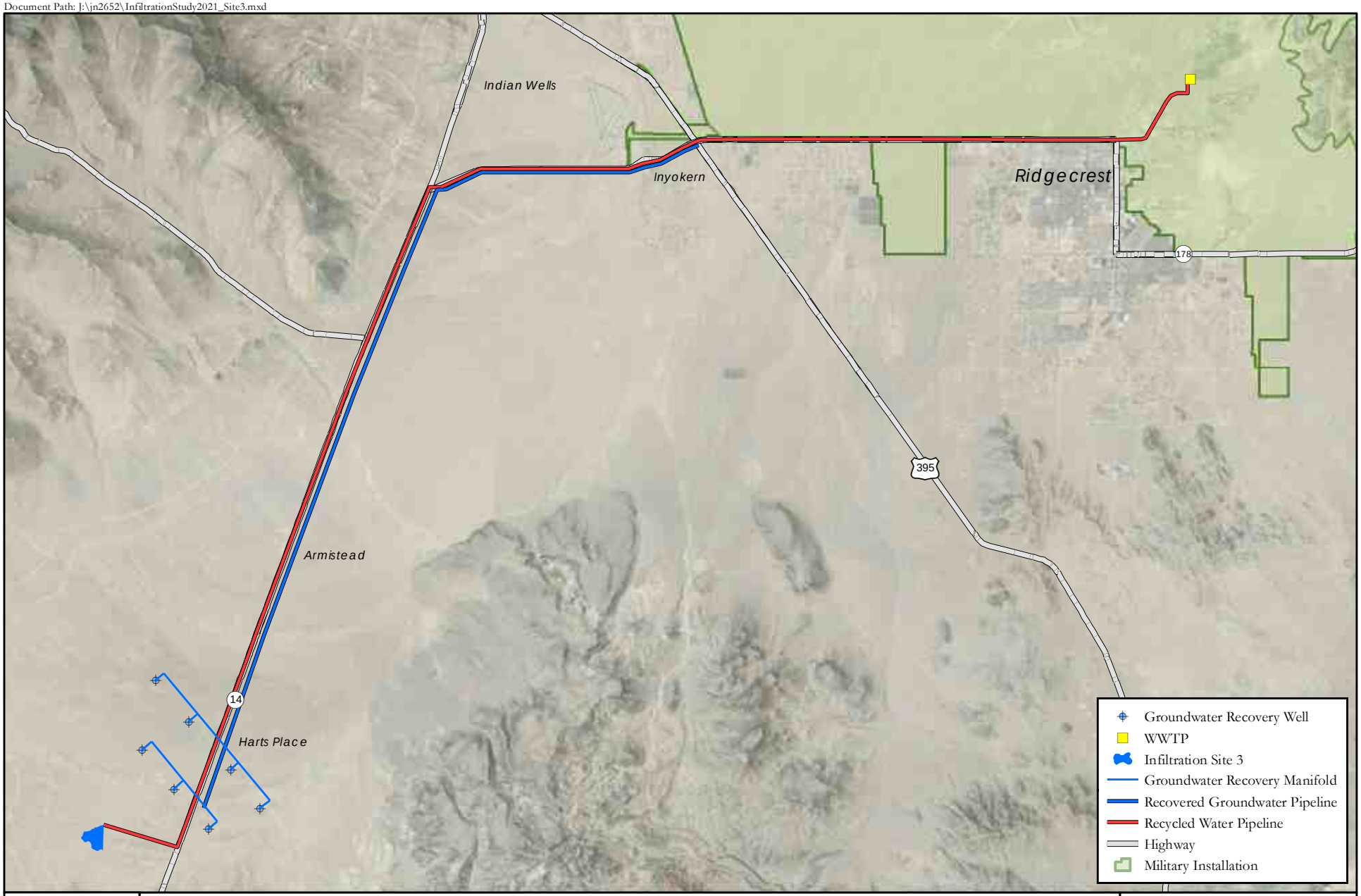
N

0 1 2

Miles

FIGURE 3-2

Document Path: J:\jn2652\InfiltrationStudy2021_Site3.mxd



STETSON ENGINEERS INC.

SITE 3
OPTION 1 IPR FACILITIES
OPTION 2 IMPORT RECHARGE FACILITIES
INDIAN WELLS VALLEY, CA

N

0 1.5 3

Miles

FIGURE 3-3

TABLE 3-1 COSTS FOR IPR OF RECYCLED WATER (OPTION 1)
($ Million)

Facility	Site 1	Site 2	Site 3
Recycled Water Pipeline	$28.0	$44.3	$51.1
Pump Station	3.6	4.0	4.0
Levee and Berm[1]	0.5	0.4	0.3
Groundwater Wells	n/a	3.2	3.2
Potable Water Pipeline	n/a	28.0	34.1
Total	$32.1	$79.9	$92.7
Annual O&M	$1.2	$2.1	$2.4

Note(s): (1) Levee and Berm includes land acquisition costs
Potable Water Pipeline terminates in Inyokern.
See Attachment C for detailed costs.

3.2 Imported Water Recharge Option 2 Facilities

Imported Water Recharge Option 2 facilities only include recharge ponds, collection wells, and return flow pipeline to Inyokern. No allowance has been made for the cost to deliver 10,000 AFY of imported water to each of the sites. Based on an infiltration rate of 1.7 feet per day (20.4 inches per day) and the delivery of 10,000 AFY, approximately 16.2 acres of recharge ponds are required for infiltration. An additional 50% recharge area has been added to provide operational flexibility for managing the recharge rates, resulting in a total required recharge area of 24.3 acres. Sites 2, and 3 include recovery wells, a manifold between wells, and a 24-inch pipeline from the manifold to the intersection of highways 395 and 14 in Inyokern. Site 1 has been excluded from this option due to poor hydrogeologic conditions for recharge and recovery of imported water. The estimated capital cost of Import Water Recharge Facilities is $41.7 million and $48.8 million for Option 2 at Sites 2 and 3, respectively (Table 3-2). Annual Operation and Maintenance costs, which includes power and repair, are $0.9 million and $1.0 million at Sites 2 and 3, respectively. The estimated capital and O&M costs represent the minimum investment to recharge and recover imported water to Sites 1 and 2 for eventual delivery of an equivalent amount to Inyokern.

TABLE 3-2 COSTS FOR IMPORTED WATER RECHARGE (OPTION 2)
($ Million)

Facility	Site 1	Site 2	Site 3
Imported Water Pipeline	n/a	n/a	n/a
Pump Station	n/a	n/a	n/a
Levee and Berm[1]	n/a	0.8	0.8
Groundwater Wells		6.4	6.4
Potable Water Pipeline		33.5	41.6
Total	n/a	$40.7	$48.8
Annual O&M	n/a	$0.9	$1.0

Note(s): (1) Levee and Berm includes land acquisition costs
Potable Water Pipeline terminates in Inyokern.
See Attachment C for detailed costs.

3.3 Evaporative Water Losses

Water loss from recharge ponds located within the IWV Basin will vary depending on the infiltration rate and required surface area of the recharge pond. Higher infiltration rates will require smaller recharge ponds and result in higher efficiencies and less evaporative losses. Similarly, wind can also impact evaporation rates by reducing both humidity and vapor pressure above a water body, resulting in additional evaporative losses. Both high wind and high daytime temperatures and related solar radiation will adversely impact water loss from recharge ponds in the IWV Basin.

Actual evaporation data from the 2003/2004 Recharge Study (IWVWD, 2005) was compared to 2020/2021 ETo data for the Ridgecrest Station #257. During the October through April months, the ETo data were higher than that which was recorded at during the recharge study. Although the discrepancy may be explained by the different years that represented by the data, they show a similar and expected trend of higher evaporation rates in the fall and spring months and less during the winter months. The evaporation from an open water body varies based on time of year, depth, area, temperature, topography, and vegetation surrounding the

water (Brown). Based on these factors, monthly evaporation can range from ETo to 1.4 times ETo. In order to estimate evaporation from infiltration ponds, ETo for Ridgecrest was multiplied by a factor of 1.2 as shown in the last column of Table 3-3. The recommended annual evaporation rate of 90.1 inches (7.5 feet) represents a conservative estimate greater than that recorded during the 2003/2004 Recharge Study by IWVWD.

TABLE 3-3 ESTIMATED EVAPORATION FROM INFILTRATION PONDS
(inches)

Month	ETo	2003/2004 Pilot Study	Recommended Evaporation Rate
Oct	4.7	9.8	5.7
Nov	3.0	2.7	3.6
Dec	2.0	2.1	2.4
Jan	2.5	1.5	3.0
Feb	3.4	2.7	4.1
Mar	5.6	3.7	6.8
Apr	8.0	8.2	9.6
May	9.4	*9.9*	11.3
Jun	10.0	*10.4*	11.9
Jul	9.8	*10.3*	11.8
Aug	9.4	*9.9*	11.3
Sep	7.2	*7.5*	8.6
Total	75.1	78.8	90.1

Notes: ETo is reported CIMS data for 2020-2021.
2003/2004 Pilot Study values estimated for May through Sept.

Total evaporative losses from either the IPR Recharge Project (Option 1) or the Imported Water Recharge Project (Option 2) are estimated to be 25 AFY and 122 AFY, respectively. Both these losses equate to approximately 1.2% of the delivered 2,095 AFY and 10,000 AFY under Options 1 and 2. The annual loss due to evaporation may be quantified in operation and maintenance costs associated with the final project.

4.0. SUMMARY AND RECOMMENDATIONS

The purpose of this reconnaissance-level investigation was to identify potential groundwater recharge sites in the IWV Basin for further investigation and collection of new data. Previous studies investigated soils, hydrogeology, infiltration rates, and other factors affecting groundwater recharge using surface application methods. This investigation relied on existing data and previous studies' results to identify specific locations that would be suitable for detailed field investigation and potential recharge pond pilot testing.

In general, the IWV Basin's valley floor is characterized by low infiltration rates due to the presence of fine-grained low-permeability materials. Because of the presence of these materials, this investigation focused on areas outside of the valley floor along the base of the Sierra Nevada Mountains. Detailed review of the previous studies eliminated areas north of Inyokern due to the depth to groundwater, fault barriers, existing production wells, and the availability of land. Areas on the east and southeast side of the IWV Basin were eliminated from further investigation due to land ownership and distance from production wells and sources of imported water. Therefore, this investigation focused on areas within the El Paso Subbasin where recharge and recovery operations would be physically supported by available land, hydrogeology, and surface conditions.

A large portion of the El Paso Subbasin is managed by the BLM, not including 3,512 acres owned by LA DWP and other privately owned parcels. The floor of the El Paso Subbasin is characterized by slopes of less than 5% and range in elevation from 2,500 feet msl to more than 3,330 feet msl. The soils are predominantly characterized by well drained sandy loam that formed in material weathered mainly from granitic alluvium. The upper 80 inches of the soil column is predominantly composed of coarse sandy loam and gravelly sand and loam (2 inches to 79 inches). Estimated infiltration rates in the El Paso Subbasin averaged 1.7 feet per day and ranged from 0.2 to 2.5 feet per day (LADWP, 2018).

Geologic borehole information shows thick sequences of lakebed or fine-grained material at depths greater than 250 feet in the southernmost portion of the El Paso Subbasin and thicker sequences of coarser gained material to the north. The coarse-grained sand and gravelly fanglomerate sequences located in the center and northern portions of the El Paso Subbasin are suitable for groundwater storage and recovery. Based on available borehole information, there are no known near surface continuous clay or low permeable layers that would restrict groundwater recharge. The depth to groundwater is least along the east side of the El Paso Subbasin and increases along its western margins as ground surface rises at a faster rate than the

groundwater table. Generally, groundwater levels south of the Freeman Fault may be expected to range from 200 to 400 feet bgs.

Three site locations were investigated to estimate capital costs for delivering and recharging either recycled or imported water to the IWV Basin. The engineering analysis was based on delivering either 2,095 AFY of recycled water (Option 1) or up to a maximum of 10,000 AFY of imported water (Option 2). Similarly, the engineering analysis was based on recovering all of the recycled water, but only 50%[4] (5,000 AFY) of recharged imported water. Of the three sites investigated, only Sites 2 and 3 included the use of new recovery wells and a conveyance pipeline to deliver up to 5,000 AFY of water to Inyokern. Site 1 relied on existing production wells to manage groundwater storage and recovery of recycled water only since this site was not analyzed for imported water recharge (Option 2). The capital costs for Option 1 recharge of recycled water, not including pre-treatment requirements, ranged from $32.1 million to $92.7 million, while the capital cost for Option 2 recharge of imported water ranged from $40.7 million to $48.8 million.

Annual O&M costs were also investigated for each of the options at the three sites. O&M costs were greatest for Option 1 due to power costs and booster station maintenance for facilities associated with delivering recycled water from the WWTP to the recharge facilities. The O&M costs for Option 1, Sites 1, 2, and 3 were $1.2 million, $2.1 million, and $2.4 million respectively. The equivalent per acre-foot costs, not including capital costs, for the same sites based on 2,095 acre-feet delivered are $560, $1,020, and $1,130, respectively. The O&M costs for Option 2, Sites 2 and 3 were $0.9 million and $1.0 million, respectively. The equivalent per acre-foot costs, not including capital costs, for the same sites based on 5,000 AFY recovered and delivered to Inyokern, are $190 and $200, respectively.

Evaporative losses from a MAR project in the El Paso Subbasin are estimated to be about 1.2%, which equates to about 25 AFY for Option 1 and 122 AFY for Option 2. The evaporative losses were based on actual October through April data collected during the recharge pilot study at the Southwest Wellfield (IWVWD, 2005) and adjusted for year-around losses. Water supply losses due to evaporation should be accounted for in annual operation and maintenance costs estimated as part of project feasibility.

[4] The recharge ponds are sized for a maximum delivery year of 10,000 AFY, while recovery was assumed to average 5,000 AFY due to long-term variability in supply subject to availability.

Site 2 provides the most likely areas to develop a MAR project based on land ownership, hydrogeology, and surface infiltration rates. Site 1 may be suitable for IPR of recycled water to supplement groundwater storage, but depth to water and the proximity to the Sierra Nevada boundary fault makes it less desirable for recovering imported recharge water. Site 3 is also less preferable due to its distance from the wastewater treatment plant (Option 1) and the regional groundwater level occurring at the top of the clay layer at a depth of approximately 250 feet bgs. Therefore, Site 2 represents the best area for developing a MAR project based on surface conditions, thick sequences of coarse-grained aquifer material, depth to groundwater, and available land.

4.1 Field Investigation Recommendations

Future field investigations required to assess suitability for a MAR should include geophysical, hydrogeologic, and operational pilot studies. A high-definition seismic survey is recommended to identify whether continuous clays or fine-grained material are present between the surface and the top of the groundwater. The hydrogeologic investigation is intended to identify soil infiltration rates, lithology, aquifer properties, and groundwater conditions related to both the recharge and recovery of groundwater. The hydrogeologic investigation will assess both the movement of water through the aquifer as well as potential water quality concerns. The pilot recharge study is intended to demonstrate the feasibility of operating a MAR based on the results from the hydrogeologic investigation.

4.1.1 Geophysical Investigation

High-resolution seismic techniques may be employed to identify horizontal and vertical anisotropies using shear wave reflection methods that employ three component geophones. The geophysical investigation study area should extend from the recharge basin to the recovery wells to map potential low permeability confining layers not identified in existing well logs. Results from this type of investigation may be used to relocate the infiltration basin or determine if other recharge techniques would be more suitable. Based on the results of this investigation, downhole seismic techniques could be employed during the Hydrogeologic Investigation.

4.1.2 Hydrogeologic Investigation

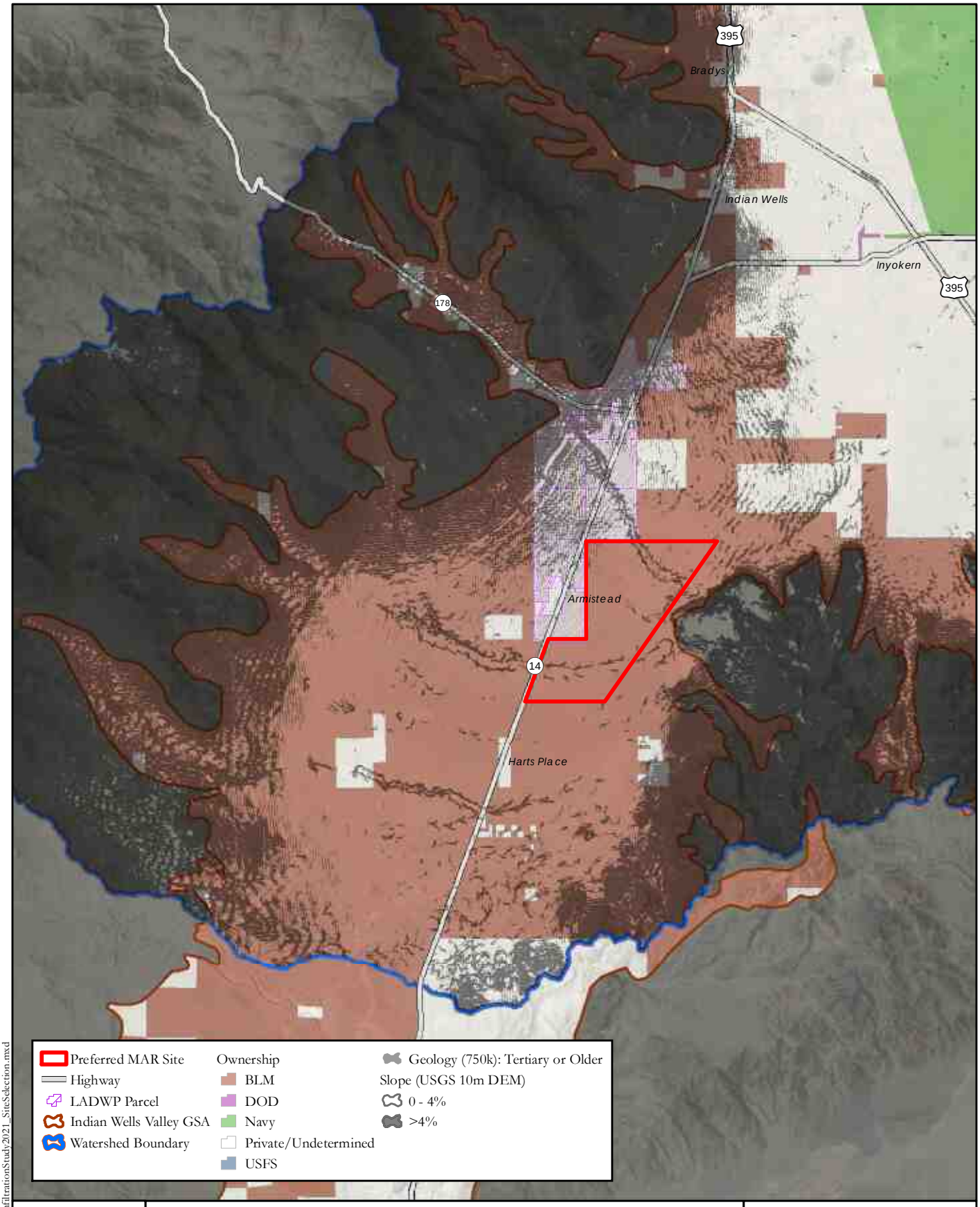
The hydrogeologic investigation includes the construction and development of monitoring and test wells to assess the aquifer properties in the vicinity of the proposed MAR project. The success of a proposed MAR project relies on both the ability to recharge water as

well as to recover water added to basin storage. Therefore, core samples and soil analysis of the near surface layers will be performed to assess whether low permeability layers (i.e., hardpan, clays, fine-grained sediments) exists. Additionally, water quality samples will be collected to determine whether sodic soils exist and if the potential exists for low-permeability layers to be created over time.

Project proponents should work with the BLM to assess the potential for developing a right of way or land exchange for up to 30 acres of land in the vicinity of Site 2. Land will be required for a minimum of 24 acres of recharge ponds, eight production wells, electrical facilities, pipelines, and appurtenant facilities. The location of the proposed MAR project could be on either side of the Highway 14 in the vicinity of Armistead, outside of existing LADWP owned lands (Figure 4-1). Following initial determination of a proposed site, the following investigation should be performed.

- Construct up to three (3) two-inch monitoring wells to 600 feet.
- Construct one (1) 8-inch test well to 800 feet bgs.
- Perform down-hole geophysical logging
- Perform Soil and Water Quality Sampling
- Perform an aquifer test
- Perform surface soil infiltration tests
- Trenching in select locations

FIGURE 4-1



Document Path: J:\jn2652\InfiltrationStudy2021_SiteSelection.mxd

STETSON ENGINEERS INC.

SITE SELECTION
INFILTRATION STUDY
INDIAN WELLS VALLEY, CA

N

0 1.5 3

Miles

4.1.3 Pilot Testing

Following geophysical and hydrogeologic investigations, approximately five acres of land could be acquired to construct two one-acre infiltration basins (to allow cycling of ponds during operation), with site piping, control valves, and instrumentation and monitoring equipment. Monitoring and production wells constructed as part of the hydrogeologic investigation should be used to monitor changes in groundwater levels and flow directions. Flow meters, sampling equipment, climatic recording instruments (precipitation and evaporation), and down-hole data loggers for the test well and monitoring wells. The pilot test should be performed for a minimum of one year or until groundwater mounding is observed.

5.0. BIBLIOGRAPHY

Brown, Paul W., AZMET Evapotranspiration Estimates: A Tool for Improving Water Management of Turfgrass. Located at: https://cals.arizona.edu/azmet/et1.htm

BSK Associates, 2011. Draft Preliminary Soil Investigation Report, Ridgecrest Wastewater Treatment Plan, Ridgecrest, California. Prepared for Provost & Pritchard Engineering Group, January 7, 2011.

Conserve Consultants Southwest, Inc., 1991. Preliminary Slow Rate Infiltration Study Inactive Sewage Treatment Facility, Ridgecrest, California. Prepared for the City of Ridgecrest, April 12, 1991.

Garner, C., Bacon, S., Pohll, G., and Chapman, J., 2017. *Technical memorandum: Indian Wells Valley Groundwater Model Update.* Prepared by Desert Research Institute. November 17, 2017.

IWVGA, 2021. GSP Annual Report Water Year 2020. April, 2021.

Indian Wells Valley Water District, 2005. Southwest Well Field Recharge Feasibility Study. Prepared by IWVWD, November 2005.

Krieger & Stewart, Inc., 1996. Results of the 1996 Southwest Well Field Aquifer Test Program. Prepared for Indian Wells Valley Water District, document not dated.

Krieger & Stewart, Inc., 1989. Southwest Well Field Test and Monitoring Wells Construction and Development. Prepared for Indian Wells Valley Water District, September 1989.

Krieger & Stewart, Inc. and Cato Geoscience Inc., 2008. Ground Water Banking Site Selection Report, Geologic and Engineering Considerations. Prepared for Indian Wells Valley Water District, September 2008.

Kunkel, Fred and G.H. Chase, 1969. *Geology and Ground Water in Indian Wells Valley, California.* USGS Open-File Report 69-329. Prepared in cooperation with the Naval Weapons Center, China Lake, California.

LADWP, 2018. *Draft TM-2: Detailed Hydrogeologic Review of Antelope Valley and Indian Wells Valley Groundwater Basins.* Task Order 013. July 2018.

Provost & Pritchard Consulting Group, 2015. Wastewater Treatment Plant Facility Plan, City of Ridgecrest, CA, Review Draft. Prepared for the City of Ridgecrest, October 2015.

Ramboll, 2019. Hydrogeologic Conceptual Framework, Indian Wells Valley. Prepared for Indian Wells Valley Water District and the Brackish Groundwater Resources Study Group. Final Report, June 2019.

SWRCB, 2021 Statutory Water Rights Law, 2021. C.C.R WAT §§13560. -13569. State Water Resources Control Board. January 2021.

SWRCB, 2018. Regulation Related to Recycled Water. Title 22 Code of Regulations §§60320.100-60320.130. State Water Resources Control Board, Division of Drinking Water. October 2018.

SWRCB, Regulation Related to Recycled Water, 2018. Title 22 Code of Regulations §60323. State Water Resources Control Board, Division of Drinking Water. October 2018.

RWQCB, Lahontan Region, 2016. *Palmdale Draft Environmental Impact Report.* Executive Officer's Report. February 2016.

RWQCB, Colorado River Basin Region, 2015. *Waste Discharge Requirements for Hi-Desert Water District, Owner/Operator Yucca Valley Wastewater Reclamation Plant, Yucca Valley-San Bernardino County.* Adopted by the CRWQCB, Colorado River Basin Region on September 17, 2015.

RWQCB, Lahontan Region, 2015. *Littlerock Creek Groundwater Recharge and Recovery Project.* Executive Officer's Report. April 2015.

TTEMI, 2003. *Groundwater Management in the Indian Wells Valley Basin, Ridgecrest, California.* AB 303 Grant State of California Water Resources Department. June 2003.

USBR, 1993. *Indian Wells Valley Groundwater Project: USBR Technical Report Volume II*. A cooperative effort among the BOR, IWVWD, North American Chemical Company, and NAWS. December 1993. Prepared by USBR Lower Colorado Region.

U.S. Geological Survey, 2019. USGS 1 arc-second n36w118 1 x 1 degree: U.S. Geological Survey.

Attachment A

Excerpt from Ramboll Hydrogeologic Conceptual Framework

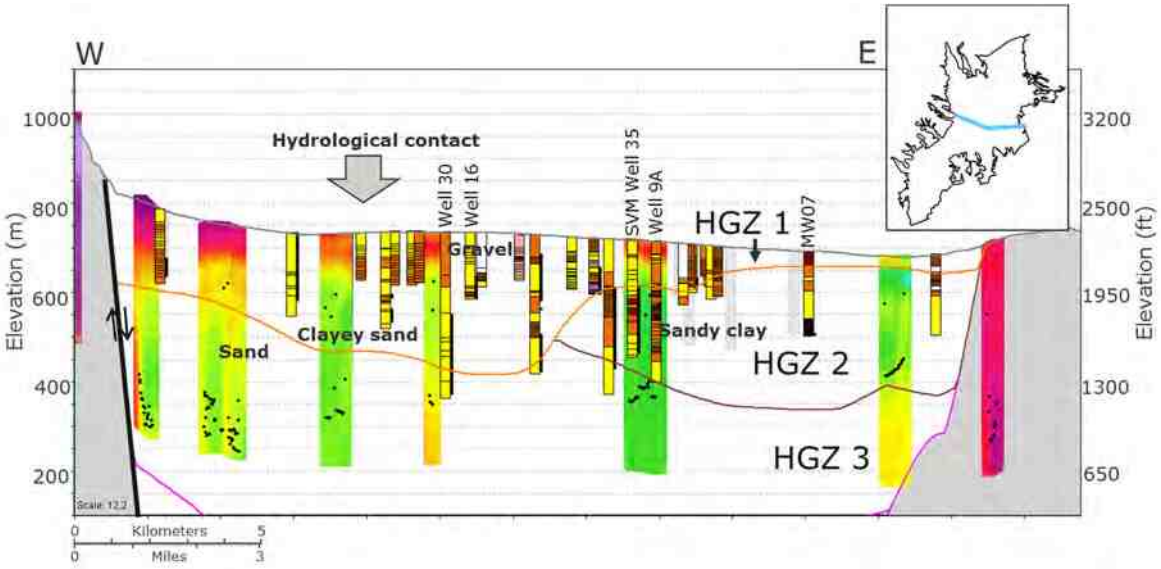


Figure 6-12. Cross-section showing the well lithology and SkyTEM data
In the west, direct hydrological contact between HGZ 1 and HGZ 3 is seen both in the well lithologies and SkyTEM data. In the center of the profile, a residual channel that has eroded into the clayey material in HGZ 2 is observed in the SkyTEM data. The orange line shows the bottom of HGZ 1, the brown line shows the bottom of HGZ 2 and the small dots show the depth of investigation for the SkyTEM data.

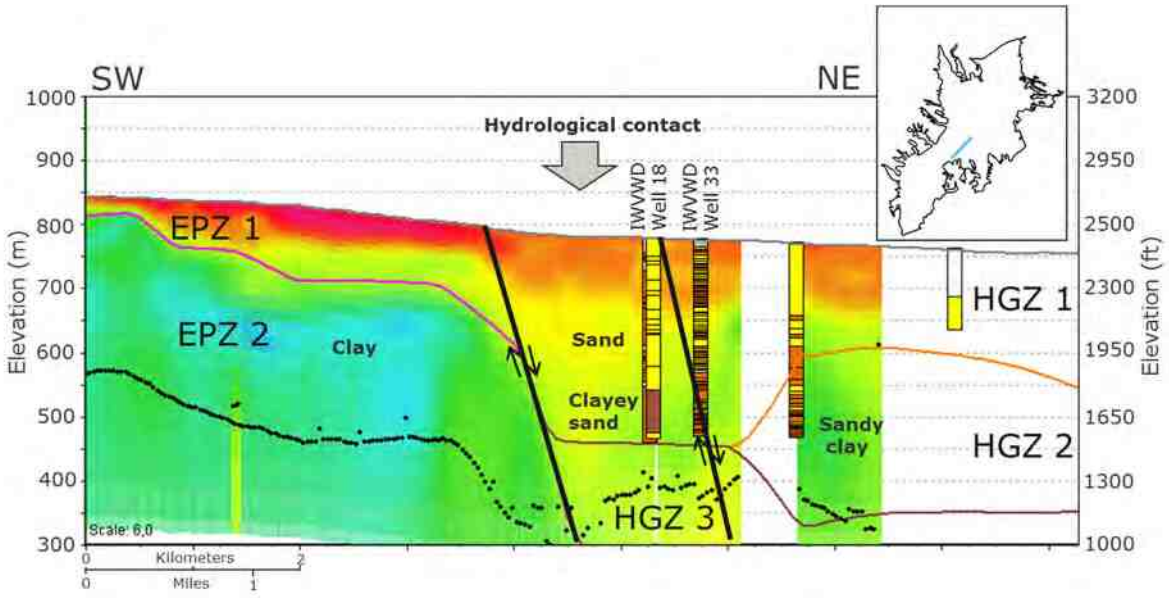


Figure 6-13. Cross-section showing the well lithology and SkyTEM data
The two interpreted faults dividing El Paso area (southwest) from the China Lake area are seen in the middle of the cross-section. To the northeast of the faults there is direct hydrological contact between HGZ 1 and HGZ 3, likely a paleochannel where coarser materials were deposited. The orange line shows the bottom of HGZ 1, the brown line shows the bottom of HGZ 2 and the small dots show the depth of investigation for the SkyTEM data.

6.3.3 Alluvial fan deposits in the El Paso area

Two separate alluvial fans are mapped in the older alluvium in the El Paso area; one coming out of Freeman Canyon in the northern part of the areas, and one coming out of Bird Spring Canyon (Figure 6-9). The cross-section in Figure 6-14 shows the profile and interpretation of the fan coming out of Bird Spring Canyon and Figure 6-15 shows the interpretation of the fan coming out of Freeman Canyon. In both fans, the coarser fan deposits are observed in the SkyTEM data, where resistivity in the saturated zone ranges from 30 to 50 ohmm (yellow to orange colors in

Figure 6-14). These deposits overly the Ricardo Group deposits consisting of finer sediments, as indicated by a resistivity of 5 – 15 ohmm (green to yellow-green colors in Figure 6-14).

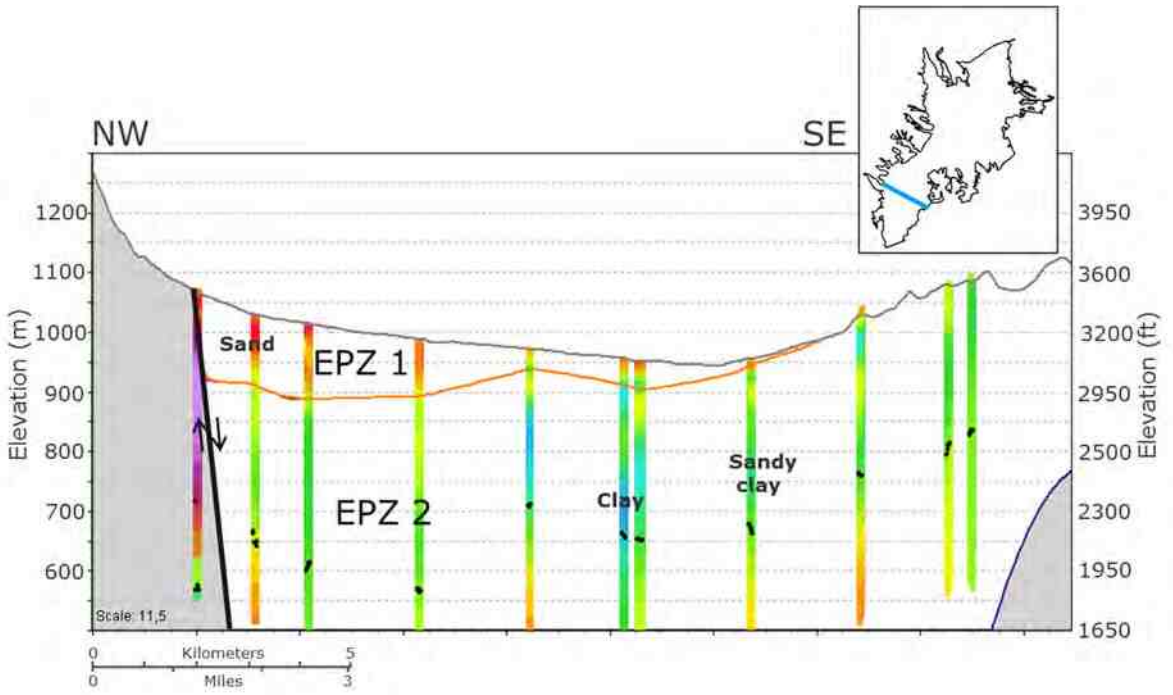


Figure 6-14. Cross-section showing the interpreted SkyTEM data in the El Paso area
The deposits of the coarser EPZ 1 material is interpreted as fan deposits coming off of the Sierra Nevada frontal fault. The uneven terrain to the southeast is where the Ricardo Group crops out. The orange line shows the bottom of HGZ 1 and the small dots show the depth of investigation for the SkyTEM data.

6.3.4 Potential barriers to groundwater flow

The most prominent structure in the Indian Wells Valley groundwater basin, which poses a barrier to groundwater flow, occurs right at the boundary between the China Lake area and the El Paso area. Just to the southwest of the fault that divides the China Lake area from the El Paso area, SkyTEM data show an area containing low resistivities (5 – 10 ohmm) that come within 100 feet (30 m) of the surface (Figure 6-15). Resistivity in this range indicate finer deposits, likely consisting of clay and shale. A map showing the SkyTEM resistivity at an elevation of 2,500 feet (770 m) shows the spatial extent of the hydrological barrier (Figure 6-16). The mapped barrier coincides with the previously reported horizontal flow barrier, as suggested by Clark (1999) and Kern County (2008).

The SkyTEM data also shows that the barrier influences groundwater flow in the valley. Resistivity from the SkyTEM can be used to approximate the groundwater table in the area of the barrier seen within the Freeman Canyon fan; resistivity over 60 ohmm (red and purple colors in Figure 6-15) show where the sediments remain unsaturated; whereas, resistivity between 20 and 60 ohmm (yellow to orange colors) show the saturated zone. Using this relationship in the SkyTEM data, the groundwater table within the Freeman Canyon fan is seen to decrease towards the northeast, as it approaches the barrier (Figure 6-15). However, at the barrier, the water table is seen to be as much as 100 feet (30 m) lower than the top of the barrier. This suggests that the barrier is holding the water back and it is likely diverting groundwater around the barrier towards the north.

In addition to the horizontal flow barrier at the boundary between the China Lake area and the El Paso area, previous studies, beginning with Kunkel and Chase (1969), have suggested the faults within the basin could pose a hydrological barrier to groundwater flow. However, Tetra Tech (2003) disputed this, indicating that groundwater level measurements from the Fence Line Monitoring Project do not show this. This study has not looked at whether the faults will pose a barrier to groundwater flow. However, several faults are seen to affect the depositional environment in the basin, particularly seen in the location of the paleo-channel deposits and the thickness of the three upper hydrogeologic zones. The abrupt change in the sediments will influence the groundwater flow in the basin. This data could be incorporated into the flow models for the groundwater basin.

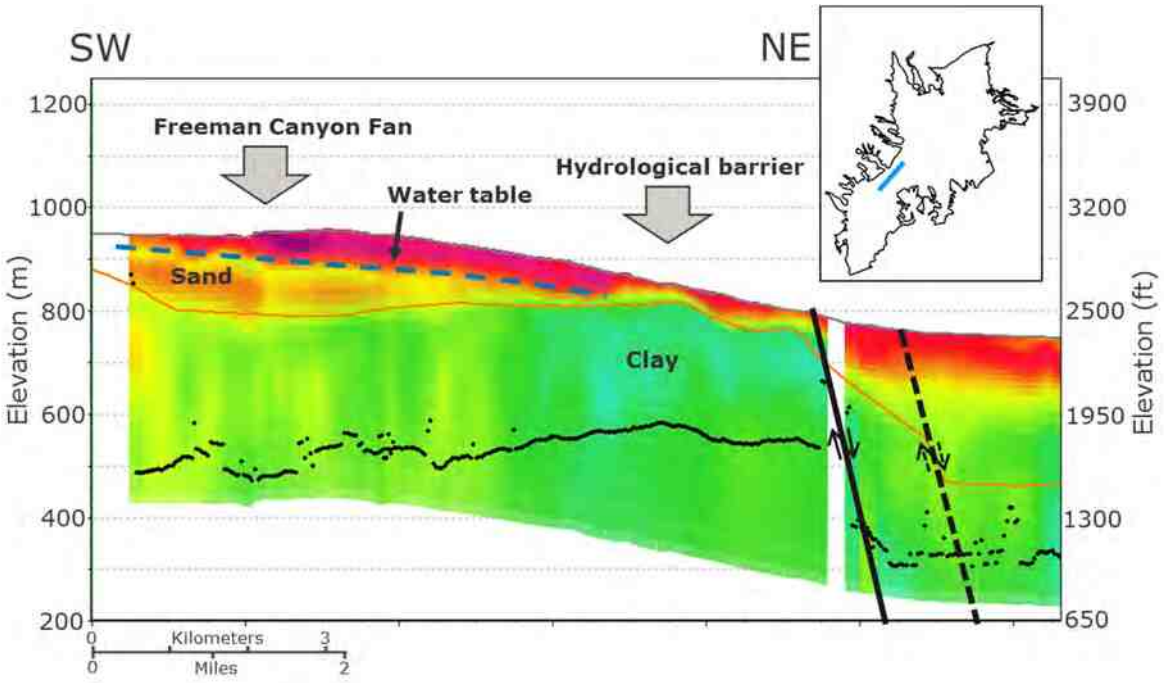
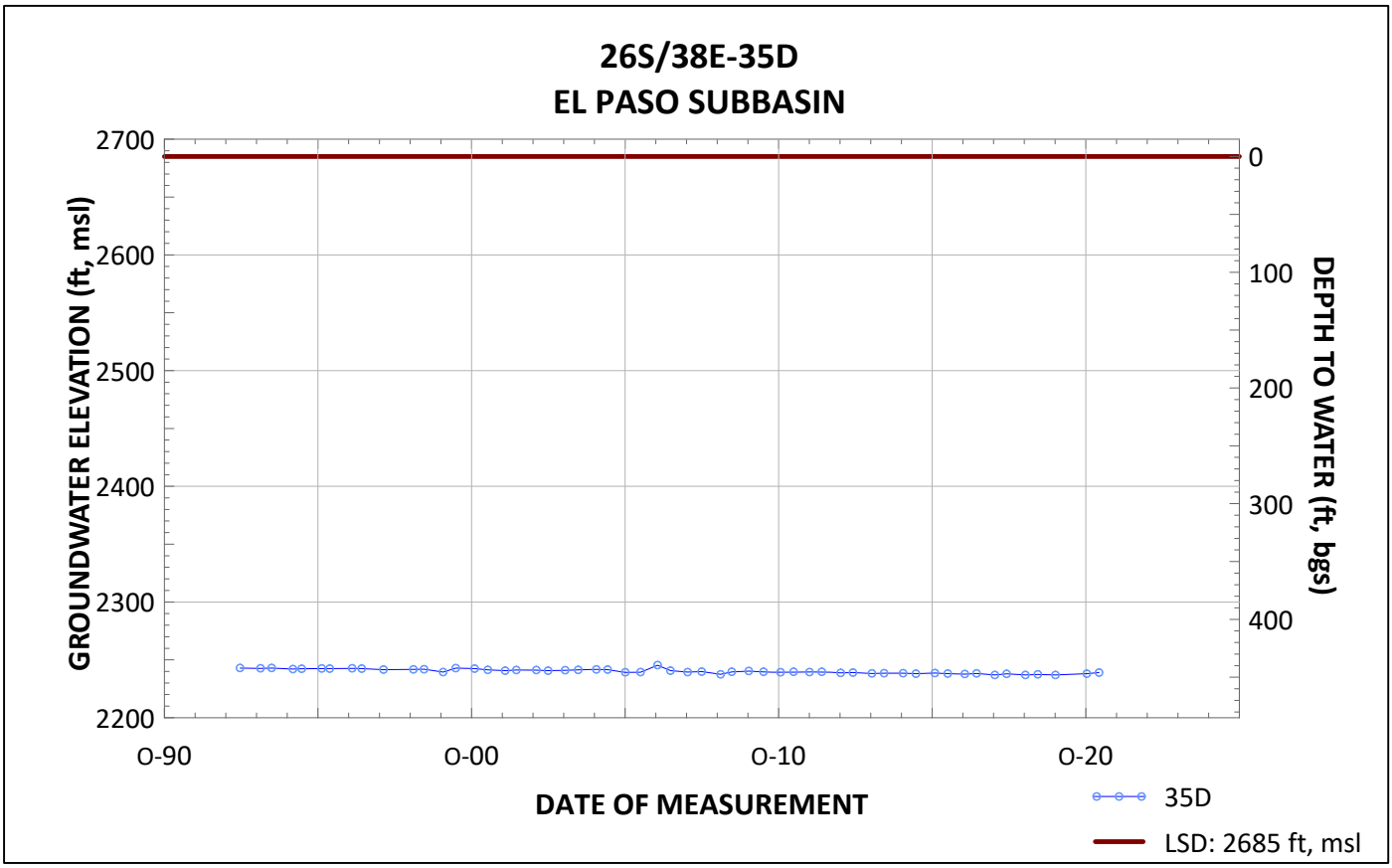
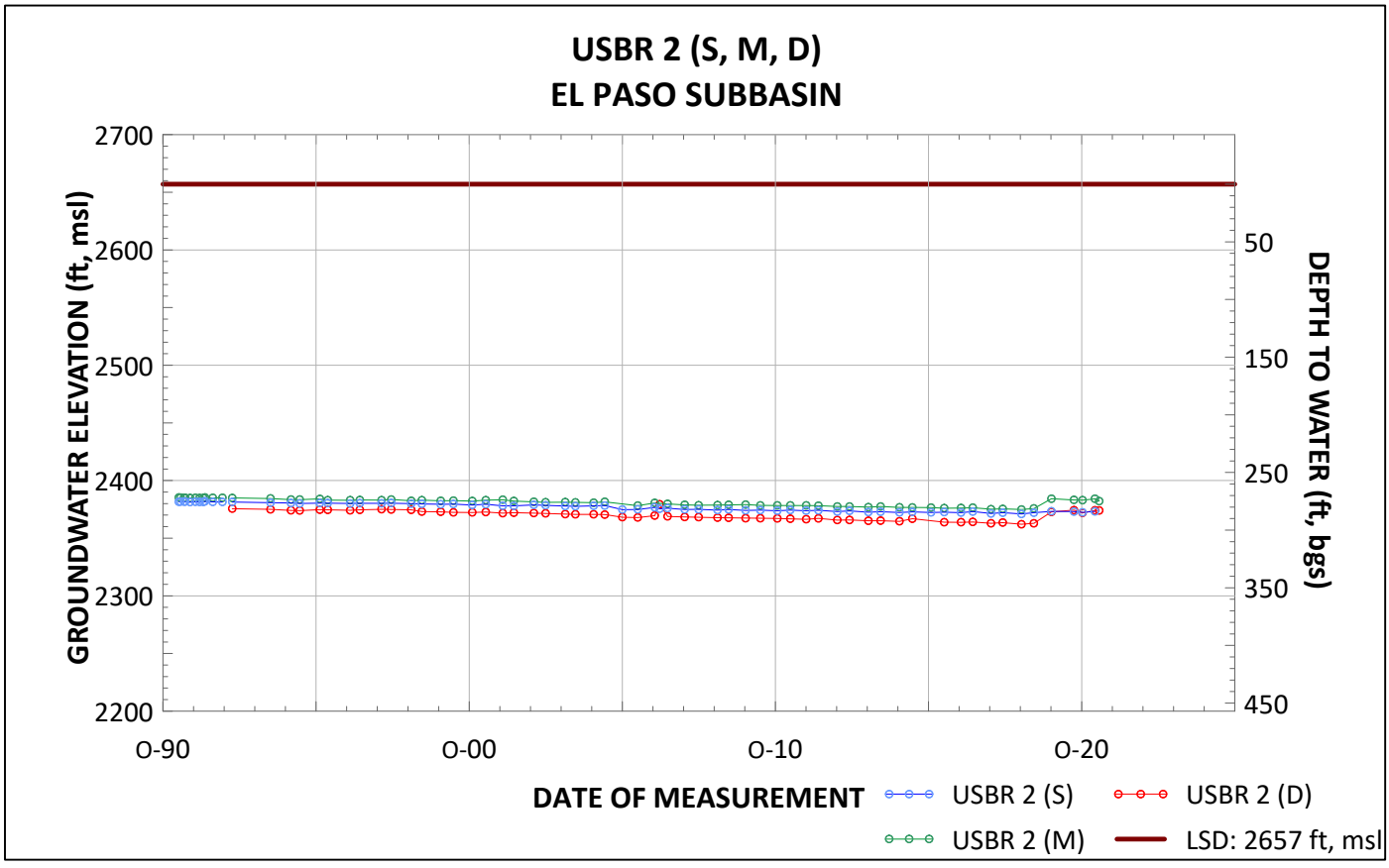


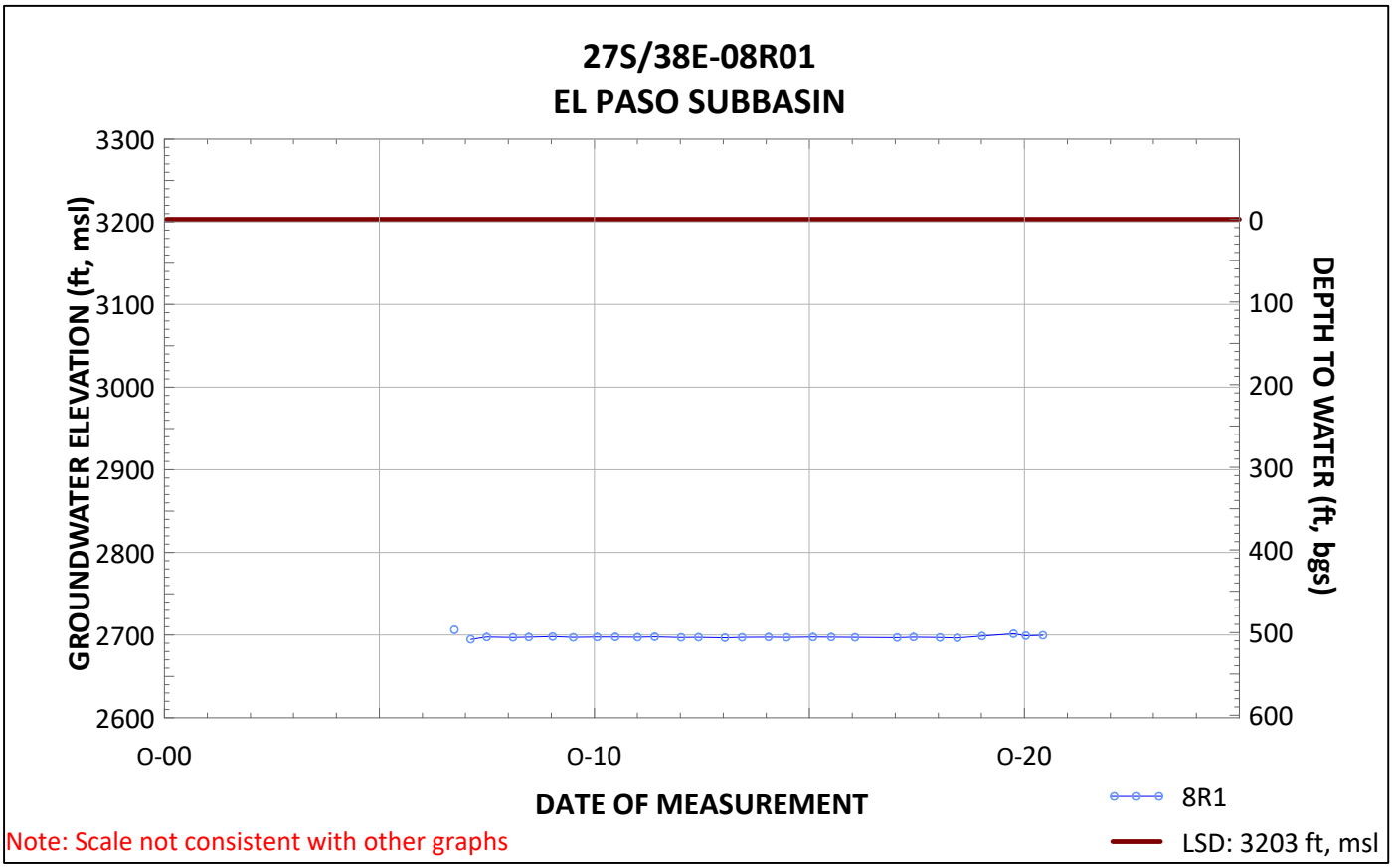
Figure 6-15. Cross-section showing the SkyTEM data, where the resistivity shows fine materials nearly reaching the surface
This is interpreted as a hydrological barrier. The barrier occurs just southwest of the two faults defining the boundary between the China Lake area and the El Paso area. The black dots represent the depth of investigation in the SkyTEM data. The dark blue dashed line shows the approximate location of the water table in EPZ 1, as mapped by SkyTEM resistivity.

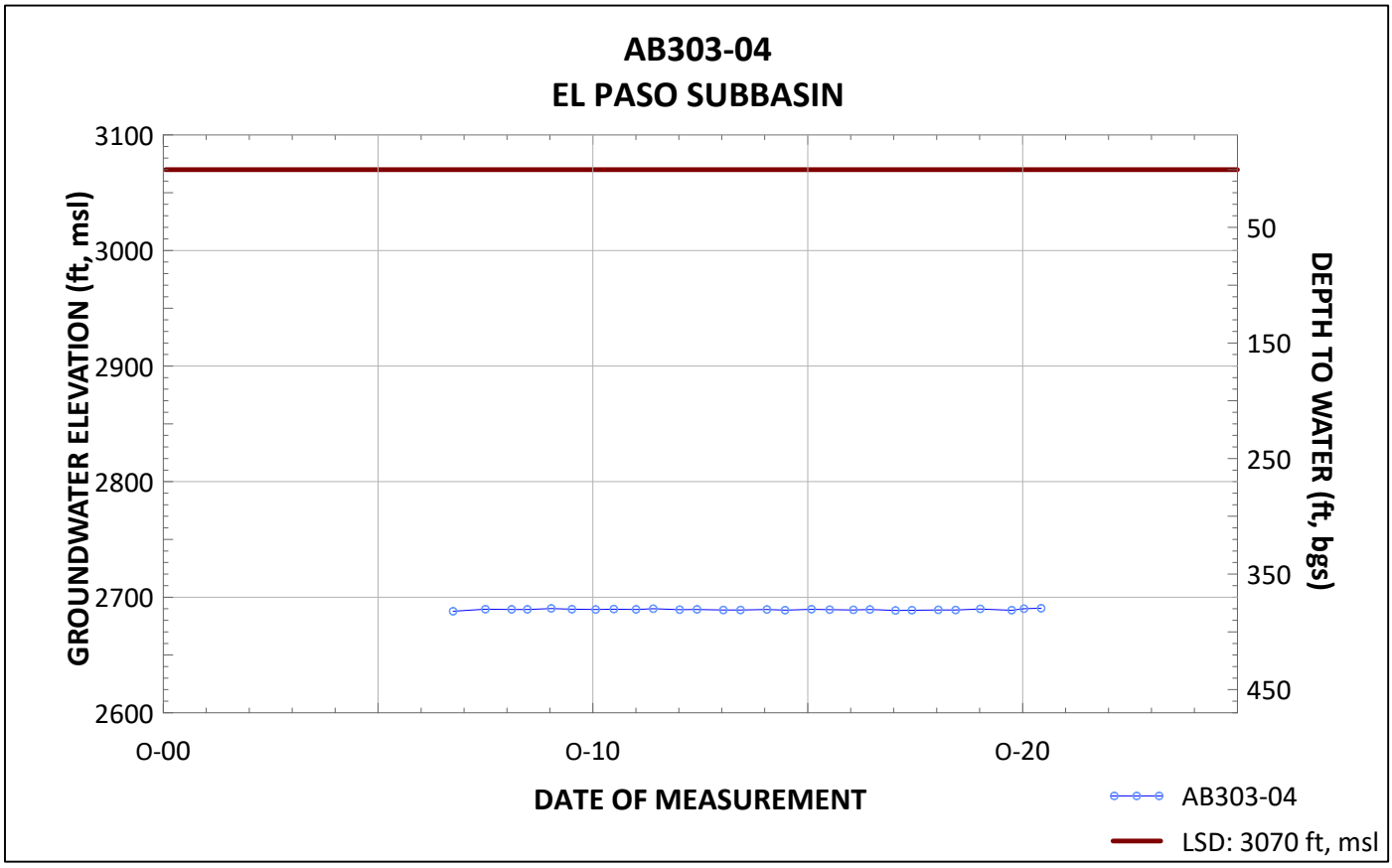
Attachment B

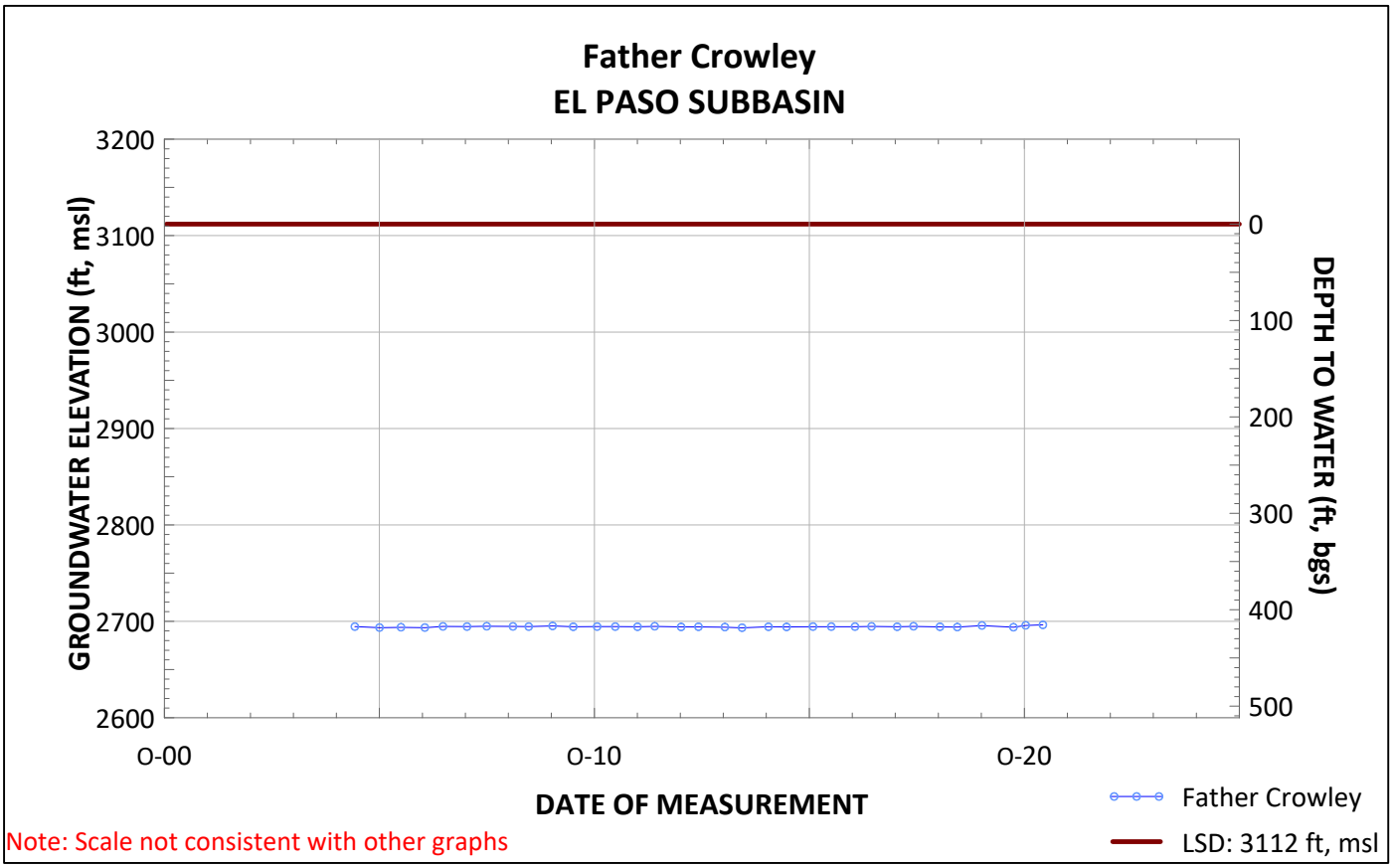
El Paso Subbasin Hydrographs


26S/38E-35D
EL PASO SUBBASIN
GROUNDWATER ELEVATION (ft, msl)
DEPTH TO WATER (ft, bgs)
2700
2600
2500
2400
2300
2200
0
100
200
300
400
O-90
O-00
O-10
O-20
DATE OF MEASUREMENT
35D
LSD: 2685 ft, msl

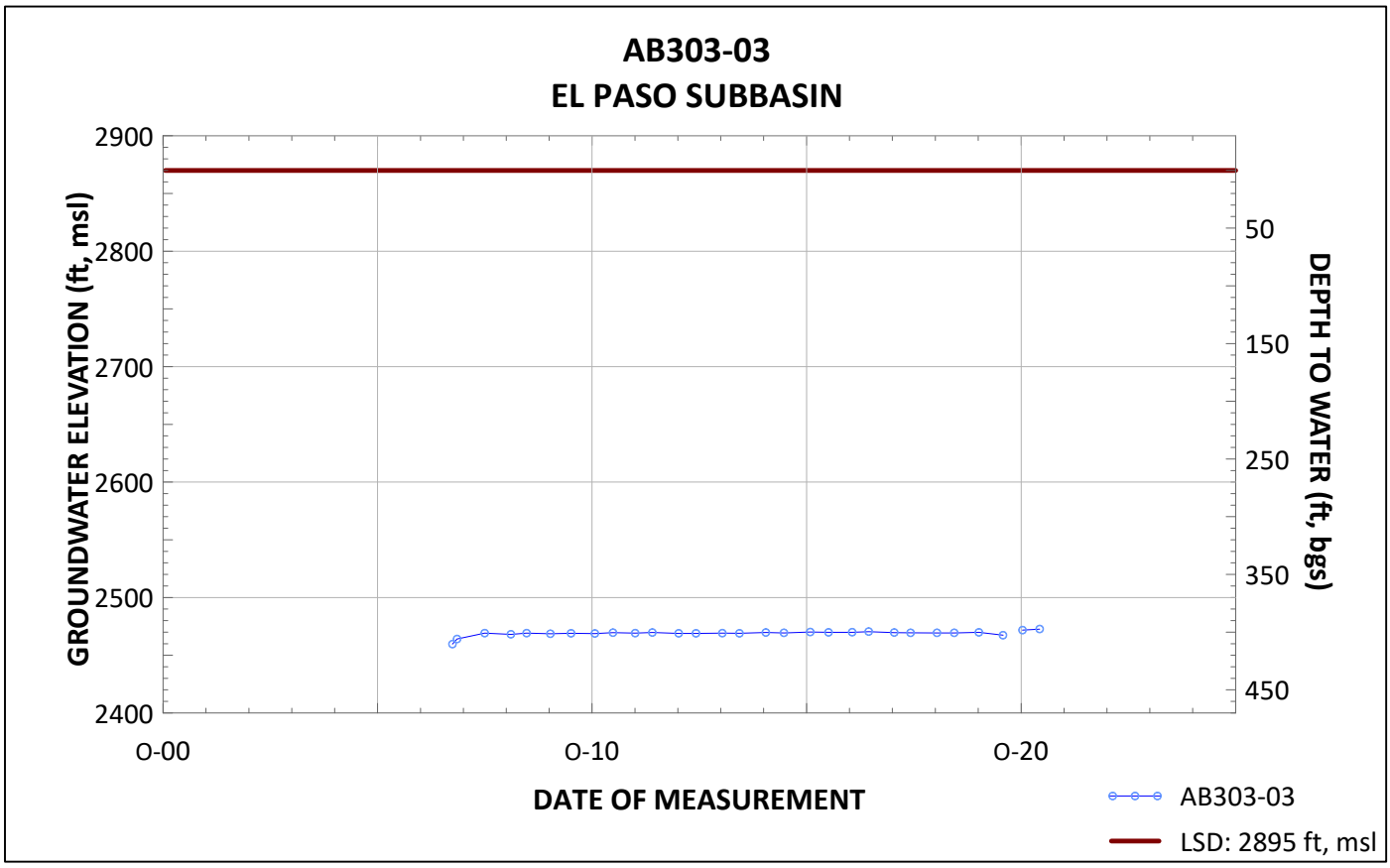

USBR 2 (S, M, D)
EL PASO SUBBASIN
GROUNDWATER ELEVATION (ft, msl)
DEPTH TO WATER (ft, bgs)
2700
2600
2500
2400
2300
2200
50
150
250
350
450
O-90
O-00
O-10
O-20
DATE OF MEASUREMENT
USBR 2 (S)
USBR 2 (D)
USBR 2 (M)
LSD: 2657 ft, msl

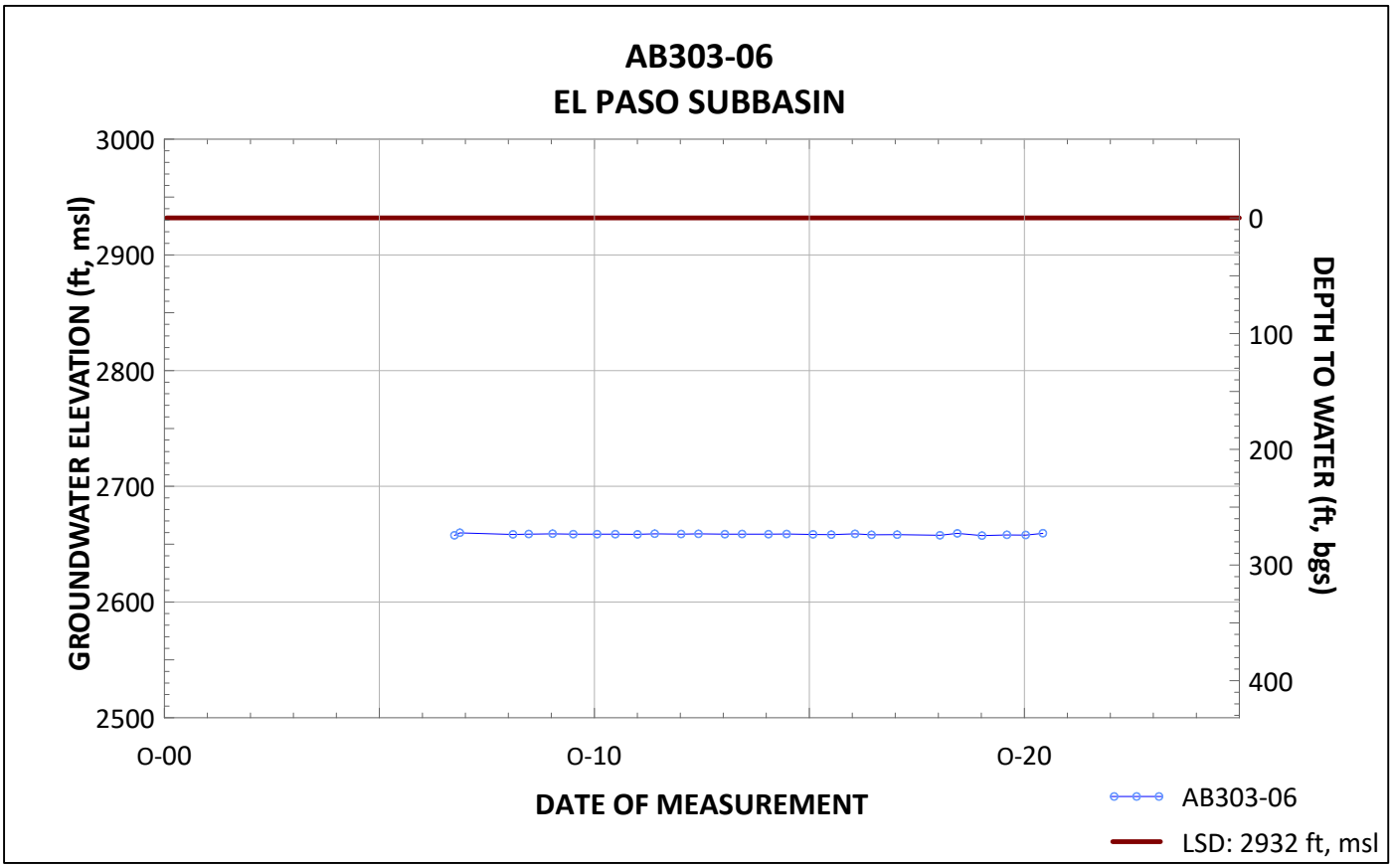

27S/38E-08R01
EL PASO SUBBASIN
GROUNDWATER ELEVATION (ft, msl)
3300
3200
3100
3000
2900
2800
2700
2600
DEPTH TO WATER (ft, bgs)
0
100
200
300
400
500
600
O-00
O-10
O-20
DATE OF MEASUREMENT
8R1
LSD: 3203 ft, msl
Note: Scale not consistent with other graphs

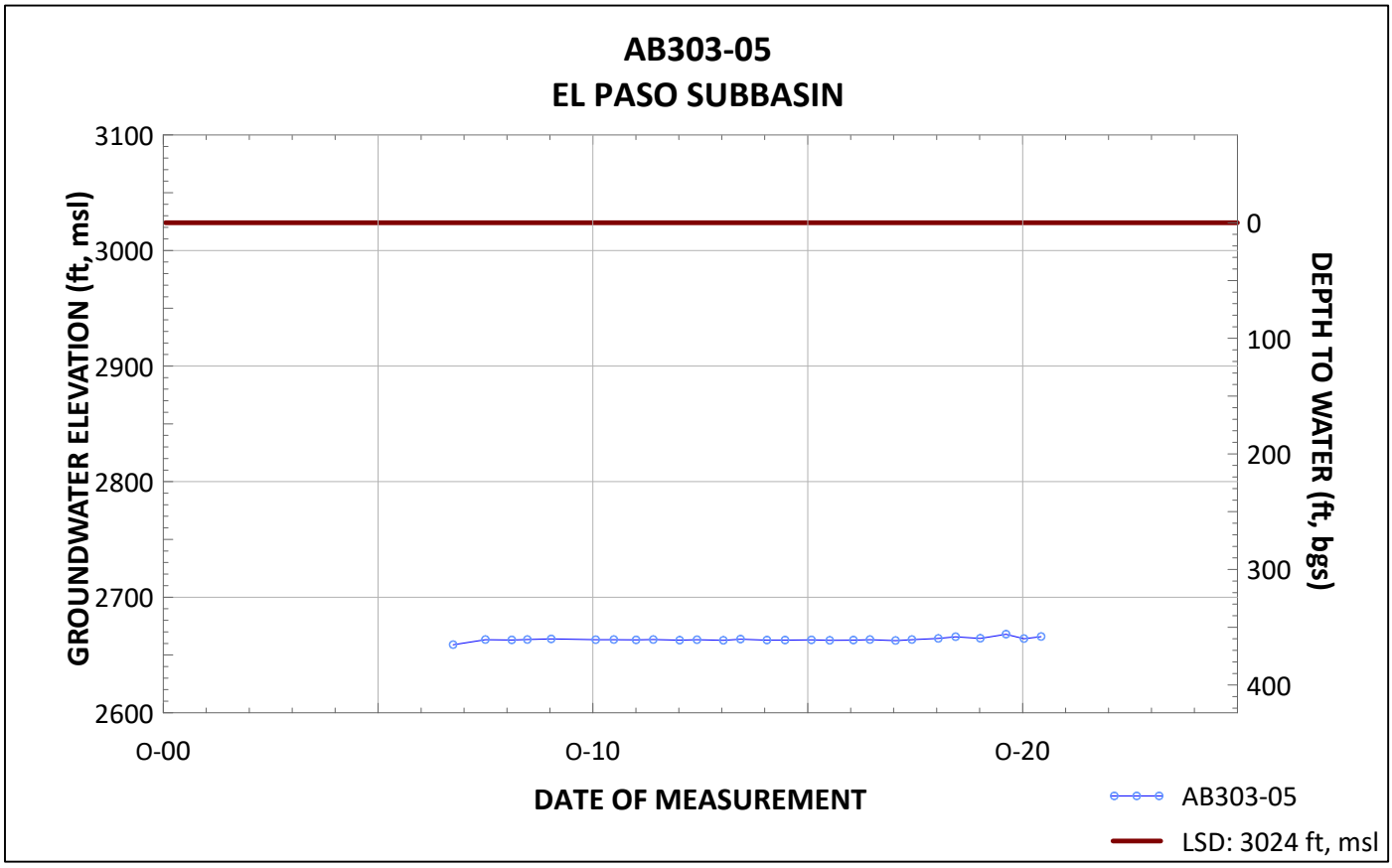

AB303-04
EL PASO SUBBASIN
GROUNDWATER ELEVATION (ft, msl)
3100
3000
2900
2800
2700
2600
DEPTH TO WATER (ft, bgs)
50
150
250
350
450
O-00
O-10
O-20
DATE OF MEASUREMENT
AB303-04
LSD: 3070 ft, msl

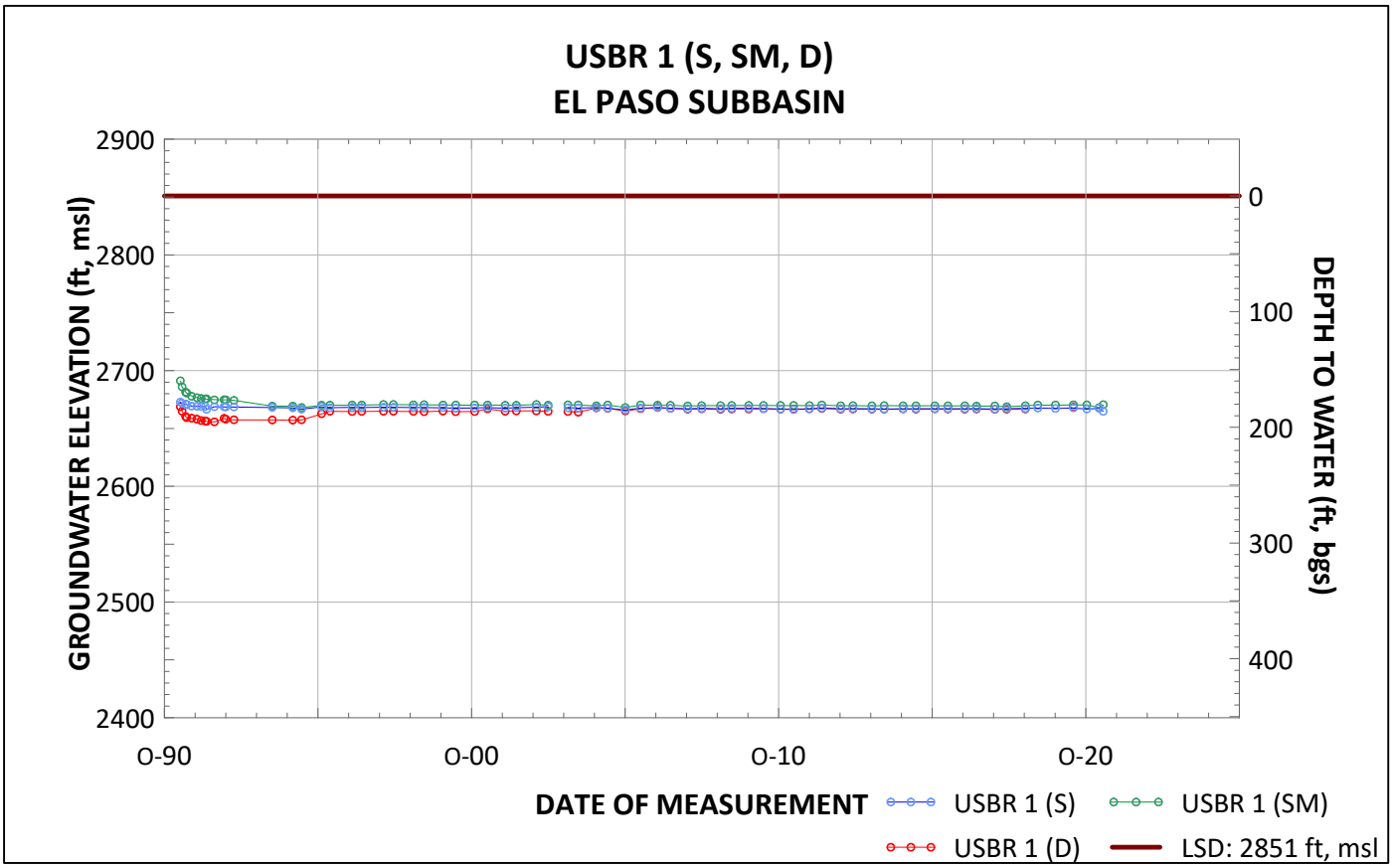


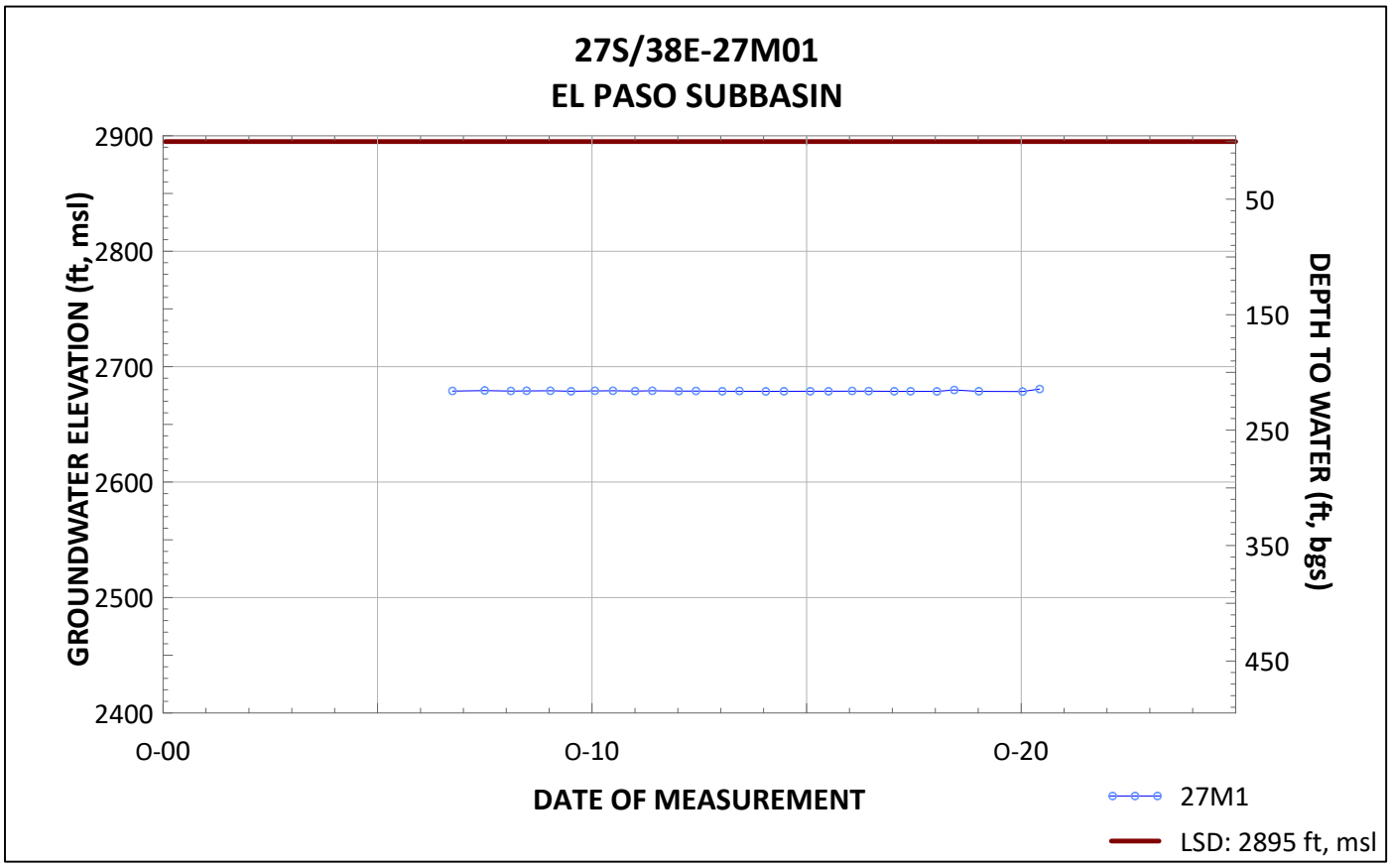
Note: Scale not consistent with other graphs

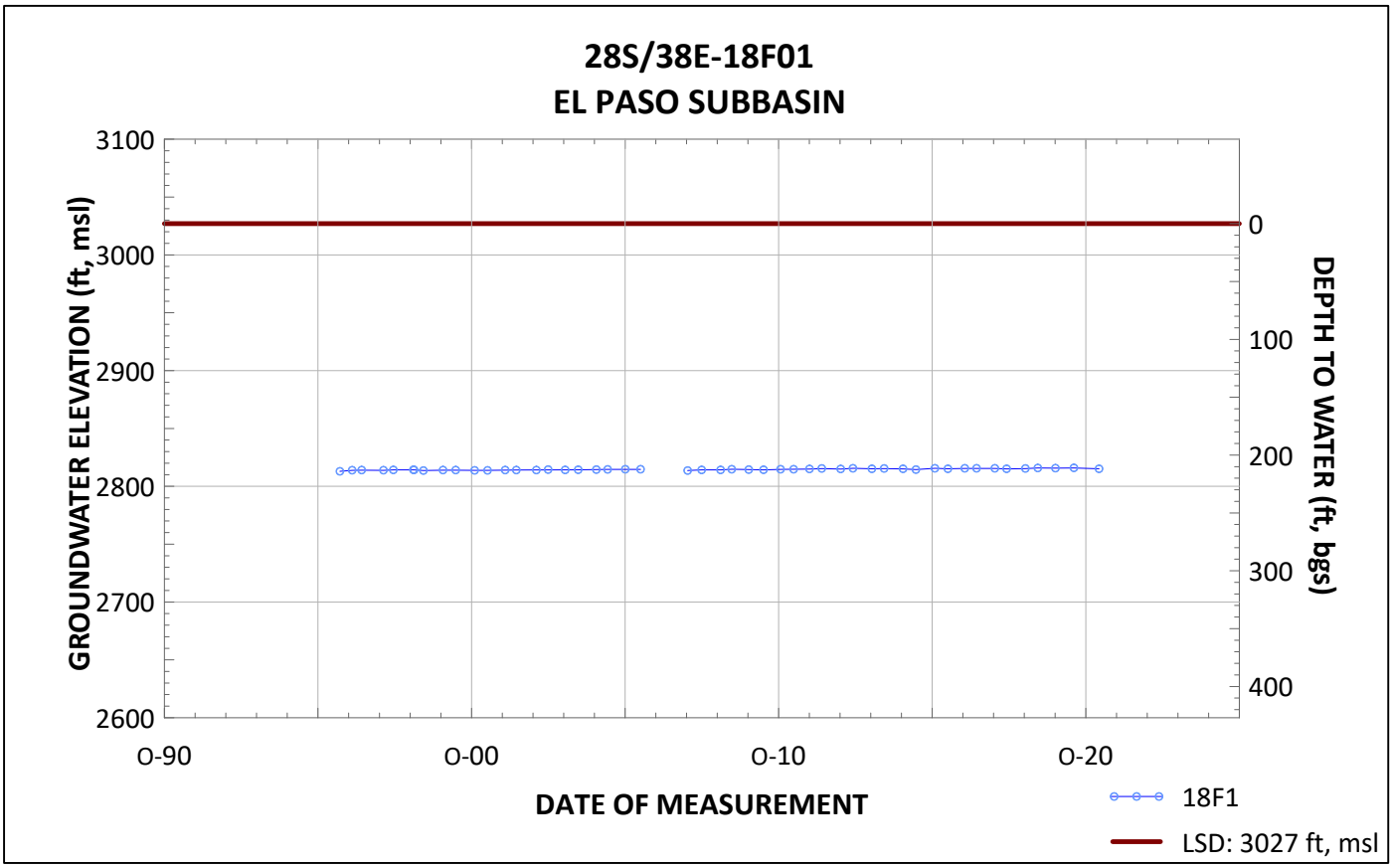


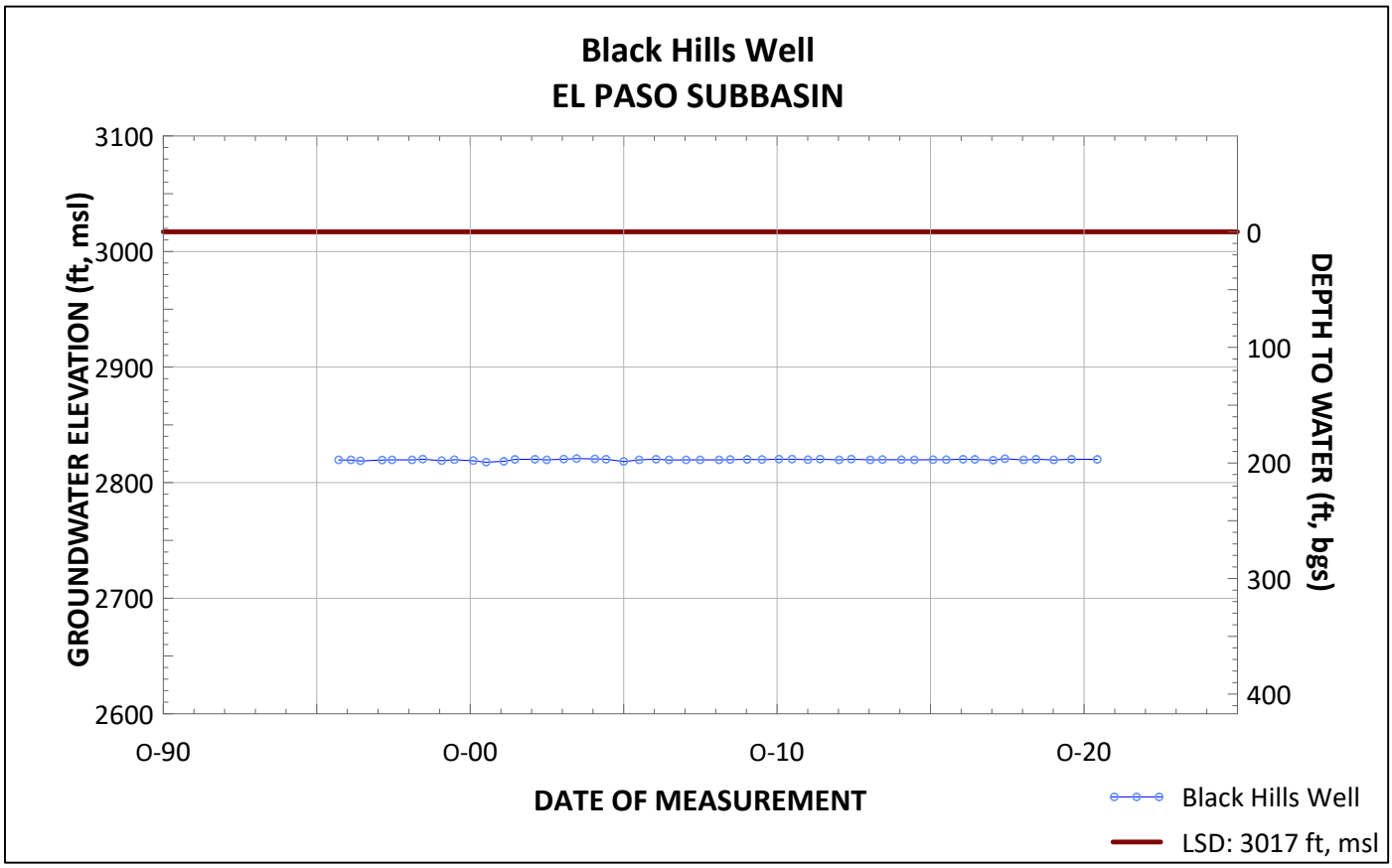

AB303-06
EL PASO SUBBASIN
GROUNDWATER ELEVATION (ft, msl)
3000
2900
2800
2700
2600
2500
DEPTH TO WATER (ft, bgs)
0
100
200
300
400
O-00
O-10
O-20
DATE OF MEASUREMENT
AB303-06
LSD: 2932 ft, msl


AB303-05
EL PASO SUBBASIN
GROUNDWATER ELEVATION (ft, msl)
3100
3000
2900
2800
2700
2600
DEPTH TO WATER (ft, bgs)
0
100
200
300
400
O-00
O-10
O-20
DATE OF MEASUREMENT
AB303-05
LSD: 3024 ft, msl


USBR 1 (S, SM, D)
EL PASO SUBBASIN
GROUNDWATER ELEVATION (ft, msl)
2900
2800
2700
2600
2500
2400
DEPTH TO WATER (ft, bgs)
0
100
200
300
400
O-90
O-00
O-10
O-20
DATE OF MEASUREMENT
USBR 1 (S)
USBR 1 (SM)
USBR 1 (D)
LSD: 2851 ft, msl


27S/38E-27M01
EL PASO SUBBASIN
GROUNDWATER ELEVATION (ft, msl)
2900
2800
2700
2600
2500
2400
DEPTH TO WATER (ft, bgs)
50
150
250
350
450
O-00
O-10
O-20
DATE OF MEASUREMENT
27M1
LSD: 2895 ft, msl


28S/38E-18F01
EL PASO SUBBASIN
GROUNDWATER ELEVATION (ft, msl)
3100
3000
2900
2800
2700
2600
DEPTH TO WATER (ft, bgs)
0
100
200
300
400
O-90
O-00
O-10
O-20
DATE OF MEASUREMENT
18F1
LSD: 3027 ft, msl


Black Hills Well
EL PASO SUBBASIN
GROUNDWATER ELEVATION (ft, msl)
3100
3000
2900
2800
2700
2600
DEPTH TO WATER (ft, bgs)
0
100
200
300
400
O-90
O-00
O-10
O-20
DATE OF MEASUREMENT
Black Hills Well
LSD: 3017 ft, msl

Attachment C

Detailed Engineering Costs for Sites 1, 2, and 3

Indian Wells Valley - Percolation Basins and Pipelines *October 7, 2022*

Percolation Site #1 - assuming percolation rate of 20.4 in/day (3142 AFY Recycled Water)

Capital Costs

Item	Description	Units	Quantity	Base Unit Cost	Unit Cost	Total Cost
1.	**Purchase Site**					
1.01	Purchase Site	AC	10.1	$ 5,000	$ 5,000	$ 50,600
1.02	Contingency				25%	$ 13,000
1.03	**Total Purchase Site**					**$ 64,000**
2.	**Percolation Basin - Site #1**					
2.01	Mobilization	LS	1	$ 12,090	$ 12,000	$ 12,000
2.02	Clear & Grub	AC	5.1	$ 5,826.75	$ 5,826.75	$ 29,500
2.03	Scarify	SY	2,500	$ 8.51	$ 8.51	$ 21,300
2.04	Excavation	CY	8,900	$ 2.36	$ 2.36	$ 21,000
2.05	Berm Fill	CY	8,900	$ 8.39	$ 8.39	$ 74,700
2.06	Berm Compaction	CY	8,900	$ 0.60	$ 0.60	$ 5,300
2.07	Inlet Works	LS	1	$ 10,000	$ 10,000	$ 10,000
2.08	Emergency Overflow	LS	1	$ 20,000	$ 20,000	$ 20,000
2.09	Access Road	LF	3,000	$ 20	$ 20	$ 60,000
2.10	**Subtotal**					**$ 254,000**
2.11	Contingency				25%	$ 64,000
2.12	**Subtotal with Contingency**					**$ 318,000**
2.13	Planning/Permitting				10%	$ 32,000
2.14	Design				10%	$ 32,000
2.15	Construction Management				10%	$ 32,000
2.16	**Total**					**$ 414,000**
3.	**Pipeline - Recycled Water from Ridgecrest**					
3.01	Mobilization	LS	1	$ 864,520	$ 865,000	$ 865,000
3.02	Furnish 12" CMLCSP	LF	79,900	$ 127	$ 127	$ 10,152,100
3.03	Install 12" CMLCSP	LF	79,900	$ 7.57	$ 8	$ 639,200
3.04	Furnish and Install 12" Isolation Gate Valves	EA	40	$ 9,461	$ 9,461	$ 377,900
3.05	Furnish and Install 2" Combination Air Relief Valves	EA	40	$ 3,400	$ 4,600	$ 183,800
3.06	Furnish and Install 2" Blowoff Assemblies	EA	40	$ 3,225	$ 4,370	$ 174,600
3.07	AC Paving Repair	LF	79,900	$ 53	$ 72	$ 5,752,800
3.08	Startup Testing	LS	1	$ 10,000	$ 10,000	$ 10,000
3.09	**Subtotal**					**$ 18,155,000**
3.10	Contingency				25%	$ 4,539,000
3.11	**Subtotal with Contingency**					**$ 22,694,000**
3.12	Planning/Permitting				8%	$ 1,816,000
3.13	Design				8%	$ 1,816,000
3.14	Construction Management				8%	$ 1,816,000
3.15	**Total**					**$ 28,142,000**
4.	**Booster Pump Station**					
4.01	Mobilization	LS	1	$ 55,250	$ 55,000	$ 55,000
4.02	Furnish and Install Booster Pumps (75 hp)	EA	3	$ 33,031	$ 33,031	$ 99,100
4.03	Furnish and Install Site Piping and Valves	LS	1	$ 100,000	$ 100,000	$ 100,000
4.04	Electrical Power, Conduits, Wiring	LS	1	$ 252,000	$ 277,400	$ 277,400
4.05	Furnish and Install Brick Building and Foundation	SF	780	$ 719	$ 790	$ 616,200
4.06	Startup Testing	LS	1	$ 10,000	$ 12,300	$ 12,300
4.07	**Subtotal (1 pump station)**					**$ 1,160,000**
4.08	**Subtotal (2 pump stations)**	EA	2	$ 1,160,000	$ 1,160,000	**$ 2,320,000**
4.09	Contingency				25%	$ 580,000
4.10	**Subtotal with Contingency**					**$ 2,900,000**
4.11	Planning/Permitting				8%	$ 232,000
4.12	Design				8%	$ 232,000

Percolation Site #1 - assuming percolation rate of 20.4 in/day (3142 AFY Recycled Water)

Capital Costs

Item	Description	Units	Quantity	Base Unit Cost	Unit Cost	Total Cost
4.13	Construction Management				8%	$ 232,000
4.14	**Total**					**$ 3,596,000**
	GRAND TOTAL					**$ 32,216,000**

Indian Wells Valley - Percolation Basins and Pipelines *October 7, 2022*

Percolation Site #2 - assuming percolation rate of 20.4 in/day (3142 AFY Recycled Water)

Item	Description	Units	Quantity	Base Unit Cost	Unit Cost	Total Cost
1.	**Purchase Site**					
1.01	Purchase Site	AC	10.1	$ 5,000	$ 5,000	$ 50,600
1.02	Contingency				25%	$ 13,000
1.03	**Total Purchase Site**					**$ 64,000**
2.	**Percolation Basin - Site #2**					
2.01	Mobilization	LS	1	$ 8,790	$ 9,000	$ 9,000
2.02	Clear & Grub	AC	5.1	$ 5,826.75	$ 5,826.75	$ 29,500
2.03	Scarify	SY	2,000	$ 8.51	$ 8.51	$ 17,000
2.04	Excavation	CY	1,700	$ 2.36	$ 2.36	$ 4,000
2.05	Berm Fill	CY	1,700	$ 8.39	$ 8.39	$ 14,300
2.06	Berm Compaction	CY	1,700	$ 0.60	$ 0.60	$ 1,000
2.07	Inlet Works	LS	1	$ 10,000	$ 10,000	$ 10,000
2.08	Emergency Overflow	LS	1	$ 20,000	$ 20,000	$ 20,000
2.09	Access Road	LF	4,000	$ 20	$ 20	$ 80,000
2.10	**Subtotal**					**$ 185,000**
2.11	Contingency				25%	$ 46,000
2.12	**Subtotal with Contingency**					**$ 231,000**
2.13	Planning/Permitting				10%	$ 23,000
2.14	Design				10%	$ 23,000
2.15	Construction Management				10%	$ 23,000
2.16	**Total**					**$ 300,000**
3.	**Pipeline - Recycled Water from Ridgecrest**					
3.01	Mobilization	LS	1	$ 1,360,080	$ 1,360,000	$ 1,360,000
3.02	Furnish 12" CMLCSP	LF	126,900	$ 127	$ 127	$ 16,123,900
3.03	Install 12" CMLCSP	LF	126,900	$ 7.57	$ 8	$ 1,015,200
3.04	Furnish and Install 12" Isolation Gate Valves	EA	63	$ 9,461	$ 9,461	$ 600,300
3.05	Furnish and Install 2" Combination Air Relief Valves	EA	63	$ 3,400	$ 4,600	$ 291,900
3.06	Furnish and Install 2" Blowoff Assemblies	EA	63	$ 3,225	$ 4,370	$ 277,300
3.07	AC Paving Repair	LF	126,900	$ 53	$ 70	$ 8,883,000
3.08	Startup Testing	LS	1	$ 10,000	$ 10,000	$ 10,000
3.09	**Subtotal**					**$ 28,562,000**
3.10	Contingency				25%	$ 7,141,000
3.11	**Subtotal with Contingency**					**$ 35,703,000**
3.12	Planning/Permitting				8%	$ 2,856,000
3.13	Design				8%	$ 2,856,000
3.14	Construction Management				8%	$ 2,856,000
3.15	**Total**					**$ 44,271,000**
4.	**Booster Pump Station**					
4.01	Mobilization	LS	1	$ 61,230	$ 61,000	$ 61,000
4.02	Furnish and Install Booster Pumps (100 hp)	EA	3	$ 66,607	$ 73,680	$ 221,000
4.03	Furnish and Install Site Piping and Valves	LS	1	$ 100,000	$ 100,000	$ 100,000
4.04	Electrical Power, Conduits, Wiring	LS	1	$ 252,000	$ 277,400	$ 277,400
4.05	Furnish and Install Brick Building and Foundation	SF	780	$ 719	$ 790	$ 616,200
4.06	Startup Testing	LS	1	$ 10,000	$ 10,000	$ 10,000
4.07	**Subtotal (1 pump station)**					**$ 1,286,000**
4.08	**Subtotal (2 pump stations)**	EA	2	$ 1,286,000	$ 1,286,000	**$ 2,572,000**
4.09	Contingency				25%	$ 643,000
4.10	**Subtotal with Contingency**					**$ 3,215,000**
4.11	Planning/Permitting				8%	$ 257,000
4.12	Design				8%	$ 257,000
4.13	Construction Management				8%	$ 257,000

Percolation Site #2 - assuming percolation rate of 20.4 in/day (3142 AFY Recycled Water)

Item	Description	Units	Quantity	Base Unit Cost	Unit Cost	Total Cost
4.14	**Total**					**$ 3,986,000**
5.	**Pipeline - Groundwater Gravity to Inyokern**					
5.01	Mobilization	LS	1	$ 741,895	$ 742,000	$ 742,000
5.02	Furnish 12" CMLCSP	LF	69,200	$ 127	$ 127	$ 8,792,600
5.03	Install 12" CMLCSP	LF	69,200	$ 8	$ 8	$ 553,600
5.04	Furnish and Install 12" Isolation Gate Valves	EA	35	$ 9,461	$ 9,461	$ 327,300
5.05	Furnish and Install 2" Combination Air Relief Valves	EA	35	$ 3,400	$ 4,600	$ 159,200
5.06	Furnish and Install 2" Blowoff Assemblies	EA	35	$ 3,225	$ 4,370	$ 151,200
5.07	AC Paving Repair	LF	69,200	$ 53	$ 70	$ 4,844,000
5.08	Startup Testing	LS	1	$ 10,000	$ 10,000	$ 10,000
5.09	**Subtotal**					**$ 15,580,000**
5.10	Contingency				25%	$ 3,895,000
5.11	**Subtotal with Contingency**					**$ 19,475,000**
5.12	Planning/Permitting				8%	$ 2,856,000
5.13	Design				8%	$ 2,856,000
5.14	Construction Management				8%	$ 2,856,000
5.15	**Total**					**$ 28,043,000**
	GRAND TOTAL					**$ 76,664,000**

Indian Wells Valley - Percolation Basins and Pipelines *October 7, 2022*

Percolation Site #3 - assuming percolation rate of 20.4 in/day (3142 AFY Recycled Water)

Item	Description	Units	Quantity	Base Unit Cost	Unit Cost	Total Cost
1.	**Purchase Site**					
1.01	Purchase Site	AC	10.1	$ 5,000	$ 5,000	$ 50,600
1.02	Contingency				25%	$ 13,000
1.03	**Total Purchase Site**					**$ 64,000**
2.	**Percolation Basin - Site #3**					
2.01	Mobilization	LS	1	$ 7,695	$ 8,000	$ 8,000
2.02	Clear & Grub	AC	5.1	$ 5,826.75	$ 5,826.75	$ 29,500
2.03	Scarify	SY	2,000	$ 8.51	$ 8.51	$ 17,000
2.04	Excavation	CY	1,000	$ 2.36	$ 2.36	$ 2,400
2.05	Berm Fill	CY	1,000	$ 8.39	$ 8.39	$ 8,400
2.06	Berm Compaction	CY	1,000	$ 0.60	$ 0.60	$ 600
2.07	Inlet Works	LS	1	$ 10,000	$ 10,000	$ 10,000
2.08	Emergency Overflow	LS	1	$ 20,000	$ 20,000	$ 20,000
2.09	Access Road	LF	3,300	$ 20	$ 20	$ 66,000
2.10	**Subtotal**					**$ 162,000**
2.11	Contingency				25%	$ 41,000
2.12	**Subtotal with Contingency**					**$ 203,000**
2.13	Planning/Permitting				10%	$ 20,000
2.14	Design				10%	$ 20,000
2.15	Construction Management				10%	$ 20,000
2.16	**Total**					**$ 263,000**
3.	**Pipeline - Recycled Water from Ridgecrest**					
3.01	Mobilization	LS	1	$ 1,569,025	$ 1,569,000	$ 1,569,000
3.02	Furnish 12" CMLCSP	LF	146,700	$ 127	$ 127	$ 18,639,700
3.03	Install 12" CMLCSP	LF	146,700	$ 7.57	$ 8	$ 1,110,000
3.04	Furnish and Install 12" Isolation Gate Valves	EA	73	$ 9,461	$ 9,461	$ 693,900
3.05	Furnish and Install 2" Combination Air Relief Valves	EA	73	$ 3,400	$ 4,600	$ 337,400
3.06	Furnish and Install 2" Blowoff Assemblies	EA	73	$ 3,225	$ 4,370	$ 320,500
3.07	AC Paving Repair	LF	146,700	$ 53	$ 70	$ 10,269,000
3.08	Startup Testing	LS	1	$ 10,000	$ 10,000	$ 10,000
3.09	**Subtotal**					**$ 32,950,000**
3.10	Contingency				25%	$ 8,238,000
3.11	**Subtotal with Contingency**					**$ 41,188,000**
3.12	Planning/Permitting				8%	$ 3,295,000
3.13	Design				8%	$ 3,295,000
3.14	Construction Management				8%	$ 3,295,000
3.15	**Total**					**$ 51,073,000**
4.	**Booster Pump Station**					
4.01	Mobilization	LS	1	$ 61,230	$ 61,000	$ 61,000
4.02	Furnish and Install Booster Pumps (100 hp)	EA	3	$ 66,607	$ 73,680	$ 221,000
4.03	Furnish and Install Site Piping and Valves	LS	1	$ 100,000	$ 100,000	$ 100,000
4.04	Electrical Power, Conduits, Wiring	LS	1	$ 252,000	$ 277,400	$ 277,400
4.05	Furnish and Install Brick Building and Foundation	SF	780	$ 719	$ 790	$ 616,200
4.06	Startup Testing	LS	1	$ 10,000	$ 10,000	$ 10,000
4.07	**Subtotal (1 pump station)**					**$ 1,286,000**
4.08	**Subtotal (2 pump stations)**	EA	2	$ 1,286,000	$ 1,286,000	**$ 2,572,000**
4.09	Contingency				25%	$ 643,000
4.10	**Subtotal with Contingency**					**$ 3,215,000**
4.11	Planning/Permitting				8%	$ 257,000
4.12	Design				8%	$ 257,000
4.13	Construction Management				8%	$ 257,000

Percolation Site #3 - assuming percolation rate of 20.4 in/day (3142 AFY Recycled Water)

Item	Description	Units	Quantity	Base Unit Cost	Unit Cost	Total Cost
4.14	**Total**					**$ 3,986,000**
5.	**Pipeline - Groundwater Gravity to Inyokern**					
5.01	Mobilization	LS	1	$ 921,090	$ 921,000	$ 921,000
5.02	Furnish 12" CMLCSP	LF	86,100	$ 127	$ 127	$ 10,939,900
5.03	Install 12" CMLCSP	LF	86,100	$ 8	$ 8	$ 651,500
5.04	Furnish and Install 12" Isolation Gate Valves	EA	43	$ 9,461	$ 9,461	$ 407,300
5.05	Furnish and Install 2" Combination Air Relief Valves	EA	43	$ 3,400	$ 4,600	$ 198,000
5.06	Furnish and Install 2" Blowoff Assemblies	EA	43	$ 3,225	$ 4,370	$ 188,100
5.07	AC Paving Repair	LF	86,100	$ 53	$ 70	$ 6,027,000
5.08	Startup Testing	LS	1	$ 10,000	$ 10,000	$ 10,000
5.09	**Subtotal**					**$ 19,343,000**
5.10	Contingency				25%	$ 4,836,000
5.11	**Subtotal with Contingency**					**$ 24,179,000**
5.12	Planning/Permitting				8%	$ 3,295,000
5.13	Design				8%	$ 3,295,000
5.14	Construction Management				8%	$ 3,295,000
5.15	**Total**					**$ 34,064,000**
	GRAND TOTAL					**$ 89,450,000**

Indian Wells Valley - Percolation Basins and Pipelines *October 7, 2022*

Percolation Site #1 - assuming percolation rate of 20.4 in/day (15,083 AFY Imported Water)

Item	Description	Units	Quantity	Base Unit Cost	Unit Cost	Total Cost
1.	**Purchase Site**					
1.01	Purchase Site	AC	49	$ 5,000	$ 5,000	$ 243,100
1.02	Contingency				25%	$ 61,000
1.03	**Total Purchase Site**					**$ 304,000**
2.	**Percolation Basin - Site #1**					
2.01	Mobilization	LS	1	$ 38,210	$ 38,000	$ 38,000
2.02	Clear & Grub	AC	24	$ 5,826.75	$ 5,826.75	$ 141,600
2.03	Scarify	SY	7,500	$ 8.51	$ 8.51	$ 63,800
2.04	Excavation	CY	41,300	$ 2.36	$ 2.36	$ 97,500
2.05	Berm Fill	CY	41,300	$ 8.39	$ 8.39	$ 346,500
2.06	Berm Compaction	CY	41,300	$ 0.60	$ 0.60	$ 24,800
2.07	Inlet Works	LS	1	$ 10,000	$ 10,000	$ 10,000
2.08	Emergency Overflow	LS	1	$ 20,000	$ 20,000	$ 20,000
2.09	Access Road	LF	3,000	$ 20	$ 20	$ 60,000
2.10	**Subtotal**					**$ 802,000**
2.11	Contingency				25%	$ 201,000
2.12	**Subtotal with Contingency**					**$ 1,003,000**
2.13	Planning/Permitting				10%	$ 100,000
2.14	Design				10%	$ 100,000
2.15	Construction Management				10%	$ 100,000
2.16	**Total**					**$ 1,303,000**
~~**3.**~~	~~**Pipeline - Imported Water from ???**~~					
~~3.01~~	~~Mobilization~~	~~LS~~	~~1~~	~~$ 500~~	~~$ 1,000~~	~~$ 1,000~~
~~3.02~~	~~Furnish 24" CMLCSP~~	~~LF~~			~~$ -~~	~~$ -~~
~~3.03~~	~~Install 24" CMLCSP~~	~~LF~~			~~$ -~~	~~$ -~~
~~3.04~~	~~Furnish and Install 24" Isolation Gate Valves~~	~~EA~~	~~0~~		~~$ -~~	~~$ -~~
~~3.05~~	~~Furnish and Install 2" Combination Air Relief Valves~~	~~EA~~	~~0~~	~~$ 3,400~~	~~$ 3,900~~	~~$ -~~
~~3.06~~	~~Furnish and Install 2" Blowoff Assemblies~~	~~EA~~	~~0~~	~~$ 3,225~~	~~$ 3,700~~	~~$ -~~
~~3.07~~	~~AC Paving Repair~~	~~LF~~	~~0~~	~~$ 53~~	~~$ 61~~	~~$ -~~
~~3.08~~	~~Startup Testing~~	~~LS~~	~~1~~	~~$ 10,000~~	~~$ 10,000~~	~~$ 10,000~~
~~**3.09**~~	~~**Subtotal**~~					~~**$ 11,000**~~
~~3.10~~	~~Contingency~~				~~25%~~	~~$ 3,000~~
~~**3.11**~~	~~**Subtotal with Contingency**~~					~~**$ 14,000**~~
~~3.12~~	~~Planning/Permitting~~				~~8%~~	~~$ 1,000~~
~~3.13~~	~~Design~~				~~8%~~	~~$ 1,000~~
~~3.14~~	~~Construction Management~~				~~8%~~	~~$ 1,000~~
~~**3.15**~~	~~**Total**~~					
4.	**Booster Pump Station**					
4.01	Mobilization	LS	1	$ 48,420	$ 48,000	$ 48,000
4.02	Furnish and Install Booster Pumps (150 hp)	EA	1	$ 99,910	$ 110,520	$ 110,500
4.03	Furnish and Install Site Piping and Valves	LS	1	$ 100,000	$ 100,000	$ 100,000
4.04	Electrical Power, Conduits, Wiring	LS	1	$ 378,000	$ 416,110	$ 416,100
4.05	Furnish and Install Brick Building and Foundation	SF	420	$ 719	$ 790	$ 331,800
4.06	Startup Testing	LS	1	$ 10,000	$ 10,000	$ 10,000
4.07	**Subtotal (1 pump station)**					**$ 1,016,000**
4.08	**Subtotal (2 pump stations)**	EA	0	$ 1,016,000	$ 1,016,000	**$ -**
4.09	Contingency				25%	$ 254,000
4.10	**Subtotal with Contingency**					**$ 1,270,000**
4.11	Planning/Permitting				8%	$ 102,000
4.12	Design				8%	$ 102,000
4.13	Construction Management				8%	$ 102,000

Percolation Site #1 - assuming percolation rate of 20.4 in/day (15,083 AFY Imported Water)

Item	Description	Units	Quantity	Base Unit Cost	Unit Cost	Total Cost
4.14	Total					$ 1,576,000
	GRAND TOTAL					$ 3,183,000

Indian Wells Valley - Percolation Basins and Pipelines *October 7, 2022*

Percolation Site #2 - assuming percolation rate of 20.4 in/day (15,083 AFY Imported Water)

Item	Description	Units	Quantity	Base Unit Cost	Unit Cost	Total Cost
1.	**Purchase Site**					
1.01	Purchase Site	AC	49	$ 5,000	$ 5,000	$ 243,100
1.02	Contingency				25%	$ 61,000
1.03	**Total Purchase Site**					**$ 304,000**
2.	**Percolation Basin - Site #2**					
2.01	Mobilization	LS	1	$ 16,155	$ 16,000	$ 16,000
2.02	Clear & Grub	AC	24	$ 5,826.75	$ 5,826.75	$ 141,600
2.03	Scarify	SY	4,000	$ 8.51	$ 8.51	$ 34,000
2.04	Excavation	CY	3,300	$ 2.36	$ 2.36	$ 7,800
2.05	Berm Fill	CY	3,300	$ 8.39	$ 8.39	$ 27,700
2.06	Berm Compaction	CY	3,300	$ 0.60	$ 0.60	$ 2,000
2.07	Inlet Works	LS	1	$ 10,000	$ 10,000	$ 10,000
2.08	Emergency Overflow	LS	1	$ 20,000	$ 20,000	$ 20,000
2.09	Access Road	LF	4,000	$ 20	$ 20	$ 80,000
2.10	**Subtotal**					**$ 339,000**
2.11	Contingency				25%	$ 85,000
2.12	**Subtotal with Contingency**					**$ 424,000**
2.13	Planning/Permitting				10%	$ 42,000
2.14	Design				10%	$ 42,000
2.15	Construction Management				10%	$ 42,000
2.16	**Total**					**$ 550,000**
~~**3.**~~	~~**Pipeline - Imported Water from ???**~~					
~~3.01~~	~~Mobilization~~	~~LS~~	~~1~~	~~$ 500~~	~~$ 1,000~~	~~$ 1,000~~
~~3.02~~	~~Furnish 24" CMLCSP~~	~~LF~~			~~$ -~~	~~$ -~~
~~3.03~~	~~Install 24" CMLCSP~~	~~LF~~			~~$ -~~	~~$ -~~
~~3.04~~	~~Furnish and Install 24" Isolation Gate Valves~~	~~EA~~	~~0~~		~~$ -~~	~~$ -~~
~~3.05~~	~~Furnish and Install 2" Combination Air Relief Valves~~	~~EA~~	~~0~~	~~$ 3,400~~	~~$ 4,600~~	~~$ -~~
~~3.06~~	~~Furnish and Install 2" Blowoff Assemblies~~	~~EA~~	~~0~~	~~$ 3,225~~	~~$ 4,370~~	~~$ -~~
~~3.07~~	~~AC Paving Repair~~	~~LF~~	~~0~~	~~$ 53~~	~~$ 70~~	~~$ -~~
~~3.08~~	~~Startup Testing~~	~~LS~~	~~1~~	~~$ 10,000~~	~~$ 10,000~~	~~$ 10,000~~
~~**3.09**~~	~~**Subtotal**~~					~~**$ 11,000**~~
~~3.10~~	~~Contingency~~				~~25%~~	~~$ 3,000~~
~~**3.11**~~	~~**Subtotal with Contingency**~~					~~**$ 14,000**~~
~~3.12~~	~~Planning/Permitting~~				~~8%~~	~~$ 1,000~~
~~3.13~~	~~Design~~				~~8%~~	~~$ 1,000~~
~~3.14~~	~~Construction Management~~				~~8%~~	~~$ 1,000~~
~~**3.15**~~	~~**Total**~~					
4.	**Booster Pump Station**					
4.01	Mobilization	LS	1	$ 55,605	$ 56,000	$ 56,000
4.02	Furnish and Install Booster Pumps (150 hp)	EA	1	$ 99,910	$ 110,520	$ 110,500
4.03	Furnish and Install Site Piping and Valves	LS	1	$ 100,000	$ 100,000	$ 100,000
4.04	Electrical Power, Conduits, Wiring	LS	1	$ 504,000	$ 554,810	$ 554,800
4.05	Furnish and Install Brick Building and Foundation	SF	420	$ 719	$ 790	$ 331,800
4.06	Startup Testing	LS	1	$ 15,000	$ 15,000	$ 15,000
4.07	**Subtotal (1 pump station)**					**$ 1,168,000**
4.08	**Subtotal (2 pump stations)**	EA	0	$ 1,168,000	$ 1,168,000	**$ -**
4.09	Contingency				25%	$ 292,000
4.10	**Subtotal with Contingency**					**$ 1,460,000**
4.11	Planning/Permitting				8%	$ 117,000
4.12	Design				8%	$ 117,000
4.13	Construction Management				8%	$ 117,000

Percolation Site #2 - assuming percolation rate of 20.4 in/day (15,083 AFY Imported Water)

Item	Description	Units	Quantity	Base Unit Cost	Unit Cost	Total Cost
4.14	**Total**					**$ 1,811,000**
5.	**Pipeline - Groundwater Gravity to Inyokern**					
5.01	Mobilization	LS	1	$ 1,274,240	$ 1,274,000	$ 1,274,000
5.02	Furnish 24" CMLCSP	LF	69,200	$ 251	$ 251	$ 17,349,100
5.03	Install 24" CMLCSP	LF	69,200	$ 10.09	$ 10	$ 698,200
5.04	Furnish and Install 24" Isolation Gate Valves	EA	35	$ 65,695	$ 65,695	$ 2,273,100
5.05	Furnish and Install 2" Combination Air Relief Valves	EA	35	$ 3,400	$ 4,600	$ 159,200
5.06	Furnish and Install 2" Blowoff Assemblies	EA	35	$ 3,225	$ 4,370	$ 151,200
5.07	AC Paving Repair	LF	69,200	$ 53	$ 70	$ 4,844,000
5.08	Startup Testing	LS	1	$ 10,000	$ 10,000	$ 10,000
5.09	**Subtotal**					**$ 26,759,000**
5.10	Contingency				25%	$ 6,690,000
5.11	**Subtotal with Contingency**					**$ 33,449,000**
5.12	Planning/Permitting				8%	$ 1,000
5.13	Design				8%	$ 1,000
5.14	Construction Management				8%	$ 1,000
5.15	**Total**					**$ 33,452,000**
	GRAND TOTAL					**$ 36,117,000**

Indian Wells Valley - Percolation Basins and Pipelines *October 7, 2022*

Percolation Site #3 - assuming percolation rate of 20.4 in/day (15,083 AFY Imported Water)

Item	Description	Units	Quantity	Base Unit Cost	Unit Cost	Total Cost
1.	**Purchase Site**					
1.01	Purchase Site	AC	49	$ 5,000	$ 5,000	$ 243,100
1.02	Contingency				25%	$ 61,000
1.03	**Total Purchase Site**					**$ 304,000**
2.	**Percolation Basin - Site #3**					
2.01	Mobilization	LS	1	$ 14,775	$ 15,000	$ 15,000
2.02	Clear & Grub	AC	24	$ 5,826.75	$ 5,826.75	$ 141,600
2.03	Scarify	SY	4,000	$ 8.51	$ 8.51	$ 34,000
2.04	Excavation	CY	2,100	$ 2.36	$ 2.36	$ 5,000
2.05	Berm Fill	CY	2,100	$ 8.39	$ 8.39	$ 17,600
2.06	Berm Compaction	CY	2,100	$ 0.60	$ 0.60	$ 1,300
2.07	Inlet Works	LS	1	$ 10,000	$ 10,000	$ 10,000
2.08	Emergency Overflow	LS	1	$ 20,000	$ 20,000	$ 20,000
2.09	Access Road	LF	3,300	$ 20	$ 20	$ 66,000
2.10	**Subtotal**					**$ 311,000**
2.11	Contingency				25%	$ 78,000
2.12	**Subtotal with Contingency**					**$ 389,000**
2.13	Planning/Permitting				10%	$ 39,000
2.14	Design				10%	$ 39,000
2.15	Construction Management				10%	$ 39,000
2.16	**Total**					**$ 506,000**
3.	**Pipeline - Imported Water from ???**					
~~3.01~~	~~Mobilization~~	~~LS~~	~~1~~	~~$ 500~~	~~$ 1,000~~	~~$ 1,000~~
~~3.02~~	~~Furnish 24" CMLCSP~~	~~LF~~			~~$ -~~	~~$ -~~
~~3.03~~	~~Install 24" CMLCSP~~	~~LF~~			~~$ -~~	~~$ -~~
~~3.04~~	~~Furnish and Install 24" Isolation Gate Valves~~	~~EA~~	~~0~~		~~$ -~~	~~$ -~~
~~3.05~~	~~Furnish and Install 2" Combination Air Relief Valves~~	~~EA~~	~~0~~	~~$ 3,400~~	~~$ 3,900~~	~~$ -~~
~~3.06~~	~~Furnish and Install 2" Blowoff Assemblies~~	~~EA~~	~~0~~	~~$ 3,225~~	~~$ 3,700~~	~~$ -~~
~~3.07~~	~~AC Paving Repair~~	~~LF~~	~~0~~	~~$ 53~~	~~$ 61~~	~~$ -~~
~~3.08~~	~~Startup Testing~~	~~LS~~	~~1~~	~~$ 10,000~~	~~$ 10,000~~	~~$ 10,000~~
~~**3.09**~~	~~**Subtotal**~~					~~**$ 11,000**~~
~~3.10~~	~~Contingency~~				~~25%~~	~~$ 3,000~~
~~**3.11**~~	~~**Subtotal with Contingency**~~					~~**$ 14,000**~~
~~3.12~~	~~Planning/Permitting~~				~~8%~~	~~$ 1,000~~
~~3.13~~	~~Design~~				~~8%~~	~~$ 1,000~~
~~3.14~~	~~Construction Management~~				~~8%~~	~~$ 1,000~~
~~**3.15**~~	~~**Total**~~					~~**$ 17,000**~~
4.	**Booster Pump Station**					
4.01	Mobilization	LS	1	$ 55,605	$ 56,000	$ 56,000
4.02	Furnish and Install Booster Pumps (150 hp)	EA	1	$ 99,910	$ 110,520	$ 110,500
4.03	Furnish and Install Site Piping and Valves	LS	1	$ 100,000	$ 100,000	$ 100,000
4.04	Electrical Power, Conduits, Wiring	LS	1	$ 504,000	$ 554,810	$ 554,800
4.05	Furnish and Install Brick Building and Foundation	SF	420	$ 719	$ 790	$ 331,800
4.06	Startup Testing	LS	1	$ 15,000	$ 15,000	$ 15,000
4.07	**Subtotal (1 pump station)**					**$ 1,168,000**
4.08	**Subtotal (2 pump stations)**	EA	0	$ 1,168,000	$ 1,168,000	**$ -**
4.09	Contingency				25%	$ 292,000
4.10	**Subtotal with Contingency**					**$ 1,460,000**
4.11	Planning/Permitting				8%	$ 117,000
4.12	Design				8%	$ 117,000
4.13	Construction Management				8%	$ 117,000

Percolation Site #3 - assuming percolation rate of 20.4 in/day (15,083 AFY Imported Water)

Item	Description	Units	Quantity	Base Unit Cost	Unit Cost	Total Cost
4.14	**Total**					**$ 1,811,000**
5.	**Pipeline - Groundwater Gravity to Inyokern**					
5.01	Mobilization	LS	1	$ 1,585,305	$ 1,585,000	$ 1,585,000
5.02	Furnish 24" CMLCSP	LF	86,100	$ 251	$ 251	$ 21,586,100
5.03	Install 24" CMLCSP	LF	86,100	$ 10.09	$ 10	$ 868,700
5.04	Furnish and Install 24" Isolation Gate Valves	EA	43	$ 65,695	$ 65,695	$ 2,828,200
5.05	Furnish and Install 2" Combination Air Relief Valves	EA	43	$ 3,400	$ 4,600	$ 198,000
5.06	Furnish and Install 2" Blowoff Assemblies	EA	43	$ 3,225	$ 4,370	$ 188,100
5.07	AC Paving Repair	LF	86,100	$ 53	$ 70	$ 6,027,000
5.08	Startup Testing	LS	1	$ 10,000	$ 10,000	$ 10,000
5.09	**Subtotal**					**$ 33,291,000**
5.10	Contingency				25%	$ 8,323,000
5.11	**Subtotal with Contingency**					**$ 41,614,000**
5.12	Planning/Permitting				8%	$ 1,000
5.13	Design				8%	$ 1,000
5.14	Construction Management				8%	$ 1,000
5.15	**Total**					**$ 41,617,000**
	GRAND TOTAL					**$ 44,255,000**

ATTACHMENT B

This Attachment summarizes the three hydrogeologic zones identified in the Indian Wells Valley (IWV) Groundwater Basin and incorporated into the model updates performed for the 2025 Periodic Evaluation. These three zones are comprised of: (1) shallow hydrogeologic zone, (2) intermediate hydrogeologic zone, and (3) deep hydrogeologic zone.

The Indian Wells Valley Groundwater Authority's (IWVGA) Technical Modeling Group (TMG) reviewed and analyzed Airborne Electromagnetic (AEM) survey data, deep well logs, and geophysical survey results (Shah et al., 2018) to delineate the lateral and vertical extent of the three hydrogeologic zones. Results are shown in four cross sections AA' through DD'. Cross section locations, deep boreholes used in this analysis, areal distribution of the clay layer, and mapped faults are shown in Figure 1.

The lateral extent of the intermediate hydrogeologic zone (deep clay layer) is shown in Figure 1. In general, the intermediate hydrogeologic zone is a confining layer, though at locations sand stringers create transmissive water-bearing sediments and can produce groundwater in significant quantities (TriEcoTt, 2013).

CROSS SECTION AA'

Cross section AA' (Figure 2) passes through 6 deep and 5 shallower wells (from west to east): BR-5, NR-2, SNORT-2, 26S39E05F01, 26S39E09G01, 26S39E10E01, 26S39E10E01, 26S39E11E01, MW02-03, TGCH-1, and TTIWV-SB06. This cross section also intercepts two faults: the Sierra Frontal Fault near the west side, and Little Lake Fault Zone near the center of the basin.

The thickness of the shallow hydrogeologic zone pinches out at both ends as shown on cross-section AA', with a maximum thickness of 460 feet logged at NR-2. The thickness also decreases in the middle at the Little Lake Fault Zone. The land surface elevation on the west side (at BR-5) is approximately 2,520 feet above mean sea level (ft amsl). The surface elevation progressively decreases (about 360 feet) to the east side of this cross section to approximately 2,163 ft amsl at TTIWV-SB06 (Figure 2). No sediment sample was collected in the top 60 feet at BR-5. Predominantly sand with some silt was logged for the remaining depth of borehole to 2,000 ft bgs in this area along the western side of the basin.

Both top and bottom of the intermediate hydrogeologic zone are well defined at three deep boreholes NR-2, SNORT-2, and TGCH-1 in the middle of the cross-section AA'. Drilled to a total depth of 473 ft bgs, bedrock was encountered at a depth of 339 ft bgs in TTIWV-SB06, defining the thickness of the intermediate hydrogeologic zone on the eastern side of the basin (cross-section AA').

CROSS SECTION BB''

Pinched out at both ends of the cross-section BB', the thickness of the shallow hydrogeologic zone varies from 252 feet at TTIWV-SB03 to 425 feet at SNORT-2 and then decreases to 340 feet at NR-1, 370 feet at BR-6 and 310 feet at TTIWV-SB01 (Figure 3). The intermediate hydrogeologic zone is shaped like a wedge in the middle of the cross-section BB' and a maximum thickness of 1,480 feet was logged at NR-1.

CROSS SECTION CC'

Both the shallow and intermediate hydrogeologic zones can be identified to the eastern end of the cross-section CC' (Figure 4). No borehole has been penetrated through the intermediate hydrogeologic zone. The bottom of the intermediate hydrogeologic zone is interpreted. For the shallow hydrogeologic zone, a maximum thickness of 166 feet is logged at MW02-03.

CROSS SECTION DD'

Both the shallow and intermediate hydrogeologic zones are well defined in the middle of the cross-section DD' (Figure 5). The thickness of the shallow hydrogeologic zone varies from 131 feet at TTIWV-SB10 to 196 feet at TGCH-1 and then decreases to 65 feet at TTBK-MW13. To the northern end, the thickness increases to 190 feet at TTIWV-MW15. Pinched out at both ends of the cross-section DD', The intermediate hydrogeologic zone is shaped like a wedge in the middle and a maximum thickness of 961 feet was logged at TGCH-1.

DISCUSSION

The shallow hydrogeologic zone contains coarse sediments near the Sierra Nevada, to the eastern and northern portions of the IWV with increased interbedded silts and clays towards the center of the IWVGB associated with the lacustrine deposits and includes China Lake's playa deposits (USBR, 1993; TriEcoTt, 2013). Groundwater occurs under unconfined conditions on top of the clay layer (TriEcoTt, 2013).

The intermediate hydrogeologic zone consists primarily of low-permeability lacustrine silts and clays, which separates the shallow hydrogeologic zone from the regional aquifer (TriEcoTt, 2013). Sand stringers within this aquifer create transmissive water-bearing zones which can produce groundwater in significant quantities.

The deep hydrogeologic zone is also composed of gravel, sand, silt and clay. It is strongly connected to the shallow aquifer in the west and southwest of the Basin; and is confined in other parts of the Basin. The best quality water is at shallow to medium depths in the southwestern part of the valley, closer to the Sierra Nevada (Dutcher et al., 1973).

For comparison, Ramboll (2019) subdivided the main IWV basin into four hydrogeologic zones (HGZ 1 through 4), where HGZ 1 and HGZ 2 are roughly equivalent to the shallow hydrogeologic zone and intermediate zone, respectively. The deep hydrogeologic zone was divided into two zones: HGZ 3 and HGZ 4. Consisting predominantly of consolidated deposits, HGZ 4 lies beneath the deep hydrogeologic zone and overlies the basement. In the El Paso management area, only two hydrogeologic zones were identified by Ramboll (2019).

References

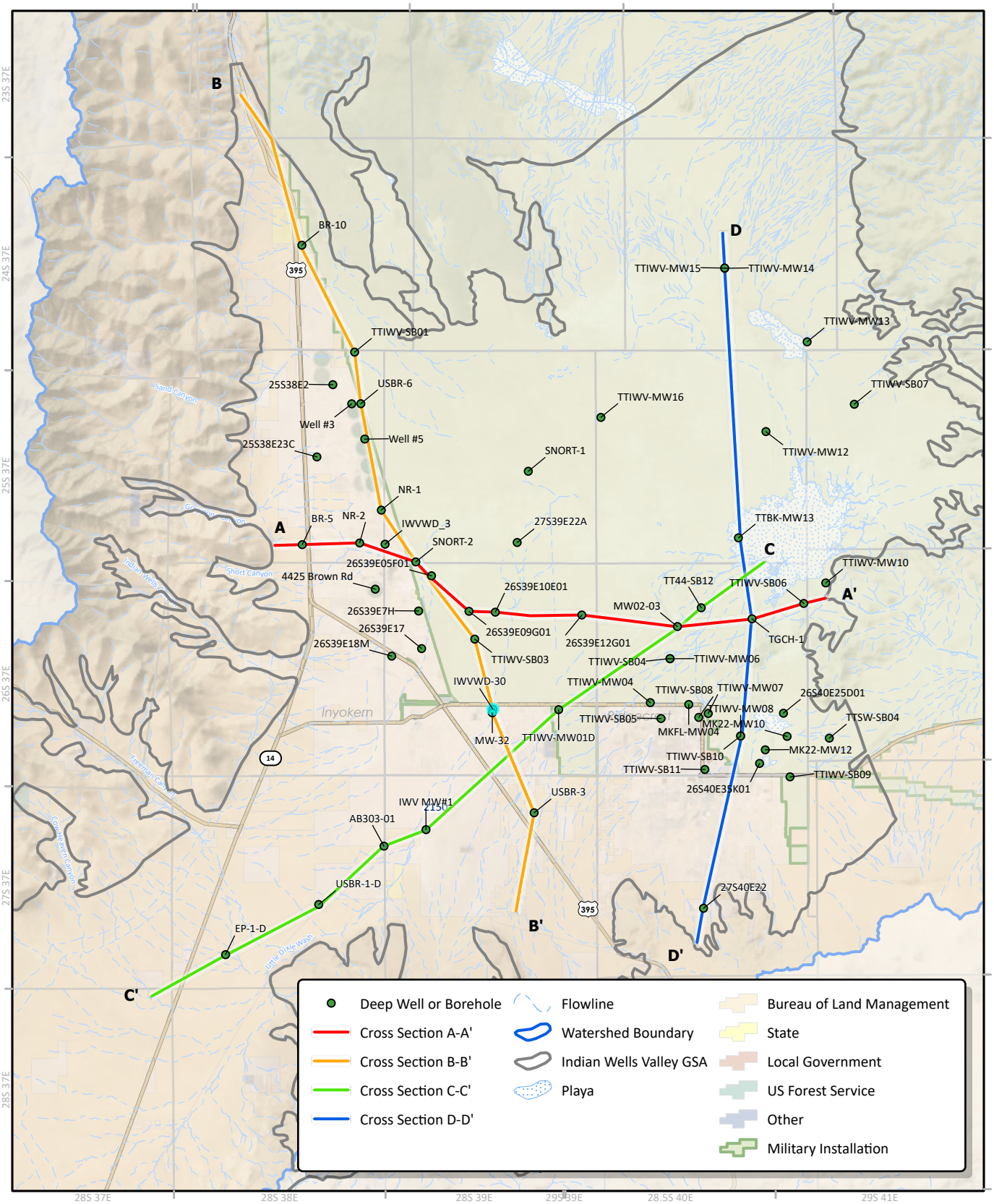
Shah, A.K, and Boyd, O.S., 2018. Depth to basement and thickness of unconsolidated sediments for the western United States—Initial estimates for layers of the U.S. Geological Survey National Crustal Model: U.S. Geological Survey Open-File Report 2018–1115, 13 p.

TriEcoTt, Joint Venture, 2013. Technical Justification for Beneficial Use Changes for Groundwater in Salt Wells Valley and Shallow Groundwater in Eastern Indian Wells Valley. Prepared for Department of the Navy, Naval Facilities Engineering Command Southwest, San Diego, California.

Ramboll, 2019, Hydrogeologic Conceptual Framework, Indian Wells Valley. Prepared for Indian Wells Valley Water District and the Brackish Groundwater Resources Study Group, Final Report, June 2019.

U.S. Bureau of Reclamation (USBR), 1993. Indian Wells Valley Groundwater Project: USBR Technical Report Volume II. A cooperative effort among the BOR, IWVWD, North American Chemical Company, and NAWS. December 1993. Prepared by USBR Lower Colorado Region.

Dutcher, L.C., and Moyle, Jr., W.R., (1973). Geologic and Hydrologic Features of the Indian Wells Valley, California. USGS Water Supply Paper 2007.



DEEP WELL AND BOREHOLE LOCATIONS
INDIAN WELLS VALLEY, CA

DRAFT
12/20/2024

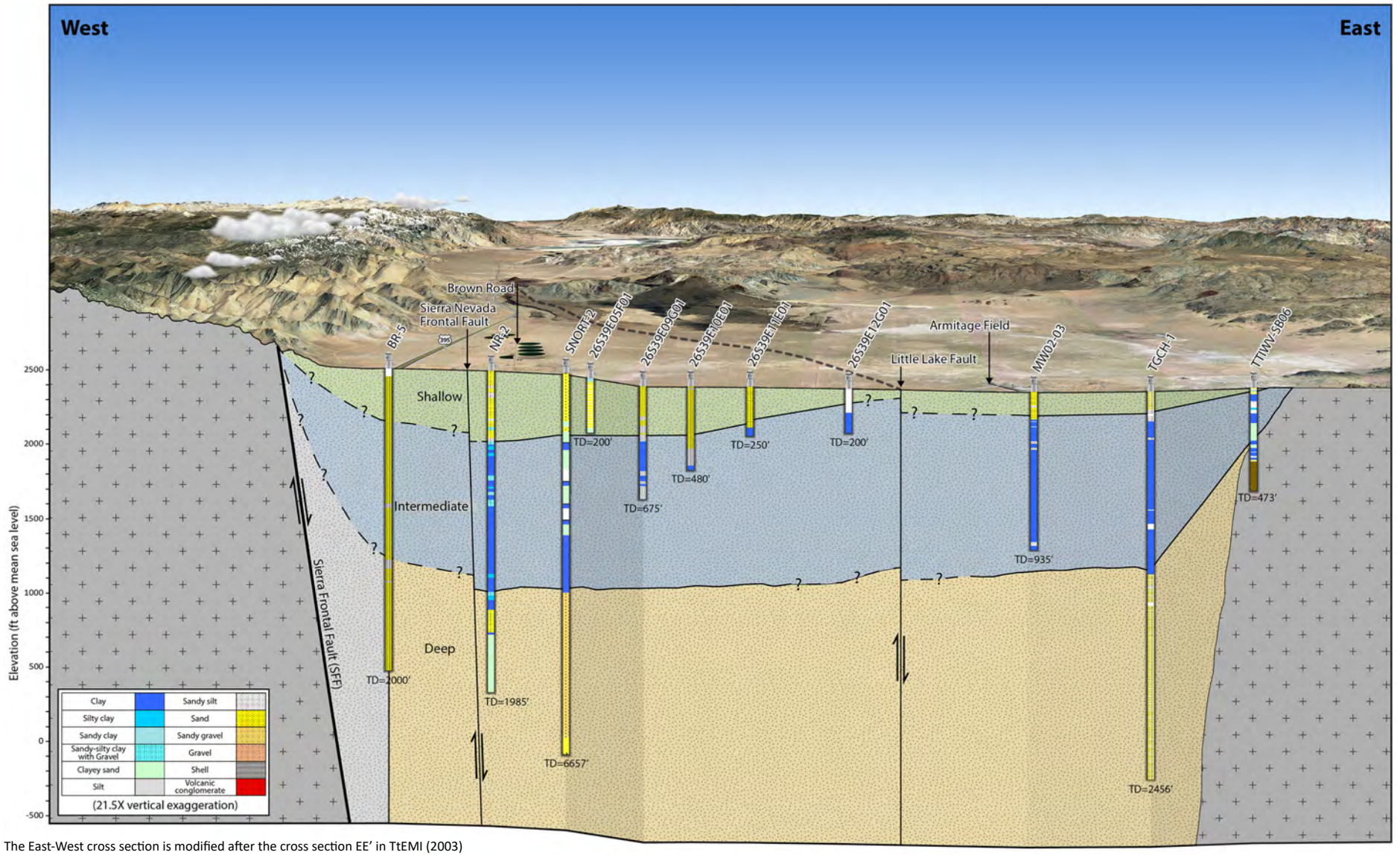
STETSON ENGINEERS INC.

N

0 2.5 5
Miles

Path: j:\jn2652\PeriodicEval2024_Appendix.aprx Layout: Appx4AFig1_DeepWellBore

Path: j:\jn2652\PeriodicEval2024_Appendix.aprx Layout: Appx4AFig2_AA'



The East-West cross section is modified after the cross section EE' in TtEMI (2003)

Reference: Tetra Tech EM, Inc, 2003. Draft Basinwide Hydrogeologic Characterization Summary Report, NAWS China Lake, California. Prepared under CLEAN II Contract for Department of the Navy.

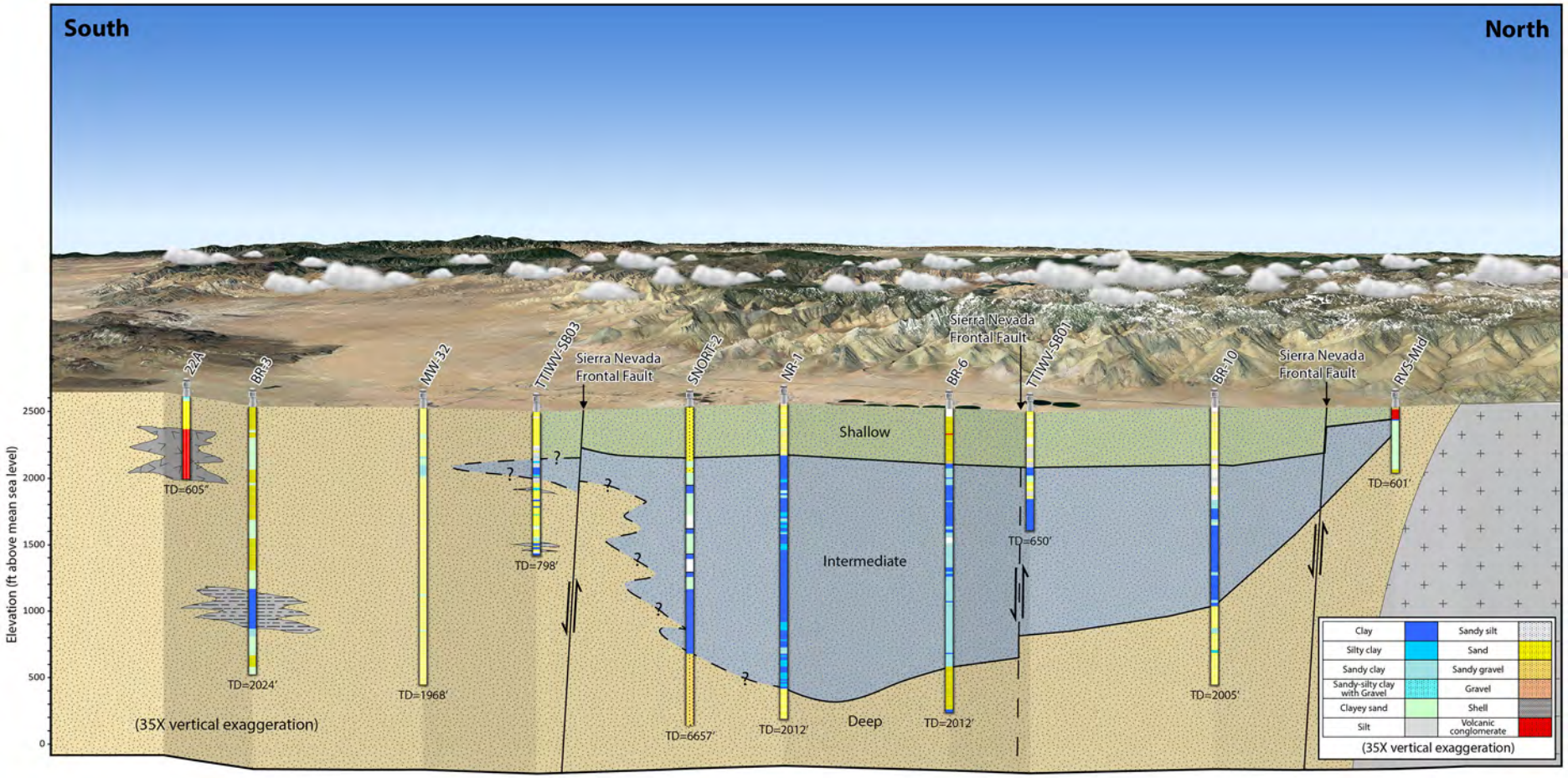
STETSON ENGINEERS INC.

GEOLOGIC CROSS SECTION AA'

INDIAN WELLS VALLEY, CA

DRAFT
12/20/2024

FIGURE 2



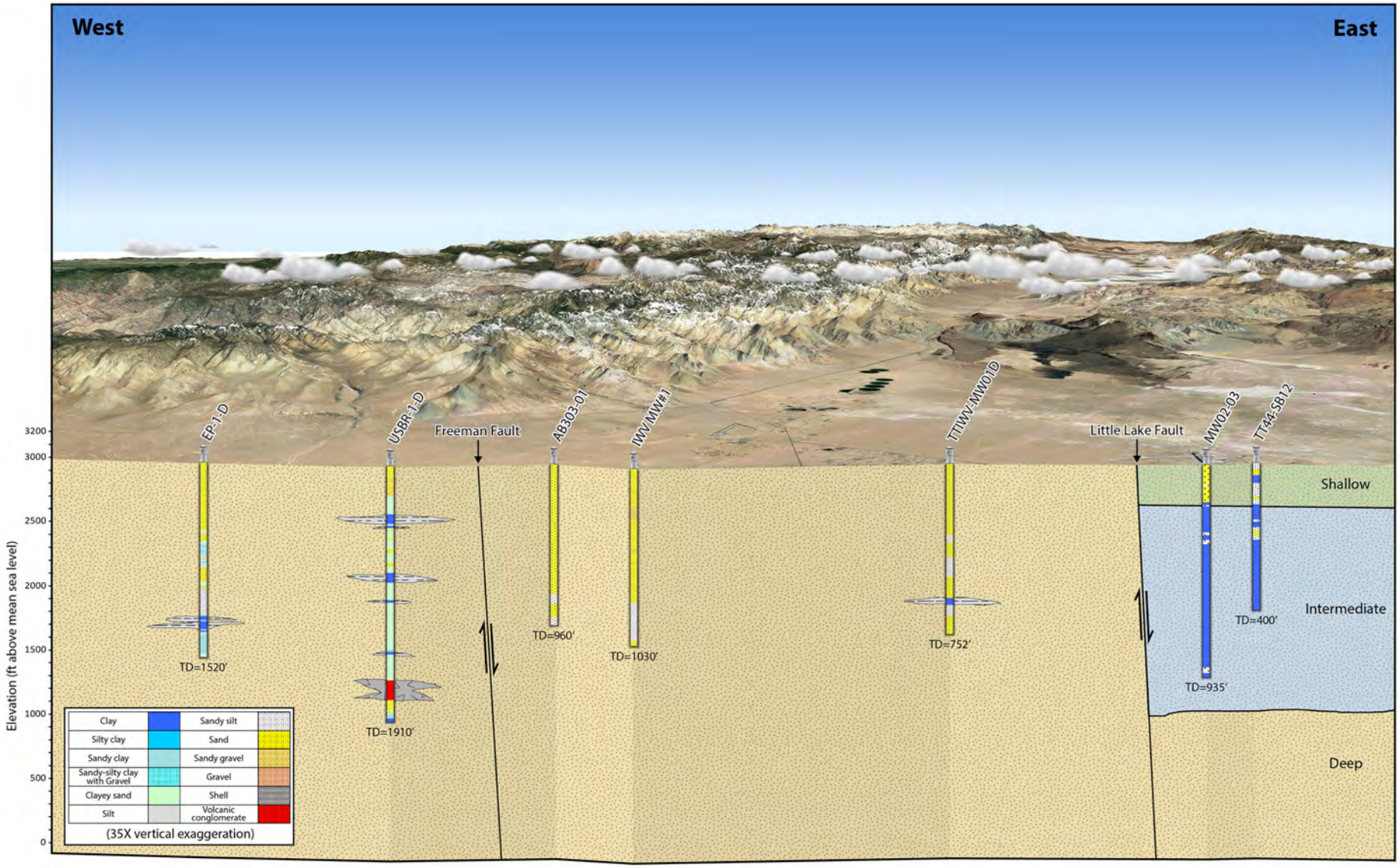
STETSON ENGINEERS INC.

GEOLOGIC CROSS SECTION BB'
INDIAN WELLS VALLEY, CA

DRAFT
12/20/2024

FIGURE 3

Path: j:\jn2652\PeriodicEval2024_Appendix.aprx Layout: Appx4AFig4_CC'



STETSON ENGINEERS INC.

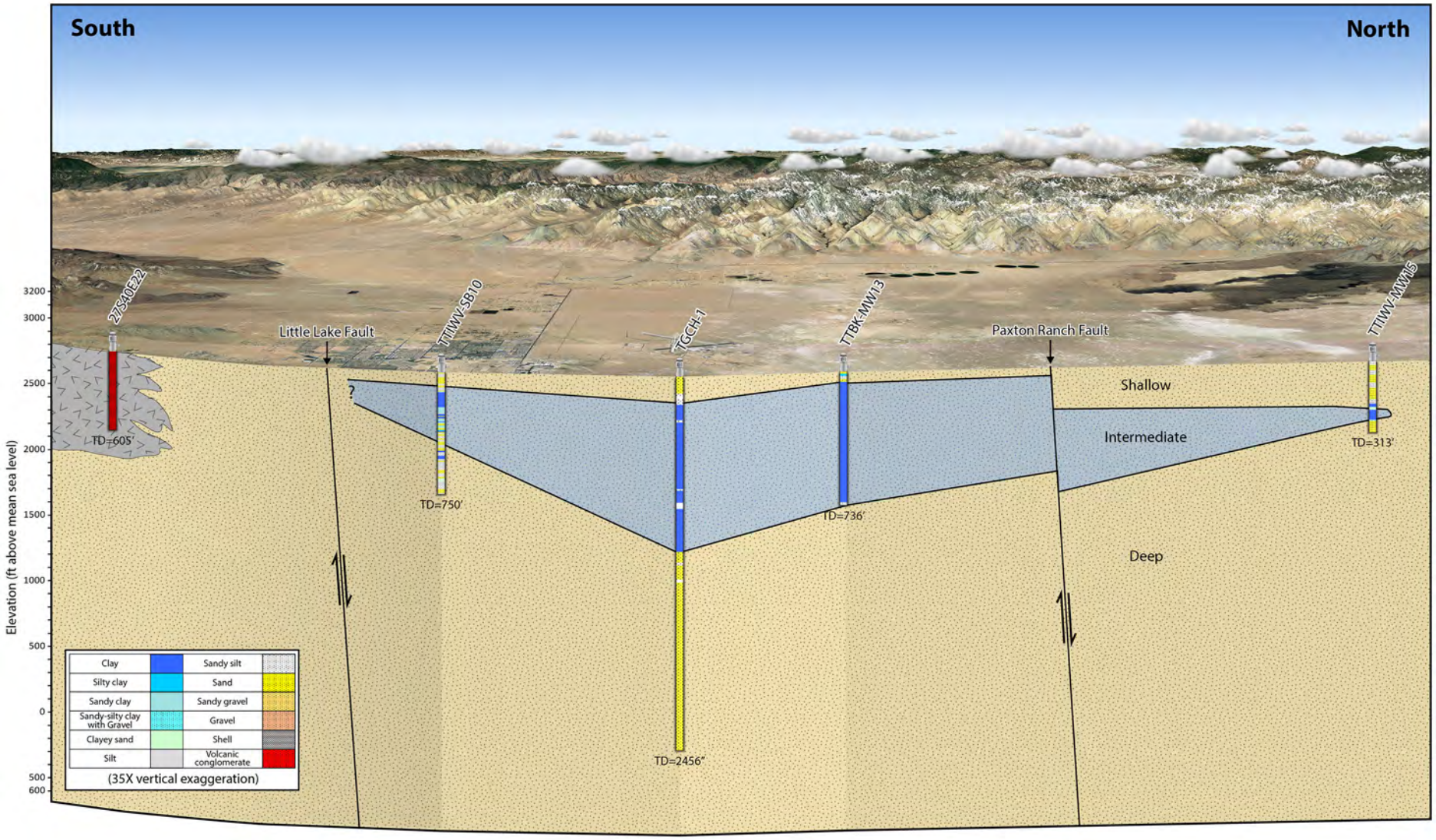
GEOLOGIC CROSS SECTION CC'

INDIAN WELLS VALLEY, CA

DRAFT
12/20/2024

FIGURE 4

Path: j:\jn2652\PeriodicEval2024_Appendix.aprx Layout: Appx4AFig5_DD'



STETSON ENGINEERS INC.

GEOLOGIC CROSS SECTION DD'
INDIAN WELLS VALLEY, CA

DRAFT
12/20/2024

FIGURE 5

ATTACHMENT C

FIELD DATA: Aquifer Properties												
137		107	107			70	70	79	79	61		
	Other	UTM - NAD83 - Zone 11				Specific	Specific					
Well Name	Name	Easting	Northing	Test Type	Screen Interval	Capacity	Capacity	T	T	K	Source	Notes
					(ft bgs)	(gpm/ft)	(m^2/day)	(m^2/day)	(ft^2/day)	(ft/day)		
BR-5 deep	n/a	421152.7	3953022.4	Slug Testing	1960-1980	n/a	n/a	n/a	n/a	13.04	TetraTech Report	2
BR-5 medium	n/a	421152.7	3953022.4	Slug Testing	1590-1610	n/a	n/a	n/a	n/a	10.77	TetraTech Report	2
BR-5 shallow	n/a	421152.7	3953022.4	Slug Testing	850-870	n/a	n/a	n/a	n/a	16.44	TetraTech Report	2
BR-10 deep	n/a	421199.0	3966702.2	Slug Testing	1930-1950	n/a	n/a	n/a	n/a	6.52	TetraTech Report	2
BR-10 med deep	n/a	421199.0	3966702.2	Slug Testing	1560-1580	n/a	n/a	n/a	n/a	10.20	TetraTech Report	2
BR-10 med shlw	n/a	421199.0	3966702.2	Slug Testing	1180-1200	n/a	n/a	n/a	n/a	1.45	TetraTech Report	2
BR-10 shallow	n/a	421199.0	3966702.2	Slug Testing	640-660	n/a	n/a	n/a	n/a	13.61	TetraTech Report	2
BR-1 deep	n/a	421986.7	3937048.2	Slug Testing	1750-1770	n/a	n/a	n/a	n/a	0.28	TetraTech Report	2
BR-1 med deep	n/a	421986.7	3937048.2	Slug Testing	1500-1520	n/a	n/a	n/a	n/a	0.71	TetraTech Report	2
BR-1 med shlw	n/a	421986.7	3937048.2	Slug Testing	1040-1060	n/a	n/a	n/a	n/a	17.29	TetraTech Report	2
BR-1 shallow	n/a	421986.7	3937048.2	Slug Testing	615-635	n/a	n/a	n/a	n/a	15.02	TetraTech Report	2
NR-2 deep	n/a	421986.7	3937048.2	Slug Testing	1910-1930	n/a	n/a	n/a	n/a	8.50	TetraTech Report	2
NR-2 medium	n/a	421986.7	3937048.2	Slug Testing	1540-1560	n/a	n/a	n/a	n/a	10.20	TetraTech Report	2
NR-2 shallow	n/a	421986.7	3937048.2	Slug Testing	330-350	n/a	n/a	n/a	n/a	34.02	TetraTech Report	2
BR-2 deep	n/a	422266.6	3942444.5	Slug Testing	1940-1960	n/a	n/a	n/a	n/a	1.16	TetraTech Report	2
BR-2 medium	n/a	422266.6	3942444.5	Slug Testing	1460-1480	n/a	n/a	n/a	n/a	13.61	TetraTech Report	2
BR-2 shallow	n/a	422266.6	3942444.5	Slug Testing	620-640	n/a	n/a	n/a	n/a	0.71	TetraTech Report	2
BR-6 deep	n/a	423998.4	3959176.6	Slug Testing	1400-1420	n/a	n/a	n/a	n/a	14.46	TetraTech Report	2
BR-6 medium	n/a	423998.4	3959176.6	Slug Testing	1190-1910	n/a	n/a	n/a	n/a	18.14	TetraTech Report	2
NR-1 deep	n/a	424803.1	3954348.6	Slug Testing	1960-1980	n/a	n/a	n/a	n/a	3.69	TetraTech Report	2
26S39E19P01	n/a	425494.5	3945924.8	Spec. Cap. Testing	unk	358	6402	5432	9810	n/a	kunkel_chase_1969	
26S39E19P01	n/a	425494.5	3945924.8	Spec. Cap. Testing	unk	296	5294	4782	7989	n/a	kunkel_chase_1969	
26S39E30C01	n/a	425494.5	3945522.5	Spec. Cap. Testing	unk	35	626	1144	796	n/a	kunkel_chase_1969	
26S39E30C01	n/a	425494.5	3945522.5	Spec. Cap. Testing	unk	55	984	1548	1297	n/a	kunkel_chase_1969	
26S39E30F01	n/a	425607.7	3945094.9	Spec. Cap. Testing	unk	81	1449	2007	1971	n/a	kunkel_chase_1969	
26S39E19Q01	n/a	426010.1	3945899.6	Spec. Cap. Testing	unk	58	1037	1604	1374	n/a	kunkel_chase_1969	
26S39E19Q01	n/a	426010.1	3945899.6	Spec. Cap. Testing	unk	105	1878	2388	2608	n/a	kunkel_chase_1969	
26S39E19Q01	n/a	426010.1	3945899.6	Spec. Cap. Testing	unk	84	1502	2056	2050	n/a	kunkel_chase_1969	
26S39E19Q01	n/a	426010.1	3945899.6	Spec. Cap. Testing	unk	99	1770	2296	2448	n/a	kunkel_chase_1969	
27S39E08L01	Well-18	427047.5	3939865.3	Spec. Cap. Testing	unk	86	1533	2084	2095	n/a	Borehole Test Data USBR 1993 Study	2
27S39E08L01	Well-18	427047.5	3939865.3	Spec. Cap. Testing	unk	87	1563	2112	2139	n/a	Borehole Test Data USBR 1993 Study	2
27S39E08L01	Well-18	427047.5	3939865.3	Spec. Cap. Testing	unk	91	1624	2166	2229	n/a	Borehole Test Data USBR 1993 Study	2
27S39E08L01	Well-18	427047.5	3939865.3	Spec. Cap. Testing	unk	97	1738	2268	2400	n/a	Borehole Test Data USBR 1993 Study	2
27S39E08L02	Well-33	427322.3	3939858.9	Spec. Cap. Testing	unk	49	874	1431	1142	n/a	Borehole Test Data USBR 1993 Study	2
27S39E08L02	Well-32	427322.3	3939858.9	Spec. Cap. Testing	unk	59	1055	1623	1400	n/a	Borehole Test Data USBR 1993 Study	2
27S39E08L02	Well-32	427322.3	3939858.9	Spec. Cap. Testing	unk	55	982	1547	1295	n/a	Borehole Test Data USBR 1993 Study	2
27S39E08L02	Well-32	427322.3	3939858.9	Spec. Cap. Testing	unk	57	1027	1593	1359	n/a	Borehole Test Data USBR 1993 Study	2
27S39E08A	Well-34	427763.2	3940635.3	Spec. Cap. Testing	unk	25	441	904	545	n/a	Borehole Test Data USBR 1993 Study	2
26S39E28R	Well-31	429386.1	3944148.5	Spec. Cap. Testing	unk	28	509	996	637	n/a	Borehole Test Data USBR 1993 Study	2
26S39E28R	Well-31	429386.1	3944148.5	Spec. Cap. Testing	unk	62	1100	1669	1464	n/a	Borehole Test Data USBR 1993 Study	2
26S39E28R	Well-31	429386.1	3944148.5	Spec. Cap. Testing	unk	61	1084	1652	1441	n/a	Borehole Test Data USBR 1993 Study	2
26S39E28R	Well-31	429386.1	3944148.5	Spec. Cap. Testing	unk	58	1030	1597	1364	n/a	Borehole Test Data USBR 1993 Study	2
26S39E28R	Well-31	429386.1	3944148.5	Spec. Cap. Testing	unk	63	1127	1696	1502	n/a	Borehole Test Data USBR 1993 Study	2
26S39E28R	Well-31	429386.1	3944148.5	Spec. Cap. Testing	unk	63	1120	1689	1492	n/a	Borehole Test Data USBR 1993 Study	2
26S39E28R	Well-31	429386.1	3944148.5	Spec. Cap. Testing	unk	61	1098	1667	1461	n/a	Borehole Test Data USBR 1993 Study	2
25S39E04R01	n/a	429570.9	3960483.8	Spec. Cap. Testing	unk	73	1306	1872	1761	n/a	kunkel_chase_1969	

Well Name	Other Name	UTM - NAD83 - Zone 11 Easting	Northing	Test Type	Screen Interval	Specific Capacity	Specific Capacity	T	T	K	Source	Notes
					(ft bgs)	(gpm/ft)	(m^2/day)	(m^2/day)	(ft^2/day)	(ft/day)		
MW-32 deep	n/a	429760.4	3945247.6	Slug Testing	1900-1920	n/a	n/a	n/a	n/a	7.94	TetraTech Report	
MW-32 med deep	n/a	429760.4	3945247.6	Slug Testing	1240-1260	n/a	n/a	n/a	n/a	16.44	TetraTech Report	
MW-32 med shlw	n/a	429760.4	3945247.6	Slug Testing	880-900	n/a	n/a	n/a	n/a	22.39	TetraTech Report	
26S39E27D01	Well-30	429942.2	3945344.2	Spec. Cap. Testing	unk	50	894	1453	1170	n/a	Borehole Test Data USBR 1993 Study	2
BR-3 deep	n/a	431560.9	3940643.0	Slug Testing	1850-1870	n/a	n/a	n/a	n/a	0.43	TetraTech Report	
BR-3 shallow	n/a	431560.9	3940643.0	Slug Testing	650-670	n/a	n/a	n/a	n/a	4.25	TetraTech Report	
25S39E35N01	n/a	431625.4	3952301.0	Spec. Cap. Testing	unk	21	376	812	459	n/a	kunkel_chase_1969	
26S39E11E01	n/a	431642.8	3949922.9	Spec. Cap. Testing	unk	33	590	1100	747	n/a	kunkel_chase_1969	
26S39E26	Well-17	432411.6	3945560.7	Spec. Cap. Testing	unk	39	703	1237	903	n/a	Borehole Test Data USBR 1993 Study	2
26S39E26	Well-17	432411.6	3945560.7	Spec. Cap. Testing	unk	61	1098	1667	1461	n/a	Borehole Test Data USBR 1993 Study	2
26S39E26	Well-17	432411.6	3945560.7	Spec. Cap. Testing	unk	60	1068	1636	1418	n/a	Borehole Test Data USBR 1993 Study	2
26S39E26	Well-17	432411.6	3945560.7	Spec. Cap. Testing	unk	64	1150	1719	1536	n/a	Borehole Test Data USBR 1993 Study	2
BR-4	n/a	432728.7	3945348.0	Slug Testing	1190-1200	n/a	n/a	n/a	n/a	39.69	TetraTech Report	
26S39E25E01	n/a	433050.1	3945001.4	Spec. Cap. Testing	unk	46	823	1374	1070	n/a	kunkel_chase_1969	
26S39E25E01	n/a	433050.1	3945001.4	Spec. Cap. Testing	unk	46	823	1374	1070	n/a	kunkel_chase_1969	
26S39E25E01	n/a	433050.1	3945001.4	Spec. Cap. Testing	unk	38	680	1209	870	n/a	kunkel_chase_1969	
26S39E25D02	n/a	433252.1	3945497.2	Spec. Cap. Testing	unk	45	805	1354	1045	n/a	kunkel_chase_1969	
26S39E25D02	n/a	433252.1	3945497.2	Spec. Cap. Testing	unk	34	608	1122	772	n/a	kunkel_chase_1969	
26S39E24K01	n/a	434056.8	3946301.9	Spec. Cap. Testing	unk	143	2557	2937	3641	n/a	kunkel_chase_1969	
26S39E24K01	n/a	434056.8	3946301.9	Spec. Cap. Testing	unk	28	501	985	626	n/a	kunkel_chase_1969	
26S39E24Q01	n/a	434056.8	3945899.6	Spec. Cap. Testing	unk	28	501	985	626	n/a	kunkel_chase_1969	
25S39E12R01	Well-22	434441.8	3958738.4	Spec. Cap. Testing	unk	37	662	1187	846	n/a	kunkel_chase_1969	
26S39E24R01	n/a	434459.1	3945899.6	Spec. Cap. Testing	unk	41	733	1272	945	n/a	kunkel_chase_1969	
26S39E24R01	n/a	434459.1	3945899.6	Spec. Cap. Testing	unk	28	501	985	626	n/a	kunkel_chase_1969	
26S39E24R01	n/a	434459.1	3945899.6	Spec. Cap. Testing	unk	13	225	577	264	n/a	kunkel_chase_1969	
26S40E19N01	n/a	434794.2	3945790.8	Spec. Cap. Testing	unk	14	250	619	296	n/a	kunkel_chase_1969	
26S40E19P01	n/a	435267.7	3945839.6	Spec. Cap. Testing	unk	18	322	733	388	n/a	kunkel_chase_1969	
26S40E30C	Well-9A	435432.6	3944419.4	Spec. Cap. Testing	unk	42	753	1295	972	n/a	Borehole Test Data USBR 1993 Study	2
26S40E30C	Well-9A	435432.6	3944419.4	Spec. Cap. Testing	unk	44	782	1327	1012	n/a	Borehole Test Data USBR 1993 Study	2
26S40E30C	Well-9A	435432.6	3944419.4	Spec. Cap. Testing	unk	46	821	1372	1067	n/a	Borehole Test Data USBR 1993 Study	2
26S40E30K01	Well-10	435543.2	3944587.4	Spec. Cap. Testing	unk	42	753	1295	972	n/a	Borehole Test Data USBR 1993 Study	2
26S40E30K01	Well-10	435543.2	3944587.4	Spec. Cap. Testing	unk	41	733	1272	945	n/a	Borehole Test Data USBR 1993 Study	2
26S40E30K01	Well-10	435543.2	3944587.4	Spec. Cap. Testing	unk	41	737	1276	950	n/a	Borehole Test Data USBR 1993 Study	2
26S40E20N01	n/a	436479.6	3945839.6	Spec. Cap. Testing	unk	10	179	494	206	n/a	kunkel_chase_1969	
26S40E32K	Well-11	437063.6	3942939.0	Spec. Cap. Testing	unk	25	449	915	556	n/a	Borehole Test Data USBR 1993 Study	2
26S40E32K	Well-11	437063.6	3942939.0	Spec. Cap. Testing	unk	25	452	920	561	n/a	Borehole Test Data USBR 1993 Study	2
26S40E32K	Well-11	437063.6	3942939.0	Spec. Cap. Testing	unk	27	474	949	590	n/a	Borehole Test Data USBR 1993 Study	2
26S40E32G	Well-13	437068.6	3943457.8	Spec. Cap. Testing	unk	13	239	599	281	n/a	Borehole Test Data USBR 1993 Study	2
26S40E32G	Well-13	437068.6	3943457.8	Spec. Cap. Testing	unk	17	308	711	370	n/a	Borehole Test Data USBR 1993 Study	2
26S40E32G	Well-13	437068.6	3943457.8	Spec. Cap. Testing	unk	16	293	688	351	n/a	Borehole Test Data USBR 1993 Study	2
26S40E32G	Well-13	437068.6	3943457.8	Spec. Cap. Testing	unk	16	284	674	340	n/a	Borehole Test Data USBR 1993 Study	2
27S40E04L01	n/a	438356.2	3941574.2	Spec. Cap. Testing	unk	47	841	1394	1095	n/a	kunkel_chase_1969	
27S40E04L01	n/a	438356.2	3941574.2	Spec. Cap. Testing	unk	38	680	1209	870	n/a	kunkel_chase_1969	
26S40E33A01	n/a	439176.9	3943988.0	Spec. Cap. Testing	unk	16	286	677	342	n/a	kunkel_chase_1969	
26S40E33A01	n/a	439176.9	3943988.0	Spec. Cap. Testing	unk	31	554	1055	698	n/a	kunkel_chase_1969	
26S40E34N01	n/a	439622.2	3942781.0	Spec. Cap. Testing	unk	47	841	1394	1095	n/a	kunkel_chase_1969	
JMM31-MW01	n/a	439788.0	3944826.0	Spec. Cap. Testing	unk	n/a	n/a	n/a	n/a	11.00	TetraTech Beneficial Use	
JMM31-MW01	n/a	439788.0	3944826.0	unk	33-48	n/a	n/a	n/a	n/a	11.06	TetraTech Report	

Well Name	Other Name	UTM - NAD83 - Zone 11 Easting	Northing	Test Type	Screen Interval	Specific Capacity	Specific Capacity	T	T	K	Source	Notes
					(ft bgs)	(gpm/ft)	(m^2/day)	(m^2/day)	(ft^2/day)	(ft/day)		
26S40E34P	Well-19 abn	440073.4	3942641.5	Spec. Cap. Testing	unk	19	345	768	419	n/a	Borehole Test Data USBR 1993 Study	
26S40E34P	Well-19 abn	440073.4	3942641.5	Spec. Cap. Testing	unk	21	379	817	463	n/a	Borehole Test Data USBR 1993 Study	
26S40E22P01	n/a	440079.0	3945839.6	Spec. Cap. Testing	unk	1	14	91	13	n/a	kunkel_chase_1969	
MK69-MW01	n/a	440121.7	3945079.4	Spec. Cap. Testing	unk	n/a	n/a	n/a	n/a	4.00	TetraTech Beneficial Use	
MK69-MW01	n/a	440121.7	3945079.4	unk	92-102	n/a	n/a	n/a	n/a	2.83	TetraTech Report	
26S40E22P4	n/a	440215.0	3946364.0	Aquifer Test	200-215	n/a	n/a	65.03	700	46.67	1996 Houghton / Stoner Aquifer Testing	1
TTIWV-MW14	n/a	440595.3	3965460.4	Slug Testing	Unknown	n/a	n/a	n/a	n/a	14.20	TetraTech Beneficial Use	
26S40E35H2	n/a	441772.0	3943079.0	Aquifer Test	340-480	n/a	n/a	51.38	553	3.95	1996 Houghton / Stoner Aquifer Testing	1
26S40E23D1	n/a	441809.0	3946342.0	Aquifer Test	385-400	n/a	n/a	0.17	1.87	0.12	1996 Houghton / Stoner Aquifer Testing	1
TTIWV-MW12	n/a	442406.6	3957977.8	Slug Testing	unk	n/a	n/a	n/a	n/a	65.20	TetraTech Beneficial Use	
26S40E36A01	n/a	444022.1	3943831.9	Spec. Cap. Testing	unk	12	215	558	251	n/a	kunkel_chase_1969	
TTIWV-MW13	n/a	444332.1	3962059.8	Slug Testing	unk	n/a	n/a	n/a	n/a	2.83	TetraTech Beneficial Use	
TTIWV-MW09	n/a	445071.2	3951044.1	Slug Testing	unk	n/a	n/a	n/a	n/a	2.44	TetraTech Beneficial Use	
26S39E15J1	n/a	unk	unk	Aquifer Test	unk	n/a	n/a	243.87	2625	n/a	1996 Houghton / Stoner Aquifer Testing	
26S40E13A1	n/a	unk	unk	Aquifer Test	unk	n/a	n/a	15.42	166	n/a	1996 Houghton / Stoner Aquifer Testing	
26S40E13Q1	n/a	unk	unk	Aquifer Test	unk	n/a	n/a	51.28	552	n/a	1996 Houghton / Stoner Aquifer Testing	
26S40E14A1	n/a	unk	unk	Aquifer Test	unk	n/a	n/a	54.16	583	n/a	1996 Houghton / Stoner Aquifer Testing	
26S40E17Q1	n/a	unk	unk	Aquifer Test	unk	n/a	n/a	27.87	300	n/a	1996 Houghton / Stoner Aquifer Testing	
26S40E23B2	n/a	unk	unk	Aquifer Test	unk	n/a	n/a	14.21	153	n/a	1996 Houghton / Stoner Aquifer Testing	
JMM01-MW03	n/a	unk	unk	unk	33-48	n/a	n/a	n/a	n/a	2.01	TetraTech Report	
JMM01-MW04	n/a	unk	unk	unk	33-48	n/a	n/a	n/a	n/a	0.74	TetraTech Report	
JMM01-MW05	n/a	unk	unk	unk	34-49	n/a	n/a	n/a	n/a	1.81	TetraTech Report	
JMM01-MW06	n/a	unk	unk	unk	34-49	n/a	n/a	n/a	n/a	0.51	TetraTech Report	
MK69-SB01	n/a	unk	unk	unk	unk	n/a	n/a	n/a	n/a	0.94	TetraTech Beneficial Use	
MK70-SB02	n/a	unk	unk	unk	unk	n/a	n/a	n/a	n/a	0.028	TetraTech Beneficial Use	
MK72-SB02	n/a	unk	unk	unk	unk	n/a	n/a	n/a	n/a	0.013	TetraTech Beneficial Use	
MKFL-SB01	n/a	unk	unk	unk	unk	n/a	n/a	n/a	n/a	0.050	TetraTech Beneficial Use	
TT07-MW01	n/a	unk	unk	Slug Testing	unk	n/a	n/a	n/a	n/a	2.17	TetraTech Beneficial Use	
TT07-MW02	n/a	unk	unk	Slug Testing	unk	n/a	n/a	n/a	n/a	34.60	TetraTech Beneficial Use	
TT07-SB01	n/a	unk	unk	unk	unk	n/a	n/a	n/a	n/a	0.0002	TetraTech Beneficial Use	
TT07-SB03	n/a	unk	unk	unk	unk	n/a	n/a	n/a	n/a	0.0001	TetraTech Beneficial Use	
TT07-SB04	n/a	unk	unk	unk	unk	n/a	n/a	n/a	n/a	0.0017	TetraTech Beneficial Use	
TT07-SB06	n/a	unk	unk	unk	unk	n/a	n/a	n/a	n/a	0.52	TetraTech Beneficial Use	
TT07-SB11	n/a	unk	unk	unk	unk	n/a	n/a	n/a	n/a	0.000004	TetraTech Beneficial Use	
TT33-MW01	n/a	unk	unk	Slug Testing	unk	n/a	n/a	n/a	n/a	7.34	TetraTech Beneficial Use	
TT33-SB01	n/a	unk	unk	unk	unk	n/a	n/a	n/a	n/a	0.021	TetraTech Beneficial Use	
TT33-SB03	n/a	unk	unk	unk	unk	n/a	n/a	n/a	n/a	0.001	TetraTech Beneficial Use	
TT70-MW01	n/a	unk	unk	Slug Testing	unk	n/a	n/a	n/a	n/a	1.64	TetraTech Beneficial Use	
TT70-MW02	n/a	unk	unk	Slug Testing	unk	n/a	n/a	n/a	n/a	2.39	TetraTech Beneficial Use	
TT71-MW01	n/a	unk	unk	Slug Testing	unk	n/a	n/a	n/a	n/a	3.01	TetraTech Beneficial Use	
TT71-SB02	n/a	unk	unk	unk	unk	n/a	n/a	n/a	n/a	0.52	TetraTech Beneficial Use	
TT71-SB02	n/a	unk	unk	unk	unk	n/a	n/a	n/a	n/a	0.006	TetraTech Beneficial Use	
TT71-SB05	n/a	unk	unk	unk	unk	n/a	n/a	n/a	n/a	0.057	TetraTech Beneficial Use	

SUMMARY

Count	Test Type
36	Slug Testing
72	Spec. Cap. Testing
20	unk
9	Aquifer Test
137	

Count	Data Source
32	TetraTech Report
34	kunkel_chase_1969
36	Borehole Test Data USBR 1993 Study
26	TetraTech Beneficial Use
9	1996 Houghton / Stoner Aquifer Testing
137	

NOTES

1 Exact location not known; used center of section

2 The U.S. Bureau of Reclamation (USBR) reported transmissivities using the Cooper method, with the aquifer thickness assumed to be the same as the screen length. Aquifer thickness is typically much greater, resulting in low transmissivity estimates. USBR hydraulic conductivity values were backcalculated for this table by dividing transmissivity by screen length. Five of the wells slug tested during the USBR study had anomalously low results. The authors of the study deemed these results nonrepresentative, probably due to inadequate well development. The five wells are: BR-3 (medium), BR-6 (shallow), BR-10 (shallow/medium), NR-1 (shallow), and MW-31 (shallow).

ATTACHMENT D

This Attachment provides a summary of aquifer testing conducted at monitoring and production wells located in Indian wells Valley.

Pumping Tests

Three groups of pumping test data have been collected and reviewed:

- IWVWD-18 (Krieger & Stewart, 1989)
- Ten wells in the eastern and central portions of the basin (Houghton, 1996)
- IWVWD-10 and Quist Ranch Tests (DRI, 2020)

In 1989, Indian Wells Valley Water District (IWVWD) installed one test well (27S39E08M04M, IWVWD-18) and three monitoring wells (IWV MW-01, IWV MW-02 and IWV MW-03) to determine aquifer characteristics (Krieger & Stewart, 1989). These two monitoring wells along with the Inyo well were used to monitor water levels during a 24-hour constant rate pumping test at IWVWD-18. The pumping rate was approximately 3,000 gpm. Test results are summarized in Table 1. In average, the transmissivity is approximately 310,167 gpd/ft or 41,466 ft^2/day. Storativity is averaged to be 0.00035. Considering the perforation length of 440 feet in IWVWD-18, calculated hydraulic conductivity value is 94.24 feet/day and specific storage (S_s) is $7.95E^{-7}$ ft^{-1}.

Table 1 Pumping Test Results at IWVWD-18 (Krieger & Stewart, 1989)

Transmissivity (gpd/ft)	Storativity (-)	Method
293,000		Theis (1935) Time-Drawdown
293,000		Theis (1935) Time-Recovery
368,000	0.0003	Drawdown, Non-Leaky aquifer
287,000	0.0003	Drawdown, Leaky Aquifer
360,000	0.0004	Recovery, non-leaky aquifer
260,000	0.0004	Recovery, leaky aquifer

Pumping tests reported by Houghton (1996) were performed on ten wells located in the eastern and central portions of the Indian Wells Valley groundwater basin. These results are summarized in Table 2. Tests were conducted for a minimum of 12 hours, except at 26S/40E-23D1. It's suggested that the low transmissivity value at this well may be the result of a plugged gravel pack or well screen (Houghton, 1996). Thus, this low T value at well 26S/40E-23D1 was not considered representative of the aquifer property in this area. Since the screen setting at 26S/40E-13A1, 13Q1 and 14A1 is unknow, aquifer thickness in Table 2 is assumed and represents the interval between the static water level and a depth of

100 feet for all three wells. Screen intervals were used for aquifer thickness for calculating T at the other seven (7) well locations.

Table 2 Pumping Test Results at Ten Monitoring Wells (Houghton, 1996)

State ID	Well Depth (ft)	Depth to Top of Screen (ft)	Depth to Bottom of Screen (ft)	Depth to Water (ft)	T (ft^2/day)	Aquifer Thickness (ft)	K (ft/day)
26S/39E-11E02	190	135	191	124.4	14,000	56	250
26S/39E-15J	720	600	700	196.4	2,625	100	26.25
26S/40E-13A1	<100			22.75	166.7	77*	2.16
26S/40E-13Q1	<100			33.05	552.6	67*	8.25
26S/40E-14A1	<100			9.9	583.3	90*	6.48
26S/40E-17Q2	450	370	430	141.45	300	60	5
26S/40E-22P4	215	200	215	113.1	700	15	46.67
26S/40E-23B2	220	180	220	31.4	153.1	40	3.83
26S/40E-23D1	400	385	400	39.7	1.87	15	0.12
26S/40E-35H2	500	340	480	90.8	553	140	3.95

DWR Prop 1 funding was used to address this data gap, and three aquifer tests were conducted to better characterize the hydrogeologic properties of an unconfined basin-fill aquifer in Indian Wells Valley (DRI, 2020). These three tests are summarized below:

- IWVWD-10 was pump tested at a flow rate of 1,109±10.7 gpm for a total of 100.6 hours. Pumping test results are summarized in Table 3.
- A constant rate pumping test was conducted at 26S39E35G01. The flow rate was 285 gpm and test duration was 21 hours. Results are summarized in Table 4.
- Well 26S39E35G02 was pump tested at a constant rate of 285 gpm for 48 hours. A saturated aquifer thickness of 225 feet is assumed. Results are summarized in Table 5.

Table 3 Pumping Test Results at IWVWD-10 (26S40E30K03, DRI, 2020)

T (gpd/ft)	K (ft/day)	Storativity (-)	Method
58,750	13.83	0.00313	Theis (1935) Distance-drawdown (24 hours)
62,530	14.72	0.00537	Theis (1935) Distance-drawdown (4 days)
83,866	19.74	0.00057	Cooper and Jacob (1946) Time Drawdown (Well 9A)
88,054	20.73	0.00099	Cooper and Jacob (1946) Time Drawdown (Well 8)
79,551	18.73	0.00045	Cooper and Jacob (1946) Time Recovery (Well 9A)
82,429	19.4	0.0009	Cooper and Jacob (1946) Time Recovery (Well 8)
95,074	22.34	0.0004	Theis (1935) Type-curve (Well 9A)
103,425	24.34	0.00072	Theis (1935) Type-curve (Well 8)

It is assumed that saturated aquifer thickness at IWVWD-10 is 568 feet which represents the interval between the static water level and the total depth of this well (DRI, 2020). From Table 3, the average hydraulic conductivity value is 19.23 feet/day and the averaged storativity is 0.0016. The S_s value is 2.76E-6 ft^{-1}.

Table 4 Pumping Test Results at 26S39E35G01 (DRI, 2020)

T (gpd/ft)	K (ft/day)	Storativity (-)	Method
84,530	66.48	0.0019	Theis (1935) Distance-drawdown (24 hours)
171,603	135	0.00076	Cooper and Jacob (1946) Time Drawdown (26S39E35G02)
148,690	116.9	0.00073	Cooper and Jacob (1946) Time Recovery (26S39E35G02)
93,213	73.31		Theis (1935) Time recovery (26S39E35G01)
167,988	132.1	0.00085	Theis (1935) Type-curve (26S39E35G02)

The assumed aquifer thickness at 26S39E35G01 is 170 feet (DRI, 2020). It represents the interval between the static water level and the total screened depth. From Table 4, an average hydraulic conductivity value of 104.76 feet/day is calculated. The storativity and S_s values are 0.0011 and 6.24E-6 ft^{-1}, respectively.

Table 5 Pumping Test Results at 26S39E35G02 (DRI, 2020)

T (gpd/ft)	K (ft/day)	Storativity (-)	Method
62,808	37.32	0.0032	Theis (1935) Distance-drawdown (24 hours)
196,506	116.8	0.00093	Cooper and Jacob (1946) Time Drawdown (26S39E35G01)
161,231	95.81	0.00076	Cooper and Jacob (1946) Time Recovery (26S39E35G01)
34,314	20.39		Theis (1935) Time recovery (26S39E35G02)
196,149	116.6	0.0012	Theis (1935) Type-curve (26S39E35G01)

At 26S39E35G02, a saturated aquifer thickness of 225 feet is assumed (DRI, 2020). It represents the interval between the static water level and the total screened depth. From Table 5, an average hydraulic conductivity value of 77.38 feet/day is calculated. The storativity and S_s values are 0.0015 and 6.76E-6 ft^{-1}, respectively.

Slug Tests

USBR (1993) installed 10 nested monitoring wells to monitor groundwater conditions in the IWV basin. Slug tests were conducted to determine hydraulic conductivity.

Table 6 Slug Test Results at 10 Nested Monitoring Wells (USBR, 1993)

Well Name	X NAD83 Zone 11 (m)	Y NAD83 Zone 11 (m)	LS Elevation (ft amsl)	Well Depth (ft)	Depth to Top of Screen (ft)	Depth to Bot. of Scrn. (ft)	Hydraulic Conductivity (ft/day)
MW 32-SM	429848	3945241	2418.53	900	880	900	22.39
MW 32-DM	429759	3945248	2418.53	1260	1240	1260	16.44
MW 32-D	429759	3945248	2418.53	1920	1900	1920	7.93
NR 1-D	424782	3954562	2275.7	2000	1960	1980	3.68
NR 2-D	423778	3953073	2314.7	350	330	350	34.01
NR 2-D	423778	3953073	2314.7	1930	1910	1930	8.5
USBR 1-S	421808	3936553	2850.5	635	615	635	15.12
USBR 1-SM	421736	3936564	2850.5	1060	1040	1060	17.29
USBR 1-DM	421808	3936553	2850.5	1540	1500	1520	0.72
USBR 1-D	421736	3936564	2850.5	1771	1750	1770	0.29
USBR 2-S	422338	3942451	2654.95	640	620	640	0.7
USBR 2-M	422265	3942445	2654.95	1480	1460	1480	13.6
USBR 2-D	422265	3942445	2654.95	1960	1940	1960	1.16
USBR 3-S	431630	3940657	2510.4	670	650	670	4.25
USBR 3-M	431560	3940643	2510.4	1340	1320	1340	4.32
USBR 3-D	431560	3940643	2510.4	1870	1850	1870	0.42
USBR 4	432818	3945345	2377.09	1200	1190	1200	40.32
USBR 5-S	421228	3953035	2520.42	870	850	870	16.56
USBR 5-M	421151	3953022	2520.42	1610	1590	1610	10.8
USBR 5-D	421151	3953022	2520.42	1980	1960	1980	12.96
USBR 6-M	423894	3959438	2352.92	1210	1190	1210	18.14
USBR 6-D	423894	3959438	2352.92	1660	1640	1660	14.45
USBR 10-S	421272	3966711	2559.39	660	640	660	13.6
USBR 10-SM	421198	3966702	2559.39	1200	1180	1200	1.44
USBR 10-DM	421198	3966702	2559	1600	1560	1580	10.08
USBR 10-D	421198	3966702	2559.39	1950	1930	1950	6.51

Slug tests at 25 environmental monitoring wells (Tetra Tech, 2003) were conducted by the Navy to estimate hydraulic conductivity and specific storage. These data are summarized below in Table 7.

Table 7 Slug Test Results at Environmental Monitoring Wells (Tetra Tech, 2003)

Well Name	X NAD83 Zone 11 (m)	Y NAD83 Zone 11 (m)	Well Depth (ft)	Depth to Top of Screen (ft)	Depth to Bottom of Screen (ft)	Hydraulic Conductivity (ft/day)	Specific Storage S_s (ft^{-1})
JMM01-MW03	438,660	3,949,554		33	48	2.01	
JMM01-MW04	438,658	3,949,550		33	48	0.73	
JMM01-MW05	438,624	3,949,537		34	49	1.81	
JMM01-MW06	438,627	3,949,531		34	49	0.51	
JMM31-MW01	439,788	3,944,826		33	48	11.05	
MK69-MW01	440,122	3,945,079		92	102	3.96	
TTIWV-MW09	445,071	3,951,044	30	18	28	2.43	
TTIWV-MW12	442,407	3,957,978	23	11	21	65.19	
TTIWV-MW13	444,332	3,962,060	27	15	25	2.83	
TTIWV-MW14	440,595	3,965,460	72	60	70	14.17	9.84E-06
TTSWV-MW01	456,845	3,945,314	27	15	25	9.35	
TTSWV-MW02	455,157	3,946,359	48	36	46	2.26	
TTSWV-MW04	453,382	3,947,058	32	20	30	6.51	6.15E-06
TTSWV-MW05	452,388	3,944,778	142	120	140	0.48	2.11E-05
TTSWV-MW06	450,997	3,946,995	52	40	50	1.13	
TTSWV-MW09	449,400	3,948,667	42	30	40	10.48	
TTIWV-MW15	440,595	3,965,473	302	280	300	45.35	
TTIWV-MW01I	432,800	3,945,360	372	350	370	4.81	
TTIWV-MW02I	434,993	3,945,662	422	400	420	11.62	2.11E-06
TTIWV-MW08	441,106	3,944,073	422	400	420	42.51	
TTIWV-MW01D	432,800	3,945,360	752	730	750	12.75	
TTIWV-MW04	436,994	3,945,639	657	635	655	18.99	
TTIWV-MW07	439,640	3,945,155	622	600	620	56.69	
TTIWV-MW06	437,918	3,947,634	960	938	958	20.97	
TTIWV-MW16	434,866	3,958,701	990	948	988	2.01	

References

Krieger & Stewart, 1989. Indian Wells Valley Water District Southwest Well Field Test and Monitoring Wells Construction and Development. December 1989.

Houghton, HydroGeo-Logic, 1996. Geohydrologic investigation report Naval Air Weapons Station, Indian Wells Valley, China Lake, California. Prepared for Naval Air Weapons Station Environmental Projects Office, China Lake, California. November 1996.

Chapman et al., 2020, Isotopic Evaluation of Groundwater Recharge and Flow in Indian Wells Valley. Desert Research Institute, Publication No. 41281, December 2020.

U.S. Bureau of Reclamation (USBR), 1993. Indian Wells Valley Groundwater Project: USBR Technical Report Volume II. A cooperative effort among the BOR, IWVWD, North American Chemical Company, and NAWS. December 1993. Prepared by USBR Lower Colorado Region.

Tetra Tech, (2003). Basewide hydrogeologic characterization summary report Naval Air Weapons Station China Lake, California. Report prepared by Tetra Tech Em Inc., for Department of the Navy, Naval Facilities Engineering Command, Southwest Divion. January 2003, p. 62, plus tables, figures, and appendices.

ATTACHMENT E

Hydraulic Conductivity Values Derived from Specific Capacity Data

State ID	Well Name	X NAD83, UTM Zone 11 (m)	Y NAD83, UTM Zone 11 (m)	Ground Surface Elevation (ft amsl)	Borehole Depth (ft bgs)	Well Depth (ft bgs)	Depth to Screen Top (ft bgs)	Depth to Screen Bottom (ft bgs)	Length of Perforation (ft)	Pumping Rate (gpm)	Specific Capacity (gpm/ft)	K (ft/day)	Source
26S40E34N1	IWVWD_19	439483.8356	3942479.72	2289.58	232	232	135	181	33	350	21.21	128.90	Layne (2010)
25S38E13M		423387.1135	3957800.594	2354.46	400	400	360	400	40	30	2.00	10.02	DWR Well Completion Report
25S38E25		424124	3954586	2311.76	255	250	125	250	125	50	1.61	2.58	DWR Well Completion Report
25S38E25A1	IWVWD_1	425044.2222	3955118.203	2269.3	300	300	140	300	160	1300	10.08	12.63	Well Log from Owner
25S38E25K		424329	3954420	2302.6	255	250	190	250	60	70	0.54	1.79	DWR Well Completion Report
25S38E25R	IWVWD_3	424938.2569	3953004.164	2289.13	480	330	120	330	210	2350	15.67	14.96	Well Log from Owner
26S39E6		425634	3951278	2299.84	205	202	142	202	60	75	0.77	2.58	DWR Well Completion Report
26S38E1H1		424664	3951623	2319.96	217	217	157	217	60	30	0.75	2.50	DWR Well Completion Report
26S39E06D	4301 Marvin Gardens	425225.9779	3950949.701	2316.36	410	340	140	300	160	2000	35.09	43.97	Well Log from Owner
26S39E7_01		425102.0306	3950446.167	2336.25	270	260	150	260	110	15	0.50	0.91	DWR Well Completion Report
26S39E7H		426439.738	3949934.185	2322.65	500	250	210	250	40	20	2.00	10.02	DWR Well Completion Report
26S39E8		426665	3949543	2331.83	255	250	190	250	60	80	0.73	2.43	DWR Well Completion Report
26S39E7L		425285.6321	3949339.188	2373.77	400	400	360	400	40	30	2.00	10.02	DWR Well Completion Report
25S38E26_01		421829	3955248	2505.17	301	301	180	300	120	60	60.00	100.26	DWR Well Completion Report
26S38E22		421504	3947034	2643.06	545	539	380	545	165	23	0.23	0.27	DWR Well Completion Report
26S38E12		424062.1269	3949738.779	2413.61	300	300	150	300	150	25	0.31	0.41	DWR Well Completion Report
26S39E18M		425190	3947884	2415.5	300	300	140	300	160	1350	39.71	49.76	DWR Well Completion Report
26S38E35B		422670.4026	3943921.009	2577.82	402	402	342	402	60	20	1.00	3.34	DWR Well Completion Report
26S38E35L		422337	3943048	2630.87	500	500	400	500	100	20	6.67	13.36	DWR Well Completion Report
25S38E11		422779.2902	3958747.935	2410.01	425	425	220	425	205	50	1.67	1.63	DWR Well Completion Report
26S39E7_02		425536	3948951	2377.16	300	300	220	300	80	425	21.25	53.26	DWR Well Completion Report
26S38E01K	4425 Brown Rd	424468.716	3950954	2339.21	652	400	180	340	160	1500	23.44	29.37	Well Log from Owner
26S39E18_01		425778	3947450	2401.59	305	302	242	302	60	50	0.47	1.57	DWR Well Completion Report
26S39E17		426561	3948215	2359.6	280	280	200	280	80	30	7.50	18.80	DWR Well Completion Report
26S38E-12		424558	3950185	2368.03	270	265	205	265	60	50	0.60	2.01	DWR Well Completion Report
24S38E34		421319	3963467	2504.87	405	400	340	400	60	40	0.36	1.21	DWR Well Completion Report
26S38E2Q		422703	3950775	2413.11	345	339	279	339	60	60	0.48	1.61	DWR Well Completion Report
25S38E14	25S40E14	422253.8311	3957809.687	2430	451	451	304	451	147	30	10.00	13.64	DWR Well Completion Report
26S38E1		423296.4867	3950902.041	2386.38	320	320	260	320	60	30	0.50	1.67	DWR Well Completion Report
25S38E26_02		422587	3954460	2439.08	420	420	400	420	20	15	0.75	7.52	DWR Well Completion Report
26S38E2F		422357.317	3951523.153	2401.39	400	400	360	400	40	25	1.67	8.35	DWR Well Completion Report
26S38E26_01		422316	3944771	2621.6	500	500	440	500	60	35	0.21	0.69	DWR Well Completion Report
25S38E14M		421966.1148	3957240.852	2443.88	400	400	380	400	20	13	0.26	2.60	DWR Well Completion Report
25S38E35		421754.323	3953679.334	2492.93	460	460	420	460	40	20	1.00	5.01	DWR Well Completion Report
24S38E16J02		421080.1465	3967535.334	2587.3	611	611	251	611	360	940	52.22	29.08	DWR Well Completion Report
25S38E36B	IWVWD_4	424412.7704	3953755.567	2294.64	400	400	200	400	200	1750	67.31	67.48	Well Log from Owner
26S39E23H	Well 28	432714.5828	3946462.078	2362	1030	1030	470	510	490	2400	60.00	41.48	Well Log from Owner
26S40E30A		435852.3974	3945434.768	2322.57	440	440	400	440	40	43	2.15	10.77	DWR Well Completion Report

Hydraulic Conductivity Values Derived from Specific Capacity Data (Continued)

State ID	Well Name	XNAD83, UTM Zone 11(m)	YNAD83, UTM Zone 11(m)	Ground Surface Elevation(ft amsl)	Borehole Depth(ft bgs)	Well Depth(ft bgs)	Depth to Screen Top(ft bgs)	Depth to Screen Bottom(ft bgs)	Length of Perforation(ft)	Pumping Rate (gpm)	Specific Capacity(gpm/ft)	K(ft/day)	Source
26S40E29K		437182	3944560	2310.65	255	250	190	250	60	65	0.68	2.26	DWR Well Completion Report
25S40E31		435423	3952847	2191.05	340	340	274	334	60	30	0.33	1.11	DWR Well Completion Report
26S40E7G		435553	3949793	2257.62	365	360	300	360	60	20	0.29	0.95	DWR Well Completion Report
26S40E30_01		435833.7798	3944861.574	2334.32	405	405	185	405	220	50	25.00	22.78	DWR Well Completion Report
26S39E20R1	Well 30	428007.8232	3945914.05	2420	1015	1015	600	900	300	1250	27.78	18.56	Well Log from Owner
27S40E6_01	IWVWD_12	434572.8555	3942258.161	2404.06	910	720	580	700	120	2000	62.50	104.44	Layne (2010)
26S39E26C		431836.8409	3945332.962	2394.18	340	340	260	340	80	24	12.00	30.08	DWR Well Completion Report
26S39E26		432396	3944686	2391.94	325	323	263	323	60	60	10.00	33.42	DWR Well Completion Report
26S39E24P01	Well 18C	433682.1211	3945679.833	2358	1020	1020	503	583	487	1500	166.67	68.62	Well Log from Owner
26S40E30H		435754	3944969	2332.76	450	450	430	450	20	30	1.00	10.02	DWR Well Completion Report
26S40E29M		436184.6373	3944474.282	2334.31	460	460	420	460	40	25	2.50	12.53	DWR Well Completion Report
26S39E26B	IWVWD_17	432411.8173	3945558.681	2385.14	1035	1030	410	490	370	997	64.32	34.86	Layne (2010)
26S39E35		432605.477	3942823.26	2434.23	485	485	445	485	40	30	3.00	15.04	DWR Well Completion Report
26S39E34_01		434598.0374	3943208.481	2382.78	400	400	380	400	20	15	1.50	15.04	DWR Well Completion Report
26S40E31R		435765.9647	3942589.386	2383.22	420	420	380	420	40	25	1.00	5.01	DWR Well Completion Report
26S39E30R		426277.4271	3944149.518	2463.45	500	500	460	500	40	25	1.25	6.26	DWR Well Completion Report
26S40E31G		435460.3993	3943236.684	2369.83	400	400	360	400	40	25	1.00	5.01	DWR Well Completion Report
26S39E27B		430765.5895	3945335.908	2408.63	400	400	380	400	20	15	1.50	15.04	DWR Well Completion Report
27S39E2B		432292	3942257	2440.87	420	420	400	420	20	15	1.00	10.02	DWR Well Completion Report
26S40E30_02		434672	3944034	2370.65	325	320	260	320	60	50	0.49	1.63	DWR Well Completion Report
26S39E20C		427093	3947031	2387.17	380	380	340	380	40	25	0.83	4.17	DWR Well Completion Report
26S40E30K02	IWVWD_9A	435433.0205	3944405.943	2349.25	1040	796	300	460	356	2800	46.74	26.33	Well Log from Owner
27S39E3C		430230	3942200	2483.55	440	440	420	440	20	20	1.00	10.02	DWR Well Completion Report
26S39E34_02		430769.9704	3942906.995	2464.85	420	420	400	420	20	40	2.67	26.73	DWR Well Completion Report
26S39E34_03		429850.9541	3943741.524	2450.24	440	440	380	440	60	20	1.00	3.34	DWR Well Completion Report
26S40E32K01	IWVWD_11	436993.8629	3942948.745	2332.19	700	620	260	310	200	1200	40.34	40.44	Well Log from Owner
26S39E28E		428228.5595	3945277.922	2432.59	400	400	360	400	40	20	1.33	6.68	DWR Well Completion Report
26S39E34_04		430568.0916	3942555.183	2468.05	420	420	380	420	40	15	1.50	7.52	DWR Well Completion Report
26S39E27	IWVWD_16	430445.1347	3945216.434	2412.95	500	500	320	500	180	1350	67.50	75.20	Layne (2010)
26S39E34_05		430770.7685	3943161.101	2463.2	400	400	360	400	40	20	0.40	2.00	DWR Well Completion Report
25S38E13L	Well #5	424058.4785	3957820.882	2325.27	456	444	109	444	335	3000	63.83	38.20	Well Log from Owner
26S38E13Q	Well #6	424307.0639	3957012.019	2307.04	495	490	120	490	370	3000	47.62	25.80	Well Log from Owner
25S38E24K	Well #7	424475.7478	3956201.517	2294.55	495	490	120	490	370	3000	71.43	38.71	Well Log from Owner
25S38E12M	Well #3	423477.2025	3959438.251	2374.55	700	700	140	700	560	4030	67.17	24.05	Well Log from Owner
25S38E2L		423845	3960703	2384.98	705	700	200	700	500	4000	32.00	12.83	DWR Well Completion Report
26S40E32F01	IWVWD_13	436795.0251	3943443.706	2322.54	849	720	520	700	180	1288	17.20	19.15	Well Log from Owner
26S39E27D01	IWVWD_30	429792.7745	3945406.421	2414.51	1230	1220	600	1200	600	1500	45.45	15.19	Well Log from Owner
26S39E28R01	IWVWD_31	429631.4234	3944082.838	2446.44	1220	1220	600	1200	600	1500	41.67	13.92	Well Log from Owner

Hydraulic Conductivity Values Derived from Specific Capacity Data (Continued)

State ID	Well Name	X NAD83, UTM Zone 11 (m)	Y NAD83, UTM Zone 11 (m)	Ground Surface Elevation (ft amsl)	Borehole Depth (ft bgs)	Well Depth (ft bgs)	Depth to Screen Top (ft bgs)	Depth to Screen Bottom (ft bgs)	Length of Perforation (ft)	Pumping Rate (gpm)	Specific Capacity (gpm/ft)	K (ft/day)	Source
27S39E8_01	IWV-MW-1, DBID-23	426677.3741	3939935.519	2558.82	1030	1020	600	1000	400	50	12.50	6.26	DWR Well Completion Report
27S38E09A	IWVWD_35	428517.2488	3940671.712	2532.16	1023	1020	560	1000	440	3000	36.14	16.47	Well Log from Owner
27S39E8_02	IWV-MW-2, DBID-21	427193.2271	3939208.105	2583.32	1030	1020	600	1000	400	50	0.65	0.32	DWR Well Completion Report
26S39E33R	IWVWD_36	428394.3151	3942473.011	2487.41	1010	1002	500	1002	502	4000	56.34	22.50	Well Log from Owner
27S39E08L01M	IWVWD_33	427182.7717	3939912.274	2557.63	1030	770	570	760	440	2000	21.28	9.69	Well Log from Owner
27S39E08A02M	IWVWD_34	427701.8735	3940622.855	2539.14	1010	955	550	935	355	1750	24.65	13.92	Well Log from Owner
27S40E8_01		436527.6364	3939559.808	2439.76	460	460	420	460	40	30	1.50	7.52	DWR Well Completion Report
25S38E2		422624.0351	3960322.287	2426.62	1020	1000	400	988	588	3600	100.00	34.10	DWR Well Completion Report
26S40E30K02R	IWVWD-35	434783.4292	3945078.731	2348.18	860	850	320	830	510	1500	71.43	28.08	DWR Well Completion Report
26S39E36G01	Well-36	433875	3943228	2396.32	1145	982	362	962	600	2000	85.11	28.44	DWR Well Completion Report
27S39E8_03	IWV-MW-3	424821	3937033	2641.06	1030	1020	600	1000	400	50	0.25	0.12	DWR Well Completion Report
27S40E6_02		435426	3942151	2407.31	410	410	350	410	60	40	0.35	1.18	DWR Well Completion Report
27S40E2		442472.3608	3941075.261	2301.98	400	400	240	400	160	60	1.00	1.25	DWR Well Completion Report
26S39E18_02		425390.6804	3948787.586	2384.82	455	455	300	455	155	15	1.50	1.94	DWR Well Completion Report
27S40E4L		438098	3941297	2331.42	305	304	244	304	60	60	0.48	1.61	DWR Well Completion Report
26S39E19P02	Well 15A	425688.5136	3945732.798	2416	620	620	320	360	270	2500	135.87	100.91	Well Log from Owner
26S39E30F002	16A	425569.7644	3944588.546	2450.35	460	455	352	455	103	2240	29.09	56.63	DWR Well Completion Report
26S38E12L		423703.4133	3949684.949	2429.72	850	830	320	810	490	3500	233.33	95.49	DWR Well Completion Report
26S38E35_01		422525	3943234	2605.5	560	555	495	555	60	15	0.10	0.32	DWR Well Completion Report
26S39E31		425832.319	3943727.839	2474.71	400	400	360	400	40	15	0.75	3.76	DWR Well Completion Report
26S39E19Q2	12-A	425711	3945808	2417.1	560	510	300	510	210	2300	20.54	19.61	DWR Well Completion Report
25S38E23C		421860.7848	3957025.814	2452.51	850	820	330	810	480	4200	110.53	46.17	DWR Well Completion Report
27S39E02K		431852.9241	3942134.645	2473.87	400	400	340	400	60	40	0.35	1.18	DWR Well Completion Report
27S40E9_01		438632.9434	3940507.933	2314.43	260	260	180	260	80	20	0.36	0.91	DWR Well Completion Report
26S39E30_01	Well #3	426012.9659	3944751.674	2445.43	499	480	310	470	160	76	6.33	7.93	DWR Well Completion Report
27S40E9_02		438615	3939180	2358.3	329	329	219	329	110	50	2.50	4.55	DWR Well Completion Report
26S39E28		428706.8537	3945617.148	2420.43	365	365	280	365	85	320	21.33	50.33	DWR Well Completion Report
26S39E30_02		426318.2751	3944796.282	2443.2	520	500	300	500	200	1250	138.89	139.26	DWR Well Completion Report
26S39E29		427312.9638	3944743.292	2447.61	400	400	300	400	100	15	0.15	0.30	DWR Well Completion Report
27S40E6_03		435262	3941449	2429.87	325	320	280	320	40	50	0.60	2.98	DWR Well Completion Report
27S40E7F		435382	3940227	2454.55	333	332	293	333	40	15	5.00	25.06	DWR Well Completion Report
27S40E11_01		442252	3940329	2343.23	200	198	178	198	20	8	0.40	4.01	DWR Well Completion Report
24S38E28		420820	3963629	2566.85	500	500	400	500	100	20	0.20	0.40	DWR Well Completion Report
27S40E10_01		440538	3939371	2350.21	220	220	180	220	40	30	6.00	30.08	DWR Well Completion Report
26S39E31K		425900	3943101	2491.68	405	405	320	405	85	60	0.58	1.37	DWR Well Completion Report
27S40E		438673.1083	3942132.11	2308.77	273	195	131	190	59	615	34.17	116.12	DWR Well Completion Report
27S40E10_02		440844	3939788	2335.24	185	185	155	185	30	10	0.38	2.57	DWR Well Completion Report
23S40E28	PMTC Range	439488.6257	3973187.963	2591.18	610	600	410	600	190	755	30.20	31.87	DWR Well Completion Report

Hydraulic Conductivity Values Derived from Specific Capacity Data (Continued)

State ID	Well Name	X NAD83, UTM Zone 11 (m)	Y NAD83, UTM Zone 11 (m)	Ground Surface Elevation (ft amsl)	Borehole Depth (ft bgs)	Well Depth (ft bgs)	Depth to Screen Top (ft bgs)	Depth to Screen Bottom (ft bgs)	Length of Perforation (ft)	Pumping Rate (gpm)	Specific Capacity (gpm/ft)	K (ft/day)	Source
26S39E31Q		425451	3942603	2505.94	600	600	320	600	280	100	4.00	2.86	DWR Well Completion Report
27S40E05M		436535.9381	3941437.994	2386.3	360	360	200	360	160	565	5.77	7.22	DWR Well Completion Report
27S40E11_02		442000	3940310	2335.53	187	187	147	187	40	12	1.20	6.01	DWR Well Completion Report
26S38E26_02		421742.6308	3945136.82	2714.25	700	700	520	700	180	10	0.10	0.11	DWR Well Completion Report
27S38E1		424478	3941285	2563.02	428	425	365	425	60	20	0.27	0.91	DWR Well Completion Report
25S38E02M	Well #2	422136.3965	3960700.041	2442.92	705	700	240	700	460	4000	160.00	69.75	Well Log from Owner
27S40E8_02		436035	3939521	2463.35	325	320	260	320	60	30	0.38	1.25	DWR Well Completion Report
25S38E02D	Well #1	422144.3061	3961517.143	2417.11	700	700	200	700	500	3200	128.00	51.33	Well Log from Owner
27S39E4		428682.4288	3942341.48	2487.19	420	420	260	420	160	20	0.25	0.31	DWR Well Completion Report
26S40E31K		435686	3942872	2380.46	300	300	150	300	150	618	18.18	24.30	DWR Well Completion Report
25S38E15J		421458	3957572	2477.53	701	630	240	630	390	2700	62.79	32.28	DWR Well Completion Report
27S40E18		435402	3938299	2582.11	525	362	320	360		25	0.12	0.35	DWR Well Completion Report
26S38E35_02		422480.2702	3943726.001	2592.74	600	600	300	600	300	15	0.75	0.50	DWR Well Completion Report
25S38E34		420930	3953061	2567.3	337	331	240	331	91	30	10.00	22.03	DWR Well Completion Report
26S38E26G01		451536.4529	3915759.235	3182.99	502	502	442	502	60	50	0.37	1.23	DWR Well Completion Report
28S40E5H		437902.5257	3932330.92	3094.5	200	199	120	199	79	7	0.11	0.29	DWR Well Completion Report
28S40E16_02		439340.9763	3929042.001	3285.68	223	205	100	200	100	12	0.20	0.39	DWR Well Completion Report
28S40E16_01		439395.7249	3928648.998	3334.38	243	235	120	235	115	7	0.05	0.08	DWR Well Completion Report
25S39E35N1		431625.4425	3952300.984	2247.72		152						84.43	Kunkel and Chase (1969) Appendix 4-B
25S39E12R1		434441.7945	3958738.36	2202.04		180.5	60	140				50.69	Kunkel and Chase (1969); Periodic Evaluation Appendix 4-B
26S39E11E1	Sandquist Spa	431642.776	3949922.92	2304.82		250	135	191				104.78	Kunkel and Chase (1969); Periodic Evaluation Appendix 4-B
25S39E4R1		429570.864	3960483.824	2253.7		200						81.33	Kunkel and Chase (1969); Periodic Evaluation Appendix 4-B
26S39E24K1		434056.792	3946301.896	2346.2		480						59.5	Kunkel and Chase (1969); Periodic Evaluation Appendix 4-B

ATTACHMENT F

STETSON
ENGINEERS INC.

861 Village Oaks Drive, Suite 100 • Covina , California 91724
Phone: (626) 967-6202 • FAX: (626) 331-7065 • Web site: www.stetsonengineers.com
Northern California • Southern California • Arizona • Colorado

FINAL

TECHNICAL MEMORANDUM

TO: **Technical Advisory Committee (TAC),**
Indian Wells Valley Groundwater Authority

FROM: **Stetson Engineers Inc.**

SUBJECT: **Evaluation of the El Paso Subarea as a Separate Indian Wells Valley Management Area**

JOB NO.: **2652-2023-22**

DATE: **July 2024**

1.0 INTRODUCTION

The 2020 Groundwater Sustainability Plan (GSP) addresses groundwater resources in the entire Indian Wells Valley Groundwater Basin (IWVGB), including the El Paso Subarea. This is consistent with the groundwater basins described in California Department of Water Resources (DWR) Bulletin 118. Through development and implementation of the GSP and preparation of the GSP Annual Reports, hydrogeologic data have been collected that support the El Paso Subarea (**Figure 1**) becoming a separate "management area" for the Indian Wells Valley Groundwater Authority (IWVGA) management purposes.

DWR (2017) guidelines state that management areas may be defined by natural or jurisdictional boundaries and may be based on differences in water use sector, water source type, geology, or aquifer characteristics. Management areas may have different minimum thresholds and measurable objectives than the basin at large and may be monitored to a different level. It is required that if a Groundwater Sustainability Agency (GSA) in the basin decides to define management areas, the GSA must provide descriptions of why those differences are appropriate for the management area, relative

to the rest of the basin. This Technical Memorandum has been prepared to provide these descriptions and comparisons.

IWVGB underlies approximately 382,000 acres (536 square miles) of land area in Kern, Inyo, and San Bernardino counties. The proposed El Paso Management Area is located in the southwest area of the GSA. It is highlighted in green on **Figure 1** and covers 30% (113,432 acres) of the IWVGB. The remaining 70% of IWVGB highlighted in blue on **Figure 1,** and includes Ridgecrest, Navy, and main pumping areas within the basin. Table 1 summarizes the areal extent of these proposed management areas.

TABLE 1 AREAL EXTENT OF PROPOSED MANAGEMENT AREAS

IWV Groundwater Basin Proposed Management Area	Surface Area (acres)	Surface Area (square miles)
Main IWVGB Management Area	268,313	419
El Paso Management Area	113,432	117
Total IWVGB	381,745	536

The two proposed management areas can be separated by a mapped surficial fault and a steep hydraulic gradient determined by semi-annual groundwater level measurements since 1995. The surficial fault trace trends northwest/southeast and is called out as the Freeman Fault for this report[1]. More recent Airborne Electro Magnetic (AEM) survey data (Stanford, 2019; Ramboll, 2019) also indicate fine-grained subsurface material on the southwest side of the fault that impedes groundwater flow.

Moyle (1963) reported that the Black Hills Well on **Figure 1** (28S38E18F1) had a depth of 930 feet bgs. Note that the screen interval in this well is unknown. A pumping test at this well indicated a specific capacity of 0.33 gpm/ft. Using the empirical relationship between specific capacity and transmissivity (Driscoll,1986), a transmissivity value of 66 ft^2/day or 0.046 ft^2/min is estimated. Similar results were obtained for the two deep aquifers at USBR-1 (USBR, 1993). Interpreted as continental deposits, hard and cemented clay at the bottom of the drill hole was noted.

[1] This unnamed surficial fault is included in California Geological Survey (CGS) 2010 fault mapping. It has been previously mislabeled as the El Paso Fault, which is located south of El Paso Subarea in the Garlock Fault Zone. The IWV Technical Model Group refers to this fault as the Freeman Fault.

As summarized in **Table 2**, these features separate the IWVGB into two hydrogeologic areas: the main IWVGB and the El Paso Subarea. This Technical Memorandum (TM) reviews hydrogeologic features and groundwater chemistry to evaluate if the southwestern portion of IWVGB should be considered a separate groundwater management area.

TABLE 2 HYDROGEOLOGIC FEATURES SEPARATING THE EL PASO SUBAREA FROM THE MAIN IWVGB

Features	Characteristics
Steep Hydraulic Gradient across the Freeman Fault	Measured groundwater elevations indicate restricted flow from the El Paso Subarea towards the main IWVGB. These measurements show 520-feet difference in groundwater elevations over 3.6 miles (gradient of 27 ft / 1,000 ft; or 0.273 ft/ft) across the Freeman fault. This results in a steep hydraulic gradient between the El Paso Subarea (higher groundwater levels) and the main IWVGB (lower groundwater levels).
Groundwater Production	There is no significant groundwater pumping in the El Paso Subarea. All major pumping occurs in the main IWVGB.
Groundwater Condition	Relatively stable groundwater levels have been observed in the El Paso Subarea since 2005 at four monitoring wells (AB303-04, AB303-03, AB303-06 and USBR-1) to the southwest of the fault – indicating that the El Paso Subarea aquifer is in a quasi-steady state condition. This is in contrast to the overdraft condition in the main IWVGB to the north and east of the faulted area where groundwater level has been declining.
Geochemistry	Groundwater geochemistry between samples collected from the El Paso Subarea and the main IWVGB show groundwater type differences based on Stiff and Piper diagrams.
Sustainable Management Criteria	Hydrogeologic monitoring of the El Paso Subarea, when included with the main IWVGB, will distort the evaluation results.

2.0 HYDROGEOLOGY

This section presents the hydrogeologic review of the southwestern part of IWVGB, including a discussion of its geologic framework, hydrogeologic units, water levels, and water quality. The study area is located near the Freeman fault where the hydrogeologic differences between the two proposed management areas occur.

2.1 Geologic Framework

Surface geology of the study area, including faults and monitoring well locations are shown in the map insert on **Figure 1**. Indian Wells Valley is largely bounded by pre-Tertiary crystalline basement rock and continental deposits of Paleocene age that most likely correlate to the Goler and Ricardo Formations (St. Amand, 1986). It is likely that

these continental and marine formations overlie the granitic crystalline basement on the basin floor, forming a relatively impervious unit below the more recent alluvial gravel and sand, older alluvium and fanglomerate, fan alluvium, and fluvial fill along the major washes (TTEMI, 2003).

In order to characterize the deep aquifers in the southwest and western regions of Indian Wells Valley, the United States Bureau of Reclamation (USBR), in cooperation with the Indian Wells Valley Water District (IWVWD), the Naval Air Weapons Station (NAWS), and the North American Chemical Company, drilled nine multiple piezometer observation wells to depths from 1,910 to 2,024 and a geothermal test hole to a depth of 7,394 feet, providing detailed information on deeper subsurface lithology in the basin. In 2021, DWR drilled a borehole to a maximum depth of 1,520 feet at EP-1 and installed three nested monitoring wells to depths of 490, 897 and 1,120 ft bgs, respectively. The location of USBR-1, USBR-2, EP-1, some deep boreholes (IWVCWMG / GTC, 2008) drilled using AB303 grant funding, and other monitoring wells are shown in **Figure 2**.

2.2 Hydrogeologic Units

Lithologic units in the Indian Wells Valley area can be grouped into three categories: (1) consolidated rocks or bedrock, which commonly have low porosity and permeability and do not readily transmit water (except where highly fractured), (2) deeper sedimentary formations of the Ricardo and Goler Formations that do not yield groundwater readily, and (3) shallow unconsolidated alluvial deposits (up to 1,500 feet thick), which transmit water readily in a few areas where coarse grained deposits occur.

A geologic cross section in the El Paso Subarea, across the Freeman fault, and into the main IWVGB is shown in **Figure 3**. The cross section passes through 3 deep wells, EP-1 (27S38E-32C), USBR-1 (27S38E-23F) and AB303-01 (27S38E-13A02). Land surface elevations on this cross section begin at approximately 2,965 feet above mean sea level (ft amsl) and decrease to the northeast toward the main IWVGB to 2,650 ft amsl. At EP-1, 20-ft of sandy silt was logged at various depths from 540 to 560 feet below ground surface (ft bgs) and alternative sandy lean clay and sandy silt were encountered between the depth intervals of 640 to 820 ft bgs. Lean clay, and lean clay with sand, dominate the depth interval from 1,190 to 1,490 ft bgs. In the middle of the cross section at USBR-1, clay was first encountered at a shallow depth of 230 ft bgs, followed by alternate layers of coarse-grained and fine-grained deposits between 230 and 1,610 ft bgs, the depth interval from 1,610 to 1,760 consists of volcanic conglomerate with clay lenses and fine

to medium sand. On the northeastern side of Freeman fault, the cross section at AB303-01 shows the top 770 feet consists of poorly graded sands.

This cross section shows a lithologic difference between the sediments in the El Paso Subarea and the sediments in the main IWVGB. This cross section in **Figure 3** also shows a difference in groundwater levels measured at monitoring wells located on different sides of the Freeman fault.

2.3 Groundwater Level

The estimated groundwater table is shown on the cross section in **Figure 3**. In general, the groundwater gradient follows ground-surface elevation. The rate of water level drop between USBR-1 and Freeman Fault increases.

Spring 2023 water level contours are shown in **Figure 4**. A steep hydraulic gradient zone is well defined between USBR-1 and Inyo well to the south and between AB303-04 and 35D to the north. The calculated hydraulic gradient values ranged from 20 to 30 feet per thousand feet (2 to 3 percent). For comparison, this is more than twice the typical hydraulic gradient range of 0.5 to 10 feet per thousand feet (0.05 to 1.0 percent) (Harter, 2003) in most areas of California's valleys and basins.

Hydrographs for eight monitoring wells with long term data are compiled in **Attachment A**. Similar characteristics are observed among the four monitoring wells (AB303-03, AB303-04, AB303-06 and USBR-1 (pages A1 and A2)) to the southwest of the Freeman fault, where in general, water levels have been stable since 2005. To the east of the Freeman Fault, groundwater levels have been declining continuously at AB303-01 and IWV MW#3 (page A3) since 2007. A similar trend has been observed at USBR-2 (Page A4), though there was a groundwater level rise observed in October 2019 during a wet year. Drilled in compacted alluvial material, the Rock Quarry (page A4) well is located near Black Hills and to the east of the Freeman fault also shows stable groundwater levels.

The groundwater level hydrographs show a different hydrogeologic behavior occurring in the El Paso Subarea compared with the groundwater levels in the main IWVGB. Wells located in the El Paso Subarea show stable groundwater levels to the southwest of the Freeman fault indicate that the El Paso Subarea is in a quasi-steady state. Wells located in the main IWVGB to the northeast of the Freeman fault show declining groundwater

levels. **These groundwater level data support having a separate management area for the southwest portion of IWVGB.**

2.4 Groundwater Chemistry

A total of 18 sets of general groundwater chemistry data were collected, reviewed, and analyzed at 14 well locations (**Attachment B**). Note that USBR-1 and USBR-2 are each triple nested wells. Measured Total Dissolved Solids (TDS) concentration are below the secondary maximum contaminant level (SMCL) of 500 mg/L, with exceptions at Father Crowley, Abandoned Well, and USBR-2S. Most of the measured water quality samples are below 300 mg/L.

Stiff diagrams were constructed for each of these groundwater samples to show a graphical representation of chemical analyses. These graphs provide a visual comparison between water from different sources. **Figures 5 and 6** show stiff diagrams for groundwater samples collected from twelve monitoring wells. On each stiff diagram, cations are plotted in milliequivalents per liter on the left side of the zero axis, one to each horizontal axis, and anions are plotted on the right side. Depending on the dominant cations and anions, a variety of groundwater types can be defined as sodium bicarbonate ($Na\text{-}HCO_3$), sodium-calcium-bicarbonate-sulfate ($Na\text{-}Ca\text{-}HCO_3\text{-}SO_4$), calcium-bicarbonate ($Ca\text{-}HCO_3$), sodium-chloride (Na-Cl) and calcium-sulfate ($Ca\text{-}SO_4$) and others.

The stiff diagrams depicted in **Figure 5** show groundwater composition at USBR-1-S, USBR-2-S and AB303-05 has similar hydro-geo-chemical characteristics ($Na\text{-}HCO_3$, type), with Total TDS values ranging from 190 to 548 mg/L. A typical groundwater chemistry of a shallow freshwater aquifer is magnesium/calcium-bicarbonate ($Mg/Ca\text{-}HCO_3$) type water. The sodium-bicarbonate ($Na\text{-}HCO_3$) type water for wells to the west of the Freeman fault is the result of replacing the dominant cation Mg/Ca with Na, often resulting from groundwater flow through shallow fractured or weathered granitic and gneiss rocks and their associated alluvial deposits, or mountain front recharge or surface water (Little Dixie). It is noted that all these three wells are located to the west of the Freeman fault.

Figure 5 shows that historical water quality data in the Indian Wells Valley Water District's (IWVWD) southwest wellfield represents a sodium-calcium-bicarbonate-sulfate ($Na\text{-}Ca\text{-}HCO_3\text{-}SO_4$) type water with a TDS concentration from 190 to 548 mg/L. This type of water

is indicative of ion exchange of mountain front recharge to a Na-rich groundwater (Lipfert et al., 2004), or reaction with gypsum groundwaters. **Figure 5** shows the stiff diagram for EP-1-S. Though EP-1-S is associated with similar water type as those wells to the west of the Freeman Fault, calcium concentration is elevated.

Other variations of sodium-bicarbonate (Na-HCO_3) water type are presented at AB303-04, AB303-06 and Father Crowley (**Figure 6**), which are the results of mountain front recharge as indicated by the ion exchange to Na-rich groundwater or reaction with gypsum groundwaters. Groundwater at the Abandoned Well (**Figure 6)** is also the result of mountain front recharge as indicated Mg to Na ion exchange or reaction with gypsum groundwaters.

3.0 El Paso Subarea as a Separate Management Area

DWR (2017) recommended that management areas may be defined by natural or jurisdictional boundaries and may be based on differences in water use sector, water source type, geology, or aquifer characteristics. Management areas may have different minimum thresholds and measurable objectives than the basin at large and may be monitored to a different level. It is required that if GSAs in the basin decide to define management areas, the GSAs must provide descriptions of why those differences are appropriate for the management area, relative to the rest of the basin.

Though its hydraulic properties haven't been well understood, the Freeman Fault is inferred between the El Paso Subarea and the main IWVGB from the groundwater level contours developed since 1995. Groundwater flows from the El Paso Subarea into the main IWVGB through a steep hydraulic gradient zone located in the same area as the Freeman Fault.

Similar characteristics are observed among the four monitoring wells (AB303-04, AB303-03, AB303-06 and USBR-1) to the southwest of the Freeman Fault, where in general, groundwater levels have been stable, indicating the El Paso Subarea is in a quasi-steady state condition. To the north and east of the Freeman Fault, groundwater level has been declining continuously and the main IWVGB is in overdraft conditions. Additionally, twelve sets of groundwater quality data have been analyzed to show where the groundwater chemistry is different between the two proposed management areas.

Given this evaluation, it is recommended that the El Paso Subarea be considered as a separate management area for the IWVGA GSP.

Action

If the TAC concurs with this Technical Memorandum, and separate "management" of the El Paso Subarea (**Figure 7**), the IWVGA staff will: (1) confirm with IWVGA Board; and (2) include this "separate" El Paso Subarea management approach in the Periodic Evaluation and any subsequent GSP Amendments to the DWR-approved GSP.

4.0 REFERENCES

Allen, D.M., Grasby, S.E. and Voormeij, D.A., 2006, Determining the circulation depth of thermal springs in the southern Rocky Mountain Trench, south-eastern British Columbia, Canada using geothermometry and borehole temperature logs, Hydrogeology Journal, February 2006.

Driscoll, F.G., 1986, Groundwater and Wells, Second Edition, Published by Johnson Filtration Systems Inc.

DWR (2017), Best Management Practices (BMP) for the Sustainable Management of Groundwater – Sustainable Management Criteria (SMC). *https://water.ca.gov/-/media/DWR-Website/Web-Pages/Programs/Groundwater-Management/Sustainable-Groundwater-Management/Best-Management-Practices-and-Guidance-Documents/Files/BMP-6-Sustainable-Management-Criteria-DRAFT_ay_19.pdf.*

Harter, Thomas, 2003, Basic concepts of groundwater hydrology, University of California, Division of Agriculture and Natural Resources, in partnership with USDA natural Resources Conservation Services.

IWVCWMG and GTC, 2008. Installation and Implementation of a Comprehensive Groundwater Monitoring Program for the Indian Wells Valley, California. Prepared for: Local Groundwater Assistance Program AB303. Prepared by: IWV Cooperative Groundwater Technical Advisory Committee and Geochemical Technologies Corporation (GTC). March 2008.

LADWP, 2018. Draft TM-2: Detailed Hydrogeologic Review of Antelope Valley and Indian Wells Valley Groundwater Basins. Task Order 013. July 2018.

Lipfert, G., Reeve, A., 2004, Characterization of Three Water Types in a Fractured Schist, High Arsenic, Watershed in Main. *https://clu-in.org/products/siteprof/2004fracrockconf/cdr_pdfs/indexed/group1/638.pdf*

Moyle, 1963. Data on Water Wells in Indian Wells Valley Area. Prepared for DWR Bulletin No. 91-9; prepared by United States Department of Interior Geological Survey.

Ramboll, 2019. Hydrogeologic Conceptual Framework, Indian Wells Valley. Prepared for Indian Wells

Valley Water District and the Brackish Groundwater Resources Study Group. March 2019.Saint-Amand, P., 1986. Water Supply of Indian Wells Valley, California: NWC Technical Publication 6404.

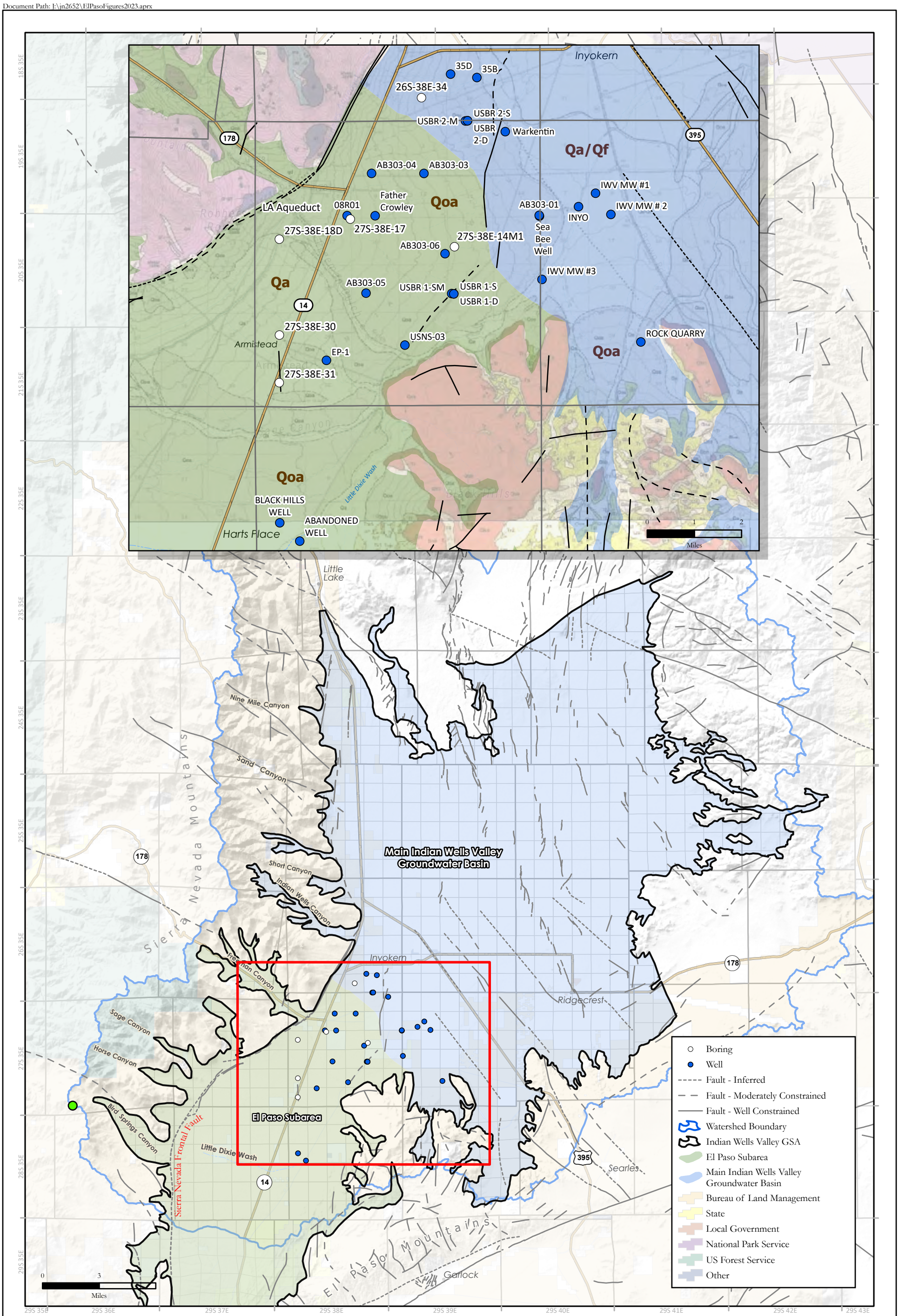
Stanford, 2018. Behroozmand. A., Knight, R., Halkjaer, M., 2018, Analysis of SkyTEM Data from Indian Wells Valley, California, Report for Stanford Contract May-August 2018.

Saint-Amand, P., 1986. Water Supply of Indian Wells Valley, California: NWC

Technical Publication 6404.TTEMI, 2003. Groundwater Management in the Indian Wells Valley Basin, Ridgecrest, California. AB 303 Grant State of California Water Resources Department. June 2003.

U.S. Bureau of Reclamation (USBR), 1993. Indian Wells Valley Groundwater Project: USBR Technical Report Volume II. A cooperative effort among the BOR, IWVWD, North American Chemical Company, and NAWS. December 1993. Prepared by USBR Lower Colorado Region.

Document Path: J:\jn2652\ElPasoFigures2023.aprx



STETSON ENGINEERS INC.

SURFACE GEOLOGY OF STUDY AREA

INDIAN WELLS VALLEY, CA

DRAFT 8/7/2024

Geology: Dibblee-Minch 2008
Faults: Ca. Geological Survey 2010; USGS 2019; USGS 2020

FIGURE 1

Document Path: J:\jn2652\ElPasoFigures2023.aprx

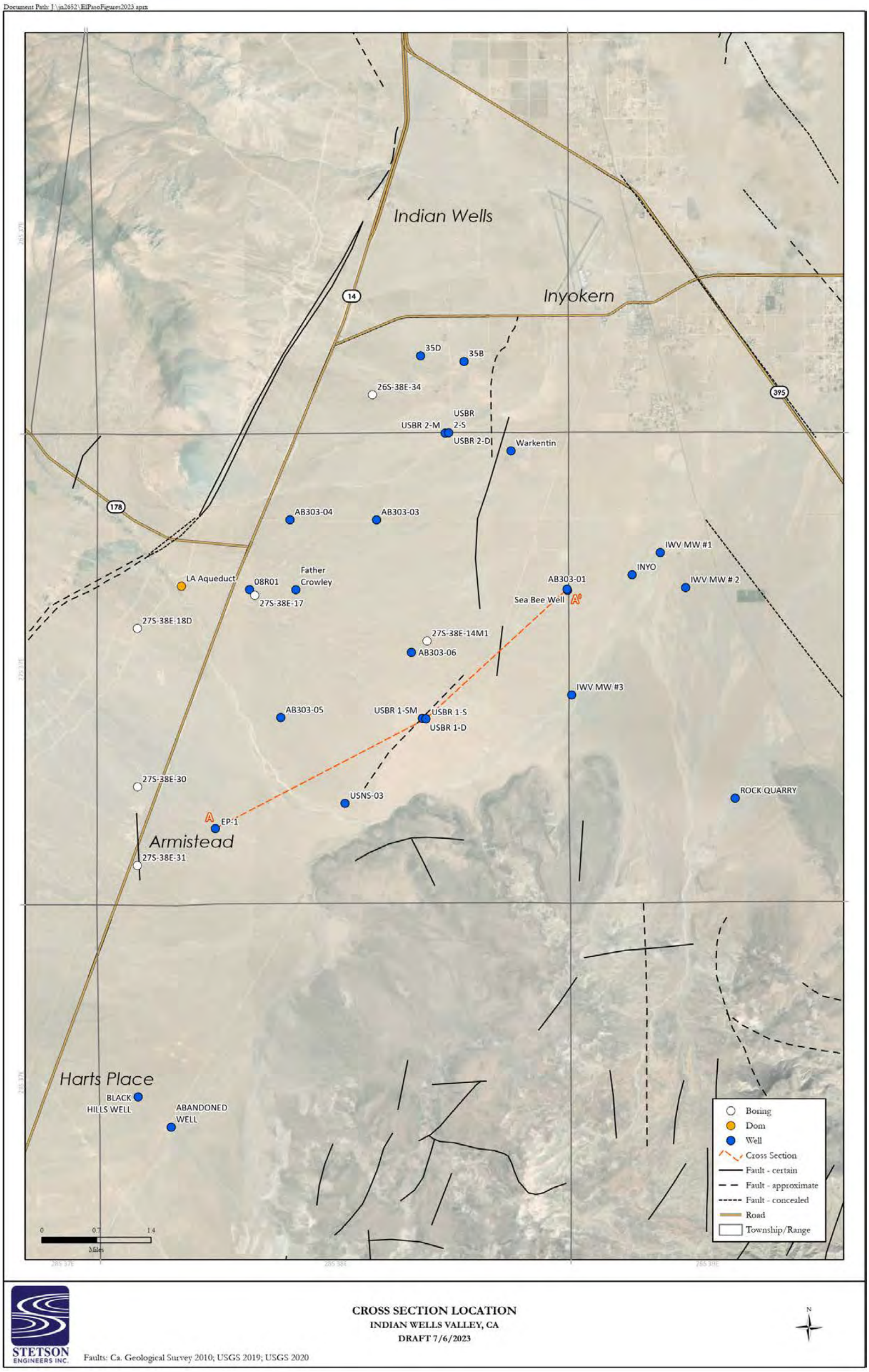


Figure 2

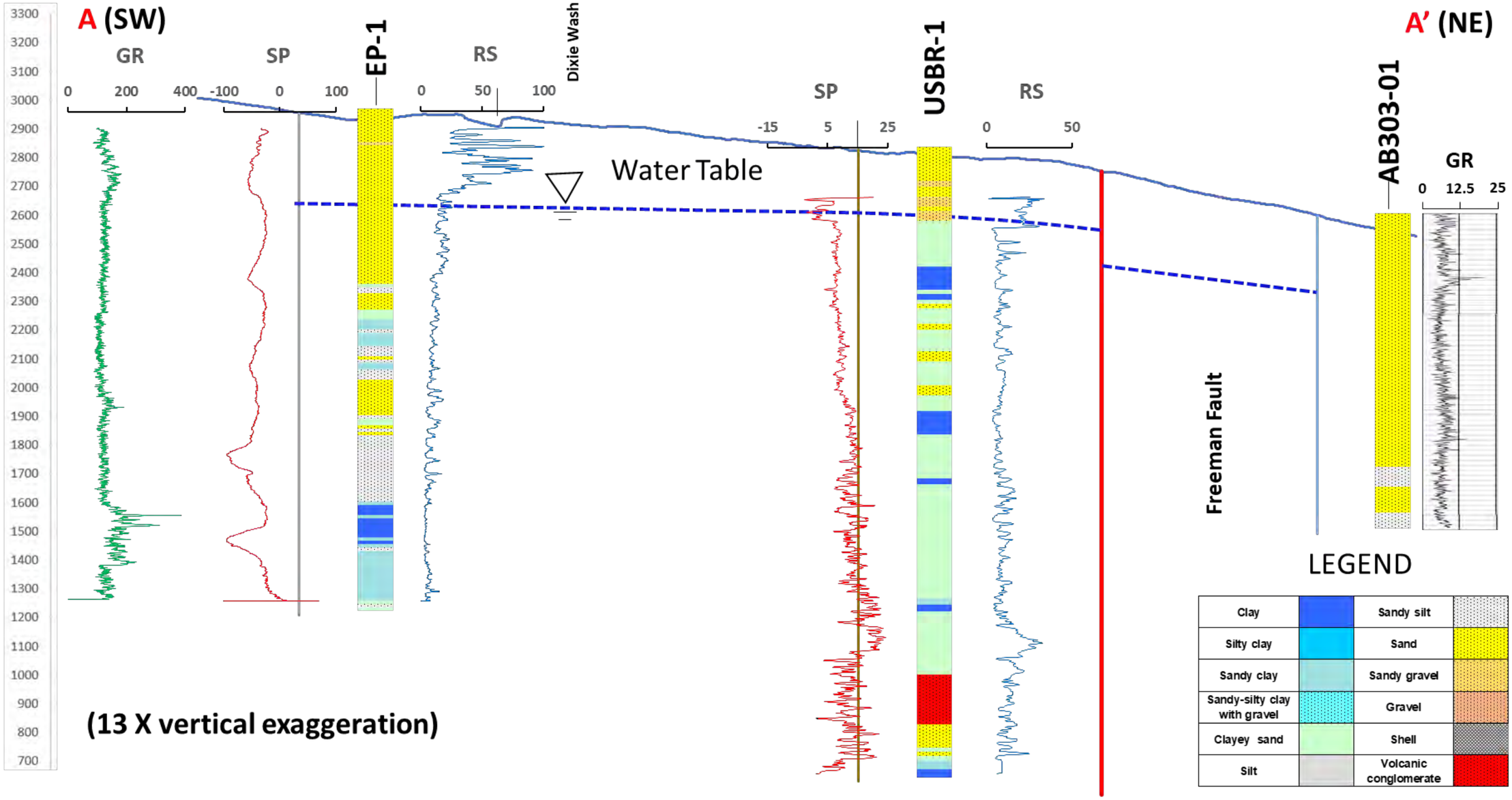
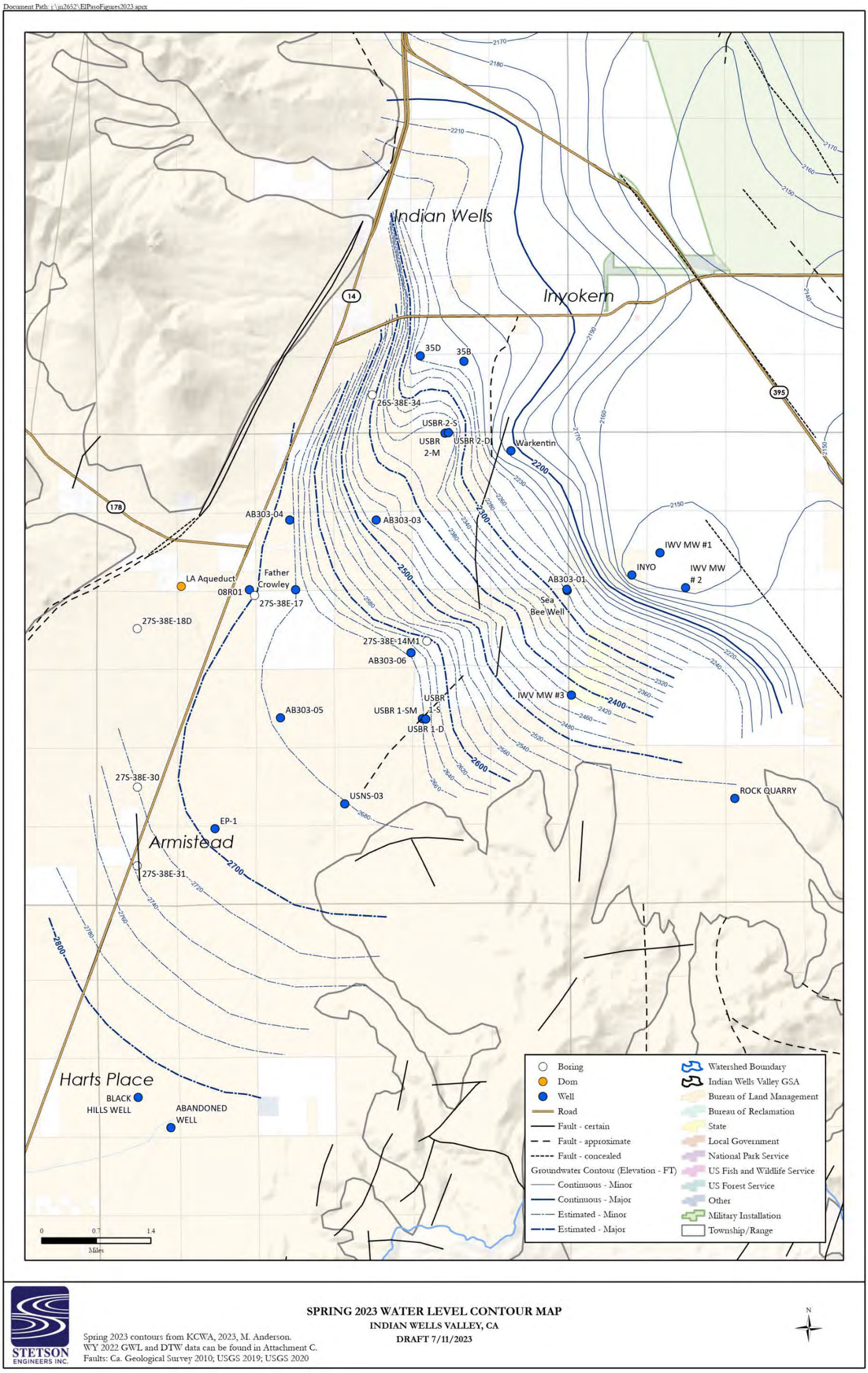


Figure 3 Cross Section AA'

Document Path: j:\jn2652\ElPasoFigures2023.aprx



STETSON ENGINEERS INC.

SPRING 2023 WATER LEVEL CONTOUR MAP
INDIAN WELLS VALLEY, CA
DRAFT 7/11/2023

Spring 2023 contours from KCWA, 2023, M. Anderson.
WY 2022 GWL and DTW data can be found in Attachment C.
Faults: Ca. Geological Survey 2010; USGS 2019; USGS 2020

Figure 4

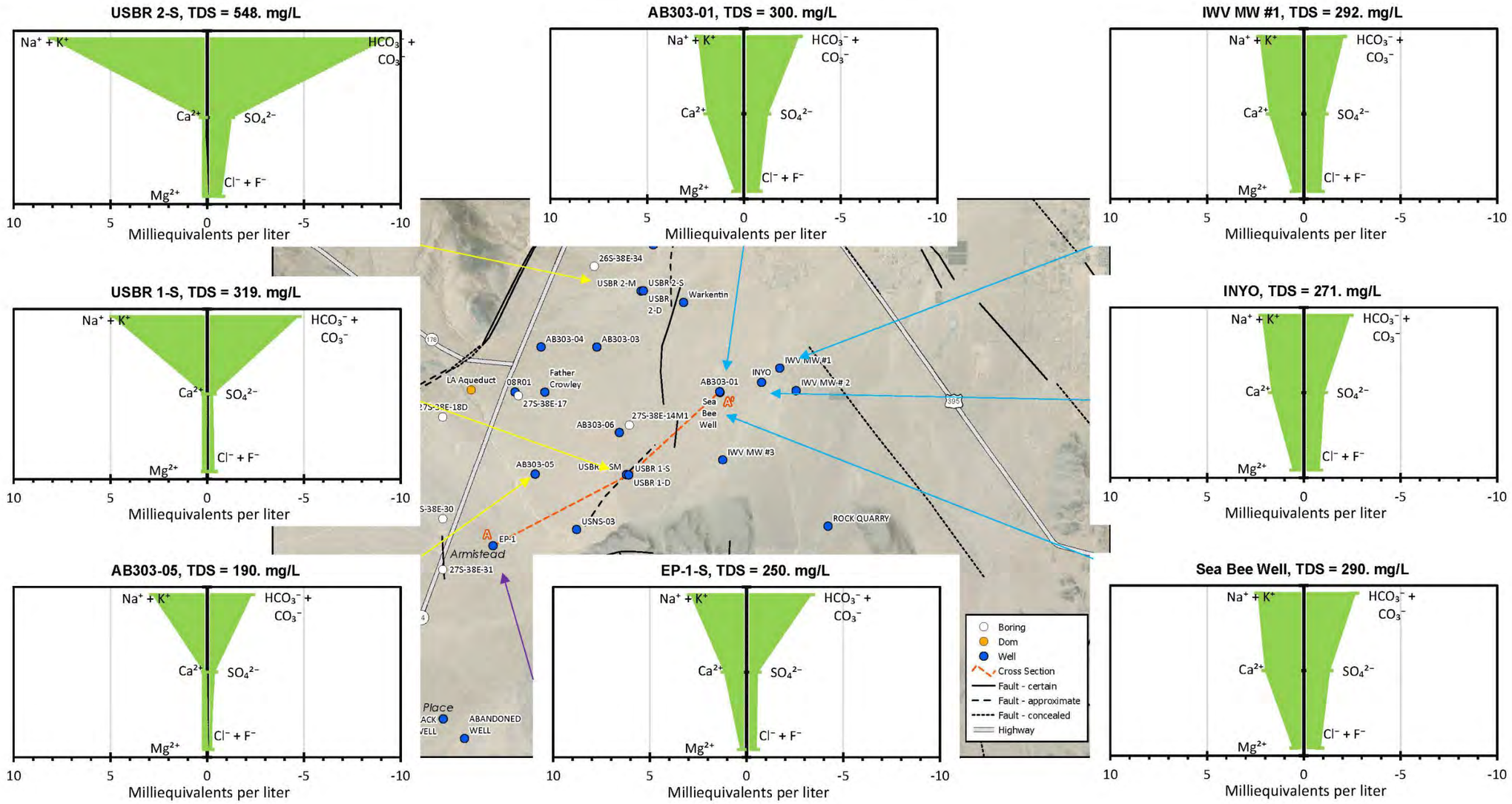


Figure 5. Stiff Diagrams for Selected Wells to the West of the Freeman Fault and near the Southwest Wellfield

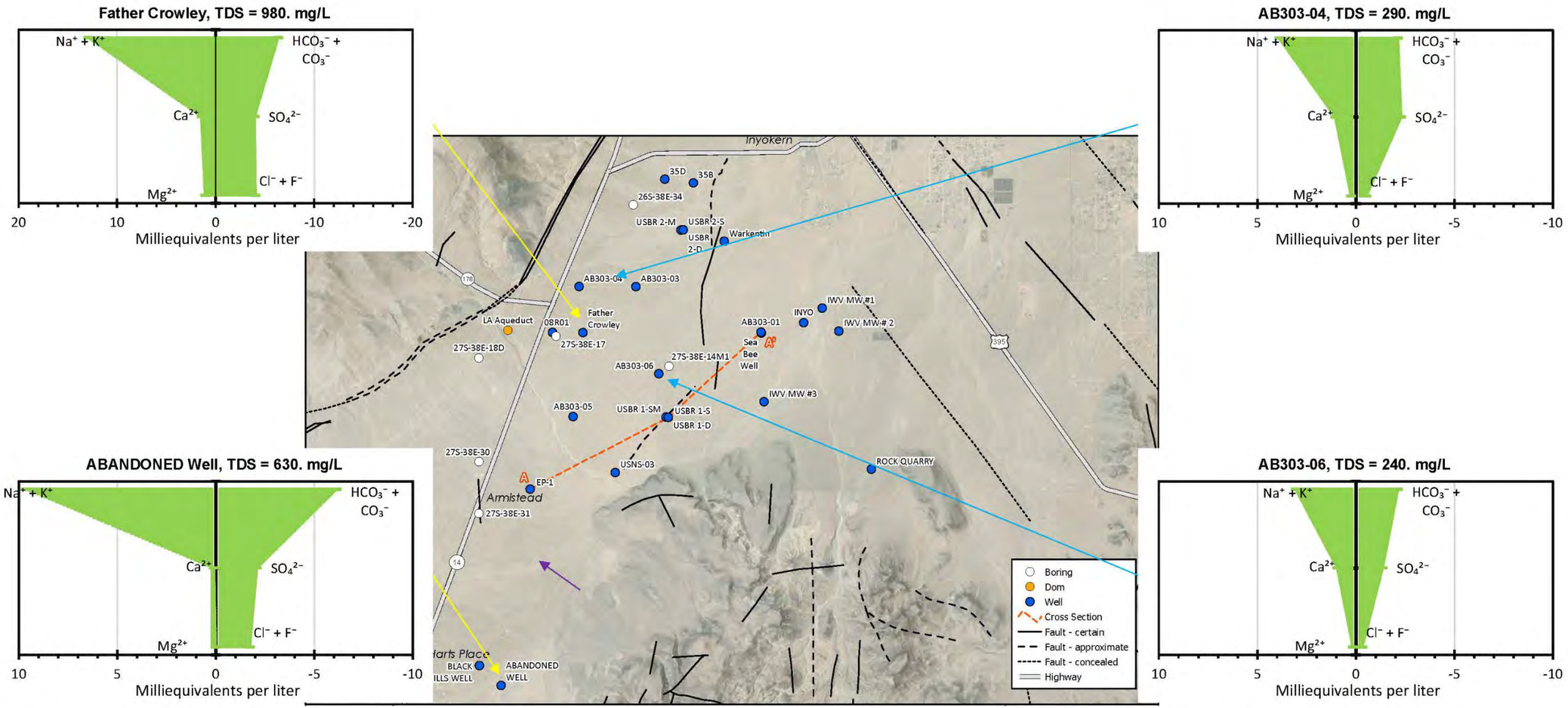
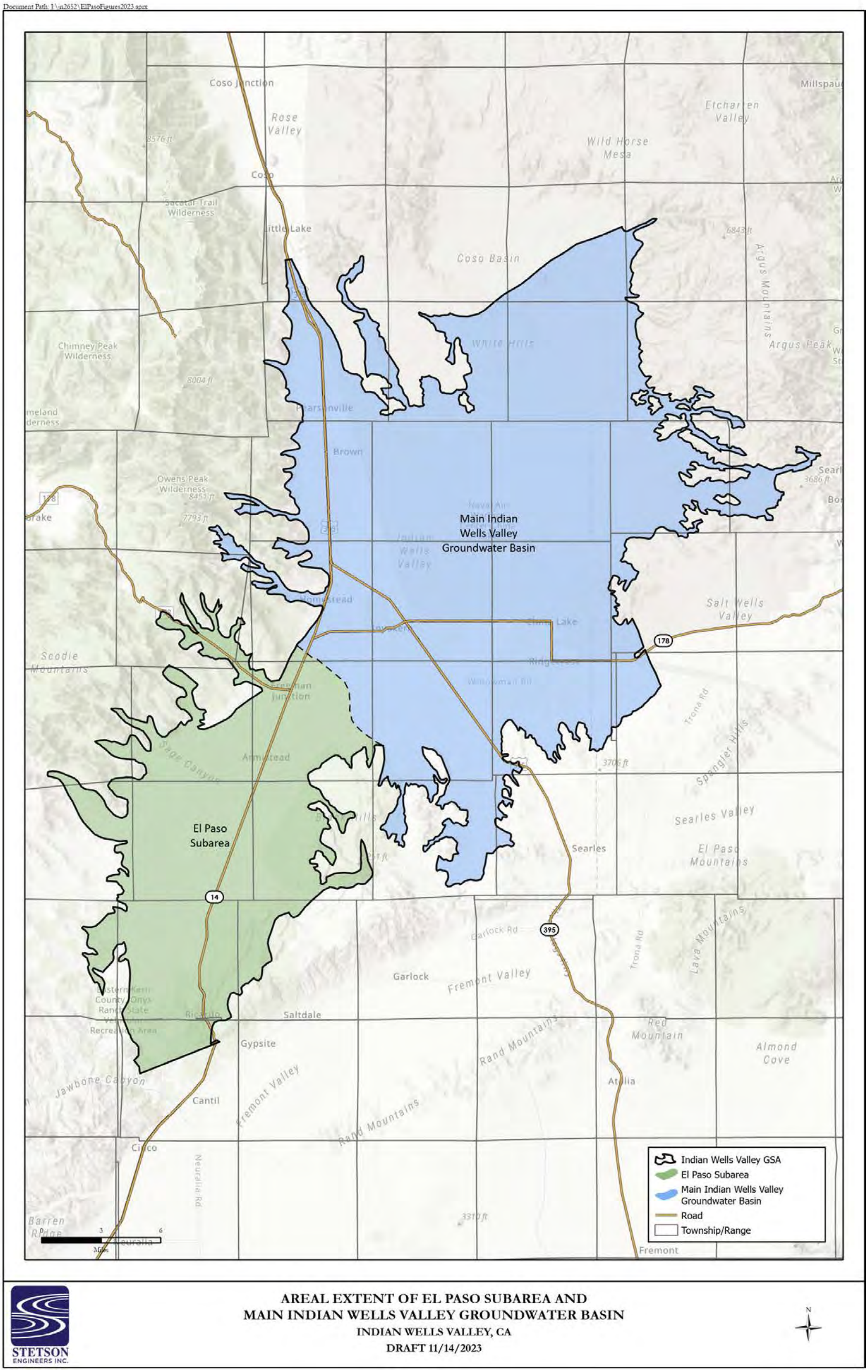


Figure 6 Stiff Diagrams for AB303-04, AB303-06, Father Crowley and Abandoned Well

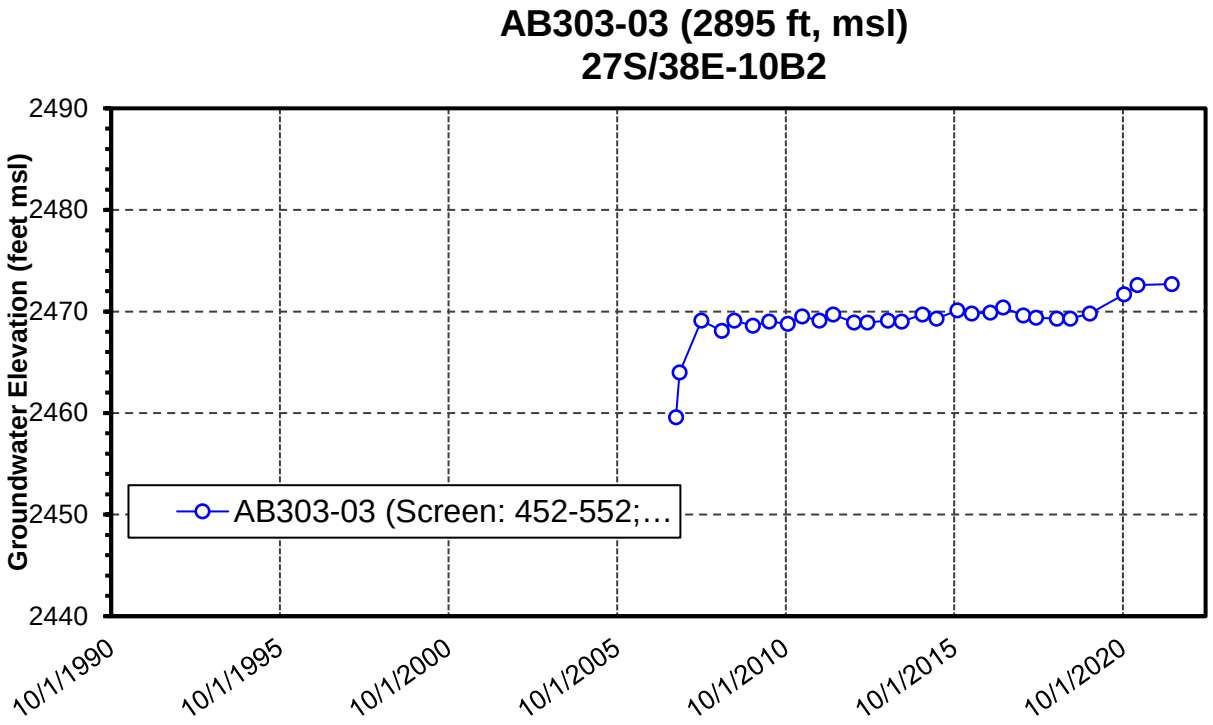
Document Path: I:\in2652\ElPasoFigures2023.aprx

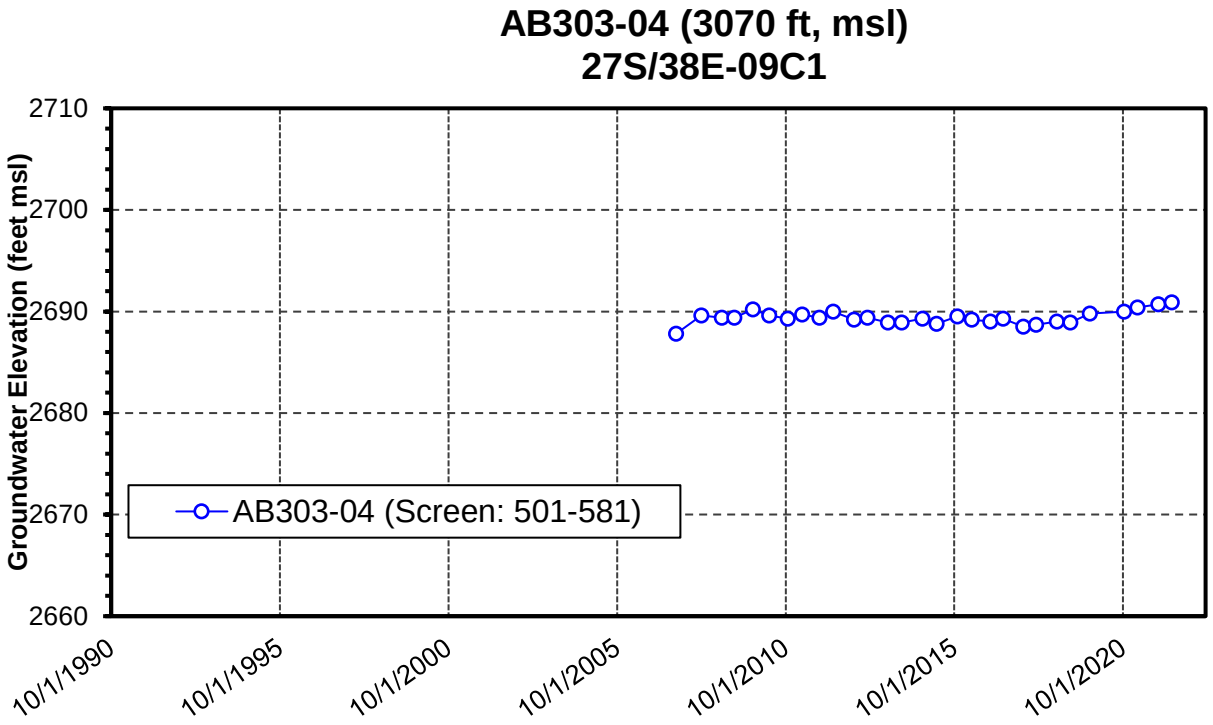


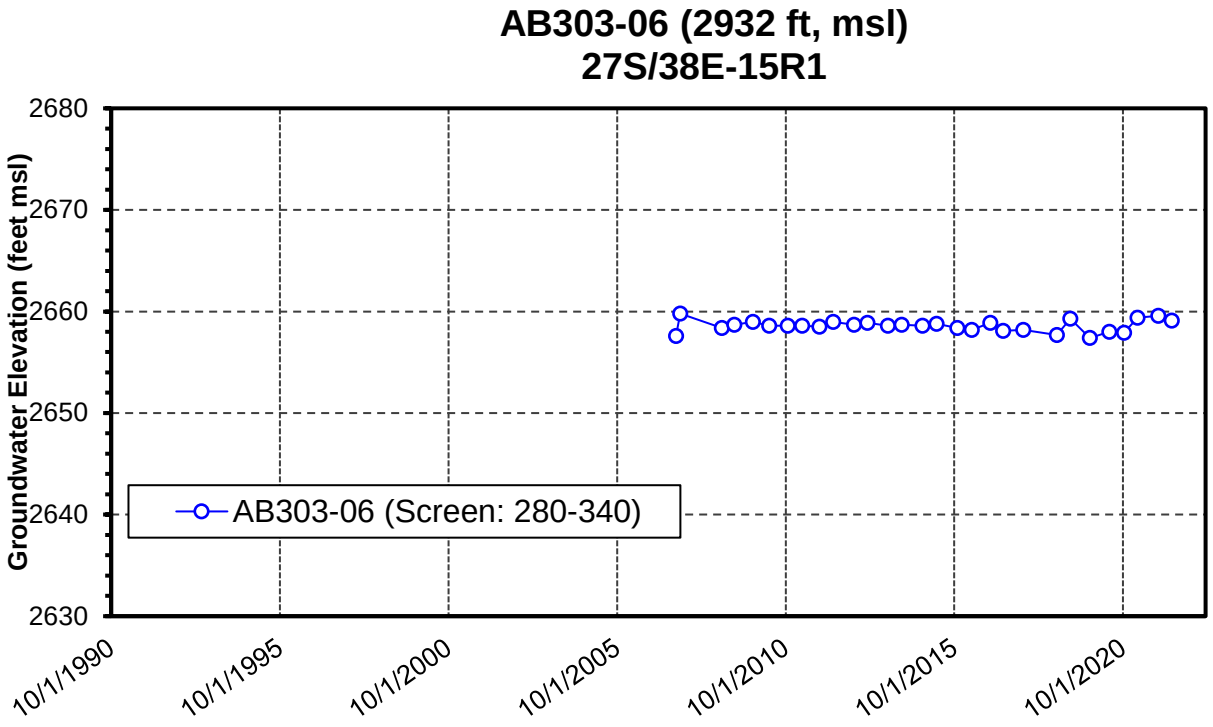
STETSON ENGINEERS INC.

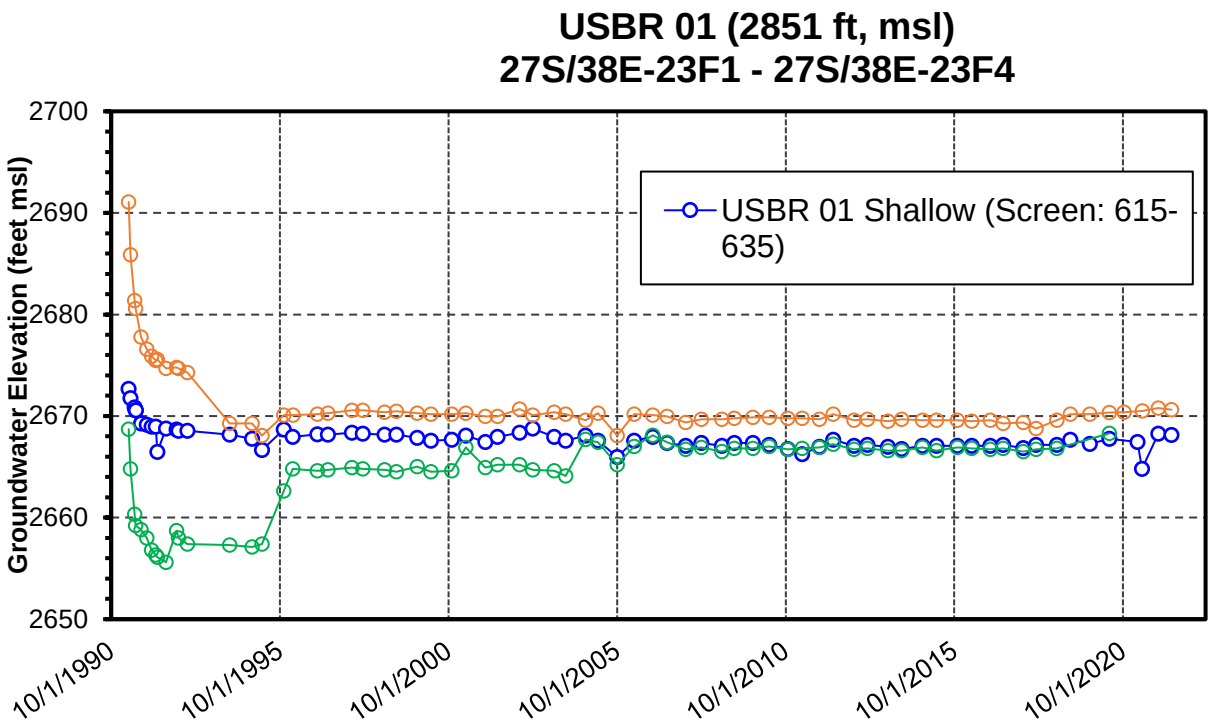
AREAL EXTENT OF EL PASO SUBAREA AND MAIN INDIAN WELLS VALLEY GROUNDWATER BASIN
INDIAN WELLS VALLEY, CA
DRAFT 11/14/2023

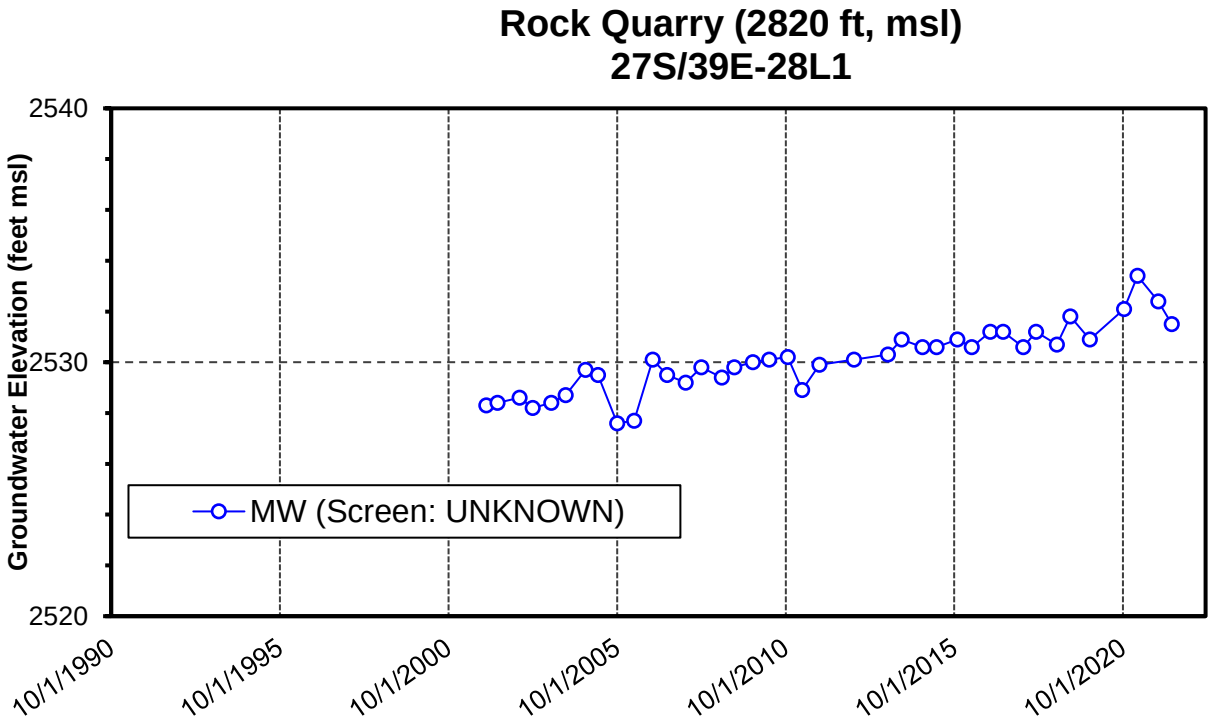
Figure 7

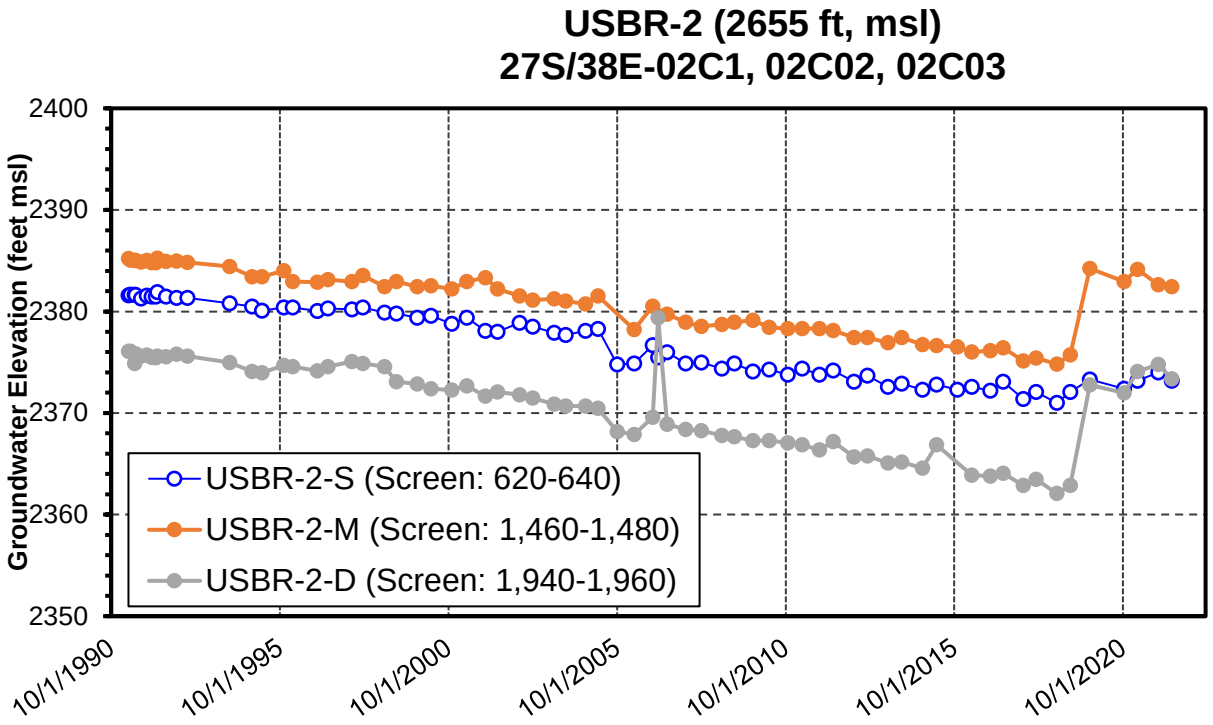

AB303-03 (2895 ft, msl)
27S/38E-10B2
Groundwater Elevation (feet msl)
2490
2480
2470
2460
2450
2440
AB303-03 (Screen: 452-552;...
10/1/1990
10/1/1995
10/1/2000
10/1/2005
10/1/2010
10/1/2015
10/1/2020

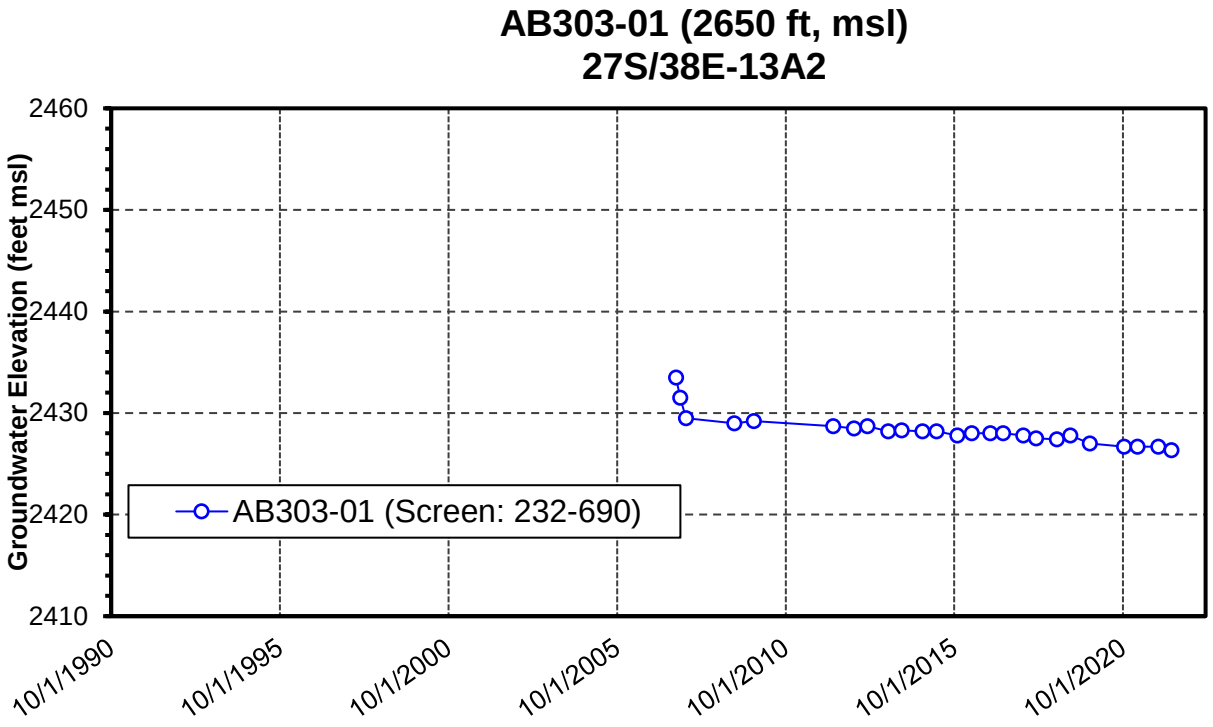

AB303-04 (3070 ft, msl)
27S/38E-09C1
Groundwater Elevation (feet msl)
2710
2700
2690
2680
2670
2660
AB303-04 (Screen: 501-581)
10/1/1990
10/1/1995
10/1/2000
10/1/2005
10/1/2010
10/1/2015
10/1/2020

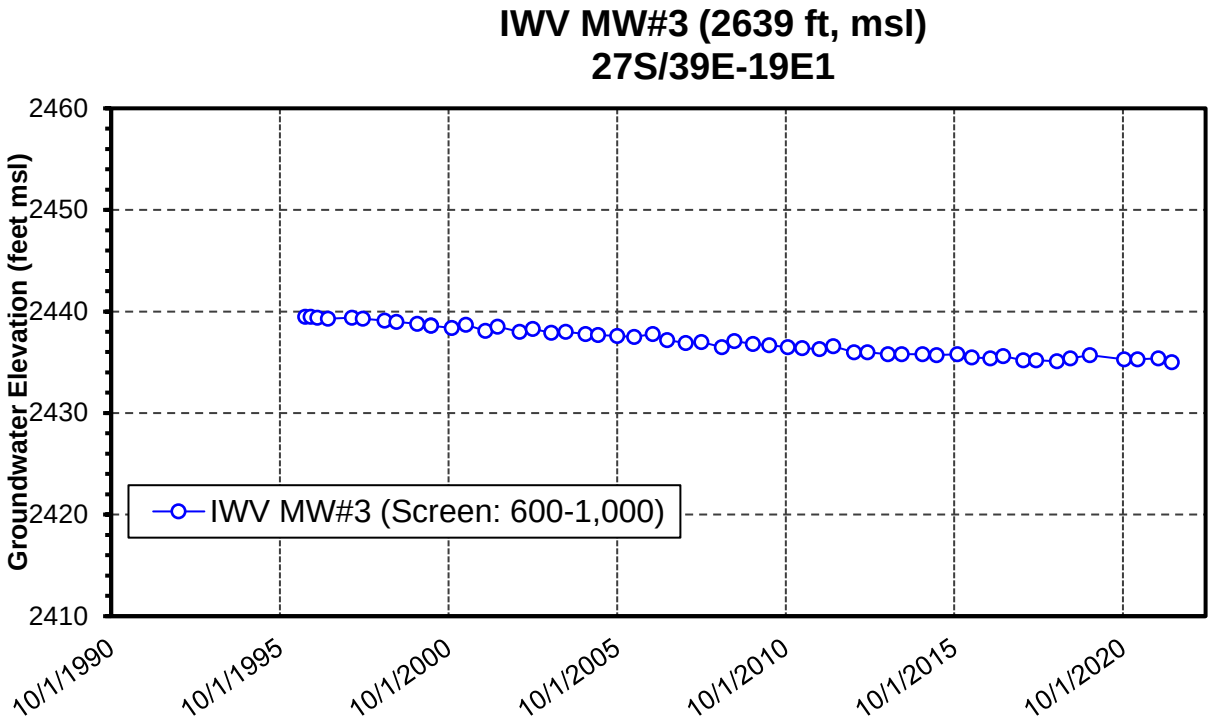

AB303-06 (2932 ft, msl)
27S/38E-15R1
Groundwater Elevation (feet msl)
2680
2670
2660
2650
2640
2630
AB303-06 (Screen: 280-340)
10/1/1990
10/1/1995
10/1/2000
10/1/2005
10/1/2010
10/1/2015
10/1/2020


USBR 01 (2851 ft, msl)
27S/38E-23F1 - 27S/38E-23F4
Groundwater Elevation (feet msl)
2700
2690
2680
2670
2660
2650
10/1/1990
10/1/1995
10/1/2000
10/1/2005
10/1/2010
10/1/2015
10/1/2020
USBR 01 Shallow (Screen: 615-635)


Rock Quarry (2820 ft, msl)
27S/39E-28L1
Groundwater Elevation (feet msl)
2540
2530
2520
MW (Screen: UNKNOWN)
10/1/1990
10/1/1995
10/1/2000
10/1/2005
10/1/2010
10/1/2015
10/1/2020


USBR-2 (2655 ft, msl)
27S/38E-02C1, 02C02, 02C03
Groundwater Elevation (feet msl)
2400
2390
2380
2370
2360
2350
10/1/1990
10/1/1995
10/1/2000
10/1/2005
10/1/2010
10/1/2015
10/1/2020
USBR-2-S (Screen: 620-640)
USBR-2-M (Screen: 1,460-1,480)
USBR-2-D (Screen: 1,940-1,960)


AB303-01 (2650 ft, msl)
27S/38E-13A2
Groundwater Elevation (feet msl)
2460
2450
2440
2430
2420
2410
AB303-01 (Screen: 232-690)
10/1/1990
10/1/1995
10/1/2000
10/1/2005
10/1/2010
10/1/2015
10/1/2020


IWV MW#3 (2639 ft, msl)
27S/39E-19E1
Groundwater Elevation (feet msl)
2460
2450
2440
2430
2420
2410
IWV MW#3 (Screen: 600-1,000)
10/1/1990
10/1/1995
10/1/2000
10/1/2005
10/1/2010
10/1/2015
10/1/2020

Attachment B

Sample ID	State ID	Screen Interval (ft bgs)	Calcium (mg/L)	Magnesium (mg/L)	Sodium (mg/L)	Potassium (mg/L)	Bicarbonate HCO_3 (mg/L)	Carbonate CO_3 (mg/L)	Chloride (mg/L)	Sulfate (mg/L)	Fluoride (mg/L)	Total Filterable Residue/TDS (mg/L)
Maximum Contaminant Level (MCL)			*n/a*	*n/a*	*n/a*	*n/a*	*n/a*	*n/a*	*500*	*500*	*2*	*1,000*
USBR 1-S	27S-38E-23F01	*615-635*	1.5	1	110	0.8	80	100	9.8	12	0.77	318.83
USBR 1-SM	27S-38E-23F02	1040-1060	0.63	0.022	94	0.28	110	73	7	9.5	0.62	280
USBR 1-D	27S-38E-23F04	1750-1770	1	0.21	110	0.4	82	97	12	11	1.2	315.73
USBR 2-S	27S-38E-02C01	640-680	3.8	0.01	180	6.2	ND	276	23	58	0.59	547.64
USBR 2-M	27S-38E-02C02	1460-1480	4	2.9	75.1	3.2	144	1	20.8	27.6	1.4	240
USBR 2-D	27S-38E-02C03	1940-1960	7.6	6.7	69	2.1	47	57	11	22	0.77	236.48
AB303-01	27S-38E-13A02	232-272; 372-472; 632-690	37	4.9	52	1.8	160	5	24	57	0.88	300
AB303-03	27S-38E-10B02	452-552, 752-852	76	0.72	58	1	35	41	4.9	23	0.36	160
AB303-04	27S-38E-09C01	502-582	21	3	88	2.8	120	5	18	110	0.29	290
AB303-05	27S-38E-21L01	905-1005	1.6	0.029	63	0.47	94	21	4.4	16	0.38	190
AB303-06	27S-38E-15R01	280-340	19	1.9	69	2	120	5	11	65	0.27	240
INYO	27S-39E-07R01	457-477	32	6	47	2.3	140	1	25	48	1	271
IWV MW #1	27S-39E-08M02	600-1000	34.5	5.82	49.8	2.08	120	1	27.7	49.4	0.97	292
IWV MW #3	27S-39E-19E01	600-1000	4	1	72	1	51	1	20	35	4	240
Sea Bee Well	27S-38E-13A01	*460-610*	39	6.1	52	2.1	150	5	27	62	0.88	290
Father Crowley	27S-38E-09P01	357-457	29	13	290	12	350	18	140	190	1.9	980
ABANDONED Well	28S/38E-18F01	*unknown*	1.9	0.25	220	2	240	66	35	100	14	630
EP-1-S	27S/38E-32C01	450-470	22	3.1	64	2.1	190	5	15	25	0.64	250

n/a - Non applicable to dataset

ND - Analyte not detected at or above the reporting limit

ATTACHMENT G

Indian Wells Valley
GSP

Appendix

Total Dissolved Solids (TDS) Database

DRAFT TECHNICAL MEMORANDUM

785 Grand Avenue, Suite 202 • Carlsbad, California • 92008
Phone: (760) 730-0701 Web site: www.stetsonengineers.com

FOR:	Appendix to Groundwater Sustainability Plan	DATE:	August 9, 2019
FROM:	Stetson Engineers, Inc.	JOB NO:	2652-001:08.03
RE:	Development of Indian Wells Valley Water Quality Database: Total Dissolved Solids (TDS)		

A Water Quality Database was developed for Indian Wells Valley Groundwater Authority to evaluate the occurrence and impacts of salinity within the groundwater basin. Total Dissolved Solids (TDS) data were collected from historical documents and verified to laboratory reports when available. The TDS database is part of the Groundwater Sustainability Plan (GSP) and will be updated as new data become available. The data will be used to evaluate changes within the basin from the management actions addressed in the GSP.

This appendix describes the data processing and review of available TDS data that was collected from groundwater wells within Indian Wells Valley groundwater basin. The initial version of the database (January 24, 2019) was reviewed by Desert Research Institute (DRI) and the Technical Advisory Committee's (TAC) Model Ad Hoc Group, and used in the TDS Transport Model developed for Indian Wells Valley's GSP. Updating of the TDS database is ongoing as new data becomes available and is added. Below is a summary of how data were compiled for the January 2019 transport model, as well as the most recent (June 2019) version of the database.

1.0. TDS SPREADSHEET DATABASE

The TDS spreadsheet database was established and formatted to easily provide data for the GSP, the Indian Wells Valley groundwater model, and other studies[1] for analysis of the salinity within the groundwater basin. For the model, the database contains (1) well construction information/locations and spring/surface water locations where TDS samples were collected and analyzed, and (2) date and sample results. The horizontal and vertical distribution of measured TDS data was established based on surveyed well locations and well completion records where available[2]. In addition, the database has a record of all changes and updates, as well as a place to

[1] The Brackish Water Group has used this TDS Database for their analysis of potential saline groundwater projects within the Indian Wells Valley basin.
[2]

contain incomplete data that still needs to be verified. The TDS spreadsheet database contains the following worksheet tabs:

1. "Wells+SW" 551 wells and 13 surface water sampling locations
2. "TDS" 2,044 TDS sample results from 1/26/1920 to 3/5/2019
3. "References" 20 referenced reports or databases
4. "Open Items" 12 open items of potential data sources to follow-up
5. "Notes" journal of data processing conducted Oct 2018 through Jun 2019
6. "Incomplete (+Suspect) TDS Data" data that is questionable and could not be verified.

The accompanied tables and figure to this appendix contain the data and information available in the first five worksheet tabs within the TDS spreadsheet database and demonstrate the database setup. Table 1 shows the elements that define the location of the sample (well, spring, or surface water) and the total depth and screen interval data available for wells. Table 2 provides an example of the TDS data including sample location name, sample date and result, analysis type, the reference of where the data came from, and the confidence level of the data. Table 3 lists the 20 references from which the TDS data was compiled. Table 4 lists 12 open items of potential data that require more research. And, Table 5 contains the journal notes of the work completed on the database through June 2019. TDS data from the June 2019 database are displayed on Figure 1, which shows the horizontal extent and concentration distribution of the most recent TDS measured within the Indian Wells Valley basin.

2.0. DATA PROCESSING

TDS data were initially compiled into a spreadsheet by the Brackish Water Group (BWG) for a study of saline water use within Indian Wells Valley[3]. The data were given to the Groundwater Authority's Water Resource Manager to develop into a TDS database for the GSP and to develop the initial TDS conditions for the Indian Wells Valley model evaluation of salinity conditions within the groundwater basin. Historical documents and databases were collected and TDS data were cross checked with referenced material. Sample dates were updated from report date to sample date, and duplicate TDS samples were removed.

An 'Analysis Type' column was added to differentiate between TDS samples that were the sum of constituents (calc), total filterable residue at 180°C (lab), or if analysis type was not specified (unk). TDS data were also given confidence levels dependent on 1) if data underwent a QA/QC check against the original report (confidence level 1); 2) data were sourced to reports that

[3] Received from Wade Major, AquiLogic, October 2018

were unavailable for QA/QC checks by Stetson (confidence level 2), or 3) data was unverified (confidence level 3). Concurrent with these crosschecks, missing data were added to the database.

Following verification of data with original published reports, data from the Groundwater Ambient Monitoring and Assessment Program (GAMA) were added to the database. Additional verification was completed of original report data and GAMA data. Duplicate samples were removed. When two samples from different sources were collected on the same date TDS values from the most trusted source were used in the database. On occasions where sources and sample date were the same a conservative approach was taken and the highest TDS value was kept.

As new TDS sample data are added to the database, data are crosschecked against data in the TDS database before being added. If data are currently in the database, sources may be updated. However, if TDS samples are not in the database, data are added. Currently, there are 2,044 TDS sample results from 1/26/1920 to 3/5/2019.

3.0. Inventory of Sampled Wells and Surface Water Locations

Well and surface water sample sites were compiled into a separate table, and a unique list of TDS sample locations was developed. Duplicate sites were removed and remaining sites were given unique names. Coordinates and construction data for these wells were compiled to provide the horizontal and vertical water quality location for mapping (Figure 1) and modeling. As new TDS data are added to the database, sample locations for new data are cross checked against location data in the database. New sample locations are appended to the database with unique database IDs. The June 2019 TDS database has 551 wells and 13 surface water sampling locations with measured TDS data.

4.0. References, Open Items, and Notes

The References, Open Items, and Notes tabs of the TDS database contain data sources, a running list of open items to make the database more complete, and a journal of all changes and updates made to the database. These sections maintain the integrity of the spreadsheet database and are key components of keeping it organized and maintaining a record of changes and edits. The most recent June 2019 version of the database contains data sourced from 20 references. Each reference listed on Table 3 indicates the number of TDS samples attributed to it. The Open Items worksheet tab contains a list of open items of some incomplete data that needs to be resolved before it can be included in the TDS database.

The Notes section contains a record of all changes and updates made in the TDS database beginning with the original data compilation provided by the Brackish Water Group. Since the January 2019 iteration (model run) the database has been updated 4 times.

Table 1: TDS Sample Locations

Depth and screen intervals are given in feet below ground surface

Notes: PLScntr - center point of corresponding Township/Range-Section & Tract (if available)

Unique Well Name	Latitude	Longitude	X_UTM	Y_UTM	Depth	Screen Interval[1]	Screen Interval[2]	Screen Interval[3]	Screen Interval[4]	Screen Interval[5]	Notes
24S38E16J02	35.84889	-117.87306	421162.772	3967540.019	611	251-611					
24S38E21A01	35.84144	-117.87177	421271.165	3966712.737	660	640-660					
24S38E21A02	35.84144	-117.87177	421271.165	3966712.737	1200	1180-1200					
24S38E21A03	35.84144	-117.87177	421271.165	3966712.737	1580	1560-1580					
24S38E21A04	35.84144	-117.87177	421271.165	3966712.737	1950	1930-1950					
24S38E28Q01	35.81412	-117.87452			450						
24S38E33J02	35.80194	-117.87167	421241.823	3962332.036	375	240-375					
24S38E35E01	35.80690	-117.85090									
24S39E33D01	35.80773	-117.77812									
24S39E33N01	35.79940	-117.77868									
24S39E34D01	35.80215	-117.75898			325	205-305					
24S40E06A01	35.88328	-117.69368									
24S40E20J01	35.83190	-117.67451			28	58-60					
24S40E21K01	35.83151	-117.65774	440592.878	3965460.296	72	60-70					
24S40E33N01	35.79930	-117.66820	439624.477	3961894.250	16						
24S40E34E01	35.80662	-117.65006			21						
24S40E36A	35.80108	-117.61616	444327.135	3962060.345	27	15-25					
24S40E36M01	35.80024	-117.61486	444443.989	3961967.211	8						
25S38E02E	35.79097	-117.86160			765	310-753					
25S38E02L01	35.79465	-117.86160	422144.413	3961514.811	765						
25S38E03G01	35.79551	-117.87291	421122.734	3961619.689							
25S38E10G	35.77678	-117.87274	421120.046	3959541.507							
25S38E11K02	35.77551	-117.85063									
25S38E11L01	35.77578	-117.86063			400						
25S38E12E	35.77982	-117.84723	423428.145	3959858.948	300						
25S38E12L01	35.77606	-117.84201	423896.400	3959437.926	350	330-350					
25S38E12L02	35.77606	-117.84201	423896.400	3959437.926	1210	1190-1210					
25S38E12L03	35.77611	-117.84111	423978.090	3959442.602	1660	1640-1660					
25S38E12M	35.77575	-117.84655			700	140-700					
25S38E12M01	35.77600	-117.84634	423505.310	3959434.414							
25S38E12Mct	35.75501	-117.84550									
25S38E13C	35.76909	-117.84322			430	260-600					
25S38E13D01	35.76884	-117.84424									
25S38E13J01	35.75833	-117.83389	424614.094	3957465.218	155						
25S38E13L	35.76125	-117.84012			444	109-444					
25S38E13L01	35.75831	-117.83814	424229.868	3957466.152	444						
25S38E13M	35.75998	-117.84689									
25S38E13Q	35.75418	-117.83730				120-490					
25S38E14M02	35.75906	-117.86291	421990.841	3957568.244	405	109-444					
25S38E14N01	35.75740	-117.86271	422007.545	3957384.300	405						
25S38E23G01	35.74895	-117.85644	422565.848	3956441.987	259						
25S38E23J01	35.74690	-117.84813									
25S38E24H	35.71894	-117.86983	421325.663	3953124.732							
25S38E24K	35.74693	-117.83530			490	120-490					
25S38E24K01	35.74511	-117.83702									PLScntr
25S38E24L	35.74368	-117.84160			517	117-571					
25S38E25C	35.73938	-117.84233	423832.878	3955369.942							
25S38E25C01	35.73811	-117.84007	424035.925	3955227.239	305						
25S38E25G01	35.73605	-117.83563	424435.795	3954994.714	305						
25S38E25J	35.73050	-117.83256	424707.961	3954376.772	330	120-330					PLScntr; Elev 2275'
25S38E25J01	35.73217	-117.83174	424784.137	3954562.235	270	250-270					
25S38E25J02	35.73217	-117.83174	424784.137	3954562.235	1150	1130-1150					
25S38E25J03	35.73217	-117.83174	424784.137	3954562.235	1980	1960-1980					
25S38E25Q	35.72477	-117.83008	424927.278	3953740.082							
25S38E34A01	35.72457	-117.86932	421377.590	3953747.942	485						
25S38E34G01	35.71703	-117.86609	421662.927	3952909.855	870	850-870					
25S38E34G02	35.71806	-117.87083	421234.469	3953026.891	1610	1590-1610					
25S38E34G03	35.71806	-117.87083	421234.469	3953026.891	1980	1960-1980					
25S38E34J02	35.71648	-117.86581	421687.582	3952848.499							
25S38E34J03	35.71648	-117.86581	421687.663	3952848.528							
25S38E35A	35.72250	-117.84917	423198.498	3953502.665							
25S38E35H	35.71832	-117.85221	422918.956	3953041.383							
25S38E35M01	35.71557	-117.86159	422068.514	3952743.813	350						

Table 1: TDS Sample Locations

Depth and screen intervals are given in feet below ground surface

Notes: PLScntr - center point of corresponding Township/Range-Section & Tract (if available)

Unique Well Name	Latitude	Longitude	X_UTM	Y_UTM	Depth	Screen Interval[1]	Screen Interval[2]	Screen Interval[3]	Screen Interval[4]	Screen Interval[5]	Notes
25S38E36A01	35.72134	-117.83062			285						
25S38E36B01	35.72495	-117.83674	2048734.884	809805.814	400	130-170	200-220	240-260			
25S38E36D	35.72323	-117.84588	423496.905	3953580.929							
25S38E36G01	35.71869	-117.84268	423781.325	3953074.734	350	330-350					
25S38E36G02	35.71869	-117.84268	423781.325	3953074.734	1560	1540-1560					
25S38E36G03	35.71869	-117.84268	423781.325	3953074.734	1930	1910-1930					
25S38E36Q01	35.71277	-117.83801	424198.053	3952414.935	285	139-285					
25S39E01N01	35.78440	-117.73840				12.8-18.8					
25S39E02E01	35.71924	-117.80844	426879.072	3953110.190	211						
25S39E04R01	35.78645	-117.77834			200	100-200					
25S39E07K01	35.77359	-117.81789	426074.295	3959145.384	122						
25S39E09J01	35.77441	-117.77789			200						
25S39E10E01	35.77690	-117.77479									
25S39E10Q01	35.76940	-117.76618									
25S39E12R02	35.77028	-117.72500	434467.935	3958711.752	150	65-140					
25S39E13E01	35.76356	-117.73979									
25S39E14H01	35.76208	-117.84792	423349.533	3957892.087							
25S39E17D01	35.76829	-117.80979			88						
25S39E19K01	35.74634	-117.82007									
25S39E21B01	35.75273	-117.78423									
25S39E22B01	35.75329	-117.76479									
25S39E22J01	35.74278	-117.76194	431104.797	3955686.968							
25S39E23G01	35.74809	-117.75740	431520.200	3956273.227		850-870					
25S39E23G02	35.74809	-117.75740	431520.200	3956273.227		3300-3320					
25S39E23G03	35.74809	-117.75740	431520.200	3956273.227		5550-5570					
25S39E23G04	35.74809	-117.75740	431520.200	3956273.227		7120-7140					
25S39E24D01	35.75235	-117.73757	433316.313	3956731.329	27						
25S39E26H01	35.73341	-117.74243	432861.438	3954634.191	302						
25S39E28P01	35.72523	-117.78562			161						
25S39E30L01	35.73041	-117.82340									PLScntr
25S39E30N01	35.72745	-117.82757									
25S39E31D01	35.71770	-117.82140			300						PLScntr
25S39E31E01	35.71884	-117.82979									
25S39E31M03	35.71606	-117.82924									
25S39E31R01	35.71056	-117.81444	426327.969	3952151.250	480	120-180					
25S39E35N01	35.71032	-117.75858	431381.500	3952084.992							
25S40E08A01	35.78586	-117.66842	439593.651	3960403.118	17						
25S40E11K01	35.77344	-117.63879	442262.853	3959008.516	62	140-300					
25S40E12M01	35.77347	-117.62642	443381.082	3959004.813	59						
25S40E14H01	35.76417	-117.63716	442403.727	3957979.628	23	11-21					
25S40E18R01	35.75969	-117.60148	445625.691	3957461.829	31.3						
25S40E19L01	35.74458	-117.69887	436809.254	3955844.280	24						
25S40E20F01	35.74889	-117.67835	438668.003	3956309.815	183						
25S40E24H01	35.75572	-117.61493	444406.881	3957029.156	40						
25S40E24N01	35.73995	-117.62923			31						
25S40E25H01	35.73273	-117.61729									
25S40E27E01	35.73134	-117.64562	441614.568	3954342.635	19						
25S40E30E01	35.73254	-117.72033	434859.246	3954522.796	72						
25S40E33L01	35.71288	-117.65800	440481.525	3952302.729	171	70-90	110-130				
25S40E33L02	35.71674	-117.67923	438563.755	3952743.842	22	2-22					
25S40E35D01	35.72064	-117.65140	441083.880	3953159.847	15	10-15					
25S40E35P01	35.71152	-117.64259	441873.942	3952142.791	18	10-15					
25S41E18Q01	35.76790	-117.61430									PLScntr
25S41E19L01	35.74990	-117.60864	444971.386	3956380.295	24						
25S41E21E01	35.75356	-117.57367			188						
25S41E31C01	35.72819	-117.60532	445257.084	3953969.901	14						
26S38E01G02	35.70377	-117.83564	424404.679	3951414.622	365						
26S38E01H03	35.70580	-117.83102	424824.396	3951636.827							
26S38E02Q01	35.70000	-117.85639	422523.507	3951012.794							
26S38E11P02	35.68303	-117.85931			515						
26S38E12R01	35.68175	-117.82912	424973.058	3948967.631							
26S38E17E01	35.67662	-117.91229			110						
26S38E27G01	35.64523	-117.87424			723						
26S38E35B01	35.63567	-117.85504			289						PLScntr

Table 1: TDS Sample Locations

Depth and screen intervals are given in feet below ground surface

Notes: PLScntr - center point of corresponding Township/Range-Section & Tract (if available)

Unique Well Name	Latitude	Longitude	X_UTM	Y_UTM	Depth	Screen Interval[1]	Screen Interval[2]	Screen Interval[3]	Screen Interval[4]	Screen Interval[5]	Notes
26S38E35L	35.62824	-117.85875	422240.002	3943055.734							
26S39E01A02	35.70940	-117.72312	434587.972	3951958.206		200-298					
26S39E02C01	35.70912	-117.75034									
26S39E02N01	35.69662	-117.75562									
26S39E03D01	35.70773	-117.77590									
26S39E05F01	35.70500	-117.80667	427026.473	3951529.258	200	100-200					
26S39E06F01	35.70454	-117.82441	425420.512	3951491.050	305						
26S39E06G01	35.70576	-117.81752	426045.685	3951622.209	285						
26S39E07B	35.69317	-117.81919				205-215					
26S39E07K05	35.68729	-117.81928	425868.852	3949574.611	305						
26S39E07L	35.68163	-117.81839	425944.686	3948945.929	235						
26S39E07M02	35.68757	-117.82818	425064.213	3949612.018	400						
26S39E07M1	35.68696	-117.83003				200-400					
26S39E07M2	35.68732	-117.82997				0-16					
26S39E07N01	35.68317	-117.82567	425287.052	3949122.575							
26S39E07P02	35.68172	-117.82446	425395.065	3948960.061	300						
26S39E07P03	35.68345	-117.82278	425548.568	3949151.727	305						
26S39E08E01	35.69059	-117.80706	426977.822	3949931.755	880						
26S39E08K01	35.68801	-117.79951									
26S39E09H01	35.69116	-117.77669	429726.588	3949972.784		570-880					
26S39E09M01	35.69080	-117.79362	428194.355	3949944.290							
26S39E10E01	35.69127	-117.77660	429733.986	3949984.014							
26S39E10N01	35.69005	-117.75660	431542.946	3949834.591							
26S39E11E01	35.69005	-117.75660	431542.946	3949834.591	250						
26S39E11E02	35.68857	-117.75646	431554.791	3949670.293	191						
26S39E11Q01	35.68107	-117.74868									
26S39E12E01	35.68829	-117.72118									
26S39E12G01	35.68884	-117.73062									
26S39E12N01	35.68245	-117.73812									
26S39E13R03	35.66662	-117.72423	434452.520	3947214.494	300						
26S39E13R04	35.66662	-117.72423	434452.520	3947214.494	800	640-800					
26S39E14E01	35.67551	-117.75757			242						
26S39E14P01	35.66676	-117.74889	432221.263	3947246.791							
26S39E17F02	35.67612	-117.80247	427380.155	3948322.457	881						
26S39E17L01	35.67213	-117.80564				681-881					PLScntr
26S39E18A01	35.67962	-117.81588	426169.715	3948721.395	300						
26S39E18C03	35.67836	-117.82381	425451.147	3948587.678	405						
26S39E18F01	35.67580	-117.82350									PLScntr
26S39E18K01	35.67134	-117.81812			330						
26S39E18K02	35.67257	-117.81792	425978.410	3947940.885	310						
26S39E18R01	35.66830	-117.81225	426487.830	3947463.452	305	290-310					
26S39E19K01	35.65564	-117.82056			803	270-666	590-625	700-790			
26S39E19P01	35.65273	-117.82062			446						
26S39E19P02	35.65264	-117.82092			600	320-360	390-590				
26S39E19Q01	35.64306	-117.81256	426436.600	3944663.332	371						
26S39E20C01	35.66361	-117.80750	426913.344	3946939.340	245						
26S39E20F01	35.66162	-117.80507									
26S39E20K03	35.65654	-117.79921	427657.295	3946148.827	360						
26S39E20Q01	35.65218	-117.80229									
26S39E20R01	35.65445	-117.79532			920	600-900					
26S39E20R02	35.65329	-117.79507			920						
26S39E21Q01	35.65428	-117.78609			1000	700-1000					
26S39E23E01	35.65718	-117.75840									
26S39E23H02	35.65917	-117.74250									
26S39E23H02a	35.65972	-117.74337			1000	470-510	580-650	730-850	900-960		
26S39E23J01	35.66023	-117.74395			660						Note two TD: 660 and 800
26S39E24E01	35.65968	-117.73979									
26S39E24K01	35.65841	-117.72763	434138.241	3946306.191	323	600-900					
26S39E24M	35.65611	-117.73889									
26S39E24M01	35.65975	-117.73966	433050.710	3946462.889	800						
26S39E24P01	35.65301	-117.73340			825	250-350	490-580	640-780			
26S39E24P03	35.65273	-117.73262			1002	503-583	651-731	808-888	930-990		

Table 1: TDS Sample Locations

Depth and screen intervals are given in feet below ground surface

Notes: PLScntr - center point of corresponding Township/Range-Section & Tract (if available)

Unique Well Name	Latitude	Longitude	X_UTM	Y_UTM	Depth	Screen Interval[1]	Screen Interval[2]	Screen Interval[3]	Screen Interval[4]	Screen Interval[5]	Notes
26S39E24Q01	35.64367	-117.71566	435209.790	3944663.673	345						Note two TD: 345 and 361
26S39E24R01	35.65481	-117.72315	434540.396	3945903.877	460						
26S39E25D01	35.63941	-117.72421	434431.841	3944196.250							
26S39E25E	35.64656	-117.73953			387	179-387					
26S39E25E01	35.63597	-117.72399	434449.830	3943815.050	387	179-260	268-284	291-384			
26S39E26A01	35.64967	-117.74214	432817.049	3945346.810	1200	1190-1200					
26S39E26A02-D	35.64980	-117.74234	432799.545	3945360.806	752	730-750					
26S39E26A02-I	35.64980	-117.74234	432799.545	3945360.806	372	350-370					
26S39E26B	35.65151	-117.74670	432405.574	3945553.195	1030	410-490	540-560	735-1015			
26S39E26B1	35.64835	-117.74803				263-323					
26S39E26B2	35.65065	-117.74833			320						
26S39E26C01	35.63993	-117.73989	2077563.420	778915.630	349	190-197	230-278	287-301			
26S39E26D01	35.64860	-117.75760									
26S39E26D02	35.65121	-117.75548	431611.010	3945526.931	1030						
26S39E26L04	35.64136	-117.74913	432177.559	3944430.042	385						
26S39E27C01	35.64830	-117.76900			500						
26S39E27D	35.65024	-117.77578	429773.046	3945433.238	1220	600-1200					
26S39E27D01	35.64844	-117.77495	429846.237	3945233.092	380	360-380					
26S39E27D02	35.64844	-117.77495	429846.237	3945233.092	900	880-900					
26S39E27D03	35.64844	-117.77495	429846.237	3945233.092	1260	1240-1260					
26S39E27D04	35.64844	-117.77495	429846.237	3945233.092	1920	1900-1920					
26S39E27J	35.64176	-117.76212				300-360					
26S39E27L1	35.64321	-117.76863				0-20					
26S39E27L2	35.64334	-117.76866									
26S39E27Q	35.63830	-117.76648				320-360					
26S39E28A01	35.65012	-117.77875									PLScntr
26S39E28B02	35.65051	-117.78284			300						
26S39E28B1	35.65076	-117.78256				0-85					
26S39E28B2	35.65048	-117.78226				0-85					
26S39E28B3	35.65067	-117.78253									
26S39E28C02	35.64086	-117.77906	429467.342	3944394.998	364						
26S39E28D01	35.64864	-117.79067	428423.197	3945266.703	385						
26S39E28G03	35.64521	-117.78397	429026.512	3944881.554	405						
26S39E28P01	35.63920	-117.78760			400						
26S39E28R01	35.63806	-117.77741	429614.648	3944083.645	1220	600-1200					
26S39E29L1	35.64206	-117.80625				0-10					
26S39E29L2	35.64209	-117.80435									
26S39E29P01	35.63953	-117.80380	427226.212	3944266.213	405						
26S39E30C01	35.64857	-117.82146			338						
26S39E30F01	35.64745	-117.82146			386						
26S39E30F03	35.64745	-117.82146			420						
26S39E30J01	35.64425	-117.81385			430	294-298	306-325	330-343	360-370	393-413	location from GAMA (does not agree w previous reports)
26S39E30J02	35.64360	-117.81620									
26S39E30K	35.64379	-117.81723									
26S39E30L	35.64399	-117.81394				300-327					
26S39E31A02	35.63681	-117.81409	426292.276	3943972.160	405						
26S39E31G	35.63148	-117.81871				320-330					
26S39E31H	35.63152	-117.81640									
26S39E31R01	35.62389	-117.81551	426151.708	3942540.317							
26S39E32K	35.62841	-117.80100				320-380					
26S39E32L	35.62905	-117.80464									
26S39E32L01	35.62998	-117.81057	426604.270	3943211.016							
26S39E32M	35.62790	-117.81075				370-380					
26S39E32N	35.62377	-117.80867				366-376					note: two sources for screen intervals: 366-376 and 266-276
26S39E32Q01	35.62577	-117.79902	427646.667	3942735.650	426						
26S39E33B	35.63546	-117.78407									

Table 1: TDS Sample Locations

Depth and screen intervals are given in feet below ground surface

Notes: PLScntr - center point of corresponding Township/Range-Section & Tract (if available)

Unique Well Name	Latitude	Longitude	X_UTM	Y_UTM	Depth	Screen Interval[1]	Screen Interval[2]	Screen Interval[3]	Screen Interval[4]	Screen Interval[5]	Notes
26S39E34F05	35.63054	-117.76836	430427.337	3943242.939	505						
26S39E34H02	35.63104	-117.76082	431110.042	3943293.561	400						
26S39E34Q01	35.62438	-117.76334			465	399-459					
26S39E36B	35.63386	-117.73144			982	362-962					
26S40E01A01	35.71042	-117.61376	444481.173	3952004.534	15						
26S40E01A02	35.70933	-117.61693	444193.669	3951885.434	198						
26S40E01J01	35.70558	-117.61690	444193.652	3951469.365	18						
26S40E01Q01	35.69742	-117.62818	443168.142	3950570.355	22						
26S40E01Q02	35.69843	-117.62015	443894.999	3950677.979	22						
26S40E04Q01	35.69739	-117.67526	438908.664	3950595.981	290						
26S40E05F01	35.70440	-117.70007			25						
26S40E05P01	35.69566	-117.69591	437038.807	3950416.395	98	40-98					
26S40E05P03	35.69634	-117.69562									
26S40E06C01	35.70834	-117.71459	435359.162	3951834.753	620	30-50	70-90	110-130			
26S40E06D01	35.70987	-117.72119	434762.803	3952008.956	320	500-600					
26S40E06D02	35.70934	-117.72235	434657.643	3951951.230	260	276-300					
26S40E06E01	35.70301	-117.72257									
26S40E07E01	35.68822	-117.71507	435298.747	3949603.885	86	120-200					
26S40E07N01	35.68107	-117.68840									
26S40E08N01	35.68162	-117.68618									
26S40E08Q01	35.68134	-117.69145									
26S40E09A01	35.69470	-117.67190	439206.252	3950297.550	100						
26S40E10E01	35.68857	-117.66923									
26S40E10F01	35.69100	-117.66097	440196.513	3949877.499	43	37-43					
26S40E10N01	35.68363	-117.66551	439780.363	3949063.707	134						
26S40E11A01	35.69229	-117.63241	442781.052	3950004.525	5						
26S40E11J01	35.68755	-117.63476	442565.650	3949479.784	18						
26S40E11J03	35.68579	-117.63645			8						
26S40E11N02	35.68162	-117.65090									
26S40E12A01	35.69218	-117.61701			21						
26S40E12G01	35.69058	-117.62216	443707.469	3949808.060	22						
26S40E12Q01	35.68333	-117.62417	443520.946	3949005.868	22						
26S40E12R01	35.68250	-117.61889	443997.940	3948910.420	21						
26S40E13C01	35.67690	-117.62645			22						
26S40E13C02	35.67752	-117.62725	443238.101	3948362.842							
26S40E13D03	35.68163	-117.63077	442921.970	3948820.588							
26S40E13M01	35.67306	-117.63004	442981.828	3947869.794	22						
26S40E14B01	35.67778	-117.64194	441908.237	3948400.064	22	20-22					
26S40E14B02	35.67892	-117.64102									PLScntr
26S40E14H01	35.67246	-117.63923									
26S40E14L01	35.67194	-117.64611	441526.921	3947755.556	57	55-57					
26S40E15E01	35.67646	-117.66545	439780.492	3948267.713	110						
26S40E15E02	35.67646	-117.66545	439780.496	3948267.718	198						
26S40E15N01	35.66722	-117.66944	439411.654	3947245.948	225						
26S40E15N02	35.66889	-117.66778	439563.755	3947429.773	101	99-101					
26S40E16K	35.67063	-117.68598	437917.412	3947634.564	960	938-958					
26S40E16M01	35.67221	-117.68411	438088.437	3947808.383							
26S40E17J01	35.67111	-117.69389	437202.312	3947692.617	97	95-97					
26S40E17N01	35.66690	-117.70479			178						
26S40E17Q01	35.66638	-117.69659	436953.848	3947169.641							
26S40E17R01	35.66746	-117.68979			101						
26S40E18E01	35.67412	-117.72173			119						
26S40E18N01	35.65953	-117.70475	436210.587	3946415.019	158						note: two TD: 158 and 555
26S40E19N	35.65385	-117.71944	434875.761	3945795.012	257	235-255					
26S40E19N01	35.65417	-117.72068	434764.178	3945831.011	306						
26S40E19P01	35.65432	-117.71422	435348.948	3945844.031	261	192-220	253-259				
26S40E20A	35.66619	-117.68874	437664.313	3947143.717							
26S40E20J01	35.65715	-117.68998									PLScntr
26S40E20L01	35.65861	-117.70056	436589.078	3946310.510							
26S40E20N01	35.64310	-117.68558	437932.182	3944580.565	190						
26S40E21A01	35.66329	-117.67173			99						
26S40E21E01	35.66143	-117.68770	437754.946	3946614.948	114						
26S40E21K01	35.65579	-117.67784									

Table 1: TDS Sample Locations

Depth and screen intervals are given in feet below ground surface

Notes: PLScntr - center point of corresponding Township/Range-Section & Tract (if available)

Unique Well Name	Latitude	Longitude	X_UTM	Y_UTM	Depth	Screen Interval[1]	Screen Interval[2]	Screen Interval[3]	Screen Interval[4]	Screen Interval[5]	Notes
26S40E22A01	35.66496	-117.65312			153	33-75					
26S40E22B01	35.66523	-117.65951			63	61-63					
26S40E22H01	35.66190	-117.65423	440784.733	3946646.356	49	47-49					
26S40E22H02	35.66190	-117.65423	440784.733	3946646.356	77	75-77					
26S40E22H03	35.66190	-117.65423	440784.733	3946646.356	97	95-97					
26S40E22J01	35.65829	-117.65590			71	69-71					
26S40E22K01	35.65634	-117.65812			52						
26S40E22N01	35.65417	-117.66944	439401.791	3945797.946	203						
26S40E22P01	35.65250	-117.66556	439752.567	3945610.704	1358	530-830					
26S40E22P02	35.65190	-117.66312	439972.683	3945542.663	75	73-75					
26S40E22P03	35.65355	-117.66371			415						PLScntr
26S40E22P04	35.65347	-117.66378			215	400-415					PLScntr
26S40E23A01	35.66339	-117.63661	442380.485	3946801.321	52	50-52					
26S40E23A02	35.66339	-117.63658	442383.205	3946801.388	77	75-77					
26S40E23B02	35.66526	-117.64147	441942.213	3947011.105	360	300-340					
26S40E23B03	35.66572	-117.63808	442249.018	3947060.355	240	180-220					
26S40E23C01	35.66384	-117.64673			40	200-215					
26S40E23D01	35.66318	-117.65028	441143.438	3946785.506	400	385-400					
26S40E23D02	35.66317	-117.65015	441155.315	3946785.291	185	170-185					
26S40E23G01	35.66162	-117.64284			57	55-57					
26S40E23J01	35.66361	-117.64611	441520.843	3946831.300	60						
26S40E23L01	35.65801	-117.64395			65						
26S40E24B01	35.66434	-117.62320									PLScntr
26S40E24C01	35.66579	-117.62449	443478.878	3947060.341	45	43.5-45.5					
26S40E24M01	35.65800	-117.63123	442863.733	3946199.859	67						
26S40E24R01	35.65343	-117.61875			149						PLScntr
26S40E25C	35.65164	-117.62824	443130.024	3945492.871							
26S40E25C02	35.64857	-117.62867			160						
26S40E25P	35.63874	-117.62704	443229.486	3944061.749							
26S40E26B01	35.64912	-117.64173			50						
26S40E26F01	35.64746	-117.64506	441603.958	3945038.872	77	75-77					
26S40E26N02	35.63857	-117.65046	441109.072	3944057.105	77	72-77					
26S40E27D01	35.65051	-117.66729	439594.451	3945391.174	160	75-77					
26S40E27D02	35.64940	-117.66784	439543.318	3945268.284							
26S40E27E03	35.64662	-117.66590			480						
26S40E28A03	35.65107	-117.67367				100-140					
26S40E28C01	35.65134	-117.68034			147						
26S40E28H01	35.64523	-117.67423									
26S40E28J01	35.64111	-117.67139	439215.888	3944351.147							
26S40E29D01	35.65051	-117.70229									
26S40E29F01	35.64551	-117.69923									
26S40E29N01	35.63773	-117.70256	436390.704	3943996.246							
26S40E30C02	35.64968	-117.71673									
26S40E30E	35.64740	-117.72039			850	320-490	530-830				
26S40E30E01	35.64579	-117.72145									
26S40E30E02	35.64718	-117.71895			378						
26S40E30J01	35.63816	-117.70367	436291.264	3944044.246	405	205-378					
26S40E30K01	35.64287	-117.71374			800	250-800					
26S40E30K02	35.64135	-117.71358			802	220-470	600-760				note: two screen interval sources: other one is 220-630
26S40E30K03	35.64222	-117.71217			800	250-800					
26S40E30K04	35.64138	-117.71318			796	300-460	600-796				
26S40E31D01	35.63500	-117.72111	434709.247	3943705.237	330						
26S40E31J01	35.61704	-117.68892	437609.728	3941692.144	380						
26S40E31K01	35.62611	-117.71361	435381.169	3942714.412							
26S40E31Q01	35.62472	-117.71119	435598.950	3942559.005	385						
26S40E32D01	35.63551	-117.70506			279						
26S40E32E01	35.63246	-117.70451			300						
26S40E32E02	35.63329	-117.70312			280						
26S40E32E06	35.63444	-117.70430	436230.717	3943631.613	405						
26S40E32F	35.63306	-117.69778									
26S40E32F01	35.63305	-117.69826	436774.557	3943475.422	720	520-700					

Table 1: TDS Sample Locations

Depth and screen intervals are given in feet below ground surface

Notes: PLScntr - center point of corresponding Township/Range-Section & Tract (if available)

Unique Well Name	Latitude	Longitude	X_UTM	Y_UTM	Depth	Screen Interval[1]	Screen Interval[2]	Screen Interval[3]	Screen Interval[4]	Screen Interval[5]	Notes
26S40E32K01	35.62833	-117.69602	436976.179	3942956.824	620	260-310	340-380	470-500	520-600		
26S40E32K02	35.62800	-117.69360									
26S40E33A02	35.63690	-117.67062			350						
26S40E33P01	35.62305	-117.67957				169-304					
26S40E33P02	35.62329	-117.67951			250						
26S40E33P03	35.62357	-117.68173									
26S40E33P04	35.61078	-117.65643	440547.952	3940978.398	304	169-182	198-216	233-252	256-272	275-290	
26S40E34N	35.62454	-117.66916				145-227					
26S40E34N01	35.62702	-117.66589	439703.368	3942785.357	232						
26S40E34R01	35.62357	-117.65451									
26S40E35H	35.63474	-117.64345	441741.120	3943627.401							
26S40E35H01	35.63194	-117.63806	442227.162	3943314.376	160	135-142	146-155	176-181			
26S40E35H02	35.63194	-117.63778	442252.313	3943314.212	500	55-70	110-130				
26S40E35Q01	35.62357	-117.64173									
26S40E35Q02	35.62278	-117.64167	441893.556	3942299.828	127	125-127					
26S40E36A01	35.63361	-117.62083	443787.737	3943489.245	270	80-90	107-127	187-195	240-260		
26S40E36K01	35.62800	-117.62240									
26S41E06P01	35.70181	-117.60719	445069.626	3951045.080	30	18-28					
26S41E07D01	35.69829	-117.61117			21						
26S41E07E01	35.69549	-117.61283	444555.418	3950347.873	32						
26S41E07G01	35.69559	-117.60008			32	30-32					PLScntr
27S37E30K	35.55656	-118.03475	406219.674	3935258.284							
27S38E01G01	35.61746	-117.83868			400						
27S38E02B01	35.62118	-117.85481				29.5-31.5					PLScntr
27S38E02C01	35.62278	-117.85750	422348.247	3942448.772	640	620-640					
27S38E02C02	35.62278	-117.85750	422348.247	3942448.772	1480	1460-1480					
27S38E02C03	35.62278	-117.85750	422348.247	3942448.772	1960	1940-1960					
27S38E09C01	35.60662	-117.89375	419049.338	3940686.033		501-581					
27S38E09Q01	35.59363	-117.89259	419140.892	3939244.748							
27S38E09Q02	35.59367	-117.89245	419154.249	3939248.517		380-480					
27S38E10C02	35.60667	-117.87310	420919.683	3940675.129							
27S38E13A01	35.59345	-117.83059	424758.015	3939174.996	770						
27S38E13A02	35.59366	-117.83065	424752.327	3939198.100		232-272	372-472	632-690			
27S38E14M01	35.58201	-117.86525	421606.591	3937933.038		452-552	752-852				
27S38E17A01	35.59371	-117.90204	418285.492	3939260.856		280-340					
27S38E21L01	35.56991	-117.89499	418900.215	3936615.252		905-1005					
27S38E23F01	35.56972	-117.86278	421818.720	3936568.493	635	615-635					
27S38E23F02	35.56972	-117.86278	421818.720	3936568.493	1060	1040-1060					
27S38E23F03	35.56972	-117.86278	421818.720	3936568.493	1520	1500-1520					
27S38E23F04	35.56972	-117.86278	421818.720	3936568.493	1770	1750-1770					
27S38E23R01	35.56633	-117.85026			300	580-680					PLScntr
27S38E27M01	35.55388	-117.88131	420123.519	3934826.511		320-360					
27S38E28R01	35.55135	-117.88229									
27S38E31D01	35.54780	-117.93410									
27S39E02K	35.61222	-117.74722	432325.865	3941196.588	400						
27S39E03B01	35.62126	-117.76578	430652.596	3942212.201	400						
27S39E03C01	35.62177	-117.77066	430211.391	3942272.457	425						
27S39E03C02	35.62205	-117.76993	430277.417	3942302.994	420						
27S39E04C01	35.62173	-117.77156	2068168.000	772267.000	425						
27S39E07R01	35.59634	-117.81673	426015.650	3939485.620		434-514					
27S39E08A02	35.60672	-117.79819			955	550-905					
27S39E08E01	35.60285	-117.81018									PLScntr
27S39E08L01	35.60051	-117.80419	427158.421	3939926.447	1020	560-1000					
27S39E08M01	35.58315	-117.80089	2059479.310	758203.220							
27S39E08M04	35.60055	-117.81151	426492.908	3939938.315	1020	560-1000					
27S39E11D01	35.60722	-117.75472	431642.341	3940647.220	670	650-670					
27S39E11D02	35.60722	-117.75472	431642.341	3940647.220	1340	1320-1340					
27S39E11D03	35.60722	-117.75472	431642.341	3940647.220	1870	1850-1870					
27S39E12M01	35.77600	-117.84634									PLScntr
27S39E19E01	35.57389	-117.82972	424818.038	3937004.883							
27S40E01G02	35.61579	-117.62478									
27S40E01K01	35.61440	-117.62506			400						
27S40E01K02	35.61472	-117.62472	443422.315	3941396.512	164						
27S40E01M01	35.61357	-117.63145			199						

Table 1: TDS Sample Locations

Depth and screen intervals are given in feet below ground surface

Notes: PLScntr - center point of corresponding Township/Range-Section & Tract (if available)

Unique Well Name	Latitude	Longitude	X_UTM	Y_UTM	Depth	Screen Interval[1]	Screen Interval[2]	Screen Interval[3]	Screen Interval[4]	Screen Interval[5]	Notes
27S40E01M02	35.61357	-117.63145			210						
27S40E02A01	35.61885	-117.63617			127						
27S40E02F01	35.61690	-117.64728			127						
27S40E02G01	35.61690	-117.64145			127						
27S40E02G03	35.61857	-117.63923									
27S40E02H01	35.61167	-117.63500	442489.313	3941063.580	200	119-197					
27S40E02J01	35.61167	-117.63500	442489.313	3941063.580	220						
27S40E02N01	35.60940	-117.64923									
27S40E03J01	35.61246	-117.65340									
27S40E03P01	35.60829	-117.66451			120						
27S40E03R01	35.60833	-117.65306	440851.581	3940704.584	162						
27S40E04B01	35.62218	-117.67451			230						
27S40E04B02	35.62218	-117.67451			288	128-278					
27S40E04B3	35.62210	-117.67500			288	138-288					
27S40E04C01	35.62246	-117.67867			300						
27S40E04C02	35.61880	-117.67840	438563.704	3941880.480	280						
27S40E04E02	35.61707	-117.68566			375	150-210					PLScntr
27S40E04F01	35.61667	-117.68333									
27S40E04F02	35.61667	-117.68333									
27S40E04F03	35.61667	-117.68333									
27S40E04F04	35.61667	-117.68333									
27S40E04L01	35.60038	-117.66023	440195.504	3939827.051	252						
27S40E04L02	35.61440	-117.67920									
27S40E05C01	35.62111	-117.69750									
27S40E05D	35.64656	-117.73953			556	251-555					
27S40E05D01	35.62190	-117.70284			555						
27S40E05F	35.61667	-117.70000									this location may have wrong longitude
27S40E06D01	35.60793	-117.70591	2087695.780	767293.420	720	580-700					
27S40E06E02	35.61817	-117.71999	434796.947	3941838.017	445						
27S40E06F01	35.61639	-117.71806	434970.839	3941639.045							
27S40E06H01	35.61579	-117.70618			402	220-400					
27S40E06L01	35.59919	-117.69945	436641.827	3939719.273							
27S40E06R	35.60861	-117.70611									
27S40E06R02	35.60996	-117.70590				255-555					
27S40E07G01	35.60162	-117.71368			410						
27S40E08A01	35.60801	-117.68895			440						
27S40E08B01	35.60635	-117.69645			400						
27S40E08B02	35.60746	-117.69367			400	200-400					
27S40E08F01	35.60107	-117.69729			400	200-400					
27S40E08Q02	35.59440	-117.69617			367						
27S40E09B01	35.60635	-117.67867									
27S40E09K03	35.59990	-117.67414	438935.224	3939782.404	305						
27S40E09L01	35.59712	-117.68164	438253.986	3939478.876	300						
27S40E09L02	35.59829	-117.68034									
27S40E09P01	35.59357	-117.68229			230						
27S40E10A01	35.60773	-117.65312			150						
27S40E10A02	35.60662	-117.65534			126						
27S40E10A07	35.60773	-117.65312									
27S40E10B01	35.60440	-117.65756									
27S40E10C01	35.60440	-117.66395			250						
27S40E10D01	35.60468	-117.66951									
27S40E10E01	35.60385	-117.66951									
27S40E10H01	35.60496	-117.65340									
27S40E10J01	35.59912	-117.65451			180						
27S40E10R01	35.59355	-117.65154	440977.769	3939064.045	263						
27S40E11C02	35.60718	-117.64701									
27S40E11D03	35.60523	-117.64951			165						
27S40E15L01	35.58396	-117.65805	440381.274	3938004.253							
27S40E17G01	35.58885	-117.69284									
28S37E13F01	35.50107	-117.94924			400						
28S37E18R01	35.49347	-118.02861			284						PLScntr
28S38E18F01	35.49912	-117.92923	415722.695	3928793.109	247						

Table 1: TDS Sample Locations

Depth and screen intervals are given in feet below ground surface

Notes: PLScntr - center point of corresponding Township/Range-Section & Tract (if available)

Unique Well Name	Latitude	Longitude	X_UTM	Y_UTM	Depth	Screen Interval[1]	Screen Interval[2]	Screen Interval[3]	Screen Interval[4]	Screen Interval[5]	Notes
ETC44-MW01	35.69228	-117.67267	439138.418	3950027.023							
ITC02-MW21	35.68634	-117.68020	438453.278	3949373.415							
ITC45-MW25	35.69213	-117.68011	438465.209	3950015.390							
JMM07-MW11	35.65979	-117.65885	440365.110	3946415.468							
JMM07-MW13	35.66044	-117.65682	440549.184	3946486.452							
JMM12-MW08			437105.321	3945617.392	153	138-153					
JMM31-MW01	35.64556	-117.66503	439795.337	3944840.264							
JMM32-MW02	35.66070	-117.64329	441774.115	3946506.338							
MK12-MW12	35.65591	-117.68691	437822.051	3946002.461							
MK12-MW16	35.65217	-117.68893	437636.665	3945588.328							
MK29-MW13	35.76967	-117.71967	434949.385	3958640.669	300	280-300					
MK62-MW01	35.64731	-117.66097	440164.189	3945032.501							
MK69-MW01	35.64777	-117.66054	440202.967	3945082.999	66	51-66					
MK69-MW02			440202.818	3945083.877	211	196-210					
MKFL-MW01	35.63894	-117.65353	440830.918	3944099.292	59	48-59					
MKFL-MW02			440438.842	3945312.585	203	182-202					
MKFL-MW03	35.66445	-117.67571	438842.116	3946942.497							
MW01-13	35.68954	-117.67701	438743.863	3949726.002							
RLS07-MW02	35.66443	-117.66238	440048.736	3946932.156							
RLS07-MW03	35.66185	-117.65810	440434.172	3946643.408							
RLS07-MW04	35.66685	-117.65024	441149.138	3947193.472							
RLS12-MW01	35.65779	-117.69139	437418.436	3946213.933							
RLS12-MW04	35.65314	-117.69507	437081.549	3945700.265	136	119-139					
RLS13-MW05	35.67043	-117.63222	442783.194	3947579.438							
RLS15-MW03	35.68946	-117.63417	442620.097	3949691.533							
RLS22-MW07	35.63307	-117.62868	443077.073	3943433.740							
RLS22-MW08 (64')	35.63983	-117.63352	442643.023	3944186.032							
RLS29-MW01	35.76959	-117.72126	434805.079	3958633.278	32	17-32					
RLS34-MW05	35.66836	-117.65678	440559.119	3947364.457							
RLS34-MW06	35.66987	-117.66335	439965.221	3947535.489							
RLS43-MW06	35.66987	-117.66335	439965.221	3947535.489							
26S38E15Q01	35.66829	-117.87285									Spring
5_Mile_Cyn	35.88164	-117.91946	417006.502	3971210.715							Surface
9_Mile_Cyn	35.84321	-117.92573	416400.251	3966954.247							Surface
Big_Spring	35.62483	-117.95818	413233.110	3942760.734							Surface
Bird_Spring_S	35.49959	-118.07795	402234.937	3928982.417							Surface - Source
Cow_Haven_Cyn	35.58598	-117.98849									Surface; PLScntr
Dead_Foot_Cyn	35.86275	-117.92126	416823.859	3969117.599							Surface
Grapevine_Cyn	35.73273	-117.90814	417874.808	3954685.231							Surface
Indian_Wells_Cyn	35.69295	-117.92926	415923.210	3950290.831							Surface
Indian_Wells_Lodge	35.66819	-117.87433									Surface Spring
Little_Lake_Outlet	35.93145	-117.90614	418259.866	3976724.948							Surface
Sand_Canyon	35.77830	-117.9220									Surface
Short_Canyon	35.71074	-117.91780	416978.866	3952253.822							Surface
TT37-MW01	35.65884	-117.62880	443084.483	3946291.596							
TT37-MW02	35.65674	-117.62767	443184.942	3946058.298							
TT37-MW03	35.65551	-117.63221	442773.319	3945925.025							
TTBK-MW03	35.63360	-117.66183	440075.276	3943512.417							
TTBK-MW06	35.65735	-117.68686	437827.836	3946161.761							
TTBK-MW08	35.76000	-117.75378	431857.908	3957591.052							
TTBK-MW09	35.74912	-117.74028	433068.994	3956374.868							
TTBK-MW10	35.63893	-117.64017	442041.105	3944090.541							
TTIWV-MW02-D			434875.761	3945795.012	802	780-800					
TTIWV-MW02-I			434875.761	3945795.012	422	400-420					
TTIWV-MW04			437075.765	3945643.499	657	635-655					
TTIWV-MW07			439616.478	3945223.345	622	600-620					
TTIWV-MW08			441101.066	3944074.928	422	400-420					
TTIWV-MW10			445072.265	3951030.290	342	260-340					
TTIWV-MW15			440588.757	3965479.490	302	280-300					
TTIWV-MW16	35.77026	-117.71969	434947.779	3958705.951	990	948-988					
TTSWV-MW01			456845.390	3945313.950	27	15-25					
TTSWV-MW02			455157.400	3946358.550	48	36-46					
TTSWV-MW03			455153.230	3946349.740	372	350-370					
TTSWV-MW04			453382.460	3947058.060	32	20-30					

Table 1: TDS Sample Locations

Depth and screen intervals are given in feet below ground surface

Notes: PLScntr - center point of corresponding Township/Range-Section & Tract (if available)

Unique Well Name	Latitude	Longitude	X_UTM	Y_UTM	Depth	Screen Interval[1]	Screen Interval[2]	Screen Interval[3]	Screen Interval[4]	Screen Interval[5]	Notes
TTSWV-MW05			452388.380	3944778.270	142	120-140					
TTSWV-MW06			450996.700	3946994.880	52	40-50					
TTSWV-MW07			451010.090	3946998.360	272	250-270					
TTSWV-MW09			449400.410	3948667.120	42	30-40					
TTSWV-MW10			449422.100	3948660.940	197	175-195					

Table 2: IWV TDS Data

Sample Dates in red indicate — min 1/26/1920 — 100
only sample month/year is known — max 3/5/2019 — 232000
count 2,044

Unique Well Name	alternateName	Sample Date	TDS (mg/L)	Analysis Type	TDS Reference	Confidence Level
24S38E16J02	Sawmill Well #1	6/15/1982	1300	Calc	B	1
24S38E16J02	Sawmill Well #1	2/4/2007	1100	Lab	FR: AB	1
24S38E21A01	USBR-10-S	4/14/1995	1140	Ukn	AB	2
24S38E21A01	USBR-10-S	11/30/1995	1120	Ukn	AB	2
24S38E21A01	USBR-10-S	3/18/1993	950	Lab	H	1
24S38E21A01	USBR-10-S	5/30/1996	980	Lab	H96	1
24S38E21A01	USBR-10-S	9/1/1992	1000	Lab	USBR	1
24S38E21A02	USBR-10-S/M	4/14/1995	745	Ukn	AB	2
24S38E21A02	USBR-10-S/M	11/30/1995	995	Ukn	AB	2
24S38E21A02	USBR-10-S/M	6/5/1996	750	Lab	H96	1
24S38E21A02	USBR-10-S/M	9/1/1992	580	Lab	USBR	1
24S38E21A03	USBR-10-M/D	4/14/1995	1140	Ukn	AB	2
24S38E21A03	USBR-10-M/D	6/5/1996	880	Lab	H96	1
24S38E21A03	USBR-10-M/D	9/1/1992	1220	Lab	USBR	1
24S38E21A04	USBR-10-D	4/14/1995	1120	Ukn	AB	2
24S38E21A04	USBR-10-D	12/1/1995	1120	Ukn	AB	2
24S38E21A04	USBR-10-D	6/5/1996	1100	Lab	H96	1
24S38E21A04	USBR-10-D	9/2/1992	1330	Lab	USBR	1
24S38E28Q01	USGS-354851117522501	8/5/1953	615	Ukn	GAMA	1
24S38E33J02	Pearsonville Well	6/15/1982	710	Calc	B	1
24S38E35E01	USGS-354825117510001	4/24/1946	852	Ukn	GAMA	1
24S39E33D01	USGS-354828117463801	2/3/1920	704	Ukn	GAMA	1
24S39E33D01	USGS-354828117463801	4/23/1946	1040	Ukn	GAMA	1
24S39E33N01	USGS-354758117464001	4/23/1946	530	Ukn	GAMA	1
24S39E34D01	N. Baker Well	3/11/1993	500	Lab	H	1
24S39E34D01	N. Baker Well	8/21/2008	480	Ukn	KCWA WQ	3
24S40E06A01	USGS-355300117413401	4/29/1946	3070	Ukn	GAMA	1
24S40E20J01		5/15/1953	1160	Calc	Moyle	1
24S40E21K01	TTIWV-MW14	12/14/2002	3200	Lab	Tri	1
24S40E21K01	TTIWV-MW14	2/17/2002	2560	Lab	TTEMI	1
24S40E33N01		7/6/1953	5120	Calc	Moyle	1
24S40E34E01		7/8/1953	1790	Calc	Moyle	1
24S40E36A	TTIWV-MW13	2/16/2002	3090	Lab	TTEMI	1
24S40E36M01		7/6/1953	1820	Calc	Moyle	1
25S38E02E	Meadowbrook - Big Horn	9/11/2018	920	Lab	MD	1
25S38E02L01		3/18/1993	960	Lab	H	1
25S38E03G01		2/7/2007	520	Lab	FR: AB	1
25S38E10G	Quarry Well	3/7/1990	352	Ukn	H-WQ	2
25S38E11K02		6/5/1953	350	Lab	Moyle	1
25S38E11K02		8/5/1953	304	Calc	Moyle	1
25S38E11L01		9/20/1987	296	Calc	B&S	1
25S38E11L01		7/9/1988	306	Calc	B&S	1
25S38E12E		6/9/1987	760	Ukn	KCWA WQ	3
25S38E12L01	USBR-06-S	5/30/1996	380	Lab	H96	1
25S38E12L01	USBR-06-S	4/14/2004	641	Ukn	L/H-WQ	2
25S38E12L01	USBR-06-S	1/10/1992	596	Lab	USBR	1

Table 2: IWV TDS Data

Sample Dates in red indicate — min 1/26/1920 — 100
only sample month/year is known — max 3/5/2019 — 232000
count 2,044

Unique Well Name	alternateName	Sample Date	TDS (mg/L)	Analysis Type	TDS Reference	Confidence Level
25S38E12L02	USBR-06-M	6/18/1996	850	Lab	H96	1
25S38E12L02	USBR-06-M	4/14/2004	1200	Ukn	L/H-WQ	2
25S38E12L02	USBR-06-M	1/10/1992	481	Lab	USBR	1
25S38E12L03	USBR-06-D	6/18/1996	600	Lab	H96	1
25S38E12L03	USBR-06-D	4/14/2004	864	Ukn	L/H-WQ	2
25S38E12L03	USBR-06-D	1/10/1992	540	Lab	USBR	1
25S38E12M	Meadowbrook Well 3	9/11/2018	940	Lab	MD	1
25S38E12M01	LM #3?	3/18/1993	830	Lab	H	1
25S38E12Mct	Meadowbrook - Coyote Trail	9/11/2018	380	Lab	MD	1
25S38E13C	Meadowbrook Well 4	9/11/2018	880	Lab	MD	1
25S38E13D01	USGS-354608117503601	4/24/1946	400	Ukn	GAMA	1
25S38E13J01		7/6/1988	343	Calc	B&S	1
25S38E13J01		1/12/2007	280	Lab	FR: AB	1
25S38E13J01		3/10/1993	330	Lab	H	1
25S38E13J01		3/18/1993	330	Ukn	KCWA WQ	3
25S38E13L	Meadowbrook Well 5	9/11/2018	690	Lab	MD	1
25S38E13L01		6/15/1982	510	Calc	B	1
25S38E13M	Meadowbrook - Headquarters	9/11/2018	760	Lab	MD	1
25S38E13Q	Meadowbrook Well 6	9/11/2018	680	Lab	MD	1
25S38E14M02		8/12/2008	380	Ukn	H-WQ	2
25S38E14N01		5/1/2007	420	Ukn	H-WQ	2
25S38E23G01		4/24/1946	354	Calc	Moyle	1
25S38E23J01	USGS-354449117505001	4/16/1986	430	Ukn	GAMA	1
25S38E24H	Old Man John Well	4/21/1996	640	Ukn	AB	2
25S38E24K	Meadowbrook Well 7	9/11/2018	620	Lab	MD	1
25S38E24K01		3/18/1993	620	Lab	H	1
25S38E24L	Meadowbrook Well 8	9/11/2018	900	Lab	MD	1
25S38E25C	PEACHIE	6/7/2005	710	Ukn	KCWA WQ	3
25S38E25C01		6/7/2005	710	Ukn	H-WQ	2
25S38E25G01		3/26/2008	610	Ukn	H-WQ	2
25S38E25J	B&S Hist. 1988 (25S38E25J01)	8/25/1988	875	Lab	B&S	1
25S38E25J01	NR1-S (Neal Ranch-1-S)	2/2/1991	2406	Lab	USBR	1
25S38E25J02	NR1-M (Neal Ranch-1-M)	2/2/1991	3660	Lab	USBR	1
25S38E25J03	NR1-D (Neal Ranch-1-D)	2/2/1991	3251	Lab	USBR	1
25S38E25Q		1/6/1998	677	Ukn	H-WQ	2
25S38E34A01	Means Well	4/11/2006	260	Ukn	H-WQ	2
25S38E34G01	USBR-05-S	6/5/1996	440	Lab	H96	1
25S38E34G01	USBR-05-S	10/22/2004	412	Ukn	L/H-WQ	2
25S38E34G01	USBR-05-S	1/6/1992	534	Lab	USBR	1
25S38E34G02	USBR-05-M	6/5/1996	1100	Lab	H96	1
25S38E34G02	USBR-05-M	10/22/2004	935	Ukn	L/H-WQ	2
25S38E34G02	USBR-05-M	1/6/1992	837	Lab	USBR	1
25S38E34G03	USBR-05-D	6/5/1996	1200	Lab	H96	1
25S38E34G03	USBR-05-D	10/22/2004	1200	Ukn	L/H-WQ	2

Table 2: IWV TDS Data

Sample Dates in red indicate
only sample month/year is known

min	1/26/1920	100	
max	3/5/2019	232000	
count	2,044		

Unique Well Name	alternateName	Sample Date	TDS (mg/L)	Analysis Type	TDS Reference	Confidence Level
25S38E34G03	USBR-05-D	1/6/1992	891	Lab	USBR	1
25S38E35A	HLEDIK	10/8/2002	610	Ukn	KCWA WQ	3
25S38E35H	HOFFMAN	2/9/1988	520	Ukn	KCWA WQ	3
25S38E35M01		8/5/1953	589	Calc	Moyle	1
25S38E36A01		8/25/1988	3210	Lab	B&S	1
25S38E36B01	WELL-27 (NWWF 04)	7/29/1988	755	Lab	B&S	1
25S38E36B01	WELL-27 (NWWF 04)	4/17/1986	827	Ukn	GAMA	1
25S38E36D	WOOD	5/8/1984	560	Ukn	KCWA WQ	3
25S38E36D	WOOD	3/7/1989	670	Ukn	KCWA WQ	3
25S38E36D	WOOD	4/3/1989	670	Ukn	KCWA WQ	3
25S38E36D	WOOD	12/21/1992	650	Ukn	KCWA WQ	3
25S38E36D	WOOD	12/8/1994	1790	Ukn	KCWA WQ	3
25S38E36D	WOOD	7/20/1999	946	Ukn	KCWA WQ	3
25S38E36G01	NR2-S (Neal Ranch-2-S)	2/26/1991	808	Lab	USBR	1
25S38E36G02	NR2-M (Neal Ranch-2-M)	2/26/1991	1367	Lab	USBR	1
25S38E36G03	NR2-D (Neal Ranch-2-D)	2/26/1991	3305	Lab	USBR	1
25S38E36Q01		8/12/2008	560	Ukn	H-WQ	2
25S39E01N01	USGS-354704117441501	4/25/1946	602	Ukn	GAMA	1
25S39E02E01		4/23/1946	501	Calc	Moyle	1
25S39E04R01	NAWS Well LB	7/31/1978	690	Calc	B	1
25S39E04R01	NAWS Well LB	3/29/1980	780	Calc	B	1
25S39E04R01	NAWS Well LB	6/1/1987	764	Lab	B&S	1
25S39E04R01	NAWS Well LB	7/8/1988	792	Calc	B&S	1
25S39E04R01	NAWS Well LB	3/27/1990	775	Lab	GAMA	1
25S39E04R01	NAWS Well LB	7/20/1990	810	Lab	GAMA	1
25S39E04R01	NAWS Well LB	5/18/1993	780	Lab	GAMA	1
25S39E04R01	NAWS Well LB	4/11/2002	782	Lab	GAMA	1
25S39E04R01	NAWS Well LB	5/20/2009	730	Lab	GAMA	1
25S39E04R01	NAWS Well LB	12/20/2011	740	Lab	GAMA	1
25S39E04R01	NAWS Well LB	8/5/1953	681	Calc	Moyle	1
25S39E04R01	NAWS Well LB	6/6/1972	644	Calc	W	1
25S39E07K01		4/23/1946	842	Calc	Moyle	1
25S39E09J01	NAWS Well B-1	7/31/1978	540	Calc	B	1
25S39E09J01	NAWS Well B-1	5/4/1979	580	Calc	B	1
25S39E09J01	NAWS Well B-1	3/29/1980	540	Calc	B	1
25S39E09J01	NAWS Well B-1	1/19/1989	584	Calc	B&S	1
25S39E09J01	NAWS Well B-1	10/10/1961	565	Ukn	GAMA	1
25S39E09J01	NAWS Well B-1	7/18/1962	602	Ukn	GAMA	1
25S39E09J01	NAWS Well B-1	10/14/1963	626	Ukn	GAMA	1
25S39E09J01	NAWS Well B-1	9/15/1964	564	Ukn	GAMA	1
25S39E09J01	NAWS Well B-1	5/16/1966	596	Ukn	GAMA	1
25S39E09J01	NAWS Well B-1	9/7/1966	608	Ukn	GAMA	1
25S39E09J01	NAWS Well B-1	6/5/1968	600	Ukn	GAMA	1
25S39E09J01	NAWS Well B-1	5/22/1969	570	Ukn	GAMA	1
25S39E09J01	NAWS Well B-1	10/25/1973	525	Ukn	GAMA	1
25S39E09J01	NAWS Well B-1	5/1/1975	494	Ukn	GAMA	1

Table 2: IWV TDS Data

Sample Dates in red indicate
only sample month/year is known

min	1/26/1920	100	
max	3/5/2019	232000	
count	2,044		

Unique Well Name	alternateName	Sample Date	TDS (mg/L)	Analysis Type	TDS Reference	Confidence Level
25S39E09J01	NAWS Well B-1	5/12/1976	518	Ukn	GAMA	1
25S39E09J01	NAWS Well B-1	11/19/1985	560	Lab	GAMA	1
25S39E09J01	NAWS Well B-1	3/27/1990	575	Lab	GAMA	1
25S39E09J01	NAWS Well B-1	7/2/1990	610	Lab	GAMA	1
25S39E09J01	NAWS Well B-1	5/18/1993	600	Lab	GAMA	1
25S39E09J01	NAWS Well B-1	4/17/1995	540	Lab	GAMA	1
25S39E09J01	NAWS Well B-1	4/11/2002	525	Lab	GAMA	1
25S39E09J01	NAWS Well B-1	8/23/2012	500	Lab	GAMA	1
25S39E09J01	NAWS Well B-1	8/3/1953	578	Calc	Moyle	1
25S39E09J01	NAWS Well B-1	6/6/1972	516	Calc	W	1
25S39E10E01	USGS-354637117462601	4/23/1946	608	Ukn	GAMA	1
25S39E10Q01	USGS-354610117455501	4/24/1946	584	Ukn	GAMA	1
25S39E12R02	NAWS Well 22	7/31/1978	650	Calc	B	1
25S39E12R02	NAWS Well 22	5/4/1979	680	Calc	B	1
25S39E12R02	NAWS Well 22	3/29/1980	760	Calc	B	1
25S39E12R02	NAWS Well 22	4/28/1987	692	Lab	B&S	1
25S39E12R02	NAWS Well 22	7/8/1988	760	Calc	B&S	1
25S39E12R02	NAWS Well 22	10/11/1961	780	Ukn	GAMA	1
25S39E12R02	NAWS Well 22	7/18/1962	752	Ukn	GAMA	1
25S39E12R02	NAWS Well 22	6/21/1965	776	Ukn	GAMA	1
25S39E12R02	NAWS Well 22	5/16/1966	776	Ukn	GAMA	1
25S39E12R02	NAWS Well 22	9/7/1966	769	Ukn	GAMA	1
25S39E12R02	NAWS Well 22	11/7/1967	746	Ukn	GAMA	1
25S39E12R02	NAWS Well 22	6/5/1968	764	Ukn	GAMA	1
25S39E12R02	NAWS Well 22	11/4/1968	721	Ukn	GAMA	1
25S39E12R02	NAWS Well 22	10/20/1969	768	Ukn	GAMA	1
25S39E12R02	NAWS Well 22	6/1/1970	748	Ukn	GAMA	1
25S39E12R02	NAWS Well 22	10/20/1970	704	Ukn	GAMA	1
25S39E12R02	NAWS Well 22	10/25/1973	776	Ukn	GAMA	1
25S39E12R02	NAWS Well 22	5/1/1975	692	Ukn	GAMA	1
25S39E12R02	NAWS Well 22	5/12/1976	675	Ukn	GAMA	1
25S39E12R02	NAWS Well 22	8/3/1953	676	Calc	Moyle	1
25S39E12R02	NAWS Well 22	4/20/1955	684	Calc	Moyle	1
25S39E12R02	NAWS Well 22	6/6/1972	723	Calc	W	1
25S39E13E01	USGS-354549117442001	4/25/1946	612	Ukn	GAMA	1
25S39E14H01	Childers Well	2/3/2007	600	Lab	FR: AB	1
25S39E17D01	USGS-354606117483201	4/24/1946	264	Ukn	GAMA	1
25S39E19K01	USGS-354447117490901	4/25/1946	446	Lab	GAMA-USGS	1
25S39E21B01	USGS-354510117470001	4/24/1946	349	Ukn	GAMA	1
25S39E22B01	USGS-354512117455001	4/25/1946	450	Ukn	GAMA	1
25S39E22J01	USGS-354435117454001	4/25/1946	778	Lab	GAMA-USGS	1
25S39E22J01	USGS-354435117454001	8/21/2008	840	Ukn	KCWA WQ	3
25S39E23G01	SNORT #1 -S	8/25/1992	9890	Lab	USBR	1
25S39E23G02	SNORT #1-S/M	8/25/1992	9350	Lab	USBR	1
25S39E23G03	SNORT #1-D/M	8/24/1992	12500	Lab	USBR	1
25S39E23G04	SNORT #1-D	8/24/1992	8900	Lab	USBR	1

Table 2: IWV TDS Data

Sample Dates in red indicate — min 1/26/1920 — 100
only sample month/year is known — max 3/5/2019 — 232000
count 2,044

Unique Well Name	alternateName	Sample Date	TDS (mg/L)	Analysis Type	TDS Reference	Confidence Level
25S39E24D01		4/25/1945	386	Calc	Moyle	1
25S39E26H01	USGS-354359117443201	10/14/1963	6530	Lab	GAMA-USGS	1
25S39E26H01	USGS-354359117443201	9/15/1964	1910	Lab	GAMA-USGS	1
25S39E26H01	USGS-354359117443201	10/20/1970	990	Lab	GAMA-USGS	1
25S39E26H01	USGS-354359117443201	6/23/1971	1050	Lab	GAMA-USGS	1
25S39E26H01	USGS-354359117443201	10/27/1971	1560	Lab	GAMA-USGS	1
25S39E26H01	USGS-354359117443201	2/29/1956	841	Calc	Moyle	1
25S39E26H01	USGS-354359117443201	6/6/1972	696	Calc	W	1
25S39E28P01		4/26/1946	484	Calc	Moyle	1
25S39E30L01		3/10/1993	91500	Lab	H	1
25S39E30N01	USGS-354339117493601	12/29/1967	734	Lab	GAMA-USGS	1
25S39E31D01		7/29/1988	845	Lab	B&S	1
25S39E31E01	USGS-354308117494401	4/26/1946	533	Lab	GAMA-USGS	1
25S39E31M03	USGS-354258117494201	5/22/1969	633	Lab	GAMA-USGS	1
25S39E31R01	USGS-354240117485301	5/31/1987	1890	Calc	B&S	1
25S39E31R01	USGS-354240117485301	1/11/2007	550	Lab	FR: AB	1
25S39E31R01	USGS-354240117485301	10/23/1986	2680	Ukn	GAMA	1
25S39E31R01	USGS-354240117485301	3/21/1989	1910	Ukn	GAMA	1
25S39E31R01	USGS-354240117485301	4/11/1990	1900	Ukn	GAMA	1
25S39E31R01	USGS-354240117485301	3/14/1991	1770	Ukn	GAMA	1
25S39E31R01	USGS-354240117485301	3/10/1993	590	Lab	H	1
25S39E31R01	USGS-354240117485301	3/18/1993	590	Ukn	KCWA WQ	3
25S39E31R01	USGS-354240117485301	4/15/1995	550	Ukn	KCWA WQ	3
25S39E31R01	USGS-354240117485301	11/17/1998	980	Ukn	KCWA WQ	3
25S39E35N01	USGS-354242117452701	7/31/1978	430	Calc	B	1
25S39E35N01	USGS-354242117452701	3/29/1980	460	Calc	B	1
25S39E35N01	USGS-354242117452701	10/25/1973	420	Ukn	GAMA	1
25S39E35N01	USGS-354242117452701	5/12/1976	508	Ukn	GAMA	1
25S39E35N01	USGS-354242117452701	4/30/1946	450	Lab	GAMA-USGS	1
25S39E35N01	USGS-354242117452701	5/22/1969	460	Lab	GAMA-USGS	1
25S39E35N01	USGS-354242117452701	10/20/1970	469	Calc	GAMA-USGS	1
25S39E35N01	USGS-354242117452701	6/23/1971	503	Lab	GAMA-USGS	1
25S39E35N01	USGS-354242117452701	10/27/1971	530	Lab	GAMA-USGS	1
25S39E35N01	USGS-354242117452701	7/31/1953	398	Calc	Moyle	1
25S39E35N01	USGS-354242117452701	6/6/1972	463	Calc	W	1
25S40E08A01	USGS-354658117411201	6/20/1978	1100	Calc	B	1
25S40E08A01	USGS-354658117411201	5/16/1979	1200	Calc	B	1
25S40E08A01	USGS-354658117411201	5/20/1980	1100	Calc	B	1
25S40E08A01	USGS-354658117411201	6/9/1982	1200	Calc	B	1
25S40E08A01	USGS-354658117411201	3/5/1974	1160	Ukn	GAMA	1
25S40E08A01	USGS-354658117411201	3/24/1975	1040	Ukn	GAMA	1
25S40E08A01	USGS-354658117411201	8/17/1976	1080	Ukn	GAMA	1
25S40E08A01	USGS-354658117411201	7/9/1953	1100	Calc	Moyle	1
25S40E11K01		6/9/1982	1400	Calc	B	1
25S40E11K01		5/14/1953	1470	Calc	Moyle	1
25S40E11K01		7/6/1953	1340	Calc	Moyle	1

Table 2: IWV TDS Data

Sample Dates in red indicate — min 1/26/1920 — 100
only sample month/year is known — max 3/5/2019 — 232000
count 2,044

Unique Well Name	alternateName	Sample Date	TDS (mg/L)	Analysis Type	TDS Reference	Confidence Level
25S40E12M01		5/14/1953	2740	Calc	Moyle	1
25S40E14H01	TTIWV-MW12	5/28/2002	2640	Lab	Tri	1
25S40E14H01	TTIWV-MW12	2/16/2002	1730	Lab	TTEMI	1
25S40E18R01	TTBK-MW12	6/21/1978	7700	Calc	B	1
25S40E18R01	TTBK-MW12	5/16/1979	1800	Calc	B	1
25S40E18R01	TTBK-MW12	5/20/1980	940	Calc	B	1
25S40E18R01	TTBK-MW12	6/9/1982	650	Calc	B	1
25S40E18R01	TTBK-MW12	3/5/1974	601	Ukn	GAMA	1
25S40E18R01	TTBK-MW12	3/24/1975	583	Ukn	GAMA	1
25S40E18R01	TTBK-MW12	8/17/1976	637	Ukn	GAMA	1
25S40E18R01	TTBK-MW12	5/12/1999	2600	Lab	Tri	1
25S40E19L01		7/9/1953	12400	Calc	Moyle	1
25S40E20F01	USGS-354450117415301	6/20/1978	580	Calc	B	1
25S40E20F01	USGS-354450117415301	5/16/1979	430	Calc	B	1
25S40E20F01	USGS-354450117415301	5/20/1980	460	Calc	B	1
25S40E20F01	USGS-354450117415301	6/9/1982	490	Calc	B	1
25S40E20F01	USGS-354450117415301	3/7/1974	507	Ukn	GAMA	1
25S40E20F01	USGS-354450117415301	3/24/1975	508	Ukn	GAMA	1
25S40E20F01	USGS-354450117415301	8/18/1976	514	Ukn	GAMA	1
25S40E24H01		5/15/1953	66400	Calc	Moyle	1
25S40E24N01		7/8/1953	5270	Calc	Moyle	1
25S40E25H01	USGS-354358117365901	5/15/1953	66400	Lab	GAMA-USGS	1
25S40E27E01	USGS-354405117395301	7/9/1953	887	Calc	Moyle	1
25S40E27E01	USGS-354405117395301	6/28/1972	799	Calc	W	1
25S40E30E01	TTBK-MW14	2/10/1999	720	Lab	Tri	1
25S40E33L01	USGS-354258117403901	6/21/1978	48000	Calc	B	1
25S40E33L01	USGS-354258117403901	5/21/1980	55000	Calc	B	1
25S40E33L01	USGS-354258117403901	6/9/1982	45000	Calc	B	1
25S40E33L01	USGS-354258117403901	3/7/1974	21300	Ukn	GAMA	1
25S40E33L01	USGS-354258117403901	3/25/1975	38400	Ukn	GAMA	1
25S40E33L01	USGS-354258117403901	8/17/1976	38100	Ukn	GAMA	1
25S40E33L02	USGS-354258117403902	6/21/1978	1400	Calc	B	1
25S40E33L02	USGS-354258117403902	5/31/1979	1300	Calc	B	1
25S40E33L02	USGS-354258117403902	5/22/1980	1400	Calc	B	1
25S40E33L02	USGS-354258117403902	6/9/1982	1400	Calc	B	1
25S40E33L02	USGS-354258117403902	3/7/1974	1270	Ukn	GAMA	1
25S40E33L02	USGS-354258117403902	3/25/1975	1290	Ukn	GAMA	1
25S40E33L02	USGS-354258117403902	8/17/1976	1230	Ukn	GAMA	1
25S40E35D01	TTBK-MW13	11/5/1998	5000	Lab	Tri	1
25S40E35D01	TTBK-MW13	2/16/2002	4830	Lab	TTEMI	1
25S40E35P01	USGS-354240117383501	7/9/1953	6790	Calc	Moyle	1
25S40E35P01	USGS-354240117383501	6/18/1972	7620	Lab	W	1
25S41E18Q01		6/3/1993	7870	Lab	H	1
25S41E19L01		6/19/1996	8100	Lab	H96	1
25S41E19L01		7/9/1953	12400	Calc	Moyle	1
25S41E21E01	USGS-354513117342201	7/31/1978	2900	Calc	B	1

Table 2: IWV TDS Data

Sample Dates in red indicate — min 1/26/1920 — 100
only sample month/year is known — max 3/5/2019 — 232000
count 2,044

Unique Well Name	alternateName	Sample Date	TDS (mg/L)	Analysis Type	TDS Reference	Confidence Level
25S41E21E01	USGS-354513117342201	12/9/1969	4040	Ukn	GAMA	1
25S41E21E01	USGS-354513117342201	10/20/1970	2950	Ukn	GAMA	1
25S41E21E01	USGS-354513117342201	6/23/1971	2050	Ukn	GAMA	1
25S41E21E01	USGS-354513117342201	10/27/1971	2590	Ukn	GAMA	1
25S41E21E01	USGS-354513117342201	10/25/1973	2820	Ukn	GAMA	1
25S41E21E01	USGS-354513117342201	5/1/1975	2710	Ukn	GAMA	1
25S41E21E01	USGS-354513117342201	5/12/1976	2890	Ukn	GAMA	1
25S41E31C01		7/9/1953	232000	Calc	Moyle	1
26S38E01G02	USGS-354215117500701	1/26/1973	546	Lab	GAMA-USGS	1
26S38E01G02	USGS-354215117500701	5/26/2009	500	Ukn	H-WQ	2
26S38E01H03	STANDARD	2/3/2007	560	Lab	FR: AB	1
26S38E02Q01	USGS-354146117512001	4/26/1946	516	Lab	GAMA-USGS	1
26S38E02Q01	USGS-354146117512001	4/11/1991	590	Ukn	KCWA WQ	3
26S38E11P02		5/4/2007	670	Ukn	H-WQ	2
26S38E12R01	Campbell	2/2/2007	560	Lab	FR: AB	1
26S38E17E01		1/12/1955	585	Lab	Moyle	1
26S38E27G01	USGS-353843117522401	9/17/1985	313	Ukn	GAMA	1
26S38E35B01		6/15/1982	190	Calc	B	1
26S38E35L	Marquardt Well.	2/7/2007	180	Lab	FR: AB	1
26S39E01A02		8/22/2008	26000	Ukn	KCWA WQ	3
26S39E02C01	USGS-354233117445801	4/26/1946	360	Lab	GAMA-USGS	1
26S39E02N01	USGS-354148117451701	4/27/1946	774	Lab	GAMA-USGS	1
26S39E03D01	USGS-354228117463001	4/27/1946	609	Lab	GAMA-USGS	1
26S39E05F01	NAWS Well 23	7/31/1978	560	Calc	B	1
26S39E05F01	NAWS Well 23	3/29/1980	590	Calc	B	1
26S39E05F01	NAWS Well 23	7/8/1988	594	Calc	B&S	1
26S39E05F01	NAWS Well 23	10/25/1973	586	Ukn	GAMA	1
26S39E05F01	NAWS Well 23	5/1/1975	522	Ukn	GAMA	1
26S39E05F01	NAWS Well 23	5/12/1976	555	Ukn	GAMA	1
26S39E05F01	NAWS Well 23	5/6/1987	100	Lab	GAMA	1
26S39E05F01	NAWS Well 23	3/27/1990	570	Lab	GAMA	1
26S39E05F01	NAWS Well 23	7/2/1990	600	Lab	GAMA	1
26S39E05F01	NAWS Well 23	5/18/1993	565	Lab	GAMA	1
26S39E05F01	NAWS Well 23	4/17/1995	585	Lab	GAMA	1
26S39E05F01	NAWS Well 23	9/15/1964	564	Lab	GAMA-USGS	1
26S39E05F01	NAWS Well 23	6/21/1965	490	Calc	GAMA-USGS	1
26S39E05F01	NAWS Well 23	5/16/1966	604	Lab	GAMA-USGS	1
26S39E05F01	NAWS Well 23	9/7/1966	628	Lab	GAMA-USGS	1
26S39E05F01	NAWS Well 23	10/23/1967	576	Lab	GAMA-USGS	1
26S39E05F01	NAWS Well 23	6/5/1968	560	Lab	GAMA-USGS	1
26S39E05F01	NAWS Well 23	11/4/1968	556	Lab	GAMA-USGS	1
26S39E05F01	NAWS Well 23	10/20/1969	624	Lab	GAMA-USGS	1
26S39E05F01	NAWS Well 23	6/1/1970	752	Lab	GAMA-USGS	1
26S39E05F01	NAWS Well 23	10/20/1970	574	Calc	GAMA-USGS	1
26S39E05F01	NAWS Well 23	6/23/1971	633	Lab	GAMA-USGS	1
26S39E05F01	NAWS Well 23	10/27/1971	609	Lab	GAMA-USGS	1

Table 2: IWV TDS Data

Sample Dates in red indicate — min 1/26/1920 — 100
only sample month/year is known — max 3/5/2019 — 232000
count 2,044

Unique Well Name	alternateName	Sample Date	TDS (mg/L)	Analysis Type	TDS Reference	Confidence Level
26S39E05F01	NAWS Well 23	8/3/1953	629	Calc	Moyle	1
26S39E05F01	NAWS Well 23	6/6/1972	602	Calc	W	1
26S39E06F01		8/19/2008	690	Ukn	H-WQ	2
26S39E06G01		5/24/2005	550	Ukn	H-WQ	2
26S39E07B	Sweet Water CO-OP Well 01	3/20/1989	390	Lab	GAMA	1
26S39E07B	Sweet Water CO-OP Well 01	7/20/1999	480	Lab	GAMA	1
26S39E07B	Sweet Water CO-OP Well 01	5/14/2003	440	Lab	GAMA	1
26S39E07B	Sweet Water CO-OP Well 01	6/9/2006	450	Lab	GAMA	1
26S39E07B	Sweet Water CO-OP Well 01	6/11/2009	460	Lab	GAMA	1
26S39E07B	Sweet Water CO-OP Well 01	7/11/2012	390	Lab	GAMA	1
26S39E07B	Sweet Water CO-OP Well 01	7/20/2015	440	Lab	GAMA	1
26S39E07B	Sweet Water CO-OP Well 01	7/10/2018	430	Lab	GAMA	1
26S39E07K05		2/19/2008	380	Ukn	H-WQ	2
26S39E07L		4/7/1998	536	Ukn	H-WQ	2
26S39E07M02		7/27/2010	470	Ukn	H-WQ	2
26S39E07M1	West Valley Mutual Well 01	3/20/1989	475	Lab	GAMA	1
26S39E07M1	West Valley Mutual Well 01	5/28/1996	470	Lab	GAMA	1
26S39E07M1	West Valley Mutual Well 01	6/8/1999	483	Lab	GAMA	1
26S39E07M1	West Valley Mutual Well 01	6/24/2002	490	Lab	GAMA	1
26S39E07M1	West Valley Mutual Well 01	8/10/2006	500	Lab	GAMA	1
26S39E07M1	West Valley Mutual Well 01	4/20/2009	570	Lab	GAMA	1
26S39E07M1	West Valley Mutual Well 01	8/21/2012	480	Lab	GAMA	1
26S39E07M1	West Valley Mutual Well 01	9/2/2015	480	Lab	GAMA	1
26S39E07M1	West Valley Mutual Well 01	11/19/2018	490	Lab	GAMA	2
26S39E07M2	West Valley Mutual Well 02	12/19/2011	430	Lab	GAMA	1
26S39E07M2	West Valley Mutual Well 02	5/13/2014	420	Lab	GAMA	1
26S39E07M2	West Valley Mutual Well 02	8/7/2017	480	Lab	GAMA	1
26S39E07N01	USGS-354055117494401	4/26/1946	358	Lab	GAMA-USGS	1
26S39E07N01	USGS-354055117494401	1/18/1971	335	Lab	GAMA-USGS	1
26S39E07N01	USGS-354055117494401	8/26/1949	302	Calc	Moyle	1
26S39E07N01	USGS-354055117494401	3/27/1951	332	Calc	Moyle	1
26S39E07P02	Campbell	4/3/2003	347	Ukn	L/H-WQ	2

Table 2: IWV TDS Data

Sample Dates in red indicate — min 1/26/1920 — 100
only sample month/year is known — max 3/5/2019 — 232000
count 2,044

Unique Well Name	alternateName	Sample Date	TDS (mg/L)	Analysis Type	TDS Reference	Confidence Level
26S39E07P03		5/7/2002	490	Ukn	KCWA WQ	3
26S39E08E01		5/31/1987	724	Calc	B&S	1
26S39E08E01		6/27/2006	300	Ukn	H-WQ	2
26S39E08K01	USGS-354117117475501	4/27/1946	386	Lab	GAMA-USGS	1
26S39E09H01		1/11/2007	340	Lab	FR: AB	1
26S39E09M01		1/1/2003	190	Ukn	AB	2
26S39E09M01		1/11/2007	180	Lab	FR: AB	1
26S39E10E01	98020-2	3/9/1999	525	Ukn	AB	2
26S39E10N01	USGS-354054117463001	1/24/1946	316	Lab	GAMA-USGS	1
26S39E11E01	USGS-354118117451501	11/17/1998	490	Ukn	AB	2
26S39E11E01	USGS-354118117451501	7/31/1978	400	Calc	B	1
26S39E11E01	USGS-354118117451501	5/4/1979	430	Calc	B	1
26S39E11E01	USGS-354118117451501	3/29/1980	430	Calc	B	1
26S39E11E01	USGS-354118117451501	10/25/1973	406	Ukn	GAMA	1
26S39E11E01	USGS-354118117451501	5/1/1975	414	Ukn	GAMA	1
26S39E11E01	USGS-354118117451501	5/12/1976	509	Ukn	GAMA	1
26S39E11E01	USGS-354118117451501	4/30/1946	288	Lab	GAMA-USGS	1
26S39E11E01	USGS-354118117451501	9/15/1964	263	Lab	GAMA-USGS	1
26S39E11E01	USGS-354118117451501	6/21/1965	316	Lab	GAMA-USGS	1
26S39E11E01	USGS-354118117451501	5/16/1966	312	Lab	GAMA-USGS	1
26S39E11E01	USGS-354118117451501	9/7/1966	328	Lab	GAMA-USGS	1
26S39E11E01	USGS-354118117451501	10/23/1967	356	Lab	GAMA-USGS	1
26S39E11E01	USGS-354118117451501	6/5/1968	312	Lab	GAMA-USGS	1
26S39E11E01	USGS-354118117451501	11/4/1968	452	Lab	GAMA-USGS	1
26S39E11E01	USGS-354118117451501	10/20/1969	368	Lab	GAMA-USGS	1
26S39E11E01	USGS-354118117451501	6/1/1970	360	Lab	GAMA-USGS	1
26S39E11E01	USGS-354118117451501	6/23/1971	391	Lab	GAMA-USGS	1
26S39E11E01	USGS-354118117451501	10/27/1971	423	Lab	GAMA-USGS	1
26S39E11E01	USGS-354118117451501	7/29/1953	248	Calc	Moyle	1
26S39E11E01	USGS-354118117451501	6/6/1972	366	Calc	W	1
26S39E11E02	96020-1	8/15/1996	490	Lab	H96	1
26S39E11Q01	USGS-354052117445201	4/27/1946	236	Lab	GAMA-USGS	1
26S39E12E01	USGS-354118117431301	1/22/1946	899	Ukn	GAMA	1
26S39E12E01	USGS-354118117431301	4/28/1946	1010	Ukn	GAMA	1
26S39E12G01	USGS-354120117434701	4/27/1946	270	Lab	GAMA-USGS	1
26S39E12N01	USGS-354057117441401	4/27/1946	274	Lab	GAMA-USGS	1
26S39E13R03	USNS-01	5/30/1987	223	Calc	B&M	1
26S39E13R03	USNS-01	4/10/1990	217	Ukn	GAMA	1
26S39E13R03	USNS-01	3/13/1991	225	Ukn	GAMA	1
26S39E13R03	USNS-01	4/16/1992	234	Ukn	GAMA	1
26S39E13R03	USNS-01	4/5/1993	228	Ukn	GAMA	1
26S39E13R03	USNS-01	3/21/1993	250	Lab	H	1
26S39E13R03	USNS-01	8/22/2008	230	Ukn	KCWA WQ	3
26S39E13R04	USGS-353959117431903	1/18/1989	826	Calc	B&M	1
26S39E13R04	USGS-353959117431903	3/21/1989	368	Ukn	GAMA	1
26S39E13R04	USGS-353959117431903	3/13/1991	272	Ukn	GAMA	1

Table 2: IWV TDS Data

Sample Dates in red indicate — min 1/26/1920 — 100
only sample month/year is known — max 3/5/2019 — 232000
count 2,044

Unique Well Name	alternateName	Sample Date	TDS (mg/L)	Analysis Type	TDS Reference	Confidence Level
26S39E13R04	USGS-353959117431903	4/16/1992	296	Ukn	GAMA	1
26S39E13R04	USGS-353959117431903	4/5/1993	237	Ukn	GAMA	1
26S39E14E01	USGS-354032117452401	4/27/1946	209	Lab	GAMA-USGS	1
26S39E14E01	USGS-354032117452401	1/22/1946	209	Calc	Moyle	1
26S39E14P01		1/11/2007	250	Lab	FR: AB	1
26S39E17F02	NACC-17-1; Kerr McGee 17-1; 17G02	5/31/1987	173	Calc	B&S	1
26S39E17F02	NACC-17-1; Kerr McGee 17-1; 17G02	3/21/1993	200	Ukn	H-WQ	2
26S39E17F02	NACC-17-1; Kerr McGee 17-1; 17G02	5/7/1983	143	Lab	Other	1
26S39E17L01		3/21/1993	200	Lab	H	1
26S39E18A01		6/16/2005	340	Ukn	H-WQ	2
26S39E18C03		2/8/2011	240	Ukn	H-WQ	2
26S39E18F01		3/11/1993	770	Lab	H	1
26S39E18K01	USGS-354017117490201	5/13/1970	255	Lab	GAMA-USGS	1
26S39E18K02		7/1/1988	312	Calc	B&S	1
26S39E18R01		6/4/2002	390	Ukn	H-WQ	2
26S39E19K01	NAWS Well 27	7/31/1978	410	Calc	B	1
26S39E19K01	NAWS Well 27	5/4/1979	410	Calc	B	1
26S39E19K01	NAWS Well 27	3/29/1980	410	Calc	B	1
26S39E19K01	NAWS Well 27	5/1/1975	423	Ukn	GAMA	1
26S39E19K01	NAWS Well 27	5/12/1976	450	Ukn	GAMA	1
26S39E19K01	NAWS Well 27	4/1/1987	393	Lab	GAMA	1
26S39E19K01	NAWS Well 27	3/27/1990	450	Lab	GAMA	1
26S39E19K01	NAWS Well 27	7/2/1990	465	Lab	GAMA	1
26S39E19K01	NAWS Well 27	5/18/1993	480	Lab	GAMA	1
26S39E19K01	NAWS Well 27	6/19/2003	332	Lab	GAMA	1
26S39E19K01	NAWS Well 27	12/27/2006	350	Lab	GAMA	1
26S39E19K01	NAWS Well 27	5/19/2009	330	Lab	GAMA	1
26S39E19K01	NAWS Well 27	12/21/2011	340	Lab	GAMA	1
26S39E19K01	NAWS Well 27	12/9/2014	380	Lab	GAMA	1
26S39E19K01	NAWS Well 27	11/15/2017	390	Lab	GAMA	1
26S39E19K01	NAWS Well 27	10/14/1963	1250	Lab	GAMA-USGS	1
26S39E19K01	NAWS Well 27	9/15/1964	707	Lab	GAMA-USGS	1
26S39E19K01	NAWS Well 27	1/10/1965	1170	Lab	GAMA-USGS	1
26S39E19K01	NAWS Well 27	1/11/1965	1400	Lab	GAMA-USGS	1
26S39E19K01	NAWS Well 27	1/12/1965	1090	Lab	GAMA-USGS	1
26S39E19K01	NAWS Well 27	8/12/1965	798	Lab	GAMA-USGS	1
26S39E19K01	NAWS Well 27	5/16/1966	716	Lab	GAMA-USGS	1
26S39E19K01	NAWS Well 27	9/7/1966	792	Lab	GAMA-USGS	1
26S39E19K01	NAWS Well 27	6/21/1967	456	Lab	GAMA-USGS	1
26S39E19K01	NAWS Well 27	10/23/1967	712	Lab	GAMA-USGS	1
26S39E19K01	NAWS Well 27	6/5/1968	632	Lab	GAMA-USGS	1
26S39E19K01	NAWS Well 27	11/4/1968	840	Lab	GAMA-USGS	1
26S39E19K01	NAWS Well 27	10/20/1969	572	Lab	GAMA-USGS	1
26S39E19K01	NAWS Well 27	6/1/1970	736	Lab	GAMA-USGS	1

Table 2: IWV TDS Data

Sample Dates in red indicate
only sample month/year is known

min	1/26/1920	100	
max	3/5/2019	232000	
count	2,044		

Unique Well Name	alternateName	Sample Date	TDS (mg/L)	Analysis Type	TDS Reference	Confidence Level
26S39E19K01	NAWS Well 27	10/20/1970	503	Calc	GAMA-USGS	1
26S39E19K01	NAWS Well 27	6/23/1971	624	Lab	GAMA-USGS	1
26S39E19K01	NAWS Well 27	10/27/1971	589	Lab	GAMA-USGS	1
26S39E19K01	NAWS Well 27	10/10/1960	697	Lab	Moyle	1
26S39E19K01	NAWS Well 27	5/1/1964	770	Lab	USGS	1
26S39E19K01	NAWS Well 27	6/6/1972	503	Calc	W	1
26S39E19P01	USGS-353910117491101	7/31/1978	320	Calc	B	1
26S39E19P01	USGS-353910117491101	5/4/1979	350	Calc	B	1
26S39E19P01	USGS-353910117491101	3/29/1980	410	Calc	B	1
26S39E19P01	USGS-353910117491101	10/25/1973	349	Ukn	GAMA	1
26S39E19P01	USGS-353910117491101	5/12/1976	313	Ukn	GAMA	1
26S39E19P01	USGS-353910117491101	9/18/1985	331	Ukn	GAMA	1
26S39E19P01	USGS-353910117491101	9/27/1986	318	Ukn	GAMA	1
26S39E19P01	USGS-353910117491101	12/12/1986	329	Ukn	GAMA	1
26S39E19P01	USGS-353910117491101	8/1/1961	355	Lab	GAMA-USGS	1
26S39E19P01	USGS-353910117491101	6/7/1962	415	Lab	GAMA-USGS	1
26S39E19P01	USGS-353910117491101	9/15/1964	291	Lab	GAMA-USGS	1
26S39E19P01	USGS-353910117491101	6/21/1965	368	Lab	GAMA-USGS	1
26S39E19P01	USGS-353910117491101	5/16/1966	332	Lab	GAMA-USGS	1
26S39E19P01	USGS-353910117491101	9/7/1966	336	Lab	GAMA-USGS	1
26S39E19P01	USGS-353910117491101	10/23/1967	320	Lab	GAMA-USGS	1
26S39E19P01	USGS-353910117491101	6/5/1968	336	Lab	GAMA-USGS	1
26S39E19P01	USGS-353910117491101	11/4/1968	304	Lab	GAMA-USGS	1
26S39E19P01	USGS-353910117491101	10/20/1969	368	Lab	GAMA-USGS	1
26S39E19P01	USGS-353910117491101	6/1/1970	328	Lab	GAMA-USGS	1
26S39E19P01	USGS-353910117491101	10/20/1970	325	Lab	GAMA-USGS	1
26S39E19P01	USGS-353910117491101	6/23/1971	358	Lab	GAMA-USGS	1
26S39E19P01	USGS-353910117491101	10/27/1971	342	Lab	GAMA-USGS	1
26S39E19P01	USGS-353910117491101	6/1/1953	320	Calc	Moyle	1
26S39E19P01	USGS-353910117491101	4/1/1963	441	Lab	USGS	1
26S39E19P01	USGS-353910117491101	5/1/1964	370	Lab	USGS	1
26S39E19P01	USGS-353910117491101	6/6/1972	300	Calc	W	1
26S39E19P02	NAWS Well 15	11/19/1985	335	Lab	GAMA	1
26S39E19P02	NAWS Well 15	9/27/1986	323	Lab	GAMA	1
26S39E19P02	NAWS Well 15	3/27/1990	355	Lab	GAMA	1
26S39E19P02	NAWS Well 15	7/2/1990	345	Lab	GAMA	1
26S39E19P02	NAWS Well 15	5/18/1993	255	Lab	GAMA	1
26S39E19P02	NAWS Well 15	6/19/2003	346	Lab	GAMA	1
26S39E19P02	NAWS Well 15	12/27/2006	380	Lab	GAMA	1
26S39E19P02	NAWS Well 15	5/19/2009	370	Lab	GAMA	1
26S39E19P02	NAWS Well 15	12/21/2011	370	Lab	GAMA	1
26S39E19P02	NAWS Well 15	12/9/2014	400	Lab	GAMA	1
26S39E19P02	NAWS Well 15	11/15/2017	410	Lab	GAMA	1
26S39E19Q01	USGS-354408117485801	7/31/1978	380	Calc	B	1
26S39E19Q01	USGS-354408117485801	5/4/1979	520	Calc	B	1
26S39E19Q01	USGS-354408117485801	3/29/1980	380	Calc	B	1

Table 2: IWV TDS Data

Sample Dates in red indicate
only sample month/year is known

min	1/26/1920	100	
max	3/5/2019	232000	
count	2,044		

Unique Well Name	alternateName	Sample Date	TDS (mg/L)	Analysis Type	TDS Reference	Confidence Level
26S39E19Q01	USGS-354408117485801	5/1/1975	544	Ukn	GAMA	1
26S39E19Q01	USGS-354408117485801	5/12/1976	599	Ukn	GAMA	1
26S39E19Q01	USGS-354408117485801	8/1/1961	395	Lab	GAMA-USGS	1
26S39E19Q01	USGS-354408117485801	6/7/1962	430	Lab	GAMA-USGS	1
26S39E19Q01	USGS-354408117485801	10/14/1963	518	Lab	GAMA-USGS	1
26S39E19Q01	USGS-354408117485801	5/5/1964	410	Lab	GAMA-USGS	1
26S39E19Q01	USGS-354408117485801	9/15/1964	382	Lab	GAMA-USGS	1
26S39E19Q01	USGS-354408117485801	6/21/1965	496	Lab	GAMA-USGS	1
26S39E19Q01	USGS-354408117485801	5/16/1966	348	Lab	GAMA-USGS	1
26S39E19Q01	USGS-354408117485801	9/7/1966	352	Lab	GAMA-USGS	1
26S39E19Q01	USGS-354408117485801	6/6/1972	470	Lab	GAMA-USGS	1
26S39E19Q01	USGS-354408117485801	4/5/1955	365	Calc	Moyle	1
26S39E19Q01	USGS-354408117485801	10/17/1956	431	Calc	Moyle	1
26S39E19Q01	USGS-354408117485801	9/19/1957	365	Calc	Moyle	1
26S39E19Q01	USGS-354408117485801	9/18/1958	343	Calc	Moyle	1
26S39E19Q01	USGS-354408117485801	11/20/1959	203	Calc	Moyle	1
26S39E19Q01	USGS-354408117485801	8/11/1960	346	Calc	Moyle	1
26S39E19Q01	USGS-354408117485801	4/1/1963	515	Lab	USGS	1
26S39E20C01	CLODT OLD WELL	4/7/1998	378	Ukn	H-WQ	2
26S39E20F01	USGS-353942117481501	9/15/1964	263	Lab	GAMA-USGS	1
26S39E20F01	USGS-353942117481501	5/22/1969	270	Lab	GAMA-USGS	1
26S39E20K03		11/19/2007	290	Ukn	H-WQ	2
26S39E20Q01	USGS-353908117480501	4/26/1946	246	Lab	GAMA-USGS	1
26S39E20R01	NAWS Well 30	3/27/1990	225	Lab	GAMA	1
26S39E20R01	NAWS Well 30	5/18/1993	225	Lab	GAMA	1
26S39E20R01	NAWS Well 30	4/17/1995	195	Lab	GAMA	1
26S39E20R01	NAWS Well 30	6/19/2003	200	Lab	GAMA	1
26S39E20R01	NAWS Well 30	12/27/2006	270	Lab	GAMA	1
26S39E20R01	NAWS Well 30	5/19/2009	220	Lab	GAMA	1
26S39E20R01	NAWS Well 30	12/21/2011	220	Lab	GAMA	1
26S39E20R01	NAWS Well 30	12/9/2014	300	Lab	GAMA	1
26S39E20R01	NAWS Well 30	11/15/2017	230	Lab	GAMA	1
26S39E20R02		5/29/1987	199	Lab	B&S	1
26S39E21Q01	NAWS Well 31	5/18/1993	215	Lab	GAMA	1
26S39E21Q01	NAWS Well 31	4/17/1995	225	Lab	GAMA	1
26S39E21Q01	NAWS Well 31	6/19/2003	192	Lab	GAMA	1
26S39E21Q01	NAWS Well 31	12/27/2006	220	Lab	GAMA	1
26S39E21Q01	NAWS Well 31	3/12/2010	240	Lab	GAMA	1
26S39E21Q01	NAWS Well 31	12/21/2011	210	Lab	GAMA	1
26S39E21Q01	NAWS Well 31	12/9/2014	230	Lab	GAMA	1
26S39E21Q01	NAWS Well 31	11/15/2017	220	Lab	GAMA	1
26S39E23E01	USGS-353926117452701	4/27/1946	240	Lab	GAMA-USGS	1
26S39E23H02	NAWS Well 28	3/27/1990	250	Lab	GAMA	1
26S39E23H02	NAWS Well 28	7/2/1990	245	Lab	GAMA	1
26S39E23H02	NAWS Well 28	5/18/1993	265	Lab	GAMA	1
26S39E23H02	NAWS Well 28	6/19/2003	161	Lab	GAMA	1

Table 2: IWV TDS Data

Sample Dates in red indicate
only sample month/year is known

min	1/26/1920	100	
max	3/5/2019	232000	
count	2,044		

Unique Well Name	alternateName	Sample Date	TDS (mg/L)	Analysis Type	TDS Reference	Confidence Level
26S39E23H02	NAWS Well 28	12/16/2009	170	Lab	GAMA	1
26S39E23H02a	NAWS Well 28A	4/17/2007	190	Lab	GAMA	1
26S39E23H02a	NAWS Well 28A	12/20/2011	180	Lab	GAMA	1
26S39E23H02a	NAWS Well 28A	12/9/2014	210	Lab	GAMA	1
26S39E23H02a	NAWS Well 28A	11/15/2017	210	Lab	GAMA	1
26S39E23J01	USGS-353937117443501	7/31/1978	230	Calc	B	1
26S39E23J01	USGS-353937117443501	5/4/1979	250	Calc	B	1
26S39E23J01	USGS-353937117443501	10/25/1973	233	Ukn	GAMA	1
26S39E23J01	USGS-353937117443501	5/1/1975	245	Ukn	GAMA	1
26S39E23J01	USGS-353937117443501	5/12/1976	248	Ukn	GAMA	1
26S39E23J01	USGS-353937117443501	4/13/1986	250	Ukn	GAMA	1
26S39E23J01	USGS-353937117443501	10/14/1963	251	Lab	GAMA-USGS	1
26S39E23J01	USGS-353937117443501	9/15/1964	263	Lab	GAMA-USGS	1
26S39E23J01	USGS-353937117443501	6/21/1965	268	Lab	GAMA-USGS	1
26S39E23J01	USGS-353937117443501	5/16/1966	236	Lab	GAMA-USGS	1
26S39E23J01	USGS-353937117443501	9/7/1966	276	Lab	GAMA-USGS	1
26S39E23J01	USGS-353937117443501	10/23/1967	236	Lab	GAMA-USGS	1
26S39E23J01	USGS-353937117443501	6/5/1968	228	Lab	GAMA-USGS	1
26S39E23J01	USGS-353937117443501	11/4/1968	224	Lab	GAMA-USGS	1
26S39E23J01	USGS-353937117443501	10/20/1969	280	Lab	GAMA-USGS	1
26S39E23J01	USGS-353937117443501	6/1/1970	216	Lab	GAMA-USGS	1
26S39E23J01	USGS-353937117443501	10/20/1970	270	Lab	GAMA-USGS	1
26S39E23J01	USGS-353937117443501	10/27/1971	256	Lab	GAMA-USGS	1
26S39E23J01	USGS-353937117443501	10/17/1960	247	Lab	Moyle	1
26S39E23J01	USGS-353937117443501	4/1/1963	308	Lab	USGS	1
26S39E23J01	USGS-353937117443501	5/1/1964	295	Lab	USGS	1
26S39E23J01	USGS-353937117443501	6/6/1972	218	Calc	W	1
26S39E24E01	USGS-353935117442001	4/27/1946	257	Lab	GAMA-USGS	1
26S39E24K01		5/4/1979	580	Calc	B	1
26S39E24M	NAWS Well 29	4/21/1987	212	Lab	GAMA	1
26S39E24M	NAWS Well 29	3/27/1990	230	Lab	GAMA	1
26S39E24M	NAWS Well 29	7/2/1990	235	Lab	GAMA	1
26S39E24M	NAWS Well 29	5/18/1993	265	Lab	GAMA	1
26S39E24M	NAWS Well 29	4/17/1995	260	Lab	GAMA	1
26S39E24M01	USGS-353922117442301	7/31/1978	200	Calc	B	1
26S39E24M01	USGS-353922117442301	5/4/1979	220	Calc	B	1
26S39E24M01	USGS-353922117442301	3/29/1980	210	Calc	B	1
26S39E24M01	USGS-353922117442301	9/15/1964	249	Ukn	GAMA	1
26S39E24M01	USGS-353922117442301	10/20/1970	250	Ukn	GAMA	1
26S39E24M01	USGS-353922117442301	10/25/1973	217	Ukn	GAMA	1
26S39E24M01	USGS-353922117442301	5/1/1975	214	Ukn	GAMA	1
26S39E24M01	USGS-353922117442301	5/12/1976	250	Ukn	GAMA	1
26S39E24M01	USGS-353922117442301	9/18/1985	235	Ukn	GAMA	1
26S39E24M01	USGS-353922117442301	10/14/1963	209	Lab	GAMA-USGS	1
26S39E24M01	USGS-353922117442301	5/16/1966	216	Lab	GAMA-USGS	1
26S39E24M01	USGS-353922117442301	9/7/1966	256	Lab	GAMA-USGS	1

Table 2: IWV TDS Data

Sample Dates in red indicate
only sample month/year is known

min	1/26/1920	100	
max	3/5/2019	232000	
count	2,044		

Unique Well Name	alternateName	Sample Date	TDS (mg/L)	Analysis Type	TDS Reference	Confidence Level
26S39E24M01	USGS-353922117442301	10/23/1967	196	Lab	GAMA-USGS	1
26S39E24M01	USGS-353922117442301	6/5/1968	184	Lab	GAMA-USGS	1
26S39E24M01	USGS-353922117442301	11/4/1968	204	Lab	GAMA-USGS	1
26S39E24M01	USGS-353922117442301	10/20/1969	236	Lab	GAMA-USGS	1
26S39E24M01	USGS-353922117442301	6/1/1970	176	Lab	GAMA-USGS	1
26S39E24M01	USGS-353922117442301	6/23/1971	246	Lab	GAMA-USGS	1
26S39E24M01	USGS-353922117442301	10/27/1971	223	Lab	GAMA-USGS	1
26S39E24M01	USGS-353922117442301	5/18/1993	265	Ukn	H-WQ	2
26S39E24M01	USGS-353922117442301	10/27/1960	231	Lab	Moyle	1
26S39E24M01	USGS-353922117442301	4/1/1963	203	Lab	USGS	1
26S39E24M01	USGS-353922117442301	5/1/1964	200	Lab	USGS	1
26S39E24M01	USGS-353922117442301	6/6/1972	218	Calc	W	1
26S39E24P01	USGS-353911117435701	5/4/1979	210	Calc	B	1
26S39E24P01	USGS-353911117435701	5/29/1987	215	Calc	B&S	1
26S39E24P01	USGS-353911117435701	10/25/1973	218	Ukn	GAMA	1
26S39E24P01	USGS-353911117435701	8/1/1961	310	Lab	GAMA-USGS	1
26S39E24P01	USGS-353911117435701	6/7/1962	260	Lab	GAMA-USGS	1
26S39E24P01	USGS-353911117435701	10/14/1963	221	Lab	GAMA-USGS	1
26S39E24P01	USGS-353911117435701	9/15/1964	249	Lab	GAMA-USGS	1
26S39E24P01	USGS-353911117435701	6/21/1965	284	Lab	GAMA-USGS	1
26S39E24P01	USGS-353911117435701	5/16/1966	208	Lab	GAMA-USGS	1
26S39E24P01	USGS-353911117435701	9/7/1966	244	Lab	GAMA-USGS	1
26S39E24P01	USGS-353911117435701	10/23/1967	212	Lab	GAMA-USGS	1
26S39E24P01	USGS-353911117435701	6/5/1968	252	Lab	GAMA-USGS	1
26S39E24P01	USGS-353911117435701	11/4/1968	232	Lab	GAMA-USGS	1
26S39E24P01	USGS-353911117435701	6/1/1970	244	Lab	GAMA-USGS	1
26S39E24P01	USGS-353911117435701	6/23/1971	254	Lab	GAMA-USGS	1
26S39E24P01	USGS-353911117435701	10/27/1971	242	Lab	GAMA-USGS	1
26S39E24P01	USGS-353911117435701	3/6/1958	237	Lab	Moyle	1
26S39E24P01	USGS-353911117435701	9/18/1958	201	Calc	Moyle	1
26S39E24P01	USGS-353911117435701	11/20/1959	210	Calc	Moyle	1
26S39E24P01	USGS-353911117435701	8/11/1960	191	Calc	Moyle	1
26S39E24P01	USGS-353911117435701	5/1/1964	240	Lab	USGS	1
26S39E24P01	USGS-353911117435701	6/6/1972	211	Calc	W	1
26S39E24P03	NAWS Well 18	11/19/1985	215	Lab	GAMA	1
26S39E24P03	NAWS Well 18	3/27/1990	215	Lab	GAMA	1
26S39E24P03	NAWS Well 18	7/2/1990	230	Lab	GAMA	1
26S39E24P03	NAWS Well 18	6/19/2003	180	Lab	GAMA	1
26S39E24P03	NAWS Well 18	4/17/2007	230	Lab	GAMA	1
26S39E24P03	NAWS Well 18	5/19/2009	160	Lab	GAMA	1
26S39E24P03	NAWS Well 18	12/21/2011	200	Lab	GAMA	1
26S39E24P03	NAWS Well 18	3/1/2017	190	Lab	GAMA	1
26S39E24P03	NAWS Well 18	11/15/2017	200	Lab	GAMA	1
26S39E24Q01	USGS-353911117434001	10/14/1963	221	Lab	GAMA-USGS	1
26S39E24Q01	USGS-353911117434001	6/6/1952	219	Calc	Moyle	1
26S39E24Q01	USGS-353911117434001	10/14/1955	226	Calc	Moyle	1

Table 2: IWV TDS Data

Sample Dates in red indicate
only sample month/year is known

min	1/26/1920	100	
max	3/5/2019	232000	
count	2,044		

Unique Well Name	alternateName	Sample Date	TDS (mg/L)	Analysis Type	TDS Reference	Confidence Level
26S39E24Q01	USGS-353911117434001	10/17/1956	197	Calc	Moyle	1
26S39E24Q01	USGS-353911117434001	9/19/1957	218	Calc	Moyle	1
26S39E24Q01	USGS-353911117434001	9/18/1958	231	Calc	Moyle	1
26S39E24R01	USGS-353911117432601	9/18/1957	164	Ukn	GAMA	1
26S39E24R01	USGS-353911117432601	4/5/1955	146	Calc	Moyle	1
26S39E24R01	USGS-353911117432601	10/14/1955	158	Calc	Moyle	1
26S39E24R01	USGS-353911117432601	10/17/1956	141	Calc	Moyle	1
26S39E24R01	USGS-353911117432601	9/18/1958	152	Calc	Moyle	1
26S39E25D01	26S39E25D001M	4/30/1958	390	Ukn	GAMA	1
26S39E25D01	26S39E25D001M	5/30/1996	180	Ukn	H-WQ	2
26S39E25E	Searles Valley Minerals Op Well 30	6/4/2002	250	Lab	GAMA	1
26S39E25E	Searles Valley Minerals Op Well 30	9/20/2005	290	Lab	GAMA	1
26S39E25E	Searles Valley Minerals Op Well 30	9/16/2008	240	Lab	GAMA	1
26S39E25E	Searles Valley Minerals Op Well 30	6/16/2009	250	Lab	GAMA	1
26S39E25E	Searles Valley Minerals Op Well 30	6/7/2011	250	Lab	GAMA	1
26S39E25E	Searles Valley Minerals Op Well 30	6/3/2014	270	Lab	GAMA	1
26S39E25E	Searles Valley Minerals Op Well 30	6/6/2017	260	Lab	GAMA	1
26S39E25E01	USGS-353849117441701	5/29/1987	261	Calc	B&S	1
26S39E25E01	USGS-353849117441701	6/12/1987	251	Lab	B&S	1
26S39E25E01	USGS-353849117441701	2/17/1967	281	Lab	GAMA-USGS	1
26S39E25E01	USGS-353849117441701	9/22/1967	290	Lab	GAMA-USGS	1
26S39E25E01	USGS-353849117441701	6/8/1999	237	Ukn	H-WQ	2
26S39E26A01	USBR-04	5/30/1996	180	Lab	H96	1
26S39E26A01	USBR-04	10/31/1990	183	Lab	USBR	1
26S39E26A02-D	TTIWV-MW01-D	2/17/2002	199	Lab	TTEMI	1
26S39E26A02-I	TTIWV-MW01-I	2/17/2002	278	Lab	TTEMI	1
26S39E26B	IWVWD Well 17	1/7/1988	251	Lab	B&S	1
26S39E26B	IWVWD Well 17	3/8/1990	218	Lab	GAMA	1
26S39E26B	IWVWD Well 17	5/10/1990	168	Lab	GAMA	1
26S39E26B	IWVWD Well 17	1/22/1991	180	Lab	GAMA	1
26S39E26B	IWVWD Well 17	2/5/1992	190	Lab	GAMA	1
26S39E26B	IWVWD Well 17	10/8/1992	154	Lab	GAMA	1
26S39E26B	IWVWD Well 17	12/3/1992	154	Lab	GAMA	1
26S39E26B	IWVWD Well 17	1/21/1993	170	Lab	GAMA	1
26S39E26B	IWVWD Well 17	3/1/1993	169	Lab	GAMA	1
26S39E26B	IWVWD Well 17	2/2/1994	558	Lab	GAMA	1
26S39E26B	IWVWD Well 17	8/8/1994	167	Lab	GAMA	1
26S39E26B	IWVWD Well 17	9/1/1994	162	Lab	GAMA	1
26S39E26B	IWVWD Well 17	6/22/1995	173	Lab	GAMA	1
26S39E26B	IWVWD Well 17	1/24/1996	182	Lab	GAMA	1
26S39E26B	IWVWD Well 17	1/13/1997	190	Lab	GAMA	1
26S39E26B	IWVWD Well 17	2/6/1998	192	Lab	GAMA	1

Table 2: IWV TDS Data

Sample Dates in red indicate
only sample month/year is known

min	1/26/1920	100	
max	3/5/2019	232000	
count	2,044		

Unique Well Name	alternateName	Sample Date	TDS (mg/L)	Analysis Type	TDS Reference	Confidence Level
26S39E26B	IWVWD Well 17	9/9/1998	168	Lab	GAMA	1
26S39E26B	IWVWD Well 17	9/15/1999	164	Lab	GAMA	1
26S39E26B	IWVWD Well 17	8/7/2000	175	Lab	GAMA	1
26S39E26B	IWVWD Well 17	8/21/2001	190	Lab	GAMA	1
26S39E26B	IWVWD Well 17	8/1/2002	180	Lab	GAMA	1
26S39E26B	IWVWD Well 17	9/10/2003	210	Lab	GAMA	1
26S39E26B	IWVWD Well 17	8/12/2004	190	Lab	GAMA	1
26S39E26B	IWVWD Well 17	8/7/2007	200	Lab	GAMA	1
26S39E26B	IWVWD Well 17	4/1/2008	220	Lab	GAMA	1
26S39E26B	IWVWD Well 17	4/5/2011	190	Lab	GAMA	1
26S39E26B	IWVWD Well 17	5/27/2014	210	Lab	GAMA	1
26S39E26B	IWVWD Well 17	5/23/2017	200	Lab	GAMA	1
26S39E26B	IWVWD Well 17	11/13/1967	203	Lab	GAMA-USGS	1
26S39E26B1	Hometown Water Assoc. Well 01	1/9/2002	230	Lab	GAMA	1
26S39E26B1	Hometown Water Assoc. Well 01	8/17/2005	240	Lab	GAMA	1
26S39E26B1	Hometown Water Assoc. Well 01	10/29/2008	300	Lab	GAMA	1
26S39E26B1	Hometown Water Assoc. Well 01	4/20/2009	290	Lab	GAMA	1
26S39E26B1	Hometown Water Assoc. Well 01	8/23/2012	310	Lab	GAMA	1
26S39E26B1	Hometown Water Assoc. Well 01	9/16/2015	370	Lab	GAMA	1
26S39E26B1	Hometown Water Assoc. Well 01	9/6/2018	330	Lab	GAMA	1
26S39E26B2	Buttermilk Acr Water System Well 1	3/29/1994	280	Lab	GAMA	1
26S39E26B2	Buttermilk Acr Water System Well 1	12/17/2003	270	Lab	GAMA	1
26S39E26C01		8/5/2010	310	Ukn	H-WQ	2
26S39E26D01	26S39E26D001M	11/1/1982	256	Ukn	GAMA	1
26S39E26D01	26S39E26D001M	1/26/1920	285	Lab	GAMA-USGS	1
26S39E26D02	USGS-353905117444901	3/22/2005	550	Ukn	GAMA	1
26S39E26D02	USGS-353905117444901	2/2/1994	558	Ukn	H-WQ	2
26S39E26L04		10/27/2009	280	Ukn	H-WQ	2
26S39E27C01	26S39E27C001M	1/7/1988	269	Lab	B&S	1
26S39E27C01	26S39E27C001M	11/1/1982	250	Ukn	GAMA	1
26S39E27C01	26S39E27C001M	7/25/1985	255	Ukn	KCWA WQ	3
26S39E27C01	26S39E27C001M	9/1/1988	242	Ukn	KCWA WQ	3
26S39E27C01	26S39E27C001M	12/20/1989	248	Ukn	KCWA WQ	3
26S39E27C01	26S39E27C001M	3/5/1992	232	Ukn	KCWA WQ	3
26S39E27C01	26S39E27C001M	2/2/1994	235	Ukn	KCWA WQ	3
26S39E27C01	26S39E27C001M	2/15/1995	257	Ukn	KCWA WQ	3
26S39E27C01	26S39E27C001M	1/24/1996	238	Ukn	KCWA WQ	3
26S39E27C01	26S39E27C001M	1/13/1997	248	Ukn	KCWA WQ	3
26S39E27C01	26S39E27C001M	1/26/1998	244	Ukn	KCWA WQ	3
26S39E27C01	26S39E27C001M	9/9/1998	229	Ukn	KCWA WQ	3

Table 2: IWV TDS Data

Sample Dates in red indicate — min 1/26/1920 — 100
only sample month/year is known — max 3/5/2019 — 232000
count 2,044

Unique Well Name	alternateName	Sample Date	TDS (mg/L)	Analysis Type	TDS Reference	Confidence Level
26S39E27C01	26S39E27C001M	9/15/1999	240	Ukn	KCWA WQ	3
26S39E27D	IWVWD Well 30	1/1/2008	560	Ukn	AB	2
26S39E27D	IWVWD Well 30	4/4/2007	220	Lab	FR: AB	1
26S39E27D	IWVWD Well 30	1/21/1993	179	Lab	GAMA	1
26S39E27D	IWVWD Well 30	2/2/1994	186	Lab	GAMA	1
26S39E27D	IWVWD Well 30	2/15/1995	228	Lab	GAMA	1
26S39E27D	IWVWD Well 30	1/24/1996	194	Lab	GAMA	1
26S39E27D	IWVWD Well 30	1/13/1997	206	Lab	GAMA	1
26S39E27D	IWVWD Well 30	1/26/1998	192	Lab	GAMA	1
26S39E27D	IWVWD Well 30	9/9/1998	183	Lab	GAMA	1
26S39E27D	IWVWD Well 30	9/15/1999	181	Lab	GAMA	1
26S39E27D	IWVWD Well 30	8/7/2000	189	Lab	GAMA	1
26S39E27D	IWVWD Well 30	8/21/2001	180	Lab	GAMA	1
26S39E27D	IWVWD Well 30	8/1/2002	190	Lab	GAMA	1
26S39E27D	IWVWD Well 30	9/10/2003	240	Lab	GAMA	1
26S39E27D	IWVWD Well 30	8/12/2004	220	Lab	GAMA	1
26S39E27D	IWVWD Well 30	3/29/2005	210	Lab	GAMA	1
26S39E27D	IWVWD Well 30	4/1/2008	220	Lab	GAMA	1
26S39E27D	IWVWD Well 30	4/5/2011	220	Lab	GAMA	1
26S39E27D	IWVWD Well 30	5/27/2014	240	Lab	GAMA	1
26S39E27D	IWVWD Well 30	5/23/2017	240	Lab	GAMA	1
26S39E27D01	MW-32-S	4/28/1993	270	Ukn	AB	2
26S39E27D01	MW-32-S	4/4/2007	220	Ukn	AB	2
26S39E27D01	MW-32-S	1/21/1993	179	Ukn	KCWA WQ	3
26S39E27D01	MW-32-S	2/2/1994	186	Ukn	KCWA WQ	3
26S39E27D01	MW-32-S	2/15/1995	228	Ukn	KCWA WQ	3
26S39E27D01	MW-32-S	1/24/1996	194	Ukn	KCWA WQ	3
26S39E27D01	MW-32-S	5/30/1996	140	Ukn	KCWA WQ	3
26S39E27D01	MW-32-S	1/26/1998	192	Ukn	KCWA WQ	3
26S39E27D01	MW-32-S	9/9/1998	183	Ukn	KCWA WQ	3
26S39E27D01	MW-32-S	9/15/1999	181	Ukn	KCWA WQ	3
26S39E27D01	MW-32-S	10/17/1991	252	Lab	USBR	1
26S39E27D02	MW-32-S/M	5/30/1996	140	Lab	H96	1
26S39E27D02	MW-32-S/M	10/18/1991	169	Lab	USBR	1
26S39E27D03	MW-32-D/M	6/4/1996	160	Lab	H96	1
26S39E27D03	MW-32-D/M	10/21/1991	176	Lab	USBR	1
26S39E27D04	MW-32-D	10/21/1991	526	Lab	USBR	1
26S39E27J	Dune 3 Mutual Well 02	3/13/1997	280	Lab	GAMA	1
26S39E27J	Dune 3 Mutual Well 02	6/12/2002	280	Lab	GAMA	1
26S39E27J	Dune 3 Mutual Well 02	6/9/2006	300	Lab	GAMA	1
26S39E27J	Dune 3 Mutual Well 02	3/4/2009	280	Lab	GAMA	1
26S39E27J	Dune 3 Mutual Well 02	2/9/2012	280	Lab	GAMA	1
26S39E27J	Dune 3 Mutual Well 02	2/2/2015	310	Lab	GAMA	1
26S39E27J	Dune 3 Mutual Well 02	1/9/2018	280	Lab	GAMA	1
26S39E27L1	China Lakes Mutual Well 01	10/12/1990	245	Lab	GAMA	1

Table 2: IWV TDS Data

Sample Dates in red indicate — min 1/26/1920 — 100
only sample month/year is known — max 3/5/2019 — 232000
count 2,044

Unique Well Name	alternateName	Sample Date	TDS (mg/L)	Analysis Type	TDS Reference	Confidence Level
26S39E27L1	China Lakes Mutual Well 01	3/25/1991	296	Lab	GAMA	1
26S39E27L1	China Lakes Mutual Well 01	8/8/1995	305	Lab	GAMA	1
26S39E27L1	China Lakes Mutual Well 01	6/15/1999	300	Lab	GAMA	1
26S39E27L1	China Lakes Mutual Well 01	5/4/2005	290	Lab	GAMA	1
26S39E27L1	China Lakes Mutual Well 01	10/29/2008	310	Lab	GAMA	1
26S39E27L1	China Lakes Mutual Well 01	4/20/2009	320	Lab	GAMA	1
26S39E27L1	China Lakes Mutual Well 01	9/17/2012	170	Lab	GAMA	1
26S39E27L1	China Lakes Mutual Well 01	8/5/2015	330	Lab	GAMA	1
26S39E27L1	China Lakes Mutual Well 01	7/9/2018	300	Lab	GAMA	1
26S39E27L2	China Lakes Mutual Well 02	3/16/2011	290	Lab	GAMA	1
26S39E27L2	China Lakes Mutual Well 02	6/9/2014	310	Lab	GAMA	1
26S39E27L2	China Lakes Mutual Well 02	7/10/2017	300	Lab	GAMA	1
26S39E27Q	Dune 3 Mutual Well 01	6/12/2002	270	Lab	GAMA	1
26S39E27Q	Dune 3 Mutual Well 01	6/9/2006	260	Lab	GAMA	1
26S39E27Q	Dune 3 Mutual Well 01	3/4/2009	280	Lab	GAMA	1
26S39E27Q	Dune 3 Mutual Well 01	2/9/2012	320	Lab	GAMA	1
26S39E27Q	Dune 3 Mutual Well 01	2/2/2015	300	Lab	GAMA	1
26S39E27Q	Dune 3 Mutual Well 01	1/9/2018	310	Lab	GAMA	1
26S39E28A01		4/28/1993	270	Lab	H	1
26S39E28B02	USGS-353902117465501	10/7/1970	212	Lab	GAMA-USGS	1
26S39E28B1	Sierra Breeze mutual Well 01	11/8/1995	420	Lab	GAMA	1
26S39E28B1	Sierra Breeze mutual Well 01	6/15/1999	453	Lab	GAMA	1
26S39E28B1	Sierra Breeze mutual Well 01	9/6/2005	450	Lab	GAMA	1
26S39E28B1	Sierra Breeze mutual Well 01	10/29/2008	510	Lab	GAMA	1
26S39E28B2	Sierra Breeze mutual Well 02	9/6/2005	310	Lab	GAMA	1
26S39E28B2	Sierra Breeze mutual Well 02	10/29/2008	350	Lab	GAMA	1
26S39E28B2	Sierra Breeze mutual Well 02	9/14/2011	530	Lab	GAMA	1
26S39E28B2	Sierra Breeze mutual Well 02	7/7/2014	520	Lab	GAMA	1
26S39E28B2	Sierra Breeze mutual Well 02	7/18/2017	480	Lab	GAMA	1
26S39E28B3	Sierra Breeze mutual Well 03	8/2/2010	330	Lab	GAMA	1

Table 2: IWV TDS Data

Sample Dates in red indicate
only sample month/year is known

min	1/26/1920	100	
max	3/5/2019	232000	
count	2,044		

Unique Well Name	alternateName	Sample Date	TDS (mg/L)	Analysis Type	TDS Reference	Confidence Level
26S39E28B3	Sierra Breeze mutual Well 03	10/3/2013	320	Lab	GAMA	1
26S39E28B3	Sierra Breeze mutual Well 03	12/11/2016	330	Lab	GAMA	1
26S39E28C02		5/1/1957	278	Calc	Moyle	1
26S39E28D01		1/4/2005	280	Ukn	H-WQ	2
26S39E28G03		4/8/2008	310	Ukn	H-WQ	2
26S39E28P01		8/21/2001	260	Ukn	H-WQ	2
26S39E28R01	IWVWD Well 31	4/4/2007	260	Lab	FR: AB	1
26S39E28R01	IWVWD Well 31	7/10/1992	197	Lab	GAMA	1
26S39E28R01	IWVWD Well 31	1/21/1993	200	Lab	GAMA	1
26S39E28R01	IWVWD Well 31	2/2/1994	197	Lab	GAMA	1
26S39E28R01	IWVWD Well 31	2/15/1995	215	Lab	GAMA	1
26S39E28R01	IWVWD Well 31	1/24/1996	206	Lab	GAMA	1
26S39E28R01	IWVWD Well 31	1/13/1997	210	Lab	GAMA	1
26S39E28R01	IWVWD Well 31	2/24/1998	216	Lab	GAMA	1
26S39E28R01	IWVWD Well 31	3/17/1998	215	Lab	GAMA	1
26S39E28R01	IWVWD Well 31	9/9/1998	199	Lab	GAMA	1
26S39E28R01	IWVWD Well 31	9/15/1999	198	Lab	GAMA	1
26S39E28R01	IWVWD Well 31	8/7/2000	204	Lab	GAMA	1
26S39E28R01	IWVWD Well 31	8/21/2001	210	Lab	GAMA	1
26S39E28R01	IWVWD Well 31	8/1/2002	200	Lab	GAMA	1
26S39E28R01	IWVWD Well 31	9/10/2003	270	Lab	GAMA	1
26S39E28R01	IWVWD Well 31	8/12/2004	240	Lab	GAMA	1
26S39E28R01	IWVWD Well 31	3/29/2005	240	Lab	GAMA	1
26S39E28R01	IWVWD Well 31	4/1/2008	550	Lab	GAMA	1
26S39E28R01	IWVWD Well 31	4/5/2011	230	Lab	GAMA	1
26S39E28R01	IWVWD Well 31	5/27/2014	250	Lab	GAMA	1
26S39E28R01	IWVWD Well 31	5/23/2017	220	Lab	GAMA	1
26S39E29L1	E. Inyokern Mutual Well 01	12/20/1989	295	Lab	GAMA	1
26S39E29L1	E. Inyokern Mutual Well 01	3/18/2003	290	Lab	GAMA	1
26S39E29L1	E. Inyokern Mutual Well 01	3/1/2006	280	Lab	GAMA	1
26S39E29L1	E. Inyokern Mutual Well 01	4/20/2009	320	Lab	GAMA	1
26S39E29L1	E. Inyokern Mutual Well 01	10/25/2012	200	Lab	GAMA	1
26S39E29L1	E. Inyokern Mutual Well 01	9/2/2015	310	Lab	GAMA	1
26S39E29L1	E. Inyokern Mutual Well 01	7/9/2018	310	Lab	GAMA	1
26S39E29L2	E. Inyokern Mutual Well 02	3/22/1993	300	Lab	GAMA	1
26S39E29L2	E. Inyokern Mutual Well 02	3/17/2003	150	Lab	GAMA	1
26S39E29L2	E. Inyokern Mutual Well 02	3/1/2006	280	Lab	GAMA	1

Table 2: IWV TDS Data

Sample Dates in red indicate
only sample month/year is known

min	1/26/1920	100	
max	3/5/2019	232000	
count	2,044		

Unique Well Name	alternateName	Sample Date	TDS (mg/L)	Analysis Type	TDS Reference	Confidence Level
26S39E29L2	E. Inyokern Mutual Well 02	4/20/2009	320	Lab	GAMA	1
26S39E29L2	E. Inyokern Mutual Well 02	10/25/2012	290	Lab	GAMA	1
26S39E29L2	E. Inyokern Mutual Well 02	9/2/2015	300	Lab	GAMA	1
26S39E29P01		9/28/2010	270	Ukn	H-WQ	2
26S39E30C01	USGS-353855117491401	5/1/1975	377	Ukn	GAMA	1
26S39E30F01	USGS-353851117491401	5/1/1975	306	Ukn	GAMA	1
26S39E30F01	USGS-353851117491401	5/12/1976	350	Ukn	GAMA	1
26S39E30F01	USGS-353851117491401	8/1/1961	335	Lab	GAMA-USGS	1
26S39E30F01	USGS-353851117491401	6/7/1962	420	Lab	GAMA-USGS	1
26S39E30F01	USGS-353851117491401	9/15/1964	329	Lab	GAMA-USGS	1
26S39E30F01	USGS-353851117491401	6/21/1965	318	Calc	GAMA-USGS	1
26S39E30F01	USGS-353851117491401	5/16/1966	360	Lab	GAMA-USGS	1
26S39E30F01	USGS-353851117491401	9/7/1966	336	Lab	GAMA-USGS	1
26S39E30F03	USGS-353851117491403	10/25/1973	384	Ukn	GAMA	1
26S39E30F03	USGS-353851117491403	5/25/1967	400	Lab	GAMA-USGS	1
26S39E30F03	USGS-353851117491403	10/16/1967	368	Lab	GAMA-USGS	1
26S39E30F03	USGS-353851117491403	11/4/1968	296	Lab	GAMA-USGS	1
26S39E30F03	USGS-353851117491403	10/20/1969	336	Lab	GAMA-USGS	1
26S39E30F03	USGS-353851117491403	6/1/1970	332	Lab	GAMA-USGS	1
26S39E30F03	USGS-353851117491403	10/20/1970	335	Calc	GAMA-USGS	1
26S39E30F03	USGS-353851117491403	6/23/1971	360	Lab	GAMA-USGS	1
26S39E30F03	USGS-353851117491403	10/27/1971	350	Lab	GAMA-USGS	1
26S39E30F03	USGS-353851117491403	6/6/1972	385	Calc	W	1
26S39E30J01	ICSD-WELL-01	7/7/1988	283	Calc	B&S	1
26S39E30J01	ICSD-WELL-01	5/14/1987	253	Lab	GAMA	1
26S39E30J01	ICSD-WELL-01	3/29/1990	260	Lab	GAMA	1
26S39E30J01	ICSD-WELL-01	6/23/1994	244	Lab	GAMA	1
26S39E30J01	ICSD-WELL-01	6/17/1997	259	Lab	GAMA	1
26S39E30J01	ICSD-WELL-01	6/20/2000	298	Lab	GAMA	1
26S39E30J01	ICSD-WELL-01	4/17/1961	264	Lab	GAMA-USGS	1
26S39E30J01	ICSD-WELL-01	3/11/1993	290	Lab	H	1
26S39E30J01	ICSD-WELL-01	9/13/1982	550	Ukn	KCWA WQ	3
26S39E30J01	ICSD-WELL-01	11/1/1982	256	Ukn	KCWA WQ	3
26S39E30J01	ICSD-WELL-01	3/26/1984	265	Ukn	KCWA WQ	3
26S39E30J01	ICSD-WELL-01	3/8/1990	244	Ukn	KCWA WQ	3
26S39E30J01	ICSD-WELL-01	6/5/1953	253	Calc	Moyle	1
26S39E30J02	26S39E30J002M	9/13/1982	412	Ukn	GAMA	1
26S39E30K	Inyokern CSD Well 03	11/21/1995	295	Lab	GAMA	1
26S39E30K	Inyokern CSD Well 03	12/15/1998	240	Lab	GAMA	1
26S39E30K	Inyokern CSD Well 03	6/17/2003	250	Lab	GAMA	1
26S39E30K	Inyokern CSD Well 03	6/20/2006	270	Lab	GAMA	1
26S39E30K	Inyokern CSD Well 03	6/23/2009	320	Lab	GAMA	1
26S39E30K	Inyokern CSD Well 03	6/17/2014	290	Lab	GAMA	1
26S39E30K	Inyokern CSD Well 03	6/12/2017	330	Lab	GAMA	1

Table 2: IWV TDS Data

Sample Dates in red indicate
only sample month/year is known

min	1/26/1920	100	
max	3/5/2019	232000	
count	2,044		

Unique Well Name	alternateName	Sample Date	TDS (mg/L)	Analysis Type	TDS Reference	Confidence Level
26S39E30L	Inyokern CSD Well 02	6/29/1989	284	Lab	GAMA	1
26S39E30L	Inyokern CSD Well 02	12/21/1989	285	Lab	GAMA	1
26S39E30L	Inyokern CSD Well 02	2/6/1992	223	Lab	GAMA	1
26S39E30L	Inyokern CSD Well 02	6/23/1994	248	Lab	GAMA	1
26S39E30L	Inyokern CSD Well 02	6/17/1997	245	Lab	GAMA	1
26S39E30L	Inyokern CSD Well 02	6/20/2000	277	Lab	GAMA	1
26S39E30L	Inyokern CSD Well 02	6/17/2003	280	Lab	GAMA	1
26S39E30L	Inyokern CSD Well 02	6/20/2006	310	Lab	GAMA	1
26S39E30L	Inyokern CSD Well 02	6/23/2009	310	Lab	GAMA	1
26S39E30L	Inyokern CSD Well 02	6/17/2014	310	Lab	GAMA	1
26S39E31A02		8/25/2009	270	Ukn	H-WQ	2
26S39E31G	Life Water CO-OP Well 01	1/2/1990	185	Lab	GAMA	1
26S39E31G	Life Water CO-OP Well 01	12/31/1996	295	Lab	GAMA	1
26S39E31G	Life Water CO-OP Well 01	7/15/2002	280	Lab	GAMA	1
26S39E31G	Life Water CO-OP Well 01	8/2/2005	280	Lab	GAMA	1
26S39E31G	Life Water CO-OP Well 01	10/29/2008	300	Lab	GAMA	1
26S39E31G	Life Water CO-OP Well 01	4/20/2009	310	Lab	GAMA	1
26S39E31G	Life Water CO-OP Well 01	12/10/2012	270	Lab	GAMA	1
26S39E31H	Life Water CO-OP Well 02	7/21/2011	280	Lab	GAMA	1
26S39E31H	Life Water CO-OP Well 02	5/13/2014	390	Lab	GAMA	1
26S39E31H	Life Water CO-OP Well 02	8/7/2017	270	Lab	GAMA	1
26S39E31R01	Pennix	2/7/2007	290	Lab	FR: AB	1
26S39E32K	S. Desert Mutual Well 01	5/12/1988	250	Lab	GAMA	1
26S39E32K	S. Desert Mutual Well 01	6/2/1999	268	Lab	GAMA	1
26S39E32K	S. Desert Mutual Well 01	2/26/2003	276	Lab	GAMA	1
26S39E32K	S. Desert Mutual Well 01	4/9/2007	270	Lab	GAMA	1
26S39E32K	S. Desert Mutual Well 01	8/9/2011	300	Lab	GAMA	1
26S39E32K	S. Desert Mutual Well 01	11/4/2014	300	Lab	GAMA	1
26S39E32K	S. Desert Mutual Well 01	8/7/2017	290	Lab	GAMA	1
26S39E32L	148 East Water System Well 1	2/22/2018	320	Lab	GAMA	1
26S39E32L01	Robert Steele	8/17/1983	290	Ukn	KCWA WQ	3
26S39E32L01	Robert Steele	12/13/1985	290	Ukn	KCWA WQ	3
26S39E32L01	Robert Steele	8/9/1988	265	Ukn	KCWA WQ	3
26S39E32L01	Robert Steele	1/19/1990	280	Ukn	KCWA WQ	3
26S39E32M	Owens Peak West Well 01	3/29/1989	285	Lab	GAMA	1
26S39E32M	Owens Peak West Well 01	12/21/1992	285	Lab	GAMA	1
26S39E32M	Owens Peak West Well 01	7/15/1996	290	Lab	GAMA	1
26S39E32M	Owens Peak West Well 01	8/11/1999	280	Lab	GAMA	1
26S39E32M	Owens Peak West Well 01	8/14/2002	280	Lab	GAMA	1
26S39E32M	Owens Peak West Well 01	8/17/2005	310	Lab	GAMA	1
26S39E32M	Owens Peak West Well 01	8/14/2008	270	Lab	GAMA	1
26S39E32M	Owens Peak West Well 01	8/11/2011	280	Lab	GAMA	1
26S39E32M	Owens Peak West Well 01	8/6/2014	300	Lab	GAMA	1
26S39E32M	Owens Peak West Well 01	8/8/2017	290	Lab	GAMA	1
26S39E32N	Owens Peak South Well 01	3/27/1995	275	Lab	GAMA	1
26S39E32N	Owens Peak South Well 01	9/9/1998	300	Lab	GAMA	1

Table 2: IWV TDS Data

Sample Dates in red indicate
only sample month/year is known

min	1/26/1920	100	
max	3/5/2019	232000	
count	2,044		

Unique Well Name	alternateName	Sample Date	TDS (mg/L)	Analysis Type	TDS Reference	Confidence Level
26S39E32N	Owens Peak South Well 01	8/14/2002	280	Lab	GAMA	1
26S39E32N	Owens Peak South Well 01	8/17/2005	330	Lab	GAMA	1
26S39E32N	Owens Peak South Well 01	8/14/2008	290	Lab	GAMA	1
26S39E32N	Owens Peak South Well 01	8/11/2011	270	Lab	GAMA	1
26S39E32N	Owens Peak South Well 01	8/6/2014	300	Lab	GAMA	1
26S39E32N	Owens Peak South Well 01	8/15/2017	240	Lab	GAMA	1
26S39E32Q01		8/12/2008	250	Ukn	H-WQ	2
26S39E33B	Dixie Water Co Well 01	8/9/1989	270	Lab	GAMA	1
26S39E33B	Dixie Water Co Well 01	5/1/2003	272	Lab	GAMA	1
26S39E33B	Dixie Water Co Well 01	7/31/2012	250	Lab	GAMA	1
26S39E34F05		11/10/2008	250	Ukn	H-WQ	2
26S39E34H02		3/6/2007	290	Ukn	KCWA WQ	3
26S39E34Q01	26S/39E-34Q01; DeMay	1/25/2005	270	Lab	Other	1
26S39E36B	GAMA:SVM Well 35 & Well 36IW; loc = Well 36	8/9/1990	224	Lab	GAMA	1
26S39E36B	GAMA:SVM Well 35 & Well 36IW; loc = Well 36	7/2/1992	204	Lab	GAMA	1
26S39E36B	GAMA:SVM Well 35 & Well 36IW; loc = Well 36	4/4/1996	210	Lab	GAMA	1
26S39E36B	GAMA:SVM Well 35 & Well 36IW; loc = Well 36	6/8/1999	209	Lab	GAMA	1
26S39E36B	GAMA:SVM Well 35 & Well 36IW; loc = Well 36	6/4/2002	210	Lab	GAMA	1
26S39E36B	GAMA:SVM Well 35 & Well 36IW; loc = Well 36	9/20/2005	230	Lab	GAMA	1
26S39E36B	GAMA:SVM Well 35 & Well 36IW; loc = Well 36	9/16/2008	230	Lab	GAMA	1
26S39E36B	GAMA:SVM Well 35 & Well 36IW; loc = Well 36	6/16/2009	290	Lab	GAMA	1
26S39E36B	GAMA:SVM Well 35 & Well 36IW; loc = Well 36	6/7/2011	290	Lab	GAMA	1
26S39E36B	GAMA:SVM Well 35 & Well 36IW; loc = Well 36	6/3/2014	290	Lab	GAMA	1
26S39E36B	GAMA:SVM Well 35 & Well 36IW; loc = Well 36	6/6/2017	210	Lab	GAMA	1
26S40E01A01		7/8/1953	165000	Calc	Moyle	1
26S40E01A02		6/9/1982	11000	Calc	B	1
26S40E01A02		9/17/1986	11400	Calc	B&M	1
26S40E01A02		6/1/1987	11700	Calc	B&S	1
26S40E01A02		3/9/1954	13800	Calc	Moyle	1
26S40E01J01	USGS-354155117370201	6/22/1978	46000	Calc	B	1
26S40E01J01	USGS-354155117370201	5/16/1979	67000	Calc	B	1
26S40E01J01	USGS-354155117370201	5/21/1980	65000	Calc	B	1
26S40E01J01	USGS-354155117370201	6/10/1982	54000	Calc	B	1
26S40E01J01	USGS-354155117370201	7/8/1953	48500	Calc	Moyle	1
26S40E01J01	USGS-354155117370201	6/13/1972	43600	Lab	W	1
26S40E01Q01		6/22/1978	4300	Calc	B	1
26S40E01Q01		5/16/1979	3200	Calc	B	1
26S40E01Q01		5/20/1980	3100	Calc	B	1
26S40E01Q02		6/22/1978	6000	Calc	B	1

Table 2: IWV TDS Data

Sample Dates in red indicate — min 1/26/1920 — 100
only sample month/year is known — max 3/5/2019 — 232000
count 2,044

Unique Well Name	alternateName	Sample Date	TDS (mg/L)	Analysis Type	TDS Reference	Confidence Level
26S40E01Q02		5/15/1979	6100	Calc	B	1
26S40E01Q02		5/20/1980	5700	Calc	B	1
26S40E01Q02		6/11/1982	6500	Calc	B	1
26S40E01Q02		5/24/1996	13000	Lab	H96	1
26S40E04Q01		5/30/1987	481	Calc	B&S	1
26S40E05F01	USGS-354216117415701	4/28/1946	376	Lab	GAMA-USGS	1
26S40E05F01	USGS-354216117415701	2/1/1946	325	Calc	Moyle	1
26S40E05P01	USGS-354147117414101	7/31/1978	610	Calc	B	1
26S40E05P01	USGS-354147117414101	3/29/1980	540	Calc	B	1
26S40E05P01	USGS-354147117414101	10/20/1970	588	Ukn	GAMA	1
26S40E05P01	USGS-354147117414101	10/25/1973	677	Ukn	GAMA	1
26S40E05P01	USGS-354147117414101	5/1/1975	666	Ukn	GAMA	1
26S40E05P01	USGS-354147117414101	5/12/1976	734	Ukn	GAMA	1
26S40E05P01	USGS-354147117414101	9/15/1964	634	Lab	GAMA-USGS	1
26S40E05P01	USGS-354147117414101	5/16/1966	628	Lab	GAMA-USGS	1
26S40E05P01	USGS-354147117414101	9/8/1966	836	Lab	GAMA-USGS	1
26S40E05P01	USGS-354147117414101	6/5/1968	588	Lab	GAMA-USGS	1
26S40E05P01	USGS-354147117414101	11/4/1968	648	Lab	GAMA-USGS	1
26S40E05P01	USGS-354147117414101	10/20/1969	876	Lab	GAMA-USGS	1
26S40E05P01	USGS-354147117414101	6/1/1970	624	Lab	GAMA-USGS	1
26S40E05P01	USGS-354147117414101	6/23/1971	710	Lab	GAMA-USGS	1
26S40E05P01	USGS-354147117414101	10/27/1971	879	Lab	GAMA-USGS	1
26S40E05P01	USGS-354147117414101	8/4/1953	562	Calc	Moyle	1
26S40E05P01	USGS-354147117414101	5/15/1958	530	Calc	Moyle	1
26S40E05P01	USGS-354147117414101	6/6/1972	699	Calc	W	1
26S40E05P03	USGS-354147117414103	4/28/1946	1500	Lab	GAMA-USGS	1
26S40E06C01		5/30/1987	60700	Calc	B&M	1
26S40E06D01		5/30/1987	9050	Calc	B&M	1
26S40E06D02		5/30/1987	8710	Calc	B&M	1
26S40E06D02		3/10/1993	24300	Lab	H	1
26S40E06D02		6/18/1996	26000	Lab	H96	1
26S40E06E01	USGS-354211117431801	4/26/1946	348	Lab	GAMA-USGS	1
26S40E07E01		1/22/1946	898	Calc	Moyle	1
26S40E07E01		4/28/1946	1010	Lab	USGS	1
26S40E07N01	USGS-354052117411501	1/28/1920	242	Lab	GAMA-USGS	1
26S40E07N01	USGS-354052117411501	4/29/1946	219	Lab	GAMA-USGS	1
26S40E08N01	USGS-354054117410701	4/28/1946	788	Lab	GAMA-USGS	1
26S40E08Q01	USGS-354053117412601	4/28/1946	298	Lab	GAMA-USGS	1
26S40E09A01		5/29/1987	535	Calc	B&S	1
26S40E09A01		3/19/1993	620	Lab	H	1
26S40E10E01	USGS-354119117400601	1/29/1920	2010	Lab	GAMA-USGS	1
26S40E10E01	USGS-354119117400601	4/28/1946	1450	Lab	GAMA-USGS	1
26S40E10F01	USGS-354125117393701	6/22/1978	490	Calc	B	1
26S40E10F01	USGS-354125117393701	6/5/1979	490	Calc	B	1
26S40E10F01	USGS-354125117393701	5/20/1980	480	Calc	B	1
26S40E10F01	USGS-354125117393701	6/9/1982	500	Calc	B	1

Table 2: IWV TDS Data

Sample Dates in red indicate — min 1/26/1920 — 100
only sample month/year is known — max 3/5/2019 — 232000
count 2,044

Unique Well Name	alternateName	Sample Date	TDS (mg/L)	Analysis Type	TDS Reference	Confidence Level
26S40E10F01	USGS-354125117393701	3/6/1974	436	Ukn	GAMA	1
26S40E10F01	USGS-354125117393701	3/25/1975	451	Ukn	GAMA	1
26S40E10F01	USGS-354125117393701	8/18/1976	465	Ukn	GAMA	1
26S40E10F01	USGS-354125117393701	7/9/1953	504	Calc	Moyle	1
26S40E10F01	USGS-354125117393701	6/13/1972	520	Lab	W	1
26S40E10N01	USGS-354055117400401	4/28/1946	647	Lab	GAMA-USGS	1
26S40E10N01	USGS-354055117400401	7/6/1953	1010	Calc	Moyle	1
26S40E11A01		7/6/1953	69500	Calc	Moyle	1
26S40E11J01	USGS-354108117380801	6/22/1978	7600	Calc	B	1
26S40E11J01	USGS-354108117380801	5/28/1980	2400	Calc	B	1
26S40E11J01	USGS-354108117380801	6/11/1985	9670	Calc	B&M	1
26S40E11J01	USGS-354108117380801	3/7/1974	3720	Ukn	GAMA	1
26S40E11J01	USGS-354108117380801	3/25/1975	3080	Ukn	GAMA	1
26S40E11J01	USGS-354108117380801	8/18/1976	2040	Ukn	GAMA	1
26S40E11J01	USGS-354108117380801	7/9/1953	1060	Calc	Moyle	1
26S40E11J01	USGS-354108117380801	6/13/1972	5880	Lab	W	1
26S40E11J03	USGS-354109117380803	8/9/1984	9700	Calc	B	1
26S40E11J03	USGS-354109117380803	7/1/1988	8090	Calc	B&S	1
26S40E11J03	USGS-354109117380803	6/11/1985	9670	Ukn	GAMA	1
26S40E11N02		8/9/1984	1300	Calc	B	1
26S40E12A01		6/29/1978	4400	Calc	B	1
26S40E12A01		5/17/1979	4100	Calc	B	1
26S40E12A01		5/21/1980	3700	Calc	B	1
26S40E12G01		5/15/1979	2400	Calc	B	1
26S40E12G01		5/27/1980	2400	Calc	B	1
26S40E12G01		6/11/1982	2800	Calc	B	1
26S40E12Q01	USGS-354101117372201	6/29/1978	1400	Calc	B	1
26S40E12Q01	USGS-354101117372201	5/15/1979	1400	Calc	B	1
26S40E12Q01	USGS-354101117372201	5/27/1980	1200	Calc	B	1
26S40E12Q01	USGS-354101117372201	6/12/1985	1330	Ukn	GAMA	1
26S40E12Q01	USGS-354101117372201	5/24/1996	1000	Lab	H96	1
26S40E12R01		6/29/1978	2000	Calc	B	1
26S40E12R01		6/6/1979	1700	Calc	B	1
26S40E12R01		5/27/1980	1900	Calc	B	1
26S40E12R01		5/24/1996	1500	Lab	H96	1
26S40E13C01	USGS-354037117373201	6/29/1978	2100	Calc	B	1
26S40E13C01	USGS-354037117373201	6/6/1979	2200	Calc	B	1
26S40E13C01	USGS-354037117373201	5/21/1980	2000	Calc	B	1
26S40E13C01	USGS-354037117373201	6/11/1982	2000	Calc	B	1
26S40E13C01	USGS-354037117373201	6/14/1972	2680	Lab	W	1
26S40E13C02	USGS well; ""China Lake Playa""	11/16/1999	1300	Lab	Tri	1
26S40E13D03		8/8/1999	1600	Lab	Tri	1
26S40E13M01	USGS-354010117375601	6/23/1978	1300	Calc	B	1
26S40E13M01	USGS-354010117375601	5/21/1980	1500	Calc	B	1
26S40E13M01	USGS-354010117375601	5/24/1996	1500	Lab	H96	1
26S40E13M01	USGS-354010117375601	6/14/1972	1180	Lab	W	1

Table 2: IWV TDS Data

Sample Dates in red indicate — min 1/26/1920 — 100
only sample month/year is known — max 3/5/2019 — 232000
count 2,044

Unique Well Name	alternateName	Sample Date	TDS (mg/L)	Analysis Type	TDS Reference	Confidence Level
26S40E14B01	USGS-354039117382801	6/20/1978	1600	Calc	B	1
26S40E14B01	USGS-354039117382801	5/15/1979	1600	Calc	B	1
26S40E14B01	USGS-354039117382801	5/20/1980	1300	Calc	B	1
26S40E14B01	USGS-354039117382801	6/9/1982	1600	Calc	B	1
26S40E14B01	USGS-354039117382801	8/6/1984	3300	Calc	B	1
26S40E14B01	USGS-354039117382801	5/27/1987	3500	Calc	B&S	1
26S40E14B01	USGS-354039117382801	7/6/1988	2930	Calc	B&S	1
26S40E14B01	USGS-354039117382801	6/11/1985	2470	Ukn	GAMA	1
26S40E14B01	USGS-354039117382801	4/16/1986	3220	Ukn	GAMA	1
26S40E14B01	USGS-354039117382801	5/24/1996	1900	Lab	H96	1
26S40E14B01	USGS-354039117382801	8/8/1999	26000	Lab	Tri	1
26S40E14B01	USGS-354039117382801	6/12/1972	3780	Lab	W	1
26S40E14B02		3/19/1993	1080	Lab	H	1
26S40E14H01	USGS-354021117381801	6/21/1972	1770	Lab	W	1
26S40E14L01	USGS-354020117384201	6/20/1978	1700	Calc	B	1
26S40E14L01	USGS-354020117384201	5/15/1979	1700	Calc	B	1
26S40E14L01	USGS-354020117384201	5/20/1980	2000	Calc	B	1
26S40E14L01	USGS-354020117384201	8/9/1984	1800	Calc	B	1
26S40E14L01	USGS-354020117384201	6/30/1988	1420	Calc	B&S	1
26S40E14L01	USGS-354020117384201	6/11/1985	1650	Ukn	GAMA	1
26S40E14L01	USGS-354020117384201	5/15/1978	1700	Ukn	KCWA WQ	3
26S40E14L01	USGS-354020117384201	6/12/1972	1070	Lab	W	1
26S40E15E01	USGS-354036117400701	6/20/1978	560	Calc	B	1
26S40E15E01	USGS-354036117400701	5/31/1979	530	Calc	B	1
26S40E15E01	USGS-354036117400701	5/22/1980	550	Calc	B	1
26S40E15E01	USGS-354036117400701	6/10/1982	530	Calc	B	1
26S40E15E01	USGS-354036117400701	3/5/1974	499	Ukn	GAMA	1
26S40E15E01	USGS-354036117400701	3/26/1975	466	Ukn	GAMA	1
26S40E15E01	USGS-354036117400701	8/18/1976	485	Ukn	GAMA	1
26S40E15E01	USGS-354036117400701	4/28/1946	620	Lab	GAMA-USGS	1
26S40E15E01	USGS-354036117400701	7/6/1953	495	Calc	Moyle	1
26S40E15E01	USGS-354036117400701	4/4/1955	464	Calc	Moyle	1
26S40E15E01	USGS-354036117400701	6/29/1972	463	Calc	W	1
26S40E15E02	USGS-354033117400601	6/20/1978	4900	Calc	B	1
26S40E15E02	USGS-354033117400601	5/31/1979	4800	Calc	B	1
26S40E15E02	USGS-354033117400601	3/5/1974	4730	Ukn	GAMA	1
26S40E15E02	USGS-354033117400601	3/26/1975	4730	Ukn	GAMA	1
26S40E15E02	USGS-354033117400601	8/18/1976	4600	Ukn	GAMA	1
26S40E15E02	USGS-354033117400601	4/28/1946	3750	Lab	GAMA-USGS	1
26S40E15E02	USGS-354033117400601	4/4/1955	3900	Calc	Moyle	1
26S40E15N01	USGS-354002117400601	6/21/1978	1200	Calc	B	1
26S40E15N01	USGS-354002117400601	5/31/1979	1300	Calc	B	1
26S40E15N01	USGS-354002117400601	5/22/1980	1200	Calc	B	1
26S40E15N01	USGS-354002117400601	4/28/1946	1340	Lab	GAMA-USGS	1
26S40E15N02	USGS-354011117400001	6/14/1982	840	Calc	B	1
26S40E15N02	USGS-354011117400001	6/11/1985	2890	Calc	B&M	1

Table 2: IWV TDS Data

Sample Dates in red indicate — min 1/26/1920 — 100
only sample month/year is known — max 3/5/2019 — 232000
count 2,044

Unique Well Name	alternateName	Sample Date	TDS (mg/L)	Analysis Type	TDS Reference	Confidence Level
26S40E15N02	USGS-354011117400001	7/9/1988	3170	Calc	B&S	1
26S40E15N02	USGS-354011117400001	8/8/1984	2800	Ukn	GAMA	1
26S40E15N02	USGS-354011117400001	5/29/1996	3000	Lab	H96	1
26S40E16K	TTIWV-MW06	2/17/2002	1980	Lab	TTEMI	1
26S40E16M01	TTBK-MW07	8/5/1999	380	Lab	Tri	1
26S40E17J01	USGS-354022117412201	8/7/1984	250	Calc	B	1
26S40E17J01	USGS-354022117412201	7/2/1988	282	Calc	B&S	1
26S40E17J01	USGS-354022117412201	6/10/1985	267	Ukn	GAMA	1
26S40E17J01	USGS-354022117412201	5/29/1996	260	Lab	H96	1
26S40E17J01	USGS-354022117412201	6/18/1972	308	Lab	W	1
26S40E17N01		10/13/1955	223	Calc	Moyle	1
26S40E17Q01	96030-1	8/6/1996	2400	Lab	H96	1
26S40E17R01	USGS-354003117412001	8/7/1984	290	Calc	B	1
26S40E17R01	USGS-354003117412001	6/10/1985	299	Ukn	GAMA	1
26S40E17R01	USGS-354003117412001	7/2/1988	282	Ukn	GAMA	1
26S40E17R01	USGS-354003117412001	6/18/1972	304	Lab	W	1
26S40E18E01	USGS-354027117431501	4/29/1946	898	Lab	GAMA-USGS	1
26S40E18N01	USGS-353959117431501	4/29/1946	648	Lab	GAMA-USGS	1
26S40E18N01	USGS-353959117431501	4/5/1955	213	Calc	Moyle	1
26S40E19N	TTIWV-MW02-S	2/18/2002	218	Lab	TTEMI	1
26S40E19N01	USGS-353917117431401	2/18/2002	218	Ukn	AB	2
26S40E19N01	USGS-353917117431401	4/30/1946	242	Lab	GAMA-USGS	1
26S40E19N01	USGS-353917117431401	3/19/1993	230	Lab	H	1
26S40E19P01	USGS-353910117430201	3/29/1980	310	Calc	B	1
26S40E19P01	USGS-353910117430201	11/20/1959	210	Ukn	GAMA	1
26S40E19P01	USGS-353910117430201	11/20/1955	210	Calc	Moyle	1
26S40E20A	TTBK-MW04	2/10/1999	350	Lab	Tri	1
26S40E20J01		3/19/1993	360	Lab	H	1
26S40E20L01		3/9/1999	1150	Ukn	KCWA WQ	3
26S40E20N01	USGS-353910117420801	4/30/1946	261	Lab	GAMA-USGS	1
26S40E20N01	USGS-353910117420801	6/1/1953	220	Calc	Moyle	1
26S40E21A01	USGS-353948117401501	8/8/1984	540	Calc	B	1
26S40E21A01	USGS-353948117401501	6/10/1985	481	Ukn	GAMA	1
26S40E21A01	USGS-353948117401501	4/17/1986	644	Ukn	GAMA	1
26S40E21A01	USGS-353948117401501	6/13/1972	612	Lab	W	1
26S40E21E01	USGS-353941117411101	8/7/1984	230	Calc	B	1
26S40E21E01	USGS-353941117411101	6/10/1985	178	Ukn	GAMA	1
26S40E21E01	USGS-353941117411101	6/18/1972	280	Lab	W	1
26S40E21K01	USGS-353921117403701	4/30/1946	430	Lab	GAMA-USGS	1
26S40E22A01	USGS-353954117390801	5/31/1987	8080	Calc	B&S	1
26S40E22A01	USGS-353954117390801	7/6/1988	5830	Calc	B&S	1
26S40E22A01	USGS-353954117390801	3/23/1989	8230	Ukn	GAMA	1
26S40E22B01	USGS-353955117393101	8/9/1984	5200	Calc	B	1
26S40E22B01	USGS-353955117393101	6/2/1987	5290	Calc	B&S	1
26S40E22B01	USGS-353955117393101	7/7/1988	5280	Calc	B&S	1
26S40E22B01	USGS-353955117393101	6/12/1985	5230	Ukn	GAMA	1

Table 2: IWV TDS Data

Sample Dates in red indicate — min 1/26/1920 — 100
only sample month/year is known — max 3/5/2019 — 232000
count 2,044

Unique Well Name	alternateName	Sample Date	TDS (mg/L)	Analysis Type	TDS Reference	Confidence Level
26S40E22B01	USGS-353955117393101	4/17/1986	5070	Ukn	GAMA	1
26S40E22B01	USGS-353955117393101	3/22/1989	5170	Ukn	GAMA	1
26S40E22B01	USGS-353955117393101	6/18/1972	5480	Lab	W	1
26S40E22H01	USGS-353942117390801	6/19/1978	5000	Calc	B	1
26S40E22H01	USGS-353942117390801	5/15/1979	4700	Calc	B	1
26S40E22H01	USGS-353942117390801	5/20/1980	4300	Calc	B	1
26S40E22H01	USGS-353942117390801	6/8/1982	5200	Calc	B	1
26S40E22H01	USGS-353942117390801	8/8/1984	4800	Calc	B	1
26S40E22H01	USGS-353942117390801	6/29/1988	4870	Calc	B&S	1
26S40E22H01	USGS-353942117390801	6/12/1985	5140	Ukn	GAMA	1
26S40E22H01	USGS-353942117390801	3/21/1993	5670	Lab	H	1
26S40E22H01	USGS-353942117390801	5/24/1996	4800	Lab	H96	1
26S40E22H01	USGS-353942117390801	8/1/2001	4520	Lab	Tri	1
26S40E22H01	USGS-353942117390801	6/12/1972	7160	Lab	W	1
26S40E22H02	USGS-353942117390802	6/19/1978	13000	Calc	B	1
26S40E22H02	USGS-353942117390802	5/15/1979	12000	Calc	B	1
26S40E22H02	USGS-353942117390802	5/20/1980	13000	Calc	B	1
26S40E22H02	USGS-353942117390802	6/8/1982	14000	Calc	B	1
26S40E22H02	USGS-353942117390802	10/31/1983	12000	Calc	B	1
26S40E22H02	USGS-353942117390802	6/29/1988	12300	Calc	B&S	1
26S40E22H02	USGS-353942117390802	6/12/1985	12900	Ukn	GAMA	1
26S40E22H02	USGS-353942117390802	6/12/1972	16500	Lab	W	1
26S40E22H03	USGS-353942117390803	6/19/1978	5300	Calc	B	1
26S40E22H03	USGS-353942117390803	5/15/1979	5700	Calc	B	1
26S40E22H03	USGS-353942117390803	5/20/1980	6800	Calc	B	1
26S40E22H03	USGS-353942117390803	6/8/1982	6800	Calc	B	1
26S40E22H03	USGS-353942117390803	8/7/1984	2800	Calc	B	1
26S40E22H03	USGS-353942117390803	8/9/1984	5400	Calc	B	1
26S40E22H03	USGS-353942117390803	6/2/1987	8350	Calc	B&S	1
26S40E22H03	USGS-353942117390803	7/7/1988	7820	Calc	B&S	1
26S40E22H03	USGS-353942117390803	6/12/1985	4830	Ukn	GAMA	1
26S40E22H03	USGS-353942117390803	4/17/1986	5860	Ukn	GAMA	1
26S40E22H03	USGS-353942117390803	3/22/1989	8520	Ukn	GAMA	1
26S40E22H03	USGS-353942117390803	6/13/1972	5400	Lab	W	1
26S40E22J01	USGS-353930117391801	10/31/1983	2700	Calc	B	1
26S40E22J01	USGS-353930117391801	8/8/1984	2800	Calc	B	1
26S40E22J01	USGS-353930117391801	7/1/1988	2330	Calc	B&S	1
26S40E22J01	USGS-353930117391801	6/11/1985	2550	Ukn	GAMA	1
26S40E22J01	USGS-353930117391801	6/2/1972	4180	Lab	W	1
26S40E22K01	USGS-353923117392601	10/31/1983	1300	Calc	B	1
26S40E22K01	USGS-353923117392601	8/8/1984	1400	Calc	B	1
26S40E22K01	USGS-353923117392601	6/12/1985	1480	Ukn	GAMA	1
26S40E22K01	USGS-353923117392601	6/1/1972	1040	Lab	W	1
26S40E22N01	USGS-353913117400601	6/20/1978	1000	Calc	B	1
26S40E22N01	USGS-353913117400601	5/31/1979	1100	Calc	B	1
26S40E22N01	USGS-353913117400601	5/23/2008	2100	Calc	B	1

Table 2: IWV TDS Data

Sample Dates in red indicate — min 1/26/1920 — 100
only sample month/year is known — max 3/5/2019 — 232000
count 2,044

Unique Well Name	alternateName	Sample Date	TDS (mg/L)	Analysis Type	TDS Reference	Confidence Level
26S40E22N01	USGS-353913117400601	3/6/1974	654	Ukn	GAMA	1
26S40E22N01	USGS-353913117400601	3/26/1975	726	Ukn	GAMA	1
26S40E22N01	USGS-353913117400601	8/19/1976	762	Ukn	GAMA	1
26S40E22N01	USGS-353913117400601	5/23/1980	2130	Ukn	GAMA	1
26S40E22N01	USGS-353913117400601	11/15/1968	432	Lab	GAMA-USGS	1
26S40E22N01	USGS-353913117400601	7/9/1953	520	Calc	Moyle	1
26S40E22N01	USGS-353913117400601	4/4/1955	429	Calc	Moyle	1
26S40E22N01	USGS-353913117400601	6/28/1972	581	Calc	W	1
26S40E22P01	USGS-353908117395201	6/22/1978	1000	Calc	B	1
26S40E22P01	USGS-353908117395201	5/17/1979	830	Calc	B	1
26S40E22P01	USGS-353908117395201	5/28/1980	1100	Calc	B	1
26S40E22P01	USGS-353908117395201	5/27/1987	1070	Calc	B&M	1
26S40E22P01	USGS-353908117395201	8/9/1988	1090	Calc	B&S	1
26S40E22P01	USGS-353908117395201	3/21/1989	1090	Ukn	GAMA	1
26S40E22P01	USGS-353908117395201	4/10/1990	1080	Ukn	GAMA	1
26S40E22P01	USGS-353908117395201	3/12/1991	1120	Ukn	GAMA	1
26S40E22P01	USGS-353908117395201	4/15/1992	1110	Ukn	GAMA	1
26S40E22P01	USGS-353908117395201	4/5/1993	1110	Ukn	GAMA	1
26S40E22P01	USGS-353908117395201	6/18/1996	860	Lab	H96	1
26S40E22P01	USGS-353908117395201	3/11/1954	1090	Ukn	KCWA WQ	3
26S40E22P01	USGS-353908117395201	11/17/1998	1150	Ukn	KCWA WQ	3
26S40E22P01	USGS-353908117395201	2/23/1954	1000	Calc	Moyle	1
26S40E22P01	USGS-353908117395201	6/17/1972	1050	Lab	W	1
26S40E22P02	USGS-353908117394001	10/31/1983	1100	Calc	B	1
26S40E22P02	USGS-353908117394001	8/8/1984	1200	Calc	B	1
26S40E22P02	USGS-353908117394001	6/10/1986	1240	Calc	B&M	1
26S40E22P02	USGS-353908117394001	7/1/1988	1660	Calc	B&S	1
26S40E22P02	USGS-353908117394001	6/10/1985	1240	Ukn	GAMA	1
26S40E22P02	USGS-353908117394001	5/29/1996	1400	Lab	H96	1
26S40E22P02	USGS-353908117394001	6/1/1972	1200	Lab	W	1
26S40E22P03		8/8/1984	1400	Calc	B	1
26S40E22P03		5/26/1987	1230	Calc	B&M	1
26S40E22P03		8/8/1988	1470	Calc	B&S	1
26S40E22P03		6/18/1996	1400	Lab	H96	1
26S40E22P03		5/26/1984	1230	Ukn	KCWA WQ	3
26S40E22P04		8/9/1984	780	Calc	B	1
26S40E22P04		5/26/1987	1890	Calc	B&M	1
26S40E22P04		8/9/1988	1260	Calc	B&S	1
26S40E22P04		6/18/1996	460	Lab	H96	1
26S40E22P04		8/8/1984	780	Ukn	KCWA WQ	3
26S40E23A01	USGS-353948117381001	6/19/1978	2100	Calc	B	1
26S40E23A01	USGS-353948117381001	5/17/1979	2200	Calc	B	1
26S40E23A01	USGS-353948117381001	5/21/1980	2500	Calc	B	1
26S40E23A01	USGS-353948117381001	6/10/1982	3900	Calc	B	1
26S40E23A01	USGS-353948117381001	5/26/1972	2140	Lab	W	1
26S40E23A02	USGS-353948117381002	6/19/1978	1200	Calc	B	1

Table 2: IWV TDS Data

Sample Dates in red indicate — min 1/26/1920 — 100
only sample month/year is known — max 3/5/2019 — 232000
count 2,044

Unique Well Name	alternateName	Sample Date	TDS (mg/L)	Analysis Type	TDS Reference	Confidence Level
26S40E23A02	USGS-353948117381002	5/17/1979	1200	Calc	B	1
26S40E23A02	USGS-353948117381002	6/10/1982	1200	Calc	B	1
26S40E23A02	USGS-353948117381002	5/29/1996	2400	Lab	H96	1
26S40E23A02	USGS-353948117381002	5/26/1972	1400	Lab	W	1
26S40E23B02	USGS-353955117381601	5/27/1987	1190	Calc	B&M	1
26S40E23B02	USGS-353955117381601	1/18/1989	1220	Calc	B&S	1
26S40E23B02	USGS-353955117381601	10/23/1986	1100	Ukn	GAMA	1
26S40E23B02	USGS-353955117381601	3/20/1989	1260	Ukn	GAMA	1
26S40E23B02	USGS-353955117381601	4/10/1990	1320	Ukn	GAMA	1
26S40E23B02	USGS-353955117381601	3/13/1991	1330	Ukn	GAMA	1
26S40E23B02	USGS-353955117381601	4/16/1992	1340	Ukn	GAMA	1
26S40E23B02	USGS-353955117381601	4/5/1993	1220	Ukn	GAMA	1
26S40E23B02	USGS-353955117381601	8/23/1996	1300	Lab	H96	1
26S40E23B03	USGS-353955117381602	5/27/1987	1240	Calc	B&M	1
26S40E23B03	USGS-353955117381602	5/27/1988	1240	Calc	B&S	1
26S40E23B03	USGS-353955117381602	7/7/1988	1140	Calc	B&S	1
26S40E23B03	USGS-353955117381602	3/20/1989	1170	Ukn	GAMA	1
26S40E23B03	USGS-353955117381602	4/10/1990	1360	Ukn	GAMA	1
26S40E23B03	USGS-353955117381602	3/13/1991	1200	Ukn	GAMA	1
26S40E23B03	USGS-353955117381602	4/16/1992	1390	Ukn	GAMA	1
26S40E23B03	USGS-353955117381602	4/5/1993	1080	Ukn	GAMA	1
26S40E23C01		7/9/1953	4060	Calc	Moyle	1
26S40E23D01	USGS-353948117385601	10/31/1983	1400	Calc	B	1
26S40E23D01	USGS-353948117385601	5/26/1987	2090	Calc	B&M	1
26S40E23D01	USGS-353948117385601	6/25/1986	2020	Ukn	GAMA	1
26S40E23D01	USGS-353948117385601	8/26/1996	2000	Lab	H96	1
26S40E23D02	USGS-353948117385602	10/31/1983	4900	Calc	B	1
26S40E23D02	USGS-353948117385602	5/26/1987	5420	Calc	B&M	1
26S40E23D02	USGS-353948117385602	1/9/1986	4620	Ukn	GAMA	1
26S40E23D02	USGS-353948117385602	6/25/1986	5260	Ukn	GAMA	1
26S40E23G01	USGS-353942117383101	8/7/1984	7100	Calc	B	1
26S40E23G01	USGS-353942117383101	6/11/1985	6750	Calc	B&M	1
26S40E23G01	USGS-353942117383101	7/7/1988	6260	Calc	B&S	1
26S40E23G01	USGS-353942117383101	5/29/1996	4400	Lab	H96	1
26S40E23G01	USGS-353942117383101	5/24/1972	10900	Lab	W	1
26S40E23J01	WWTF	8/9/1984	620	Calc	B	1
26S40E23J01	WWTF	5/24/1972	1720	Lab	W	1
26S40E23L01	USGS-353929117383501	6/2/1972	2100	Lab	W	1
26S40E24B01		7/8/1953	1360	Calc	Moyle	1
26S40E24C01	USGS-353953117373701	6/23/1978	1900	Calc	B	1
26S40E24C01	USGS-353953117373701	5/21/1980	1500	Calc	B	1
26S40E24C01	USGS-353953117373701	6/10/1982	2100	Calc	B	1
26S40E24C01	USGS-353953117373701	7/9/1953	675	Calc	Moyle	1
26S40E24C01	USGS-353953117373701	5/26/1972	2500	Lab	W	1
26S40E24M01	USGS-353929117374901	6/12/1972	6080	Lab	W	1
26S40E24R01		3/9/1954	745	Calc	Moyle	1

Table 2: IWV TDS Data

Sample Dates in red indicate — min 1/26/1920 — 100
only sample month/year is known — max 3/5/2019 — 232000
count 2,044

Unique Well Name	alternateName	Sample Date	TDS (mg/L)	Analysis Type	TDS Reference	Confidence Level
26S40E25C	TTBK-MW01	5/13/1999	610	Lab	Tri	1
26S40E25C02		5/28/1987	956	Calc	B&M	1
26S40E25P	RLS22-MW01 (83')	5/18/1999	1100	Lab	Tri	1
26S40E26B01	USGS-353857117382701	7/8/1953	1360	Ukn	GAMA	1
26S40E26F01		6/14/1982	1300	Calc	B	1
26S40E26F01		7/8/1988	1320	Calc	B&M	1
26S40E26F01		3/21/1993	1500	Lab	H	1
26S40E26F01		5/24/1996	1400	Lab	H96	1
26S40E26F01		5/26/1972	952	Lab	W	1
26S40E26N02	TTBK-MW02	5/13/1999	1100	Lab	Tri	1
26S40E26N02	TTBK-MW02	2/18/2002	668	Lab	TTEMI	1
26S40E27D01		7/8/1988	1940	Calc	B&S	1
26S40E27D01		5/31/1996	1660	Lab	H	1
26S40E27D01		8/22/2008	1700	Ukn	KCWA WQ	3
26S40E27D02	35H2 on inside of cap	7/8/1988	1490	Calc	B&S	1
26S40E27E03	USGS-353848117395402	2/26/1989	479	Ukn	GAMA	1
26S40E28A03		6/1/1953	298	Calc	Moyle	1
26S40E28C01		6/1/1953	277	Calc	Moyle	1
26S40E28H01	USGS-353843117402401	11/19/1959	357	Ukn	GAMA	1
26S40E28H01	USGS-353843117402401	6/1/1953	356	Calc	Moyle	1
26S40E28J01	USGS-353828117401301	6/29/1978	330	Calc	B	1
26S40E28J01	USGS-353828117401301	6/1/1979	410	Calc	B	1
26S40E28J01	USGS-353828117401301	5/27/1980	400	Calc	B	1
26S40E28J01	USGS-353828117401301	6/11/1982	590	Calc	B	1
26S40E28J01	USGS-353828117401301	8/10/1984	630	Calc	B	1
26S40E28J01	USGS-353828117401301	9/17/1987	595	Calc	B&M	1
26S40E28J01	USGS-353828117401301	9/1/1987	595	Lab	B&S	1
26S40E28J01	USGS-353828117401301	6/17/1972	298	Lab	W	1
26S40E29D01	USGS-353902117420501	6/17/1972	262	Lab	W	1
26S40E29F01	USGS-353844117415401	11/2/1970	246	Lab	GAMA-USGS	1
26S40E29N01	KLEINSCHMIDT	4/28/2009	180	Ukn	KCWA WQ	3
26S40E30C02	USGS-353859117425702	4/30/1946	202	Lab	GAMA-USGS	1
26S40E30E	GAMA:SVM Well 34	6/11/1987	255	Lab	GAMA	1
26S40E30E	GAMA:SVM Well 34	6/2/1988	179	Lab	GAMA	1
26S40E30E01	USGS-353845117431401	4/30/1946	202	Lab	GAMA-USGS	1
26S40E30E02		5/29/1987	234	Calc	B&S	1
26S40E30E02		6/11/1987	216	Calc	B&S	1
26S40E30E02		8/5/1953	184	Calc	Moyle	1
26S40E30J01		12/11/2007	150	Ukn	H-WQ	2
26S40E30K01	IWVWD Well 08	1/7/1988	237	Lab	B&S	1
26S40E30K01	IWVWD Well 08	4/4/2007	280	Lab	FR: AB	1
26S40E30K01	IWVWD Well 08	6/4/1975	264	Ukn	GAMA	1
26S40E30K01	IWVWD Well 08	3/23/1977	242	Ukn	GAMA	1
26S40E30K01	IWVWD Well 08	7/30/1981	210	Ukn	GAMA	1
26S40E30K01	IWVWD Well 08	3/2/1982	230	Ukn	GAMA	1
26S40E30K01	IWVWD Well 08	7/9/1982	243	Ukn	GAMA	1

Table 2: IWV TDS Data

Sample Dates in red indicate
only sample month/year is known

min	1/26/1920	100	
max	3/5/2019	232000	
count	2,044		

Unique Well Name	alternateName	Sample Date	TDS (mg/L)	Analysis Type	TDS Reference	Confidence Level
26S40E30K01	IWVWD Well 08	11/21/1983	223	Ukn	GAMA	1
26S40E30K01	IWVWD Well 08	1/22/1985	260	Lab	GAMA	1
26S40E30K01	IWVWD Well 08	8/1/1986	703	Lab	GAMA	1
26S40E30K01	IWVWD Well 08	12/20/1989	238	Lab	GAMA	1
26S40E30K01	IWVWD Well 08	1/22/1991	207	Lab	GAMA	1
26S40E30K01	IWVWD Well 08	3/6/1992	167	Lab	GAMA	1
26S40E30K01	IWVWD Well 08	1/21/1993	175	Lab	GAMA	1
26S40E30K01	IWVWD Well 08	2/2/1994	190	Lab	GAMA	1
26S40E30K01	IWVWD Well 08	6/22/1995	196	Lab	GAMA	1
26S40E30K01	IWVWD Well 08	1/24/1996	205	Lab	GAMA	1
26S40E30K01	IWVWD Well 08	1/13/1997	223	Lab	GAMA	1
26S40E30K01	IWVWD Well 08	1/26/1998	200	Lab	GAMA	1
26S40E30K01	IWVWD Well 08	9/9/1998	212	Lab	GAMA	1
26S40E30K01	IWVWD Well 08	9/15/1999	227	Lab	GAMA	1
26S40E30K01	IWVWD Well 08	8/7/2000	173	Lab	GAMA	1
26S40E30K01	IWVWD Well 08	8/21/2001	190	Lab	GAMA	1
26S40E30K01	IWVWD Well 08	8/1/2002	200	Lab	GAMA	1
26S40E30K01	IWVWD Well 08	9/10/2003	260	Lab	GAMA	1
26S40E30K01	IWVWD Well 08	8/12/2004	250	Lab	GAMA	1
26S40E30K01	IWVWD Well 08	3/29/2005	240	Lab	GAMA	1
26S40E30K01	IWVWD Well 08	8/21/1964	200	Lab	USGS	1
26S40E30K01	IWVWD Well 08	3/31/1970	207	Lab	USGS	1
26S40E30K02	IWVWD 09 (Abandoned)	5/14/1987	240	Calc	B&S	1
26S40E30K02	IWVWD 09 (Abandoned)	1/7/1988	207	Calc	B&S	1
26S40E30K02	IWVWD 09 (Abandoned)	2/28/1977	296	Ukn	GAMA	1
26S40E30K02	IWVWD 09 (Abandoned)	11/9/1978	240	Ukn	GAMA	1
26S40E30K02	IWVWD 09 (Abandoned)	7/9/1982	270	Ukn	GAMA	1
26S40E30K02	IWVWD 09 (Abandoned)	1/22/1985	263	Lab	GAMA	1
26S40E30K02	IWVWD 09 (Abandoned)	1/14/1988	539	Lab	GAMA	1
26S40E30K02	IWVWD 09 (Abandoned)	6/29/1989	244	Lab	GAMA	1
26S40E30K02	IWVWD 09 (Abandoned)	2/2/1990	217	Lab	GAMA	1
26S40E30K02	IWVWD 09 (Abandoned)	1/22/1991	238	Lab	GAMA	1
26S40E30K02	IWVWD 09 (Abandoned)	3/6/1992	181	Lab	GAMA	1
26S40E30K02	IWVWD 09 (Abandoned)	4/13/1994	215	Lab	GAMA	1
26S40E30K02	IWVWD 09 (Abandoned)	2/15/1995	224	Lab	GAMA	1
26S40E30K02	IWVWD 09 (Abandoned)	1/24/1996	218	Lab	GAMA	1
26S40E30K02	IWVWD 09 (Abandoned)	1/13/1997	287	Lab	GAMA	1
26S40E30K02	IWVWD 09 (Abandoned)	1/26/1998	178	Lab	GAMA	1
26S40E30K02	IWVWD 09 (Abandoned)	9/9/1998	218	Lab	GAMA	1
26S40E30K02	IWVWD 09 (Abandoned)	9/15/1999	212	Lab	GAMA	1
26S40E30K02	IWVWD 09 (Abandoned)	8/7/2000	217	Lab	GAMA	1
26S40E30K02	IWVWD 09 (Abandoned)	8/21/2001	220	Lab	GAMA	1
26S40E30K02	IWVWD 09 (Abandoned)	8/1/2002	240	Lab	GAMA	1
26S40E30K02	IWVWD 09 (Abandoned)	3/31/1970	246	Lab	GAMA-USGS	1
26S40E30K03	IWVWD Well 10	4/4/2007	280	Lab	FR: AB	1
26S40E30K03	IWVWD Well 10	10/24/1974	238	Ukn	GAMA	1

Table 2: IWV TDS Data

Sample Dates in red indicate
only sample month/year is known

min	1/26/1920	100	
max	3/5/2019	232000	
count	2,044		

Unique Well Name	alternateName	Sample Date	TDS (mg/L)	Analysis Type	TDS Reference	Confidence Level
26S40E30K03	IWVWD Well 10	6/4/1975	304	Ukn	GAMA	1
26S40E30K03	IWVWD Well 10	3/23/1977	317	Ukn	GAMA	1
26S40E30K03	IWVWD Well 10	11/9/1978	350	Ukn	GAMA	1
26S40E30K03	IWVWD Well 10	5/1/1980	330	Ukn	GAMA	1
26S40E30K03	IWVWD Well 10	7/30/1981	255	Ukn	GAMA	1
26S40E30K03	IWVWD Well 10	7/9/1982	377	Ukn	GAMA	1
26S40E30K03	IWVWD Well 10	11/12/1983	267	Ukn	GAMA	1
26S40E30K03	IWVWD Well 10	1/22/1985	323	Lab	GAMA	1
26S40E30K03	IWVWD Well 10	1/7/1988	286	Lab	GAMA	1
26S40E30K03	IWVWD Well 10	1/14/1988	532	Lab	GAMA	1
26S40E30K03	IWVWD Well 10	12/20/1989	377	Lab	GAMA	1
26S40E30K03	IWVWD Well 10	1/22/1991	256	Lab	GAMA	1
26S40E30K03	IWVWD Well 10	3/6/1992	234	Lab	GAMA	1
26S40E30K03	IWVWD Well 10	10/8/1992	232	Lab	GAMA	1
26S40E30K03	IWVWD Well 10	1/22/1993	226	Lab	GAMA	1
26S40E30K03	IWVWD Well 10	2/2/1994	214	Lab	GAMA	1
26S40E30K03	IWVWD Well 10	2/15/1995	234	Lab	GAMA	1
26S40E30K03	IWVWD Well 10	1/24/1996	245	Lab	GAMA	1
26S40E30K03	IWVWD Well 10	1/13/1997	266	Lab	GAMA	1
26S40E30K03	IWVWD Well 10	1/26/1998	248	Lab	GAMA	1
26S40E30K03	IWVWD Well 10	9/9/1998	191	Lab	GAMA	1
26S40E30K03	IWVWD Well 10	9/15/1999	235	Lab	GAMA	1
26S40E30K03	IWVWD Well 10	8/7/2000	217	Lab	GAMA	1
26S40E30K03	IWVWD Well 10	8/21/2001	220	Lab	GAMA	1
26S40E30K03	IWVWD Well 10	8/1/2002	240	Lab	GAMA	1
26S40E30K03	IWVWD Well 10	9/10/2003	290	Lab	GAMA	1
26S40E30K03	IWVWD Well 10	8/12/2004	260	Lab	GAMA	1
26S40E30K03	IWVWD Well 10	3/29/2005	260	Lab	GAMA	1
26S40E30K03	IWVWD Well 10	4/1/2008	280	Lab	GAMA	1
26S40E30K03	IWVWD Well 10	4/5/2011	260	Lab	GAMA	1
26S40E30K03	IWVWD Well 10	7/11/2013	253	Ukn	GAMA	1
26S40E30K03	IWVWD Well 10	5/27/2014	210	Lab	GAMA	1
26S40E30K03	IWVWD Well 10	5/23/2017	250	Lab	GAMA	1
26S40E30K04	IWVWD Well 09A	7/16/2003	290	Lab	GAMA	1
26S40E30K04	IWVWD Well 09A	8/12/2004	280	Lab	GAMA	1
26S40E30K04	IWVWD Well 09A	3/29/2005	310	Lab	GAMA	1
26S40E30K04	IWVWD Well 09A	6/20/2006	416	Ukn	GAMA	1
26S40E30K04	IWVWD Well 09A	3/31/2008	440	Lab	GAMA	1
26S40E30K04	IWVWD Well 09A	6/17/2008	290	Lab	GAMA	1
26S40E30K04	IWVWD Well 09A	4/5/2011	300	Lab	GAMA	1
26S40E30K04	IWVWD Well 09A	5/27/2014	290	Lab	GAMA	1
26S40E30K04	IWVWD Well 09A	5/23/2017	340	Lab	GAMA	1
26S40E31D01	HOPPER	11/27/1981	355	Ukn	H-WQ	2
26S40E31D01	HOPPER	9/30/1997	228	Ukn	KCWA WQ	3
26S40E31J01		3/13/2001	270	Ukn	H-WQ	2
26S40E31K01	BURNS	10/22/2002	520	Ukn	H-WQ	2

Table 2: IWV TDS Data

Sample Dates in red indicate
only sample month/year is known

min	1/26/1920	100	
max	3/5/2019	232000	
count	2,044		

Unique Well Name	alternateName	Sample Date	TDS (mg/L)	Analysis Type	TDS Reference	Confidence Level
26S40E31Q01		3/20/2007	410	Ukn	H-WQ	2
26S40E32D01	USGS-353808117421501	4/30/1946	162	Lab	GAMA-USGS	1
26S40E32D01	USGS-353808117421501	9/24/1946	160	Lab	GAMA-USGS	1
26S40E32D01	USGS-353808117421501	7/10/1953	178	Calc	Moyle	1
26S40E32E01		7/9/1953	249	Calc	Moyle	1
26S40E32E02	USGS-353800117420801	6/17/1972	306	Lab	W	1
26S40E32E06		7/27/2010	160	Ukn	H-WQ	2
26S40E32F	IWVWD Well 12 (Abandoned)	1/22/1985	293	Lab	GAMA	1
26S40E32F	IWVWD Well 12 (Abandoned)	1/7/1988	279	Lab	GAMA	1
26S40E32F	IWVWD Well 12 (Abandoned)	12/20/1989	220	Lab	GAMA	1
26S40E32F	IWVWD Well 12 (Abandoned)	1/22/1991	260	Lab	GAMA	1
26S40E32F	IWVWD Well 12 (Abandoned)	3/6/1992	208	Lab	GAMA	1
26S40E32F	IWVWD Well 12 (Abandoned)	10/8/1992	195	Lab	GAMA	1
26S40E32F	IWVWD Well 12 (Abandoned)	1/21/1993	223	Lab	GAMA	1
26S40E32F	IWVWD Well 12 (Abandoned)	3/14/1994	198	Lab	GAMA	1
26S40E32F	IWVWD Well 12 (Abandoned)	2/15/1995	255	Lab	GAMA	1
26S40E32F	IWVWD Well 12 (Abandoned)	1/24/1996	252	Lab	GAMA	1
26S40E32F	IWVWD Well 12 (Abandoned)	1/13/1997	274	Lab	GAMA	1
26S40E32F	IWVWD Well 12 (Abandoned)	1/26/1998	181	Lab	GAMA	1
26S40E32F	IWVWD Well 12 (Abandoned)	9/8/1998	177	Lab	GAMA	1
26S40E32F	IWVWD Well 12 (Abandoned)	9/15/1999	229	Lab	GAMA	1
26S40E32F	IWVWD Well 12 (Abandoned)	8/7/2000	194	Lab	GAMA	1
26S40E32F01	IWVWD Well 13	5/28/1987	446	Calc	B&S	1
26S40E32F01	IWVWD Well 13	1/7/1988	561	Lab	B&S	1
26S40E32F01	IWVWD Well 13	1/22/1985	507	Lab	GAMA	1
26S40E32F01	IWVWD Well 13	12/20/1989	330	Lab	GAMA	1
26S40E32F01	IWVWD Well 13	1/23/1991	439	Lab	GAMA	1
26S40E32F01	IWVWD Well 13	3/6/1992	399	Lab	GAMA	1
26S40E32F01	IWVWD Well 13	10/26/1992	751	Lab	GAMA	1
26S40E32F01	IWVWD Well 13	11/19/1992	486	Lab	GAMA	1
26S40E32F01	IWVWD Well 13	12/17/1992	534	Lab	GAMA	1
26S40E32F01	IWVWD Well 13	1/21/1993	412	Lab	GAMA	1
26S40E32F01	IWVWD Well 13	2/3/1994	418	Lab	GAMA	1
26S40E32F01	IWVWD Well 13	2/15/1995	506	Lab	GAMA	1
26S40E32F01	IWVWD Well 13	1/24/1996	483	Lab	GAMA	1
26S40E32F01	IWVWD Well 13	1/13/1997	807	Lab	GAMA	1

Table 2: IWV TDS Data

Sample Dates in red indicate
only sample month/year is known

min	1/26/1920	100	
max	3/5/2019	232000	
count	2,044		

Unique Well Name	alternateName	Sample Date	TDS (mg/L)	Analysis Type	TDS Reference	Confidence Level
26S40E32F01	IWVWD Well 13	1/26/1998	633	Lab	GAMA	1
26S40E32F01	IWVWD Well 13	9/8/1998	433	Lab	GAMA	1
26S40E32F01	IWVWD Well 13	9/15/1999	441	Lab	GAMA	1
26S40E32F01	IWVWD Well 13	8/7/2000	485	Lab	GAMA	1
26S40E32F01	IWVWD Well 13	8/21/2001	460	Lab	GAMA	1
26S40E32F01	IWVWD Well 13	8/1/2002	420	Lab	GAMA	1
26S40E32F01	IWVWD Well 13	9/10/2003	530	Lab	GAMA	1
26S40E32F01	IWVWD Well 13	8/12/2004	490	Lab	GAMA	1
26S40E32F01	IWVWD Well 13	3/29/2005	600	Lab	GAMA	1
26S40E32F01	IWVWD Well 13	4/1/2008	670	Lab	GAMA	1
26S40E32F01	IWVWD Well 13	4/5/2011	570	Lab	GAMA	1
26S40E32F01	IWVWD Well 13	5/27/2014	890	Lab	GAMA	1
26S40E32F01	IWVWD Well 13	5/23/2017	890	Lab	GAMA	1
26S40E32K01	IWVWD Well 11	1/7/1988	268	Lab	B&S	1
26S40E32K01	IWVWD Well 11	4/4/2007	470	Lab	FR: AB	1
26S40E32K01	IWVWD Well 11	5/1/1980	260	Ukn	GAMA	1
26S40E32K01	IWVWD Well 11	6/26/1981	410	Ukn	GAMA	1
26S40E32K01	IWVWD Well 11	7/9/1982	353	Ukn	GAMA	1
26S40E32K01	IWVWD Well 11	11/22/1983	217	Ukn	GAMA	1
26S40E32K01	IWVWD Well 11	1/22/1985	463	Lab	GAMA	1
26S40E32K01	IWVWD Well 11	12/20/1989	434	Lab	GAMA	1
26S40E32K01	IWVWD Well 11	1/22/1991	409	Lab	GAMA	1
26S40E32K01	IWVWD Well 11	3/6/1992	393	Lab	GAMA	1
26S40E32K01	IWVWD Well 11	10/8/1992	378	Lab	GAMA	1
26S40E32K01	IWVWD Well 11	1/22/1993	220	Lab	GAMA	1
26S40E32K01	IWVWD Well 11	2/3/1994	400	Lab	GAMA	1
26S40E32K01	IWVWD Well 11	2/15/1995	221	Lab	GAMA	1
26S40E32K01	IWVWD Well 11	1/24/1996	302	Lab	GAMA	1
26S40E32K01	IWVWD Well 11	1/13/1997	404	Lab	GAMA	1
26S40E32K01	IWVWD Well 11	1/26/1998	399	Lab	GAMA	1
26S40E32K01	IWVWD Well 11	9/8/1998	386	Lab	GAMA	1
26S40E32K01	IWVWD Well 11	9/15/1999	392	Lab	GAMA	1
26S40E32K01	IWVWD Well 11	8/7/2000	252	Lab	GAMA	1
26S40E32K01	IWVWD Well 11	8/21/2001	320	Lab	GAMA	1
26S40E32K01	IWVWD Well 11	8/1/2002	390	Lab	GAMA	1
26S40E32K01	IWVWD Well 11	9/10/2003	290	Lab	GAMA	1
26S40E32K01	IWVWD Well 11	8/12/2004	430	Lab	GAMA	1
26S40E32K01	IWVWD Well 11	3/29/2005	440	Lab	GAMA	1
26S40E32K01	IWVWD Well 11	4/1/2008	530	Lab	GAMA	1
26S40E32K01	IWVWD Well 11	4/5/2011	500	Lab	GAMA	1
26S40E32K01	IWVWD Well 11	5/27/2014	500	Lab	GAMA	1
26S40E32K01	IWVWD Well 11	5/23/2017	530	Lab	GAMA	1
26S40E32K01	IWVWD Well 11	3/19/1993	240	Lab	H	1
26S40E32K02	26S40E32K002M	5/1/1980	290	Ukn	GAMA	1
26S40E32K02	26S40E32K002M	6/26/1981	270	Ukn	GAMA	1
26S40E32K02	26S40E32K002M	11/12/1983	297	Ukn	GAMA	1

Table 2: IWV TDS Data

Sample Dates in red indicate — min 1/26/1920 — 100
only sample month/year is known — max 3/5/2019 — 232000
count 2,044

Unique Well Name	alternateName	Sample Date	TDS (mg/L)	Analysis Type	TDS Reference	Confidence Level
26S40E33A02		6/1/1953	215	Calc	Moyle	1
26S40E33P01	IWVWD 07 (Destroyed)	8/1/1986	674	Lab	GAMA	1
26S40E33P01	IWVWD 07 (Destroyed)	6/29/1989	378	Lab	GAMA	1
26S40E33P01	IWVWD 07 (Destroyed)	1/23/1991	360	Lab	GAMA	1
26S40E33P01	IWVWD 07 (Destroyed)	3/6/1992	377	Lab	GAMA	1
26S40E33P01	IWVWD 07 (Destroyed)	1/20/1993	387	Lab	GAMA	1
26S40E33P01	IWVWD 07 (Destroyed)	2/3/1994	373	Lab	GAMA	1
26S40E33P01	IWVWD 07 (Destroyed)	2/16/1995	403	Lab	GAMA	1
26S40E33P01	IWVWD 07 (Destroyed)	1/24/1996	401	Lab	GAMA	1
26S40E33P01	IWVWD 07 (Destroyed)	1/13/1997	460	Lab	GAMA	1
26S40E33P01	IWVWD 07 (Destroyed)	2/24/1998	480	Lab	GAMA	1
26S40E33P01	IWVWD 07 (Destroyed)	3/17/1998	475	Lab	GAMA	1
26S40E33P01	IWVWD 07 (Destroyed)	9/8/1998	476	Lab	GAMA	1
26S40E33P01	IWVWD 07 (Destroyed)	9/15/1999	519	Lab	GAMA	1
26S40E33P01	IWVWD 07 (Destroyed)	8/7/2000	539	Lab	GAMA	1
26S40E33P01	IWVWD 07 (Destroyed)	8/21/2001	560	Lab	GAMA	1
26S40E33P01	IWVWD 07 (Destroyed)	8/1/2002	570	Lab	GAMA	1
26S40E33P01	IWVWD 07 (Destroyed)	9/10/2003	680	Lab	GAMA	1
26S40E33P01	IWVWD 07 (Destroyed)	8/12/2004	630	Lab	GAMA	1
26S40E33P01	IWVWD 07 (Destroyed)	2/7/1945	346	Lab	GAMA-USGS	1
26S40E33P01	IWVWD 07 (Destroyed)	1/1/1945	306	Calc	Moyle	1
26S40E33P01	IWVWD 07 (Destroyed)	6/1/1953	280	Calc	Moyle	1
26S40E33P02	USGS-353724117404302	2/7/1945	735	Lab	GAMA-USGS	1
26S40E33P02	USGS-353724117404302	1/8/1951	303	Lab	GAMA-USGS	1
26S40E33P02	USGS-353724117404302	11/19/1959	257	Lab	GAMA-USGS	1
26S40E33P02	USGS-353724117404302	3/31/1970	349	Lab	GAMA-USGS	1
26S40E33P02	USGS-353724117404302	1/1/1945	670	Calc	Moyle	1
26S40E33P03	USGS-353725117405101	4/30/1946	372	Lab	GAMA-USGS	1
26S40E33P03	USGS-353725117405101	9/25/1946	330	Lab	GAMA-USGS	1
26S40E33P03	USGS-353725117405101	7/14/1967	283	Lab	GAMA-USGS	1
26S40E33P04	RC HGTS WELL #7	5/28/1987	343	Calc	B&M	1
26S40E33P04	RC HGTS WELL #7	1/17/1989	353	Calc	B&S	1
26S40E33P04	RC HGTS WELL #7	3/23/1977	324	Ukn	GAMA	1
26S40E33P04	RC HGTS WELL #7	11/13/1978	290	Ukn	GAMA	1
26S40E33P04	RC HGTS WELL #7	5/1/1980	370	Ukn	GAMA	1
26S40E33P04	RC HGTS WELL #7	6/26/1981	440	Ukn	GAMA	1
26S40E33P04	RC HGTS WELL #7	7/30/1981	440	Ukn	GAMA	1
26S40E33P04	RC HGTS WELL #7	7/9/1982	220	Ukn	GAMA	1
26S40E33P04	RC HGTS WELL #7	11/22/1983	330	Ukn	GAMA	1
26S40E33P04	RC HGTS WELL #7	4/17/1992	420	Ukn	GAMA	1
26S40E33P04	RC HGTS WELL #7	4/6/1993	445	Ukn	GAMA	1
26S40E33P04	RC HGTS WELL #7	5/18/1964	306	Lab	GAMA-USGS	1
26S40E33P04	RC HGTS WELL #7	3/31/1970	320	Lab	GAMA-USGS	1
26S40E33P04	RC HGTS WELL #7	8/1/1986	674	Ukn	H-WQ	2
26S40E34N	IWVWD Well 19 (Destroyed)	1/22/1991	458	Lab	GAMA	1

Table 2: IWV TDS Data

Sample Dates in red indicate — min 1/26/1920 — 100
only sample month/year is known — max 3/5/2019 — 232000
count 2,044

Unique Well Name	alternateName	Sample Date	TDS (mg/L)	Analysis Type	TDS Reference	Confidence Level
26S40E34N	IWVWD Well 19 (Destroyed)	3/6/1992	408	Lab	GAMA	1
26S40E34N	IWVWD Well 19 (Destroyed)	1/20/1993	411	Lab	GAMA	1
26S40E34N	IWVWD Well 19 (Destroyed)	4/14/1993	419	Lab	GAMA	1
26S40E34N	IWVWD Well 19 (Destroyed)	4/29/1993	410	Lab	GAMA	1
26S40E34N	IWVWD Well 19 (Destroyed)	2/3/1994	413	Lab	GAMA	1
26S40E34N	IWVWD Well 19 (Destroyed)	2/15/1995	453	Lab	GAMA	1
26S40E34N	IWVWD Well 19 (Destroyed)	1/24/1996	457	Lab	GAMA	1
26S40E34N	IWVWD Well 19 (Destroyed)	1/13/1997	438	Lab	GAMA	1
26S40E34N	IWVWD Well 19 (Destroyed)	2/6/1998	496	Lab	GAMA	1
26S40E34N	IWVWD Well 19 (Destroyed)	9/8/1998	505	Lab	GAMA	1
26S40E34N	IWVWD Well 19 (Destroyed)	9/15/1999	534	Lab	GAMA	1
26S40E34N	IWVWD Well 19 (Destroyed)	8/7/2000	596	Lab	GAMA	1
26S40E34N	IWVWD Well 19 (Destroyed)	8/21/2001	650	Lab	GAMA	1
26S40E34N	IWVWD Well 19 (Destroyed)	8/1/2002	570	Lab	GAMA	1
26S40E34N	IWVWD Well 19 (Destroyed)	9/10/2003	11000	Lab	GAMA	1
26S40E34N	IWVWD Well 19 (Destroyed)	8/12/2004	640	Lab	GAMA	1
26S40E34N	IWVWD Well 19 (Destroyed)	3/29/2005	700	Lab	GAMA	1
26S40E34N	IWVWD Well 19 (Destroyed)	4/1/2008	720	Lab	GAMA	1
26S40E34N01		7/31/1978	400	Calc	B	1
26S40E34N01		3/29/1980	440	Calc	B	1
26S40E34N01		1/18/1989	442	Calc	B&M	1
26S40E34N01		9/10/2003	11000	Ukn	H-WQ	2
26S40E34N01		6/2/1953	225	Calc	Moyle	1
26S40E34N01		4/6/1955	206	Calc	Moyle	1
26S40E34N01		10/17/1956	221	Calc	Moyle	1
26S40E34N01		9/18/1957	228	Calc	Moyle	1
26S40E34N01		9/18/1958	258	Calc	Moyle	1
26S40E34N01		11/20/1959	292	Calc	Moyle	1
26S40E34N01		8/11/1960	324	Calc	Moyle	1
26S40E34N01		4/30/1946	259	Lab	USGS	1
26S40E34N01		9/24/1946	260	Lab	USGS	1
26S40E34N01		8/1/1961	375	Lab	USGS	1
26S40E34N01		7/18/1962	346	Lab	USGS	1
26S40E34N01		10/14/1963	375	Lab	USGS	1

Table 2: IWV TDS Data

Sample Dates in red indicate — min 1/26/1920 — 100
only sample month/year is known — max 3/5/2019 — 232000
count 2,044

Unique Well Name	alternateName	Sample Date	TDS (mg/L)	Analysis Type	TDS Reference	Confidence Level
26S40E34N01		9/15/1964	343	Lab	USGS	1
26S40E34N01		6/21/1965	328	Lab	USGS	1
26S40E34N01		5/16/1966	296	Lab	USGS	1
26S40E34N01		9/7/1966	316	Lab	USGS	1
26S40E34N01		10/23/1967	268	Lab	USGS	1
26S40E34N01		6/21/1968	352	Lab	USGS	1
26S40E34N01		11/4/1968	292	Lab	USGS	1
26S40E34N01		10/20/1969	324	Lab	USGS	1
26S40E34N01		6/1/1970	360	Lab	USGS	1
26S40E34N01		10/20/1970	349	Calc	USGS	1
26S40E34N01		6/23/1971	277	Lab	USGS	1
26S40E34N01		10/27/1971	391	Lab	USGS	1
26S40E34N01		6/6/1972	321	Calc	W	1
26S40E34R01	USGS-353725117391301	5/1/1946	732	Lab	GAMA-USGS	1
26S40E34R01	USGS-353725117391301	9/24/1946	800	Lab	GAMA-USGS	1
26S40E35H	RLS22-MW02	5/14/1996	1080	Lab	Tri	1
26S40E35H01		5/28/1987	662	Calc	B&M	1
26S40E35H02		8/6/1996	2200	Ukn	AB	2
26S40E35H02		7/8/1988	285	Calc	B&M	1
26S40E35H02		8/5/1996	2200	Lab	H96	1
26S40E35Q01	USGS-353725117382701	9/24/1946	355	Lab	GAMA-USGS	1
26S40E35Q02	S. Boundary	1/19/1989	894	Calc	B&M	1
26S40E35Q02	S. Boundary	3/10/1993	670	Lab	H	1
26S40E35Q02	S. Boundary	6/16/1972	1050	Lab	W	1
26S40E36A01	USGS-353801117370701	6/29/1978	730	Calc	B	1
26S40E36A01	USGS-353801117370701	6/6/1979	750	Calc	B	1
26S40E36A01	USGS-353801117370701	5/27/1980	770	Calc	B	1
26S40E36A01	USGS-353801117370701	6/14/1982	970	Calc	B	1
26S40E36A01	USGS-353801117370701	5/28/1987	1310	Calc	B&S	1
26S40E36A01	USGS-353801117370701	3/6/1974	462	Ukn	GAMA	1
26S40E36A01	USGS-353801117370701	3/25/1975	464	Ukn	GAMA	1
26S40E36A01	USGS-353801117370701	8/19/1976	549	Ukn	GAMA	1
26S40E36A01	USGS-353801117370701	6/17/1985	1140	Ukn	GAMA	1
26S40E36A01	USGS-353801117370701	3/8/1954	1620	Calc	Moyle	1
26S40E36K01	26S40E36K001M	3/30/1982	210	Ukn	GAMA	1
26S41E06P01	TTIWV-MW09	12/12/2002	7190	Lab	Tri	1
26S41E06P01	TTIWV-MW09	2/16/2002	5980	Lab	TTEMI	1
26S41E07D01		6/29/1978	15000	Calc	B	1
26S41E07D01		5/17/1979	15000	Calc	B	1
26S41E07D01		5/21/1980	15000	Calc	B	1
26S41E07D01		3/19/1993	5650	Lab	H	1
26S41E07E01		6/29/1978	4500	Calc	B	1
26S41E07E01		5/17/1979	4600	Calc	B	1
26S41E07E01		5/20/1980	4200	Calc	B	1
26S41E07E01		6/10/1982	5100	Calc	B	1
26S41E07E01		7/9/1953	838	Calc	Moyle	1

Table 2: IWV TDS Data

Sample Dates in red indicate — min 1/26/1920 — 100
only sample month/year is known — max 3/5/2019 — 232000
count 2,044

Unique Well Name	alternateName	Sample Date	TDS (mg/L)	Analysis Type	TDS Reference	Confidence Level
26S41E07G01		6/29/1978	7200	Calc	B	1
26S41E07G01		5/17/1979	7100	Calc	B	1
26S41E07G01		7/9/1953	7890	Calc	Moyle	1
27S37E30K	Horse Canyon Well	1/15/1996	348	Ukn	AB	2
27S37E30K	Horse Canyon Well	4/23/1996	355	Ukn	AB	2
27S37E30K	Horse Canyon Well	7/9/2007	360	Lab	FR: AB	1
27S38E01G01	USGS-353703117501601	9/17/1985	356	Ukn	GAMA	1
27S38E01G01	USGS-353703117501601	11/9/1985	358	Ukn	GAMA	1
27S38E02B01		3/17/1993	310	Lab	H	1
27S38E02C01	USBR-02-S	6/4/1996	240	Ukn	AB	2
27S38E02C01	USBR-02-S	6/4/1996	450	Lab	H96	1
27S38E02C01	USBR-02-S	3/17/1993	310	Ukn	H-WQ	2
27S38E02C01	USBR-02-S	10/20/2004	303	Ukn	KCWA WQ	3
27S38E02C02	USBR-02-M	6/4/1996	330	Lab	H96	1
27S38E02C02	USBR-02-M	10/20/2004	358	Ukn	KCWA WQ	3
27S38E02C02	USBR-02-M	10/30/1990	240	Lab	USBR	1
27S38E02C03	USBR-02-D	6/4/1996	500	Lab	H96	1
27S38E02C03	USBR-02-D	10/20/2004	164	Ukn	KCWA WQ	3
27S38E02C03	USBR-02-D	10/30/1990	354	Lab	USBR	1
27S38E09C01	AB303-03	2/3/2007	460	Lab	FR: AB	1
27S38E09Q01	Father Crowley E.	2/2/2007	430	Lab	FR: AB	1
27S38E09Q02	Father Crowley W.	2/2/2007	980	Lab	FR: AB	1
27S38E10C02		2/3/2007	300	Lab	FR: AB	1
27S38E13A01	SWCB01	3/8/1999	360	Ukn	KCWA WQ	3
27S38E13A02	AB303-01	8/27/2007	300	Lab	FR: AB	1
27S38E14M01		10/11/2007	290	Lab	FR: AB	1
27S38E17A01		10/11/2007	390	Lab	FR: AB	1
27S38E21L01	AB303-05	8/27/2007	510	Lab	FR: AB	1
27S38E23F01	USBR-01-S	3/17/1993	370	Lab	H	1
27S38E23F01	USBR-01-S	6/4/1996	270	Lab	H96	1
27S38E23F01	USBR-01-S	3/18/1993	370	Ukn	KCWA WQ	3
27S38E23F01	USBR-01-S	5/14/2004	282	Ukn	KCWA WQ	3
27S38E23F01	USBR-01-S	3/2/1991	213	Lab	USBR	1
27S38E23F02	USBR-01-S/M	6/4/1996	230	Lab	H96	1
27S38E23F02	USBR-01-S/M	5/14/2004	206	Ukn	KCWA WQ	3
27S38E23F02	USBR-01-S/M	3/2/1991	244	Lab	USBR	1
27S38E23F03	USBR-01-M/D	6/4/1996	230	Lab	H96	1
27S38E23F03	USBR-01-M/D	5/14/2004	246	Ukn	KCWA WQ	3
27S38E23F03	USBR-01-M/D	3/2/1991	354	Lab	USBR	1
27S38E23F04	USBR-01-D	8/27/2007	190	Lab	FR: AB	1
27S38E23F04	USBR-01-D	6/4/1996	240	Lab	H96	1
27S38E23F04	USBR-01-D	5/14/2004	254	Ukn	L/H-WQ	2
27S38E23F04	USBR-01-D	3/2/1991	285	Lab	USBR	1
27S38E23R01		3/29/1960	262	Lab	Moyle	1
27S38E27M01	AB303-07	10/11/2007	260	Lab	FR: AB	1
27S38E28R01	USGS-353305117525301	3/22/1946	380	Lab	GAMA-USGS	1

Table 2: IWV TDS Data

Sample Dates in red indicate
only sample month/year is known

min	1/26/1920	100
max	3/5/2019	232000
count	2,044	

Unique Well Name	alternateName	Sample Date	TDS (mg/L)	Analysis Type	TDS Reference	Confidence Level
27S38E28R01	USGS-353305117525301	3/29/1960	262	Lab	GAMA-USGS	1
27S38E31D01	27S38E31D001M	4/20/1962	205	Lab	GAMA-USGS	1
27S38E31D01	27S38E31D001M	6/5/1953	181	Calc	Moyle	1
27S39E02K	ASPHALT CONST. CO	3/7/1990	240	Ukn	KCWA WQ	3
27S39E02K	ASPHALT CONST. CO	10/29/2012	350	Ukn	KCWA WQ	3
27S39E02K	ASPHALT CONST. CO	6/25/2013	350	Ukn	KCWA WQ	3
27S39E03B01	Eugene Curry	3/30/1986	253	Ukn	H-WQ	2
27S39E03C01	Farrell	10/29/2012	300	Ukn	H-WQ	2
27S39E03C01	Farrell	5/6/2013	280	Ukn	KCWA WQ	3
27S39E03C02	Dewhurst	3/6/2001	260	Ukn	H-WQ	2
27S39E04C01	Padgett Well	5/23/2005	274	Ukn	H-WQ	2
27S39E07R01	INYO	3/22/1946	298	Lab	B&S	1
27S39E07R01	INYO	3/14/1955	275	Lab	B&S	1
27S39E07R01	INYO	3/29/1960	271	Lab	B&S	1
27S39E07R01	INYO	8/31/1988	259	Lab	B&S	1
27S39E08A02	IWVWD Well 34	2/13/2007	290	Lab	GAMA	1
27S39E08A02	IWVWD Well 34	2/14/2012	280	Lab	GAMA	1
27S39E08A02	IWVWD Well 34	5/27/2014	290	Lab	GAMA	1
27S39E08A02	IWVWD Well 34	5/23/2017	240	Lab	GAMA	1
27S39E08E01		3/17/1993	230	Lab	H	1
27S39E08L01	IWVWD Well 33	8/21/2001	260	Lab	GAMA	1
27S39E08L01	IWVWD Well 33	8/1/2002	250	Lab	GAMA	1
27S39E08L01	IWVWD Well 33	9/10/2003	310	Lab	GAMA	1
27S39E08L01	IWVWD Well 33	8/12/2004	290	Lab	GAMA	1
27S39E08L01	IWVWD Well 33	3/29/2005	280	Lab	GAMA	1
27S39E08L01	IWVWD Well 33	4/1/2008	280	Lab	GAMA	1
27S39E08L01	IWVWD Well 33	4/5/2011	260	Lab	GAMA	1
27S39E08L01	IWVWD Well 33	5/27/2014	310	Lab	GAMA	1
27S39E08L01	IWVWD Well 33	7/5/2017	250	Lab	GAMA	1
27S39E08M01	TEST WELL	7/2/1987	274	Lab	B&S	1
27S39E08M01	TEST WELL	7/6/1987	262	Lab	B&S	1
27S39E08M01	TEST WELL	5/30/1996	140	Lab	H96	1
27S39E08M04	IWVWD Well 18	8/21/2001	250	Lab	GAMA	1
27S39E08M04	IWVWD Well 18	8/1/2002	240	Lab	GAMA	1
27S39E08M04	IWVWD Well 18	9/10/2003	300	Lab	GAMA	1
27S39E08M04	IWVWD Well 18	10/19/2004	270	Lab	GAMA	1
27S39E08M04	IWVWD Well 18	3/29/2005	270	Lab	GAMA	1
27S39E08M04	IWVWD Well 18	4/1/2008	290	Lab	GAMA	1
27S39E08M04	IWVWD Well 18	4/5/2011	270	Lab	GAMA	1
27S39E08M04	IWVWD Well 18	5/27/2014	280	Lab	GAMA	1
27S39E08M04	IWVWD Well 18	5/23/2017	260	Lab	GAMA	1
27S39E11D01	USBR-03-S	6/4/1996	300	Ukn	AB	2
27S39E11D01	USBR-03-S	6/25/1996	290	Lab	H96	1
27S39E11D01	USBR-03-S	3/18/1991	360	Lab	USBR	1
27S39E11D02	USBR-03-M	6/25/1996	6500	Lab	H96	1
27S39E11D02	USBR-03-M	3/18/1991	955	Lab	USBR	1

Table 2: IWV TDS Data

Sample Dates in red indicate
only sample month/year is known

min	1/26/1920	100
max	3/5/2019	232000
count	2,044	

Unique Well Name	alternateName	Sample Date	TDS (mg/L)	Analysis Type	TDS Reference	Confidence Level
27S39E11D03	USBR-03-D	6/25/1996	9400	Lab	H96	1
27S39E11D03	USBR-03-D	3/18/1991	6634	Lab	USBR	1
27S39E12M01		6/1/1987	365	Lab	B&S	1
27S39E12M01		9/1/1987	340	Lab	B&S	1
27S39E19E01	IWV WD MW03	3/17/1993	240	Lab	H	1
27S39E19E01	IWV WD MW03	3/18/1993	240	Ukn	KCWA WQ	3
27S40E01G02	USGS-353657117372602	9/23/1946	1540	Lab	GAMA-USGS	1
27S40E01K01	USGS-353652117372701	9/3/1929	983	Lab	GAMA-USGS	1
27S40E01K01	USGS-353652117372701	1/1/1929	920	Calc	Moyle	1
27S40E01K02	George Air Corridor	9/18/1986	452	Ukn	KCWA WQ	3
27S40E01K02	George Air Corridor	6/1/1953	1130	Calc	Moyle	1
27S40E01K02	George Air Corridor	6/17/1972	1510	Lab	W	1
27S40E01M01	USGS-353649117375001	5/1/1946	523	Lab	GAMA-USGS	1
27S40E01M01	USGS-353649117375001	9/23/1946	502	Lab	GAMA-USGS	1
27S40E01M01	USGS-353649117375001	6/4/1953	517	Calc	Moyle	1
27S40E01M02		7/8/1988	599	Calc	B&S	1
27S40E02A01	USGS-353708117380701	6/14/1972	1130	Lab	W	1
27S40E02F01	USGS-353701117384701	6/16/1972	374	Lab	W	1
27S40E02G01	USGS-353701117382601	6/15/1972	1880	Lab	W	1
27S40E02G03	USGS-353707117381801	7/8/1988	1350	Calc	B&M	1
27S40E02G03	USGS-353707117381801	4/12/1990	1420	Ukn	GAMA	1
27S40E02G03	USGS-353707117381801	3/14/1991	1160	Ukn	GAMA	1
27S40E02G03	USGS-353707117381801	4/16/1992	1120	Ukn	GAMA	1
27S40E02G03	USGS-353707117381801	4/6/1993	1040	Ukn	GAMA	1
27S40E02H01	USGS-353657117380101	6/30/1988	684	Calc	B&S	1
27S40E02H01	USGS-353657117380101	5/1/1975	617	Ukn	GAMA	1
27S40E02H01	USGS-353657117380101	6/18/1972	668	Lab	W	1
27S40E02J01	DMP Cemetery	6/28/1978	1100	Calc	B	1
27S40E02J01	DMP Cemetery	6/1/1979	1100	Calc	B	1
27S40E02J01	DMP Cemetery	5/23/1980	1100	Calc	B	1
27S40E02J01	DMP Cemetery	6/1/1987	1130	Calc	B&M	1
27S40E02J01	DMP Cemetery	6/30/1988	1160	Calc	B&S	1
27S40E02J01	DMP Cemetery	2/26/1968	1170	Ukn	GAMA	1
27S40E02J01	DMP Cemetery	4/3/1969	1110	Ukn	GAMA	1
27S40E02J01	DMP Cemetery	8/19/1976	1150	Ukn	GAMA	1
27S40E02J01	DMP Cemetery	3/6/1974	1130	Calc	GAMA-USGS	1
27S40E02J01	DMP Cemetery	3/25/1975	1120	Calc	GAMA-USGS	1
27S40E02J01	DMP Cemetery	3/7/1990	1026	Ukn	KCWA WQ	3
27S40E02J01	DMP Cemetery	6/17/1972	1230	Lab	W	1
27S40E02N01	USGS-353634117385401	4/27/1946	774	Lab	GAMA-USGS	1
27S40E03J01	USGS-353645117390901	3/2/1959	4780	Lab	GAMA-USGS	1
27S40E03P01	USGS-353630117394901	9/25/1946	2200	Lab	GAMA-USGS	1
27S40E03P01	USGS-353630117394901	6/1/1953	4340	Calc	Moyle	1
27S40E03P01	USGS-353630117394901	6/5/1953	4230	Calc	Moyle	1
27S40E03R01	USGS-353630117390901	6/29/1978	700	Calc	B	1
27S40E03R01	USGS-353630117390901	6/6/1979	820	Calc	B	1

Table 2: IWV TDS Data

Sample Dates in red indicate
only sample month/year is known

min	1/26/1920	100
max	3/5/2019	232000
count	2,044	

Unique Well Name	alternateName	Sample Date	TDS (mg/L)	Analysis Type	TDS Reference	Confidence Level
27S40E03R01	USGS-353630117390901	5/27/1980	820	Calc	B	1
27S40E03R01	USGS-353630117390901	6/15/1982	920	Calc	B	1
27S40E03R01	USGS-353630117390901	8/19/1976	923	Ukn	GAMA	1
27S40E03R01	USGS-353630117390901	3/7/1974	469	Calc	GAMA-USGS	1
27S40E03R01	USGS-353630117390901	3/25/1975	660	Calc	GAMA-USGS	1
27S40E04B01	USGS-353720117402501	7/14/1967	640	Ukn	GAMA	1
27S40E04B02	USGS-353720117402502	5/29/1987	717	Calc	B&M	1
27S40E04B02	USGS-353720117402502	6/11/1987	676	Calc	B&S	1
27S40E04B02	USGS-353720117402502	6/1/1953	224	Ukn	GAMA	1
27S40E04B02	USGS-353720117402502	5/12/1965	435	Ukn	GAMA	1
27S40E04B02	USGS-353720117402502	7/14/1967	404	Ukn	GAMA	1
27S40E04B3	Searles Valley Minerals Op Well 02	6/11/1987	743	Lab	GAMA	1
27S40E04B3	Searles Valley Minerals Op Well 02	7/2/1992	851	Lab	GAMA	1
27S40E04B3	Searles Valley Minerals Op Well 02	4/4/1996	884	Lab	GAMA	1
27S40E04B3	Searles Valley Minerals Op Well 02	6/8/1999	936	Lab	GAMA	1
27S40E04B3	Searles Valley Minerals Op Well 02	3/19/2002	1000	Lab	GAMA	1
27S40E04B3	Searles Valley Minerals Op Well 02	6/4/2002	1000	Lab	GAMA	1
27S40E04B3	Searles Valley Minerals Op Well 02	9/11/2002	1100	Lab	GAMA	1
27S40E04B3	Searles Valley Minerals Op Well 02	12/17/2002	1100	Lab	GAMA	1
27S40E04B3	Searles Valley Minerals Op Well 02	3/11/2003	1100	Lab	GAMA	1
27S40E04B3	Searles Valley Minerals Op Well 02	3/16/2004	1400	Lab	GAMA	1
27S40E04B3	Searles Valley Minerals Op Well 02	9/7/2004	1200	Lab	GAMA	1
27S40E04B3	Searles Valley Minerals Op Well 02	12/14/2004	1100	Lab	GAMA	1
27S40E04B3	Searles Valley Minerals Op Well 02	3/1/2005	1100	Lab	GAMA	1
27S40E04B3	Searles Valley Minerals Op Well 02	6/14/2005	1100	Lab	GAMA	1
27S40E04B3	Searles Valley Minerals Op Well 02	9/13/2005	1200	Lab	GAMA	1
27S40E04B3	Searles Valley Minerals Op Well 02	9/20/2005	1100	Lab	GAMA	1
27S40E04B3	Searles Valley Minerals Op Well 02	12/13/2005	1000	Lab	GAMA	1
27S40E04B3	Searles Valley Minerals Op Well 02	2/28/2006	1100	Lab	GAMA	1
27S40E04B3	Searles Valley Minerals Op Well 02	6/13/2006	1000	Lab	GAMA	1
27S40E04B3	Searles Valley Minerals Op Well 02	9/5/2006	1100	Lab	GAMA	1
27S40E04B3	Searles Valley Minerals Op Well 02	12/5/2006	1100	Lab	GAMA	1

Table 2: IWV TDS Data

Sample Dates in red indicate
only sample month/year is known

min	1/26/1920	100
max	3/5/2019	232000
count	2,044	

Unique Well Name	alternateName	Sample Date	TDS (mg/L)	Analysis Type	TDS Reference	Confidence Level
27S40E04B3	Searles Valley Minerals Op Well 02	3/6/2007	700	Lab	GAMA	1
27S40E04B3	Searles Valley Minerals Op Well 02	9/4/2007	830	Lab	GAMA	1
27S40E04B3	Searles Valley Minerals Op Well 02	12/4/2007	1200	Lab	GAMA	1
27S40E04B3	Searles Valley Minerals Op Well 02	9/16/2008	1100	Lab	GAMA	1
27S40E04B3	Searles Valley Minerals Op Well 02	6/16/2009	1200	Lab	GAMA	1
27S40E04B3	Searles Valley Minerals Op Well 02	6/8/2010	1300	Lab	GAMA	1
27S40E04B3	Searles Valley Minerals Op Well 02	6/7/2011	1100	Lab	GAMA	1
27S40E04B3	Searles Valley Minerals Op Well 02	6/3/2014	1100	Lab	GAMA	1
27S40E04B3	Searles Valley Minerals Op Well 02	6/6/2017	1200	Lab	GAMA	1
27S40E04B3	Searles Valley Minerals Op Well 02	8/8/2017	1100	Lab	GAMA	1
27S40E04B3	Searles Valley Minerals Op Well 02	12/11/2018	1300	Lab	GAMA	1
27S40E04B3	Searles Valley Minerals Op Well 02	3/5/2019	1300	Lab	GAMA	1
27S40E04C01	USGS-353721117404001	5/22/1969	282	Ukn	GAMA	1
27S40E04C01	USGS-353721117404001	3/31/1970	347	Ukn	GAMA	1
27S40E04C01	USGS-353721117404001	11/19/1959	282	Lab	GAMA-USGS	1
27S40E04C02	USGS-353714117403901	11/19/1959	282	Ukn	GAMA	1
27S40E04C02	USGS-353714117403901	3/31/1970	342	Ukn	GAMA	1
27S40E04C02	USGS-353714117403901	3/23/1977	506	Ukn	GAMA	1
27S40E04C02	USGS-353714117403901	11/13/1978	510	Ukn	GAMA	1
27S40E04C02	USGS-353714117403901	12/27/1978	560	Ukn	GAMA	1
27S40E04C02	USGS-353714117403901	8/1/1986	899	Ukn	H-WQ	2
27S40E04E02		6/1/1953	232	Calc	Moyle	1
27S40E04F01	IWVWD 01 (RCH 01; Destroyed)	12/20/1989	499	Lab	GAMA	1
27S40E04F01	IWVWD 01 (RCH 01; Destroyed)	1/1/1949	276	Calc	Moyle	1
27S40E04F02	IWVWD 02 (RCH 02; Destroyed)	6/29/1989	360	Lab	GAMA	1
27S40E04F02	IWVWD 02 (RCH 02; Destroyed)	12/20/1989	499	Lab	GAMA	1
27S40E04F02	IWVWD 02 (RCH 02; Destroyed)	1/22/1991	360	Lab	GAMA	1
27S40E04F02	IWVWD 02 (RCH 02; Destroyed)	3/6/1992	344	Lab	GAMA	1
27S40E04F02	IWVWD 02 (RCH 02; Destroyed)	1/20/1993	336	Lab	GAMA	1
27S40E04F02	IWVWD 02 (RCH 02; Destroyed)	2/2/1994	337	Lab	GAMA	1
27S40E04F02	IWVWD 02 (RCH 02; Destroyed)	2/15/1995	341	Lab	GAMA	1
27S40E04F03	IWVWD 03 (Destroyed)	8/1/1986	899	Lab	GAMA	1

Table 2: IWV TDS Data

Sample Dates in red indicate — min 1/26/1920 — 100
only sample month/year is known — max 3/5/2019 — 232000
count 2,044

Unique Well Name	alternateName	Sample Date	TDS (mg/L)	Analysis Type	TDS Reference	Confidence Level
27S40E04F03	IWVWD 03 (Destroyed)	6/29/1989	434	Lab	GAMA	1
27S40E04F03	IWVWD 03 (Destroyed)	2/2/1990	443	Lab	GAMA	1
27S40E04F03	IWVWD 03 (Destroyed)	1/22/1991	471	Lab	GAMA	1
27S40E04F03	IWVWD 03 (Destroyed)	3/6/1992	401	Lab	GAMA	1
27S40E04F03	IWVWD 03 (Destroyed)	1/20/1993	390	Lab	GAMA	1
27S40E04F04	IWVWD 04 (Destroyed)	8/1/1986	728	Lab	GAMA	1
27S40E04F04	IWVWD 04 (Destroyed)	6/29/1989	215	Lab	GAMA	1
27S40E04F04	IWVWD 04 (Destroyed)	2/2/1990	236	Lab	GAMA	1
27S40E04F04	IWVWD 04 (Destroyed)	3/6/1992	237	Lab	GAMA	1
27S40E04F04	IWVWD 04 (Destroyed)	1/22/1993	236	Lab	GAMA	1
27S40E04L01	USGS-353652117404201	11/9/1978	540	Ukn	GAMA	1
27S40E04L01	USGS-353652117404201	11/19/1959	277	Lab	GAMA-USGS	1
27S40E04L01	USGS-353652117404201	3/31/1970	338	Lab	GAMA-USGS	1
27S40E04L01	USGS-353652117404201	10/1/1971	397	Calc	GAMA-USGS	1
27S40E04L01	USGS-353652117404201	8/1/1986	728	Ukn	H-WQ	2
27S40E04L01	USGS-353652117404201	7/1/1950	303	Calc	Moyle	1
27S40E04L01	USGS-353652117404201	6/1/1953	358	Calc	Moyle	1
27S40E04L01	USGS-353652117404201	4/7/1955	317	Calc	Moyle	1
27S40E04L02	27S40E04L002M	7/9/1982	680	Ukn	GAMA	1
27S40E05C01	IWVWD Well 14 (RCH 13; Destroyed)	12/20/1989	390	Lab	GAMA	1
27S40E05C01	IWVWD Well 14 (RCH 13; Destroyed)	1/22/1991	400	Lab	GAMA	1
27S40E05C01	IWVWD Well 14 (RCH 13; Destroyed)	3/6/1992	365	Lab	GAMA	1
27S40E05C01	IWVWD Well 14 (RCH 13; Destroyed)	1/21/1993	349	Lab	GAMA	1
27S40E05C01	IWVWD Well 14 (RCH 13; Destroyed)	2/2/1994	339	Lab	GAMA	1
27S40E05C01	IWVWD Well 14 (RCH 13; Destroyed)	2/15/1995	364	Lab	GAMA	1
27S40E05C01	IWVWD Well 14 (RCH 13; Destroyed)	5/24/2002	1500	Lab	GAMA	1
27S40E05D	Searles Valley Minerals Op Well 04	6/4/2002	350	Lab	GAMA	1
27S40E05D	Searles Valley Minerals Op Well 04	9/20/2005	380	Lab	GAMA	1
27S40E05D	Searles Valley Minerals Op Well 04	9/16/2008	370	Lab	GAMA	1
27S40E05D	Searles Valley Minerals Op Well 04	6/16/2009	410	Lab	GAMA	1
27S40E05D	Searles Valley Minerals Op Well 04	6/7/2011	410	Lab	GAMA	1
27S40E05D	Searles Valley Minerals Op Well 04	6/3/2014	430	Lab	GAMA	1
27S40E05D	Searles Valley Minerals Op Well 04	6/6/2017	430	Lab	GAMA	1
27S40E05D	Searles Valley Minerals Op Well 04	8/8/2017	390	Lab	GAMA	1
27S40E05D01		5/29/1987	352	Calc	B&S	1

Table 2: IWV TDS Data

Sample Dates in red indicate — min 1/26/1920 — 100
only sample month/year is known — max 3/5/2019 — 232000
count 2,044

Unique Well Name	alternateName	Sample Date	TDS (mg/L)	Analysis Type	TDS Reference	Confidence Level
27S40E05F	IWVWD 05 (RCH 07; Destroyed)	2/2/1990	519	Lab	GAMA	1
27S40E05F	IWVWD 05 (RCH 07; Destroyed)	3/6/1992	495	Lab	GAMA	1
27S40E05F	IWVWD 05 (RCH 07; Destroyed)	1/20/1993	482	Lab	GAMA	1
27S40E05F	IWVWD 05 (RCH 07; Destroyed)	2/2/1994	490	Lab	GAMA	1
27S40E05F	IWVWD 05 (RCH 07; Destroyed)	2/15/1995	474	Lab	GAMA	1
27S40E06D01	Dist. Well 12	3/10/1999	252	Ukn	AB	2
27S40E06D01	Dist. Well 12	5/28/1987	235	Lab	B&S	1
27S40E06D01	Dist. Well 12	1/7/1988	239	Lab	B&S	1
27S40E06D01	Dist. Well 12	1/22/1985	293	Ukn	KCWA WQ	3
27S40E06D01	Dist. Well 12	4/18/1986	275	Ukn	KCWA WQ	3
27S40E06D01	Dist. Well 12	12/20/1989	220	Ukn	KCWA WQ	3
27S40E06D01	Dist. Well 12	3/12/1990	212	Ukn	KCWA WQ	3
27S40E06D01	Dist. Well 12	1/22/1991	260	Ukn	KCWA WQ	3
27S40E06D01	Dist. Well 12	3/6/1992	208	Ukn	KCWA WQ	3
27S40E06D01	Dist. Well 12	10/8/1992	195	Ukn	KCWA WQ	3
27S40E06D01	Dist. Well 12	1/21/1993	223	Ukn	KCWA WQ	3
27S40E06D01	Dist. Well 12	3/14/1994	198	Ukn	KCWA WQ	3
27S40E06D01	Dist. Well 12	2/15/1995	255	Ukn	KCWA WQ	3
27S40E06D01	Dist. Well 12	1/24/1996	252	Ukn	KCWA WQ	3
27S40E06D01	Dist. Well 12	1/13/1997	274	Ukn	KCWA WQ	3
27S40E06D01	Dist. Well 12	1/26/1998	181	Ukn	KCWA WQ	3
27S40E06D01	Dist. Well 12	9/8/1998	177	Ukn	KCWA WQ	3
27S40E06D01	Dist. Well 12	9/15/1999	229	Ukn	KCWA WQ	3
27S40E06E02	TURNER #2	4/24/2007	300	Ukn	H-WQ	2
27S40E06F01	FRISBEE	10/6/1998	673	Ukn	H-WQ	2
27S40E06H01	USGS-353657117421901	6/2/1987	321	Calc	B&S	1
27S40E06H01	USGS-353657117421901	1/14/1988	318	Lab	B&S	1
27S40E06H01	USGS-353657117421901	2/19/1972	264	Lab	GAMA-USGS	1
27S40E06L01	27S40E06L001M	1/26/1983	357	Ukn	GAMA	1
27S40E06L01	27S40E06L001M	11/22/1983	267	Ukn	GAMA	1
27S40E06R	IWVWD Well 15 (RCH 12; Destroyed)	2/11/1988	740	Lab	GAMA	1
27S40E06R	IWVWD Well 15 (RCH 12; Destroyed)	2/2/1990	467	Lab	GAMA	1
27S40E06R	IWVWD Well 15 (RCH 12; Destroyed)	1/22/1991	537	Lab	GAMA	1
27S40E06R	IWVWD Well 15 (RCH 12; Destroyed)	3/6/1992	327	Lab	GAMA	1
27S40E06R	IWVWD Well 15 (RCH 12; Destroyed)	1/22/1993	620	Lab	GAMA	1
27S40E06R02		2/11/1988	760	Lab	B&S	1
27S40E07G01	USGS-353606117424601	8/11/1960	2040	Lab	Moyle	1
27S40E08A01	USGS-353629117411701	1/14/1988	398	Lab	B&S	1
27S40E08A01	USGS-353629117411701	10/25/1949	399	Lab	GAMA-USGS	1

Table 2: IWV TDS Data

Sample Dates in red indicate — min 1/26/1920 — 100
only sample month/year is known — max 3/5/2019 — 232000
count 2,044

Unique Well Name	alternateName	Sample Date	TDS (mg/L)	Analysis Type	TDS Reference	Confidence Level
27S40E08A01	USGS-353629117411701	7/2/1970	185	Lab	GAMA-USGS	1
27S40E08A01	USGS-353629117411701	6/1/1953	342	Calc	Moyle	1
27S40E08B01		6/2/1987	398	Calc	B&S	1
27S40E08B01		1/14/1988	420	Lab	B&S	1
27S40E08B02	USGS-353627117413401	1/14/1988	432	Lab	B&S	1
27S40E08B02	USGS-353627117413401	5/19/1970	310	Lab	GAMA-USGS	1
27S40E08F01		1/14/1988	532	Lab	B&S	1
27S40E08Q02		6/2/1987	645	Calc	B&M	1
27S40E08Q02		1/14/1988	559	Lab	B&S	1
27S40E09B01	USGS-353623117404001	4/30/1946	388	Ukn	GAMA	1
27S40E09K03		1/25/2011	1700	Ukn	H-WQ	2
27S40E09L01		6/16/2005	1200	Ukn	H-WQ	2
27S40E09L02	USGS-353554117404601	9/11/1964	923	Lab	GAMA-USGS	1
27S40E09P01	USGS-353537117405301	10/10/1951	498	Lab	GAMA-USGS	1
27S40E09P01	USGS-353537117405301	6/1/1953	508	Calc	Moyle	1
27S40E09P01	USGS-353537117405301	6/29/1972	632	Calc	W	1
27S40E10A01		6/1/1953	712	Calc	Moyle	1
27S40E10A01		4/6/1955	637	Calc	Moyle	1
27S40E10A01		9/18/1958	632	Calc	Moyle	1
27S40E10A02		6/1/1953	1700	Calc	Moyle	1
27S40E10A07	USGS-353628117390804	6/17/1972	896	Lab	W	1
27S40E10B01	USGS-353616117392403	4/29/1946	2670	Lab	GAMA-USGS	1
27S40E10C01	USGS-353616117394701	9/25/1946	1800	Lab	GAMA-USGS	1
27S40E10C01	USGS-353616117394701	7/9/1953	2210	Calc	Moyle	1
27S40E10C01	USGS-353616117394701	4/6/1955	2180	Calc	Moyle	1
27S40E10D01	USGS-353617117400701	9/24/1946	1230	Lab	GAMA-USGS	1
27S40E10E01	USGS-353614117400701	6/19/1962	1340	Lab	GAMA-USGS	1
27S40E10H01	USGS-353618117390901	3/8/1967	427	Ukn	GAMA	1
27S40E10H01	USGS-353618117390901	10/11/1961	441	Lab	GAMA-USGS	1
27S40E10H01	USGS-353618117390901	7/20/1962	442	Lab	GAMA-USGS	1
27S40E10H01	USGS-353618117390901	10/24/1963	421	Calc	GAMA-USGS	1
27S40E10H01	USGS-353618117390901	9/8/1964	445	Lab	GAMA-USGS	1
27S40E10H01	USGS-353618117390901	3/23/1966	452	Lab	GAMA-USGS	1
27S40E10H01	USGS-353618117390901	8/11/1960	466	Lab	Moyle	1
27S40E10J01		4/1/1953	425	Calc	Moyle	1
27S40E10J01		8/5/1953	682	Calc	Moyle	1
27S40E10R01	USGS-353540117390601	6/28/1978	3200	Calc	B	1
27S40E10R01	USGS-353540117390601	6/6/1979	2600	Calc	B	1
27S40E10R01	USGS-353540117390601	5/28/1980	2800	Calc	B	1
27S40E10R01	USGS-353540117390601	8/19/1976	3230	Ukn	GAMA	1
27S40E10R01	USGS-353540117390601	3/7/1974	9340	Lab	GAMA-USGS	1
27S40E10R01	USGS-353540117390601	3/25/1975	2710	Calc	GAMA-USGS	1
27S40E11C02	USGS-353626117384602	4/29/1946	1210	Lab	GAMA-USGS	1
27S40E11C02	USGS-353626117384602	9/23/1946	518	Lab	GAMA-USGS	1
27S40E11D03		6/1/1953	474	Calc	Moyle	1
27S40E15L01	27S40E15L001M; USGS-353504117394401	3/7/1974	1500	Ukn	GAMA	1

Table 2: IWV TDS Data

Sample Dates in red indicate — min 1/26/1920 — 100
only sample month/year is known — max 3/5/2019 — 232000
count 2,044

Unique Well Name	alternateName	Sample Date	TDS (mg/L)	Analysis Type	TDS Reference	Confidence Level
27S40E15L01	27S40E15L001M; USGS-353504117394401	6/27/1961	1110	Lab	GAMA-USGS	1
27S40E15L01	27S40E15L001M; USGS-353504117394401	6/29/1972	1370	Calc	W	1
27S40E17G01	USGS-353520117413101	10/6/1969	741	Calc	GAMA-USGS	1
27S40E17G01	USGS-353520117413101	1/29/1970	660	Lab	GAMA-USGS	1
28S37E13F01	USGS-353004117565401	9/25/1990	450	Ukn	GAMA	1
28S37E13F01	USGS-353004117565401	6/5/1953	432	Calc	Moyle	1
28S37E18R01		3/22/1946	230	Calc	Moyle	1
28S37E18R01		3/29/1960	447	Lab	Moyle	1
28S38E18F01	Oil Exploration Well	2/2/2007	630	Lab	FR: AB	1
28S38E18F01	Oil Exploration Well	11/18/1999	657	Ukn	H-WQ	2
ETC44-MW01	ETC44-MW01	4/4/1992	523	Lab	Tri	1
ITC02-MW21	ITC02-MW21	8/5/1999	1300	Lab	Tri	1
ITC45-MW25	ITC45-MW25	5/11/1999	550	Lab	Tri	1
JMM07-MW11	JMM07-MW11	12/4/2002	6220	Lab	Tri	1
JMM07-MW13	JMM07-MW13	12/3/2002	8390	Lab	Tri	1
JMM12-MW08	JMM12-MW08	2/19/2002	350	Lab	TTEMI	1
JMM31-MW01	JMM31-MW01	2/23/1992	3200	Lab	Tri	1
JMM32-MW02	JMM32-MW02	2/22/1992	3000	Lab	Tri	1
MK12-MW12	MK12-MW12	11/12/1999	460	Lab	Tri	1
MK12-MW16	MK12-MW16	4/11/2005	2680	Lab	Tri	1
MK29-MW13	MK29-MW13	2/15/2002	656	Lab	TTEMI	1
MK62-MW01	MK62-MW01	6/11/1998	529	Lab	Tri	1
MK69-MW01	MK69-MW01	12/13/2002	1390	Lab	Tri	1
MK69-MW01	MK69-MW01	2/18/2002	588	Lab	TTEMI	1
MK69-MW02	MK69-MW02	2/18/2002	244	Lab	TTEMI	1
MKFL-MW01	MKFL-MW01	2/25/1999	3600	Lab	Tri	1
MKFL-MW01	MKFL-MW01	2/20/2002	3050	Lab	TTEMI	1
MKFL-MW02	MKFL-MW02	2/20/2002	1330	Lab	TTEMI	1
MKFL-MW03	MKFL-MW03	4/5/2005	2810	Lab	Tri	1
MW01-13	MW01-13	8/25/2009	735	Lab	Tri	1
RLS07-MW02	RLS07-MW02	12/3/2002	5110	Lab	Tri	1
RLS07-MW03	RLS07-MW03	12/3/2002	4310	Lab	Tri	1
RLS07-MW04	RLS07-MW04	2/5/1992	6900	Lab	Tri	1
RLS12-MW01	RLS12-MW01	2/19/1992	320	Lab	Tri	1
RLS12-MW04	RLS12-MW04	12/17/2002	682	Lab	Tri	1
RLS12-MW04	RLS12-MW04	2/19/2002	282	Lab	TTEMI	1
RLS13-MW05	RLS13-MW05	12/5/2002	986	Lab	Tri	1
RLS15-MW03	RLS15-MW03	5/19/2011	3360	Lab	Tri	1
RLS22-MW07	RLS22-MW07	5/14/1996	1140	Lab	Tri	1
RLS22-MW08 (64')	RLS22-MW08 (64')	5/1/1996	982	Lab	Tri	1
RLS29-MW01	RLS29-MW01	2/16/2002	1400	Lab	TTEMI	1
RLS34-MW05	RLS34-MW05	12/4/2002	3960	Lab	Tri	1
RLS34-MW06	RLS34-MW06	2/10/1992	7300	Lab	Tri	1
RLS43-MW06	RLS43-MW06	4/14/2000	11000	Lab	Tri	1
Spring_26S38E15Q01		8/5/1953	519	Calc	Moyle	1

Table 2: IWV TDS Data

Sample Dates in red indicate
only sample month/year is known

min	1/26/1920	100	
max	3/5/2019	232000	
count	2,044		

Unique Well Name	alternateName	Sample Date	TDS (mg/L)	Analysis Type	TDS Reference	Confidence Level
Surface_5_Mile_Canyon	5 Mile Canyon	11/21/1995	658	Ukn	AB	2
Surface_5_Mile_Canyon	5 Mile Canyon	11/26/1995	731	Ukn	AB	2
Surface_5_Mile_Canyon	5 Mile Canyon	5/4/1996	633	Ukn	AB	2
Surface_5_Mile_Canyon	5 Mile Canyon	2/19/2007	740	Lab	FR: AB	1
Surface_9_Mile_Canyon	9 Mile Canyon	4/2/1995	560	Ukn	AB	2
Surface_9_Mile_Canyon	9 Mile Canyon	12/2/1995	842	Ukn	AB	2
Surface_9_Mile_Canyon	9 Mile Canyon	5/13/1996	703	Ukn	AB	2
Surface_9_Mile_Canyon	9 Mile Canyon	2/19/2007	640	Lab	FR: AB	1
Surface_9_Mile_Canyon	9 Mile Canyon	3/21/1993	570	Lab	H	1
Surface_Big_Spring	Big Spring	4/9/2007	270	Lab	FR: AB	1
Surface_Bird_Spring_Source	Bird Spring-Source	4/23/1995	245	Ukn	AB	2
Surface_Bird_Spring_Source	Bird Spring-Source	1/15/1996	199	Ukn	AB	2
Surface_Bird_Spring_Source	Bird Spring-Source	5/5/1996	244	Ukn	AB	2
Surface_Cow_Haven_Cyn	Cow Haven Cyn	7/9/2007	240	Lab	FR: AB	1
Surface_Dead_Foot_Canyon	Dead Foot Canyon	4/2/1995	675	Ukn	AB	2
Surface_Dead_Foot_Canyon	Dead Foot Canyon	11/21/1995	668	Ukn	AB	2
Surface_Grapevine_Canyon	Grapevine Canyon	1/20/1995	743	Lab	FR: AB	1
Surface_Grapevine_Canyon	Grapevine Canyon	4/8/1995	490	Lab	FR: AB	1
Surface_Grapevine_Canyon	Grapevine Canyon	5/13/1996	552	Lab	FR: AB	1
Surface_Grapevine_Canyon	Grapevine Canyon	3/10/1999	384	Lab	FR: AB	1
Surface_Grapevine_Canyon	Grapevine Canyon	3/21/1993	590	Lab	H	1
Surface_Indian_Wells_Canyon	Indian Wells Canyon	4/9/2007	610	Lab	FR: AB	1
Surface_Indian_Wells_Canyon	Indian Wells Canyon	3/21/1993	460	Lab	H	1
Surface_Indian_Wells_Lodge_Spring 01	Indian Wells Lodge Spring 01	5/25/1989	550	Lab	GAMA	1
Surface_Indian_Wells_Lodge_Spring 01	Indian Wells Lodge Spring 01	4/29/1997	560	Lab	GAMA	1
Surface_Little_Lake_Outlet	Little Lake Outlet	2/4/2007	1300	Lab	FR: AB	1
Surface_Sand_Canyon	Sand Canyon	4/9/1995	375	Lab	FR: AB	1
Surface_Sand_Canyon	Sand Canyon	11/20/1995	782	Lab	FR: AB	1
Surface_Sand_Canyon	Sand Canyon	5/13/1996	360	Lab	FR: AB	1
Surface_Sand_Canyon	Sand Canyon	2/19/2007	480	Lab	FR: AB	1
Surface_Short_Canyon	Short Canyon	4/8/1995	350	Ukn	AB	2
Surface_Short_Canyon	Short Canyon	1/12/1996	322	Ukn	AB	2
Surface_Short_Canyon	Short Canyon	4/21/1996	492	Ukn	AB	2
Surface_Short_Canyon	Short Canyon	5/13/1996	435	Ukn	AB	2
Surface_Short_Canyon	Short Canyon	4/9/2007	390	Lab	FR: AB	1
Surface_Short_Canyon	Short Canyon	3/21/1993	360	Lab	H	1
TT37-MW01	TT37-MW01	7/11/2001	2340	Lab	Tri	1
TT37-MW02	TT37-MW02	7/10/2001	1500	Lab	Tri	1
TT37-MW03	TT37-MW03	7/11/2001	1720	Lab	Tri	1
TTBK-MW03	TTBK-MW03	11/15/1999	3200	Lab	Tri	1
TTBK-MW06	TTBK-MW06	8/10/1999	340	Lab	Tri	1
TTBK-MW08	TTBK-MW08	5/13/1999	350	Lab	Tri	1
TTBK-MW09	TTBK-MW09	8/4/1999	420	Lab	Tri	1
TTBK-MW10	TTBK-MW10	5/13/1999	640	Lab	Tri	1
TTIWV-MW02-D	TTIWV-MW02-D	2/18/2002	208	Lab	TTEMI	1

Table 2: IWV TDS Data

Sample Dates in red indicate
only sample month/year is known

min	1/26/1920	100	
max	3/5/2019	232000	
count	2,044		

Unique Well Name	alternateName	Sample Date	TDS (mg/L)	Analysis Type	TDS Reference	Confidence Level
TTIWV-MW02-I	TTIWV-MW02-I	2/18/2002	152	Lab	TTEMI	1
TTIWV-MW04	TTIWV-MW04	2/20/2002	464	Lab	TTEMI	1
TTIWV-MW07	TTIWV-MW07	2/21/2002	608	Lab	TTEMI	1
TTIWV-MW08	TTIWV-MW08	2/18/2002	376	Lab	TTEMI	1
TTIWV-MW10	TTIWV-MW10	2/16/2002	6320	Lab	TTEMI	1
TTIWV-MW15	TTIWV-MW15	2/17/2002	2000	Lab	TTEMI	1
TTIWV-MW16	TTIWV-MW16	2/16/2002	33900	Lab	TTEMI	1
TTSWV-MW01	TTSWV-MW01	2/13/2002	25800	Lab	TTEMI	1
TTSWV-MW02	TTSWV-MW02	2/13/2002	28800	Lab	TTEMI	1
TTSWV-MW03	TTSWV-MW03	2/14/2002	28100	Lab	TTEMI	1
TTSWV-MW04	TTSWV-MW04	2/15/2002	13700	Lab	TTEMI	1
TTSWV-MW05	TTSWV-MW05	2/15/2002	3030	Lab	TTEMI	1
TTSWV-MW06	TTSWV-MW06	2/14/2002	9780	Lab	TTEMI	1
TTSWV-MW07	TTSWV-MW07	2/14/2002	12100	Lab	TTEMI	1
TTSWV-MW09	TTSWV-MW09	2/15/2002	12500	Lab	TTEMI	1
TTSWV-MW10	TTSWV-MW10	2/15/2002	12300	Lab	TTEMI	1

Table 3: TDS References Used in TDS Data Tab

Year	Reference Abbreviation	Record Count	Report	Author	Confidence Level	Stetson has Ref	Notes
1963	Moyle	134	DWR Bulletin No 91-9: Data on Water Wells in IWV Area	USGS, Moyle	1	x	
1975	W	60	WRI 8-75 Groundwater Quality in Indian Wells Valley	Warner	1	x	
1987	B	196	USGS OFR 86-315	Berenbrock	1	x	
1991	B&M	29	USGS Water Resources Investigation Report 89-4191	Berenbrock and Martin	1	x	
1993	USBR	34	IWV Groundwater Project	USBR	1	x	
1994	B&S	87	USGSWater Resources Investigation Report 93-4003	Berenbrock and Schroeder	1	x	
1996	H96	46	Geohydrologic Investigation Report, NAWS China Lanke, CA	Houghton HydroGeo-Logic	1	x	
1995	H	33	GW Geochemistry of IWV	Houghton	1	x	
2003	TTEMI	35	Basewide Hydrogeologic Characterization Summary Report	Tetra Tech EMI	1	x	
2008	AB	36	Appendix C of AB 303 Final Report (historical report summary)	IWVCGTAC & GTC	2	x	
2008	FR: AB	44	AB303 Final Report (samples collected for report)	IWVCGTAC & GTC	1	x	
2013	Tri	50	Tech Justification of Beneficial Use Changes	TriEco Tt	1	x	Stetson has Final (2013) the 2012 referenced is draft
2015	H-WQ	55	Historical IWV Water Quality 2015 Spreadsheet	Navy, Stephan Bork	2		Compilation of historical data
2018	MD	9	MeadowbrookWaterQualityResults_20180911	from Eddy Teasdale	1	x	
2018	GAMA	828	https://geotracker.waterboards.ca.gov/gama/gamamap/public/	CA Water Boards (DHS)	1	x	accessed database November 2018
2018	KCWA WQ	87	KCWA BaseWQ Spreadsheet (unique, not found in other reports)		3	x	Stetson received 12/17/18 from Michelle Anderson
2018/19	GAMA-USGS	242	GAMA & USGS Inyokern and Ridgecrest Quads Well Data	USGS	1	x	Compilation of data received from Stephan Bork (3/7/2019)
2019	USGS	29	USGS Inyokern and Ridgecrest Quads Well Data	USGS	1	x	Compilation of data received from Stephan Bork (3/7/2019)
variable	Other	2	Other - Well logs or other hard data		1	x	
2009/15	L/H-WQ	8	historical compilations from reports		2		Both Layne 2009 and Historical IWV WQ 2015 Spreadsheet

Table 4: Open Items

Year	Reference Abbreviation	Record Count	Report	Author	Confidence Level	Stetson has Ref	Notes
1975	W		WRI 8-75 Groundwater Quality in Indian Wells Valley	Warner			Determine the x,y location of 26S39E19Q02 to add to database
1986	M/B		1986 Study	Muir & Birman			12/9/18 Email - Earl has hard copy to give to Stetson January 2019 for scanning
1987	W/B		1987 Geochemistry Study (U of Utah)	Whalen & Baskin		x	received January 2019 from Earl for scanning
1996	H96		Geohydrologic Investigation Report, NAWS China Lanke, CA	Houghton HydroGeo-Logic		x	Determine following well locations: 26S39E15J01; 26S40E12D01; 26S40E13A01; 26S40E14A01; 26S40E35G01; 27S40E01G
1996	H96		Geohydrologic Investigation Report, NAWS China Lanke, CA	Houghton HydroGeo-Logic		x	Add surface water and spring TDS samples to database
1999			Evidence for Interbasin Flow through Bedrock in SE Sierra NV	Thyne, Gillespie, Ostdick			Water Quality data is not included in report (see footnote 1 on p. 1 for more info)
2008	AB		Appendix C of AB 303 Final Report (historical report summary)	IWVCGTAC & GTC		x	all historical entries in Apx C table have not been confirmed for this database (only BWG entries checked)
2008	AB		Appendix C of AB 303 Final Report (historical report summary)	IWVCGTAC & GTC		x	new data collected for AB303 Phase II entered into TDS data; check original AB Apx C sources for data (confidence level 2)
2009	L		(report unknown; probably working map?)	Layne			1 figure from report IWVWD (recvd 11/30/2018; Renee)
2018	BWG	31	BWG Sampling Event	BWG		x	Not included yet, need to verify screen intervals to place SC/TDS value into DB
2018	RMC		IWV Groundwater Basin SNMP	RMC & Parker GW Inc.		x	this data is a compilation of historical data; currently in incomplete and shund be cross checked for unique values
variable	Other		Other - Well logs or other hard data			x	Add PMTC Range Well (x,y location and TDS sample) into database

Table 5: TDS Reporting Notes

Data Processing Notes

BWG spreadsheet received October 9, 2018

- 1,207 total data entries were gathered from 15 reports/spreadsheets and 1 field sampling event by the BWG
- 31 data entries from field sampling were omitted due to sampling methods
- Stetson performed a QA/QC on the remaining 1,176 entries and their references
    - 15 of the references used by the BWG were focused to 13
        - Stetson has 10 of the 13 references in their files
        - missing reports requested from BWG on 11/19/2018 and received 11/30/18
    - 334 duplicate entries were deleted
    - AB 303 entries were cross-checked against the original AB 303 Final Report (2008) completed by IWVCGTAC & GTC
        - Sample dates were changed from summarizing reports to actual date of sample
        - When comparing actual sample dates, additional duplicate entries (41) were removed
        - 9 missing entries from the AB 303 Final Report (2008) were added to 'TDS Data' tab
    - Berenbrock and Schroeder enteries were cross-checked against the original USGS OFR 93-4003 (1994)
        - TDS values in orange are 'Solids, sum of constituents, dissolved' (DSC) rather than 'Solids, residue @ 180°C, dissolved' (TDS) - for an explanation on the difference see p. 8 of USGS OFR 93-4003 (Noted in 'Analysis Type' column)
        - 51 missing entries from the USGS OFR 93-4003 (1994) were added 'TDS Data' tab
    - Berenbrock entries were cross-checked against the original USGS OFR 86-315 (1987)
        - TDS values from report are 'Solids, sum of constituents, dissolved' (DSC) rather than 'Solids, residue @ 180°C, dissolved' (TDS) - for an explanation on the difference see p. 8 of USGS OFR 93-4003 (Noted in 'Analysis Type' column)
        - 53 missing entries from the USGS OFR 86-315 were added 'TDS Data' tab
    - Berenbrock & Martin entries were cross-checked against the original USGS WRI 89-4191 (1991)
        - TDS values from report are 'Solids, sum of constituents, dissolved' (DSC) rather than 'Solids, residue @ 180°C, dissolved' (TDS) - for an explanation on the difference see p. 8 of USGS OFR 93-4003 (Noted in 'Analysis Type' column)
        - 14 missing entries from the USGS WRI 89-4191 (1991) were added 'TDS Data' tab
    - Houghton entries were cross-checked against the original GW Geochemistry of IWV (1995) Report
        - 21 missing entries from GW Geochemistry of IWV (1995) were added 'TDS Data' tab
    - TriEco entries were cross-checked against the original Tech Justification of Beneficial Use Changes (2013)
        - 28 missing entries from Tech Justification of Beneficial Use Changes (2013) were added 'TDS Data' tab
- During QA/QC 83 entries were found in Appendix C of the AB 303 Final Report (2008).
  This 2008 report contains both a compilation of historical and new TDS data.
  A confidence level of 1 was given to 44 TDS data that could be verified.
  A confidence level of 2 was given to 39 TDS data that could not be verified.
  We are missing the tables from the AB 303 Phase I Report (2003) which may identify the data source and could improve the data's confidence level
- Data from references RMC and Layne were removed because they were unable to be cross-checked
    - 1 entry from Layne (2009) was based on DRAFT IWVWD figure with 18 TDS values
        - no report was available to effectively QA/QC data - moved to the 'Suspect TDS Data' tab
    - 102 entries from RMC (2018) by BWG were moved to the 'Suspect TDS Data' tab - report did not source TDS data, therefore Stetson was unable to effectively QA/QC data
        - an additional 28 TDS data points were added from the RMC report
        - 20 of the 130 entries entered by the BWG were entered with the incorrect location TDS data assigned to IWVWD wells that should have been assigned to NAWS wells with same well #
        - 26 of the 130 entries have well names indicating that the TDS data were taken from the shallow screen interval. RMC Apx B table listed data without depth; p41 of texts says 'deep aquifer'
        - after accounting for historical report duplicates, there are 52 incomplete (without verifiable source) TDS values in RMC's SNMP remaining.

Additional TDS data added or changes made to TDS database

GAMA

- TDS values for 1,963 entries from the GAMA website were added to the DB & and additional QA/AC was performed
  - 90 TDS entries were moved to the 'Incomplete (+Suspect) TDS Data' tab
  - 752 duplicate entries were deleted
    - Note: where duplicate samples were listed on the same date the TDS value from the most trusted reference/source was used. Where the sources were the same, the highest TDS value was kept

AB303 (2003 and 2008)

- The AB 303 Apx C table listed TDS value of 501 mg/L for both NR-2S and NR-1D. The correct values could not be verified
- TDS values for 38 samples from AB 303 (2003) report by Tetra Tech were added to TDS DB
  - 6 duplicate entries were removed
  - 1 entry from TriEco Tt (2012) was moved to 'Suspect or Incomplete TDS Data' tab due to date

TDS Data from Analysis or Calculation

- the 'analysis type' column was included to clarify the TDS value:
  calc' = TDS valuesare sum of constituents (note, sometimes does not include silica)
  Lab = 'total filterable resudue' from lab analysis; or 'Solids, residue @ 180°C, dissolved' (TDS)'
  SC-calc = multiplying Specific Conductance by TDS/SC ratio where known/measured
  unk = not specified

Confidence Levels

1 TDS data have been cross-checked against original report; or data were downloaded directly from the GAMA website

2 TDS data have been found in AB303 Apx C (2008) report summary tables,
however report was unable to be appropriately cross-checked
Confidence level 2 also applies to (1) unverified Navy's compilation of WQ and (2) Draft Layne figure (ref by BWG)

3 KCWA's water quality database is a compilation of many data sources that have not been verified.
There may be errors in this.

Other Notes

- Dates listed as 1/1/xxxx in red were originally only given as a year
- Cells with unusually low TDS values (i.e. 1-75) that were unable to be cross-checked were moved to suspect data tab
- USGS WRIR 93-4003 references two other reports (Koehler, 1971 & Warner, 1975) that may have additional TDS data, however we do not have these references yet to add to the DB
- To verify unique TDS values for IWVWD and Navy production wells with similar well numbers,
  The SDWIS number (water system #) was enterend into the following website
  https://sdwis.waterboards.ca.gov/PDWW/index.jsp
- Requested GIS providecentroid location (x,y of the coordinates of the center of the section) where lat/long not available
  These are noted as "PLScntr" in the "Notes" Column of the Well Information Tab

1/28/2019 Database Update

1 ● 1988 B&S TDS sample well ID (25S38E25J01; 8/25/1988; 875 mg/L) changed to 25S38E25J because 25J01 is assigned to NR-1
1988 historical well 25S38E25J had a total depth of 330 & screen interval of 120-330 from Table 1 (Page 10) of B&S

2 ● 25S38E36G01 (NR2-S) TDS sample (2/26/1991; 808 mg/L) was moved from the incomplete tab into the TDS tab
The BWG (NR2-S) conflicted with RMC (NR2-D), however, the sample was re-sourced to USBR (NR2-S)

3 ● 1995 AB 27S38E23F01 (USBR-01S) TDS sample (12/15/1995 617 mg/L) was moved into the incomplete tab (#208)
AB ref has a conflicting TRSt (27S38E23F01) and Alternate Name (NR-2)
A true location will need to be determined for this sample

4 ● 27S39E11D02 (USBR-03-M) TDS sample (6/25/1996; 6500 mg/L) is inconsistent with historical samples.
Original H-WQ reference not available to verify; TDS value moved to incomplete tab

5 ● USBR-05-S (25S38E34G01; 1/6/1992; 534 mg/L) from USBR, 1993 was added to the DB

6 ● USBR-10-S/M (24S38E21A02; 9/1/1992; 580 mg/L) from USBR, 1993 was added to the DB

7 ● USBR-10 (24S38E21A; 10/30/1995; 1480 mg/L) from AB 303 Appx C not clear on depth zone; moved to incomplete tab

8 ● MW-32-S/M 900 feet (26S39E27D02) 10/18/1991 TDS sample has 2 values in the USBR report:
172.8 mg/L and 168.6 mg/L in lab reports (Apx VIII), and 169 mg/L on Table 2 of the main report
TDS was changed from the Apx VIII highest value to the Report Table 2 value (169 mg/L)

9 ● MW-32-M/D 1200 feet (26S39E27D02) 10/18/1991 TDS sample has 2 values in the USBR report:
179.3 mg/L and 176.3 mg/L in lab reports (Apx VIII), and 176 mg/L on Table 2 of the main report
TDS was changed from the Apx VIII highest value to the Report Table 2 value (176 mg/L)

10 ● 25S38E34G01 (USBR-05-S) TDS sample (3/18/1993; 5690 mg/L) was moved to incomplete TDS Data tab
due to inconsistency between historical data and well names. Houghton TDS sample for 25S38E34J01 was classified as USBR-05-S (25S38E34G01) because this well was historically mislabeled. True location and depth unknown.

11 ● USBR-10 (24S38E21A) - 4 TDS samples were added from the AB 303 Appx C database. These values were given a confidence level of 2 (cannot locate original source (T) referenced in AB303 Appx C table)

12 ● USBR-10 (24S38E21A01; 12/1/1995; 1120 mg/L (BWG)) sample depth was corrected
original BWG value listed as shallow; changed to USBR-10-D (24S38E21A04; AB303 Apx C table elev 630' (depth 1930'))

13 ● Houghton Hydro-Geologic, 1996 Table A2 Labaratory data for groundwater samples from wells added to database
corrected AB303 Apx C alternated names/well ID to match original H96 source (USBR-02 S & M, USBR-01 S & S/M)
updated 28 TDS samples with new Reference Source of H96 and confidence level to 1 from earlier compiled data reference
added 15 TDS samples from H96 reference not included from other compiled data.
6 additional H96 TDS samples that we do not have well locations for. These are listed under Reference tab as an Open Items
Samples for 25S38E34J02 and J03 were referenced as USBR-05; State ID's were corrected to 34G02 and 34G03.

14 ● Alternate name NACC-17-1; Kerr McGee 17-1; 17G02 added for Well 26S39E17F02
added TDS sample (143 mg/L; 5/7/1983) from well report

15 ● Well 26S39E19Q02 sourced from GAMA gives a lat/long (near N Brown Road) that does not agree with the TRS (near Inhokern airport)
the 3 datapoints for this well from 1968 and 1973 were moved to incomplete TDS data

Feb 2019 Database Update

1 ● Added data from 1975 Warner report and QA/QC-ed data
51 entries originally attributed to GAMA were changed to Warner
9 of the 51 entries had TDS values that were updated to match Warner '75
1 26S40E22N01 6/28/1972 TDS sample updated from 582 mg/L (GAMA) to 581 mg/L (Warner)
2 26S40E23G01 5/24/1972 TDS sample updated from 11,000 mg/L (GAMA) to 10,900 mg/L (Warner)
3 26S39E30F03 6/6/1972 TDS sample updated from 385 mg/L (GAMA) to 302 mg/L (Warner)
4 26S39E23J01 6/6/1972 TDS sample updated from 252 mg/L (GAMA) to 218 mg/L (Warner)
5 26S39E24M01 6/6/1972 TDS sample updated from 231 mg/L (GAMA) to 218 mg/L (Warner)
6 26S39E24P01 6/6/1972 TDS sample updated from 238 mg/L (GAMA) to 211 mg/L (Warner)
7 25S39E26H01 6/6/1972 TDS sample updated from 826 mg/L (GAMA) to 696 mg/L (Warner)
8 26S40E17J01 6/18/1972 TDS sample updated from 312 mg/L (GAMA) to 308 mg/L (Warner)
9 26S39E11E01 6/6/1972 TDS sample updated from 812 mg/L (GAMA) to 366 mg/L (Warner)
2 entries originally attributed to KCWA were changed to Warner
2 entries originally attributed to H-WQ were changed to Warner
6 entries from not previously in the database were added
1 26S39E19K01 6/6/1972
2 26S39E19P01 6/6/1972
3 26S40E34N01 6/6/1972
4 25S39E04R01 6/6/1972
5 25S39E09J01 6/6/1972
6 26S39E11E01 6/6/1972

Mar 2019 Database Update

1 ● Addition & QA/QC of data compiled by the Navy (provided by Stephan Bork)
242 entries originally attributed to GAMA were updated to GAMA-Navy based on corresponding Navy data
29 new entries were added as 'Navy' reference

2 ● GAMA duplicate entry for 27S40E07G01 (2040 mg/L) removed

May 2019 Database Update

1 ● Addition of TDS data for the 26S39E34Q01 provided by Tom & Annette DeMay on 5/8/2019
1 new entry was added as 'Other' reference

June 2019 Database Update

1 ● Addition of 3 TDS values from GAMA 6/21/2019 data download
Searles Valley Minerals Op Well 02 (27S40E04B3) 12/11/2018 & 3/5/2019 TDS Samples
West Valley Mutual Well 01 (26S39E07M1) 11/19/2018 TDS Sample

Aug 2019 Database Update

ATTACHMENT H

TECHNICAL MEMORANDUM

785 Grand Avenue, Suite 202 • Carlsbad, California • 92008
Phone: (760) 730-0701 FAX: (415) 457-1638 Web site: www.stetsonengineers.com

TO:	IWV TAC	DATE:	December 31, 2021
FROM:	Stetson Engineers, Inc.	JOB NO:	2652-001: 59
RE:	DRAFT Groundwater Dependent Ecosystem Monitoring Plan		

CONTENTS

1.0. BACKGROUND 1

2.0. INTRODUCTION 1

3.0. OVERVIEW OF GROUNDWATER DEPENDENT ECOSYSTEMS IN IWV 1

4.0. EXISTING GDE VEGETATION DATA 2

5.0. AUGUST 11, 2021 FIELD RECONNAISSANCE 4

6.0. ADDITIONAL PLANNED RECONNAISSANCE IN 2022 5

7.0. GDE MONITORING PLAN 6

7.1 FUTURE PLANNED GDE BASELINE DETERMINATION AND ANNUAL SURVEYS 6
7.2 GDE ANNUAL VEGETATION SURVEYS 6
7.3 GDE-RELATED GROUNDWATER MONITORING 7
7.4 REPORTING 7

FIGURES

ATTACHMENT A FIVE RECON SITES VISITED ON AUGUST 11, 2021: VEGETATION MAPS, WELL DATA, AND PHOTOS

ATTACHMENT B PROPOSED RECON SITES TO EVALUATE IN 2022

1.0. BACKGROUND

In compliance with 2014 California's Sustainable Groundwater Management Act (SGMA) the Indian Wells Valley (IWV) Groundwater Authority (GA) was established as the local Groundwater Sustainability Agency (GSA) for the Indian Wells Valley Groundwater Basin (Basin). Subsequently, a Groundwater Sustainability Plan (GSP)[1] was developed to ensure consistent and effective protection of the Basin. SGMA requires that GSPs include "…where appropriate and in collaboration with the appropriate local agencies […] impacts on groundwater dependent ecosystems" (CWC §10727.4(l)). Groundwater dependent ecosystems (GDEs) are defined in the GSP Regulations as "…ecological communities or species that depend on groundwater emerging from aquifers or on groundwater occurring near the ground surface" (23 CCR §351(m)). As discussed in Section 3.4.7 of the GSP, GDEs on the valley floor are vulnerable and susceptible to impacts related to the chronic lowering of groundwater levels. While modelling has shown a possible lowering of groundwater levels in the vicinity of GDEs near the China Lake Playa in the future (see GSP Appendix 3-H), the potential negative effects of such a lowering on GDEs is currently unknown and has been identified in the GSP as a data gap.

2.0. INTRODUCTION

A reconnaissance field trip was conducted on August 11, 2021 to identify a few key areas containing viable GDE communities within NAWS where groundwater characteristics could also be measured to establish representative GDE monitoring areas. This report summarizes the findings from this initial field visit to five potential GDE areas, and makes recommendations for investigating four additional sites in 2022 to develop an ongoing GDE Monitoring Program. Mapping, groundwater level measurements, and observations from this initial investigation are included for each of the evaluated sites.

3.0. OVERVIEW OF GROUNDWATER DEPENDENT ECOSYSTEMS IN IWV

There are two principal aquifer units defined by Kunkel and Chase (1969)[2]. The shallow aquifer contains coarse sediments near the Sierra Nevada with increased interbedded silts and clays towards the center of the Basin associated with the lacustrine deposits and includes China Lake's playa deposits. The best quality of water is at shallow to medium depths in the southwestern part

[1] Stetson Engineers Inc, 2020. *Indian Wells Valley Groundwater Authority;* Groundwater Sustainability Plan for the Indian Wells Valley Groundwater Basin, Bulletin 118 Basin No. 6-054

[2] Kunkel, Fred, and G.H. Chase, 1969. Geology and Ground Water in Indian Wells Valley, California. USGS Open-File Report 69-329. Prepared in cooperation with the Naval Weapons Center, China Lake, California. 89pp.

of the valley, closer to the Sierra Nevada (Dutcher and Moyle, 1973)[3]. The deeper aquifer is also composed of gravel, sand, silt and clay. It is strongly connected to the shallow aquifer in the west and southwest portions of the IWV, and is confined in other parts of the Basin. Existing multi-level CASGEM monitoring wells (USBR, 1993)[4] show semi-confined artesian conditions within the deeper aquifer where it occurs beneath the lacustrine and other fine-grained sediments.

Ephemeral streams exist in the mountain canyons, but typically do not flow past the mouths of the canyon except for in very wet years. There are multiple natural springs in the mountain and canyon areas surrounding the IWV (see Figure 3-11 in the GSP). There is currently no data documenting any undesirable results or Basin impacts related to depletions of interconnected surface water.

There are no significant interconnected surface water systems that interact with groundwater in the Basin. Streams in the valley are typically ephemeral and the majority of recharge occurs as mountain front recharge.

4.0. EXISTING GDE VEGETATION DATA

To assist GSAs in identifying GDEs, the California Department of Water Resources (DWR) hosts the online *Natural Communities Commonly Associated with Groundwater Dataset*[5] (NCCAG Dataset). The NCCAG Dataset is a compilation of 48 publicly available State and Federal agency datasets that map vegetation, wetlands, springs, and seeps in California. A working group comprised of DWR, the California Department of Fish and Wildlife (CDFW), and The Nature Conservancy (TNC) reviewed the compiled dataset and conducted a screening process to exclude vegetation and wetland types less likely to be associated with groundwater and retain types commonly associated with groundwater, based on criteria described in Klausmeyer et al, (2018)[6]. Two habitat classes are included in the dataset: (1) wetland features commonly associated with the surface expression of groundwater under natural, unmodified conditions; and (2) vegetation types commonly associated with the sub-surface presence of groundwater (phreatophytes). Plant communities mapped in the NCCAG Dataset do not represent the confirmed presence of GDEs.

---

[3] Dutcher L.C. and W.R. Moyle, 1973. Geologic and Hydrologic Features of Indian Wells Valley, California. USGS Water Supply Paper 2007. Prepared in cooperation with the California Department of Water Resources.

[4] U.S. Bureau of Reclamation (USBR), 1993. Indian Wells Valley Groundwater Project: USBR Technical Report Volume II. A cooperative effort among the USBR, IWVWD, North American Chemical Company, and NAWS. December 1993. Prepared by USBR Lower Colorado Region.

[5] https://gis.water.ca.gov/app/NCDatasetViewer/

[6] Klausmeyer, K., Howard, J., Keeler-Wolf, T., Davis-Fadtke, K., Hull, R., Lyons, A., 2018. *Mapping Indicators of Groundwater Dependent Ecosystems in California: Methods Report*. San Francisco, California.

Instead the dataset is intended to illustrate the potential existence of GDEs which can be used by GSAs as a starting point for identifying GDEs within a groundwater basin.

Mapping produced by the NCCAG Dataset indicates the vast majority of GDEs within the IWV are located on NAWS on the broad margins of the China Lake Playa (Figure 1). The Navy's Integrated Natural Resources Monitoring Plan (Tierra Data, 2014) [7] illustrates a similar distribution of GDEs around the playa but with some variation and less apparent detail. Given the lack of perennial surface water in these areas, these GDEs can only be supported by the vertical upward gradient under the Playa which causes groundwater to discharge to the surface. A field visit by representatives of the Navy, TNC and Stetson on November 1, 2018 verified the presence of GDEs in the China Lake Playa region, but no formal assessment or survey was conducted at that time.

TNC's web-based GDE Pulse application[8] provides tools to view long-term trends of moisture and photosynthetic chlorophyll present in vegetation based on satellite data. This information serves as an indicator of vegetative health for GDEs. The online GDE Pulse maps and data show little to no change in vegetative moisture or photosynthetic chlorophyll present in the Playa areas from 1985 to 2018.

Smaller, scattered communities of GDEs may be present in the canyons along the Sierra Nevada, Argus Range and El Paso Mountains, and in the southwest region of the IWV along ephemeral streams. GDEs located in the mountain canyons are not considered vulnerable to the effects of groundwater pumping because they are supported by mountain block recharge. Likewise, GDEs located in the El Paso region are not considered vulnerable due to the lack of groundwater pumping in that area and the consequently stable groundwater levels. GDEs located in the valley floor, including those near the China Lake Playa, are likely more vulnerable than other GDEs in the IWV due to chronic lowering of groundwater levels. This is supported by research (Lancaster, 2019)[9] documenting vegetation loss in well-established GDEs near the Supersonic Naval Ordnance Research Track (SNORT), east of the Little Lake Fault Zone on NAWS due to chronic lowering of groundwater levels. These GDE communities, which currently stabilize sand dunes, are vulnerable to destabilization if groundwater levels continue to decline. Considering the relative vulnerabilities of GDEs within the Basin, only the GDEs within NAWS are addressed by this plan.

---

[7] Tierra Data, Inc. 2014. *Integrated Natural Resource Management Plan.* Naval Air Weapons Station China Lake.

[8] https://groundwaterresourcehub.org/sgma-tools/gde-pulse/

[9] Lancaster, Nicholas, et al, 2019. *Eolian Hazard Assessment for the SNORT Facility*. Prepared for Naval Air Warfare Center Weapons Division China Lake, CA. Prepared by Desert Research Institute. NAWCWD TP. 8840. May 2019.

5.0. AUGUST 11, 2021 FIELD RECONNAISSANCE

A field trip was set up to verify potential GDE Monitoring Sites. Each site was evaluated by (1) NAWS biologist confirming if the NCCAG vegetation types were present, (2) staff geologist measuring depth to groundwater in adjacent wells, and (3) performing an overall site evaluation. Field maps were constructed using DWR's NCCAG data to identify vegetated areas where GDEs (Figure 1) potentially exist in the vicinity of China Lake Playa. Existing monitoring wells at a GDE site would provide depth-to-water data that could be correlated with ecosystem health. NAWS groundwater monitoring wells were matched with the NCCAG vegetated areas to develop potential GDE monitoring sites (Figure 2).

As an initial step in that process, representatives of the WRM and the Navy met on August 11, 2021 for a reconnaissance of five potential GDE areas within NAWS where existing monitoring wells are also located. The purpose of the reconnaissance was to field evaluate well integrity and characteristics and to have a biologist briefly inspect areas surrounding the wells for potential GDE species. Attachment A contains (1) detailed maps of each Recon Area, (2) field observations and available construction details of selected wells, and (3) photos taken at each site. Determination of whether observed species are considered GDE species is based on the Navy's review of Klausmeyer et al, (2018).

Recon Area 1: Several viable monitoring wells exist in this area, although no obvious GDEs were observed. Tamarisk trees (salt cedar) exist in the area and were clearly established along the perimeter of the former 'Charley Tower" compound. However, given that all Tamarisk species found on NAWSCL are non-native and there is no wide consensus that these species are strictly groundwater dependent, these plants are not considered GDE indicators.

Recon Area 2: Two viable monitoring wells were identified in the center of this area but no obvious GDEs were observed near the wells. The northern portion of this area, where the NCCAG Dataset mapped a possible *Atriplex parryi* community, was not investigated.

Recon Area 3: This area is situated along the west edge of the China Lake Playa. Although two viable wells exist in this area, no obvious GDE communities were observed in their vicinity. One well (35E01) exhibits flowing artesian conditions but is capped with an inoperable gate valve. An active "seep" exists near well TTBK-MW13 and is surrounded by grass. The "seep" is a point source of water and there are no other obvious seeps in the surrounding vicinity. Given these conditions, the seep may be due to an artificial conduit, possibly from an old well or an improperly sealed soil boring.

Recon Area 4: Although two viable wells exist in this area along Centerline Road, no obvious GDE indicator species were observed. However, in an area near wells 21K01 and 21K02 located near the north end of Centerline Road, several examples of Parry's Saltbush (*Atroplex parryi*) and Iodine bush (*Allenrolfea occidentalis*) were observed. Both of these species are broadly considered to be phreatophytes.

Recon Area 5: Several viable monitoring wells and several species of GDE and surface water dependent plant species exist in this area. However, local surface water and near-surface groundwater are largely controlled by, and are the result of, infiltration from the nearby wastewater treatment plant ponds. Given the artificial and variable nature of surface and groundwater in this area, and the near-term plans to replace the treatment plant and substantially change artificial water infiltration rates, GDE monitoring in this area is not recommended.

6.0. ADDITIONAL PLANNED RECONNAISSANCE IN 2022

As summarized above, no viable GDE communities were observed near inspected monitoring wells in Recon Areas 1 through 4 and Recon Area 5 is not recommended for GDE monitoring. However, some GDE indicator species were observed near monitoring wells 24S/40E-21K01 and K02 north of Recon Area 4. Based on these results, additional field reconnaissance is recommended to be conducted in 2022 to more fully evaluate Recon Area 4 and investigate other potential areas where GDEs can be effectively monitored. Some areas preliminarily identified for further reconnaissance are shown on Figure 2 and detailed maps are included as Attachment B.

Planned Recon Area 6 - the northern portion of Recon Area 2 mapped by the NCCAG Dataset as potentially containing *Atriplex parryi*,

Planned Recon Area 7 - an area between Recon Areas 2 and 5 mapped by the NCCAG Dataset as potentially containing *Suaeda moquinii*,

Planned Recon Area 8 - the area near the east edge of Recon Area 4 mapped by the NCCAG Dataset as potentially containing *Allenrolfea occidentalis*,

Planned Recon Area 9 - the area surrounding well 21K01, north of Recon Area 4.

Other areas may be investigated by Navy staff at their discretion if insufficient GDE communities are encountered at the above areas.

7.0. GDE MONITORING PLAN

Though we have not yet identified a site to monitor GDE groundwater levels and vegetation health, we are hopeful that at least one of the sites identified for investigation during 2022 will work. Once GDE monitoring sites are chosen, a baseline determination will be performed and annual surveys will be conducted to evaluate any impacts from groundwater level changes. Monitoring wells at each GDE monitoring site will be included in the GSP GWMP and measurements will be taken at least semi-annually.

7.1 *Future Planned GDE Baseline Determination and Annual Surveys*

Baseline GDE surveys will be conducted in each area that is determined to have existing GDE plant communities with nearby groundwater monitoring wells. The surveys will be conducted following guidance provided by U.S. Forest Service's *Groundwater-Dependent Ecosystems: Level I Inventory Field Guide* (USDA, 2012)[10], although the full scope of the survey will be determined by the lead surveyor based on conditions at each site. At minimum, the shape, size and location of each survey area will be measured and recorded and all GDE species within each area will be identified and characterized by apparent health, distribution density, and other parameters as outlined in the Forest Service guidance. Each area will be assigned a unique identification label and site name. The initial baseline survey and subsequent annual surveys will be conducted during the middle of the growing season when plant types and their relative abundance is easiest to observe. For plants around the China Lake Playa this is expected to be in mid to late March.

7.2 *GDE Annual Vegetation Surveys*

Annual GDE vegetation surveys will be performed at each of the established GDE areas at roughly the same time of year as the baseline survey. This is expected to be in mid to late March. Following the GDE baseline and subsequent annual surveys, the Navy shall submit a brief report of findings to the IWVGA Technical Advisory Committee (TAC). The baseline survey report will include maps of surveyed areas, descriptions of survey methodology used, lists of GDE species, their distribution and relative health, etc. As with the survey activities, the elements included in the survey reports will depend on the given site conditions and will be at the discretion of the Navy personnel managing the surveys.

[10] U.S. Department of Agriculture, Forest Service (USDA), March 2012. Groundwater-Dependent Ecosystems: Level I Inventory Field Guide, Inventory Methods for Assessment and Planning, Gen. Tech. Report WO-86a

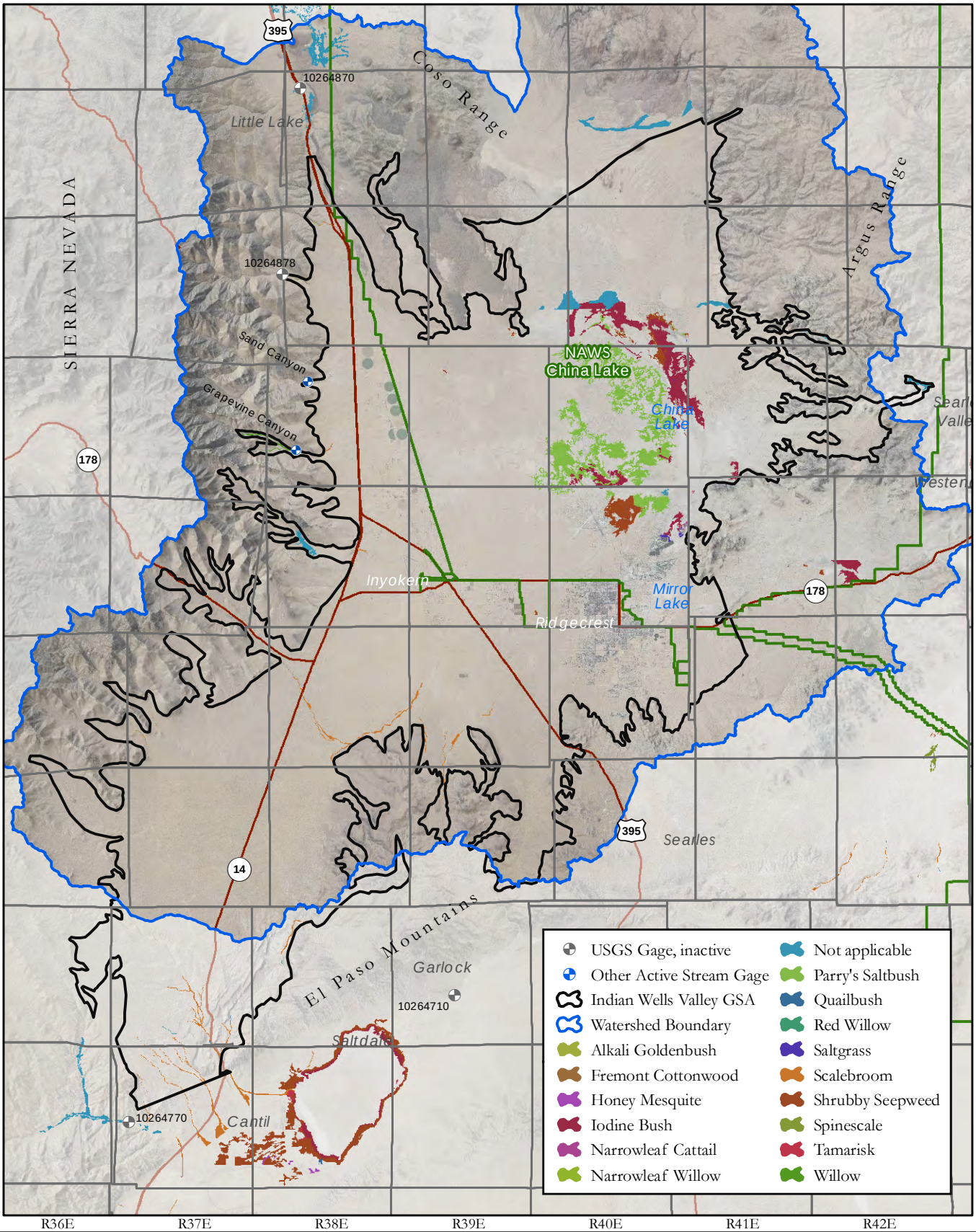
7.3 *GDE-Related Groundwater Monitoring*

A final list of monitoring wells and their construction details will be compiled and presented in an updated monitoring plan once final GDE areas are selected. Wells will be selected based on their capacity to measure shallow groundwater levels and potential differential gradients between the lower and shallow aquifers. The wells will be added to the IWV GWMP established in the GSP and will be monitored on the same semi-annual schedule. Additional wells may be added and/or installed as necessary to address future identified data gaps. Pressure transducer/data loggers may also be used in selected GDE monitoring wells. These will provide relatively continuous water level measurement to illustrate potential short-term variability due to evapotranspiration or other factors. All well monitoring data collection and reporting standards for this project shall be consistent with the Technical Memorandum entitled "Monitoring Protocols and Reporting Standards", dated October 26, 2018 and included in Appendix 4-C of the GSP.

7.4 *Reporting*

GDE vegetation surveys and groundwater elevation data will be made available to the TAC as part of the Annual Reporting required by SGMA. The TAC will review these data and the GDE survey reports for evidence of groundwater level impacts and will report to the WRM as appropriate.

FIGURES



STETSON ENGINEERS INC.

GROUNDWATER DEPENDENT ECOSYSTEMS (GDE)

INDIAN WELLS VALLEY

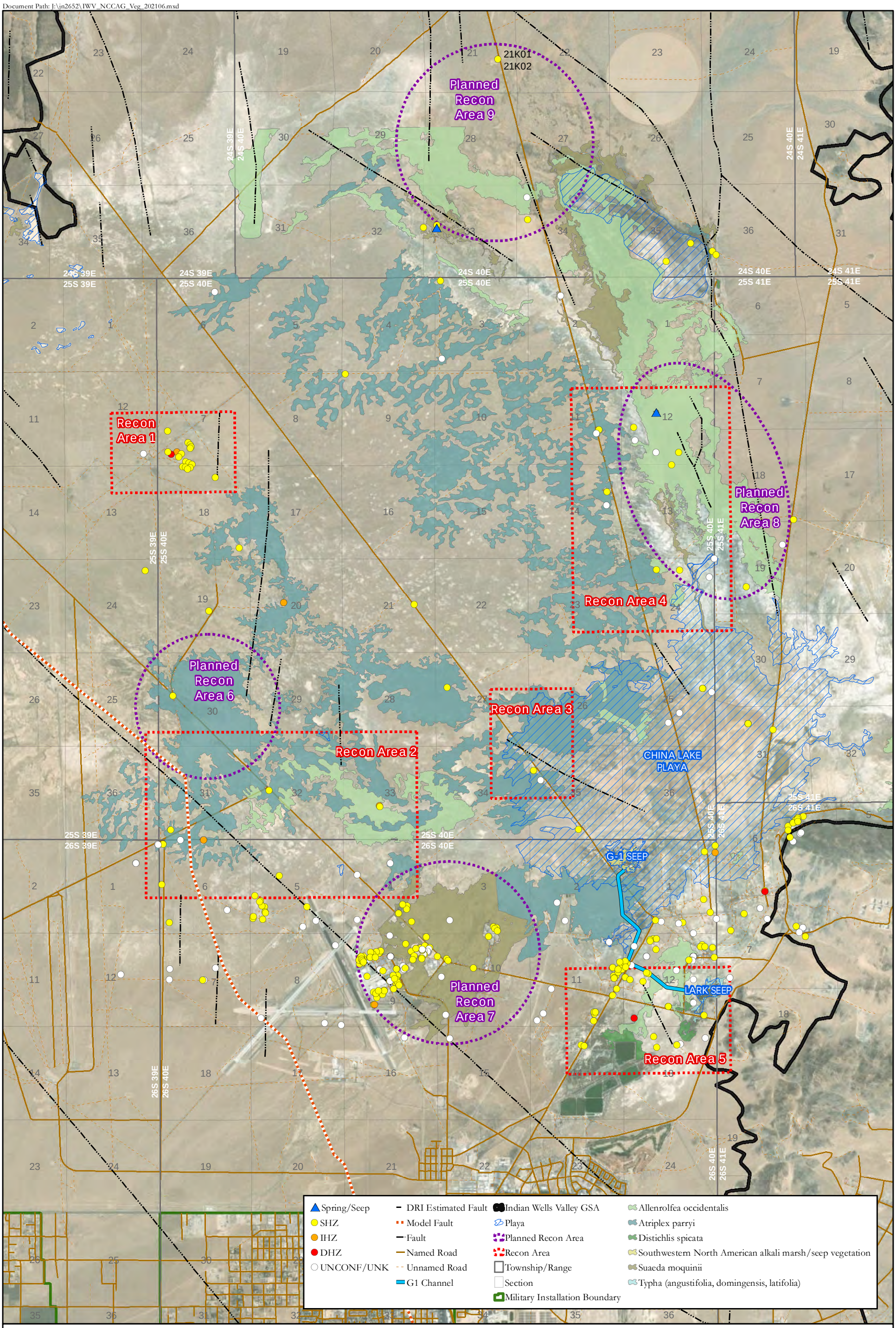
Source: DWR Natural Communities Commonly Associated with Groundwater

N

0 3 6 Miles

Document Path: J:\jn2652\IWV_NCDataset_vegetation.mxd

Document Path: J:\jn2652\IWV_NCCAG_Veg_202106.mxd



STETSON ENGINEERS INC.

RECONNAISSANCE OVERVIEW MAP

0 0.5 1 Miles

N

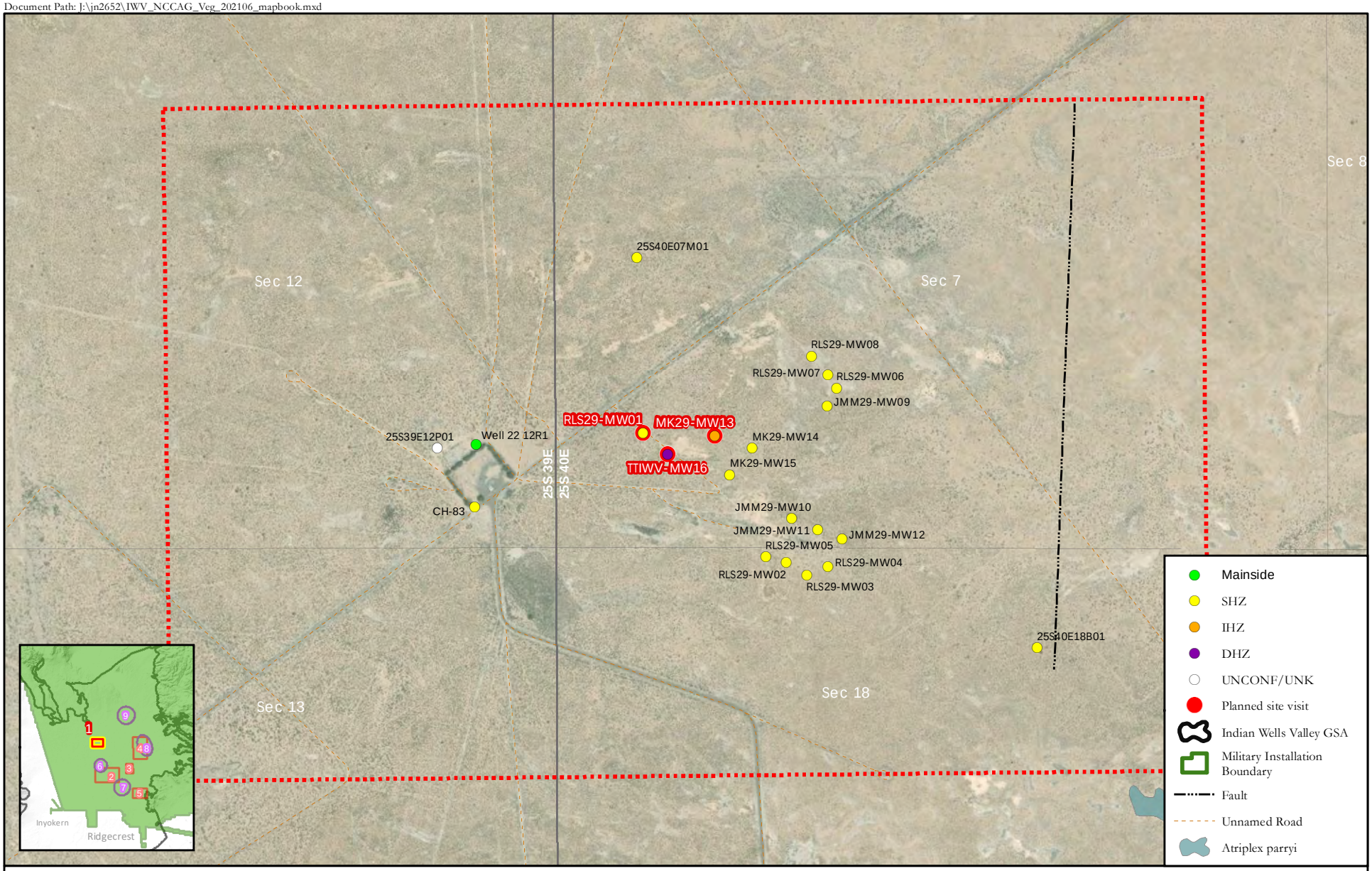
FIGURE 2

Attachment A

FIVE RECON SITES VISITED ON AUGUST 11, 2021:

VEGETATION MAPS, WELL DATA, AND PHOTOS

Document Path: J:\jn2652\IWV_NCCAG_Veg_202106_mapbook.mxd



STETSON ENGINEERS INC.

RECON AREA 1

0 550 1,100 Feet

N

GDE and Well Reconnaissance on NAWS China Lake, Indian Wells Valley Groundwater Basin

GDE and Monitoring Well Data

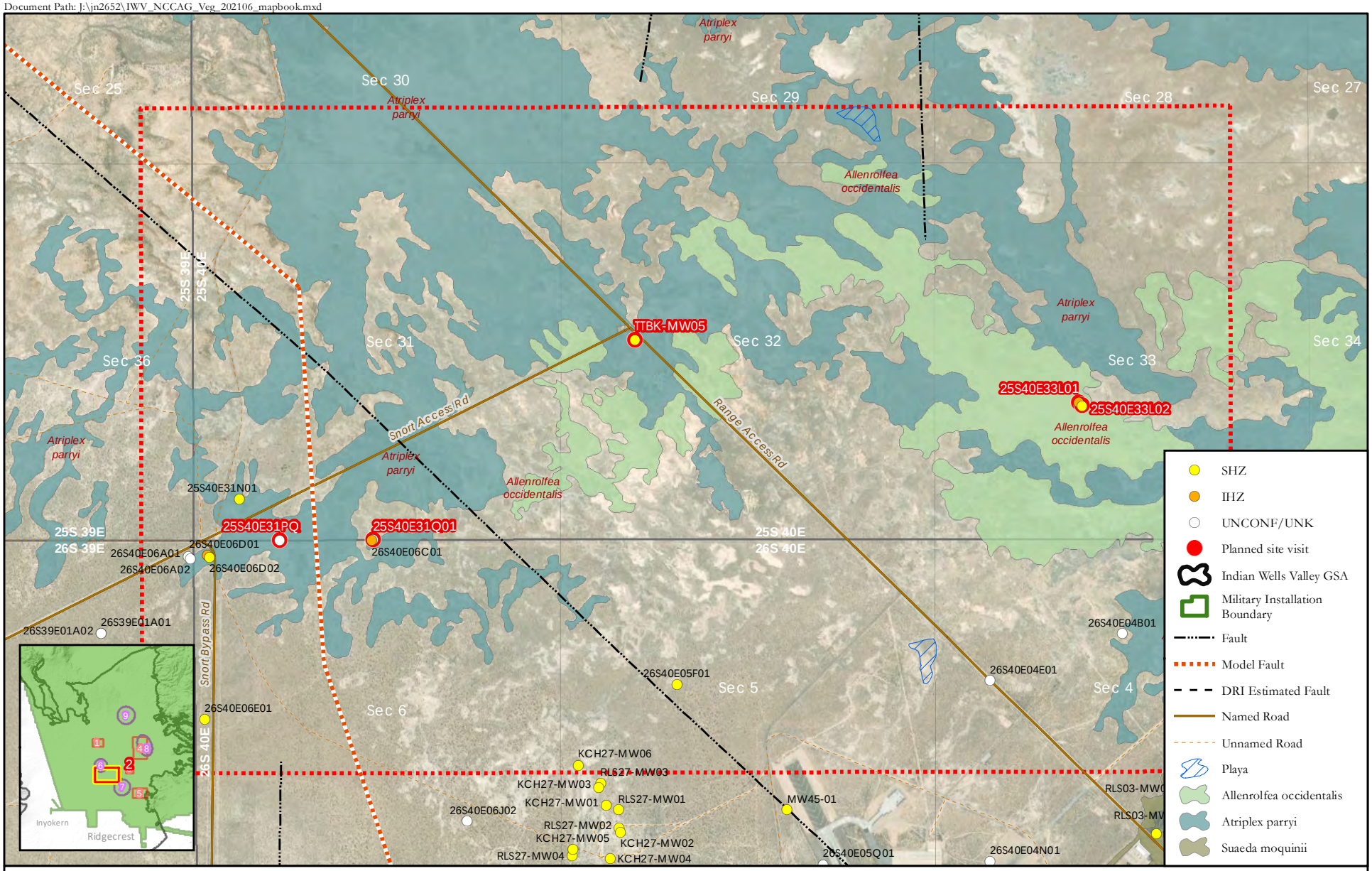
Table 1 - Recon Area 1					
Well Number	RLS29 -MW01	TTIWV -MW16	MK29 -MW13	25S/39E 12R1; Well 22	CH-83
Date Drilled		10/21/2001	8/31/1999	Jan-55	
Casing Material	PVC	Steel	PVC	Steel	PVC
Casing Diameter (inches)	2	4	2	10	4
Screened Interval (feet)	17 - 31.5		280 - 300	65 - 140	
Total Well Depth (feet)	32.7 from MP 32.0'	990	300 from MP - 302	150 (145 measured, soft)	38.9 (soft)
Well Log	Yes	Yes	Yes	Yes	
MP Description		N. side casing	TOC mark inside	N. side casing	N. side casing
DTW (ft below MP)	27.09	32.24	21.19	25.76	26.4
DTW Date, Time	8/11/2021	8/11/2021, 0924	8/11/2021, 0930	8/11/2021, 1000	8/11/2021, 1019
GDE Vegetation Types	Creosote, salt cedar at distance (not GDE indicators)	Annuals, Alkali Golden Bush (not GDE indicators)		Tamarisk (salt cedar) (not a GDE indicator)	
Field Notes	GS elev. Noted as 2200.4	KM - historical info Does not have confining clay like east	9/2/99 DTW 16.10'	Nearby notes: "Drawdown 20' when pumped, 104' pump, Historic DTW 18' "	New IRP site monitoring well.

RECON AREA 1; AUGUST 11, 2021 SITE VISIT





Document Path: J:\jn2652\IWV_NCCAG_Veg_202106_mapbook.mxd



STETSON ENGINEERS INC.

RECON AREA 2

0 1,100 2,200 Feet

N

GDE and Well Reconnaissance on NAWS China Lake, Indian Wells Valley Groundwater Basin

GDE and Monitoring Well Data

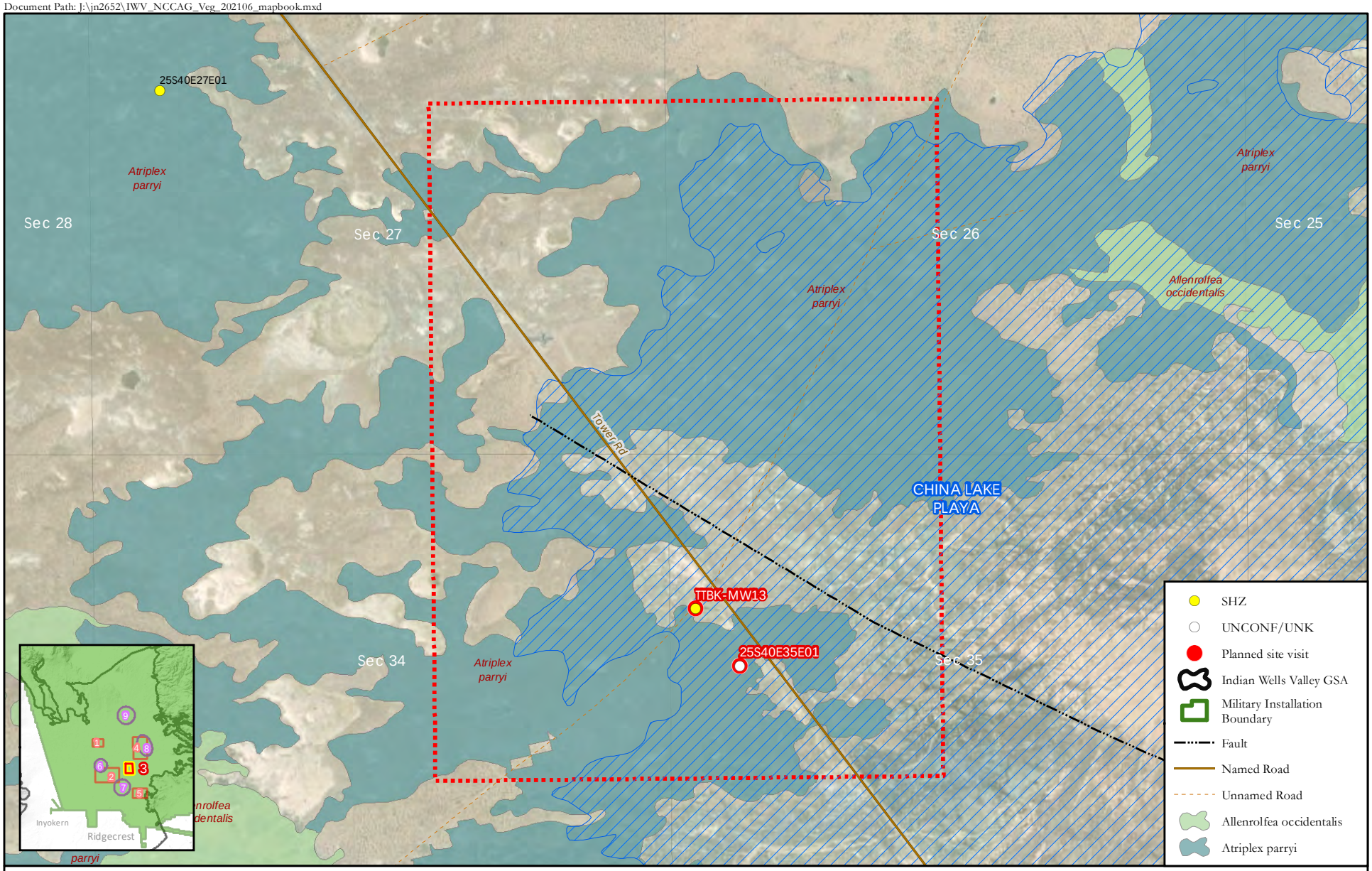
Table 2 - Recon Area 2					
Well Number	26S/40E 31PQ	26S/40E 06C01	25S/40E 33L01	25/40E 33L02	TTBK- MW05
Date Drilled		TTEMI 3/9/99			9/26/1998
Casing Material		PVC			PVC
Casing Diameter (inches)	6	6			2
Screened Interval (feet)	500-600	500 - 600	110-130, 70-90		9.1 - 14.1
Total Well Depth (feet)	640	640	Not Reported	Not Reported	14.5 (per log) 17.3 (meas from TOC)
Well Log		check with Tetra Tech	Yes (soil boring log)	Yes (soil boring log)	Yes
MP Description		N. mark			N. side of casing
DTW (ft below MP)		21.43			12.55
DTW Date, Time		8/11/2021, 1057			8/11/2021, 1037
GDE Vegetation Types					Salt cedars (Not a GDE indicator)
Field Notes	Well not found GS - 2195 Deep zone	Loc. LSD 2195	Well not found	Well not found	GS 2180.302

RECON AREA 2; AUGUST 11, 2021 SITE VISIT





Document Path: J:\jn2652\IWV_NCCAG_Veg_202106_mapbook.mxd



STETSON ENGINEERS INC.

RECON AREA 3

0 740 1,480 Feet

N

GDE and Well Reconnaissance on NAWS China Lake, Indian Wells Valley Groundwater Basin

GDE and Monitoring Well Data

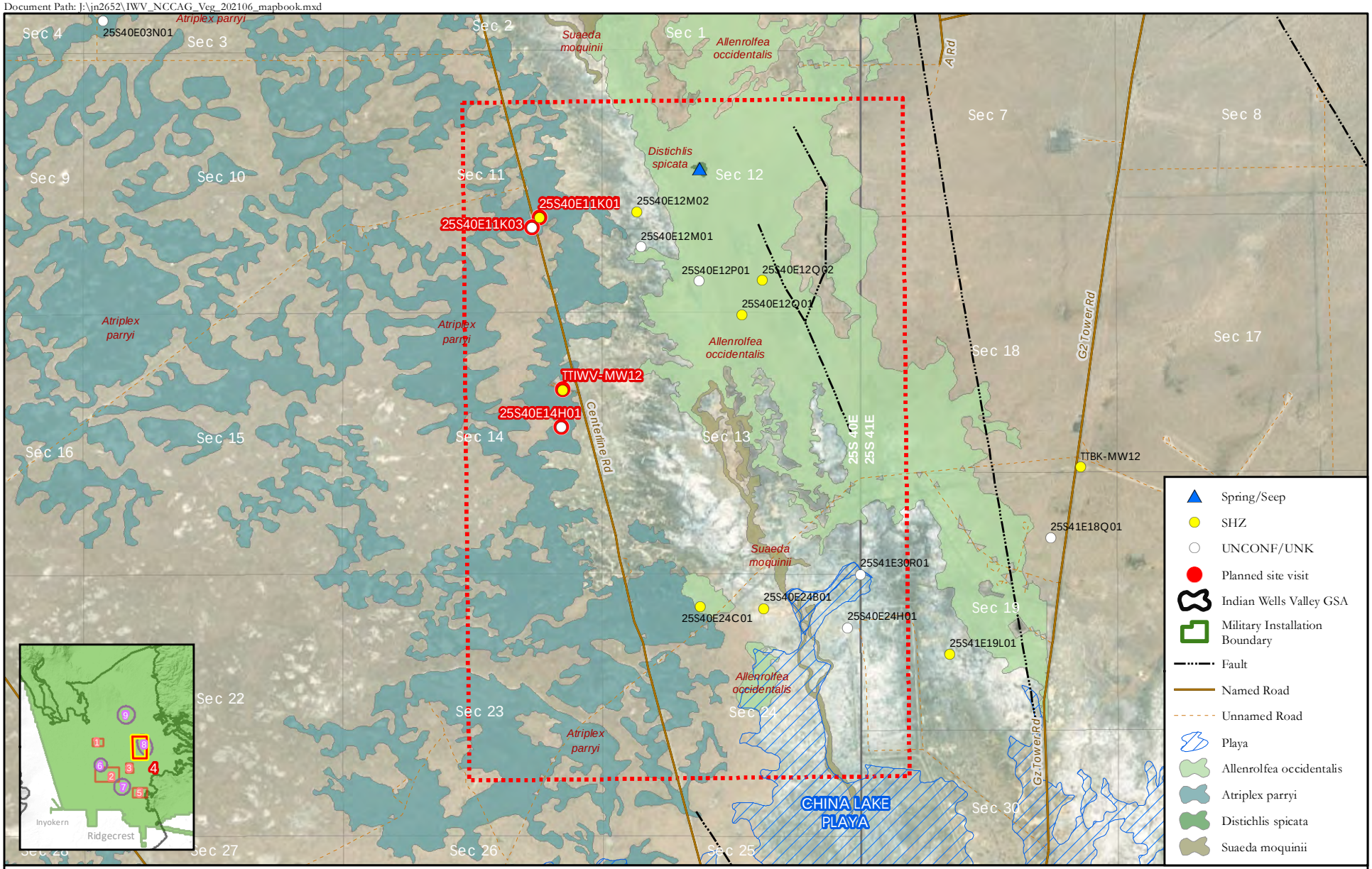
Table 3 - Recon Area 3				
Well Number	TTBK- MW13	25S/40E 35E01		
Date Drilled	9/23/1998	7/3-7/13/1982		
Casing Material	PVC			
Casing Diameter (inches)	2	2.5		
Screened Interval (feet)	11.5 - 14.65	29-59		
Total Well Depth (feet)	18' from MP	TBD		
Well Log	Yes			
MP Description	PVC			
DTW (ft below MP)	6.31	Flowing		
DTW Date, Time	8/11/2021	8/11/2021		
GDE Vegetation Types	Carpet of salt grass 3 Killdear invertebrates Bobcat tracks, Coyote scat			
Field Notes	GS 2154.50 Well has dedicated sample tubing. Nearby bubbling seep surrounded by grass, 18' from well. (seep may be an old well or failed boring?) Recommend to use magnetometer to check for steel well casing at seep.	Flowing well, 2.5" pipe with closed gate valve (not functional) Surface elev: 2154.1 ft (Per KM: Log indicates artesian conditions encountered at 29 ft.) Recommend to make gate valve functional so well can be accessed.		

RECON AREA 3; AUGUST 11, 2021 SITE VISIT





Document Path: J:\jn2652\IWV_NCCAG_Veg_202106_mapbook.mxd



STETSON ENGINEERS INC.

RECON AREA 4

0 1,600 3,200 Feet

N

GDE and Well Reconnaissance on NAWS China Lake, Indian Wells Valley Groundwater Basin

GDE and Monitoring Well Data

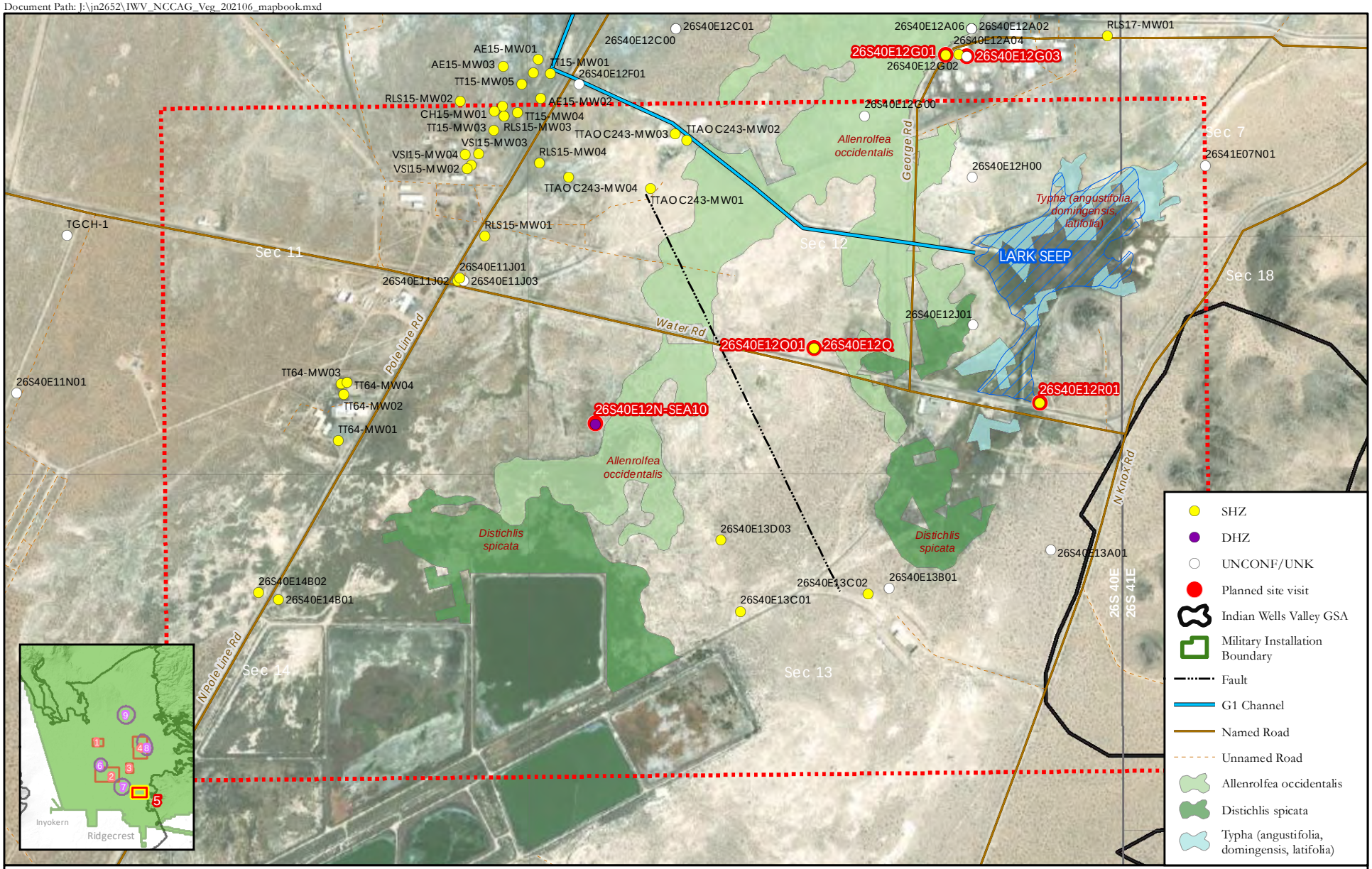
Table 4 - Recon Area 4					
Well Number	24S/40E 21K01	24S/40E 21K02	25S/40E 14H01	TTIWV- MW12	
Date Drilled				9/7/2001	
Casing Material	PVC	Steel		PVC	
Casing Diameter (inches)	4	4		4	
Screened Interval (feet)				21-Nov	
Total Well Depth (feet)	76.4 (soft bottom)	310 (soft bottom)		23 (from log) 26.3 (measured)	
Well Log				Yes	
MP Description	TOC mark north side	TOC mark north side		PVC mark north side	
DTW (ft below MP)	53.31	52.40		8.05	
DTW Date, Time	8/11/2021, 0847	8/11/2021, 0852		8/11/2021, 0808	
GDE Vegetation Types	Parry's Saltbush, Iodine Bush (recognized GDE indicators) Creosote, salt bush (not GDE indicators)			Salt grass (not a GDE indicator)	
Field Notes	13" stand pipe	13" stand pipe			

RECON AREA 4; AUGUST 11, 2021 SITE VISIT





Document Path: J:\jn2652\IWV_NCCAG_Veg_202106_mapbook.mxd



STETSON ENGINEERS INC.

RECON AREA 5

0 725 1,450 Feet

N

GDE and Well Reconnaissance on NAWS China Lake, Indian Wells Valley Groundwater Basin

GDE and Monitoring Well Data

Table 5 - Recon Area 5					
Well Number	26S/40E-12N-SEA10 (Notes: 26S40E14A01)	26S/40E 12Q01	26/40E 12R01		
Date Drilled					
Casing Material	PVC	PVC	Steel		
Casing Diameter (inches)	6	2	2		
Screened Interval (feet)	486.9 - 544.4				
Total Well Depth (feet)	555.2	48.7 (soft bottom)	21.8		
Well Log		Boring log for Q02			
MP Description	Mark on PVC	Top of threaded pipe			
DTW (ft below MP)	10.57	10.10	4.76		
DTW Date, Time	8/11/2021, 0645	8/11/2021, 0704	8/11/2021, 0714		
GDE Vegetation Types	Tamarisk (not a GDE indicator)	Salt Bush, Iodine Bush, (recognized GDE indicators) Salt Grass	Iodine Bush (a recognized GDE indicator) Cattail		
Field Notes	Notes on well cap: "Blanks 0-486.9 and 544.4-555.2; TD 555.2; Video 8/3/10 SVMC-NAWS"	JM Note: Q02 Artesian Flow. KM Note: "Surface Water Dependant" Do not use Q01 for GDE monitoring	Square metal stand pipe completion		

RECON AREA 5; AUGUST 11, 2021 SITE VISIT



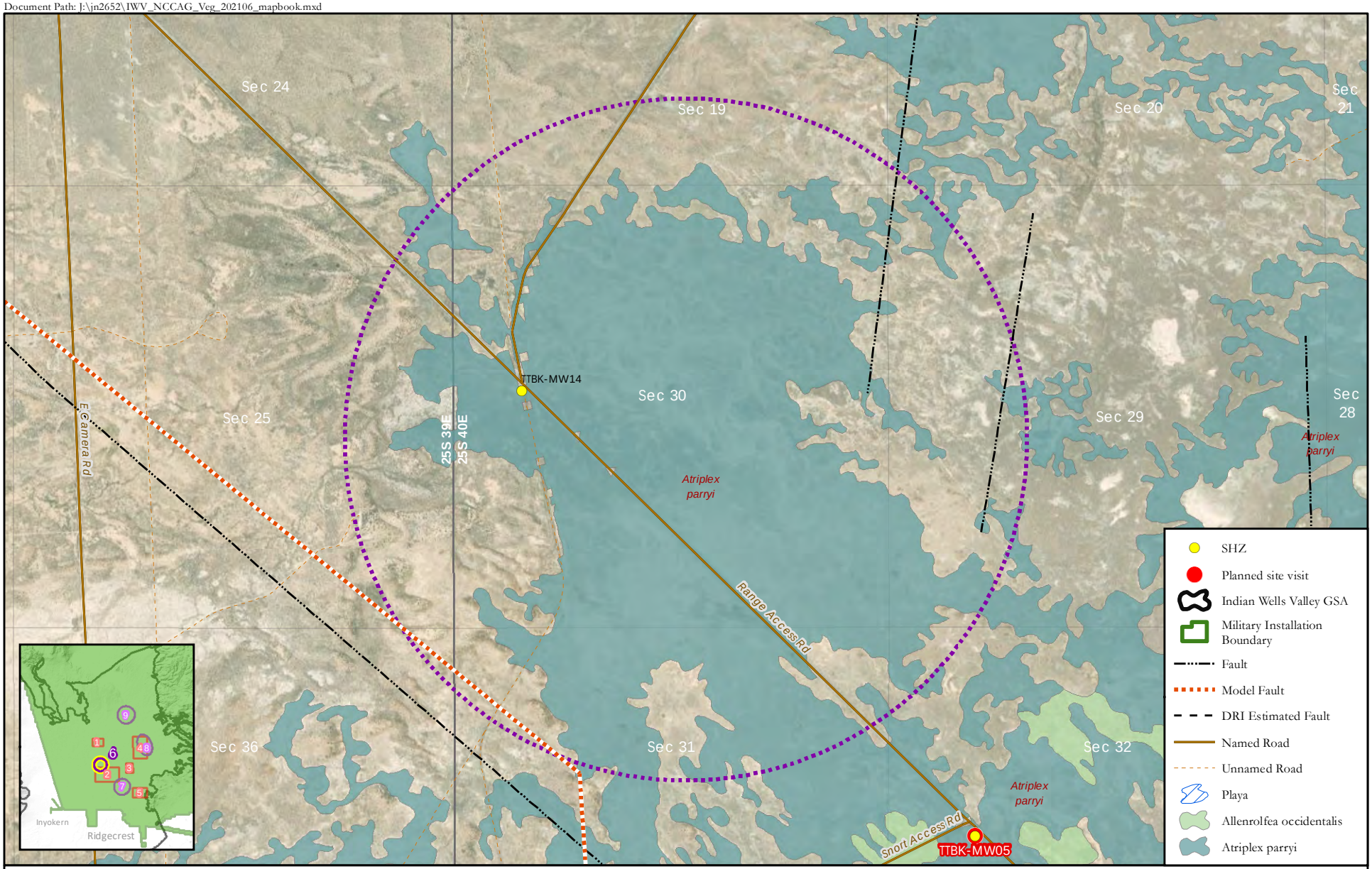


Attachment B

PROPOSED RECON SITES

TO EVALUATE IN 2022

Document Path: J:\jn2652\IWV_NCCAG_Veg_202106_mapbook.mxd



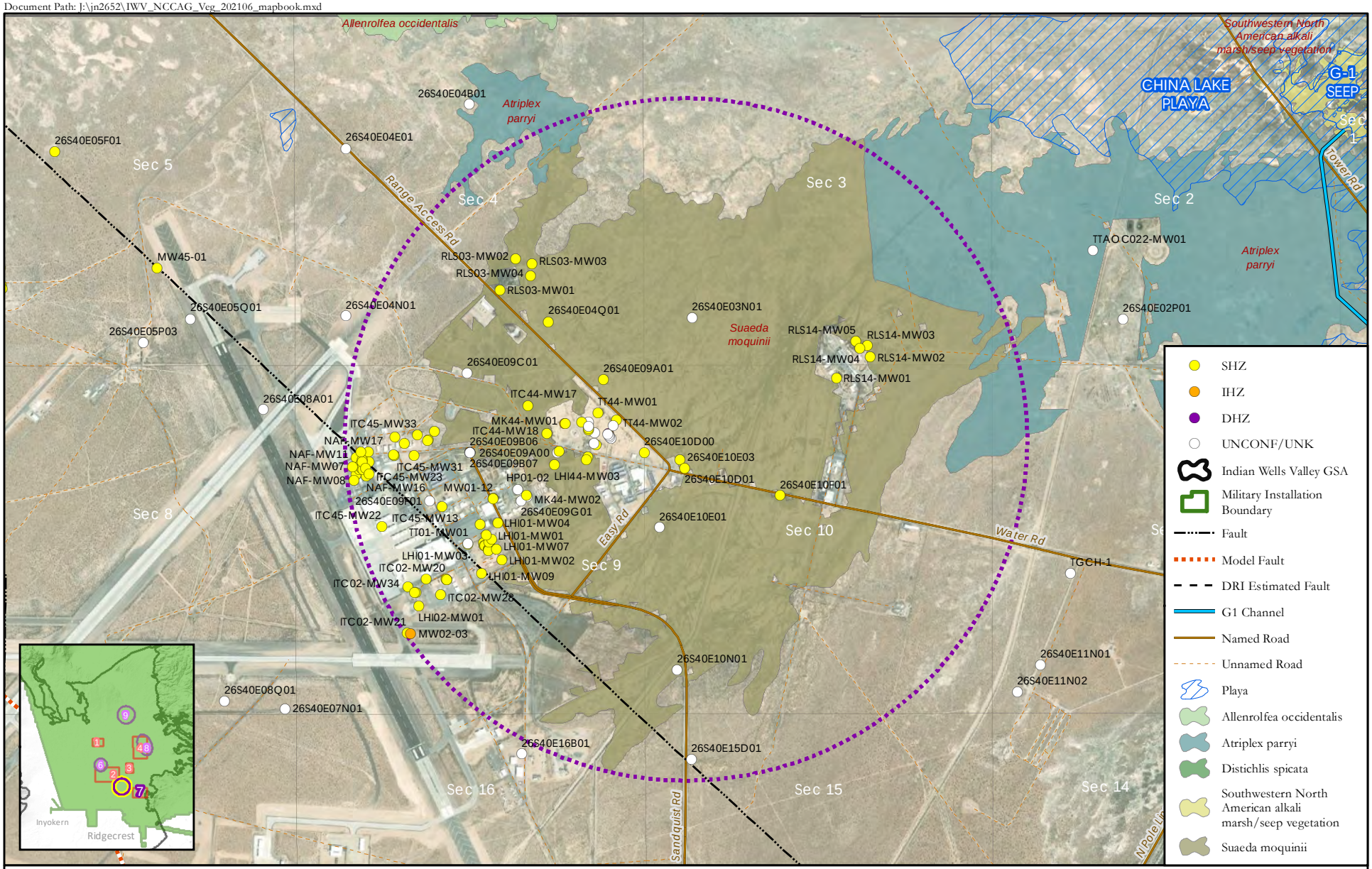
STETSON ENGINEERS INC.

PLANNED RECON AREA 6

0 975 1,950 Feet

N

Document Path: J:\jn2652\IWV_NCCAG_Veg_202106_mapbook.mxd



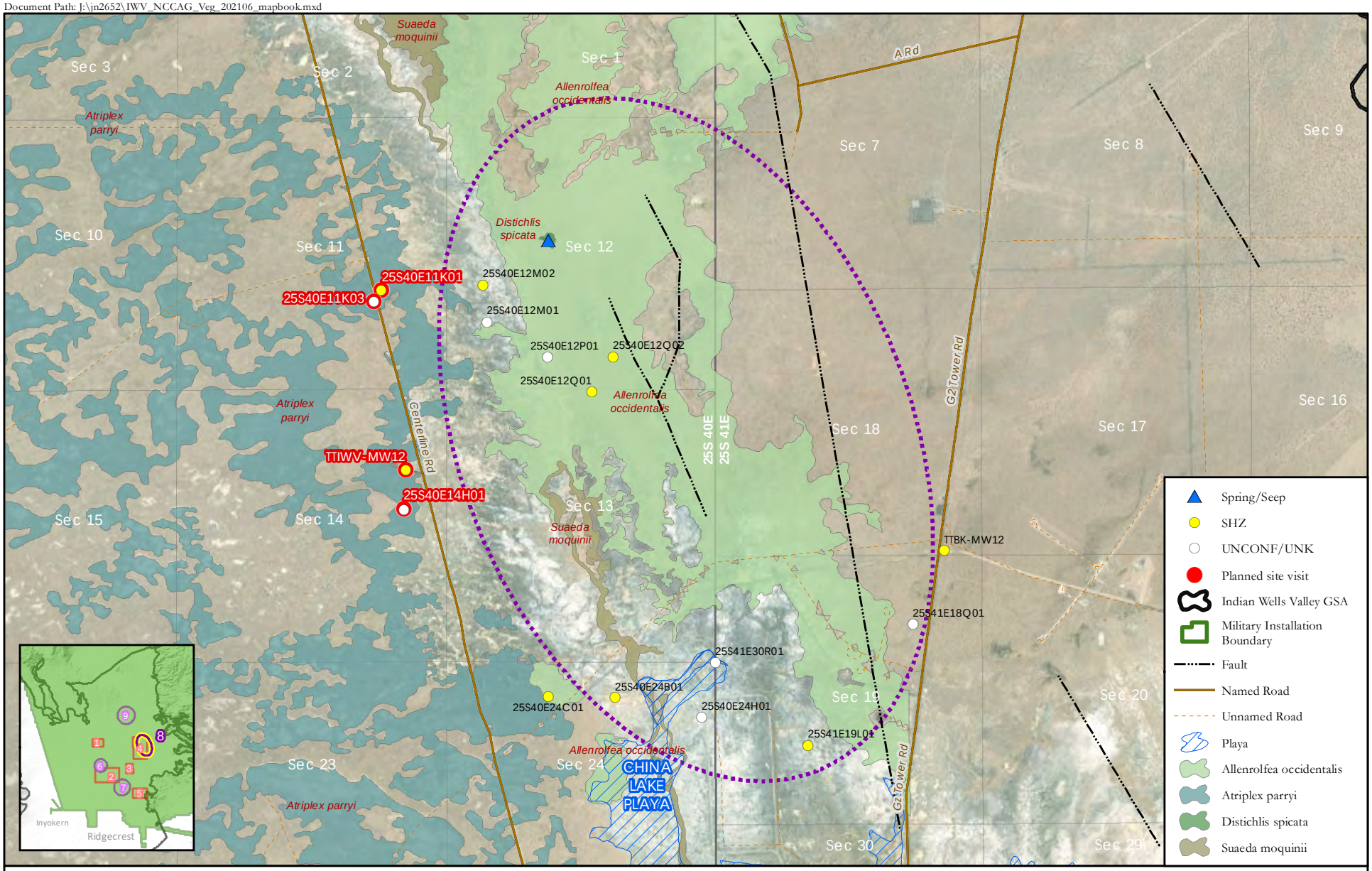
STETSON ENGINEERS INC.

PLANNED RECON AREA 7

0 1,200 2,400 Feet

N

Document Path: J:\jn2652\IWV_NCCAG_Veg_202106_mapbook.mxd



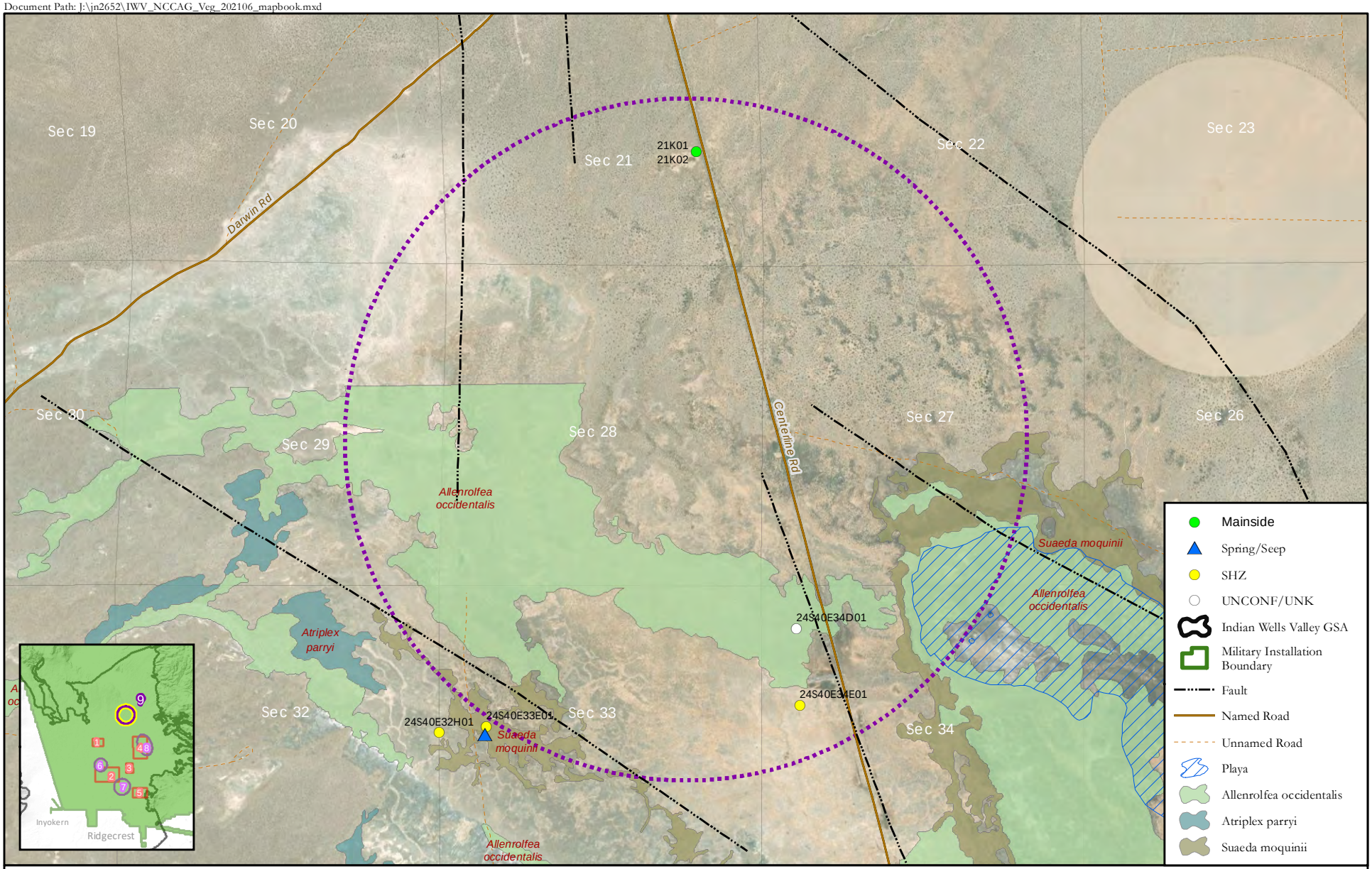
STETSON ENGINEERS INC.

PLANNED RECON AREA 8

0 1,600 3,200 Feet

N

Document Path: J:\jn2652\IWV_NCCAG_Veg_202106_mapbook.mxd



STETSON ENGINEERS INC.

PLANNED RECON AREA 9

0 1,300 2,600 Feet

N

ATTACHMENT I

Groundwater Dependent Ecosystem Vegetation Monitoring Report

Naval Air Weapons Stations China Lake

Combined 2022 and 2023 Report



Prepared for:
Indian Wells Valley Groundwater Authority
100 W California Ave., Ridgecrest CA 93555

Prepared By:
Naval Air Weapons Station China Lake
Environmental Management Division
429 E. Bowen Road, Mail Stop 4014
China Lake, California 93555

INTRODUCTION

As part of its coordination with the Indian Wells Valley Groundwater Authority (IWVGA), Naval Air Weapons Station China Lake's (NAWSCL) Environmental Management Division (EMD) performed vegetation surveys of groundwater dependent ecosystems (GDEs) in 2022 and 2023. This report summarizes the information collected. Two years of information is not sufficient to do any trend analysis and will not provide conclusive evidence of the effect of groundwater levels over time. Additionally, both 2022 and 2023 were unusually wet years for this desert region.

GDEs hold vegetation that are termed phreatophytes (Table 1.), which are plant species that can serve as an indicator of shallow groundwater (Glenn et al., 2013). Since phreatophytes depend directly upon groundwater (Robinson, 1958), they become an important component in identifying potential shifts in groundwater levels. Decreasing groundwater levels can put more stress on these species and could restrict or reduce plant growth (Naumburg et al., 2005).

The aim of this study is to identify GDEs on NAWSCL and begin to evaluate how they are affected by shifts in ground water levels and if changes can be measured through vegetation surveys. Long-term monitoring of these GDE communities, in conjunction with the semi-annual monitoring of groundwater wells within the region, may help establish trend data on the relative health of GDE vegetation communities at NAWSCL and how they are responding to changes in groundwater over time (Stetson, 2021). The survey method used for these two years of data is the line-point intercept (LPI) method. This method has been used to determine changes in plant cover and height over time. Data must be collected for multiple years to establish a correlation between plant species health and ground water levels. Initially, three (3) GDE locations were chosen with one LPI transect at each. These GDEs are located around the China Lake playa (Appendix C-1), which is an area that is typically comprised of Saltbush species due to the high alkali soil.

During the Pleistocene era, China Lake basin contained a large body of water. However, due to global climatic factors near the end of the Pleistocene, the surface water dried out and the basin transitioned into a playa (Meyer et al., 2011). In recent history, the groundwater level has been

dropping further, as recharge is diminished through prolonged drought and anthropogenic factors such as groundwater pumping.

Table 1. List of essential phreatophytes near NAWSCL playa.

Scientific Name	Common Name	Flowering Time	Elevation (meters)
Allenrolfea occidentalis	Iodine bush	June—August	< 1,450
Ambrosia dumosa	Burrobush	December—June	-80—1,700
Atriplex confertifolia	Shadscale	April—July	< 2,400
Atriplex parryi	Parry's saltbush	May—August	< 1,500
Distichlis spicata	Saltgrass	April—September	< 1,550
Isocoma acradenia	Alkali goldenbush	August-November	< 1,100
Suaeda nigra	Bush seepweed	May—September	< 1,600

METHODS

Study Area

The monitoring areas are within the North Range of NAWSCL, located in the northern Mojave Desert and is approximately 150 miles northeast of Los Angeles (INRMP, 2014; Appendix C-2). NAWSCL North Range is in portions of Kern, Inyo, and San Bernardino counties. This region has a mean annual average high temperature of 80.1 F with a mean annual average low of 47.5 F and experiences an average of 4.27 inches of precipitation each year (WRCC, n.d.). The monitoring sites themselves are located around the China Lake playa, which is on NAWSCL North Range (Appendix C-1 and C-2). Vegetation in this area is comprised of Allscale Saltbush Scrub community.

NAWSCL EMD, The Nature Conservancy, and Stetson Engineering Inc. conducted initial field visits on 11 August 2021 to multiple locations around the China Lake playa to verify presence of GDEs (Stetson, 2021). Field maps showing potential GDE locations on the China Lake Playa were used. Once on site, NAWSCL biologists confirmed the presence of GDEs at site locations. Sites were visited if they met these three parameters: presence of phreatophytes, ease of access,

and proximity to a viable monitoring well. We visited a total of nine sites, but only three sites were chosen that met the above criteria: Recon Area (RA) 6, 8, and 9 (page 7 in monitoring plan). Appendix C-3 shows the transect locations for each chosen RA.

Determining Phreatophtye Species

We used Klausmeyer et al., "Mapping Indicators of Groundwater Dependent Ecosystems in California: Methods Report" (2018), for a detailed list of phreatophyte species. We then determined which phreatophyte species occur on NAWSCL in the RA by site visits and using Jepson eFlora (2023) or Consortium California Herbaria (2023).

Line-Point Intercept

We conducted the LPI method, an accepted standard survey method, to assess variation and quantity changes in plant species height and ground cover over time (Caratti, 2006). Three sites were chosen with one transect each: 6-1, 8-1, and 9-1. Table 2 provides general location information for each transect. Transect 6-1 (Appendix C-4) was inventoried on 29 June 2022; transects 8-1 (Appendix C-5) and 9-1 (Appendix C-6) were inventoried on 5 July 2022. Each site was resurveyed on 23 October 2023. We chose a 50 meter transect with samples taken every one meter using a narrow diameter sampling pole. The pole had height classes marked at five centimeter intervals to ensure accuracy. There was a total of 18 height classes on the pole, measuring at a total of 90 centimeters tall. Data was collected from the lowest point first and the highest point last. Ground cover included bare ground, organic material, litter, standing dead, or rock fragments. The tallest point of each species that touched the sampling pole was recorded. We did not include additional height classes if the same species touched the sampling pole more than once.

For both 2022 and 2023 we chose to not include additional height classes during our surveys. Additional height classes means that measurements would be taken each time the same species touched the sampling pole more than once. We felt this data was not important to collect because we measured the length and maximum height of each phreatophyte species that was sampled in the transects.

In 2023, surveys were conducted on 23 October to ensure accurate identification of phreatophyte species. We pounded stakes at the start and end points at each transect (Table 2.) and placed orange flagging on the starting point. Stakes were placed to ensure the start and end points were exact each field season.

Table 2. GDE Vegetation Monitoring Transect Locations on NAWSCL

Transect ID	Start Latitude	Start Longitude	Azimuth	End Latitude	End Longitude
6-1	35.721910	-117.705200	156°	35.721497	-117.704973
8-1	35.775895	-117.619950	174°	35.775448	-117.619891
9-1	35.824726	-117.653306	345°	35.825160	-117.653450

RESULTS

2022

Our results for 2022 showed presence of phreatophytes at all three site locations (Table 3) and provided initial measurements of these species. Transect 6-1 and 8-1 both had *A. occidentalis* sampled during the LPI. This was the only phreatophyte species that was sampled at two different site locations. All other phreatophytes identified were only found at one of the three transects. Transect 6-1 sampled *I. acradenia*, while 8-1 had the same species nearby but was only observed in the 4 meter wide belt.

Transect 6-1 had a total of nine phreatophytes sampled, most of which were *S. nigra*. Transect 8-1 had a total of four phreatophyes, half *A. occidentalis* and *A. confertifolia*. Transect 9-1 had a total of seven phreatophyes, with one more *A. confertifolia* than *A. dumosa*. Appendix B-1 through B-3 contains full data sets from each surveyed transect.

Table 3. 2022 Presence of Phreatophytes on GDE Transects

Transect ID	Iodine Bush (*Allenrolfea occidentalis*)	Alkali Goldenbush	Burrobush (*Ambrosia dumosa*)	Shadescale (*Atriplex confertifolia*)	Bush Seepweed	Saltgrass (*Distichlis spicata*)

		(*Isocoma acradenia*)			(*Suaeda nigra*)	
6-1	X	X			X	
8-1	X	B				X
9-1			X	X		

X – Present B – Observed within a 4m wide belt of transect. Not directly surveyed on transect.

2023

Our results for 2023 were slightly different than the results from 2022. This was mainly because we did not physically mark the survey locations in 2022 and relied on GPS in 2023, which was off by several meters. More of this is discussed in the Discussion section of the paper. Transect 6-1 and 8-1 both had *A. confertifolia* sampled during the LPI (Table 4.). *A. confertifolia* was the only species present at each transect or within the 4m wide belt. *I. acradenia* was sampled in Transect 8-1 but observed in the 4m wide belt at Transect 6-1.

Transect 6-1 had a total of six phreatophytes sampled, half of which were *S. nigra*. Transect 8-1 had a total of three phreatophyes, one *A. confertifolia*, one *I. acradenia*, and one *A. occidentalis*. Only three phreatophyes were sampled on Transect 9-1 for 2023. Appendix B-4 through B-6 contains full data sets from each surveyed transect.

Table 4. 2023 Presence of Phreatophytes on GDE Transects

Transect ID	Iodine Bush (*Allenrolfea occidentalis*)	Alkali Goldenbush (*Isocoma acradenia*)	Burrobush (*Ambrosia dumosa*)	Shadescale (*Atriplex confertifolia*)	Bush Seepweed (*Suaeda nigra*)	Saltgrass (*Distichlis spicata*)
6-1		B		X	X	
8-1	X	X		X		X
9-1			X	B		

X – Present B – Observed within a 4m wide belt of transect. Not directly surveyed on transect.

DISCUSSION

Continuing these survey efforts will provide data to the IWVGA and Stetson Engineering Inc. that can be analyzed to establish trends or determine if GDEs are being affected by shifts in groundwater levels. Surveys should be conducted close to the same time each year and at each

RA/transect location. However, we decided to change the survey times from June to October in 2023 because more phreatophyte species were flowing or fruiting, this made it easier for identification. Thus, data collected in 2023 will not easily be compared to data collected in 2022. This is because surveys were not conducted on the same transect line and were surveyed at different times of year. We relied on GPS for the stop and start points of the transects, which was off by several meters. Therefore, we pounded stakes at the start and stop points of each transect to ensure data can be compared in future survey efforts. Flagging was attached to each transect start point. The 2023 data should be used to compare future survey efforts if the same methodologies are used.

Recommendations For Future GDE Evaluation

1) Add more sites to the study:

The three sites that were chosen for this study met each of the parameters as described in the methods section. This does not mean that they had the highest density of phreatophytes. There may be other sites with a better association of these species but lack a monitoring well in the vicinity or an easily accessible route. Without the monitoring well, we cannot make a correlation that lower ground water levels negatively impact phreatophyte species. Sites that had a more challenging or longer approach were also discarded even though they could potentially have a higher density of phreatophytes. However, these sites typically did not have a monitoring well in the area, which provided another reason to discard them.

Five RAs were initially selected, but four additional RAs were added to meet the study parameters. RAs 1 through 4 were discarded because no viable GDEs were observed. RA 5 met all parameters but was discarded since it was too close to the wastewater treatment ponds. Stetson Engineers did not recommend conducting GDE monitoring at this RA “given the artificial and variable nature of surface and groundwater in this area” (Stetson, 2021). RA 7 potentially contained *S. moquinii* but was rejected. No specific reason for the rejection was mentioned in Stetson Engineers Groundwater Dependent Ecosystem Monitoring Plan (2021). Transects 6-1, 8-1, and 9-1 met all parameters for GDE monitoring and phreatophytes were sampled during the LPI. Data will need to be gathered for multiple years to identify a correlation as described in the paragraph above. More transects should be established to acquire more data.

With one to two more transects per RA, more data would be gathered, and our results would provide a more accurate representation to correlate ground water and phreatophytes.

2) Compare data with precipitation changes:
Additional data should be collected to make conclusions about groundwater effects on phreatophyte species. Annual precipitation should be taken into account. Precipitation, depending on the amount, could alter the data that is collected that year. For example, if heavy rains occurred early in the year or over summer, the growth rate of plants could increase. This could be mistaken and assumed that the growth came from changes in groundwater levels. Including precipitation data in future survey efforts will allow one to analyze the effects of precipitation vs. groundwater.

3) Consider alternate survey methods:
Though LPI is a good method to quantify changes in plant species cover and height overtime, it may not be the best method to use for this study. The goal of this project is to determine if phreatophyte species are being impacted by shifts in groundwater levels. LPI is typically used to calculate plant abundance or species composition. Caratti et al. (2006) states the LPI method is best used if one is wanting to note changes in ground cover over time. An alternative method to LPI could be conducting measurements of live extremities of several marked individual phreatophyte species yearly at each chosen RA. Another method would be to measure xylem water potential to determine plant stress. This would probably provide the best results but would require a lab to generate this data, which could be expensive and time consuming. Other study designs such as those described in Orellana et al (2012) could be used but would also require more funding and time.

Literature Cited

Caratti, John F. "Point intercept (PO)." *FIREMON: Fire effects monitoring and inventory system* (2006): 1-17.

Consortium of California Herbaria (CCH). 2023. Biodiversity data provided by the participants of the Consortium of California Herbaria (https://ucjeps.berkeley.edu/consortium/ Accessed on June 16).

Desert Research Center, "China Lake NAF, California" *China Lake NAF, California – Climate Summary*, Western Regional Climate Center, https://wrcc.dri.edu/cgi-bin/cliMAIN.pl?ca1733 (Accessed on 5 May 2023).

Glenn, Edward P., et al. "Phreatophytes under Stress: Transpiration and Stomatal Conductance of Saltcedar (Tamarix Spp.) in a High-Salinity Environment." *Plant and Soil*, vol. 371, no. 1/2, 2013, pp. 655–73. *JSTOR*, http://www.jstor.org/stable/42952747. Accessed 26 July 2023.

Jepson Flora Project (eds.) 2023. Jepson eFlora, https://ucjeps.berkeley.edu/eflora/ [accessed on 16 June 2023]

Klausmeyer K., J. Howard, T. Keeler-Wolf, K. Davis-Fadtke, R. Hull, A. Lyons. 2018. Mapping Indicators of Groundwater Dependent Ecosystems in California: Methods Report. San Francisco, California.

Meyer, Jack, et al. "Constructing a Regional Historical Context for Terminal Pleistocene/Early Holocene Archaeology of the North-central Mojave Desert." *Department of Defense Legacy Resource Management Program (On file, Naval Air Weapons Station China Lake, Ridgecrest, California)* (2011).

Naumburg, Elke, et al. "Phreatophytic vegetation and groundwater fluctuations: a review of current research and application of ecosystem response modeling with an emphasis on Great Basin vegetation." *Environmental Management* 35.6 (2005): 726-740

Orellana, Felipe, et al. "Monitoring and modeling water-vegetation interactions in groundwater-dependent ecosystems." *Reviews of Geophysics* 50.3 (2012).

Robinson, Thomas William. *Phreatophytes*. US Government Printing Office, 1958.

Stetson Engineers. 2021. Groundwater Dependent Ecosystem Monitoring Plan. Carlsbad, California.

US Navy. 2014. Integrated Natural Resources Management Plan Naval Air Weapons Station China Lake. Tierra Data, Inc., Escondido, CA.

APPENDIX A: Acronyms

EMD	Environmental Management Division
GDE	Ground Water Dependent Ecosystems
INRMP	Integrated Natural Resources Management Plan
IWVGA	Indian Wells Valley Ground Water Authority
LPI	Line Point Intercept
NAWSCL	Naval Air Weapons Station China Lake
RA	Recon Area

APPENDIX B: 2022 and 2023 Transect Data (B-1 through B-6)

Appendix B-1. 2022 Transect 6-1 Survey Data

Transect 6-1						
Date: 6/29/2022		**Time:** 0708-0741		**Surveyors:** J. Sherrock, D. Layfield		
Point	**Ground Cover***	**Species**	**Height Class****	**Plant Height (cm)**	**Begin/End (m)*****	**Notes**
1	B	N/A	-	-	-	-
2	B	N/A	-	-	-	-
3	B	N/A	-	-	-	-
4	B	N/A	-	-	-	-
5	B	N/A	-	-	-	-
6	B	*Sueda nigra*	4	45	5.58/6.12	-
7	B	N/A	-	-	-	-
8	B	N/A	-	-	-	-
9	B	*Atriplex confertifolia*	8	45	8.73/9.24	-
10	B	N/A	-	-	-	-
11	B	N/A	-	-	-	-
12	B	N/A	-	-	-	-
13	B	N/A	-	-	-	-
14	B	N/A	-	-	-	-
15	B	N/A	-	-	-	-
16	B	N/A	-	-	-	-
17	B	N/A	-	-	-	-
18	B	N/A	-	-	-	-
19	B	*Schismus* sp.	2	10	N/A	-
20	B	N/A	-	-	-	-
21	B	*Sueda nigra*	5	40	21.13/24.42	-
22	B	N/A	-	-	-	-
23	B	N/A	-	-	-	-
24	B	N/A	-	-	-	-
25	B	N/A	-	-	-	-
26	B	N/A	-	-	-	-
27	B	*Isocoma acradenial*	2	25	26.44/27.16	-
28	B	N/A	-	-	-	-
29	B	*Atriplex confertifolia*	7	35	28.68/29.54	-
30	B	N/A	-	-	-	-
31	B	N/A	-	-	-	-
32	B	N/A	-	-	-	-
33	B	N/A	-	-	-	-
34	B	N/A	-	-	-	-
35	B	N/A	-	-	-	-
36	B	N/A	-	-	-	-

37	B	N/A	-	-	-	-
38	B	N/A	-	-	-	-
39	B	N/A	-	-	-	-
40	B	N/A	-	-	-	-
41	B	*Sueda nigra*	3	30	40.87/41.48	-
42	B	N/A	-	-	-	-
43	B	N/A	-	-	-	-
44	B	N/A	-	-	-	-
45	B	N/A	-	-	-	-
46	B	N/A	-	-	-	-
47	B	*Sueda nigra*	4	35	46.70/47.29	-
48	B	*Sueda nigra*	7	40	-	-
49	B	N/A	-	-	-	-
50	B	*Sueda nigra*	6	30	49.83/50.33	-
BELT (2m on each side): *Bromus tectorum* (cheatgrass), *Distichlis spicata* (saltgrass)						
*B=BARE, L=LITTER, R=ROCK, D=DEAD						
**Height classes are in 5cm increments (1 = 0-5cm, 2 = 5-10cm, etc.)						
***Start and stop points of plant species along the transect.						

Appendix B-2. 2022 Transect 8-1 Survey Data

Transect 8-1						
Date: 7/5/2022		**Time:** 0808-0832		**Surveyors:** J. Sherrock, D. Layfield		
Point	**Ground Cover***	**Species**	**Height Class****	**Plant Height**	**Begin/End (m)*****	**Notes**
1	B	N/A	-	-	-	-
2	B	N/A	-	-	-	-
3	B	N/A	-	-	-	-
4	B	*Allenrolfea occidentalis*	3	25	3.95/4.05	-
5	B	N/A	-	-	-	-
6	B	N/A	-	-	-	-
7	B	*Atriplex confertifolia*	4	30	6.93/7.46	-
8	B	N/A	-	-	-	-
9	B	N/A				-
10	B	N/A	-	-	-	-
11	B	N/A	-	-	-	-
12	B	N/A	-	-	-	-
13	B	*Atriplex confertifolia*	4	30	12.66/13.54	-
14	B	N/A	-	-	-	-
15	B	N/A	-	-	-	-

16	B	*Allenrolfea occidentalis*	3	25	15.71/16.28	-
17	B	N/A	-	-	-	Standing dead *Atriplex* sp.
18	B	N/A	-	-	-	-
19	B	N/A	-	-	-	-
20	B	N/A	-	-	-	-
21	B	N/A	-	-	-	-
22	B	N/A	-	-	-	Dead *Distichlis spicata*
23	B	N/A	-	-	-	Dead *Distichlis spicata*
24	B	N/A	-	-	-	-
25	B	N/A	-	-	-	-
26	B	N/A	-	-	-	-
27	B	N/A	-	-	-	Dead *Atriplex* sp.
28	B	N/A	-	-	-	-
29	B	N/A	-	-	-	-
30	B	N/A	-	-	-	-
31	B	N/A	-	-	-	-
32	B	N/A	-	-	-	-
33	B	N/A	-	-	-	-
34	B	N/A	-	-	-	Dead *Atriplex confertifolia*
35	B	N/A	-	-	-	-
36	B	N/A	-	-	-	-
37	B	N/A	-	-	-	-
38	B	N/A	-	-	-	-
39	B	N/A	-	-	-	-
40	B	N/A	-	-	-	-
41	B	N/A	-	-	-	-
42	B	N/A	-	-	-	-
43	B	N/A	-	-	-	-
44	B	N/A	-	-	-	-
45	B	N/A	-	-	-	-
46	B	N/A	-	-	-	-
47	B	N/A	-	-	-	-
48	B	N/A	-	-	-	-
49	B	N/A	-	-	-	-
50	B	N/A	-	-	-	-
BELT (2m on each side): *Bromus tectorum* (cheatgrass), *Isocoma acradenia* (Alkali goldenbush), *Distichlis spicata* (saltgrass), *Eriogonum inflatum* (Desert trumpet)						

*B=BARE, L=LITTER, R=ROCK, D=DEAD
**Height classes are in 5cm increments (1 = 0-5cm, 2 = 5-10cm, etc.)
***Start and stop points of plant species along the transect.

Appendix B-3. 2022 Transect 9-1 Survey Data

Transect 9-1						
Date: 7/5/2022		**Time:** 0808-0832		**Surveyors:** J. Sherrock, D. Layfield		
Point	**Ground Cover***	**Species**	**Height Class****	**Plant Height**	**Begin/End (m)*****	**Notes**
1	B	*Abrosia dumosa*	4	40	0.69/1.32	-
2	B	N/A	-	-	-	-
3	B	N/A	-	-	-	-
4	L	*Larrea tridentate*	1	135	3.41/4.92	-
5	B	N/A	-	-	-	-
6	B	N/A	-	-	-	-
7	B	N/A	-	-	-	-
8	B	N/A	-	-	-	-
9	B	*Abrosia dumosa*	4	35	8.55/9.03	-
10	B	N/A	-	-	-	-
11	B	N/A	-	-	-	-
12	B	N/A	-	-	-	-
13	B	N/A	-	-	-	-
14	B	N/A	-	-	-	-
15	B	N/A	-	-	-	-
16	B	N/A	-	-	-	-
17	B	N/A	-	-	-	-
18	B	N/A	-	-	-	-
19	B	N/A	-	-	-	-
20	L	N/A	-	-	-	-
21	L	N/A	-	-	-	-
22	B	N/A	-	-	-	-
23	B	N/A	-	-	-	-
24	B	N/A	-	-	-	-
25	B	*Atriplex confertifolia*	3	80	24.86/25.78	-
26	L	*Atriplex confertifolia*	7	70	25.71/26.38	-
27	B	N/A	-	-	-	-
28	B	*Ambrosia dumosa*	5	40	28.20/28.47	-
29	L	*Atriplex confertifolia*	8	60	28.36/29.16	-
30	B	N/A	-	-	-	-
31	B	N/A	-	-	-	-
32	B	N/A	-	-	-	-
33	B	N/A	-	-	-	-
34	B	N/A	-	-	-	-

35	B	N/A	-	-	-	-
36	B	N/A	-	-	-	-
37	L	N/A	-	-	-	Annual grass litter
38	B	N/A	-	-	-	-
39	L	*Atriplex confertifolia*	5	-	-	Standing dead
40	B	N/A	-	-	-	-
41	B	N/A	-	-	-	-
42	B	N/A	-	-	-	-
43	B	N/A	-	-	-	-
44	B	N/A	-	-	-	-
45	B	N/A	-	-	-	-
46	B	N/A	-	-	-	-
47	B	N/A	-	-	-	-
48	B	N/A	-	-	-	-
49	B	N/A	-	-	-	-
50	B	N/A	-	-	-	-
BELT (2m on each side): *Bromus* sp., *Cryptantha* sp.						
*B=BARE, L=LITTER, R=ROCK, D=DEAD						
**Height classes are in 5cm increments (1 = 0-5cm, 2 = 5-10cm, etc.)						
***Start and stop points of plant species along the transect.						

Appendix B-4. 2023 Transect 6-1 Survey Data

Transect 6-1						
Date: 10/23/2023		**Time:** 1325-1400		**Surveyors:** D. Layfield, C. Hopkins		
Point	**Ground Cover***	**Species* or Lower Layer**	**Height Class****	**Plant Height (cm)**	**Begin/End (m)*****	**Notes**
1	B	N/A	-	-	-	-
2	B	N/A	-	-	-	-
3	B	N/A	-	-	-	-
4	B	N/A	-	-	-	-
5	B	N/A	-	-	-	-
6	B	N/A	-	-	-	-
7	B	N/A	-	-	-	-
8	B	N/A	-	-	-	-
9	R	N/A	-	-	-	-
10	B	N/A	-	-	-	-
11	B	N/A	-	-	-	-
12	B	N/A	-	-	-	-
13	B	N/A	-	-	-	-

14	B	N/A	-	-	-	-
15	AD	*Atriplex confertifolia*	3	30	14.57/15.32	-
16	B	N/A	-	-	-	-
17	AD	L	-	-	-	-
18	SD	B	-	-	-	-
19	B	*CLE*	1	10	18.61/19.11	-
20	B	N/A	-	-	-	-
21	B	*Sueda nigra*	5	40	21.13/24.42	-
22	B	N/A	-	-	-	-
23	B	N/A	-	-	-	-
24	B	N/A	-	-	-	-
25	B	N/A	-	-	-	-
26	L	N/A	-	-	-	-
27	B	*Atriplex confertifolia*	52	30	26.75/27.28	-
28	L	S	-	-	-	-
29	B	N/A	-	-	-	-
30	B	N/A	-	-	-	-
31	AD	S	-	-	-	-
32	AD	S	-	-	-	-
33	B	N/A	-	-	-	-
34	R	S	-	-	-	-
35	B	N/A	-	-	-	-
36	B	N/A	-	-	-	-
37	B	N/A	-	-	-	-
38	B	*Sueda nigra*	6	40	37.51/38.18	-
39	B	N/A	-	-	-	-
40	R	S	-	-	-	-
41	B	N/A	-	-	-	-
42	R	S	-	-	-	-
43	R	S	-	-	-	-
44	B	*Sueda nigra*	1	5	43.78/44.07	-
45	B	N/A	-	-	-	-
46	R	S	-	-	-	-
47	B	N/A	-	-	-	-
48	PD	*Sueda nigra*	5	15	47.78/48.11	-
49	B	N/A	-	-	-	-
50	B	N/A	-	-	-	-

BELT (2m on each side): *Suedra nigra*, *Atriplex confertifolia*, *Isocoma acradenial*

*B=BARE, AD=ANNUAL DEAD, PERIENNIAL DEAD, SD= STANDING DEAD, L=LITTER, R=ROCK, D=DEAD

**Height classes are in 5cm increments (1 = 0-5cm, 2 = 5-10cm, etc.)

***Start and stop points of plant species along the transect.

Appendix B-5. 2023 Transect 8-1 Survey Data

Transect 8-1						
Date: 10/23/2023		**Time:** 0830-0845		**Surveyors:** D. Layfield, C. Hopkins		
Point	**Ground Cover***	**Species* or Lower Layer**	**Height Class****	**Plant Height (cm)**	**Begin/End (m)*****	**Notes**
1	B	N/A	-	-	-	-
2	B	N/A	-	-	-	-
3	B	N/A	-	-	-	-
4	AD	B	-	-	-	-
5	B	*Distichlis spicata*	N/A	N/A	N/A	-
6	B	N/A	-	-	-	-
7	N/A	*Lepidium fremontii*	N/A	N/A	N/A	-
8	B	N/A	-	-	-	-
9	B	N/A	-	-	-	-
10	B	N/A	-	-	-	-
11	PD	N/A	-	-	-	-
12	N/A	PSAANN	-	-	-	-
13	B	N/A	-	-	-	-
14	B	N/A	-	-	-	-
15	S	N/A	-	-	-	-
16	B	N/A	-	-	-	-
17	L	N/A	-	-	-	-
18	B	N/A	-	-	-	-
19	B	*Atriplex confertifolia*	3	25	18.79/19.27	-
20	L	N/A	-	-	-	-
21	B	N/A	-	-	-	-
22	B	N/A	-	-	-	-
23	SD	N/A	-	-	-	-
24	L	B	-	-	-	-
25	B	N/A	-	-	-	-
26	B	N/A	-	-	-	-
27	B	N/A	-	-	-	-
28	B	*Isocoma acradenial*	5	12	27.5/28.76	-
29	B	N/A	-	-	-	-
30	B	N/A	-	-	-	-
31	B	N/A	-	-	-	-
32	B	N/A	-	-	-	-
33	B	N/A	-	-	-	-
34	B	N/A	-	-	-	-
35	B	*Allenrolfea occidentalis*	6	11	34.3/35.55	-
36	B	N/A	-	-	-	-

37	B	N/A	-	-	-	-
38	B	N/A	-	-	-	-
39	B	N/A	-	-	-	-
40	L	B	-	-	-	-
41	B	N/A	-	-	-	-
42	B	N/A	-	-	-	-
43	AD	B	-	-	-	-
44	B	N/A	-	-	-	-
45	B	N/A	-	-	-	-
46	B	N/A	-	-	-	-
47	L	B	-	-	-	-
48	B	N/A	-			-
49	B	N/A	-	-	-	-
50	L	N/A	-	-	-	-
BELT (2m on each side): *Atriplex confertifolia*						
*B=BARE, AD=ANNUAL DEAD, PERIENNIAL DEAD, SD= STANDING DEAD, L=LITTER, R=ROCK, D=DEAD						
**Height classes are in 5cm increments (1 = 0-5cm, 2 = 5-10cm, etc.)						
***Start and stop points of plant species along the transect.						

Appendix B-1. 2023 Transect 8-1 Survey Data

Transect 9-1						
Date: 10/23/2023		**Time: 1005-1030**		**Surveyors:** D. Layfield, C. Hopkins		
Point	**Ground Cover***	**Species* or Lower Layer**	**Height Class****	**Plant Height (cm)**	**Begin/End (m)*****	**Notes**
1	B	N/A	-	-	-	-
2	AD	B	-	-	-	*Schismus* sp.
3	PD	N/A	-	-	-	*A. dumosa*
4	AD	B	-	-	-	-
5	B	N/A	-	-	-	-
6	AD	B	-	-	-	*Schismus* sp.
7	AD	B	-	-	-	*Schismus* sp.
8	B	N/A	-	-	-	-
9	B	N/A	-	-	-	-
10	B	N/A	-	-	-	-
11	B	N/A	-	-	-	-
12	B	N/A	-	-	-	-
13	B	N/A	-	-	-	-
14	B	N/A	-	-	-	-
15	B	N/A	-	-	-	-

16	PD	AD/B	-	-	-	*A. dumosa*
17	B	N/A	-	-	-	-
18	L	B	-	-	-	-
19	B	N/A	-	-	-	-
20	B	N/A	-	-	-	-
21	B	N/A	-	-	-	-
22	PD	N/A	2	25	-	21.95/22.72
23	B	N/A	-	-	-	-
24	R	N/A	-	-	-	-
25	B	N/A	-	-	-	-
26	B	N/A	-	-	-	-
27	PD	B	-	-	-	Unknown
28	B	N/A	-	-	-	-
29	AD	B	-	-	-	*Schismus* sp.
30	B	N/A	-	-	-	-
31	B	N/A	-	-	-	-
32	B	N/A	-	-	-	-
33	B	N/A	-	-	-	-
34	B	N/A	-	-	-	-
35	B	N/A	-	-	-	-
36	B	N/A	-	-	-	-
37	B	N/A	-	-	-	-
38	B	N/A	-	-	-	-
39	B	*Larrea tridentata*	21	120	38.03/41.08	-
40	SD	B	-	-	-	*A. polycarpa*
41	AD	B	-	-	-	*Schismus* sp
42	B	N/A	-	-	-	-
43	B	N/A	-	-	-	-
44	B	N/A	-	-	-	-
45	B	N/A	-	-	-	-
46	AD	L/B	-	-	-	-
47	B	*Ambrosia dumosa*	3	20	46.83/47.08	-
48	B	N/A	-			-
49	AD	B	-	-	-	-
50	L	N/A	-	-	-	-

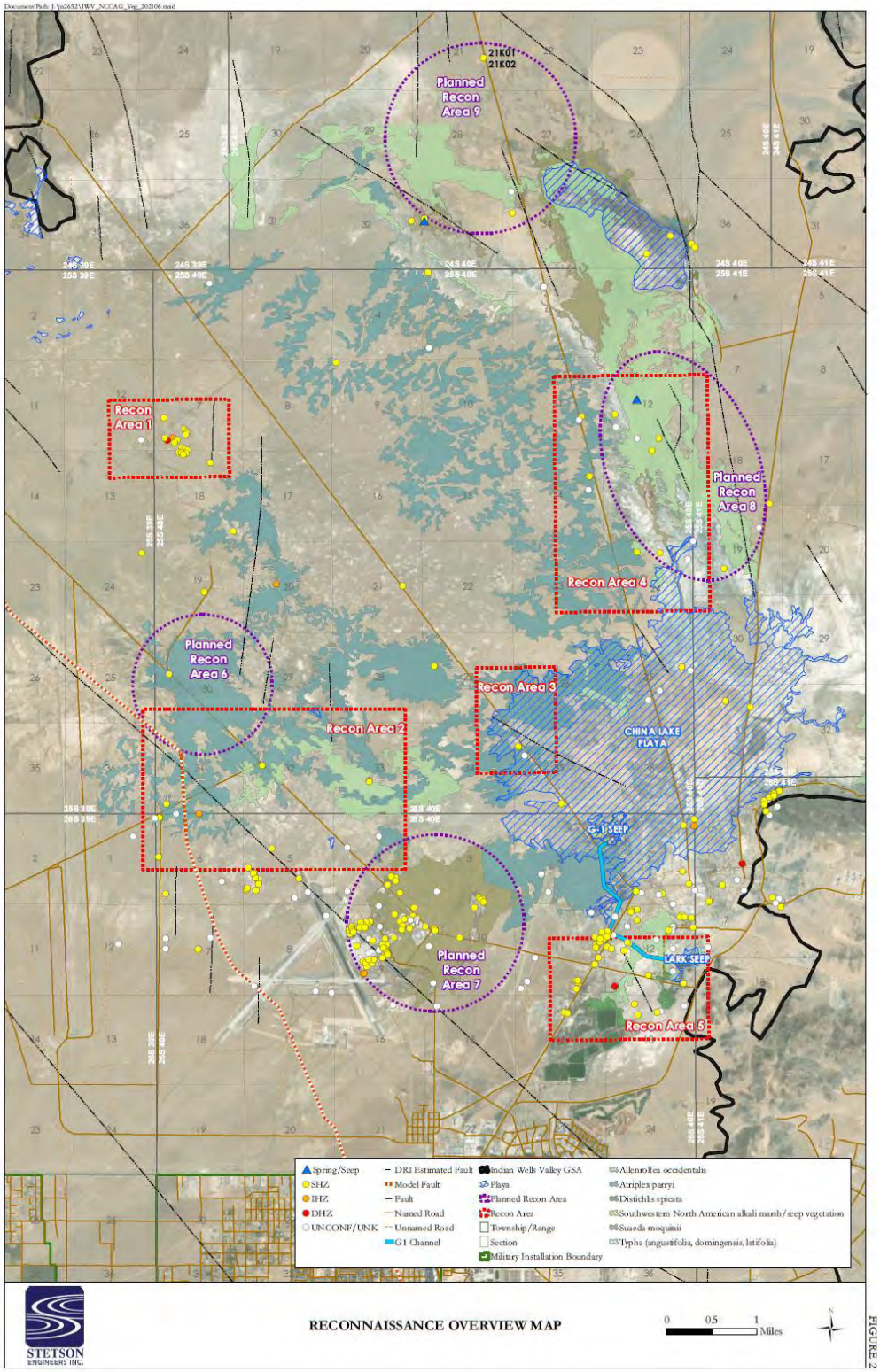
BELT (2m on each side):

*B=BARE, AD=ANNUAL DEAD, PERIENNIAL DEAD, SD= STANDING DEAD, L=LITTER, R=ROCK, D=DEAD

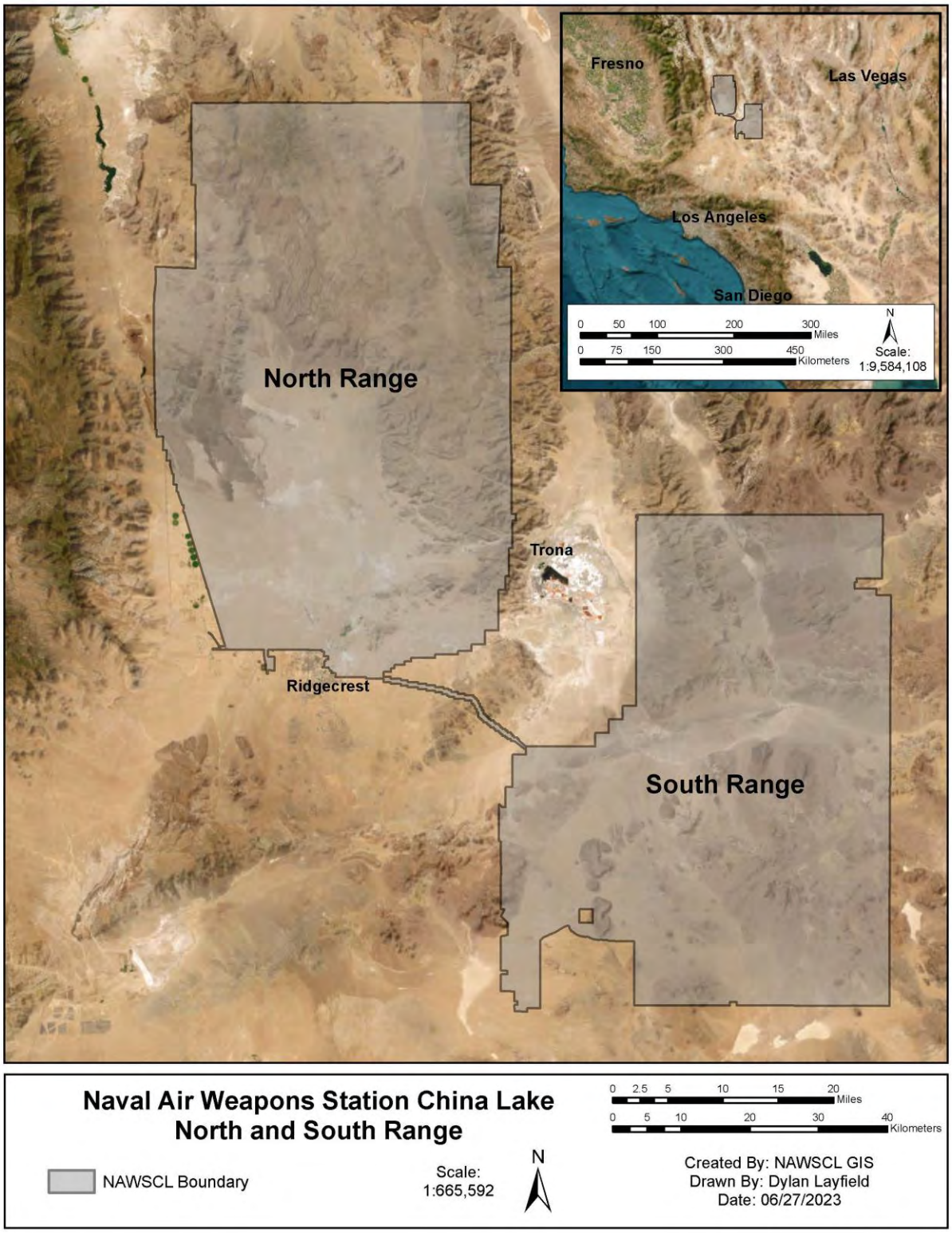
**Height classes are in 5cm increments (1 = 0-5cm, 2 = 5-10cm, etc.)

***Start and stop points of plant species along the transect.

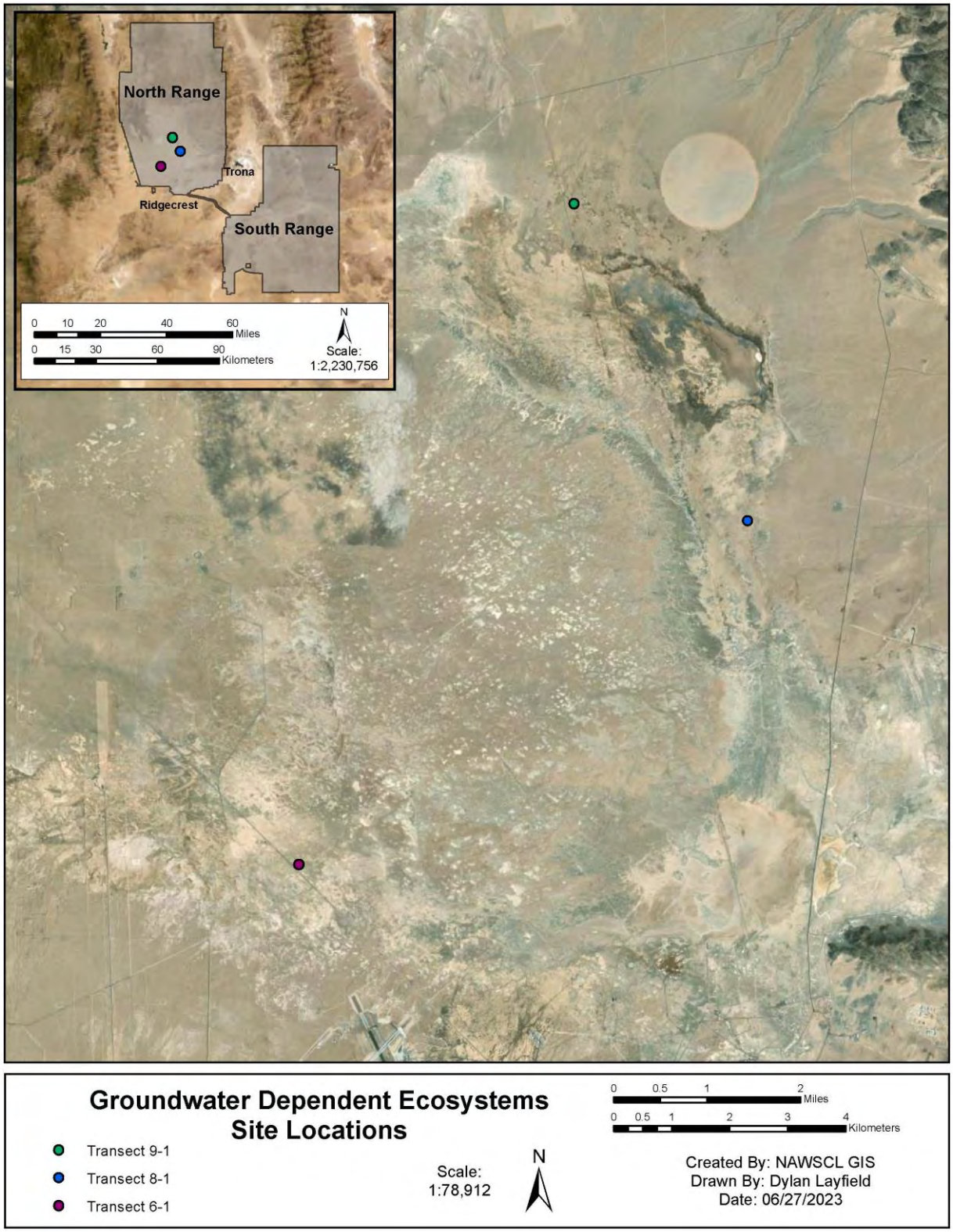
APPENDIX C: Maps



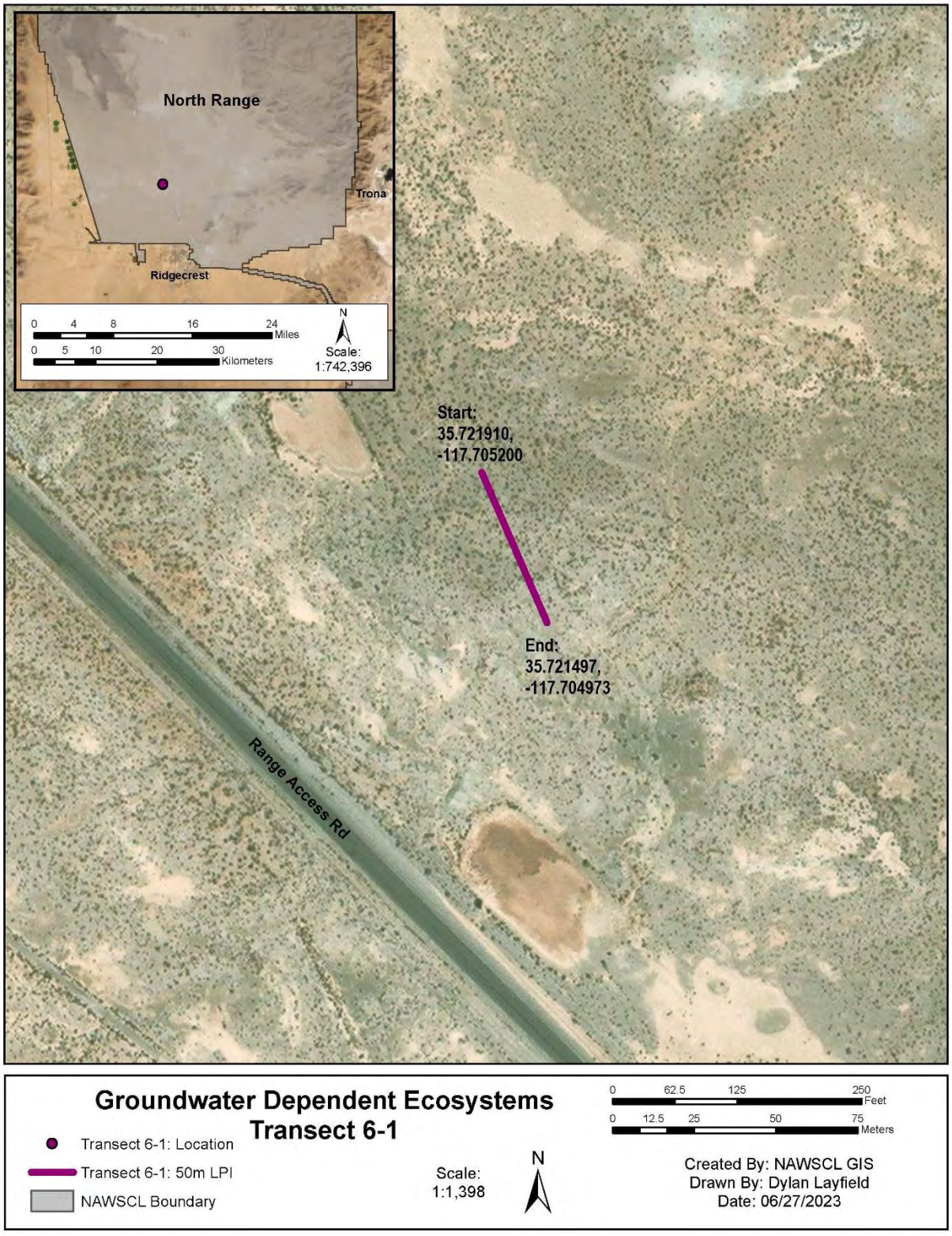
Appendix C-1. Stetson Engineer Map showing Recon areas and China Lake playa.



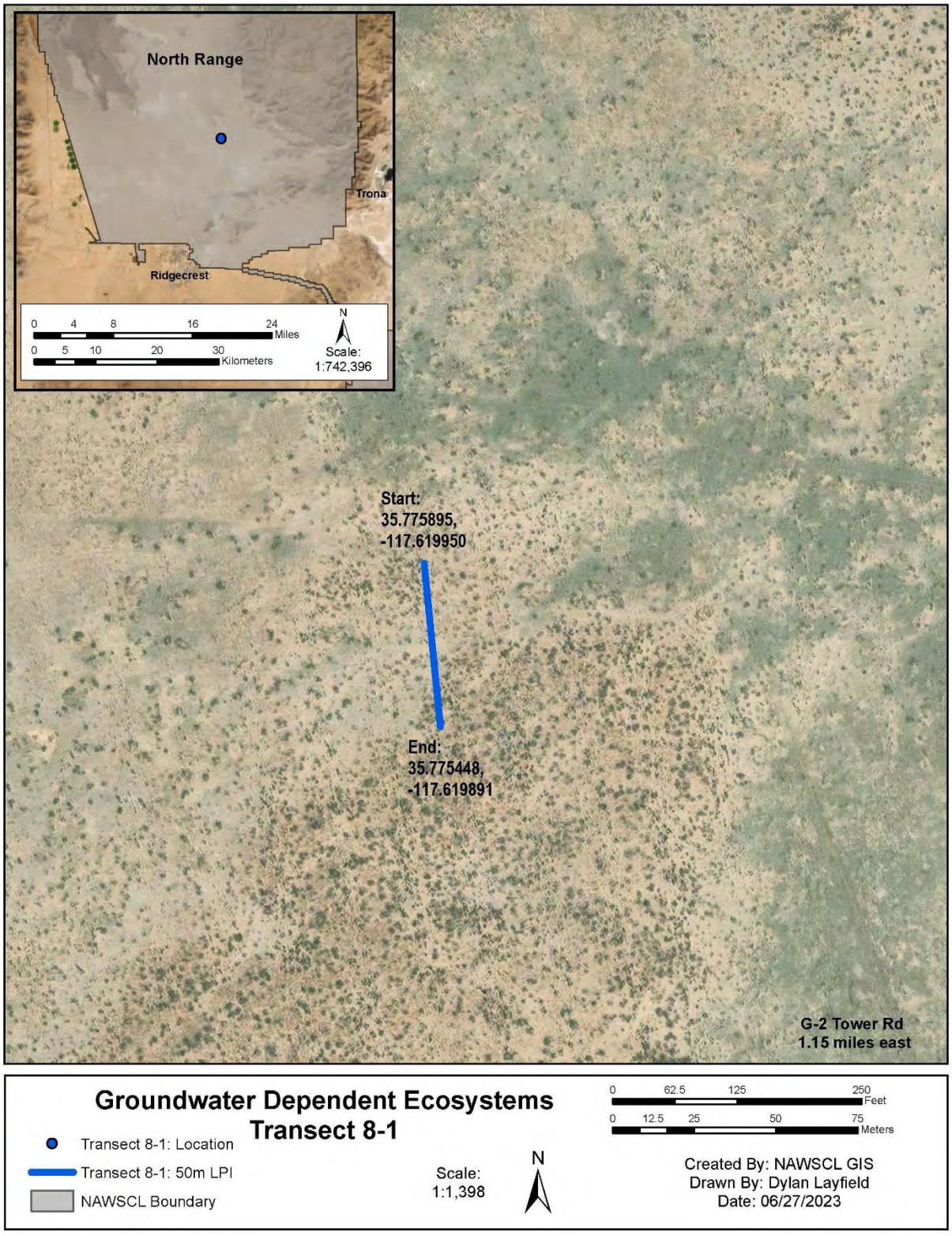
Appendix C-2. NAWSCL Installation Boundary



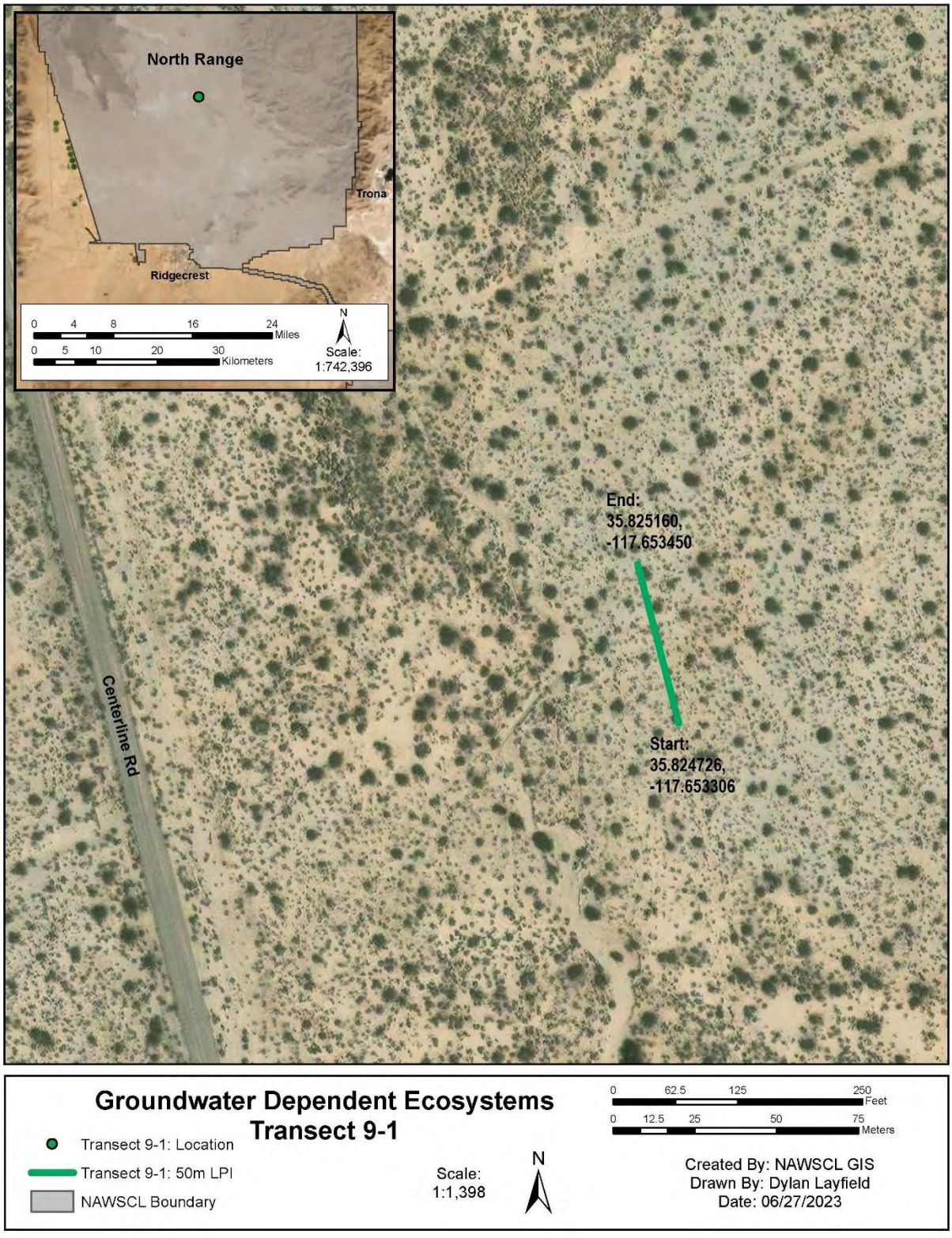
Appendix C-3. Site Locations of GDE on NAWSCL playa



Appendix C-4. Zoomed in location of transect 6-1



Appendix C-5. Zoomed in location of transect 8-1



Appendix C-6. Zoomed in location of transect 9-1

ATTACHMENT J

Indian Wells Valley GSP Model Documentation
DRAFT

Karl Pohlmann, Chris Garner, Jenny Chapman, and Greg Pohll
Desert Research Institute
Nevada System of Higher Education

January 2020

THIS PAGE LEFT INTENTIONALLY BLANK

CONTENTS

List of Figures ii
List of Tables iv
1. Introduction 1
2. Flow Model 1
2.1 Strategy and Assumptions 1
2.2 Code Selection and Documentation 1
2.3 Configuration 2
2.4 Boundary Conditions 4
2.4.1 Perimeter Boundaries 4
2.4.2 Internal Boundaries 4
2.4.3 Recharge 5
2.4.4 Evapotranspiration 7
2.4.5 Groundwater Pumping 12
2.4.6 Basin Outflow 15
2.5 Calibration 16
2.5.1 Steady-State Model 16
2.5.2 Transient-Historical Model 24
2.6 Sensitivity Analysis 36
2.7 Predictive Flow Models 42
3. Transport Model 43
3.1 Introduction 43
3.2 Code Selection and Documentation 43
3.3 Configuration 43
3.4 Initial and Boundary Conditions 44
3.5 Calibration 53
3.6 Transport Results 55
4. Model Limitations 58
References 59
Appendix A: Plots of Simulated and Measured Groundwater Level Hydrographs for Calibration of the Transient-Historical Model A-1

List of Figures

1. Domain of the Indian Wells Valley groundwater flow model showing perimeter boundary conditions. 3
2. East-West cross-section A-A' through model mesh showing the configuration of the six computational layers. 4
3. Locations of the eight fault segments simulated as hydrologic barriers. 5
4. Mountain-block recharge zones surrounding Indian Wells Valley and their associated flux values (shown in blue) on the model boundary. 6
5. Annual variability of recharge forecasted for the predictive simulations. 7
6. Distribution of vegetation and bare ground (denoted as Barren in the legend) within the area of evapotranspiration (ET) (from McGraw et al. [2016]). 8
7. Map of evapotranspiration zones used for the Evapotranspiration Segments (ETS) package in the GSP model. 10
8. The ETS segmented curve that relates the proportion of evapotranspiration extinction depth (PXDP) to the proportion of the maximum evapotranspiration rate (PETM). 11
9. Spatial distribution of two ET zones in the model and their annual ET rates as estimated from EVI values from Landsat imagery using the method of Beamer et al. (2013). 12
10. Annual groundwater withdrawals for all use categories for the period 1920 through 2016. 14
11. Groundwater-pumping wells included in the transient models. 15
12. Locations of groundwater level targets for the steady-state pre-development model (from Garner et al. [2017]). 17
13. Locations of pilot points in (a) Layer 1 and (b) Layers 2 and 3 that were used for calibration of the steady-state flow model. 18
14. Calibrated hydraulic conductivity in (a) Layer 1, (b) Layers 2 and 3, and (c) Layers 3, 4, and 5 of the steady state model. 20
15. Cross sections showing examples of the distribution of calibrated hydraulic conductivity within the layers of the steady state model. 21
16. Residuals between simulated and observed groundwater levels for the calibrated steady-state model. 22
17. Plot of simulated heads to observed heads in the calibrated steady-state model. 23
18. Groundwater flow directions and hydraulic heads simulated on Layer 1 of the pre-development steady-state model. 24
19. Locations of groundwater level targets used for calibration of the transient-historical flow model. 25
20. Example of the hydrograph slope-fitting method used for calibration of the transient-historical flow model. 27
21. Results of calibration metrics Drawdown Slope and MAE of All Heads used for calibration of the transient-historical flow model. 28

22. Spatial distribution of specific yield obtained by kriging in the calibrated transient-historical model. 29
23. Mean residuals between simulated and observed groundwater levels for the calibrated transient-historical model. 30
24. Plot of simulated heads to observed heads in the calibrated transient-historical model. 31
25. Simulated and observed heads at well 27S38E02C01 near the El Paso fault zone. 32
26. Mean residuals between simulated and observed drawdown slopes in the transient-historical model. 33
27. Comparison of water levels simulated by the transient-historical model to observed water levels for the year 2016. 34
28. Evapotranspiration (ET) simulated by the transient-historical model plotted against ET estimated by the empirical relationship established by Beamer et al. (2013) between EVI and ET. 35
29. Locations of wells used for water-level observations in the sensitivity analysis. 38
30. Results of sensitivity analysis for constant recharge rates (a) and specific yield (b). 39
31. Results of sensitivity analysis for specific storage (a) and hydraulic conductivity (b). 40
32. Results of sensitivity analysis for annually variable recharge rate. 41
33. Comparison of the sensitivity coefficients for the five parameters adjusted during the sensitivity analysis. 41
34. Annual rates of groundwater withdrawal and artificial recharge included in the Baseline and Scenario 6.2 models. 42
35. Examples of TDS temporal trends and the selection of the most recent TDS concentration for wells having multiple measurements. 45
36. Locations of wells and the most recent TDS concentrations in the three TDS zones used to develop the TDS initial conditions for the transport model. 46
37. Example of calculation of mean TDS values at wells having multiple measurements in a single TDS zone. 47
38. An example North-South cross section through the transport model illustrating the relationship between of the Shallow, Intermediate, and Deep TDS zones to the six computational layers in the flow model. 48
39. Locations of wells having multiple screens and TDS measurements in the Shallow and Deep TDS zones. 49
40. Spatial distributions of TDS concentration in the three TDS zones that are used for initial conditions in the transport model. 51
41. TDS concentrations assigned to groundwater recharge areas in the transport model. 52
42. Comparison of annual rate of change in TDS (mg/L/yr) forecasted for the years 2020 to 2070 in the Shallow TDS Zone to historical annual rates of change observed in wells 54
43. Comparison of the spatial distributions of simulated TDS concentration in the shallow TDS zone in the year 2020 (left), and the year 2070 for the baseline model (center) and the scenario 6.2 model (right). 56

44. Areas where the forecasted annual rate of change in TDS concentration exceeds 5 mg/L/yr for the years 2020 to 2070 for the baseline model (left) and scenario 6.2 model (right). 57

List of Tables

1. Values of evapotranspiration rate used to develop the segmented ETS curve for the Evapotranspiration Segments (ETS) package. 9
2. Summary of ranges of parameter values and calibrated values estimated during calibration of the steady-state model. 19
3. Groundwater budget simulated by the steady-state model. 23
4. Groundwater budget simulated by the transient-historical model for the year 2016 36
5. Values of constant parameters used in the sensitivity analysis. 37
6. Wells used for comparison of observed to simulated TDS concentration trends. 55

1. Introduction

A three-dimensional groundwater flow and salinity transport model of the groundwater system in Indian Wells Valley Groundwater Basin was developed for this Groundwater Sustainability Plan (GSP). This model was utilized to:

- develop a quantitative framework for synthesizing data and conceptualizing hydrogeologic processes,
- provide a common foundation for developing and testing conceptual models,
- testing of options for groundwater resources management, and
- evaluate compliance with the Sustainable Groundwater Management Act (SGMA).

This appendix documents how the conceptual model of the Indian Wells Valley Groundwater Basin (IWVGB) described in Section 3.3 is represented in the flow and salinity transport models. Also described here are the modeling strategy and assumptions, model simulation codes, model configuration, boundary conditions, calibration processes, and sensitivity analysis.

The IWVGB flow model is based on a groundwater flow model developed by Desert Research Institute (DRI) (McGraw et al., 2016) for the U.S. Navy to support their planning for the China Lake Naval Air Weapons Station (NAWS) in response to declining groundwater levels in Indian Wells Valley and concerns about water quality degradation and subsidence. The 2016 model was subsequently revised by DRI to include regional faults as internal hydrologic barriers and then recalibrated (Garner et al., 2017). The 2017 model was further revised and enhanced by DRI for the Indian Wells Valley GSP. This documentation provides an overview of the model construction and application, but ultimately focuses on the components and approaches incorporated for this GSP that differ from the previous versions.

2. Flow Model

2.1 Strategy and Assumptions

The primary assumptions of the model include the following:

- The groundwater system is in a transient state based on observed water level changes and the conceptualization of the groundwater budget.
- Groundwater flow can be described by the continuum approach, although several discrete hydrologic features are included to represent faults.
- Hydrogeologic units are internally heterogeneous, with variations established by calibration to local hydraulic data and conceptualizations of lithologic and structural features.
- The shallow zone of the groundwater system is unconfined below most of the basin, though discontinuous clay layers confine lower zones in some locations.

Additional model assumptions are described in subsequent sections of this documentation.

2.2 Code Selection and Documentation

The flow model utilizes the public-domain and widely-accepted MODFLOW-NWT finite-difference groundwater modeling code developed by the U.S. Geological Survey (version 1.1.3) (Niswonger et al., 2011) and its supporting modular flow packages. MODFLOW-NWT is a formulation of the MODFLOW-2005 code (Harbaugh, 2005) that provides improved solutions for complex, unconfined groundwater

flow systems. The model was constructed using the Groundwater Modeling System (GMS) environment (version 10.2) developed by Aquaveo, LLC. GMS serves as a database for all of the hydrogeologic information in the model and provides an easy to use graphical pre- and post-processor interface to MODFLOW. Although developed within GMS, the MODFLOW input and output files are in standard MODFLOW format and the model can be run without the use of GMS.

2.3 Configuration

The active domain of the IWVGB groundwater flow model encompasses 460 square miles on the valley floor of Indian Wells Valley (Figure 1). The model is aligned with and georeferenced to the Universal Transverse Mercator (UTM) coordinate system Zone 11 North, North American Datum (NAD) 1983, and is discretized on a uniform mesh of 231 rows and 207 columns. Cell dimensions are 820.2 feet (250 m) in both the easting and northing directions, corresponding to a cell area of 15.4 acres. Land surface elevations from a digital elevation model (DEM) having a resolution of 10 m were resampled to the model mesh to represent the top surface of the numerical model. The length unit is meters, but the output is converted to U.S. customary units for reporting purposes.

Six computational layers (Figure 2) vary in thickness from 100 to 500 ft to allow representation of the observed vertical and horizontal heterogeneity in hydraulic properties of unconsolidated alluvium, lacustrine, and playa deposits within the basin. Values of these properties were estimated during model calibration (Section 2.5). The model reaches its maximum thickness of 2,544 feet in the El Paso sub-basin.

The primary flux simulated on the perimeter boundary is mountain-block recharge and underflow of recharge in Rose Valley in the far northwestern corner of the model (McGraw et al., 2016) (described in Section 2.4.3). In terms of outflow, the IWVGB is considered to be a nearly hydrologically closed basin; the only interbasin groundwater discharge is thought to be a small quantity of flow toward Salt Wells Valley to the southeast (McGraw et al., 2016) (described in Section 2.4.1).

Three distinct intervals within the time period 1920 to 2070 are simulated in the GSP models to maximize the utility of available hydraulic data in the IWVGB and effectively predict changes in the groundwater system through time. A steady-state stress period, based on models constructed by DRI for the U.S. Navy (McGraw et al., 2016; Garner et al., 2017), represents hydrologic conditions prior to large-scale groundwater pumping that began in 1921 (McGraw et al., 2016) and was used for calibration. Groundwater conditions during the 96-year interval from 1921 through 2016 are simulated by the GSP transient-historical model that uses stress periods of one-year length and the results from the steady-state stress period as initial conditions. The GSP transient-predictive model predicts changes in groundwater levels and storage for the 54-year interval from 2017 through 2070 using stress periods of one-month length and the results of the 96-year transient-historical simulation as initial conditions.

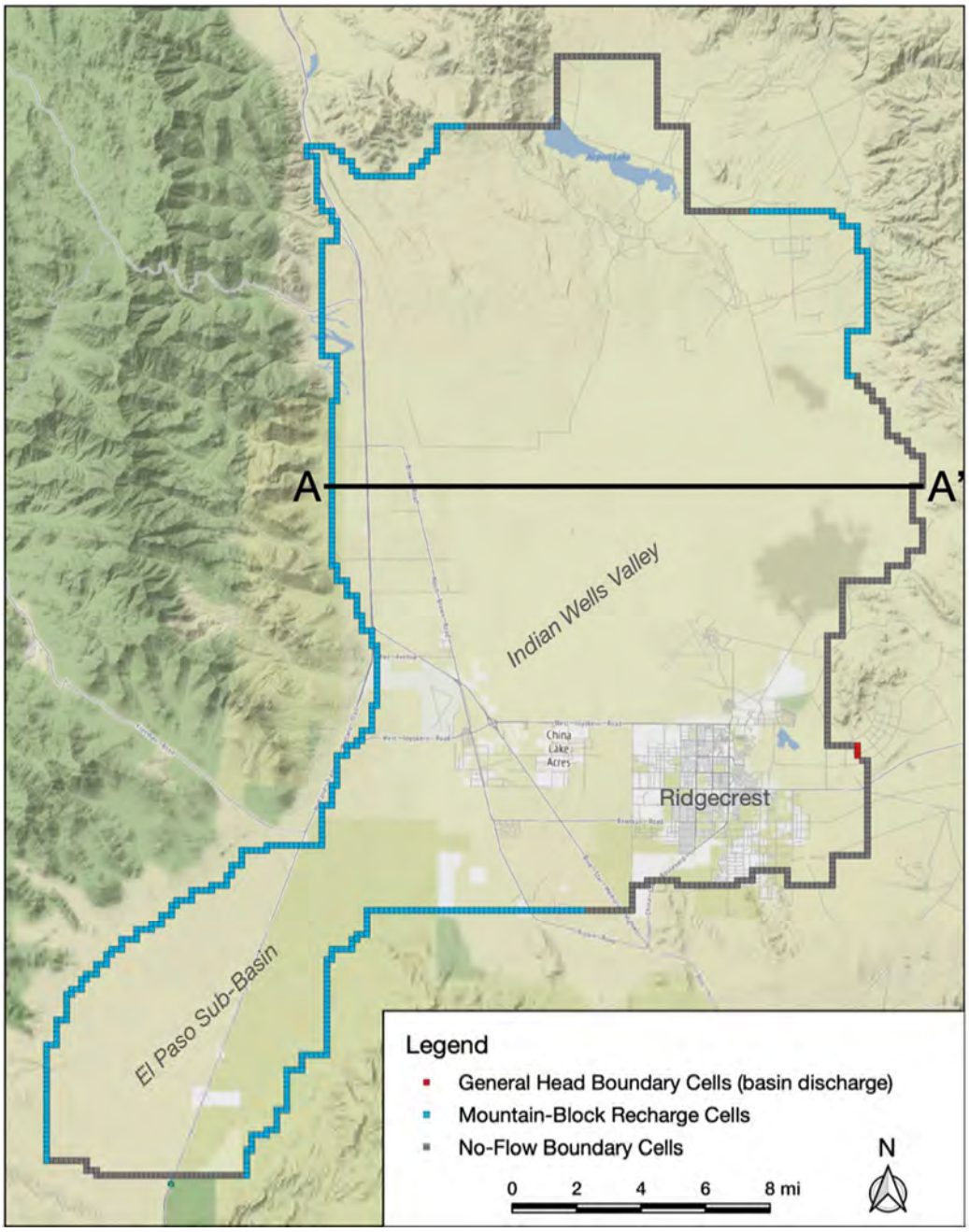


Figure 1. Domain of the Indian Wells Valley groundwater flow model showing perimeter boundary conditions. Cross-section A-A' through the model mesh is shown in Figure 2.

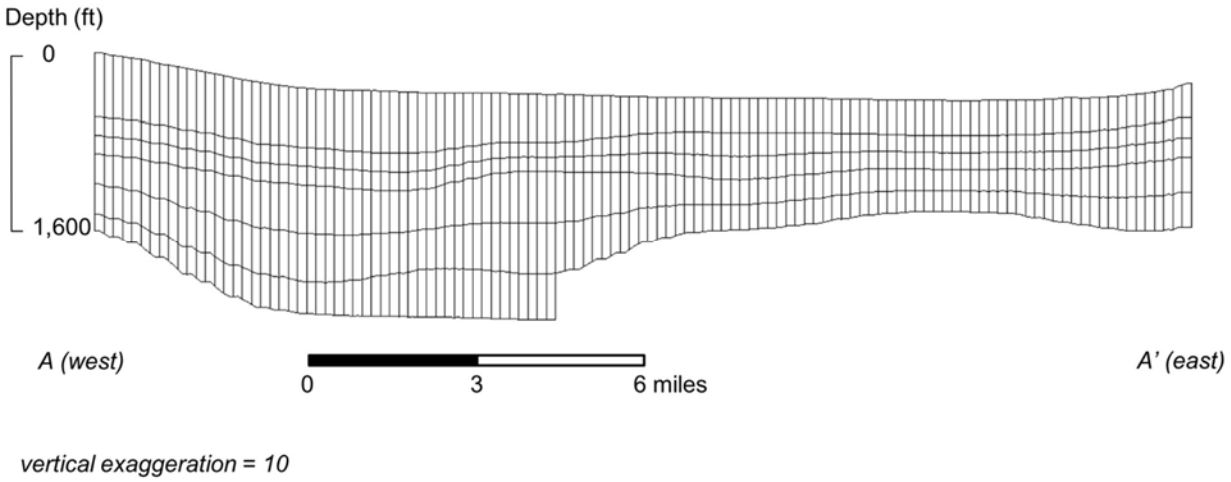


Figure 2. East-West cross-section A-A' through model mesh showing the configuration of the six computational layers.

2.4 Boundary Conditions

2.4.1 Perimeter Boundaries

The perimeter of the model is configured as interbasin flow, recharge, or no-flow boundary segments. Interbasin flow is simulated only toward Salt Wells Valley to the east using an assumed boundary head of 2,152 ft assigned to three adjoining boundary cells in Layer 1 (shown in Figure 1). Interbasin flow is only allowed to leave the model domain at this location and only in Layer 1 (Section 2.4.6).

Recharge from adjacent mountain blocks is simulated on selected perimeter boundary segments in Layers 1, 2, and 3 (shown in Figure 1) and is described further in Section 2.4.3. The remaining boundary segments are configured as no-flow in all six layers.

2.4.2 Internal Boundaries

Active faults in the IWVGB that are known to act as groundwater barriers include the Little Lake fault zone (LLFZ) and a fault that crosses the eastern margin of the El Paso Valley in the southwestern portion of IWV, informally referred to here as the El Paso fault (EPF) (Lancaster et al., 2019; Garner et al., 2017). These faults increase horizontal gradients, particularly in the vicinity of the EPF where a large groundwater gradient is present on the order of 100 ft/mile. Observations in Owens Valley, the next major hydrographic basin to the north, also find that fault systems can reduce transmissivity of aquifer materials in fault zones by a factor of 20 (Danskin, 1998).

The LLFZ and EPF are simulated as eight individual fault segments using MODFLOW's Horizontal Flow Barrier (HFB) package (Figure 3). These faults are assumed to extend vertically through all six model layers. Note that a splay of the LLFZ suggested by fault maps and water level patterns (Lancaster et al., 2019) was added to the 2017 model (Garner et al., 2017) to improve the fit of simulated head gradients in the southeastern area of the basin. Values of the fault hydraulic characteristic parameter for each fault segment were estimated during model calibration (Section 2.5).

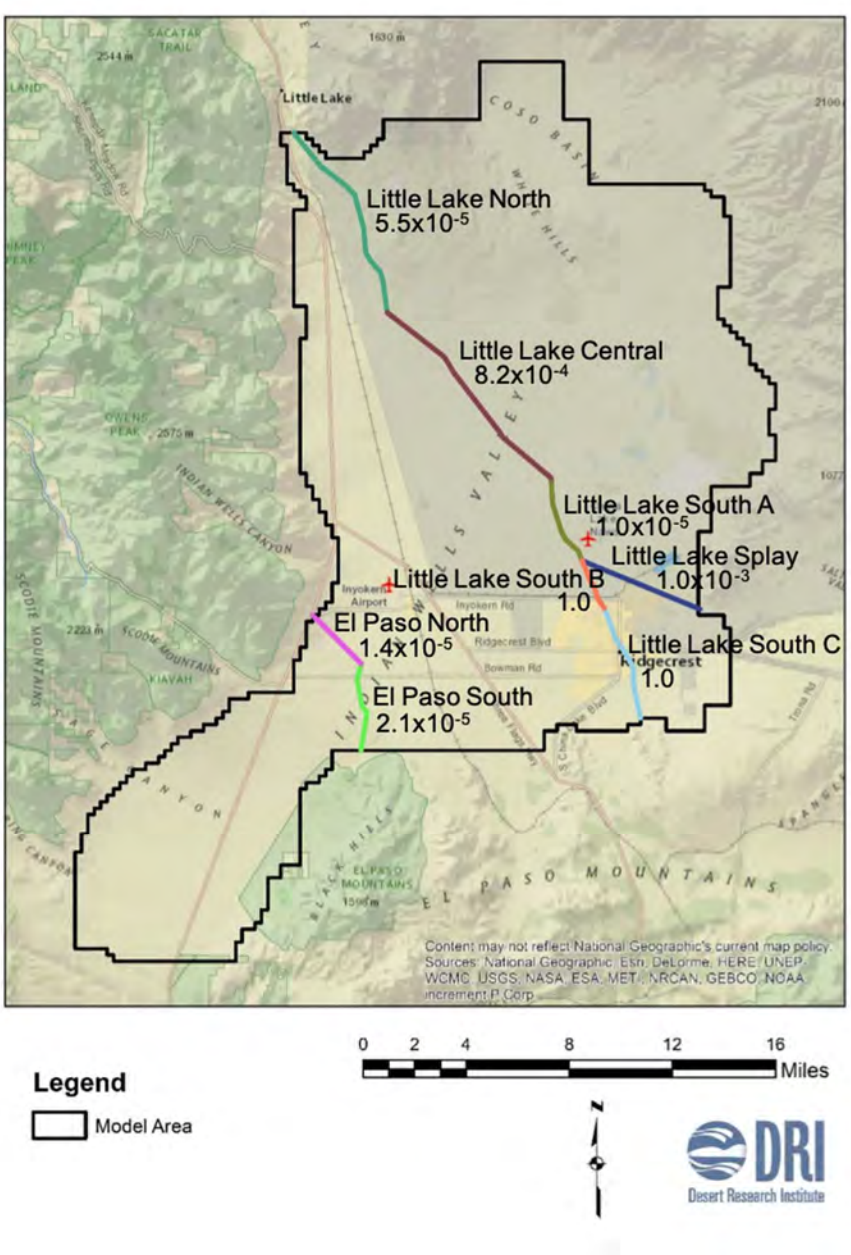


Figure 3. Locations of the eight fault segments simulated as hydrologic barriers. Values of the calibrated hydraulic characteristic parameter are shown for each segment. Units are day^{-1}.

2.4.3 Recharge

Mountain-block recharge is the primary inflow to the groundwater system and is simulated on selected segments of the perimeter boundary as a specified-flux boundary condition using the MODFLOW WEL package. Total mountain-block recharge is simulated as a constant flux of 7,650 AFY in the steady-state and transient models. This value was developed from analysis of fourteen previous recharge studies in the basin and a two-dimensional flow model constructed to assess the recharge estimates and their spatial distribution (McGraw et al., 2016). The range in estimates of total mountain-block recharge of

4,100 to 11,000 AFY from these previous studies was discussed with the Model Ad Hoc Group of the IWV Technical Advisory Committee and the best estimate value of 7,650 AFY presented by McGraw et al. (2016) was confirmed for use in the GSP model.

The recharge boundaries and their associated flux values are shown in Figure 4. Recharge flux from each recharge zone is distributed among the cells on the adjacent model boundary and is applied only to cells in Layers 1, 2, and 3 where permeabilities of the range-front and basin-fill sediments are expected to be highest. Below these recharge boundary segments, boundary cells in Layers 4, 5, and 6 are configured as no-flow. Recharge rates are constant in the steady-state and transient-historical simulations, and vary temporally in the transient-predictive simulations.

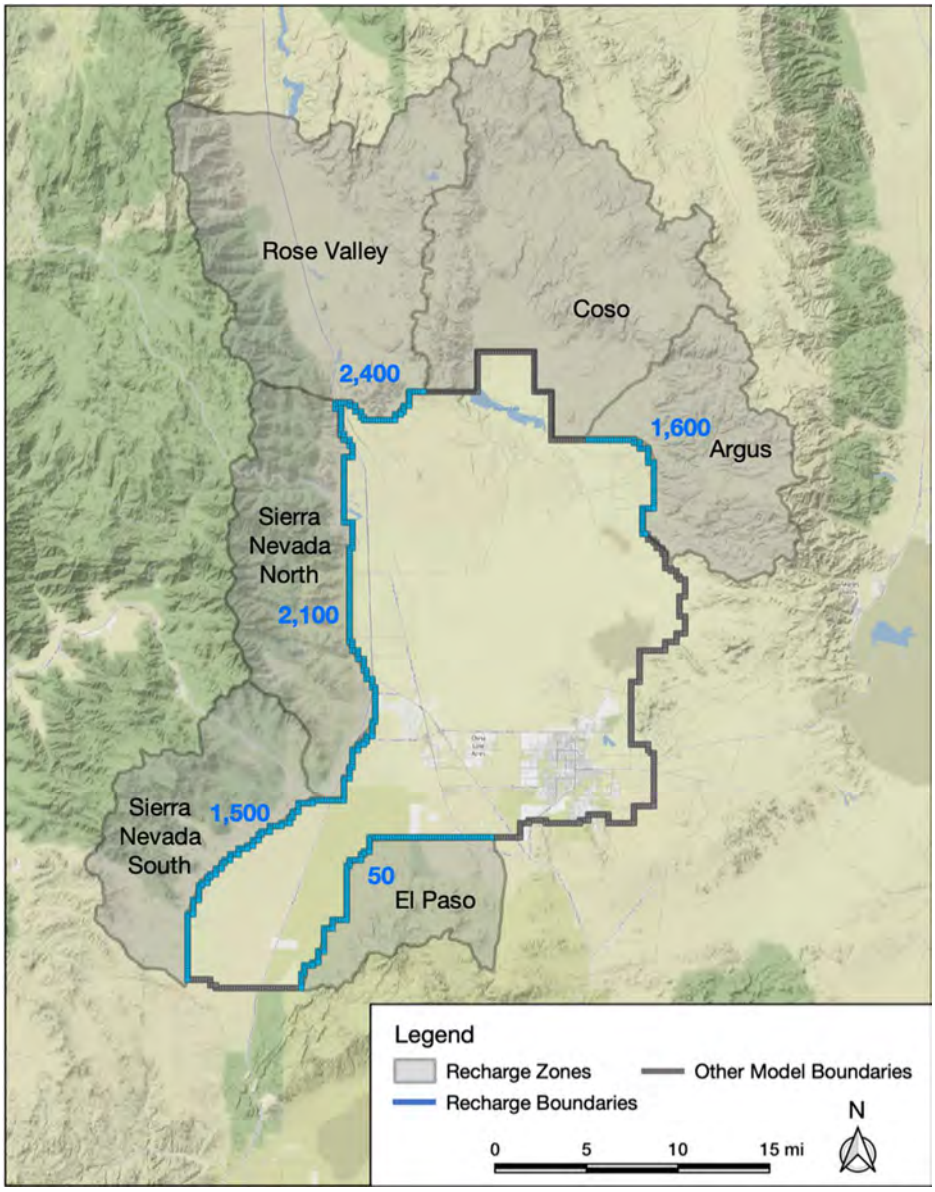


Figure 4. Mountain-block recharge zones surrounding Indian Wells Valley and their associated flux values (shown in blue) on the model boundary. Recharge units are acre-ft/year.

Annual variations in recharge rate were developed for the transient-predictive model by scaling the constant rate by the annual precipitation amounts observed in and near Indian Wells Valley over a balanced hydrologic period from 1990 through 2014 (Stetson Engineers, 2018). This 26-year period was then repeated to obtain the 51-year record (the last year of the repeated period was not included). The mean of these variations over the prediction period is equal to the annual recharge rate of 7,650 AF used for the steady-state and transient stress models (Figure 5).

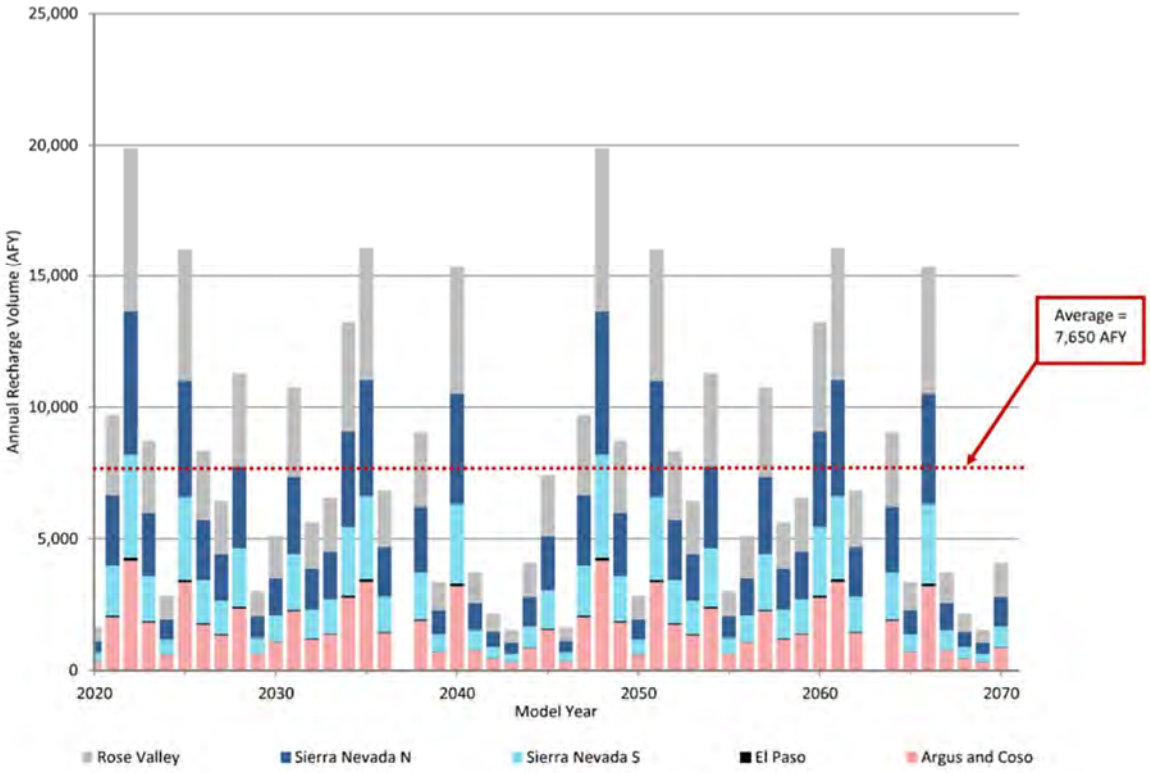


Figure 5. Annual variability of recharge forecasted for the predictive simulations. The mean of the annual recharge values is 7,650 AFY.

Other sources of groundwater recharge have been considered, such as fluid sources from deep geothermal upwelling (Bean, 1989), subsurface inflow from Sierra Nevada bedrock (Thyne et al., 1999), leakage from the Los Angeles Aqueduct (Todd Engineers, 2014), and percolation from wastewater ponds (Todd Engineers, 2014), but these have been either refuted or found to be insignificant when compared to the overall basin groundwater budget (Todd Engineers, 2014; McGraw et al., 2016).

2.4.4 Evapotranspiration

Evapotranspiration (ET) is focused in the area of the China Lake Playa where shallow groundwater levels support phreatophyte vegetation. Prior to 1921, when groundwater pumping began, ET was the predominant outflow from the IWVGB (McGraw et al., 2016), though no ET measurements are available from that time.

ET is simulated in the model using the Evapotranspiration Segments (ETS) package (Banta, 2000) that computes the volumetric ET rate in every model cell based on an input function that relates evapotranspiration to maximum ET flux at the ET surface, extinction depth, and hydraulic head. Based on the results of earlier studies in the IWVGB, McGraw et al. (2016) delineated two phreatophyte vegetation zones and estimated their associated ET rates (Figure 6) to establish a relationship of ET rate to depth to groundwater for the steady-state model. In that model, several smaller areas together represent a greasewood zone with a maximum ET rate of 2.4 ft/yr that terminates when groundwater levels are below an extinction depth of 33 ft. The second and much larger zone in the McGraw et al. (2016) model represents bare playa soil and all vegetation types outside of the greasewood zone (primarily pickleweed and saltgrass). This larger zone was assigned a maximum ET rate of 5.7 ft/yr and terminates when groundwater levels are below an extinction depth of 10 ft. The larger zone was expanded westward for the GSP model to incorporate phreatophyte vegetation mapped during subsequent hydrogeomorphic studies (Lancaster et al., 2019).

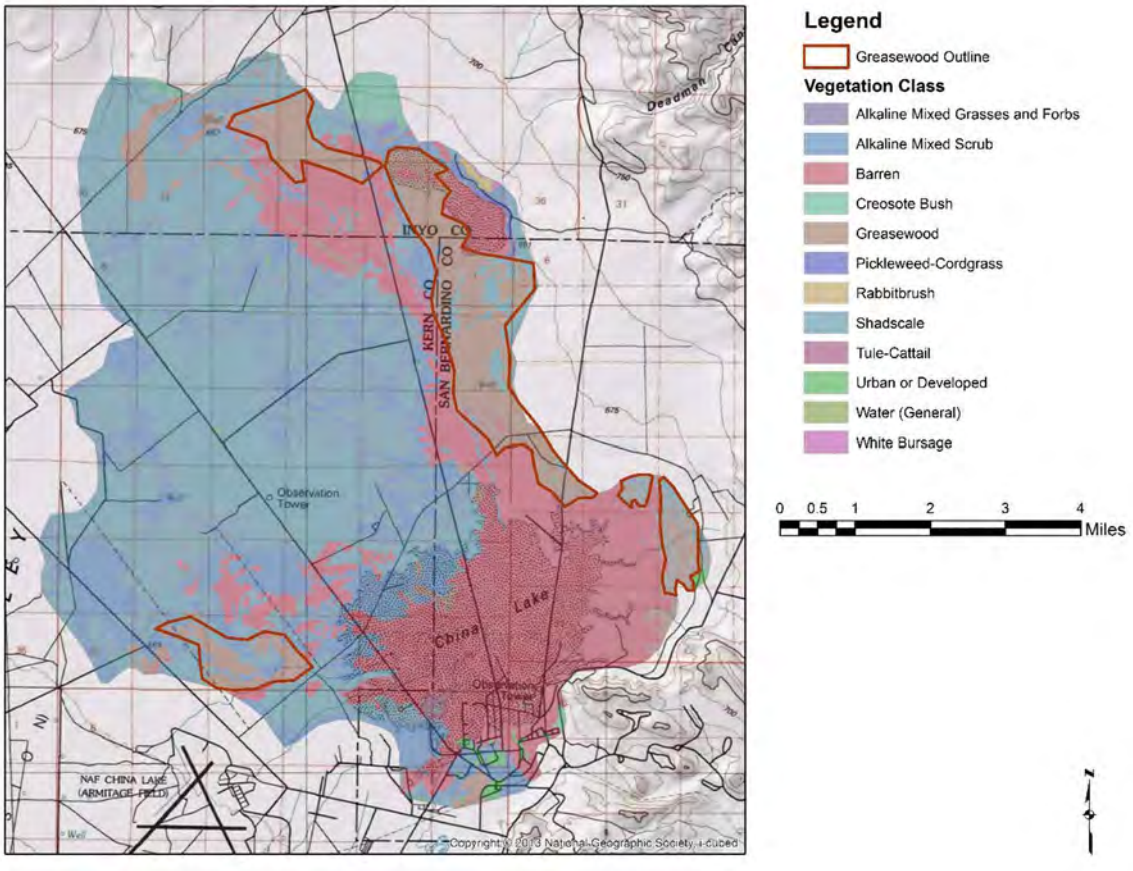


Figure 6. Distribution of vegetation and bare ground (denoted as Barren in the legend) within the area of evapotranspiration (ET) (from McGraw et al. [2016]). The two ET zones in the model are (1) greasewood (outlined in red) and (2) combination of bare playa and all other vegetation zones other than greasewood. Mapping is based on the 2013 vegetation survey of Menke et al. (2013) and correlation to geomorphic map units of Lancaster et al. (2019) in Bullard et al. (2019).

The extinction depth parameters in the GSP model were revised during calibration of the transient-historical model to better fit simulated heads to observed groundwater levels in the playa area. The final values used for the ETS package are listed in Table 1 and the associated ET zones are show in Figure 7. The ETS segmented curve that relates ET rate to hydraulic head is shown in Figure 8. ET is computed during the flow simulation by interpolating the proportion of the maximum ET rate (PETM) at the point on the appropriate segment defined by the hydraulic head (proportion of ET extinction depth, PXDP) for each cell where ET is simulated (Banta, 2000).

Table 1. Values of evapotranspiration rate used to develop the segmented ETS curve for the Evapotranspiration Segments (ETS) package.

ET Zone	Maximum ETS Rate (ft/yr)	ETS Extinction Depth (ft)
Greasewood	2.4	16.4
Dune Phreatophytes	7.2	16.4
Other Phreatophytes	7.2	4.9
Bare Playa	7.2	4.9

Rates of ET are likely to vary in relation to declines in groundwater levels and changes in the sizes and compositions of areas of phreatophyte vegetation. The results of two additional studies were employed to refine ET estimates during calibration of the transient models. Utilizing data from an eddy covariance station installed in 2014 on the southern edge of China Lake Playa, McGraw et al. (2016) estimate that ET rates for bare soil range from 0.2 to 0.4 ft/yr. The lower value accounts for removal of elevated ET measurements that often occur after precipitation events. Although these results are specific to Indian Wells Valley, they are limited to a one-year time period.

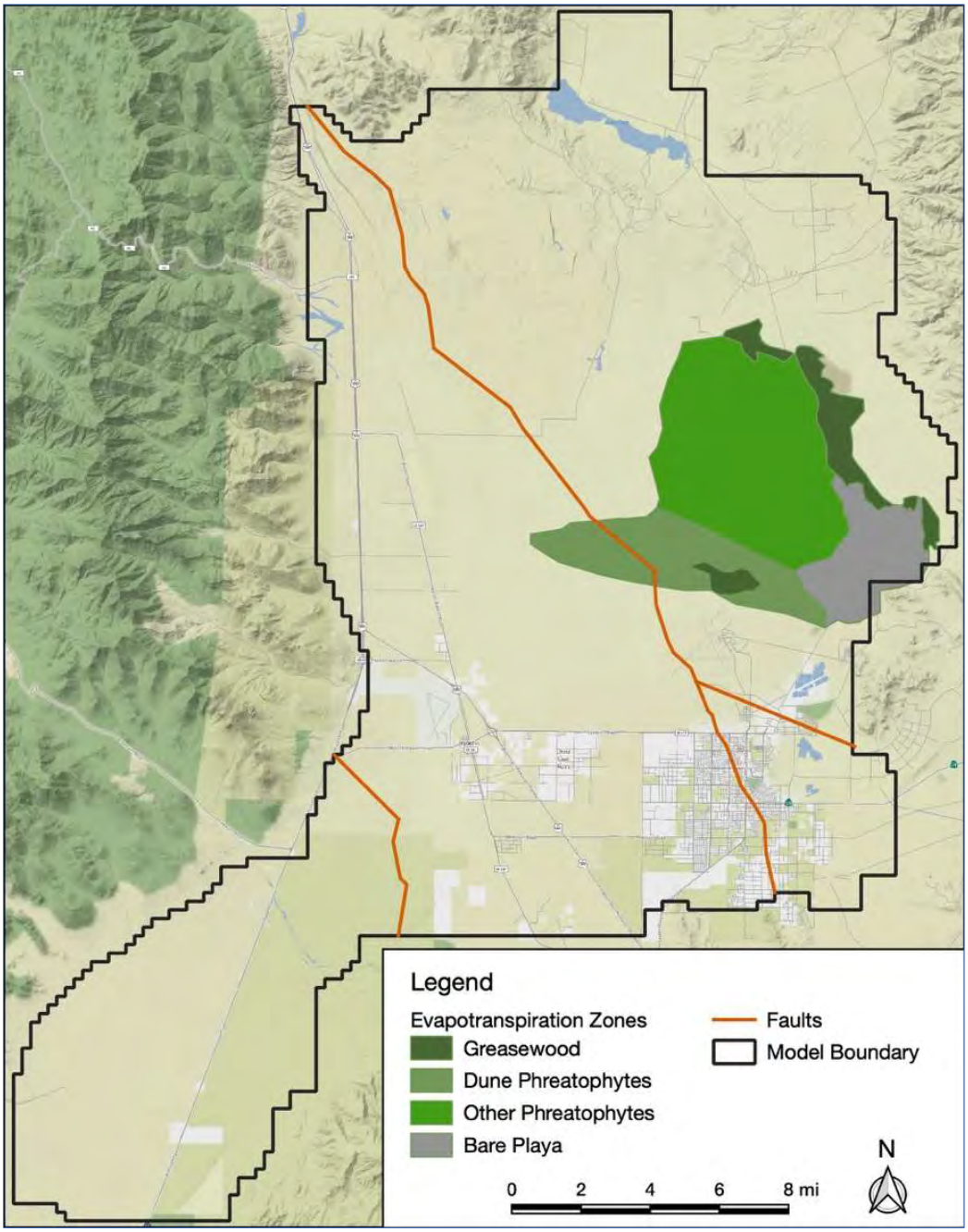


Figure 7. Map of evapotranspiration zones used for the Evapotranspiration Segments (ETS) package in the GSP model. Refer to Figure 3 for the names of the fault segments.

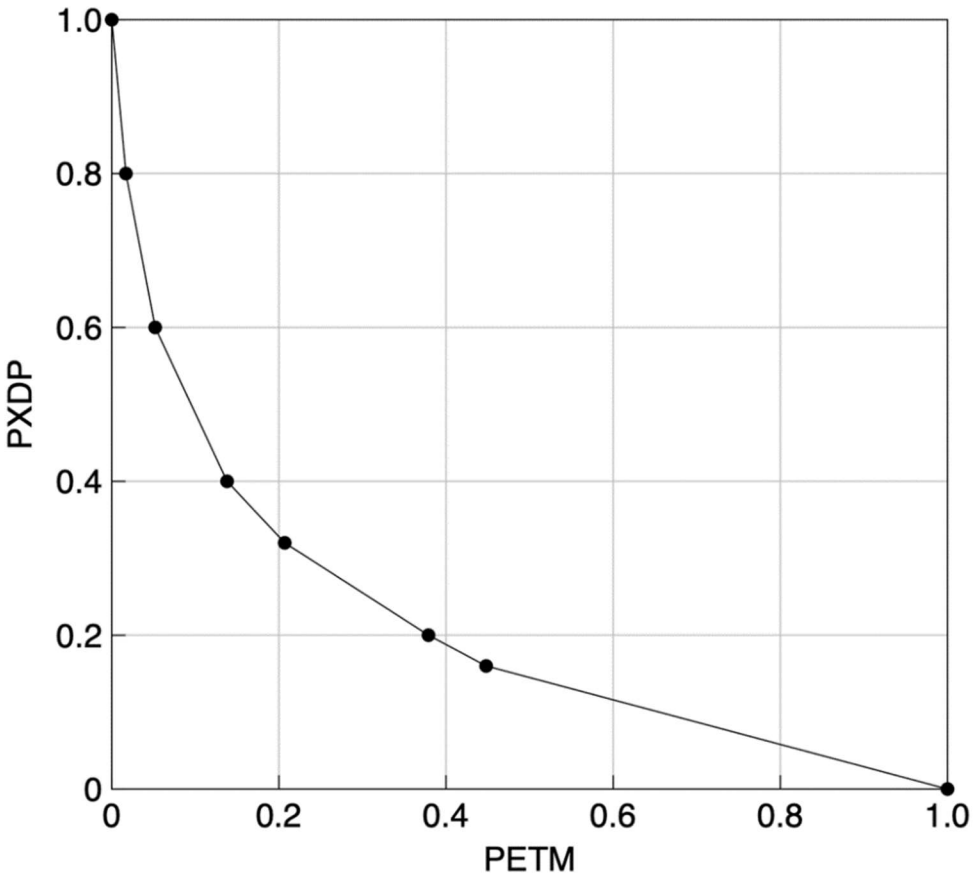


Figure 8. The ETS segmented curve that relates the proportion of evapotranspiration extinction depth (PXDP) to the proportion of the maximum evapotranspiration rate (PETM).

Beamer et al. (2013) compiled ET rates measured over the period 1997 to 2008 at 40 flux tower systems (eddy covariance and Bowen ratio) located throughout the Great Basin. By correlating the measured ET rates and enhanced vegetation index (EVI) values obtained from Landsat imagery for the same areas, Beamer developed an empirical relationship that is transferable to similar ET settings. Using EVI values from Landsat imagery covering the phreatophyte area in eastern Indian Wells Valley and the empirical relationship of Beamer et al. (2013), ET rates were estimated for the GSP model (Figure 9). The results are presented as part of model calibration in Section 2.5.

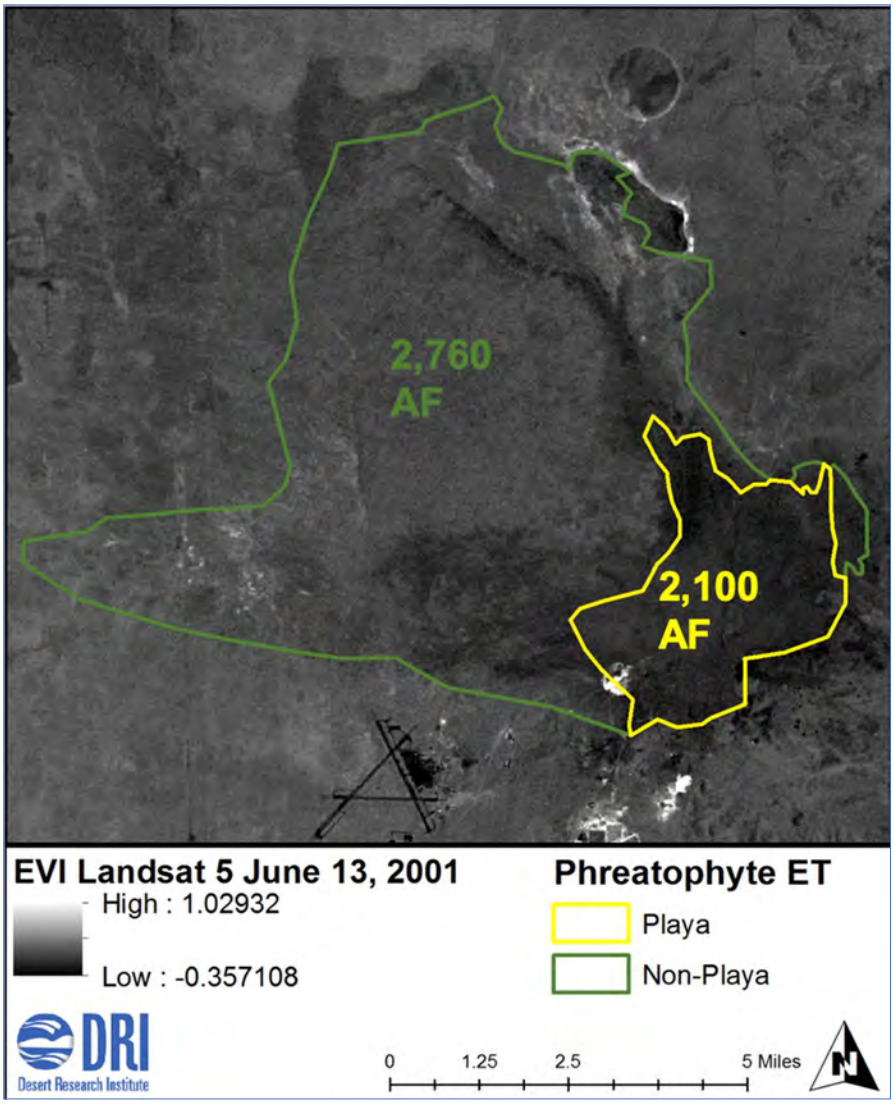


Figure 9. Spatial distribution of two ET zones in the model and their annual ET rates as estimated from EVI values from Landsat imagery using the method of Beamer et al. (2013).

2.4.5 Groundwater Pumping

Groundwater-pumping wells are simulated in the model using the MODFLOW WEL package. McGraw et al. (2016) compiled a groundwater-pumping database for the years 1920 through 2013 for use in the original transient-historical model. Pumping wells were evaluated and assigned by McGraw et al. (2016) to one of five use categories: private domestic, municipal, agriculture, Searles Valley Minerals (SVM), or NAWS. Wells were then compared to existing databases (Brown and Caldwell, 2009) and to aerial photographs to verify their use. Total annual withdrawals for each use category were digitized from Todd Engineers (2014, Figure 9) who summarized pumping data from Berenbrock and Martin (1991) and the Indian Wells Valley Cooperative Groundwater Management Group (IWVCGMG) Production Data (https://iwvgroundwater.org/iwv-production-data). Annual withdrawals were assigned to individual wells in the database when this relationship could be established. For other non-agriculture wells, the

remaining total annual withdrawal for each use category was divided equally among the wells in that category. Wells in the agriculture use category are assigned annual withdrawal rates determined by whether they are used for irrigation of alfalfa or pistachios. Pumping rates for these crops are based on estimates by Todd Engineers (2014) and the irrigated area of each crop type calculated from a geographic information system maintained by NAWS. Pumping rates for pistachio orchards increase over the 12-year period to maturity and then are held constant to account for changing water demands during their growth and mature stages (McGraw et al., 2016).

Garner et al. (2017) re-evaluated the groundwater-pumping database as part of the updates for the 2017 transient-historical model. Using annual withdrawal records for the period 1975 through 2015 available from the IWVCGMG, annual withdrawals in the model database were found to be in good agreement with the IWVCGMG data for the municipal, agriculture, SVM, and NAWS use categories. The annual rate in the database for private domestic wells of approximately 1 AF was found to be lower than the 2.5 AF rate prescribed by IWVCGMG, but is more consistent with the analysis of Todd Engineers (2014) that suggested the rate is generally less than 1 AF, with only a few parcels exceeding this amount.

Annual withdrawals in the database were updated through 2016 (Garner et al., 2017) utilizing records for individual IWCWD municipal wells and NAWS wells. Total annual withdrawals reported for private domestic wells; City of Inyokern, Ridgecrest Heights, and City of Ridgecrest municipal wells; and SVM wells were divided equally among the wells in their respective use categories. Annual withdrawals for agricultural wells were updated using estimates of alfalfa and pistachio production following the methods of McGraw et al. (2016). The domestic pumping rate of 1 AFY was used as described above. The annual groundwater withdrawals for all use categories are shown in Figure 10. Withdrawals were obtained from Berenbrock and Martin (1991) for 1920 through 1974 and from IWVCGMG estimates from 1975 through 2016. In addition, withdrawals at NAWS significantly declined in 1975. From 1980 through 2016, an annual average of approximately 25,000 AF was withdrawn from the basin. The total withdrawal for the year 2016, the last year simulated by the transient-historical model, is 24,473 AF. The locations, 2016 annual volumetric production, and use categories of the pumping wells are shown in Figure 11. Wells withdraw water from depths of up to 1,200 ft below land surface and from all six model layers.

The transient-predictive model simulations begin in the year 2020 and extend through 2070 using annual groundwater withdrawals associated with management scenarios developed by the Indian Wells Valley Groundwater Authority. The predictive flow models are described in Section 2.7.

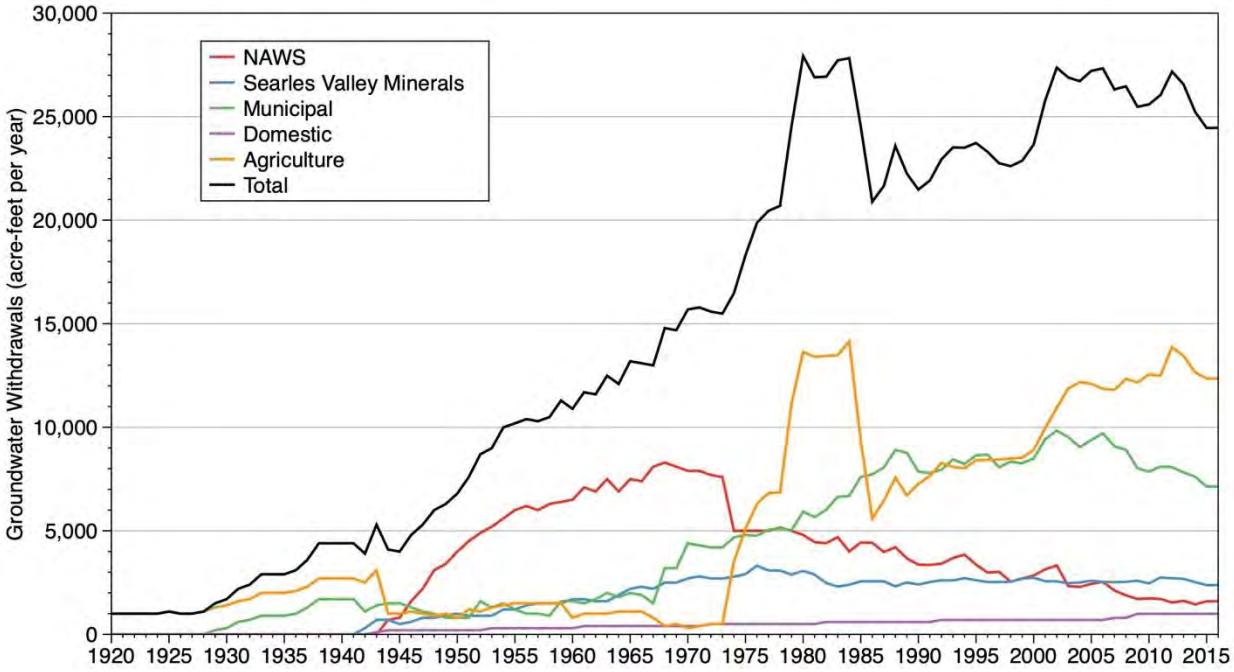


Figure 10. Annual groundwater withdrawals for all use categories for the period 1920 through 2016.

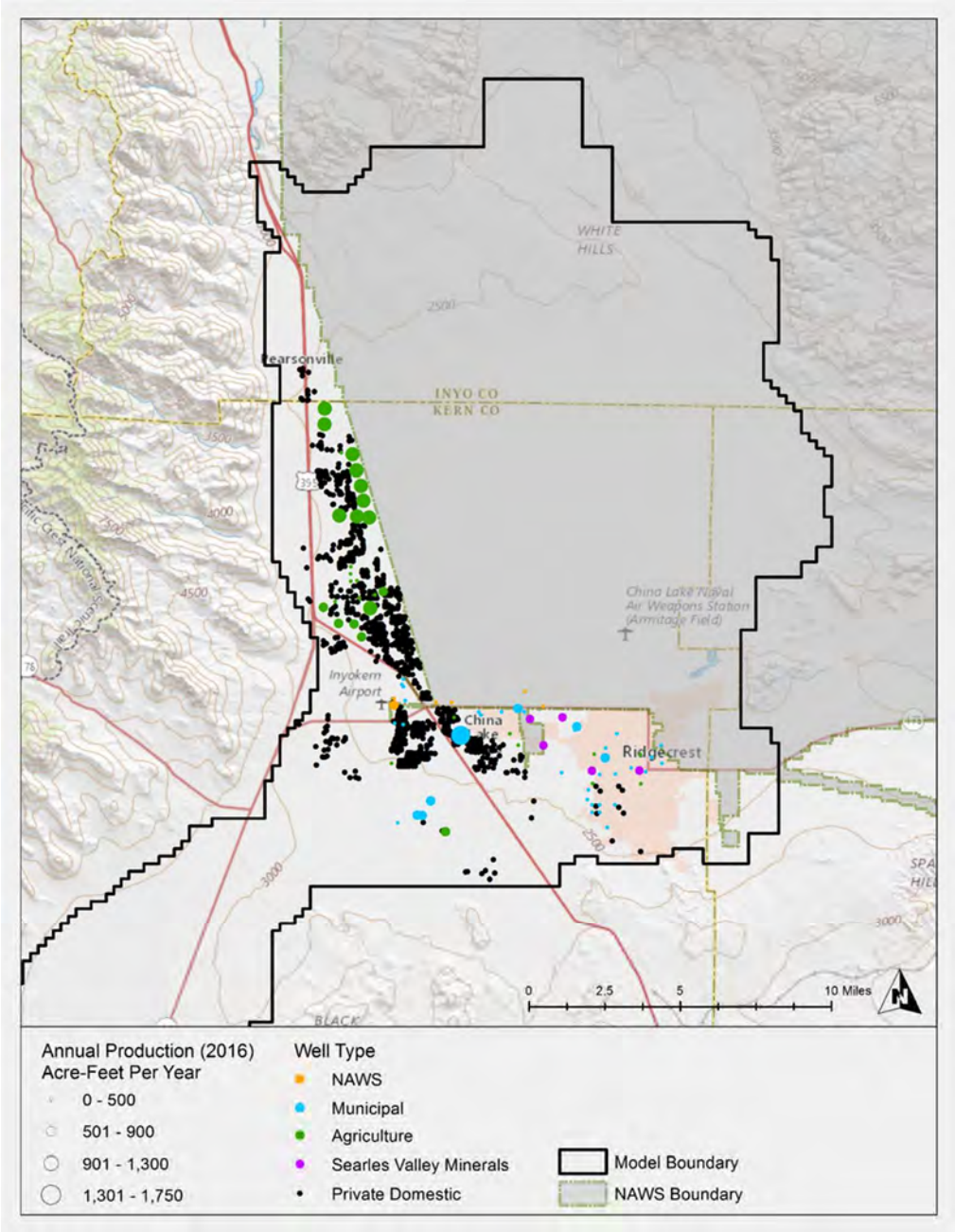


Figure 11. Groundwater-pumping wells included in the transient models.

2.4.6 Basin Outflow

Tertiary igneous and metamorphic rocks bound the IWVGB and Miocene basalts are present near the El Paso Mountains. Unless they are highly fractured, these rocks typically have low permeability and for the purposes of this and previous basin-fill groundwater models, they are not considered to be water-bearing. As a result, most studies of the IWVGB consider the pre-developed basin to be nearly hydrologically closed, with only very small or negligible underflow eastward toward Salt Wells Valley

(McGraw et al., 2016). Mass balance calculations of total dissolved solids suggest that the absence of large accumulations of salinity in the IWVGB (other than in the playa area where salinity increases through the ET process) may be indicative of interbasin groundwater outflow (McGraw et al., 2016). The possible annual magnitude of this flow was approximated as 200 AF by McGraw et al. (2016) using two-dimensional calculations incorporating hydraulic and geometric information from TriEcoTt (2012). This value was used in the original steady-state model and was adjusted downward during calibration of the transient-historical model as described in Section 2.5.

Basin outflow is simulated toward Salt Wells Valley using MODFLOW's General-Head Boundary (GHB) package with an assumed boundary head of 2,152 ft assigned to three adjoining boundary cells in Layer 1 (shown in Figure 1). This head value is revised in the GSP model from the value of 2,182 ft used by McGraw et al. (2016) based on further evaluation of water levels in this area of the basin. Interbasin flow is only allowed to leave the model domain at this location and only in Layer 1, based on the assumption that basin-fill deposits are most permeable in this area and at shallow depths.

2.5 Calibration

The general approach to GSP model calibration has been to adjust the values of selected parameters using manual and automated calibration processes until the model's simulated results are consistent with observed historic trends in Indian Wells Valley and the El Paso sub-basin. The flow model was calibrated in two stages, steady state and transient-historical, with comparisons made to observed water levels and water budgets in both cases.

2.5.1 Steady-State Model

The steady-state groundwater flow model represents hydrologic conditions before large-scale groundwater pumping began in 1921. This model is calibrated to steady-state water levels measured in 132 wells in Indian Wells Valley in 1920 and four wells in the El Paso sub-basin (Figure 12). Because pre-development water levels are not available in the El Paso sub-basin, the mean values of recent stable water levels in four wells were used (Garner et al., 2017). One artificial point, with an assigned water level elevation of 2,280 ft was added in the northwest basin (indicated in blue in Figure 12) to constrain simulated water levels to a range that would be expected in that area.

The values of two model parameters were optimized during steady-state calibration using the PEST (Parameter Estimation) software (Doherty and Hunt, 2010), (1) horizontal hydraulic conductivity (K) of the six model layers and (2) hydraulic characteristic (fault transmissivity divided by barrier width) of the fault segments identified in Figure 3. These parameters were chosen because in general they have significant effects on simulated water levels and because measurements of their values in Indian Wells Valley are limited and therefore are considered more uncertain than the other parameters. PEST was applied to optimize the selected parameter values to achieve the best fit of simulated to observed steady-state groundwater levels.

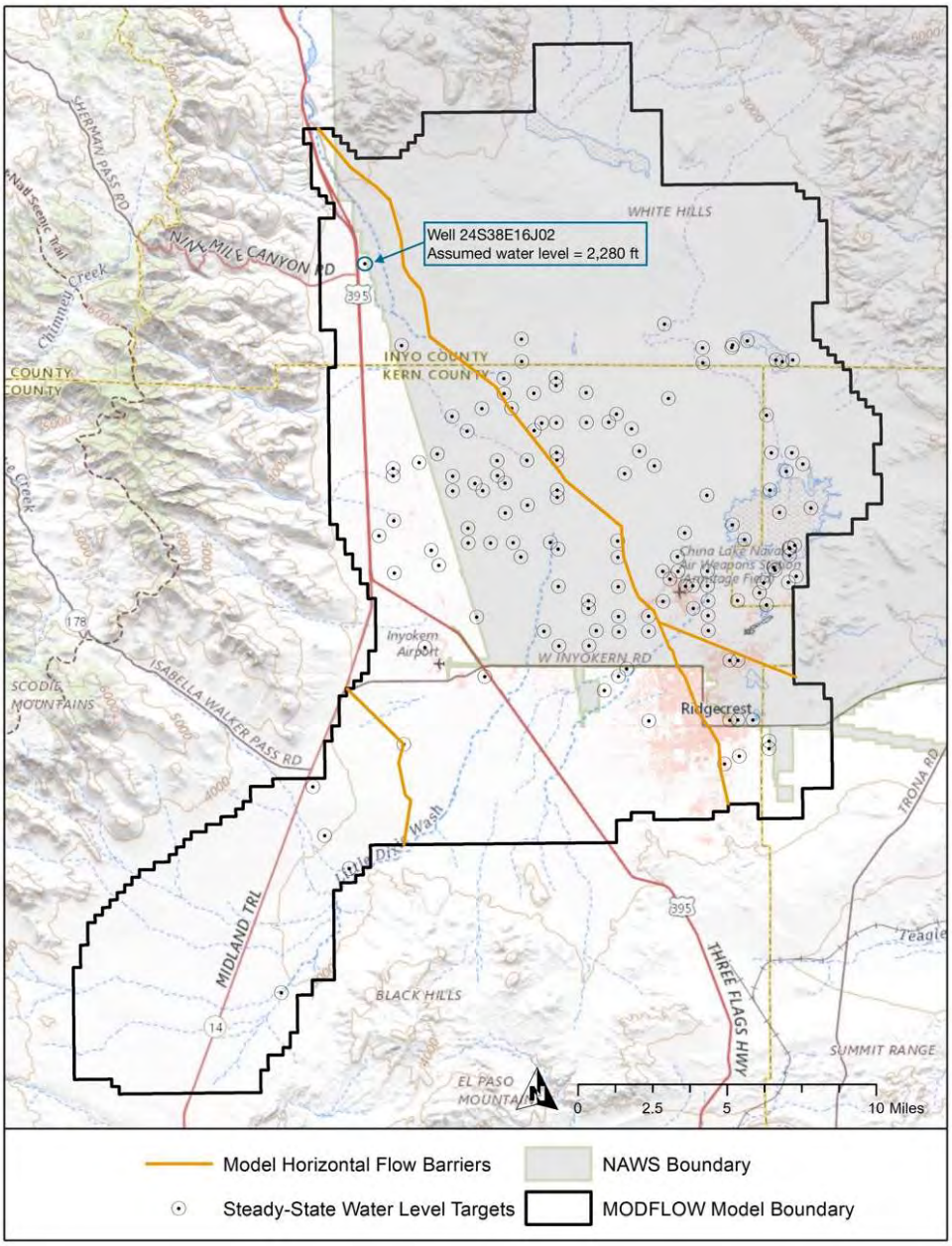


Figure 12. Locations of groundwater level targets for the steady-state pre-development model (from Garner et al. [2017]). One artifical point was included in the northwest (indicated in blue) to constrain simulated water levels to values thought to be representative of that area. There are no pre-development water levels available in the El Paso sub-basin, so mean values of recent stable water levels at the four available wells are used. Refer to Figure 3 for the names of the fault segments.

The vertical anisotropy ratio of hydraulic conductivity (K_z/K_x) is set at 0.3, the value determined during calibration of DRI's groundwater flow model for the Navy (McGraw et al., 2016). This value of anisotropy ratio is assigned throughout the model domain. Hydraulic conductivity is assumed to be laterally heterogeneous within all six model layers. Values of K in Layer 1 were calibrated using 54 pilot point

locations. Eighteen of these pilot points are located at well locations where pumping tests provide estimates of K (Figure 13), the values of which are fixed at these pilot points during calibration. In Layers 2 and 3, K was calibrated using the same 54 pilot point locations; however, no known pumping tests are available at these depths in the basin so calibration could not be guided by direct estimates of K in these layers. Instead, pilot points in these layers were used to guide calibration toward K values that were consistent with the hydrostratigraphic conceptualization of this depth interval. Lithologic logs of deep wells in the western and central portions of the basin (USBR, 1993) indicate discontinuous zones of fine-grained sediments at these depths. Pilot points were not used for Layers 4, 5, and 6. Each of these layers were divided into three horizontal zones of homogeneous K and PEST was used to adjust the K value within each zone. One zone covers the majority of the basin and two smaller zones represent the El Paso sub-basin and an area in the southeast basin surrounding Ridgecrest.

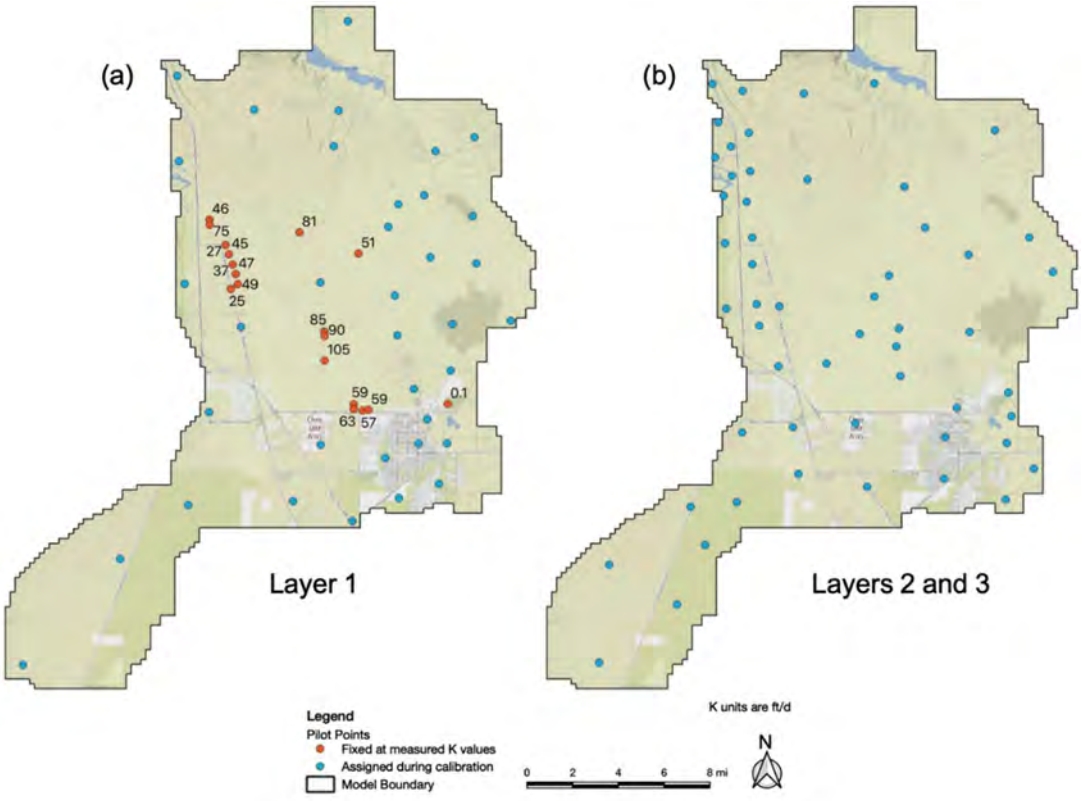


Figure 13. Locations of pilot points in (a) Layer 1 and (b) Layers 2 and 3 that were used for calibration of the steady-state flow model. Pilot points were not used in Layers 3, 4, and 5.

Values of the hydraulic characteristic parameter for the eight fault segments simulated as horizontal flow barriers were also optimized during PEST calibration. The Little Lake fault zone and a connected splay fault are divided into six segments and the El Paso fault was divided into two segments. The fault segments extend vertically through all six model layers and the values of hydraulic characteristic are vertically uniform within each segment.

The ranges in parameter values used for calibration are listed in Table 2. The initial ranges of K were chosen from the values used for the four primary hydrogeologic units by Brown and Caldwell (2009). Lacking site-specific data, initial broad ranges of fault hydraulic characteristic were chosen based on professional experience and judgement. The value of the hydraulic characteristic for the Little Lake Splay fault was chosen as 1×10^{-3} day^{-1} based on model performance and was fixed during calibration.

Table 2. Summary of ranges of parameter values and calibrated values estimated during calibration of the steady-state model.

Model Parameter	Model Element	Parameter Range		Calibrated Value
		Minimum	Maximum	
Hydraulic Conductivity (ft/day)	Layer 1	0.01	41	0.03 to 40
	Layers 2 and 3	0.01	11	0.01 to 10
	Layers 4 to 6 Main Basin	1.00E-10	100	0.51
	Layers 4 to 6 SE Main Basin	0.01	0.1	0.10
	Layers 4 to 6 El Paso	1.00E-10	100	5.00E-04
Hydraulic Characteristic of Horizontal Flow Barriers (day^{-1})	Little Lake North	1.00E-08	1.00E-04	5.54E-05
	Little Lake Central	1.00E-08	100	8.19E-04
	Little Lake South, segment A	1.00E-08	100	1.00E-05
	Little Lake South, segment B	1.00E-10	100	1.00
	El Paso South	1.00E-08	100	2.11E-05
	El Paso North	1.00E-08	100	1.42E-05

The distributions of calibrated K values in each layer are shown in Figure 14 and the values are listed in Table 2. The hydraulic conductivity values range from 0.01 to 41 ft/day in Layer 1 (Figure 14[a]) and 0.01 to 11 ft/day in Layers 2 and 3 (Figure 14[b]. Calibrated hydraulic conductivity values for layers 4, 5, and 6 are 0.5 ft/day in the main basin, 0.1 ft/day in the southeastern main basin, and 5×10^{-4} ft/day in the El Paso sub-basin (Figure 14[c]). The distribution of K is consistent with the generalized hydrostratigraphy in the basin. In the shallow subsurface, high K in the central basin represents unconsolidated coarse-grained younger alluvium, lower K in the China Lake area is associated with fine-grained playa and lacustrine deposits, and lower K in the El Paso sub-basin relates to high hydraulic gradients observed there. Information from lithologic logs of deep wells (USBR, 1993) suggest that discontinuous zones of fine-grained sediment are present at depths represented by model Layers 2 and 3. The lower K associated with this stratigraphy is captured in the calibrated K values in these layers (Figure 14[b] and Figure 15). Higher calibrated K is related to coarse-grained sediments conceptualized at greater depths throughout most of the basin (Figures 14[c] and 15), though lower K values were required in the El Paso sub-basin and the southeastern main basin to best fit water-level observations in these areas. Few deep boreholes are available in these areas to provide the lithologic information that can guide calibration.

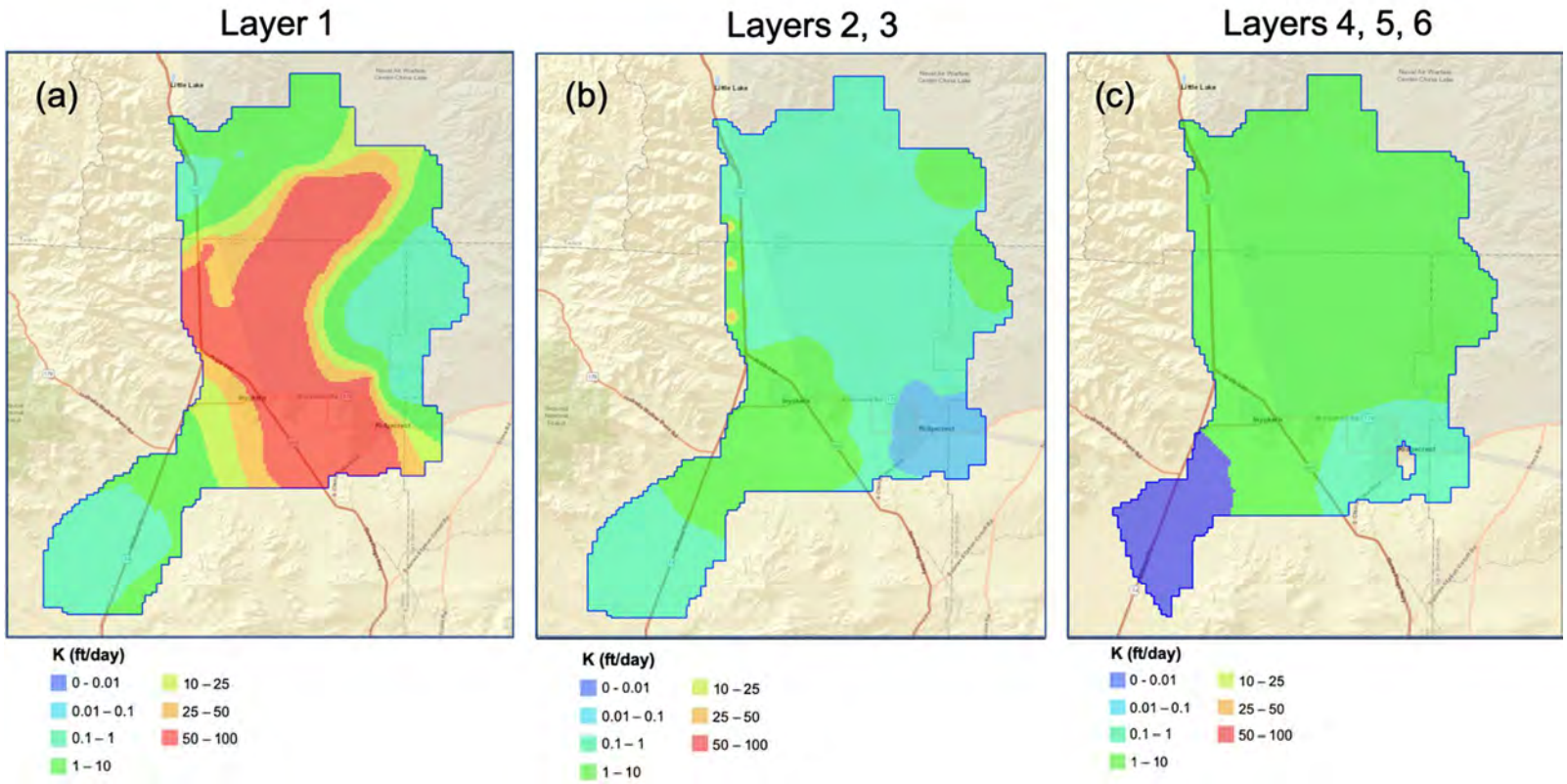


Figure 14. Calibrated hydraulic conductivity in (a) Layer 1, (b) Layers 2 and 3, and (c) Layers 3, 4, and 5 of the steady state model.

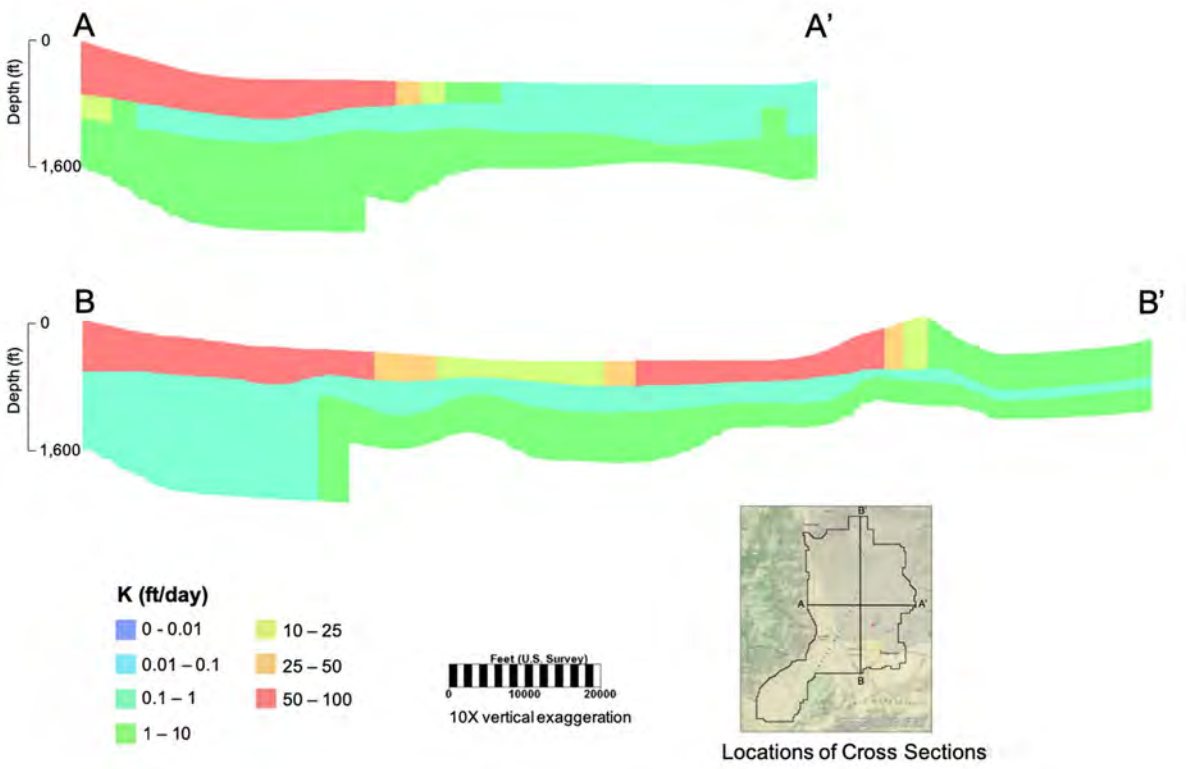


Figure 15. Cross sections showing examples of the distribution of calibrated hydraulic conductivity within the layers of the steady state model.

The results of steady-state calibration show that the model provides a good simulation of observed groundwater levels. The mean absolute error (*MAE*) in water levels was calculated using the equation

$$MAE_{water\ level} = \frac{1}{n}\sum_{w=0}^{n} abs\{h_{sim} - h_{obs}\} \quad (1)$$

where $MAE_{water\ level}$ = mean absolute error in the water level, n = number of water-level measurements, h_{sim} = simulated groundwater level, and h_{obs} = measured groundwater level.

The mean absolute error between simulated and observed water levels is 4.5 ft. The relative error in water levels, which is the MAE divided by the range in observed water levels, is one percent, which is well below the 10-percent threshold that is generally considered an acceptable maximum relative error for use of the model as a tool for water-level predictions. Models with a relative error less than five percent are considered excellent (Anderson et al., 2015). Head residuals of the steady-state model range from -15.3 to +16 feet (Figure 16), with most residuals in the range of -4.5 to +4.5 feet. There is no apparent bias between simulated and observed water levels; water levels are well simulated over the entire range of water-level observations. (Figure 17).

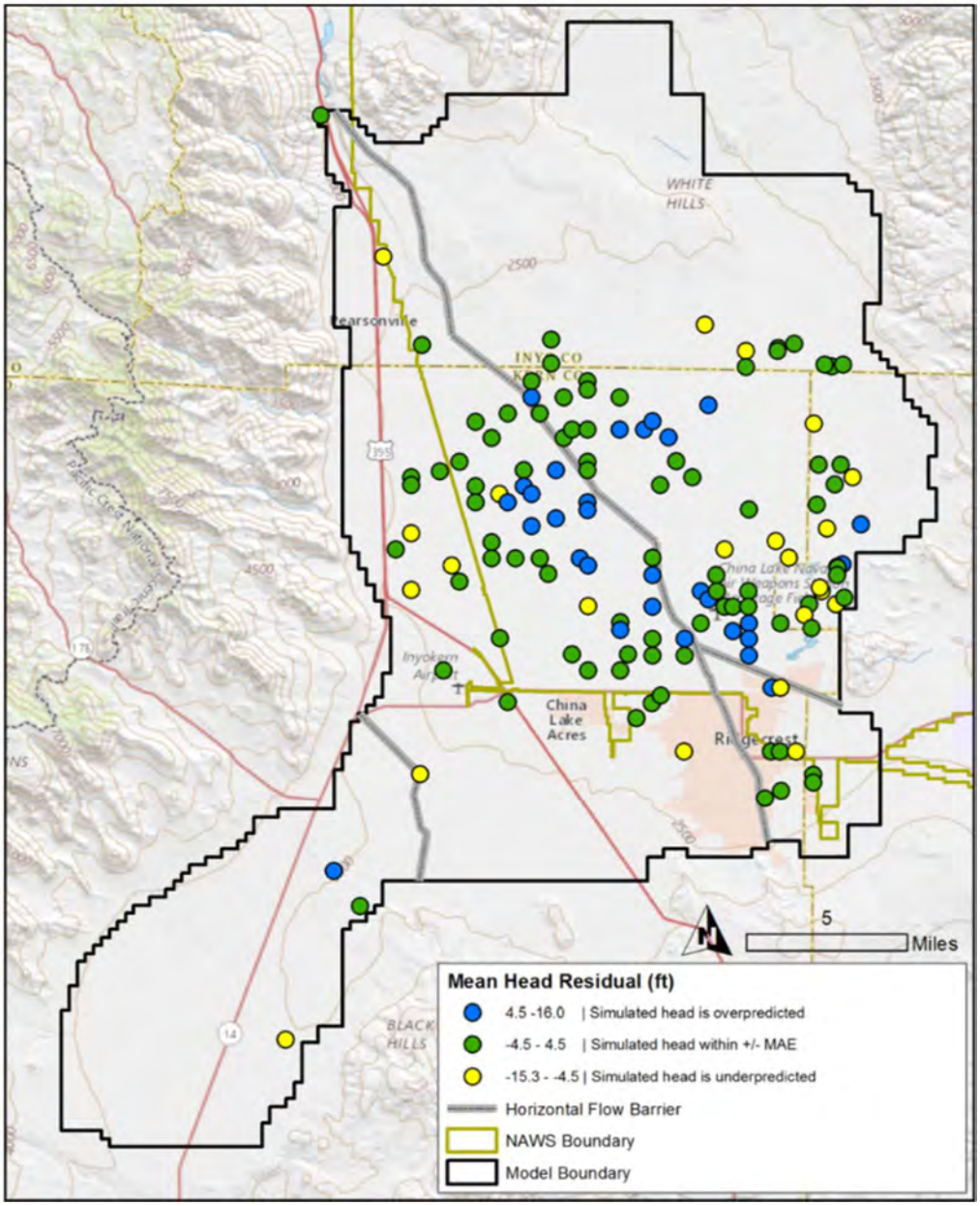


Figure 16. Residuals between simulated and observed groundwater levels for the calibrated steady-state model. Refer to Figure 3 for the names of the fault segments.

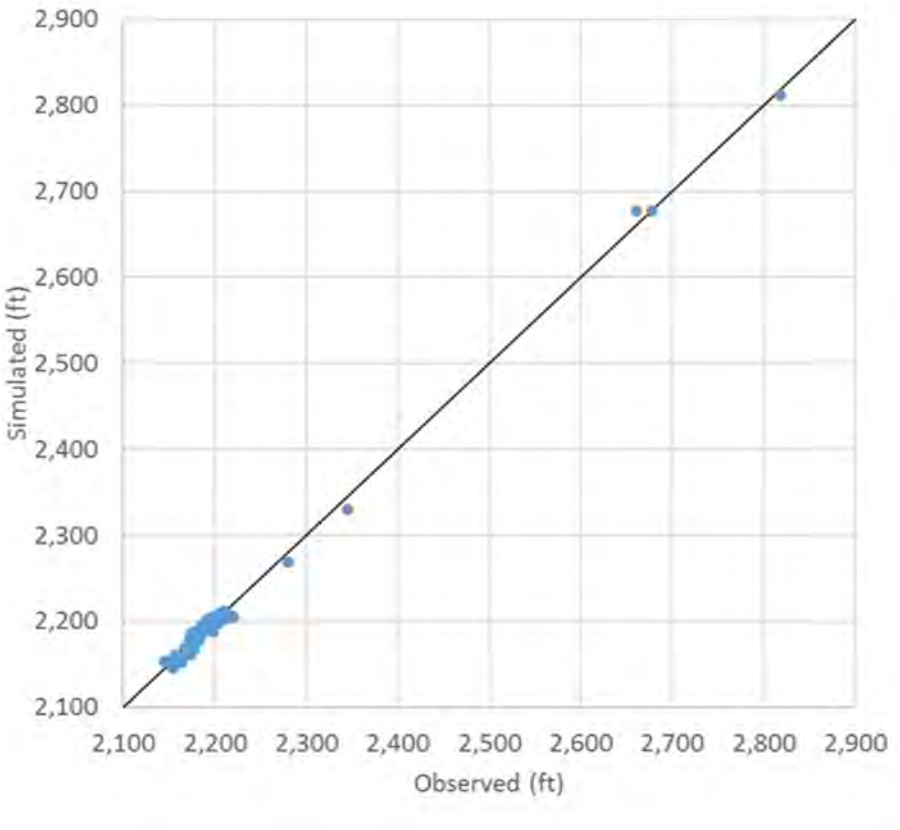


Figure 17. Plot of simulated heads to observed heads in the calibrated steady-state model.

The groundwater budget for the steady state model is tabulated in Table 3. The sole sources of inflow to the model are mountain block recharge and interbasin flow from Rose Valley, at a combined rate of 7,650 AFY. Evapotranspiration is the primary component of outflow (7,510 AFY), with interbasin flow to Salt Wells Valley (140 AFY) providing the remainder.

Table 3. Groundwater budget simulated by the steady-state model.

INFLOW	**(acre-ft/year)**
Recharge and Interbasin Flow	7,650
Coso and Argus Ranges	1,600
Rose Valley	2,400
Sierra Nevada North	2,100
Sierra Nevada South	1,500
El Paso sub-basin	50
Total:	**7,650**

OUTFLOW	**(acre-ft/year)**
Evapotranspiration	7,510
Flow to Salt Wells Valley	140
Total:	**7,650**

Groundwater flow directions prior to development as simulated by the steady state model are shown in Figure 18. Flow paths originate at recharge boundaries and as interbasin flow from Rose Valley and are directed toward areas of evapotranspiration and interbasin flow to Salt Wells Valley. Groundwater flow is parallel to northern segments of the Little Lake Fault where fault conductivity is lower and crosses the fault further south where fault conductivity is higher.

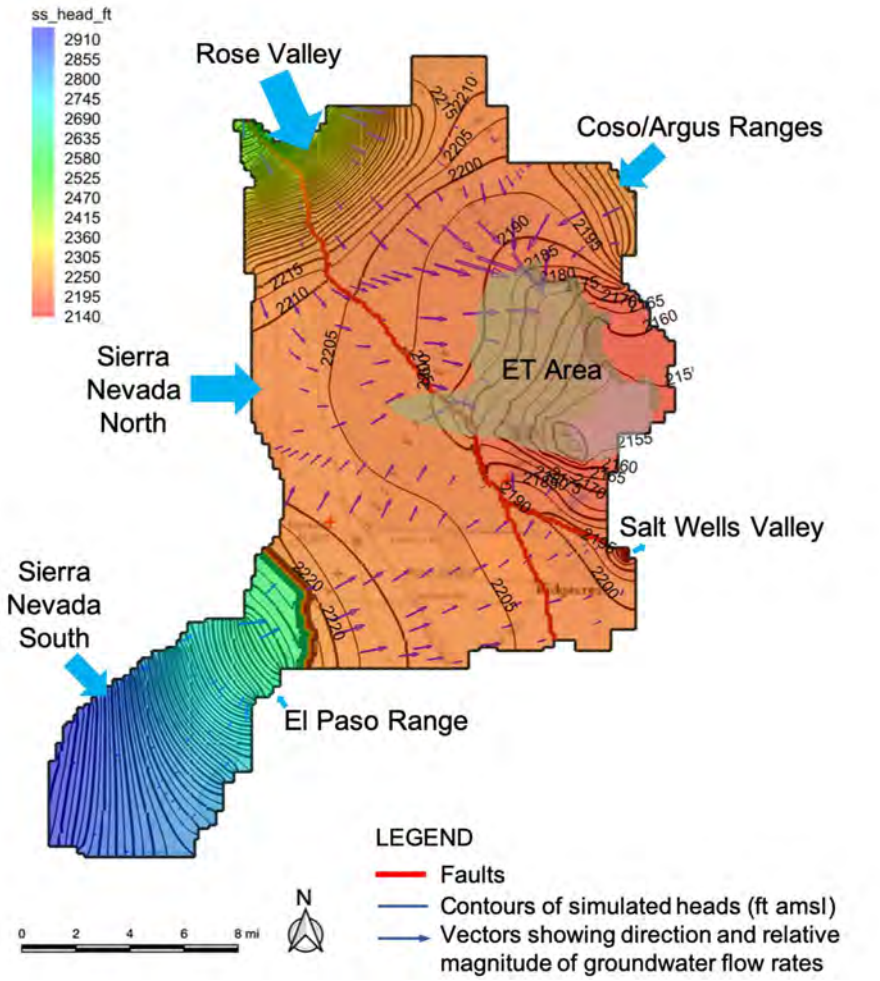


Figure 18. Groundwater flow directions and hydraulic heads simulated on Layer 1 of the pre-development steady-state model. Locations of recharge and interbasin flow boundaries are indicated by large blue arrows. Refer to Figure 3 for the names of the fault segments.

2.5.2 Transient-Historical Model

Groundwater conditions during the period 1921 through 2016 are simulated by the transient-historical flow model, which includes groundwater withdrawals at the 1,191 wells contained in the revised groundwater-pumping database (Garner et al., 2017). Mountain-block recharge rates are constant over this time period. This model is calibrated to water budget terms and historic water-level trends and altitudes observed in 36 wells (Figure 19) by adjusting values of the transient storage parameters

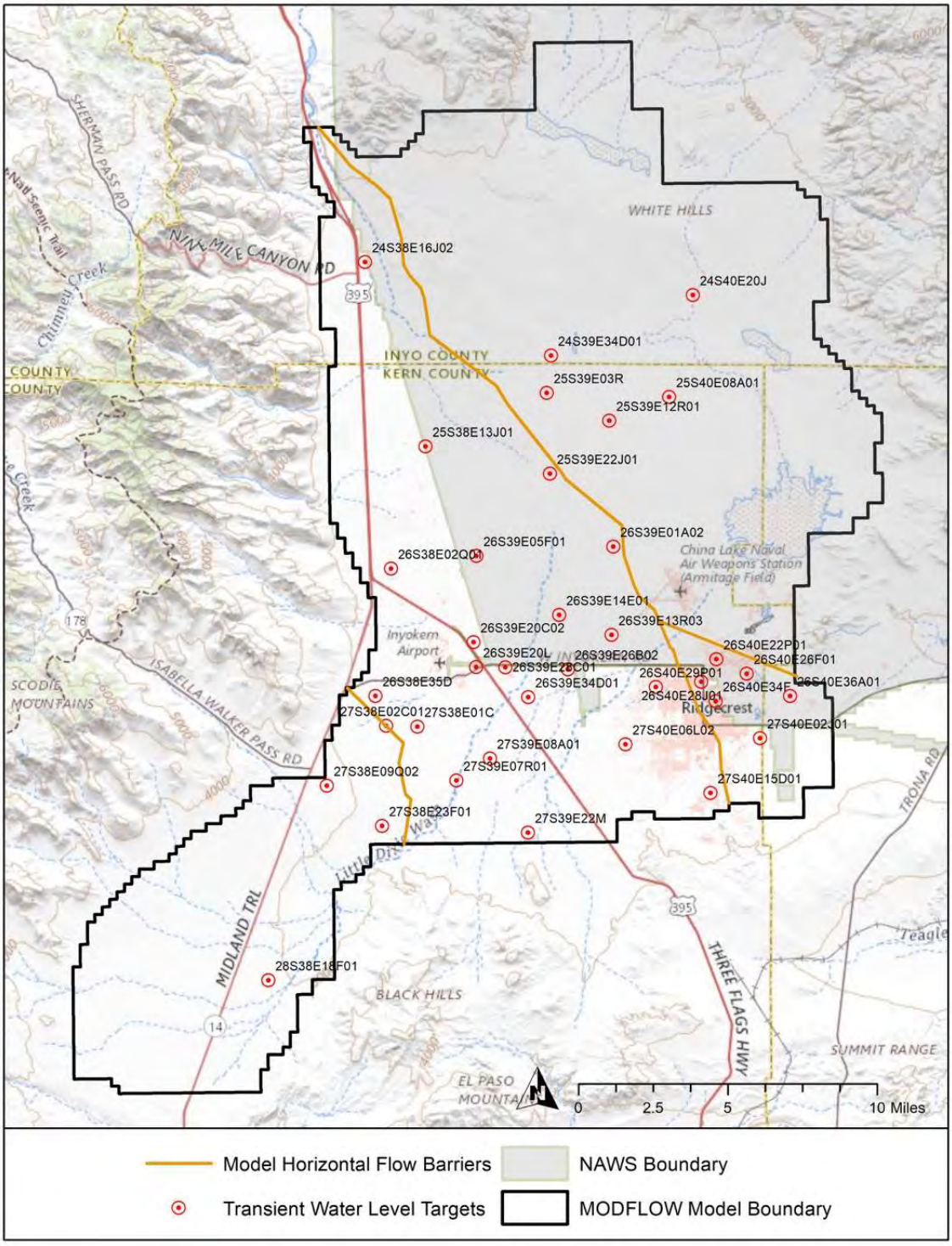


Figure 19. Locations of groundwater level targets used for calibration of the transient-historical flow model. Refer to Figure 3 for the names of the fault segments.

specific storage and specific yield. The values of the hydraulic conductivity and fault hydraulic characteristic parameters determined during calibration of the steady-state model were adopted unchanged in the transient-historical model. Model results were found to be insensitive to specific storage so this parameter was assigned a constant value of 3×10^{-6} ft^{-1} for all confined model layers.

The transient-historical model uses observed rates of water-level drawdown that resulted from groundwater withdrawals as a calibration metric to supplement the MAE of water level altitudes. This approach was used because errors in correctly simulating the rates of drawdown will have a large effect on forecasted water levels and thus is the critical factor for simulating the effect of overdraft conditions. The water-level altitude is generally controlled by hydraulic conductivity and recharge, parameters that were determined in the steady-state model, while drawdown rates are strongly affected by storage parameters. This approach minimizes errors in the calibration that might result from the model attempting to resolve offsets in water level altitudes simulated by the steady-state model.

A robust regression slope-fitting approach was used to remove observation outliers and compute the differences in slope of the simulated and observed water-level trends at the 36 observation locations. Ordinary least squares regression assumes a normal distribution of errors in the observed responses. If the data to be fitted contain erroneous or stress affected measurements, the resulting slope fit will be skewed by the outlier data points. A robust regression fit is better suited to these circumstances because the approach automatically removes outlier observations within the analysis period by assigning a weight to each data point. The weights are iteratively recomputed to exclude data points farther from model predictions.

For each simulated variation in the specific yield parameter, the difference in the slope of the head observations and the simulated head values is computed using the equation

$$MAE_{slope} = \frac{1}{n}\sum_{w=0}^{n} abs\{[\log(abs(S_{sim})) - \log(abs(S_{obs}))]\} \quad (2)$$

where MAE_{slope} = mean absolute error in the drawdown slope, n = number of monitoring wells, S_{sim} = drawdown slope (simulated), and S_{obs} = drawdown slope (observed). It was necessary to take the logarithm of the data to reduce the inherent bias of comparing values that span several orders of magnitude. This *MAE* results from taking the difference in logs and has no units.

An example result from the robust regression slope fitting approach for California state well number (SWN) 26S39E05F01 is shown in Figure 20. Red circles represent observed water levels, blue circles represent simulated water levels, and orange and green circles represent the observed and simulated water levels that were input to the regression model after outlier observations were removed. The observed drawdown slope is -2.35 ft/yr and the simulated slope is -2.56 ft/year corresponding to a slope difference of -0.21 ft/year. Plots of the simulated and measured groundwater level hydrographs over the transient-historical calibration period are provided for all monitoring wells used in the calibration in Appendix A.

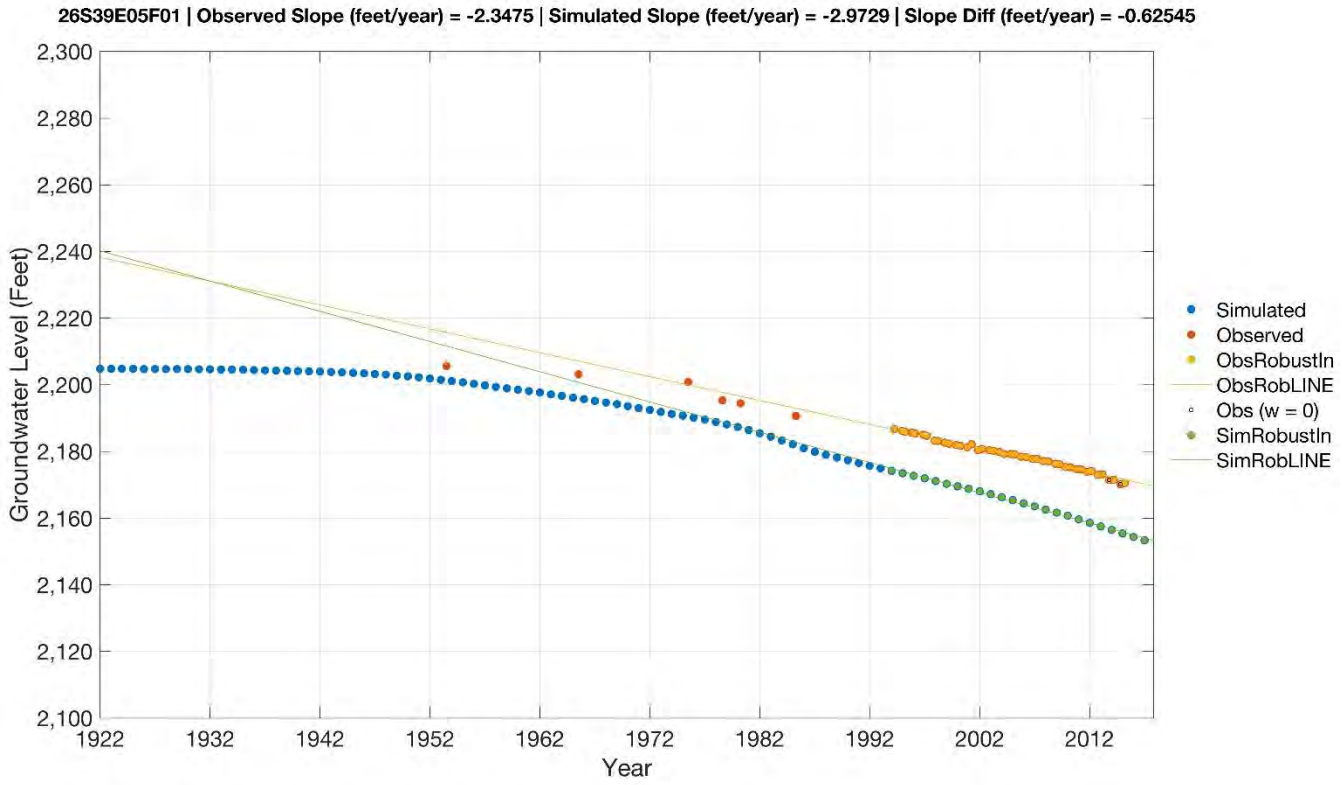


Figure 20. Example of the hydrograph slope-fitting method used for calibration of the transient-historical flow model. Plots for all monitoring wells used for the transient model calibration are provided in Appendix A.

The transient-historical model was manually calibrated using six values of specific yield that together represent a reasonable range for the basin-fill sediments. The calibration metrics that resulted from these runs are shown in Figure 21. The optimal solution using drawdown slope as the metric is obtained for a specific yield value of 0.225, whereas an optimum specific yield of 0.25 results when using MAE of water levels as the metric. Although these values are very close in magnitude, the value of 0.225 was selected because the optimal fit of drawdown slope is critical to effective forecasting of drawdowns for predictive pumping scenarios.

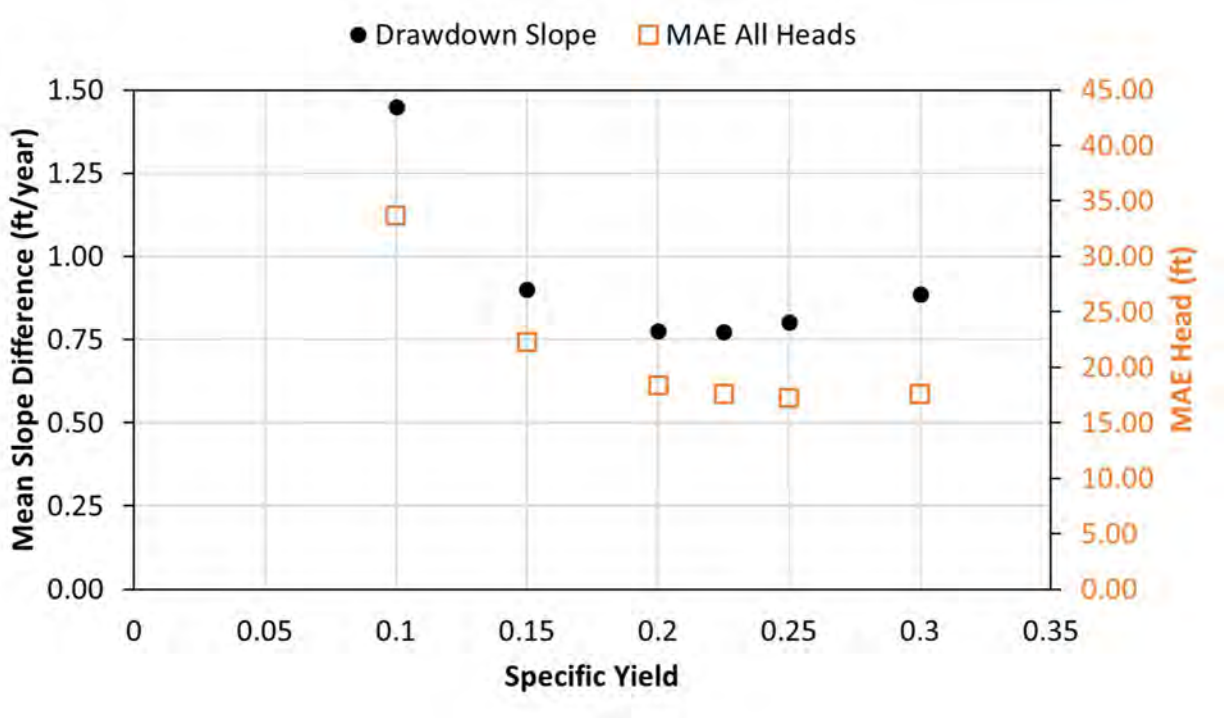


Figure 21. Results of calibration metrics Drawdown Slope and MAE of All Heads used for calibration of the transient-historical flow model.

Although the specific yield value of 0.225 was globally optimal, drawdown slopes were underpredicted in the southern portion of the basin. Manual adjustment resulted in a lower value of 0.08 that improved the fit to observed drawdowns and was found to be consistent with a value of specific yield of 0.04 estimated from the results of an aquifer testing program in the IWVWD southwest well field (Krieger & Stewart, 1996). The horizontal spatial distribution of specific yield throughout the model domain was obtained by kriging, with a value of 0.08 assigned around the IWVWD southwest well field and values of 0.225 used as constraints throughout the rest of the model. The results are shown in Figure 22. All model layers are assigned the same distribution of specific yield.

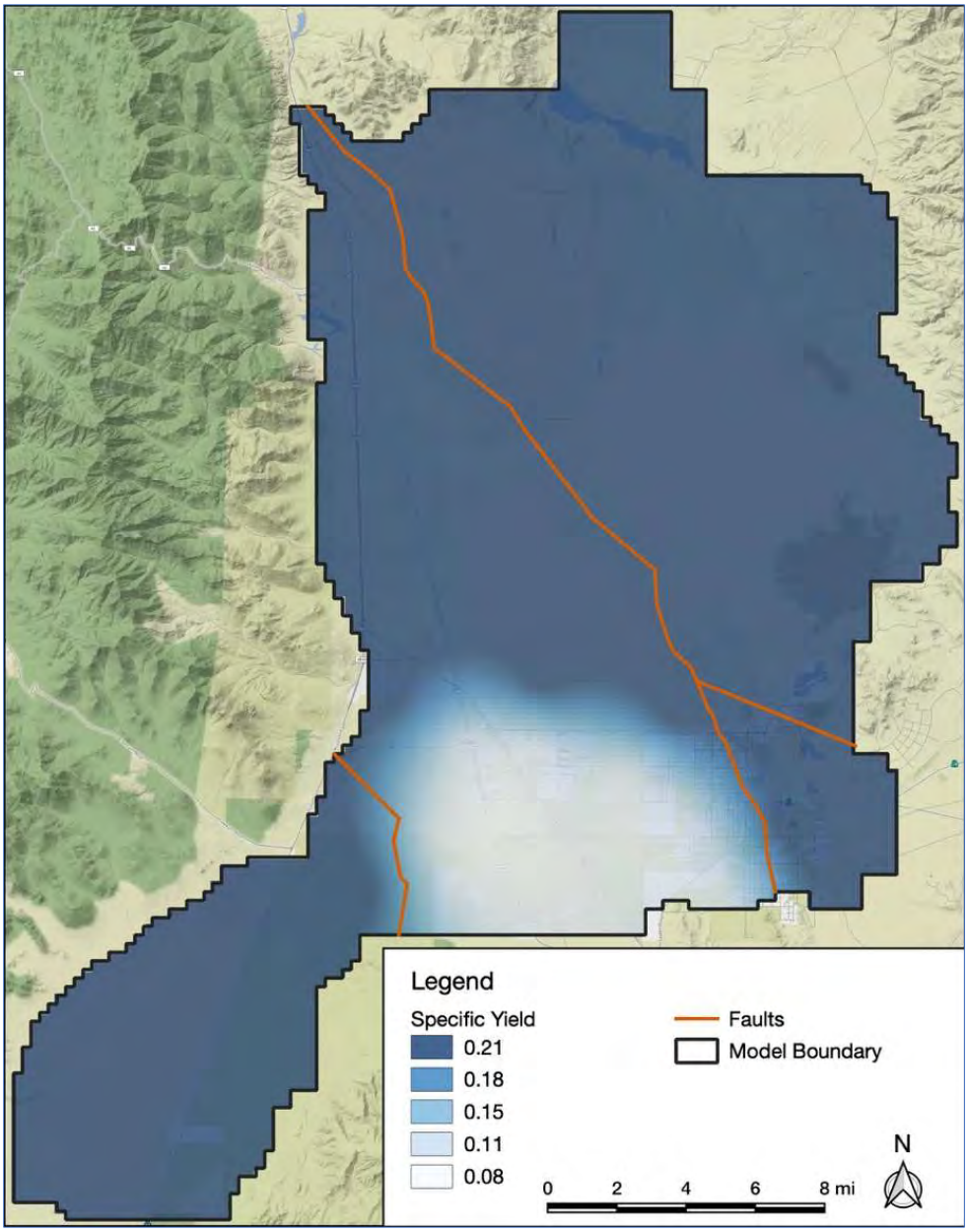


Figure 22. Spatial distribution of specific yield obtained by kriging in the calibrated transient-historical model. All model layers are assigned the same spatial distribution of specific yield. Refer to Figure 3 for the names of the fault segments.

The mean absolute error between simulated and observed water levels in the transient-historical model is 14 ft, which is higher than the value of 4.5 ft in the steady state model, but reasonable considering the challenges faced when using a regional model to fit to transient groundwater conditions measured at a local scale. The relative error in water levels is two percent, which is well below the 10-percent threshold that is generally considered an acceptable maximum relative error for use of the model as a tool for water-level predictions. Models with a relative error less than five percent are considered excellent (Anderson et al., 2015). Head residuals of the transient-historical model range from -128.4 to

+26.4 feet (Figure 23), with most residuals in the range between -14.0 and +14.1 feet. Bias between simulated and observed water levels is greater than in the steady state model; the transient-historical model shows a tendency to slightly underpredict some observed water levels (Figure 24). The underpredicted transient water levels at well 27S38E02C01 are described below. Most underpredicted water levels occur in the area where the northern El Paso joins the main basin, indicating that the hydraulic characteristics of the hydrogeologic system here are not well defined.

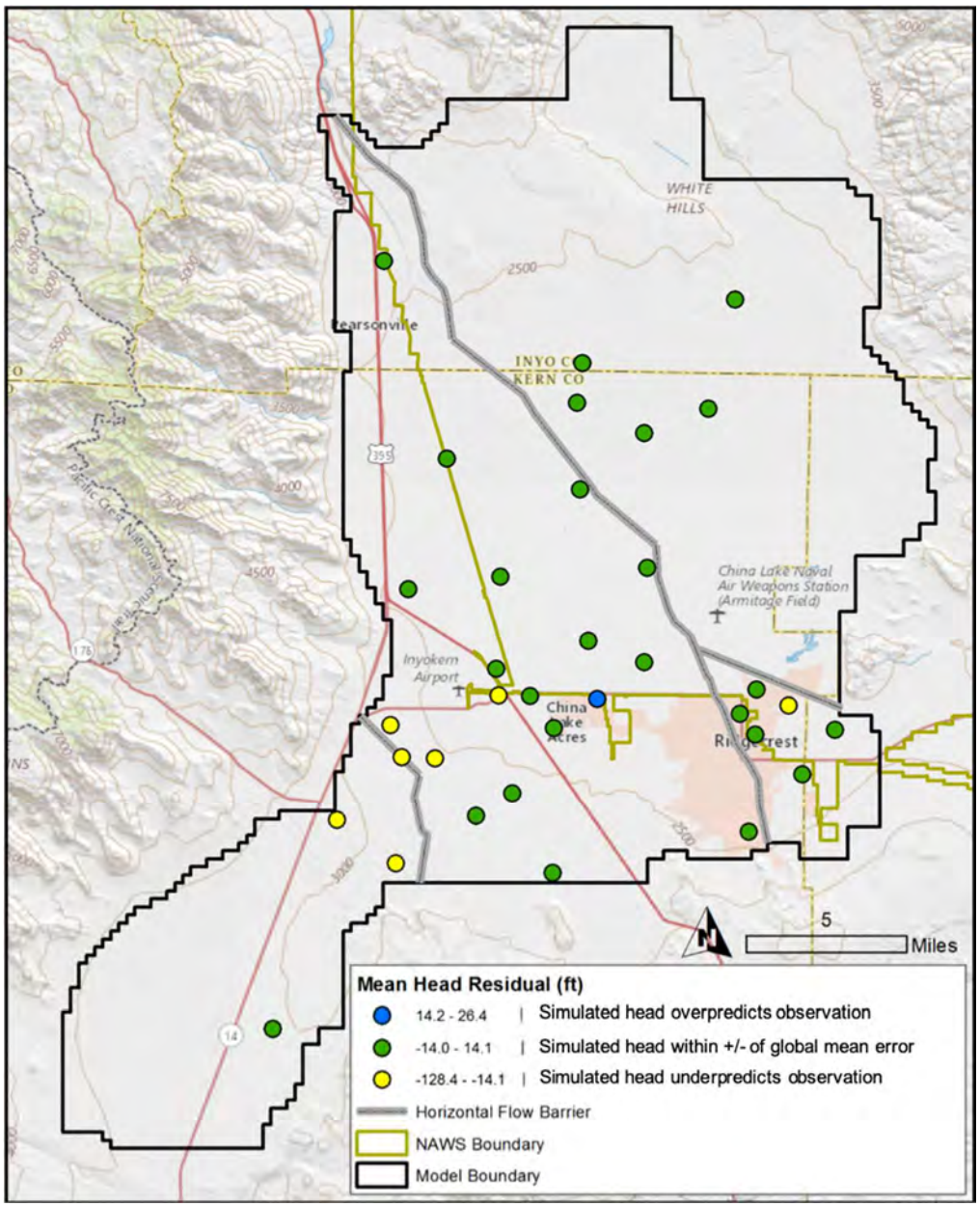


Figure 23. Mean residuals between simulated and observed groundwater levels for the calibrated transient-historical model. Refer to Figure 3 for the names of the fault segments.

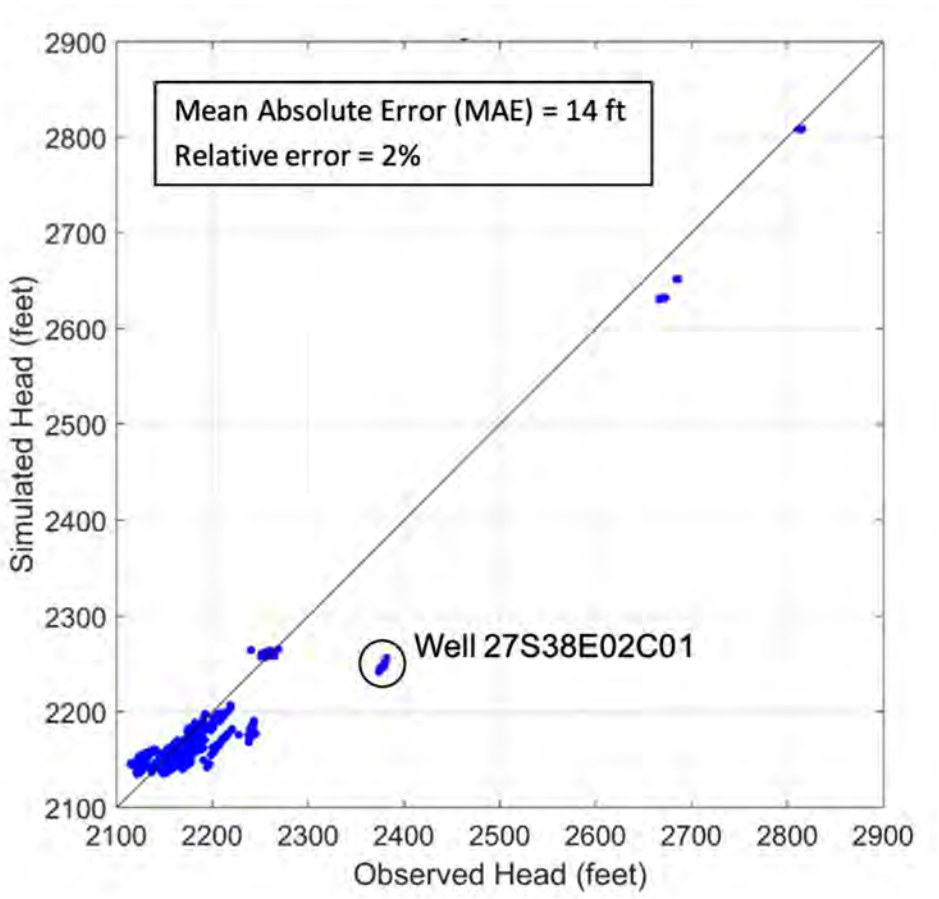


Figure 24. Plot of simulated heads to observed heads in the calibrated transient-historical model. Transient water levels at well 27S38E02C01 are described in the text.

The largest error between simulated and observed water levels occurs at well 27S38E02C01, which is located in a model cell through which also passes the El Paso Fault (Figure 25). The fault is simulated as a barrier to groundwater flow, causing a large decline in water levels as groundwater crosses the fault from southwest to northeast. The well is located in the fault zone, but the hydraulic barrier that represents the fault in the model bounds the model cell on the western and southern sides, meaning that this cell is located on the down-hydraulic-gradient side of the simulated fault barrier where heads are lower. MODFLOW simulates heads in the centroid of each cell, causing the transient heads in this cell to be simulated significantly lower than the observations at well 27S38E02C01. Mean residuals between simulated and observed drawdown slopes in the transient-historical model range from -1.99 ft/yr to +1.8 ft/yr, with most residuals in the 1.55-ft/yr range of -0.77 to +0.78 ft/yr (Figure 26).

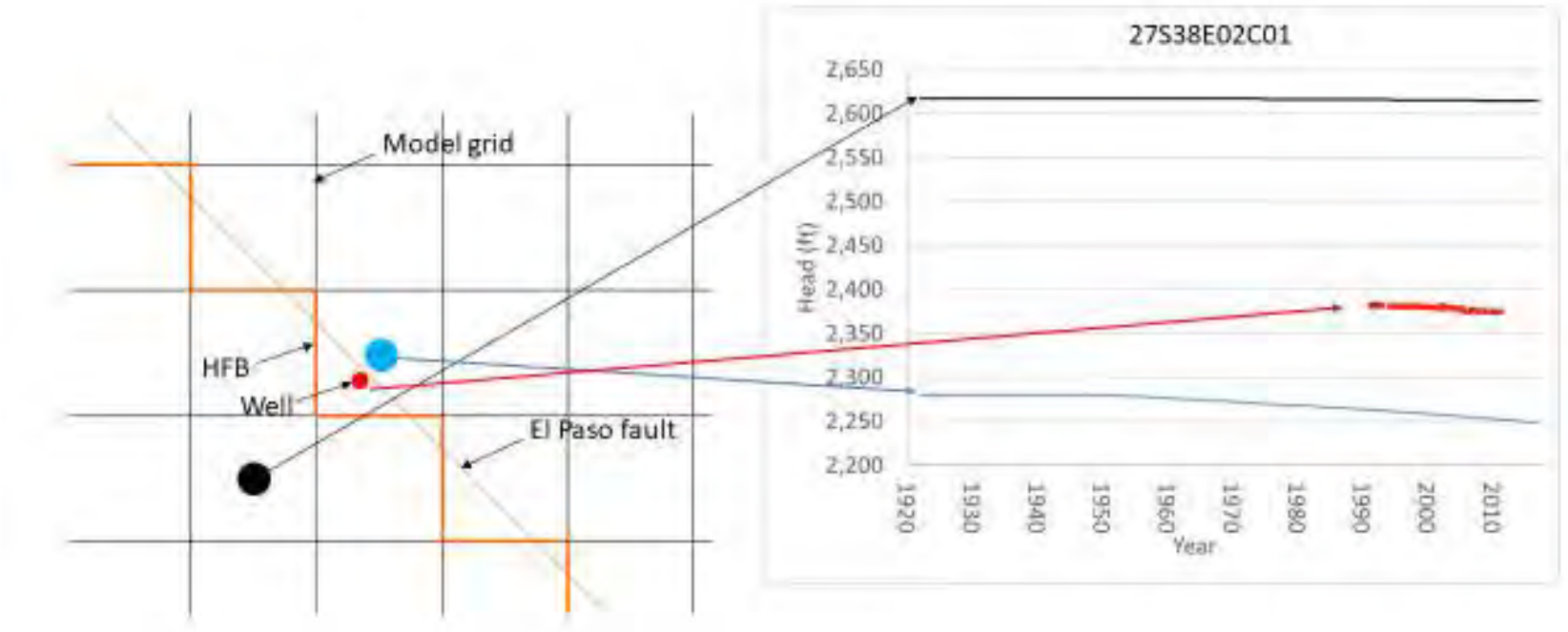


Figure 25. Simulated and observed heads at well 27S38E02C01 near the El Paso fault zone.

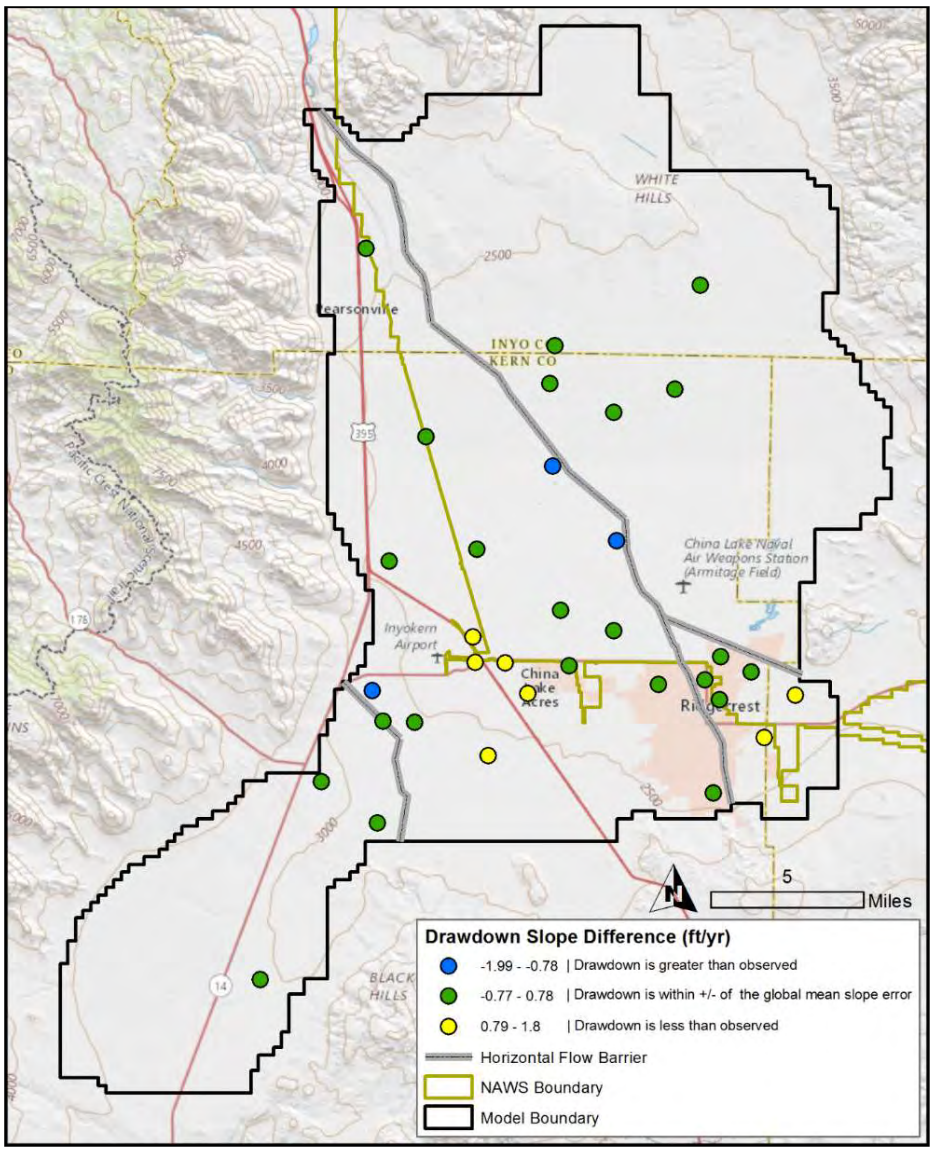


Figure 26. Mean residuals between simulated and observed drawdown slopes in the transient-historical model. Refer to Figure 3 for the names of the fault segments.

Water levels simulated by the transient-historical model in year 2016 are compared to water levels observed in 2016 in Figure 27. Groundwater flow directions and gradients are generally consistent, though local features represented by small numbers of grouped observations are not simulated by the model to the same degree because its larger scale limits accurate simulation of local detail. Note that the effects of the fault barriers are clearly seen in the contours of simulated head. The scarcity of observations points, particularly near faults, prevents the same effects from being revealed in the contours of observed water levels near most of the faults in the basin. Notably, high gradients in groundwater heads observed near the El Paso Fault indicate the barrier effect of this fault (Garner et al., 2017).

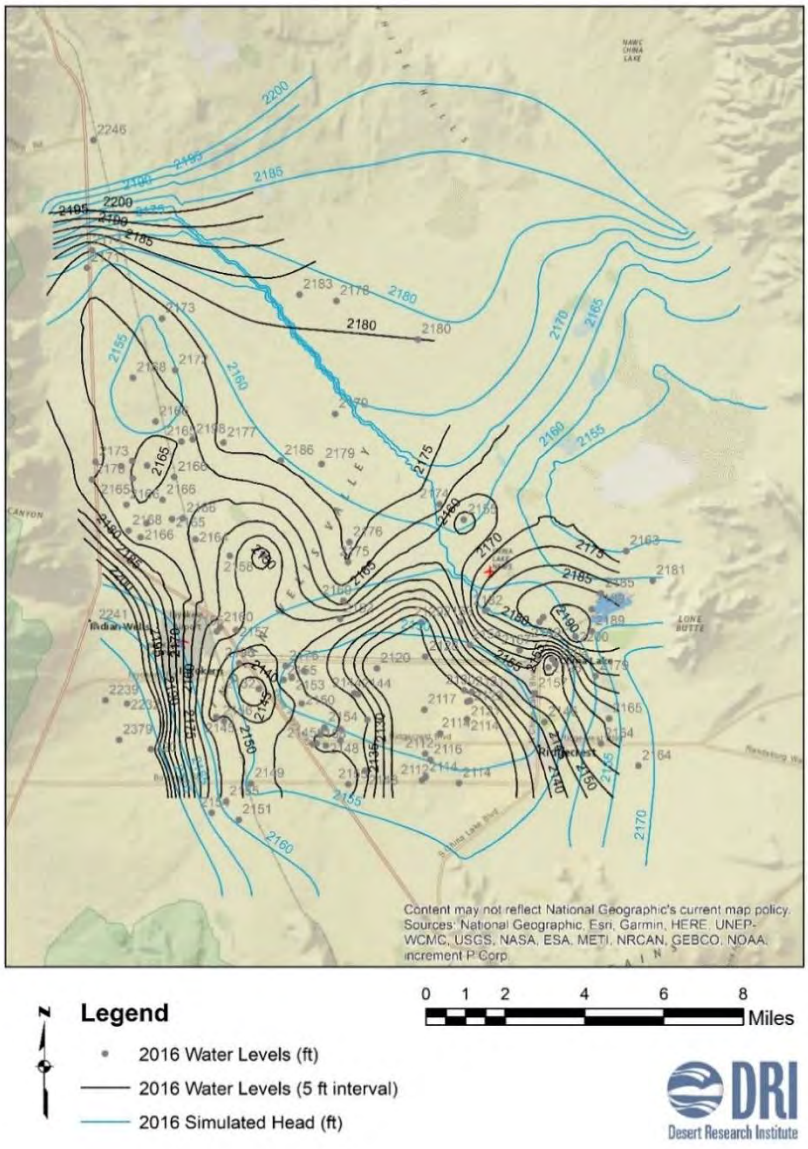


Figure 27. Comparison of water levels simulated by the transient-historical model to observed water levels for the year 2016.

As discussed previously, no direct measurements of ET over a multiple-year period are available in the basin. Instead, estimates of ET rate and ET extinction depth were made for phreatophytes and bare soil in eastern Indian Wells Valley and the model calculated ET based on depth to groundwater. The annual rate of ET computed by the transient-historical model declines from 7,600 AFY in 1922 to 2,852 AFY in 2016 (Figure 28). Also shown on Figure 28 are the ET rates estimated from enhanced vegetation index (EVI) values obtained from Landsat imagery covering the phreatophyte area in eastern Indian Wells Valley and the empirical relationship of Beamer et al. (2013). The plot shows an excellent agreement of the model-simulated ET to the EVI-estimated ET for the period 1997 through 2008. Most importantly, the similar slope of these ET trends indicates that the flow model is correctly simulating the processes that are contributing to the decline in ET observed in the eastern basin.

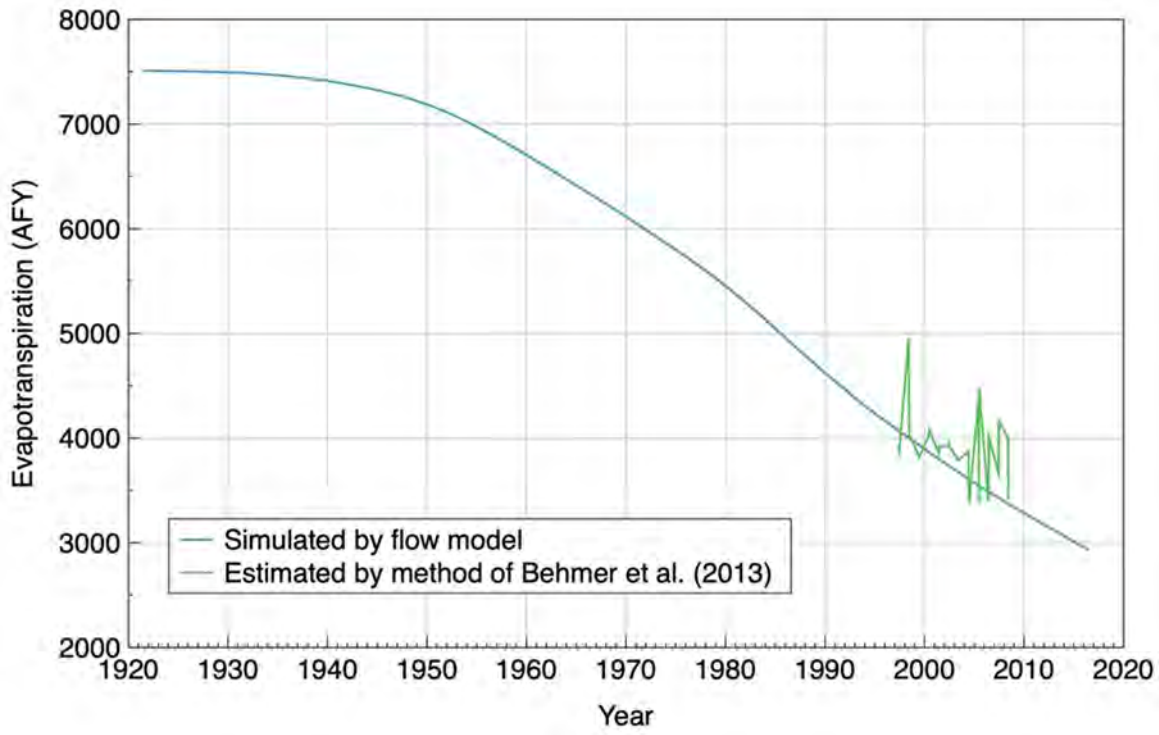


Figure 28. Evapotranspiration (ET) simulated by the transient-historical model plotted against ET estimated by the empirical relationship established by Beamer et al. (2013) between EVI and ET.

The groundwater budget for 2016, the final year simulated by transient-historical model, is tabulated in Table 4. Mountain block recharge is set at the same value of 7,650 AFY as in the steady-state model. However, drawdowns related to groundwater withdrawals during the transient stress period causes the outflow components of evapotranspiration (2,963 AFY) and interbasin flow to Salt Wells Valley (67 AFY) to be reduced from their values in the steady-state model. The area of ET and ET rates are reduced as water levels in the western basin decline below extinction depths. Similarly, hydraulic gradients near the boundary with Salt Wells Valley are reduced by declines in groundwater levels caused by pumping centers near Ridgecrest, which reduces the eastward-directed hydraulic gradient. The largest component of the transient-historical groundwater budget is groundwater pumping at a value of 24,472 AFY in 2016.

Table 4. Groundwater budget simulated by the transient-historical model for the year 2016.

INFLOW	**(acre-ft/year)**
Recharge	7,650
Coso and Argus Ranges	1,600
Rose Valley	2,400
Sierra Nevada North	2,100
Sierra Nevada South	1,500
El Paso sub-basin	50
Total:	**7,650**

OUTFLOW	**(acre-ft/year)**
Pumping (total)	24,473
Agricultural	12,363
Domestic	993
Municipal	7,142
NAWS	1,596
SVM	2,379
Evapotranspiration	2,934
Flow to Salt Wells Valley	74
Total:	**27,481**
CHANGE IN STORAGE	**-19,831**

2.6 Sensitivity Analysis

A sensitivity analysis of the flow model was performed to identify the parameters and boundary conditions that model results are particularly responsive to. For this analysis, a version of the transient-historical flow model was run in forward mode for the years 2018 through 2067. Five model parameters were adjusted in individual model runs using values that were 50 percent and 150 percent of their calibrated values and the effects of these adjustments on simulated heads were evaluated. Values of three of the parameters, specific yield, specific storage, and recharge, are constant throughout the simulation period and model domain or in specific zones within the model domain. The base values of these parameters are the values used in the transient-historical model previously described and their values as used in the sensitivity runs are shown in Table 5. Hydraulic conductivity varies spatially in the model, by cell in Layer 1 and by zones in Layers 2 through 6, so their many values are not included in Table 5. However, this parameter was adjusted in the same way, the base K value in every model cell was adjusted by 50 percent and 150 percent. The annual variation in recharge rate used in the transient-predictive models was also incorporated in this analysis by adjusting each yearly rate by 50 percent and 150 percent. Groundwater withdrawals were set at a constant rate of 24,473 AFY, the rate used in the final year of the transient model.

Table 5. Values of constant parameters used in the sensitivity analysis. Separate sensitivity runs addressed hydraulic conductivity and annual variation in recharge rate. See text for explanation.

Parameter	Parameter Value		
	50%	Base	150%
Constant Recharge Total	3,825	7,650	11,474
Coso and Argus Ranges	800	1,600	2,400
Rose Valley	1,200	2,400	3,600
Sierra Nevada North	1,050	2,100	3,150
Sierra Nevada South	750	1,500	2,250
El Paso sub-basin	25	50	75
Specific Yield	0.1125	0.225	0.3375
Specific Storage	5.00E-07	1.00E-06	1.50E-06

Simulated heads were evaluated at four wells, three in the main basin and one in the El Paso sub-basin (Figure 29). These locations were chosen to represent areas of the model of particular interest for management of groundwater resources, including important municipal and agricultural pumping centers. The effects of the adjusted parameters are shown in Figures 30 through 32. The sensitivity coefficient, defined as the difference between the drawdown for 50 percent and 150 percent of the base values, is calculated for each of the four wells for each parameter and then averaged to provide an overall sensitivity coefficient for each parameter. Model sensitivity is dominated by specific yield, all other parameters have moderate to low effect on simulated heads (Figure 33). The value of specific yield is an important factor for forecasting drawdowns in response to future pumping scenarios, but data supporting the choice of this parameter are limited in the basin. Conducting additional pumping tests with one or more observation wells can reduce the uncertainty in this parameter and provide information of how it varies within the basin-fill aquifers. The uncertainty in hydraulic conductivity can also be reduced through analysis of additional pumping tests.

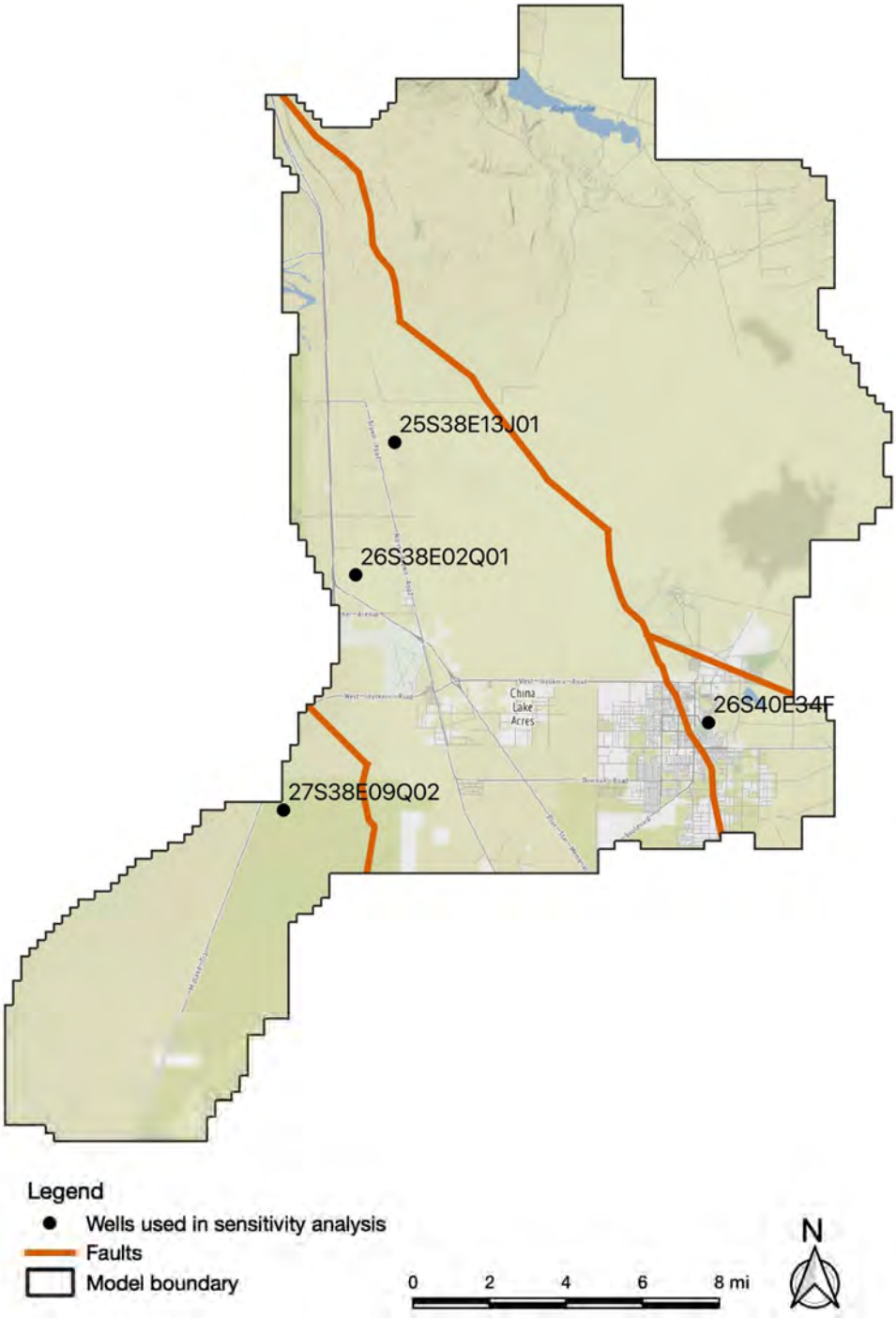


Figure 29. Locations of wells used for water-level observations in the sensitivity analysis. Refer to Figure 3 for the names of the fault segments.

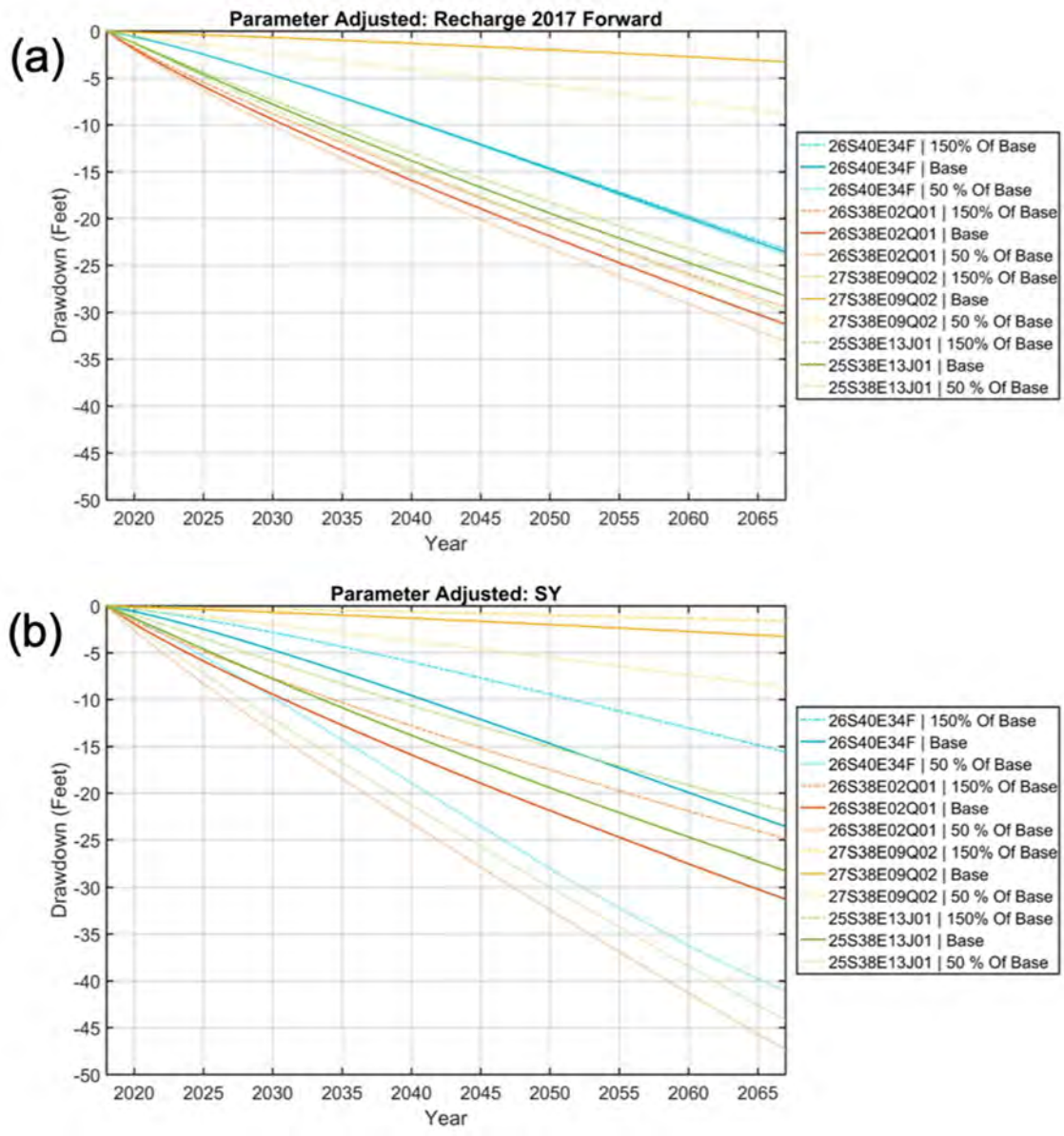


Figure 30. Results of sensitivity analysis for constant recharge rates (a) and specific yield (b). The sensitivity coefficient for each parameter is defined as the difference between the drawdown for 50 percent and 150 percent of the base values.

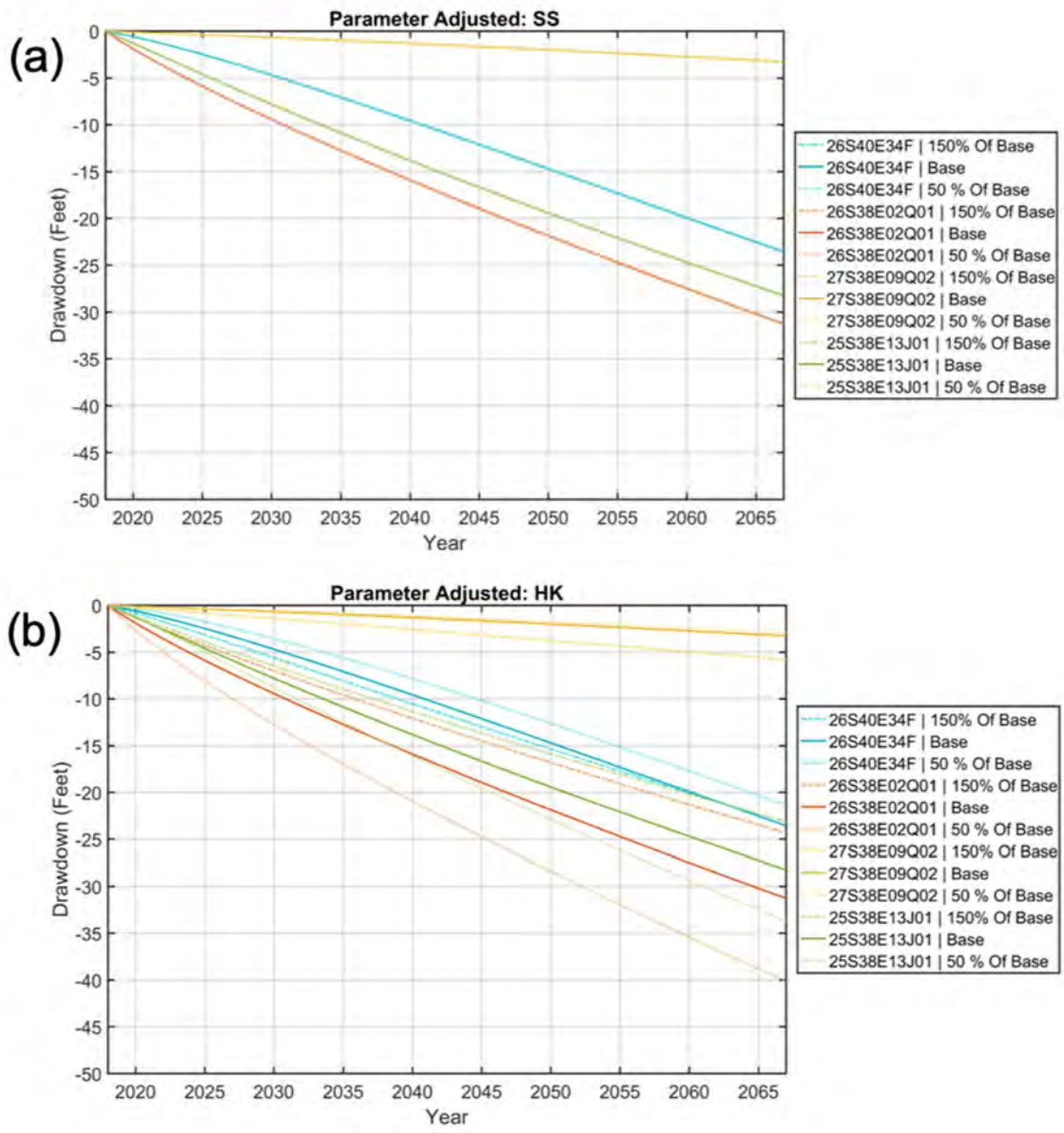


Figure 31. Results of sensitivity analysis for specific storage (a) and hydraulic conductivity (b). The sensitivity coefficient for each parameter is defined as the difference between the drawdown for 50 percent and 150 percent of the base values.

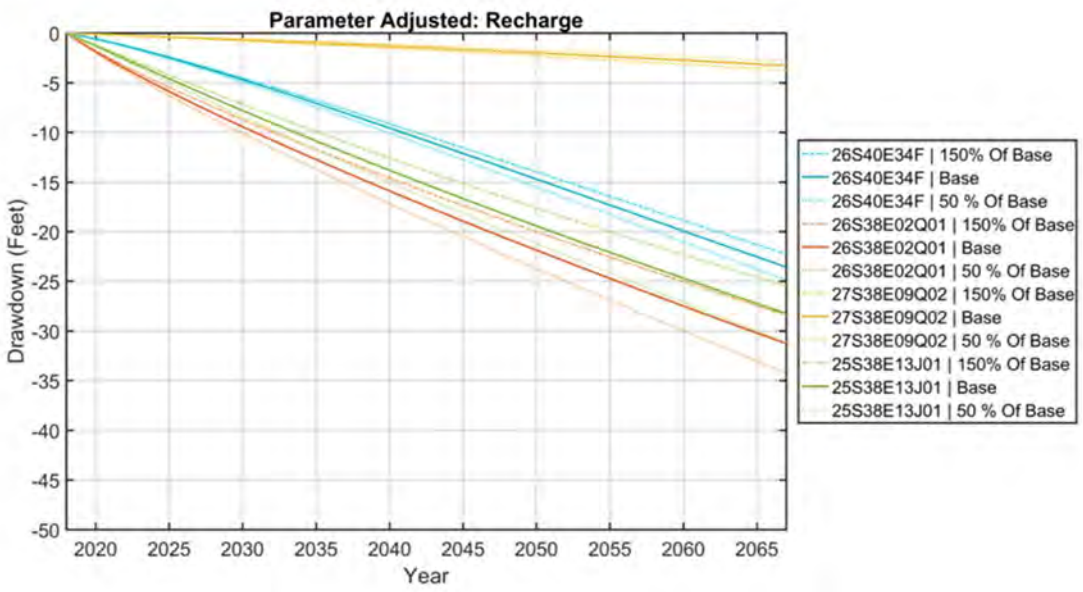


Figure 32. Results of sensitivity analysis for annually variable recharge rate. The sensitivity coefficient for each parameter is defined as the difference between the drawdown for 50 percent and 150 percent of the base values.

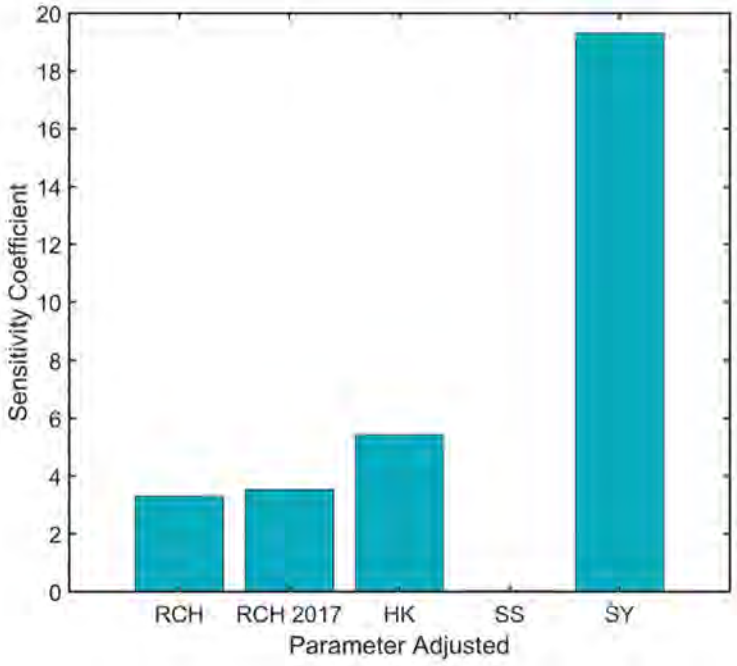


Figure 33. Comparison of the sensitivity coefficients for the five parameters adjusted during the sensitivity analysis.

2.7 Predictive Flow Models

Two predictive flow models were developed from the calibrated transient-historical model to forecast responses of the groundwater flow system to possible future alternative groundwater management scenarios. The baseline flow model simulates a "no action" alternative, where most groundwater withdrawal rates and locations that occurred in 2016 are continued into the future with annual increases to account for modest population growth. The scenario 6.2 flow model simulates the groundwater allocation and management plans described in the Groundwater Sustainability Plan, and includes artificial recharge of imported and recycled water. In both models, a three-year transition period from 2017 through 2019 is used to equilibrate the model to a withdrawal rate of 35,000 AFY that is held constant during the 3-year transition. The predictive model simulations then begin in the year 2020 and extend through 2070 utilizing the annual rates of groundwater withdrawal and artificial recharge shown in Figure 34. Groundwater withdrawals are simulated at the 938 wells included in the pumping allocations for the baseline and 6.2 scenarios, as described in the GSP.

As discussed in Section 2.4.3, natural recharge rates in the predictive models are varied by scaling the constant rate of 7,650 AFY by the annual precipitation amounts observed in and near Indian Wells Valley over a balanced hydrologic period from 1990 through 2014 (Stetson Engineers, 2018). This 26-year period is then repeated to obtain the natural recharge input for the predictive models. Other than this variability in natural recharge and the two scenarios of groundwater withdrawal and artificial recharge, there are no differences between the predictive flow models and the calibrated transient-historical flow model.

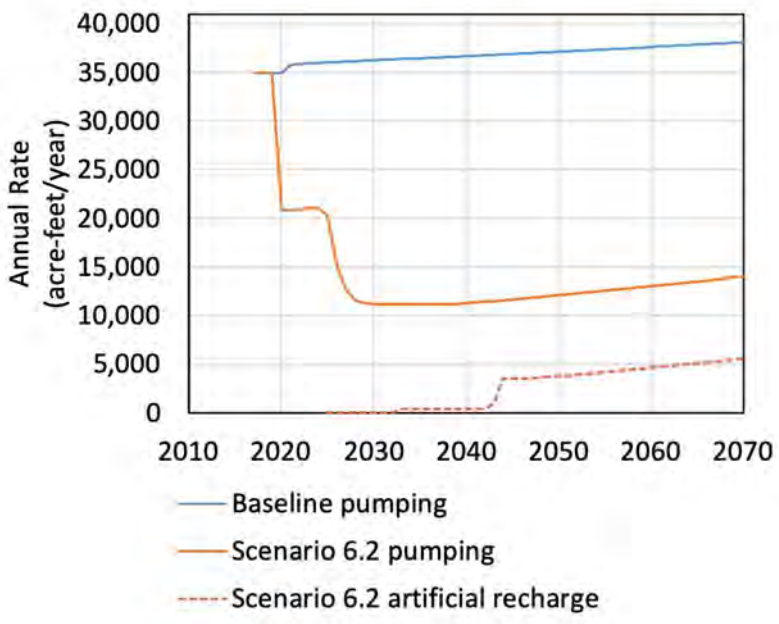


Figure 34. Annual rates of groundwater withdrawal and artificial recharge included in the Baseline and Scenario 6.2 models.

The results forecast by the baseline and scenario 6.2 predictive flow models were presented to the Technical Advisory Committee (TAC). These presentations are included in Appendix 3-H of the Groundwater Management Plan. Included are comparisons of changes in groundwater levels from 2020 through 2070 as maps and hydrographs for selected wells, plots of the change in groundwater storage, plots of evapotranspiration, and the groundwater budgets for the entire basin.

3. Transport Model

3.1 Introduction

Saline groundwater that underlies portions of Indian Wells Valley may reduce water quality in production wells if these poor-quality groundwaters are drawn toward pumping centers. Evidence of increasing salinity in some production wells in the southeastern basin near Ridgecrest has been shown by Berenbrock and Schroeder (1994) and Todd Engineers (2014). Solutes in groundwater within Indian Wells Valley are conceptualized as originating from recharge from surrounding mountain ranges, groundwater flow from surrounding basins, mixing with remnant evaporative brines and geothermal fluids, and concentration by evaporation. Solutes are removed from the groundwater system by discharge to Searles Valley to the southeast. McGraw et al. (2016) summarized numerous studies that together identify areas of generally higher salinity groundwater to the east near China Lake Playa, to the northwest toward Rose Valley, around eastern Ridgecrest, and in several other locations associated with clay horizons or geothermal zones. Evidence of increasing salinity in wells in the Ridgecrest area has been documented by Berenbrock and Schroeder (1994) and Todd Engineers (2014). The Indian Wells Valley transport model was developed to investigate how the distribution of salinity within the groundwater system may be influenced by alternative scenarios for groundwater management.

3.2 Code Selection and Documentation

The MT3D-USGS: Groundwater Solute Transport Simulator for MODFLOW was applied to assess the effects of pumping on groundwater quality over time. The model was constructed using the Groundwater Modeling System (GMS) environment (version 10.2) developed by Aquaveo, LLC. As for the flow model, GMS serves as a database for all of the hydrogeologic information in the model and provides an easy to use graphical pre- and post-processor interface to MODFLOW/MT3D-USGS. Although developed within GMS, the MT3D-USGS input and output files are in standard MODFLOW format and the model can be run without the use of GMS.

3.3 Configuration

The framework of the transport model coincides with the groundwater flow model of Indian Wells Valley, employing the same model domain, grid structure, and layers. MT3D solves the transport equations using the groundwater flow rates and directions simulated by the groundwater flow model. The transport model uses total dissolved solids (TDS) concentrations as a surrogate for groundwater salinity to forecast TDS concentrations from the present to the year 2070 by incorporating the volumetric groundwater flow rates simulated by the flow model for the GSP management scenario. Stress periods of one month are used to be consistent with the transient-predictive flow model. The results are presented as maps showing the spatial distribution of forecasted TDS concentrations for selected times, and maps showing rates of change of TDS concentration for selected times. The concentration units in the model and in the plots are mg/L.

Two transport models were developed using the flow results from the predictive groundwater flow models described in Section 2.7 to forecast movement of solutes in response to possible alternative scenarios for groundwater management. The baseline model simulates a “no action” alternative, where most groundwater withdrawal rates and locations in place in 2016 are continued into the future with annual increases to account for modest population growth. The scenario 6.2 model simulates the groundwater allocation and management plan described in Section 3.5.5 of the GSP, and includes artificial recharge of imported and recycled water. The transport simulations begin in the year 2020 and extend through 2070.

3.4 Initial and Boundary Conditions

A database of wells and groundwater TDS concentrations over time was developed by Stetson Engineers Inc. from TDS measurements compiled from numerous sources, with the majority obtained from the Groundwater Ambient Monitoring and Assessment Program (GAMA) database (California Water Board, 2018), publications by the U.S. Geological Survey (including Moyle, 1963; Berenbrock, 1987, and Berenbrock and Schroeder, 1994), data from Meadowbrook Dairy (E. Teasdale, personal communication, Sept. 11, 2018), and a database by the Kern County Water Agency (2018). The database includes 563 locations and 2,006 TDS values, with data collected over a 70-year period.

The TDS initial condition dataset for the transport model was developed from a subset of the full database. Wells with unknown depth or screened interval were excluded from the initial condition data set. Historical TDS measurements did not provide uniform coverage over time and therefore the most-recent TDS concentration was selected at each well as the initial value (Figure 35). This approach provides an approximation of initial conditions for the basin for forecasts into the future, but does not account for historical variation or trends in TDS concentrations at individual wells. The TDS concentrations of the most recent measurements and their locations are shown in Figure 36.

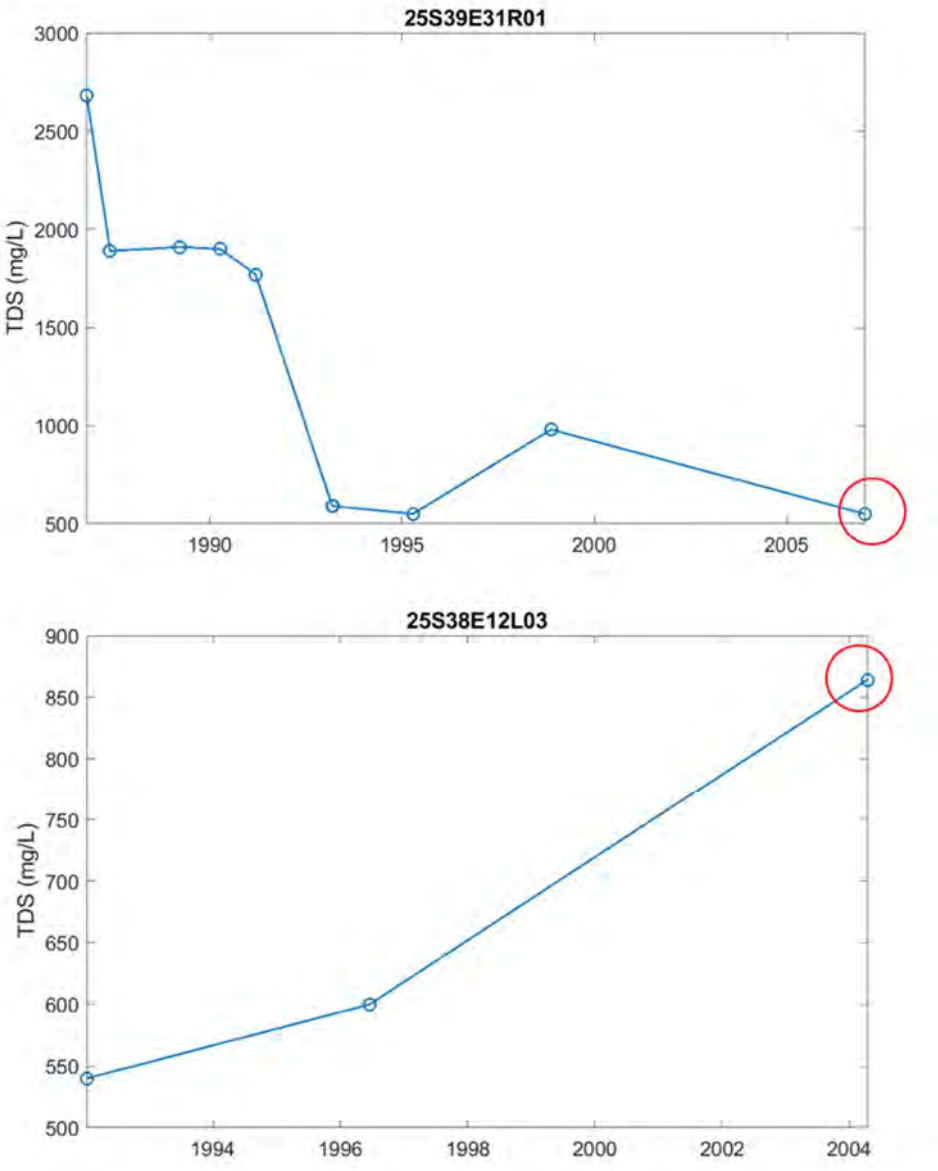


Figure 35. Examples of TDS temporal trends and the selection of the most recent TDS concentration (indicated by red circles) for wells having multiple measurements. Using this approach, the initial TDS data set represents the most recent data for the basin, though historical trends at individual wells are not explicitly included.

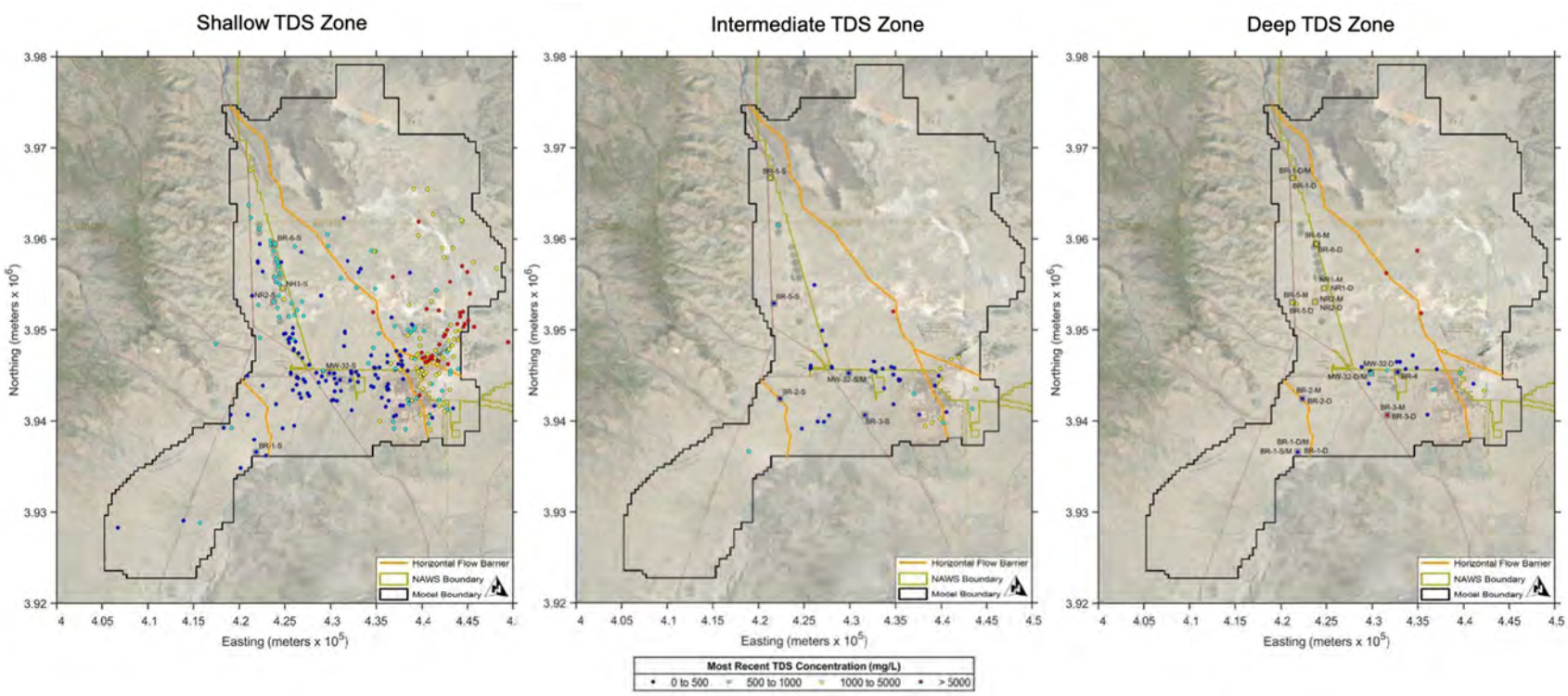


Figure 36. Locations of wells and the most recent TDS concentrations in the three TDS zones used to develop the TDS initial conditions for the transport model. The TDS scale shown applies to all three TDS Zones. Refer to Figure 3 for the names of the fault segments.

Because of sparse horizontal and vertical data coverage, particularly for model layers 2 through 6, it wasn't possible to interpolate the measurements to each model layer independently, so the measurements were assigned to one of three vertical zones (Shallow, Intermediate, and Deep). The Shallow TDS zone includes measurements within the depth range of flow model layer 1, where most measurements are located. TDS measurements are limited below layer 1, so the lower portion of the model was divided into two TDS zones. The Intermediate TDS zone corresponds to flow model layers 2 and 3, and the Deep TDS zone includes measurements within the depth ranges of flow model layers 4, 5, and 6. Each well was assigned to one of the zones based on the centroid of the depth of its screened interval. In the case of the fourteen wells that have multiple screens within a single TDS zone, the arithmetic mean of their measured concentrations was computed and used as the initial condition in that zone (Figure 37). The mean TDS values were not weighted by the relative flow rates contributed by screens at multiple depths because flow-rate data were generally unavailable. An example cross section through the model showing the configuration of the three TDS zones is shown in Figure 38. The locations of wells where the means of multiple TDS concentrations were calculated for a single zone are shown in Figure 39. The refined database is comprised of 391 well locations.

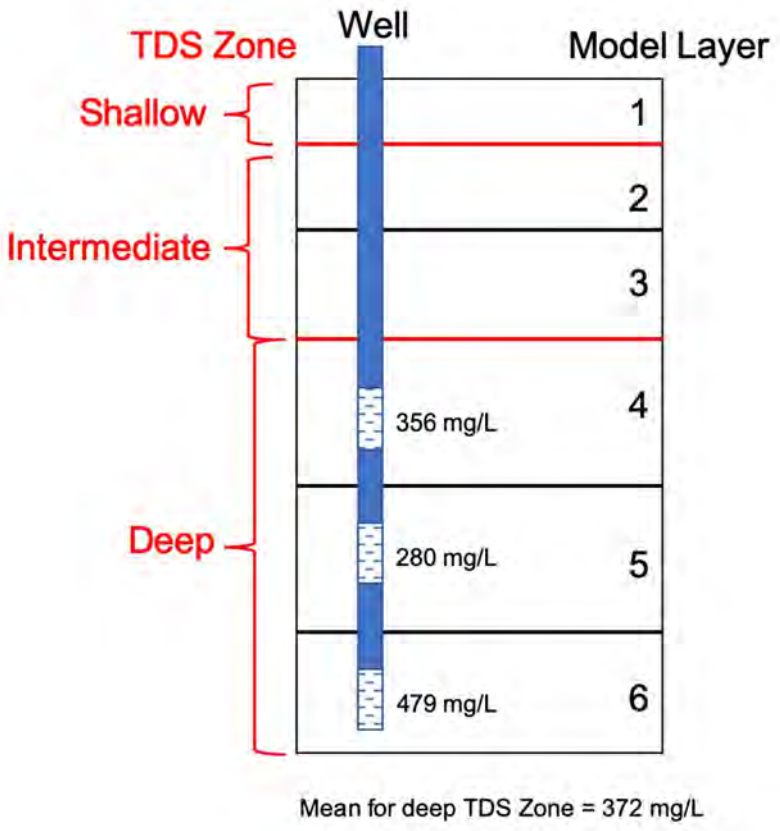


Figure 37. Example of calculation of mean TDS values at wells having multiple measurements in a single TDS zone.

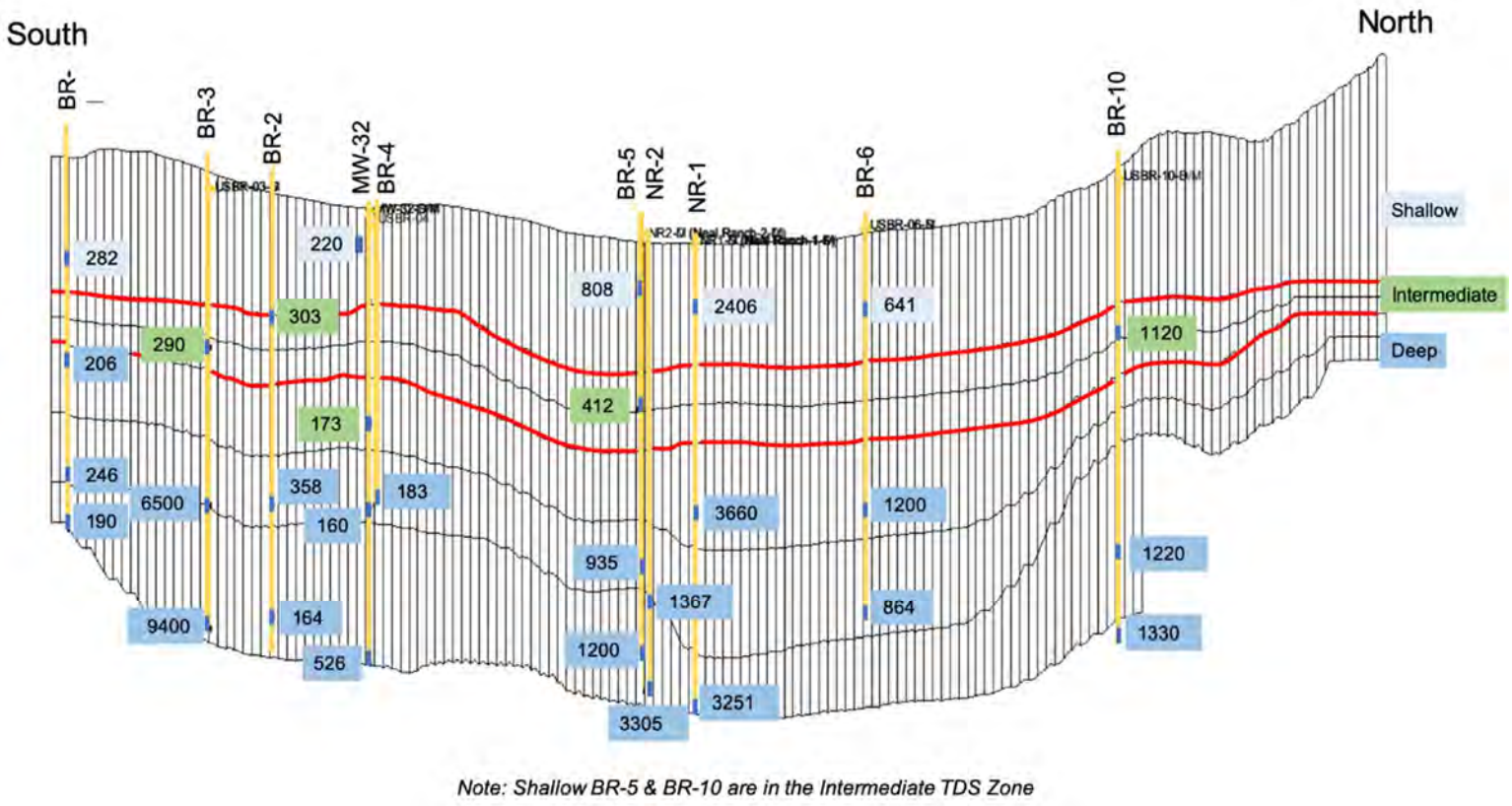


Figure 38. An example North-South cross section through the transport model illustrating the relationship between of the Shallow, Intermediate, and Deep TDS zones (separated by red lines) to the six computational layers in the flow model. TDS measurements at selected well locations are shown to illustrate the averaging of multiple values within a zone. Measured TDS concentrations were interpolated to the transport model grid cells based on the TDS zone in which they fall.

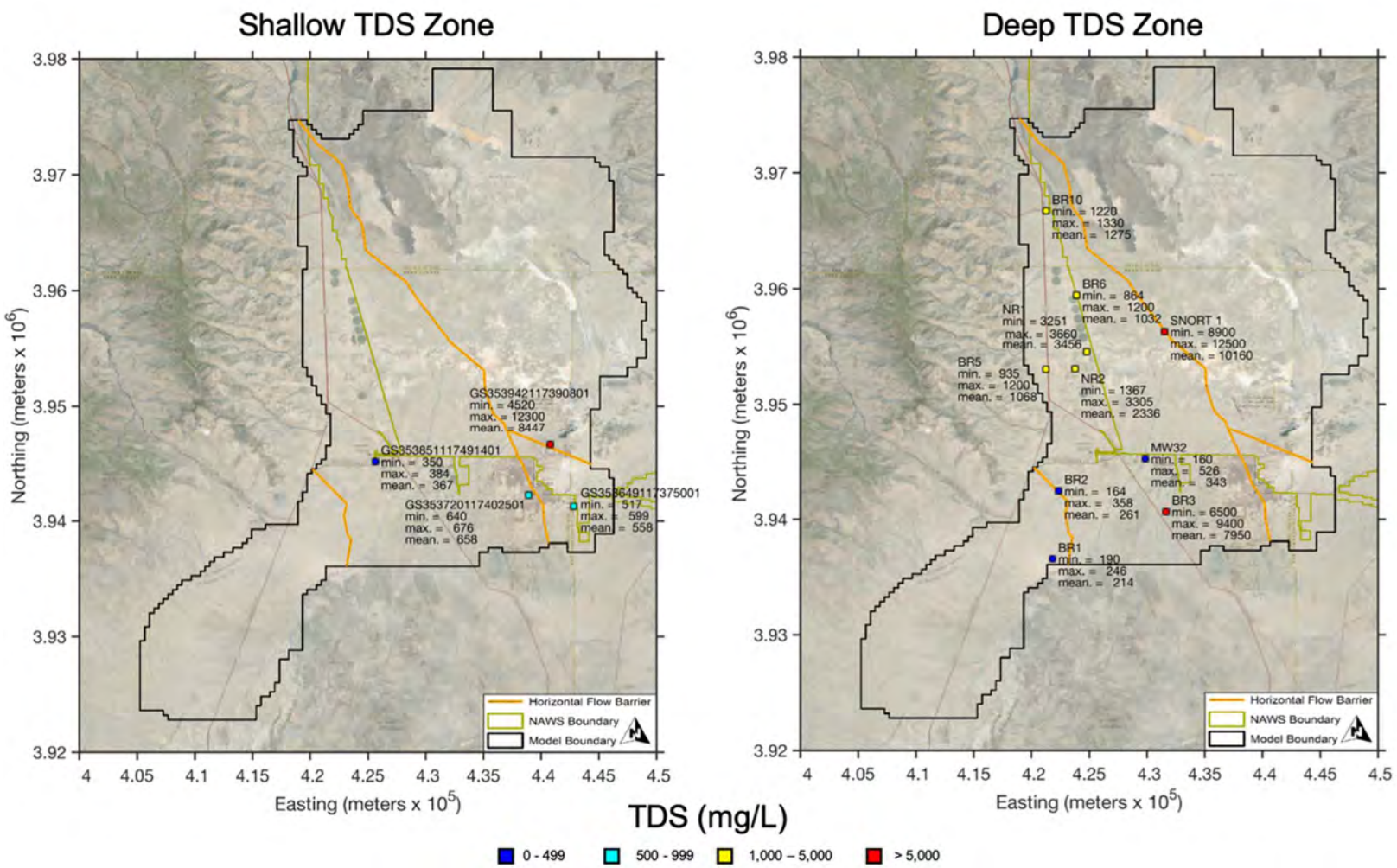


Figure 39. Locations of wells having multiple screens and TDS measurements in the Shallow and Deep TDS zones. There are no wells of this type in the Intermediate TDS zone. Refer to Figure 3 for the names of the fault segments.

Initial TDS conditions for the transport model were developed by spatial interpolation of the TDS values in the refined database within the shallow, intermediate and deep TDS zones. Each active model grid cell was assigned an initial TDS value based on the zone-layer relationship defined above. Kriging was used to interpolate the point data using a semivariogram structure with no nugget, a range of 1.1 km, and a variance of 1.9×10^7 $(mg/L)^2$ to fit the experimental variogram. Kriging interpolation was performed on the $\log_{10}$ of the TDS concentration values because of the large range in values. The interpolated TDS maps for the three TDS zones are shown in Figure 40. In areas where no TDS measurements exist, control points were established to fully populate the model domain (open squares in Figure 40) and ensure that the interpolated TDS distributions were consistent with conceptualized TDS distributions. These points were assigned a value of 1,500 mg/L in the northern basin and a value of 450 mg/L in the El Paso sub-basin. In both cases, the values were selected to be consistent with TDS measurements in nearby areas of the basin. The spatial distribution of interpolated TDS is generally consistent with the salinity patterns identified by previous studies (e.g. Berenbrock and Schroeder, 1994; Morgan, 2010). For example, TDS in the northwest and east-central portions of the basin is higher in the intermediate zone than in the shallow zone, corresponding to the finer-grained material at these depths in these areas. TDS is also higher in the area of China Lake playa, where groundwater concentrations of some major ions increase because of geochemical reactions with lacustrine deposits (Berenbrock and Schroeder, 1994).

Groundwater recharge carries dissolved solutes into the groundwater system (Figure 41). The TDS concentration of recharge along the western edge of the model was assumed to be 67 mg/L in the previous Navy model (McGraw et al., 2016), based on measurements in “recharge areas of the high Sierra Nevada” reported by Güler and Thyne (2004). However, those locations are associated with springs above 6,500 ft elevation. A value of 356 mg/L represents samples from the Sierra Nevada and other mountain ranges at elevations mostly below 6,500 ft. Citing Maxey (1968), Güler and Thyne (2004) point out that these lower elevation areas provide the majority of recharge to basin-fill aquifers. This led to the choice of 350 mg/L during initial transport model development. Following an update to the TDS database by Stetson Engineers in January 2019, the TDS concentration for the southern Sierra Nevada boundary was revised to 450 mg/L to reflect TDS measurements in the range of 447 to 630 mg/L in wells in southern El Paso sub-basin.

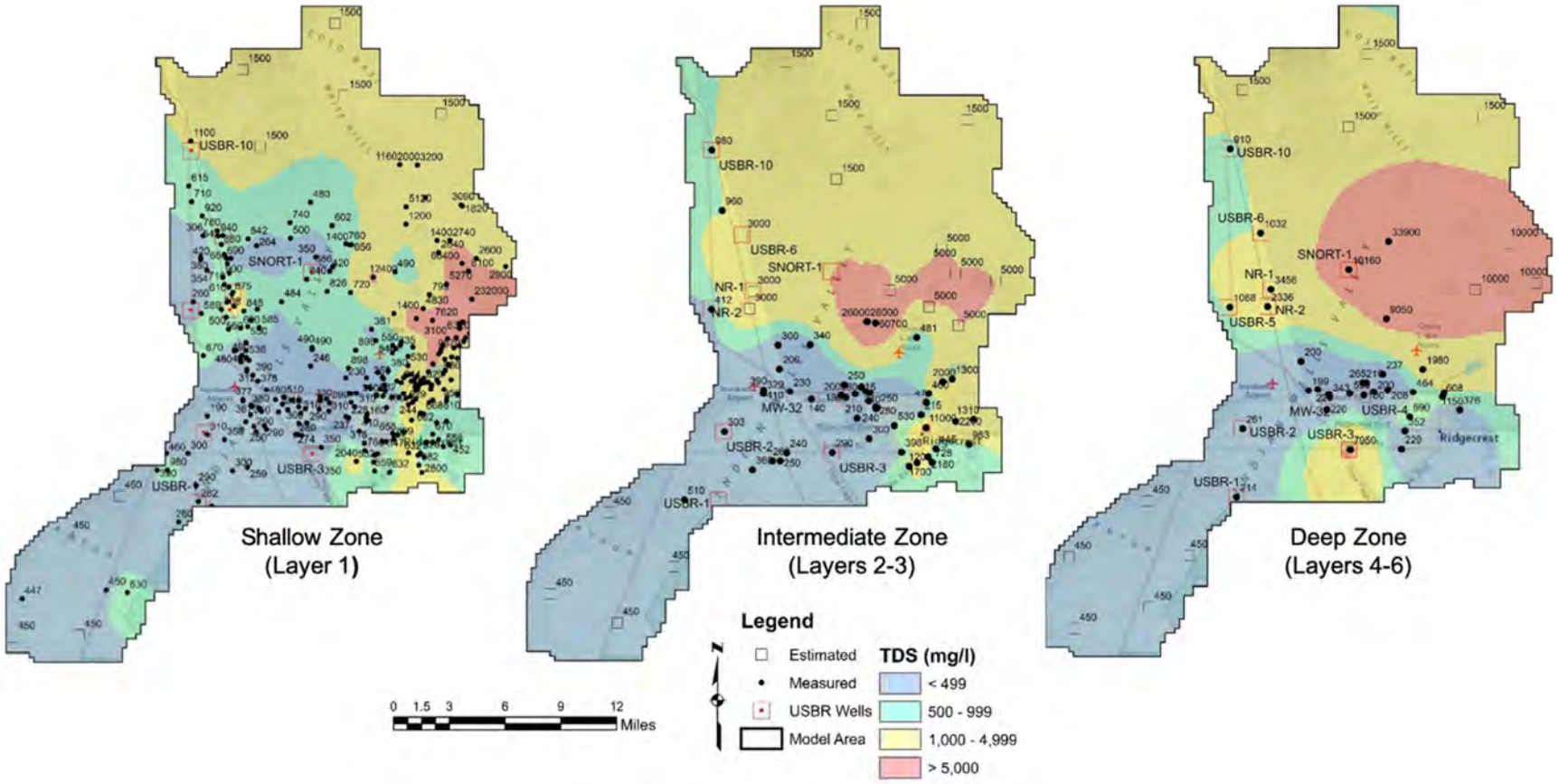


Figure 40. Spatial distributions of TDS concentration in the three TDS zones that are used for initial conditions in the transport model. Hollow squares are control points used to improve interpolation. These points were assigned a value of 1,500 mg/L in the north northern basin and a value of 450 mg/L in the El Paso sub-basin.

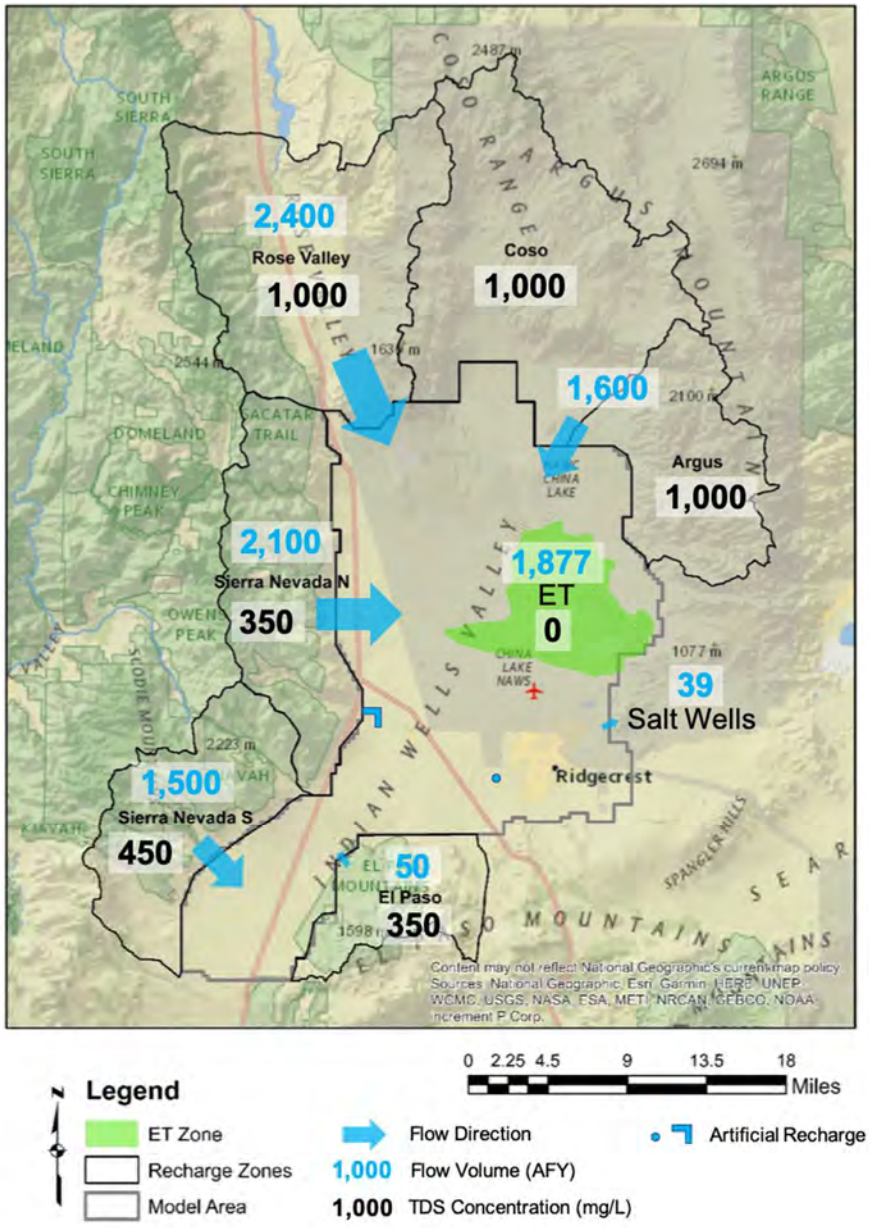


Figure 41. TDS concentrations assigned to groundwater recharge areas in the transport model. The TDS of the artificial recharge is 280 mg/L for imported water (western location) and 250 mg/L for recycled water (eastern location).

In addition to the natural sources of TDS described above, the scenario 6.2 transport model includes TDS sources in the form of artificial recharge of imported and recycled water (Figure 41). Imported water having a TDS concentration of 280 mg/L is recharged via an infiltration basin located west of the Inyokern Airport. Because site-specific infiltration data were not available, the model applies this recharge directly to the saturated zone and thus evaporation and potential subsequent concentration of TDS in the recharge water are not simulated. Recycled water having a TDS concentration of 250 mg/L is recharged directly to the saturated zone via an injection well west of Ridgecrest.

The values of TDS transport parameters are based on those used in DRI's groundwater transport model for the Navy (McGraw et al., 2016). The value of longitudinal dispersivity was chosen to be consistent with the large size of the model domain and the potential for movement of saline groundwater over substantial distances. The mean advective transport distance in model layer 1 during the 50-year simulation period is 365 m, which corresponds to a longitudinal dispersivity value of 100 m based on the relationship between the scale of field observations and values of longitudinal dispersivity presented by Gelhar et al. (1992). Horizontal transverse dispersivity was set at 10 m as defined by the typical ratio of 0.1 to longitudinal dispersivity (Dullien, 1992), and vertical transverse dispersivity was set at 1 m. Effective porosity was set at 0.225, which is the specific yield value used in the flow models and is a value typical for unconsolidated basin fill materials (Stephens et al., 1998). The value of the diffusion coefficient is set to zero and there are no geochemical reactions or sorption effects included in the transport model.

The transport model utilizes the standard finite difference (SFD) method with upstream weighting solution scheme employed in the MT3D-USGS code for solving the advection term of the transport equation. Although several solution schemes are available in MT3D-USGS, the SFD method was chosen for its efficiency. This method is considered reasonably accurate for transport models having a Peclet number less than four (Zheng and Wang, 1999). The Peclet number, P_e, is defined as

$$P_e = \frac{|v|\Delta x}{D} \tag{3}$$

where $|v|$ is the mean seepage velocity (LT^{-1}), Δx is the grid spacing (L), and D is the dispersion coefficient (L^2T^{-1}). D is the product of longitudinal dispersivity and mean seepage velocity. For the IWV predictive flow model for Scenario 6.2, Δx is 250 m, D is 100 m, and $|v|$ in model layer 1 is 0.023 m/d in 2020 and 0.017 m/d in 2070. Using the mean of these values of seepage velocity gives a Peclet number of 2.5, indicating that the SFD method is appropriate for this model.

3.5 Calibration

A quantitative calibration of the transport model was not performed because the initial TDS distribution integrates available measurements that span many decades, thus a single historic simulation period could not be developed for calibration. Instead, a qualitative calibration compared the forecasts of TDS trends simulated by the baseline transport model (described in Section 3.6) to general historic trends and spatial distributions represented by the conceptual model of groundwater salinity. Nine wells in the TDS database were selected for the comparison. These wells are among the nineteen wells used to evaluate TDS trends by Todd Engineers (2014). Though they did not identify the wells that were used, the nine wells listed in Table 6 correspond to the locations of the wells plotted in Figure 7 of Todd Engineers (2014). Historical trends were calculated from the available data using linear regression. Assuming that historical trends in TDS concentrations and groundwater withdrawals continue 50 years into the future, the baseline transport model forecasts show reasonable agreement to changes in TDS concentrations (Figure 42).

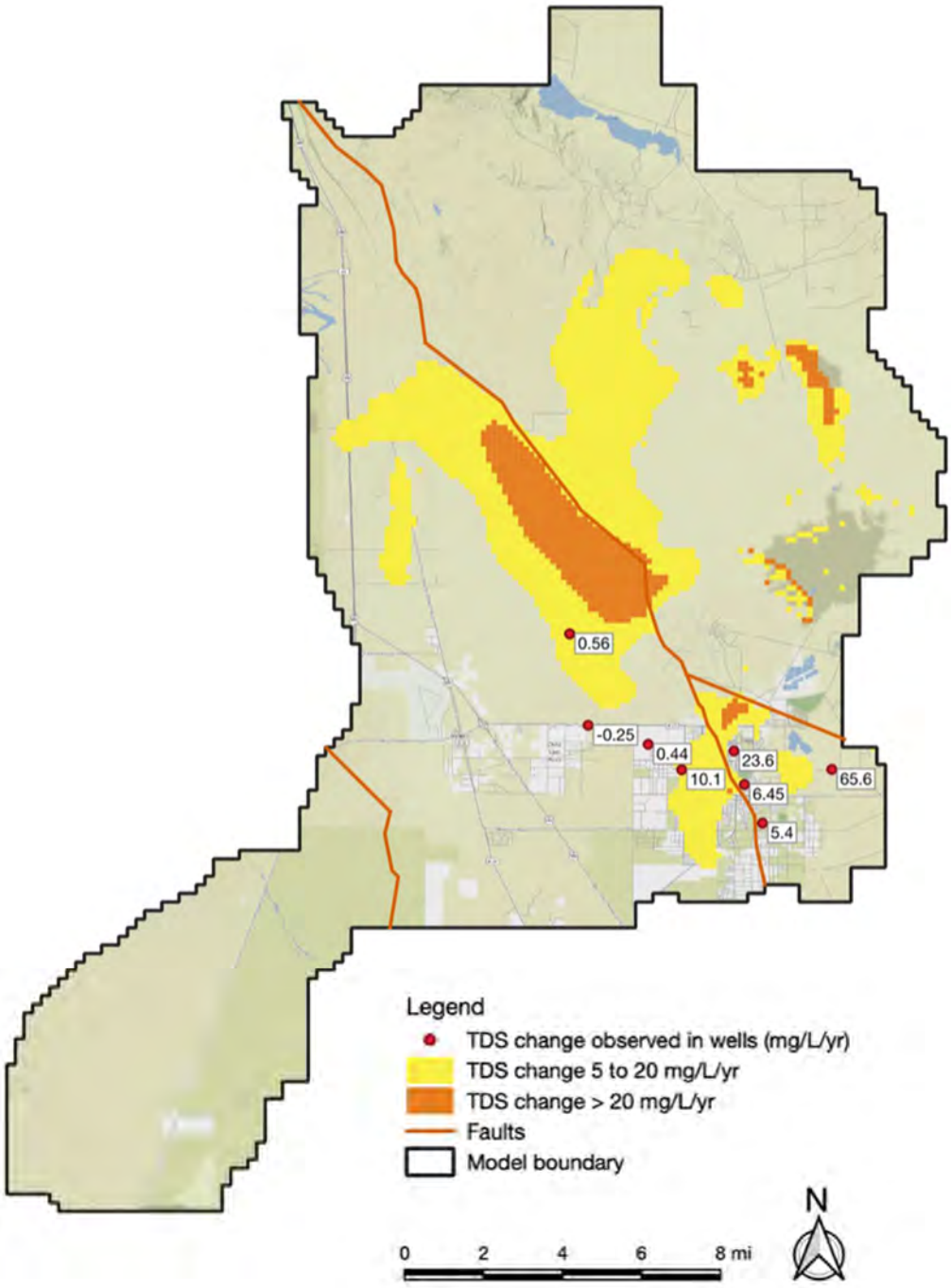


Figure 42. Comparison of annual rate of change in TDS (mg/L/yr) forecasted for the years 2020 to 2070 in the Shallow TDS Zone to historical annual rates of change observed in wells. Refer to Figure 3 for the names of the fault segments.

Table 6. Wells used for comparison of observed to simulated TDS concentration trends.

Well Name	TDS Slope (mg/L/yr)	Depth (ft)
26S/39E-11E01	6.18	250
26S/40E-36A01	65.6	270
26S/39E-10N01	0.56	--
26S/40E-28J01	23.6	--
RC HGTS WELL #7	5.40	304
26S/40E-34N01	6.45	232
IWVWD Well 17	-0.25	1030
26S/39E-24Q01	0.44	345
IWVWD Well 13	10.1	720

3.6 Transport Results

Changes in TDS concentrations forecast by the baseline and scenario 6.2 transport models were presented to the TAC. These presentations are included as Attachment B to this Appendix. The results are also summarized in Section 3.5.3 of the GSP report.

Simulated TDS concentrations in year 2070 in the shallow TDS zone for the baseline and scenario 6.2 models show similar spatial distributions to each other and to the year 2020 (Figure 43) despite 50 years of groundwater withdrawals at very different rates. This result is primarily a function of very low groundwater velocities in the basin that prevent large-scale TDS transport by advection. The largest TDS differences occur in the west-central portion of the basin where high-volume groundwater withdrawals are focused in the baseline at a rate of 38,063 AFY, but are significantly reduced to a rate of 14,011 AFA in scenario 6.2.

The largest area of TDS change is in the shallow TDS zone where most groundwater pumping takes place and where evapotranspiration increases salinity through concentration. These areas are shown in yellow for both models in Figure 44 and generally correspond to the region of highest hydraulic conductivity in model layer 1 as shown in Figure 14. The higher conductivity allows greater groundwater velocities relative to other areas in response to the high pumping rates in the central-west portion of the basin, drawing groundwater of higher salinity in the direction of the pumping centers. The area of largest TDS change is larger in the baseline model because the pumping rates are substantially higher than in scenario 6.2, which drives increased movement of salinity. In deeper zones, even low velocity groundwater movement can cause high rates of TDS change owing to the much higher salinity. Overall, however, simulated TDS concentrations change very little over the predictive time period.

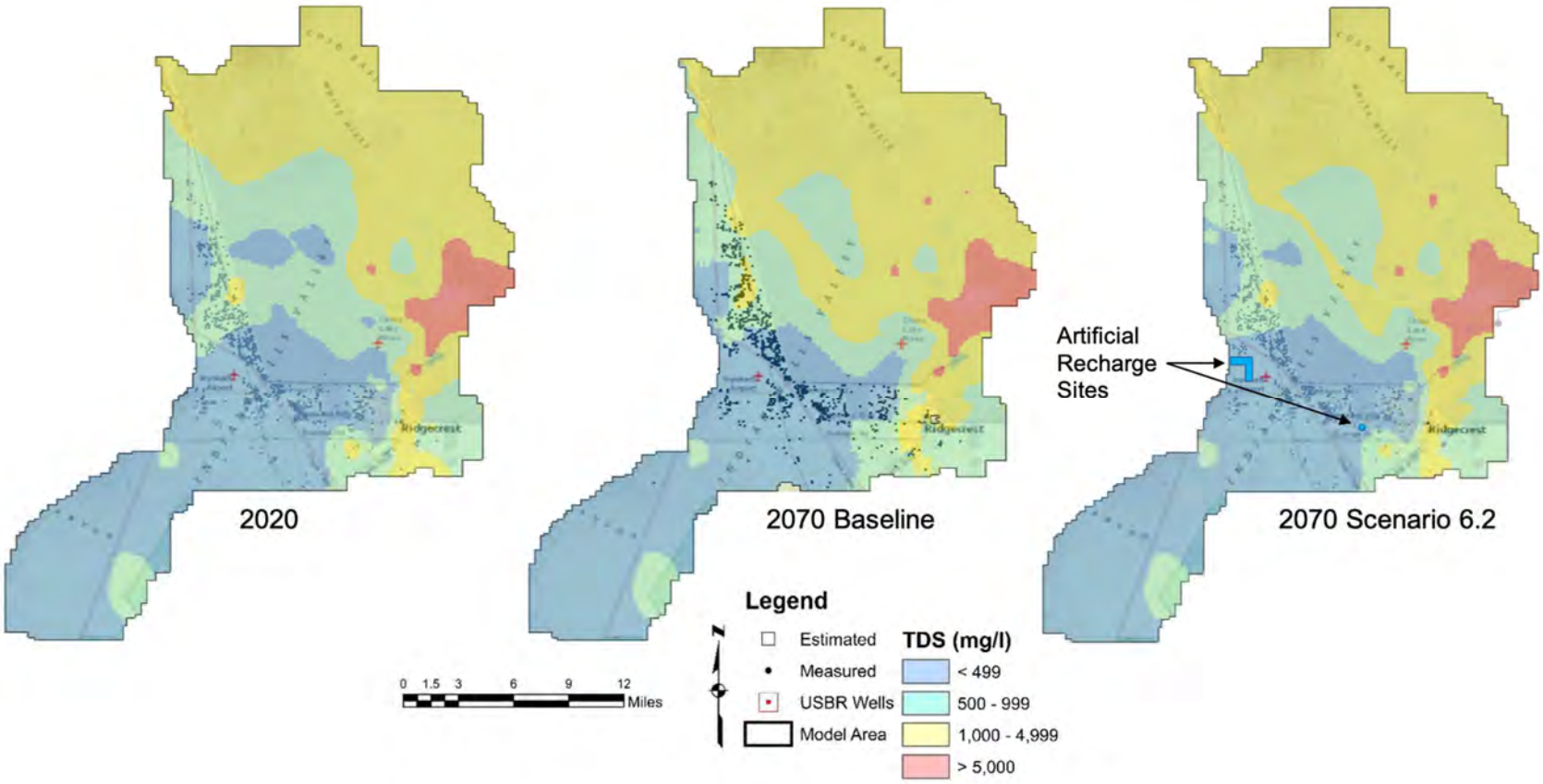


Figure 43. Comparison of the spatial distributions of simulated TDS concentration in the shallow TDS zone in the year 2020 (left), and the year 2070 for the baseline model (center) and the scenario 6.2 model (right).

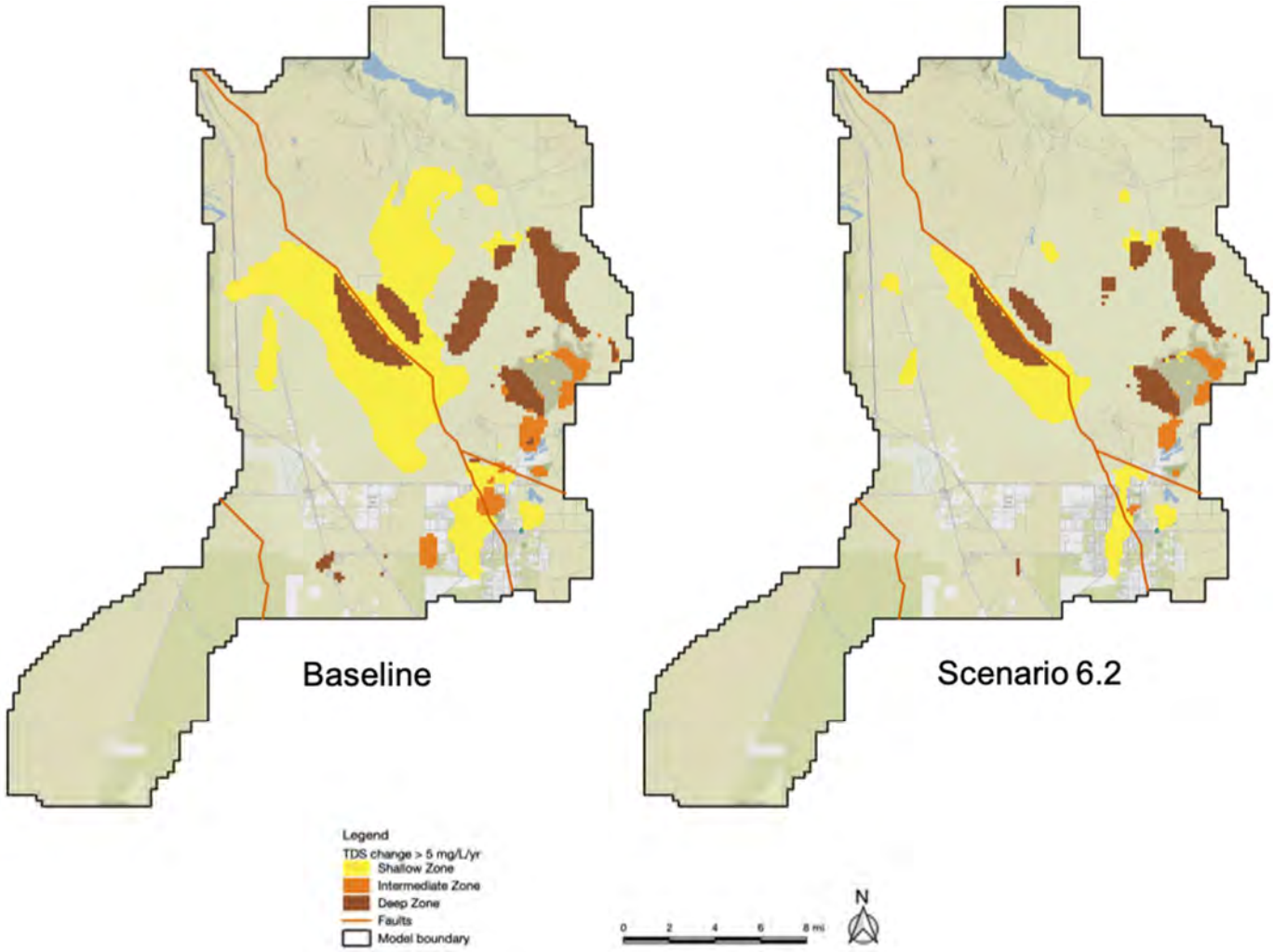


Figure 44. Areas where the forecasted annual rate of change in TDS concentration exceeds 5 mg/L/yr for the years 2020 to 2070 for the baseline model (left) and scenario 6.2 model (right). The areas for all three TDS Zones are superimposed. Refer to Figure 3 for the names of the fault segments.

4. Model Limitations

Though the Indian Wells Valley GSP model has been shown to be a reasonable representation of the conceptualization of the groundwater flow system and honors available local data, the model has limitations, including:

1. Evapotranspiration is not directly measured in the basin, and currently can only be quantified as a component of the simulated groundwater volumetric balance. In any case, the simulated ET is well characterized and shows good agreement with the results of the EVI approach.
2. The model is currently not designed to simulate the physical processes of artificial recharge from infiltration basins, instead the imported water was added directly to the saturated zone. The infiltration process can be incorporated in the model using field measurements of infiltration, soil properties, and climate data.
3. The transport model was designed to investigate how the distribution of salinity within the groundwater system may be influenced by alternative scenarios for groundwater management. Owing to limitations in the TDS dataset and the overall scale of the model, the transport model was not designed for use as a predictor of TDS concentrations at the local scale.

References

Anderson, M. P., Woessner, W. W., and Hunt R. J., 2015. Applied Groundwater Modeling, Second Edition: Simulation of Flow and Advective Transport, Elsevier, New York, 564p.

Bullard, T. F., Bacon, S. N., Adams, K. D., and Decker, D. L., 2019. Geomorphic map of China Lake basin below 700 m elevation in Support of Cultural Resource Management at Naval Air Weapons Station China Lake, prepared by Desert Research Institute for Naval Air Warfare Center Weapons Division, China Lake, California.

Lancaster, N. L., Bacon, S. N., Bullard, T. F., Baker, S. E. and Decker, D. L., 2019. Eolian Hazard Assessment for the SNORT Facility, prepared by Desert Research Institute for Naval Air Warfare Center Weapons Division, China Lake, California.

Banta, E. R., 2000. MODFLOW-2000, The U.S. Geological Survey Modular Ground- Water Model—Documentation of Packages for Simulating Evapotranspiration with a Segmented Function (ETS1) and Drains with Return Flow (DRT1). U.S. Geological Survey Open-File Report 00-466.

Beamer, J. P., Huntington, J. L., Morton, C. G., and Pohll, G. M., 2013. Estimating Annual Groundwater Evapotranspiration from Phreatophytes in the Great Basin Using LANDSAT and Flux Tower Measurements. *Journal of the American Water Resources Association*, 49(3):518-533.

Bean, R.T., 1989. Hydrogeologic Conditions in Indian Wells Valley and Vicinity, Prepared for California Department of Water Resources, 56p.

Berenbrock, C., 1987, Ground-water data for Indian Wells Valley, Kern, Inyo, and San Bernardino Counties, California, 1977-84. U.S. Geological Survey Open-File Report 86-315, 56 p.

Berenbrock, C. and Martin, P., 1991. The Ground-Water Flow System in Indian Wells Valley, Kern, Inyo, and San Bernardino Counties, California. U.S. Geological Survey Water-Resources Investigations Report 89-4191.

Berenbrock, C., and Schroeder, R. A., 1994. Ground-Water Flow and Quality, and Geochemical Processes, in Indian Wells Valley, Kern, Inyo, and San Bernardino Counties, California, 1987-88. U.S. Geological Survey, Water-Resources Investigations Report 93-4003.

Brown and Caldwell, 2009. Indian Wells Valley Basin Groundwater Model and Hydrogeologic Study, Final report. Prepared for Indian Wells Valley Water District, Ridgecrest, California.

Bullard, T. F., Bacon, S. N., Adams, K. D., and Decker, D. L., 2015. Phase II: Geomorphic Map of the China lake Basin below 700 m in Support of cultural Resource Management at NAWS China Lake. Report prepared by Desert Research Institute for Naval Air Warfare Center, Weapons Division, NAWS China Lake, CA, March 2015. DRI Division of Hydrologic Sciences, NESEP Publication No. 50011, 58 p. + 2 appendices and map.

California Water Boards, Groundwater Ambient Monitoring and Assessment Program (GAMA). https://geotracker.waterboards.ca.gov/gama/gamamap/public/ accessed November 2018.

Danskin, W.R., 1998. Evaluation of the hydrologic system and selected water-management alternatives in the Owens Valley, California, U.S. Geological Survey Water Supply Paper 2370-H.

Doherty, J. E. and Hunt, R. J., 2010. Approaches to highly parameterized inversion---A guide to using PEST for groundwater-model calibration. U.S. Geological Survey Scientific Investigations Report 2010-5169.

Dullien, F.A.L., 1992. Porous Media: Fluid Transport and Pore Structure, Academic, San Diego.

Gelhar, L. W., Welty, C., and Rehfeldt, K. R., 1992. A critical review of data on field-scale dispersion in aquifers. *Water Resources Research*, 28(7):1955-1974, doi:/10.1029/92WR00607.

Garner, C., Bacon, S., Pohll, G., and Chapman, J., 2017. Indian Wells Valley Groundwater Model Update. Desert Research Institute Technical Memorandum.

Güler, C. and Thyne, G. D., 2004. Hydrologic and geologic factors controlling surface and groundwater chemistry in Indian Wells-Owens Valley area, southeastern California, USA. *Journal of Hydrology*, 285(1):177--198, doi:/10.1016/j.jhydrol.2003.08.019.

Harbaugh, A. W., 2005. MODFLOW-2005: the U.S. Geological Survey modular ground-water model--the ground-water flow process. U.S. Geological Survey Techniques and Methods 6-A16.

Kern County Water Agency, Base WQ spreadsheet. Received by Stetson Engineers Dec. 17, 2018 from Michelle Anderson.

Krieger & Stewart, 2011. 2010 Urban Water Management Plan. Ridgecrest, California. Prepared for Indian Wells Valley Water District, Ridgecrest, California.

Maxey, G. B., 1968. Hydrogeology of Desert Basins. *Ground Water*, 6(5):10-22, doi:/10.1111/j.1745-6584.1968.tb01660.x.

McGraw, D., Carroll, R., Pohll, G., Chapman, J., Bacon, S., and Jasoni, R., 2016. Groundwater Resource Sustainability: Modeling Evaluation for the Naval Air Weapons Station, China Lake. California. prepared by Desert Research Institute for the Naval Air Warfare Center Weapons Division, Final Evaluation Report NAWCWD TP 8811.

Menke, J., Reyes, E., Glass, A., Johnson, D., and Reyes, J., 2013. 2013 California Vegetation Map in Support of the Desert Renewable Energy Conservation Plan. Final Report. Prepared for the California Department of Fish and Wildlife Renewable Energy Program and the California Energy Commission. Aerial Information Systems, Inc., Redlands, CA.

Moyle, W.R., Jr., 1963. Data on water wells in Indian Wells Valley area, Inyo, Kern, and San Bernardino Counties, California. California Department of Water Resources Bulletin 91-9, 243 p.

Niswonger, R. G., Sorab, P., and Motomu, I., 2011. MODFLOW-NWT, A Newton formulation for MODFLOW-2005. U.S. Geological Survey Techniques and Methods 6-A37, 44 p.

Stephens, D.B, K. Hsu, M.A. Prieksat, M.D. Ankeny, N. Blandford, T.L. Roth, J.A. Kelsey, and J.R. Whitworth, 1998. A comparison of estimated and calculated effective porosity, Hydrogeology Journal, 6, pp. 156-165.

Stetson Engineers, 2018. Notes on Determination of Balanced Hydrologic Period and Model Recharge Distribution. Memo to Greg Pohll, Desert Research Institute, December 12, 2018.

Thyne, G.D., Gillespe, J.M., and Ostdick, J.R., 1999. Evidence for interbasin flow through bedrock in the southeastern Sierra Nevada. Geological Society of America Bull. 111 (11): pp. 1600-1616.

Todd Engineers, 2014. Indian Wells Valley Resource Opportunity Plan - Water Availability and Conservation Report, prepared for Kern County Planning & Community Development Department.

TriEcoTt, Joint Venture, 2012. Technical Justification for Beneficial Use Changes for Groundwater in Salt Wells Valley and Shallow Groundwater in Eastern Indian Wells Valley. Prepared for Department of the Navy, Naval Facilities Engineering Command Southwest, San Diego, California.

U.S. Bureau of Reclamation, 1993. Indian Wells Valley Groundwater Project: USBR Technical Report Volumes I and II.

Zheng, C. and Wang, P. P., 1999. MT3DMS: a modular three-dimensional multispecies transport model for simulation of advection, dispersion, and chemical reactions of contaminants in groundwater systems: documentation and user's guide. Prepared for U.S. Army Corps of Engineers, Strategic Environmental Research and Development Program Contract Report SERDP-99-1.

Attachment A. Plots of Simulated and Measured Groundwater Level Hydrographs for Calibration of the Transient-Historical Model

The MATLAB robust regression slope-fitting function *robustfit* was used to automatically identify and remove observation outliers and compute the regression slopes for observed and simulated water level trends at the 36 observation locations in the transient-historical model. Observations from the years 1994 through 2016 were chosen for this analysis because sufficient data were available during this period in all wells except well 25S40E08A01. Manual screening was performed prior to the regression analysis to remove observations earlier than 1994 (except well 25S40E08A01) and observations that were clearly related to pumping activities in nearby wells (post-2012 in well 26S39E20L and Fall 1996 through Spring 2003 in well 26S39E13R03).

The title of each plot in this appendix provides the California State Well Number and gives the slopes of the regression lines for the observed and simulated water levels and the difference between these slopes.

Red circles represent all observed water levels (Observed).
Orange circles represent observed water levels used in the regression model after outliers were manually removed (ObsRobustIn).
Small black unfilled circles represent observed water levels that were automatically removed during computation of the regression (Obs [w = 0]).
Orange line is the fitted regression line for the observed water levels (ObsRobustLINE).

Blue circles represent water levels simulated by the transient-historical model (Simulated).
Green circles represent simulated water levels used in the regression model (SimRobustIn).
Small black filled circles represent simulated water levels that were automatically removed during computation of the regression (Sim [w = 0]).
Green line is the fitted regression line for the simulated water levels (SimRobLINE).

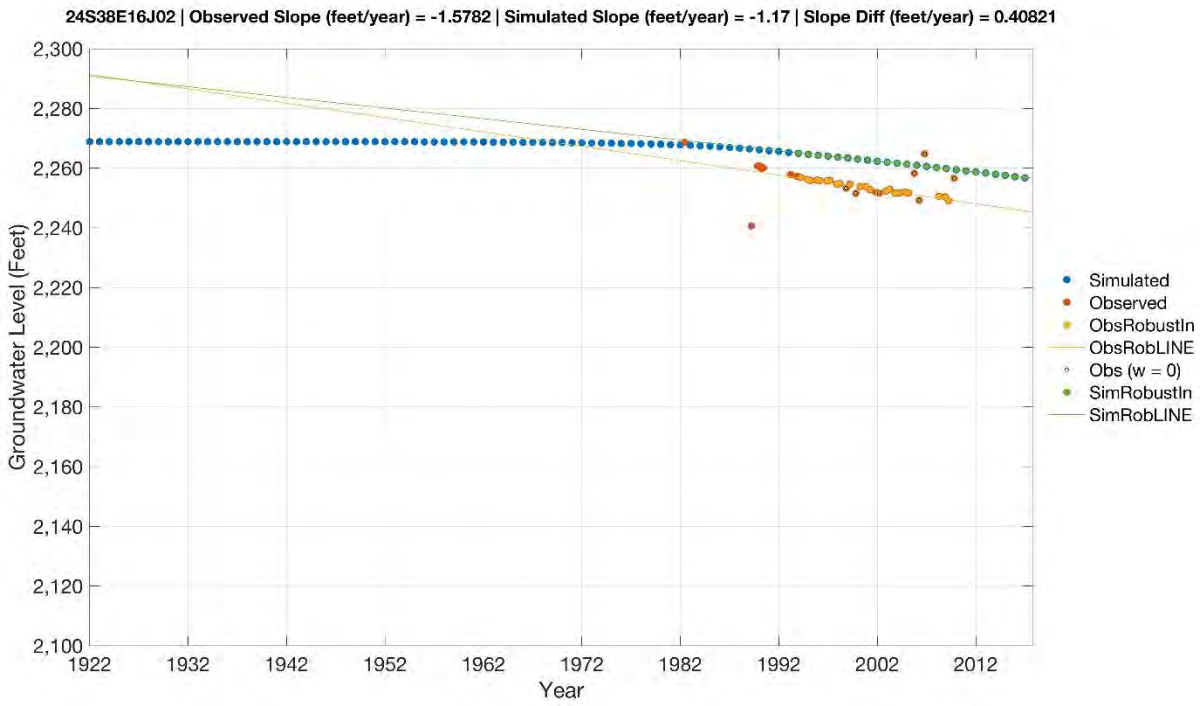


Figure A-1

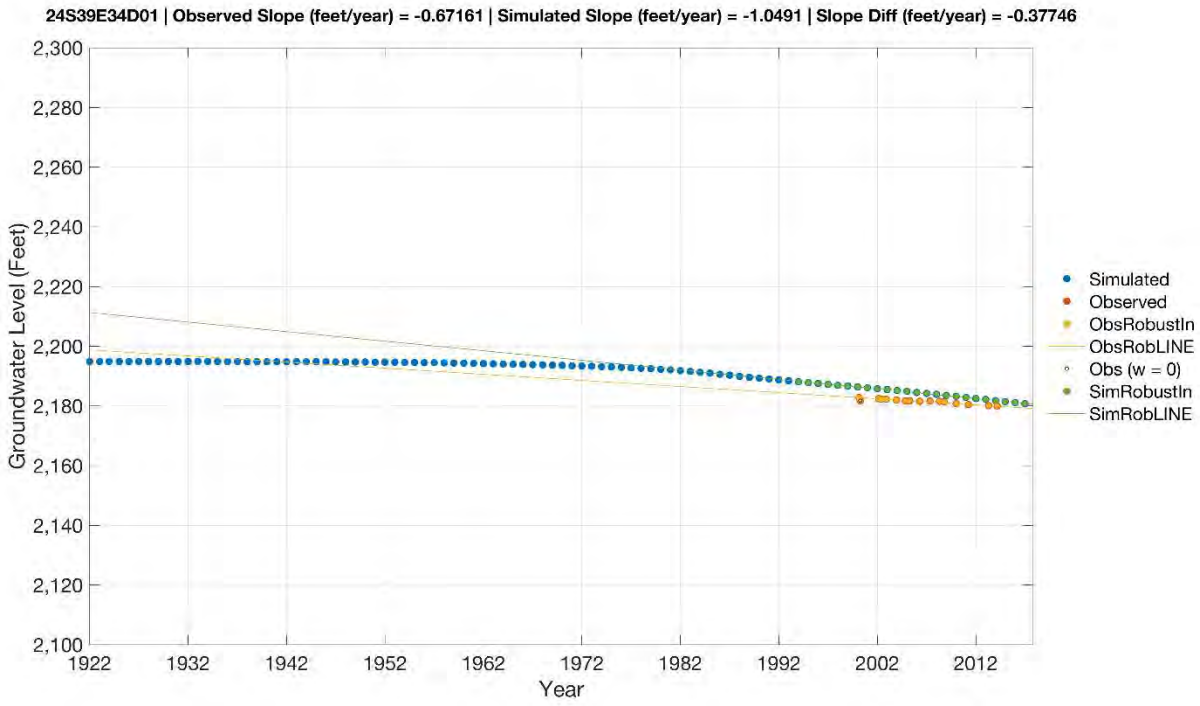


Figure A-2

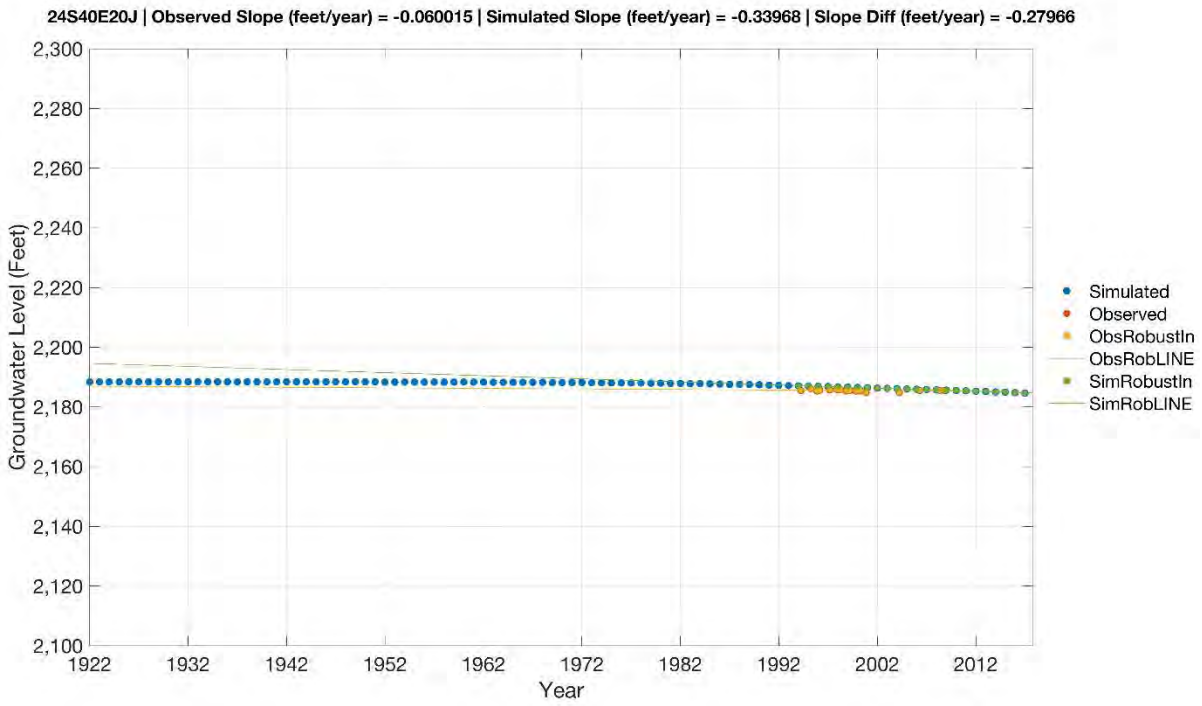


Figure A-3

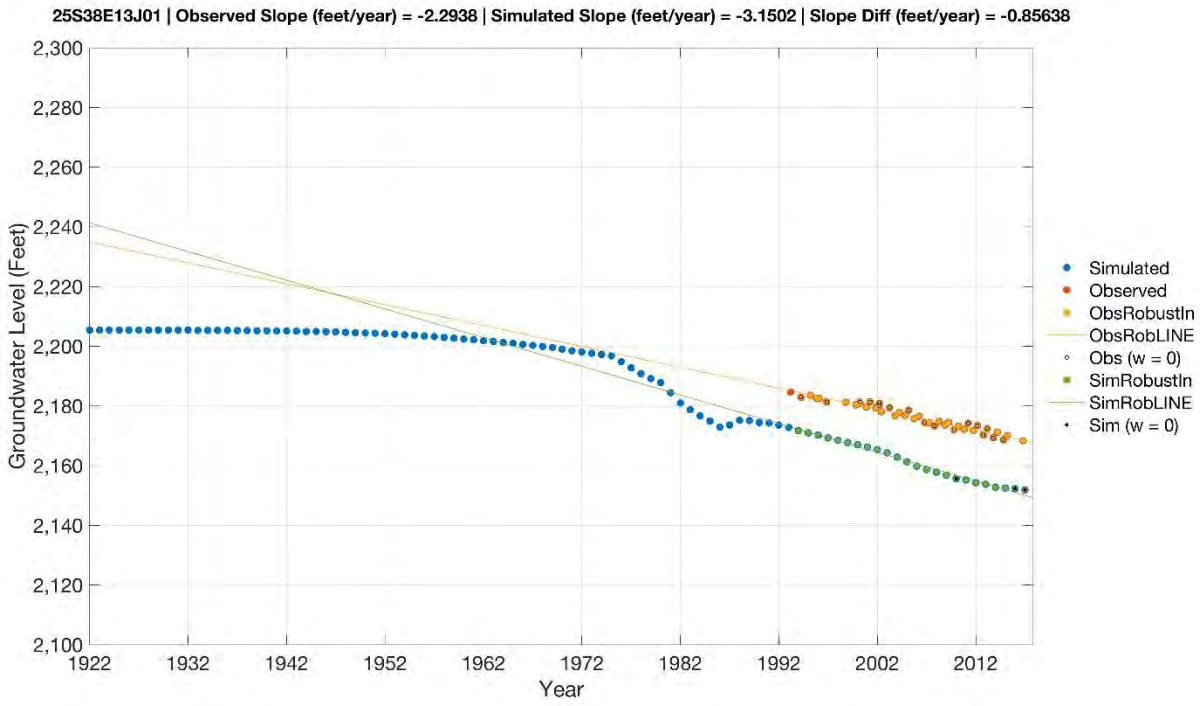


Figure A-4

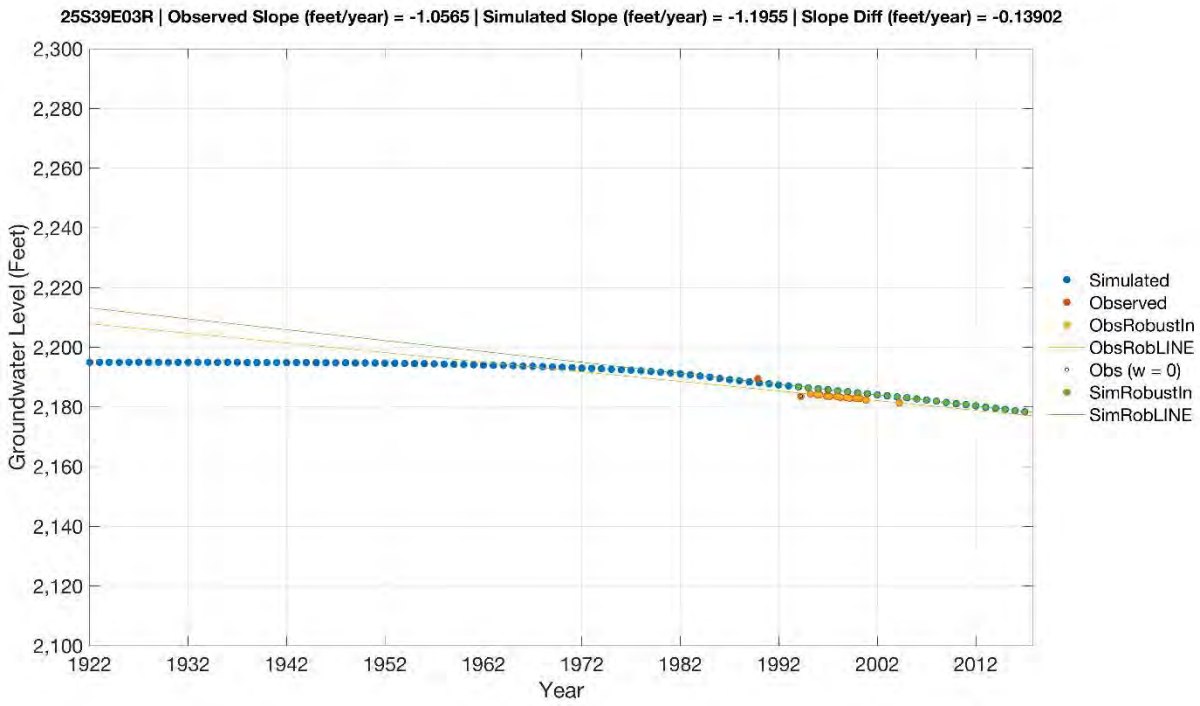


Figure A-5

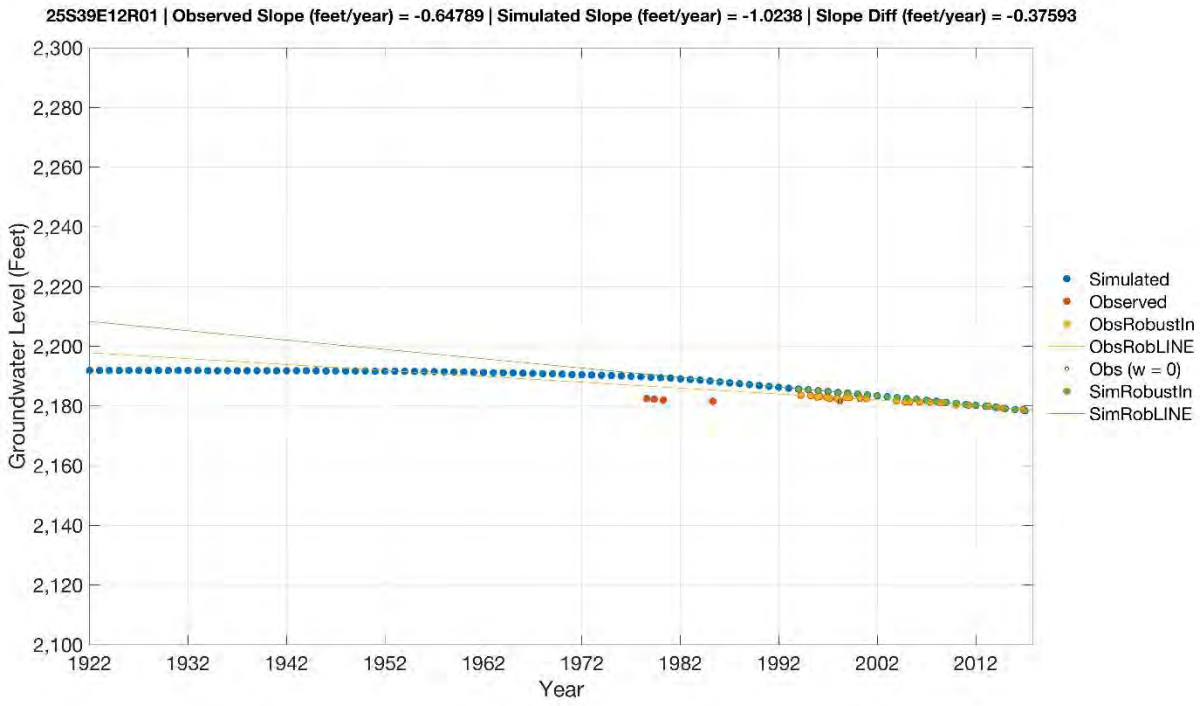


Figure A-6

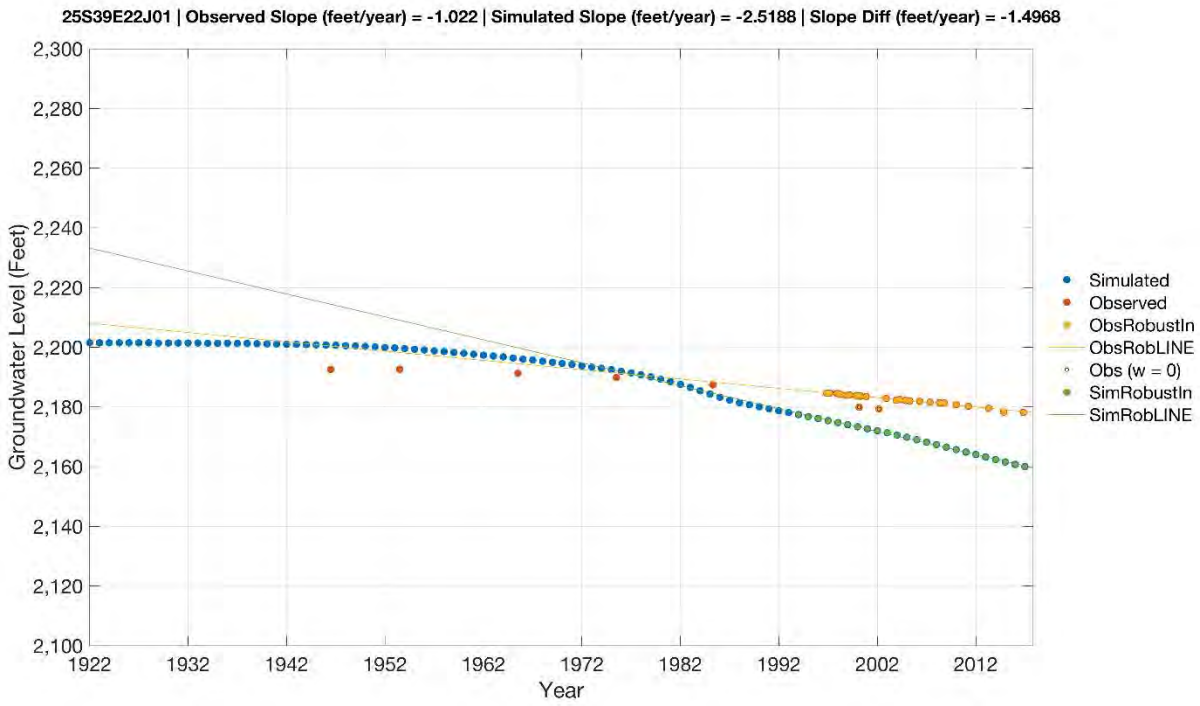


Figure A-7

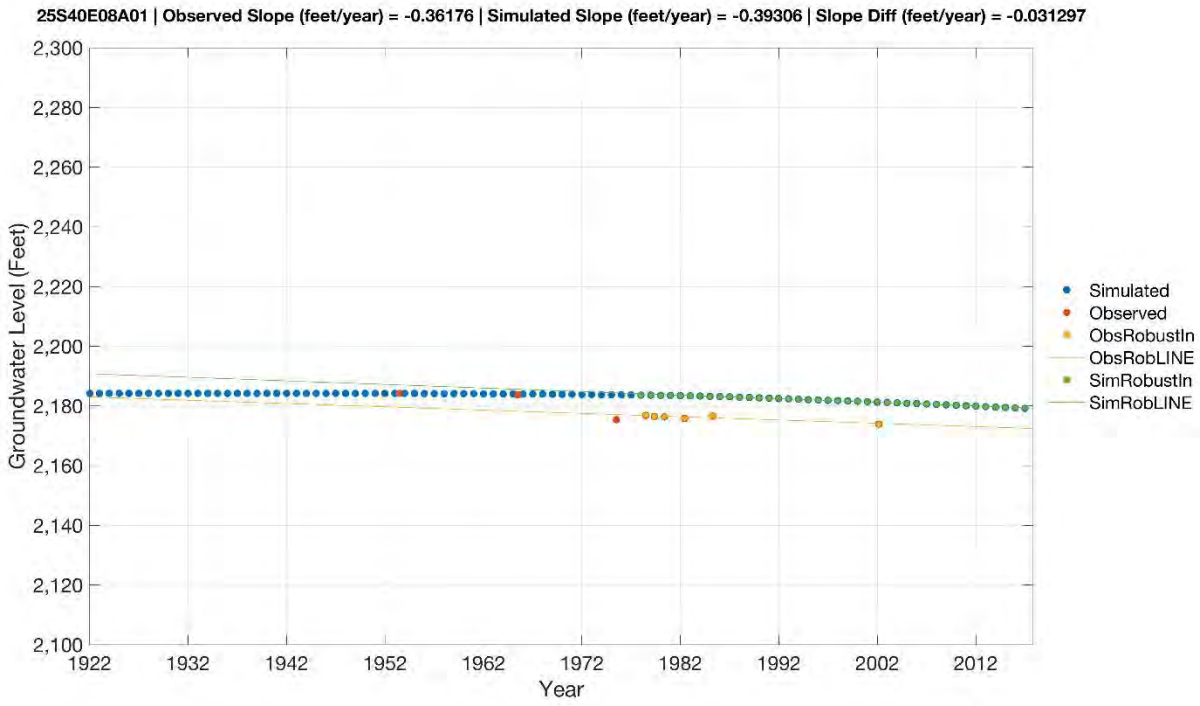


Figure A-8

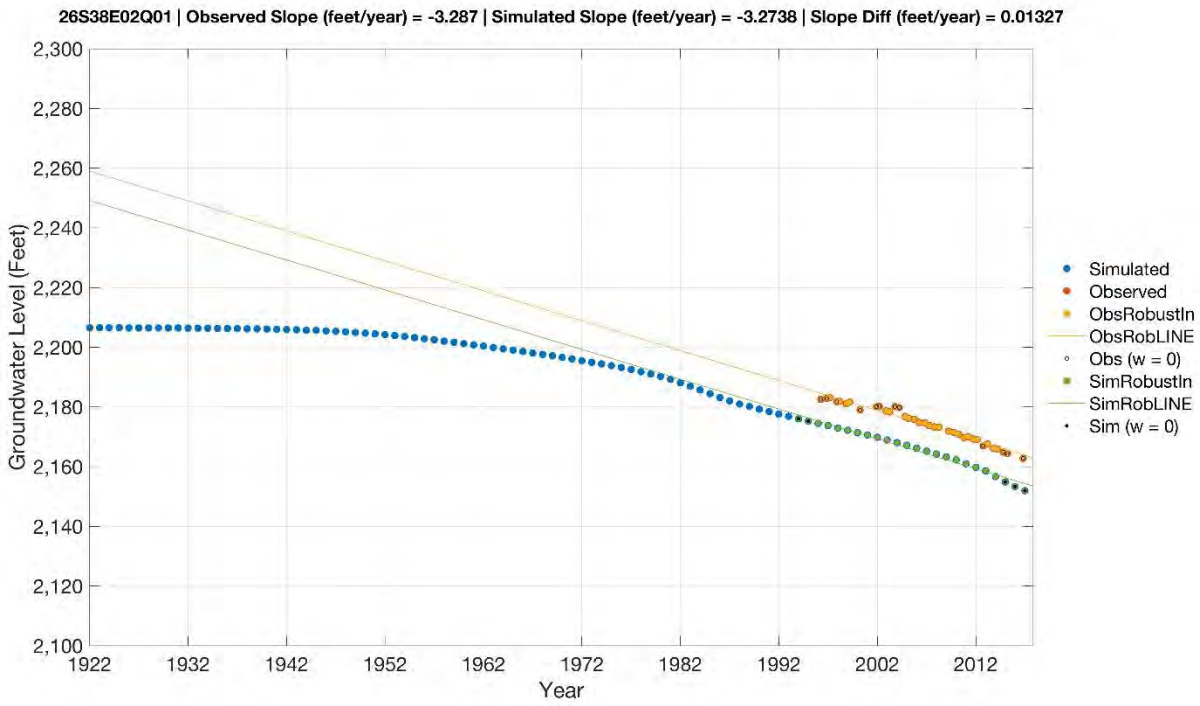


Figure A-9

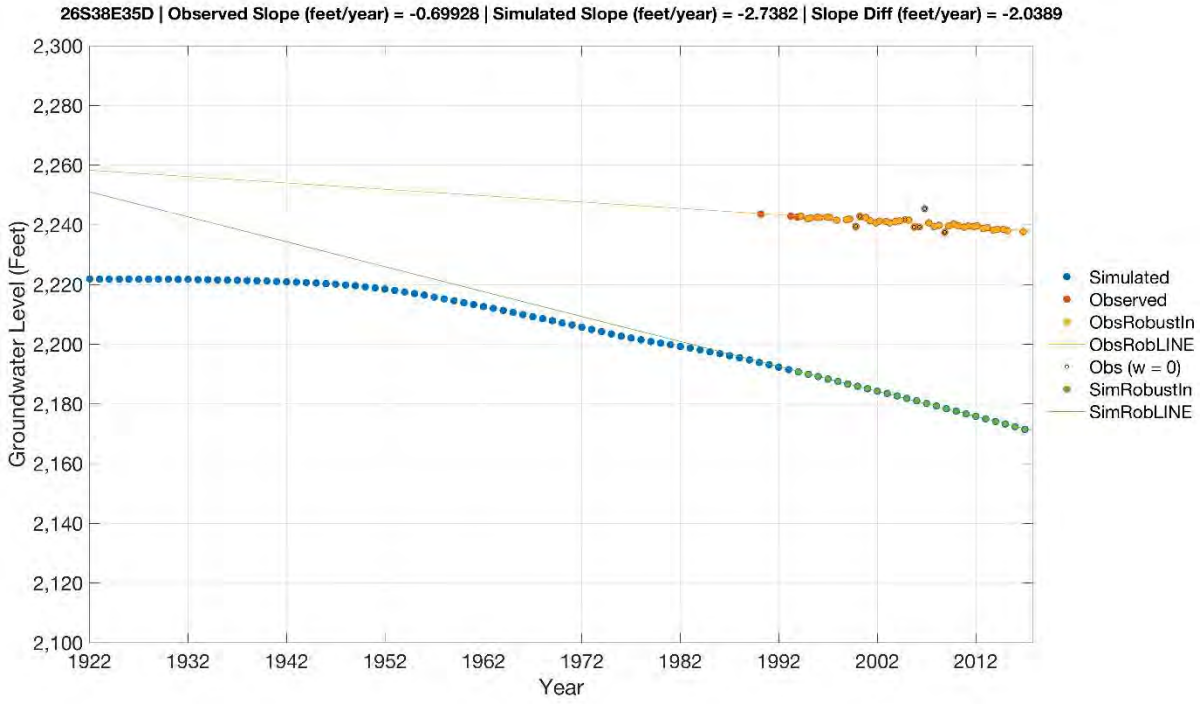


Figure A-10

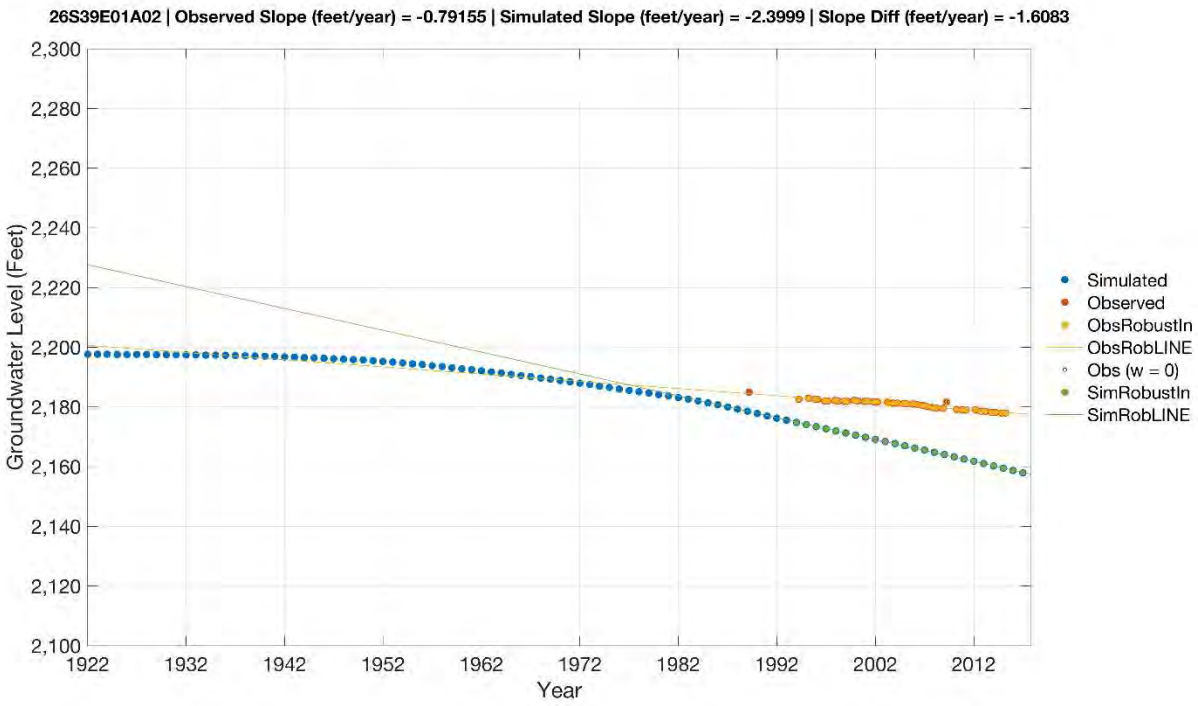


Figure A-11

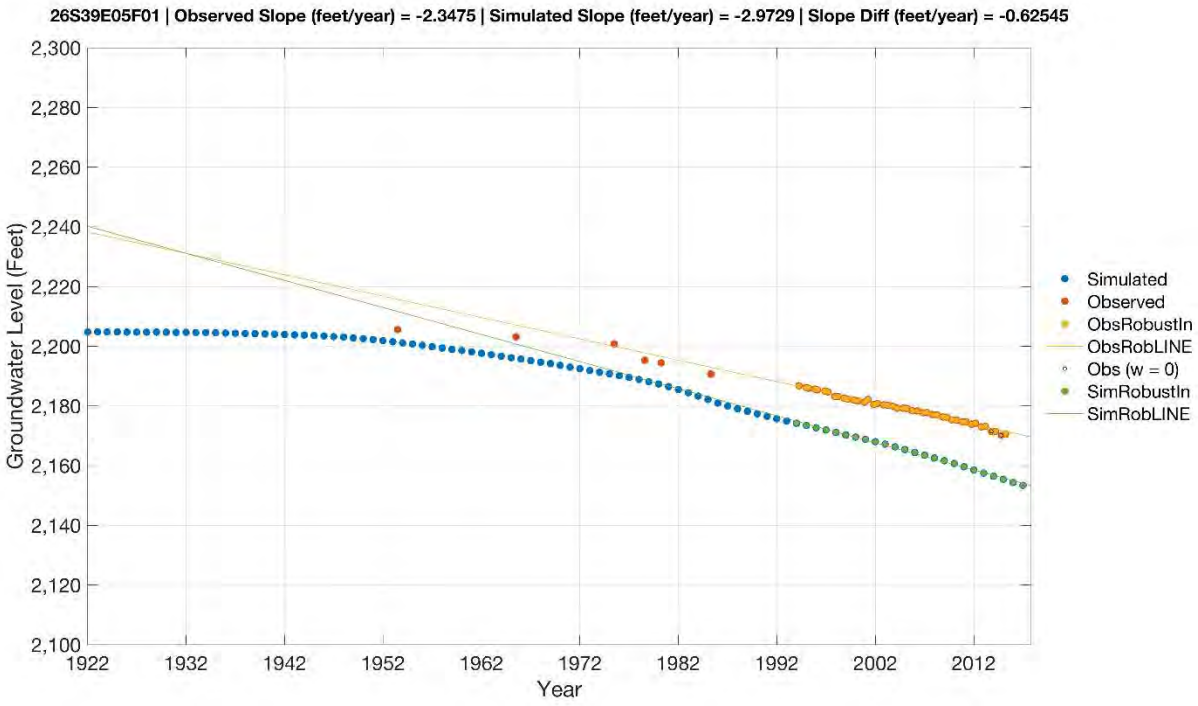


Figure A-12

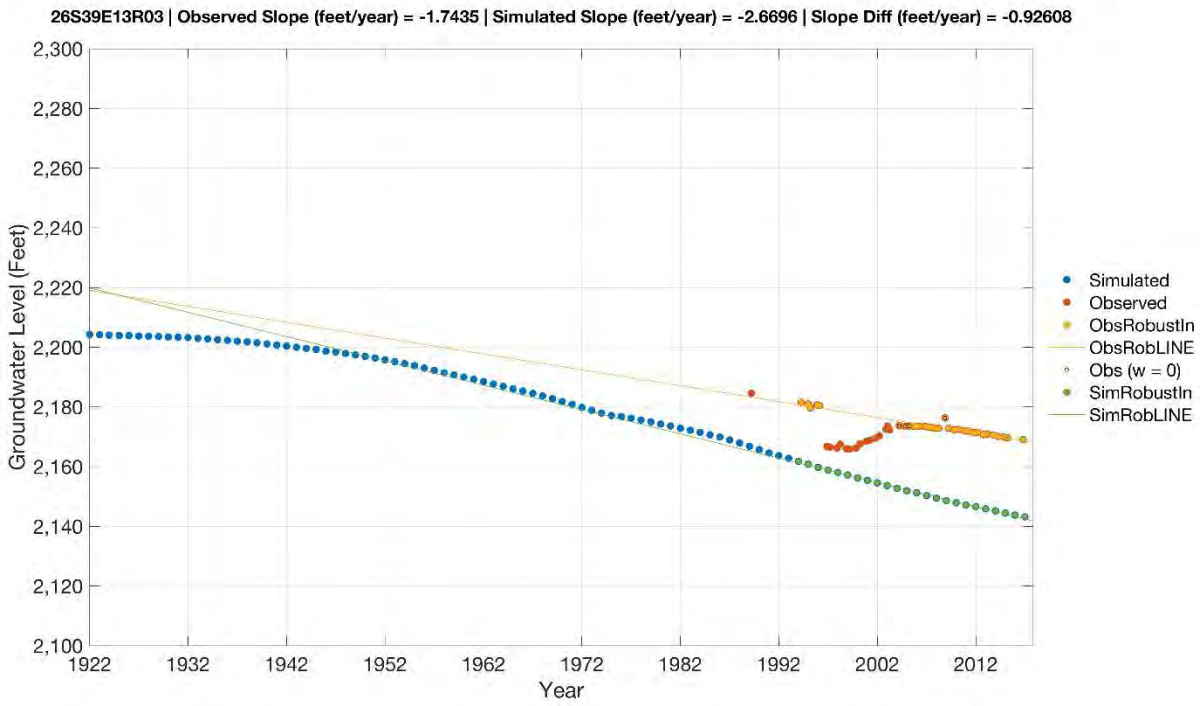


Figure A-13

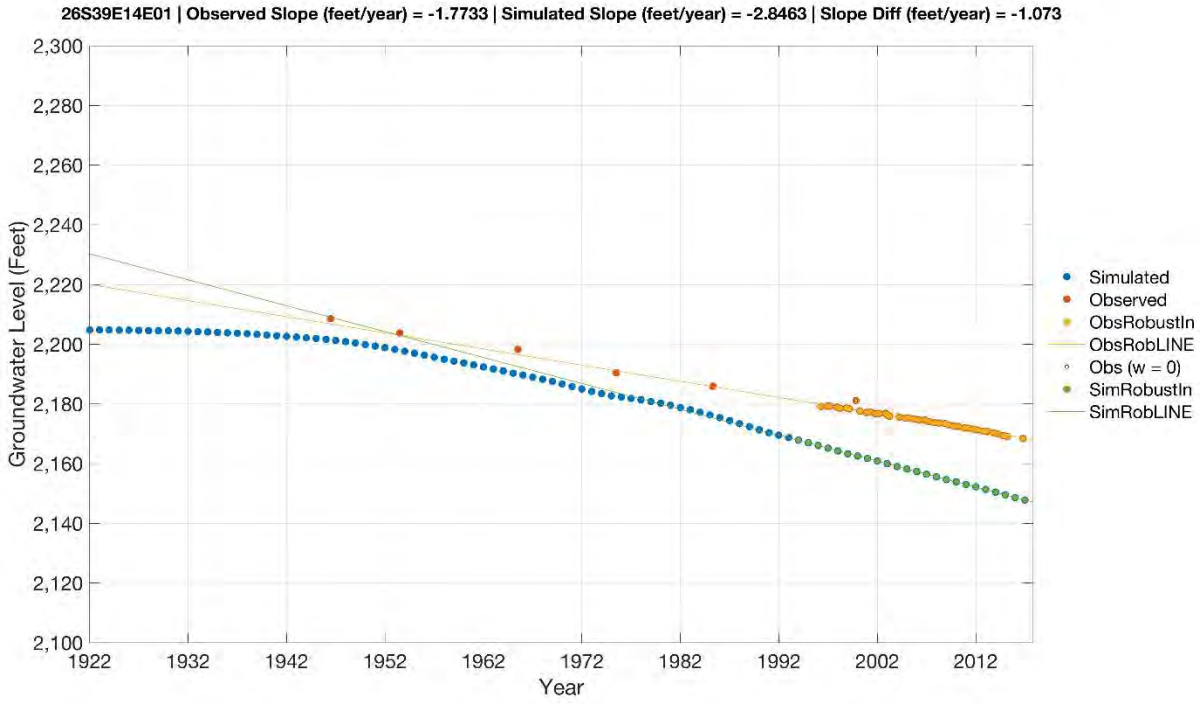


Figure A-14

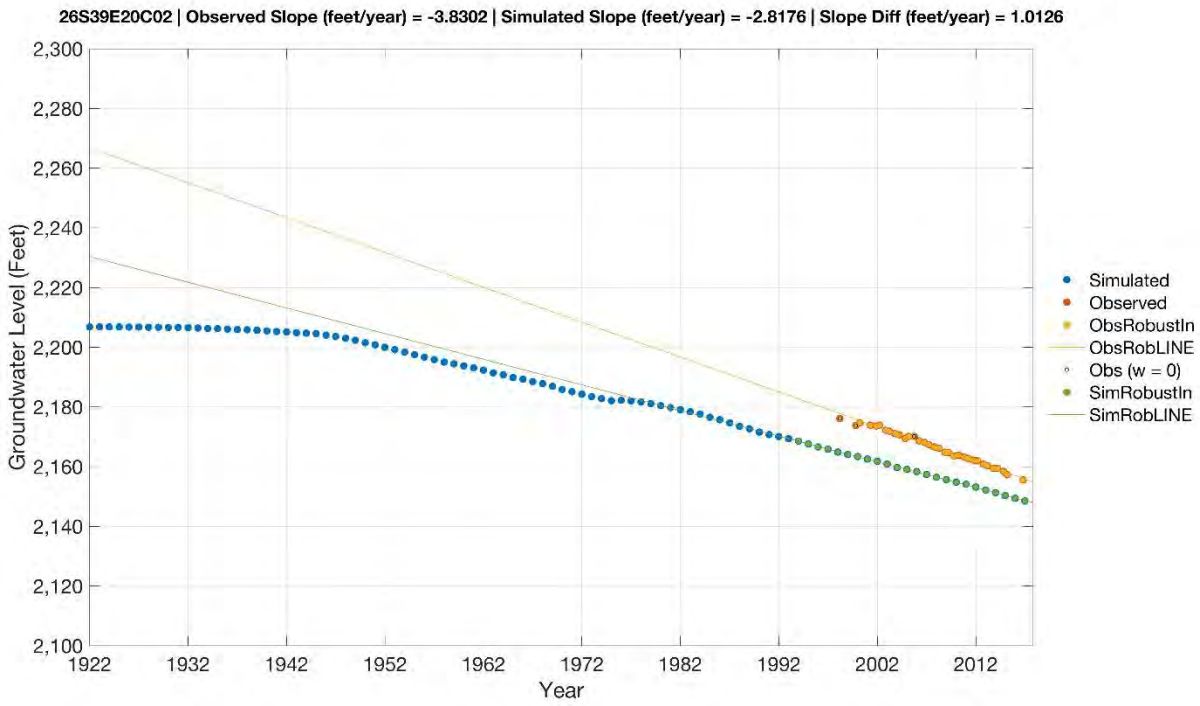


Figure A-15

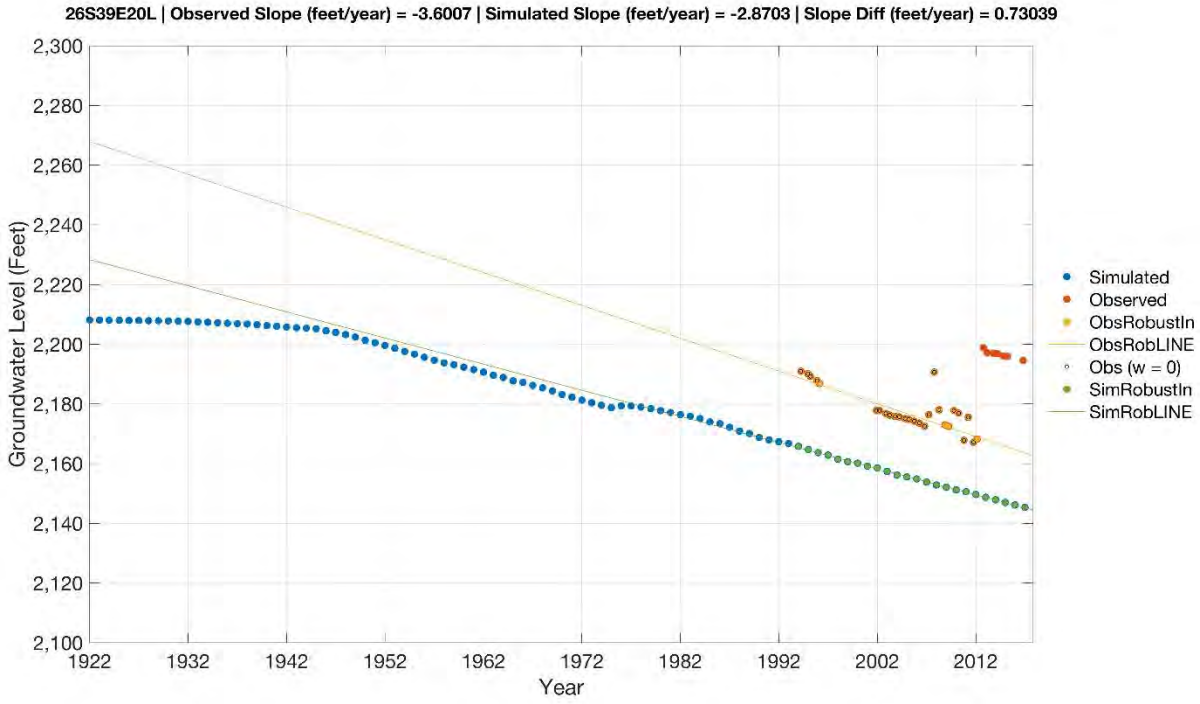


Figure A-16

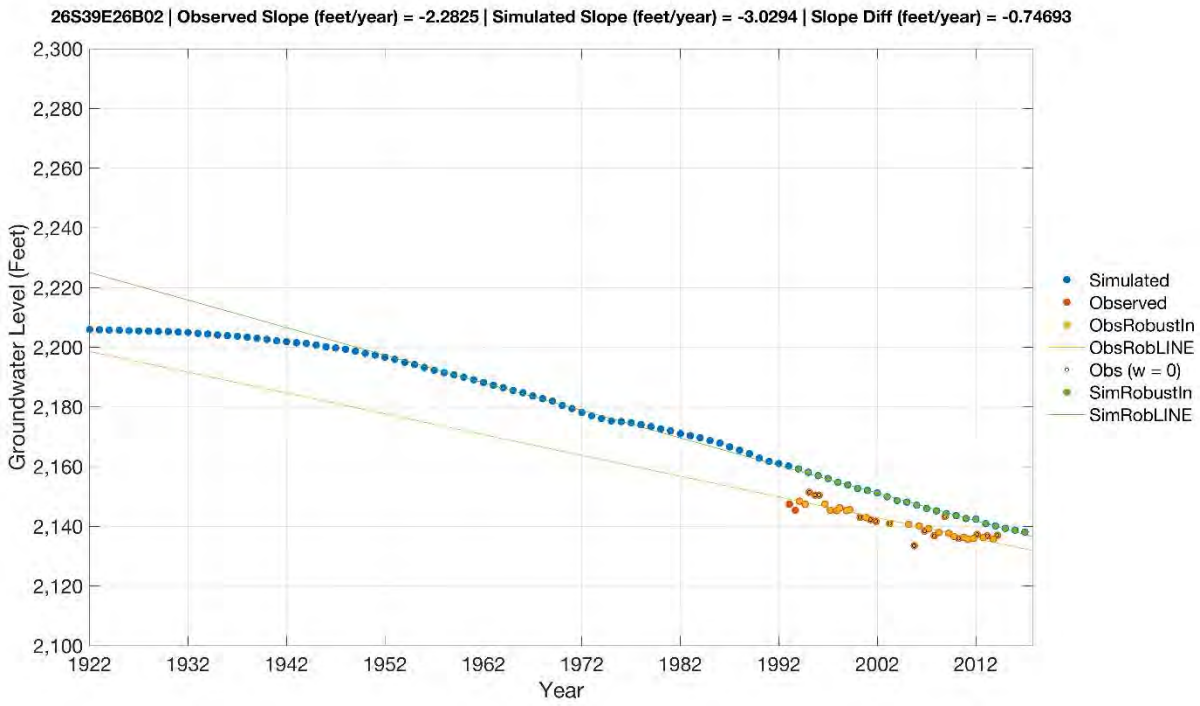


Figure A-17

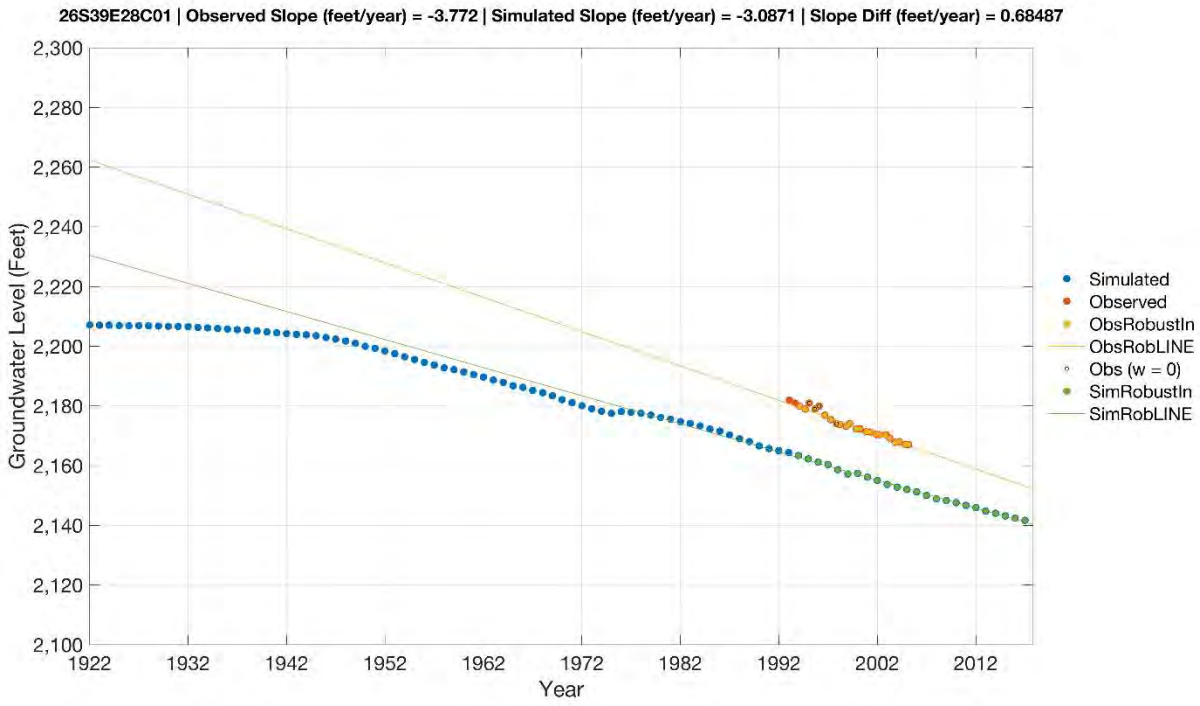


Figure A-18

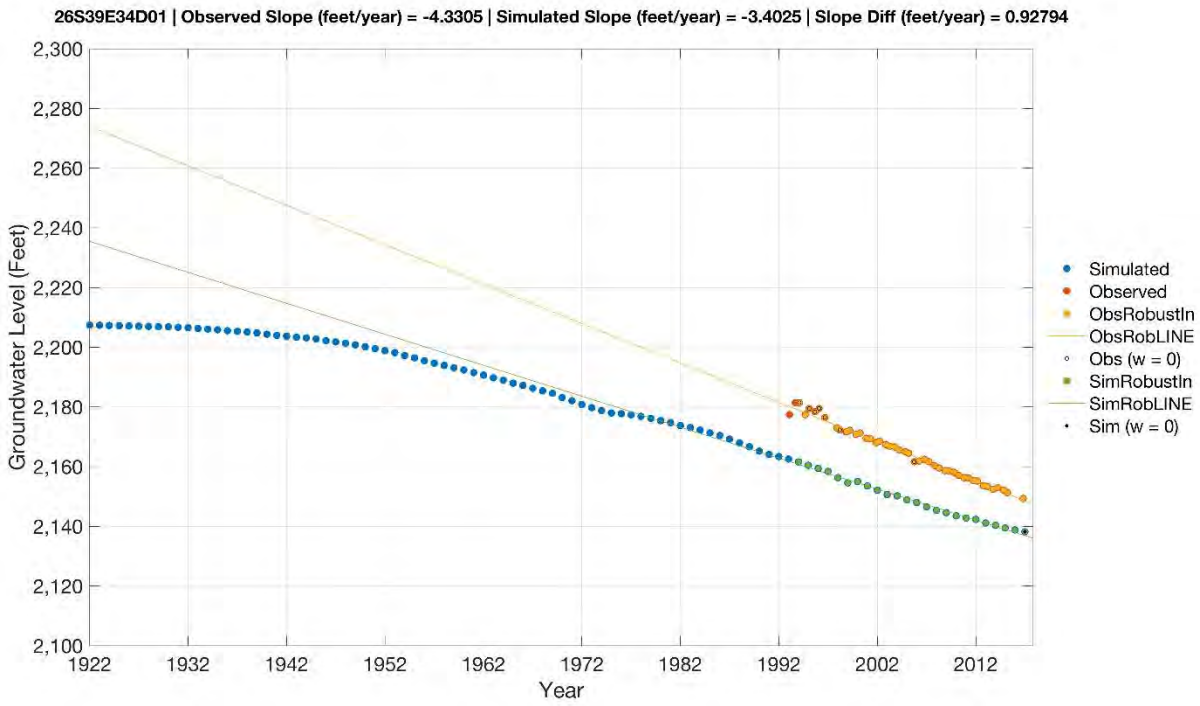


Figure A-19

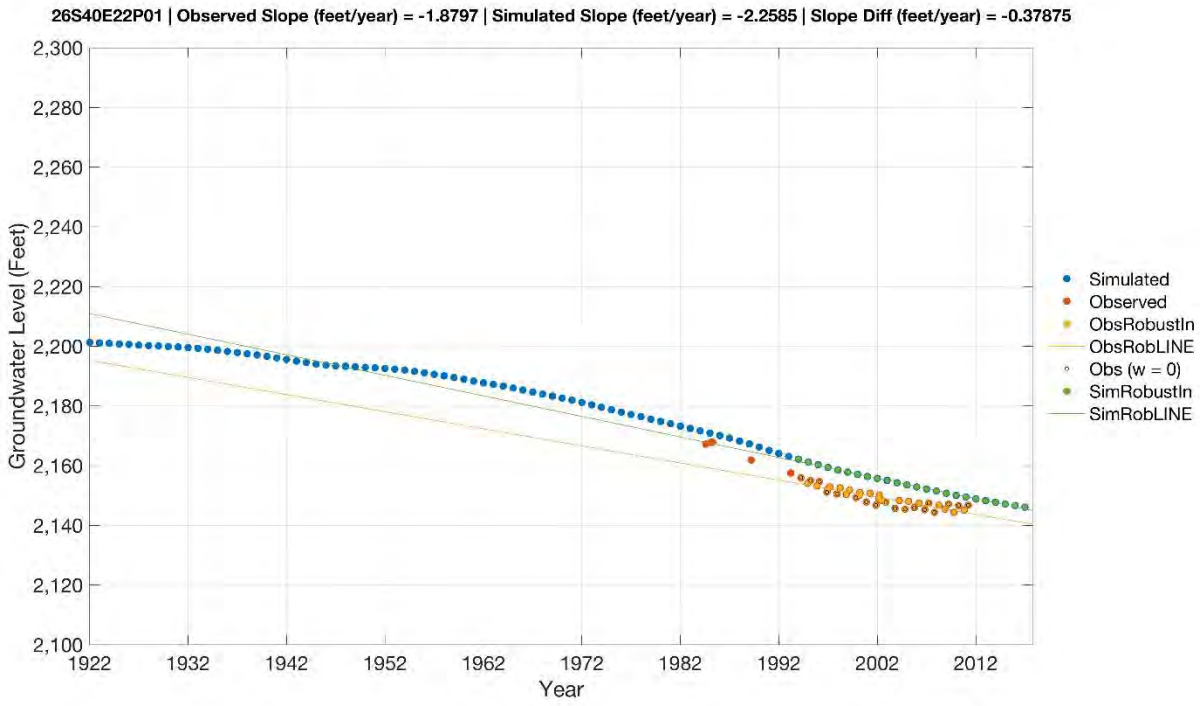


Figure A-20

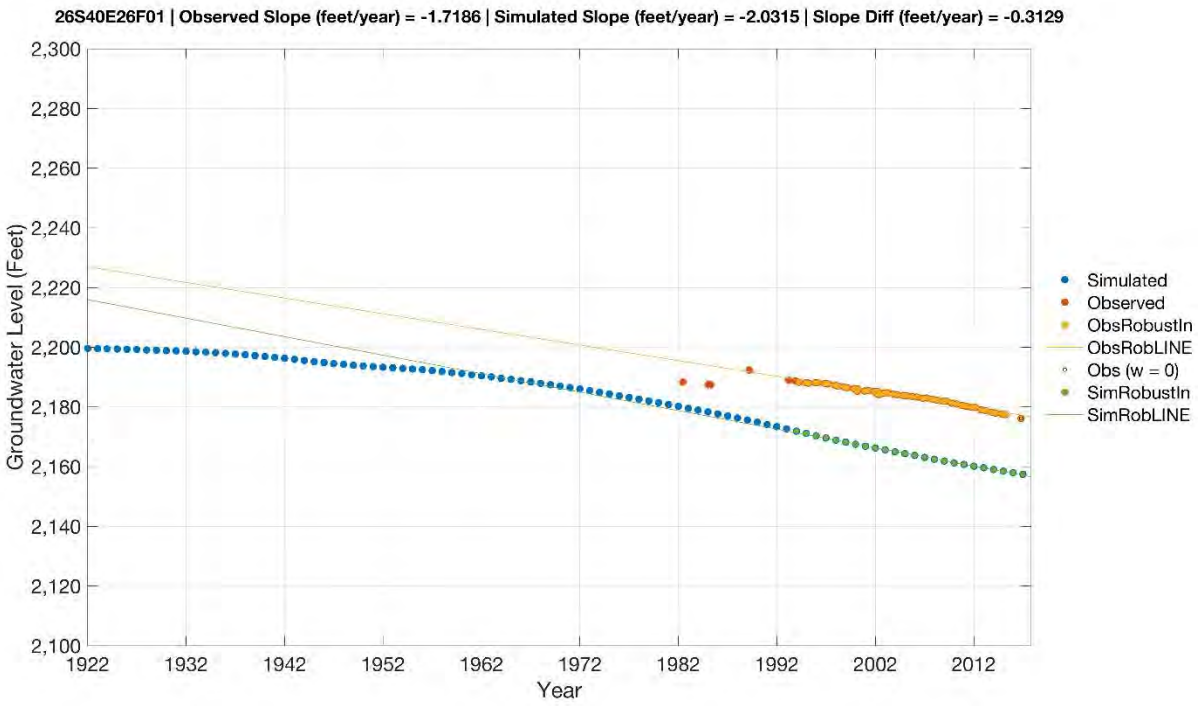


Figure A-21

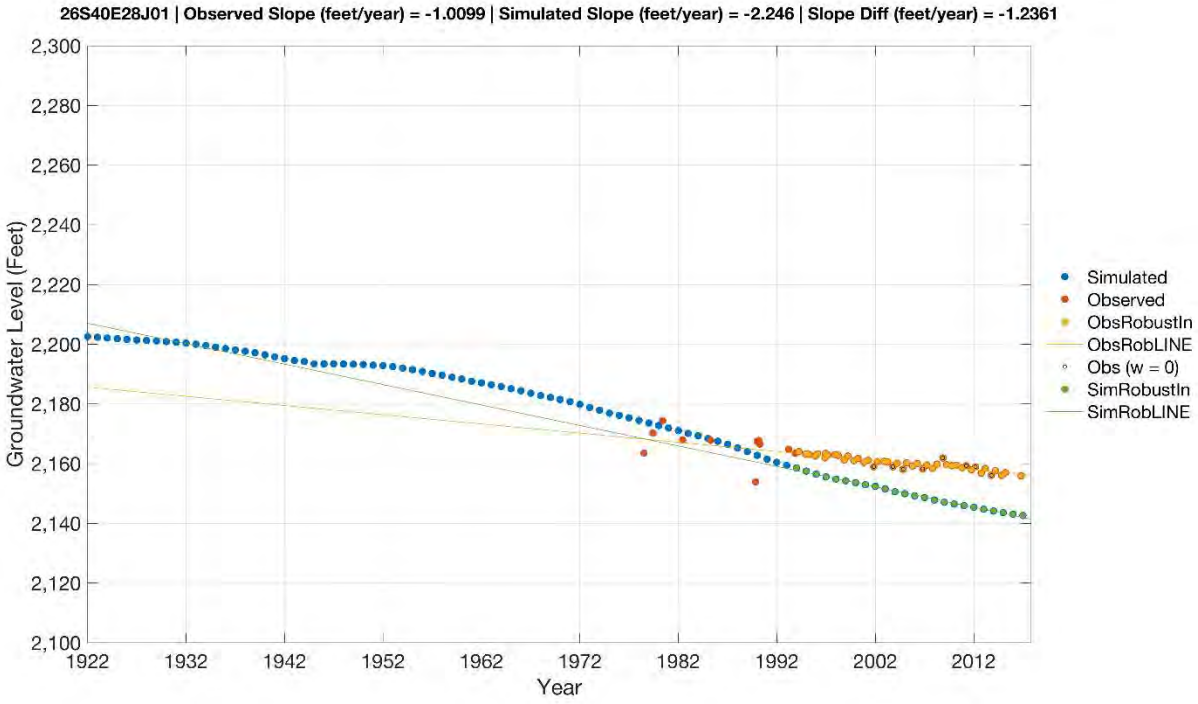


Figure A-22

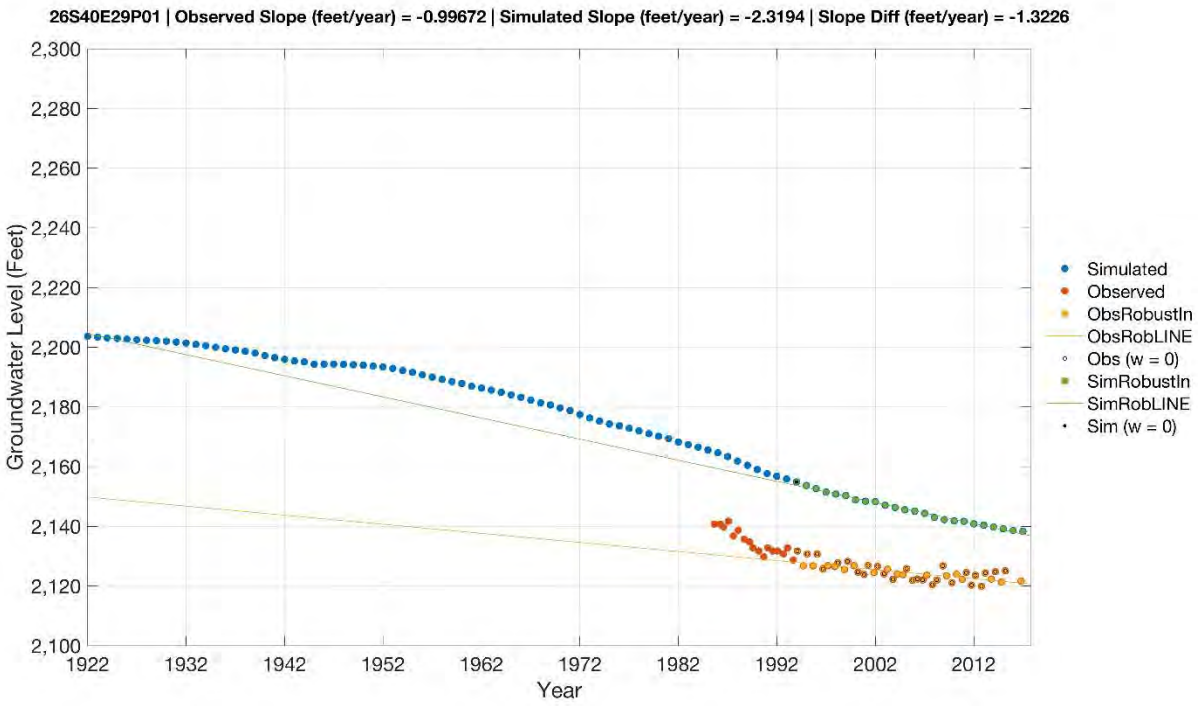


Figure A-23

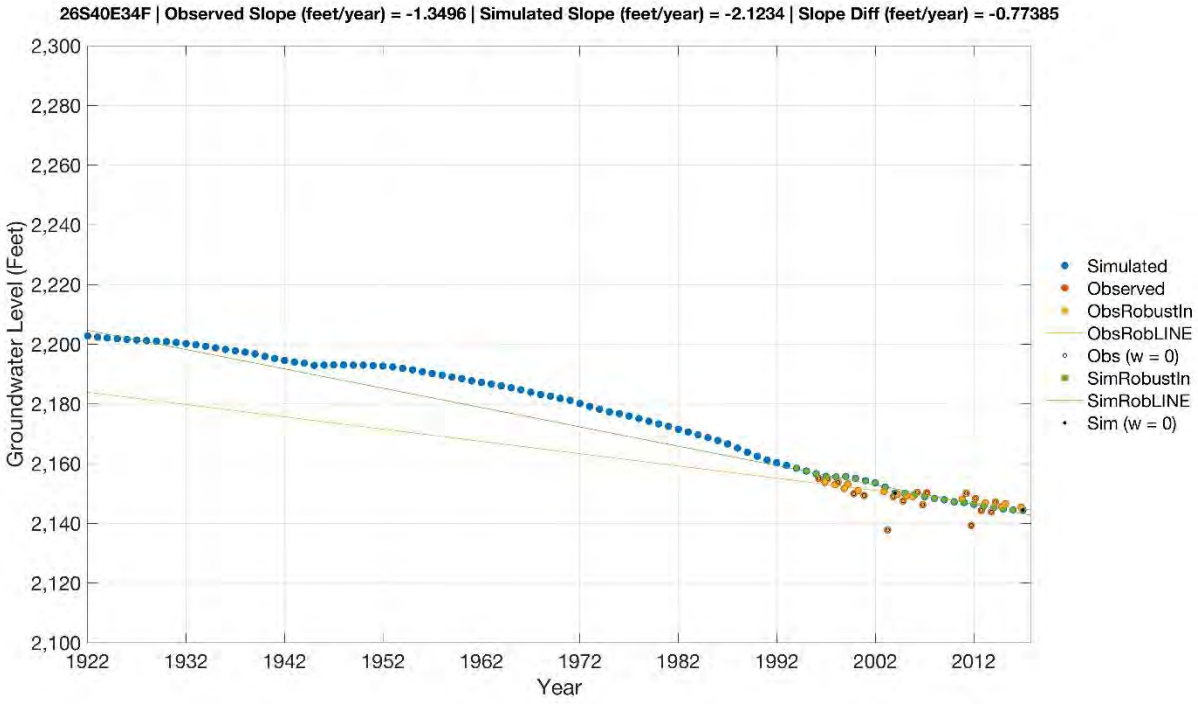


Figure A-24

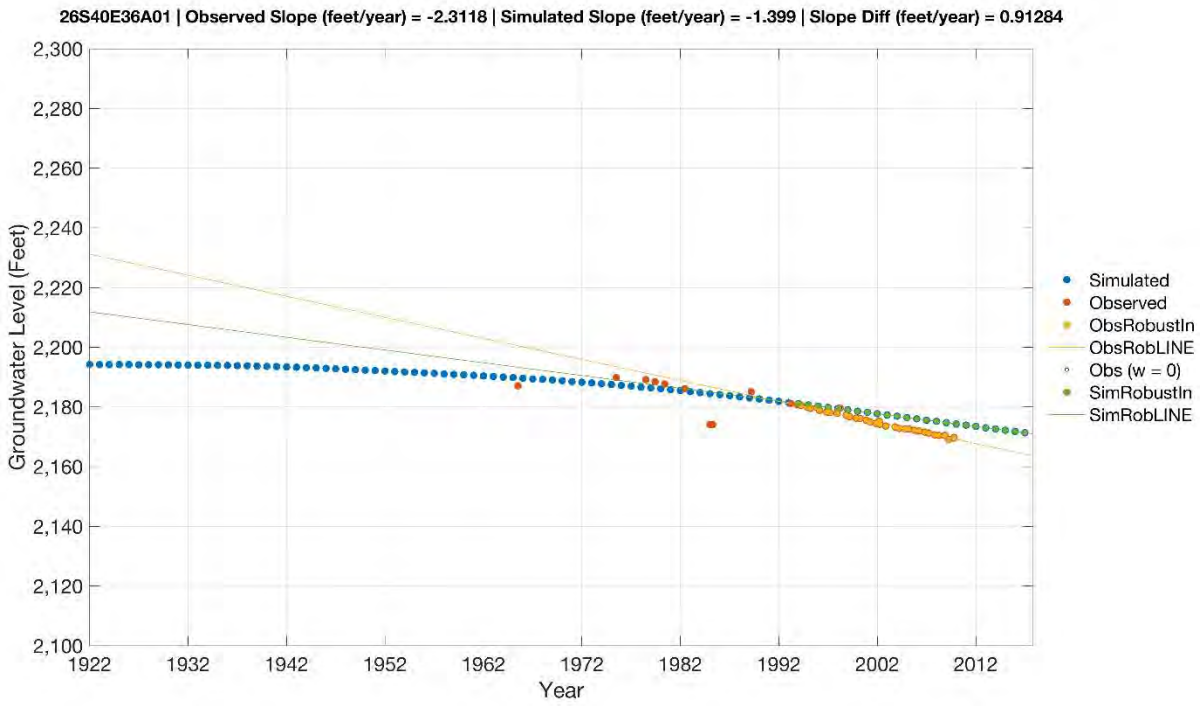


Figure A-25

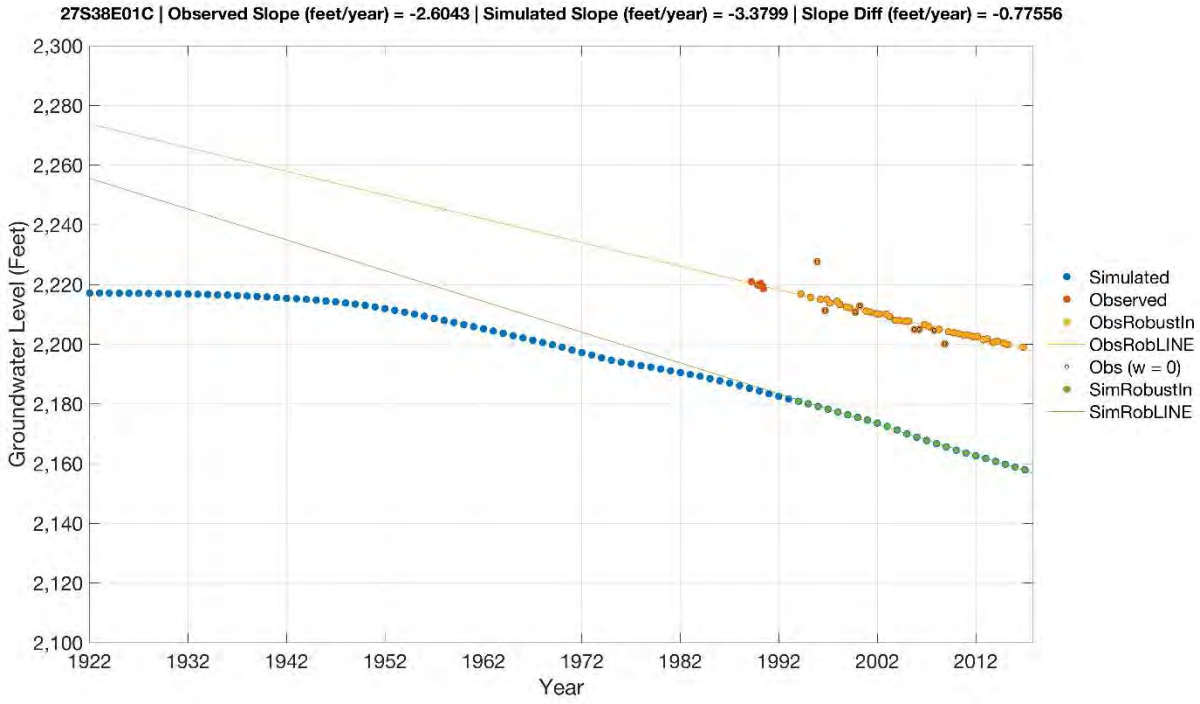


Figure A-26

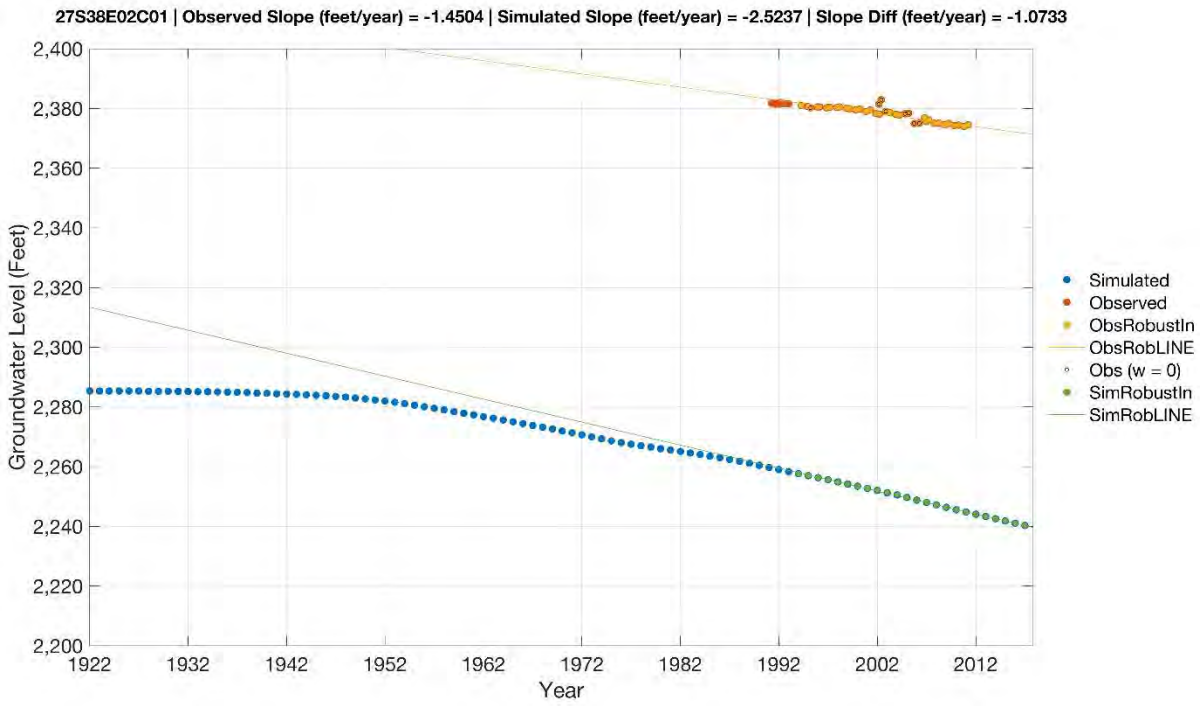


Figure A-27

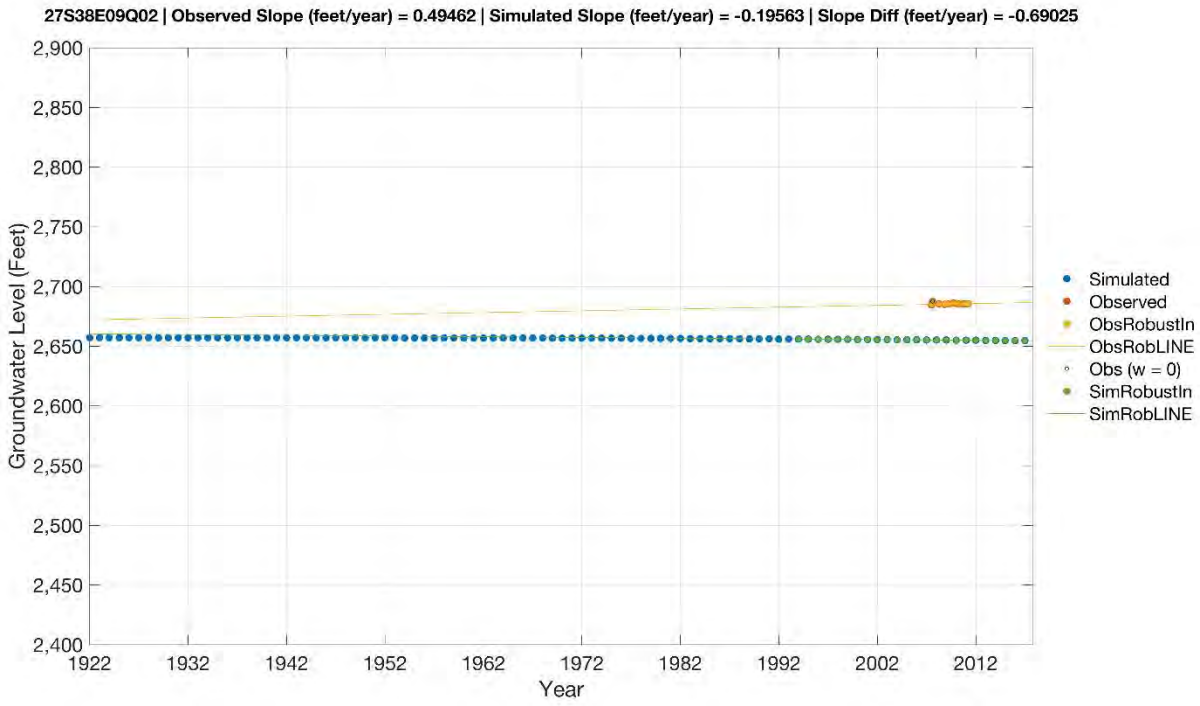


Figure A-28

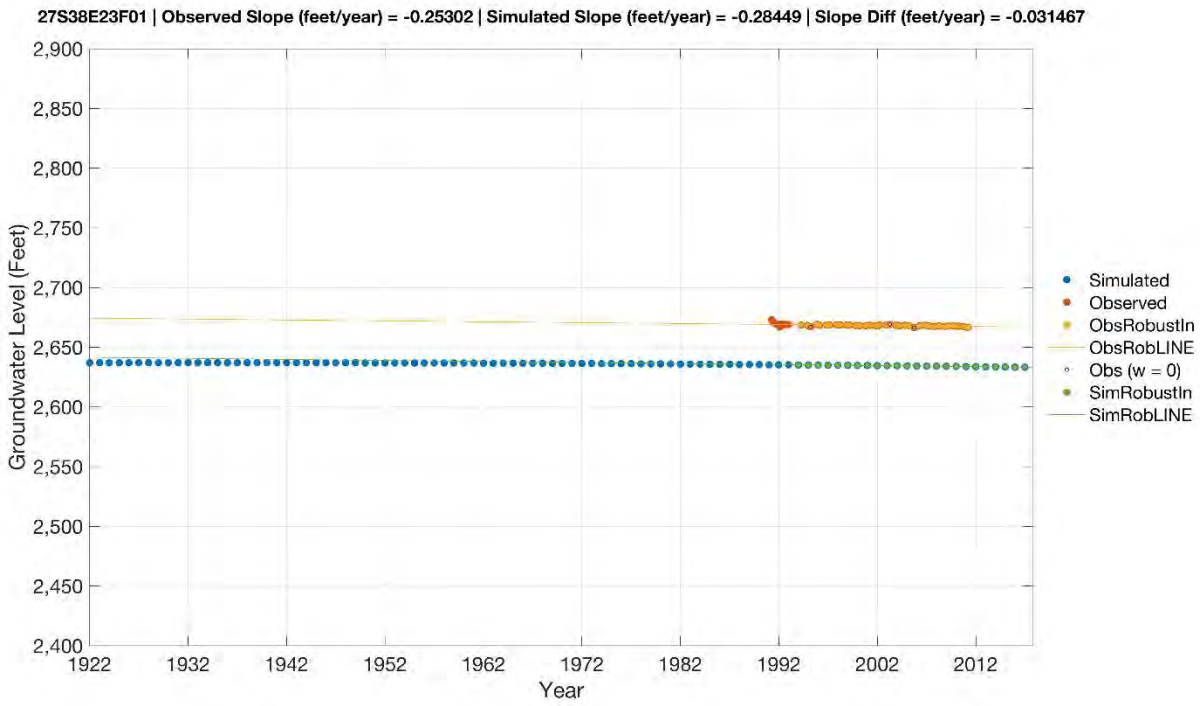


Figure A-29

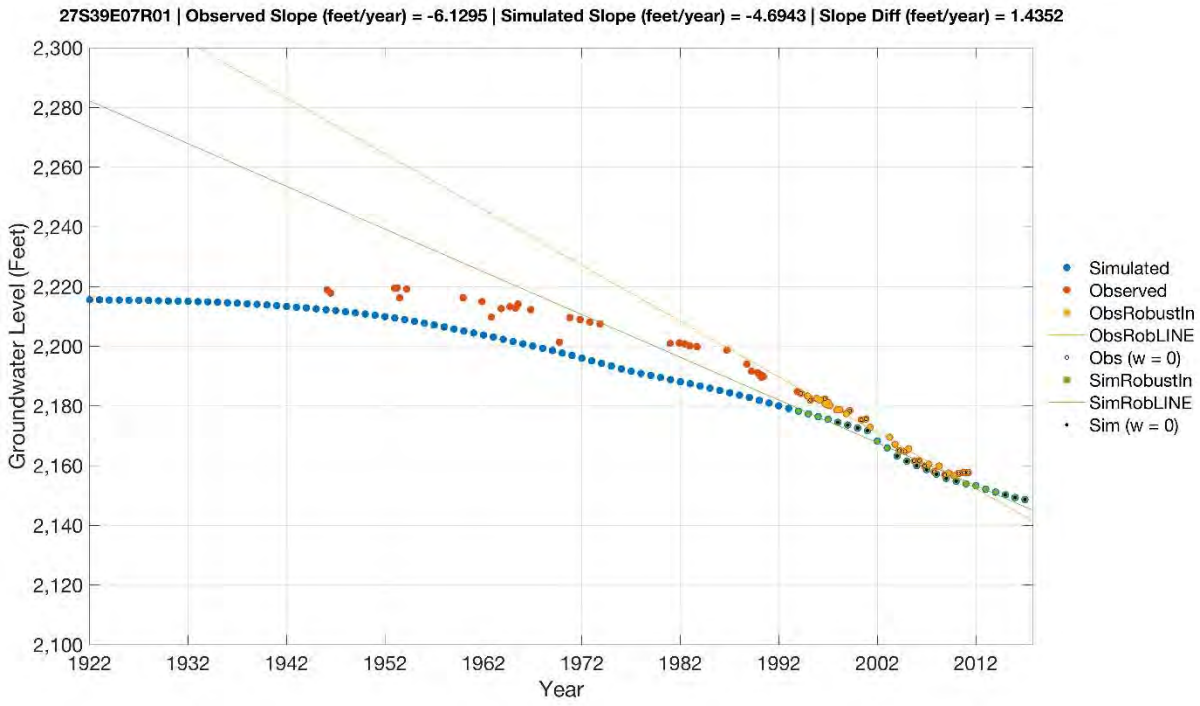


Figure A-30

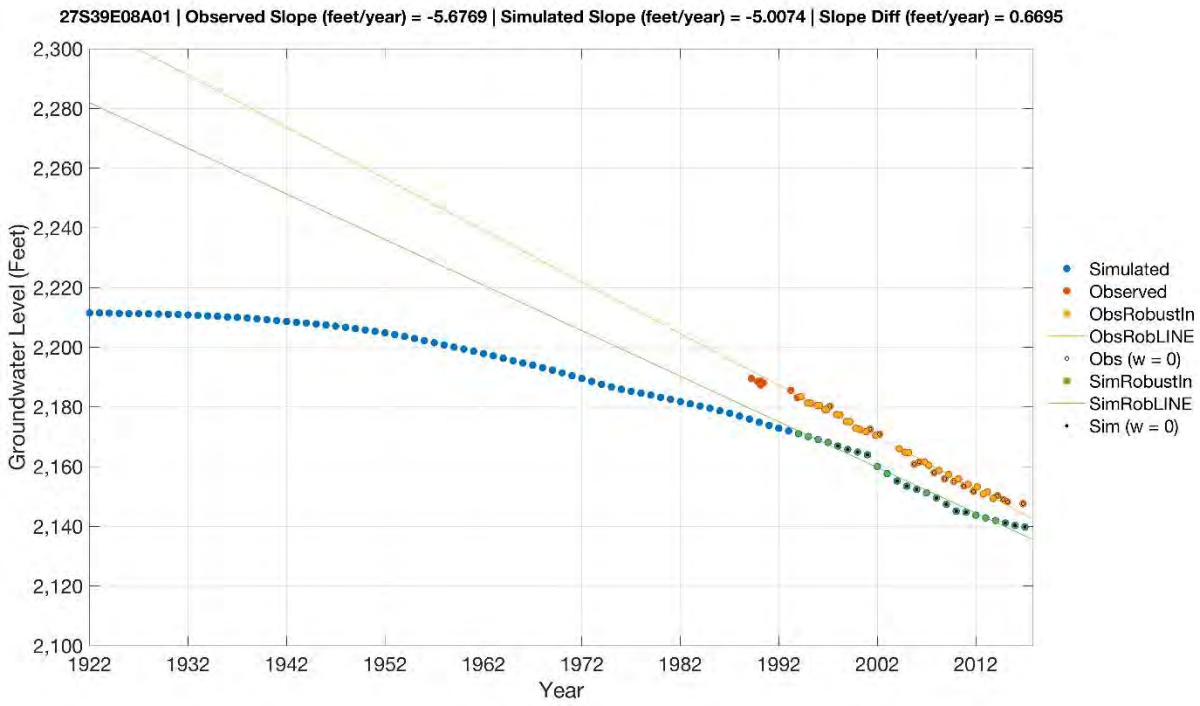


Figure A-31

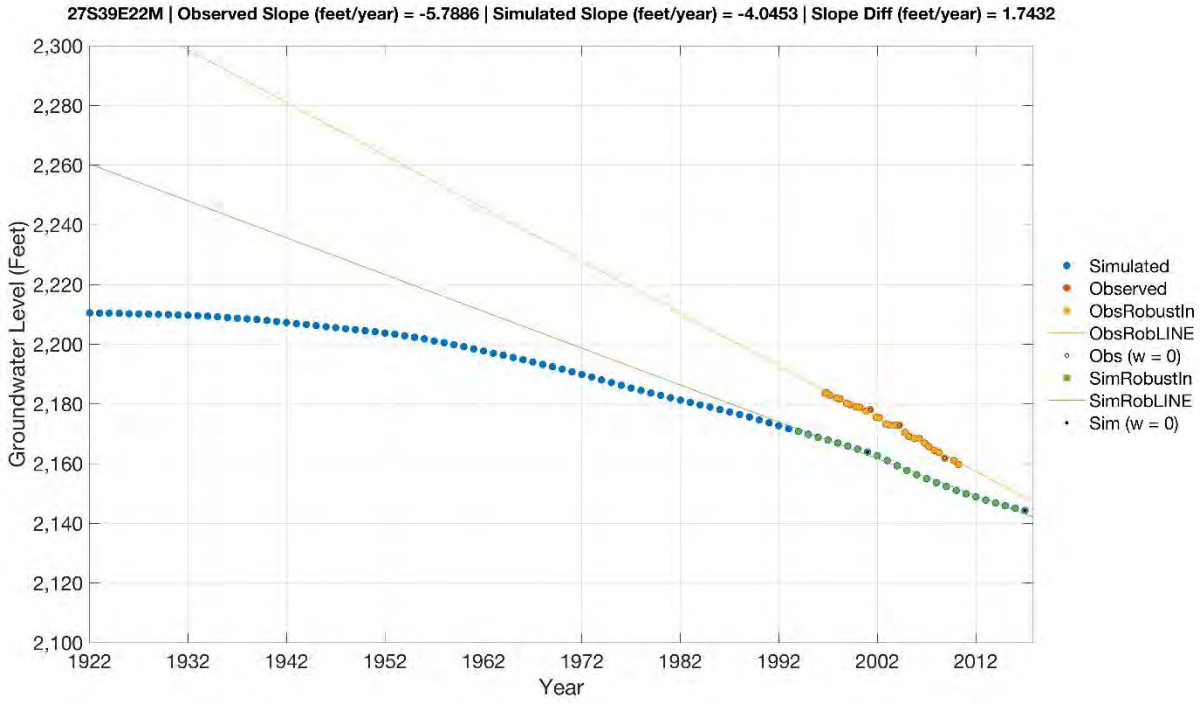


Figure A-32

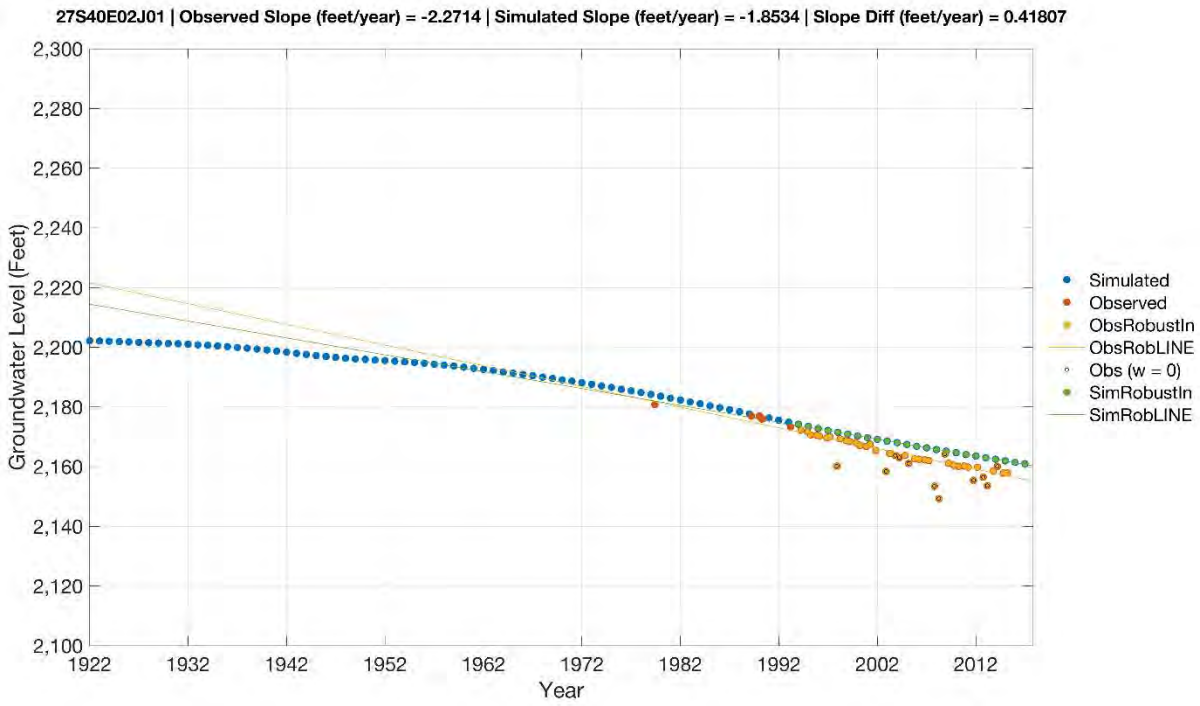


Figure A-33

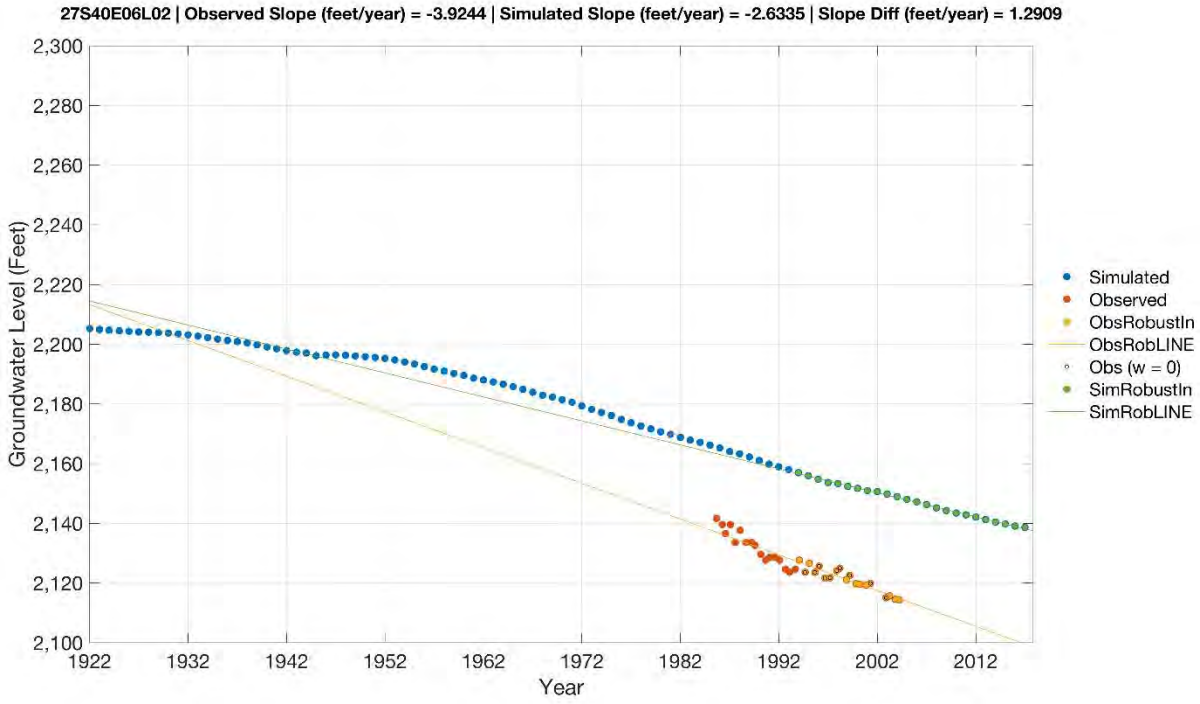


Figure A-34

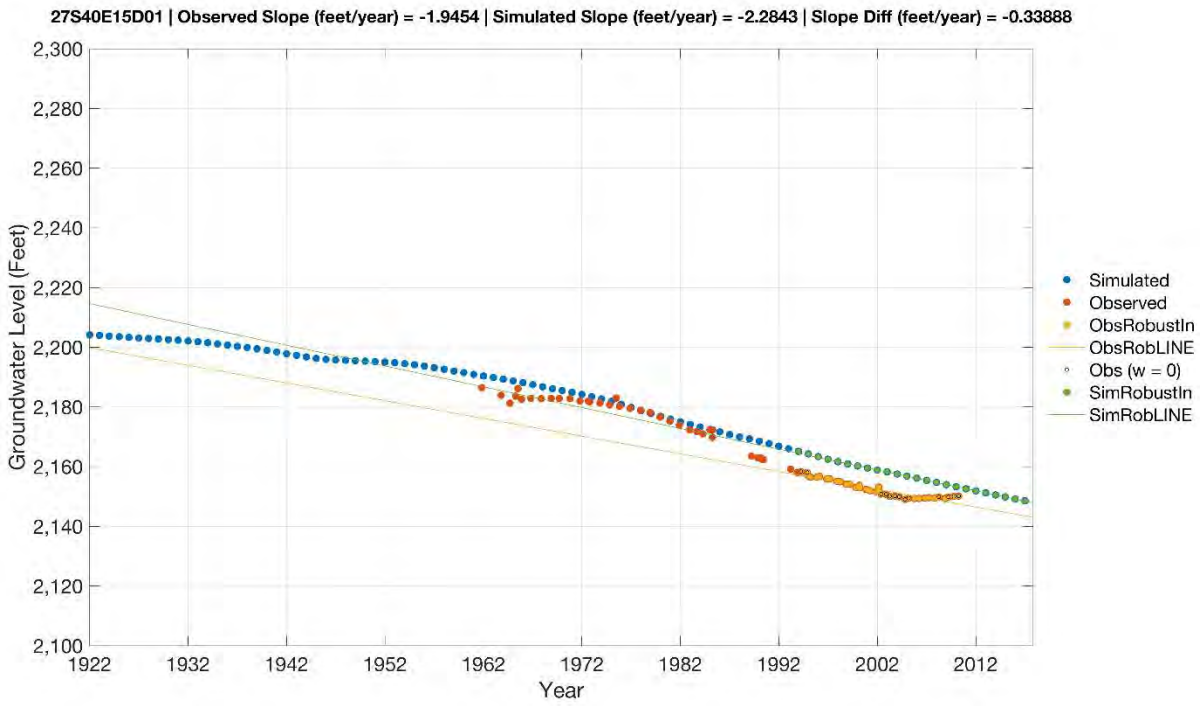


Figure A-35

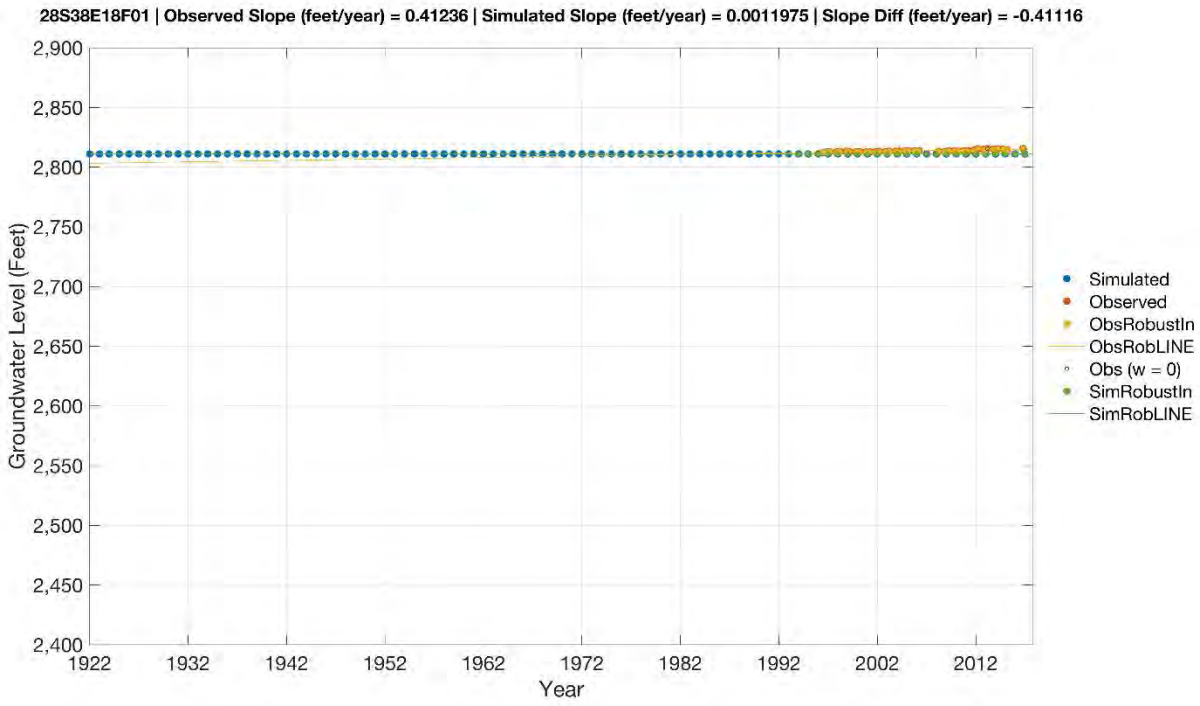


Figure A-36

Indian Wells Valley
Baseline Groundwater Model Results



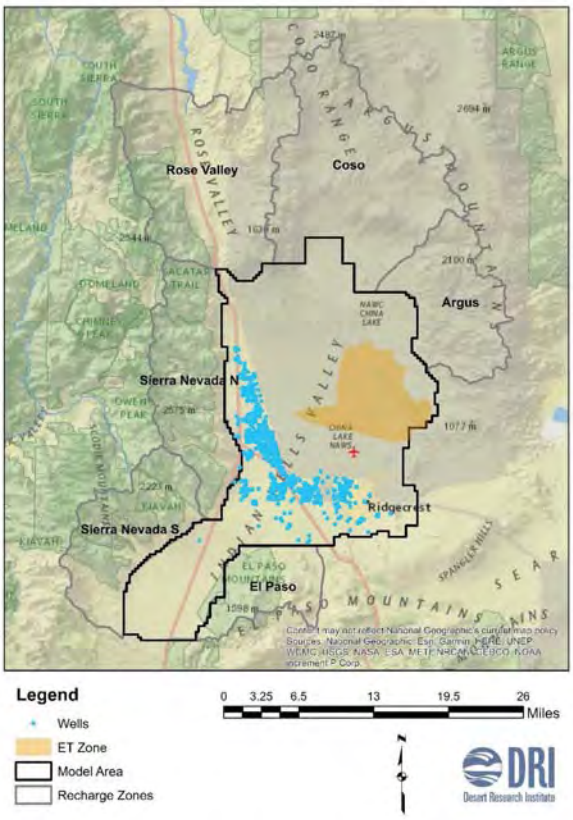
January 3, 2019

DRI
Desert Research Institute

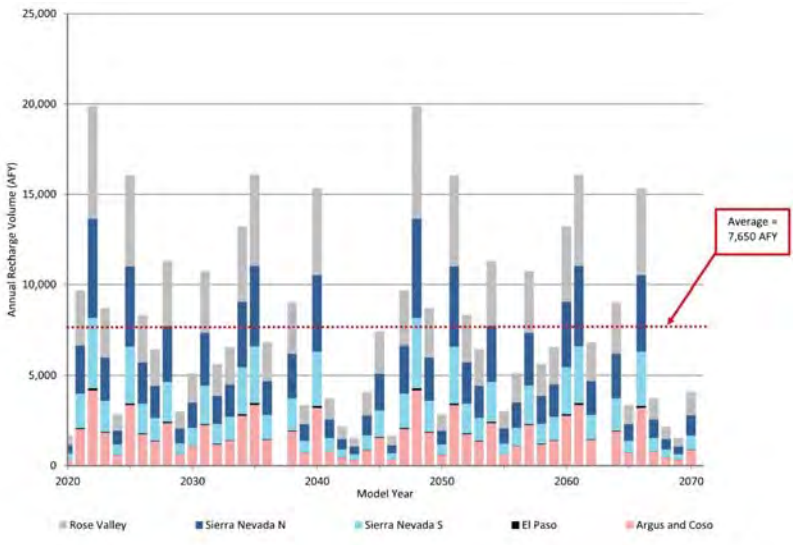
- Model assumptions
- Model results
  - Drawdown
  - Hydrographs by model analysis zone
  - Water budget

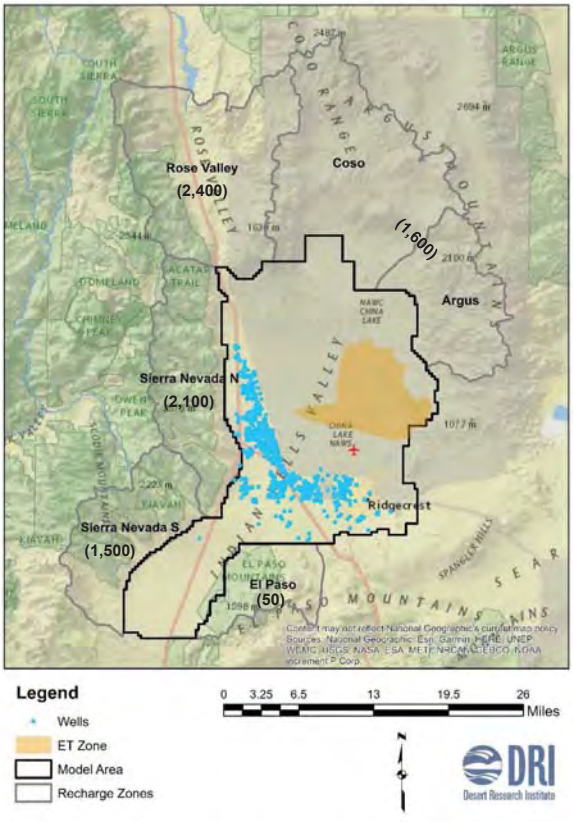
Model Assumptions

- Simulation period: 2017 – 2070
- Monthly time steps
- Water level initial condition from historical model
- Variable recharge
- Baseline pumping

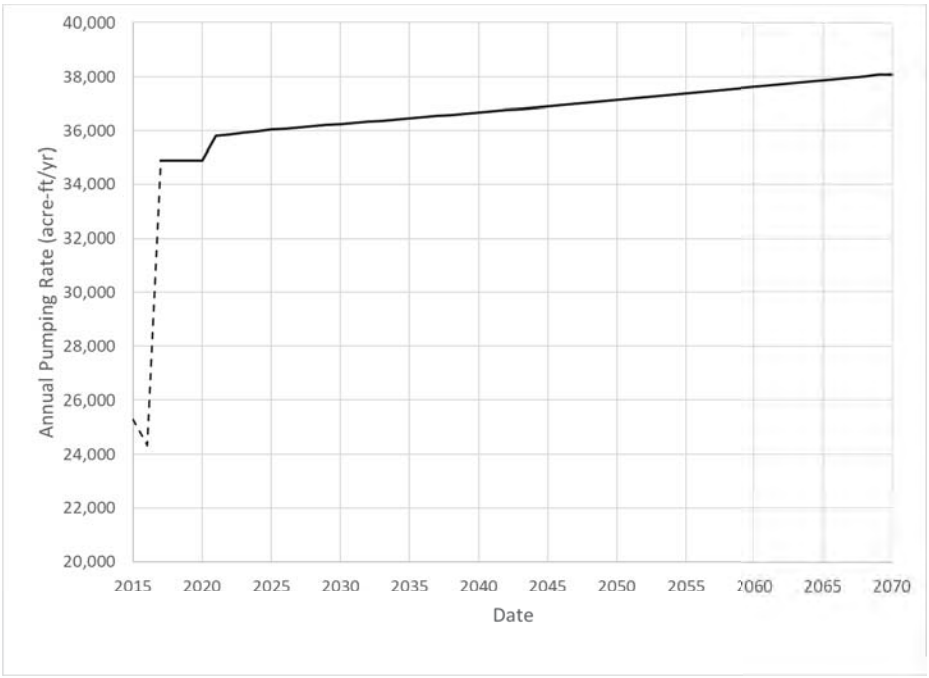


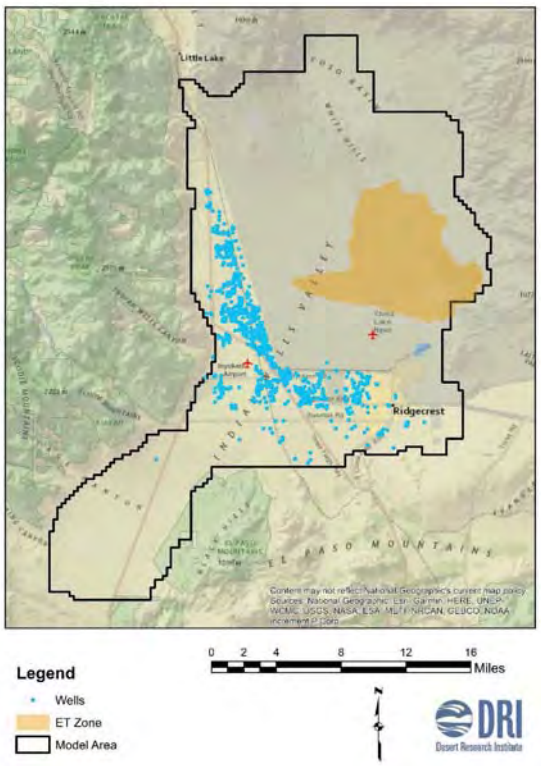
Recharge



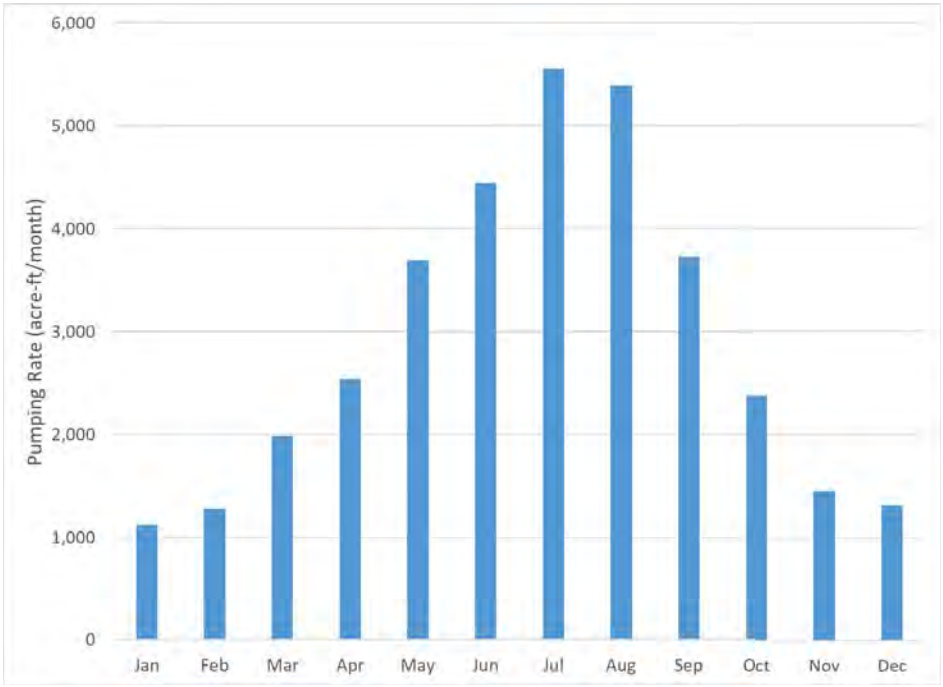


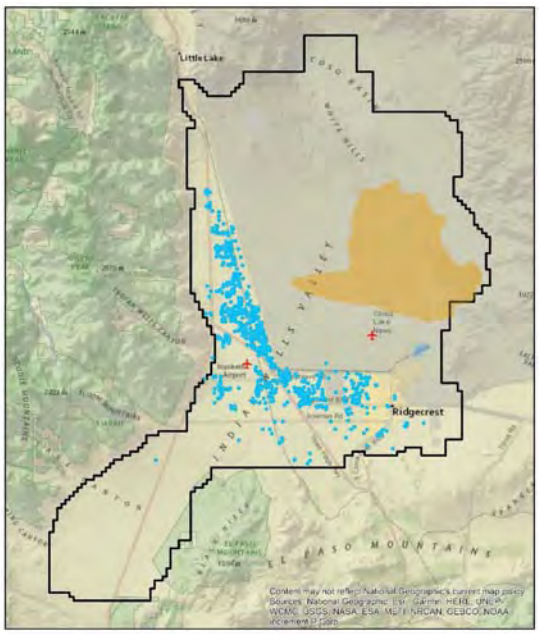
Simulated Pumping





Simulated Pumping





2020-2070 Average Water Budget

INPUTS

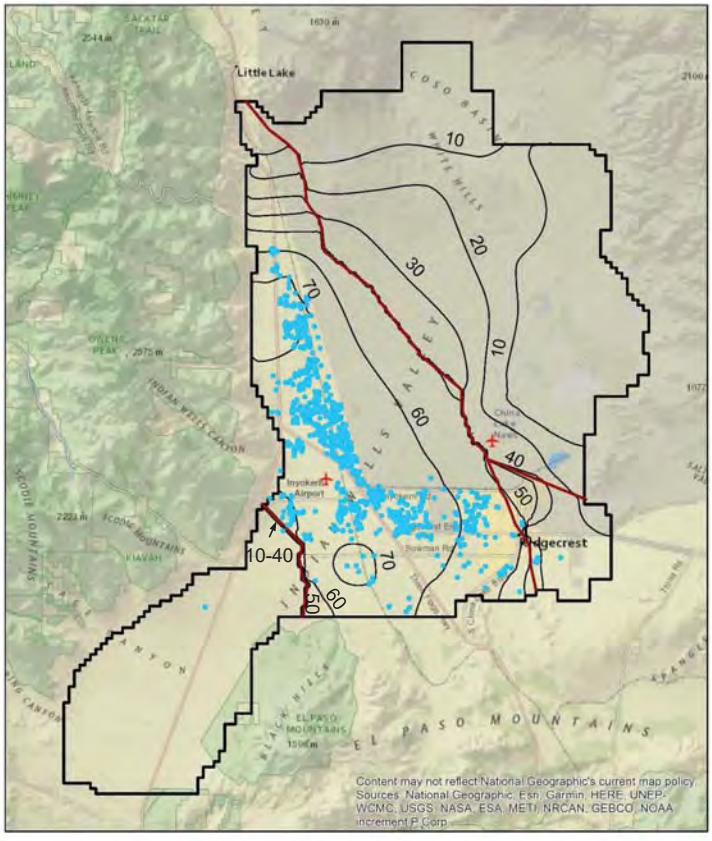
	(acre-ft/year)
Recharge	7,650
Storage	30,880
Total:	38,530

OUTPUTS

	(acre-ft/year)
Pumping	36,880
ET	1,610
Flow to Salt Wells Valley	40
Total:	38,530

Drawdown Results

- Drawdown from 2020 to 2070



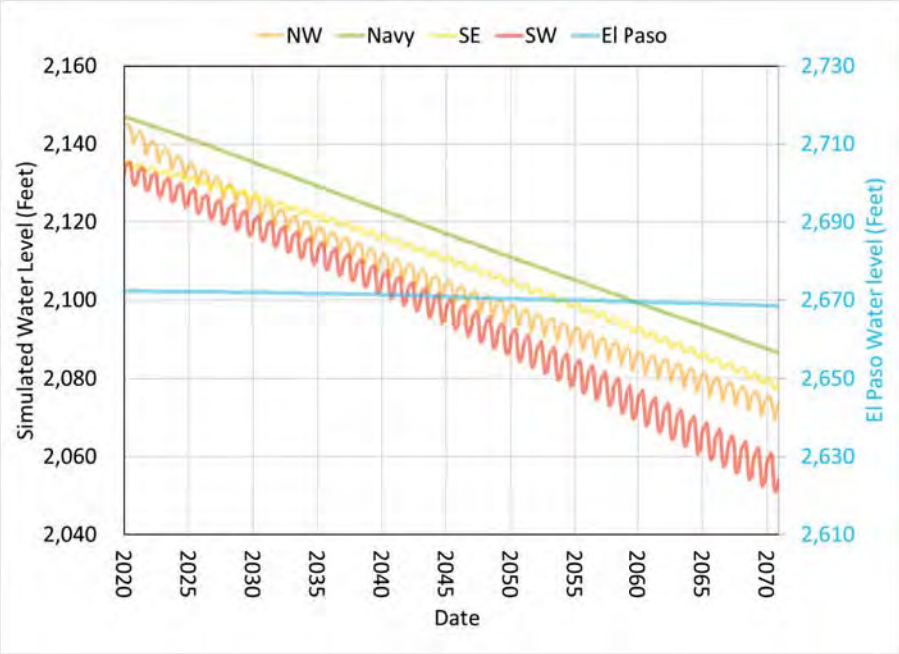
Legend
- Wells
- Geologic Faults
- Drawdown (2020-2070) ft
- Model Area

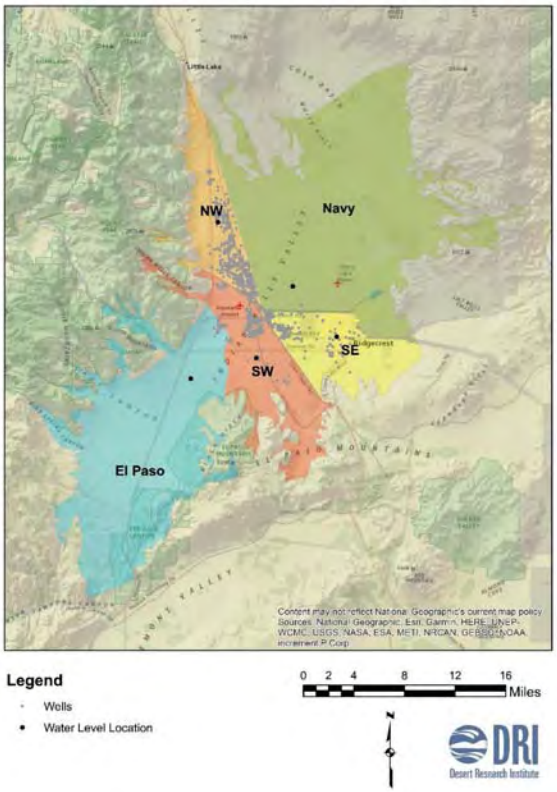
0 1.5 3 6 9 12 Miles

N

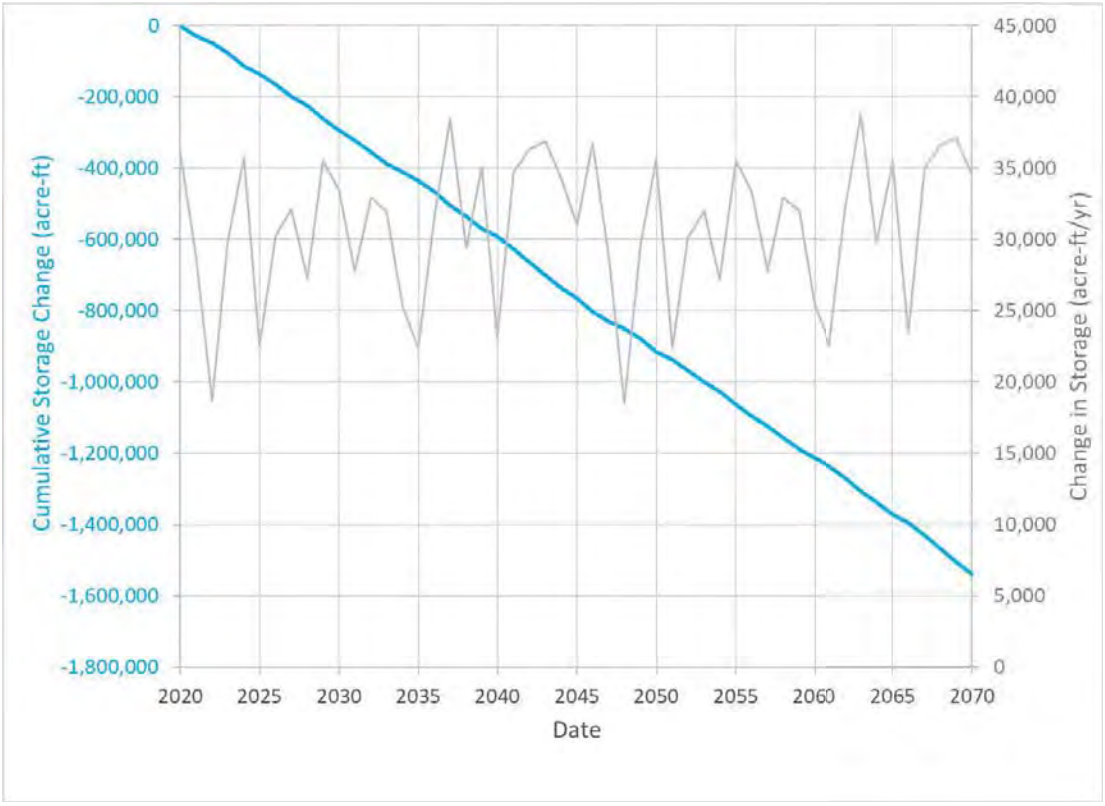
DRI Desert Research Institute

Simulated Water Levels by Model Analysis Zones

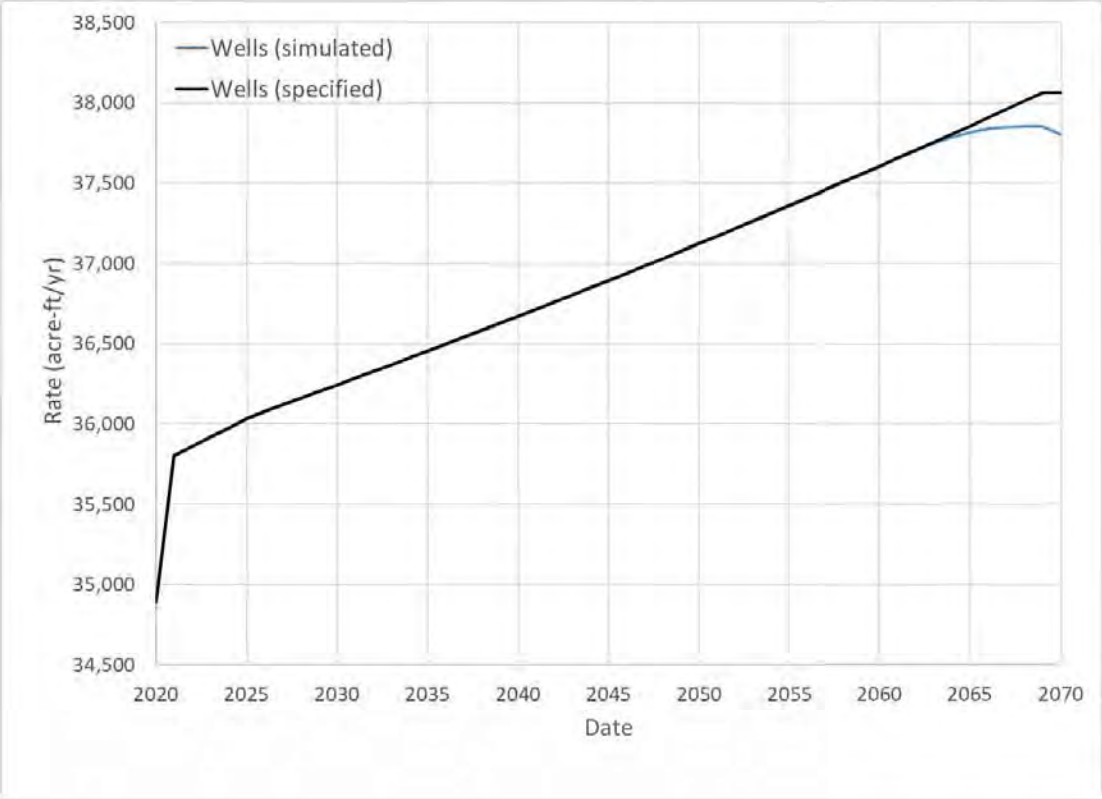




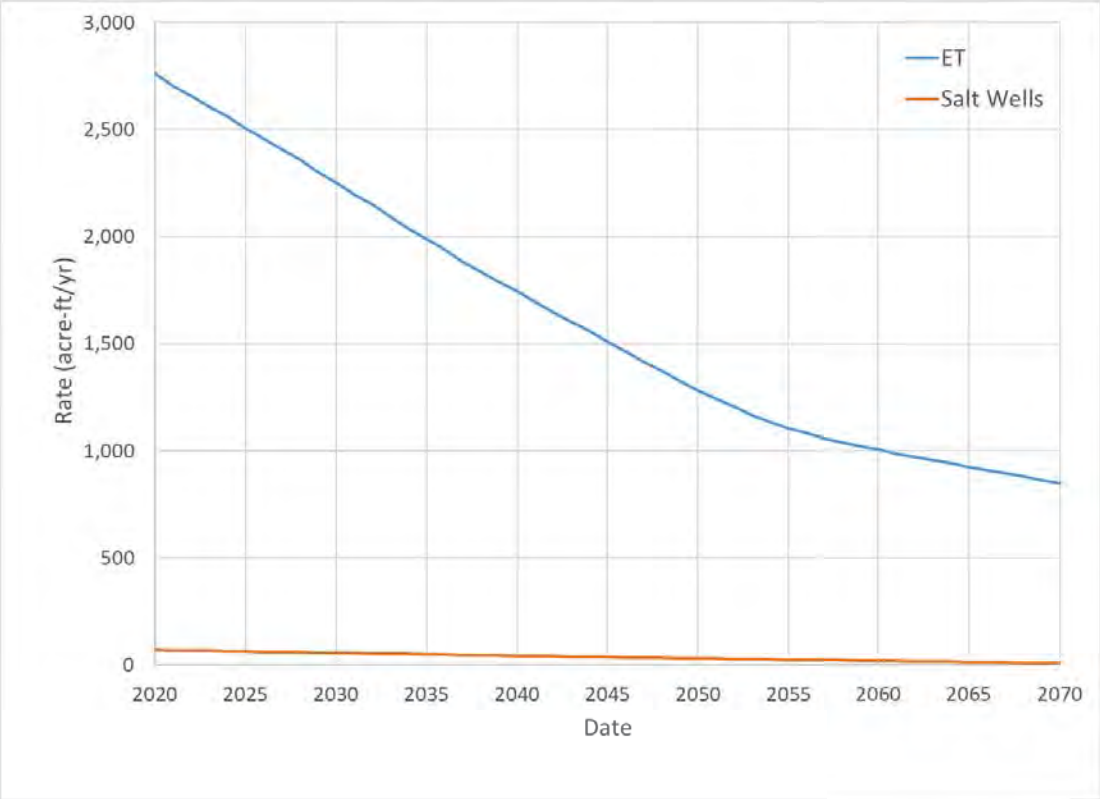
Change in Groundwater Storage



Simulated Outputs (Wells)



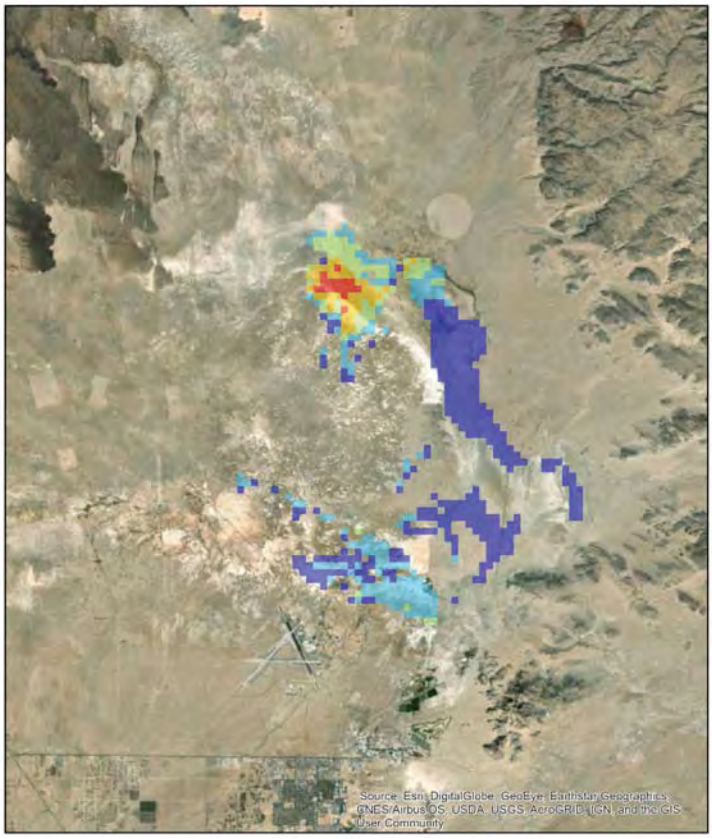
Simulated ET & Flow to Salt Wells



Questions

https://clminternship.org

ET Changes (2020 to 2070)



Scenario 6 Summary

1

Scenario 6 Development

- Results of Scenarios 3, 4, and 5 presented to the Board in May and June
  - Emphasis on minimizing loss of groundwater in storage
  - Scenario 4 identified as a potentially viably acceptable solution
- IWVGA Attorney's meeting on July 12
  - Discussion of basin water demands, groundwater in storage, use of storage, and GSP implementation
  - Agreement to proceed with a new modeling scenario (Scenario 6)
    - Modified version of Scenario 4 (Water Buyout) with "blocks" of allowed non-domestic pumping
- Draft summary of concepts for Scenario 6 was developed in coordination with the Attorneys
  - Final model inputs provided to DRI after finalizing the summary of concepts with the Attorneys
- Discussion of Scenario 6 results and goals with DRI
  - Second iteration of Scenario 6 (6.2) developed to further evaluate imported water requirement

2

Scenario 6 Objectives

- Create an allocation and management plan based on 2010-2014 pumping history and the highest beneficial uses of groundwater
- Maintain a similar cumulative loss of groundwater in storage as in Scenario 4 (Water Buyout) by replicating the total pumping volume used in Scenario 4
- Provide pumping "blocks" to non-domestic pumpers approximately equivalent to total non-domestic pumping in Scenario 4
  - More practical and feasible than the "ramp-down" in Scenario 4
- Optimize pumping locations to minimize future large drawdowns

3

Recap - Model Scenario 4 (Water Buyout)

- Start of Management Action – January 2022
  - Current pumping maintained in 2020 and 2021
- 2022: Total pumping going forward consists only of allocated rights (Federal and State rights).
  - Pumping includes reduced quantities of unprotected pumping (subject to ramp-down), plus protected pumping (not subject to ramp-down).
  - Pumpers who did not pump in each of the allocation years (2010-2014) identified during Scenario 4 preparation (Simmons, Blubaugh), were given zero allocation.
- 2023 through 2027: Unprotected allocations reduced by equal increments each year to reach Total Pumping of ~12,000 AFY in 2027
- 2025: Recycled water available to help reduce overdraft
- 2028 through 2070: Total Annual Pumping of ~12,000 AFY
- 2035 through 2070: Imported water supply available for basin recharge to operate sustainably

4

Summary of Model Scenario 6 (Modified Water Buyout)

- Discontinue all pumping that was **not continuous** from 2010-2014 (i.e. post-SGMA pumpers)
  - McGee, Blubaugh, Simmons Ranch
    - Status as post-SGMA pumpers to be verified as a post-GSP action
- Pumpers with continuous pumping from 2010 – 2014 categorized into one of two groups:

Domestic Group	Non-Domestic Group
Kern County	Meadowbrook
City of Ridgecrest	Mojave
IWVWD	SVM (industrial)
Inyokern CSD	Other small ag. (Quist, Sierra Shadows, Amberglow, Terese, Hickle, Bellino)
SVM (Trona only)	
Mutuals and domestic/private wells	
Navy	

5

5

Summary of Model Scenario 6 (Modified Water Buyout) (cont.)

Domestic group

- Starting in February 2020, allocation equal to lowest annual pumping from 2010-2014
  - Does not result in decreases in current pumping, except for a minor decrease for City of Ridgecrest
- Modeled pumping for 2020-2070 is equal to allocation, except the IWVWD
  - IWVWD pumping in 2020 equal to 6,507 AFY (based on 2017 actual pumping)
  - Assumed growth rate of 1% per year for IWVWD demands
  - IWVWD pumping above allocation due to growth will be offset by purchasing additional imported water
  - City stops pumping when recycled water becomes available

6

6

Summary of Model Scenario 6 (Modified Water Buyout) (cont.)

- Domestic group allocations
  - Navy 2,041 AFY
  - Kern County 18 AFY
  - IWVWD 7,319 AFY
  - Private/domestic wells 800 AFY
  - Mutuals 300 AFY
  - Inyokern CSD 108 AFY
  - City of Ridgecrest 339 AFY
  - SVM (Trona) 225 AFY
  - **11,150 AFY**
- Domestic group modeled 2020 pumping
  - Navy 2,041 AFY
  - Kern County 18 AFY
  - IWVWD 6,507 AFY
  - Private/domestic wells 800 AFY
  - Mutuals 300 AFY
  - Inyokern CSD 108 AFY
  - City of Ridgecrest 339 AFY
  - SVM (Trona) 225 AFY
  - **10,338 AFY**

7

Summary of Model Scenario 6 (Modified Water Buyout) (cont.)

Non-domestic group

- Pumpers have no allocations but are allowed to pump up to an assigned portion of a non-domestic pool/block volume.
- Total non-domestic pool/block volume: **63,836 AF**
  - Approximately equal to total non-domestic pumping in Scenario 4 over 8 years (2 years of current pumping and 6 years of "ramp-down" pumping)
- Agricultural pumpers: assigned portion of the pool volume is distributed proportionate to existing information on irrigated acres from 2010-2014
  - Acreage per the March 2014 Farm Group letter
- SVM (industrial): assigned portion of the pool volume is distributed proportionate to SVM's lowest pumping in 2010-2014 compared to the total of the lowest pumping by each non-domestic producer in 2010-2014
- All pumping from the non-domestic pool is required to cease by **2040**
  - For modeling purposes, non-domestic group pumpers continue to pump at current levels over a "cliff" period until their assigned portions of the pool volume are depleted
  - Assigned portion of the pool volume may be used variably until 2040, but total pumping shall not exceed assigned portion.

8

Summary of Model Scenario 6 (Modified Water Buyout) (cont.)

Name	Irrigated Acreage (acres)	Portion of Pool Volume (AF)	Estimated "Cliff" Period (months)
Meadowbrook	890	31,832	60
Mojave*	120	4,292	8
Quist	140	5,007	92
Sierra Shadows	168	6,009	94
Amberglow	12	429	83
Terese	80	2,861	111
Hickle	17	608	86
Bellino	13	465	112
SVM (industrial)**	-	12,333	62
Total	**1,440**	**63,836**	-

*Irrigated acres consists only of 120 acres of alfalfa converted to pistachio
**Does not reflect recent information provided by SVM on pumping before establishment of China Lake NAWS

9

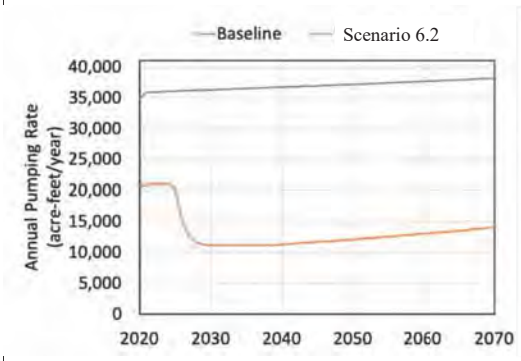
Summary of Model Scenario 6 (Modified Water Buyout) (cont.)

- Lease Market
  - Possible sellers
    - Meadowbrook
    - IWVWD (after accounting for annual growth)
    - City of Ridgecrest (demands assumed to be replaced with recycled water in 2025)
  - Possible buyers
    - Mojave
    - SVM (industrial)
    - Small Ag
  - SVM would purchase lease water or recycled water for its industrial demands until imported water becomes available in 2035.
- Some IWVWD and SVM pumping relocated towards Brown Road to optimize pumping.
- Imported water assumed to be available for basin recharge starting in 2035 to offset pumping above sustainable yield and offset increased pumping demands due to projected growth (IWVWD).
  - Included in Scenarios 6.1 and 6.2
- 2,500 AFY of additional imported water would be required for recharge to offset ongoing losses of groundwater in storage due to evapotranspiration.
  - **Only included in Scenario 6.1**

10

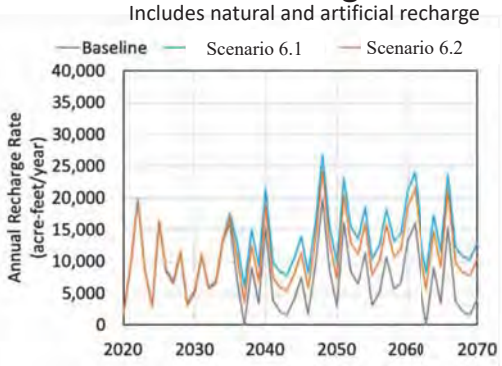
Management Scenario 6.2 - Pumping and Recharge Scenarios

Pumping



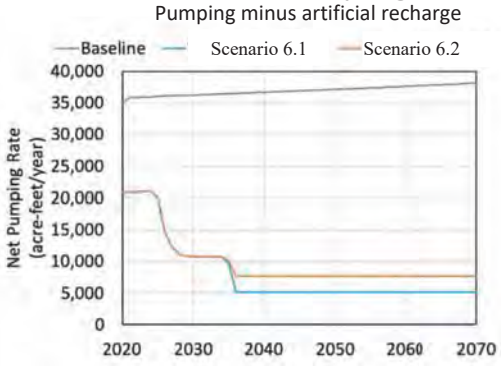
Recharge

Includes natural and artificial recharge



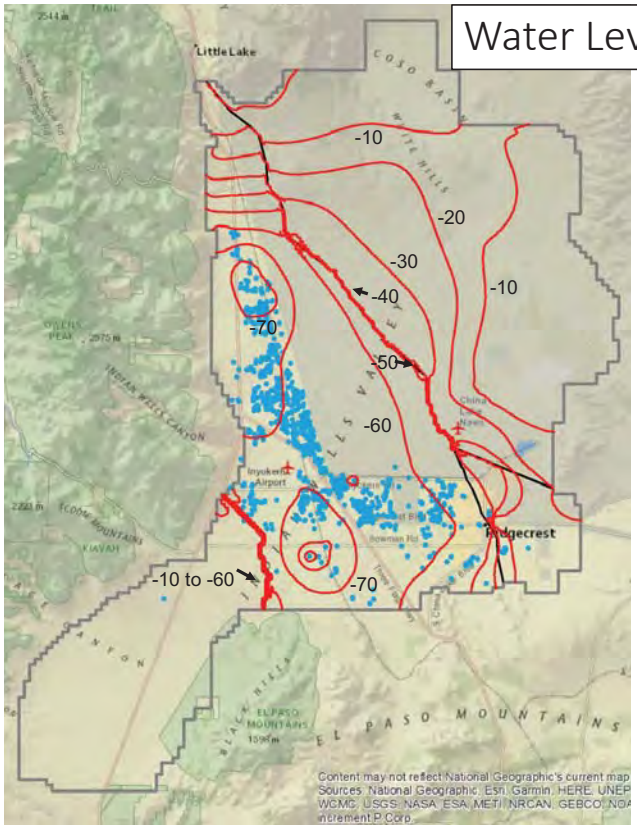
Net Pumping

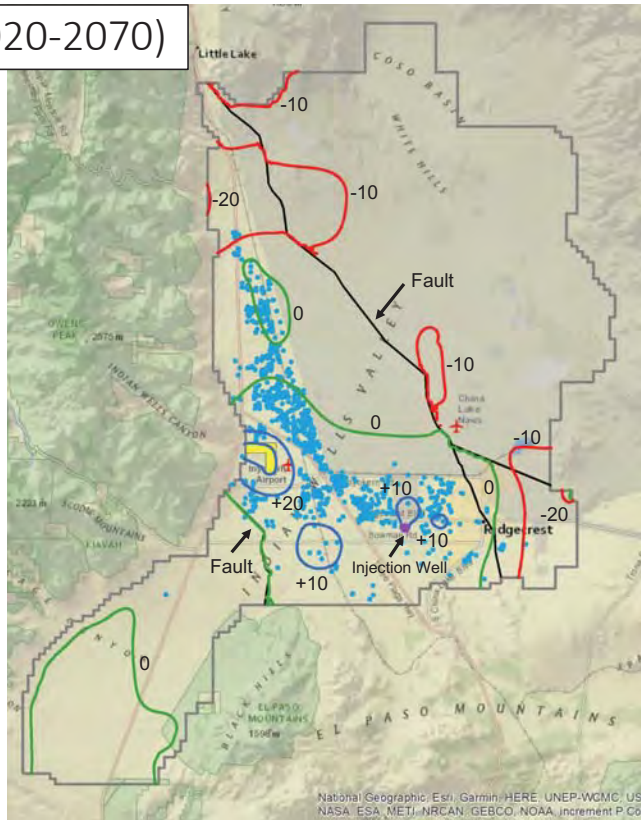
Pumping minus artificial recharge



DRAFT – Subject to change

Water Level Change (2020-2070)





DRAFT – Subject to change

Baseline

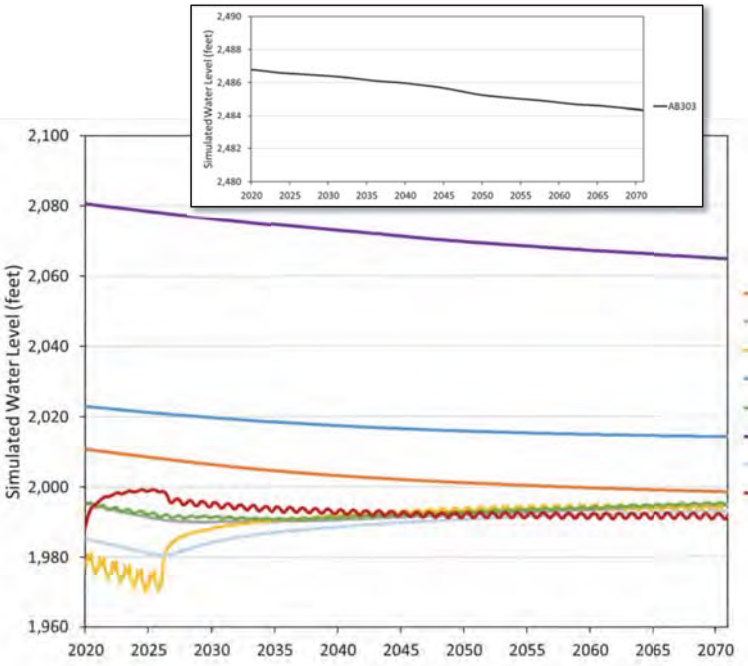
DRAFT – Subject to change

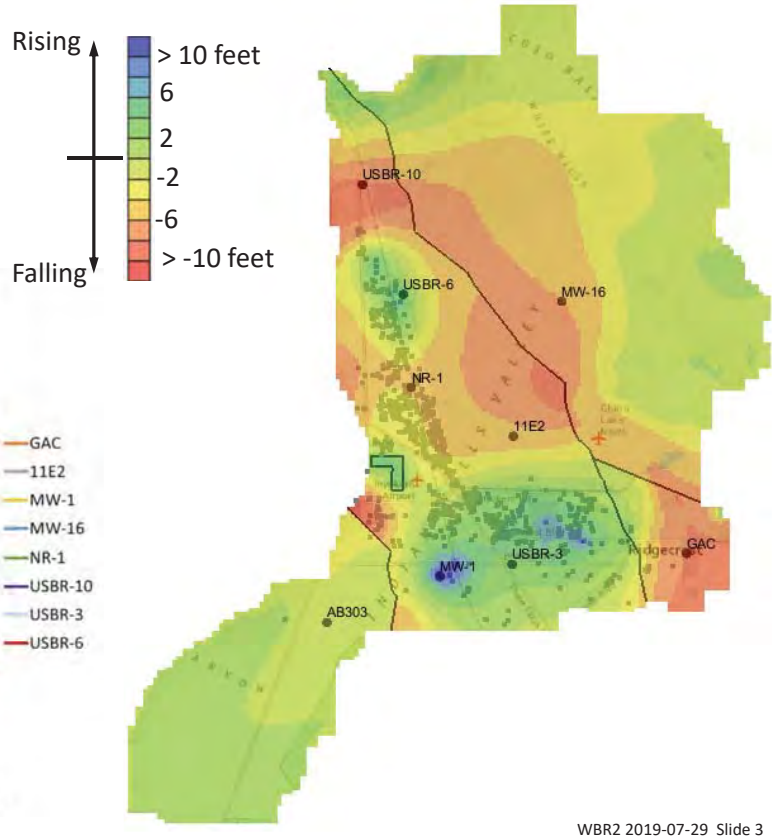
Scenario 6.2

Units: feet

Water Level Change 2020-2040

Management Scenario 6.2

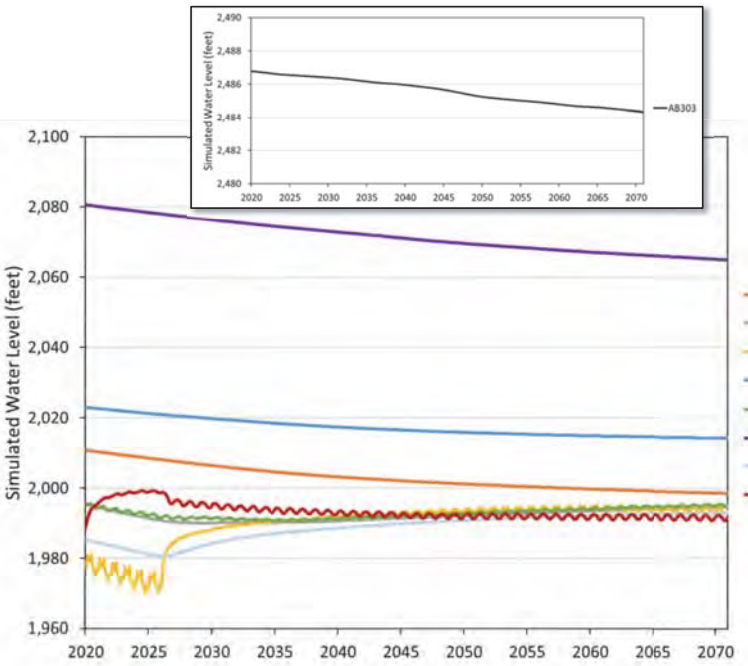


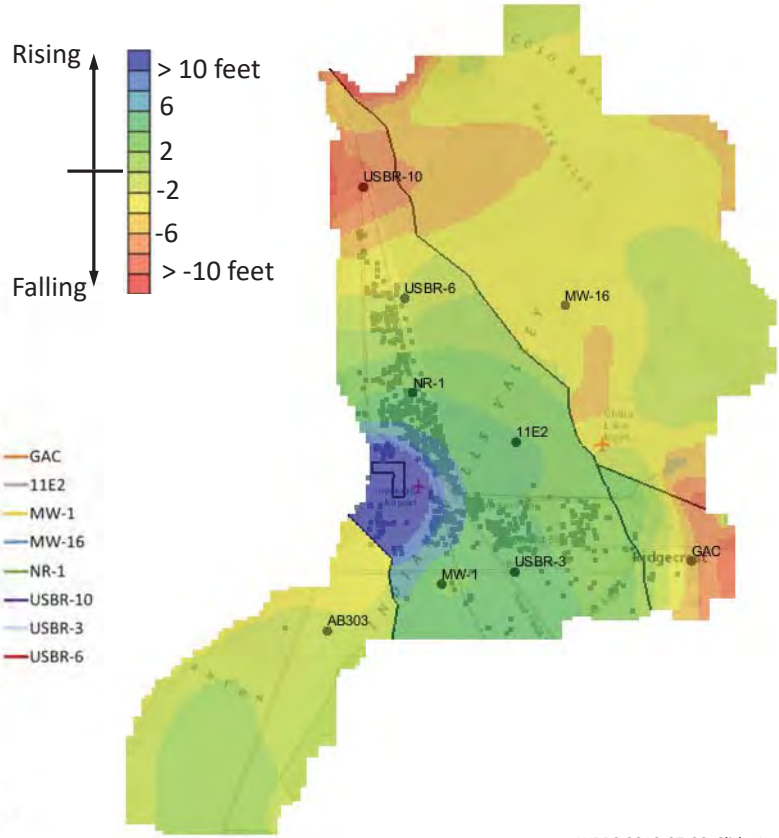


DRAFT – Subject to change

Water Level Change 2040-2070

Management Scenario 6.2

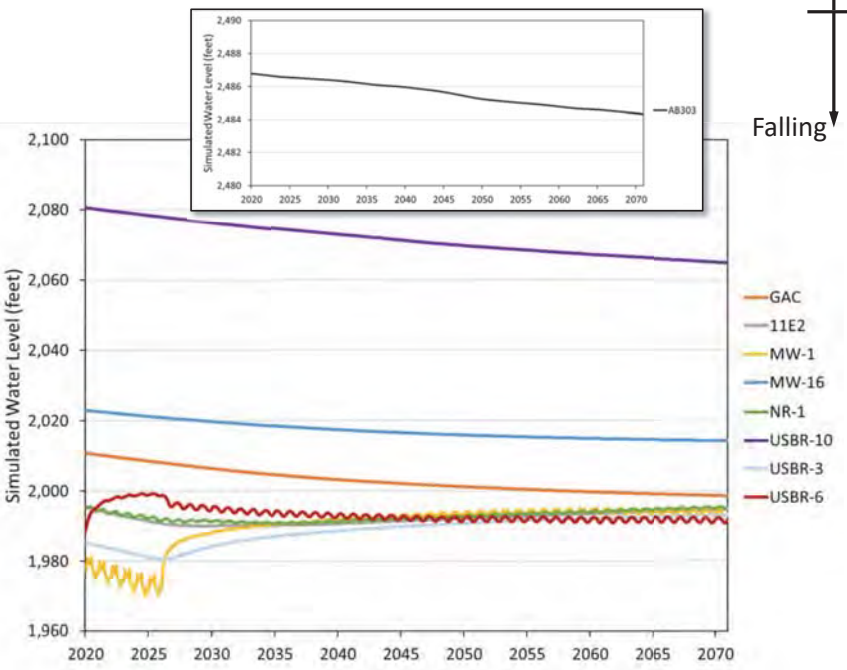


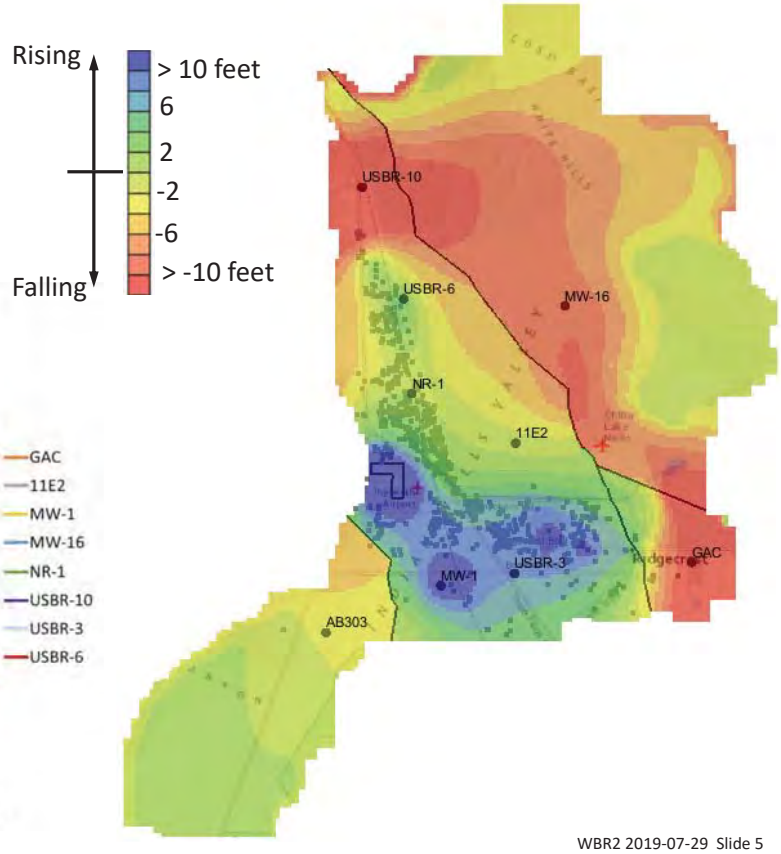


DRAFT – Subject to change

Water Level Change 2020-2070

Management Scenario 6.2





DRAFT – Subject to change

Basin Groundwater Budgets for 2020 through 2070

Annual Average (acre-feet/year)

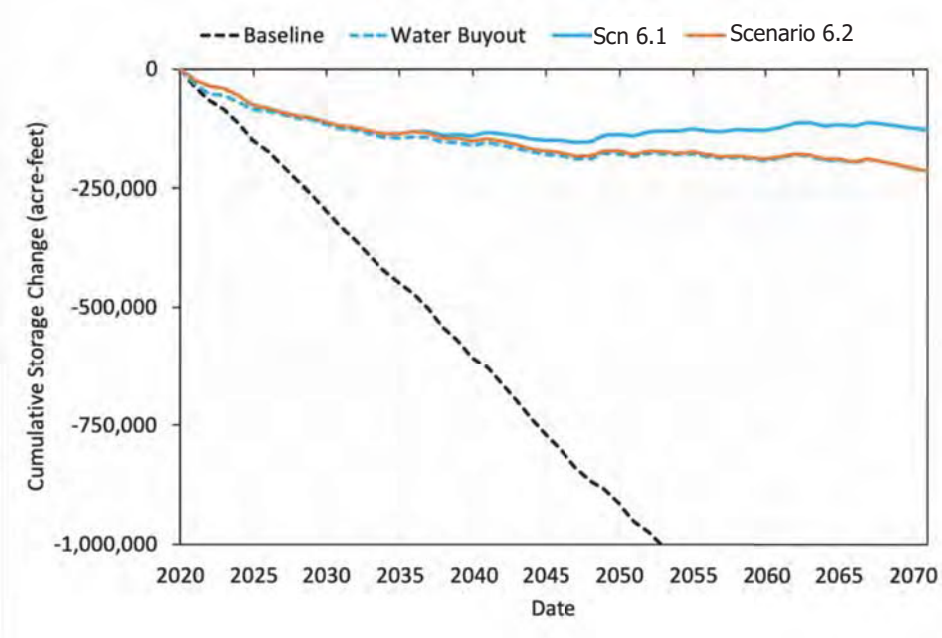
	Baseline	Water Buyout	Scenario 6.1	Scenario 6.2
INFLOW				
Recharge	7,650	10,959	12,707	10,990
TOTAL	7,650	10,959	12,707	10,990
OUTFLOW				
Pumping	36,880	13,176	13,260	13,260
Evapotranspiration	1,610	1,944	1,885	1,877
Flow to Salt Wells Valley	40	38	39	39
TOTAL	38,530	15,158	15,184	15,176
CHANGE IN GW STORAGE	-30,880	-4,199	-2,477	-4,186

Cumulative (acre-feet)

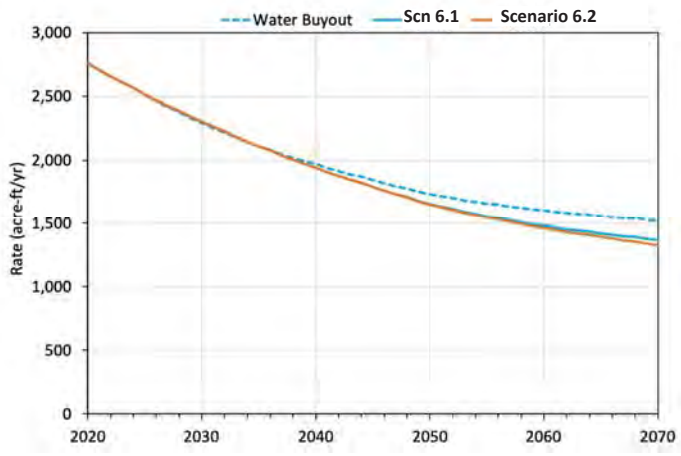
	Baseline	Water Buyout	Scenario 6.1	Scenario 6.2
INFLOW				
Recharge	390,405	558,906	648,042	560,507
TOTAL	390,405	558,906	648,042	560,507
OUTFLOW				
Pumping	1,880,898	671,973	676,270	676,270
Evapotranspiration	82,347	99,128	96,141	95,722
Flow to Salt Wells Valley	1,893	1,931	1,991	1,990
TOTAL	1,965,139	773,033	774,402	773,982
CHANGE IN GW STORAGE	-1,574,734	-214,127	-126,360	-213,475

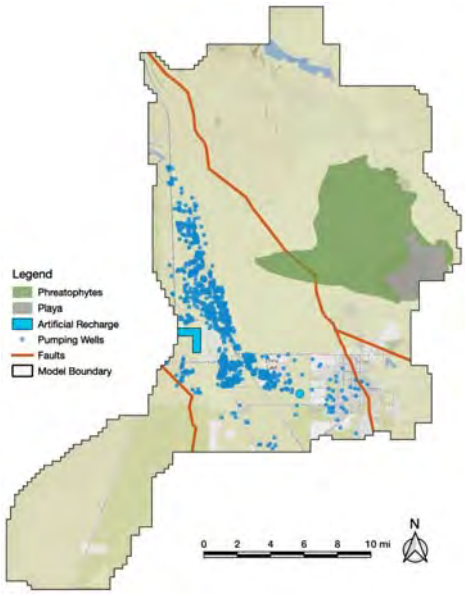
DRAFT – Subject to change

Change in Basin Groundwater Storage



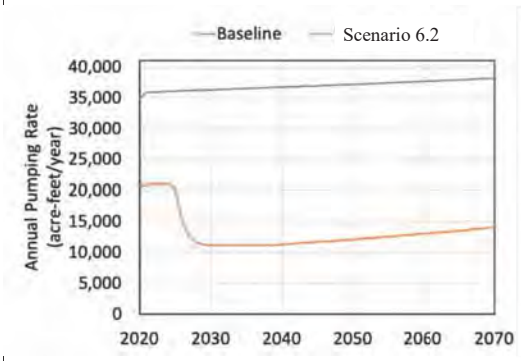
Evapotranspiration





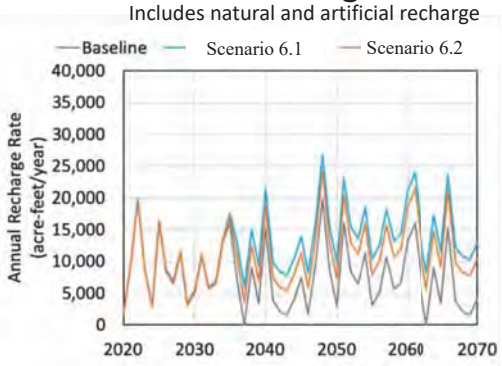
Management Scenario 6.2 - Pumping and Recharge Scenarios

Pumping



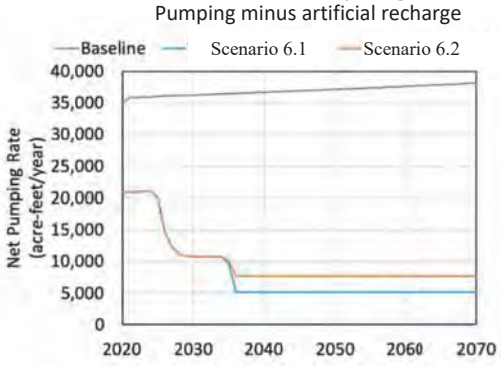
Recharge

Includes natural and artificial recharge



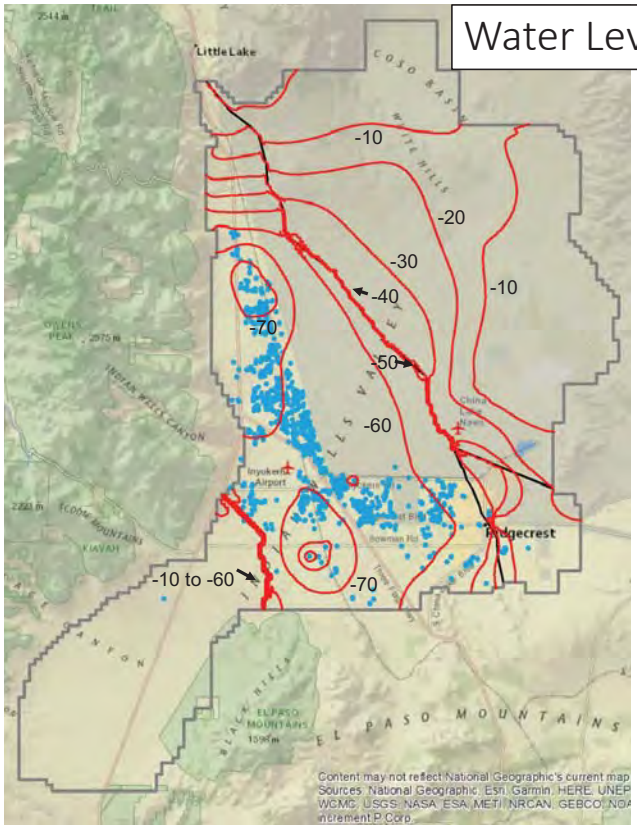
Net Pumping

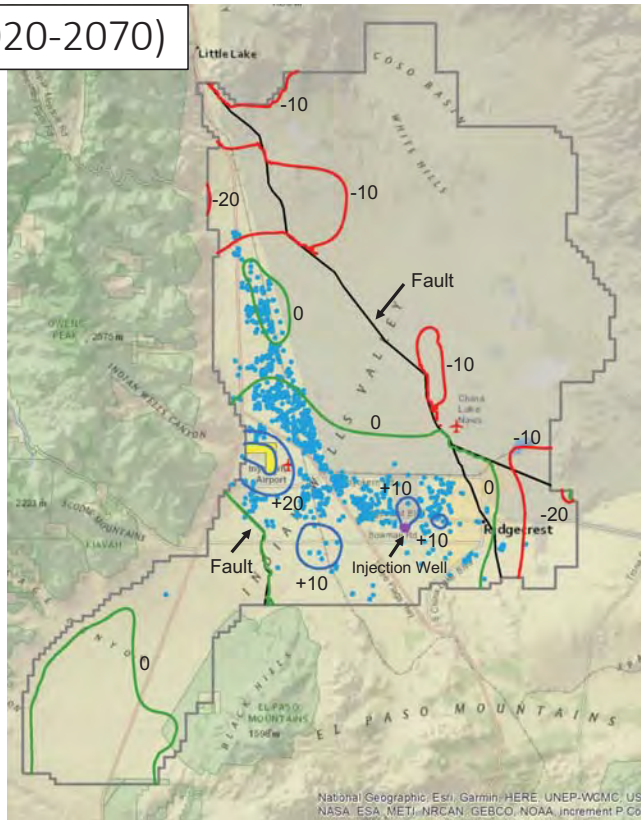
Pumping minus artificial recharge



DRAFT – Subject to change

Water Level Change (2020-2070)





DRAFT – Subject to change

Baseline

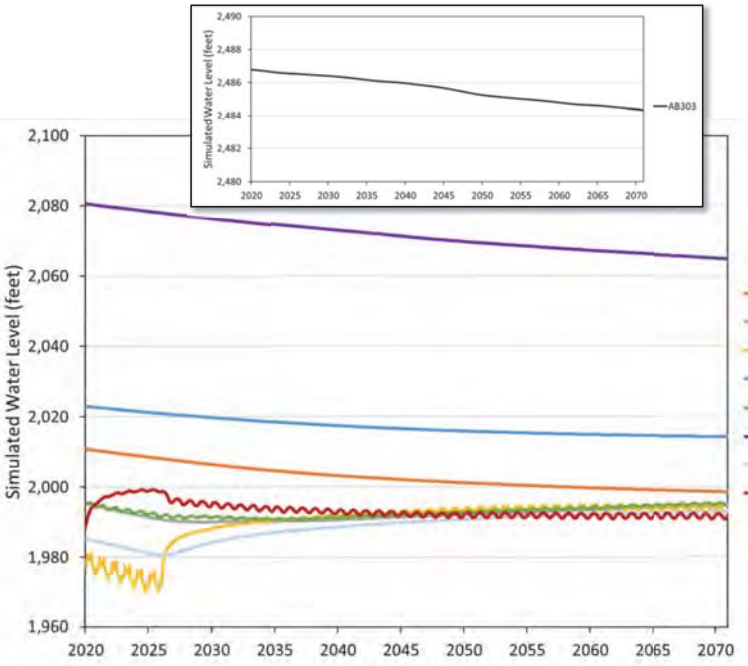
DRAFT – Subject to change

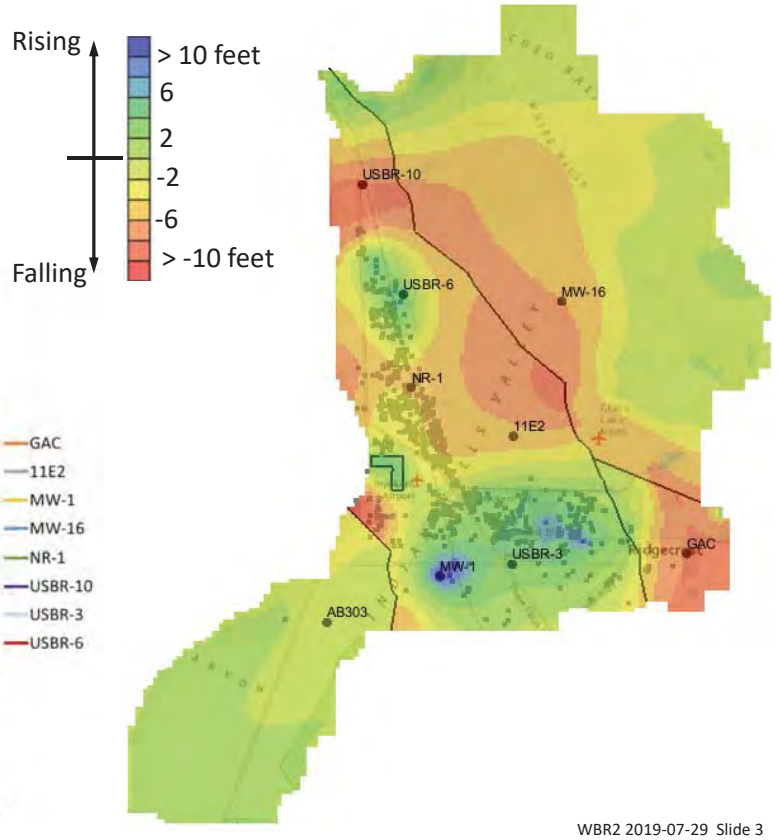
Scenario 6.2

Units: feet

Water Level Change 2020-2040

Management Scenario 6.2

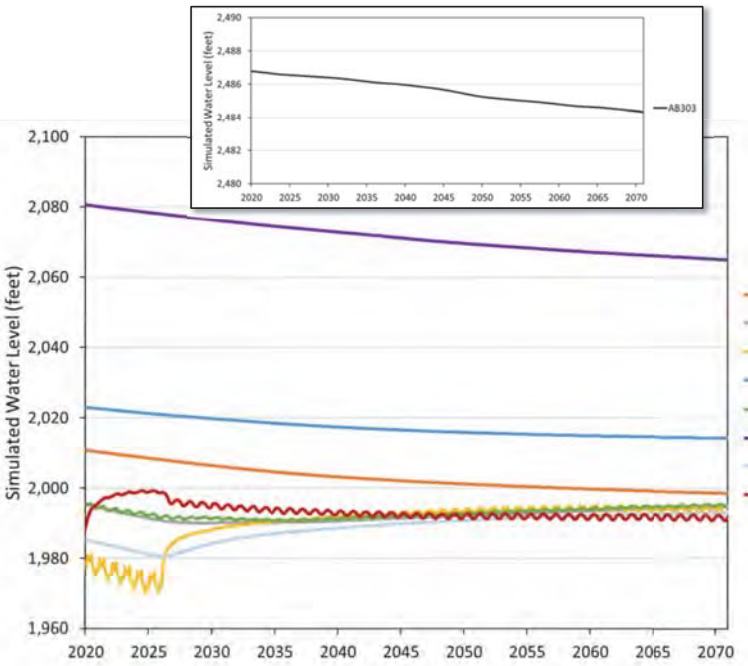


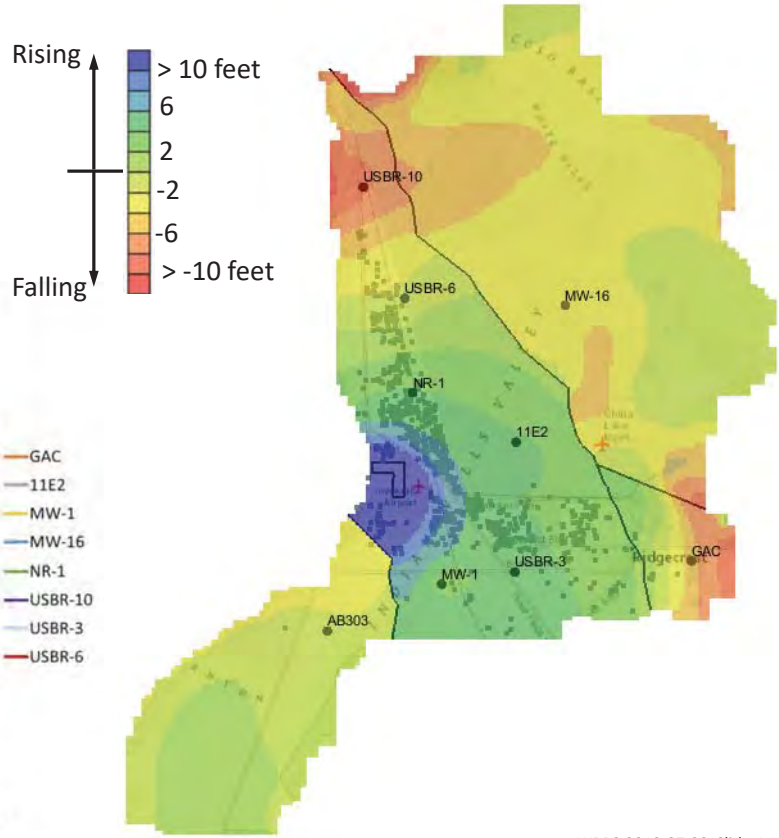


DRAFT – Subject to change

Water Level Change 2040-2070

Management Scenario 6.2

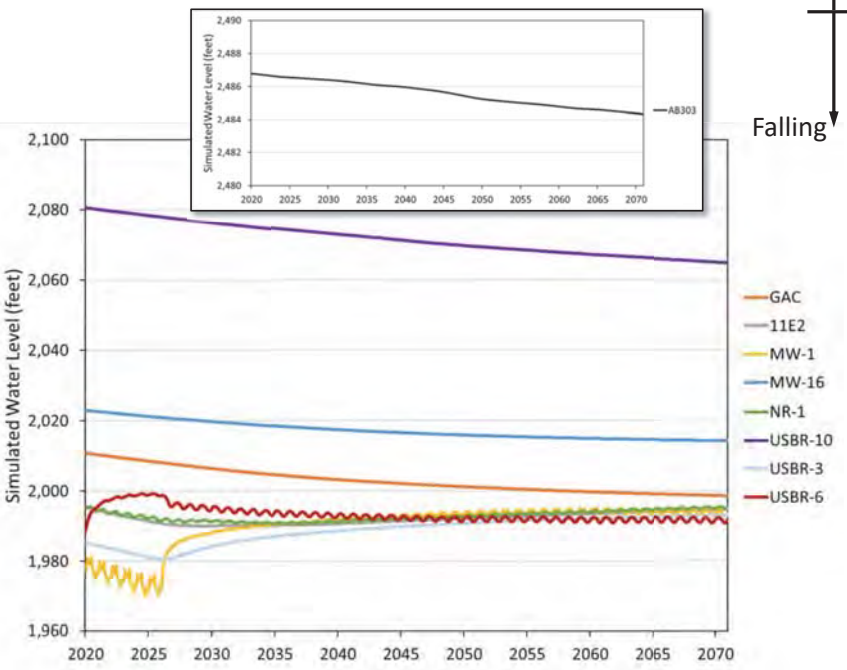


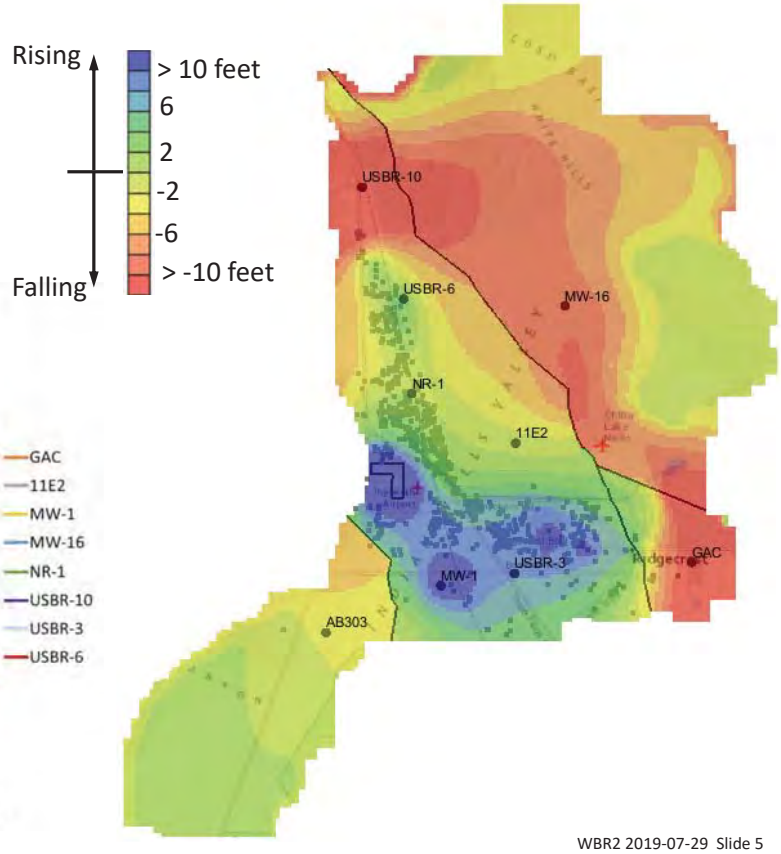


DRAFT – Subject to change

Water Level Change 2020-2070

Management Scenario 6.2





DRAFT – Subject to change

Basin Groundwater Budgets for 2020 through 2070

Annual Average (acre-feet/year)

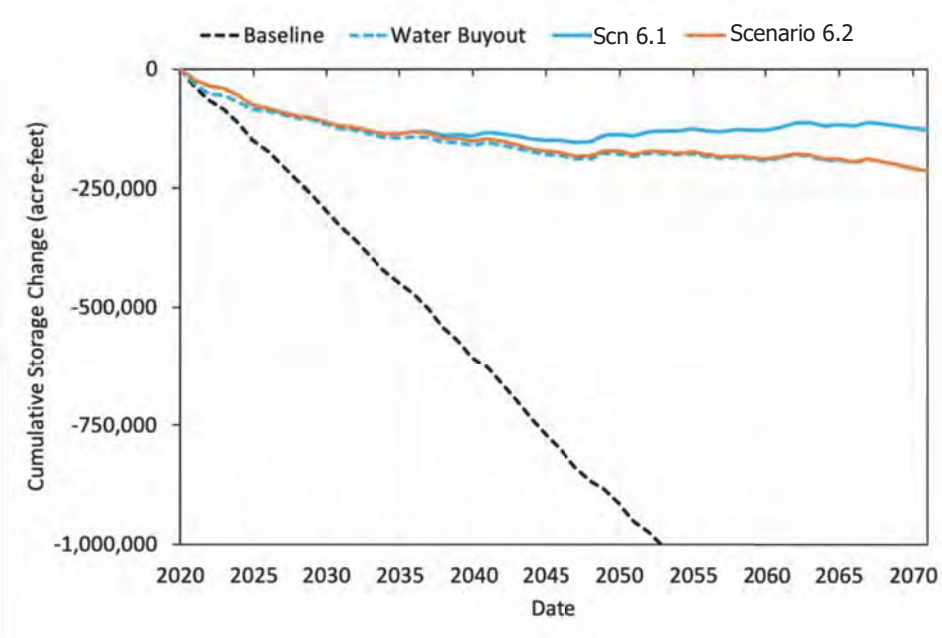
	Baseline	Water Buyout	Scenario 6.1	Scenario 6.2
INFLOW				
Recharge	7,650	10,959	12,707	10,990
TOTAL	7,650	10,959	12,707	10,990
OUTFLOW				
Pumping	36,880	13,176	13,260	13,260
Evapotranspiration	1,610	1,944	1,885	1,877
Flow to Salt Wells Valley	40	38	39	39
TOTAL	38,530	15,158	15,184	15,176
CHANGE IN GW STORAGE	-30,880	-4,199	-2,477	-4,186

Cumulative (acre-feet)

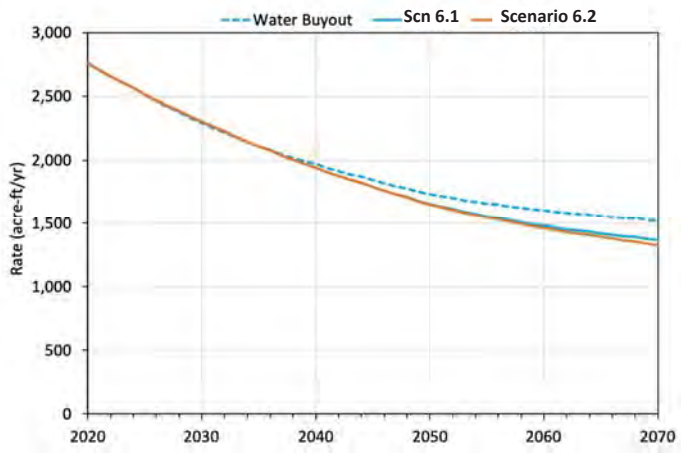
	Baseline	Water Buyout	Scenario 6.1	Scenario 6.2
INFLOW				
Recharge	390,405	558,906	648,042	560,507
TOTAL	390,405	558,906	648,042	560,507
OUTFLOW				
Pumping	1,880,898	671,973	676,270	676,270
Evapotranspiration	82,347	99,128	96,141	95,722
Flow to Salt Wells Valley	1,893	1,931	1,991	1,990
TOTAL	1,965,139	773,033	774,402	773,982
CHANGE IN GW STORAGE	-1,574,734	-214,127	-126,360	-213,475

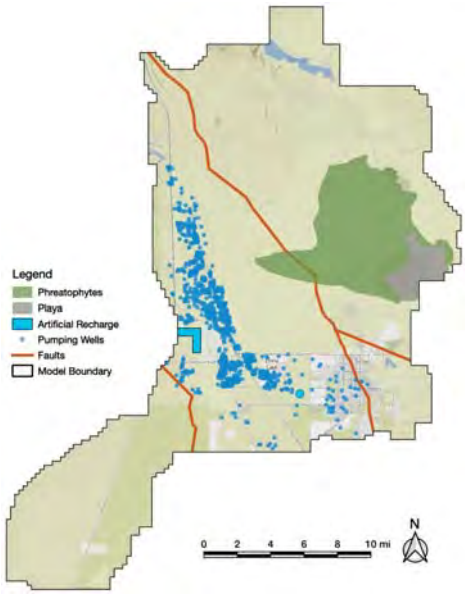
DRAFT – Subject to change

Change in Basin Groundwater Storage



Evapotranspiration





Indian Wells Valley
Draft TDS Transport Model
Baseline Pumping Conditions

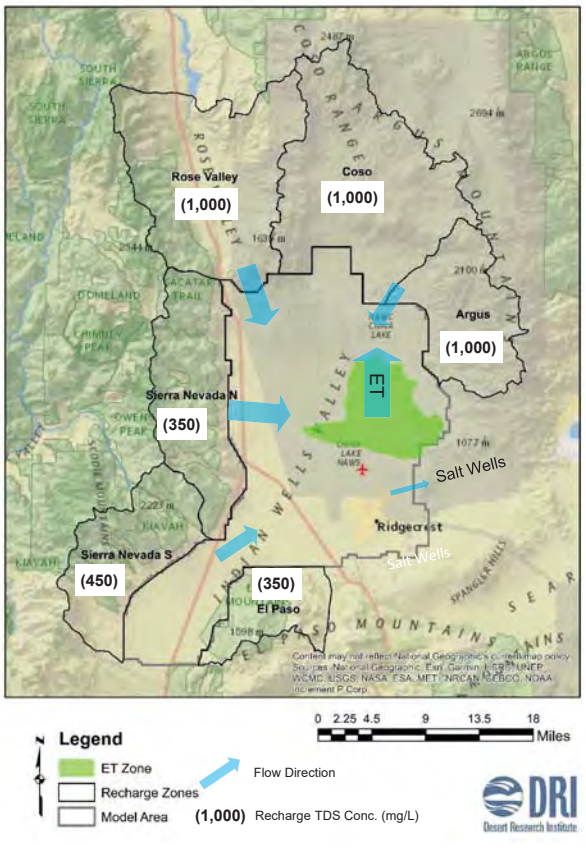


February 7, 2019

Conceptual Model

- <u>Sources:</u>
  - Solutes in recharge
  - Dissolution of minerals in basin
  - Mixing with saltier groundwater
    - Remnant evaporative brines
    - Geothermal fluids
- Concentration by evaporation

- <u>Sinks:</u>
  - Solutes in discharge to Searles valley
  - Precipitation of minerals

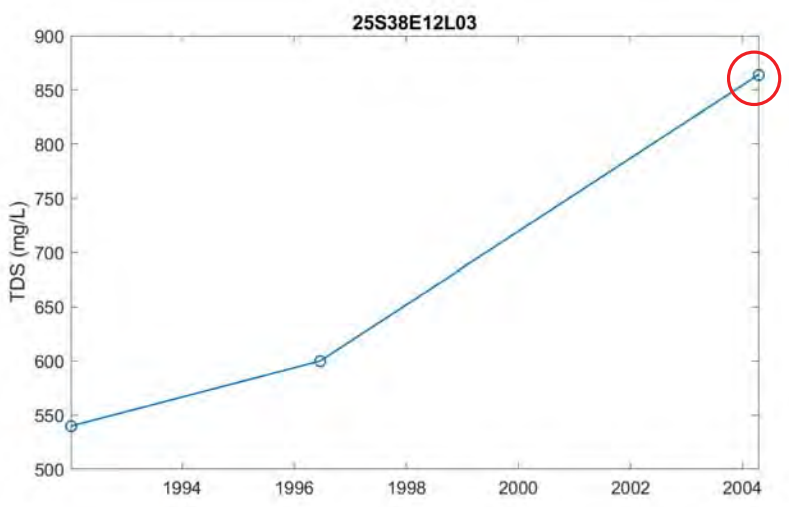


TDS Model Process

- Step #1 – Compile and QA Dataset
  - Dataset from Stetson – quality checked back to original published sources. Includes data compiled in BWG database, GAMA, and from AB303 (2003). Stetson identified 548 wells and 1,993 TDS values.
  - DRI used TDS data for 402 wells (wells missing depths were excluded). The most recent TDS measurement is used, if multiple dates are available.

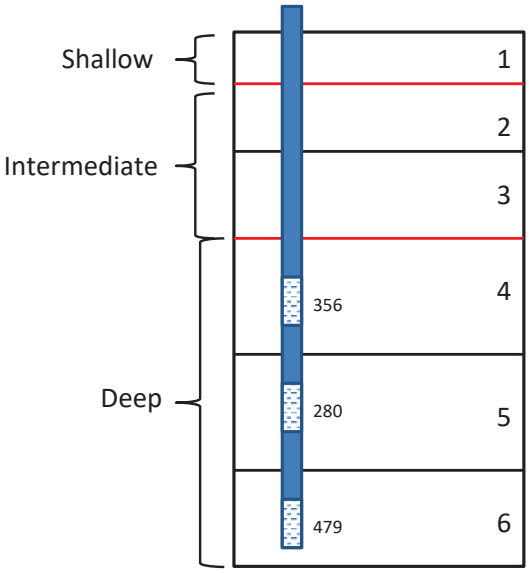
TDS Model Process

- Step #2 – Select most recent TDS value for single well

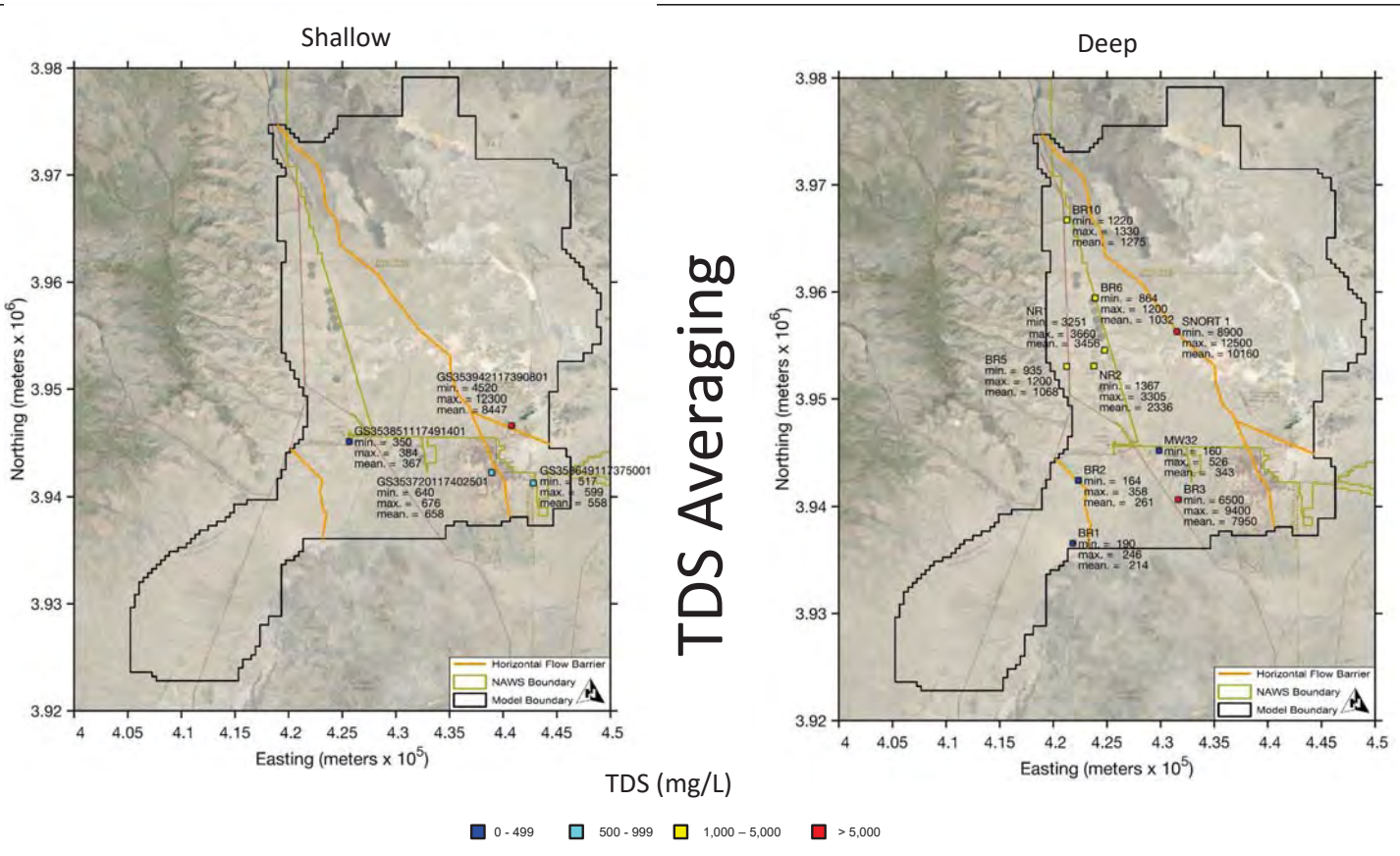


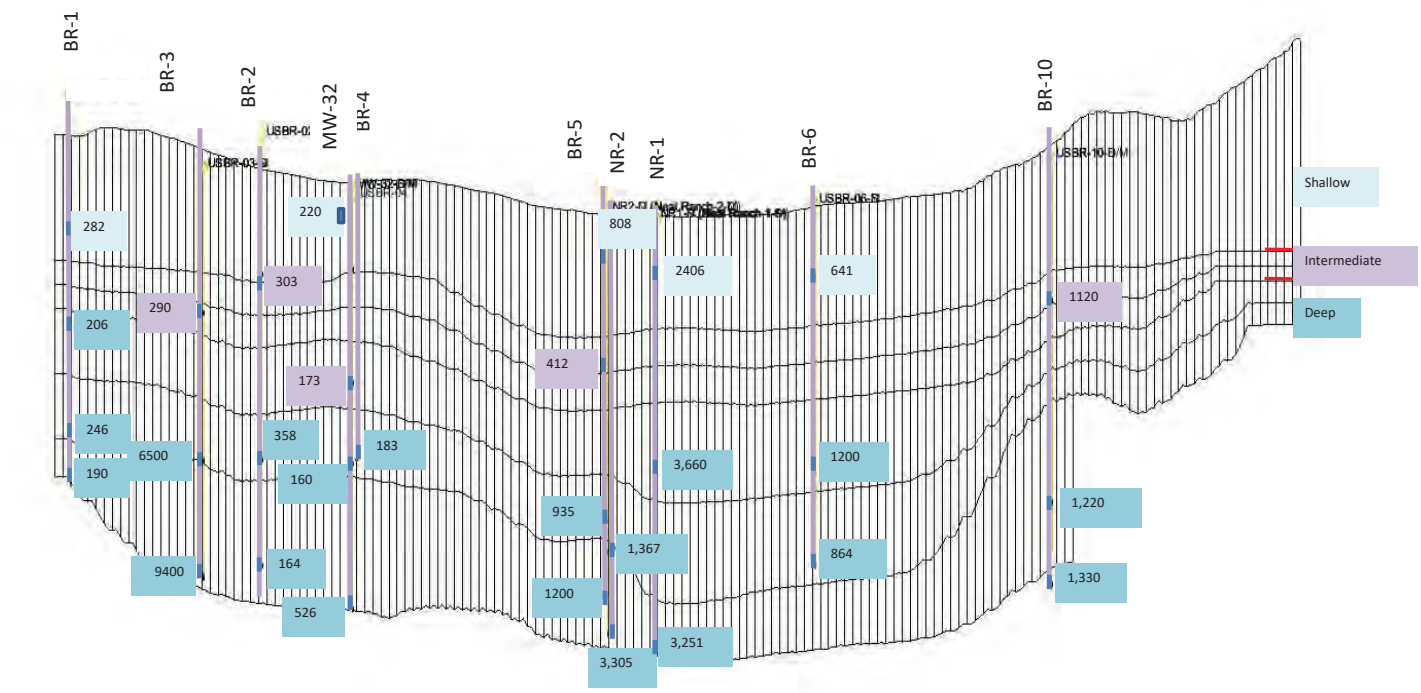
TDS Model Process

- <u>Step #3 – Partition domain into three layers</u>
  - Shallow (model layer 1)
  - Intermediate (model layers 2-3)
  - Deep (model layers 4-6)
  - Not enough TDS data to interpolate to six layers independently
- <u>Step #4 – Average TDS values</u>
  - Average TDS values if multiple values fall into single layer



Average for deep layer = 372





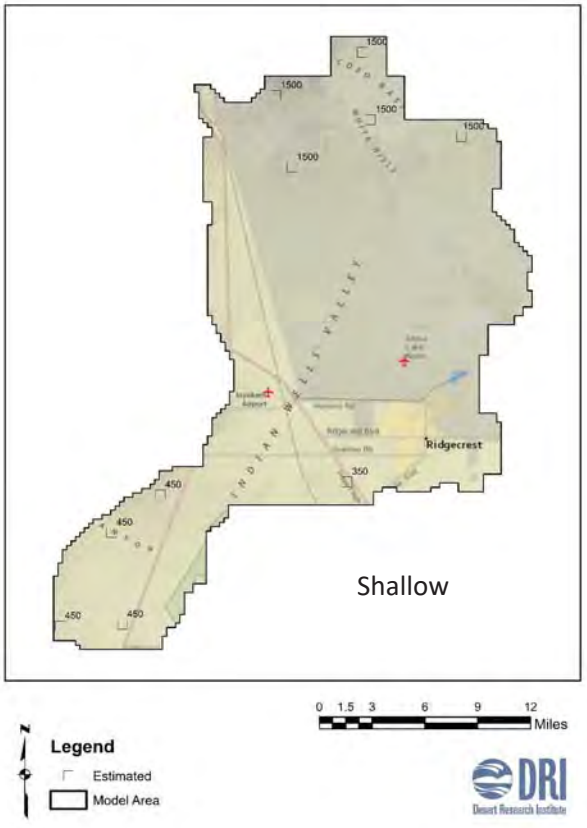
South

North

Note: Shallow BR-5 & BR-10 are in intermediate layer

TDS Model Process

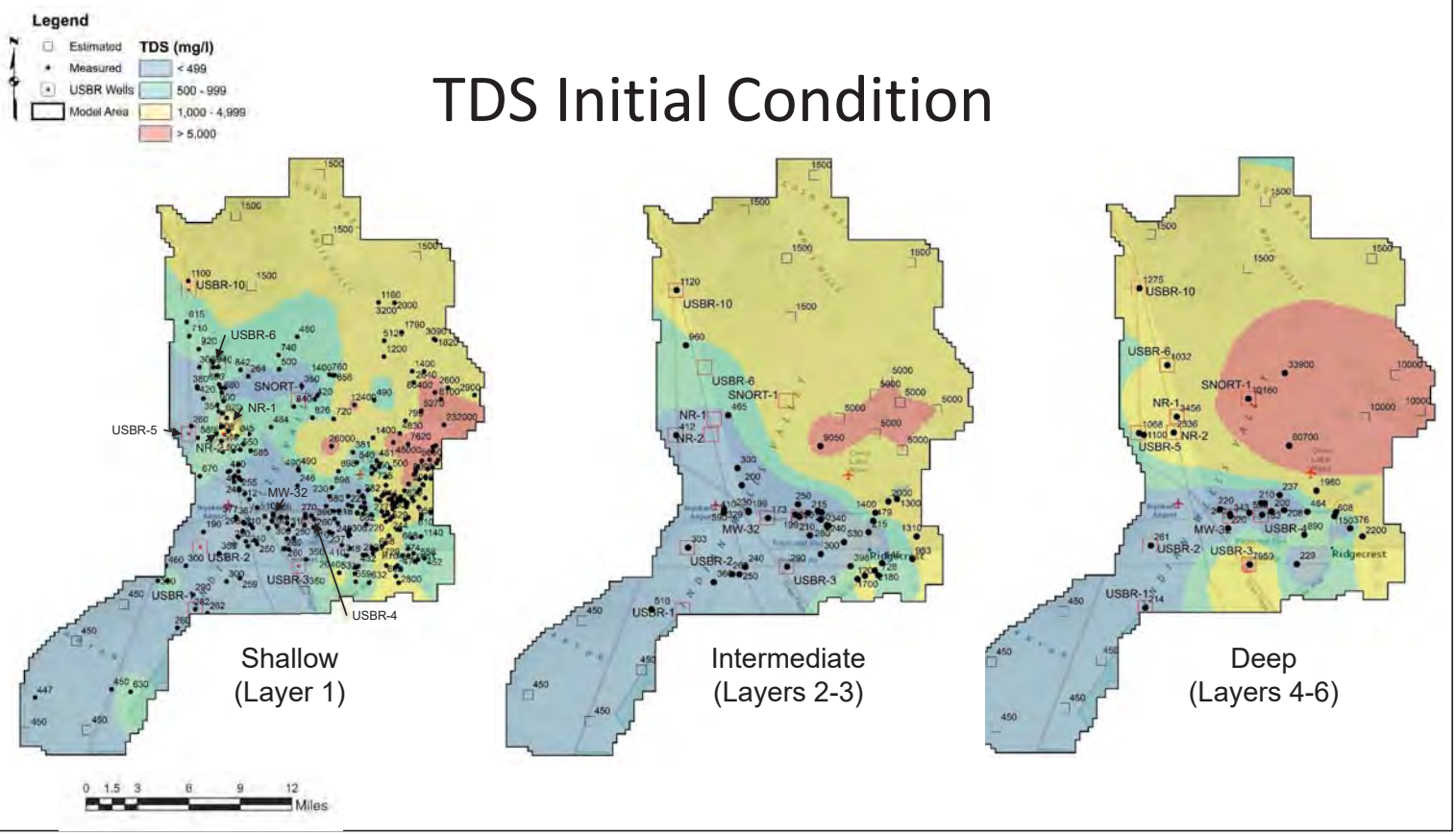
- Step #5 – Add estimated TDS points



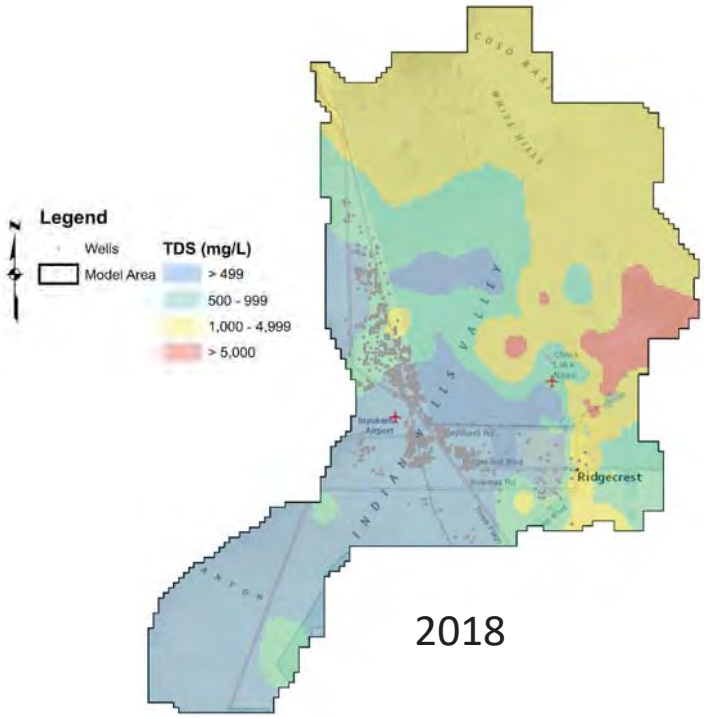
TDS Model Process

- Step #6 – Combine measured and estimated datasets
- Step #7 – Interpolate combined dataset
  - Repeat for shallow, intermediate, and deep layers
  - Interpolated values represent continuous values
- Step #8 – Setup initial conditions for transport model and run using baseline flow model (~35k pumping)

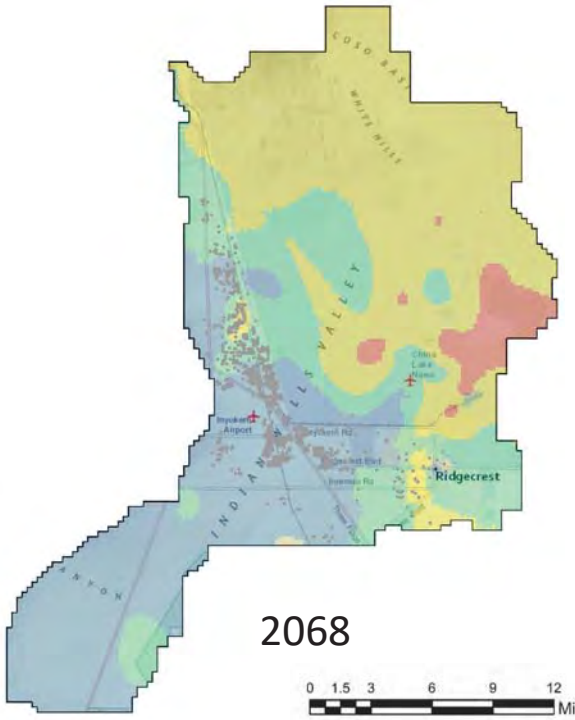
TDS Initial Condition



Simulated TDS Concentration - Shallow



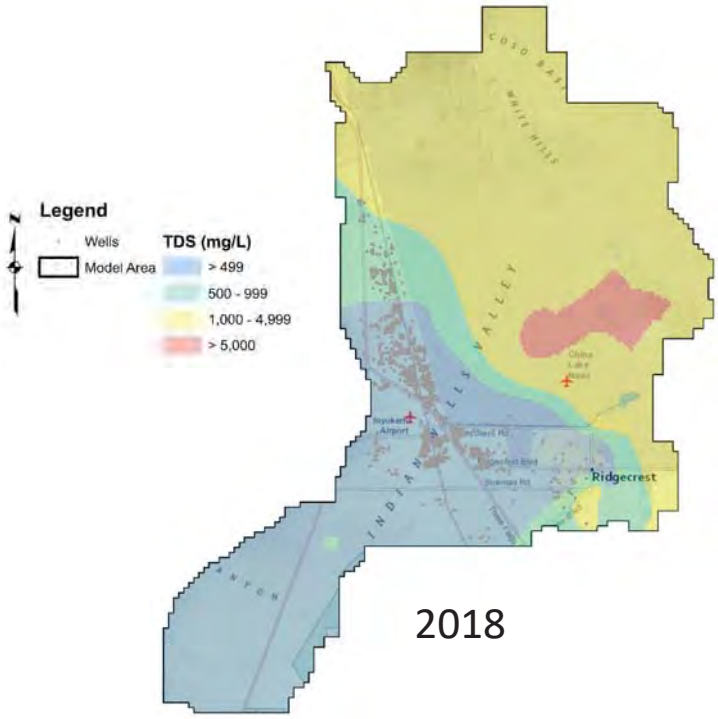
2018



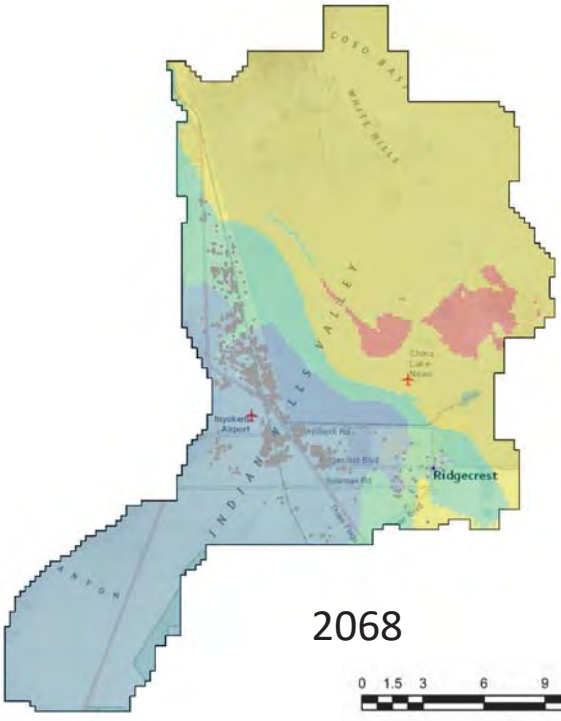
2068

0 1.5 3 6 9 12 Miles

Simulated TDS Concentration - Intermediate



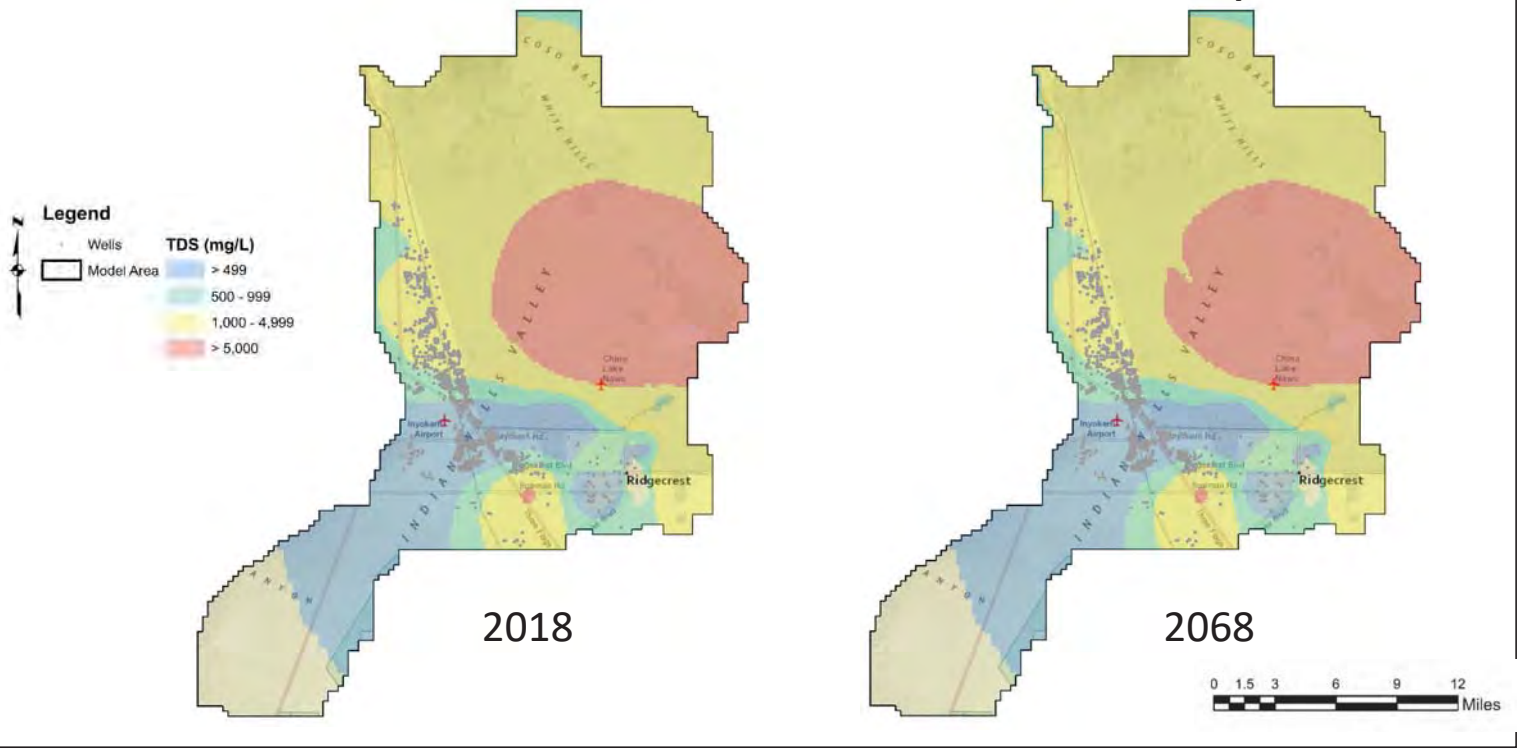
2018



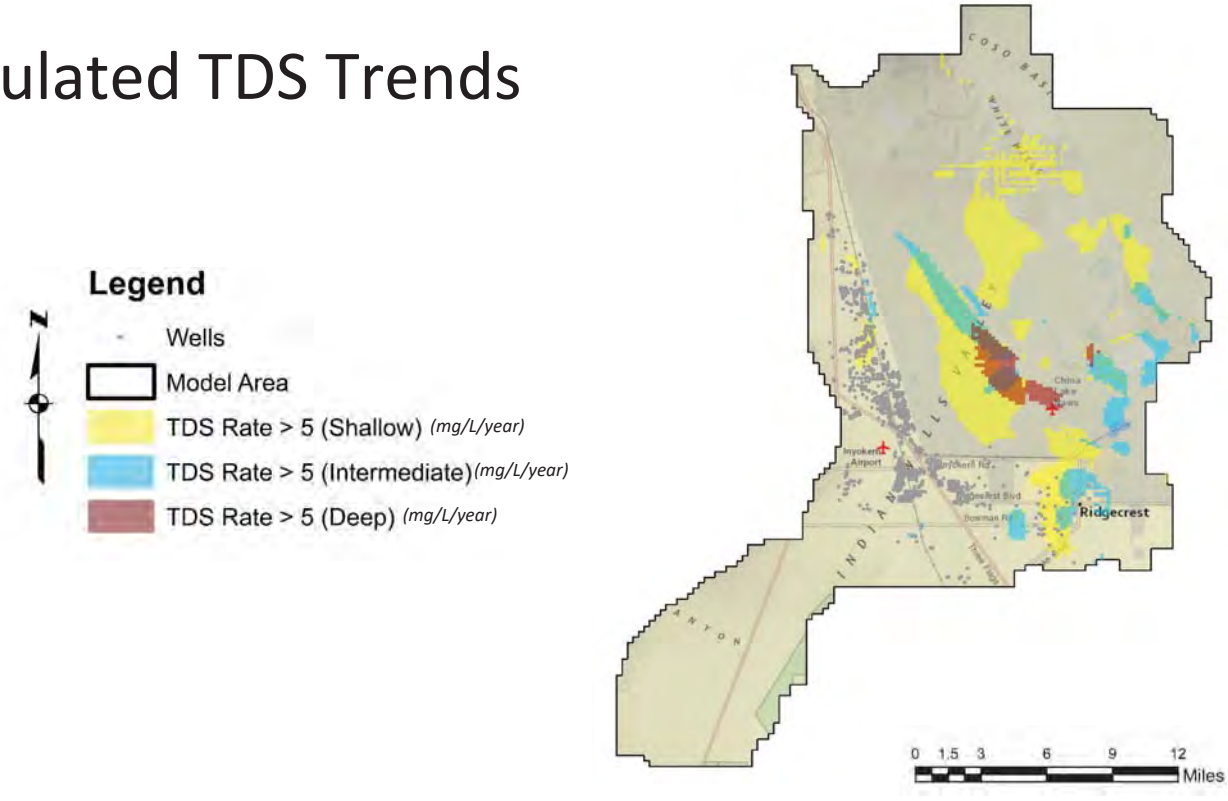
2068

0 1.5 3 6 9 12 Miles

Simulated TDS Concentration - Deep



Simulated TDS Trends



Questions

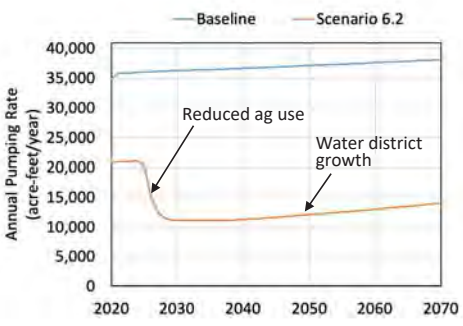


Results from Groundwater Flow and TDS Transport Model Scenario 6.2

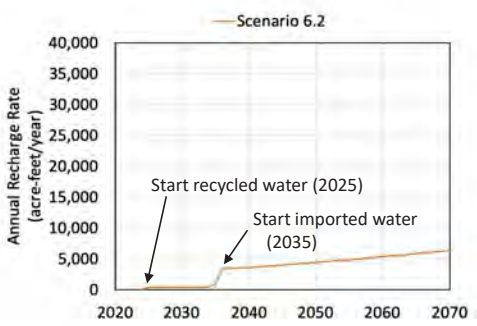
Comparison with Baseline

Pumping and Recharge Scenarios

Pumping

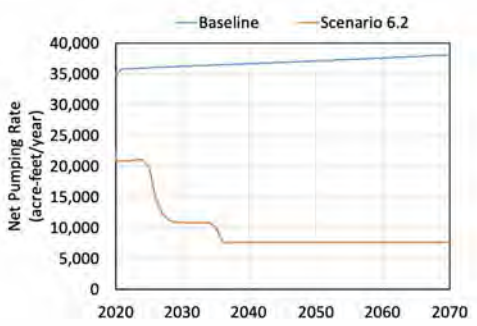


Artificial Recharge

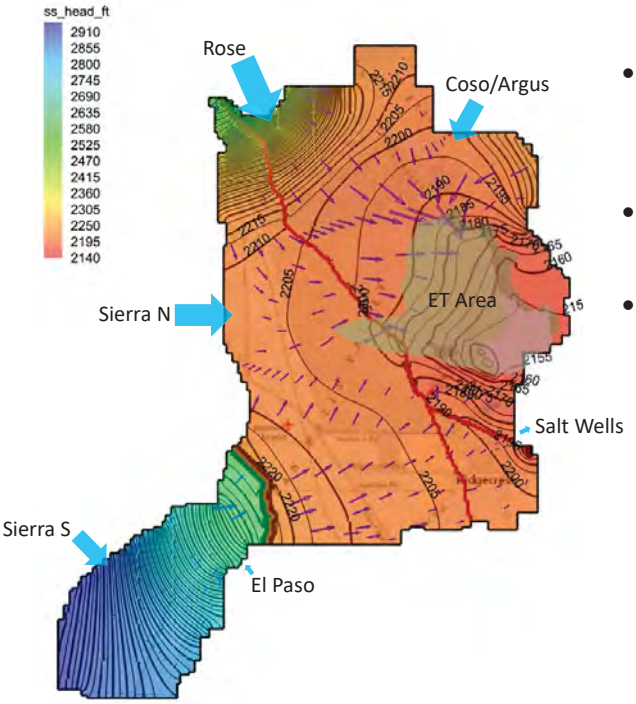


Net Pumping

Pumping minus artificial recharge



Groundwater Flow Prior to Development

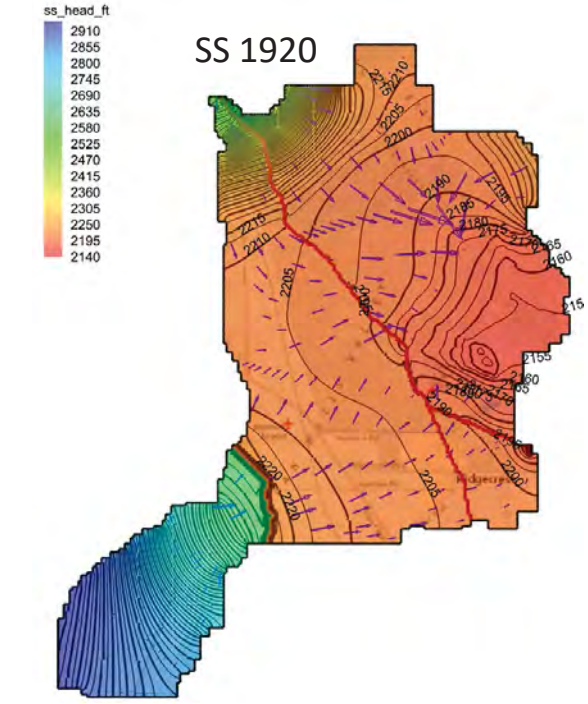


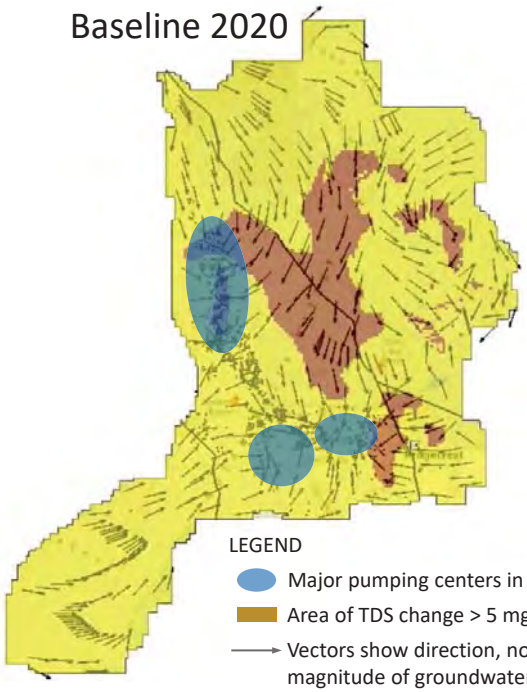
- Groundwater flow simulated from recharge areas to discharge at playa (ET) and toward Salt Wells Valley
- Flow parallel to northern Little Lake Fault where fault conductivity is lower
- Flow crosses Little Lake Fault where fault conductivity is higher

LEGEND
- Faults
- Contours of simulated heads (ft amsl)
- Vectors showing direction and relative magnitude of groundwater flow rates

Map shows results for Layer 1 of the steady-state model

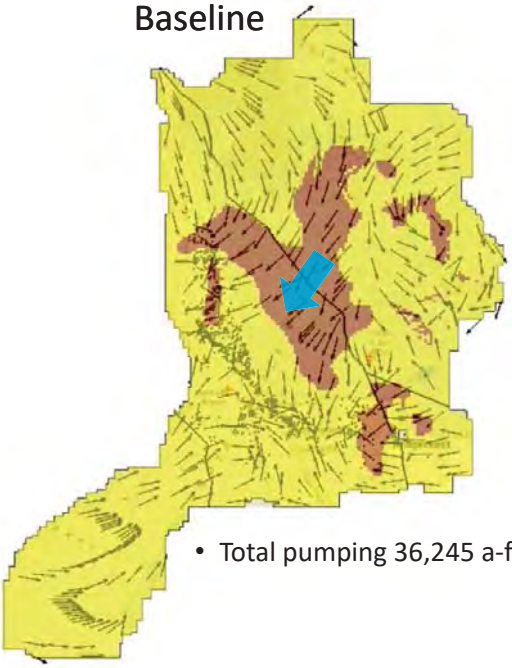
Pumping Effects on Groundwater Flow Directions





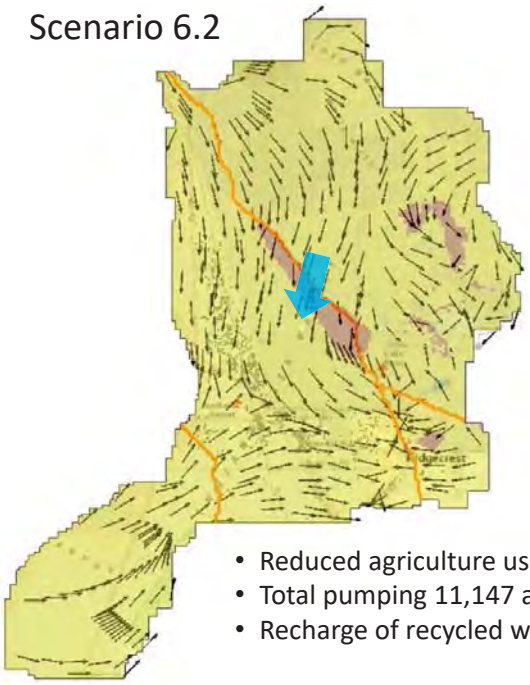
Groundwater Flow Directions in 2030

Baseline



- Total pumping 36,245 a-f/yr

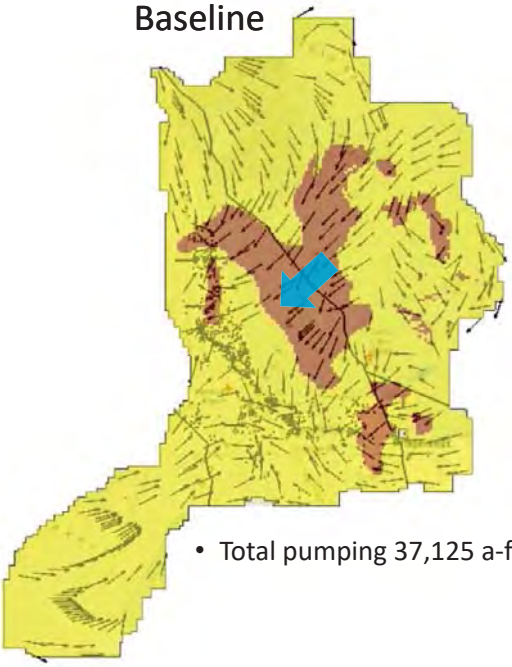
Scenario 6.2



- Reduced agriculture use
- Total pumping 11,147 a-f/yr
- Recharge of recycled water starts 2025

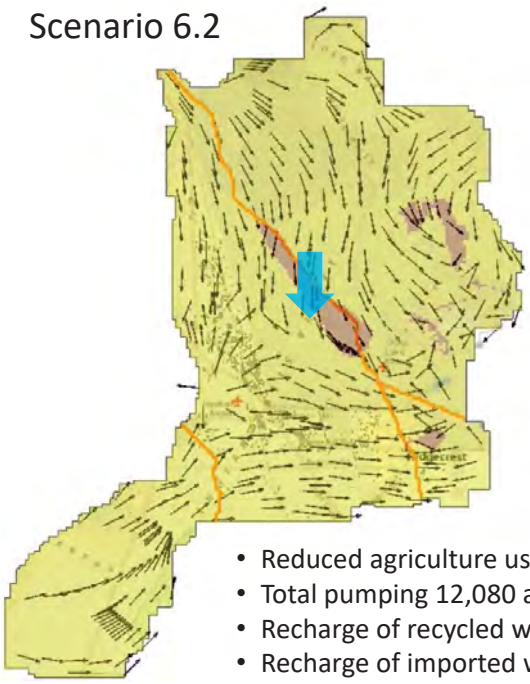
Groundwater Flow Directions in 2050

Baseline



- Total pumping 37,125 a-f/yr

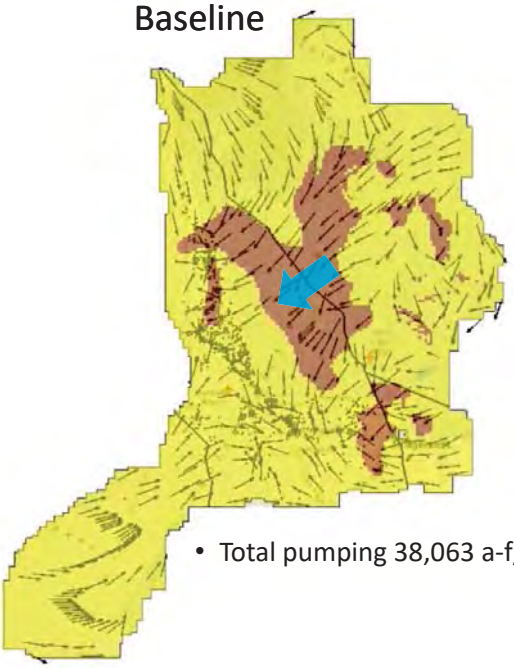
Scenario 6.2



- Reduced agriculture use
- Total pumping 12,080 a-f/yr
- Recharge of recycled water starts 2025
- Recharge of imported water starts 2035

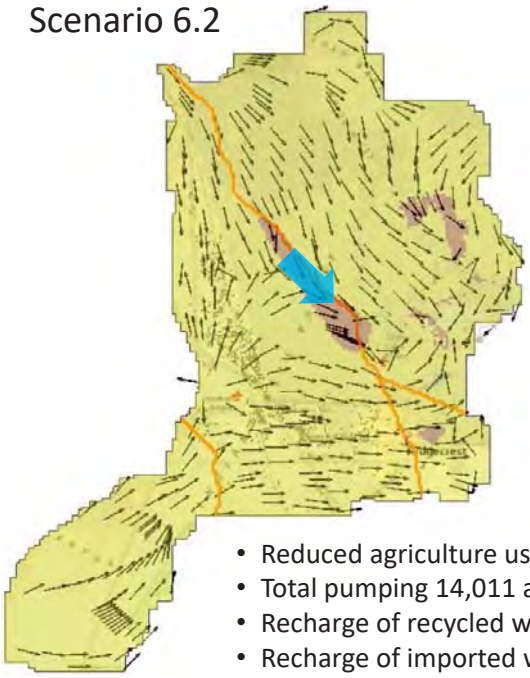
Groundwater Flow Directions in 2070

Baseline



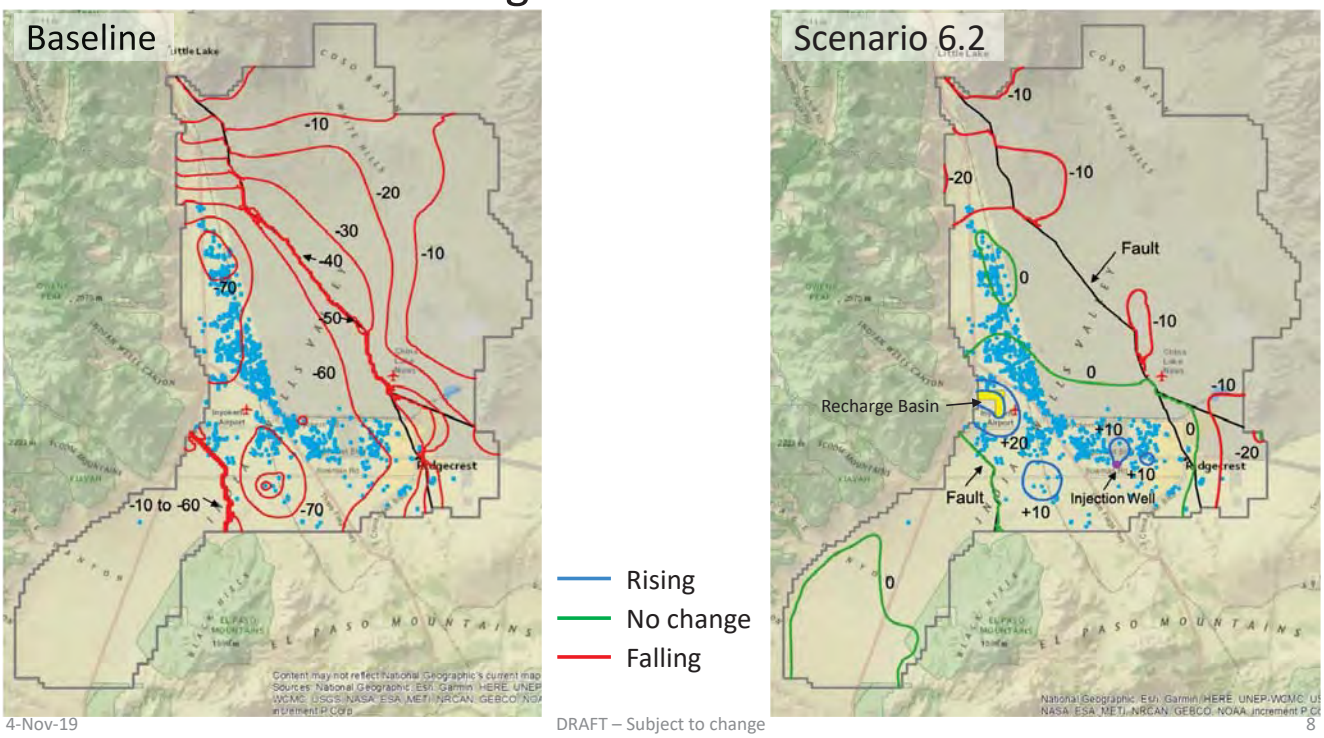
- Total pumping 38,063 a-f/yr

Scenario 6.2



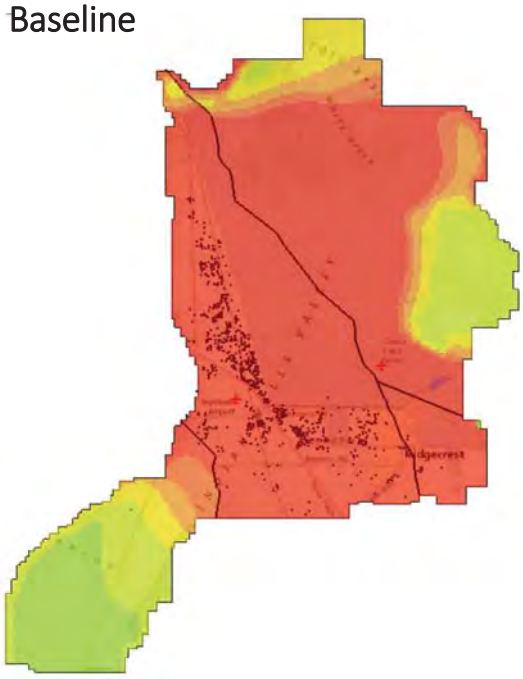
- Reduced agriculture use
- Total pumping 14,011 a-f/yr
- Recharge of recycled water starts 2025
- Recharge of imported water starts 2035

Groundwater Level Changes 2020 - 2070

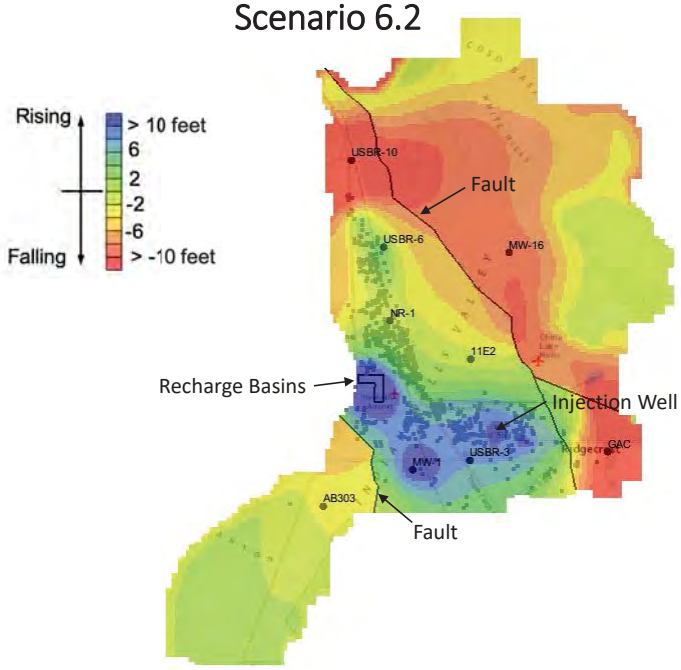


Groundwater Level Changes 2020 - 2070

Baseline



Scenario 6.2



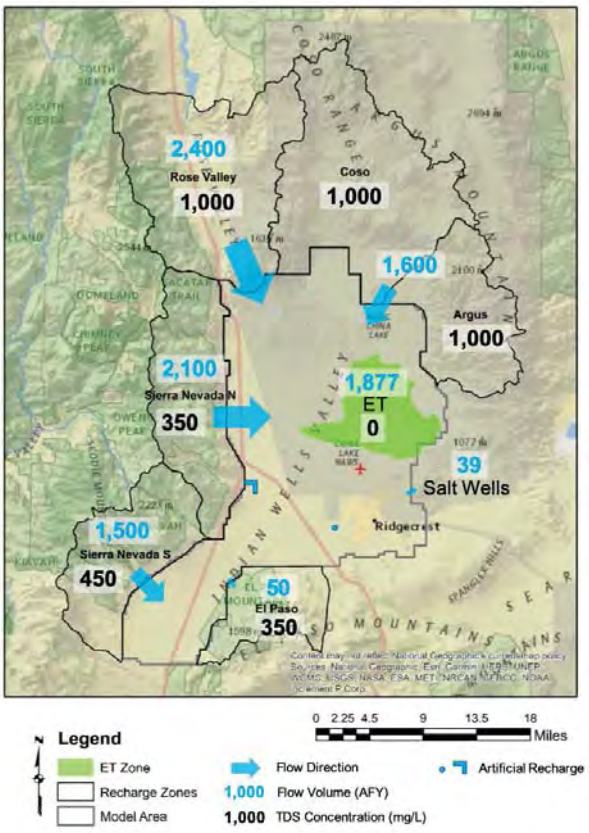
Results from TDS Transport Model Scenario 6.2

Comparison with Baseline

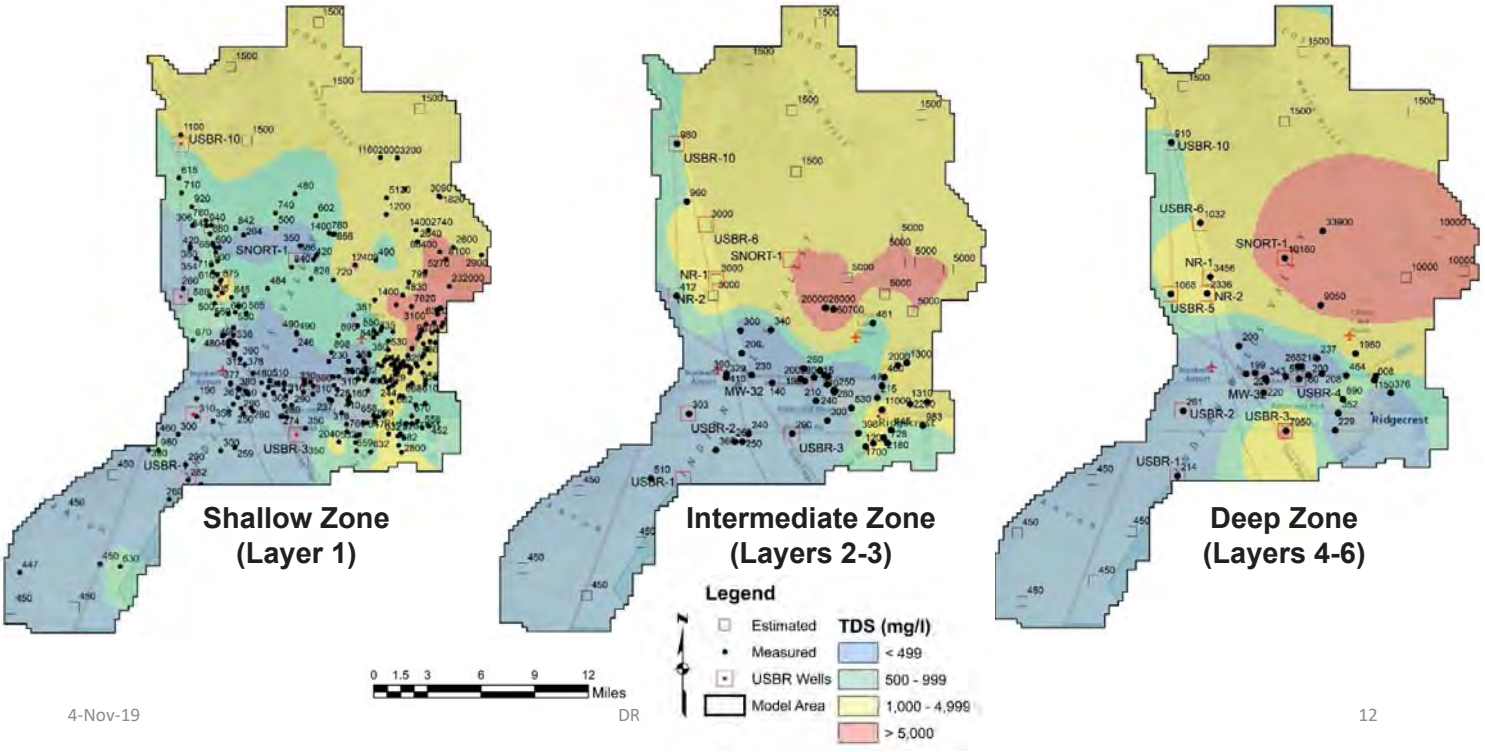
TDS Transport Models

TDS Sources
- Natural recharge
- Artificial recharge (Scenario 6.2)
  Imported: 280 mg/L
  Recycled: 250 mg/L
- Mixing with higher-TDS GW
- Concentration by evaporation

TDS Sinks
- Extraction wells
- Discharge to Salt Wells Valley

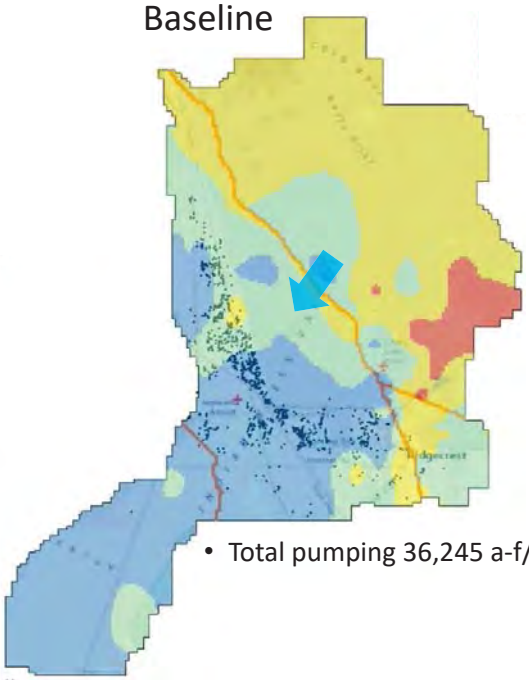


Initial Conditions for TDS Concentration



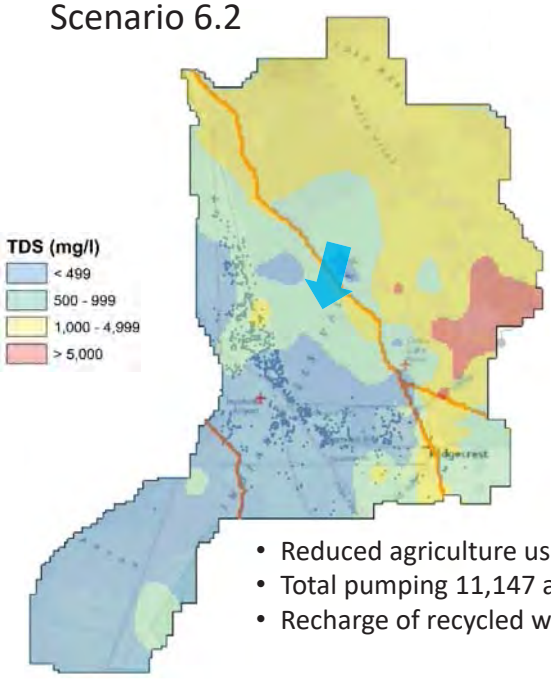
TDS Concentrations in 2030 in the Shallow Zone

Baseline



- Total pumping 36,245 a-f/yr

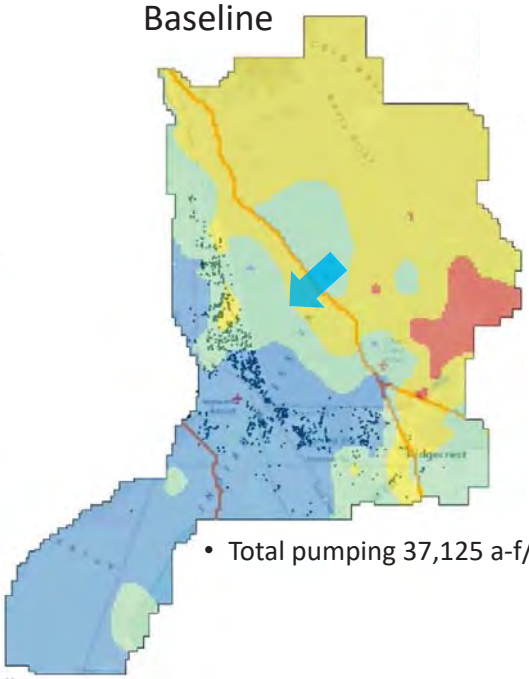
Scenario 6.2



- Reduced agriculture use
- Total pumping 11,147 a-f/yr
- Recharge of recycled water starts 2025

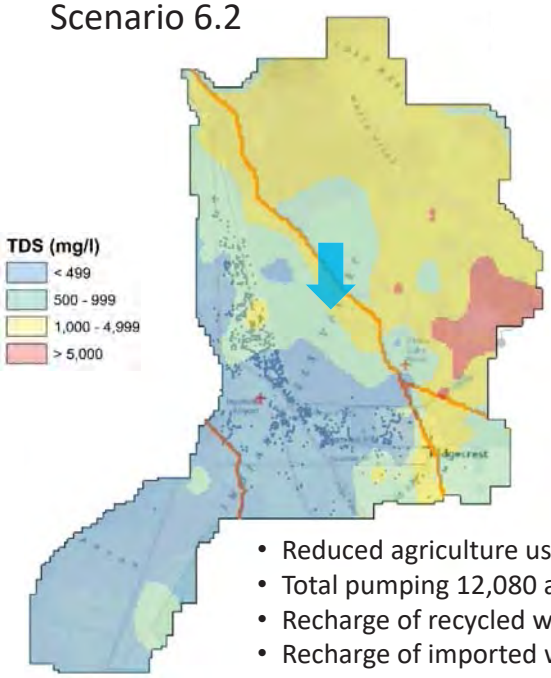
TDS Concentrations in 2050 in the Shallow Zone

Baseline



- Total pumping 37,125 a-f/yr

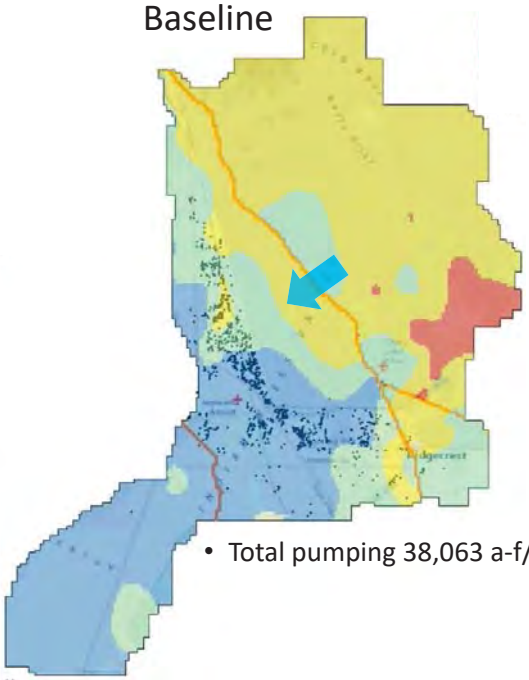
Scenario 6.2



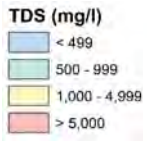
- Reduced agriculture use
- Total pumping 12,080 a-f/yr
- Recharge of recycled water starts 2025
- Recharge of imported water starts 2035

TDS Concentrations in 2070 in the Shallow Zone

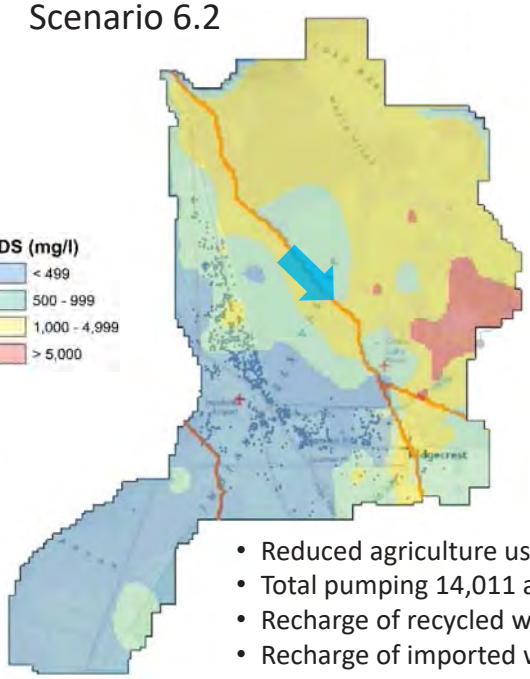
Baseline



- Total pumping 38,063 a-f/yr

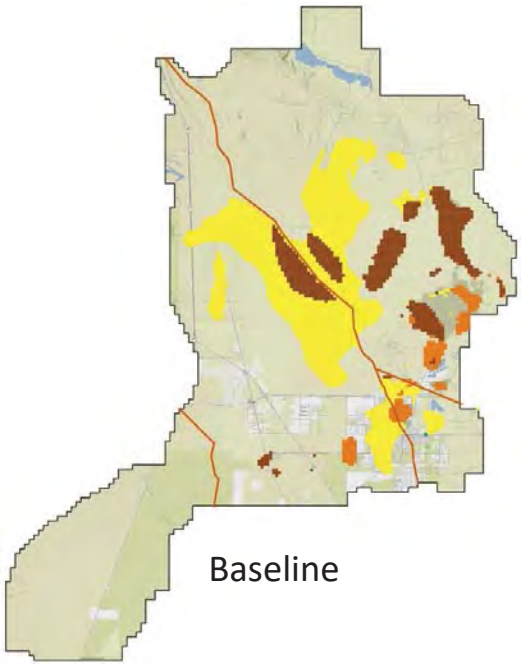


Scenario 6.2



- Reduced agriculture use
- Total pumping 14,011 a-f/yr
- Recharge of recycled water starts 2025
- Recharge of imported water starts 2035

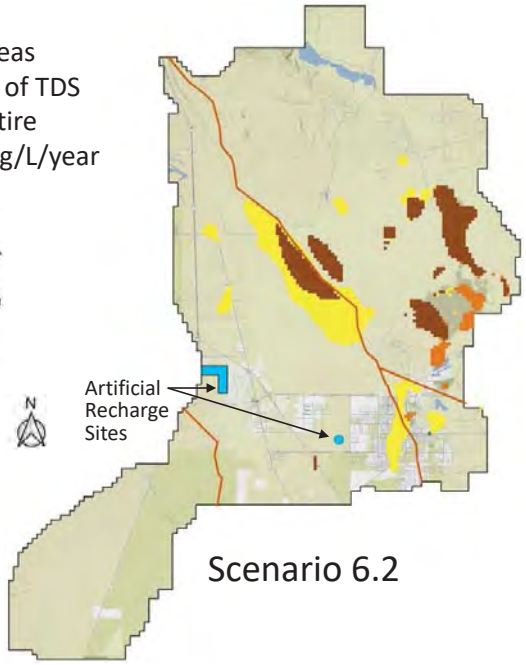
TDS Concentration Trends 2020 through 2070 – All Zones



Baseline

Color represents areas where average rate of TDS change over the entire period exceeds 5 mg/L/year





Scenario 6.2

ATTACHMENT K

DEPARTMENT OF THE NAVY
NAVAL AIR WEAPONS STATION
1 ADMINISTRATION CIRCLE
CHINA LAKE CA 93555-6100

IN REPLY REFER TO:
11011
Ser PR2/594
7 Nov 18

From: Commanding officer, Naval Air Weapons Station China Lake
To: Indian Wells Valley Groundwater Authority

Subj: INDIAN WELLS VALLEY GROUNDWATER MODEL

Ref: (a) NAWCWD-TP-8811.

1. The Navy contracted with Desert Research Institute (DRI) to develop a digital model of the Indian Wells Valley (IWV) groundwater aquifer, as initially documented in Ref(a). This model has become the basis for the IWV Groundwater Authority's (IWV GA) efforts to develop a Groundwater Sustainability Plan (GSP) pursuant to California State law, the Sustainable Groundwater Management Act of 2014. The Naval Air Weapons Station (NAWS) is an ex-officio, non-voting member of the IWV GA.

2. The Navy supports the transfer of the basin model's maintenance, further development, and configuration management to the IWV GA with a condition of this transfer that the Navy shall be a participant of the model's configuration management process that oversees, recommends, and dispositions any changes to the model's capability and functionality. The Navy will retain its unlimited use license of the basin model to support studies specific and unique to Navy interests and needs. Consequently, there shall be no condition in the relationship between DRI and the IWV GA that prohibits DRI from using the basin model to these ends. Upon the IWV GA's acceptance of these conditions, the Navy will act immediately to inform DRI of the IWV GA's authority to manage the maintenance, development, and configuration management of the basin model.

3. The IWV GA will develop a model management plan, to include configuration management, to ensure proper maintenance and vetting of future requirements requiring change to the model. The Navy shall be a participant of the model's configuration management process that oversees, recommends, and dispositions any changes to the model's capability and functionality.

4. Any questions regarding this letter should be directed to NAWS China Lake Public Works Officer, CDR Peter R. Benson at 760-939-2382.

P. R. BENSON
By direction

Place holder
Note – to be replaced by 1" Navy Logo

Document #: *Draft 2021.0825*
DATE: *August 25, 2021*

CONFIGURATION MANAGEMENT PLAN

FOR

CONTROLLED USE, MAINTENANCE, AND UPGRADE
OF THE NAVY'S NUMERICAL GROUNDWATER MODEL
DEVELOPED BY DESERT RESEARCH INSTITUTE
FOR THE
INDIAN WELLS VALLEY GROUNDWATER BASIN

FOR

INDIAN WELLS VALLEY GROUNDWATER AUTHORITY

AND

UNITED STATES NAVY

NOTICE TO REVIEWERS

This document was submitted for review and approval to the persons and organizations listed below. The date identifies when Reviewers provided comments to the Originator or Approvers gave approval of the document as submitted.

APPROVER:	_____ Name Title	_____ Date
REVIEWER:	_____ Name Title	_____ Date
ORIGINATOR:	_____ Name Title	_____ Date

RECORD OF CHANGES

This index records all revisions/reviews made to the document.

Page	Revision	A,M,D,R	Date	Authorization	Description
	-				Original Release

A=added, M=modified, D=deleted, R=review (no changes required)

Table of Contents

1.0 Introduction 1

1.1 Purpose 1
1.2 Scope 1
1.3 CM Objectives 1
1.4 Applicability 2
1.5 Plan Deviations 2
1.6 Review Cycle 2

2.0 Roles and Responsibilities 2

2.1 TMG Manager 2
2.2 TMG Members 3
2.3 Desert Research Institute (DRI) 3
2.4 Subcontractors 3
2.5 Use of Model Code 3
2.6 Applicable Documents 4

3.0 Configuration Management 4

3.1 Configuration Item Process and Technical Review 4
3.2 IWV-Model Revision and Version Tracking 5
3.3 Model Run Review, Reporting, and Tracking 5

4.0 CM Plan Updates and Revisions 5

Attachments

IWV-Model Configuration Item List

IWV-Model Revision List

IWV-Model Run List

1.0 Introduction

1.1 Purpose

This document establishes the Configuration Management (CM) Plan for the Indian Wells Valley (IWV) Groundwater Model (IWV-Model). This Plan describes the CM processes for development, maintenance, upgrade, and use of the IWV-Model that was initially developed by Desert Research Institute (DRI) under contract with the Navy; and further developed by DRI under contract with the IWV Groundwater Authority (IWVGA) to support development of the Groundwater Sustainability Plan (GSP). Pursuant to California's Sustainable Groundwater Management Act of 2014, the IWVGA is tasked with managing the sustainability of water resources for all water users within the basin. The IWV-Model is one of the primary technical tools that the IWVGA uses to understand and quantify the available groundwater resources and to develop sound groundwater management policy for the IWV Basin. This CM Plan establishes appropriate maintenance and management standards to ensure fidelity and transparency of this technical tool for the citizens of IWV.

The Navy's transfer of the IWV-Model's maintenance, further development, and CM to the IWVGA includes the Navy's participation in the model's CM process that oversees, recommends and dispositions of any changes to the model's capability and functionality. The IWVGA and Navy will retain unlimited use licenses of the model to support studies specific and unique to their respective interests and needs.

1.2 Scope

The scope of this Plan contains the procedures and processes needed to fulfill the CM requirements of all projects and resources associated with the IWV-Model. Those requirements include:

a. Provide quality assurance that data and information used in the model is accurate and appropriately represents the Hydrogeologic Conceptual Model (HCM).

b. Establish a Technical Model Group (TMG), including Navy and DRI representation, to ensure the scientific sustainment and effectiveness of the IWV-Model. The TMG's responsibilities include (a) review, evaluate, and make recommendations regarding new configuration change requests, (b) evaluate IWV-Model calibration and results, and (c) track change requests, model runs and revisions, and model documentation.

c. Establish an adequate tracking and documentation system of model codes and corresponding input/output files for historical conditions, future baseline, management scenarios, revisions, and other uses.

d. Provide peer review of model structure and analysis.

e. Offer methods for updating and improving this CM Plan to fully address its stated purpose.

1.3 CM Objectives

The IWVGA's goals in managing the IWV-Model, the configuration change process, and activity tracking are to ensure that:

a. adequate and accurate information is available to provide a transparent management tool that is professionally maintained, modified, and improved as new scientific data become available.

b. the impact of configuration management and configuration changes upon the costs of operation and maintenance of this groundwater resource tool are understood and accommodated within the IWVGA's fiscal constraints.

c. all personnel involved in managing the IWV-Model or data intended for use in the IWV-Model have reviewed and understand the CM process described herein to ensure the fullest possible support of the CM process.

1.4 Applicability

This CM Plan provides overarching guidance for model-related activities of the IWVGA, TMG, and DRI, including any subcontractors and/or service providers who will influence IWV-Model development or changes, use and/or store IWV-Model data, use the model code to run scenarios, use data output for reporting or other purposes, or in any way influence management of the IWV-Model.

This CM Plan directs the development of and/or identifies TMG's CM processes and procedures but is not a process or procedures document. The requirements in this Plan apply to all phases of the IWV-Model lifecycle to include modification, sustainment, and decommissioning.

1.5 Plan Deviations

The CM activities described in this document are core requirements for projects involving the IWV-Model. Given this policy but understanding needs of a project vary, it is permissible to deviate from the established process for a specific project. Any deviations must receive prior approval from the TMG Manager and be formally documented as part of project requirements. Project personnel charged with implementation will ensure that completed work products comply with the CM process described in this document.

1.6 Review Cycle

This IWV-Model CM Plan will be reviewed no less than annually at the end of each calendar year and the 'Record of Change' page will be updated to reflect any changes. When there are no changes deemed necessary during the review cycle, the 'Record of Change' page will be updated to reflect this.

2.0 Roles and Responsibilities

Configuration Management related responsibilities for the various roles within the TMG are described below.

2.1 TMG Manager

The TMG will have an established manager who will also serve as the configuration manager. The manager will be a representative of the IWVGA's Water Resource Manager (WRM), or an assigned subcontractor, and will ensure that the CM requirements, processes, and procedures are followed. Responsibilities of the manager include:

- Ensure overall compliance with the CM Plan
- Preside over establishment of TMG CM processes and methodologies
- Maintain a roster and contact information of TMG members and alternates for the IWVGA
- Review and comment on project documentation to ensure CM needs are met
- Manage the configuration item (CI) list to ensure entries are complete and accurate
- Process and track CM Plan change requests and variance requests
- Coordinate schedule and manage budget of IWV-Model calibration and model runs
- Assign duties to TMG members or subcontractors as needed
- Determine when TMG meeting is necessary, schedule meeting, and set meeting agenda
- Report status and activities to the TAC and at IWVGA Board meetings.

2.2 TMG Members

TMG will be established by the WRM. TMG members will consist of people knowledgeable of numerical modeling, professional geologists and hydrogeologists, and representatives from the WRM, DRI and the Navy. Members will provide technical support during consideration of CIs and comply with the CM process identified herein. Responsibilities of TMG members include:

- Review this document and comply with the established CM requirements
- Provide technical review of new CI requests
- Develop recommendations regarding CI requests (e.g. implement or not, modify the CI, etc.)
- Attend TMG meetings, as determined by the TMG Manager
- Evaluate IWV-Model revisions, re-calibration, sensitivity, and uncertainty analysis
- Perform additional duties as assigned by the TMG Manager

2.3 Desert Research Institute (DRI)

DRI shall be the principal modeler and have representation on the TMG. Modeling duties may be assigned to the WRM, or other TMG Members, through the CM Plan. DRI's responsibilities include:

- Comply with CM requirements established herein
- Attend TMG meetings, as determined by the TMG Manager
- Maintain copies of all IWV-Model versions until released from that obligation by the IWVGA and the Navy
- Provide copies of each new model version to the IWVGA's Water Resource Manager (WRM) and the Navy
- Provide technical review of new CIs,
- Develop recommendations regarding CI requests, especially considering implementation logistics
- Develop cost estimates for CI implementation
- Perform model revisions and model runs requested by the TMG Manager
- Ensure applicable cybersecurity accreditations are maintained

2.4 Subcontractors

Subcontractors or other entities working on any aspect of the IWV-Model, including data collection for inclusion in the IWV-Model, modification to model code, additional model runs, etc. must review this document and comply with CM requirements established herein.

2.5 Use of Model Code

If any entity other than DRI and the WRM is allowed to use the model code for additional model runs, a variance request shall first be submitted to the TMG Manager for consideration and approval. Any allowed variances shall be recorded on the IWV-Model Run List and documentation of model input and output provided to the TMG Manager.

2.6 Applicable Documents

The following applicable documents list will be updated as future model documentation is completed and approved by the TMG.

NAWCWD-TP-8811	Groundwater Resource Sustainability: Modeling Evaluation for the Naval Air Weapons Station, China Lake, California. By McGraw, et. al. (Desert Research Institute), September 2016
IWVGA Model Review	Review of the Indian Wells Valley Groundwater Basin Model documented in *Groundwater Resource Sustainability: Modeling Evaluation for the NAWS China Lake, California.* By Moran (Stetson Engineers Inc.) 2017
IWVGA GSP, Appendix 3-H	Indian Wells Valley GSP Model Documentation, by Pohlmann, Garner, Chapman and Pohll, Desert Research Institute, January 2020.
11011 Ser PR2/594	Letter from CDR Peter R. Benson, NAWS China Lake Public Works Officer to IWVGA re Indian Wells Valley Groundwater Model. November 7, 2018.

3.0 Configuration Management

Configuration Management (CM) is a process for managing the maintenance of, changes to, and documentation of the IWV-Model. Primary components of this CM Plan include (1) CI process with technical review, (2) model revisions with technical oversight, and (3) model run implementation and documentation.

3.1 Configuration Item Process and Technical Review

A key component of the CM process is the initial request to consider a CI. It is expected that most CI recommendations would originate from the Technical Advisory Committee (TAC) established under the IWVGA. The WRM will assign CM tasking to the TMG, subject to approval of the associated budget for the CM task by the IWVGA Board. It is the WRM assigning the CI review task to the TMG Manager that triggers the CM process described below:

1) The WRM assigns the CI review task to the TMG Manager
2) The TMG Manager requests the TMG members to review the CI considering the following questions or issues at minimum:
    - Review CI's technical information, report, and/or data.
    - What information is desired or expected from the CI?
    - Can the CI request be addressed with existing information?
    - Would the information gained from the CI be significant enough to warrant the effort?
    - Is implementing the CI practical from a model code manipulation perspective?
    - What is the approximate cost to implement the CI?
    - Determine if the budget for any changes is acceptable to the IWVGA Board, or Navy, appropriate to funding source.
    - When and in what model version should the CI be implemented?
    - Should the CI be combined with other CIs?

3) The TMG prepares a recommendation to the WRM in response to the CI request, including whether to reject, modify or implement the CI, recommended implementation timing, etc.

4) When directed to proceed with the CI, the TMG Manager logs an entry on the *IWV-Model Configuration Item List* (attached).

5) When the CI has been implemented, the TMG Manager shall complete and close out the CI tracking entry in the IWV-Model CI List. Updated lists will be posted on the IWVGA website.

3.2 IWV-Model Revision and Version Tracking

Not all CIs are expected to result in an individual IWV-Model revision, therefore IWV-Model revisions will be tracked separately in the IWV-Model Revision List (example attached). For each approved IWV-Model revision, DRI shall prepare an Interim Technical Note (ITN) summarizing the revision and the results. Following review by the TMG, the ITN shall be distributed to the TAC, presented at the IWVGA Board meeting, and uploaded to the IWVGA website for public access.

Periodically, new IWV-Model versions are expected to be created to replace the previous versions. For each new IWV-Model version created, an entry shall be logged in the IWV-Model Revision List and DRI shall prepare a Model Documentation Report. Model documentation shall provide a comprehensive summary of all changes to the IWV-Model since the previous versions, and include updated MODFLOW source code, discussions of the technical data incorporated from the CM process, and new calibration, sensitivity, and uncertainty results. DRI's Model Documentation will be peer reviewed by the TMG. Following peer review, copies of report will be distributed to the WRM, IWVGA and the Navy, and uploaded to the IWVGA website for public access.

3.3 Model Run Review, Reporting, and Tracking

Under approval of funding by the IWVGA, the TMG will work with DRI to develop model runs. Individual model runs shall be numbered sequentially and logged in the IWV-Model Run List (example attached). The log entry shall include a basic description of attributes, properties, or data changed from the most recent model version for each particular model run.

The model run process will include an initial TMG meeting with DRI to discuss what model run parameters are to be changed, and the purpose of the model run. DRI will present model results to the TMG for discussion and peer review. DRI will present peer reviewed model run to the IWVGA, and prepare a technical memorandum summarizing the model run construction and results. The technical memorandum will be distributed to the TAC and posted on the IWVGA website for public access.

4.0 CM Plan Updates and Revisions

TMG members can make recommendations to the TMG Manager for updates or revisions to the CM Plan. All proposed changes to the CM Plan will be reviewed by IWVGA and Navy staff prior to implementation. If approved, the change would be noted on the second page of this document in the Record of Changes table, and the updated version of the CM Plan will be posted on the IWVGA website.

Indian Wells Valley Groundwater Authority, Model Technical Advisory Committee

IWV-Model Configuration Item (CI) List

CI Request Number	Request Date	CI Summary	Importance Rank 1 (low) 5 (high)	Priority 1 (low) 5 (high)	Origin of CI (IWVGA, TAC, Navy, etc.)	Completed Date

Indian Wells Valley Groundwater Authority, Model Technical Advisory Committee

IWV-Model Revision List

Model Version	Revision No. *	Revision Date	Summary of Revision	Requestor

* Model Run numbering format: Model Version - Revision Number - 2-digit Model Run Number. E.g. '2020-13-05'.

Indian Wells Valley Groundwater Authority, Model Technical Advisory Committee

IWV-Model Run List

Model Run Number *	Run Date	Summary of Conditions Modeled	Requestor (IWVGA, Navy, etc.)

* Model Run numbering format: Model Version - Revision Number - 2-digit Model Run Number. E.g. '2020-13-05'.

ATTACHMENT L

IWV-MODEL CONFIGURATION ITEM (CI) LIST

CI Request Number	CI Request Date	CI Summary	Reviewed	Model Consideration/ Inclusion		Origin of CI (IWVGA, TAC, Navy, etc.)	Date Completed review order
				2025	2030		
1	5/6/22	SkyTEM Airborne Surveys, Dec 2017. SkyTEM Survey: Indian Wells, California (42 pp)	X	X		IWVGA	TMG 8/18/22 Plan outside AEM review Fall 2023 TMG 1/30/24
2	5/6/22	Ramboll, June 2019. Hydrogeologic Conceptual Framework; Indian Wells Valley, Final Report (113 pp)	X	X		IWVGA	TMG 8/18/22 Plan outside AEM review Fall 2023 TMG 1/30/24
3	5/6/22	Ramboll, June 2019. Indian Wells Valley – Boreholes; A Description of Borehole Information (532 pp)	X	X		IWVGA	Plan outside review w AEM Fall 2023
4	5/6/22	Steve Bacon, August 2020. DRI's Technical Review of Hydrogeologic Conceptual Framework, Indian Wells Valley, by P. Thorn, T. Parker, and M. Halhjaer, Ramboll	X	X		IWVGA	TMG 8/18/22
5	5/6/22	Jenny B. Chapman, James M. Thomas, Chris Garner; Applied Geochemistry 2022. Groundwater recharge timing based on ^{14}C and ^{2}H within Indian Wells Valley	X	X		IWVGA	
6	5/6/22	Aquifer Test Data/Reports: a) DRI, December 2020. Indian Wells Valley Multi-well Aquifer Test Analysis: IWVWD Well 10 and Quist Ranch 21-hour and 48-hour Tests, Ridgecrest, CA b) Aquilogic, 2020 (*do not have data or results as of 2/28/24)* c) Driller log capacity tests	X	X		IWVGA	Fall 2023 TMG 1/30/24

CI Request Number	CI Request Date	CI Summary	Reviewed	Model Consideration/ Inclusion		Origin of CI (IWVGA, TAC, Navy, etc.)	Date Completed review order
				2025	2030		
7	5/6/22	Navy/DRI Research Article (2021). Tectonic, hydrogeologic, and climatic controls on Late Holocene dune formation, China Lake basin, Indian Wells Valley, California, USA	X	X		IWVGA	TMG 7/14/22 Field 10/20/22
8	5/6/22	Review monitoring well EP-1 geologic, monitoring, and water quality data.	X	X		IWVGA	TMG 10/27/22 & 11/3/22
9	5/6/22	Review groundwater level data since 2015. a) Fall and spring contours b) Datalogger and telemetry data c) Monitoring well hydrographs	X	X		IWVGA	TMG 6/16/22 & 6/23/22
10	5/6/22	Review of annual water quality data collected since 2020.	X	X		IWVGA	TMG 9/1/22
11	5/6/22	Review of surface water gaged flow and field observations.	X	X		IWVGA	
12	5/6/22	Review large pumping well concentration and cones of depression.	X	X		IWVGA	TMG 7/14/22 S. Bacon, DRI Oct 2023 Hist Pumping to DRI
13	5/6/22	Review IWV faulting: a) Unnamed Fault separating El Paso Subarea and main IWV Basin b) 2019 Ridgecrest Earthquake (new) fault structure	X	X		IWVGA	TMG 7/14/22 TMG 1/30/24 S. Bacon, DRI
14	5/6/22	Rose Valley Subflow a) new monitoring wells Fall 2022 b) Faulting near Little Lake and Rose Valley Subflow Conceptual Model c) Little Lake surface flow from Inyo County	X	X		IWVGA	10/27/22 Ongoing w drilling program
15	5/10/22	USGS Basin Characterization Model (recharge)	X	X		T. Parker	TMG 1/12/24

CI Request Number	CI Request Date	CI Summary	Reviewed	Model Consideration/ Inclusion		Origin of CI (IWVGA, TAC, Navy, etc.)	Date Completed review order
				2025	2030		
16	9/1/22	Evaporation off of a wet playa	X	X		S. Bacon DRI	TMG 10/27/22 S. Bacon, DRI
17	10/6/22	IWV model Configuration Item List developed in 2022; Field visit the next day	X	X		DRI/WRM	TMG 10/6/22 Group discussion
18	10/27/22	Biweekly meetings to discuss changes to groundwater in storage and compare the model results to a Thiessen Polygon method.	X	X		DRI/WRM	TMG 12/15/22 Group discussion
19	1/19/23	Dr. Ryan Smith a) Presentation of how to approach Airborne Electromagnetic (AEM) survey data analysis (SkyTEM Survey Data Report) to Technical Model Group (TMG) members b) Additional data to provide for AEM interpretation	X	X		DRI/WRM	TMG 1/19/23 Group discussion
20	2/7/23	Numerous Teams meetings with Stetson, Dr. R. Smith, and some TMG members to discuss uncertainties using AEM survey data in GW models	X	X		DRI/WRM	TMG 2/24/23 Group discussion
21	3/2/23	Weekly calls between Stetson and DRI group to have technical discussions about GSP 2025 update	X	X		DRI/WRM	TMG 4/6/23 Group discussion
22	4/6/23	"DRI to present the first proposed GSP Model changes: a) Simulation period: October 1, 1920 through September 30, 2022. b) Stress period: annual stress period from October 1, 1920 to September 30, 1995; monthly stress period from October 1, 1995 to September 30, 2022. c) Six model layers d) Depth and thickness of each model layer based on Monasttero et al. (2002); Shah et al. (2018) and AEM data (2019) e) Hydraulic conductivity f) Pumping a. g. Recharge"	X	X		DRI/WRM	TMG 8/17/23 Group discussion
23	5/24/23	Group meeting a) Seismic depth to basement analysis	X	X		DRI/WRM	TMG 5/24/23 Group discussion

CI Request Number	CI Request Date	CI Summary	Reviewed	Model Consideration/ Inclusion		Origin of CI (IWVGA, TAC, Navy, etc.)	Date Completed review order
				2025	2030		
		b) Clay plug analysis					
24	6/14/23	Group meeting a) Depth to basement analysis b) Sedimentary thickness analysis	X	X		DRI/WRM	TMG 6/14/23 Group discussion
25	6/30/23	Group meeting a) Preliminary model layer delineation	X	X		DRI/WRM	TMG 6/30/23 Group discussion
26	7/21/23	a) Discussed methodology for discretizing model grid in basalt flow area below Rose Valley, and planned to delineate an aquifer property zone for the White Hills formation. b) DRI will continue work on model grid discretization using SkyTEM and well log data. DRI will complete the preliminary model discretization, define faults to be simulated, and analyze clay fraction in the clay plug to present at the next modeling group meeting.	X	X		DRI/WRM	TMG 7/31/23 Group discussion
27	8/7/23	Several Teams meetings with Stetson group and R. Smith to discuss borehole data and AEM data to define clay extent; Prepared and gave two presentations to Stetson group and TMG members: 1) Proposed Model Faults for 2025 GSP Update (August 7, 2023); and Proposed Clay Extent 2025 GSP Update (August 25, 2023)	X	X		DRI/WRM	TMG 8/25/23 Group discussion
28	9/25/23	Steve Bacon, September 25, 2023. Development of a Tectonic Block Model in Support of the Hydrogeology Conceptual Framework of IWV (2025 GSP Update)	X	X		DRI/WRM	TMG 9/25/23 Plan outside AEM review
29	10/6/23	Hydrogeologic zone and aquifer properties	X	X		DRI/WRM	Emailed on 10/6/23
30	10/23/23	Historical Calibration Pumping for model update	X	X		DRI/WRM	TMG 10/23/23 reviewing
31	10/30/23	Initial head (October 1920) and historical water levels in IWVGB	X	X		DRI/WRM	1/9/2024

CI Request Number	CI Request Date	CI Summary	Reviewed	Model Consideration/ Inclusion		Origin of CI (IWVGA, TAC, Navy, etc.)	Date Completed review order
				2025	2030		
32	12/18/23	a) Final model domain boundary. b) Final model domain layers including deep clay extent. c) Proposed aerial extent, extinction depths, and maximum rates of ET zones. d) Review 2020 GSP recharge distribution and discuss potential changes to recharge distribution in 2025 update.	X	X		DRI/WRM	TMG 12/18/2023 discussion
33	1/5/24	Mountain front recharge and aquifer connectivity	X	X		DRI/WRM	TMG 1/12/2024 discussion
34	1/12/24	Recharge and model update	X	X		DRI/WRM	TMG 1/12/2024 discussion
35	1/30/24	Recharge distribution, hydraulic conductivity zones and model update	X	X		DRI/WRM	TMG 1/30/2024 discussion
36	2/13/24	Transient water level for IWV model calibration	X	X		DRI/WRM	2/14/2024
37	2/28/24	Consider uncertainty analysis in next 2030 Model update.	X		X	DRI/WRM	3/5/2024 TMG meeting
38	2/28/24	Groundwater level data for model calibration - prioritize areal density and temporal length of well data sets. 2025 Model update uses about double the number of target wells as 2020 GSP Model. Revisit target well data sets (include target weighting) for 2030 Model update.	X		X	DRI/WRM	3/5/2024 TMG meeting
39	2/28/24	2025 Model update maintains 7,650 AFY Recharge from 2020 GSP Model. Revisit these recharge assumptions during future 2030 Model update.	X		X	DRI/WRM	3/5/2024 TMG meeting
40	2/28/24	Review of LADWP Emergency Release Draft Data Report.	X	X		WRM	3/5/2024 TMG meeting

CI Request Number	CI Request Date	CI Summary	Reviewed	Model Consideration/ Inclusion		Origin of CI (IWVGA, TAC, Navy, etc.)	Date Completed review order
				2025	2030		
41	2/28/24	Review of El Paso Subarea delineation for sub-water budget.	X	X		WRM	3/5/2024 TMG meeting
42	3/18/24	Review Rose Valley water hydrogeology and model update	X	X		WRM	TMG 3/18/2024 discussion
43	3/26/24	Develop future baseline pumping.	X	X		WRM	TMG 3/26/2024 discussion
44	4/2/24	Review 2020 GSP Scenario 6.2 modeling and discuss approach to baseline pumping.	X	X		WRM	4/2/2024 TMG meeting
45	4/16/24	Model calibration progress. Calibration mostly complete, with exception to Rose Valley area.	X	X		S. Rybarski, DRI	4/16/2024 TMG meeting
46	4/23/24	Consider sensitivity analysis by region in 2030 Model update.	X		X	DRI/WRM	4/30/2024 TMG meeting
47	4/25/24	Develop assumptions for 2025 Implemented Management pumping	X	X		WRM	5/17/2024 TMG meeting
48	5/9/24	Modify future baseline pumping	X	X		WRM/Legal	5/17/2024 TMG meeting
49	5/10/24	Develop climate change modeling approach – use of Cal-Adapt tool	X	X		DRI/WRM	5/17/2024 TMG meeting
50	5/15/24	Model calibration complete	X	X		DRI/WRM	5/17/2024 TMG meeting
51	5/24/24	Initial disclosures on current and projected pumping	X	X		WRM/Legal	6/4/2024 TMG meeting
52	5/29/24	Additional Model Runs developed - Scenario 1A: Implementation - Scenario 2: No GA	X	X		WRM/Legal	6/4/2024 TMG meeting
53	6/13/24	Modify future baseline pumping and 2025 Implemented Management pumping assumptions	X	X		WRM	6/18/2024 TMG meeting
54	6/17/24	Additional consumptive use analysis added as a data gap	X		X	WRM	6/18/2024 TMG meeting
55	7/10/24	Model Update Presentation at IWVGA Board Meeting	X	X		DRI	7/10/2024 IWVGA Board meeting
55	7/17/24	Development of additional modeling scenarios - Scenario 3: ET Study - Scenario 1B: SVM/IWVWD Pumping Balance	X	X		DRI/WRM	7/17/2024 DRI/Stetson call

CI Request Number	CI Request Date	CI Summary	Reviewed	Model Consideration/ Inclusion		Origin of CI (IWVGA, TAC, Navy, etc.)	Date Completed review order
				2025	2030		
		- Scenario 4: El Paso Pumping					
56	8/8/24	Verify model results for GDE EVT with monitoring data	X		X	WRM	8/8/2024
57	8/12/24	Well locations updated	X	X		DRI/WRM	8/12/2024
58	8/14/24	Monthly recharge updated	X	X		DRI/WRM	8/21/2024
59	8/27/24	Additional modeling runs complete		X		DRI	8/27/2024
60	9/24/24	Climate change modeling complete		X		DRI	9/24/2024
61	Oct. 2024	Sensitivity Analysis Complete	X	X		DRI	October 2024

ATTACHMENT M

Documentation of the Indian Wells Valley 2025 Basin Groundwater Model Update

Susan C. Rybarski, MS
Steven N. Bacon, PhD, PG, CEG

February 2025

Prepared by

Division of Hydrologic Sciences, Desert Research Institute,
Reno, Nevada

THIS PAGE LEFT INTENTIONALLY BLANK

ACKNOWLEDGEMENTS

The authors acknowledge the World Climate Research Programme's Working Group on Coupled Modelling, which is responsible for CMIP, and we thank the climate modeling groups (listed in Table 6-1 of this report) for producing and making available their model output. For CMIP the U.S. Department of Energy's Program for Climate Model Diagnosis and Intercomparison provides coordinating support and led development of software infrastructure in partnership with the Global Organization for Earth System Science Portals.

THIS PAGE LEFT INTENTIONALLY BLANK

CONTENT

ACKNOWLEDGEMENTS iii
LIST OF FIGURES vi
LIST OF TABLES xii
LIST OF ACRONYMS xii
1. INTRODUCTION 1
2. BASIN CONFIGURATION 1
2.1. Model Domain Boundary 1
2.2. Base of Model Domain 9
3. HYDROGEOLOGIC CONCEPTUAL MODEL 10
3.1. Inclusion of Faults 10
3.1.1. Fault Identification 12
3.1.2. 2025 Basin Model Faults 18
3.2. Hydrogeologic Stratigraphic Framework 19
3.2.1. Spatial Extent of Fine-grained “Clay” Unit 20
3.2.2. Depth of Fine-grained “Clay” Unit 22
3.2.3. Thickness of Fine-grained “Clay” Unit 25
3.2.4. Tectonic-block Model for Northern Indian Wells Valley and China Lake Basin 26
3.2.5. Methods for Developing Geologic Cross Sections 30
3.2.6. Geologic Cross Sections 36
3.2.7. 2025 Basin Model Clay Unit 42
4. CONCEPTUAL FLOW BUDGET 42
4.1. Spatial Distribution of Mountain-front Recharge 43
4.2. Spatial Distribution of Bare Soil Evaporation and Evapotranspiration 44
4.3. Historical Pumping 48
5. NUMERICAL MODELING 50
5.1. Boundary Conditions 51
5.1.1. Recharge 51
5.1.2. Evapotranspiration 54
5.1.3. Outflow to Salt Wells Valley 54
5.1.4. Pumping 57
5.2. Model Parameterization 58

5.2.1. Aquifer Property Zones 58
5.2.3. Faults 58
5.3. Model Calibration and Results 60
5.3.1. Estimated Model Parameters 60
5.3.2. Steady-state Calibration Metrics 63
5.3.3. Transient Calibration Metrics 65
5.3.4. Transient Historical Flow Budgets 73
5.4. Sensitivity Analysis 74
6. 2025 BASIN MODEL SCENARIOS 80
6.1. Baseline Scenario 80
6.2. 2025 Basin Model Pumping Scenarios 85
6.3. Climate Change Scenarios 85
6.3.1. Estimation of Change in Potential ET due to Climate Change 87
6.3.2. Estimation of Change in Mountain Front Recharge due to Climate Change 91
6.3.3. Climate Change Scenario Configuration 92
6.3.4. Climate Change Scenario Results 93
7. MODEL LIMITATIONS 104
8. CONCLUSIONS 105
9. REFERENCES 105
ATTACHMENT 1 ..... A-1
ATTACHMENT 2 ..... B-1
ATTACHMENT 3 ..... C-1
ATTACHMENT 4 ..... D-1

LIST OF FIGURES

2-1. Map showing the location of Groundwater Sustainability Agencies (GSAs) Bulletin 118 Indian Wells Valley groundwater basin, as well as other basins and subbasins in California. 2

2-2. Map showing the Groundwater Sustainability Agencies (GSAs) Bulletin 118 Indian Wells Valley groundwater basin and adjacent basins. 3

2-3. Map showing the distribution of consolidated Pliocene sedimentary rocks of the White Hills sequence and consolidated Miocene sedimentary and volcanic rocks within the northern and southern boundaries, respectively, of the Groundwater

Sustainability Agencies (GSAs) Bulletin 118 Indian Wells Valley groundwater basin… 4

2-4. Map showing the 2020 GSP model domain in relation to the distribution of consolidated Pliocene sedimentary rocks of the White Hills sequence, consolidated Miocene sedimentary and volcanic rocks, and the Groundwater Sustainability Agencies (GSAs) Bulletin 118 Coso Valley groundwater basin. 5

2-5. Map showing a comparison of the aerial extent between the 2020 GSP and 2025 Basin Model domains. 7

2-6. Map showing an updated model domain for the 2025 Basin Model that is developed from the extent of geologic data and Groundwater Sustainability Agencies (GSAs) Bulletin 118 groundwater basins (Figures 2-3 and 2-4), plus the distribution of range-front faults and depth to pre-Cenozoic basement (i.e., bedrock) from the National Crustal Model dataset. 8

2-7. Map showing the 2025 Basin Model domain in relation to the National Crustal Model unconsolidated sedimentary thickness. 9

3-1. Map showing the 2025 Basin Model domain in relation to the primary fault zones with historical, Holocene, latest Quaternary, and late Quaternary fault activity in the watershed of the Indian Wells Valley groundwater basin. 11

3-2. Map showing the 2025 Basin Model domain and the survey area of Airborne Electromagnetic (AEM) resistivity data. 13

3-3. Cross sections (EW04 and EW05) through resistivity grids of Airborne Electromagnetic (AEM) data. 15

3-4. Cross sections (N15 2 and N17 2) through resistivity grids of Airborne Electromagnetic (AEM) data in the El Paso Valley subbasin. 17

3-5. Maps showing the distribution of faults used in the 2020 GSP Model and the 2025 Basin Model. 19

3-6. Map showing the extent of the deep fine-grained “clay” unit within the 2025 Basin Model domain. 21

3-7. Map showing the extent of the deep fine-grained “clay” unit within the 2025 Basin Model domain. 22

3-8. Map showing the distribution of wells that recorded the top of the deep fine-grained “clay” unit within the 2025 Basin Model domain. 23

3-9. Map showing the distribution of wells that recorded the bottom of the deep fine-grained “clay” unit within the 2025 Basin Model domain. 24

3-10. Map showing the distribution of wells and measured thickness of the deep fine-grained “clay” unit within the 2025 Basin Model domain. 26

3-11. Map showing tectonic model of the IWV groundwater basin used to support development of geologic cross sections. 28

3-12. Idealized models for the major characteristics in cross-sectional view of the three types of flower structures present in a divergent-wrench fault zone: (A) negative, (B) positive, and (C) hybrid flower structures. 29

3-13. Map showing location of wells along geologic cross section transects 1–5 used in the development of the tectonic-block model of the deep fine-grained "clay" unit within the 2025 Basin Model domain. 31

3-14. Stratigraphic columns for deep wells SNORT-1, SNORT-2, and TGCH-1. 33

3-15. Geologic cross sections along transects 1–3 showing the configuration of the fine-grained "clay" unit represented by the lacustrine facies sedimentary unit 2 based on a simple tectonic-block model for northern IWV and China Lake basin. 37

3-16. Geologic cross sections along transects 4 and 5 showing the configuration of the fine-grained "clay" unit represented by the lacustrine facies sedimentary unit 2 based on a simple tectonic-block model for northern IWV and China Lake basin. ... 38

3-17. Map showing location of primary and secondary faults of the tectonic-block model and geologic cross section transects 1–5 within the 2025 Basin Model domain. 39

3-18. Map showing interpolated elevation of the top of clay unit in 2025 Basin Model domain based on digitized elevations from geologic cross sections along transects 1–5 (Figures 3-15 and 3-16). 40

3-19. Map showing interpolated elevation of the bottom of clay unit in 2025 Basin Model domain based on digitized elevations from geologic cross sections along transects 1–5 (Figures 3-15 and 3-16). 41

4-1. Map showing the watersheds and associated groundwater recharge areas used in the 2025 Basin Model. 44

4-2. Map showing the extent and type of evapotranspiration (ET) zones used in the 2020 GSP Model. 45

4-3. Map showing the extent and type of evapotranspiration (ET) zones used in the 2025 Basin Model Update. 47

4-4. Locations of simulated historical pumping wells. 49

4-5. Total pumping rates assigned to each well type for the Historical Calibration period (WY 1921-2022). 50

5-1. Linear distribution of historical precipitation to estimated recharge, distributed to average 7,650 AFY over WY 1921-2022. 53

5-2. Annual recharge rates estimated using the relationship between precipitation and recharge (gray) as presented in Figure 5-1, compared to the final simulated recharge rates modified to reflect fluctuations in layer 1 only (green). 53

5-3. Monthly distribution of assigned maximum ET rates for the 2025 Basin Model, defined based on monthly percentages of annual ETa from Owens Lake basin… 54

5-4. Location of General Head Boundary used to simulate outflow through overflow channel to Salt Wells Valley. 55

5-5. Distribution of aquifer property zones by material type for each of the six model layers, and locations of the faults used to define them. 56

5-6. Cross-sections of the 2025 Basin Model domain, showing layer discretization and distribution of aquifer property zones. 57

5-7. Locations of faults simulated as barriers to flow within the 2025 Basin Model, compared to all faults used in the tectonic block model. 59

5-8. Calibrated hydraulic conductivity fields for the six model layers, and the tectonic block model faults used to define aquifer property zones. 61

5-9. Calibrated specific yield fields for the six model layers, and the tectonic block model faults used to define aquifer property zone. 62

5-10. Spatial distribution of head error in the steady-state 2025 Basin Model. Negative numbers indicate that the model is under-simulating observed water levels, and positive values indicate that the model is over-simulating observed water levels. 64

5-11. One-to-one plot comparing simulated and observed heads for the steady-state 2025 Basin Model. 65

5-12. Simulated change in water level between WY 1920-2022 for the transient-historical calibration model and locations of observation wells for which comparisons of simulated and observed water levels are presented in Figures 5-13 to 5-17. 67

5-13. Simulated vs observed heads for representative wells within the model domain..... 68

5-14. Simulated vs observed heads for representative wells within the model domain..... 69

5-15. Simulated vs observed heads for representative wells within the model domain..... 70

5-16. Simulated vs observed heads for representative wells within the model domain..... 71

5-17. Simulated vs observed heads for representative wells within the model domain..... 72

5-18. Simulated flow budget for the 2025 Basin Historical Calibration Model, showing rates of mountain block/mountain front recharge (RCH), pumping (WEL), vegetated evapotranspiration (EVT vegetation), bare soil evaporation (Evap bare soil), and flow to Salt Wells Valley (Net flow to SWV). 73

5-19. Simulated cumulative change in storage for the 2025 Basin Historical Calibration Model. 74

5-20. Simulated recharge rates for the transient-historical calibration model and the two recharge sensitivity models. 74

5-21. Difference in water levels between the 2025 Basin transient-historical calibration model and the +10% Recharge Sensitivity model (left), and the -10% Recharge Sensitivity model (right) for the end of WY 2022 75

5-22. Simulated groundwater levels for the transient-historical calibration model and the two recharge sensitivity models at representative wells within the model domain. ... 76

5-23. Simulated groundwater levels for the transient-historical calibration model and the two recharge sensitivity models at representative wells within the model domain. ... 77

5-24. Simulated groundwater levels for the transient-historical calibration model and the two recharge sensitivity models at representative wells within the model domain..... 78

5-25. Simulated total evapotranspiration (bare soil + phreatophyte ET) for the transient-historical calibration model and the two recharge sensitivity models. 79

5-26. Excess storage depletion for the two recharge sensitivity models relative to the transient-historical calibration model. 79

6-1. Total pumping rates assigned to each well type for the Historical Calibration period (WY 1921-2022) and Baseline Scenario (WY 2020-2070)..... 81

6-2. Change in water levels for the Baseline Scenario between WY 2020-2070 (left) and WY 2040-2070 (right). 82

6-3. Simulated flow budget for the Baseline (No Action) Scenario, showing rates of mountain block/mountain front recharge (RCH), pumping (WEL), vegetated evapotranspiration (EVT vegetation), bare soil evaporation (Evap bare soil), and flow to Salt Wells Valley (Net flow to SWV). 83

6-4. Simulated cumulative change in storage for the Baseline Scenario. 83

6-5. Time-series plots for water year 1896 to 2021 showing mean annual temperature and range at elevations as high as Owens Peak and as low as China Lake basin..... 84

6-6. Time-series plots for water year 1896 to 2021 showing soil evaporation for mountain soil settings at elevations as high as Owens Peak and for playa soil settings at elevation as low as China Lake basin. 89

6-7. Plot showing empirical relations between estimated monthly soil evaporation derived from the Jense-Haise (1963) radiation-based empirical model versus associated mean monthly temperature. 90

6-8. Estimated change in PET calculated from temperatures from each of the twenty GCMs relative to average PET calculated using average air temperatures for 1950-2006..... 91

6-9. Cumulative recharge deficit for each of the twenty GCMs used to estimate change in recharge based on future changes in precipitation and temperature. 92

6-10. Difference maps showing the change in water levels between the RCP 8.5 (Warm/Dry) scenario and Baseline (left) and the RCP 8.5 (Average) scenario and Baseline (right), for the end of WY 2070. 94

6-11. Difference maps showing the change in water levels between the RCP 4.5 (Average) scenario and Baseline (left) and the RCP 4.5 (Cool/Wet) scenario and Baseline (right), for the end of WY 2070. 95

6-12. Difference map showing the change in water levels between the RCP 4.5 (Complement) scenario and Baseline for the end of WY 2070. 96

6-13. 25S/38E-03B (Well 1) change in water level relative to Baseline for all climate scenarios..... 96

6-14. 25S/38E-35B01 (Well 2) change in water level relative to Baseline for all climate scenarios. 97
6-15. Kerr McGee (Well 3) change in water level relative to Baseline for all climate scenarios. 97
6-16. Sandquist Spa (Well 4) change in water level relative to Baseline for all climate scenarios. 97
6-17. MW 32-SM (Well 5) change in water level relative to Baseline for all climate scenarios. 98
6-18. USBR-04 (Well 6) change in water level relative to Baseline for all climate scenarios. 98
6-19. USBR-01-S (Well 7) change in water level relative to Baseline for all climate scenarios. 98
6-20. 27S/39E-08A01 (Well 8) change in water level relative to Baseline for all climate scenarios. 99
6-21. USBR-03-S (Well 9) change in water level relative to Baseline for all climate scenarios. 99
6-22. George Air Corridor (Well 10) change in water level relative to Baseline for all climate scenarios. 99
6-23. TTBK-MW05 (Well 11) change in water level relative to Baseline for all climate scenarios. 100
6-24. TTBK-MW12 (Well 12) change in water level relative to Baseline for all climate scenarios. 100
6-25. TTIWV-MW15 (Well 13) change in water level relative to Baseline for all climate scenarios. 100
6-26. Cumulative loss of groundwater in storage for the model domain for the Baseline model and all climate scenarios. 101
6-27. Cumulative change in storage for the model domain due to climate change, calculated as the difference in storage loss between the Baseline scenario and each climate change scenario. 101
6-28. Simulated outflow to vegetated evapotranspiration zones for Baseline and climate change scenarios. 102
6-29. Simulated outflow to bare soil evapotranspiration zones for Baseline and climate change scenarios. 102
6-30. Simulated change in vegetated ET area for each climate change scenario, relative to Baseline. 103
6-31. Simulated change in bare soil ET area for each climate change scenario, relative to Baseline. 104

LIST OF TABLES

3-1. Fault information for tectonic-block model used to develop geologic cross section along transect 1. 35

4-1. Extinction depths for soil and vegetation types for evapotranspiration zones in the 2025 Basin Model. 48

5-1. Rates of mountain front recharge applied to each watershed boundary in the 2025 Basin Model (left), compared to the 2020 GSP Model (right), in acre-feet per year. 52

5-2. Comparison of steady-state flow budgets for the 2025 Basin Model and the 2020 GSP Model. 63

5-3. Comparison of steady-state model error statistics for the 2025 Basin Model and the 2020 GSP Model. 63

5-4. Comparison of transient-historical model error statistics for the 2025 Basin Model and the 2020 GSP Model. 66

6-1. Subset of CMIP5 multi-model ensemble results used to estimate the range of climate impacts within the simulated area. 86

LIST OF ACRONYMS

AEM	Airborne Electromagnetic
ALF	Airport Lake fault
CADWR	California Department of Water Resources
CDFW	California Department of Fish and Wildlife
CGS	California Geological Survey
CI	Configuration Items
CMIP5	Coupled Model Intercomparison Project Phase 5
CMP	Configuration Management Plan
CWB	climate water-balance
CY	Calendar Year
DHZ	deep hydrogeologic zone
EP-1	El Paso subarea
ETS	Evapotranspiration Segments
ET	Evapotranspiration

GA	Groundwater Authority
GCM	Global Climate Model
GHB	General Head Boundary
GMS	Groundwater Modeling System
GSAs	Groundwater Sustainability Agencies
GSP	Groundwater Sustainability Plan
GWR	groundwater recharge
HCM	hydrogeologic conceptual model
HFB	Hydrologic Flow Barrier
IHZ	intermediate hydrogeologic zone
IWV	Indian Wells Valley
LLF	Little Lake fault
MAE	mean absolute error
NAWSCL	Naval Air Weapons Station China Lake
NCM	National Crustal Model
PET	potential evapotranspiration
PEST	Parameter ESTimation software
PRISM	Parameter-elevation Regressions on Independent Slopes Model
PRF	Paxton Ranch fault
Qa	Quaternary alluvium unit
Qoa	older Quaternary alluvium units
RCPs	Representative Concentration Pathways
RVS-1	Little Lake
SGMA	Sustainable Groundwater Management Act
SHZ	shallow hydrogeologic zone
SNFF	Sierra Nevada frontal fault
TAC	Technical Advisory Committee
TMG	Technical Modeling Group

UWMP	Urban Water Management Plan
USGS	U.S. Geological Survey
WEL	Well Package
WY	water years

1. INTRODUCTION

The numerical groundwater model developed for Indian Wells Valley (IWV) Groundwater Sustainability Plan (GSP), 2020 GSP Model, has been used by the Technical Advisory Committee (TAC) and Groundwater Authority (GA) to quantify the occurrence and movement of groundwater, and to develop planning scenarios for managing the groundwater resources of the IWV groundwater basin. In 2021, a Configuration Management Plan (CMP) was developed for determining the process of technical review of new data, making recommendations to the GA Board for model updates, and documenting any model revisions. A Technical Modeling Group (TMG) was formed in early 2022 to review technical Configuration Items (CI) and make recommendations to the GA for updating the model with new data and information obtained since the development of the 2020 GSP Model.

The updated 2020 GSP numerical groundwater model, referred to as the 2025 Basin Model, was updated based on consideration of 61 CIs (Attachment 1). The CIs include relevant data recently formulated or acquired since the development of the 2020 GSP Model, as well as relevant data that was not previously considered or used. Revisions were made to four primary model elements, including: (1) basin configuration, (2) hydrogeologic conceptual model, (3) hydrologic budget, and (4) re-calibration. The calibrated 2025 Basin Model was then used to perform simulations for specific 2025 Implementation scenarios. The following sections describe in detail the sources of new data and approaches used to develop and calibrate a refined numerical groundwater model.

2. BASIN CONFIGURATION

Basin configuration is a fundamental component of groundwater storage because it defines the geometry of the aquifer. The TMG recommended that the physical configuration of the groundwater basin be evaluated and updated with existing and readily available information to represent the distribution of saturated hydrogeologic units more accurately within the IWV groundwater basin. The 2025 Basin Model consists of a revised model domain both in the horizontal and vertical dimensions, which collectively has improved the accuracy of the model's ability to simulate groundwater flow.

2.1. Model Domain Boundary

The areal extent of the model domain boundary in past groundwater models was originally defined and used in the groundwater flow model prepared for the IWV Water District (Brown and Caldwell, 2009). The extent of the same boundary was also adopted by subsequent groundwater models developed by the Desert Research Institute for Naval Air Weapons Station China Lake (NAWSCL) (McGraw et al., 2016) and later used by the GA for the 2020 GSP (Garner et al., 2017; IWVGA, 2020).

The California Department of Water Resources (CADWR) updated and defined the boundaries of a total of 517 groundwater basins/subbasins in the State of California (Bulletin 118 update 2020; Figure 2-1). The boundaries of the groundwater basins were defined to support Groundwater Sustainability Agencies (GSAs) as part of the Sustainable Groundwater Management Act (SGMA). There are four GSA groundwater basins that encompass Indian Wells Valley (6-054) that include: Rose Valley on the northwest, Coso Valley (6-055) on the

northeast, Salt Wells Valley (6-053) on the east, and Fremont Valley (6-046) on the south (Figure 2-2).

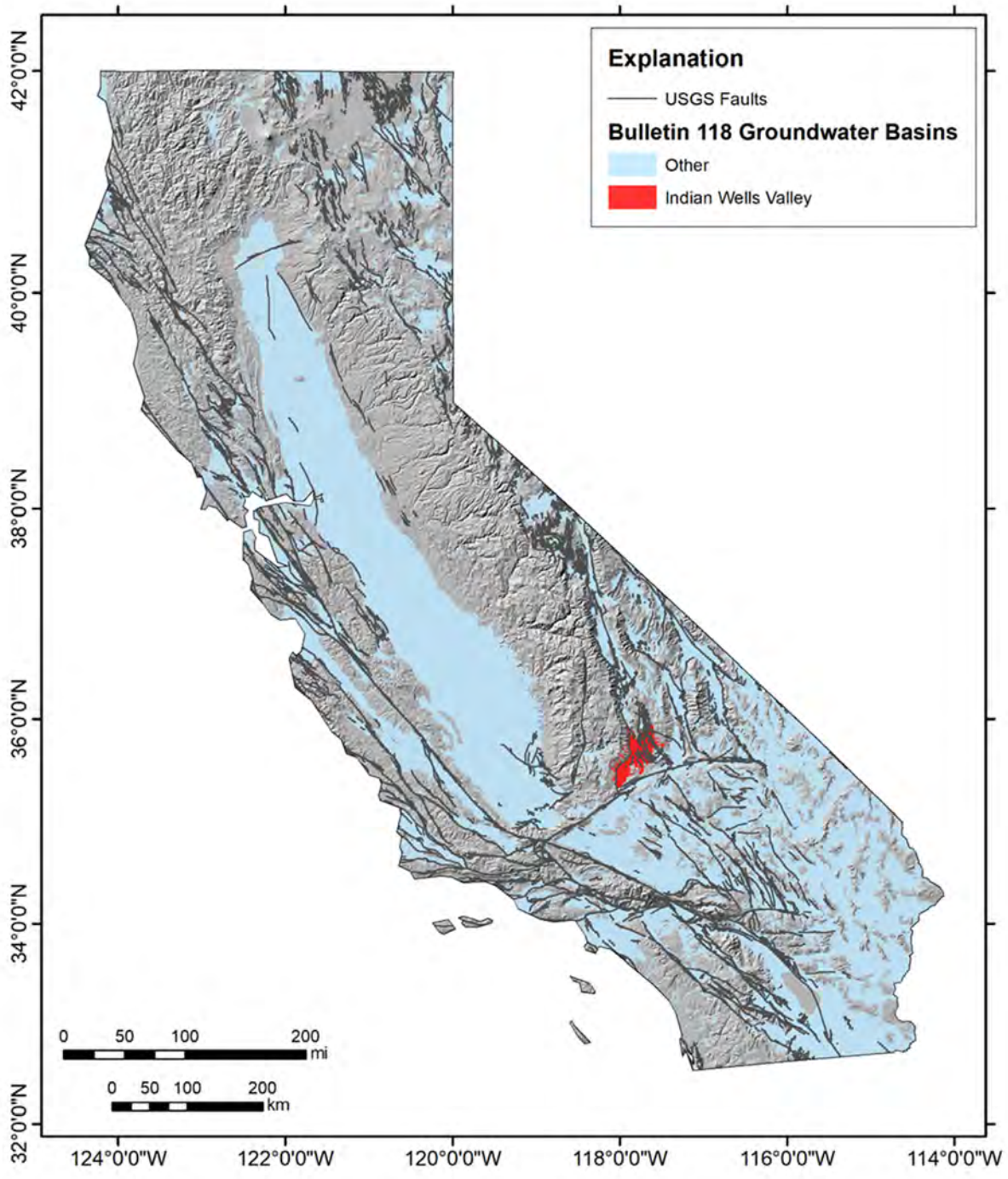


Figure 2-1. Map showing the location of Groundwater Sustainability Agencies (GSAs) Bulletin 118 Indian Wells Valley groundwater basin, as well as other basins and subbasins in California. The distribution of principal faults is also shown (USGS, 2020).

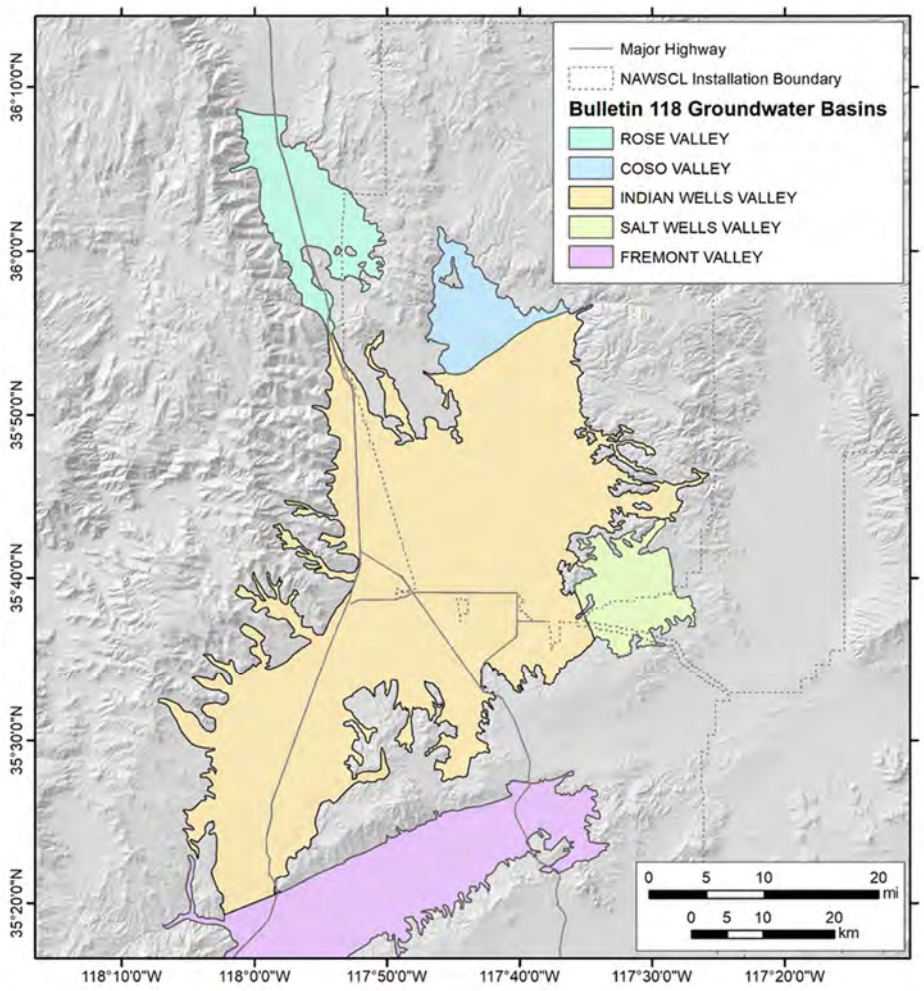


Figure 2-2. Map showing the Groundwater Sustainability Agencies (GSAs) Bulletin 118 Indian Wells Valley groundwater basin and adjacent basins.

Realistic representation of the margins of groundwater basins will yield more accurate estimates of flow from groundwater recharge areas and groundwater storage. The margins of the GSA IWV groundwater basin (6-054) were evaluated to identify any potential shortcomings in using it as an updated model domain boundary. As with most of the GSA groundwater basins in eastern California and within the Basin and Range Physiographic Province, the GSA IWV groundwater basin was defined by the distribution of sedimentary valley fill. However, most of the tributary streams that enter IWV are narrow drainages that consist of thin and unsaturated alluvium (e.g., Figures 2-2 and 2-3). Model domain boundaries that define narrowly shaped areas of unsaturated and thin valley fill are problematic in numerical models designed to simulate saturated groundwater flow. As a result, a new approach was used to delineate a realistic model domain boundary that could be used in an updated numerical groundwater model. An updated 2025 Basin Model domain boundary was developed from the integration of different components of the GSA IWV groundwater basin boundary, geologic mapping, geophysical information, and water level and lithologic logs from wells.

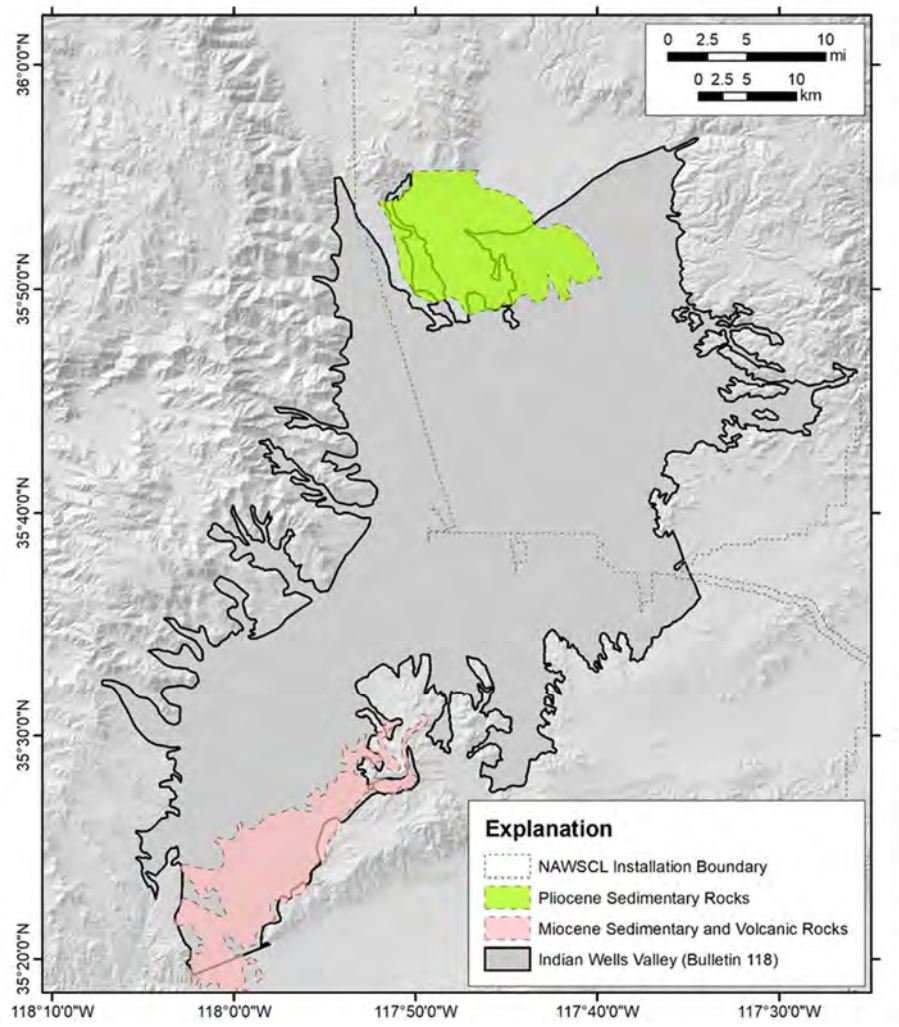


Figure 2-3. Map showing the distribution of consolidated Pliocene sedimentary rocks of the White Hills sequence (Jennings et al., 1962; Monastero et al., 2002) and consolidated Miocene sedimentary and volcanic rocks (Jennings et al., 2010) within the northern and southern boundaries, respectively, of the Groundwater Sustainability Agencies (GSAs) Bulletin 118 Indian Wells Valley groundwater basin.

The margins of the GSA IWV groundwater basin generally coincide with the extent of Quaternary alluvium and older alluvium units (Qa and Qoa) mapped on the 1:750,000-scale Geologic Map of California (Jennings et al., 2010). However, Tertiary rocks are also mapped within the boundaries of the GSA IWV groundwater basin (Figure 2-3). Areas on the northern margin of the groundwater basin include Pliocene sedimentary rocks of the White Hills sequence that are locally overlain by thin Quaternary volcanic flow rocks (Jennings et al., 1962; Monastero et al., 2002). An additional area within the southern sector of the GSA IWV groundwater basin includes Miocene sedimentary and volcanic rocks (Jennings et al., 1962; 2010). These Tertiary sedimentary and volcanic rocks are consolidated and not representative of unconsolidated sedimentary valley fill. The consolidated rock types are not part of the IWV groundwater basin unconsolidated sedimentary aquifer system.

The 2020 GSP Model domain boundary was also evaluated and compared to the GSA groundwater basins, geologic maps, and geophysical data. The majority of the 2020 GSP Model domain is within unconsolidated valley fill; however, the northern sector of the model domain includes the Pliocene sedimentary rocks of the White Hills sequence, as well as crosses into the GSA Coso Valley groundwater basin (Figure 2-4).

The 2020 GSP Model domain boundary was further evaluated for accuracy using geophysical data to determine how well the model domain represents topographic variations and shallow bedrock along the surrounding mountain fronts. Publicly available geophysical data from the U.S. Geological Survey (USGS) National Crustal Model (NCM) was used as a

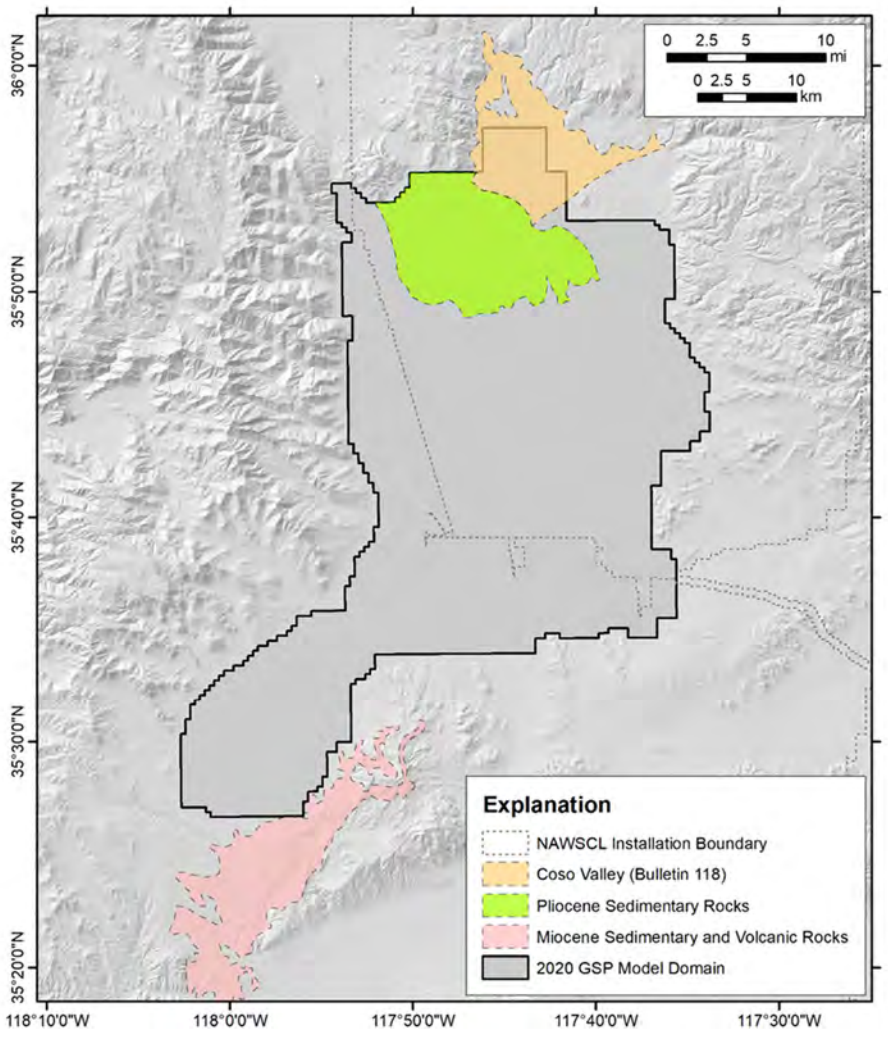


Figure 2-4. Map showing the 2020 GSP model domain in relation to the distribution of consolidated Pliocene sedimentary rocks of the White Hills sequence (Jennings et al., 1962; Monastero et al., 2002), consolidated Miocene sedimentary and volcanic rocks (Jennings et al., 2010), and the Groundwater Sustainability Agencies (GSAs) Bulletin 118 Coso Valley groundwater basin.

source of information. The NCM was developed as part of an ongoing study to characterize and improve seismic hazard assessments (Shah and Boyd, 2018). Prediction of ground motion is dependent on the vertical and horizontal heterogeneity of crustal density, seismic velocity, and wave attenuation. The NCM includes crustal properties for the western U.S. on a one-kilometer grid scale leveraging previous regional geophysical studies. The NCM data includes the depth to basement and two layers of sedimentary fill defined by the thickness of consolidated and unconsolidated sediment. The layers were developed to parameterize the NCM computational grid from regional studies that used either detailed gravity surveys, wells, or both (e.g., Jachens and Moring, 1990). For the Basin and Range region, isostatic residual gravity modeling was used to estimate sediment thickness within the numerous smaller basins associated with Cenozoic crustal extension. Techniques were used to separate gravity anomalies caused by lower density sedimentary fill from those caused by density variations within the surrounding rock. Basin-fill gravity anomalies are solved for the thickness of the fill layer from an assumed and prescribed layered density structure (Shah and Boyd, 2018).

Although a seismic hazard assessment is the primary focus of the NCM research effort, the gridded NCM spatial dataset can also provide a useful estimate of the potential aquifer thickness of sedimentary fill and depth to pre-Cenozoic basement (i.e., bedrock). However, the densities for valley fill and basement in the NCM dataset tend to be overpredicted because of limited knowledge of the subsurface geologic structure of many sedimentary basins, which commonly leads to either overestimates or underestimates in the depth to basement along valley margins where bedrock is shallow (Boyd, 2020). In other cases, such as where older sedimentary fill is overlain by volcanic flow rocks, density contrasts and gradients can be greater than what is assumed in gravity models leading to overestimates in the depth to basement (Boyd, 2020). Given the potential uncertainties in the NCM dataset, all available groundwater level information and lithologic well logs from sites along the margins of the IWV groundwater basin were also used to validate or refine the depth to bedrock, as well as determine the extent of unsaturated valley fill.

The margins of the 2025 Basin Model domain were updated from the geospatial analysis of the extent of GSA groundwater basins and geologic maps, in combination with the distribution of range-front faults and the NCM depth to bedrock. The model domain boundary was discretized at a grid resolution of 250 m. The updated 2025 Basin Model domain has an area of 363.4 mi^2 (941.1 km^2). This area is 21% less than the 2020 GSP Model domain's area of 458.6 mi^2 (1187.7 km^2) (Figure 2-5). The reduced area is primarily associated with the exclusion of the extent of Pliocene rocks of the White Hills sequence and the Coso Valley groundwater basin (Figure 2-4). Other factors that contributed to the reduction in area are related to defining the basin margins using a combination of depth to bedrock and identifying areas of unsaturated valley fill with a minimum thickness of 100 m based on available groundwater levels. The margins of the model domain are also partially controlled by the distribution of range-front faults, especially in the northwestern sector of the model domain (Figure 2-6). The final boundary of the 2025 Basin Model domain (Figure 2-5) was iteratively defined during model development and calibration (see Section 5.0).

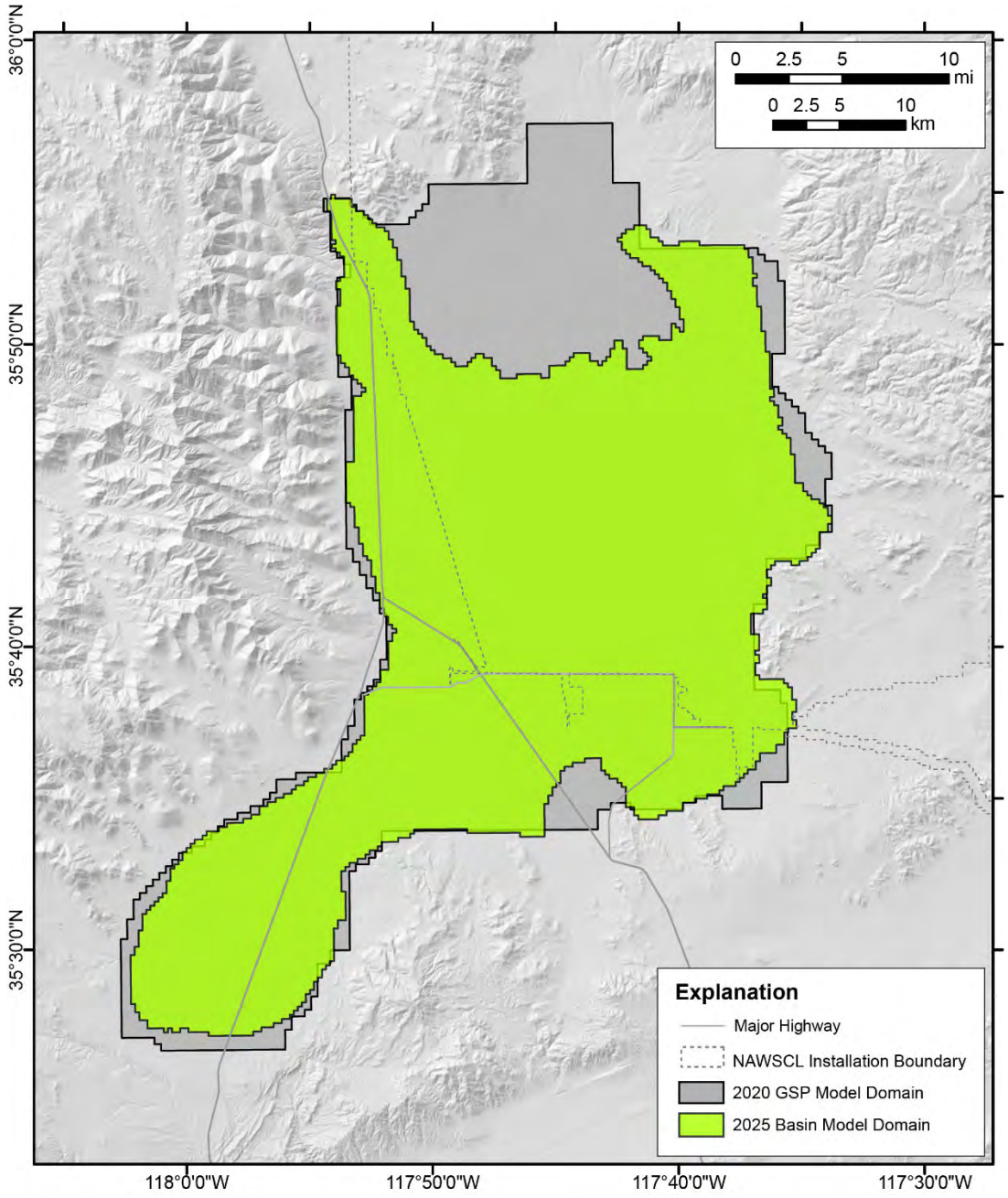


Figure 2-5. Map showing a comparison of the aerial extent between the 2020 GSP and 2025 Basin Model domains.

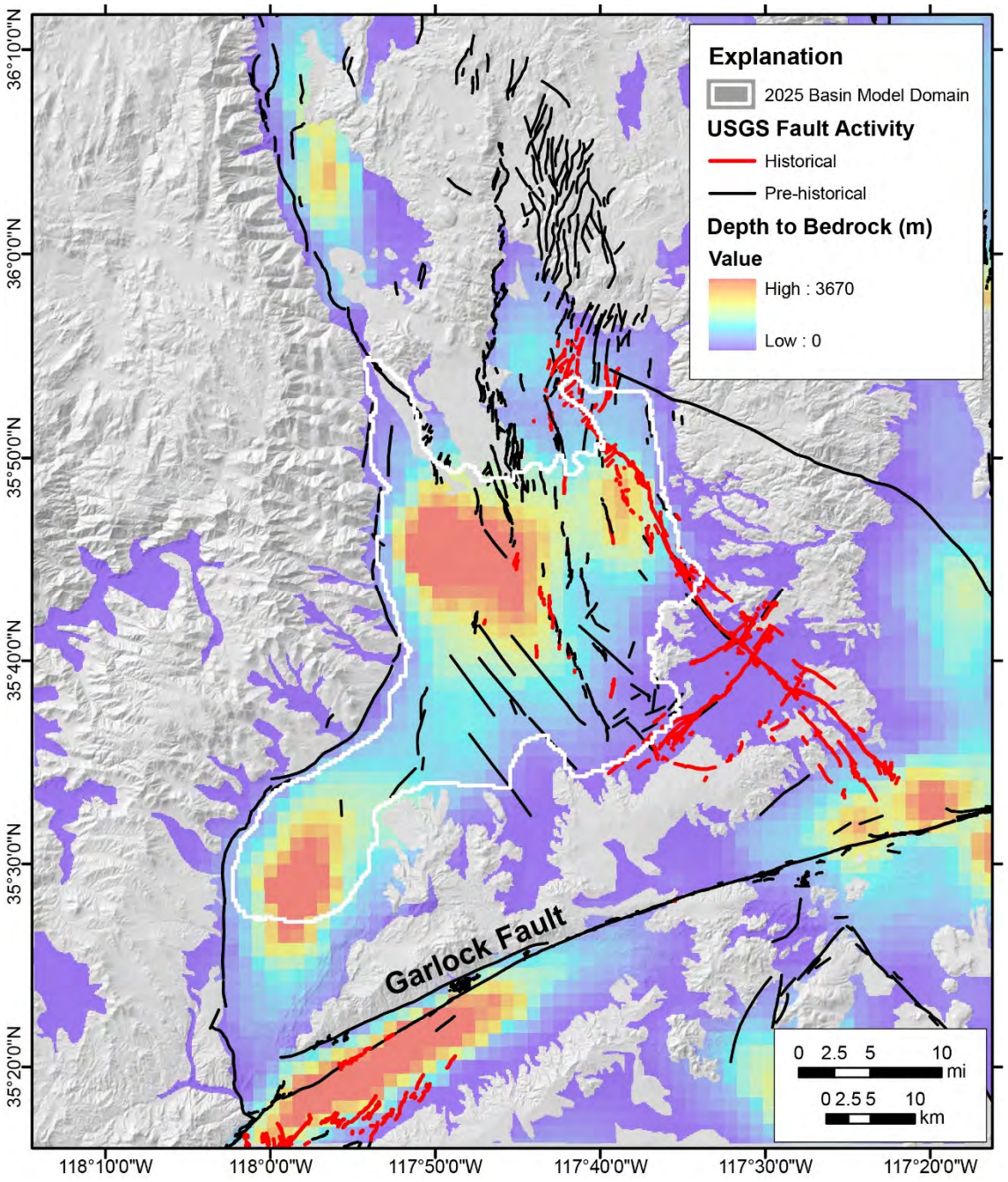


Figure 2-6. Map showing an updated model domain for the 2025 Basin Model that is developed from the extent of geologic data and Groundwater Sustainability Agencies (GSAs) Bulletin 118 groundwater basins (Figures 2-3 and 2-4), plus the distribution of range-front faults (USGS, 2020) and depth to pre-Cenozoic basement (i.e., bedrock) from the National Crustal Model dataset (Shah and Boyd, 2018). The one-kilometer gridded depth to bedrock data is shown for the GSA groundwater basins.

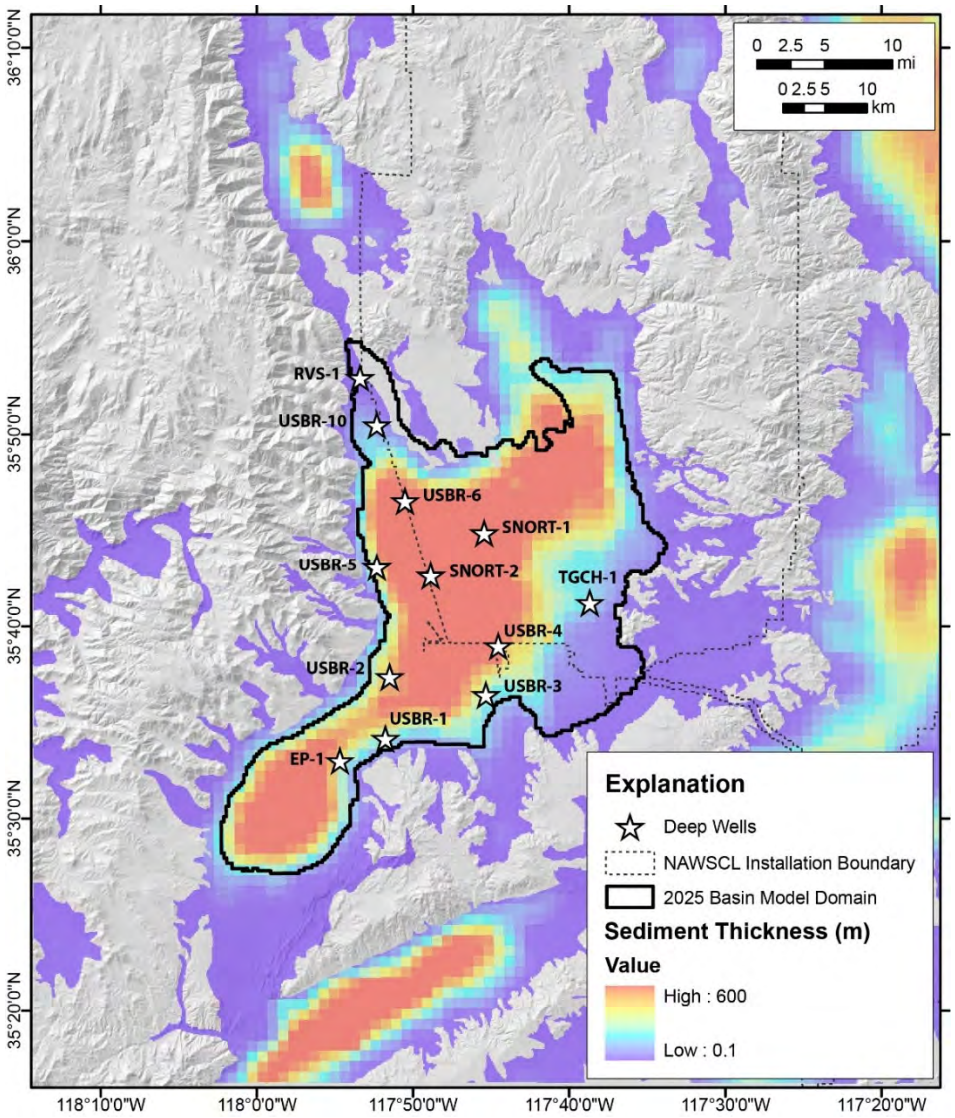


Figure 2-7. Map showing the 2025 Basin Model domain in relation to the National Crustal Model unconsolidated sedimentary thickness (Shah and Boyd, 2018). The one-kilometer gridded National Crustal Model data is shown for the GSA groundwater basins. Also shown are deep wells used to confirm unconsolidated sedimentary thickness.

2.2. Base of Model Domain

The base of the lowest layer in past groundwater models was originally defined and used in the groundwater flow model prepared for the IWV Water District by Brown and Caldwell (2009). The configuration of the same lower layer was also adopted by subsequent groundwater models constructed by the Desert Research Institute for NAWSCL (McGraw et al., 2016) and later used by the GA for the 2020 GSP (Garner et al., 2017; IWVGA, 2020).

The base of the 2025 Basin Model domain was initially defined from the geospatial analysis of both the NCM unconsolidated thickness and depth to bedrock geospatial datasets (Figures 2-6 and 2-7). Existing deep well logs (USBR, 1993) and seismic profile data (e.g.,

Monastero et al., 2002) were used to confirm the accuracy of the NCM unconsolidated thickness layer. Comparisons between the NCM unconsolidated thickness values and information presented in deep well logs and seismic profiles were reasonably close. The final base of the 2025 Basin Model domain was iteratively defined during model development and calibration (see Section 5.0) and yielded minimum and maximum thicknesses of 750 ft (229 m) and 2,482 ft (757 m), respectively, whereas the range in thickness in the 2020 GSP Model is 1,080 ft (329 m) to 3,860 ft (1177 m). The updated model domain has a volume of 123.1 mi^3 (513.1 km^3), which is 37% less than the 2020 GSP Model having a volume of 195.5 mi^3 (814.9 km^3).

3. HYDROGEOLOGIC CONCEPTUAL MODEL

A hydrogeologic conceptual model (HCM) provides an understanding of the general physical characteristics related to regional hydrology, land use, geology and geologic structure, water quality, principal aquifers, and principal aquitards of the groundwater basin setting. A HCM also provides the context to develop water budgets, mathematical (analytical or numerical) models, and monitoring networks, which taken together, provide a tool for GSA managers and stakeholder outreach and communication (CADWR, 2016). One of the principal goals of the 2025 Basin Model Update was to refine the HCM of the model domain by: 1) better characterizing the tectonic setting of the IWV groundwater basin from the inclusion of primary fault zones and secondary faults; 2) evaluate new Airborne Electromagnetic (AEM) resistivity survey data to potentially improve the overall representation of the stratigraphic framework of the basin and identify subsurface faults; and 3) refine aquifer properties using recent aquifer and specific capacity test data.

3.1. Inclusion of Faults

Faults were not simulated as barriers to flow in the first groundwater flow model prepared for the IWV Water District (Brown and Caldwell, 2009). A lack of faults was also adopted in the subsequent groundwater model constructed by the Desert Research Institute for NAWSCL (McGraw et al., 2016). This same model was later revised for the 2020 GSP to include two faults that improved model calibration (Garner et al., 2017; IWVGA, 2020). Previous studies in IWV have described many of the faults as flow barriers because of observed water-level differentials across faults (Bloyd and Robson, 1971; Dutcher and Moyle, 1973; Mallory, 1978; St.-Amand, 1986; Lancaster et al., 2022), whereas others have suggested the faults do not affect groundwater flow (Berenbrock and Martin, 1991) or that observed groundwater-level differences are reconciled by stratigraphy (Steinpress et al., 1994). Faults in groundwater flow models need to be supported by data that indicate potential barrier effects to groundwater flow, including, but not limited to, mapped surface fault traces, subsurface faults identified from geophysical data, hydraulic head differentials (i.e., groundwater compartments), vertical hydraulic gradients, responses (or lack of responses) to pumping, and differences in water quality over short distances.

There are four primary fault zones and two secondary faults in the IWV groundwater basin mapped by the USGS and California Geological Survey (CGS) with surface evidence of historical (last 200 years), Holocene (past 11,700 years), and late Quaternary (past 700,000 years) fault activity (Figure 3-1). The four primary fault zones are in IWV and include the Airport Lake fault, Little Lake fault, Paxton Ranch fault, and Sierra Nevada Frontal fault. Two secondary faults were also identified in the El Paso subarea that act as

barriers to groundwater flow and are informally named the Freeman and Armistead faults (Figure 3-1). Of note, the Freeman fault was previously used and referred to as the El Paso fault in the 2020 GSP Model. This fault is renamed the Freeman fault in the 2025 Basin Model Update to better represent its geographical location and to not be confused with a similarly named fault that is officially named the El Paso fault, which is associated with the Garlock fault zone to the south (CGS, 2010).

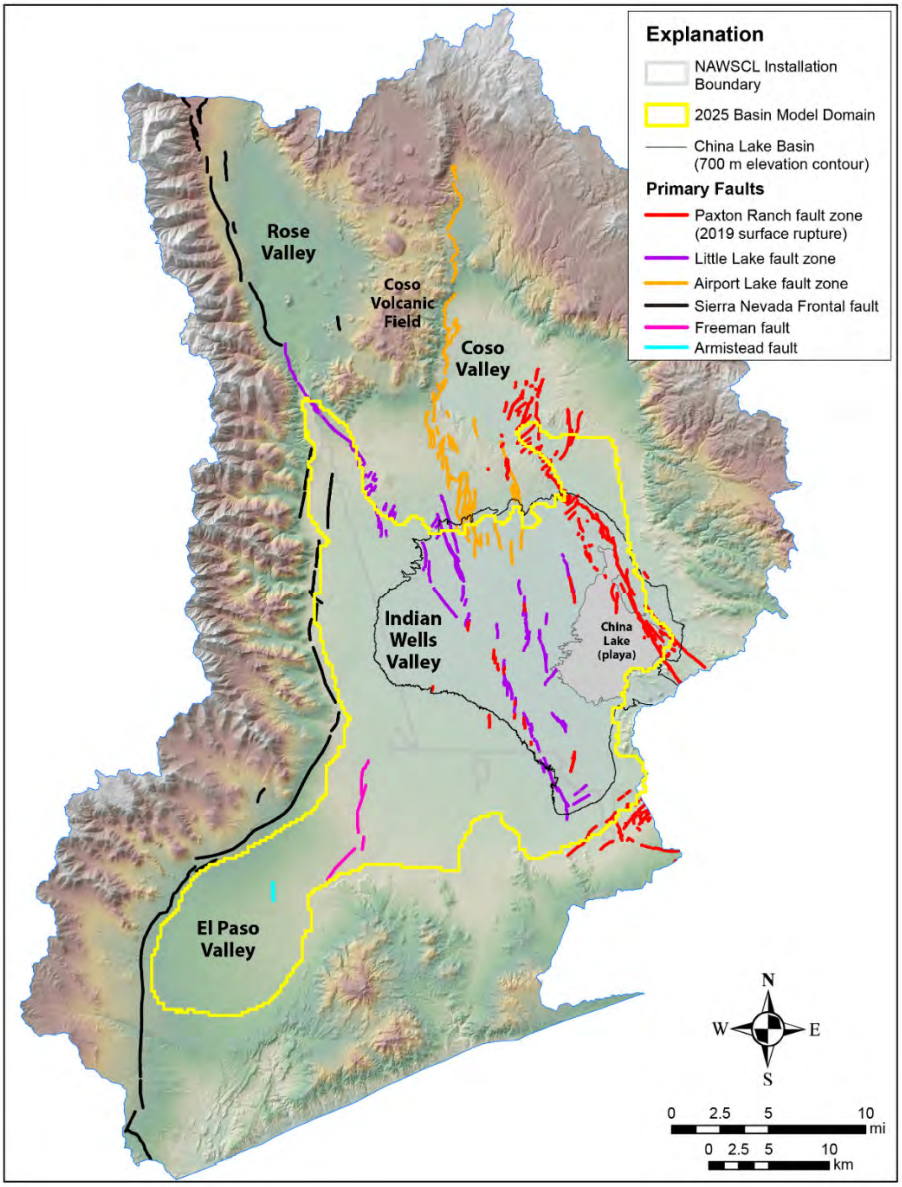


Figure 3-1. Map showing the 2025 Basin Model domain in relation to the primary fault zones with historical, Holocene, latest Quaternary, and late Quaternary fault activity in the watershed of the Indian Wells Valley groundwater basin. Surface faults are from the U.S. Geological Survey and California Geological Survey fault hazards mapping programs (CGS, 2010; DuRoss et al., 2020; Ponti et al., 2020; USGS, 2020). The extent of China Lake basin below an elevation of 700 m is also shown.

3.1.1. Fault Identification

All available geospatial fault data was evaluated to identify which faults could potentially impede groundwater flow or control the distribution of sediments and groundwater geochemistry across the Basin Model domain. The following data sources were used in the evaluation: the Fault Activity Map of California (CGS, 2010), USGS Fault and Fold Database (USGS, 2020), and the surface rupture map of the 2019 Ridgecrest earthquake sequence (DuRoss et al., 2020; Ponti et al., 2020). Selection of a particular fault for the 2025 Basin Model Update was based on meeting the following criteria, either: 1) it coincides with major groundwater level/gradient changes; 2) it coincides with sharp changes in sediment type (i.e., hydrogeologic properties) and groundwater geochemistry; or 3) it coincides with hydrogeomorphic features (i.e., springs, sag ponds, phreatophyte-vegetated dune areas). Existing groundwater reports (e.g., Dutcher and Moyle, 1973; St.-Amand, 1986; Garner et al., 2017), seismic profile data (e.g., Monastero et al., 2002), tectonic-hydrogeomorphic studies (e.g., Lancaster et al., 2022), and groundwater geochemistry (e.g., Tetra Tech, 2003; Chapman et a., 2022), collectively demonstrate that at least one of the criteria was met on each of the six faults considered in the 2025 Basin Model Update.

Airborne Electromagnetic (AEM) Survey Data

In addition to the geospatial fault data, Airborne Electromagnetic (AEM) survey data flown across the IWV groundwater basin in 2017 (Behroozmand et al., 2018) was also used in the characterization of faults. The raw AEM resistivity data was acquired and processed in 2023 by Dr. Ryan G. Smith (Colorado State University) as part of the 2025 Basin Model Update. The processed data was used to determine the spatial distribution of, and distinguish between, the fine-grained (sand/silt/clay) and coarse-grained (sand/gravel) sediment types in the subsurface of the IWV groundwater basin (Figure 3-2). Analysis of the AEM data proved useful in identifying sharp horizontal contacts and apparent vertical discontinuities in cross sections of AEM resistivity grids that commonly coincided with the surface trace of mapped faults or geomorphic features. The AEM survey data yielded resistivity grids to depths to approximately 1300 ft (400 m) (Behroozmand et al., 2018). Four unannotated cross sections of Behroozmand et al. (2018) are presented as examples of how the AEM resistivity grids were used to characterize the structural geology of the IWV groundwater basin and identify 2025 Basin Model faults.

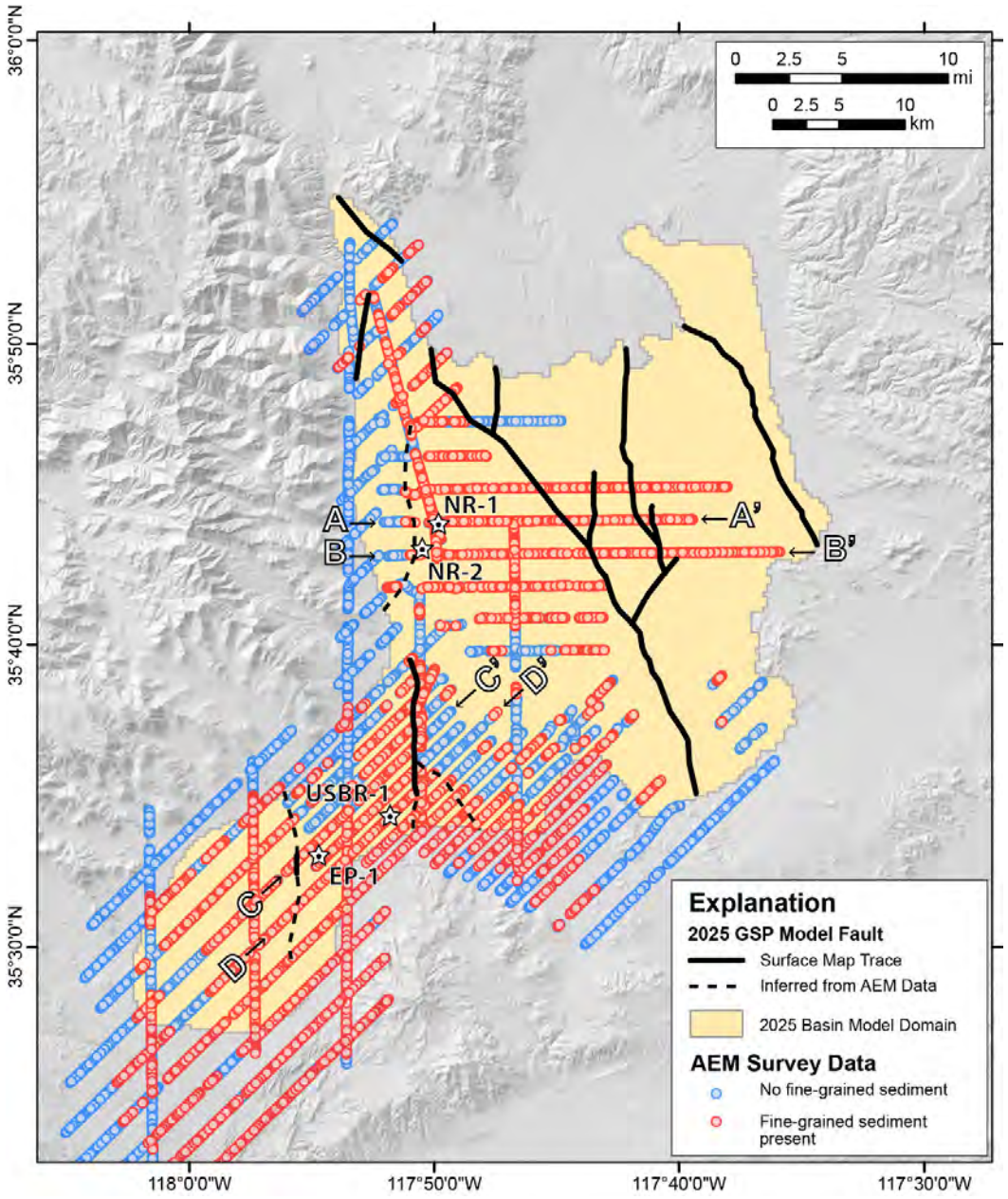


Figure 3-2. Map showing the 2025 Basin Model domain and the survey area of Airborne Electromagnetic (AEM) resistivity data (Behroozmand et al., 2018). Raw AEM data was processed as part of the 2025 Basin Model Update to determine the likely occurrence of fine-grained (sand/silt/clay) and coarse-grained (sand/gravel) sediment types within the Indian Wells Valley groundwater basin. Analysis of the AEM data also identified the location of additional faults inferred in the subsurface (dashed lines), in addition to confirming the location and geometry of mapped surface traces of fault zones (bold lines) (CGS, 2010; USGS, 2020). The location of deep wells NR-1, NR-2, USBR-1, and EP-1 are also shown with stars. Cross sections of transects A–A' to D–D' are shown on Figures 3-3 and 3-4.

AEM Data in Indian Wells Valley

Identification of the surface and subsurface location and geometry of faults, as well as vertical sedimentary erosional features (i.e., buttress unconformities) were made from the analysis of the AEM resistivity grid cross sections. Transects A–A' and B–B' in the IWV coincide with the unannotated cross sections EW04 and EW05 of Behroozmand et al. (2018) (Figures 3-2 and 3-3). In this sector of IWV, the AEM data indicate the presence of a thick and low resistivity (<10 Ohm m) layer that is overlain and truncated on the west by mostly higher resistivity (>10 Ohm m) layers (Figure 3-3). The low resistive layer was confirmed to be composed of a thick section of fine-grained (sand/silt/clay) stratified lacustrine sediment that extends deeper than the base of the resistivity grids, whereas the higher resistivity layers are predominantly composed of coarse-grained (sand/gravel) mixed alluvial sediment based on the lithologic logs of deep wells NR-1 and NR-2 on the western parts of transects A–A' and B–B', respectively (Figures 3-2 and 3-3). The lithologic log of NR-1 describes a sharp contact between the fine- and coarse-grained sediment types at a depth of 340 ft (103.6 m) having an elevation of 1935.7 ft (590 m) (USBR, 1993; Figure 3-2). The lithologic log of NR-2 describes the same sharp contact between the fine- and coarse-grained sediment types at a deeper depth of 440 ft (134.1 m) having an elevation of 1874.7 ft (571.4 m) (USBR, 1993; 3-2). The elevations of the sharp contact in logs have strong correspondence with resistivity values of about 8–10 Ohm m on cross sections.

Transects A–A' and B–B' are separated by 1.6 mi (2.5 km) and show extensive deformation of the fine-grained (low resistivity) sediment layer. The deformation is in the form of both brittle faulting and normal drag folding (i.e., bending). Active faulting on the Little Lake and Airport Lake fault zones created a well-defined graben from up to six parallel fault splays, of which up to three fault splays correspond with traces mapped at the surface (CGS, 2010; USGS, 2020; Figure 3-3). The fine-grained sediment layer is also truncated to the west by inferred normal faulting that locally forms a horst tectonic block. There are no surface fault traces mapped in the western area of the two transects (CGS, 2010; USGS, 2020). However, analysis of imagery and topographic profiles of the area generated from a 2-meter resolution digital elevation model (DEM) indicate potential faulting of older fans along a discontinuous zone of poorly defined lineaments. The tectonic-geomorphology of the area suggests west-side-down vertical movement along the zone of lineaments, which also coincides with the structural geology interpreted from the AEM resistivity data (e.g., Figure 3-3).

Based on the apparent large magnitude of west-side-down normal faulting, the western fault on transects A–A' and B–B' is likely an antithetic (i.e., secondary) fault that forms the eastern margin of a range-bounding graben associated with the primary (i.e., main) faulting on the Sierra Nevada Frontal fault system. Besides faulting, the resistivity data also shows shallow subsurface evidence of fluvial-deltaic cut-and-fill processes in the vicinity of the western margin of China Lake playa that coincides with geomorphic mapping (Bullard et al., 2019; Transect B–B', Figure 3-3).

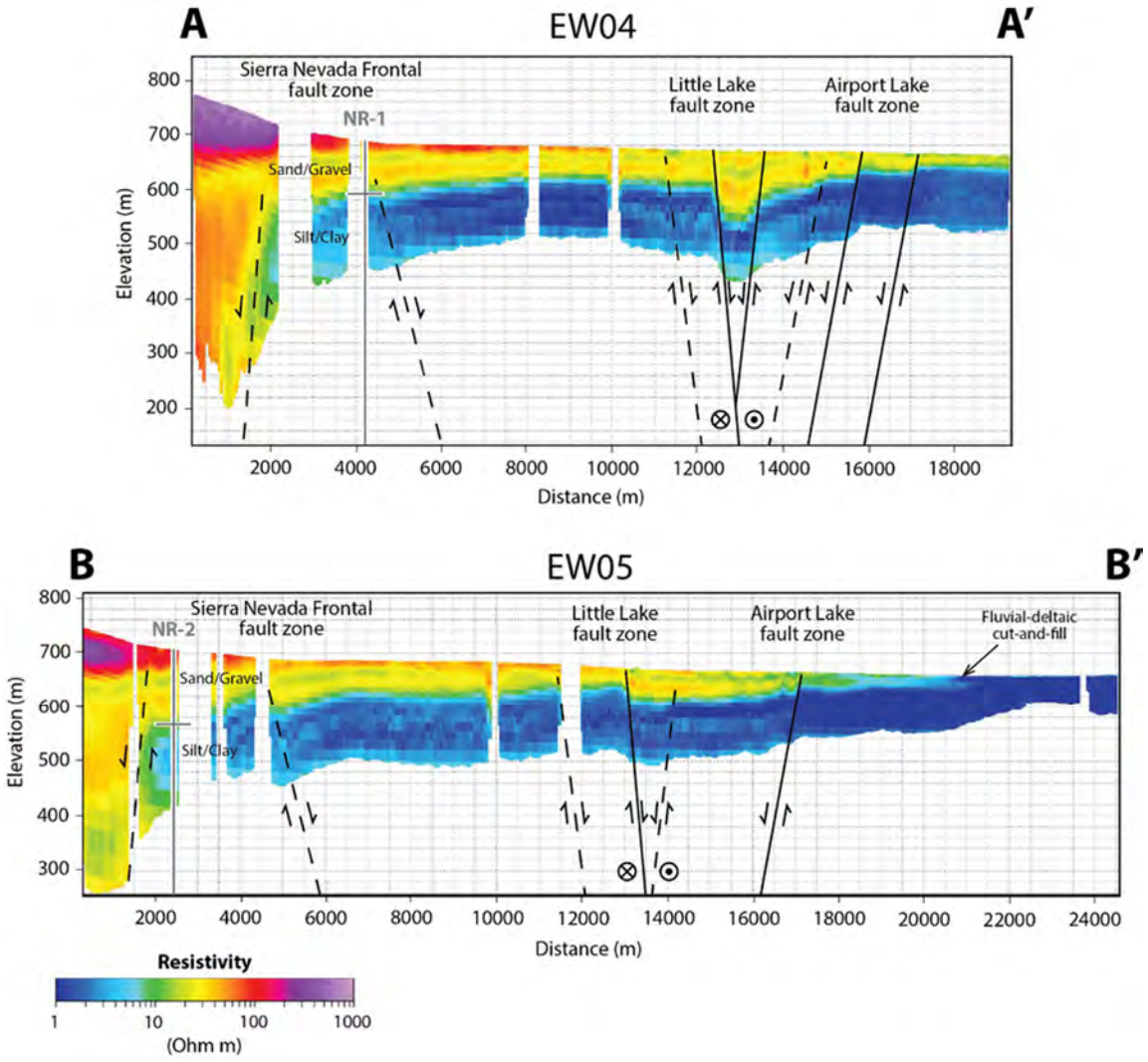


Figure 3-3. Cross sections (EW04 and EW05) through resistivity grids of Airborne Electromagnetic (AEM) data (Behroozmand et al., 2018). The unannotated cross sections of Behroozmand et al. (2018) were used to interpret the structural geology of the IWV groundwater basin for the 2025 Basin Model Update. Transects A–A' and B–B' are presented as example cross sections for IWV and locations are shown on Figure 3-2. Solid faults coincide with the surface location of individual map traces of the Little Lake and Airport Lake fault zones (CGS, 2010; USGS, 2020). Dashed faults have no surface trace but are interpreted from the apparent normal separation of the top of the low resistivity (blue) layer. Normal faulting along the eastern margin of a half-graben related to the Sierra Nevada Frontal fault system is inferred. Arrows show vertical sense of motion; dot and cross represent horizontal sense of right-lateral motion on the Little Lake fault, dot towards and cross away. The location of deep well NR-1 on western part of transect A–A' and contact between coarse-grained (sand/gravel) and fine-grained (sand/silt/clay) sediment types from the well log are also shown. Vertical exaggeration is 25x.

AEM Data in El Paso Subarea

The same approach of interpreting the AEM resistivity data was used to confirm and define the extent and style of faulting on the Freeman and Armistead faults. Transects C–C' and D–D' in the El Paso subarea coincide with unannotated cross sections N15 2 and N17 2 of Behroozmand et al. (2018) (Figures 3-2 and 3-4). In this sector of the El Paso subarea, the AEM data show relatively higher resistivity values compared to the values along Transects A–A' and B–B' in IWV. The basin settings between IWV and the El Paso subarea are markedly different, where the El Paso subarea is tectonically less active over the evolution of the basin and as a result, is geomorphically less active and the site of mostly thinly deposited low-gradient alluvial fan and marsh to shallow lake depositional environments, based on the lithologic logs of USBR-1 and EP-1. In comparison, IWV is tectonically more active and the site of a wider range of depositional environments and thicker sections of both coarse- and fine-grained deposits associated with mostly alluvial fan and plain sedimentation and fluctuating deep lake cycles. The resistivity values along transect C–C' and D–D' reflect mostly alluvial sedimentation in the El Paso subarea. The relatively lower resistivity (blue and green) layers are associated with older alluvial deposits consisting of 33–100 ft (10–30 m) thick interbeds of silt/clay and sand based on surficial geologic mapping (Jennings et al., 1962) and the lithologic logs of deep well USBR-1 on the northern part of transect D–D' (USBR, 1993) and the projection of deep well EP-1 onto both transects. The relatively higher resistivity (yellow to red) layers represent younger alluvial deposits composed of mostly mixed sand and gravel with lesser clayey interbeds (Figure 3-4).

Transects C–C' and D–D' are separated by 1.6 mi (2.5 km) and show subsurface evidence of deformed valley fill that coincides with the vertical projections of mapped surface traces of the Freeman and Armistead faults (CGS, 2010; USGS, 2020). The tectonic-geomorphology of the Freeman fault consists of a well-defined, north striking east-side-down normal fault scarp with a height of up to 33 ft (10 m) and fault length of 7.8 mi (12.6 km), whereas the Armistead fault consists of a poorly defined, north striking east-side-down normal fault scarp with a height of about 2.5 ft (2.0 m) and fault length of 1.1 mi (1.8 km) (Figure 3-1). Resistivity contrasts are interpreted to represent mostly east-side-down tilted fault blocks that have formed half grabens from normal faulting. Transect C–C' shows sharp contrasts between relatively low and high resistivity values along gently back tilted horizontal layers and two steeply dipping planes that project to the surface in the location of the mapped surface traces of the Armistead and Freeman faults (Figure 3-4). Transect D–D' also shows resistivity contrasts that define a steeply dipping plane that projects to the surface in the location of the mapped surface trace of the Freeman fault, as well as a sequence of gently back tilted horizonal layers that are separated by inferred normal fault splays. One of the fault splays vertically projects to the surface where the southerly plan view projection of the Armistead fault is located. Additional resistivity contrasts indicate the presence of fault splays that bound the surface trace of the Freeman fault (Figure 3-4).

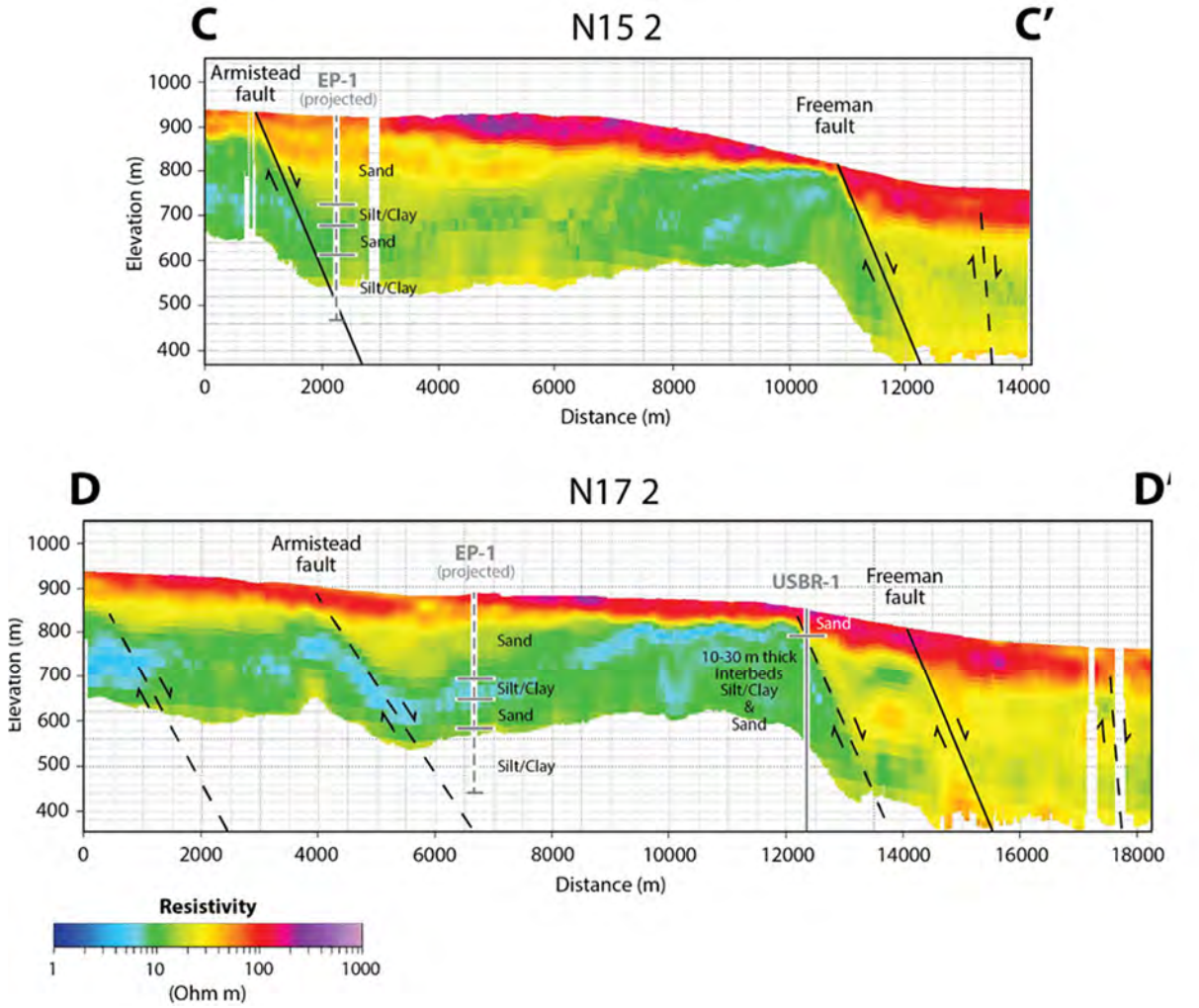


Figure 3-4. Cross sections (N15 2 and N17 2) through resistivity grids of Airborne Electromagnetic (AEM) data in the El Paso Valley subbasin (Behroozmand et al., 2018). Transects C–C' and D–D' of cross sections are presented as example cross sections and their locations are shown on Figure 3-2. Interpretation of fault location and geometry is from the analysis of AEM data for the 2025 Basin Model Update. Solid faults coincide with the surface location of individual map traces of the Freeman and Armistead faults (CGS, 2010; USGS, 2020). Dashed faults have no surface trace but are interpreted from the apparent normal separation of the top of the relatively lower resistivity (green) layer. The location of deep well USBR-1 on northern part of transect D–D' and the projected location of deep well EP-1 on both transects are shown. Contacts between coarse-grained (sands) and fine-grained (silt/clay) sediment types from well logs are also shown. Arrows show vertical sense of motion. Vertical exaggeration is 25x.

There are no surface fault traces in areas of the inferred faults because they are either concealed by younger deposits, have very slow slip rates (i.e., low fault activity), or both. The apparent thickening and thinning of the relatively higher resistivity layers west of the Freeman fault likely reflects the localized deposition of younger alluvial fan deposits within back-tilted half grabens formed between the Armistead and Freeman faults and associated fault splays, which is supported by the thickness of the upper sand units observed in deep wells EP-1 and USBR-1 on Transect D–D' (Figure 3-4). In contrast, the relatively higher resistivity layers east of the Freeman fault are much thicker and the product of long-term sedimentation within down-dropped blocks east of the Freeman fault. The Freeman fault forms a structural boundary between IWV and the El Paso subarea based on the depth to basement, which has ultimately controlled the thickness of valley fill in the area (Figures 2-6, 3-1, and 3-4).

3.1.2. 2025 Basin Model Faults

The surface map traces of faults in the IWV groundwater basin have complex fault patterns consisting of distributed zones of short and discontinuous en echelon scarps (Figure 3-1). As a result, the fault pattern complexity of each of the faults selected in the 2025 Basin Model were generalized into a single and continuous fault having associated fault splays based on a combination of available map data and structural interpretation of all the cross sections of resistivity grids generated by Behroozmand et al. (2018) and the AEM data processed in 2023 for the Basin Model Update (e.g., Figures 3-2 to 3-4). Concealed sections of the Sierra Nevada frontal fault, the northerly and southerly projections of the Armistead fault, plus the northwest-striking fault splay of the Freeman fault were identified and inferred from the AEM resistivity data (Figure 3-2). The generalization of fault complexity was performed for ease of inclusion in the numerical groundwater model, following a similar approach that was done for faults in the 2020 GSP Model. The new analysis of faults has refined the location and length of the Little Lake and Freeman faults previously used in the 2020 GSP Model, as well as added four additional faults and associated fault splays for a total of six faults in the 2025 Basin Model. The update has doubled the total fault length from 38.6 mi (62.1 km) in the 2020 GSP Model to 79.6 mi (128.1 km) in the 2025 Basin Model (Figure 3-5).

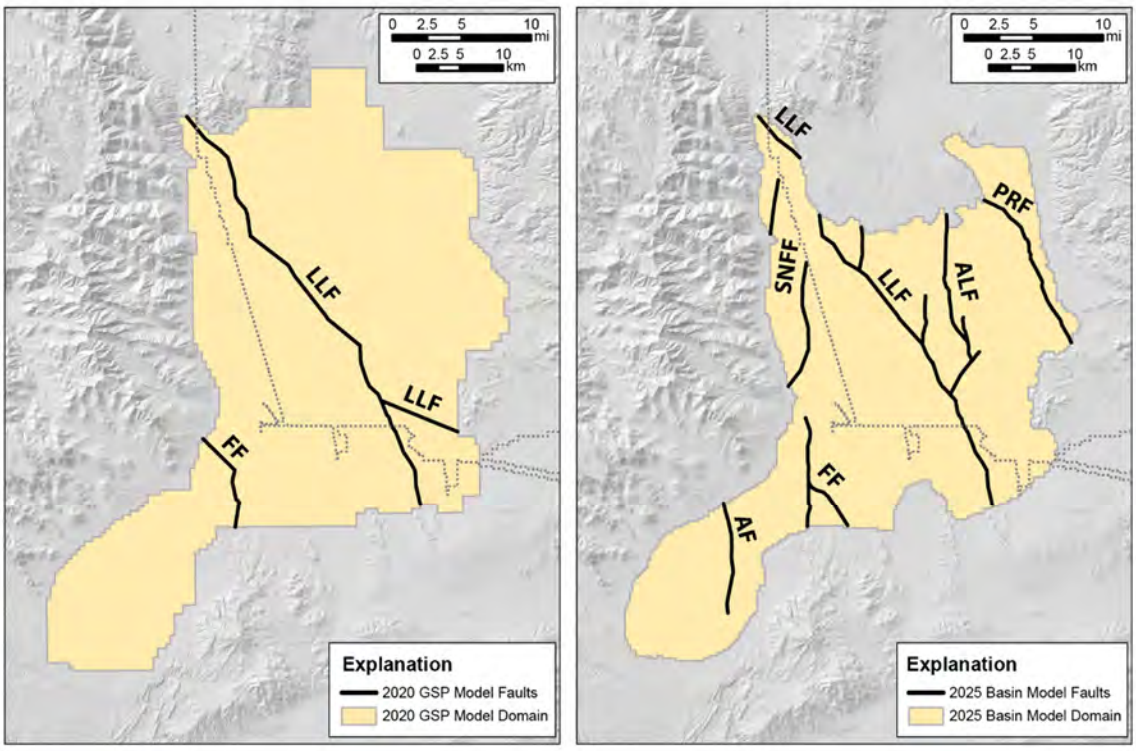


Figure 3-5. Maps showing the distribution of faults used in the 2020 GSP Model and the 2025 Basin Model. The complexity of fault patterns has been generalized into single fault strands. Fault location is based on either surface fault traces, interpretation of Airborne Electromagnetic (AEM) survey data or both (CGS, 2010; DuRoss et al., 2020; Ponti et al., 2020; USGS, 2020; Figures 3-2 to 3-4). Faults: Airport Lake fault (ALF); Armistead fault (AF); Freeman fault (FF); Little Lake fault (LLF); Paxton Ranch fault (PRF); Sierra Nevada Frontal fault (SNFF).

3.2. Hydrogeologic Stratigraphic Framework

Previous investigations have separated the hydrogeology of the IWV groundwater basin into three general hydrogeologic zones. The three zones include: a shallow hydrogeologic zone (SHZ) composed of middle to late Pleistocene and Holocene sandy to gravelly alluvium and Holocene fine-grained playa deposits; an intermediate hydrogeologic zone (IHZ) composed of a thick section of early to middle Pleistocene lacustrine sediment consisting of thick silt and clay with interbedded fine sand stringers and organic-rich layers; and a deep hydrogeologic zone (DHZ) primarily composed of early to middle Pleistocene sand and gravel with some interbedded clay (e.g., Berenbrock and Martine, 1991; Monastero et al., 2002; Tetra Tech, 2003). Although the thick lacustrine unit of the IHZ has been observed in numerous shallow and deep wells in the northern part of IWV, the spatial extent, depth, and thickness across the groundwater basin is poorly understood. As a result, previous groundwater models, including the 2020 GSP Model, did not explicitly include a layer that accurately depicted the fine-grained sediment of the IHZ (e.g., Brown and Caldwell, 2009; McGraw et al., 2016; Garner et al., 2017; IWVGA, 2020). Given that the IHZ is primarily

composed of a thick section of low-permeability silts and clays, a detailed characterization of its spatial extent, depth, and thickness considering the active tectonic setting of IWV was performed for the 2025 Basin Model Update.

3.2.1. Spatial Extent of Fine-grained "Clay" Unit

The playa of China Lake is currently the terminal basin of IWV. China Lake basin below an elevation of 700 m has generally been the long-term depocenter of fine-grained sedimentation in IWV from past water-level fluctuations of pluvial China Lake, with the latest highstand at an elevation of 690 m occurring around 14,000 years ago (e.g., Rosenthal et al., 2017) (Figure 3-1). The AEM resistivity data processed in 2023 for the 2025 Basin Model was used to characterize the spatial extent of the fine-grained sediment of the IHZ across China Lake basin (Figure 3-6). The fine-grained sediment previously placed in the IHZ is informally referred to as the "clay unit" in the 2025 Basin Model because it is described mostly as a thick lacustrine clay in lithologic well logs (e.g., Dutcher and Moyle, 1973; USBR, 1993; Tetra Tech, 2003). The lithologic logs of shallow and deep wells were also used to confirm the presence and spatial extent of the clay unit measured along AEM survey lines (Figure 3-7). The lithologic well logs and AEM survey data were used together to map the clay unit, which has an area of 147.0 mi^2 (380.8 km^2) or about 41% of the total area of the 2025 Basin Model domain. The mapped margins of the clay unit are controlled by either faults or depositional boundaries. Faults control most of the western and eastern margins of the clay unit corresponding with the Sierra Nevada Frontal fault and Paxton Ranch fault, respectively. The northern and southern margins are primarily depositional having interfingering relations (i.e., facies changes) between the clay unit (i.e., lacustrine) and alluvial sediment that coincide with the long axis of the valley (e.g., Figures 3-3, 3-5, and 3-7).

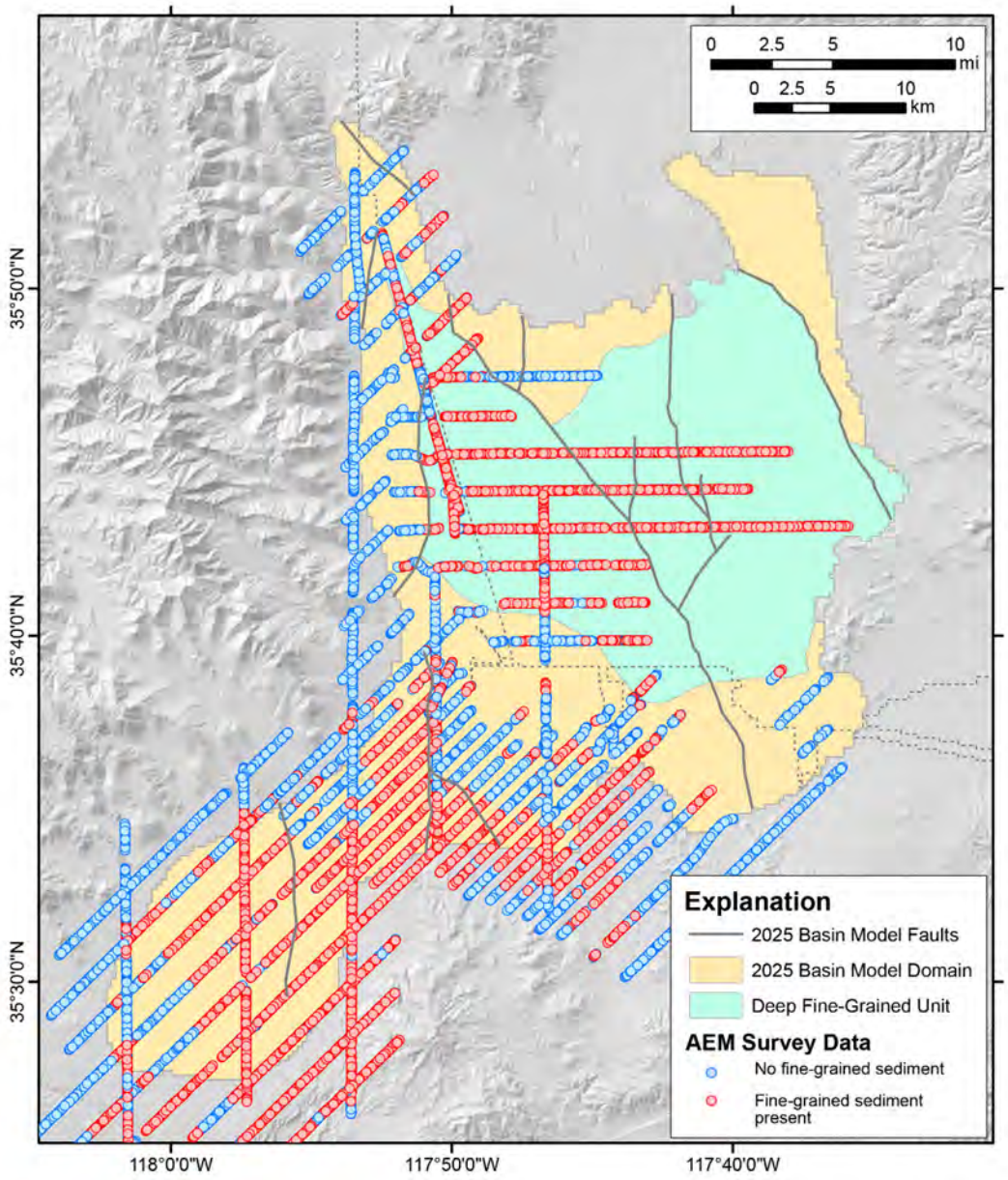


Figure 3-6. Map showing the extent of the deep fine-grained "clay" unit within the 2025 Basin Model domain. Also shown is the survey area of Airborne Electromagnetic (AEM) resistivity survey data (Behroozmand et al., 2018). Raw AEM data was processed as part of the 2025 Basin Model to determine the likely occurrence of fine-grained (silt/clay) and coarse-grained (sand/gravel) sediment types within the Indian Wells Valley groundwater basin. Analysis of the AEM data was used to identify the lateral extent of the deep fine-grained unit with either depositional or fault boundaries.

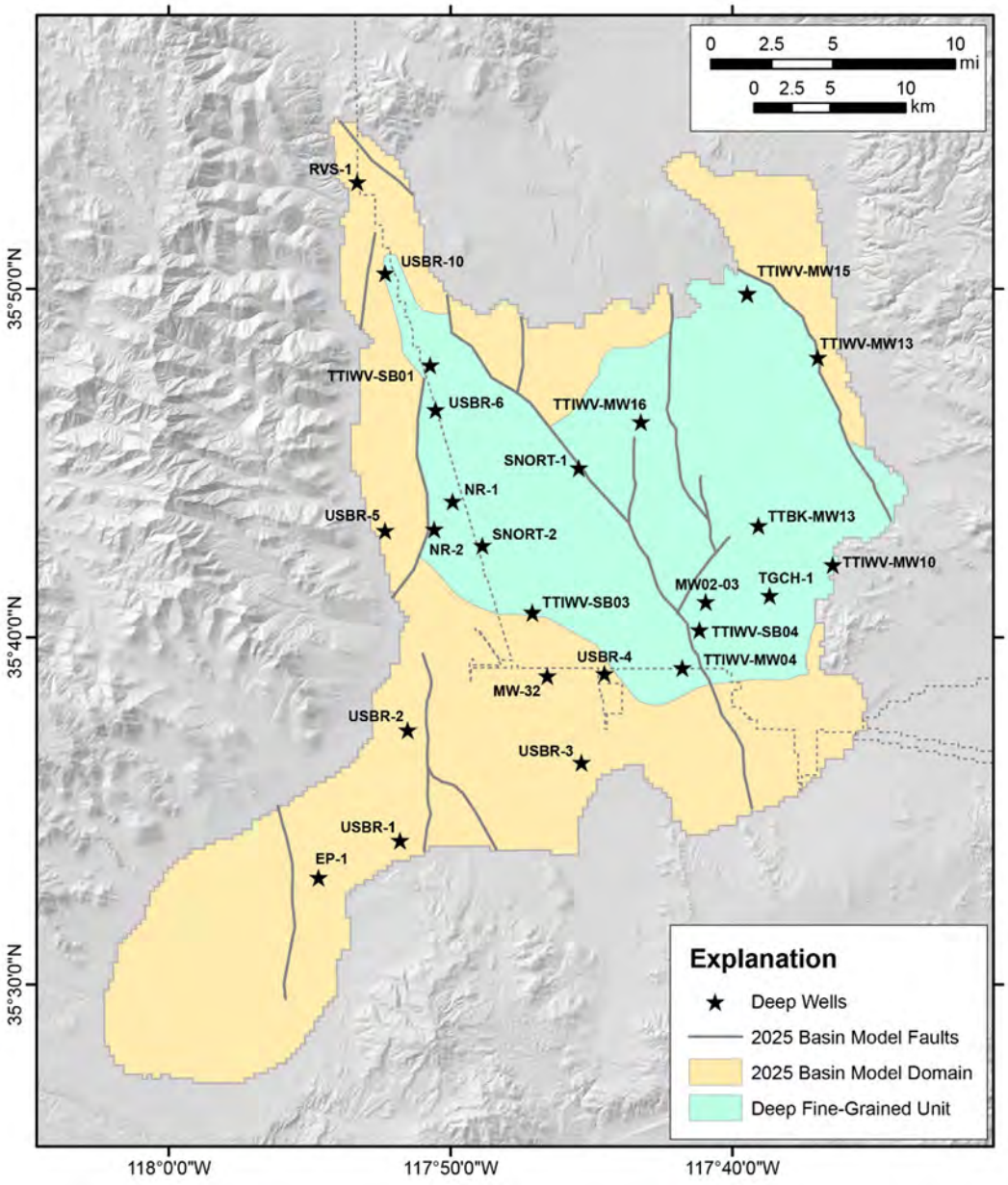


Figure 3-7. Map showing the extent of the deep fine-grained "clay" unit within the 2025 Basin Model domain. Also shown is the location of deep wells used to confirm the presence and lateral extent of the deep fine-grained unit.

3.2.2. Depth of Fine-grained "Clay" Unit

Detailed analysis of lithologic logs from 32 shallow and deep wells in the mapped clay unit was performed to determine the top and bottom depths and to better understand its variation in thickness and three-dimensional configuration (Figures 3-8 and 3-9). The clay unit is commonly overlain by Holocene to Pleistocene alluvium along the western margins of China Lake basin. The clay unit in the central sector of the lake basin is overlain by a thick section of late Pleistocene interbedded fluvial-deltaic sands and thinly bedded lacustrine clay

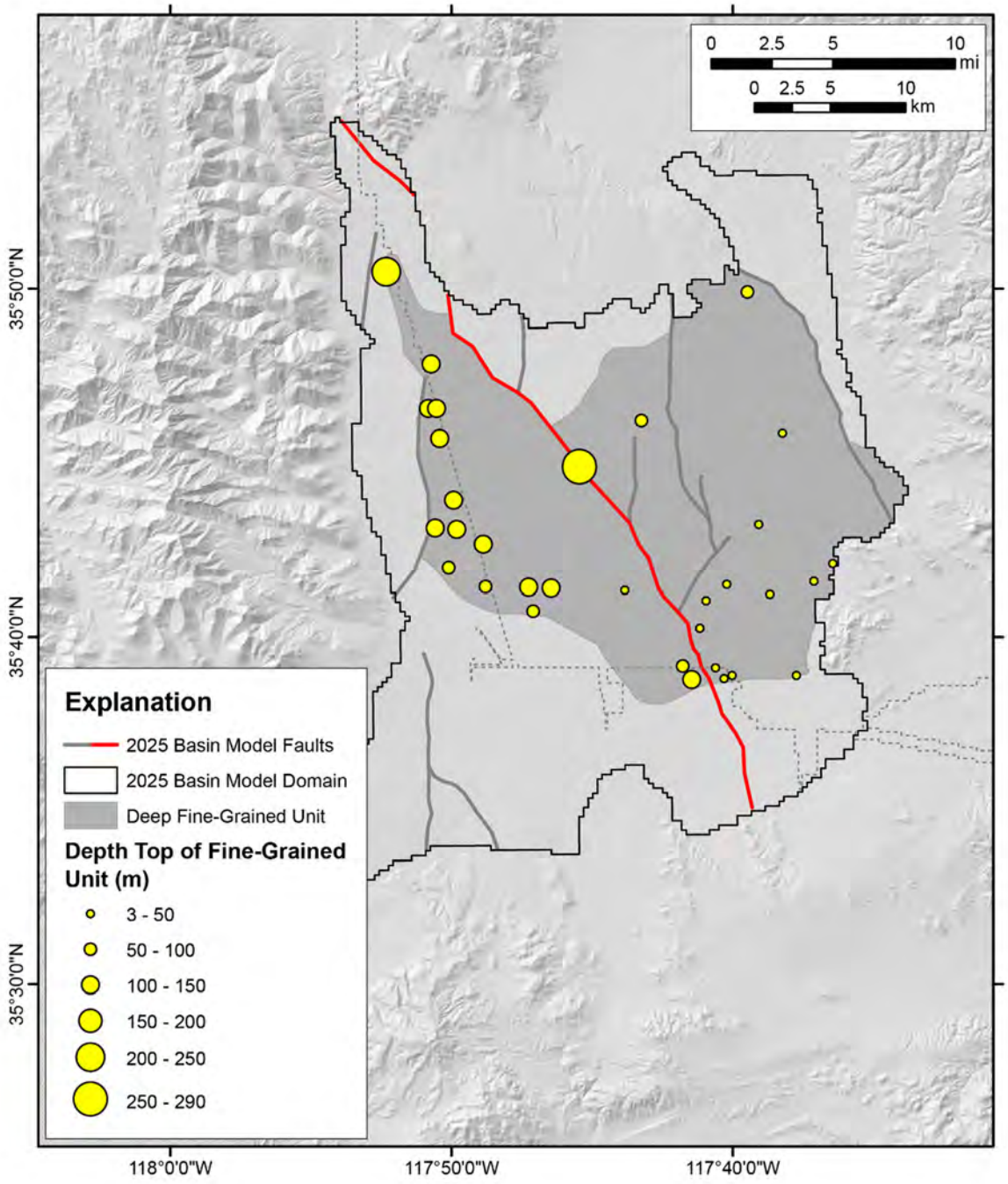


Figure 3-8. Map showing the distribution of wells that recorded the top of the deep fine-grained "clay" unit within the 2025 Basin Model domain. The depth of the top of the fine-grained unit, its lateral extent, as well as faults are also shown. The Little Lake fault is shown in red and generally defines two structural domains that separate different groups of depth of the top of the fine-grained unit.

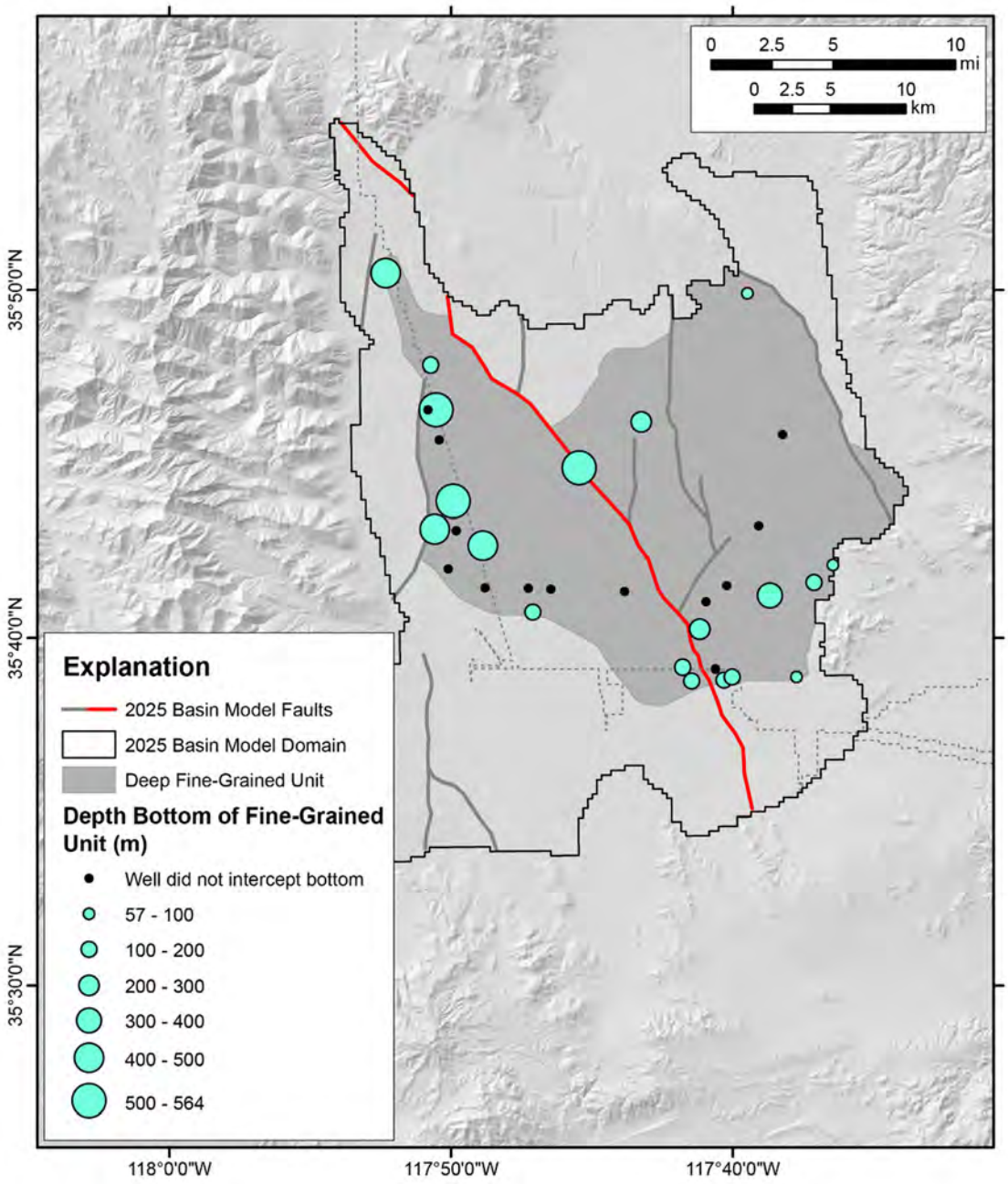


Figure 3-9. Map showing the distribution of wells that recorded the bottom of the deep fine-grained "clay" unit within the 2025 Basin Model domain. The depth of the bottom of the fine-grained unit, its lateral extent, as well as faults are also shown. The Little Lake fault is shown in red and generally defines two structural domains that separate different groups of depth of the bottom of the fine-grained unit.

subunits (Tetra Tech, 2003). The fine-grained lacustrine sediment consists of lenticular to semi-continuous horizons of micaceous silt and silty clay to plastic clays with few thinly bedded fine sands (Tetra Tech, 2003). The silty and clayey sediment appear in well logs as green, blue-green, blue, gray to black laminated mud indicative of sedimentation below

wave-base in a deep lake. The lacustrine sediment has distinctly different colors compared to alluvial sediment that are typically light brown to yellowish-brown. Fossil shell- and organic-rich horizons are also present in lacustrine sediment (USBR, 1993; Tetra Tech, 2003). Criteria used in the 2025 Basin Model to distinguish the clay unit of the IHZ from other types of clayey sediment associated with either alluvium or the thinly bedded and younger lacustrine clay subunits include: 1) a color change from light color (yellows/browns) to darker color (greens, blues, gray, and black); 2) presence of fossils and/or organic-rich horizons; and 3) a continuous thickness of greater than 10 ft (3 m).

The top of the clay unit was encountered in all 33 wells and ranges in depth from 10–950 ft (3–290 m) across northern IWV (Figure 3-8). The clay unit of the IHZ is widespread below both younger alluvium and the thinly interbedded fluvial-deltaic and lacustrine sediment in the western sector of China Lake basin, where the top of the clay unit is commonly encountered east of Sierra Nevada frontal faults at depths of 330–490 ft (100–150 m), whereas the maximum depth of 950 ft (290 m) is encountered adjacent to and west of the Little Lake fault at SNORT-1 (Figures 3-7 and 3-8). The top of the clay unit occurs at much shallower depths of 10–160 ft (3–50 m) in the eastern and southeastern sectors of China Lake basin having a minimum depth of 230 ft (70 m) in the northern sector of the lake basin. The depth of the clay is strongly controlled by the tectonic setting of northern IWV and its relation to the Little Lake fault, where the top of clay occurs at deeper depths west of the fault and shallower depths on the east (Figure 3-8).

The bottom of the clay unit was encountered in 20 of the 33 wells and ranges in depth from 190–1850 ft (57–564 m) (Figure 3-9). The bottom of the clay unit commonly occurs at depths of 1300–1640 ft (400–500 m) east of Sierra Nevada frontal faults having a maximum depth of 1850 ft (564 m) west of the Little Lake fault at SNORT-1 (Figures 3-7 and 3-9). The bottom of the clay unit occurs at shallower depths of 190–1150 ft (57–350 m) in the southeastern sector of China Lake basin with relatively deeper depths of 260–950 ft (80–290 m) in the northern sector of the lake basin. The greatest depths of the base of the clay unit occurs west of the Little Lake fault (Figure 3-9).

3.2.3. Thickness of Fine-grained “Clay” Unit

Previous hydrogeologic studies of the stratigraphy of China Lake basin document a wide range in thickness for lacustrine muddy layers observed in wells from around 13 ft (3 m) to 1480 ft (450 m) (e.g., Dutcher and Moyle, 1973; USBR, 1993; Tetra Tech, 2003). The total thickness of the clay unit of the IHZ in the 2025 Basin Model was determined from wells that encountered both the top and bottom of the unit. Thickness was calculated from 20 of the 33 wells and ranges from 43–1480 ft (13–451 m) (Figure 3-10). The greatest clay thickness occurs in the western sector of the lake basin east of Sierra Nevada frontal faults having values of 900–1480 ft (275–450 m) with the maximum thickness observed at NR-1 (Figures 3-7 and 3-10). The clay unit east of the Little Lake fault is relatively thinner but has a wider range in thickness from 122–1037 ft (37–316 m) in the southeastern sector of the lake basin to 43–700 ft (13–213 m) in the north-northeastern sectors. The clay unit also thins along the southern depositional boundaries of the map area having a range in thickness of 130–230 ft (32–70 m) (Figure 3-10).

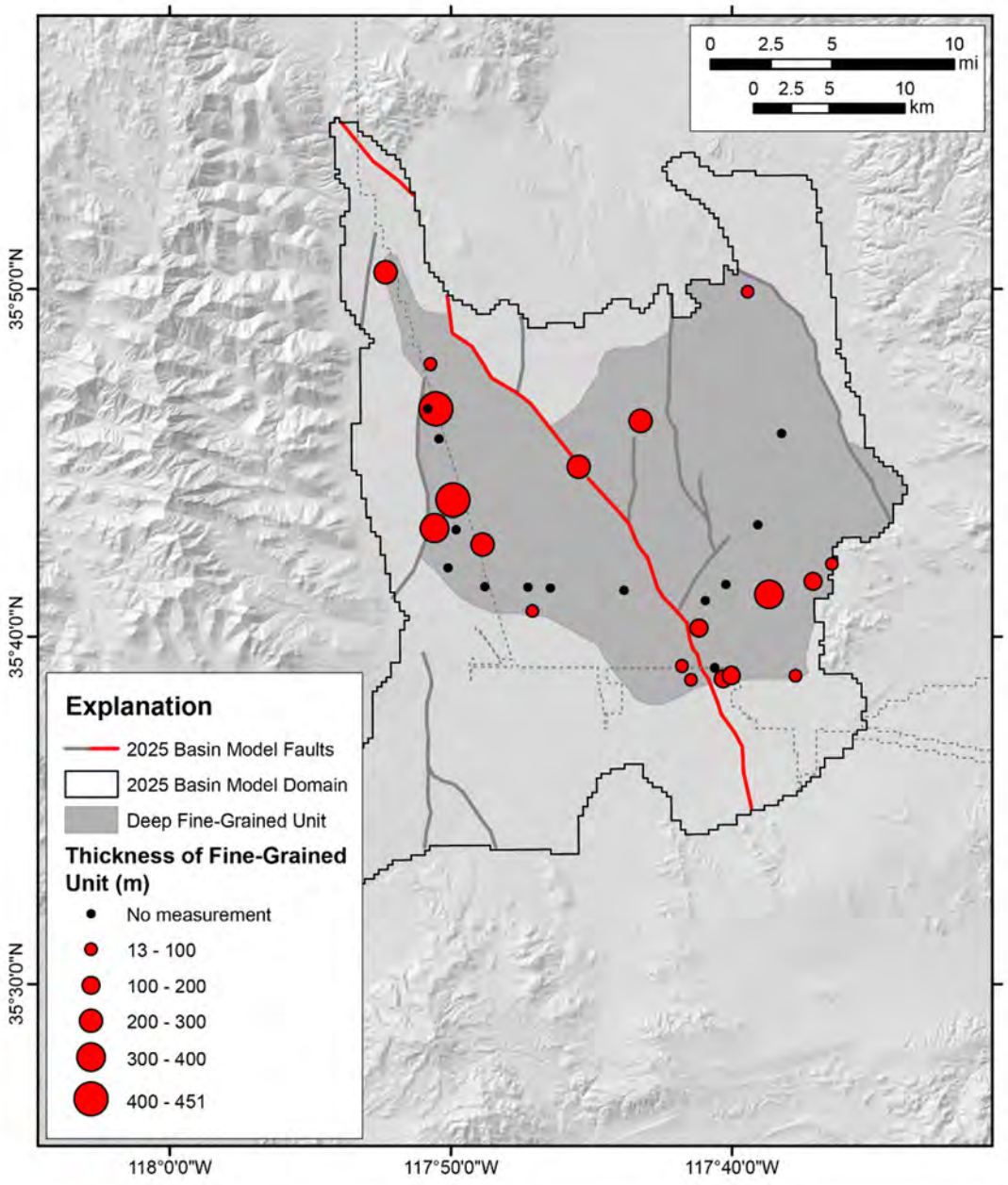


Figure 3-10. Map showing the distribution of wells and measured thickness of the deep fine-grained "clay" unit within the 2025 Basin Model domain. The thickness of the fine-grained unit, its lateral extent, as well as faults are also shown. The Little Lake fault is shown in red and generally defines two structural domains with different thicknesses.

3.2.4. Tectonic-block Model for Northern Indian Wells Valley and China Lake Basin

Previous hydrogeologic investigations did not account for long-term tectonic deformation of the thick clay unit when developing geologic conceptual frameworks and geologic cross sections of the IWV groundwater basin (e.g., Dutcher and Moyle, 1973; Berenbrock and Martin, 1991; Tetra Tech, 2003). Previous geologic and tectonic

investigations of the IWV basin fill used reflection seismic and gravity data, along with deep wells to characterize the subsurface structure and stratigraphy, as well as to define the depth to basement (Monastero et al., 2002). The base of a continuous clay layer (Horizon D) was interpreted on seismic profiles as the shallowest and laterally continuous reflector along both west-east and north-south transects through northern IWV. The top of this clay layer, however, was not identified on seismic profiles because continuous reflectors are not discernable at depths of 0–1300 ft (0–400 m) (Monastero et al., 2002). Therefore, the top of the clay unit's spatial distribution and its thickness in areas without deep well log data is poorly characterized and uncertain. As a result, geologic cross sections controlled by a simple tectonic-block model were developed to estimate the clay unit's spatial and vertical configuration across northern IWV and China Lake basin to support the hydrogeologic conceptual framework of the 2025 Basin Model.

Tectonic Setting

A complex array of four subparallel primary faults in IWV collectively form an active pull-apart basin that has developed within a right-lateral transtensional shear zone (e.g., Monastero et al., 2002; Unruh et al., 2003). The floor of northern IWV is crossed by several parallel to near parallel active, northerly striking normal-oblique, right-lateral (i.e., strike slip) faults that merge towards the north with the Sierra Nevada frontal fault system and Coso volcanic field (e.g., Roquemore and Zellmer, 1987; Monastero et al., 2002; Amos et al., 2013) (Figure 3-1). The primary faults include the normal Sierra Nevada frontal fault (SNFF) on the western margin of the valley and from west to east across the valley, the oblique-normal right-lateral Little Lake fault (LLF), Airport Lake fault (ALF), and Paxton Ranch fault (PRF). Additional parallel and secondary faults that are unnamed and identified as part of the 2025 Basin Model Update also accommodate distributed slip across the valley. Distributed slip along the eastside of the Sierra Nevada is complicated by slip partitioning between parallel normal faults of the SNFF and normal-oblique right-lateral faults in valley bottoms, such as in Owens Valley located north of IWV (e.g., Wesnousky and Jones, 1994). Slip partitioning between range-front normal faults and strike-slip faults likely also occur in IWV.

The distribution of the generalized 2025 Basin Model faults and other secondary faults coincide with variations in the depth to bedrock, where the deepest parts of northern IWV correspond to long-term oblique-normal faulting between the SNFF and LLF having depths up to 10,000 ft (3050 m) (Figure 3-11). Other areas in northeastern IWV have a well-defined zone with depths up to 6600 ft (2010 m) that have formed from oblique-normal faulting between the PRF and a parallel secondary fault (Figure 3-11). The El Paso subarea also has deep basement with depths to bedrock up to 9840 ft (3000 m) coinciding with SNFF normal faulting, back tilting along the Armistead fault, and likely transpressional structural features associated with the left-lateral Garlock fault system to the south (e.g., Monastero et al., 2002; Figures 2-6 and 3-11).

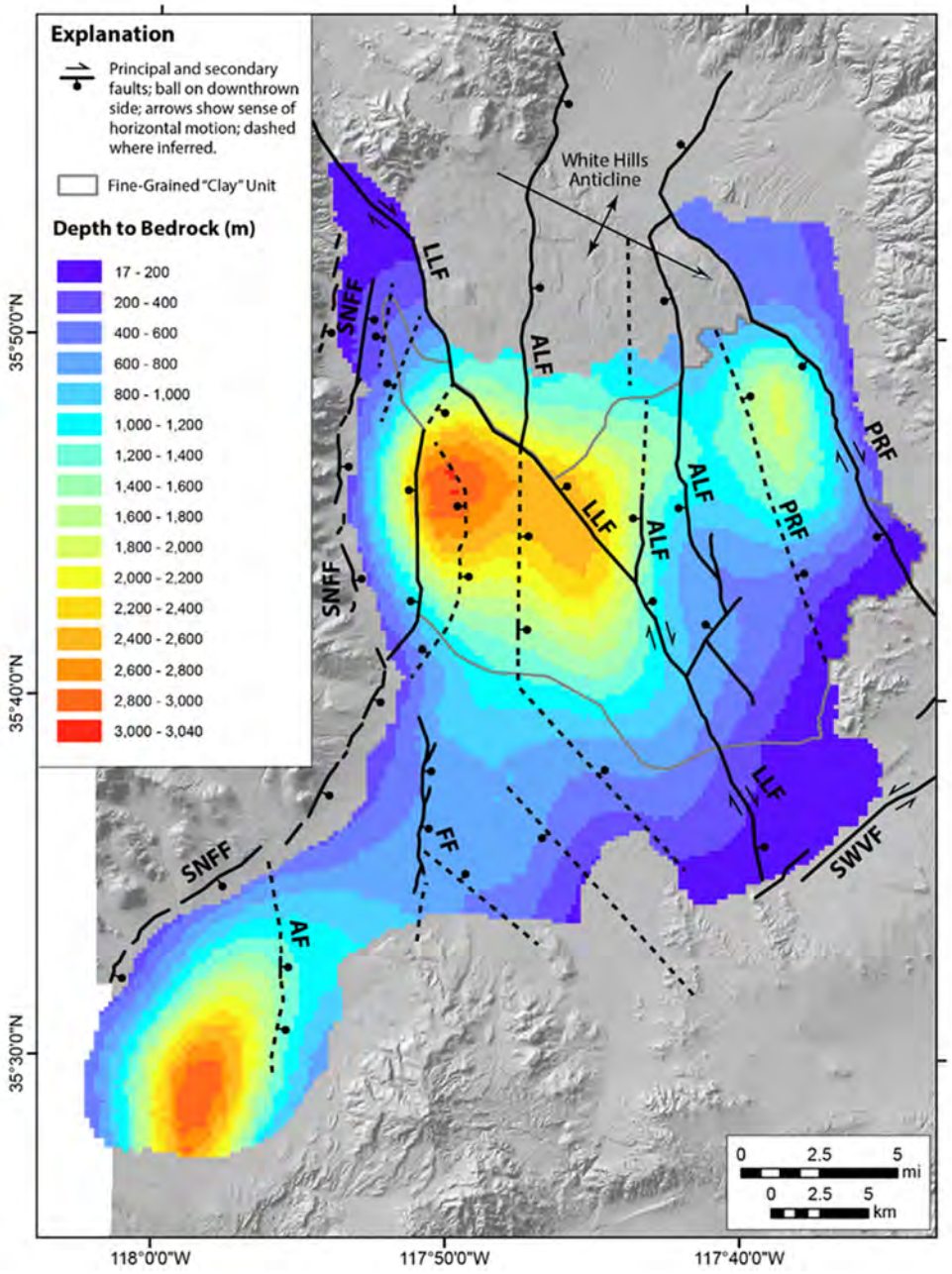


Figure 3-11. Map showing tectonic model of the IWV groundwater basin used to support development of geologic cross sections. Distribution of generalized primary and secondary faults of 2025 Basin Model and other faults (e.g., CGS, 2010; USGS, 2020) are shown in relation to the depth to pre-Cenozoic basement (i.e., bedrock) from the National Crustal Model dataset (Shah and Boyd, 2018) for the 2025 Basin Model domain. The spatial extent of the deep fine-grained "clay" unit is also shown. Faults: Airport Lake Fault (ALF); Armistead Fault (AF); Freeman Fault (FF); Little Lake Fault (LLF); Paxton Ranch Fault (PRF); Salt Wells Valley Fault (SWVF); Sierra Nevada Frontal (SNFF). The White Hills anticline is also shown (e.g., Monastero et al., 2002). Hillshade is from 2019 Ridgecrest, California Pre-Earthquake Digital Surface Model (published July 9, 2019).

Fault Structure

The mechanics and structural style of deformation across IWV can be best described by wrench fault tectonics. Wrench faults (i.e., Transcurrent faults) are major near vertical strike-slip faults which involve basement (e.g., Sylvester, 1984). Flower structures are typical structural features of wrench fault zones that develop under a simple shear deformation field. There are three distinct kinds of flower structures that have been identified in tectonic studies based on differences in their internal structural architecture: (1) negative flower structures characterized by synforms and normal separations; (2) positive flower structures characterized by antiforms and reverse separations; and (3) hybrid flower structures developed in divergent-wrench zones that result from the combined effects of extensional, compressional, and strike-slip deformation (e.g., Huang and Liu, 2017; Figure 3-12). The deformation field across IWV can be best explained by having the attributes of mostly negative flower structures in the northern sectors of the valley that produce down-dropped blocks (Figure 3-3; Transect A–A'), but also hybrid flower structures in areas proximal to the normal-oblique right-lateral LLF with anticlinal warping, as well as drag folding along normal faults in areas further to the south (Figure 3-3; Transect B–B'). Flower structures in the deep valley fill of northern IWV are identified on deep seismic profiles associated with the LLF and ALF (Monastero et al., 2002).

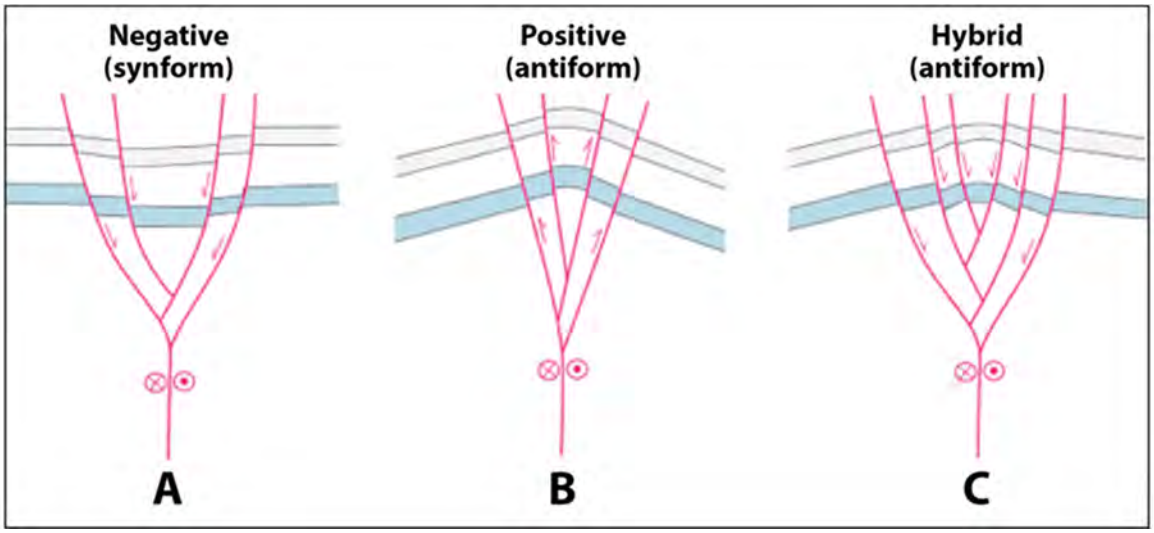


Figure 3-12. Idealized models for the major characteristics in cross-sectional view of the three types of flower structures present in a divergent-wrench fault zone: (A) negative, (B) positive, and (C) hybrid flower structures (from Huang and Liu, 2017). The Indian Wells Valley (IWV) is an active pull-apart basin that has developed within a right-lateral transtensional shear zone. The dominant structural style of tectonic deformation across the northern sector of IWV is best described by both negative (synform) flower structure and a hybrid (antiform) flower structure. Arrows show vertical sense of motion; dot and cross represent horizontal sense of right-lateral (i.e., strike slip) motion, dot towards and cross away.

3.2.5. Methods for Developing Geologic Cross Sections

Given the active tectonic setting of the IWV groundwater basin, geologic cross sections were developed by accounting for long-term deformation. Accounting for ground deformation provides the foundation to accurately depict the structure and stratigraphy and to help explain the observed differences in depth and thickness of the clay unit in wells across northern IWV and China Lake basin. A simple tectonic-block model was used to estimate the amount of displacement of the clay unit along primary and secondary faults for geologic cross sections. The tectonic-block model was developed by: (1) generalizing complex fault zones into a single fault structure, (2) deforming the thick and deep clay unit into rigid fault-bounded blocks, and (3) having the style of displacement consistent with both negative and hybrid flower structures (Figures 3-11 and 3-12).

Shallow and deep well logs, cross sections of AEM resistivity grids of Behroozmand et al. (2018), along with the AEM resistivity data processed in 2023 to determine the presence or absence of the clay unit were collectively integrated to determine the lateral extent and thickness of the clay unit. The same dataset was also used to confirm the location of mapped faults, as well as to identify unmapped or concealed faults for inclusion in the 2025 Basin Model. The entire dataset was used to develop geologic cross sections along five transects. Each transect was drawn so that it either intersected or was placed adjacent to between 5 and 10 shallow or deep wells to control clay unit thickness (Figure 3-13).

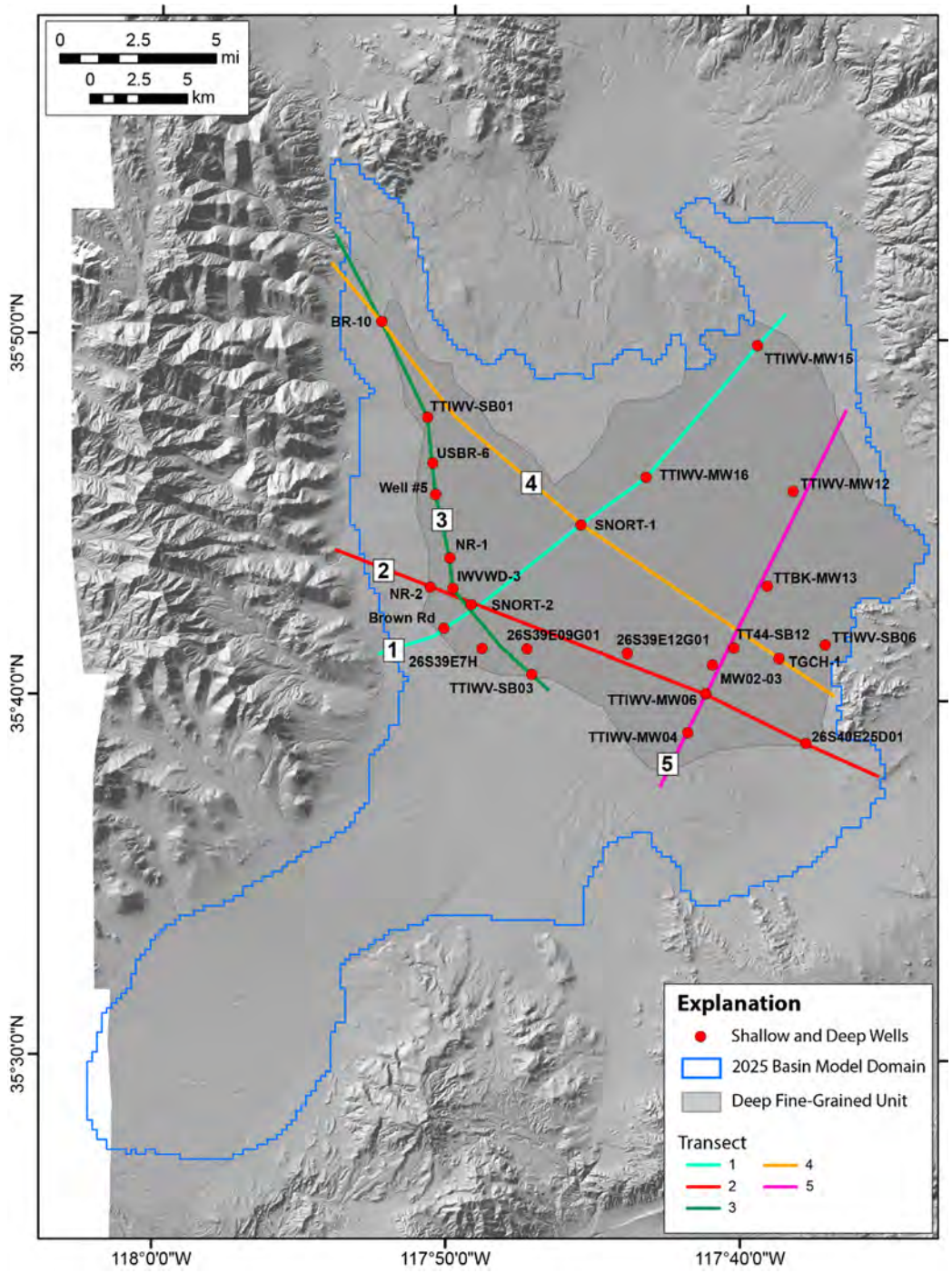


Figure 3-13. Map showing location of wells along geologic cross section transects 1–5 used in the development of the tectonic-block model of the deep fine-grained "clay" unit within the 2025 Basin Model domain. The lateral extent of the clay unit is also shown. Hillshade is from 2019 Ridgecrest, California Pre-Earthquake Digital Surface Model (published July 9, 2019).

Age Estimate of Clay Unit

Modeled deformation of the clay unit in geologic cross sections requires an age estimate for the unit to determine its magnitude of displacement along faults. The base of the clay unit has an unconformable contact with the top of the White Hills sequence, which consists of up to 2000 ft (600 m) of consolidated conglomerate to sandstone with lesser interbeds of siltstone, limestone, and shale (Figure 3-14). The age of the clay unit has not been directly determined. However, the SNORT-1 well intercepted basalt flow rocks that yielded an age of 3.9 million years ago (Ma) from samples at a depth of about 3200 ft (975 m) within the middle section of the White Hills sequence (Figure 3-14). An age for the top of the White Hill sequence was previously estimated to likely correspond to the Pliocene/Pleistocene boundary at 1.8 Ma based on inferred sedimentation rates typical of lake deposits in the region, along with the depth and age of the 3.9 Ma basalt in SNORT-1 (Monastero et al., 2002). Since Monastero et al. (2002), the age of the Pliocene/Pleistocene boundary has been revised and lowered to coincide with the beginning of the Quaternary at 2.58 Ma (Gibbard et al., 2010). If the top of the White Hills sequence represents the Pliocene/Pleistocene boundary, then the base of the clay unit has a maximum age of 2.56 Ma. The same approach used by Monastero et al. (2002) to estimate the age of the top of the White Hills sequence was also performed to confirm the minimum age of the White Hills sequence with the revised age for the Pliocene/Pleistocene boundary for the tectonic-block model. Using a thickness of 1394 ft (425 m) between the top of the White Hills sequence and the 3.9 Ma basalt, as well as the difference in age of 1.32 Ma between the basalt age of 3.9 Ma and the Pliocene/Pleistocene boundary age of 2.56 Ma, results in a sedimentation rate of about 322 m per million years (m.y.) or 32.2 cm per thousand years (k.y.). A sedimentation rate of 32.2 cm/k.y. for Tertiary sandstone deposits in the Basin and Range Province is relatively low compared to sedimentation rates of about 40 cm/k.y. typical for unconsolidated Pleistocene deep-water clay deposits, such as what is documented in Owens Lake core OL-92 over the past 800,000 years (Bischoff et al., 1997). The sedimentation rate of 32.2 cm/k.y. is considered a minimum estimate and does not account for unrecognized unconformities, as well as sediment consolidation during lithification.

An age for the top of the clay unit was also estimated following the same approach used for the top of the White Hills sequence for the tectonic-block model. An age of 1.455 Ma or 1455 k.y. for the top of the clay unit was determined by subtracting the age of the Pliocene/Pleistocene boundary of 2580 k.y. from the duration of 1225 k.y. for sedimentation of a maximum thickness of 450 m or 45,000 cm for the clay unit at well NR-1 and the 40 cm/k.y. sedimentation rate for Pleistocene clay deposition from Owens Lake core OL-92 (e.g., 45,000 cm x (k.y./40 cm). An age of 1455 k.y. or 1.46 Ma for the top of the clay is equivalent to an Early Pleistocene age. An Early Pleistocene age seems reasonable given that the IWV has been the site of a sedimentary basin in which lacustrine deposition has dominated during the past 2 million years (Monastero et al., 2002).

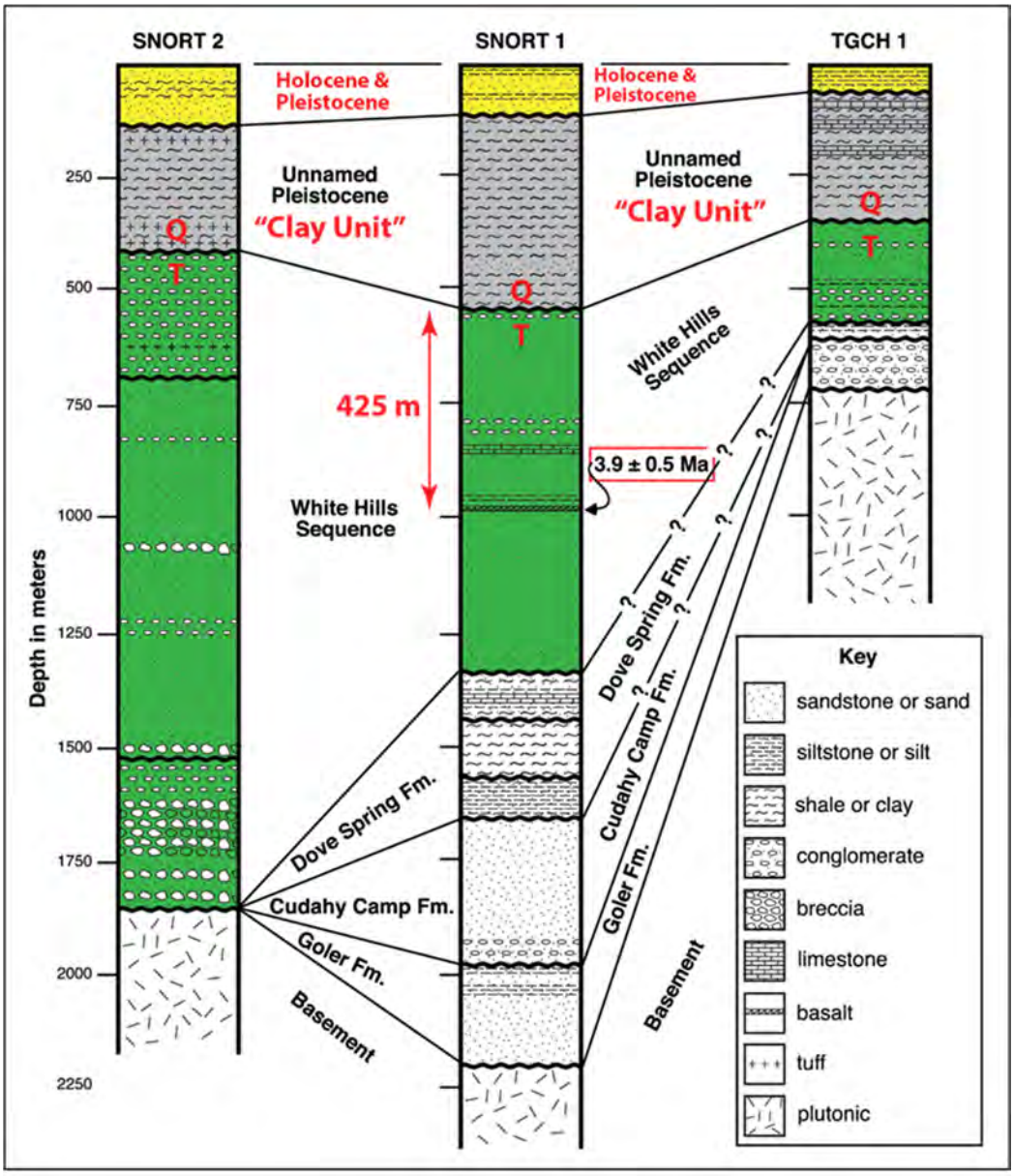


Figure 3-14. Stratigraphic columns for deep wells SNORT-1, SNORT-2, and TGCH-1 (modified after Monastero et al., 2002). Modifications are shown in red and specific geologic units are colored the same as the geologic units shown on geologic cross sections. The unnamed Pleistocene unit is referred to as the clay unit in the 2025 Basin Model Update. The unconformable contact between the White Hills sequence and the clay unit marks the Pliocene/Pleistocene or Tertiary (T)/Quaternary (Q) boundary that is estimated to have an age of 2.58 million years ago (Ma). Age of 3.9 Ma for dated basalt in SNORT-1 is highlighted with red box.

Fault Displacement and Vertical Slip Rates

Studies of the tectonics of nearby southern Owens Valley demonstrate that the vertical slip rate distribution summed across five primary faults in Owens Lake basin total 0.8 ± 0.2 m/k.y. over the past 40,000 years (Bacon et al., 2020). China Lake basin is located about 50 mi (80 km) south of Owens Lake basin and is situated in a similar seismotectonic setting where up to four primary faults also distribute slip across the basin. As a result, the tectonic-block model for China Lake basin was developed so that it would have a similar vertical slip distribution as Owens Lake basin. The amount of vertical displacement on primary and secondary faults in the tectonic-block model of China Lake basin was iteratively determined so that the vertical slip rate distribution would total about 1.0 m/k.y. across the deepest part of the basin and in a direction perpendicular to the length of IWV (i.e., extension direction). The main assumptions in the tectonic-block model include: (1) distributed vertical slip across China Lake basin has been constant since 1.45 Ma, which is the age of the top of the clay unit; (2) the primary faults in the basin (SNFF, LLF, ALF, PRF) will have higher vertical slip rates than the secondary faults; (3) there will be sharp changes in sedimentary thickness of geologic units across strike-slip faults; and (4) independently derived vertical slip rates can be used to solve for vertical displacement since 1.45 Ma.

The LLF is the only fault in IWV with published slip rate information. The LLF has a lateral slip rate of about 1.0 m/k.y., but no vertical slip rate. The LLF and the Owens Valley fault in Owens Lake basin have similar lateral slip rates (Bacon and Pezzopane, 2007; Amos et al., 2013). Both faults display similar tectonic-geomorphology and are situated in similar structural settings in the bottom of the basin relative to the SNFF system. Due to these similarities, a vertical slip rate of 0.10 m/k.y. from the Owens Valley fault was assigned to the LLF (Table 3-1).

Vertical slip rates for the SNFF and PRF in IWV were independently calculated to provide supporting data for the tectonic-block model as part of the 2025 Basin Model Update. A vertical slip rate for the SNFF was estimated from a well-defined normal fault scarp with 30 m of offset measured from a topographic profile derived from a 2-m DEM. The location of the fault scarp profile is on the northwest end of Transect 3 along the range front (see Figure 3-13). The trace of the SNFF in this area cuts Quaternary old alluvial fan (Qfo) deposits that lack direct age control (Jennings et al., 1962). A minimum age for the Qfo deposits was estimated from correlating similarly mapped Qfo deposits about 1.5 km across the valley in the Coso Volcanic Field that are overlain by a basalt flow with a $^{40}Ar/^{39}Ar$ date of 281 ka (Amos et al., 2013). A late Pleistocene vertical slip rate of 0.12 m/k.y. for the SNFF in northern IWV was derived from a 30 m scarp height, an assumed fault dip of 60°, and age of 280 k.y. (Table 3-1).

Table 3-1. Fault information for tectonic-block model used to develop geologic cross section along transect 1.

	SNFF	SNFF	Unnamed fault	LLF	ALF	ALF	Unnamed fault	PRF	Total
Kinematic role	Primary	Secondary	Secondary	Primary	Primary	Primary	Secondary	Primary	–
Fault type	Normal	Normal	Normal	Normal-oblique, right-lateral	Normal-oblique, right-lateral	Normal-oblique, right-lateral	Normal-oblique, right-lateral	Normal-oblique, right-lateral	–
Modeled fault dip (degrees)	60	60	60	80	80	80	80	80	–
Vertical displacement (m)	N/A	95	150	140	440	80	30	N/A	935 (min.)
Vertical slip rate (m/k.y.)	0.12*	0.07	0.10	0.10*	0.30	0.06	0.02	0.22*	0.98

Note: *See text for explanation of independently derived vertical slip rate.

A vertical slip rate for the PRF was calculated from the maximum vertical offset of 2.75 m measured on the 2019 surface rupture (Duross et al., 2020). The location of the maximum vertical offset is on the northeast end of Transect 5 (see Figure 3-13). A luminescence age of 12.95 ka from beach ridge deposits at an elevation 670 m in the southeastern margin of the lake basin is used to provide a maximum age constraint for faulted deposits (S.N. Bacon, unpublished data, 2024). A latest Pleistocene vertical slip rate of 0.22 m/k.y. for the PRF was derived from the 2.75 m offset, an assumed fault dip of 80°, and an age of 12.95 k.y. (Table 3-1).

A list of fault information used in the tectonic-block model is presented in Table 1. Modeled fault dip ranges from a 60° dip for primary and secondary normal faults for the SNFF system and unnamed faults to an 80° dip for primary and secondary normal-oblique right-lateral faults. The assigned range of fault dip for the normal and strike-slip faults in China Lake basin is similar to the ranges of modeled normal and strike-slip fault dips in Owens Valley (e.g., Wesnousky and Jones, 1994; Bacon et al., 2020). Vertical displacements range from as low as 30 m for an unnamed secondary normal-oblique fault to as high as 440 m for the normal-oblique ALF. Vertical slip rates also range from 0.02 to 0.30 m/k.y. (Table 3-1).

3.2.6. Geologic Cross Sections

Five geologic cross sections (transects 1–5) were developed to reflect variable magnitudes of vertical displacement of four main sedimentary units across a complex array of faults in northern IWV and China Lake basin (Figures 3-15 and 3-16). Geologic cross sections show the stratigraphy for depths above sea level (0 m elevation) that correspond to near the maximum depth of the 2025 Basin Model domain. The bottom of geologic cross sections is based on extracted depth to bedrock from the USGS National Crustal Model dataset (e.g., Figure 3-11) along transects and converted to elevations and locally adjusted with deep well information. The four main sedimentary units include: (1) Middle Pleistocene to Holocene fluvial-deltaic, lacustrine, and distal fan facies of the SHZ; (2) Early Pleistocene deltaic and lacustrine facies representing the clay unit of IHZ; (3) Pliocene fluvial-deltaic, lacustrine, and distal fan facies of the White Hills sequence; and (4) Undifferentiated Quaternary and Tertiary alluvial fan facies of the SHZ and DHZ. The geologic cross section of transect 1 was developed first because the orientation and location of the transect is nearly perpendicular to all the primary and secondary faults, as well as crosses the deepest sectors of the lake basin and intersects the deepest wells, so the maximum amount of vertical deformation of the main sedimentary units could be characterized (Figure 3-15). The tectonic-block model and interpretation of the structure and stratigraphy developed along transect 1 was used to control the magnitude of displacement and style of deformation of sedimentary units along the other transects (2–5) (Figures 3-15 and 3-16).

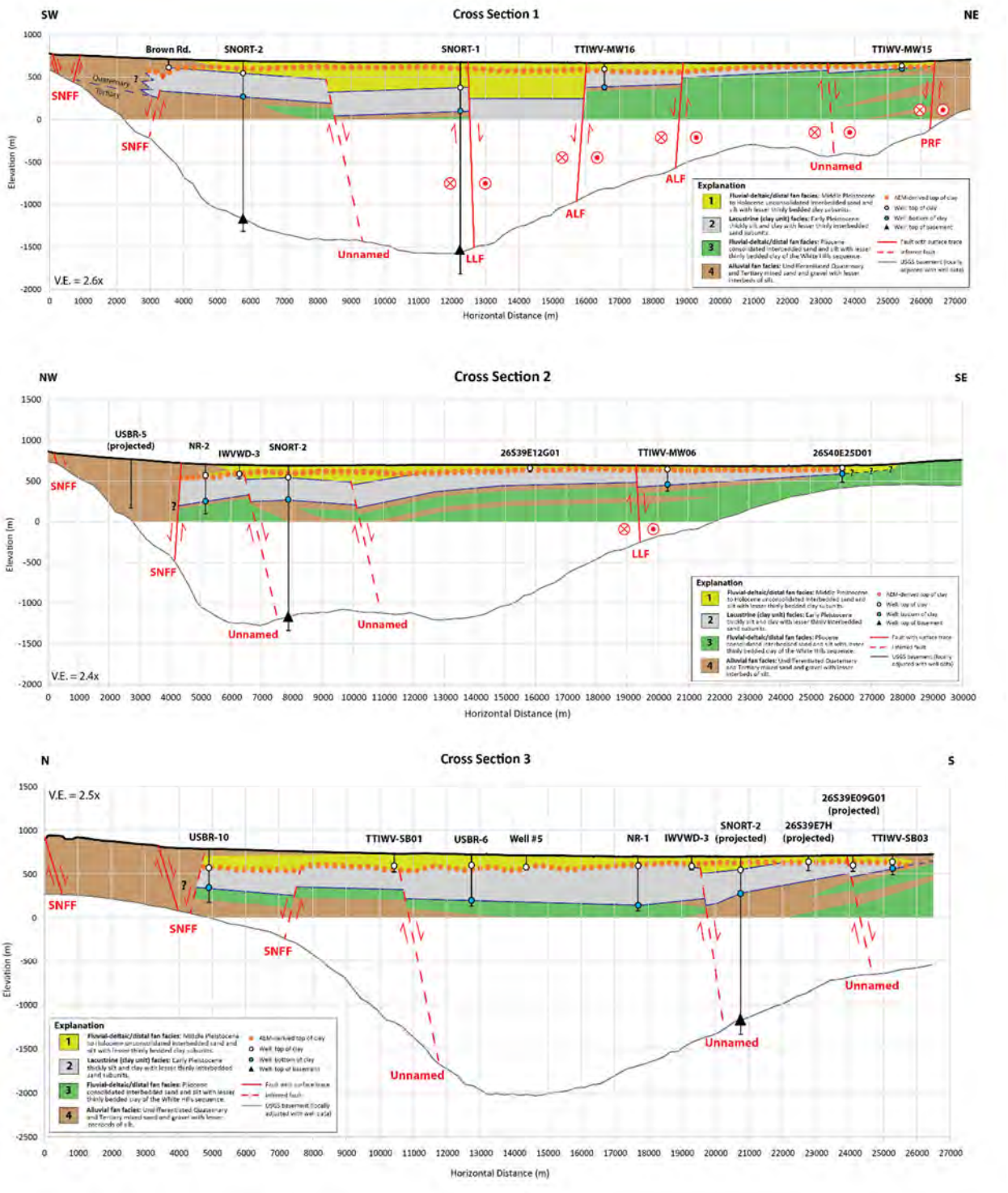


Figure 3-15. Geologic cross sections along transects 1–3 showing the configuration of the fine-grained "clay" unit represented by the lacustrine facies sedimentary unit 2 based on a simple tectonic-block model for northern IWV and China Lake basin. The location of wells and depths of the top and bottom of the clay unit from lithologic logs are shown. The top of the first fine-grained "clay" layer detected by the Airborne Electromagnetic (AEM) resistivity survey is also shown.

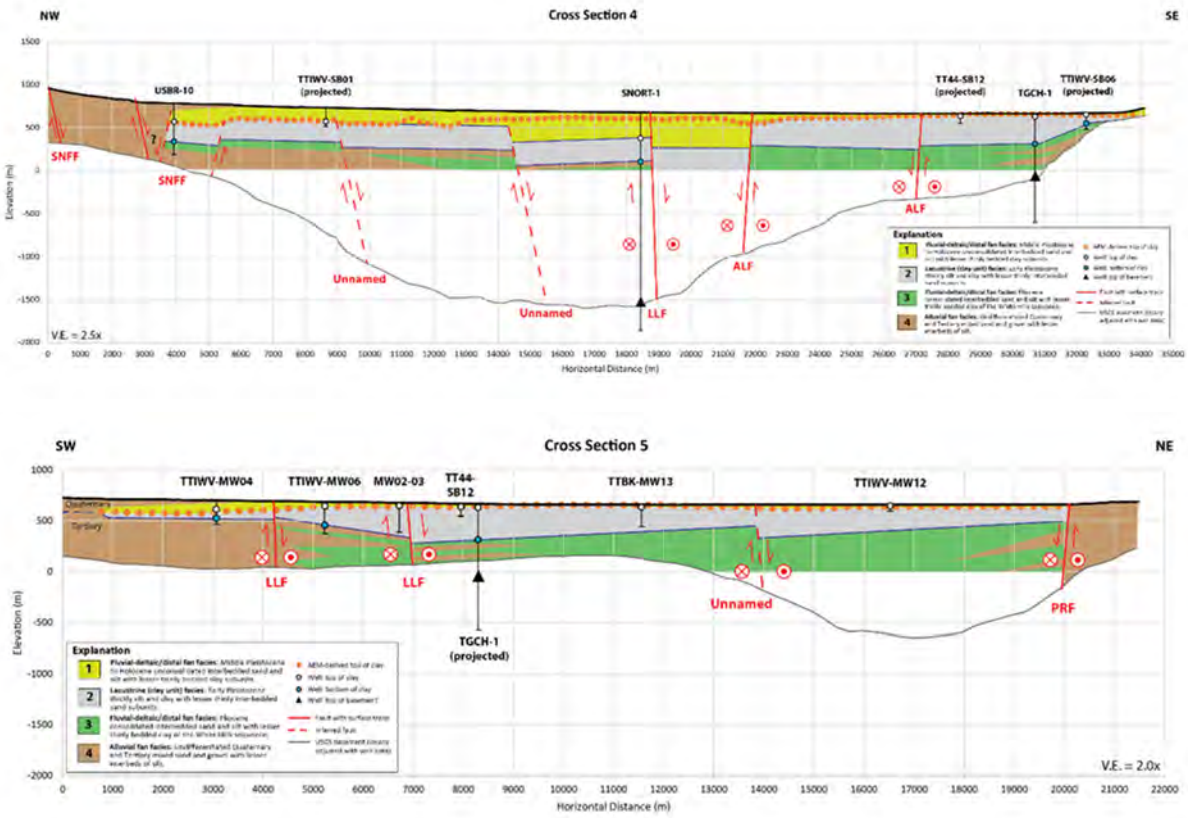


Figure 3-16. Geologic cross sections along transects 4 and 5 showing the configuration of the fine-grained "clay" unit represented by the lacustrine facies sedimentary unit 2 based on a simple tectonic-block model for northern IWV and China Lake basin. The location of wells and depths of the top and bottom of the clay unit from lithologic logs are shown. The top of the first fine-grained "clay" layer detected by the Airborne Electromagnetic (AEM) resistivity survey is also shown.

The depths of the top and bottom of the clay unit observed in wells were used as control points to model clay unit thickness in geologic cross sections. The AEM resistivity data processed in 2023 for the model update was also used to estimate the elevation of the top of the clay unit along survey lines (e.g., Figure 3-6). The AEM-derived elevations were interpolated as a gridded dataset for the mapped area of the clay unit (Figure 3-17). The purpose of the interpolation was to provide a spatially continuous dataset that could be used to better characterize the top of the clay unit for inclusion in the 2025 Basin Model. The distribution of the interpolated AEM-derived elevations of the top of the clay unit generally coincides with the deepest parts of the basin and location of primary faults (Figure 3-17).

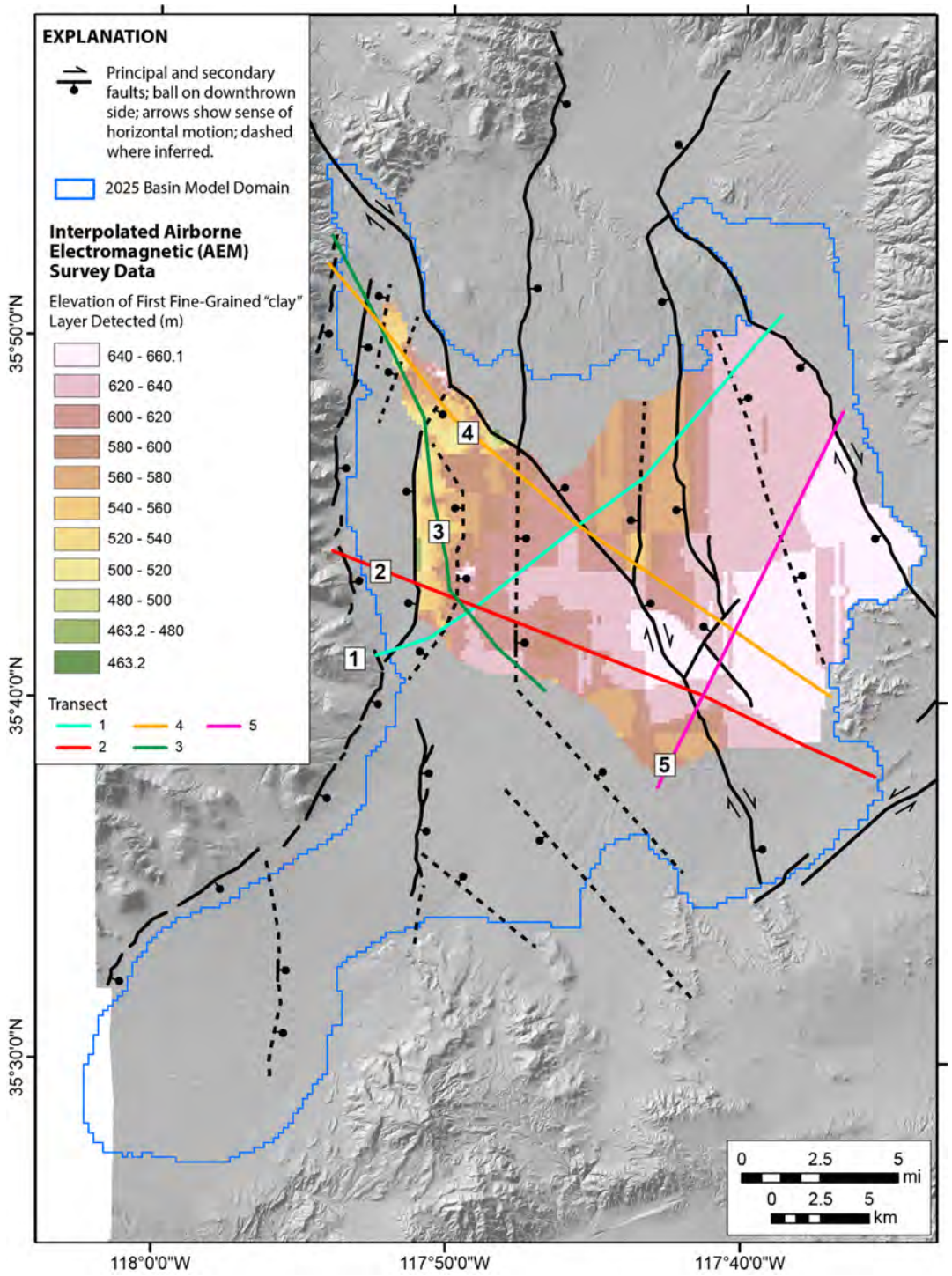


Figure 3-17. Map showing location of primary and secondary faults of the tectonic-block model and geologic cross section transects 1–5 within the 2025 Basin Model domain. The interpolated elevation of the first fine-grained "clay" layer detected by the Airborne Electromagnetic (AEM) resistivity survey is also shown for the mapped clay unit. Hillshade is from 2019 Ridgecrest, California Pre-Earthquake Digital Surface Model (published July 9, 2019).

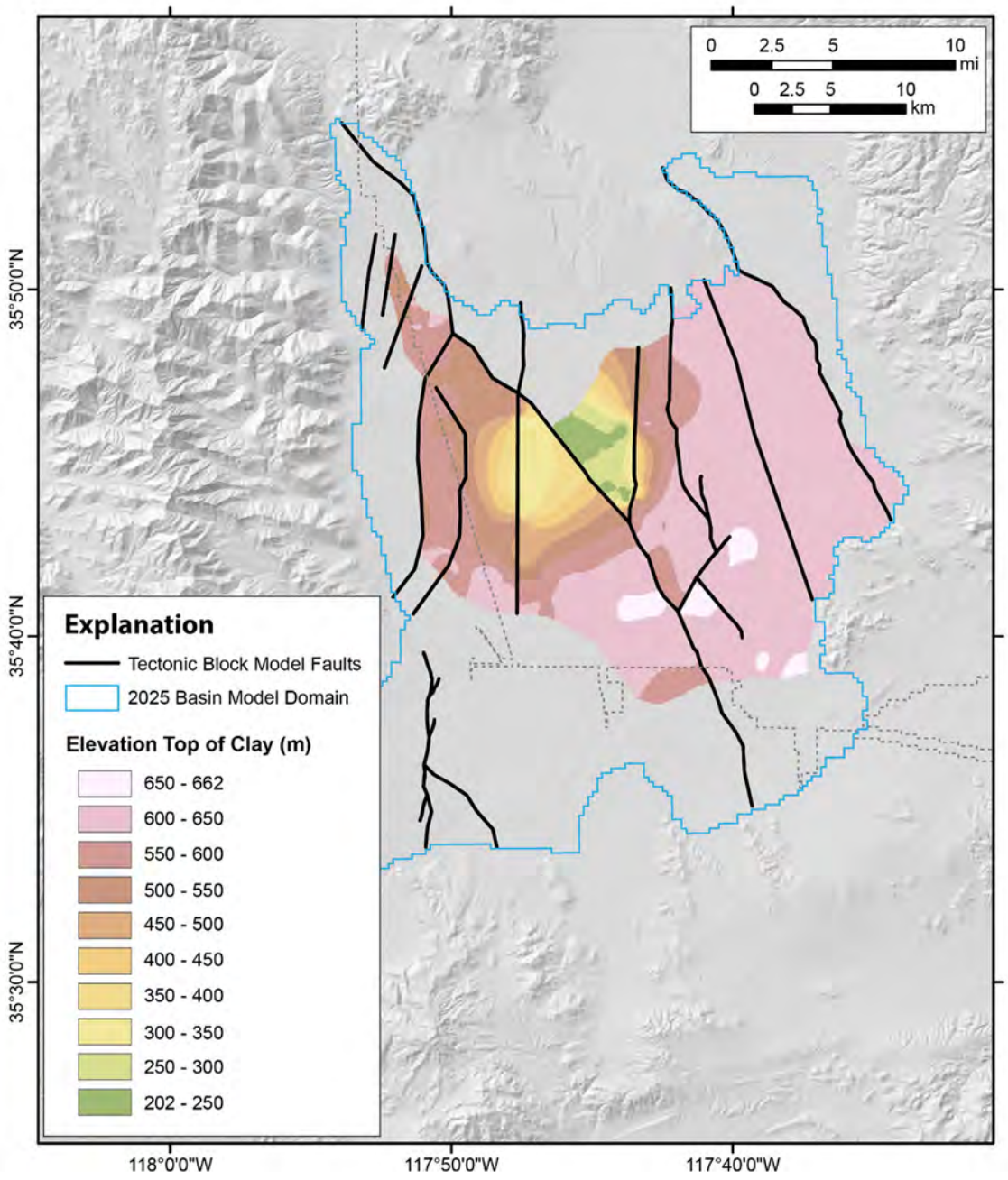


Figure 3-18. Map showing interpolated elevation of the top of clay unit in 2025 Basin Model domain based on digitized elevations from geologic cross sections along transects 1–5 (Figures 3-15 and 3-16). Faults used in the tectonic-block model are also shown.

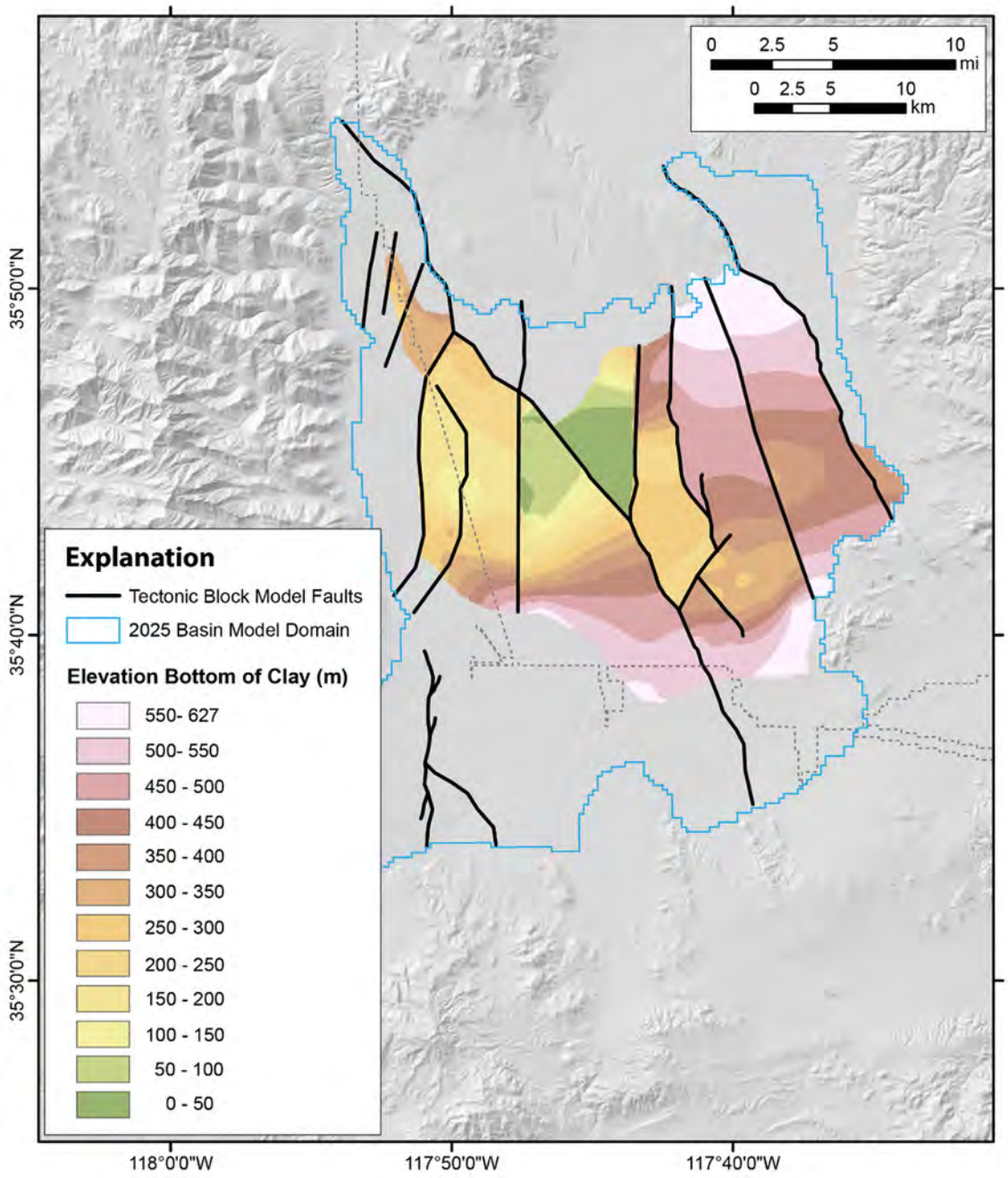


Figure 3-19. Map showing interpolated elevation of the bottom of clay unit in 2025 Basin Model domain based on digitized elevations from geologic cross sections along transects 1–5 (Figures 3-15 and 3-16). Faults used in the tectonic-block model are also shown.

Comparison of the interpolated elevations of the top of the clay unit with the elevations observed in wells indicates that the AEM-derived elevations are more accurate along the western and eastern margins of the mapped clay unit, whereas in the central sector of the mapped area near the deep well of SNORT-1, the clay unit occurs in wells at much lower elevations. A sequence of clay subunits less than 10 m thick are commonly

interbedded with sands and silts in areas near SNORT-1. The sequence of interbedded clay and sandy subunits coincide with the deepest part of the basin and is a preserved stack of alternating fluvial-deltaic and lacustrine deposits associated with fluctuating lake levels during the late Pleistocene (e.g., Tetra Tech, 2003; Rosenthal et al., 2017). It appears that the AEM resistivity data returned the first clay layer detected in the subsurface along survey lines. In the western and eastern sectors of the mapped clay unit the AEM-derived elevations are accurately depicted and shown on geologic cross sections as an erosional contact across fault-bounded blocks (Figures 3-15 and 3-16). However, in areas bound by either deep grabens or half-grabens the stratigraphy is characterized by up to 1640 ft (500 m) of basin fill deposits represented by sedimentary unit 1, which overlies the clay unit (sedimentary unit 2) (e.g., Transects 1 and 4; Figures 3-15 and 3-16).

The AEM-derived elevations for the top of the clay unit also indicate a continuous contact with rough (i.e., irregular) relief along the western margin of the lake basin, whereas the relief in the central and eastern sectors along the other transects is smooth (Figures 3-15 and 3-16). It is likely the rough contact on the western margin of the lake basin is from cut-and-fill erosional process from alluvial fans sourced from high-gradient tributary streams from the Sierra Nevada (Transect 3; Figure 3-15). The smooth relief in areas closer to the depocenter of China Lake basin is likely a product of erosional process associated with low-gradient deposition of distal alluvial fans and fluctuating lake levels across uplifted fault blocks (Transects 2, 4, and 5; Figures 3-15 and 3-16).

3.2.7. 2025 Basin Model Clay Unit

Previous groundwater models of the IWV groundwater basin including the 2020 GSP Model did not explicitly include the clay unit of the IHZ (e.g., Brown and Caldwell, 2009; McGraw et al., 2016; Garner et al., 2017; IWVGA, 2020). The elevations of the top and bottom of the clay unit were determined from geologic cross sections for the 2025 Basin Model. The elevation of the top and bottom of sedimentary unit 2 was digitized from geologic cross sections and georeferenced as point data along transects 1–5 in ArcGIS (Figures 3-15 and 3-16). The elevation point data was used to create raster elevation surfaces. The geoprocessing routine of spline interpolation with barriers was used to create the raster dataset. Interpolation was performed within the extent of the mapped clay unit and the primary and secondary faults of the tectonic-block model were included as barriers so that elevation data would not be interpolated across faults (Figures 3-17 to 3-19). The top and bottom raster datasets of the clay unit were integrated with the model grid for the 2025 Basin Model and used to update the aquifer property zones used to parameterize the model (Section 5.2.1).

4. CONCEPTUAL FLOW BUDGET

Tabulation of estimates of groundwater budget components (e.g., groundwater recharge and groundwater discharge) are part of every conceptual model in order to provide an initial understanding of model inflows and outflows (i.e., water balance) (Anderson et al., 2015). A comprehensive water budget for the entire hydrologic system of IWV was developed to identify the specific components of the groundwater budget in the groundwater flow model used for the 2020 GSP (IWVGA, 2020). The hydrologic budget of the 2020 GSP Model includes the following budget components: empirically derived mountain-front recharge from precipitation, evapotranspiration (discharge), interbasin flow (discharge), and

pumping (discharge) (McGraw et al., 2016; Garner et al., 2017). The water budget elements focused on in the 2025 Basin Model included refining the spatial and vertical distributions of mountain-front recharge along the Sierra Nevada and Coso Range, as well as bare soil evaporation and evapotranspiration from vegetation within and adjacent to China Lake playa. Updating these hydrologic budget components improved model calibration, thereby enhancing the performance of groundwater water-level simulations.

4.1. Spatial Distribution of Mountain-front Recharge

Mountain-front recharge, which generally occurs along the margins of alluvial basins, can be a large part of total recharge to the aquifer system in such basins. Mountain-front recharge occurs as the result of infiltration of flow from streams that have headwaters in the mountainous areas adjacent to alluvial basins. This streamflow is commonly assumed to be equal to mountain-front recharge because most of this streamflow infiltrates and recharges the basin-fill aquifer (e.g., Danskin, 1998). The 2020 GSP Model accounted for mountain-front recharge from five of the six watersheds that encompass the model domain. The recharge is also uniformly distributed at the mountain front within the boundary of each watershed. Evaluation and revision of the spatial distribution of the quantities of mountain-front recharge over all six of the watersheds to determine each watershed's contribution to recharge in the groundwater basin was performed for the 2025 Basin Model. An evaluation of the distribution of recharge associated with each watershed, in terms of either being uniformly distributed or distributed as a point source at the mouth of tributary streams was performed during the model update.

The spatial and vertical distributions of mountain-front recharge was revised in the 2025 Basin Model and includes an additional recharge area associated with the White Hills in the northern sector of the groundwater basin (Figure 4-1). Recent literature on the dating of both mountain tributary stream water and deep groundwater was used to support the refinement of the distribution of mountain-front recharge for each watershed (Chapman et al., 2022). Recently drilled deep wells with water-level information from the El Paso subarea (EP-1) and south of Little Lake (RVS-1) (Figure 2-7), in conjunction with water levels from wells across the model domain were used to iteratively estimate the fraction and magnitude of mountain recharge into model layers during model calibration (see Section 5.0). The total steady-state inflow of 7,650 AFY, however, did not change between the 2020 GSP Model and the 2025 Basin Model.

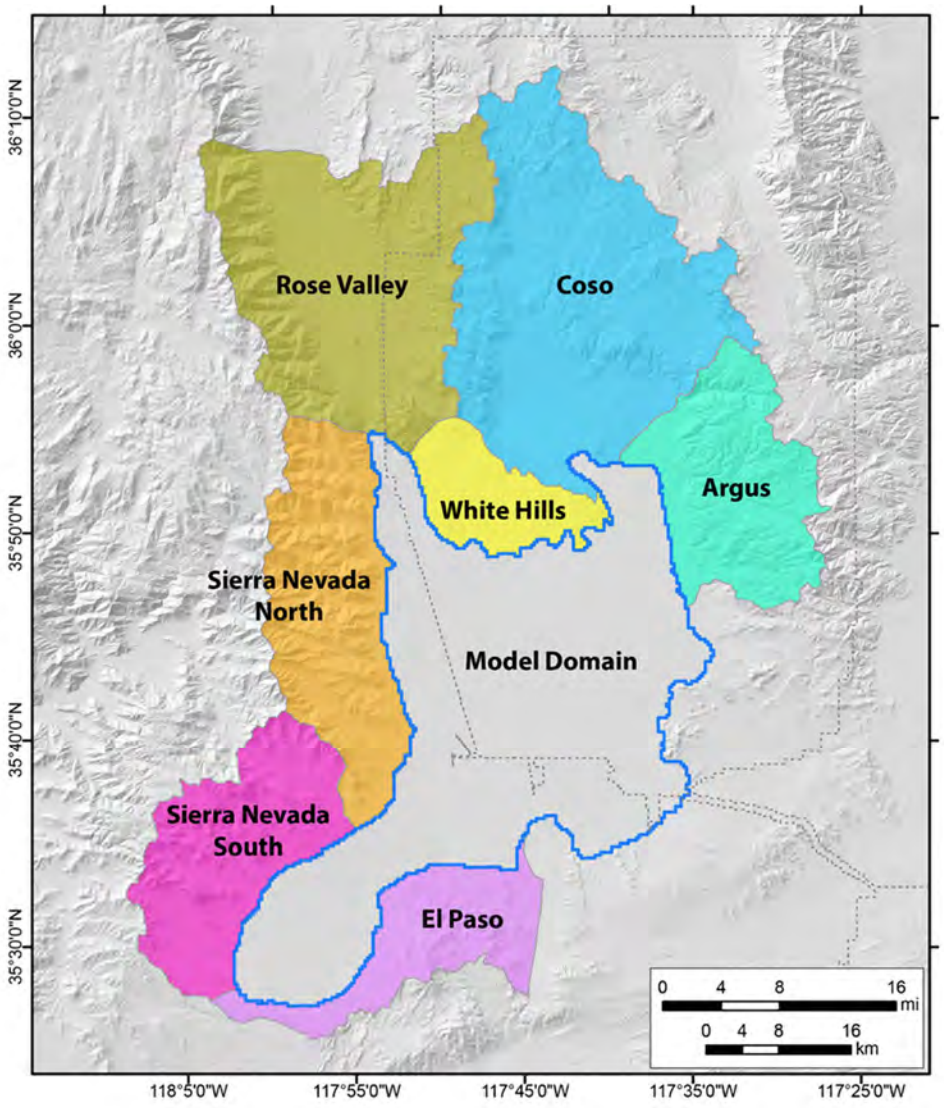


Figure 4-1. Map showing the watersheds and associated groundwater recharge areas used in the 2025 Basin Model. Also shown is a new recharge area named the White Hills that conveys groundwater sourced from Rose Valley through fracture flow within the Pliocene sedimentary rocks of the White Hills sequence.

4.2. Spatial Distribution of Bare Soil Evaporation and Evapotranspiration

Evapotranspiration (ET) from China Lake playa is the principal predevelopment groundwater outflow from the IWV groundwater basin. Four vegetation zones were used in the 2020 GSP Model to simulate the depth to water versus ET. The four zones include a large zone classified as main ET area, an area of bare soil associated with China Lake playa, a zone representing dune phreatophytes, and a smaller zone composed of greasewood (Figure 4-2). The amount of ET for each vegetation zone was modeled using a nonlinear functional shape between depth to water and ET rate (McGraw et al., 2016). This function terminates at an extinction depth where there is no longer ET when groundwater levels drop below a pre-defined threshold depth.

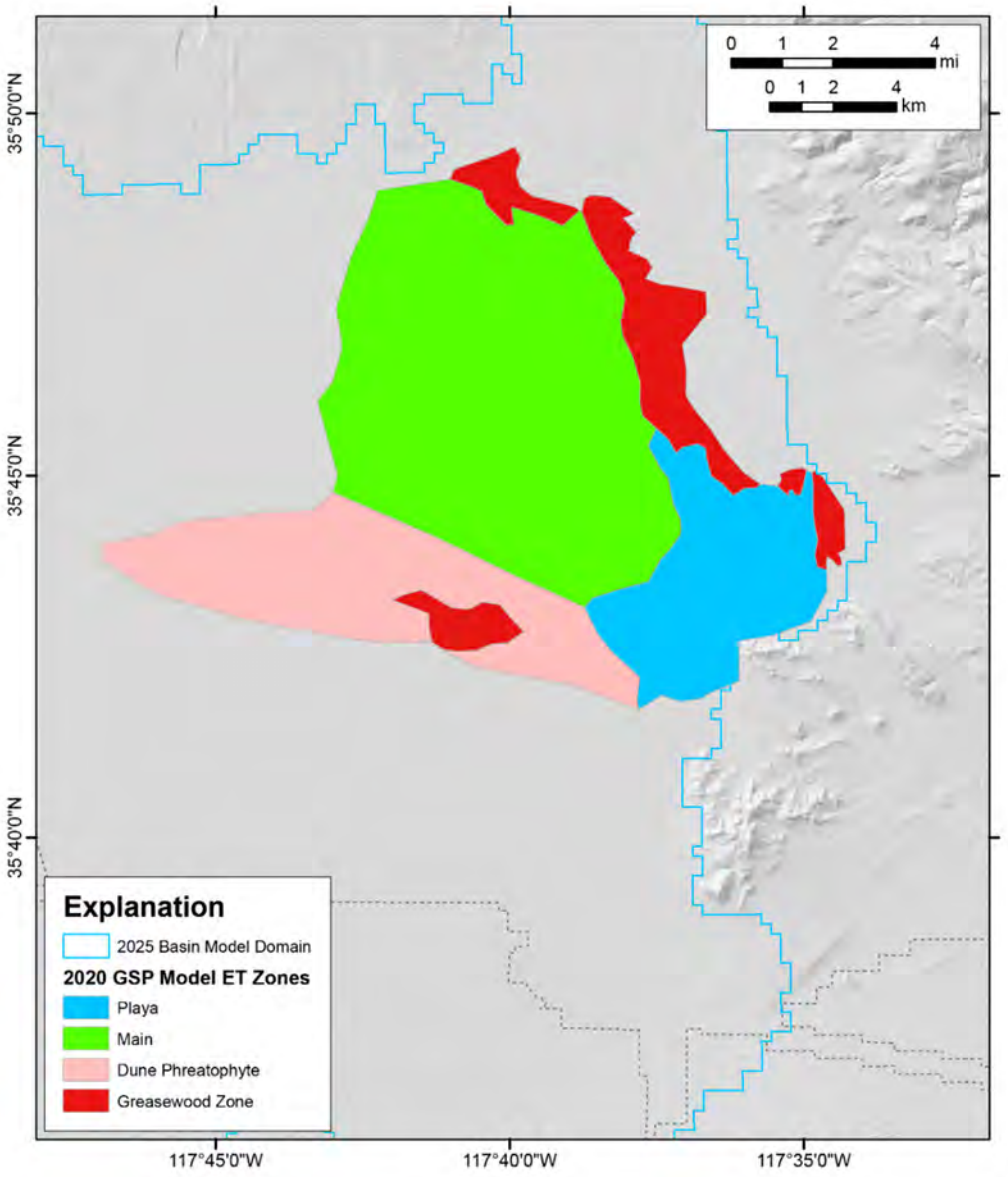


Figure 4-2. Map showing the extent and type of evapotranspiration (ET) zones used in the 2020 GSP Model.

Playas vary greatly in their geologic and hydrologic settings, leading to several classification schemes that group playas by sedimentologic or hydrologic characteristics, with the distinction between 'wet' and 'dry' playas (Rosen, 1994). In a wet playa, groundwater is near (typically <16–17 ft) or at the playa surface, through which it is lost by evaporation or fluid outflow. In a dry playa, groundwater does not interact with the surface because the water table lies far below the surface (typically >16–17 ft). In wet playas, capillary action in sediments, as controlled largely by sediment texture and structure, allows for continuous evaporation of water from shallow groundwater (Reynolds et al., 2007). China Lake playa is a wet playa based on the classification of playas (e.g., Rosen, 1994).

Given that extinction depths of bare soil evaporation from China Lake playa can be much deeper than previously considered in the 2020 GSP Model (e.g., Shen et al., 2013), a primary goal in developing the 2025 Basin Model ET zones was to refine previous estimates of the potential of bare soil evaporation from the playa zone by accounting for sediment texture and the thickness of the capillary fringe. The spatial distribution of the zones of evaporation from the playa and ET from playa margin vegetation was also refined in the 2025 Basin Model by using geomorphic mapping of China Lake basin to identify the extent of bare soil playa features more accurately, as well as groundwater-dependent vegetated areas associated with sand dunes (Bullard et al., 2019; Lancaster et al., 2021). Because desert regions typically have distinctive vegetation patterns and associations that reflect soil-geomorphic landscape position (e.g., Michaud et al., 2013), the boundaries of the geomorphic units were used with a high-degree of confidence to map vegetation by correlating to overlapping California Department of Fish and Wildlife (CDFW) vegetation map units. The principal dataset used for the delineation of vegetation is from the 2013 California vegetation map of the Mojave Desert region (Menke et al., 2013). This dataset consists of high-resolution vegetation classification in support of the desert renewable energy conservation plan of the CDFW.

Previous estimates of the rates of bare soil evaporation from playa settings and ET rates from a range of groundwater-dependent vegetation communities in nearby Owens Valley was also used to support model update efforts (Tyler et al., 1997, 2006; Danskin, 1998; Steinwand et al., 2006). An ET zone map for the 2025 Basin Model was developed that includes ten distinct ET zones. The ET zones include four silty bare soil zones associated with playa and flood plain landform types, as well as two sandy bare soil zones related to sand dunes and sandsheets. The other ET zones are covered by vegetation and include mostly shadscale saltbush (*Atriplex confertifolia*) associated with delta plain landforms, shadscale saltbush (*Atriplex parryi*) associated with vegetated sandsheets and playa margins, and Greasewood (*Sarcobatus vermiculatus*) which is commonly associated with vegetated dunes (Figure 4-3). The 2025 Basin Model includes a refined value of extinction depths between groundwater level and ET for each distinct ET zone based on either bare soil type or predominant vegetation type (Table 4-1).

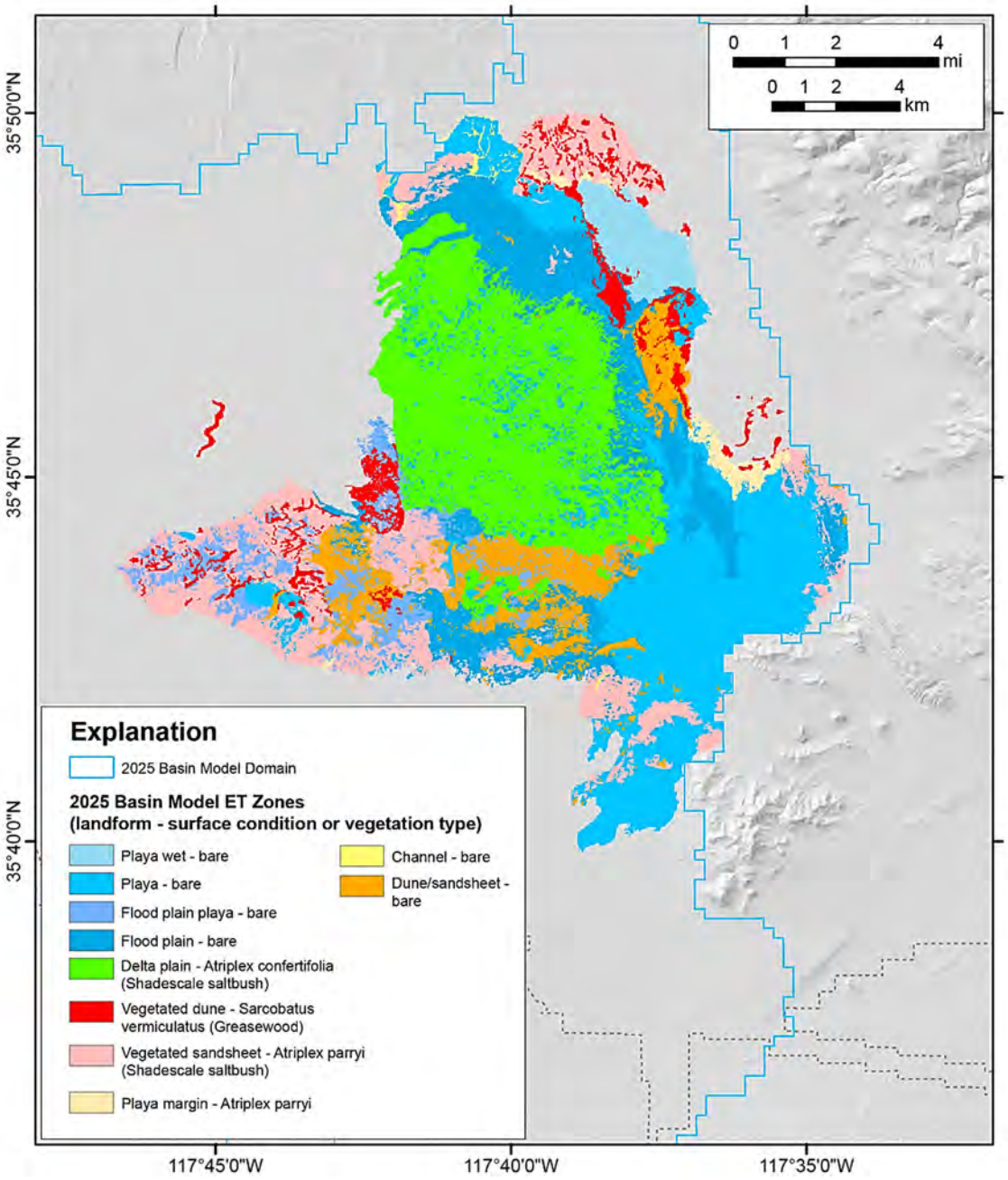


Figure 4-3. Map showing the extent and type of evapotranspiration (ET) zones used in the 2025 Basin Model Update. ET zones were developed from detailed geomorphic mapping and the assignment of dominant vegetation type from Menke et al. (2013).

Table 4-1. Extinction depths for soil and vegetation types for evapotranspiration zones in the 2025 Basin Model.

Landform	Soil Type	Soil Extinction Depth (m)	Surface Condition or Vegetation Type	Vegetation Extinction Depth (m)	Modeled Extinction Depth (m)
Channel	Sand	0.5	Bare	0	0.5
Delta plain	Sandy loam	1.3	*Atriplex confertifolia*	7	7
Dune	Sand	0.5	Bare	0	0.5
Flood plain	Silt loam	4.2	Bare	0	4.2
Flood plain playa	Silt	4.3	Bare	0	4.3
Playa	Silt	4.3	Bare	0	4.3
Playa margin	Silt loam	4.2	*Atriplex perryi*	5	5
Playa wet	Silt	4.3	Bare	0	4.3
Sandsheet	Loamy sand	0.7	Bare	0	0.7
Vegetated dune	Sand	0.5	*Sarcobatus vermiculatus*	15	15
Vegetated sandsheet	Loamy sand	0.7	*Atriplex perryi*	5	5

The extent of applied evapotranspiration zones was improved in the 2025 Basin Model. The total area of evapotranspiration zones in the updated model is 60.3 mi^2, which is 10.8% greater than the 2020 GSP Model with an area of 53.8 mi^2 (Figures 4-2 and 4-3). Although the total area of evapotranspiration between the 2020 GSP Model and the 2025 Basin Model is within about 11%, the distribution of potential groundwater loss from vegetated and bare soil zones is markedly different. The updated model includes evapotranspiration from vegetated zones having an area of 27.1 mi^2, compared to the 2020 GSP Model with an area of 45.0 mi^2. The updated model also includes a larger extent of bare soil evaporation from playa and alluvial plains surfaces with an area of 33.2 mi^2, whereas the 2020 GSP Model has a significantly smaller area of 8.8 mi^2 from playa surfaces (Figures 4-2 and 4-3). It should be noted that these values compare the areal extent of applied evapotranspiration zones, not the extent of actual simulated ET, which is a function of both the applied zones and the simulated water levels in the intersected model grid cells.

4.3. Historical Pumping

Production well locations, estimated pumping volume, and recently (2020-2023) reported monthly pumping were reviewed and updated during 2023 for the Model Update using the CMP process. Updating the model included converting pumping from calendar years to water years (WY) and simulating monthly stress periods starting in October 1995.

The 2020 GSP Model contained 1,191 production wells pumping from Calendar Year (CY) 1922 to 2016 based on estimated well locations, and 946 production wells pumping from Water Year (WY) 2020 to 2070 developed through the TAC during the GSP process. During the CMP Model Update process, these two 2020 GSP Model well location datasets were compiled and assessed for agreement using 2020-2023 reported production well data and GIS aerial photo mapping, resulting in 974 historical and 946 current/future production well locations which were incorporated into the 2025 Basin Model Update. Figure 4-4 displays pumping well locations for WY 2020.

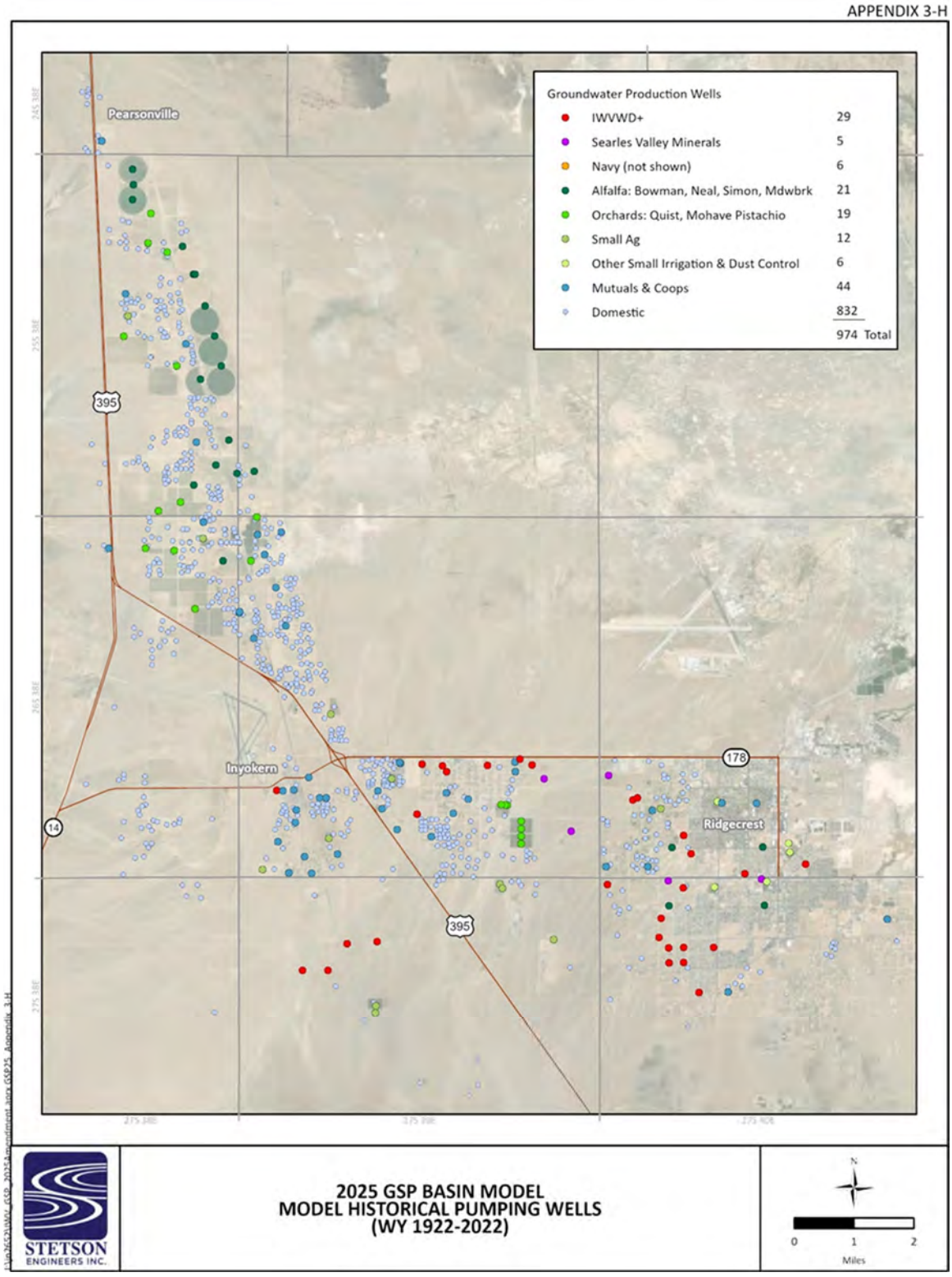


Figure 4-4. Locations of simulated historical pumping wells.

The monthly volume of pumping was reported to the GA from 2020 through 2023 by agriculture, irrigation, municipal, and navy groundwater pumpers. These new data were used to develop monthly pumping curves for estimating historical calibration. Assumptions made during the 2020 GSP TAC for the Baseline were used where measured pumping data were not available. It is recommended that these data gaps, especially domestic groundwater use, be addressed in future model updates. Figure 4-5 displays a bar graph showing the estimated annual pumping by water year and pumping group for the Historical Calibration (WY 1921-2022).

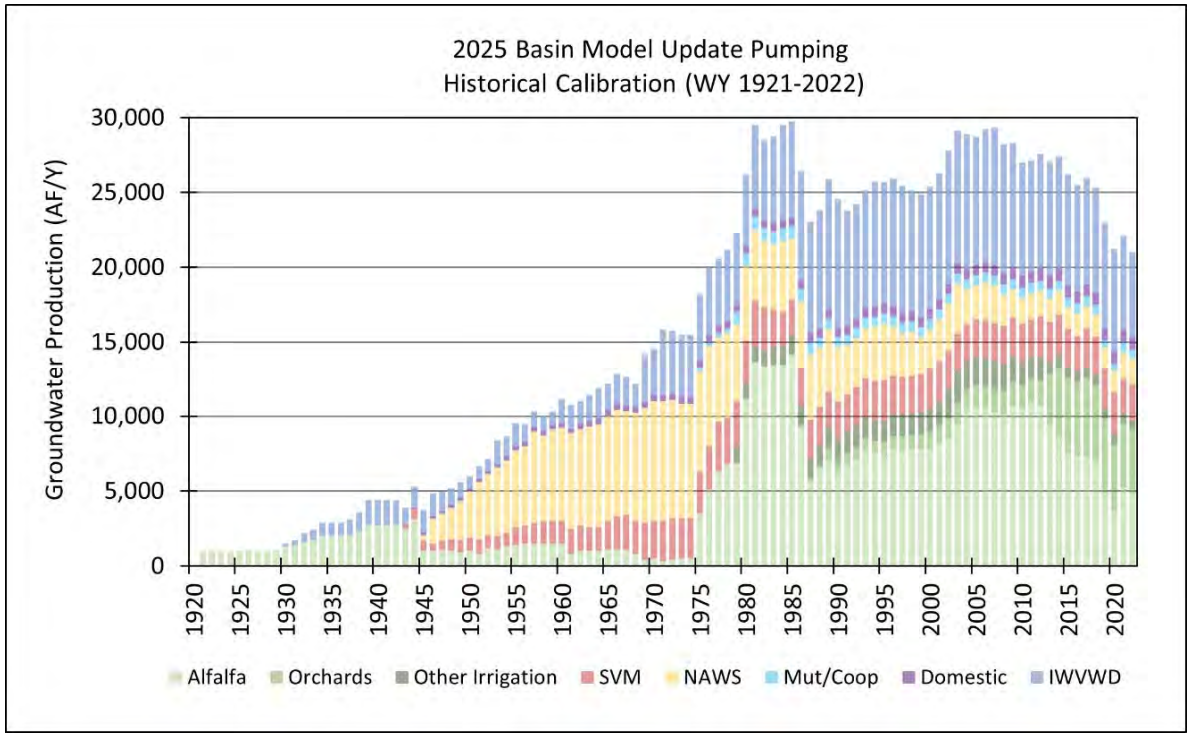


Figure 4-5. Total pumping rates assigned to each well type for the Historical Calibration period (WY 1921-2022).

5. NUMERICAL MODELING

MODFLOW-NWT (Niswonger et al., 2011) was used to simulate the three-dimensional groundwater flow system in the Pahrump basin. MODFLOW is considered the industry standard and has been extensively tested and verified by numerous hydrogeologists. The model was developed within the Groundwater Modeling System (GMS) environment (version 10.8). GMS acts as a database for all of the hydrogeologic information and provides an easy-to-use graphical pre- and post-processor to MODFLOW.

The 2025 Basin Model consists of 90,342 250 m x 250 m active grid cells over six computational layers that range in thickness from 20 m to 300 m. The geometry of the model domain was initially developed as described in Section 2.1, which produced a realistic 'bowl' structure that necessitated either clipping the areal extent of the lower model layers or the use

of very thin grid cells. To improve model stability, the areal extent of layer 1 was extended through layer 6 and a minimum layer thickness of 20 m was assigned to layers 2-6. Spatially, these added grid cells represent consolidated material or bedrock, and were parameterized as such during model calibration. The thickness of layer 1 was initially defined based on the 2020 GSP Model, and was modified as necessary to accommodate the updated model domain and to maintain a minimum thickness of 100 m to ensure the water table would be simulated within layer 1. Layers 2-5 were assigned a thickness of 75 m each through the majority of the area where transmissive materials were present, and were reduced to a minimum of 20 m along the boundaries of the model domain where the total thickness of transmissive materials could not accommodate this distribution, or as required to represent the transition from unconsolidated to consolidated materials. The remaining thickness of the model domain below the assigned base of layer 5 was assigned to layer 6, resulting in significant variability in the thickness of the grid cells in that layer, with an average thickness of 117 m, ranging from 20 m to 213 m. Additional details on the structure of the model grid and spatial distribution of parameter zones can be found in Section 5.2.

Two calibration models (steady-state and transient-historical) were developed to simulate flow and used to parameterize aquifer properties. A steady-state model representing average predevelopment conditions prior to 1921, when groundwater pumping began, was calibrated to observed heads and estimated recharge and discharge values. The results of this model were used as the initial condition for a transient model simulating WY 1921-2022, using annual stress periods through WY 1995 and monthly stress periods beginning in WY 1996. This temporal discretization represents an important departure from the 2020 GSP Model, which simulated calendar year stress periods through CY 2016.

5.1. Boundary Conditions

Boundary conditions simulated in the 2025 Basin Model include mountain front/mountain block recharge, evapotranspiration, outflow to Salt Wells Valley, and pumping. While the same boundary conditions were used in the 2020 GSP Model, modifications have been made to their configuration for use in the 2025 Basin Model.

5.1.1. Recharge

Mountain front/mountain block recharge is simulated using MODFLOW's Well (WEL) Package along the boundaries of the model domain and is simulated in layers 1-3 only. Recharge in layer 1 was associated with mountain tributary stream water and was applied only along the canyon mouths in the Sierra Nevada and El Paso recharge zones. Layer 1 recharge along the Rose Valley, White Hills, and Argus zones enters the basin as underflow and was distributed along the length of those boundaries (Figure 4-1). Recharge simulated in layers 2 and 3 was also simulated as distributed flow along the length of the recharge zone boundary. The deepest simulated recharge in layer 3 was simulated along the Sierra Nevada North zone only. The rate of recharge simulated in each of the zones was redistributed relative to the 2020 GSP Model based on model calibration (Table 5-1). The total recharge rate for the steady-state (predevelopment) model was maintained at 7,650 AFY, as previously developed by DRI in coordination with the IWV TAC (McGraw et al., 2016; Garner et al., 2017).

Table 5-1. Rates of mountain front recharge applied to each watershed boundary in the 2025 Basin Model (left), compared to the 2020 GSP Model (right), in acre-feet per year.

2025 Basin Model	
Inflows	**AFY**
Mountain Front Recharge	
Sierra Nevada North	2,995
Sierra Nevada South	377
Argus	1,739
Rose Valley	1,919
El Paso	324
White Hills	296
Total	**7,650**

2020 GSP Model	
Inflows	**AFY**
Mountain Front Recharge	
Sierra Nevada North	2,100
Sierra Nevada South	1,500
Argus	1,600
Rose Valley	2,400
El Paso	50
Total	**7,650**

The 2020 GSP Model used a constant 7,650 AFY recharge from CY 1920 to 2016. The updated 2025 Basin Model, uses estimated annual and monthly recharge rates for the transient-historical model based on the average observed precipitation at stations (Haiwee, Indian WV, Laural Mtn Stations). These stations were chosen based on representing different mountain regions (Rose Valley, Sierra Nevada North, and El Paso, respectively). Precipitation at the China Lake station was used to estimate precipitation at the Haiwee station to fill in data gaps. Observed average precipitation rates from WY 1921-2022 were initially fit to a linear distribution of recharge, such that the average recharge over that time period would equal 7,650 AFY (Figure 5-1; Attachment 2).

Deeper recharge in layers 2 and 3 was assumed to represent older, slower recharge that would more closely represent long-term averages, and was simulated using the steady-state rate for each recharge zone. As a result, the initially calculated recharge rates were modified such that changes in precipitation would affect recharge only in layer 1. To estimate changes in precipitation within layer 1 only, recharge rates were first calculated using linear distribution shown in Figure 5-1, resulting in a long-term average recharge rate of 7,650 AFY over the simulated historical time period of WY 1921-2022. These rates were then compared to the average annual recharge rate of 7,650 AFY to obtain the fraction of average for each stress period. These fractions were then applied to the steady-state recharge rates for layer 1 for each stress period. Recharge in layer 1 was distributed to each recharge zone in each stress period according to the fraction used in the steady-state model (Table 5-1). This method results in a muted signal relative to the initially estimated recharge rates, in that above average recharge is reduced, but below average recharge is increased, and zero-recharge stress periods are no longer simulated because of the steady flow occurring in layers 2 and 3. Figure 5-2 shows annual recharge rates estimated using the relationship between precipitation and recharge as presented in Figure 5-1, compared to the final simulated recharge rates modified to reflect fluctuations in layer 1 only.

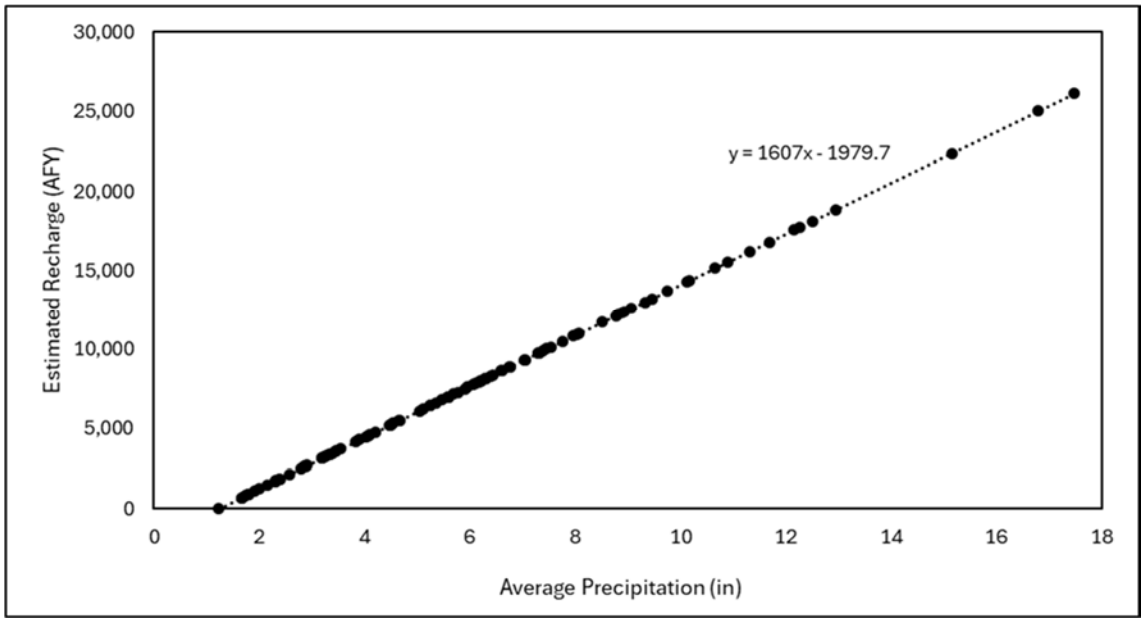


Figure 5-1. Linear distribution of historical precipitation to estimated recharge, distributed to average 7,650 AFY over WY 1921-2022.

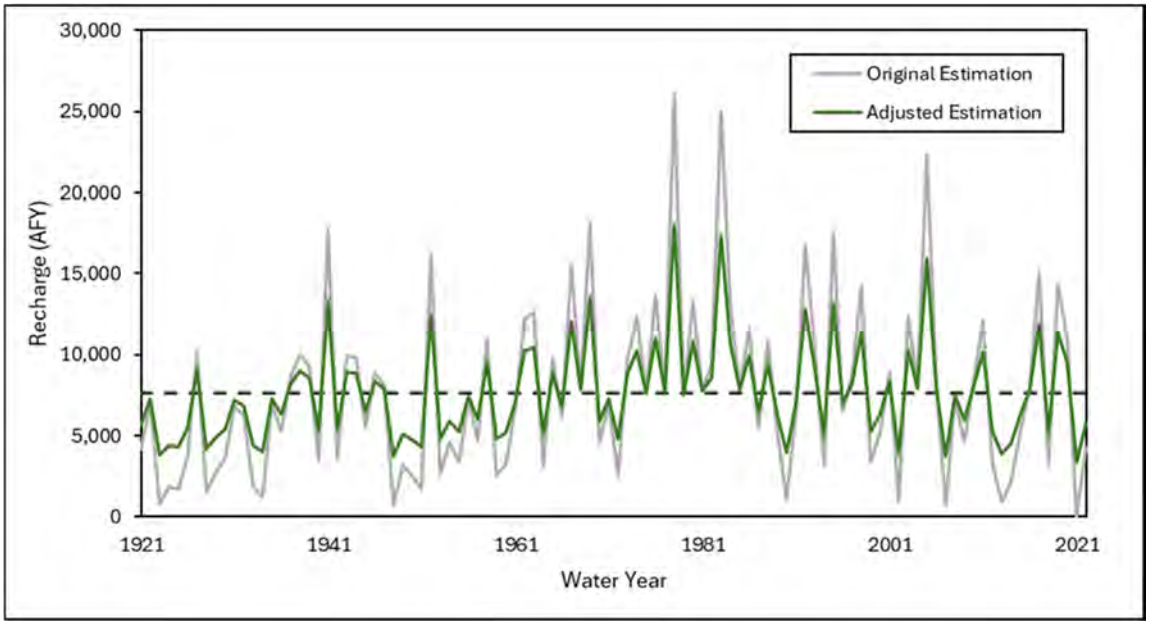


Figure 5-2. Annual recharge rates estimated using the relationship between precipitation and recharge (gray) as presented in Figure 5-1, compared to the final simulated recharge rates modified to reflect fluctuations in layer 1 only (green). The dashed line depicts the average annual recharge rate of 7,650 AFY.

5.1.2. Evapotranspiration

Vegetated and bare soil evapotranspiration are simulated using MODFLOW's Evapotranspiration Segments (ETS) Package. Vegetation and bare soil zones were applied to the model as depicted in Figure 4-3, and extinction depths were assigned to each zone as detailed in Table 4-1. A calibrated maximum ET rate of 0.0004 m/d (0.0013 ft/d) was applied to all zones for the steady-state model and for WY 1921-1995 in the transient-historical model. Beginning in WY 1996, when simulation of monthly stress periods began, a seasonal fluctuation of maximum ET rates was applied to allow for variability resulting from seasonal differences in air temperature and radiative forcing (Figure 5-3). The rates applied for each month were derived from those used in a groundwater model of the nearby Owens Lake basin (Jiao and Vogler, 2020). The monthly percentage of annual ET_a from that study was used to distribute maximum ET rates over each month, such that the annual average would be equal to the steady-state rate of 0.0004 m/d. The segmented curve used to define simulated ET based on water level for all ET zones was taken from the 2020 GSP Model.

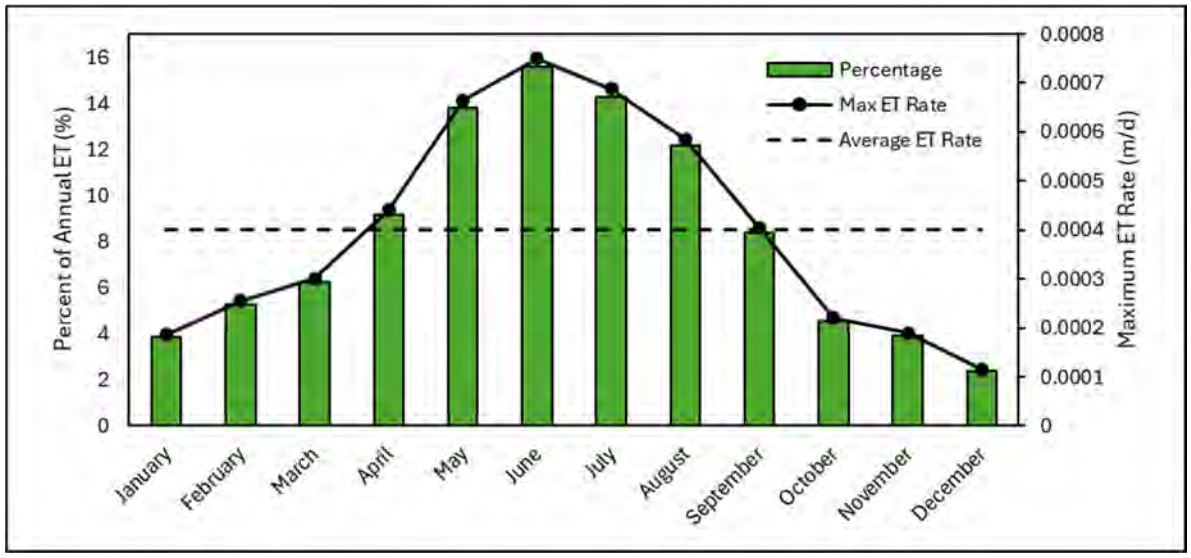


Figure 5-3. Monthly distribution of assigned maximum ET rates for the 2025 Basin Model, defined based on monthly percentages of annual ETa from Owens Lake basin (Jiao and Vogler, 2020). The average annual ET rate used for the steady-state model and all annual stress periods through WY 1995 is shown for comparison.

5.1.3. Outflow to Salt Wells Valley

Outflow to Salt Wells Valley is believed to occur primarily through an overflow channel on the eastern side of the basin, near the south end of the ET zone (Figure 5-4). Outflow was simulated using MODFLOW's General Head Boundary (GHB) package in two grid cells in layer 1 with an assigned elevation of 655 m and a conductance of 1000 m^2/d/m.

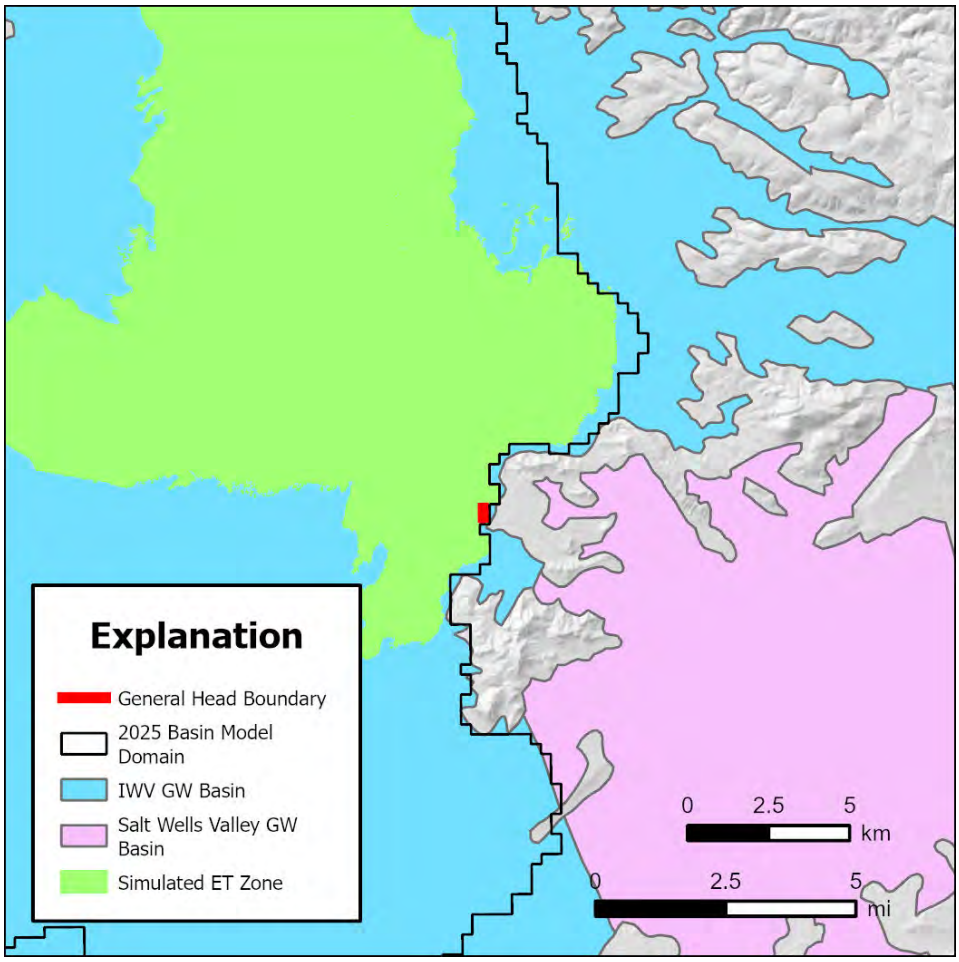


Figure 5-4. Location of General Head Boundary used to simulate outflow through overflow channel to Salt Wells Valley.

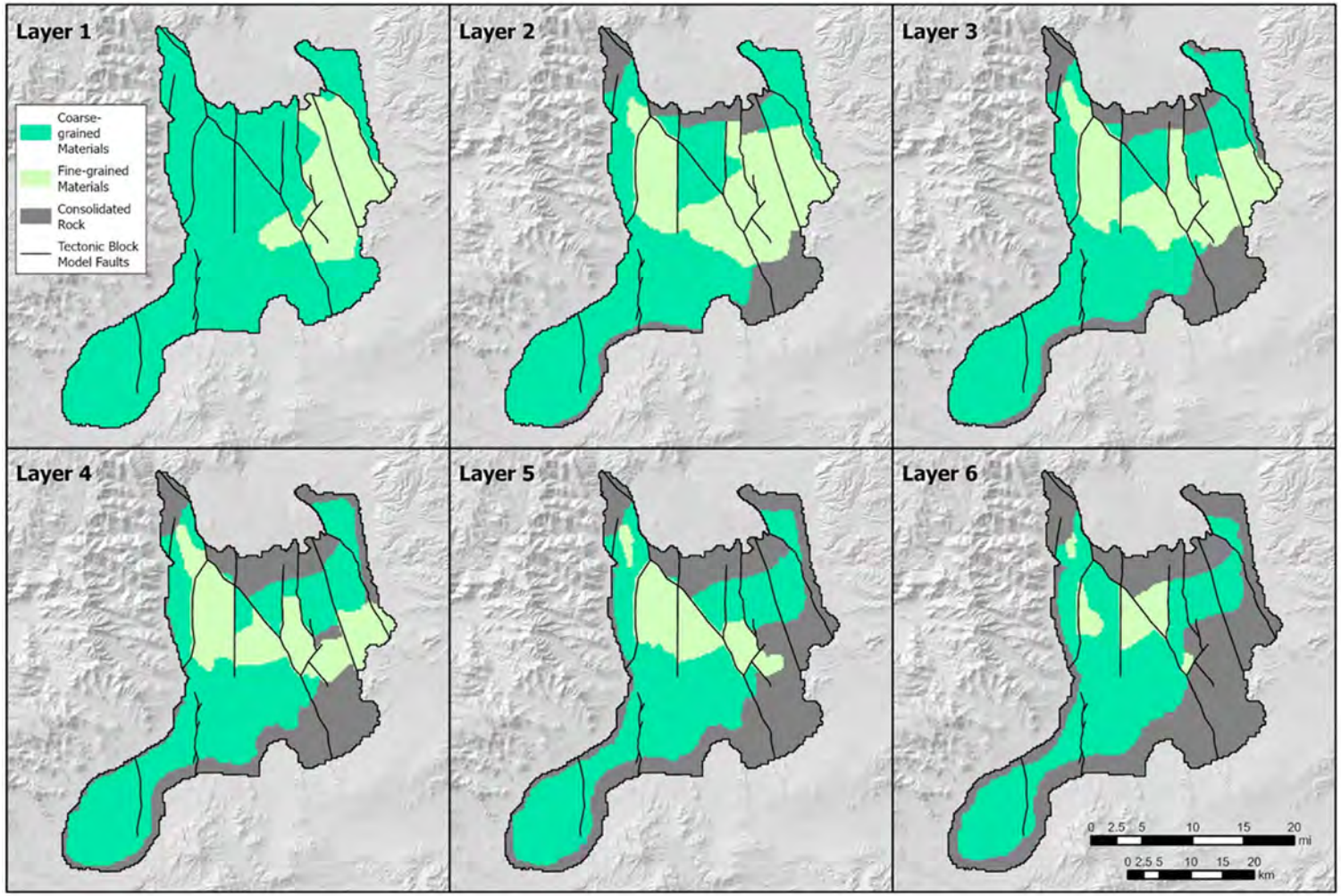


Figure 5-5. Distribution of aquifer property zones by material type for each of the six model layers, and locations of the faults used to define them.

5.1.4. Pumping

Pumping wells were simulated using MODFLOW's Well (WEL) Package, using the estimated rates described in Section 4.3. Wells were simulated using known screened intervals where available and were simulated in layer 1 where this information was unknown. All domestic wells were assumed to be screened in layer 1 only. The deepest simulated pumping intersected layer 4, and no pumping was simulated in layers 5-6.

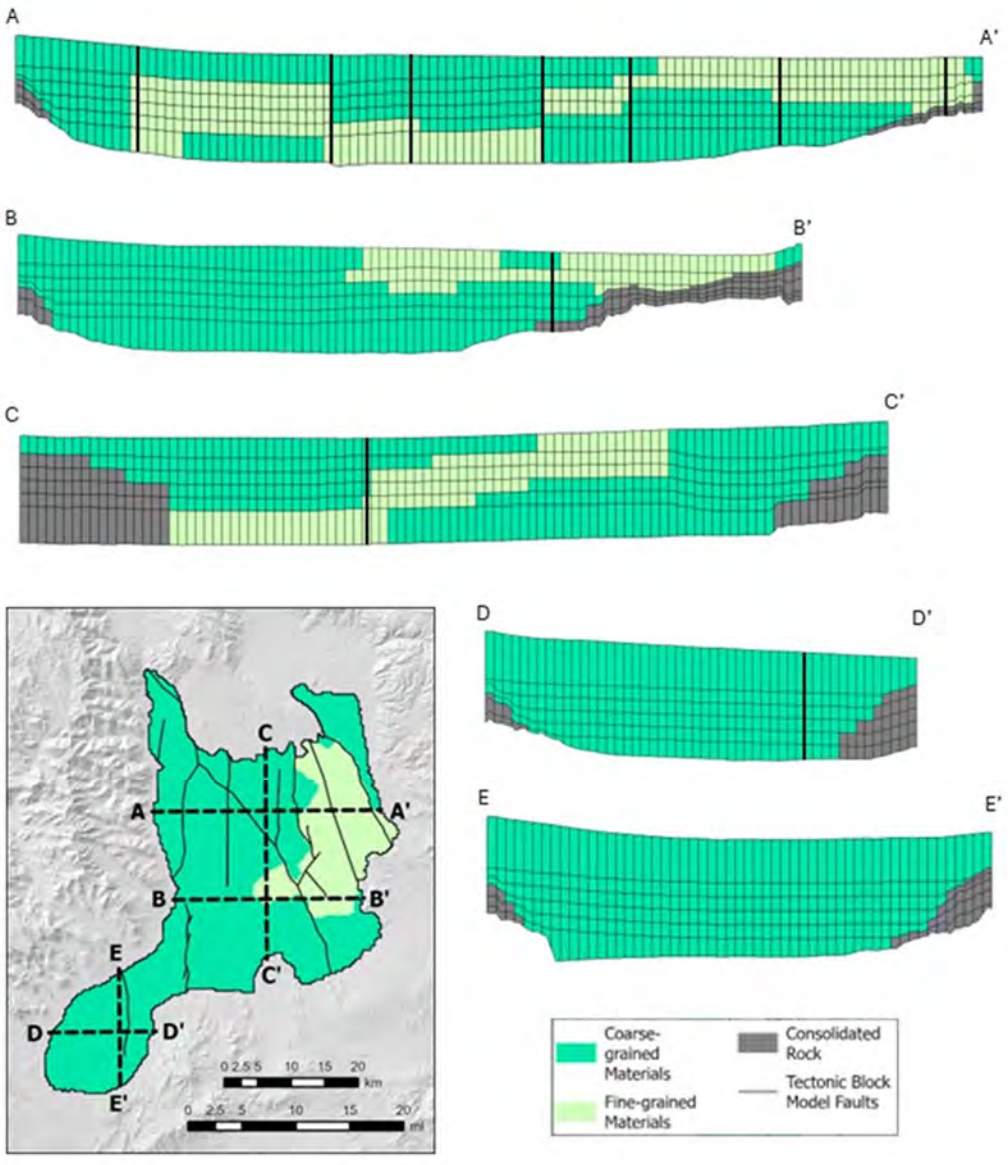


Figure 5-6. Cross-sections of the 2025 Basin Model domain, showing layer discretization and distribution of aquifer property zones.

5.2. Model Parameterization

Aquifer properties (hydraulic conductivity and storage) were parameterized by defining zones within each model layer, which were assigned either a single value or were interpolated using pilot points. Faults were also simulated as barriers to flow where indicated by observed water levels or improvement to calibration metrics.

5.2.1. Aquifer Property Zones

Aquifer property zones were generally defined as representing bedrock or consolidated material, the "clay" (fine-grained) unit, or the more transmissive (coarse-grained) materials into which most pumping wells are screened (Figures 5-5 and 5-6). Zones representing the clay unit for each model layer were defined using elevation rasters for the top and bottom of the clay unit (Section 3.2.7). For each grid cell in the model, the top and bottom elevation of the clay unit were compared to the top and bottom elevation of the grid cell. Grid cells were classified as clay where they contained greater than 50% fine-grained materials, based on this comparison. The more transmissive coarse-grained materials were further subdivided along fault lines to create additional zones in each layer, which could then be independently parameterized using either a single value or an interpolated field using pilot points. Initial values for hydraulic conductivity pilot points were taken primarily from specific capacity test data from well logs and from previous studies, or from slug test results (Moyle, 1963; Kunkel and Chase, 1969; TetraTech, 2003; Layne, 2010). A limited number of available aquifer test results were also included in the pilot point set for hydraulic conductivity (Krieger & Stewart, 1989; Houghton, 1996; DRI, 2020). The pilot point interpolation method was used to define hydraulic conductivities for specific zones in layers 1 and 2 only, as data availability was more limited for deeper layers. The same aquifer property zones used to define the hydraulic conductivity fields for each layer were also used to define the values for specific yield and specific storage.

5.2.3. Faults

While all faults depicted in Figure 5-5 were used to inform the model (defining the "clay" geometry, delineating aquifer property zones, etc.), only some were simulated as barriers to flow. Those that were simulated in the model were defined using MODFLOW's Hydrologic Flow Barrier (HFB) Package (Figure 5-7). It is important to note that while these features are referred to as "barriers," they do not prevent groundwater from flowing through them – they simply impede flow to some degree according to the conductance term assigned to them. Hydraulic characteristics (defined as the hydraulic conductivity of a barrier divided by its width) for these faults were calibrated, and observed faults were removed as barriers to flow where the model was insensitive to their simulation or where nearby observed head data was not available for use in calibration.

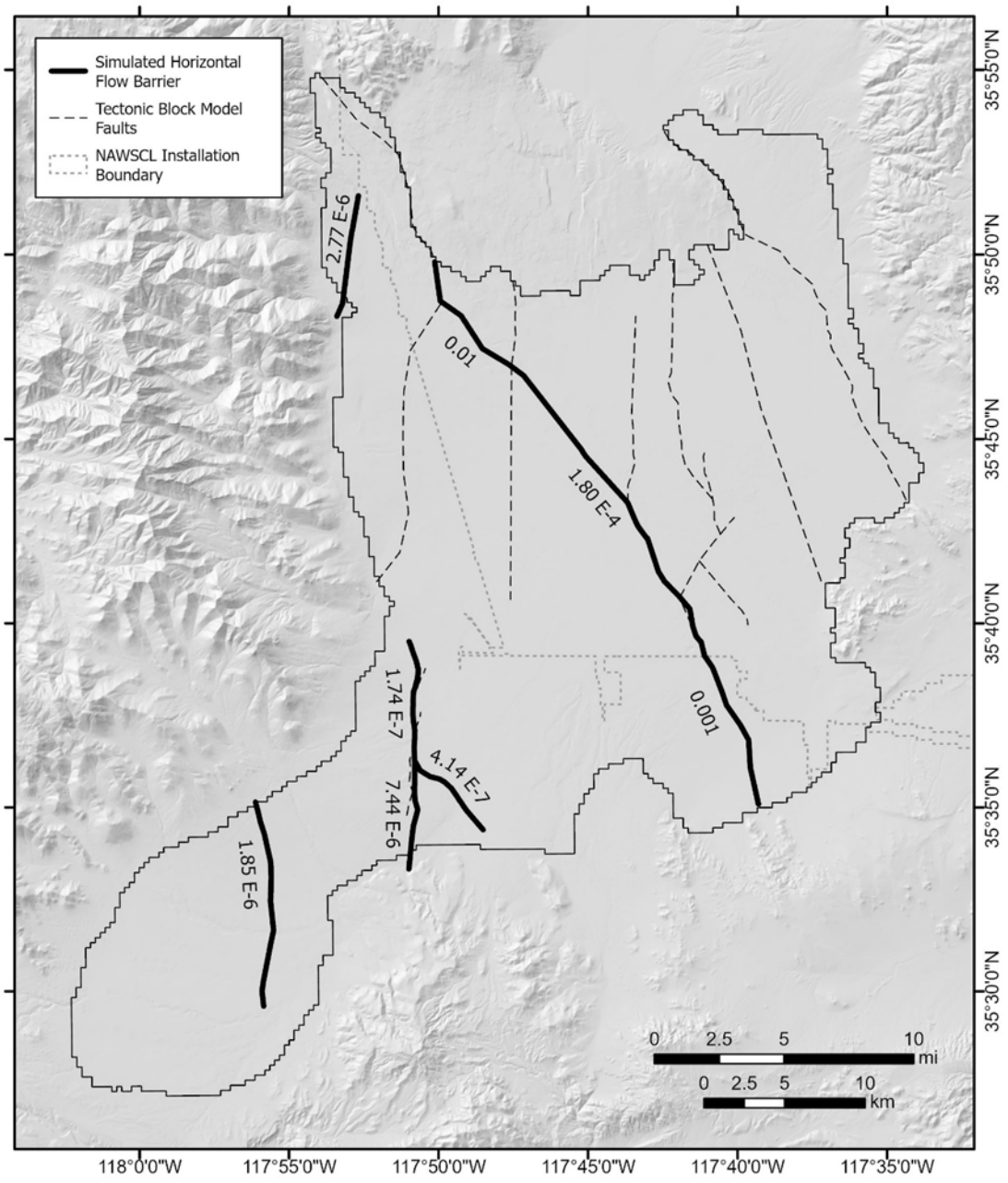


Figure 5-7. Locations of faults simulated as barriers to flow within the 2025 Basin Model, compared to all faults used in the tectonic block model. Faults simulated as barriers to flow are labeled with the calibrated hydraulic characteristic term assigned to that fault. Lower values indicate greater impedance to flow.

5.3. Model Calibration and Results

For a numerical model to produce results that can reasonably be expected to answer questions about a given system or be used in a predictive role, it must first be shown that the model can adequately simulate observed behavior in that system within a reasonable margin of error. Calibration is the iterative process of adjusting input parameter properties that are not known with certainty (such as hydraulic conductivity or storage parameters) until the computed solution matches the observed values to a reasonable level of accuracy. For this study, the model was calibrated to observed groundwater heads and estimated outflows (evapotranspiration and outflow to Salt Wells Valley).

To estimate model parameters, both trial-and-error and automatic model calibration methods using Parameter ESTimation software (PEST, Doherty and Hunt, 2010) were used. Model calibration was assessed based on head error metrics (mean error, mean absolute error, and root mean square error) and on the fit to observed trends in water levels in the transient model. Calibrated parameters include hydraulic conductivity, specific yield and specific storage, and the conductance terms applied to faults simulated as barriers to flow. Hydraulic conductivity and fault conductance terms in the steady-state and transient-historical calibration models were calibrated iteratively, using the results of the steady-state model as the initial condition for the transient-historical model, to ensure a good fit to observed heads in both models.

5.3.1. Estimated Model Parameters

Calibrated hydraulic conductivities ranged from 0.003 ft/d in the deeper layers of the El Paso subarea to 100 ft/d in the west-central portion of the Indian Wells Valley main basin, along the Sierra Nevada North recharge zone (Figure 5-8). Hydraulic conductivities in layer 1 are generally much higher than in the deeper layers, and hydraulic conductivities in the more transmissive coarse-grained materials are generally much higher than in the fine-grained “clay” materials and the zones representing bedrock (Figures 5-5 and 5-8). Calibration of hydraulic conductivities in the El Paso subarea generally required lower values than elsewhere in the Indian Wells Valley main basin in order to match observed heads. Older, consolidated alluvium has been observed in this area which is expected to reduce transmissivity (Jennings, et al., 1962).

Calibrated values for specific yield ranged from 0.001 in the zones representing bedrock to 0.25 in layer 1 in the north-central portion of the model domain (Figure 5-9). Assigned specific yield values are reduced below layer 1 and are lower in the fine-grained “clay” materials and the zones representing bedrock than in the coarse-grained materials (Figure 5-5 and 5-9). Specific yield values for layers 2-6 are estimated and uncalibrated because the simulated water table falls within layer 1 for the majority of the model domain. MODFLOW uses specific yield to calculate storativity only for grid cells that are under water table conditions, and relies on specific storage and the thickness of a given grid cell to make this calculation for grid cells that are fully saturated. Specific storage was calibrated using single values for aquifer property zones, with the exception of the south/central portions of the Indian Wells Valley main basin in layer 2, which used pilot points to interpolate the specific storage field. Calibrated values for specific storage range from 0.0005 ft^{-1} in the pilot point zone of layer 2 to 3e-7 ft^{-1} in zones representing consolidated rock.

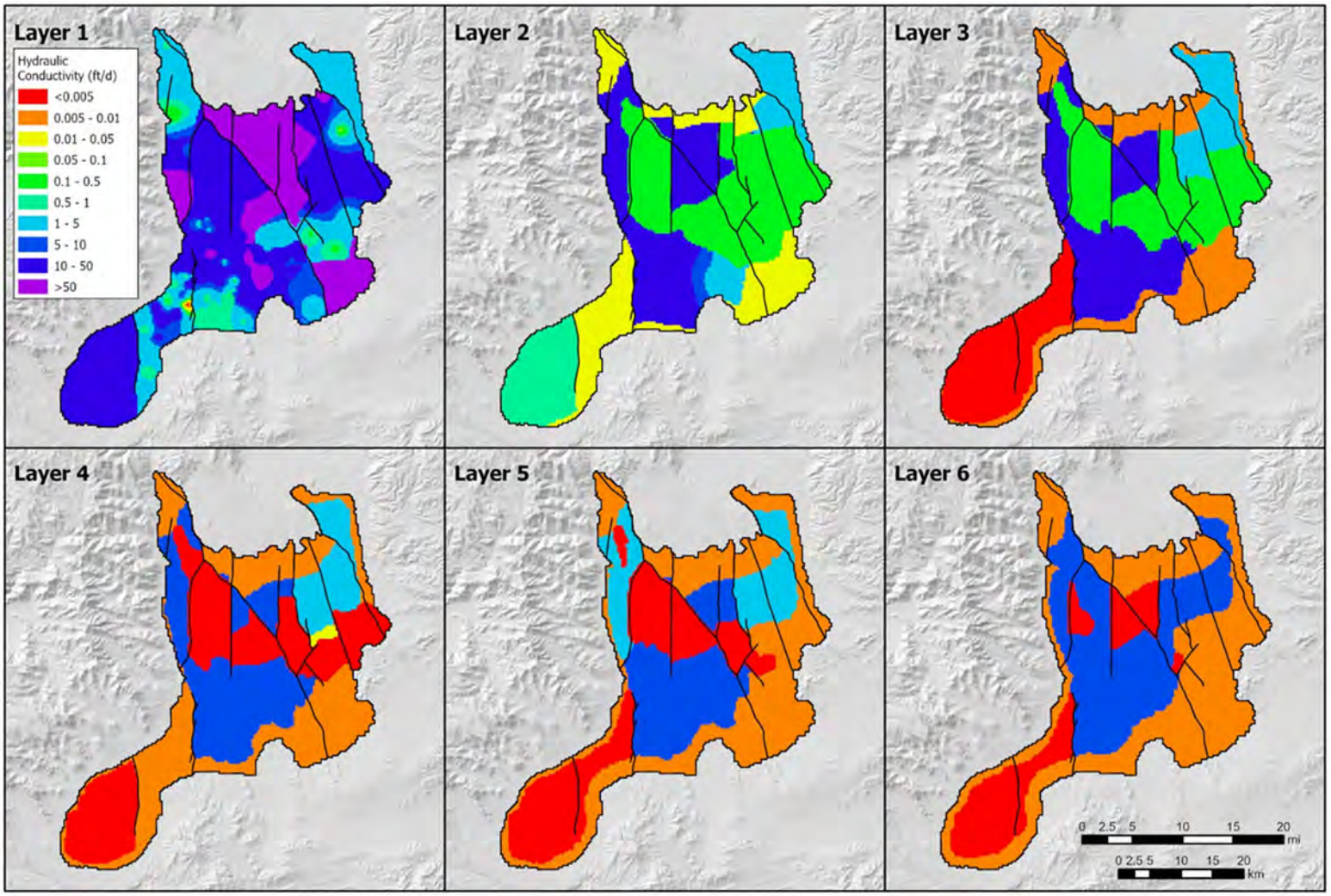


Figure 5-8. Calibrated hydraulic conductivity fields for the six model layers, and the tectonic block model faults used to define aquifer property zones.

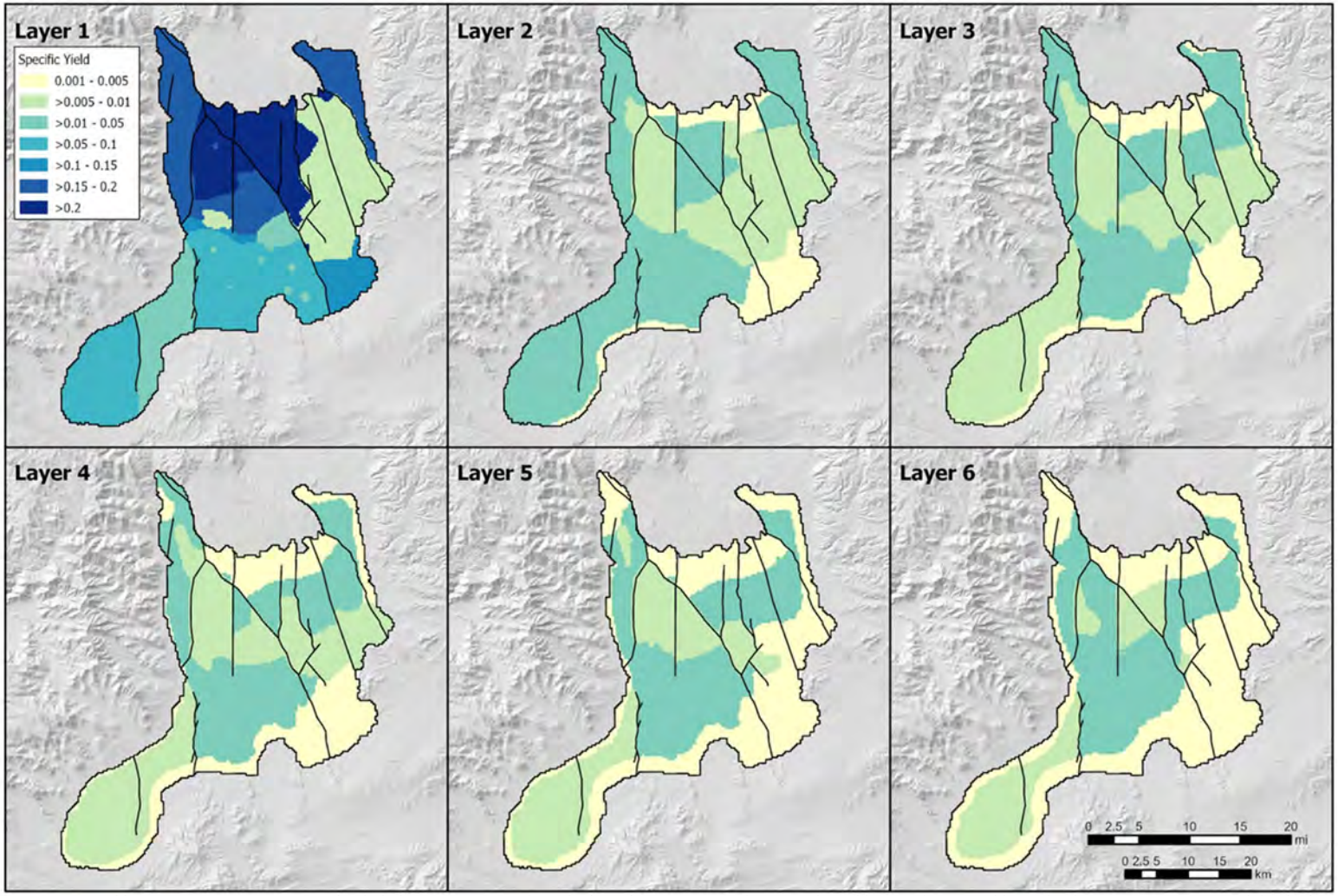


Figure 5-9. Calibrated specific yield fields for the six model layers, and the tectonic block model faults used to define aquifer property zone.

5.3.2. Steady-state Calibration Metrics

For the steady-state model calibration, the same depth-to-water measurements were used as in the 2020 GSP Model. Seven additional more recent measurements from the El Paso subarea were also included to improve model calibration in that area, under the assumption that changes in water levels in that area have been small since the predevelopment period. This was done to ensure a more appropriate initial condition for the transient-historical model; however, these water level measurements were not included in the calibration metrics as it cannot be known with certainty that these water levels are representative of the predevelopment period.

Calibrated steady-state flow rates for modeled sources and sinks are detailed in Table 5-2. The steady-state model was calibrated to within a 0.69% relative error of simulated to observed heads, based on a mean absolute error (MAE) of 4.63 feet (Table 5-3). Relative error is calculated for each error statistic (ME, MAE, RMSE) divided by the observed change between the highest observed head and lowest observed head in the system. The 0.69% relative error for MAE is very similar to the 0.67% relative error for MAE calibrated in the 2020 GSP Model. The distribution of error in the steady-state 2025 Basin Model at observation wells across the model domain is shown in Figure 5-10. A plot of simulated vs observed water levels shows points tightly clustered around the one-to-one line (Figure 5-11) and shows the distribution of observed water level data by elevation.

Table 5-2. Comparison of steady-state flow budgets for the 2025 Basin Model and the 2020 GSP Model.

2025 Basin Model	
Inflows	**AFY**
Mountain Front Recharge	7,650
Total	**7,650**

2020 GSP Model	
Inflows	**AFY**
Mountain Front Recharge	7,650
Total	**7,650**

Outflows	**AFY**
ET	7,600
Interbasin Flow	50
Total	**7,650**

Outflows	**AFY**
ET	7,510
Interbasin Flow	140
Total	**7,650**

Table 5-3. Comparison of steady-state model error statistics for the 2025 Basin Model and the 2020 GSP Model.

	2025 Steady-State Basin Model		**2020 Steady-State GSP Model**	
	Error (ft)	**Relative Error (%)**	**Error (ft)**	**Relative Error (%)**
Mean Error (ME)	1.44	0.21	-0.13	-0.02
Mean Absolute Error (MAE)	4.63	0.69	4.49	0.67
Root Mean Squared Error (RMSE)	6.66	0.99	5.77	0.86

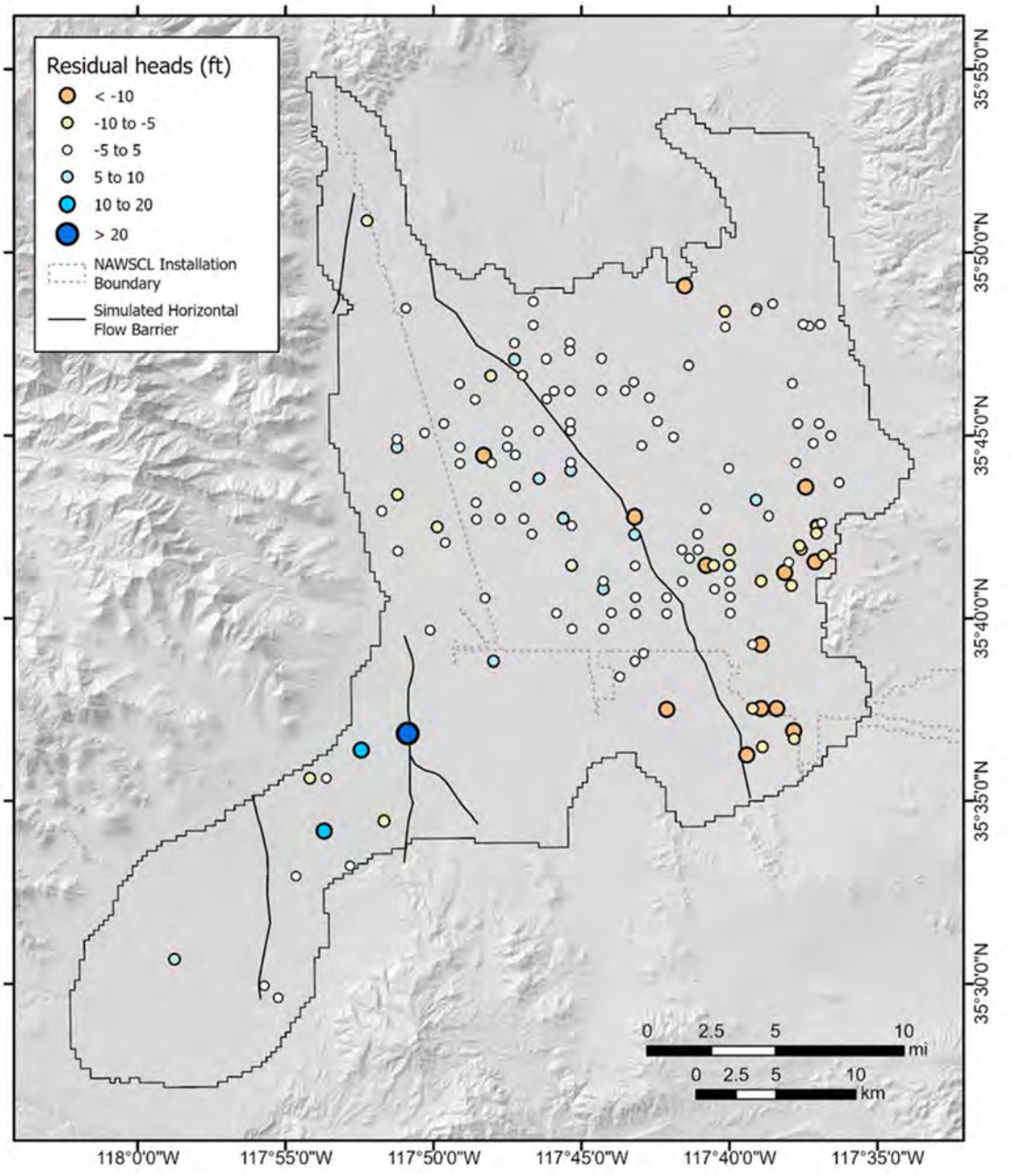


Figure 5-10. Spatial distribution of head error in the steady-state 2025 Basin Model. Negative numbers indicate that the model is under-simulating observed water levels, and positive values indicate that the model is over-simulating observed water levels.

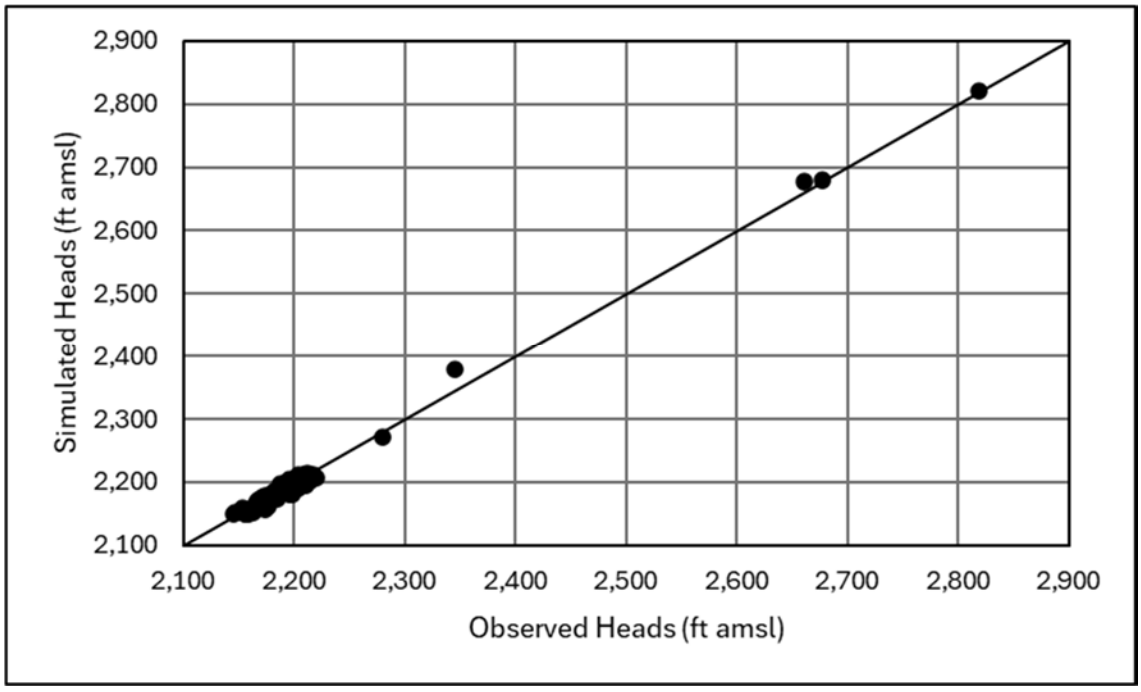


Figure 5-11. One-to-one plot comparing simulated and observed heads for the steady-state 2025 Basin Model. In a perfect model, all points would fall on the line (simulated heads are equal to observed heads). Pre-development data from areas with higher groundwater elevations is limited, and most observation data are clustered below 2,250 ft.

5.3.3. Transient Calibration Metrics

For calibration of the transient-historical model, the number of observation wells (189 wells) was greatly increased from those used in the calibration of the 2020 GSP Model (50 wells). This additional data improved the spatial distribution of targeted water levels and filled data gaps throughout the model domain. Calibration metrics are a function of the observed water level data applied to a model, so the metrics calculated for the 2020 GSP Model using the original 50 well sample are not directly comparable to the metrics calculated for the 2025 Basin Model. In order to compare the calibration of the two models, the well dataset used for the 2025 Basin Model was applied to the 2020 GSP Model, and the metrics were recalculated based on the 179 observation wells which had data available before the end of the 2020 GSP Model (CY 2016).

The transient-historical 2025 Basin Model was calibrated to within a 1.91% relative error of simulated to observed heads, based on a MAE of 14.21 feet (Table 5-4). These metrics represent a significant improvement in model calibration relative to the 2020 GSP Model, which was calibrated to a 3.58% relative error, based on a MAE of 26.44 feet, using the full set of available observation data. Model error in the 2025 Basin Model has been reduced by 12.23 feet, or 46%, relative to the 2020 GSP Model.

Table 5-4. Comparison of transient-historical model error statistics for the 2025 Basin Model and the 2020 GSP Model.

	2025 Basin Model		2020 GSP Model	
	Error (ft)	**Relative Error (%)**	**Error (ft)**	**Relative Error (%)**
Mean Error (ME)	5.94	0.80	16.14	2.18
Mean Absolute Error (MAE)	14.21	1.91	26.44	3.58
Root Mean Squared Error (RMSE)	19.55	2.63	48.75	6.59

In addition to head error statistics, it is also important to evaluate the simulated trends in water levels when assessing the calibration of a transient groundwater model. While minimizing the error in simulated heads is important, targeting observed trends in water levels ensures that a model is adequately representing an aquifers response to stress, and produces a more reliable tool for making predictions based on future stresses such as changes in pumping or recharge rates. A representative set of observation wells was selected based on spatial distribution and length of the period of record (Figure 5-12), and hydrographs comparing the observed and simulated water levels at each of these well locations are presented in Figures 5-13 to 5-17. Calibration hydrographs for all 189 observation wells used in calibration of the transient-historical model are presented in Attachment 3.

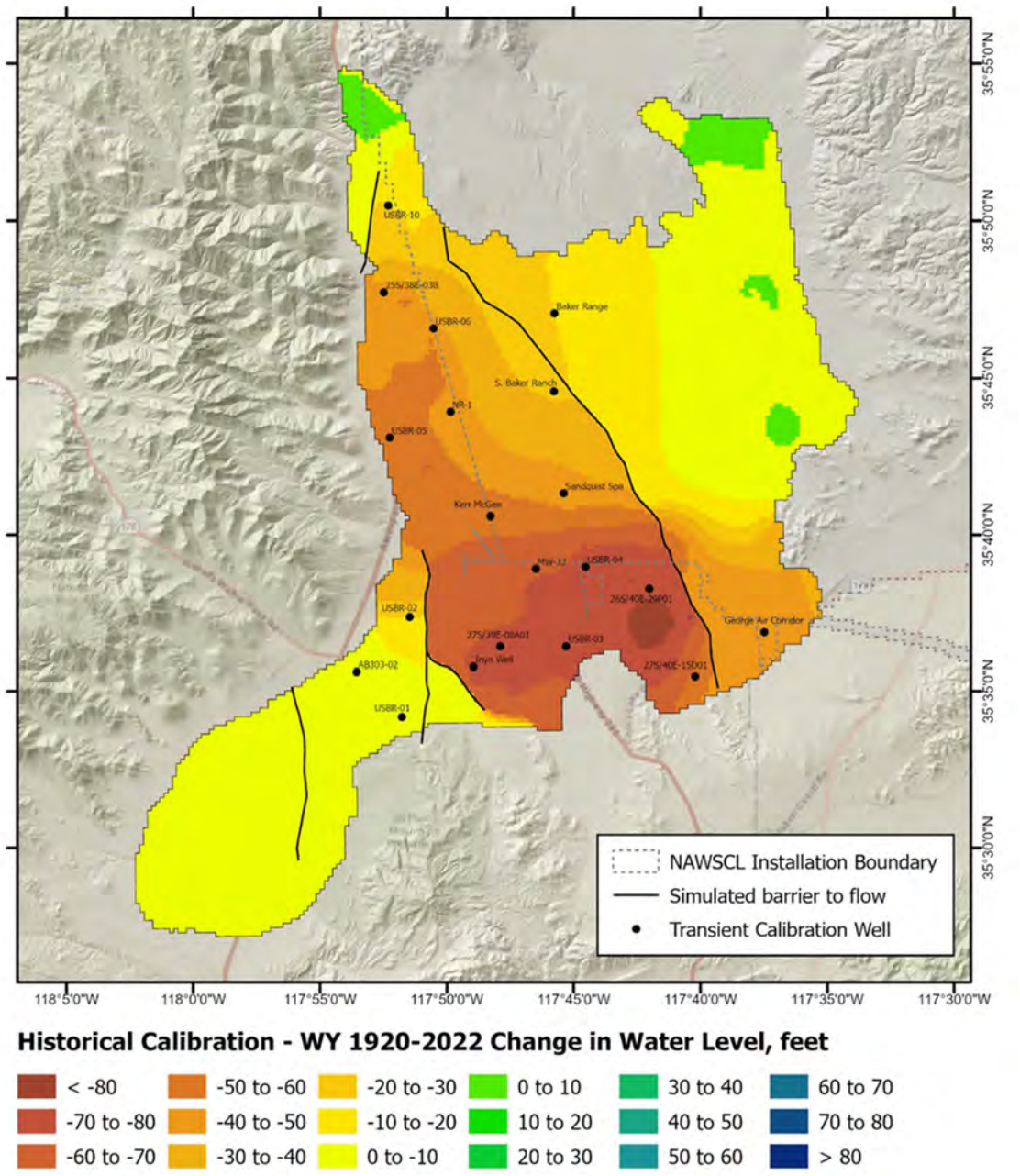


Figure 5-12. Simulated change in water level between WY 1920-2022 for the transient-historical calibration model and locations of observation wells for which comparisons of simulated and observed water levels are presented in Figures 5-13 to 5-17.

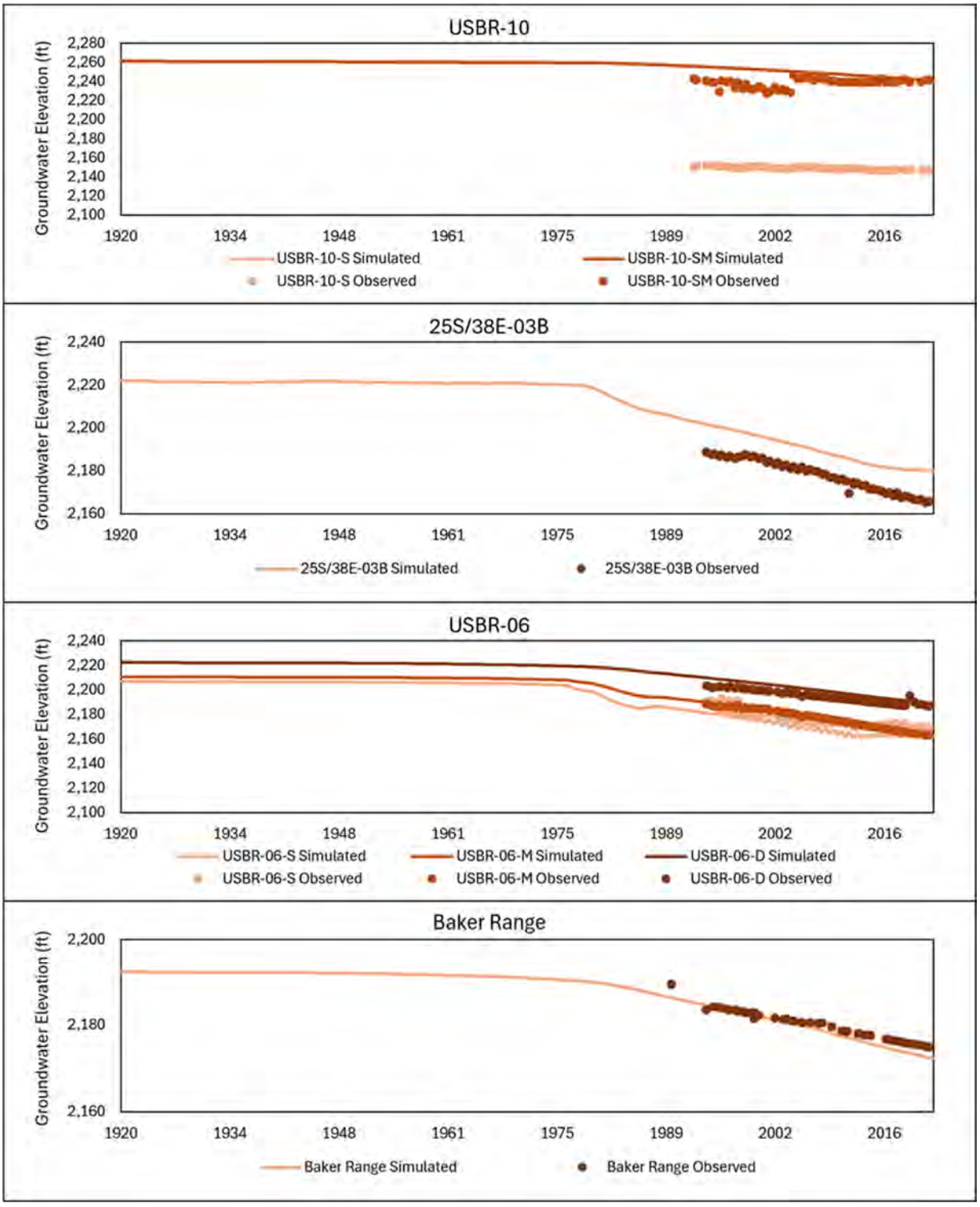


Figure 5-13. Simulated vs observed heads for representative wells within the model domain. Well locations are shown in Figure 5-12.

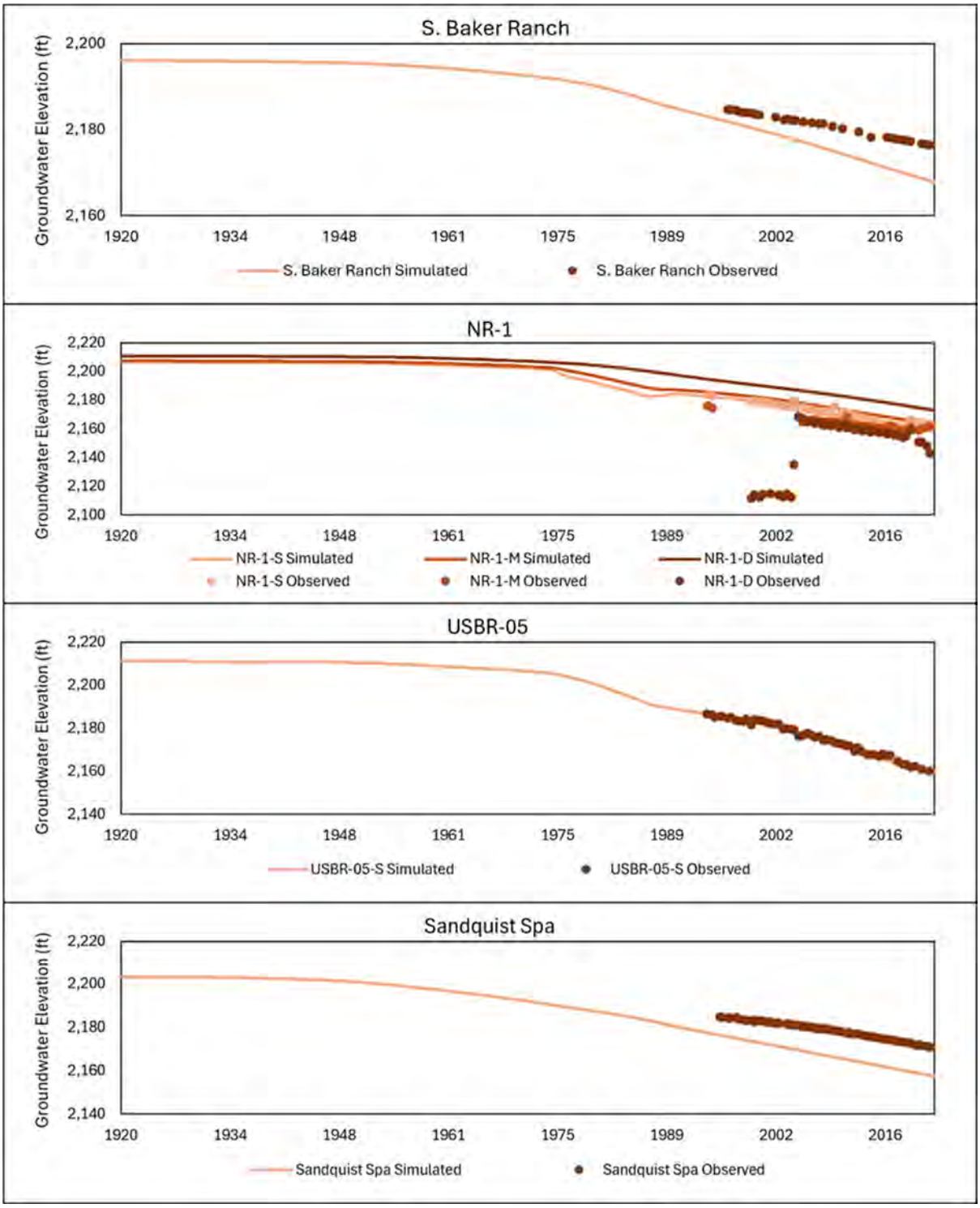


Figure 5-14. Simulated vs observed heads for representative wells within the model domain. Well locations are shown in Figure 5-12.

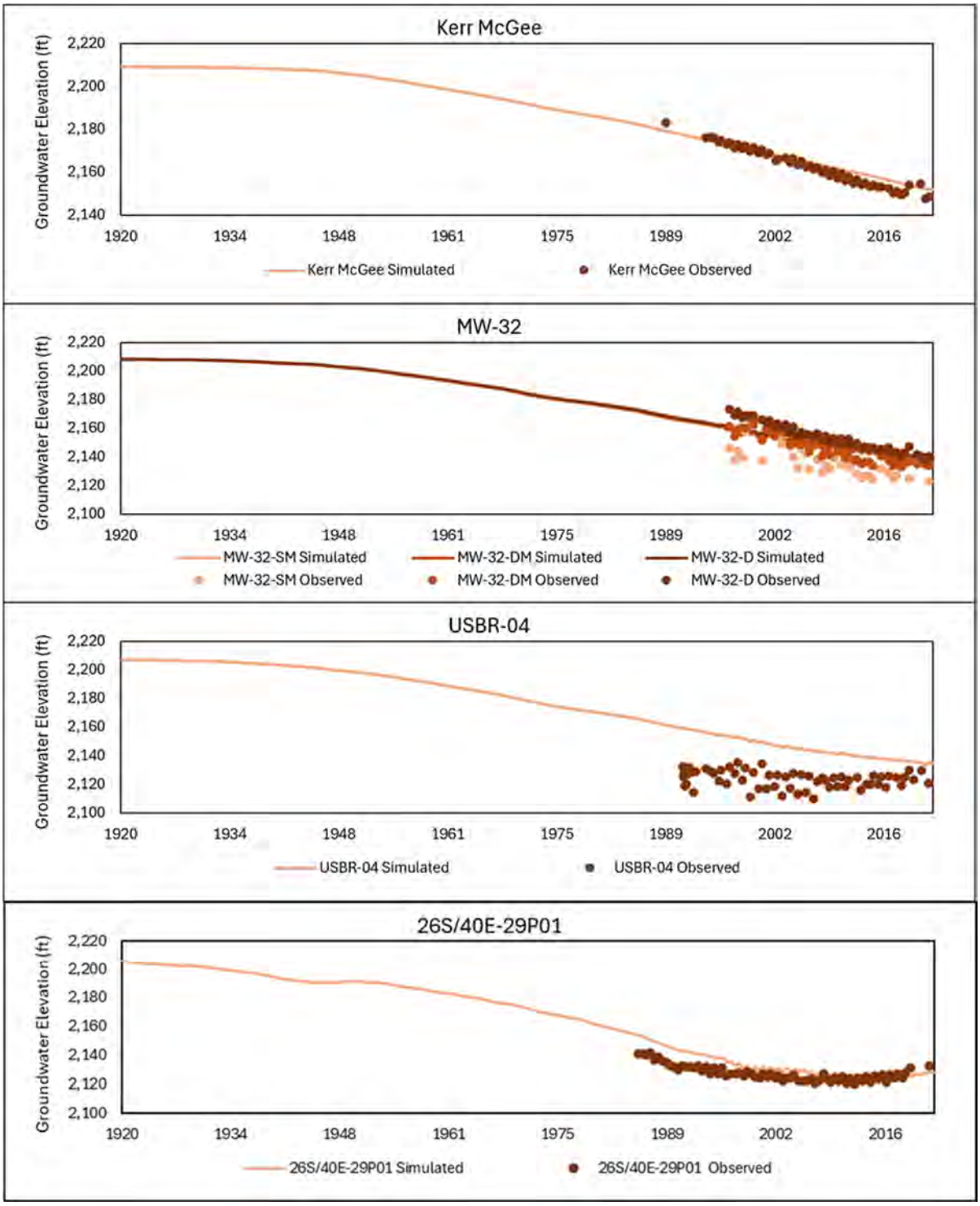


Figure 5-15. Simulated vs observed heads for representative wells within the model domain. Well locations are shown in Figure 5-12.

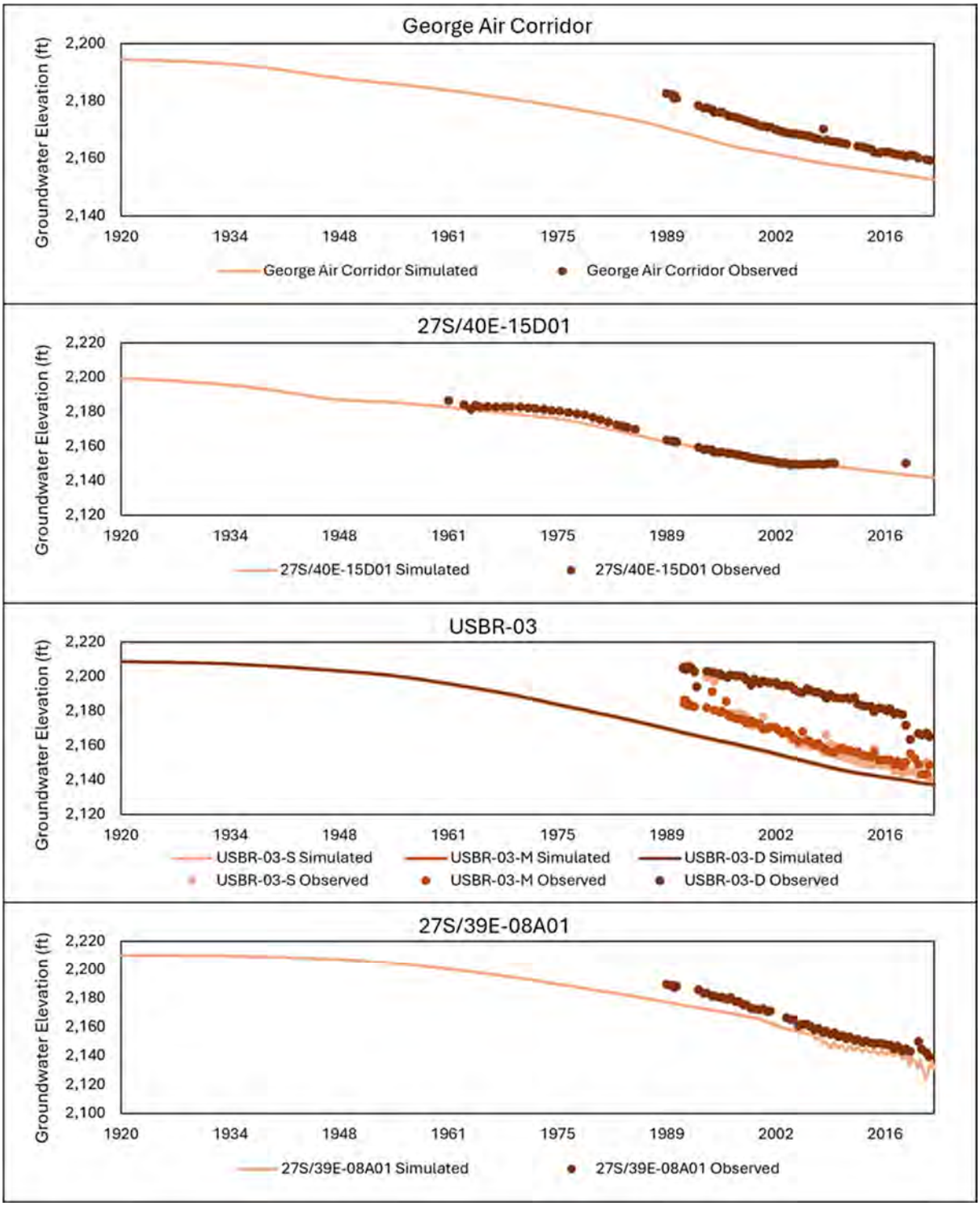


Figure 5-16. Simulated vs observed heads for representative wells within the model domain. Well locations are shown in Figure 5-12.

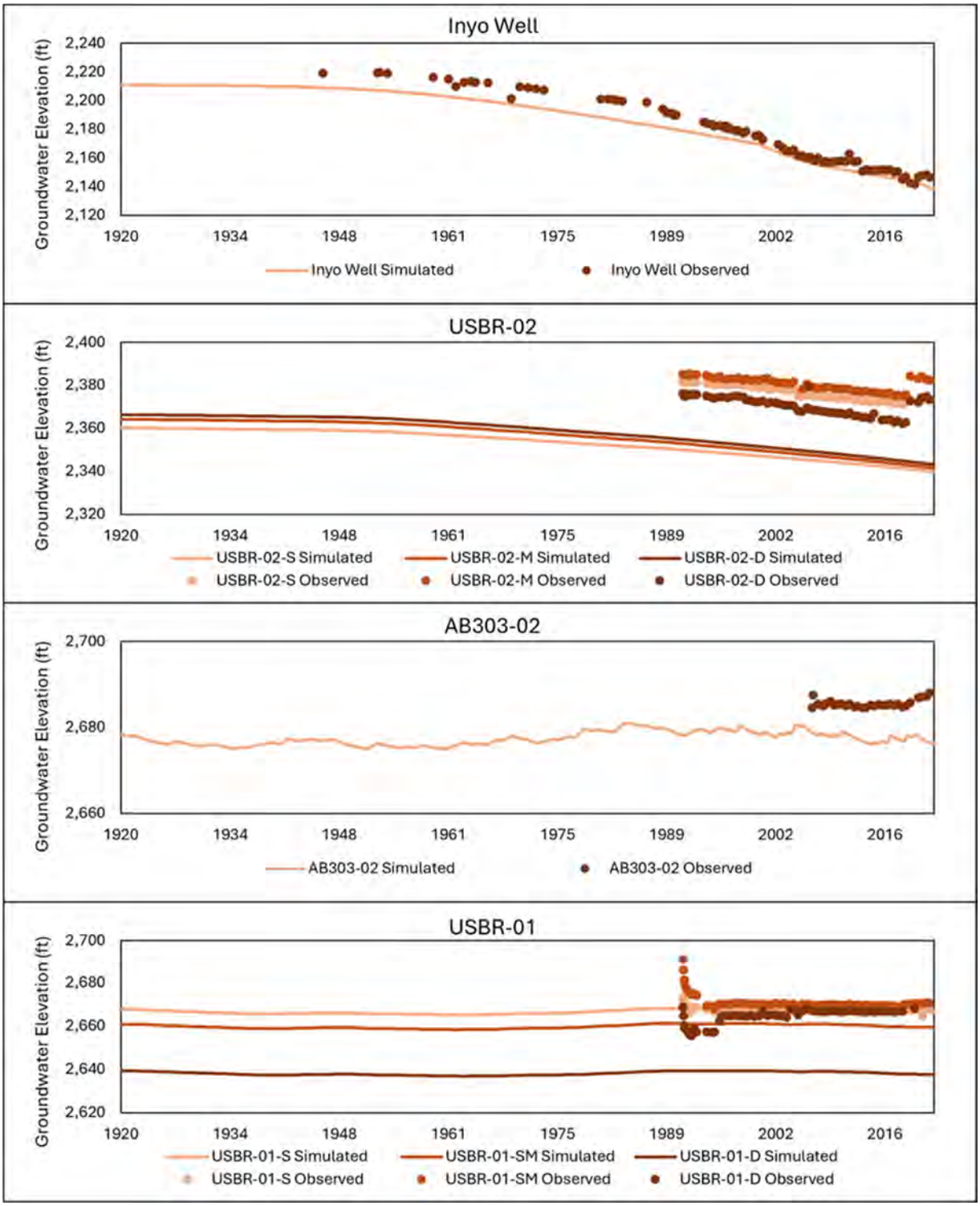


Figure 5-17. Simulated vs observed heads for representative wells within the model domain. Well locations are shown in Figure 5-12.

5.3.4. Transient Historical Flow Budgets

Using the head field generated from the steady-state calibration model as the initial condition, the transient-historical model was run simulating WY 1921-2022, using the aquifer properties and boundary conditions described in Sections 5.1, 5.2.3, and 5.3.1. The resulting simulated flow budget is dominated by the pumping discharge rate (Figure 5-18). Outflows to bare soil and vegetated ET decrease from 7,600 AFY in WY 1921 to 4,122 AFY in WY 2022. The imbalance between simulated recharge and discharge is reflected in the change in storage (Figure 5-19). The simulated cumulative loss in storage over WY 1921-2022 is approximately 1.5 million acre-feet.

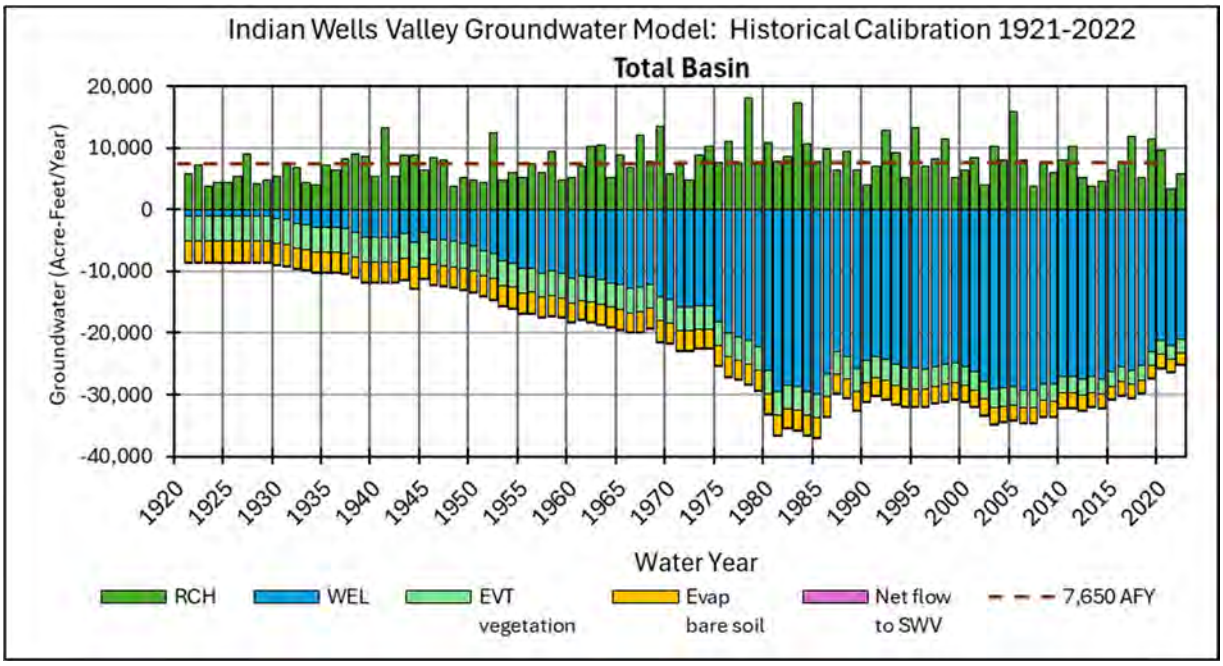


Figure 5-18. Simulated flow budget for the 2025 Basin Historical Calibration Model, showing rates of mountain block/mountain front recharge (RCH), pumping (WEL), vegetated evapotranspiration (EVT vegetation), bare soil evaporation (Evap bare soil), and flow to Salt Wells Valley (Net flow to SWV).

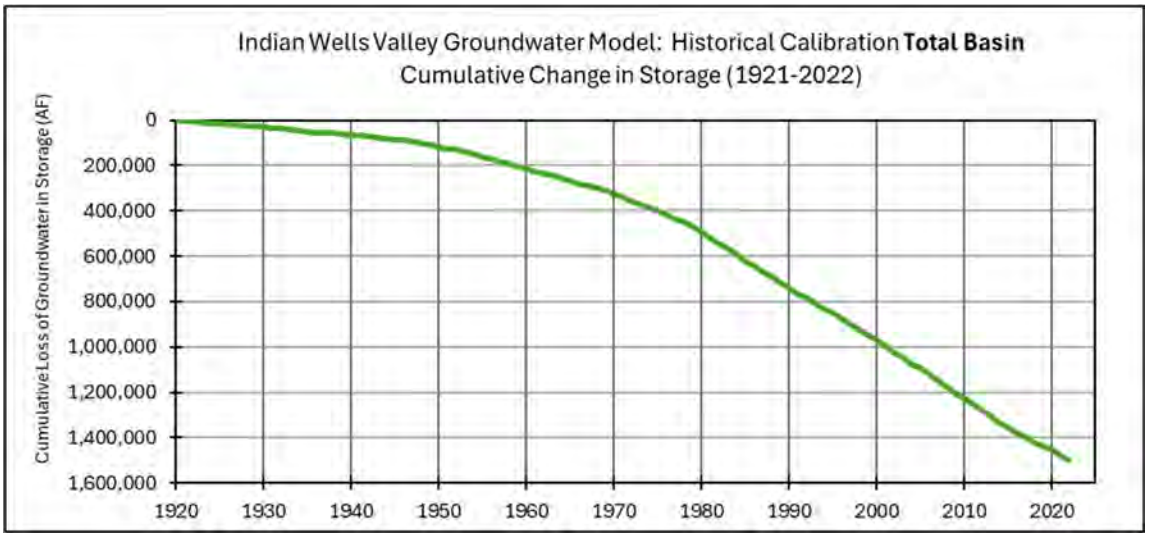


Figure 5-19. Simulated cumulative change in storage for the 2025 Basin Historical Calibration Model.

5.4. Sensitivity Analysis

A simple analysis was performed to assess the sensitivity of the model to mountain front recharge. Two simulations were run over the transient-historical time period (WY 1921-2022), simulating the effect shifting the assigned mountain front recharge rate by ±10% (Figure 5-20). For each simulation, a steady-state stress period was also run with the recharge rate adjusted by ±10% to generate a corresponding initial condition for each model – thus, these sensitivity models test the sensitivity of the model to differences in the long-term equilibrium recharge rate. All other model parameters remained the same as in the calibrated transient-historical model, and the results of the two sensitivity models were compared to the calibration model.

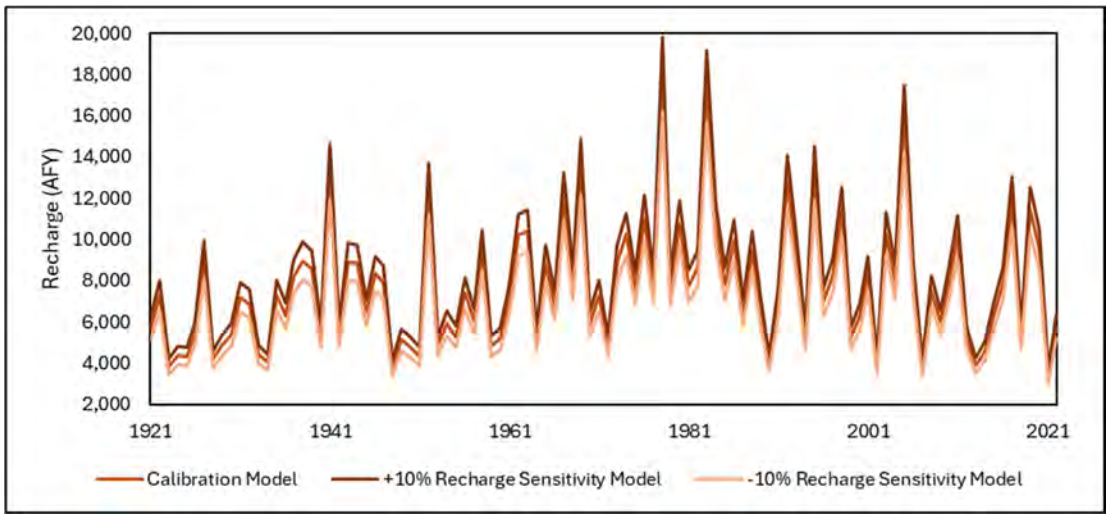


Figure 5-20. Simulated recharge rates for the transient-historical calibration model and the two recharge sensitivity models.

The resultant head fields for the two sensitivity models were assessed by subtracting the head field for the calibrated transient-historical model for the final stress period of WY 2022 (Figure 5-21). The results are near mirror images of each other. Both models show larger differences in heads in the El Paso subarea and in the northwest portion of the model domain near the boundary with Rose Valley. The smallest differences in heads occur in the eastern side of the model domain in the area of the phreatophyte and bare soil ET zones and are on the order of 0-2 ft in that area. The average difference in heads relative to the transient-historical calibration model is 9.2 and -9.6 ft for the +10% and -10% mountain-front recharge sensitivity models, respectively. The median difference in heads for the two sensitivity models is 3.9 and -4.1 ft, respectively.

Hydrographs comparing simulated water levels for the transient-historical calibration model with each of the two sensitivity models were generated to assess temporal changes in the difference in heads between these models (Figure 5-22 to 5-24). Results were assessed for each of the representative set of observation wells presented in Section 5.3.3 (Figure 5-21). At each of these wells, the temporal variability is very small in terms of the difference in heads between the transient-historical calibration model and the two sensitivity models. While the magnitude of the simulated water levels is greatly affected by the change in recharge at some of these wells, the simulated trends in water levels are overwhelmingly dominated by pumping.

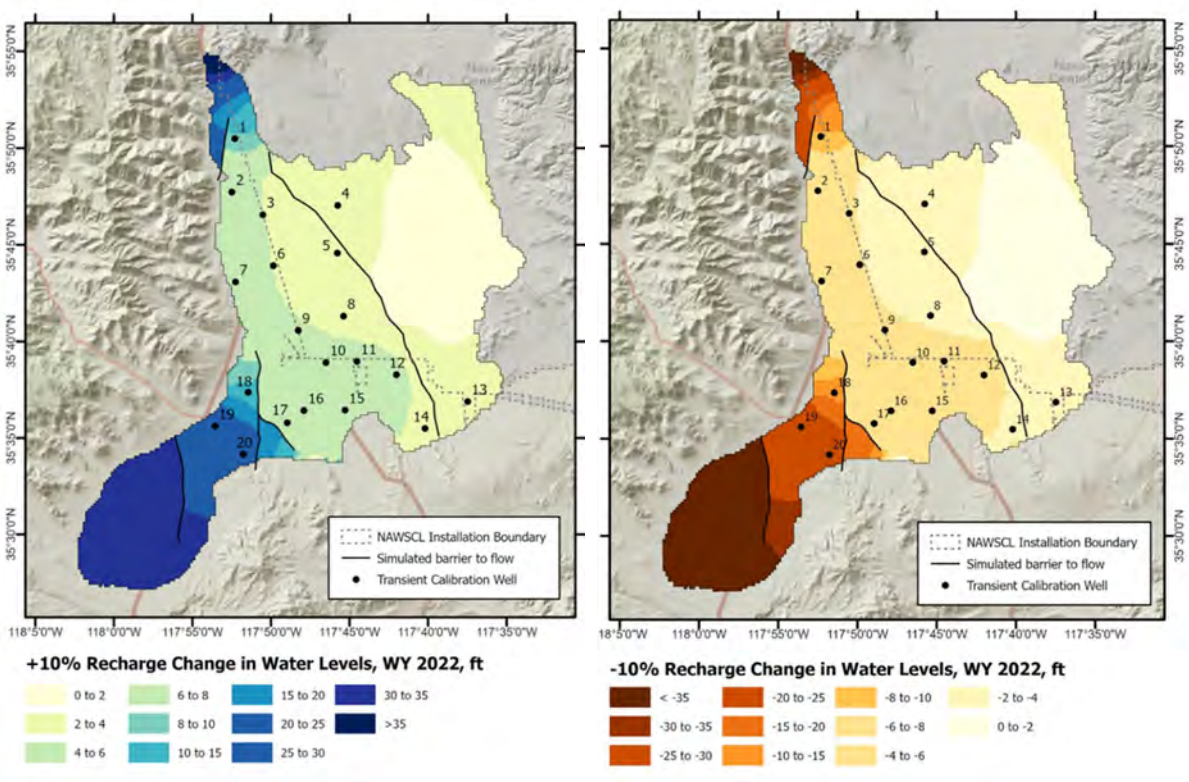


Figure 5-21. Difference in water levels between the 2025 Basin transient-historical calibration model and the +10% Recharge Sensitivity model (left), and the -10% Recharge Sensitivity model (right) for the end of WY 2022

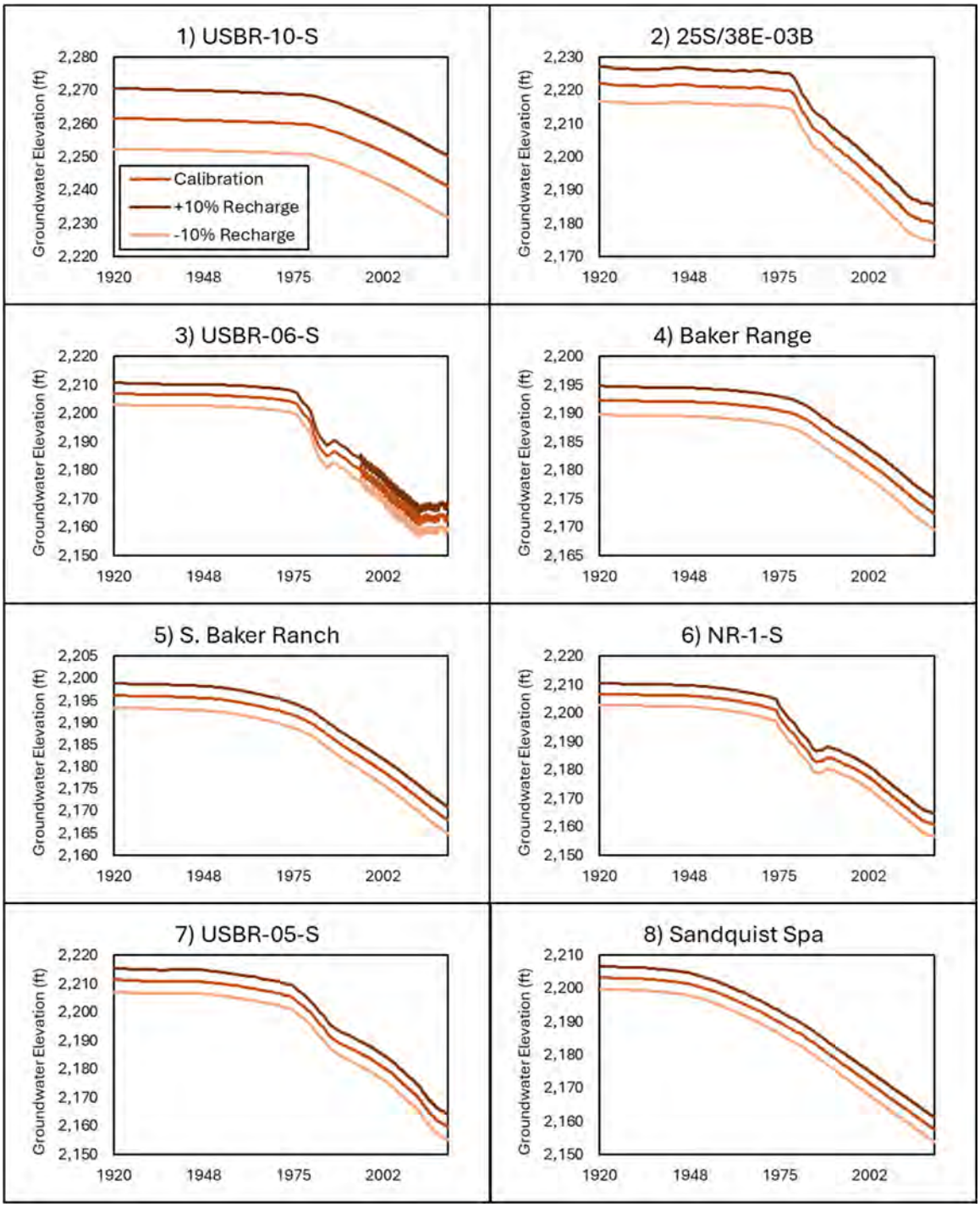


Figure 5-22. Simulated groundwater levels for the transient-historical calibration model and the two recharge sensitivity models at representative wells within the model domain. Well locations are shown in Figure 5-21.

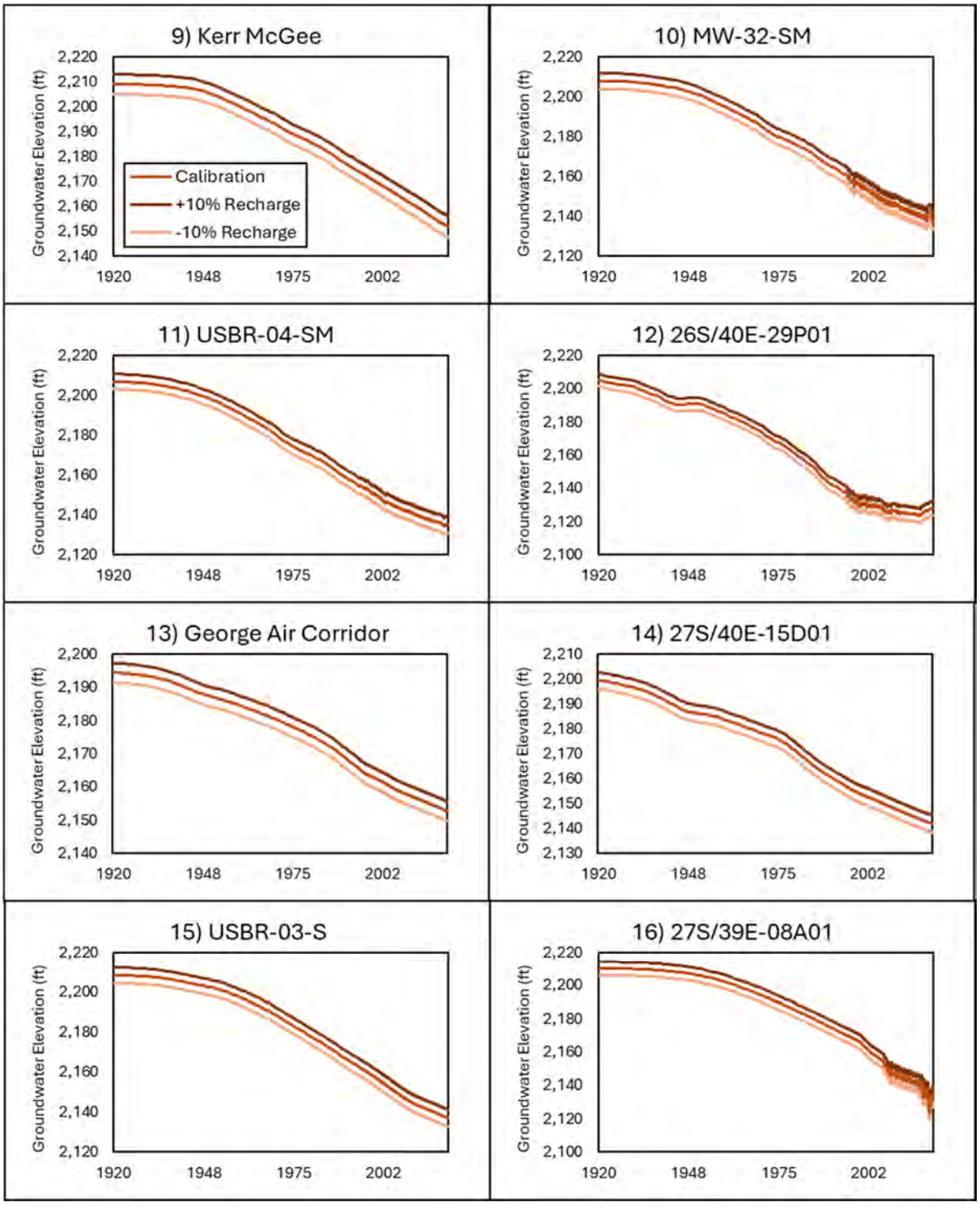


Figure 5-23. Simulated groundwater levels for the transient-historical calibration model and the two recharge sensitivity models at representative wells within the model domain. Well locations are shown in Figure 5-21.

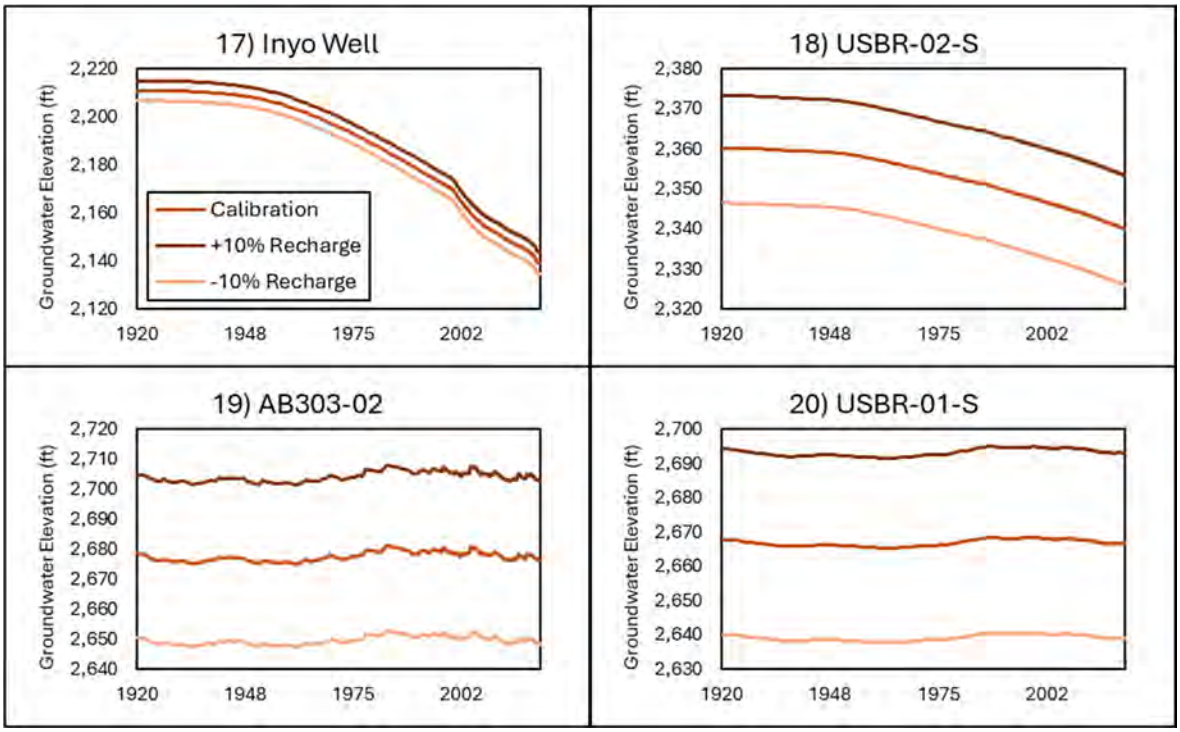


Figure 5-24. Simulated groundwater levels for the transient-historical calibration model and the two recharge sensitivity models at representative wells within the model domain. Well locations are shown in Figure 5-21.

Simulated evapotranspiration rates (Figure 5-25) and cumulative change in storage (Figure 5-26) for the two sensitivity models were also compared to the transient-historical calibration model. Trends in simulated ET in the two sensitivity models closely follow those in the transient-historical calibration model but converge towards the flow rate from the calibration model as time passes. Over the simulated time period (WY 1921-2022), the difference between ET simulated in the sensitivity models and the ET simulated in the calibration model decreases by 220-240 AFY (Figure 5-25).

Differences in the cumulative change in storage between the two sensitivity models and the transient-historical calibration model are small relative to the total cumulative change in storage but tell an interesting story. The excess storage depletion for each of the two sensitivity models is calculated as the cumulative change in storage for each model less the cumulative change in storage for the calibration model (Figure 5-26). Counterintuitively, results show that for the WY 1921-1980 time period, less water is captured from storage in the -10% Recharge Sensitivity Model relative to the calibration model, while more water is captured from storage in the +10% Recharge Sensitivity Model relative to the calibration model. Following WY 1980, the trend reverses. The reason this occurs is because increasing or decreasing mountain-front recharge results in a corresponding increase or decrease in outflows in the model – primarily ET in this case. Most pumping within the model domain occurs well away from the phreatophyte and bare soil ET zones, and on the other side of the Little Lake fault zone which acts as a barrier to flow (Figures 3-11 and 4-3). As pumping begins in WY 1921, declines in water levels (and reduction in storage) occurs primarily on

the west side of the Little Lake fault zone. In the +10% Recharge Sensitivity Model, losses in storage in the pumping areas are reduced by the higher mountain-front recharge rate. However, the evaporative demand in the ET zones has also been increased relative to the calibration model. The distance from the pumping area and the fault zone acting as a barrier to flow result in a lag between the onset of water level declines and the arrival of that signal to the ET zones. Since ET is simulated as a head-dependent boundary, the total simulated ET outflow remains relatively flat until approximately WY 1980, at which point water levels in the ET zone begin to decline and the trend reverses.

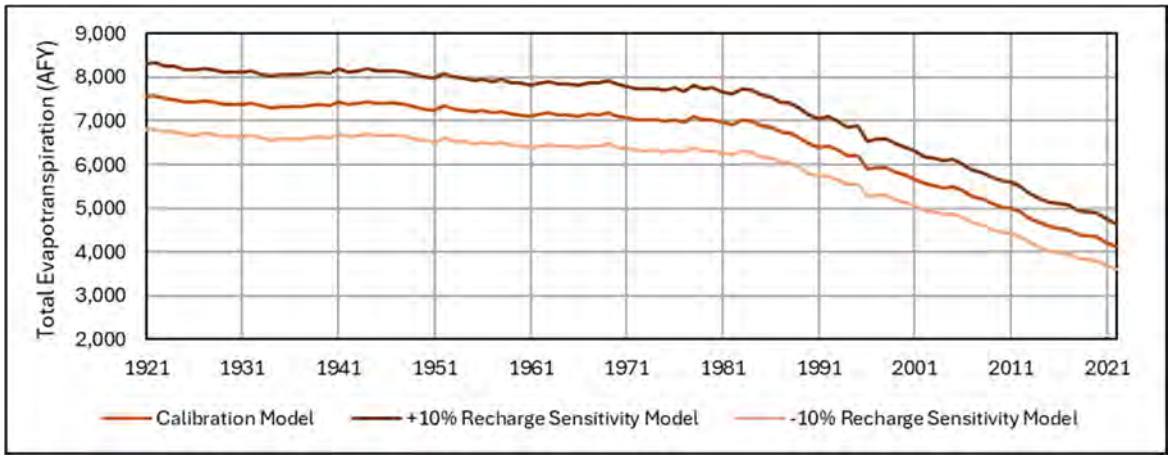


Figure 5-25. Simulated total evapotranspiration (bare soil + phreatophyte ET) for the transient-historical calibration model and the two recharge sensitivity models.

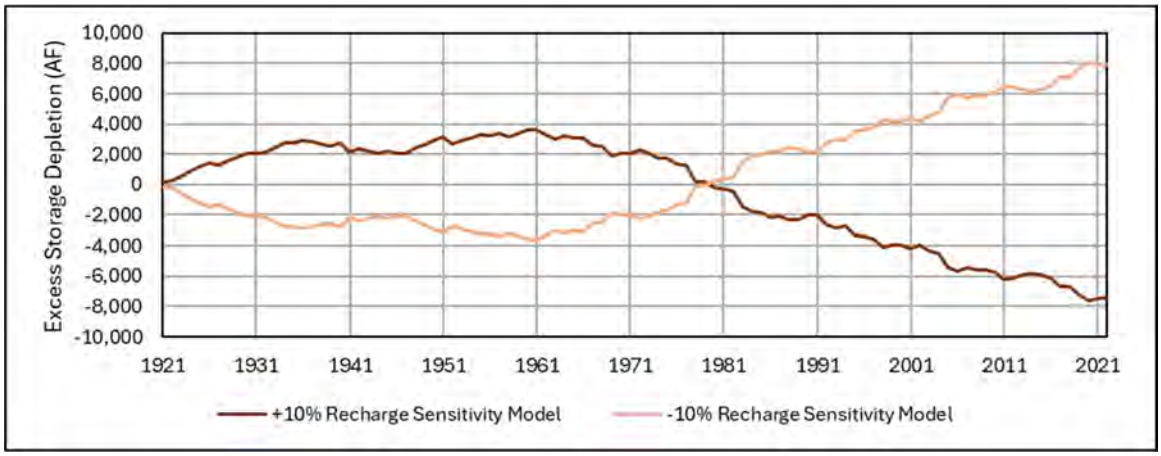


Figure 5-26. Excess storage depletion for the two recharge sensitivity models relative to the transient-historical calibration model. Negative values indicate cumulative losses from storage that are less than those from the transient-historical calibration model, positive values indicate cumulative losses from storage that are greater than those from the transient-historical calibration model.

6. 2025 BASIN MODEL SCENARIOS

Aquifer properties and simulated water levels derived from the calibration model were used to parameterize a predictive model to serve as a basis for comparison to examine the effects of 1) changes in the rates and spatial distribution of pumping and 2) changes in recharge and evapotranspiration rates due to climate change. Pumping rates for WY 2020-2022 are identical to those used in the last two years of the transient-historical calibration model, and pumping rates from WY 2023 were estimated using the same methods as described in Section 4.3 and are intended to represent actual pumping for that year. This report documents the development of the Baseline Scenario and subsequent climate change scenarios but does not detail the development of any additional pumping scenarios, though they are briefly described in Section 6.2.

6.1. Baseline Scenario

The Baseline Scenario was developed to represent a 'No Action' pumping scenario which would continue current rates of pumping while allowing for an increase in population. Pumping rates for WY 2020-2023 were defined based on historical rates as described earlier in this report. Pumping rates for WY 2024-2070 were defined for most well types using average pumping for WY 2020-2023. Total pumping at NAWSCL wells was held at a constant 2,041 AFY, rural domestic pumping was assigned an annual 1% growth rate, and IWVWD pumping was defined based on the Urban Water Management Plan (UWMP) (Figure 6-1).

Results show continued declines in water levels through the majority of the basin, with the deepest drawdowns occurring in the southwest pumping area (Figure 6-2). The maximum predicted drawdown over the WY 2020-2070 time period is 62 ft. Of this, 37 ft occurs between WY 2040-2070. Vegetated and bare soil ET decline from 2,271 and 2,078 AFY in 2020 to 967 and 958 AFY in 2070, respectively (Figure 6-3). Results show a cumulative loss of groundwater from storage of 974,516 AF over the simulated 51-year period WY 2020-2070 (Figure 6-4).

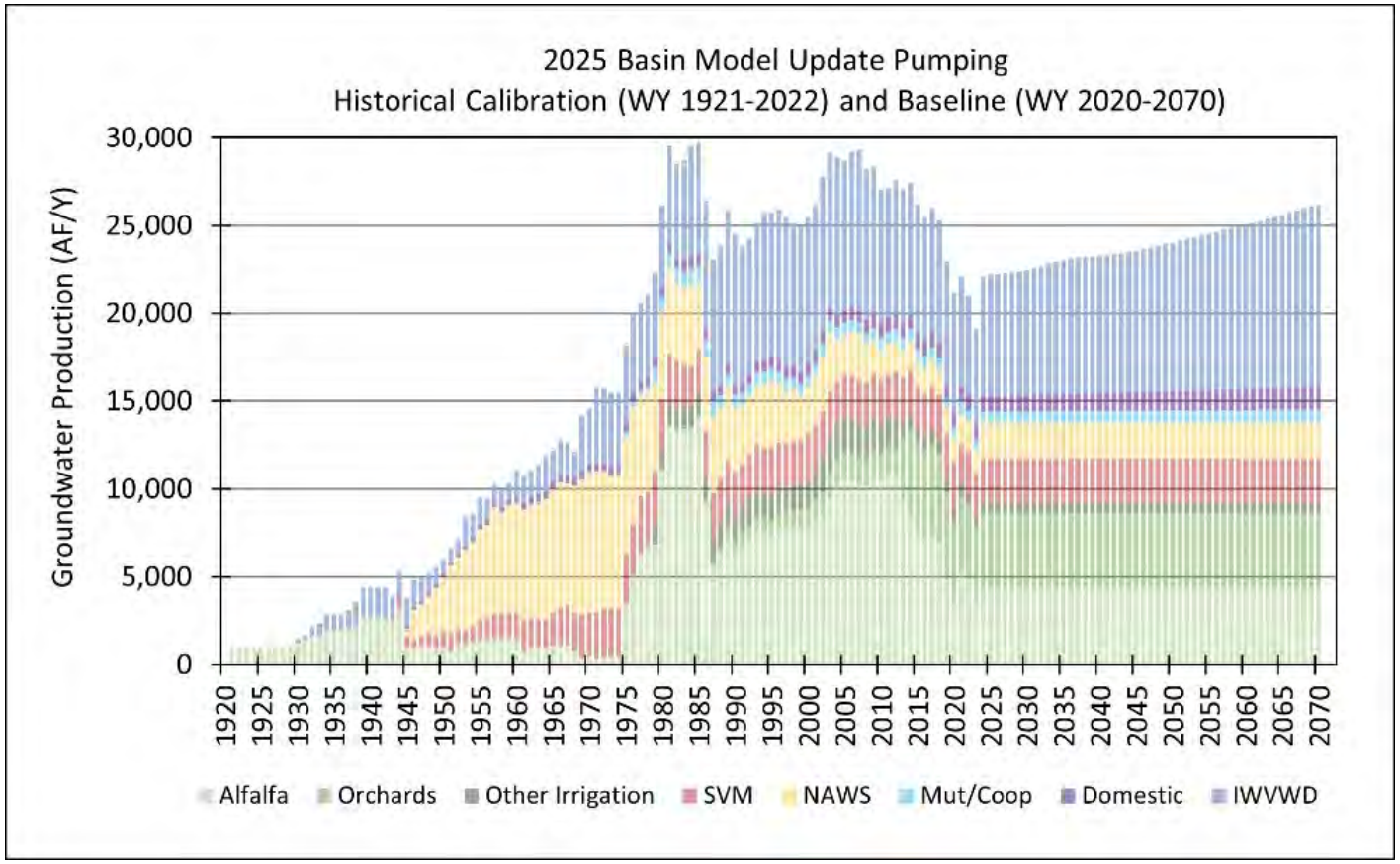


Figure 6-1. Total pumping rates assigned to each well type for the Historical Calibration period (WY 1921-2022) and Baseline Scenario (WY 2020-2070).

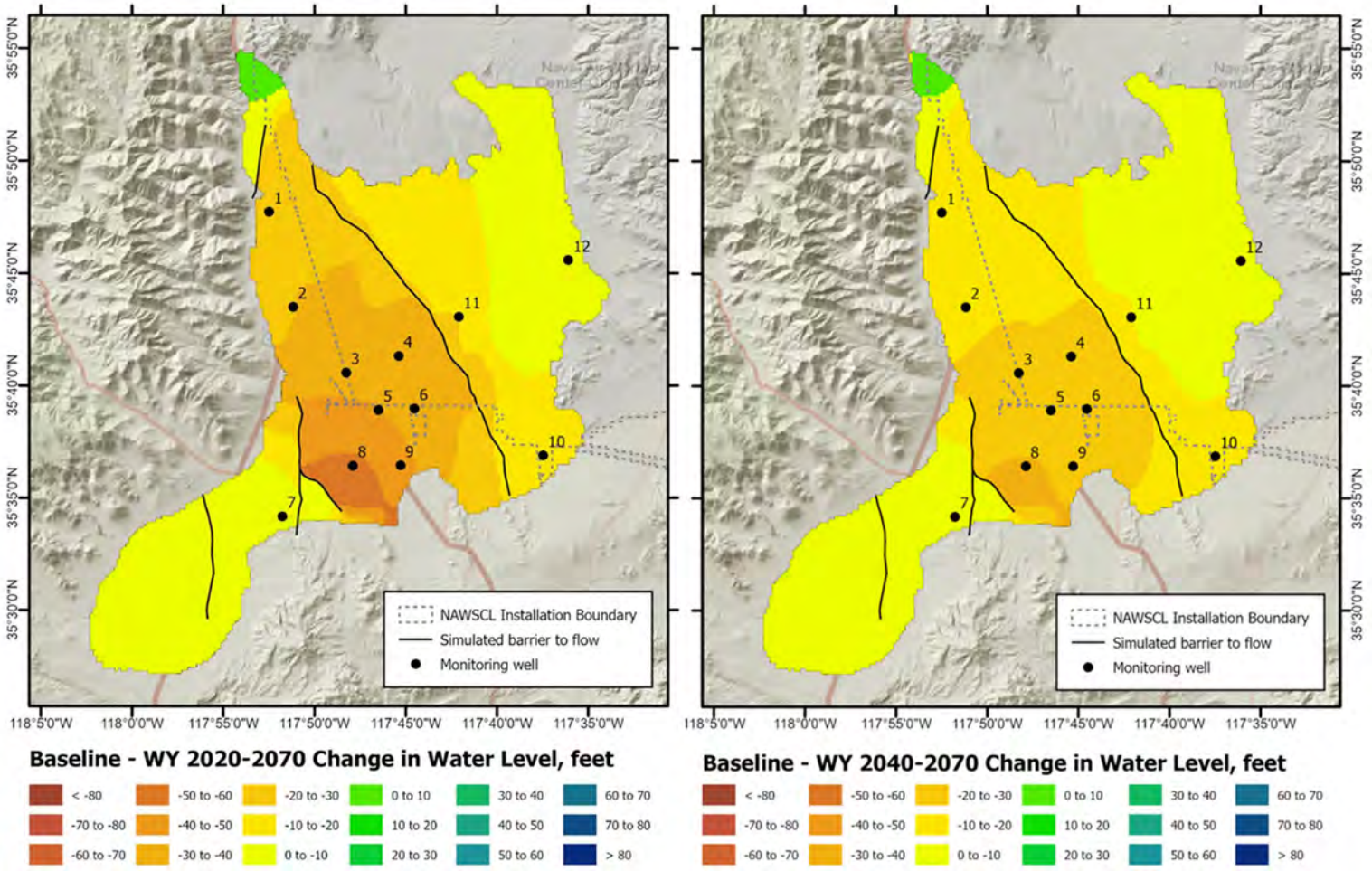


Figure 6-2. Change in water levels for the Baseline Scenario between WY 2020-2070 (left) and WY 2040-2070 (right). Hydrographs for pictured monitoring wells are presented in Attachment 2, Figures B-1 and B-2.

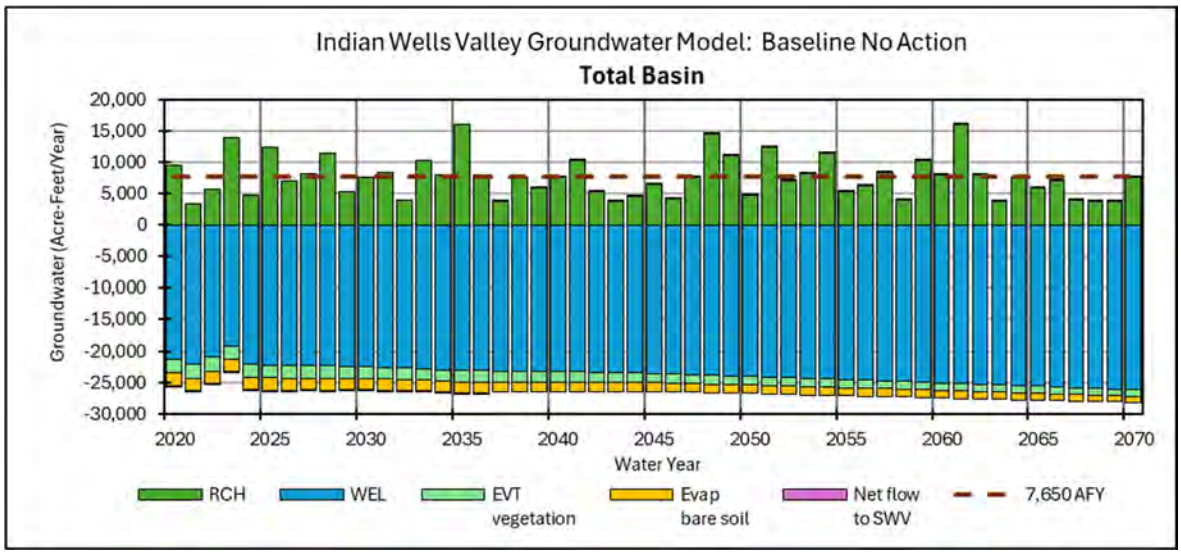


Figure 6-3. Simulated flow budget for the Baseline (No Action) Scenario, showing rates of mountain block/mountain front recharge (RCH), pumping (WEL), vegetated evapotranspiration (EVT vegetation), bare soil evaporation (Evap bare soil), and flow to Salt Wells Valley (Net flow to SWV).

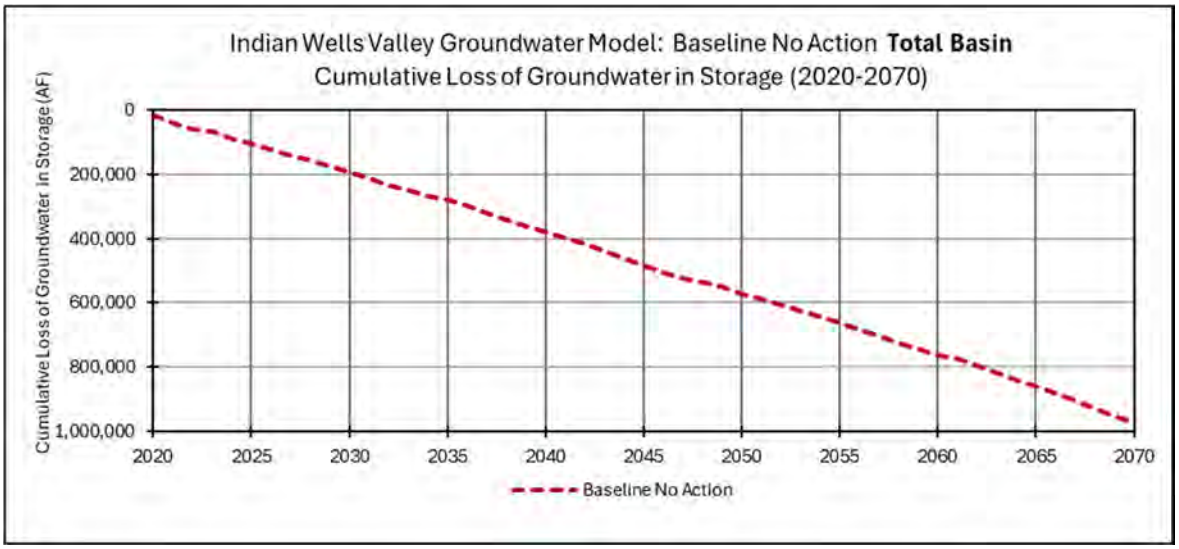


Figure 6-4. Simulated cumulative change in storage for the Baseline Scenario.

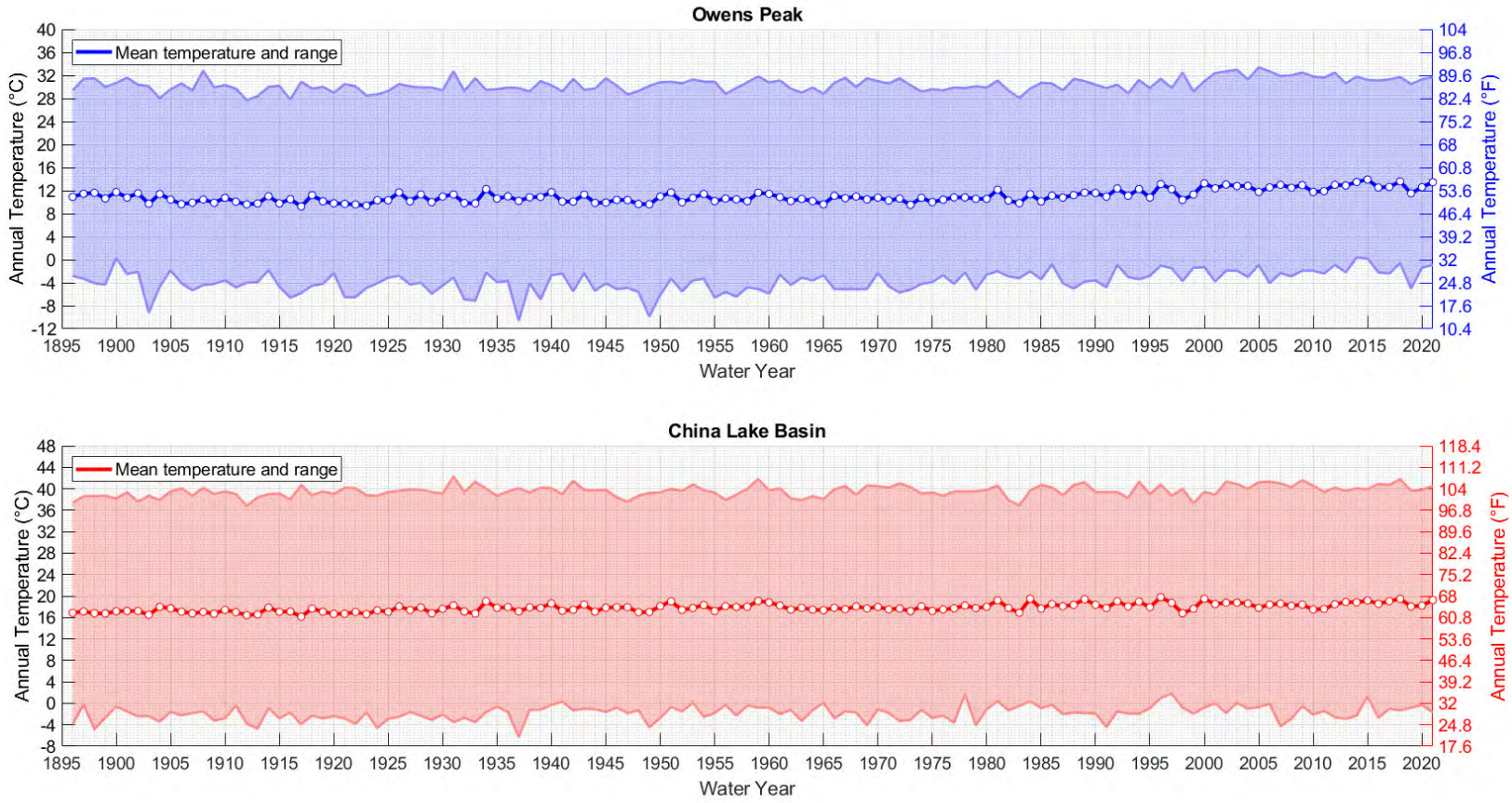


Figure 6-5. Time-series plots for water year 1896 to 2021 showing mean annual temperature and range at elevations as high as Owens Peak and as low as China Lake basin. Data are from the monthly historical Parameter-elevation Regressions on Independent Slopes Model (PRISM).

6.2. 2025 Basin Model Pumping Scenarios

The 2025 Basin Model was used to evaluate five different pumping scenarios from WY 2020-2070. Four of the scenarios contained the same recharge and evapotranspiration (except Scenario 3) assumptions used in the Baseline Scenario, with different pumping management. Scenario 1A presents the current management implementation and assumptions for reduced SVM pumping. Scenario 1B considers the current implementation with adjustments to SVM pumping. Scenario 2 considers conditions under no Groundwater Authority. Scenario 3 evaluates effects on evapotranspiration. Scenario 4 considers limited pumping in the El Paso Subarea. Scenario descriptions and simulated results from the following scenarios are included in Attachment 4:

1A	Implemented GSP
1B	Implemented GSP Adjusted SVM
2	No Groundwater Authority
3	Evapotranspiration
4	El Paso Pumping

6.3. Climate Change Scenarios

Five scenarios were simulated to assess the impact of predicted changes in precipitation and temperature resulting from climate change. Each of these scenarios was simulated using pumping rates from the Baseline model, and the effects of the potential climate change scenarios were isolated by comparing simulated results to those from the Baseline model.

Potential climate outcomes were defined using downscaled results from the Coupled Model Intercomparison Project Phase 5 (CMIP5) (Table 6-1) made available through the Cal-Adapt tool (cal-adapt.org) (Pierce et al., 2018). The Cal-Adapt tool presents a subset of downscaled Global Climate Model (GCM) results from CMIP5, selected for their ability to represent observed historical (1950-2005) climate conditions in the state of California. For each of the ten GCMs in the subset, results are presented for two Representative Concentration Pathways (RCPs). The RCP 4.5 scenario represents a medium emissions future where societies work to reduce greenhouse gas emissions, while the RCP 8.5 scenario represents a ‘business as usual’ scenario used to explore the effects of higher greenhouse gas emissions. Within the subset of ten GCMs for each RCP (4.5 and 8.5), a second subset of four models was identified that span the temperature and precipitation changes resulting in the larger subset of ten GCMs. These four models can generally be classified as warm/dry (HadGEM2-ES), cool/wet (CNRM-CM5), average (CanESM2), and ‘complement’ (MIROC5), which was chosen as the model that was most unlike the other three in order to envelope the spread of potential outcomes (Pierce et al., 2018).

Table 6-1. Subset of CMIP5 multi-model ensemble results used to estimate the range of climate impacts within the simulated area.

Modeling Center	Model	RCPs	Institution
CSIRO-BOM	ACCESS1.0	4.5, 8.5	CSIRO (Commonwealth Scientific and Industrial Research Organisation, Australia), and BOM (Bureau of Meteorology, Australia)
CCCma	CanESM2	4.5, 8.5	Canadian Centre for Climate Modelling and Analysis
NCAR	CCSM4	4.5, 8.5	National Center for Atmospheric Research
NSF-DOE-NCAR	CESM1(BGC)	4.5, 8.5	National Science Foundation, Department of Energy, National Center for Atmospheric Research
CMCC	CMCC-CMS	4.5, 8.5	Centro Euro-Mediterraneo per I Cambiamenti Climatici
CNRM-CERFACS	CNRM-CM5	4.5, 8.5	Centre National de Recherches Meteorologiques/ Centre Europeen de Recherche et de Formation Avancee en Calcul Scientifique
NOAA GFDL	GFDL-CM3	4.5, 8.5	Geophysical Fluid Dynamics Laboratory
MOHC	HadGEM2-CC	4.5, 8.5	Met Office Hadley Centre
MOHC (additional realizations by INPE)	HadGEM2-ES	4.5, 8.5	Met Office Hadley Centre (additional HadGEM2-ES realizations contributed by Instituto Nacional de Pesquisas Espaciais)
MIROC	MIROC5	4.5, 8.5	Atmosphere and Ocean Research Institute (The University of Tokyo), National Institute for Environmental Studies, and Japan Agency for Marine-Earth Science and Technology

For each of the twenty identified GCMs (10 each for RCP 4.5 and 8.5), annual maximum and minimum temperatures and precipitation totals were downloaded using the Cal-Adapt tool (Pierce et al., 2018). The Basin Model cannot directly accept temperatures or precipitation rates as inputs, so it was instead necessary to use these results to estimate changes in mountain front recharge and evapotranspiration rates over phreatophytes and bare soil, which were then used to modify the boundary conditions of the Baseline 2025 Basin model. To best replicate the methodology used to estimate recharge from precipitation applied in the transient-historical 2025 Basin model, GCM results were downloaded for the locations of the three precipitation gages relied on to estimate average mountain front precipitation for the basin (Haiwee, Laurel Mountain, and Indian Wells Canyon). The methods used to estimate changes in recharge and evapotranspiration are detailed in the following sections.

6.3.1. Estimation of Change in Potential ET due to Climate Change

Sustainable groundwater use relies on adequate rates of groundwater recharge, which are expected to be altered by climate change. Recharge is most sensitive to climate changes in arid regions where potential evapotranspiration (PET) slightly exceeds precipitation, implying that even the modest levels of aridification can substantially decrease potential groundwater recharge. (Berghuijs et al., 2024). In general, changes in precipitation and PET have disproportionately large effects on recharge rates in regions where PET slightly exceeds precipitation. The effects of future precipitation changes will likely be larger than those of future PET changes. Therefore, regional variations in total projected changes to recharge are expected to follow the patterns of precipitation-induced changes. However, it is also expected that in semi-arid to arid regions, such as in the majority of Indian Wells Valley, the effects of precipitation change on recharge are anticipated to be modulated by higher PET rates that will be predominately driven by a rising trend of increased temperature (e.g., Scanlon et al., 2006; Tillman et al., 2020; Berghuijs et al., 2024).

Observation-based recharge estimates from sites spanning most regions of the globe show that recharge fractions are strongly controlled by climate aridity (e.g., Moeck et al., 2020). In semi-arid climates, such as the higher portions of the Sierra Nevada Mountains in the groundwater basin, larger fractions of precipitation typically recharge groundwater. This recharge fraction, however, is significantly reduced with increasing aridity, often approaching nearly zero in arid climates, such as at the floors of Indian Wells Valley and China Lake basin (e.g., Berghuijs et al., 2022). On average, groundwater recharge rates estimated over large semi-arid to arid regions (40–374,000 km^2) commonly range from 0.2 to 35 mm/yr (0.008 to 1.38 in/yr), representing 0.1 to 5% of the long-term average annual precipitation (Scanlon et al., 2006).

Potential changes in groundwater recharge associated with future climate change in the updated 2025 Basin Model were accounted for by using a general approach to reduce the amount of annual precipitation available for recharge due to PET. This general approach is fundamentally based on the climate water-balance (CWB) model, which has been used to assess changes in groundwater recharge during climate change at both global and regional watershed scales (e.g., Willmott et al., 1985; Abatzoglou et al., 2018). The fundamentals of the CWB model to estimate potential groundwater recharge (GWR) are largely based on the method of Thornthwaite (1948) to derive the soil moisture budget of a given land surface area. Monthly potential *GWR/CWB* (mm) is represented by:

$$Potential\ GWR = \ CWB = P - PET \tag{1}$$

where *P* is monthly precipitation (mm), and *PET* is monthly potential evapotranspiration (mm). A major assumption in this simple model is that positive values result in a soil water surplus and therefore water is potentially available for GWR, whereas negative values represent a soil water deficit resulting in a lack of GWR. Of note, the potential for GWR is highest where groundwater levels are either shallow within thinly mantled soils, in areas of exposed rock, or along main tributary channels within mountain block settings. GWR is typically negligible to non-existent where groundwater levels are either deep in alluvial valley bottoms or shallow within playa areas in arid climates, such as across the majority of Indian Wells Valley (Flint et al., 2013).

PET was estimated using a simple radiation-based empirical model appropriate for an arid environment (Jensen and Haise, 1963). The Jensen-Haise equation is an energy-balance equation that incorporates air temperature and incoming solar radiation to predict the monthly PET rate (mm/mo) for an alfalfa reference crop, which is represented by:

$$PET = \frac{R_s}{L}[0.0252(T_{air}) + 0.078] \quad (2)$$

where R_s is incoming solar radiation at the ground surface (MJ/m^2/day) based on a site's latitude and clear sky conditions, L is latent heat of vaporization (MJ/kg) calculated from mean monthly temperature and based on empirical equations (e.g., Shuttleworth, 2012), and T_{air} is mean monthly temperature (ºC). Historical monthly temperature data for water year 1896 through 2021 were used from the 4-km grid Parameter-elevation Regressions on Independent Slopes Model (PRISM) for two sites representing some of the highest and lowest elevations in the groundwater basin. Temperature data from a site in the vicinity of Owens Peak (latitude: 35.7385; -117.9970) at an elevation of 8280 ft (2524 m) was selected to characterize mountain block recharge areas, whereas temperature data from a site at the depocenter of China Lake playa (latitude: 35.7390; -117.5983) at an elevation 2159 ft (658 m) was selected to provide maximum estimates of PET within a valley bottom setting (Figure 6-6).

Although the Jensen-Haise equation is useful for arid environments it was originally developed for reference crop ET. As a result, the equation was modified to account for bare-soil evaporation since the majority of the groundwater recharge areas in the groundwater basin are in the Sierra Nevada Mountains that are sparsely covered by vegetation and thinly mantled by colluvial soils or contain bare rock. The monthly bare-soil evaporation (E_o) rate (mm) is represented by:

$$E_o = \left[\frac{R_s}{L}[0.0252(T_{air}) + 0.078]\right] f_{soil} \quad (3)$$

where f_{soil} is a bare-soil evaporation resistance factor. The monthly PET values were aggregated at annual timesteps (mm/yr) for the 125-year period of record. The E_o model for the China Lake basin site was calibrated to eddy-covariance measurements from the margin of the playa in 2015 (McGraw et al., 2016). A value of 0.056 for f_{soil} was iteratively determined to reduce PET and match a measured eddy-covariance rate of 115.03 mm/yr for bare-soil evaporation from playa soils with relatively high moisture contents. This resistance factor was also applied to the Owens Peak site to estimate potential E_o for mountain soil settings due to a lack of site-specific eddy-covariance data from sparsely vegetated and exposed bedrock surfaces in the groundwater basin or other areas in the Sierra Nevada (Figure 6-6). It is acknowledged that there will likely be differences in E_o between playa and mountain soil types in the Sierra Nevada due to contrasting terrain and hydrologic conditions, soil textures, and vegetation type and density (e.g., Wolf et al., 2024).

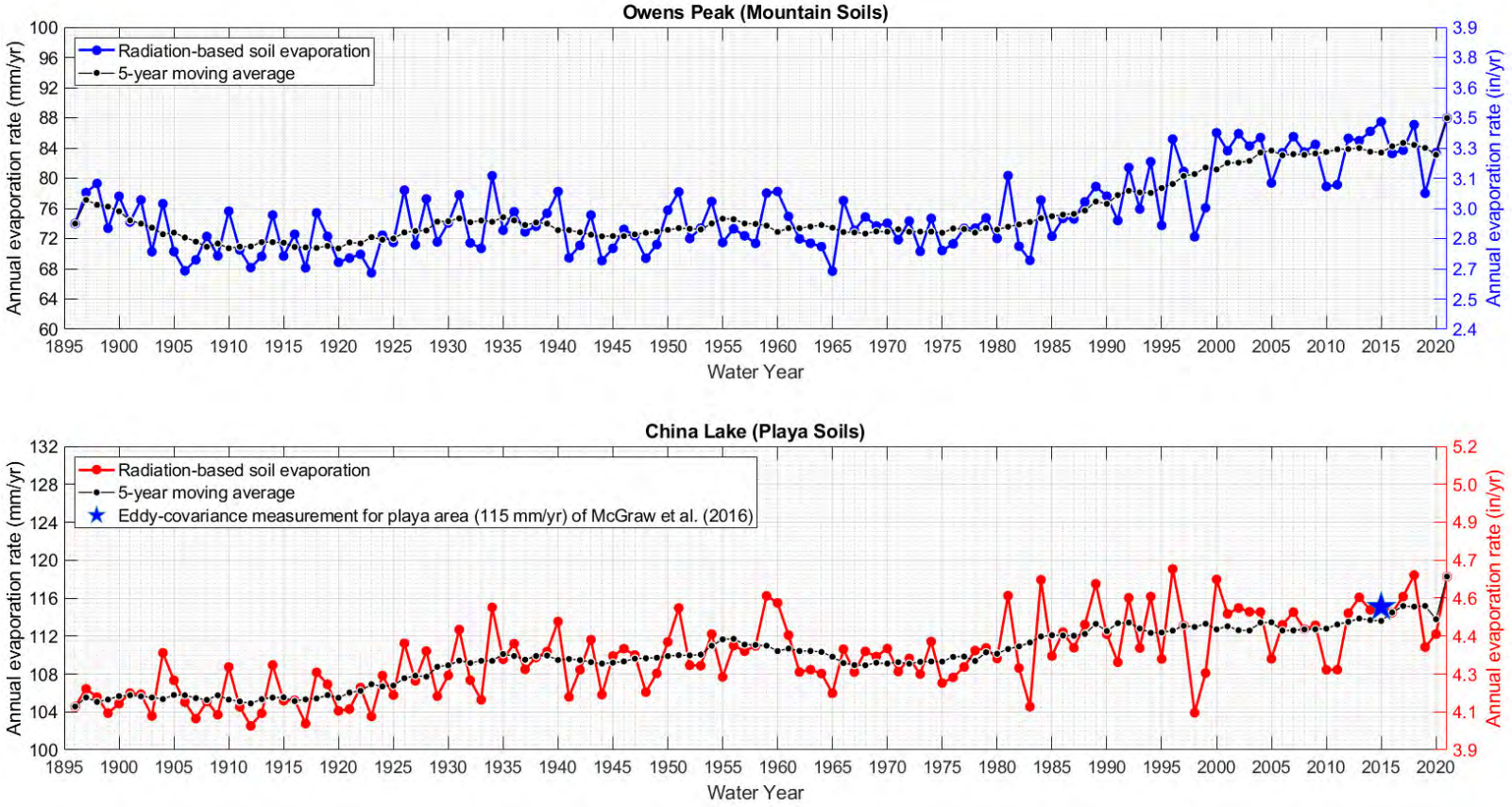


Figure 6-6. Time-series plots for water year 1896 to 2021 showing soil evaporation for mountain soil settings at elevations as high as Owens Peak and for playa soil settings at elevation as low as China Lake basin. Soil evaporation is based on Jense-Haise (1963) radiation-based empirical model that requires temperature, latent heat of vaporization, and incoming solar radiation at the ground surface. The empirical model is calibrated for annual bare-soil evaporation from eddy-covariance station measurements in 2015 for areas within and adjacent to China Lake playa (blue star).

Since projected precipitation patterns are significantly more variable compared to the steady trend of increasing temperature during future climate change, the approach used to account for climate change in the updated 2025 Basin Model involved developing empirical relations between PET and temperature. Calculated monthly bare-soil evaporation for the Owens Peak and China Lake playa sites versus associated monthly temperature from the 125-year historical period of record were plotted to develop an empirical equation from regression analysis (Figure 6-7).

Using the exponential function derived from the regression analysis, an index soil evaporation rate was calculated using the observed average annual temperature used for calibration of the GCMs over the 1950-2006 time period, taken from the locations of the three precipitation gages (Haiwee, Laurel Mountain, and Indian Wells Canyon). The same regression was used to calculate an annual average soil evaporation rate for each year in each of the twenty GCMs. The historical index soil evaporation rate (85.7 mm/yr) was subtracted from each year's calculated value to derive the change in soil evaporation due to climate change for that year. The calculated change in soil evaporation relative to the historical index rate for each of the twenty GCMs is presented in Figure 6-8. For the purposes of modeling, the change in soil evaporation was considered to be equal to the change in PET.

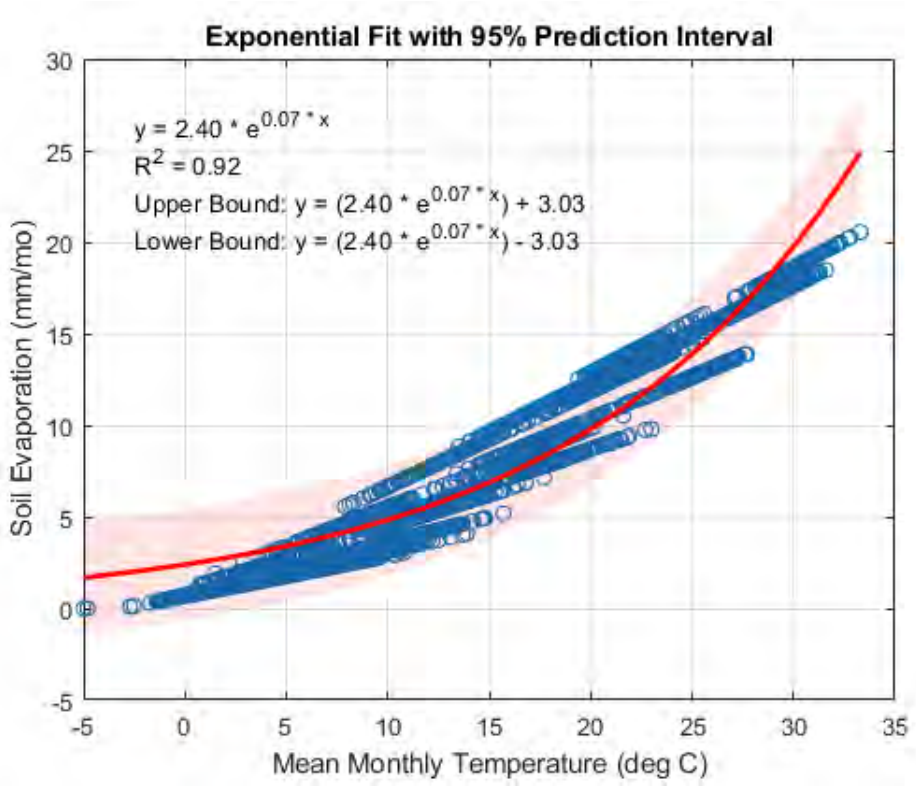


Figure 6-7. Plot showing empirical relations between estimated monthly soil evaporation derived from the Jense-Haise (1963) radiation-based empirical model versus associated mean monthly temperature. Also shown is an exponential function fit to data with 95% prediction limits. Monthly temperature data from the Parameter-elevation Regressions on Independent Slopes Model (PRISM) for Owens Peak and China Lake playa areas for the period water year 1896 to 2021 were used.

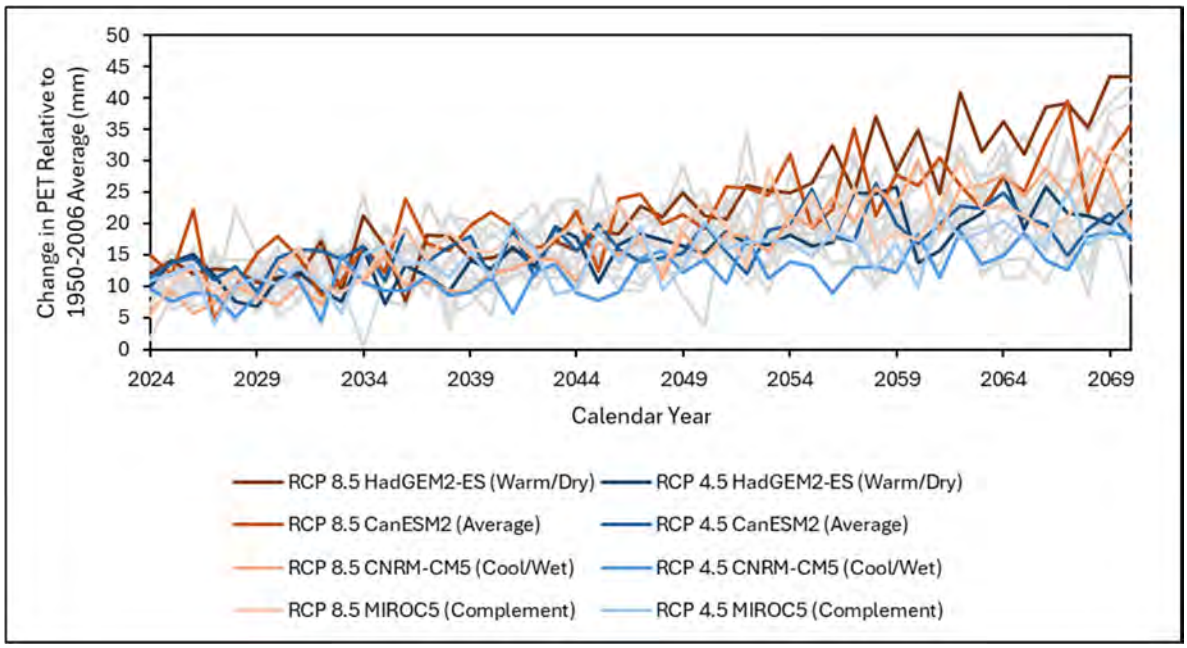


Figure 6-8. Estimated change in PET calculated from temperatures from each of the twenty GCMs relative to average PET calculated using average air temperatures for 1950-2006.

6.3.2. Estimation of Change in Mountain Front Recharge due to Climate Change

Observed average precipitation at the three gages used to estimate average mountain front precipitation for the basin (Haiwee, Laurel Mountain, and Indian Wells Canyon) for the time period 1950 to 2006 was compared to the observed average precipitation at the locations of these gages as reported in the GCM output. The average observed precipitation used for calibration of the GCM models (6.6 inches) was slightly lower than the actual average observed precipitation over the 1950-2006 time period (6.86 inches). To account for this discrepancy, all predicted precipitation rates from the GCMs were scaled by this ratio. The estimated change in PET for each year in each GCM was then subtracted from the scaled predicted precipitation rate to account for additional losses from the shallow soil zone as a result of increasing temperatures, which are expected to reduce the total rate of infiltration to the saturated zone.

Using this modified precipitation rate, mountain front recharge for each year in each GCM was then estimated using the linear relationship between precipitation and recharge used in the transient historical model, and scaled such that fluctuations in recharge would occur only in layer 1, and distributed across the six recharge zones according to the steady-state distribution as described in Section 5.1.1. As in the transient historical and Baseline models, recharge simulated in layers 2 and 3 was held constant at the steady-state rate, under the assumption that this deeper, older recharge would not yet be affected by changes in precipitation and PET over the next 50 years.

Mountain front recharge was calculated for each year in each of the twenty GCMs. To identify the set of GCMs that best encapsulate the range of potential outcomes in Indian Wells Valley, the cumulative recharge deficit was calculated for each GCM by subtracting

the long-term average rate of 7,650 AFY from each year's estimated recharge and taking the cumulative sum of the result. The cumulative recharge deficit for all twenty GCMs is shown in Figure 6-9. Positive values indicate a cumulative increase in recharge relative to the long-term average, while negative values indicate a cumulative decrease in recharge. Results from the subset of four models from RCP 4.5 and 8.5 (eight total models) are highlighted. From these results, a set of five models was identified for simulation in the 2025 Basin Model and subsequent comparison with the Baseline model: RCP 4.5 (Average), RCP 4.5 (Complement), RCP 4.5 (Cool/Wet), RCP 8.5 (Average), and RCP 8.5 (Warm/Dry).

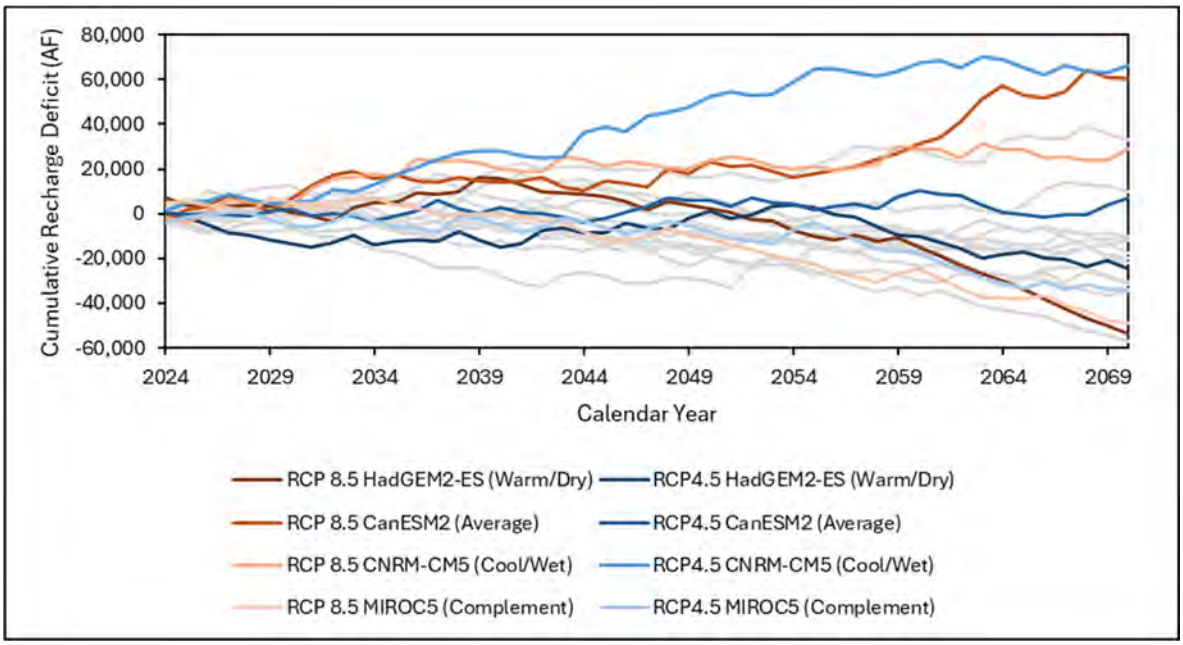


Figure 6-9. Cumulative recharge deficit for each of the twenty GCMs used to estimate change in recharge based on future changes in precipitation and temperature.

6.3.3. Climate Change Scenario Configuration

The five simulated climate change models used the pumping rates defined for the Baseline model and were simulated using the same monthly stress periods as that model. However, GCM output was acquired as calendar year average datasets. As a result, recharge rates and adjustments to the maximum ET rate over the simulated phreatophyte and bare soil ET zones were simulated using these average rates, applied to each month within that calendar year. This differs from the distribution of recharge and ET rates applied to the Baseline model, which simulated recharge following a typical annual distribution of precipitation, and simulated maximum ET rates based on the simulated monthly distribution of ET at nearby Owens Lake basin (Jiao and Vogler, 2020), as described in Section 5.1.2. Climate change scenario models simulated to the time period WY 2020-2070, but WY 2020-2023 used the same recharge and maximum ET rates as in the Baseline model.

6.3.4. Climate Change Scenario Results

For each of the five climate change scenarios, changes in water levels and flow budgets were compared to those from the Baseline model to identify those changes that can be attributed to climate change and eliminate the signal generated by pumping. Changes in water levels attributed to climate change at observation wells were very small compared to changes in water levels resulting from pumping and are difficult to see on a standard hydrograph. Simulated water levels from climate change scenarios are therefore presented as the difference between the water level at each well and the water level at that well for the Baseline scenario. Maps showing the water level difference between each climate scenario and Baseline at the end of WY 2070 are shown in Figures 6-10 to 6-12. Water level difference plots at selected monitoring wells are shown in Figures 6-13 to 6-25. The locations of these wells in the basin are shown in the maps in Figures 6-10 to 6-12. In general, the differences in water levels between the climate scenarios and Baseline are small, with a difference of less than a foot at most of the monitoring wells. The greatest variability occurs in wells that are near boundaries where mountain front recharge is simulated, near or in the simulated ET zones, or both, though even for these wells the water-level difference is less than 5 feet for all simulated stress periods.

Changes in mountain front recharge and PET resulting from climate change result in changes to storage and evapotranspiration rates within each climate change simulation. The cumulative loss of groundwater from storage for each of the climate scenarios and the Baseline model are presented in Figure 6-26. The signal is dominated by loss from groundwater due to pumping, and differences between the scenarios are difficult to see. Figure 6-27 eliminates the impact of pumping on groundwater storage and presents the cumulative change in storage for each climate change scenario, calculated as the difference between storage change in each scenario and the Baseline scenario. The cumulative change in storage resulting from climate change alone ranges from an increase of 52,800 AF in the RCP 4.5 Cool/Wet scenario to a decrease of 54,900 AF in the RCP 8.5 Warm/Dry scenario over the WY 2020-2070 time period.

Simulated changes to evapotranspiration flow rates are a function of both the simulated water level and the maximum ET rate applied to the zone. Increasing PET due to increases in air temperature was simulated by increasing the maximum ET rate over the phreatophyte and bare soil ET zones, which has the effect of increasing simulated outflows to ET. At the same time, simulated water levels within these scenarios are declining due to pumping, and in some scenarios due to a reduction in mountain front recharge. When water levels below the ET zones drop, ET outflows decrease and eventually fall to zero when the water level falls below the assigned extinction depth (Table 4-1). Simulated outflows from the vegetated and bare soil ET zones for Baseline and all climate scenarios are shown in Figures 6-28 and 6-29, respectively. The sudden increase in ET beginning in WY 2024 occurs because the effects of climate change are not simulated before that time, so the maximum ET rate assigned to the ET zones increases suddenly. In general, ET outflows over the vegetated zone in the climate change scenarios are greater than in the Baseline scenario, but follow the same approximate trend in decline. Bare soil ET from the climate scenarios matches the Baseline more closely initially, but shows a greater variability in results between scenarios as time passes.

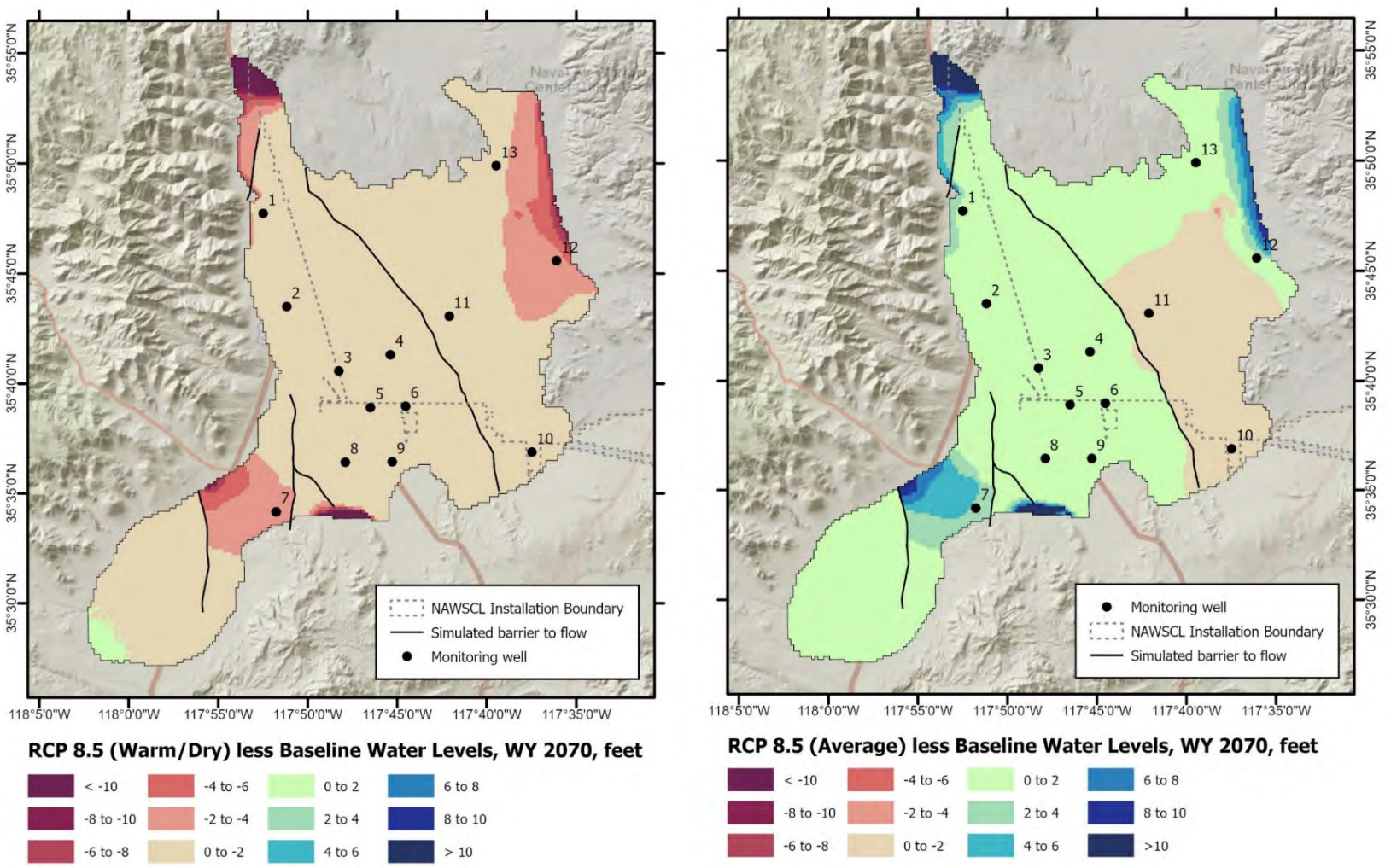


Figure 6-10. Difference maps showing the change in water levels between the RCP 8.5 (Warm/Dry) scenario and Baseline (left) and the RCP 8.5 (Average) scenario and Baseline (right), for the end of WY 2070.

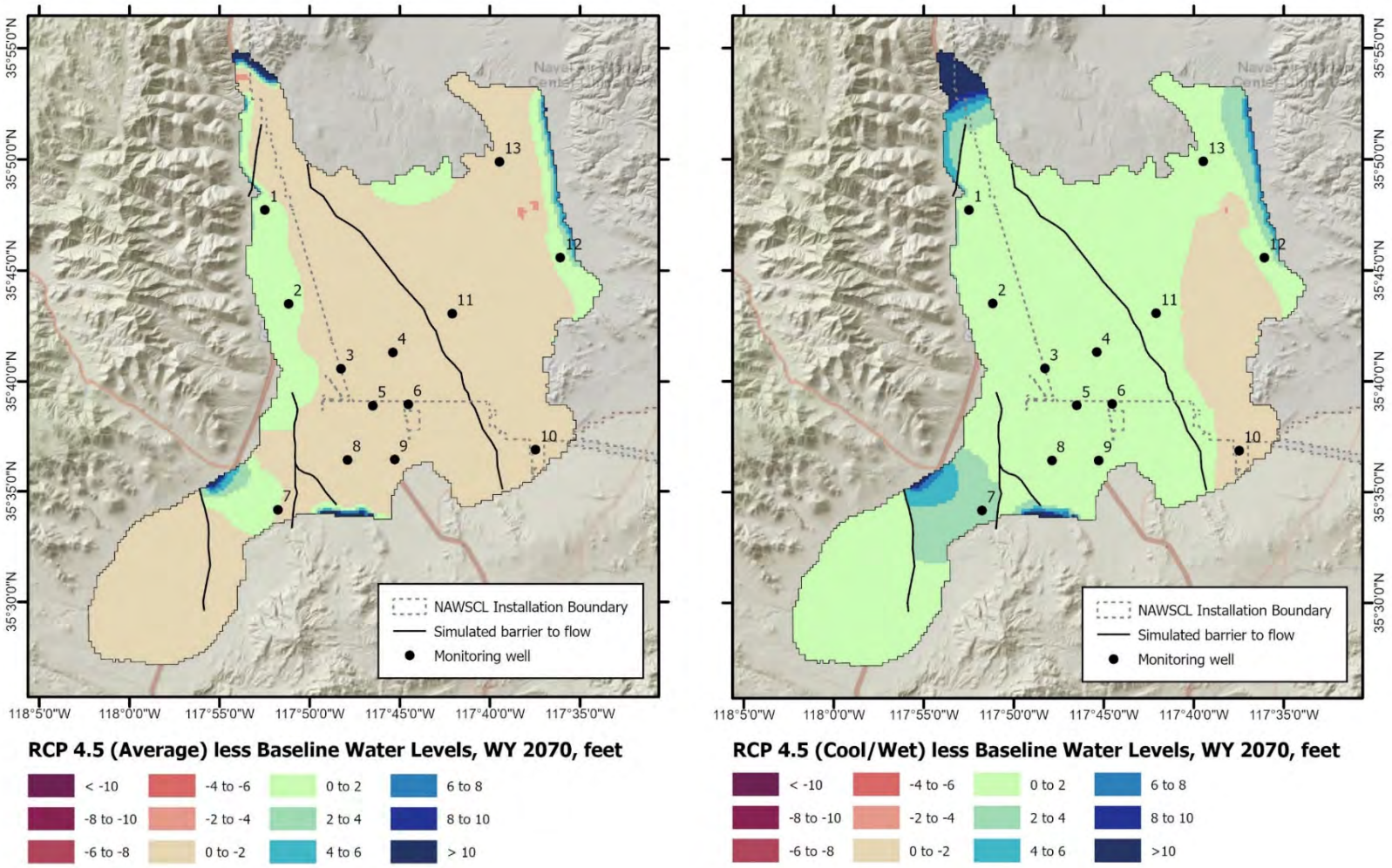


Figure 6-11. Difference maps showing the change in water levels between the RCP 4.5 (Average) scenario and Baseline (left) and the RCP 4.5 (Cool/Wet) scenario and Baseline (right), for the end of WY 2070.

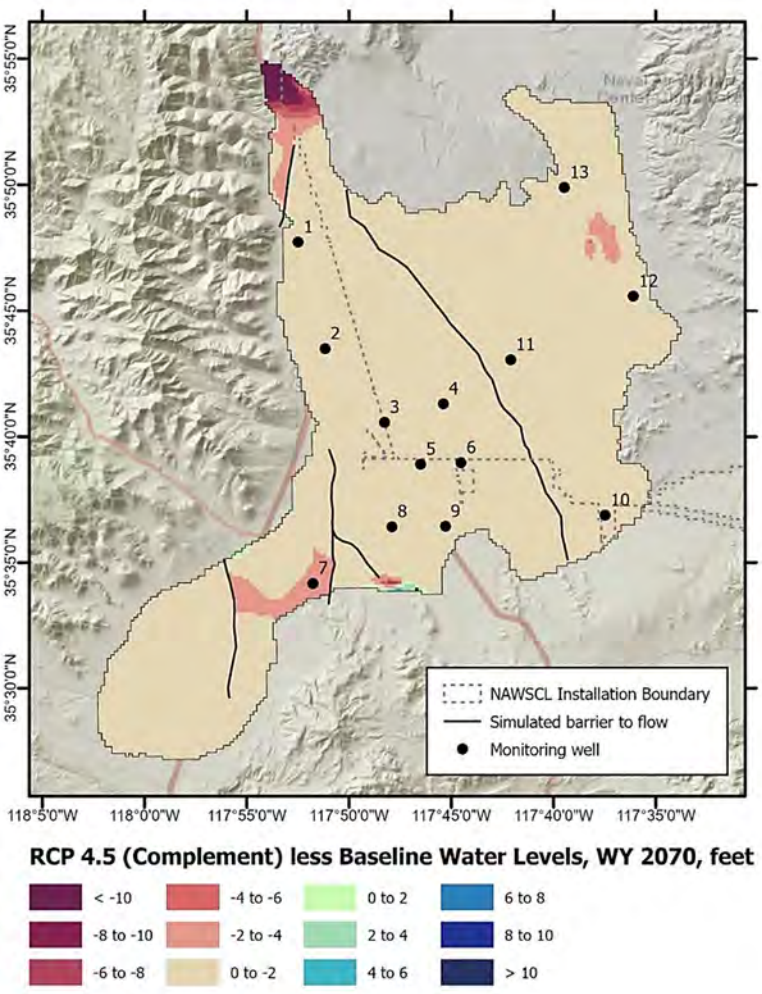


Figure 6-12. Difference map showing the change in water levels between the RCP 4.5 (Complement) scenario and Baseline for the end of WY 2070.

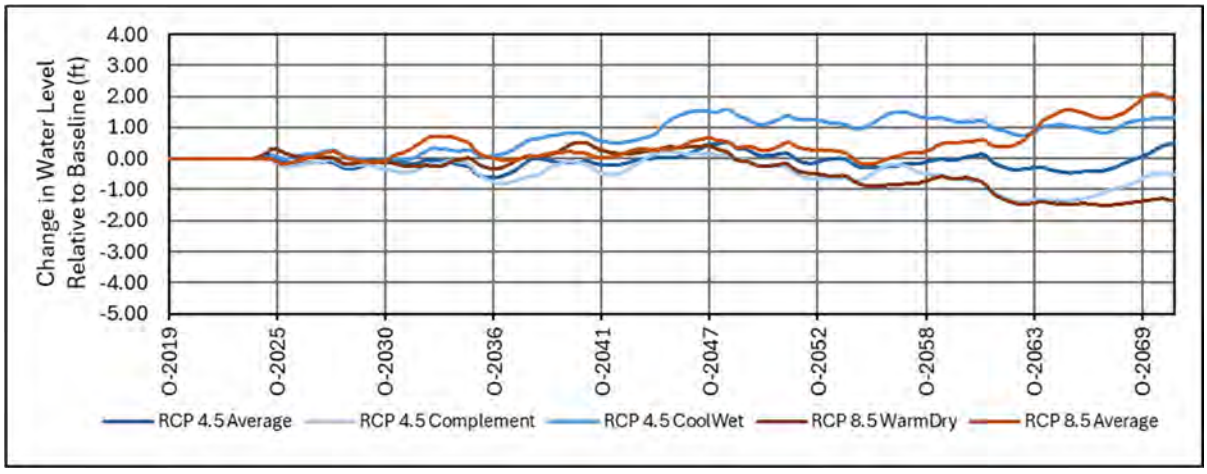


Figure 6-13. 25S/38E-03B (Well 1) change in water level relative to Baseline for all climate scenarios.

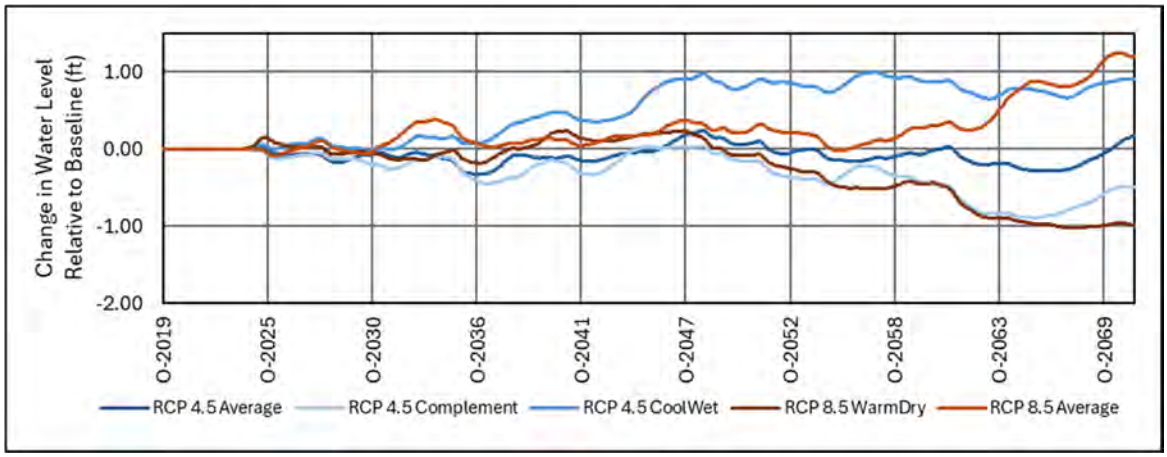


Figure 6-14. 25S/38E-35B01 (Well 2) change in water level relative to Baseline for all climate scenarios.

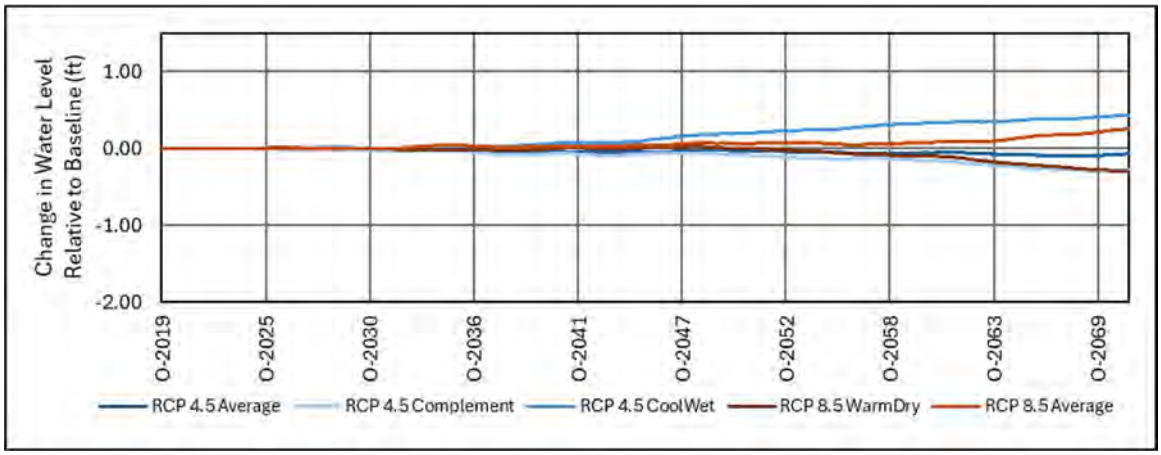


Figure 6-15. Kerr McGee (Well 3) change in water level relative to Baseline for all climate scenarios.

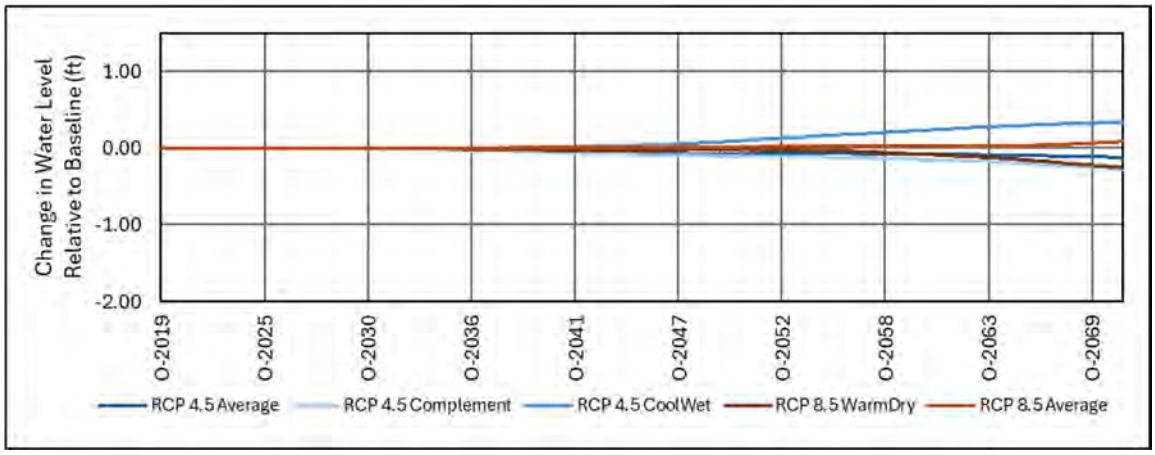


Figure 6-16. Sandquist Spa (Well 4) change in water level relative to Baseline for all climate scenarios.

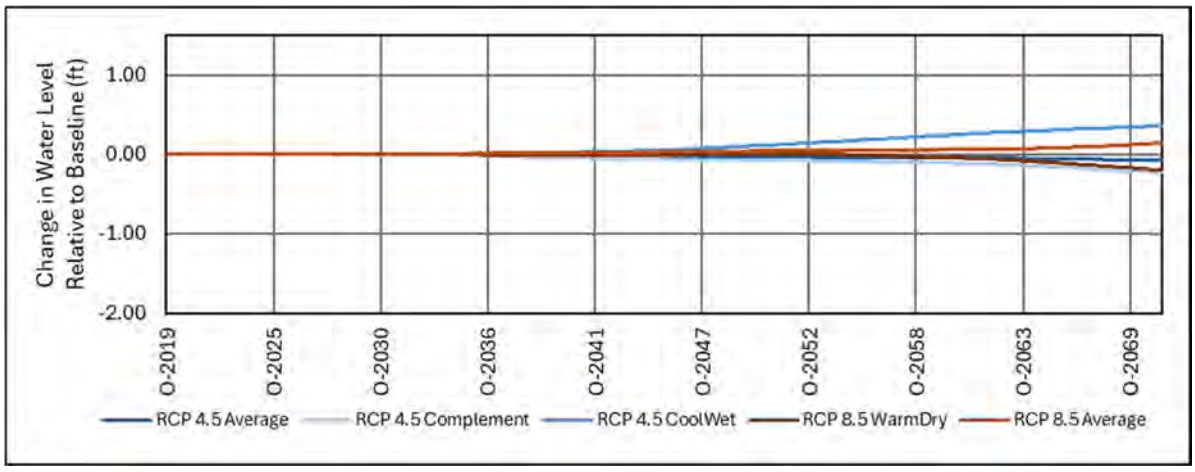


Figure 6-17. MW 32-SM (Well 5) change in water level relative to Baseline for all climate scenarios.

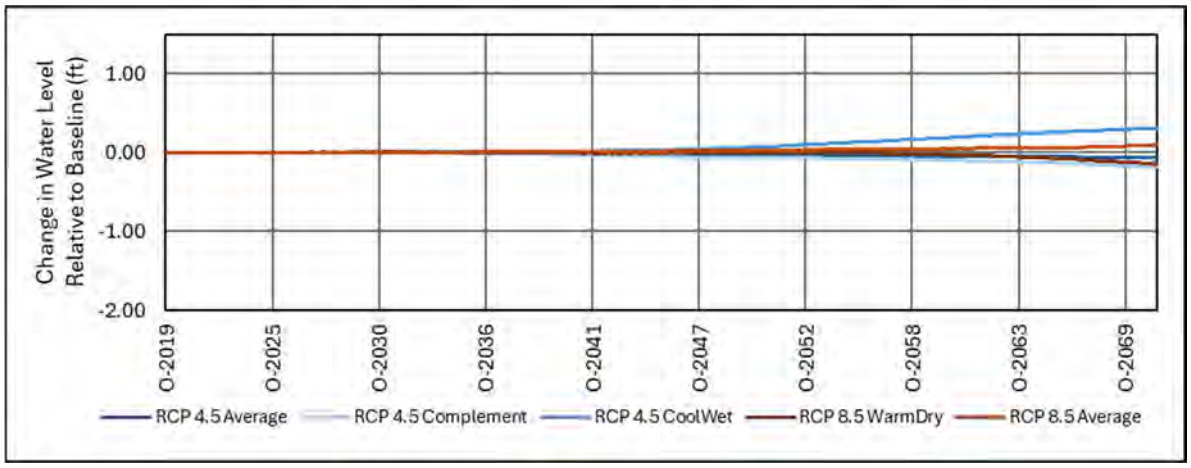


Figure 6-18. USBR-04 (Well 6) change in water level relative to Baseline for all climate scenarios.

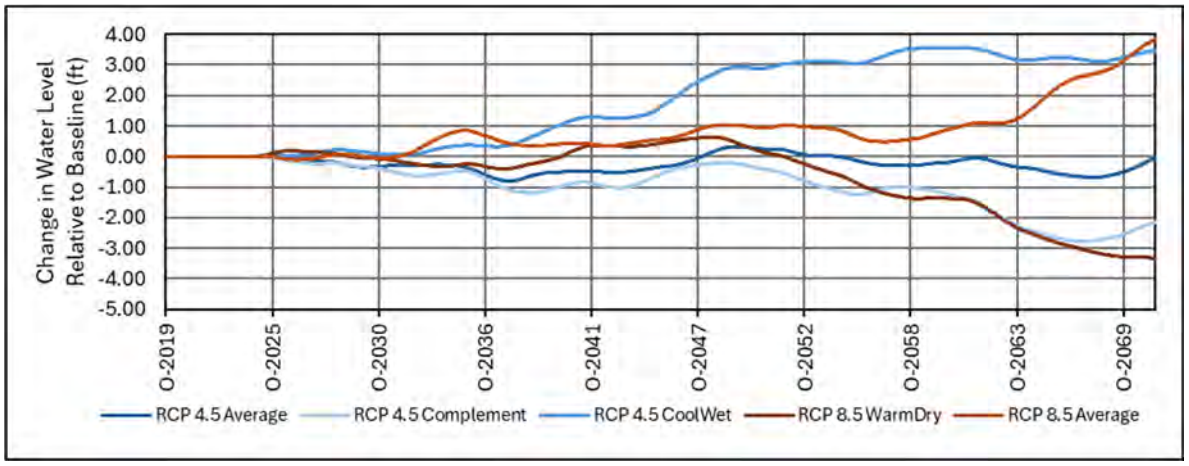


Figure 6-19. USBR-01-S (Well 7) change in water level relative to Baseline for all climate scenarios.

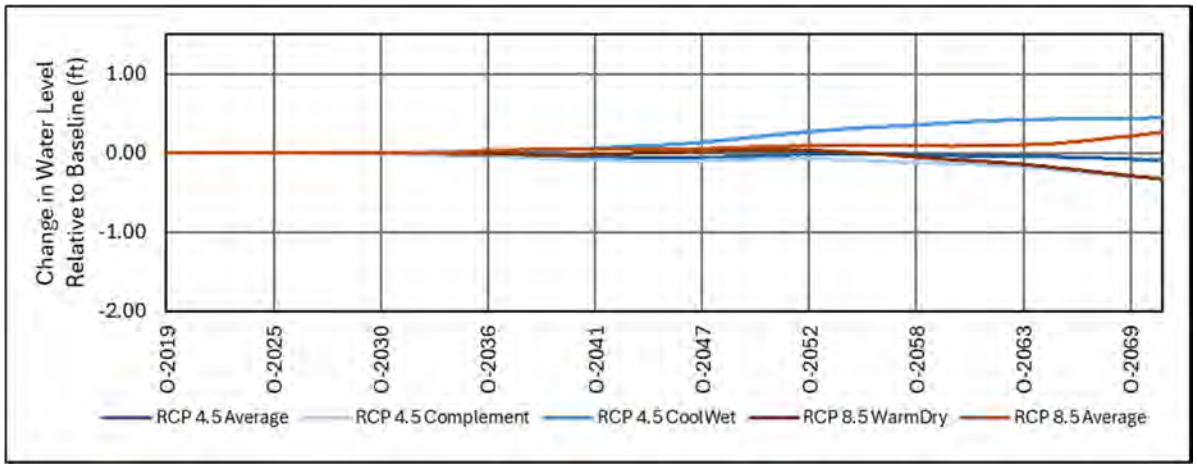


Figure 6-20. 27S/39E-08A01 (Well 8) change in water level relative to Baseline for all climate scenarios.

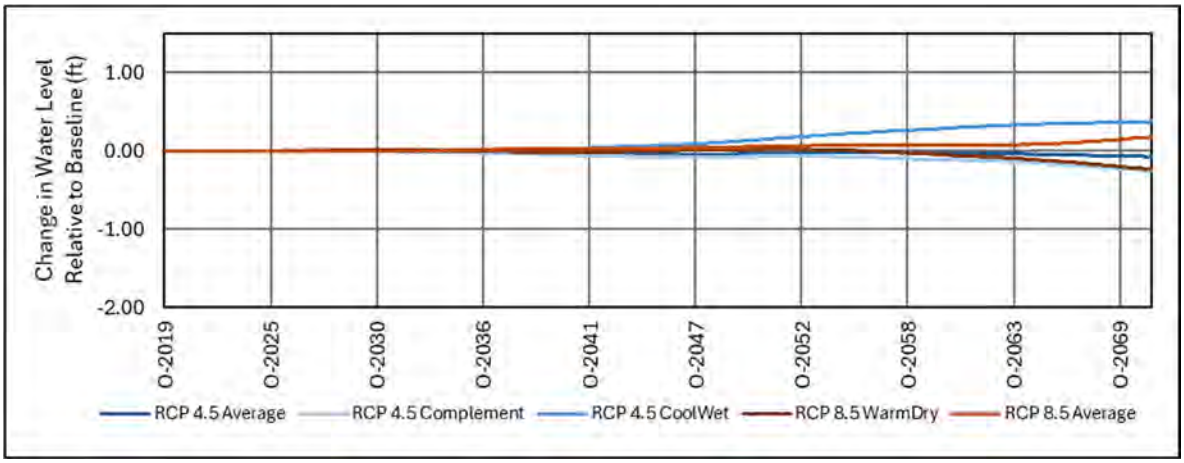


Figure 6-21. USBR-03-S (Well 9) change in water level relative to Baseline for all climate scenarios.

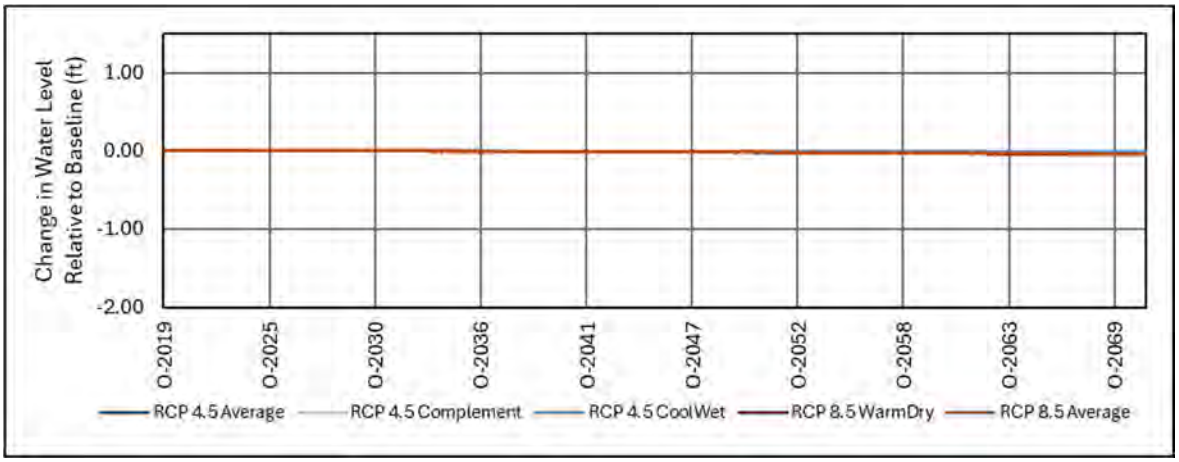


Figure 6-22. George Air Corridor (Well 10) change in water level relative to Baseline for all climate scenarios.

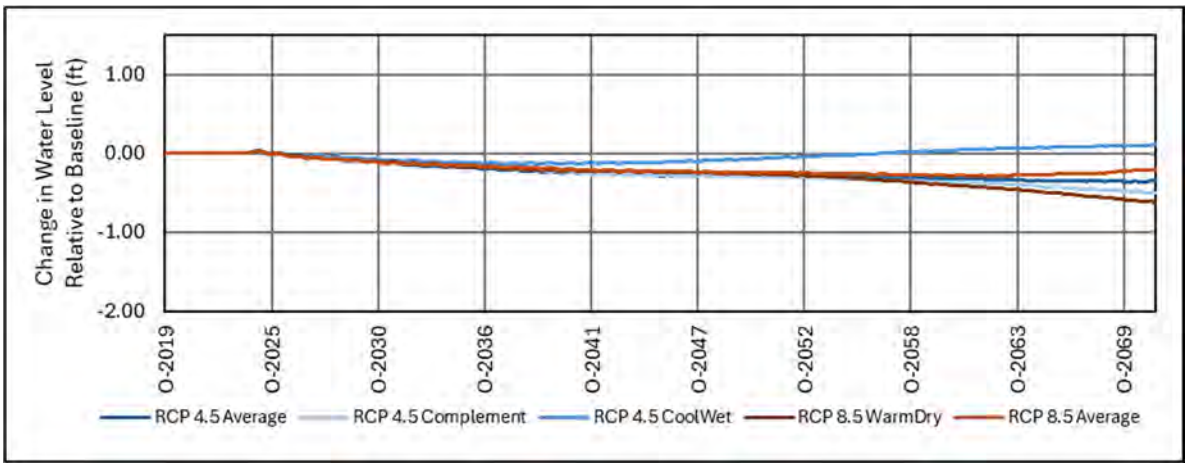


Figure 6-23. TTBK-MW05 (Well 11) change in water level relative to Baseline for all climate scenarios.

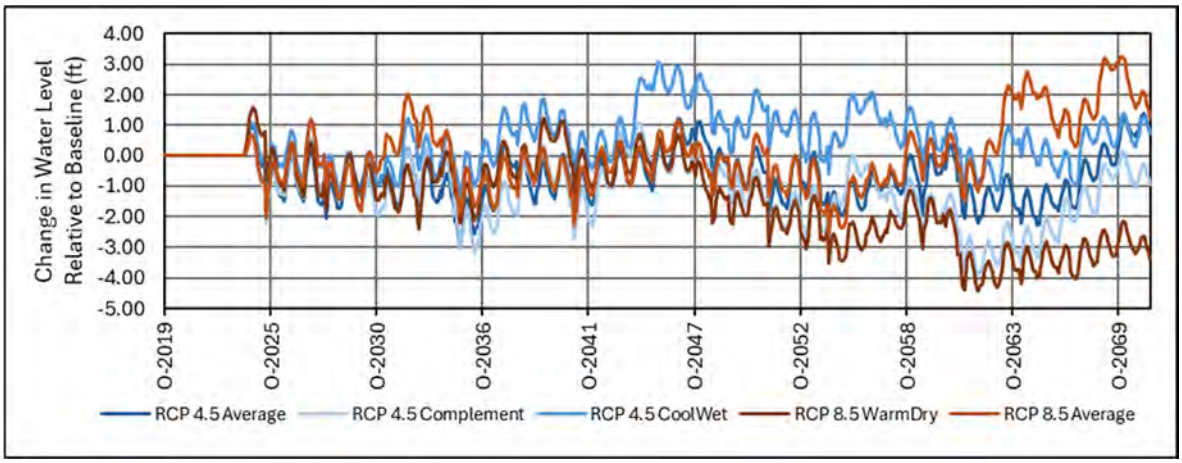


Figure 6-24. TTBK-MW12 (Well 12) change in water level relative to Baseline for all climate scenarios.

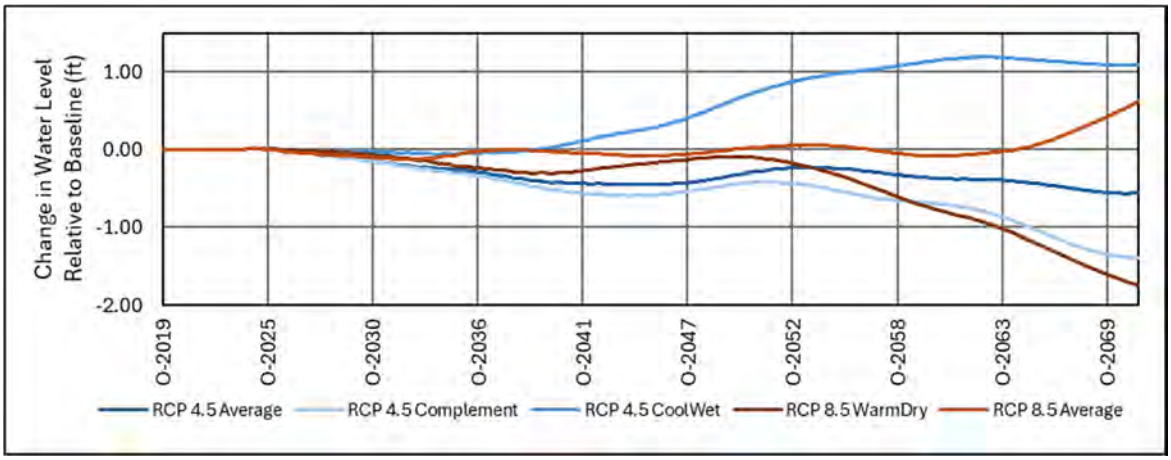


Figure 6-25. TTIWV-MW15 (Well 13) change in water level relative to Baseline for all climate scenarios.

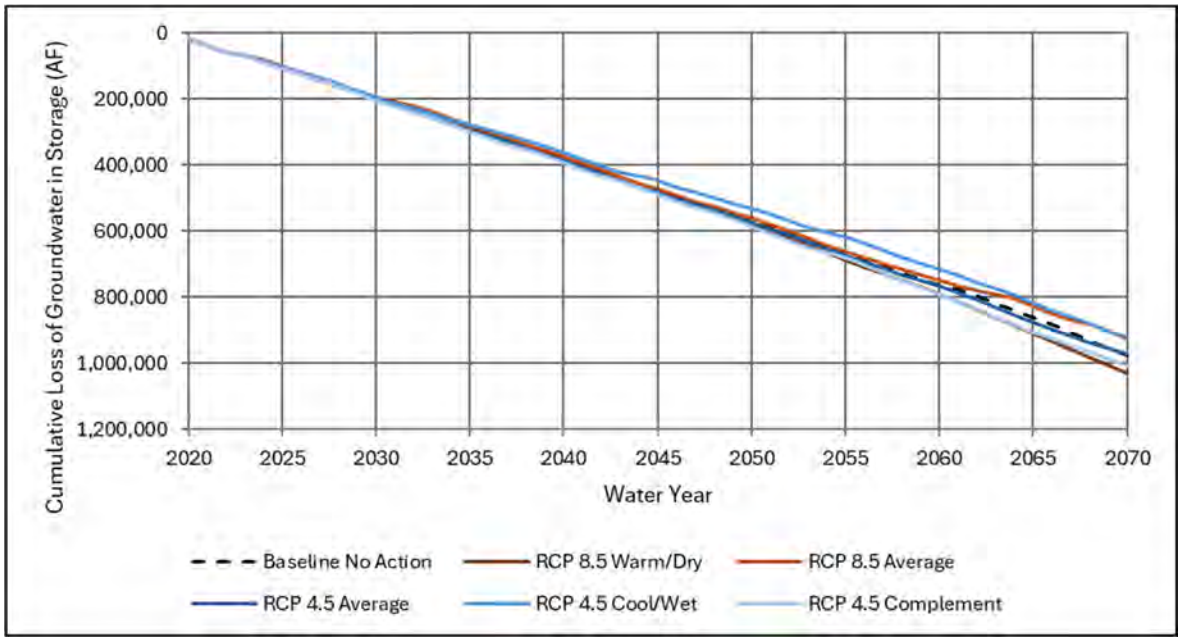


Figure 6-26. Cumulative loss of groundwater in storage for the model domain for the Baseline model and all climate scenarios.

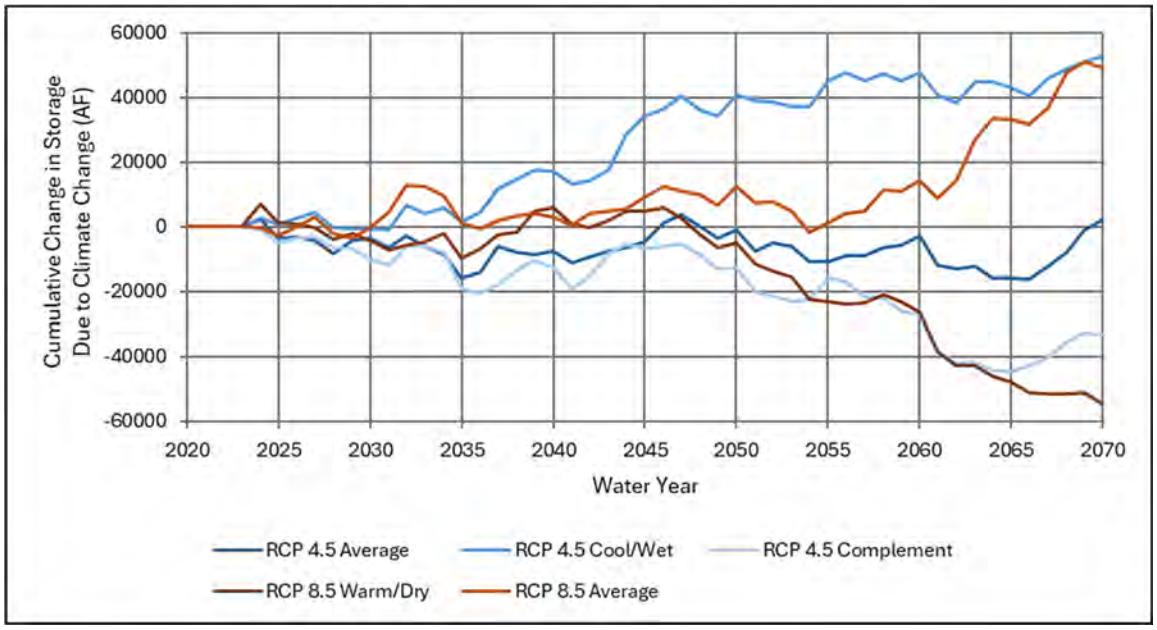


Figure 6-27. Cumulative change in storage for the model domain due to climate change, calculated as the difference in storage loss between the Baseline scenario and each climate change scenario. Positive values indicate an increase in storage relative to Baseline and negative values indicate a loss in storage relative to Baseline.

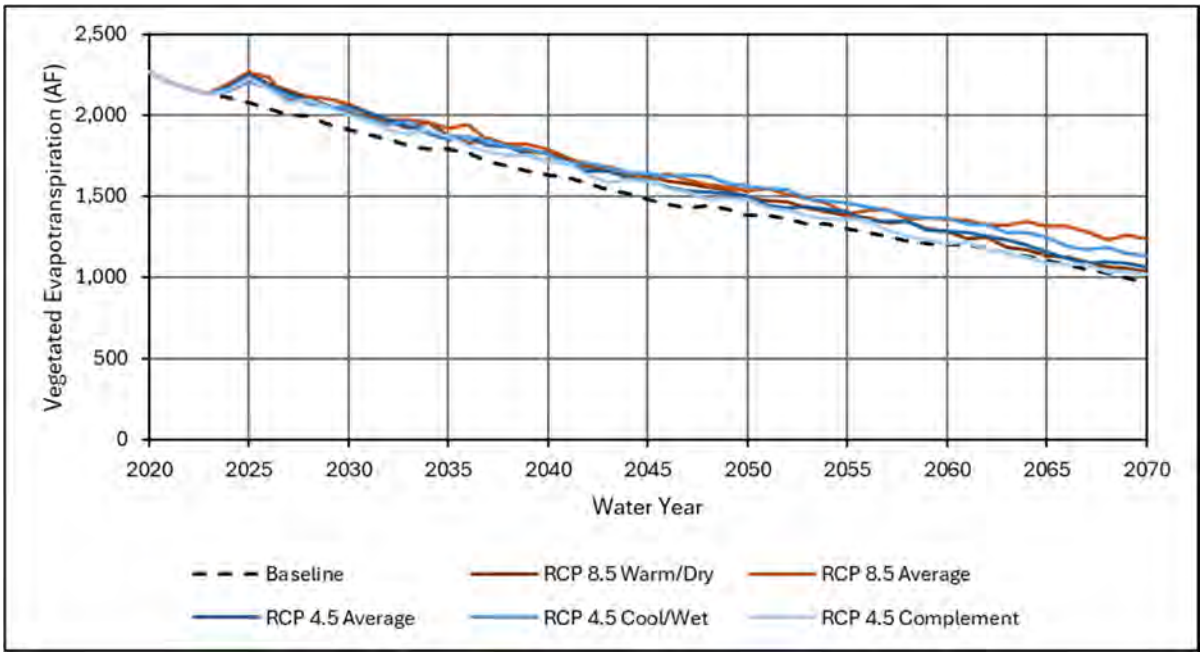


Figure 6-28. Simulated outflow to vegetated evapotranspiration zones for Baseline and climate change scenarios.

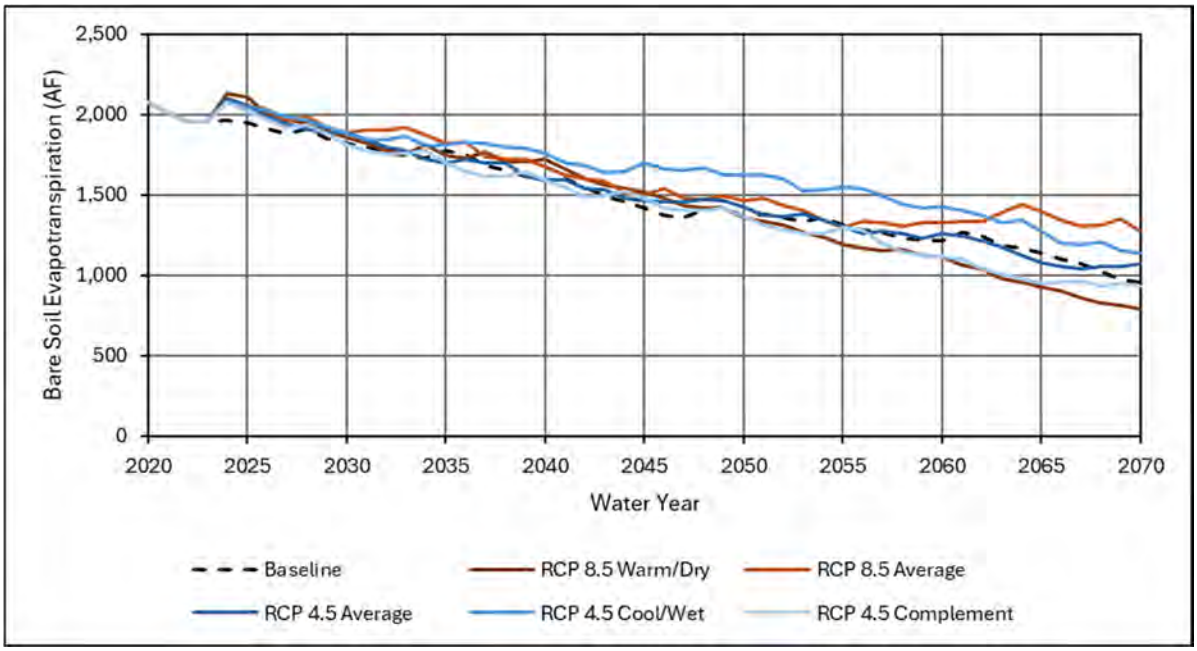


Figure 6-29. Simulated outflow to bare soil evapotranspiration zones for Baseline and climate change scenarios.

Simulated declines in outflow to ET suggest a loss in vegetated area and soil moisture. The vegetated and bare soil ET zones within the Baseline and climate change scenario models were analyzed to count the number of grid cells with a simulated ET outflow for each stress period. As water levels drop below the assigned extinction depth for a given cell, ET outflows are no longer simulated in that cell until water levels rise above the extinction depth. The difference in the count of grid cells simulating an ET outflow for each climate scenario was compared to the Baseline model to estimate the loss in vegetated or bare soil ET zone areas. Results show the change in vegetated and bare soil ET area that is attributable to climate change and are presented in Figures 6-30 and 6-31, respectively. These figures show a range of results for change in vegetated area from near zero in the RCP 4.5 Cool/Wet scenario, to a loss of 670 acres in the RCP 8.5 Warm/Dry scenario by 2070. The change in area is much greater for the bare soil ET zone, ranging from an increase of 230 acres in the RCP 4.5 Cool/Wet scenario, to a loss of 1,650 acres in the RCP 8.5 Warm/Dry scenario. It should be noted that while the bare soil ET area may shrink and later recover in size, it would be much more difficult for the vegetated ET zone to recover from a die-off. It is also important to note that these results are only applicable assuming the pumping rates simulated in the Baseline scenario because the water-level declines are primarily a function of pumping – without the simulated pumping, groundwater levels in the climate change scenarios would still change as a function of recharge and PET, but they may or may not exceed the extinction depth for a given cell. However, the overall trend in changes to ET areas between the five climate change scenarios will remain valid.

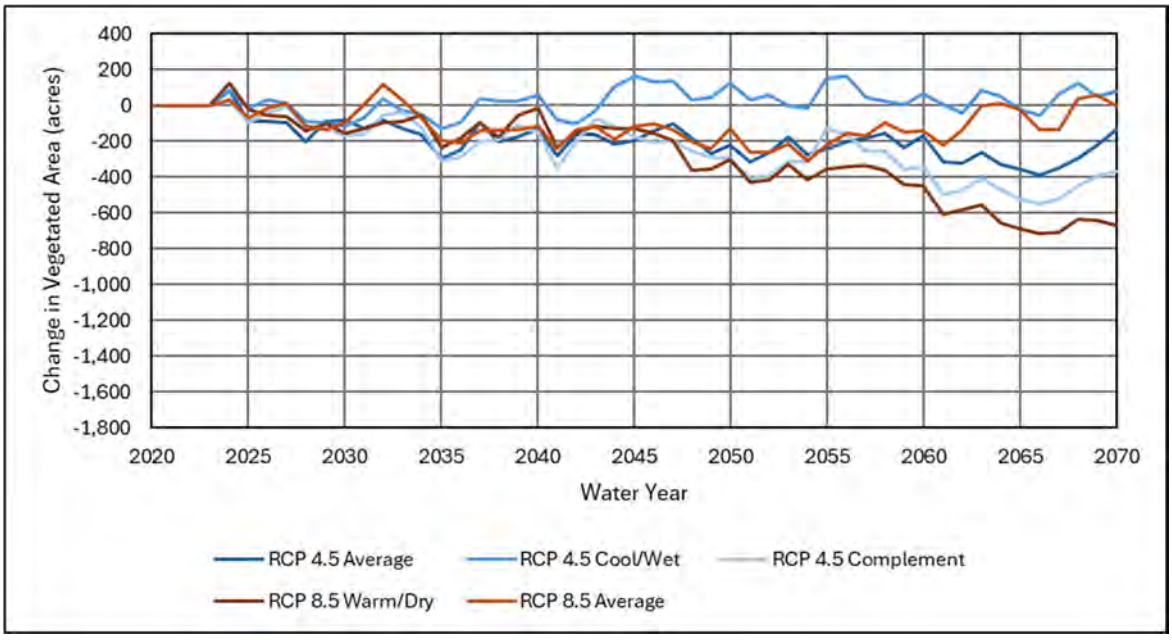


Figure 6-30. Simulated change in vegetated ET area for each climate change scenario, relative to Baseline.

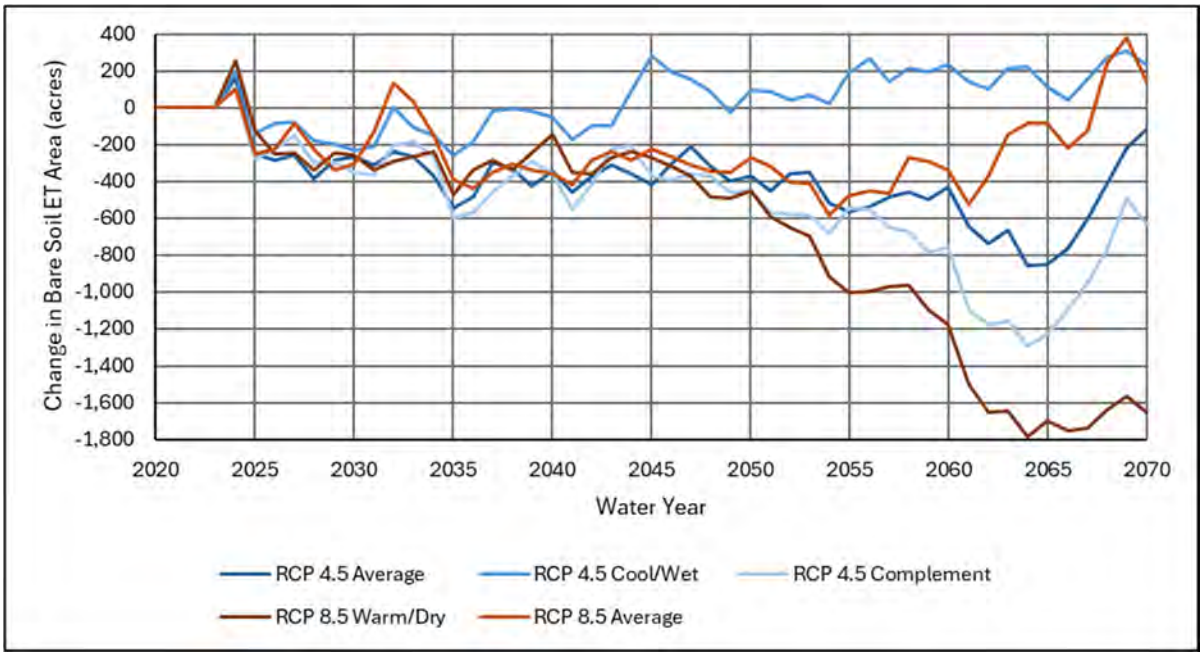


Figure 6-31. Simulated change in bare soil ET area for each climate change scenario, relative to Baseline.

7. MODEL LIMITATIONS

Limitations to model development include uncertainties in rates of historical pumping and mountain block recharge, and limited early-time (prior to 1995) water level data for the simulated time period. While some older water level data do exist, they are rare, spatially limited, and none cover the entire historical calibration period. Therefore, simulated heads cannot be compared to observed heads over the entire simulation period for much of the model domain. Combined with uncertainties in historical pumping rates and mountain block recharge, these limitations reduce the uniqueness of model results.

The majority of hydraulic conductivity data in the 2025 Basin Model is derived from specific capacity measurements taken from well logs, which may more accurately describe the properties of the small portion of the aquifer immediately surrounding the well than those of the larger surrounding aquifer. Specific capacity measurements also do not account for the storage properties of the aquifer, which must be estimated. Although some aquifer test data do exist, aquifer property data could be improved with additional aquifer tests throughout the basin for use in future modeling.

There is also considerable uncertainty in discharge rates for ET and outflow to Salt Wells Valley. The change in these flow rates over time as groundwater development has increased is also highly uncertain. Improved estimates for these terms would help in validating or recalibrating the model to increase the accuracy of results. Improved estimates for these terms may also help to validate estimates of mountain-front recharge.

8. CONCLUSIONS

Results indicate that the 2025 Basin Model presented in this report replicate observed trends in groundwater elevation within a reasonable amount of error, and calibration metrics show a great improvement in model error relative to the 2020 GSP Model. This improvement is largely attributed to updates to the hydrogeologic framework to incorporate the geometry of the "clay" unit. Modifications to the rates and spatial distribution of pumping, fault delineation, and distribution of ET zones were also critical to the improved calibration.

Predictive climate change simulations envelope the range of potential outcomes for the basin based on expected changes to mountain-front recharge and ET rates. Predicted changes in precipitation (and therefore mountain-front recharge) are uncertain. Climate models indicate that IWV may experience an increase or a decrease in mountain-front recharge. The resultant cumulative change in storage ranges from an increase of 52,800 AF to a decrease of 54,900 AF over the WY 2020-2070 time period. Changes in water levels and ET rates are also expected to affect the phreatophyte and bare soil ET zones. Model results indicate that the phreatophyte ET zone may lose up to 670 acres in area, while change in the bare soil ET zone range from an increase of 230 acres to a loss of 1,650 acres.

9. REFERENCES

Abatzoglou, J.T., Dobrowski, S.Z., Parks, S.A., and Hegewisch, K.C., (2018). Data Descriptor: TerraClimate, a high-resolution global dataset of monthly climate and climatic water balance from 1958 – 2015. Scientific Data 5, 170191.

Amos, C.B., Brownlee, S.J., Rood, D.H., Burch Fisher, G., Bürgmann, R., Renne, P.R., and Jayko, A.S., (2013). Chronology of tectonic, geomorphic, and volcanic interactions and the tempo of fault slip near Little Lake, California: Geological Society of America Bulletin, v. 125, p. 1187–1202.

Anderson, M.P., Woessner, W.W., and Hunt, R.J., (2015). Applied Groundwater Modeling: Simulation of Flow and Advective Transport, 2nd Edition, Elsevier Inc., 564 p.

Bacon, S.N., and Pezzopane, S.K., (2007). A 25,000-year record of earthquakes on the Owens Valley fault near Lone Pine, California: Implications for recurrence intervals, slip rates, and segmentation models: Geological Society of America Bulletin 119, 823–847.

Bacon, S.N., Bullard, T.F., Keen-Zebert, A.K., Jayko, A.S., Decker, D.L., (2020). Spatiotemporal patterns of distributed slip in southern Owens Valley indicated by deformation of late Pleistocene shorelines, eastern California, Geological Society of America Bulletin 132, 1681–1703.

Behroozmand, A., Knight, R., and Halkjaer, M., (2018). Analysis of SkyTEM Data from Indian Wells Valley, California. Report prepared by Standford University and Ramboll. November 6, 2018, p. 16, plus tables and appendices.

Berenbrock, C., and Martin, P., (1991). The ground-water flow system in the Indian Wells Valley, Kern, Inyo, and San Bernardino counties, California. U.S. Geological Survey Water Resources Investigations Report 89–4191, 81 pp.

Berghuijs, W.R., Luijendijk, E., Moeck, C., van der Velde, Y., and Allen, S.T. (2022). Global recharge data set indicate strengthened groundwater connection to surface fluxes. Geophysical Research Letters 49, e2022GL099010.

Berghuijs, W.R., Collenteur, R.A., Jasechko, S., Jaramillo, F., Luijendijk, E., Moeck, C., van der Velde, Y., Allen, S.T. (2024). Groundwater recharge is sensitive to changing long-term aridity. Nature Climate Change 14, 357–363.

Bischoff, J.L., Stafford, T.W. Jr., and Rubin, M., (1997). A time-depth lake scale for Owens Lake sediments of core OL-92: Radiocarbon dates and constant mass-accumulation rate, *in* G.I. Smith and J.L. Bischoff (Eds.), An 800,000-year Paleoclimatic Record from Core OL-92, Owens Lake, Southeast California. Geological Society of America Special Paper, 317, 91–98.

Bloyd, R.M., and Robson, S.G., (1971). Mathematical groundwater model of Indian Wells Valley, California, U.S. Geological Survey Open-File Report, 36 p.

Boyd, O.S., (2020). Calibration of the U.S. Geological Survey National Crustal Model, U.S. Geological Survey Open-File Report 2020–1052, 23 p.

Brown and Caldwell, (2009). Final Report, Indian Wells Valley Basin Groundwater Flow Model and Hydrogeologic Study, Prepared for the Indian Wells Valley Water District, Ridgecrest, CA.

Bullard, T.F., Bacon, S.N., Adams, K.D., and Decker, D.L., (2019). Geomorphic Map of the China Lake Basin below 700 m in Support of Cultural Resource Management at Naval Air Weapons Station China Lake. Prepared by Naval Earth Sciences and Engineering Program, Desert Research Institute for Naval Air Warfare Center, Weapons Division, China Lake, NAWCWD TP 8839, 79 pp.

CADWR [California Department of Water Resources], (2016). SGMA Best Management Practice: Hydrogeologic Conceptual Model: Sustainable Groundwater Management Program, December 2016, 25 p.

Chapman, J.B., Thomas, J.M., and Garner, C., (2022). Groundwater recharge timing based on ^{14}C and ^{2}H within Indian Wells Valley, California, USA. Applied Geochemistry 141, 105268.

CGS [California Geological Survey], (2010). Fault activity map of California. California Geologic Data Map Series, Map No. 6, scale: 1:750,000, GIS data.

DBSA [Daniel B. Stephens & Associates, Inc.], (2011). Revised Groundwater Flow Model and Predictive Simulation Results: Coso Operating Company Hay Ranch Water Extraction and Delivery System Conditional Use Permit (CUP 2007-003). Report prepared for County of Inyo, January 28, 2011, 28 p., plus tables, figures, and appendices.

Danskin, W.R., (1998). Evaluation of the Hydrologic System and Selected Water-Management Alternatives in the Owens Valley, California. U.S. Geological Survey Water-Supply Paper 2370-H, 175 p.DuRoss, C.B., Gold, R.D., Dawson, T.E., Scharer, K. M., Kendrick, K.J., Akciz, S.O., Angster, S.J., et al., (2020). Surface displacement distributions for the July 2019 Ridgecrest, California, earthquake ruptures. Bulletin of the Seismological Society of America 110, 1400–1418.

Dutcher, L.C., and Moyle, Jr., W.R., (1973). Geologic and Hydrologic Features of the Indian Wells Valley, California. USGS Water Supply Paper 2007.

Flint, L.E., Flint, A.L., Thorne, J.H., and Boynton, R. (2013). Fine-scale hydrologic modeling for regional landscape applications: the California Basin Characterization Model development and performance. Ecological Processes 2, 25.

Garner, C., Bacon, S., Pohll, G., and Chapman, J., (2017). Indian Wells Valley Groundwater Model Update. Desert Research Institute Technical Memorandum.

Gibbard, P.L., Head, M.J., Walker, M.J.C. and the Subcommission on Quaternary Stratigraphy., (2010). Formal ratification of the Quaternary System/Period and the Pleistocene Series/Epoch with a base at 2.58 Ma. Journal of Quaternary Science 25, 96–102.

Hanson, R.T., Dettinger, M.D., and Newhouse, M.W. (2006). Relations between climatic variability and hydrologic time series from four alluvial basins across the southwestern United States: Hydrogeology Journal 14, 1122–1146.

Houghton HydroGeo-Logic, (1996). Geohydrologic Investigation Report: Naval Air Weapons Station, Indian Wells Valley, China Lake, California. Prepared for Naval Air Weapons Station Environmental Projects Office, China Lake, California, November 30, 1996.

Haung, L., and Liu, C., (2017). Three types of flower structures in a divergent-wrench fault zone. Journal of Geophysical Research: Solid Earth, 122 10,478–10,497.

IWVGA [Indian Wells Valley Groundwater Authority], (2020). GSP Annual Report Water Year 2019. (October 2018 to September 2019). Prepared by Indian Wells Valley Groundwater Authority (IWVGA). SGMA Annual Report.

IWVGA [Indian Wells Valley Groundwater Authority], (2025). 2025 Periodic Evaluation of the

Jachens, R.C., and Moring, B.C., (1990). Maps of the thickness of Cenozoic deposits and the isostatic residual gravity over basement for Nevada: U.S. Geological Survey Open-File Report 90–404, 15 p.

Jennings, C.W., Burnett, J.L., and Troxel, B.W., (1962). Geologic Map of California: Trona Sheet. California Geological Survey, scale 1:250,000.

Jennings, C.W., with modifications by Gutierrez, C., Bryant, W., Saucedo, G., and Wills, C., (2010). Geologic Map of California: California Geological Survey, Geologic Data Map No. 2, scale 1:750,000.

Jensen, M.E., and Haise, H.R. (1963). Estimating evapotranspiration from solar radiation. Proceedings of the American Society of Civil Engineers, Journal of the Irrigation and Drainage Division 89, 15–41.

Jiao, C. and Vogler, E., (2020). Model documentation report for the Owens Lake groundwater model update. Prepared for Los Angeles Department of Water and Power, June 2020.

Krieger & Stewart, (1989). Indian Wells Valley Water District Southwest Well Field Test and Monitoring Wells Construction and Development. September 1989.

Kunkel, F., and G.H. Chase, 1969. Geology and Ground Water in Indian Wells Valley, California. US Geological Survey Open-File Report 69-329. Prepared in cooperation with the Naval Weapons Center China Lake, CA, dated January 23.

Lancaster, N., Bacon, S.N., Bullard, T.F., Neudorf, C.M., Keen-Zebert, A.K., Decker, D.L., and Boggs, M.L., (2022). Tectonic, hydrologic, and climatic controls on Late Holocene dune formation, China Lake basin, Indian Wells Valley, California, USA. Quaternary Research 106, 11–27. https://doi.org/10.1017/qua.2021.62

Layne Christensen Company, (2010). Water supply improvement plan, Phase 1 and 2 Final Technical Memorandum, Project No. 27-1666. Submitted to Indian Wells Valley Water District, April 16, 2010.

Mallory, J.M., (1978). Water-Level Predictions for Indian Wells Valley Ground-Water Basin, U.S. Geological Survey Open-File Report 79-254.

McGraw, D., Carroll, R., Pohll, G., Chapman, J., Bacon, S., and Jasoni, R., (2016). Groundwater Resource Sustainability: Modeling Evaluation for the Naval Air Weapons Station, China Lake, California. Prepared by Naval Earth Sciences and Engineering Program, Desert Research Institute for Naval Air Warfare Center, Weapons Division, China Lake, NAWCWD TP 8811, p. 114 (pp. including appendices).

Menke, J., E. Reyes, A. Glass, D. Johnson, and J. Reyes, (2013). 2013 California Vegetation Map in Support of the Desert Renewable Energy Conservation Plan. Final Report. Prepared for the California Department of Fish and Wildlife Renewable Energy Program and the California Energy Commission. Aerial Information Systems, Inc., Redlands, CA.

Michaud, G.A., H.C. Monger, and D.L. Anderson, (2013). Geomorphic-vegetation relationships using geopedological classification system, northern Chihuahuan Desert, USA. Journal of Arid Environments 90, 45–54.

Moeck, C., Grech-Cumbo, N., Podgorski, J., Bretzler, A., Gurdak, J. J., Berg, M., & Schirmer, M. (2020). A global-scale dataset of direct natural groundwater recharge rates: A review of variables, processes and relationships. Science of the Total Environment, 717, 137042.

Monastero, F.C., Walker, J.D., Katzenstein, A.M., Sabin, A.E., (2002). Neogene evolution of the Indian Wells Valley, east-central California. In: Glazner, A.F., Walker, J.D., Bartley, J.M. (Eds.), Geologic Evolution of the Mojave Desert and Southwestern Basin and Range: Geological Society of America Memoir 195, 199–228.

Moyle, W.R., Jr., 1963. Data on water wells in Indian Wells Valley area, Inyo, Kern, and San Bernardino Counties, California. California Department of Water Resources Bulletin 91-9, 243 p.

Pierce, D. W., J. F. Kalansky, and D. R. Cayan, (Scripps Institution of Oceanography). 2018. Climate, Drought, and Sea Level Rise Scenarios for the Fourth California Climate Assessment. California's Fourth Climate Change Assessment, California Energy Commission. Publication Number: CNRA-CEC-2018-006.

Ponti, D.J., Blair, J.L., Rosa, C.M., Thomas, K., Pickering, A.J., Akciz, S., Angster, S., et al., (2020). Documentation of surface fault rupture and ground deformation features produced by the Ridgecrest M6.4 and M7.1 earthquake sequence of July 4 and 5, 2019. Seismological Research Letters 91. https://doi.org/10.1785/0220190322.

Roquemore, G.R., Zellmer, J.T., (1987). Naval Weapons Center Active Fault Map Series, NWC TP-6828. Naval Weapons Center, China Lake, CA, 18 p., 14 maps, scale 1:24,000.

Rosen, M.R., (1994). The importance of groundwater in playas: A review of playa classifications and the sedimentology and hydrology of playas, *in* Rosen, M.R., ed., Paleoclimate and Basin Evolution of Playa Systems: Boulder, Colorado, Geological Society of America Special Paper 289.

Rosenthal, J.S., Meyer, J., Palacios-Fest, M.R., Young, D.C., Ugan, A., Byrd, B.F., Goblet, K., Giacomo, J., (2017). Paleohydrology of China Lake basin and the context of early human occupation in the northwestern Mojave Desert, USA. Quaternary Science Reviews 176, 112–139.

Reynolds, R.L., Yount, J.C., Reheis, M., Goldstein, H., Chavez, P. Jr., Fulton, R., Whitney, J., Fuller, C., and Forester, R.M., (2007). Dust emission from wet and dry playas in the Mojave Desert, USA. Earth Surface Processes and Landforms 32, https://doi.org/10.1002/esp.1515.

Scanlon, B.R., Keese, K.E., Flint, A.L., Flint, L.E., Gaye, C.B., Edmonds, W.M., and Simmers, I. (2006). Global synthesis of groundwater recharge in semiarid and arid regions. Hydrological Processes 20, 3335–3370.

Shah, A.K, and Boyd, O.S., (2018). Depth to basement and thickness of unconsolidated sediments for the western United States—Initial estimates for layers of the U.S. Geological Survey National Crustal Model: U.S. Geological Survey Open-File Report 2018–1115, 13 p.

Shen, R., Pennell, K.G., and Suuberg, E.M., (2013). Influence of soil moisture on soil gas vapor concentration for vapor intrusion. Environmental Engineering Science 30, 628–637.

Shuttle, W.J., (2012). Terrestrial Hydrometeorology. John Wiley & Sons, Ltd., 448 p.

St. Amand, P., (1986). Water Supply of Indian Wells Valley, California. NWC TP 6404. NAWS, Ridgecrest, CA.

Steinpress, M.G., Couch, R.F., and McDonald, J., (1994). The China Lake barrier: a structural or stratigraphic hydrologic feature? Geological Society of America Abstracts with Programs 26, 95.

Steinwand, A.L., Harrington, R.F. and Or, D., (2006). Water balance for Great Basin phreatophytes derived from eddy covariance, soil water, and water table measurements. Journal of Hydrology 329, 595–605.

Sylvester, A.G., (1984). Wrench Fault Tectonics. American Association of Petroleum Geologists, Reprint Series No. 28, 374 p.

Tetra Tech, (2003). Basewide hydrogeologic characterization summary report Naval Air Weapons Station China Lake, California. Report prepared by Tetra Tech Em Inc., for Department of the Navy, Naval Facilities Engineering Command, Southwest Divion. January 2003, p. 62, plus tables, figures, and appendices.

Thornthwaite, C.W. (1948). An approach toward a rational classification of climate. Geographical Review 38, 55.

Tillman, F.D., Gangopadhyay, S., and Pruitt, T. (2020). Recent and projected precipitation and temperature changes in the Grand Canyon area with implications for groundwater resources. Scientific Reports 10, 19740.

Tyler, S.W., Krantz, S., Parlange, M.B., Albertson, Katul, G.G., Cochran, G.F., Lyles, B.A., and Holder, G., (1997). Estimation of groundwater evaporation and salt flux from Owens Lake, California, USA. Ground Water 44, 329–338.

Tyler, S.W., Munoz, J.F., and Wood, W.W., (2006). The response of playa and sabkha hydraulics and mineralogy to climate forcing. Journal of Hydrology 200, 110–135.

Unruh, J., Humphrey, J., and Barron, A., (2003). Transtensional model of Sierra Nevada frontal fault system, eastern California: Geology, v. 31, p. 327–330.

USBR [U.S. Bureau of Reclamation], (1993). Indian Wells Valley Groundwater Project: USBR Technical Report Volumes I and II.

USGS [U.S. Geological Survey], (2020). Quaternary Fault and Fold Database for the United States. https://www.usgs.gov/natural-hazards/earthquakehazards/ faults. [accessed May 2020].

Wesnousky, S.G., and Jones, C.H., (1994). Oblique slip, slip partitioning, spatiotemporal changes in the regional stress field, and the relative strength of active faults in the Basin and Range, western United States: Geology 22, 1031–1034.

Wolf, S., Paul-Limoges, E., Sayler, D., and Kirchner, J.W. (2024). Dynamics of evapotranspiration from concurrent above- and below-canopy flux measurements in a montane Sierra Nevada forest. Agricultural and Forest Meteorology 346, 109864.

ATTACHMENT 1

IWV-MODEL CONFIGURATION ITEM (CI) LIST

CI Request Number	CI Request Date	CI Summary	Reviewed	Model Consideration/ Inclusion		Origin of CI (IWVGA, TAC, Navy, etc.)	Date Completed review order
				2025	2030		
1	5/6/22	SkyTEM Airborne Surveys, Dec 2017. SkyTEM Survey: Indian Wells, California (42 pp)	X	X		IWVGA	TMG 8/18/22 Plan outside AEM review Fall 2023 TMG 1/30/24
2	5/6/22	Ramboll, June 2019. Hydrogeologic Conceptual Framework; Indian Wells Valley, Final Report (113 pp)	X	X		IWVGA	TMG 8/18/22 Plan outside AEM review Fall 2023 TMG 1/30/24
3	5/6/22	Ramboll, June 2019. Indian Wells Valley – Boreholes; A Description of Borehole Information (532 pp)	X	X		IWVGA	Plan outside review w AEM Fall 2023
4	5/6/22	Steve Bacon, August 2020. DRI's Technical Review of Hydrogeologic Conceptual Framework, Indian Wells Valley, by P. Thorn, T. Parker, and M. Halhjaer, Ramboll	X	X		IWVGA	TMG 8/18/22
5	5/6/22	Jenny B. Chapman, James M. Thomas, Chris Garner; Applied Geochemistry 2022. Groundwater recharge timing based on ^{14}C and ^{2}H within Indian Wells Valley	X	X		IWVGA	Completion date to be verified
6	5/6/22	Aquifer Test Data/Reports: a) DRI, December 2020. Indian Wells Valley Multi-well Aquifer Test Analysis: IWVWD Well 10 and Quist Ranch 21-hour and 48-hour Tests, Ridgecrest, CA b) Aquilogic, 2020 (*do not have data or results as of 2/28/24)* c) Driller log capacity tests	X	X		IWVGA	Fall 2023 TMG 1/30/24

CI Request Number	CI Request Date	CI Summary	Reviewed	Model Consideration/ Inclusion		Origin of CI (IWVGA, TAC, Navy, etc.)	Date Completed review order
				2025	2030		
7	5/6/22	Navy/DRI Research Article (2021). Tectonic, hydrogeologic, and climatic controls on Late Holocene dune formation, China Lake basin, Indian Wells Valley, California, USA	X	X		IWVGA	TMG 7/14/22 Field 10/20/22
8	5/6/22	Review monitoring well EP-1 geologic, monitoring, and water quality data.	X	X		IWVGA	TMG 10/27/22 & 11/3/22
9	5/6/22	Review groundwater level data since 2015. a) Fall and spring contours b) Datalogger and telemetry data c) Monitoring well hydrographs	X	X		IWVGA	TMG 6/16/22 & 6/23/22
10	5/6/22	Review of annual water quality data collected since 2020.	X	X		IWVGA	TMG 9/1/22
11	5/6/22	Review of surface water gaged flow and field observations.	X	X		IWVGA	Completion date to be verified
12	5/6/22	Review large pumping well concentration and cones of depression.	X	X		IWVGA	TMG 7/14/22 S. Bacon, DRI Oct 2023 Hist Pumping to DRI
13	5/6/22	Review IWV faulting: a) Unnamed Fault separating El Paso Subarea and main IWV Basin b) 2019 Ridgecrest Earthquake (new) fault structure	X	X		IWVGA	TMG 7/14/22 TMG 1/30/24 S. Bacon, DRI
14	5/6/22	Rose Valley Subflow a) new monitoring wells Fall 2022 b) Faulting near Little Lake and Rose Valley Subflow Conceptual Model c) Little Lake surface flow from Inyo County	X	X		IWVGA	10/27/22 Ongoing w drilling program
15	5/10/22	USGS Basin Characterization Model (recharge)	X	X		T. Parker	TMG 1/12/24

CI Request Number	CI Request Date	CI Summary	Reviewed	Model Consideration/ Inclusion		Origin of CI (IWVGA, TAC, Navy, etc.)	Date Completed review order
				2025	2030		
16	9/1/22	Evaporation off of a wet playa	X	X		S. Bacon DRI	TMG 10/27/22 S. Bacon, DRI
17	10/6/22	IWV model Configuration Item List developed in 2022; Field visit the next day	X	X		DRI/WRM	TMG 10/6/22 Group discussion
18	10/27/22	Biweekly meetings to discuss changes to groundwater in storage and compare the model results to a Thiessen Polygon method.	X	X		DRI/WRM	TMG 12/15/22 Group discussion
19	1/19/23	Dr. Ryan Smith a) Presentation of how to approach Airborne Electromagnetic (AEM) survey data analysis (SkyTEM Survey Data Report) to Technical Model Group (TMG) members b) Additional data to provide for AEM interpretation	X	X		DRI/WRM	TMG 1/19/23 Group discussion
20	2/7/23	Numerous Teams meetings with Stetson, Dr. R. Smith, and some TMG members to discuss uncertainties using AEM survey data in GW models	X	X		DRI/WRM	TMG 2/24/23 Group discussion
21	3/2/23	Weekly calls between Stetson and DRI group to have technical discussions about 2025 update	X	X		DRI/WRM	TMG 4/6/23 Group discussion
22	4/6/23	"DRI to present the first proposed GSP Model changes: a) Simulation period: October 1, 1920 through September 30, 2022. b) Stress period: annual stress period from October 1, 1920 to September 30, 1995; monthly stress period from October 1, 1995 to September 30, 2022. c) Six model layers d) Depth and thickness of each model layer based on Monasttero et al. (2002); Shah et al. (2018) and AEM data (2019) e) Hydraulic conductivity f) Pumping a. g. Recharge"	X	X		DRI/WRM	TMG 8/17/23 Group discussion
23	5/24/23	Group meeting a) Seismic depth to basement analysis	X	X		DRI/WRM	TMG 5/24/23 Group discussion

CI Request Number	CI Request Date	CI Summary	Reviewed	Model Consideration/ Inclusion		Origin of CI (IWVGA, TAC, Navy, etc.)	Date Completed review order
				2025	2030		
		b) Clay plug analysis					
24	6/14/23	Group meeting a) Depth to basement analysis b) Sedimentary thickness analysis	X	X		DRI/WRM	TMG 6/14/23 Group discussion
25	6/30/23	Group meeting a) Preliminary model layer delineation	X	X		DRI/WRM	TMG 6/30/23 Group discussion
26	7/21/23	a) Discussed methodology for discretizing model grid in basalt flow area below Rose Valley, and planned to delineate an aquifer property zone for the White Hills formation. b) DRI will continue work on model grid discretization using SkyTEM and well log data. DRI will complete the preliminary model discretization, define faults to be simulated, and analyze clay fraction in the clay plug to present at the next modeling group meeting.	X	X		DRI/WRM	TMG 7/31/23 Group discussion
27	8/7/23	Several Teams meetings with Stetson group and R. Smith to discuss borehole data and AEM data to define clay extent; Prepared and gave two presentations to Stetson group and TMG members: 1) Proposed Model Faults for 2025 Update (August 7, 2023); and Proposed Clay Extent 2025 Update (August 25, 2023)	X	X		DRI/WRM	TMG 8/25/23 Group discussion
28	9/25/23	Steve Bacon, September 25, 2023. Development of a Tectonic Block Model in Support of the Hydrogeology Conceptual Framework of IWV (2025 Update)	X	X		DRI/WRM	TMG 9/25/23 Plan outside AEM review
29	10/6/23	Hydrogeologic zone and aquifer properties	X	X		DRI/WRM	Emailed on 10/6/23
30	10/23/23	Historical Calibration Pumping for model update	X	X		DRI/WRM	TMG 10/23/23 reviewing
31	10/30/23	Initial head (October 1920) and historical water levels in IWVGB	X	X		DRI/WRM	1/9/2024

CI Request Number	CI Request Date	CI Summary	Reviewed	Model Consideration/ Inclusion		Origin of CI (IWVGA, TAC, Navy, etc.)	Date Completed review order
				2025	2030		
32	12/18/23	a) Final model domain boundary. b) Final model domain layers including deep clay extent. c) Proposed aerial extent, extinction depths, and maximum rates of ET zones. d) Review 2020 GSP recharge distribution and discuss potential changes to recharge distribution in 2025 update.	X	X		DRI/WRM	TMG 12/18/2023 discussion
33	1/5/24	Mountain front recharge and aquifer connectivity	X	X		DRI/WRM	TMG 1/12/2024 discussion
34	1/12/24	Recharge and model update	X	X		DRI/WRM	TMG 1/12/2024 discussion
35	1/30/24	Recharge distribution, hydraulic conductivity zones and model update	X	X		DRI/WRM	TMG 1/30/2024 discussion
36	2/13/24	Transient water level for IWV model calibration	X	X		DRI/WRM	2/14/2024
37	2/28/24	Consider uncertainty analysis in next 2030 Model update.	X		X	DRI/WRM	3/5/2024 TMG meeting
38	2/28/24	Groundwater level data for model calibration - prioritize areal density and temporal length of well data sets. 2025 Model update uses about double the number of target wells as 2020 GSP Model. Revisit target well data sets (include target weighting) for 2030 Model update.	X		X	DRI/WRM	3/5/2024 TMG meeting
39	2/28/24	2025 Model update maintains 7,650 AFY Recharge from 2020 GSP Model. Revisit these recharge assumptions during future 2030 Model update.	X		X	DRI/WRM	3/5/2024 TMG meeting
40	2/28/24	Review of LADWP Emergency Release Draft Data Report.	X	X		WRM	3/5/2024 TMG meeting

CI Request Number	CI Request Date	CI Summary	Reviewed	Model Consideration/ Inclusion		Origin of CI (IWVGA, TAC, Navy, etc.)	Date Completed review order
				2025	2030		
41	2/28/24	Review of El Paso Subarea delineation for sub-water budget.	X	X		WRM	3/5/2024 TMG meeting
42	3/18/24	Review Rose Valley water hydrogeology and model update	X	X		WRM	TMG 3/18/2024 discussion
43	3/26/24	Develop future baseline pumping.	X	X		WRM	TMG 3/26/2024 discussion
44	4/2/24	Review 2020 GSP Scenario 6.2 modeling and discuss approach to baseline pumping.	X	X		WRM	4/2/2024 TMG meeting
45	4/16/24	Model calibration progress. Calibration mostly complete, with exception to Rose Valley area.	X	X		S. Rybarski, DRI	4/16/2024 TMG meeting
46	4/23/24	Consider sensitivity analysis by region in 2030 Model update.	X		X	DRI/WRM	4/30/2024 TMG meeting
47	4/25/24	Develop assumptions for 2025 Implemented Management pumping	X	X		WRM	5/17/2024 TMG meeting
48	5/9/24	Modify future baseline pumping	X	X		WRM/Legal	5/17/2024 TMG meeting
49	5/10/24	Develop climate change modeling approach – use of Cal-Adapt tool	X	X		DRI/WRM	5/17/2024 TMG meeting
50	5/15/24	Model calibration complete	X	X		DRI/WRM	5/17/2024 TMG meeting
51	5/24/24	Initial disclosures on current and projected pumping	X	X		WRM/Legal	6/4/2024 TMG meeting
52	5/29/24	Additional Model Runs developed - Scenario 1A: Implementation - Scenario 2: No GA	X	X		WRM/Legal	6/4/2024 TMG meeting
53	6/13/24	Modify future baseline pumping and 2025 Implemented Management pumping assumptions	X	X		WRM	6/18/2024 TMG meeting
54	6/17/24	Additional consumptive use analysis added as a data gap	X		X	WRM	6/18/2024 TMG meeting
55	7/10/24	Model Update Presentation at IWVGA Board Meeting	X	X		DRI	7/10/2024 IWVGA Board meeting
55	7/17/24	Development of additional modeling scenarios - Scenario 3: ET Study - Scenario 1B: SVM/IWVWD Pumping Balance	X	X		DRI/WRM	7/17/2024 DRI/Stetson call

CI Request Number	CI Request Date	CI Summary	Reviewed	Model Consideration/ Inclusion		Origin of CI (IWVGA, TAC, Navy, etc.)	Date Completed review order
				2025	2030		
		- Scenario 4: El Paso Pumping					
56	8/8/24	Verify model results for GDE EVT with monitoring data	X		X	WRM	8/8/2024
57	8/12/24	Well locations updated	X	X		DRI/WRM	8/12/2024
58	8/14/24	Monthly recharge updated	X	X		DRI/WRM	8/21/2024
59	8/27/24	Additional modeling runs complete		X		DRI	8/27/2024
60	9/24/24	Climate change modeling complete		X		DRI	9/24/2024
61	Oct. 2024	Sensitivity Analysis Complete	X	X		DRI	October 2024

ATTACHMENT 2

TECHNICAL MEMORANDUM

STETSON ENGINEERS INC.

2171 E. Francisco Blvd., Suite K • San Rafael, California • 94901

TEL: (415) 457-0701 FAX: (415) 457-1638 e-mail: curtisl@stetsonengineers.com

TO:	File	DATE:	December 2, 2024
FROM:	Stetson and DRI (Jean Moran, Curtis Lawler, Susan Rybarski)	JOB NO:	2162
RE:	Mountain Front Recharge – 2025 Model Data Preparation		

1 Introduction

This technical memorandum documents and summarizes the methodologies used to develop data for mountain front recharge used in the 2025 Basin Model for Indian Well Valley Groundwater Authority SGMA analyses. Mountain front recharge is the predominant source of inflow to the Basin. The estimated long-term average mountain front recharge of 7,650 acre-feet per year (AFY) was established for the 2020 GSP.

2 Background and Work Performed for 2020 GSP

In 2016, DRI reviewed fourteen previous studies in which recharge estimates ranged from 4,000 to 11,000 AFY. The average annual recharge developed by DRI, in coordination with the IWV TAC, is 7,650 AFY (McGraw et al., 2016; Garner et al., 2017). Mountain areas receive more precipitation than the playa and are the primary source of recharge for the Basin. For the 2020 GSP Model, the long-term average 7,650 AFY of recharge was distributed to five mountain regions: Argos and Coso, Rose Valley, Sierra Nevada North, Sierra Nevada South, and El Paso (Figure 1).

The Navy provided the initial annual calibrated model developed by DRI as in-kind services. The 2020 GSP Model calibration was based on annual stress periods, and water budget numbers were summarized by calendar year (January through December). Future Baseline (no action) and Management Model runs were developed with a monthly stress period, and the water budgets were summarized as calendar years (January 2020 through December 2070) for the 2020 GSP Model.

When examining hydrologic trends, a more recent balanced period was selected to take advantage of recent precipitation data available at stations within the recharge zones. A monthly precipitation index was computed for three recharge zones for the corresponding balanced hydrologic period of 1990 to 2015, 26 years (Stetson Engineers, 2018). The precipitation index was used to scale the average annual recharge for the groundwater model (7,650 AFY) using a linear relationship between the precipitation index and recharge. SGMA requires a 51-year (WY 2020 to WY 2070) future planning period for GSPs. Reconstruction of the required 51-year future recharge was based on repeated historical hydrology from 1990-2015, then 1990-2014. The mean of these

variations over the prediction period is equal to the annual recharge rate of 7,650 AF used for the steady-state and transient groundwater models.

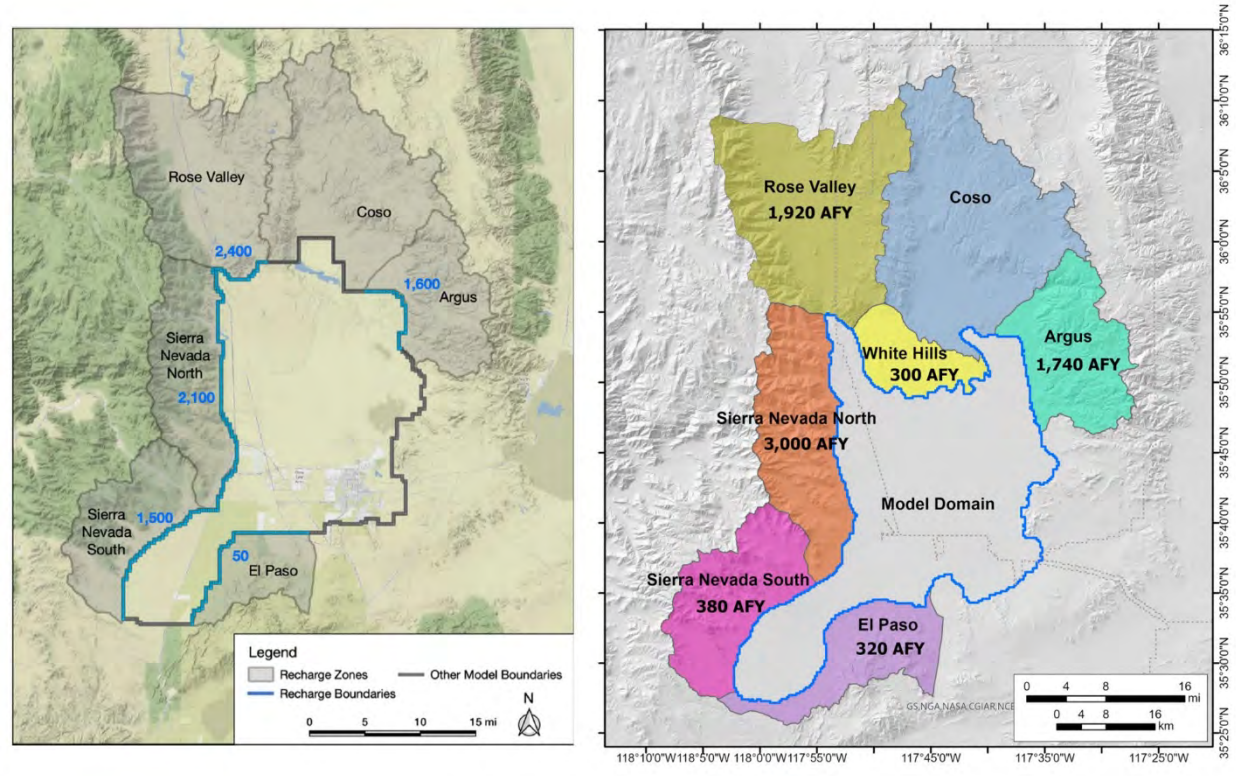


Figure 1. Recharge zones and average annual recharge rates used in the 2020 GSP Basin Model (left) and the 2025 Basin Model (right). All rates are displayed in acre-feet per year.

2.1 Filling in Missing Data in the Precipitation Gage Records

The index precipitation used for the 2020 GSP was an average of three precipitation stations (Haiwee, Indian WV, Laural Mtn Stations) based on available data from the Western Regional Climate Center. These stations were chosen based on representing different mountain regions (Rose Valley, Sierra Nevada North, and El Paso, respectively). The fill-in method[1] uses data and the ratio of long-term averages from nearby precipitation stations to the index station so that there is a complete data set for these three main precipitation stations used in the analysis.

[1] Note: The method for filling in missing precipitation data is more fully described in the 2020 GSP. WRCC stopped reporting Haiwee in 2017. We received LADWP data for the Haiwee gage after the recharge was calculated for the 2025 Basin Model. The average Haiwee precipitation from 1985 to 2016 is slightly different depending upon source (LADWP=6.2 in/year compared with 5.7 in/yr WRCC/Molly spreadsheet). For the period Haiwee estimated in WRCC database 2017-2023, the average is also different (LADWP=8.5 in/year compared with 8.3 in/yr from WRCC used in the 2020 GSP Model). It is recommended switching data sources for the next model update after both data sets are fully reviewed.

3 Additional Work for the 2025 Basin Model

The same methodology used for the 2020 GSP Model was utilized but updated to fit stress periods aligned with water years rather than calendar years, to extend historical recharge estimates through WY 2022, and to address the new distribution of recharge applied to the 2025 Basin model. The linear distribution of observed precipitation to the initially estimated recharge rate is presented in Figure 2. The 2025 Basin model also used monthly stress periods in the transient historical model beginning in WY 1995, unlike the 2020 GSP which used annual stress periods for the duration of the transient historical model, so historical recharge rates were discretized to accommodate this change.

Similar to the 2020 GSP model, recharge was applied in the upper 3 layers of the model domain, but the spatial distribution was modified for the 2025 Basin model to include an additional recharge zone (White Hills) (Figure 1). The initial monthly recharge values developed for the 2025 Basin model were further processed so that the inflows to deeper model layers 2 and 3 are constant (3,362 AFY), and only the recharge in layer 1 varies according to the precipitation. This process smoothed out the extreme minimum and maximum monthly recharge and provided better model calibration of historical groundwater level data, compared to raw estimates based only on rainfall.

To estimate changes in precipitation within layer 1 only, annual (WY 1920-1995) or monthly (WY 1996-2022) recharge rates were first calculated using the 2020 GSP methodology, resulting in a long-term average recharge rate of 7,650 AFY over the simulated historical period of WY 1921-2022. These rates were then divided by the average annual recharge rate of 7,650 AFY to obtain the fraction of the long-term annual average for each monthly or annual stress period. These fractions were then applied to the steady-state recharge rates for layer 1 to develop recharge rates for each monthly or annual stress period. Total recharge in layer 1 was distributed to each recharge zone in each stress period according to the fraction used in the steady-state model (Figure 1).

This method results in a muted signal relative to the 2020 GSP recharge rates, i.e. above average recharge is reduced, but below average recharge is increased, and zero-recharge stress periods do not occur. Figure 3 shows annual recharge rates estimated using the relationship between precipitation and recharge as presented in Figure 2, compared to the final simulated recharge rates modified to reflect fluctuations in layer 1 only.

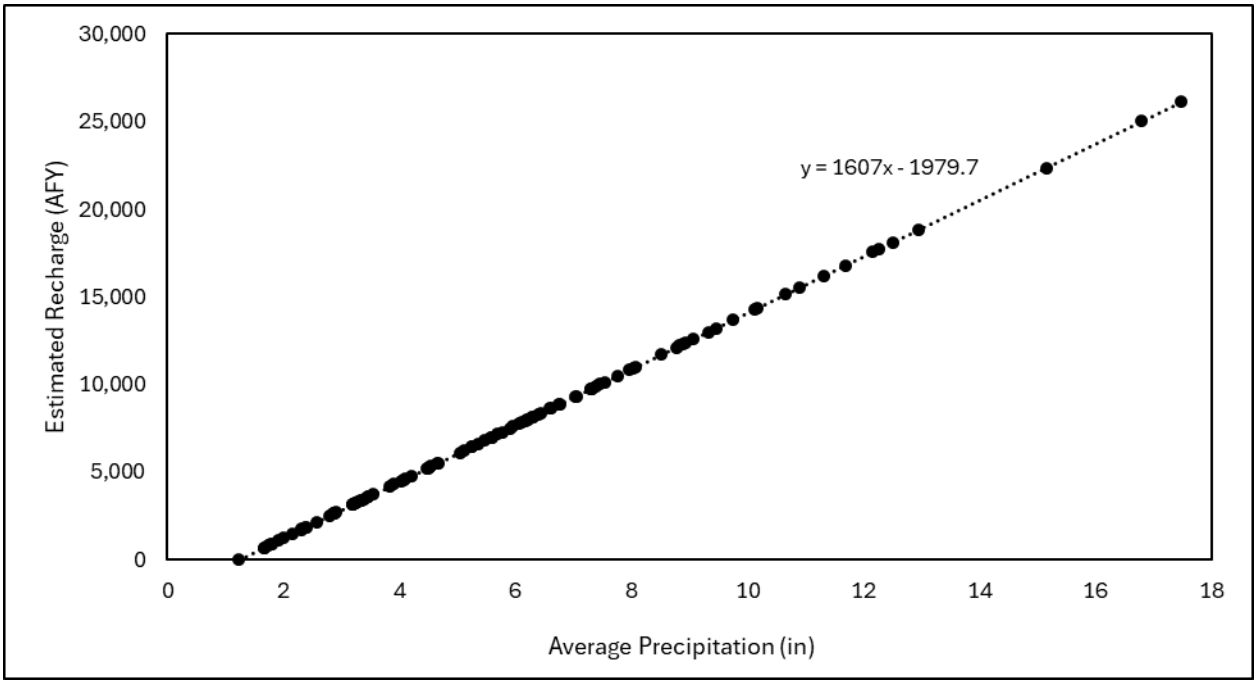
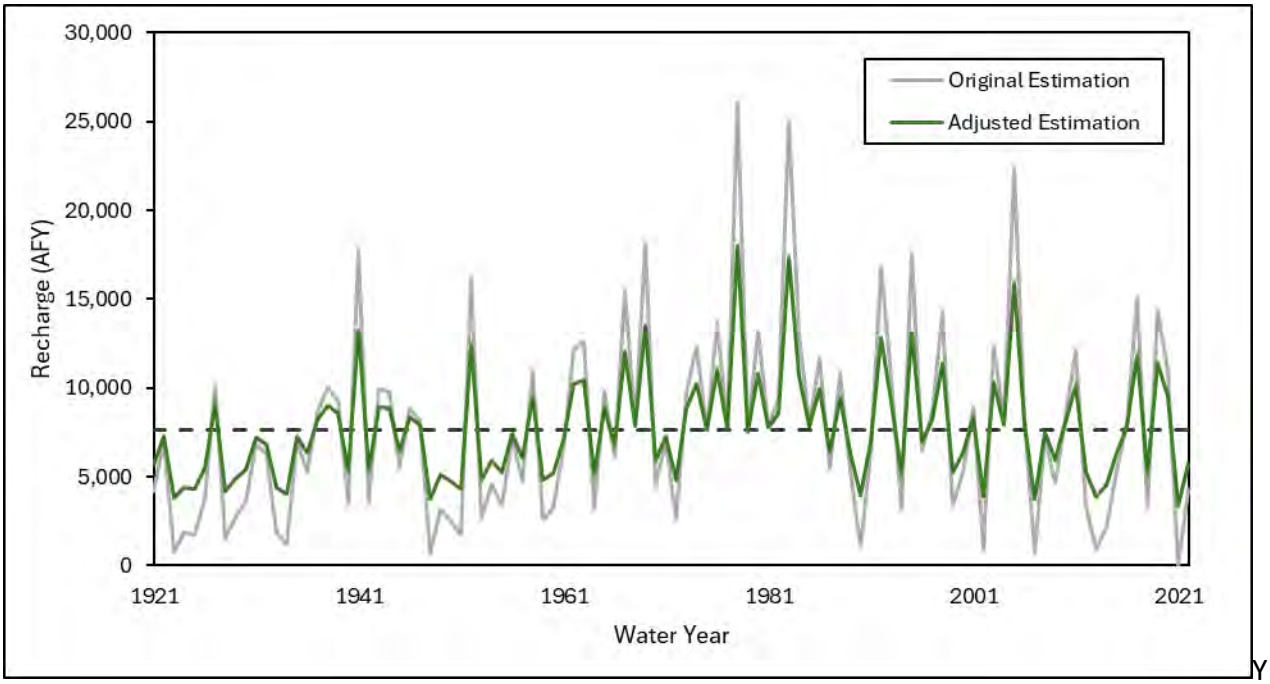


Figure 2. Linear distribution of historical precipitation to estimated recharge, distributed to average 7,650 AFY over W 1921-2022.



Y

Figure 3. Annual recharge rates estimated using the relationship between precipitation and recharge (grey) as presented in Figure 2, compared to the final simulated recharge rates modified to reflect fluctuations in layer 1 only (green). The dashed line depicts the average annual recharge rate of 7,650 AFY.

3.1 Mountain Front Recharge Estimate Using Precipitation Index

The 2025 Basin Model Baseline and Management Scenarios simulate WY 2020-2070 (51 years). WY 2020-2022 overlap in both the historical calibration and the future management scenarios. The recharge rates for those three years were replicated in the Baseline and Management Scenario models. Given the timing of model development and calibration, WY 2023 was not included in the historical calibration. However, recharge for WY 2023 in the Baseline and Management Scenarios was estimated based on observed precipitation rates for that year using the relationship derived from the WY 1921-2022 precipitation index.

To generate the distribution of annual variation, the sequence of monthly recharge rates used in the 2020 GSP (based on 1990-2015) was used as the starting point, modified to simulate fluctuations in layer 1 only, and then repeated to cover the simulation period through WY 2070. These years were then spliced with historical estimates for 2020-2023 and average values at benchmark years 2030, 2040, and 2070. Lastly, to ensure that the annual average was still 7,650 AFY with these edits, monthly recharge rates for the years 2066, 2067, and 2068 were adjusted to obtain the 51-year average. Annual totals of simulated recharge for the Baseline and Management Scenario models are shown in Figure 4.

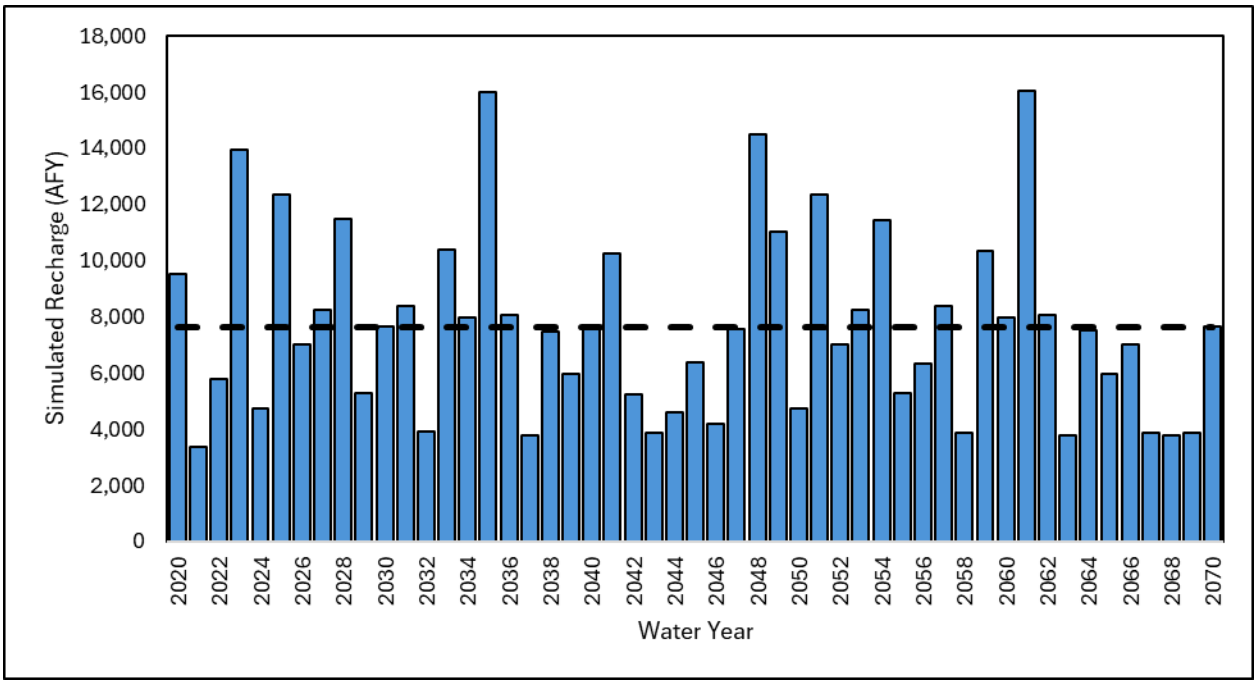


Figure 4. Annual variability of recharge forecasted for the predictive simulations. The mean of the annual recharge values is 7,650 AFY, shown with a dashed black line.

4 References

Indian Wells Valley Groundwater Basin Groundwater Sustainability Plan, January 2020

California RAWS data: https://raws.dri.edu/scaF.html

California Cooperative weather station data: https://wrcc.dri.edu/summary/Climsmsca.html

OSU PRISM Climate Normals for 1981-2010 (800-meter spatial raster for annual precipitation):

http://prism.oregonstate.edu/normals/

Garner, C., Bacon, S., Pohll, G., and Chapman, J., 2017. Indian Wells Valley Groundwater Model Update. Desert Research Institute Technical Memorandum.

McGraw, D., Carroll, R., Pohll, G., Chapman, J., Bacon, S., and Jason, R., 2016. Groundwater Resource Sustainability: Modeling Evaluation for the Naval Air Weapons Station, China Lake. California. Prepared by Desert Research Institute for the Naval Air Warfare Center Weapons Division, Final Evaluation Report NAWCWD TP 8811.

Stetson Engineers, 2018. Notes on Determination of Balanced Hydrologic Period and Model Recharge Distribution. Memo to Greg Pohll, Desert Research Institute, December 12, 2018.

ATTACHMENT 3

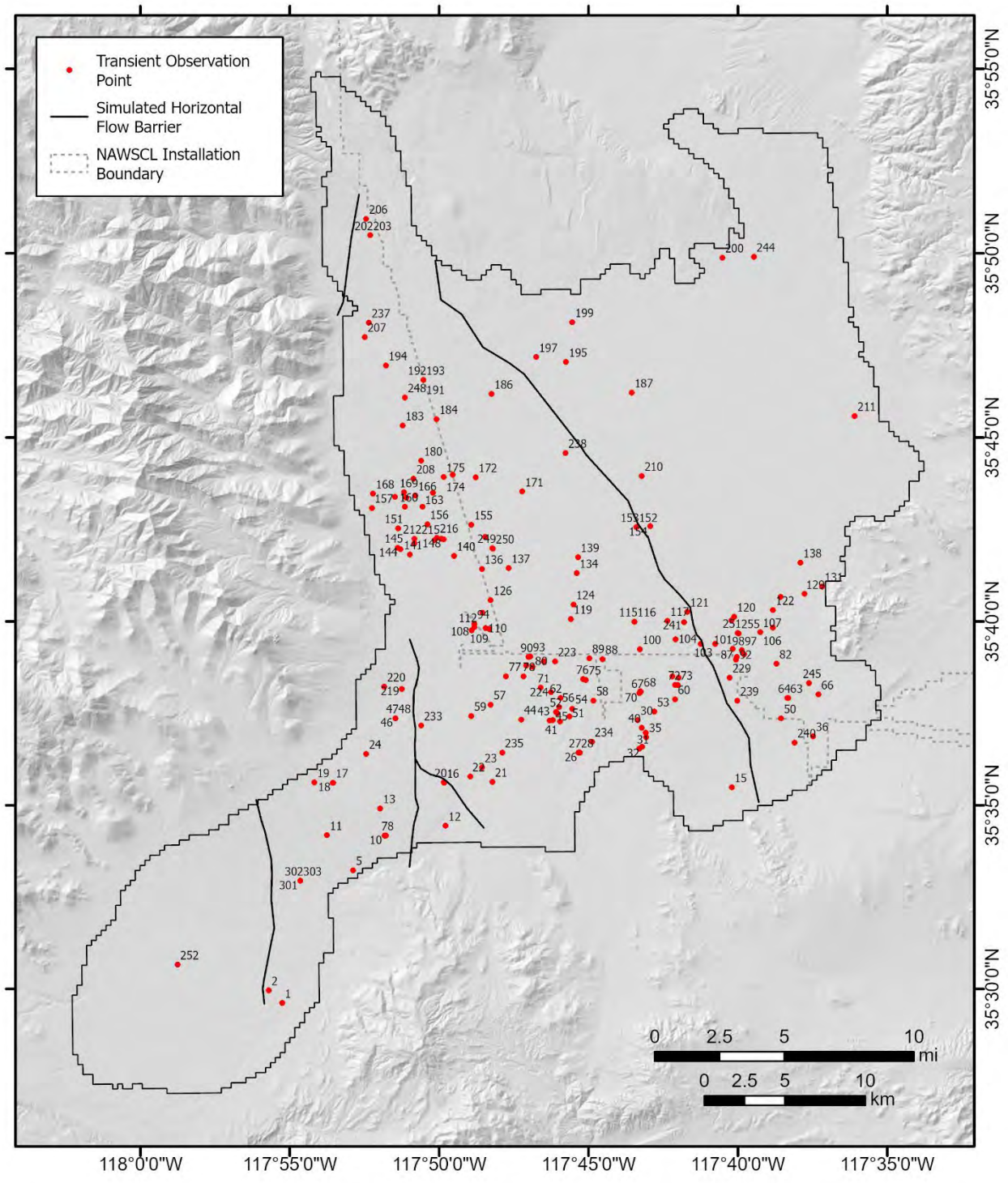


Figure A-1. Locations of observation points used in the calibration of the transient-historical model for the 2025 Basin Model. Hydrographs showing observed and simulated water levels at each point are shown in Figures A-2 to A-25.

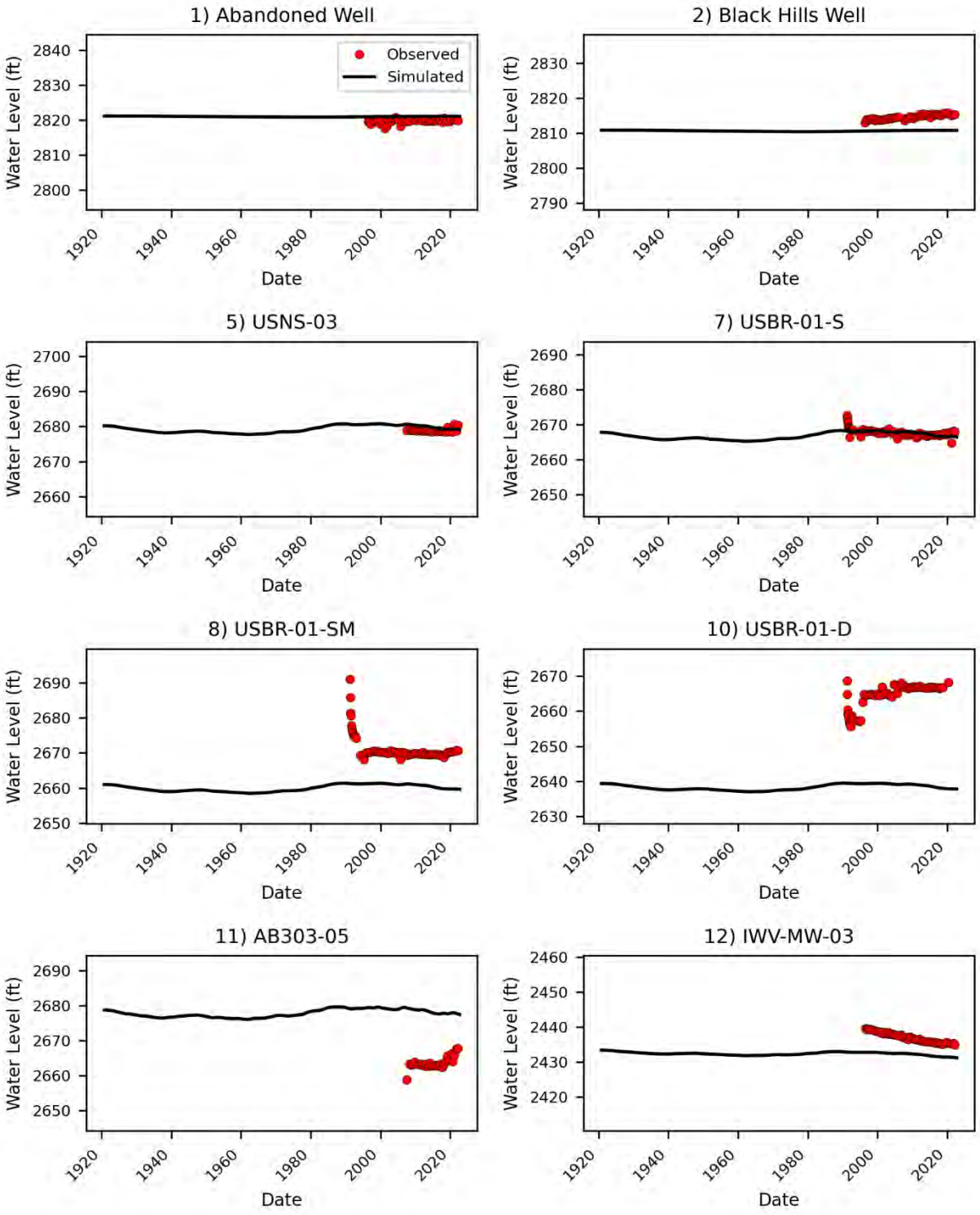


Figure A-2. Simulated and observed water levels from the transient historical calibration model for well locations indicated on Figure A-1.

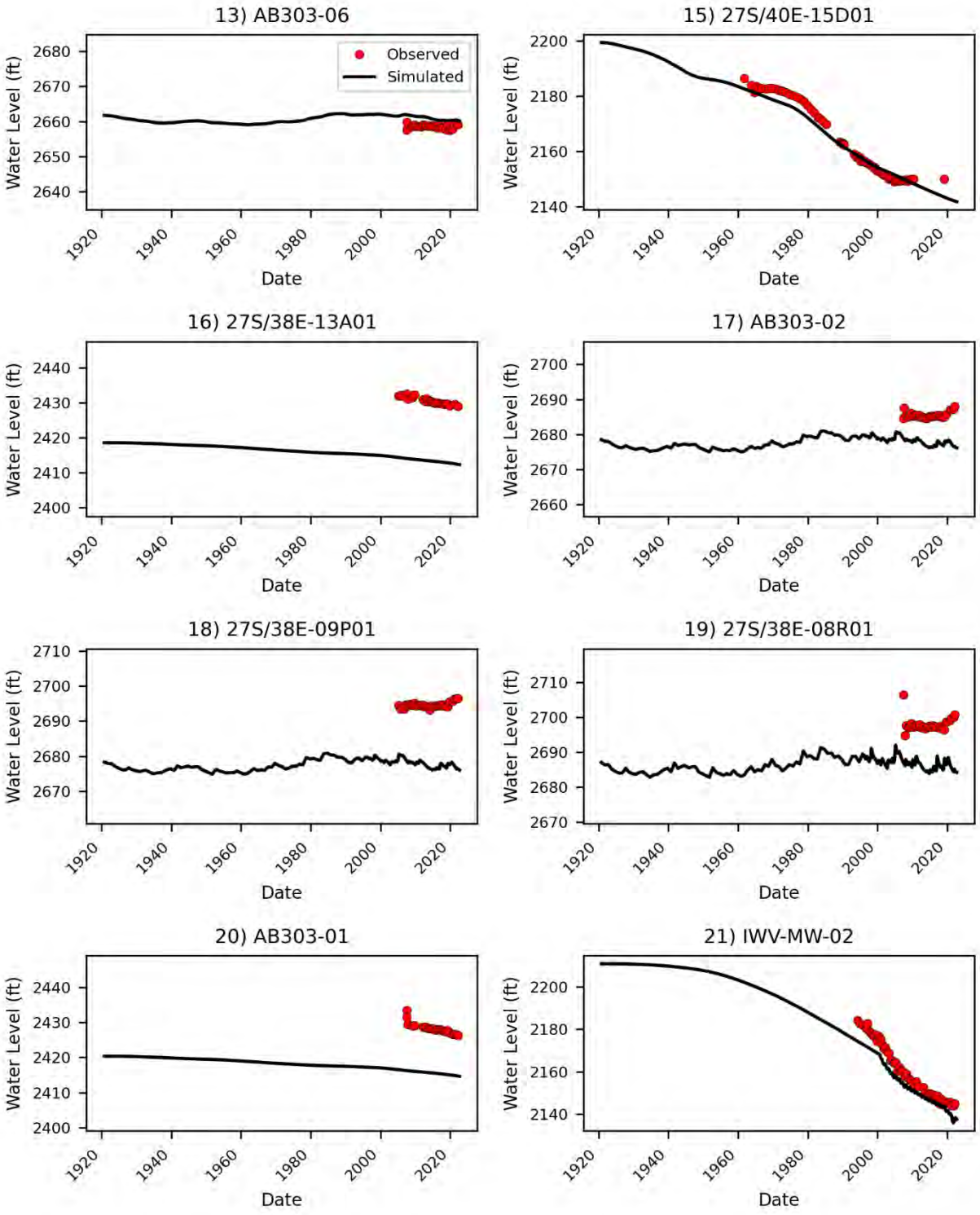


Figure A-3. Simulated and observed water levels from the transient historical calibration model for well locations indicated on Figure A-1.

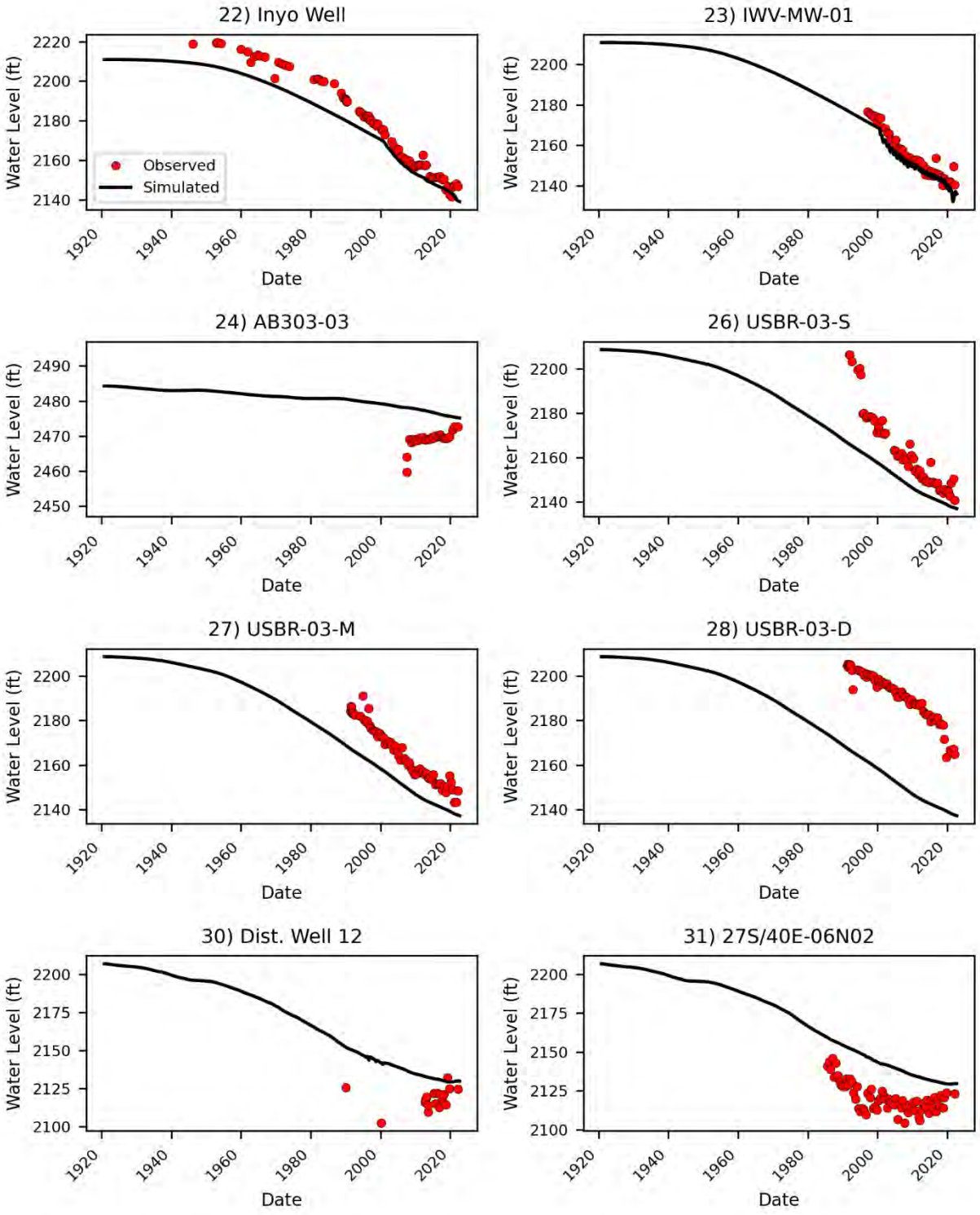


Figure A-4. Simulated and observed water levels from the transient historical calibration model for well locations indicated on Figure A-1.

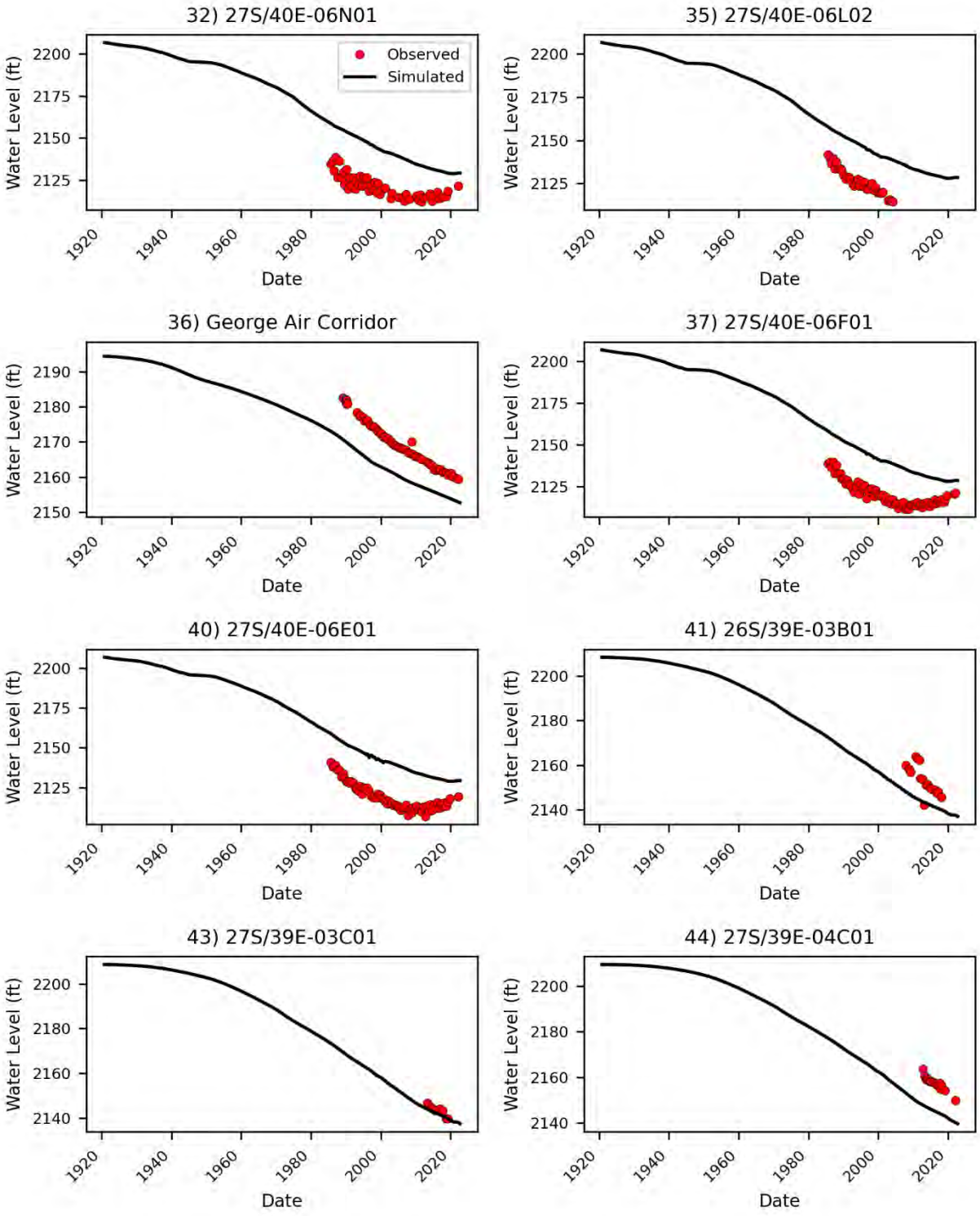


Figure A-5. Simulated and observed water levels from the transient historical calibration model for well locations indicated on Figure A-1.

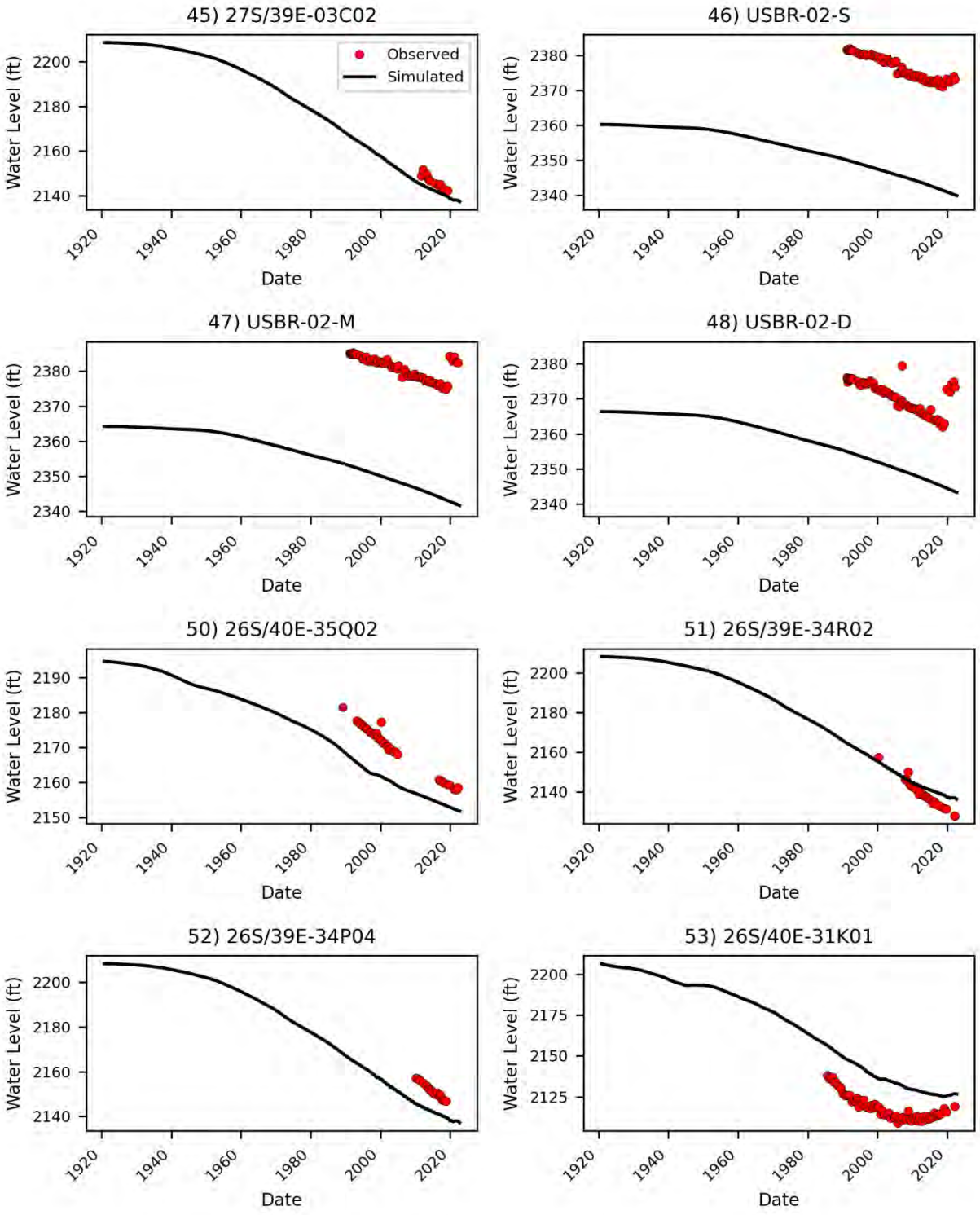


Figure A-6. Simulated and observed water levels from the transient historical calibration model for well locations indicated on Figure A-1.

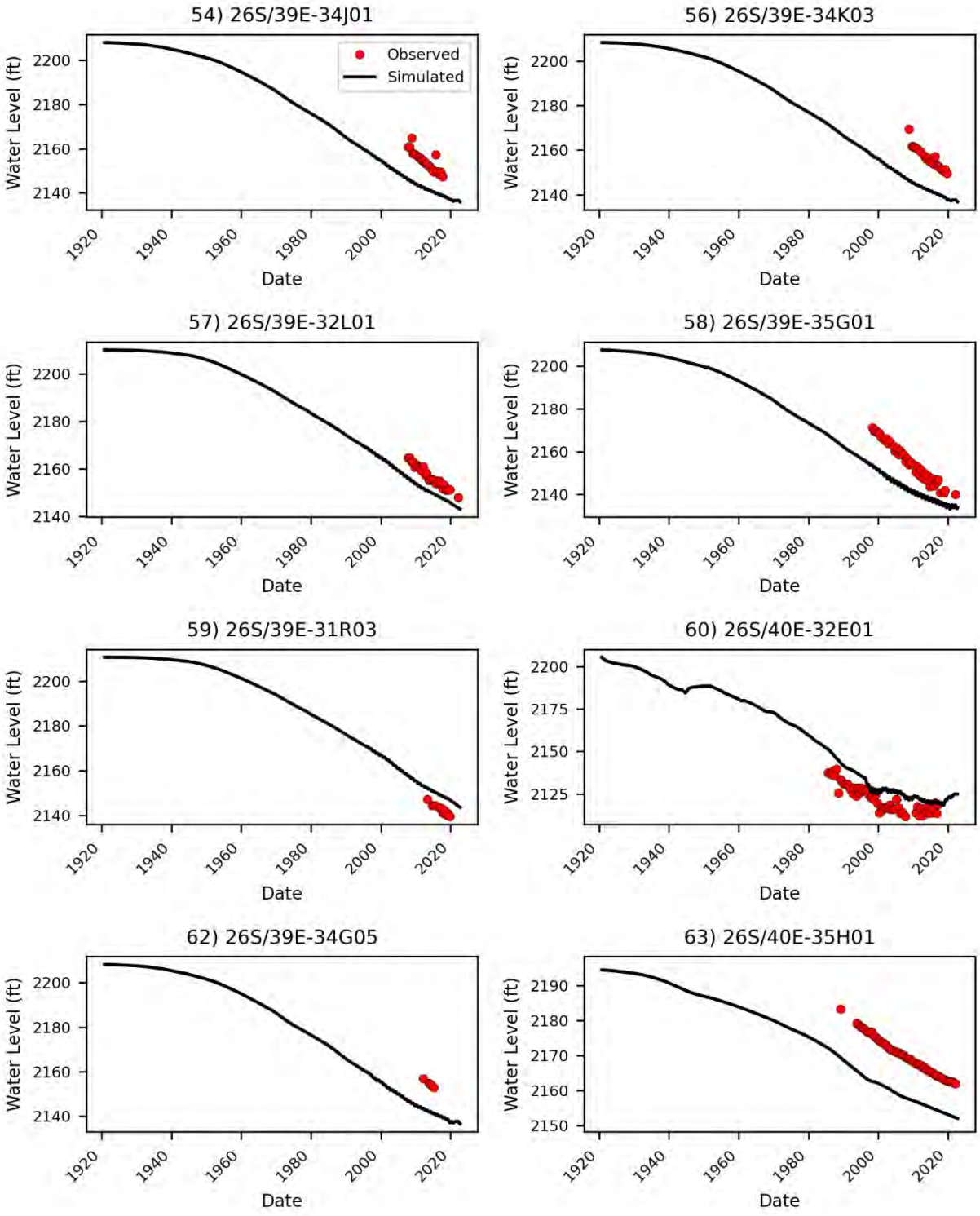


Figure A-7. Simulated and observed water levels from the transient historical calibration model for well locations indicated on Figure A-1.

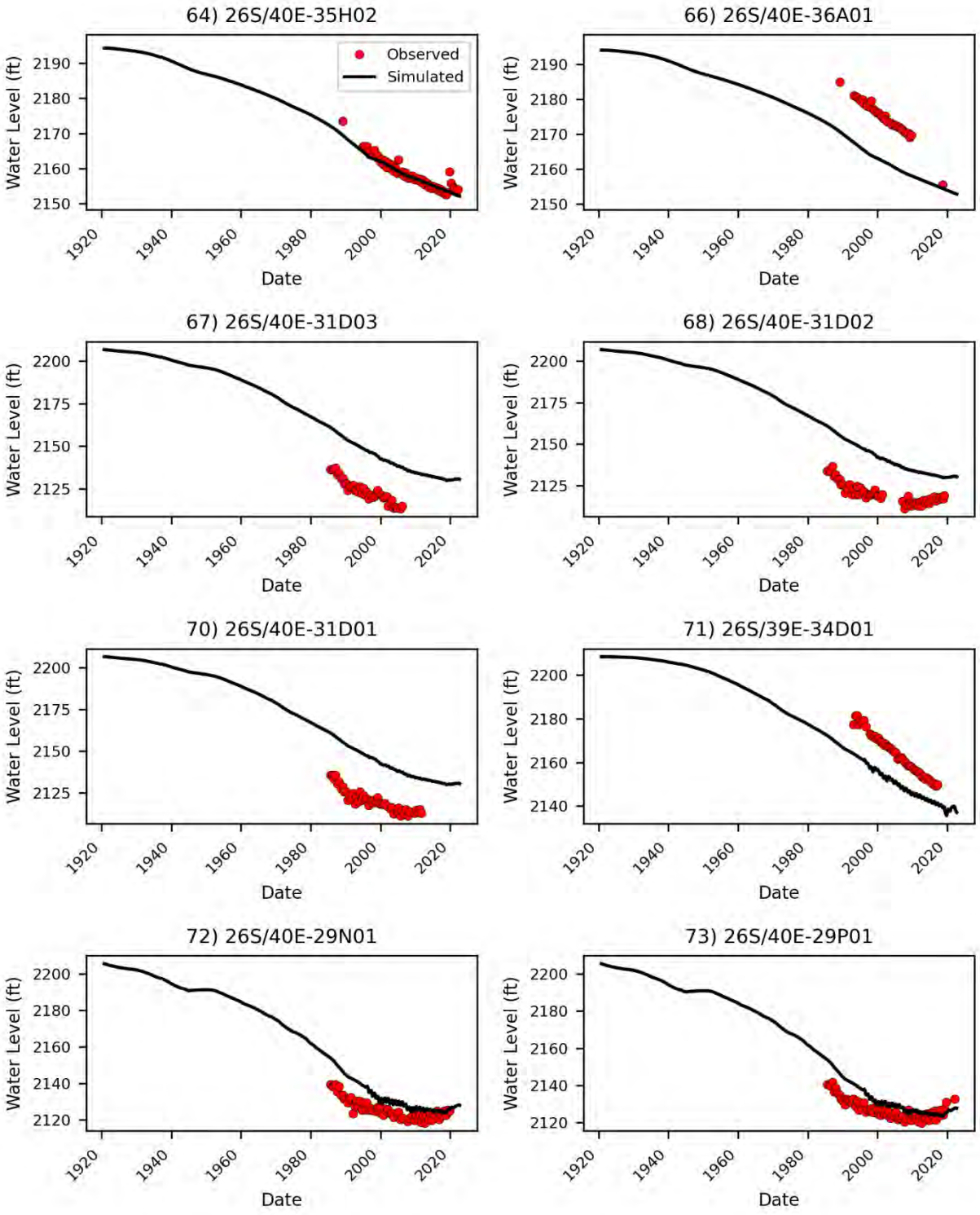


Figure A-8. Simulated and observed water levels from the transient historical calibration model for well locations indicated on Figure A-1.

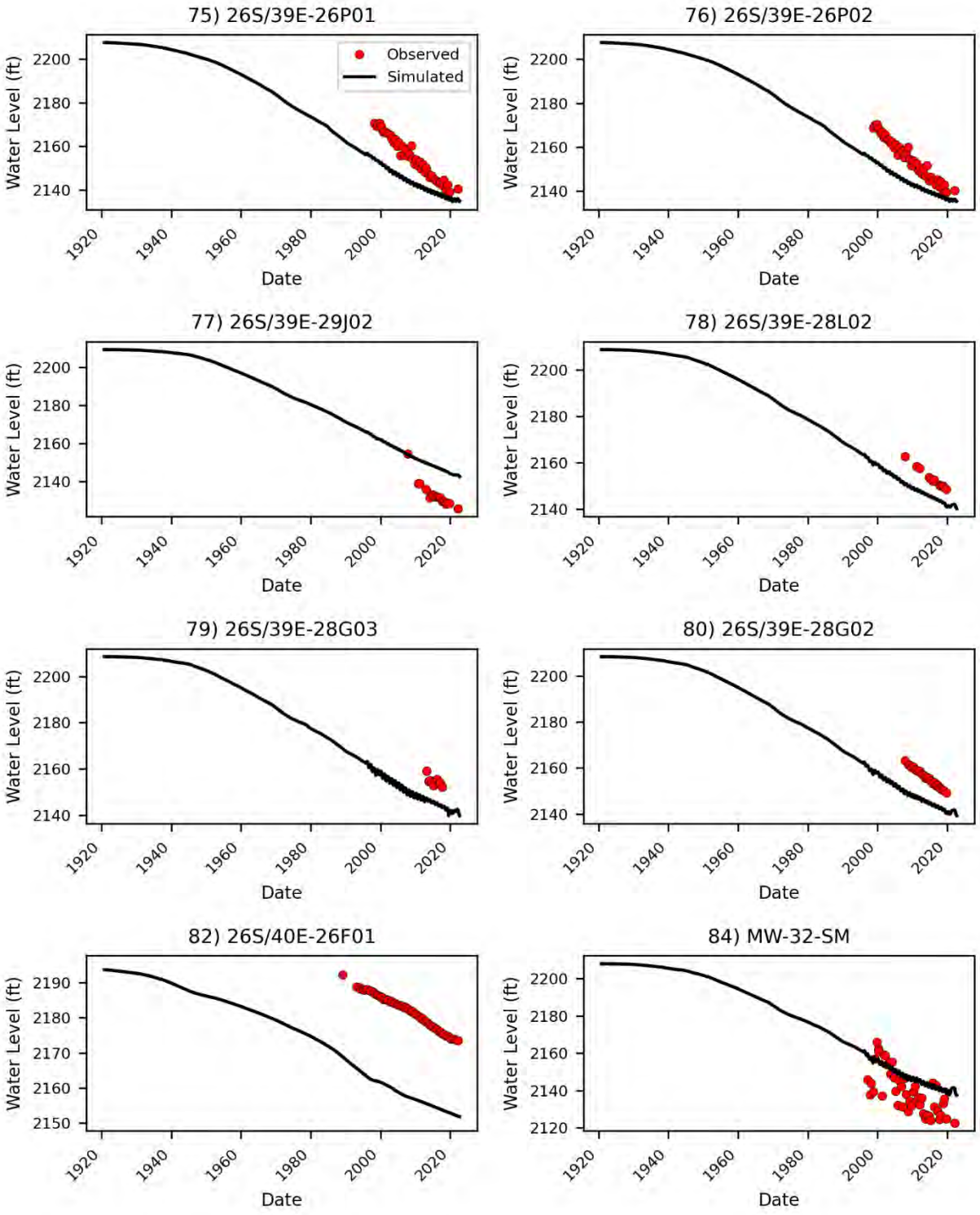


Figure A-9. Simulated and observed water levels from the transient historical calibration model for well locations indicated on Figure A-1.

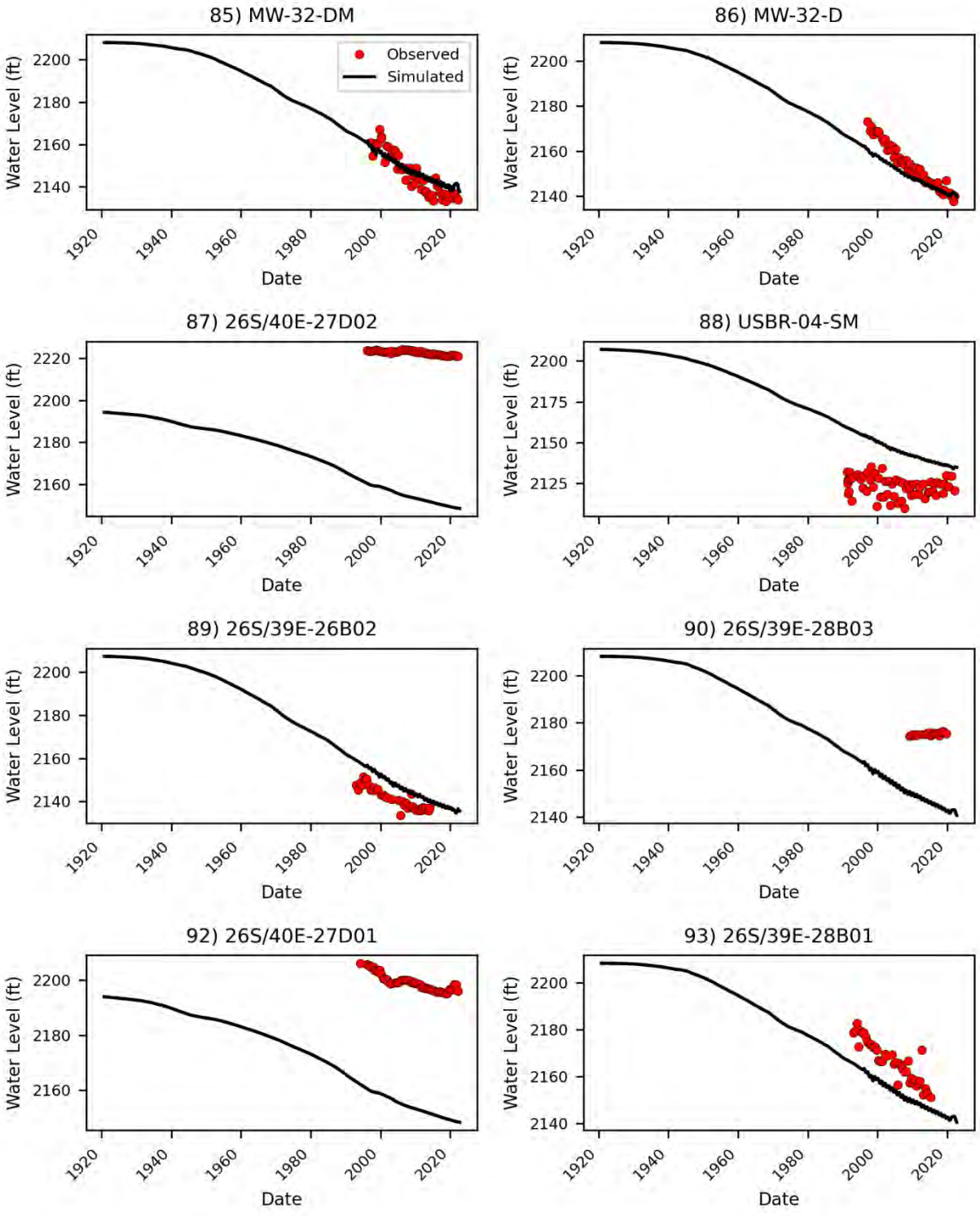


Figure A-10. Simulated and observed water levels from the transient historical calibration model for well locations indicated on Figure A-1.

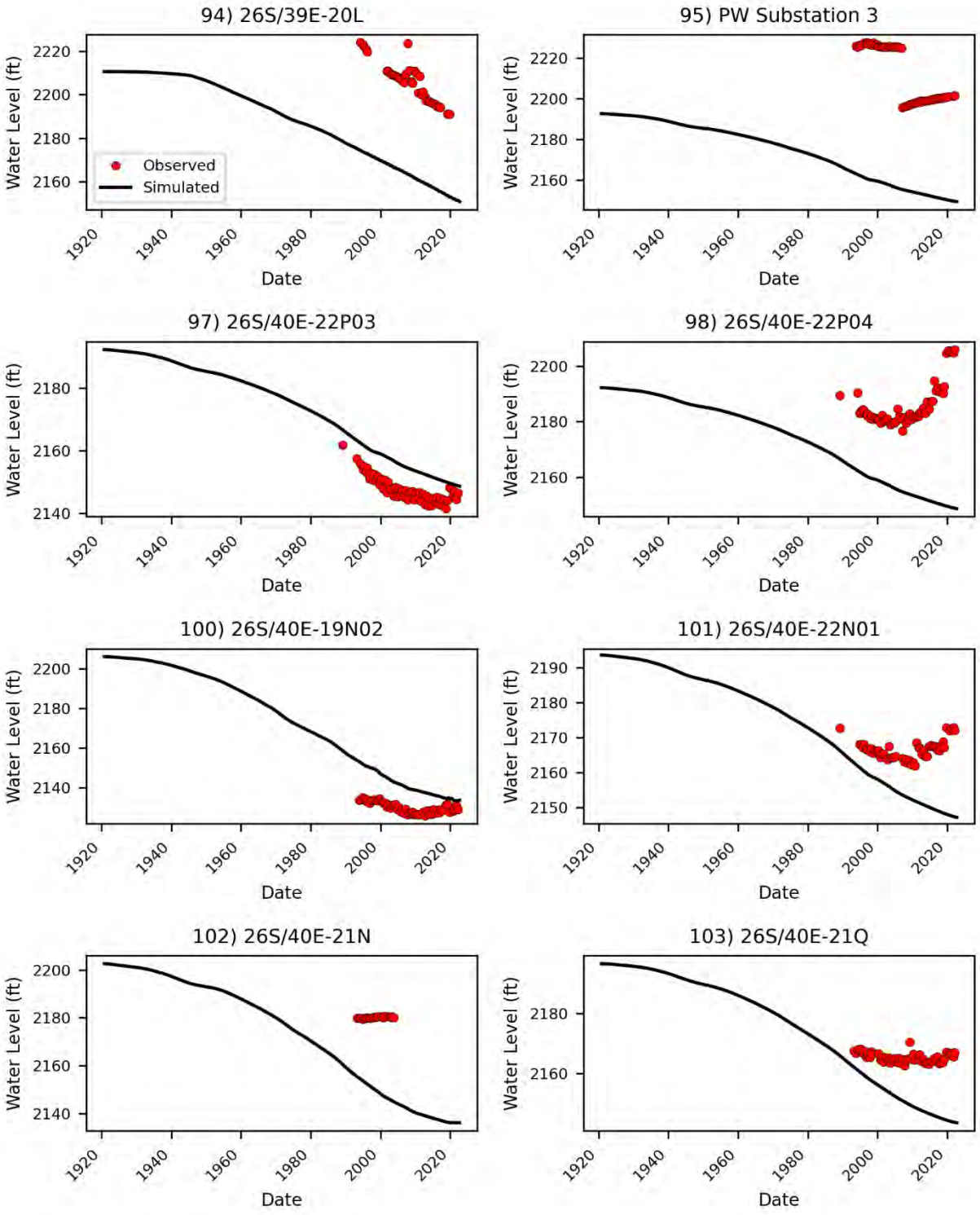


Figure A-11. Simulated and observed water levels from the transient historical calibration model for well locations indicated on Figure A-1.

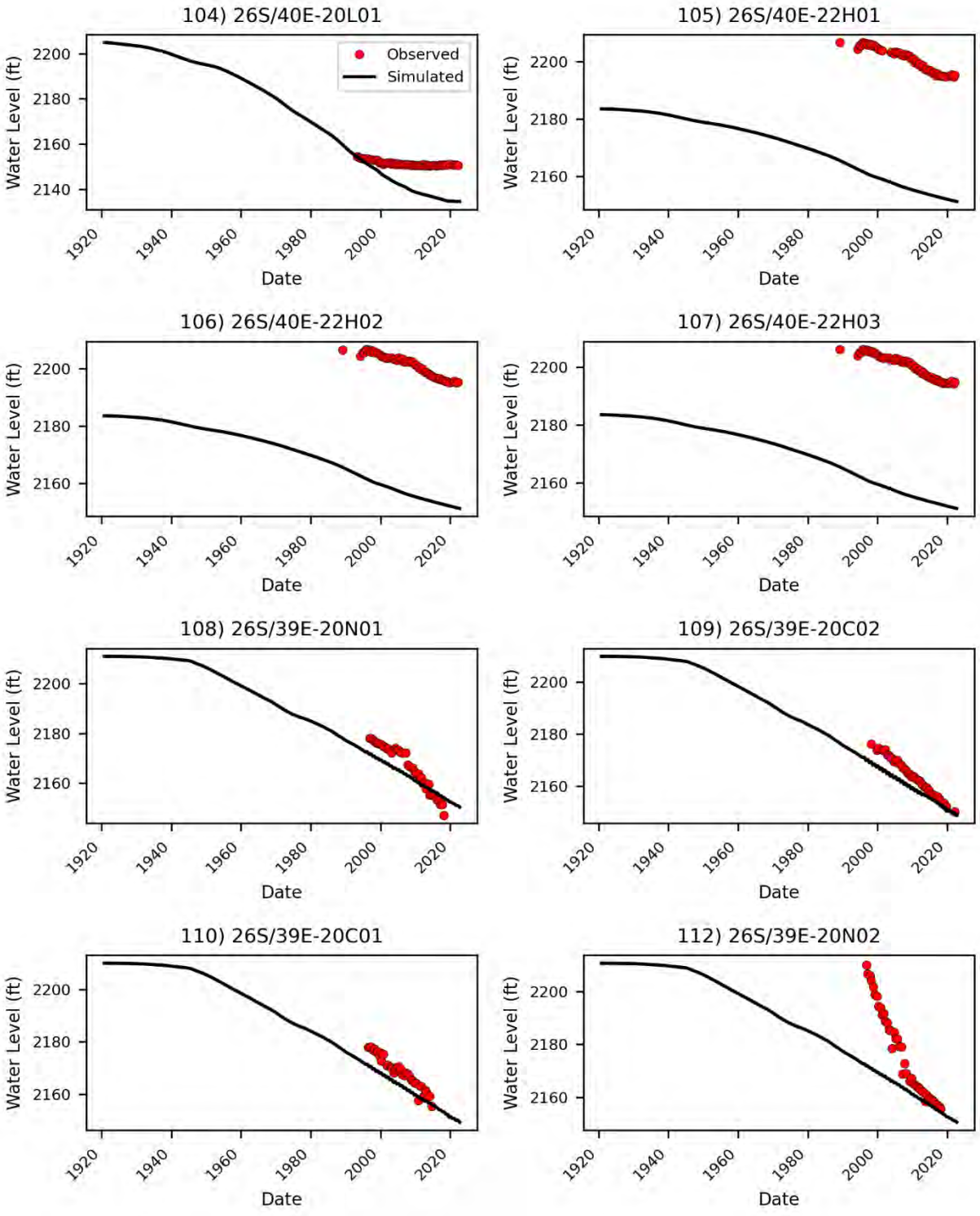


Figure A-12. Simulated and observed water levels from the transient historical calibration model for well locations indicated on Figure A-1.

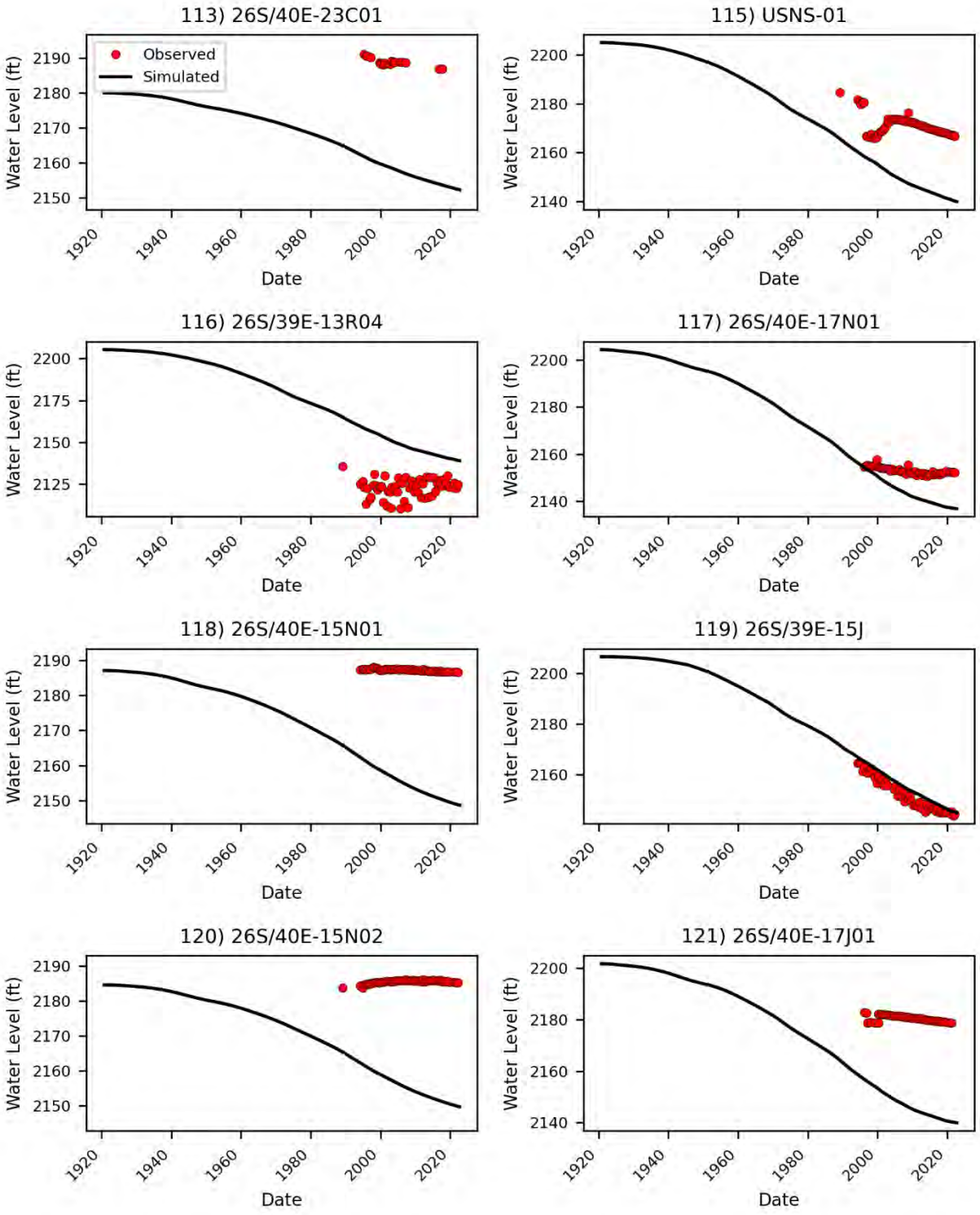


Figure A-13. Simulated and observed water levels from the transient historical calibration model for well locations indicated on Figure A-1.

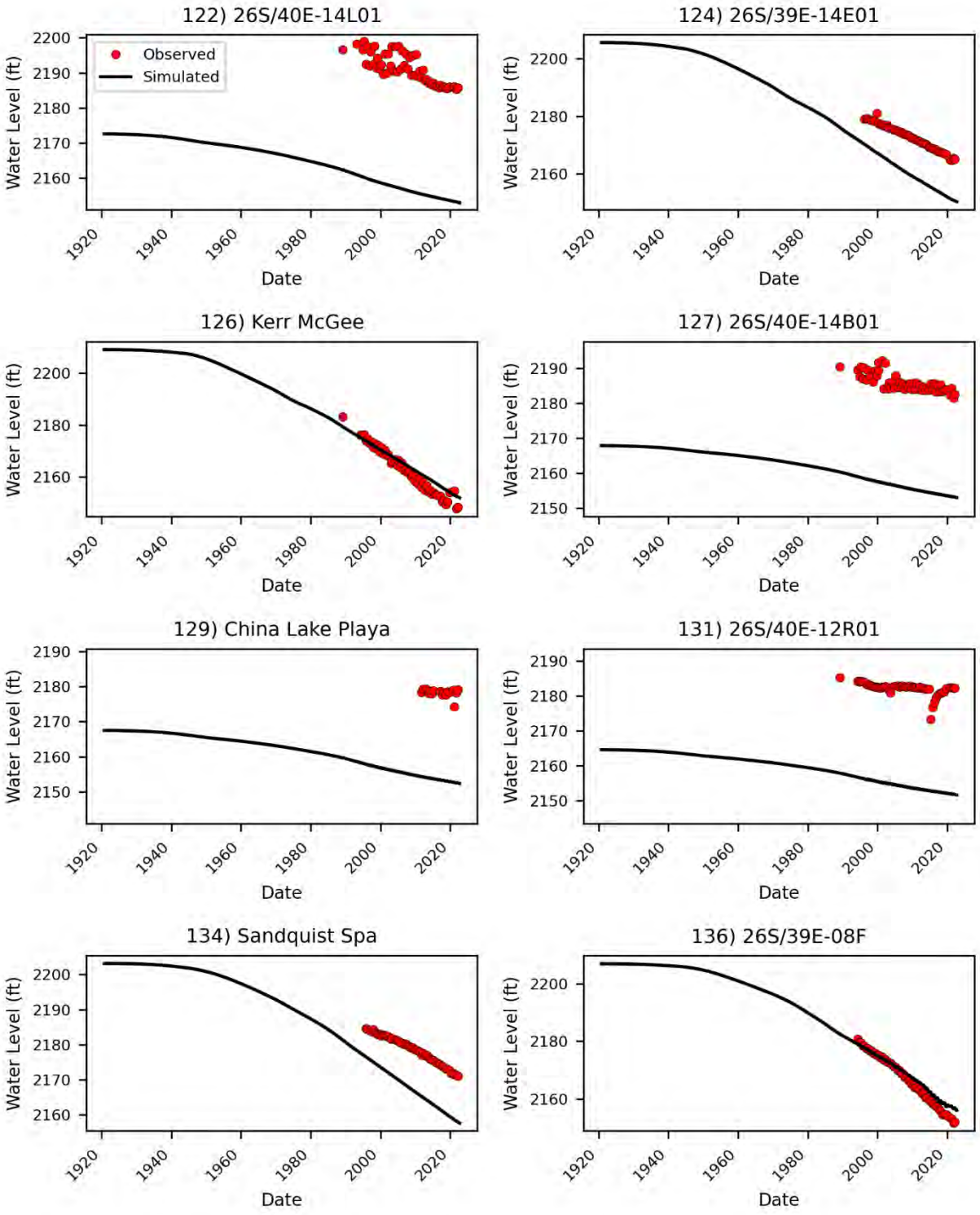


Figure A-14. Simulated and observed water levels from the transient historical calibration model for well locations indicated on Figure A-1.

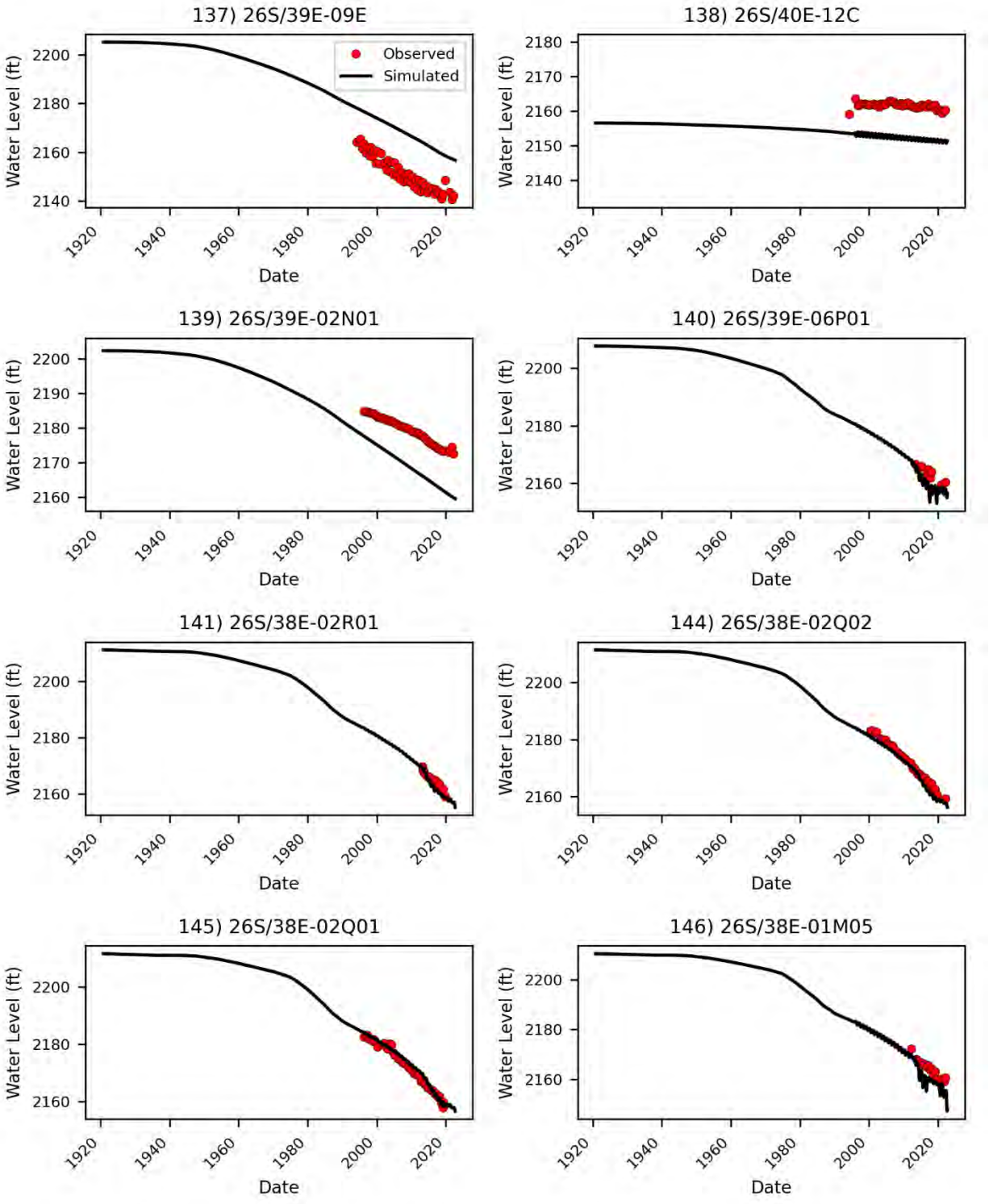


Figure A-15. Simulated and observed water levels from the transient historical calibration model for well locations indicated on Figure A-1.

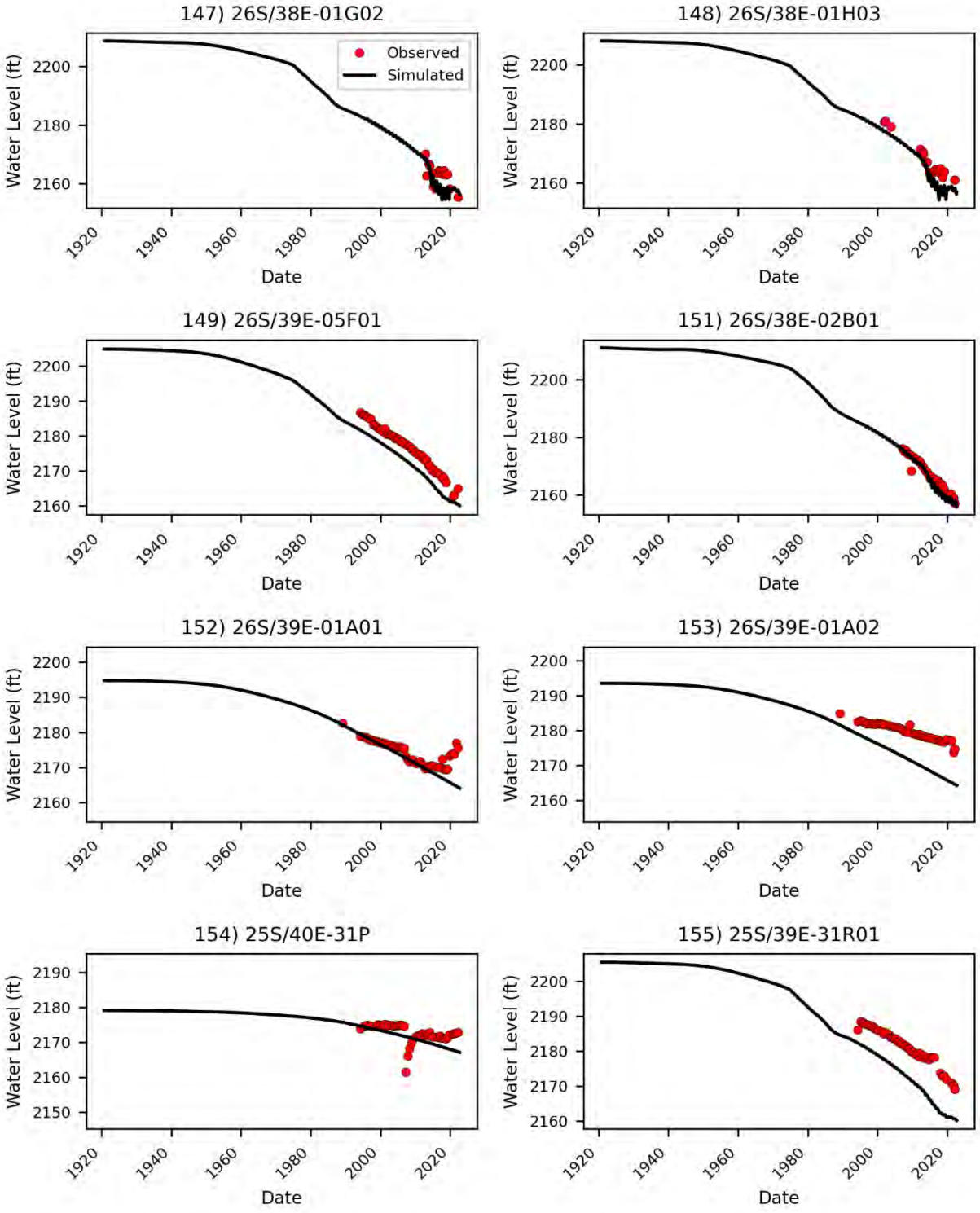


Figure A-16. Simulated and observed water levels from the transient historical calibration model for well locations indicated on Figure A-1.

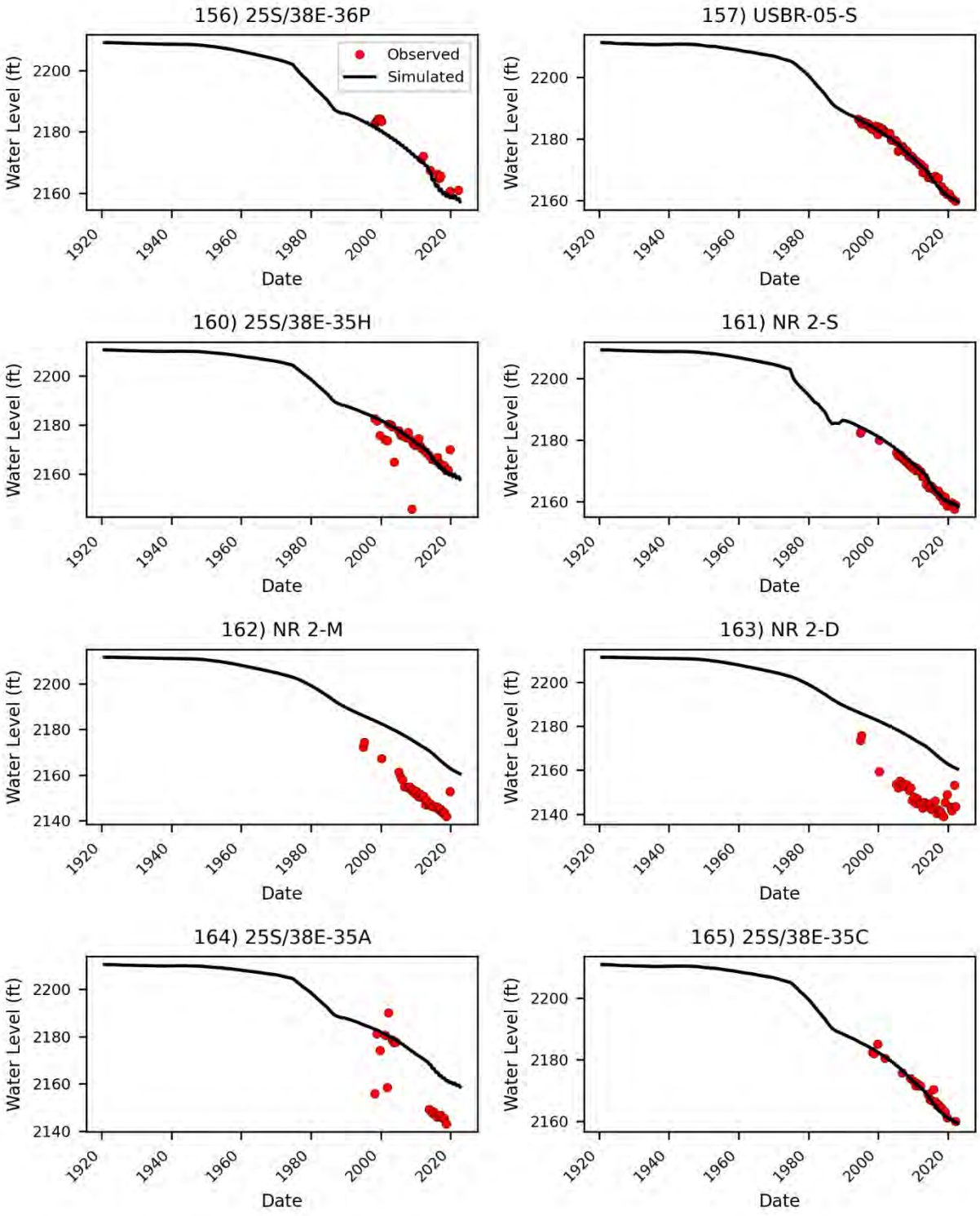


Figure A-17. Simulated and observed water levels from the transient historical calibration model for well locations indicated on Figure A-1.

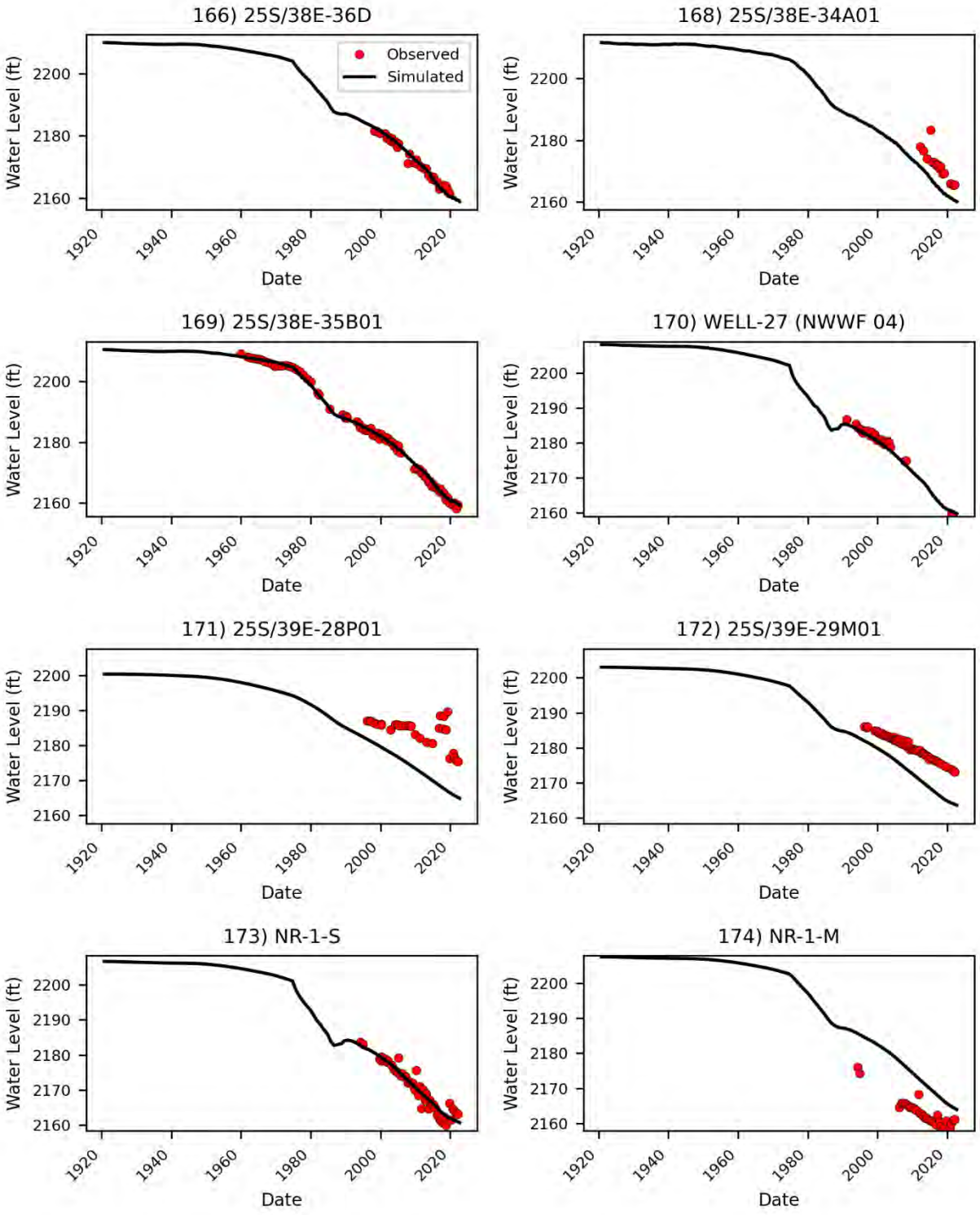


Figure A-18. Simulated and observed water levels from the transient historical calibration model for well locations indicated on Figure A-1.

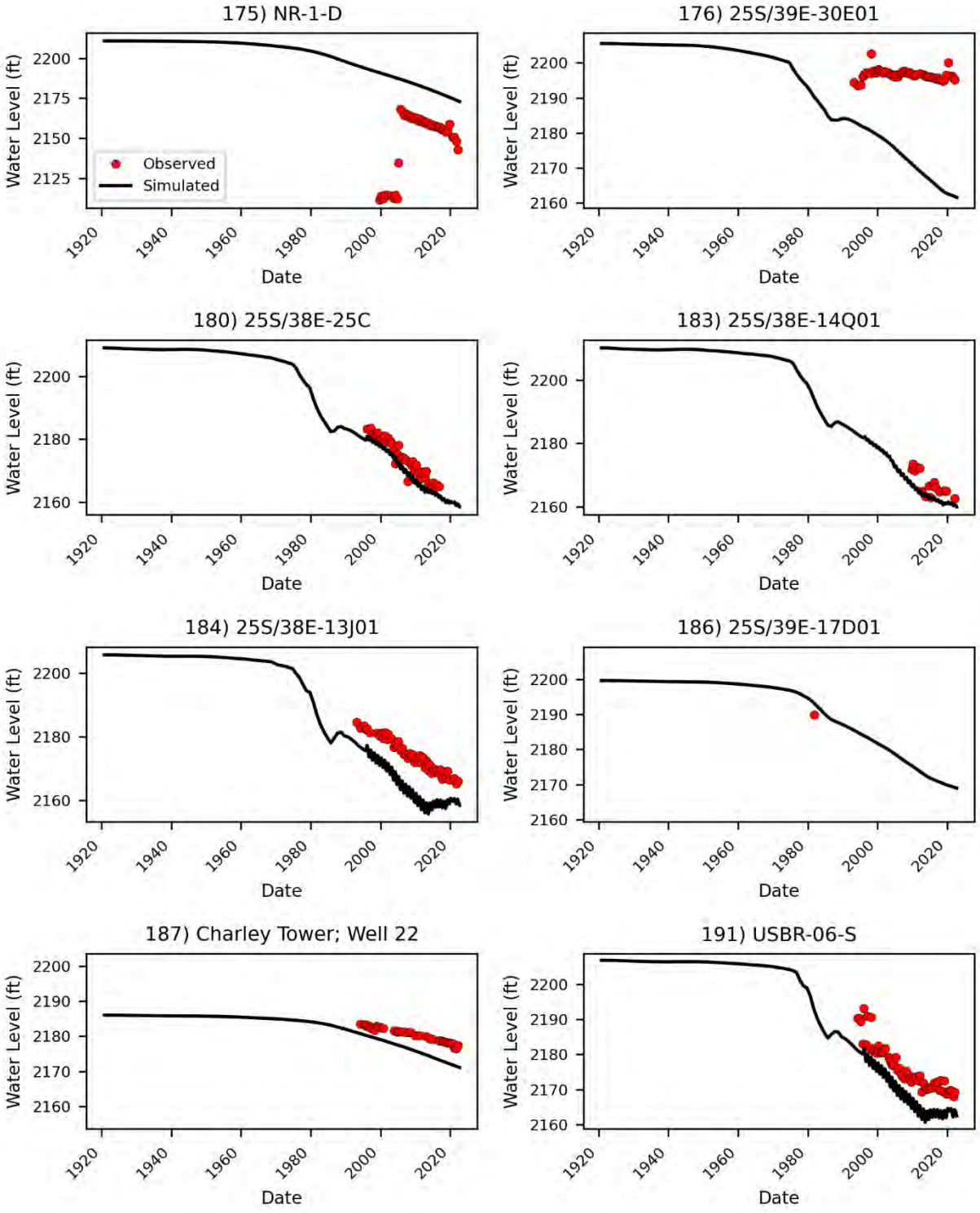


Figure A-19. Simulated and observed water levels from the transient historical calibration model for well locations indicated on Figure A-1.

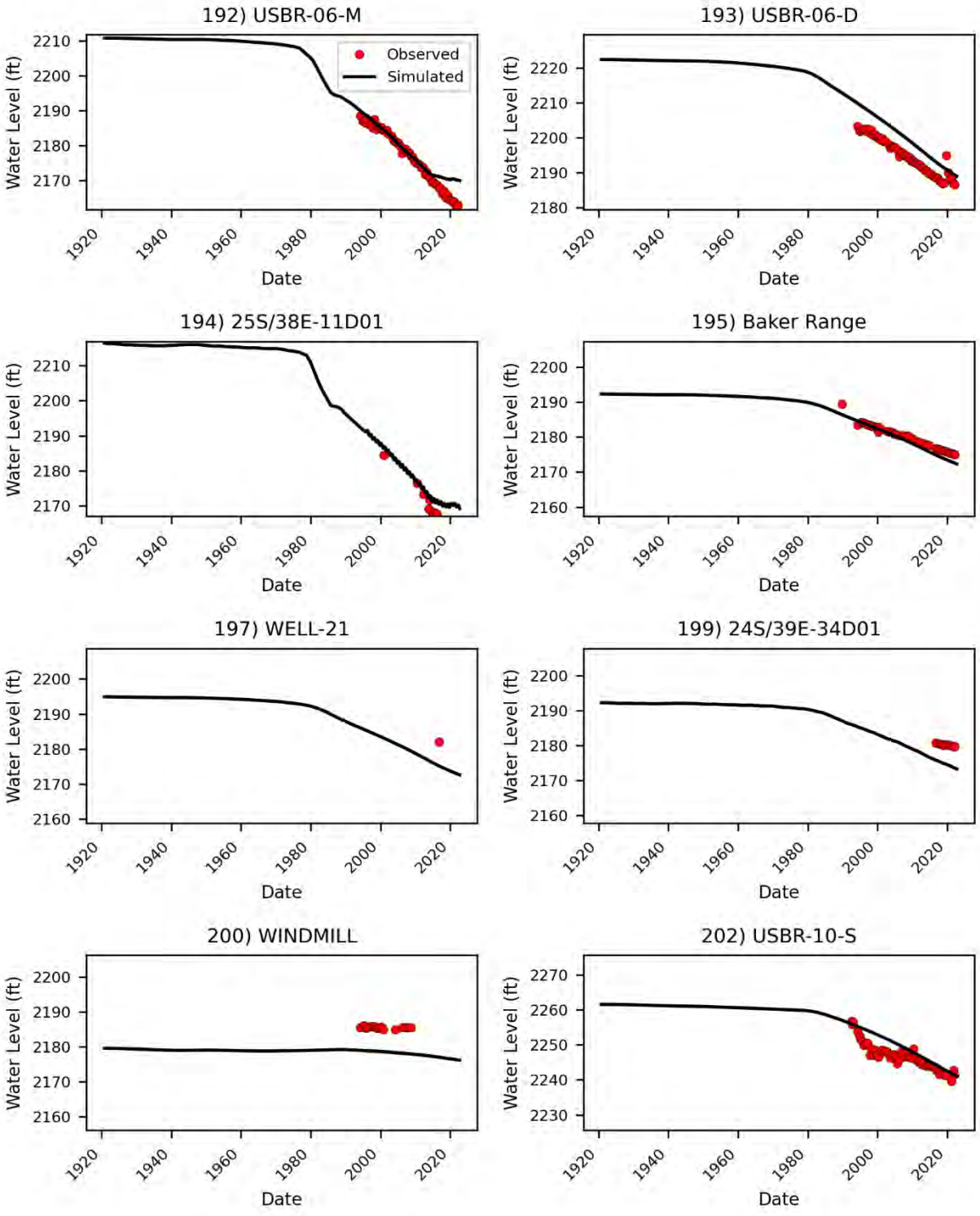


Figure A-20. Simulated and observed water levels from the transient historical calibration model for well locations indicated on Figure A-1.

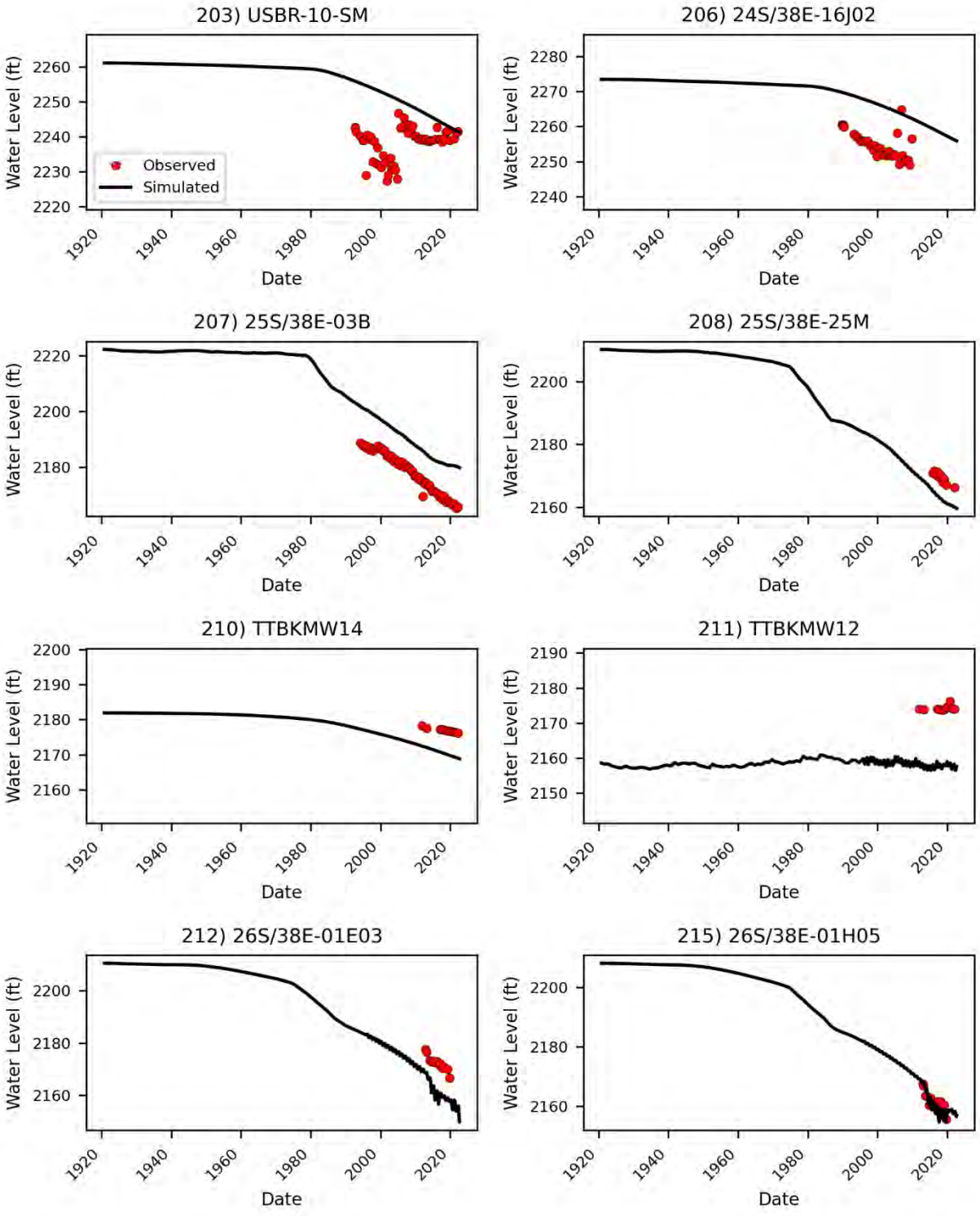


Figure A-21. Simulated and observed water levels from the transient historical calibration model for well locations indicated on Figure A-1.

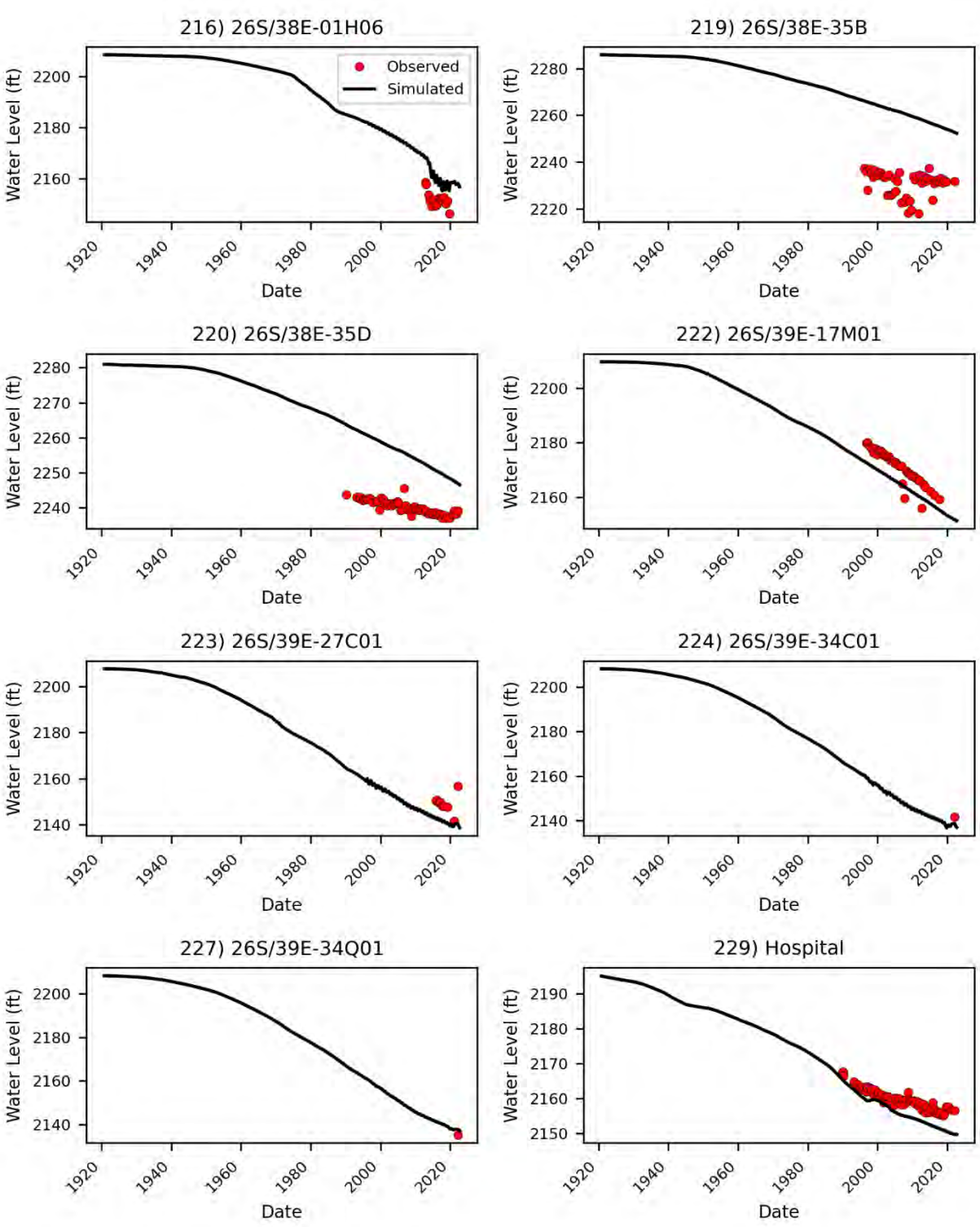


Figure A-22. Simulated and observed water levels from the transient historical calibration model for well locations indicated on Figure A-1.

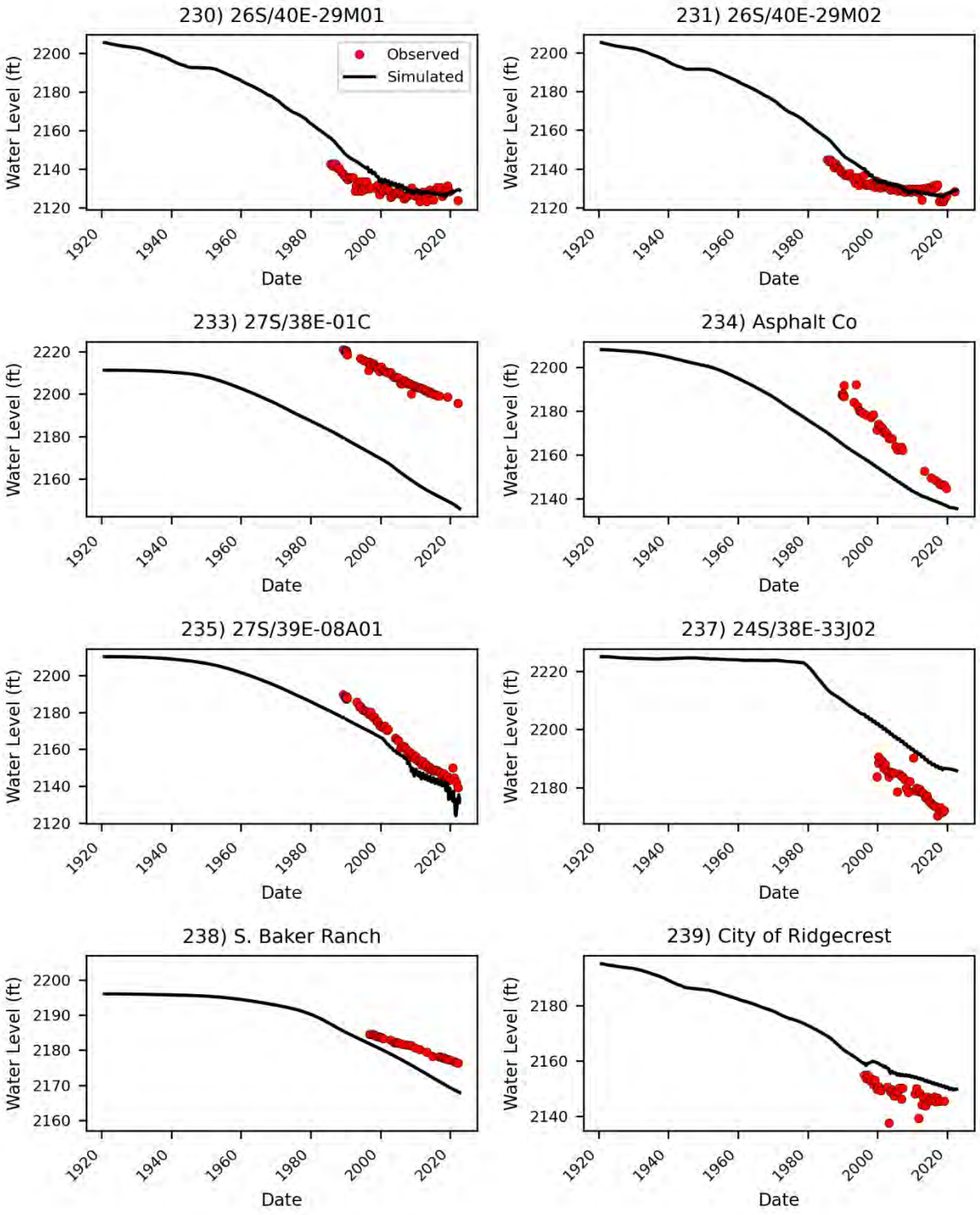


Figure A-23. Simulated and observed water levels from the transient historical calibration model for well locations indicated on Figure A-1.

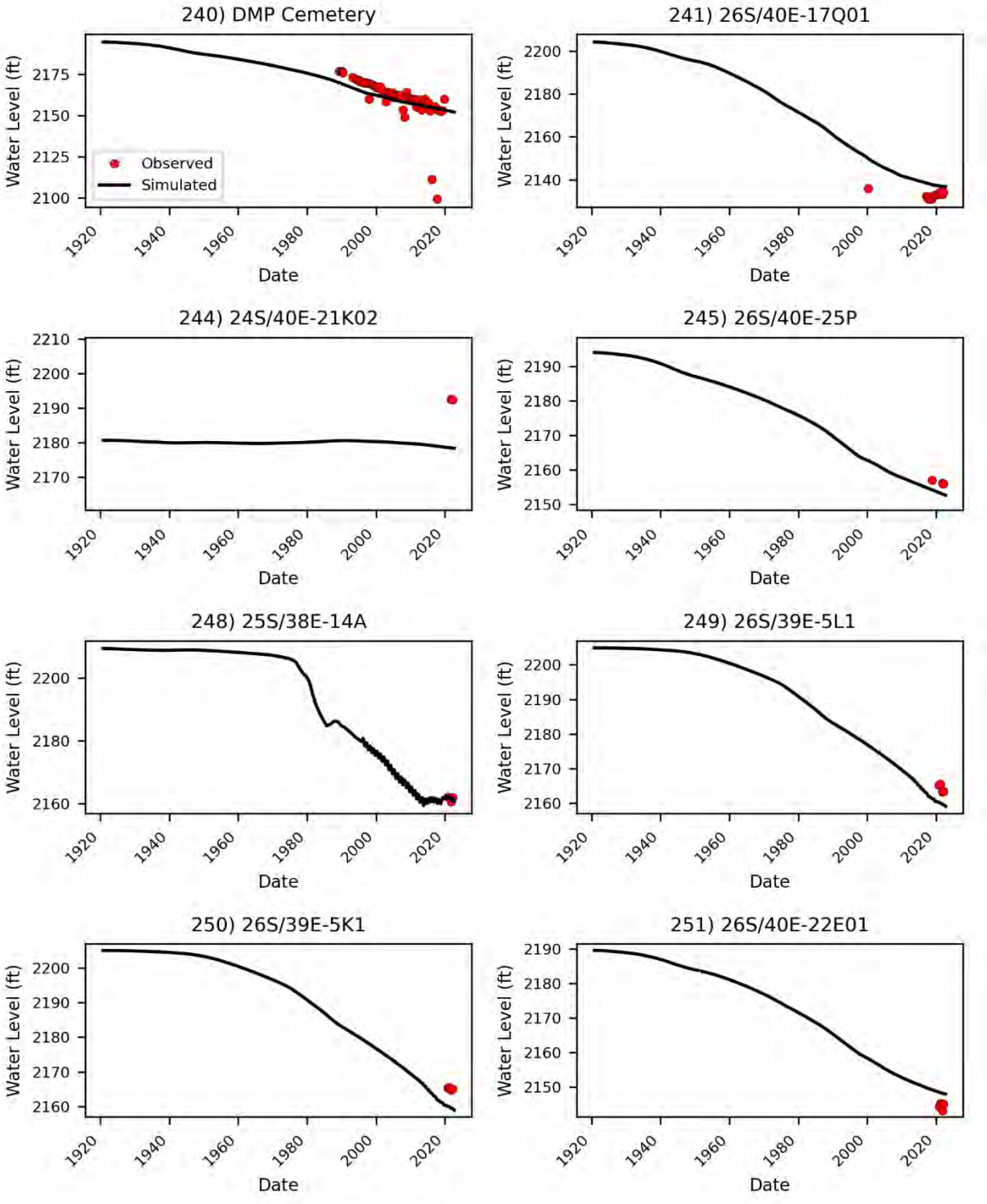


Figure A-24. Simulated and observed water levels from the transient historical calibration model for well locations indicated on Figure A-1.

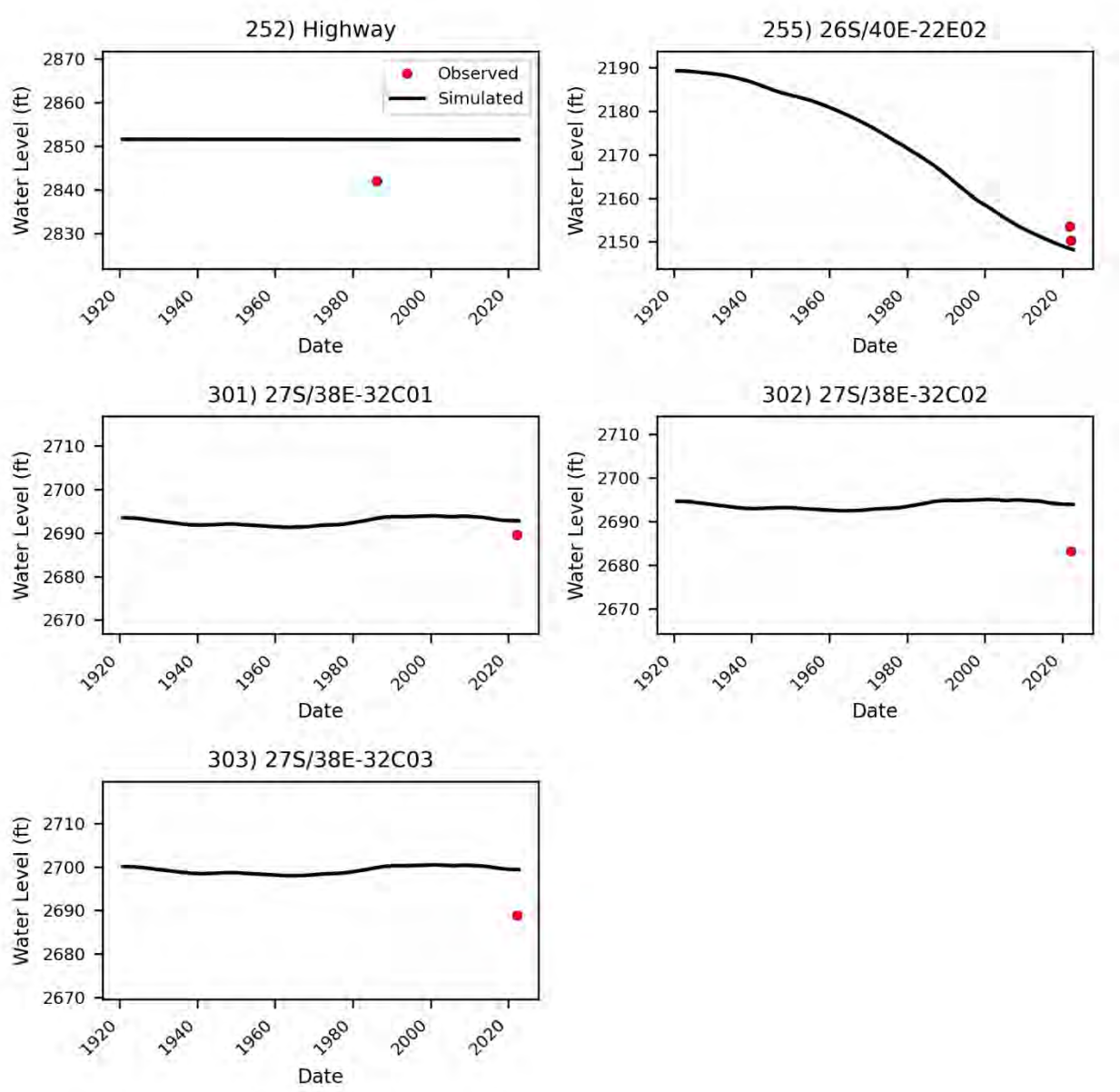


Figure A-25. Simulated and observed water levels from the transient historical calibration model for well locations indicated on Figure A-1.

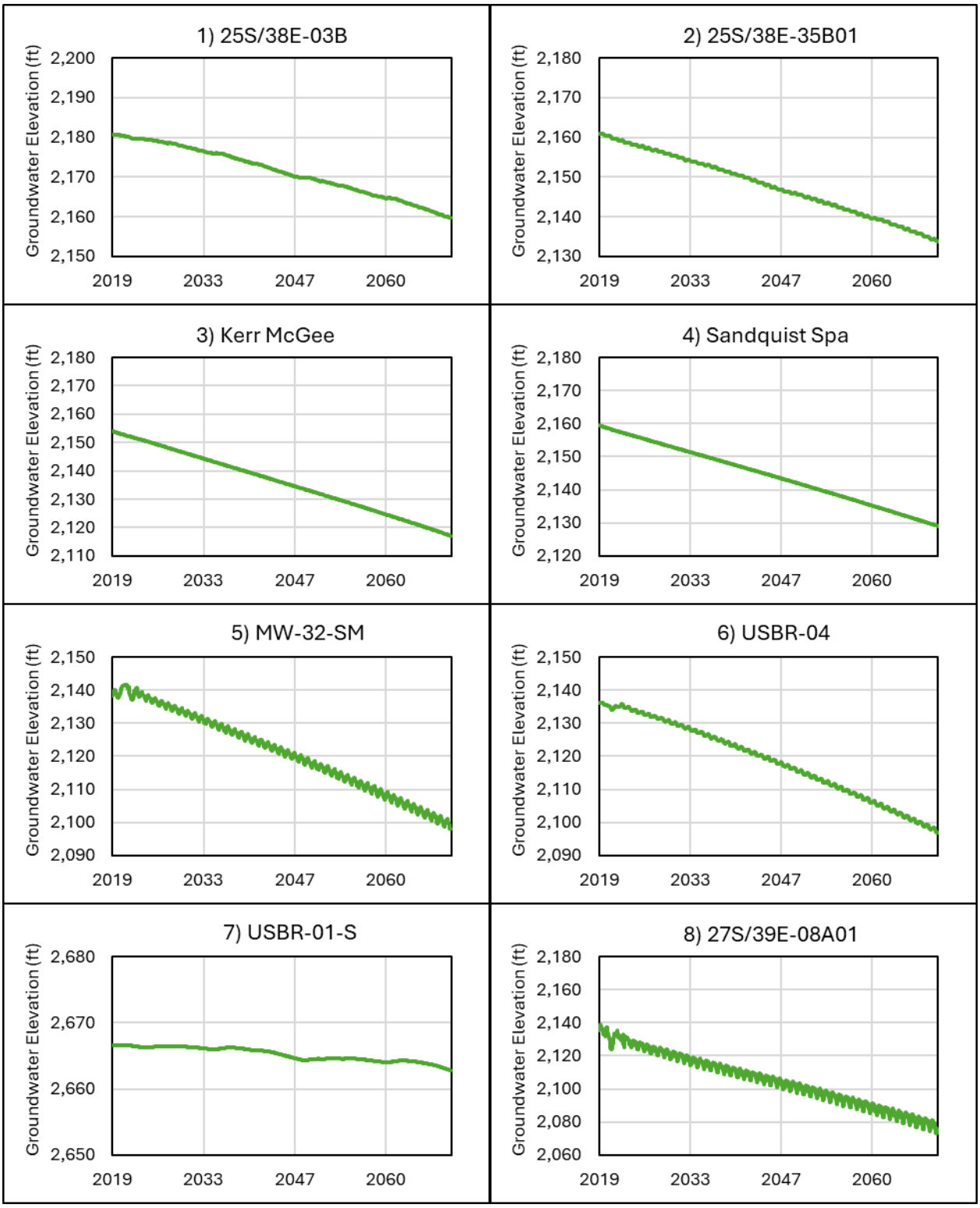


Figure B-1. Simulated water levels from the Baseline Scenario for well locations indicated on Figure 6-2.

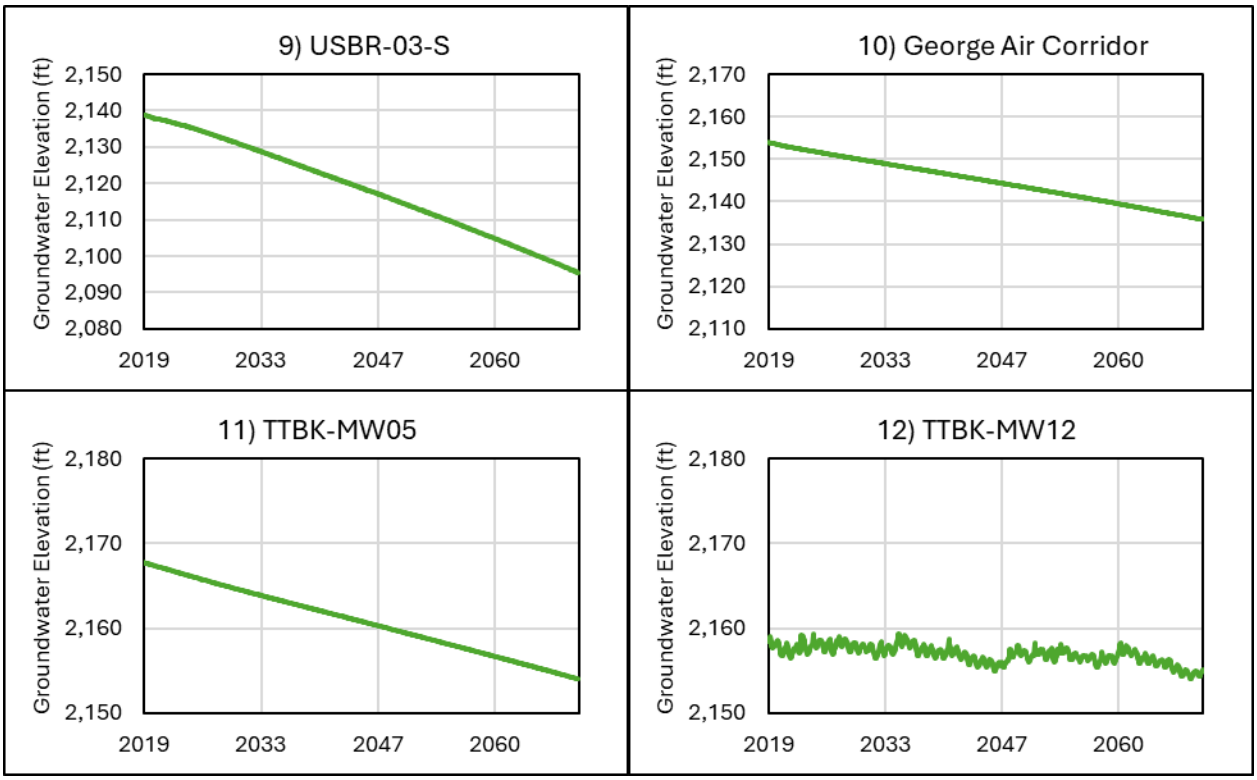


Figure B-2. Simulated water levels from the Baseline Scenario for well locations indicated on Figure 6-2.

ATTACHMENT 4

ATTACHMENT 4

IWV Model Results for:

- **Baseline**
- **Scenario 1A Implemented GSP**
- **Scenario 1B Implemented GSP Adjusted SVM**
- **Scenario 2 No GA**
- **Scenario 3 EVT**
- **Scenario 4 El Paso Pumping**

Model Baseline No Action 2020-2070

As defined by California Code of Regulations section 351(e), Baseline is defined as "historical information used to project future conditions for hydrology, water demand, and availability of surface water and to evaluate potential sustainable management practices of a basin". Since 2020 GSP adoption, monthly pumping data has been reported and estimated for all pumpers in the Basin to establish Baseline pumping conditions in the Basin.

The Baseline Model Run simulates 51 years from WY 2020 through WY 2070 with monthly stress periods. Future estimated recharge is variable by month and year, with an average of 7,650 AFY ranging from 3,360 AFY to 16,028 AFY. Groundwater pumping is estimated based on WY 2020 through WY 2023 reported pumping where available. Population growth with a subsequent 1% water use increase is included for IWVWD, Inyokern CSD, and domestic wells. Consistent with the 2020 GSP, the Navy's pumping is set to 2,401 AFY. All other pumping is maintained at the WY 2020-2023 average to simulate the Baseline 'no action' Model Run.

Groundwater Pumping for Model Scenario Baseline No Action 2020-2070

Pumper	Starting Pumping WY 2024 (AF)	Pumping WY 2030 (AF)	Pumping WY 2040 (AF)	Pumping WY 2070 (AF)	Assumptions
IWVWD	6,821	7,130	7,830	10,342	Growth consistent with IWVWD 2020 UWMP up to 2045, 1% growth until 2070
Navy	2,041	2,041	2,041	2,041	Requested by the Navy for future uses
City of Ridgecrest	188	188	188	188	WY 2020-2023 Average, static
Kern County	22	22	22	22	WY 2020-2023 Average, static
Searles Valley Minerals	2,544	2,544	2,544	2,544	WY 2020-2023 Average, static
Mojave Pistachios	3,561	3,561	3,561	3,561	WY 2020-2023 Average, static
Meadowbrook Dairy	4,352	4,352	4,352	4,352	WY 2020-2023 Average, static
Other Large Ag	762	762	762	762	WY 2020-2023 Average, static
Small Ag	320	320	320	320	WY 2020-2023 Average, static
Inyokern CSD	205	218	241	324	WY 2020-2023 Average in WY 2024, 1% growth
Mutuals	414	414	414	414	WY 2020-2023 Average, static
Domestic	864	913	1,003	1,336	Historical (832 AFY) + 1% growth of 8.32 AF per year.
TOTAL PUMPING*	**22,094**	**22,465**	**23,277**	**26,206**	

* Errors in totals reflect rounding

BASELINE No Action 2020-2070 WY Annual Water Budget (AFY)

Indian Wells Valley - Total

WY Range	Recharge AF/WY	Flow in from SWV AF/WY	Pumping AF/WY	EVT vegetation AF/WY	Evap bare soil AF/WY	Flow to SWV AF/WY	NET Change of GW in Storage AF/WY	Cumulative Change of GW in Storage AF/WY
2020	9,534	0	(21,232)	(2,271)	(2,078)	(11)	(16,059)	(16,059)
2030	7,650	1	(22,465)	(1,911)	(1,821)	(5)	(18,550)	(194,550)
2040	7,672	4	(23,277)	(1,635)	(1,597)	(1)	(18,835)	(379,797)
2050	4,715	10	(24,036)	(1,384)	(1,364)	-	(22,060)	(573,144)
2060	7,994	18	(25,067)	(1,198)	(1,218)	-	(19,471)	(763,443)
2070	7,650	28	(26,206)	(967)	(958)	-	(20,453)	(974,516)
2020-2070	7,650	9	(23,708)	(1,549)	(1,509)	(2)	(19,108)	(974,516)
2041-2070	7,373	18	(24,642)	(1,286)	(1,285)	(0)	(19,824)	(594,719)

IWV Main Basin

WY Range	Recharge AF/WY	Flow in from SWV AF/WY	Flow in from El Paso SA AF/WY	Pumping AF/WY	EVT vegetation AF/WY	Evap bare soil AF/WY	Flow to SWV AF/WY	Flow out to El Paso SA AF/WY	NET Change of GW in Storage AF/WY	Cumulative Change of GW in Storage AF
2020	7,894	0	1,613	(21,231)	(2,271)	(2,078)	(10.93)	(0.26)	(16,085)	(16,085)
2030	6,102	1	1,615	(22,463)	(1,911)	(1,821)	(5.21)	(0.35)	(18,482)	(194,077)
2040	6,120	4	1,624	(23,276)	(1,635)	(1,597)	(0.96)	-	(18,761)	(378,763)
2050	3,305	10	1,617	(24,035)	(1,384)	(1,364)	-	(0.23)	(21,852)	(571,187)
2060	6,427	18	1,626	(25,066)	(1,198)	(1,218)	-	-	(19,411)	(760,973)
2070	6,102	28	1,624	(26,204)	(967)	(958)	-	-	(20,375)	(970,853)
2020-2070	6,102	9	1,619	(23,706)	(1,549)	(1,509)	(2.28)	(0.23)	(19,036)	(970,853)
2041-2070	5,838	15	1,622	(24,640)	(1,286)	(1,285)	(0.05)	(0.17)	(19,736)	(592,091)

El Paso Subarea

WY Range	Recharge AF/WY	Inflow from IWV Main AF/WY	Pumping AF/WY	Outflow to IWV Main AF/WY	NET Change of GW in Storage AF/WY	Cumulative Change of GW in Storage AF
2020	1,639	0.26	(1.00)	(1,613)	26	26
2030	1,548	0.35	(1.10)	(1,615)	(473)	(68)
2040	1,552	-	(1.21)	(1,624)	(1,034)	(74)
2050	1,410	0.23	(1.33)	(1,617)	(1,958)	(208)
2060	1,567	-	(1.46)	(1,626)	(2,470)	(60)
2070	1,548	-	(1.61)	(1,624)	(3,662)	(78)
2020-2070	1,549	0.23	(1.28)	(1,619)	(1,503)	(78)
2041-2070	1,536	0.17	(1.40)	(1,622)	(2,215)	(4)

BASELINE No Action 2020-2070 CY Annual Water Budget (AFY)

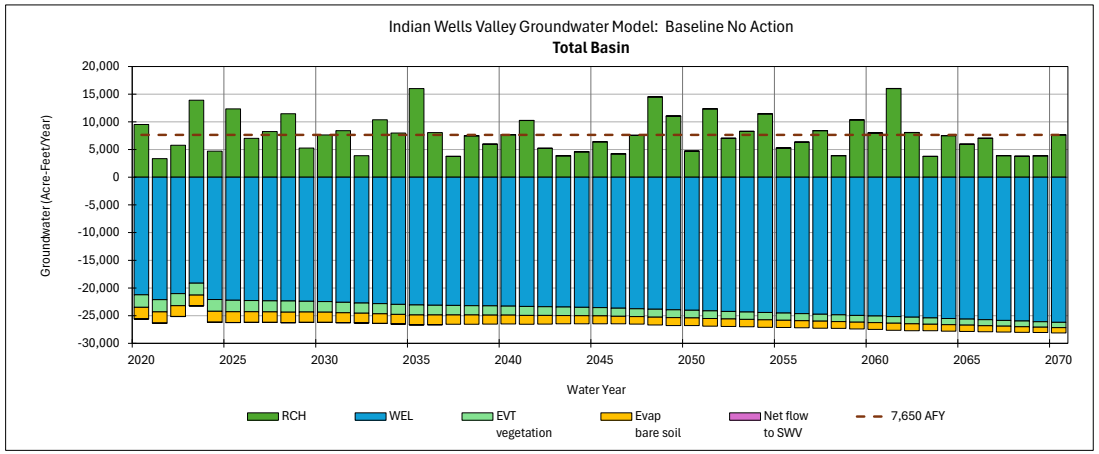
Calander Year

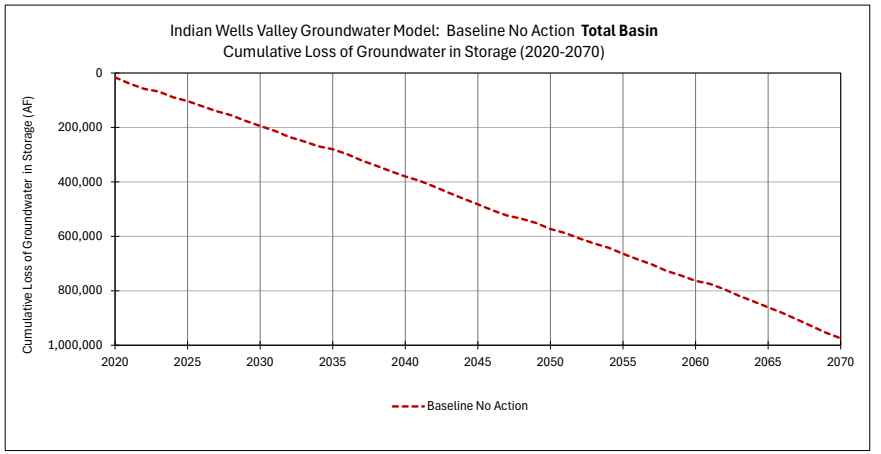
Indian Wells Valley - Total

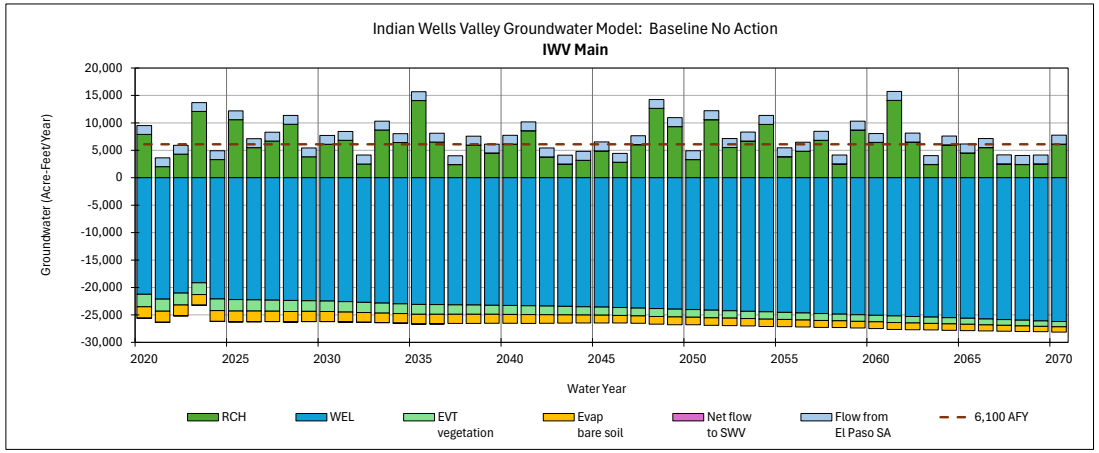
CY Range	Recharge AF/CY	Flow in from SWV AF/CY	Pumping AF/CY	EVT vegetation AF/CY	Evap bare soil AF/CY	Flow to SWV AF/CY	NET Change of GW in Storage AF/CY	Cumulative Change of GW in Storage AF/CY
2020	7,110	0	(21,272)	(2,263)	(2,071)	(11)	(18,506)	(20,018)
2030	6,465	1	(22,493)	(1,903)	(1,814)	(5)	(19,749)	(198,390)
2040	11,289	4	(23,290)	(1,634)	(1,598)	(1)	(15,230)	(378,916)
2050	5,025	10	(24,059)	(1,378)	(1,354)	-	(21,755)	(576,737)
2060	11,240	18	(25,092)	(1,197)	(1,219)	-	(16,249)	(763,464)
2069	5,022	27	(26,114)	(987)	(969)	-	(23,020)	(957,178)
2020-2069	7,627	9	(23,676)	(1,556)	(1,515)	(2)	(19,113)	(957,178)
2040-2069	7,374	14	(24,566)	(1,304)	(1,301)	(0)	(19,783)	(578,262)

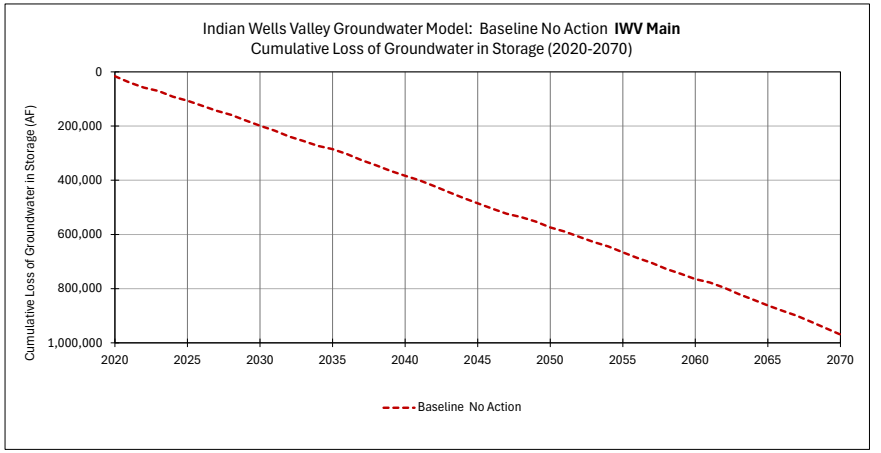
IWV Model is Oct 2019 through Sep 2070

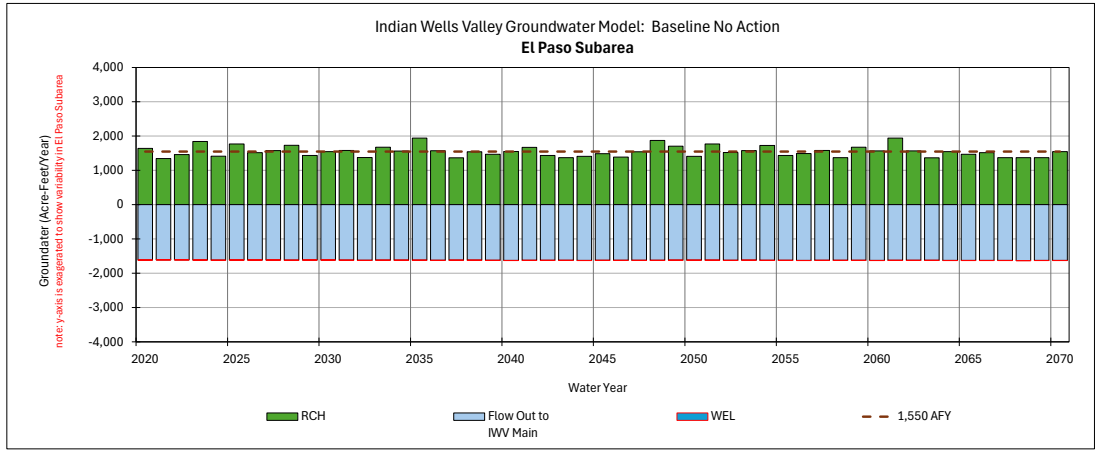
note: partial years for 2019 and 2070 not used in summary table

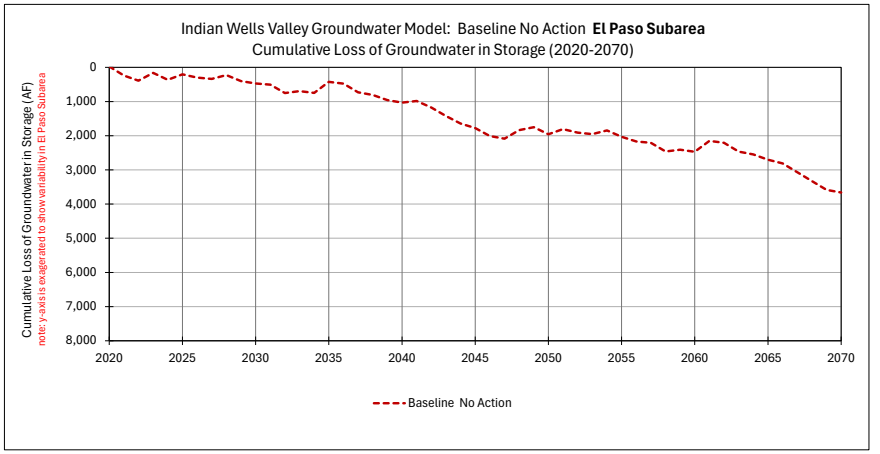




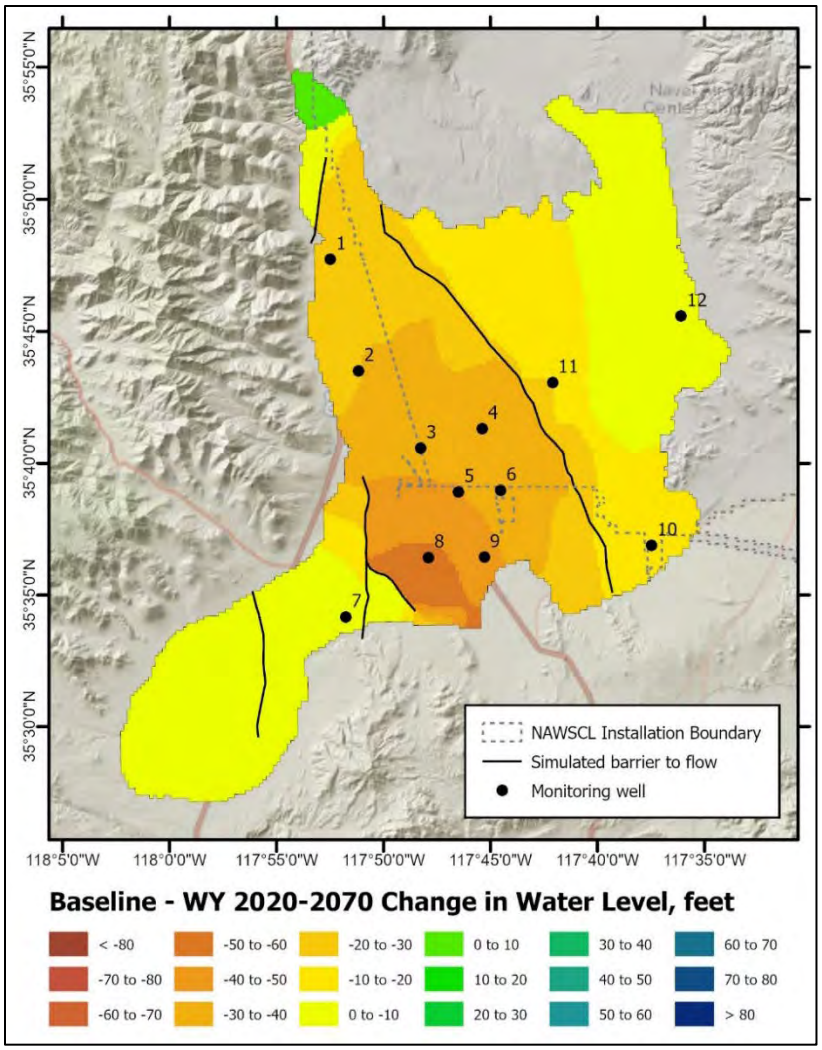


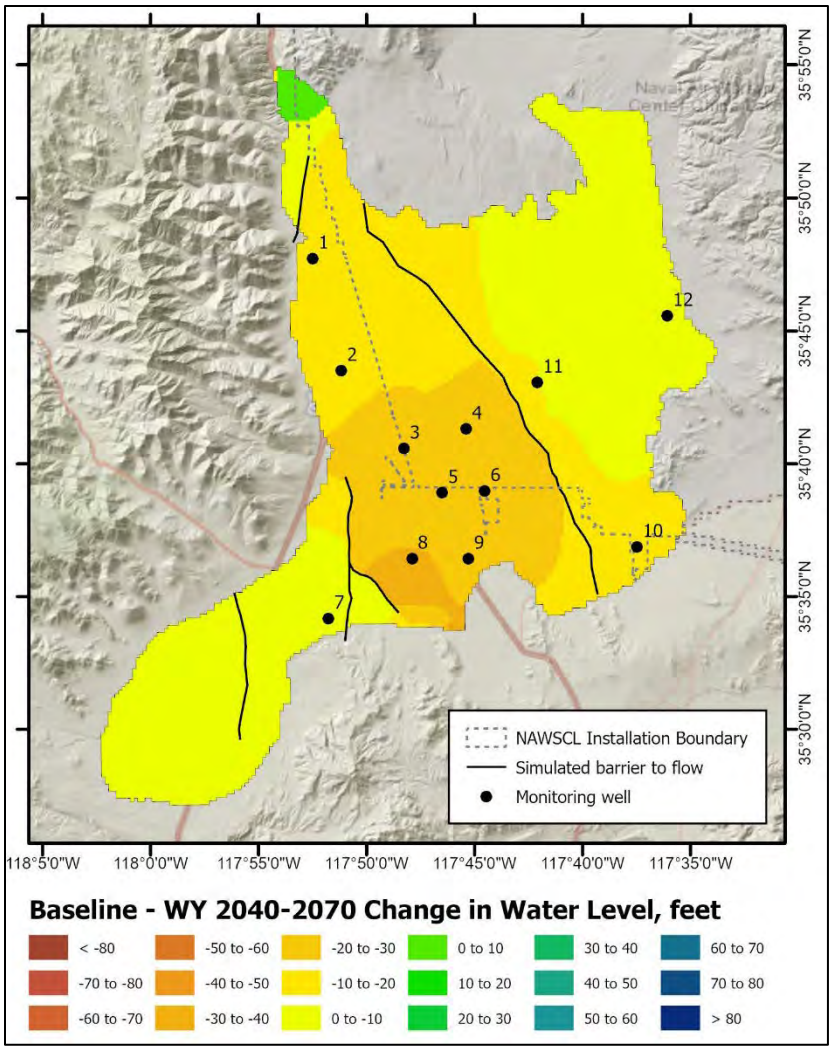






IWV Model Baseline No Action





BASELINE NO ACTION Change in Groundwater Levels.

Maps of simulated change in water level from WY 2020-2070 (left) and WY 2040-2070 (right). Hydrographs for numbered monitoring wells are presented in IWV Model Results: page 1 of 4: **1**) 25S/38E-03B, **2**) 25S/38E-35B01, **3**) Kerr McGee,
Page 2 of 4: **4**) Sandquist Spa, **5**) MW 32-SM, **6**) USBR-04,
Page 3 of 4: **7**) USBR-01-S, **8**) 27S/39E-08A01, **9**) USBR-03-S
Page 4 of 4: **10**) George Air Corridor, **11**) TTBK-MW05, **12**) TTBK-MW12.

Model Scenario 1A Implemented GSP (2020-2070)

This model scenario represents current Basin conditions since the start of GSP implementation. Since 2020 GSP adoption, the IWVGA has implemented several projects and management actions as outlined in the 2020 GSP. The IWVGA has implemented voluntary Basin-wide conservation, the Transient Pool, and Shallow Well Mitigation Program, and is currently on track to implement the Imported Water Project, with imported water expected to be available in 2030. Once imported water is available, total pumping in the Basin will be reduced to the sustainable yield of 7,650 AF. This model scenario uses the same model code, 51-year time frame, and 7,650 AFY average annual recharge from the Model Baseline. The only changes are to the volume of pumped groundwater.

- Basin-wide conservation since SGMA and GSP implementation has reduced pumping within the Basin significantly, especially shown in IWVWD pumping.
- The Transient Pool Program limits total pumping to 51,000 AF from Basin storage from several agriculture pumpers, with allocations set to expire in 2040. However, this modeling scenario assumed pumpers in the Transient Pool Program would cease pumping by 2027, as it would be uneconomical for small agricultural pumpers to continue agricultural activities.
- Any agricultural pumpers not in the Transient Pool Program would cease pumping immediately in WY 2024. Current litigation with Mojave Pistachios was assumed to be completed and that Mojave Pistachios would cease pumping by 2027.
- Pumping by Searles Valley Minerals (SVM) will be reduced to its pre-Navy (1943) pumping of 300 AFY.
- City of Ridgecrest park expansions are planned to increase water use from 188 AFY to 325 AFY. The remainder of the pumping would follow baseline conditions and be assumed to not change.

GSP implementation that has yet to occur and not simulated in Run 1A include the Recycled Water Project, Pumping Optimization, and the Dust Control Mitigation Program.

Groundwater Pumping for Model Scenario 1A Implemented GSP

Pumper	Pumping WY 2024 (AF)	Pumping WY 2030 (AF)	Pumping WY 2040 (AF)	Pumping WY 2070 (AF)	Assumptions
IWVWD	6,821	3,417	3,304	2,888	Pumping reduced to meet Sustainable Yield in 2030
Navy	2,041	2,041	2,041	2,041	Baseline Pumping
City of Ridgecrest	325	325	325	325	Initial Disclosure Pumping, static
Kern County	22	22	22	22	Baseline Pumping
Searles Valley Minerals	2,544	300	300	300	Baseline Pumping until reduced to pre-Navy pumping in 2030
Mojave Pistachios	3,561	0	0	0	Baseline Pumping until 2027, litigation
Meadowbrook Dairy	4,352	0	0	0	Baseline Pumping until 2027, litigation
Other Large Ag	762	0	0	0	Transient Pool until 2027
Small Ag	281	0	0	0	Transient Pool until 2027
Inyokern CSD	205	218	241	324	Baseline Pumping
Mutuals	414	414	414	414	Baseline Pumping
Domestic	864	913	1,003	1,336	Baseline Pumping

TOTAL PUMPING*	**22,192**	**7,650**	**7,650**	**7,650**	

* Errors in totals reflect rounding

Scenario 1A GSP Implementation WY Annual Water Budget (AFY)

Indian Wells Valley - Total

WY Range	Recharge AF/WY	Flow in from SWV AF/WY	Pumping AF/WY	EVT vegetation AF/WY	Evap bare soil AF/WY	Flow to SWV AF/WY	NET Change of GW in Storage AF/WY	Cumulative Change of GW in Storage AF/WY
2020	9,534	0	(21,232)	(2,271)	(2,078)	(11)	(16,059)	(16,059)
2030	7,650	1	(7,650)	(1,911)	(1,820)	(5)	(3,735)	(153,456)
2040	7,672	4	(7,650)	(1,662)	(1,612)	(1)	(3,250)	(185,166)
2050	4,715	7	(7,650)	(1,491)	(1,437)	(0)	(5,857)	(219,695)
2060	7,994	10	(7,650)	(1,414)	(1,376)	-	(2,436)	(243,430)
2070	7,650	15	(7,650)	(1,300)	(1,203)	-	(2,488)	(279,161)
2020-2070	7,650	6	(9,893)	(1,652)	(1,582)	(2)	(5,474)	(279,161)
2041-2070	7,373	10	(7,650)	(1,457)	(1,408)	(0)	(3,133)	(93,995)

IWV Main Basin

WY Range	Recharge AF/WY	Flow in from SWV AF/WY	Flow in from El Paso SA AF/WY	Pumping AF/WY	EVT vegetation AF/WY	Evap bare soil AF/WY	Flow to SWV AF/WY	Flow out to El Paso SA AF/WY	NET Change of GW in Storage AF/WY	Cumulative Change of GW in Storage AF
2020	7,894	0	1,613	(21,231)	(2,271)	(2,078)	(10.93)	(0.26)	(16,085)	(16,085)
2030	6,102	1	1,615	(7,649)	(1,911)	(1,820)	(5.16)	(0.35)	(3,667)	(152,984)
2040	6,120	4	1,620	(7,649)	(1,662)	(1,612)	(1.11)	-	(3,181)	(184,153)
2050	3,305	7	1,606	(7,649)	(1,491)	(1,437)	(0.03)	(0.25)	(5,660)	(217,834)
2060	6,427	10	1,610	(7,649)	(1,414)	(1,376)	-	(0.02)	(2,391)	(241,190)
2070	6,102	15	1,604	(7,648)	(1,300)	(1,203)	-	-	(2,430)	(275,912)
2020-2070	6,102	6	1,611	(9,892)	(1,652)	(1,582)	(2.30)	(0.25)	(5,410)	(275,912)
2041-2070	5,838	9	1,609	(7,649)	(1,457)	(1,408)	(0.09)	(0.19)	(3,059)	(91,758)

El Paso Subarea

WY Range	Recharge AF/WY	Inflow from IWV Main AF/WY	Pumping AF/WY	Outflow to IWV Main AF/WY	NET Change of GW in Storage AF/WY	Cumulative Change of GW in Storage AF
2020	1,639	0.26	(1.00)	(1,613)	26	26
2030	1,548	0.35	(1.10)	(1,615)	(473)	(68)
2040	1,552	-	(1.21)	(1,620)	(1,013)	(74)
2050	1,410	0.25	(1.33)	(1,606)	(1,861)	(208)
2060	1,567	0.02	(1.46)	(1,610)	(2,240)	(60)
2070	1,548	-	(1.61)	(1,604)	(3,250)	(78)
2020-2070	1,549	0.25	(1.28)	(1,611)	(1,394)	(78)
2041-2070	1,536	0.19	(1.40)	(1,609)	(2,032)	(4)

Scenario 1A GSP Implementation 2020-2070 CY Annual Water Budget (AFY)

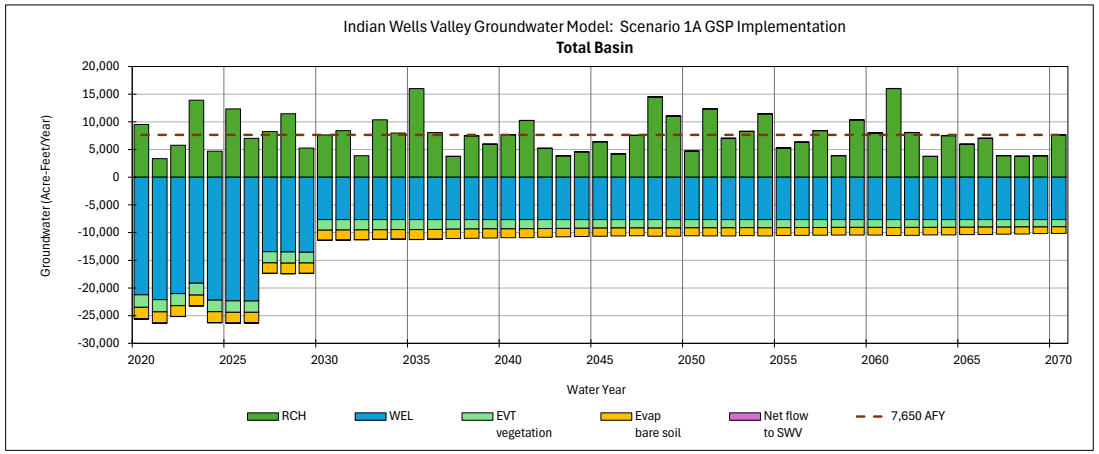
Calander Year

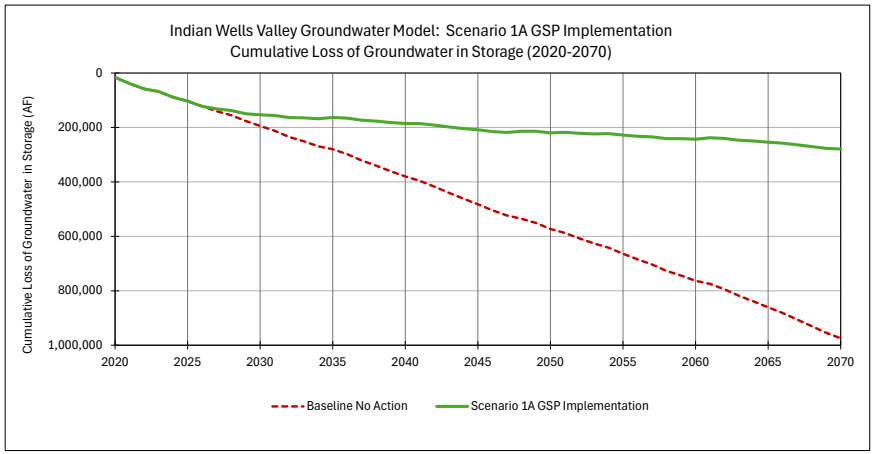
Indian Wells Valley - Total

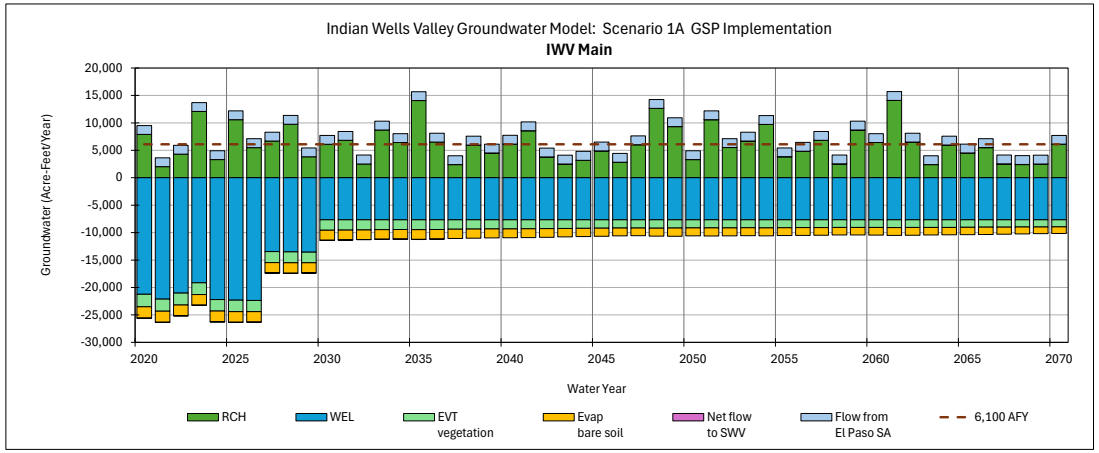
CY Range	Recharge AF/CY	Flow in from SWV AF/CY	Pumping AF/CY	EVT vegetation AF/CY	Evap bare soil AF/CY	Flow to SWV AF/CY	NET Change of GW in Storage AF/CY	Cumulative Change of GW in Storage AF/CY
2020	7,110	0	(21,272)	(2,263)	(2,071)	(11)	(18,506)	(20,018)
2030	6,465	1	(7,650)	(1,904)	(1,814)	(5)	(4,906)	(155,017)
2040	11,289	4	(7,650)	(1,661)	(1,614)	(1)	366	(181,843)
2050	5,025	7	(7,650)	(1,487)	(1,428)	-	(5,533)	(220,690)
2060	11,240	10	(7,650)	(1,415)	(1,379)	-	807	(240,655)
2069	5,022	15	(7,650)	(1,313)	(1,209)	-	(5,135)	(276,796)
2020-2069	7,627	6	(9,894)	(1,655)	(1,586)	(2)	(5,506)	(276,796)
2040-2069	7,374	9	(7,650)	(1,467)	(1,419)	(0)	(3,153)	(94,953)

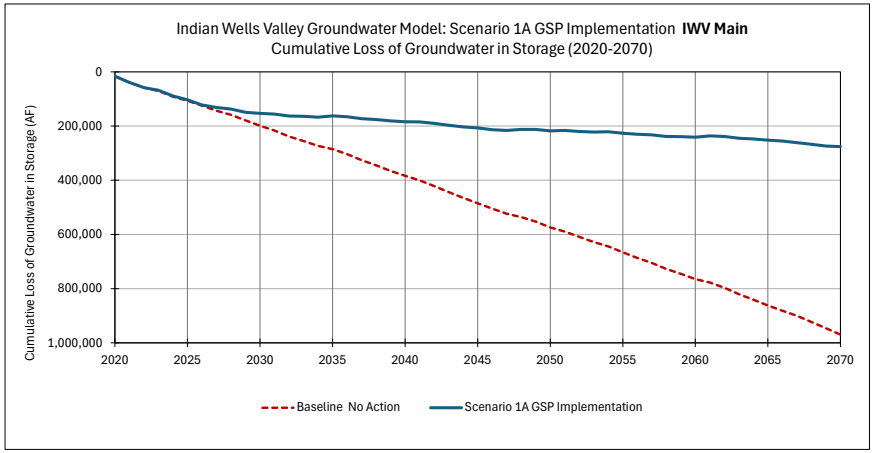
IWV Model is Oct 2019 through Sep 2070

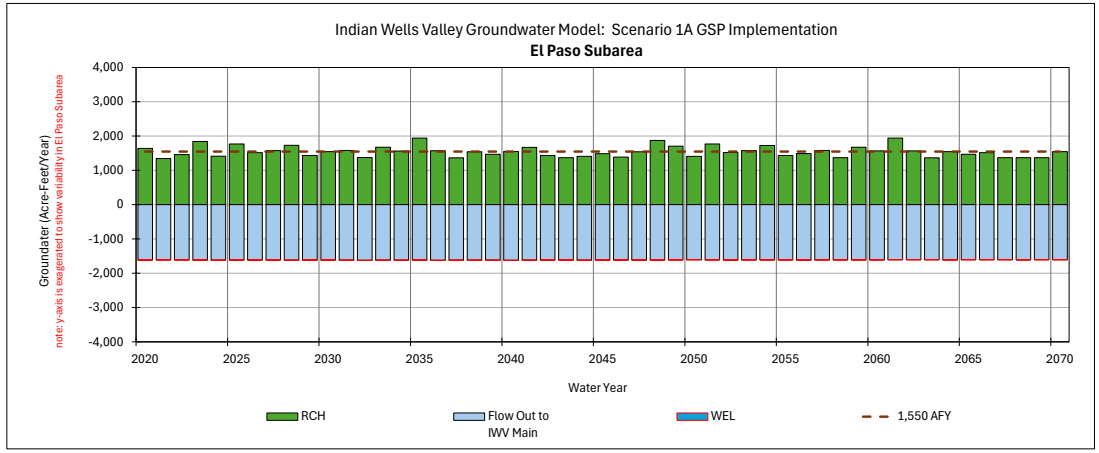
note: partial years for 2019 and 2070 not used in summary table

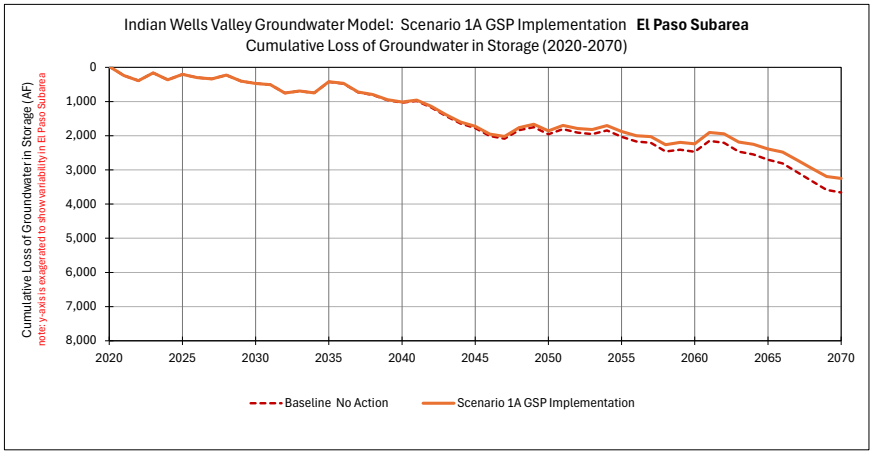




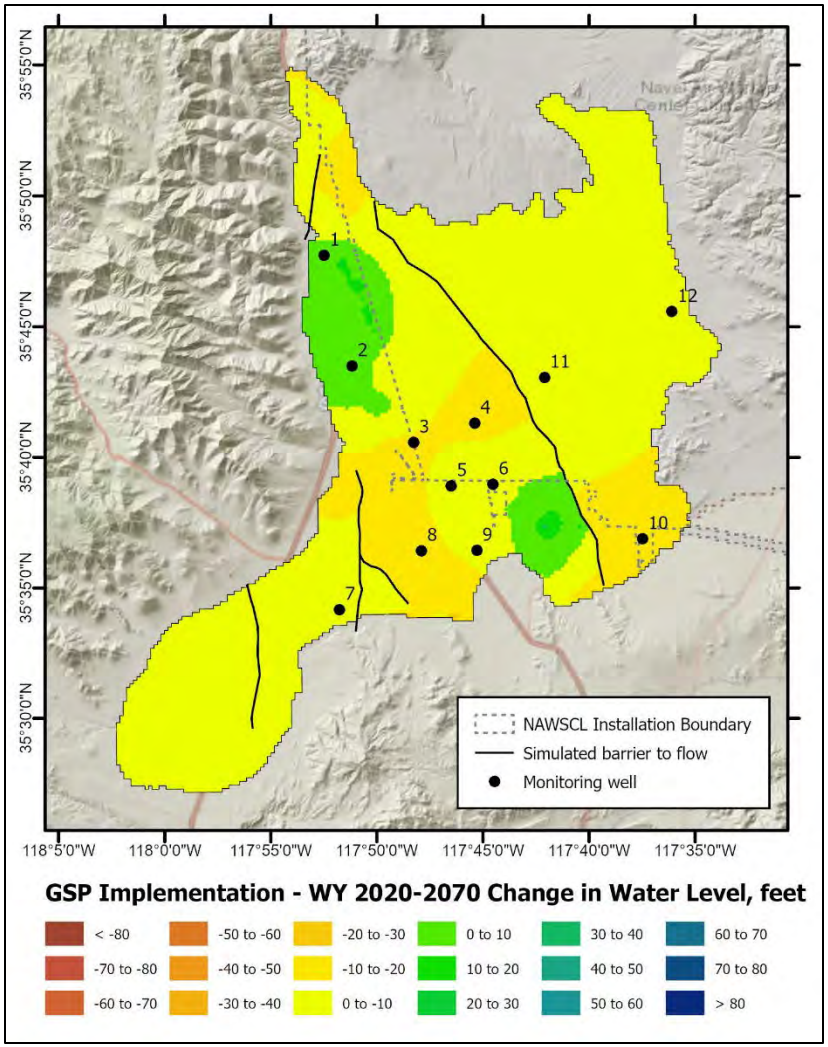


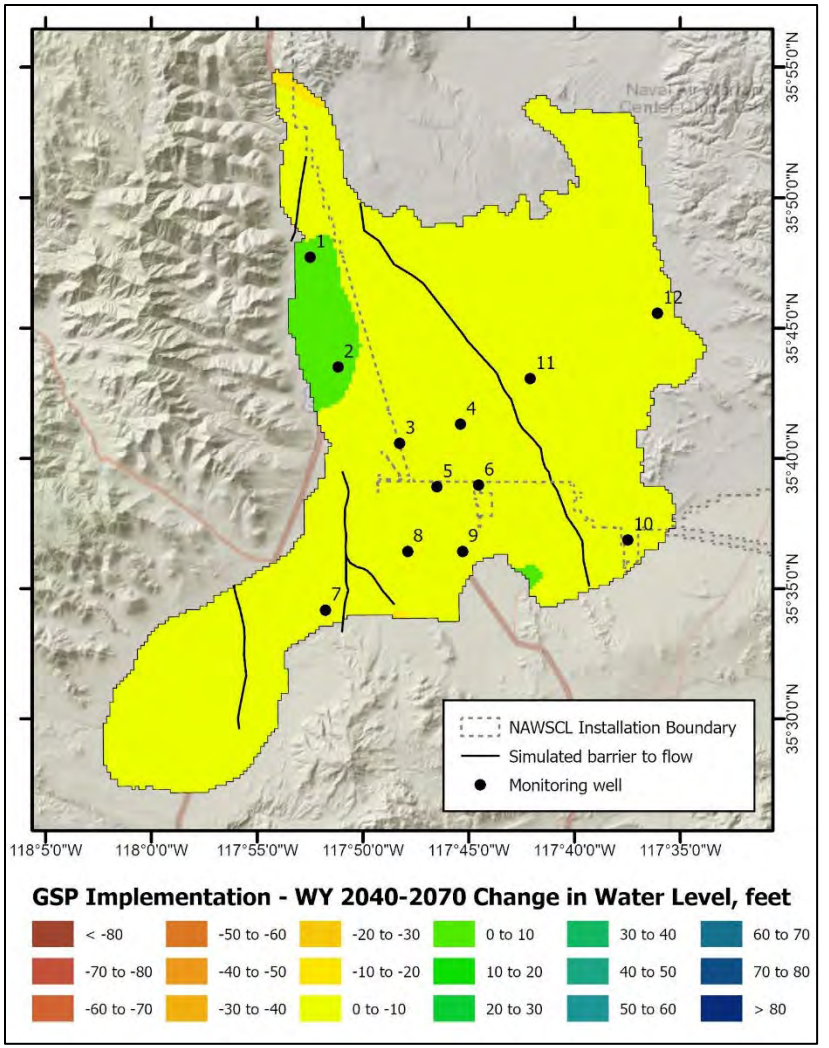






IWV Model Scenario 1A GSP Implementation





SCENARIO 1A IMPLEMENTED GSP Change in Groundwater Levels.

Maps of simulated change in water level from WY 2020-2070 (left) and WY 2040-2070 (right). Hydrographs for numbered monitoring wells are presented in IWV Model Results:

Page 1 of 4: **1**) 25S/38E-03B, **2**) 25S/38E-35B01, **3**) Kerr McGee,
Page 2 of 4: **4**) Sandquist Spa, **5**) MW 32-SM, **6**) USBR-04,
Page 3 of 4: **7**) USBR-01-S, **8**) 27S/39E-08A01, **9**) USBR-03-S
Page 4 of 4: **10**) George Air Corridor, **11**) TTBK-MW05, **12**) TTBK-MW12.

Model Scenario 1B Implemented GSP Adjusted SVM

This model scenario is an iteration of Model Scenario 1A GSP Implementation 2020-2070. It represents current Basin conditions since the start of GSP implementation but includes adjustments in pumping by Searles Valley Minerals (SVM) to its current average WY 2020 to 2023 pumping of 2,544 AFY. This model scenario once again includes currently implemented 2020 GSP projects and managements such as voluntary Basin-wide conservation, the Transient Pool, Shallow Well Mitigation Program, and the Imported Water Project which will allow imported water to be available in 2030. Once imported water is available, total pumping in the Basin will be reduced to the sustainable yield of 7,650 AF. This model scenario uses the same model code, 51-year time frame, and 7,650 AFY average annual recharge from the Model Baseline. The only changes are to the volume of pumped groundwater.

Groundwater Pumping for Model Scenario 1B Implemented GSP Adjusted SVM

Pumper	Pumping WY 2024 (AF)	Pumping WY 2030 (AF)	Pumping WY 2040 (AF)	Pumping WY 2070 (AF)	Assumptions
IWVWD	6,821	1,173	1,060	643	Pumping reduced to meet Sustainable Yield in 2030
Navy	2,041	2,041	2,041	2,041	Baseline Pumping
City of Ridgecrest	325	325	325	325	Initial Disclosure Pumping, static
Kern County	22	22	22	22	Baseline Pumping
Searles Valley Minerals	2,544	2,544	2,544	2,544	Baseline Pumping
Mojave Pistachios	3,561	0	0	0	Baseline Pumping until 2027, litigation
Meadowbrook Dairy	4,352	0	0	0	Baseline Pumping until 2027, litigation
Other Large Ag	762	0	0	0	Transient Pool until 2027
Small Ag	281	0	0	0	Transient Pool until 2027
Inyokern CSD	205	218	241	324	Baseline Pumping
Mutuals	414	414	414	414	Baseline Pumping
Domestic	864	913	1,003	1,336	Baseline Pumping
TOTAL PUMPING*	**22,192**	**7,650**	**7,650**	**7,650**	

* Errors in totals reflect rounding

Scenario 1B GSP adjusted SVM 2020-2070 WY Annual Water Budget (AFY)

Indian Wells Valley - Total

WY Range	Recharge AF/WY	Flow in from SWV AF/WY	Pumping AF/WY	EVT vegetation AF/WY	Evap bare soil AF/WY	Flow to SWV AF/WY	NET Change of GW in Storage AF/WY	Cumulative Change of GW in Storage AF/WY
2020	9,534	0	(21,232)	(2,271)	(2,078)	(11)	(16,059)	(16,059)
2030	7,650	1	(7,650)	(1,911)	(1,820)	(5)	(3,735)	(153,456)
2040	7,672	4	(7,650)	(1,661)	(1,611)	(1)	(3,247)	(185,157)
2050	4,715	8	(7,650)	(1,489)	(1,432)	-	(5,848)	(219,625)
2060	7,994	13	(7,650)	(1,410)	(1,368)	-	(2,422)	(243,244)
2070	7,650	18	(7,650)	(1,295)	(1,194)	-	(2,472)	(278,823)
2020-2070	7,650	7	(9,893)	(1,650)	(1,579)	(2)	(5,467)	(278,823)
2041-2070	7,373	13	(7,650)	(1,454)	(1,402)	(0)	(3,122)	(93,666)

IWV Main Basin

WY Range	Recharge AF/WY	Flow in from SWV AF/WY	Flow in from El Paso SA AF/WY	Pumping AF/WY	EVT vegetation AF/WY	Evap bare soil AF/WY	Flow to SWV AF/WY	Flow out to El Paso SA AF/WY	NET Change of GW in Storage AF/WY	Cumulative Change of GW in Storage AF
2020	7,894	0	1,613	(21,231)	(2,271)	(2,078)	(10.93)	(0.26)	(16,085)	(16,085)
2030	6,102	1	1,615	(7,649)	(1,911)	(1,820)	(5.16)	(0.35)	(3,667)	(152,984)
2040	6,120	4	1,620	(7,649)	(1,661)	(1,611)	(0.97)	-	(3,178)	(184,146)
2050	3,305	8	1,605	(7,649)	(1,489)	(1,432)	-	(0.26)	(5,652)	(217,775)
2060	6,427	13	1,609	(7,649)	(1,410)	(1,368)	-	(0.02)	(2,379)	(241,028)
2070	6,102	18	1,602	(7,648)	(1,295)	(1,194)	-	-	(2,416)	(275,612)
2020-2070	6,102	7	1,610	(9,892)	(1,650)	(1,579)	(2.27)	(0.25)	(5,404)	(275,612)
2041-2070	5,838	11	1,608	(7,649)	(1,454)	(1,402)	(0.06)	(0.20)	(3,049)	(91,466)

El Paso Subarea

WY Range	Recharge AF/WY	Inflow from IWV Main AF/WY	Pumping AF/WY	Outflow to IWV Main AF/WY	NET Change of GW in Storage AF/WY	Cumulative Change of GW in Storage AF
2020	1,639	0.26	(1.00)	(1,613)	26	26
2030	1,548	0.35	(1.10)	(1,615)	(473)	(68)
2040	1,552	-	(1.21)	(1,620)	(1,011)	(74)
2050	1,410	0.26	(1.33)	(1,605)	(1,850)	(208)
2060	1,567	0.02	(1.46)	(1,609)	(2,216)	(60)
2070	1,548	-	(1.61)	(1,602)	(3,211)	(78)
2020-2070	1,549	0.25	(1.28)	(1,610)	(1,383)	(78)
2041-2070	1,536	0.19	(1.40)	(1,608)	(2,013)	(4)

Scenario 1B GSP adjusted SVM GSP 2020-2070 CY Annual Water Budget (AFY)

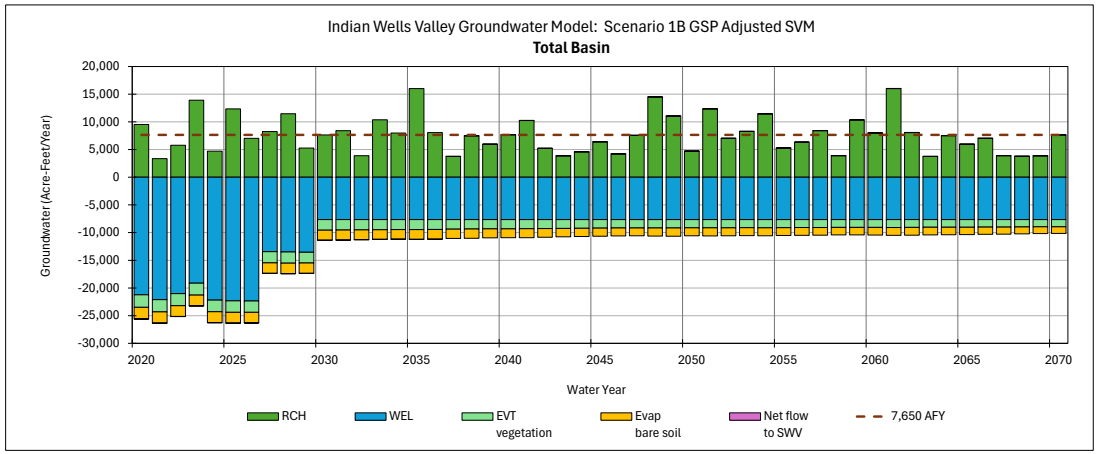
Calander Year

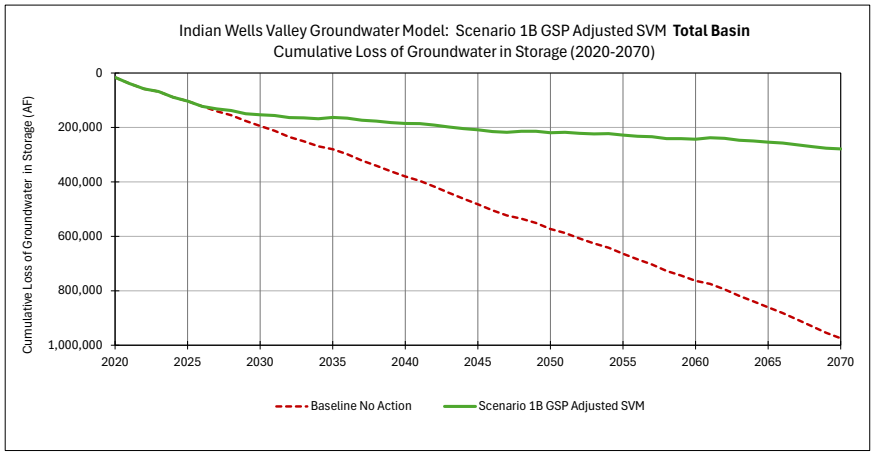
Indian Wells Valley - Total

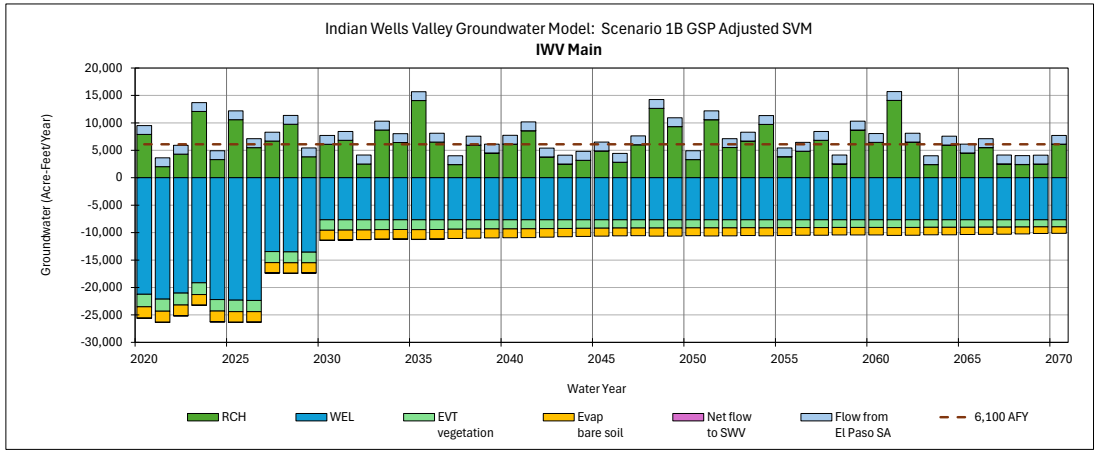
CY Range	Recharge AF/CY	Flow in from SWV AF/CY	Pumping AF/CY	EVT vegetation AF/CY	Evap bare soil AF/CY	Flow to SWV AF/CY	NET Change of GW in Storage AF/CY	Cummulative Change of GW in Storage AF/CY
2020	7,110	0	(21,272)	(2,263)	(2,071)	(11)	(18,506)	(20,018)
2030	6,465	1	(7,650)	(1,904)	(1,814)	(5)	(4,906)	(155,068)
2040	11,289	4	(7,650)	(1,661)	(1,613)	(1)	369	(181,884)
2050	5,025	8	(7,650)	(1,484)	(1,423)	-	(5,524)	(220,669)
2060	11,240	13	(7,650)	(1,411)	(1,372)	-	820	(240,517)
2069	5,022	17	(7,650)	(1,308)	(1,201)	-	(5,119)	(276,521)
2020-2069	7,627	7	(9,895)	(1,654)	(1,582)	(2)	(5,500)	(276,521)
2040-2069	7,374	10	(7,650)	(1,464)	(1,413)	(0)	(3,142)	(94,637)

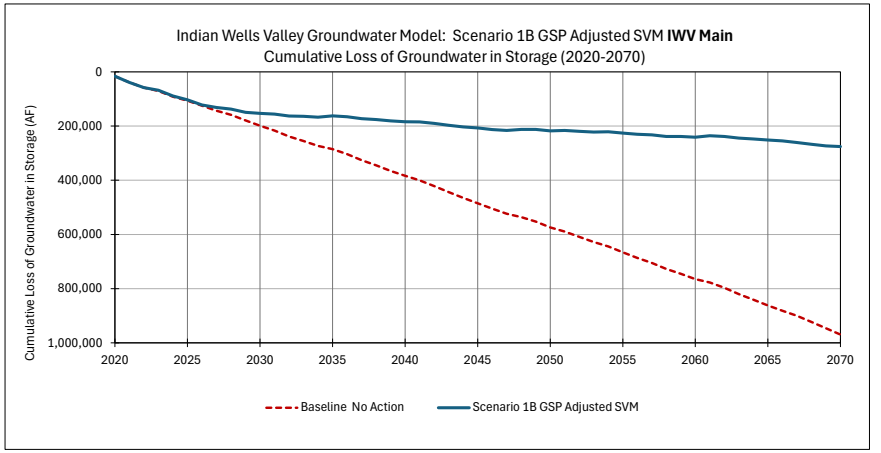
IWV Model is Oct 2019 through Sep 2070

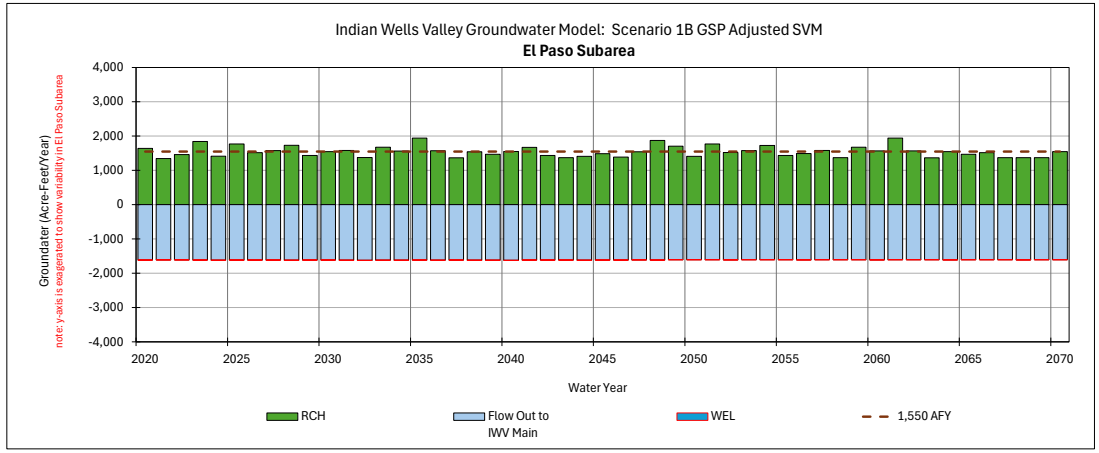
note: partial years for 2019 and 2070 not used in summary table

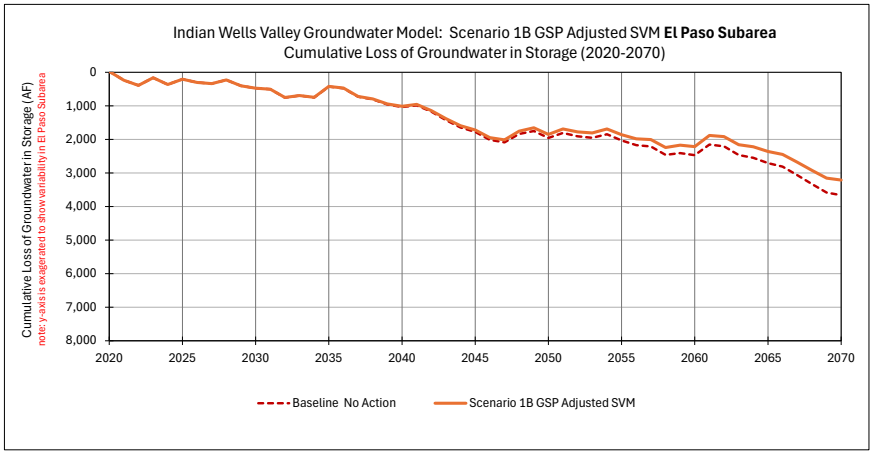




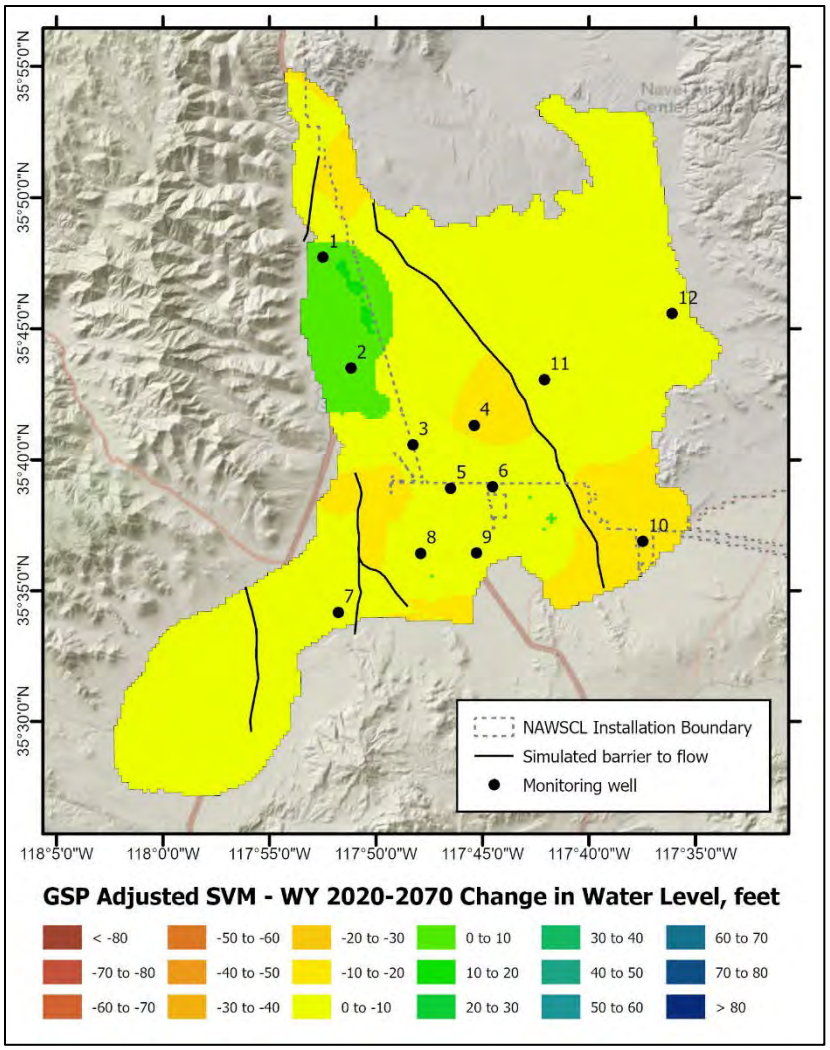


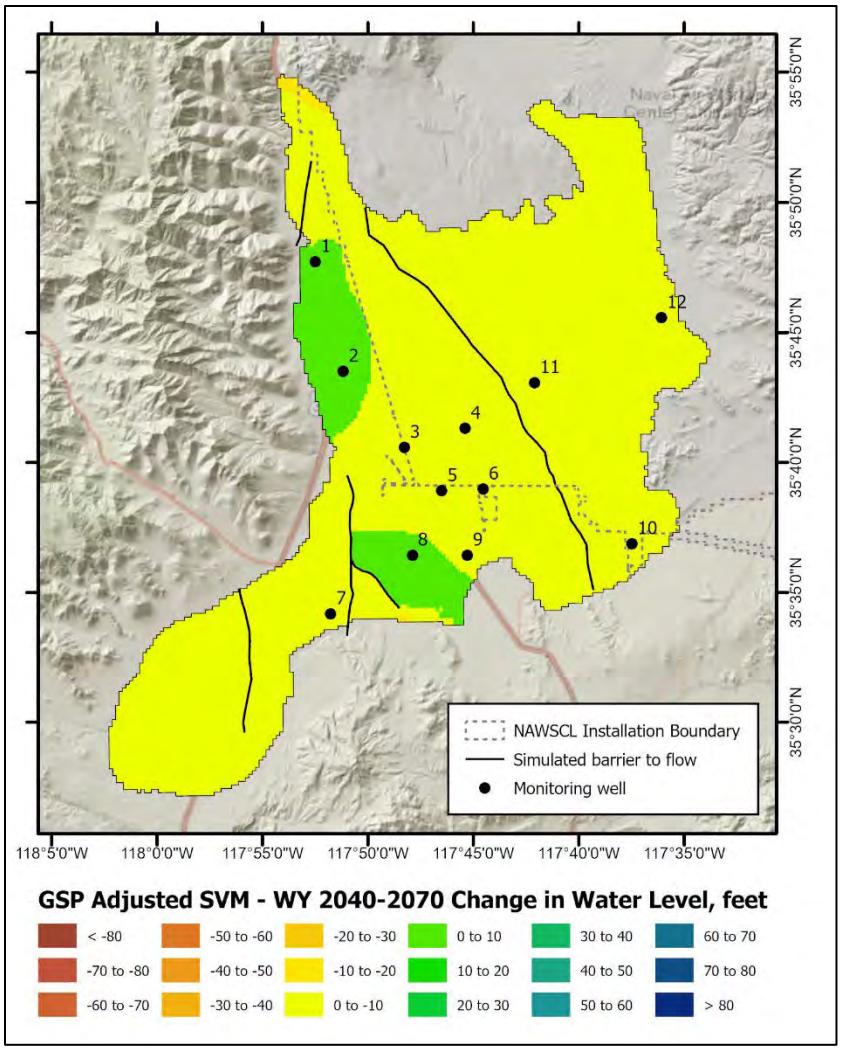






IWV Model Scenario 1B GSP Adjusted SVM





SCENARIO 1B IMPLEMENTED GSP ADJUSTED SVM Change in Groundwater Levels.

Maps of simulated change in water level from WY 2020-2070 (left) and WY 2040-2070 (right). Hydrographs for numbered monitoring wells are presented in IWV Model Results: page 1 of 4: **1**) 25S/38E-03B, **2**) 25S/38E-35B01, **3**) Kerr McGee,
Page 2 of 4: **4**) Sandquist Spa, **5**) MW 32-SM, **6**) USBR-04,
Page 3 of 4: **7**) USBR-01-S, **8**) 27S/39E-08A01, **9**) USBR-03-S
Page 4 of 4: **10**) George Air Corridor, **11**) TTBK-MW05, **12**) TTBK-MW12.

Model Scenario 2 "No GA"

This model scenario portrays conditions in the Basin if the IWVGA stopped implementation and all groundwater extractors in the Basin pumped at their current or desired pumping. Much of the projected pumping came from initial disclosures included in IWVGA litigation. Remaining pumpers are expected to continue at their current Baseline pumping. Initial disclosure documents by the City of Ridgecrest, Kern County, Mojave Pistachios, IWVWD, Inyokern CSD, Meadowbrook Dairy, Searles Valley Minerals, Sierra Shadows Ranch and the Navy, submitted to the Superior Court of the State of California, County of Orange on May 17, 2024 provide the 'planned' groundwater use for this model scenario.

This model scenario uses the same model code, 51-year time frame, and 7,650 AFY average annual recharge from the Baseline Model Run. The only changes are to the volume of pumped groundwater.

Groundwater Pumping for Model Scenario 2 "No GA"

Pumper	Starting Pumping WY 2024 (AF)	Pumping WY 2030 (AF)	Pumping WY 2040 (AF)	Pumping WY 2070 (AF)	Assumptions
IWVWD	6,821	7,130	7,830	10,342	Initial Disclosure Pumping up to 2045, Baseline Pumping to 2070
Navy*	6,503	6,503	6,503	6,503	1st Initial Disclosure Pumping, static
City of Ridgecrest	325	325	325	325	Initial Disclosure Pumping, static
Kern County	24	24	24	24	Initial Disclosure Pumping, static
Searles Valley Minerals	2,712	2,712	2,712	2,712	Initial Disclosure Pumping, static
Mojave Pistachios	12,109	12,109	12,109	12,109	Initial Disclosure Pumping, static
Meadowbrook Dairy	10,995	10,995	10,995	10,995	Initial Disclosure Pumping, static
Other Large Ag	1,446	1,446	1,446	1,446	Initial Disclosures Pumping, static/Baseline Pumping
Small Ag	320	320	320	320	Baseline Pumping
Inyokern CSD	196	208	228	304	Initial Disclosure Pumping, static
Mutuals	414	414	414	414	Baseline Pumping
Domestic	864	913	1,003	1,336	Baseline Pumping
TOTAL PUMPING**	**42,728**	**43,098**	**43,908**	**46,829**	

* Not representative of the Navy's full federally reserved water rights; subsequent amendments have been made to the Navy's initial disclosure pumping.

** Errors in total are due to rounding

Scenario 2 'No GA' 2020-2070 WY Annual Water Budget (AFY)

Indian Wells Valley - Total

WY Range	Recharge AF/WY	Flow in from SWV AF/WY	Pumping AF/WY	EVT vegetation AF/WY	Evap bare soil AF/WY	Flow to SWV AF/WY	NET Change of GW in Storage AF/WY	Cumulative Change of GW in Storage AF/WY
2020	9,534	0	(21,232)	(2,271)	(2,078)	(11)	(16,059)	(16,059)
2030	7,650	1	(43,098)	(1,907)	(1,819)	(5)	(39,178)	(338,979)
2040	7,672	5	(43,908)	(1,555)	(1,549)	(0)	(39,336)	(729,951)
2050	4,715	15	(44,665)	(1,175)	(1,221)	-	(42,331)	(1,127,078)
2060	7,994	30	(45,693)	(861)	(973)	-	(39,504)	(1,518,739)
2070	7,650	49	(46,823)	(575)	(603)	-	(40,301)	(1,929,079)
2020-2070	7,650	15	(42,719)	(1,384)	(1,386)	(2)	(37,825)	(1,929,079)
2041-2070	7,373	31	(45,269)	(1,017)	(1,083)	(0)	(39,971)	(1,199,129)

IWV Main Basin

WY Range	Recharge AF/WY	Flow in from SWV AF/WY	Flow in from El Paso SA AF/WY	Pumping AF/WY	EVT vegetation AF/WY	Evap bare soil AF/WY	Flow to SWV AF/WY	Flow out to El Paso SA AF/WY	NET Change of GW in Storage AF/WY	Cumulative Change of GW in Storage AF
2020	7,894	0	1,613	(21,231)	(2,271)	(2,078)	(10.93)	(0.26)	(16,085)	(16,085)
2030	6,102	1	1,618	(43,097)	(1,907)	(1,819)	(5.13)	(0.35)	(39,107)	(338,498)
2040	6,120	5	1,637	(43,907)	(1,555)	(1,549)	(0.40)	-	(39,250)	(728,821)
2050	3,305	15	1,633	(44,664)	(1,175)	(1,221)	-	(0.22)	(42,106)	(1,124,875)
2060	6,427	30	1,645	(45,692)	(861)	(973)	-	-	(39,425)	(1,515,842)
2070	6,102	49	1,643	(46,821)	(575)	(603)	-	-	(40,203)	(1,924,794)
2020-2070	6,102	15	1,632	(42,718)	(1,384)	(1,386)	(2.18)	(0.23)	(37,741)	(1,924,794)
2041-2070	5,838	24	1,639	(45,267)	(1,017)	(1,083)	(0.01)	(0.17)	(39,866)	(1,195,972)

El Paso Subarea

WY Range	Recharge AF/WY	Inflow from IWV Main AF/WY	Pumping AF/WY	Outflow to IWV Main AF/WY	NET Change of GW in Storage AF/WY	Cumulative Change of GW in Storage AF
2020	1,639	0.26	(1.00)	(1,613)	26	26
2030	1,548	0.35	(1.10)	(1,618)	(481)	(68)
2040	1,552	-	(1.21)	(1,637)	(1,129)	(74)
2050	1,410	0.22	(1.33)	(1,633)	(2,203)	(208)
2060	1,567	-	(1.46)	(1,645)	(2,897)	(60)
2070	1,548	-	(1.61)	(1,643)	(4,286)	(78)
2020-2070	1,549	0.23	(1.28)	(1,632)	(1,719)	(78)
2041-2070	1,536	0.16	(1.40)	(1,639)	(2,566)	(4)

Scenario 2 No GA 2020-2070 CY Annual Water Budget (AFY)

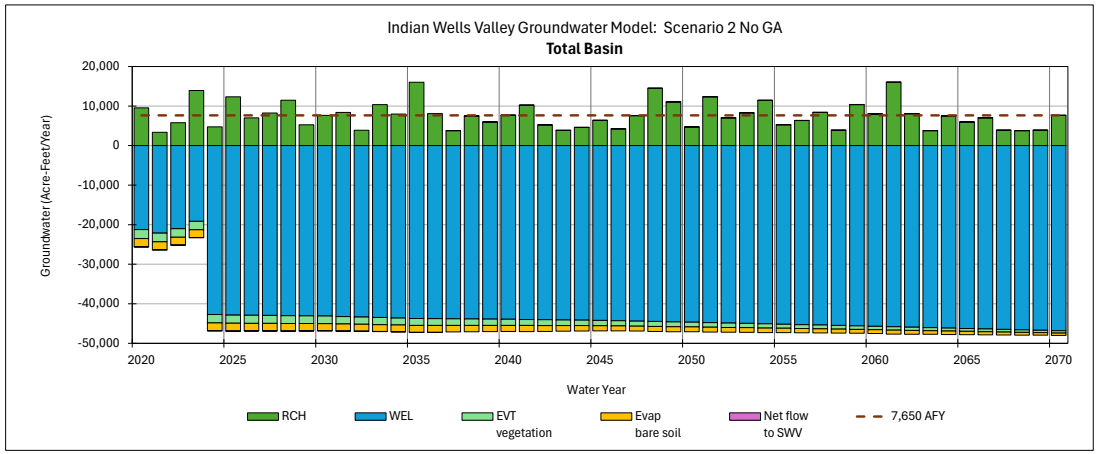
Calander Year

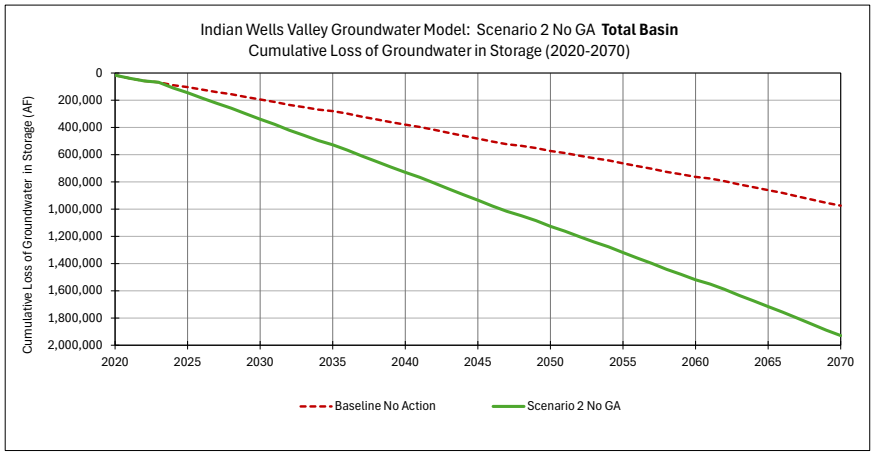
Indian Wells Valley - Total

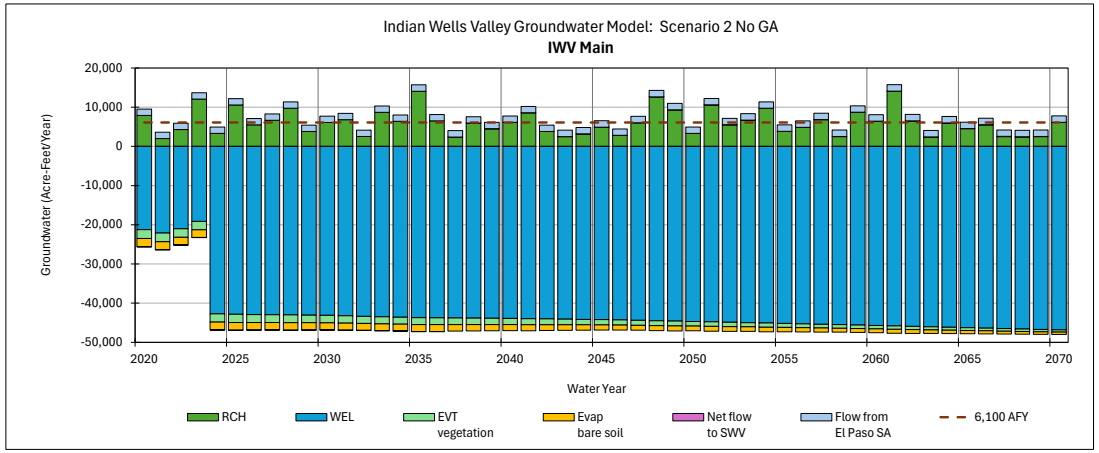
CY Range	Recharge AF/CY	Flow in from SWV AF/CY	Pumping AF/CY	EVT vegetation AF/CY	Evap bare soil AF/CY	Flow to SWV AF/CY	NET Change of GW in Storage AF/CY	Cumulative Change of GW in Storage AF/CY
2020	7,110	0	(21,272)	(2,263)	(2,071)	(11)	(18,506)	(20,018)
2030	6,465	1	(43,127)	(1,899)	(1,812)	(5)	(40,376)	(345,148)
2040	11,289	5	(43,921)	(1,551)	(1,548)	(0)	(35,727)	(731,369)
2050	5,025	16	(44,688)	(1,166)	(1,208)	-	(42,021)	(1,132,920)
2060	11,240	30	(45,718)	(858)	(972)	-	(36,278)	(1,520,958)
2069	5,022	48	(46,736)	(595)	(622)	-	(42,882)	(1,894,055)
2020-2069	7,627	15	(42,702)	(1,393)	(1,395)	(2)	(37,851)	(1,894,055)
2040-2069	7,374	23	(45,194)	(1,043)	(1,108)	(0)	(39,947)	(1,162,686)

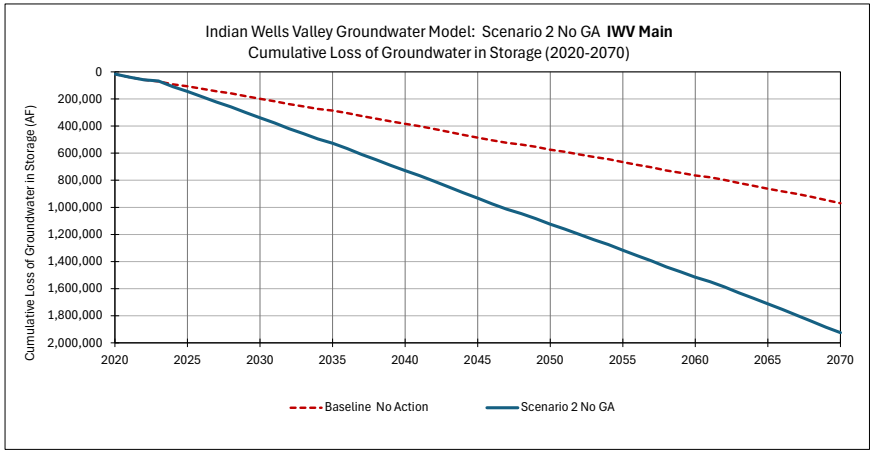
IWV Model is Oct 2019 through Sep 2070

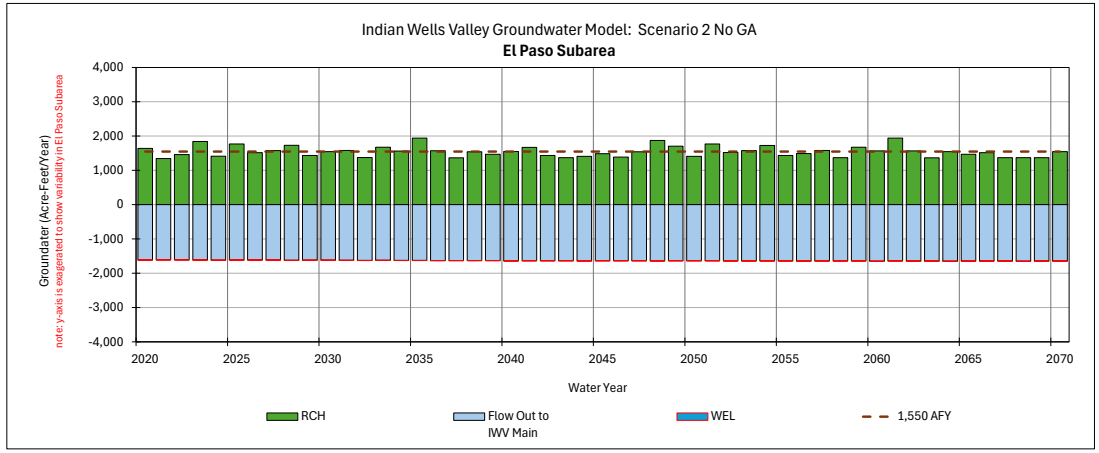
note: partial years for 2019 and 2070 not used in summary table

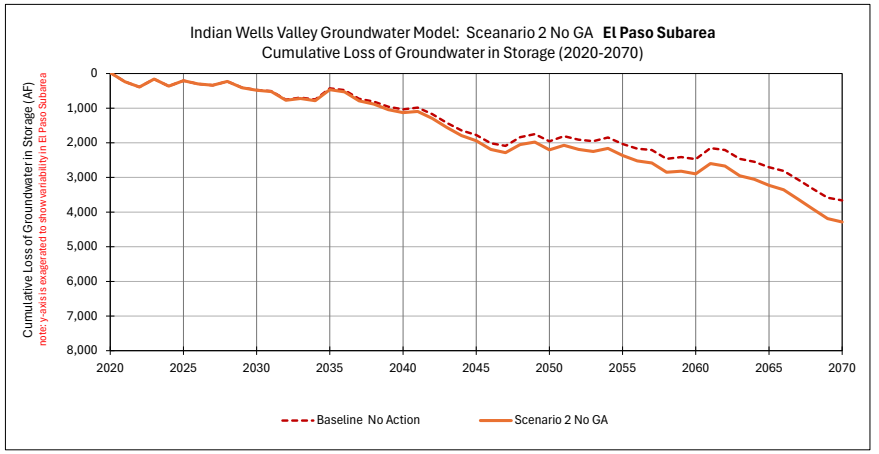




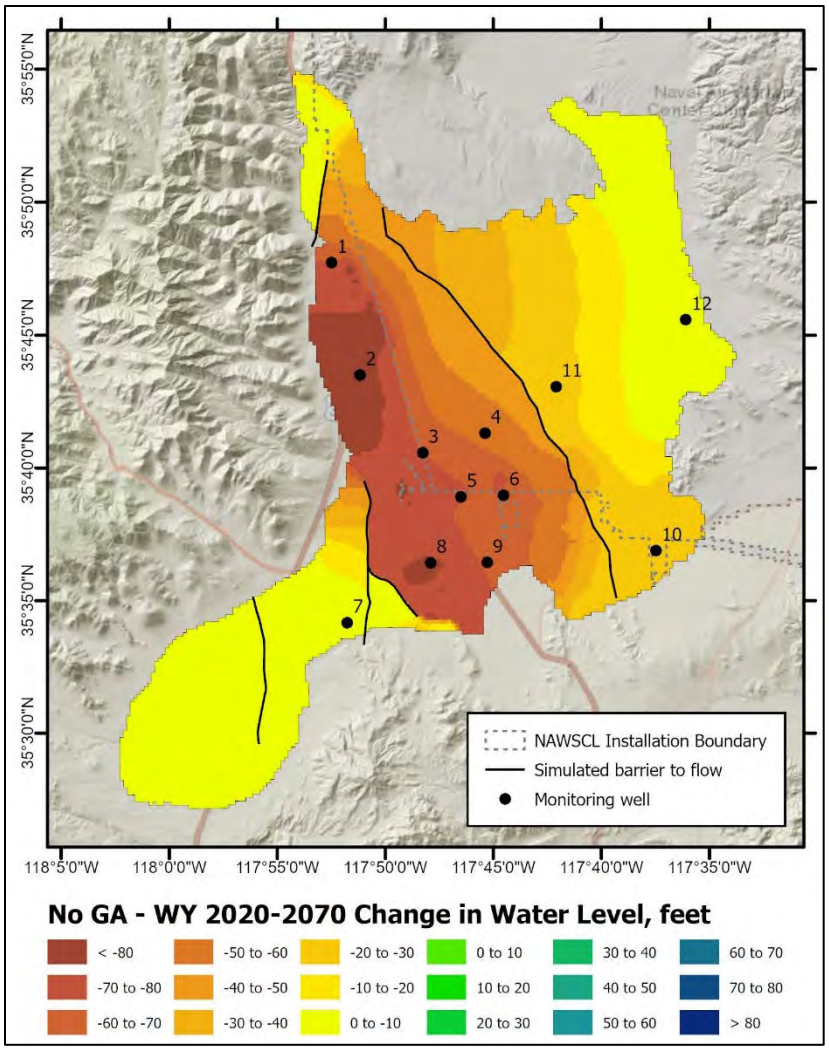


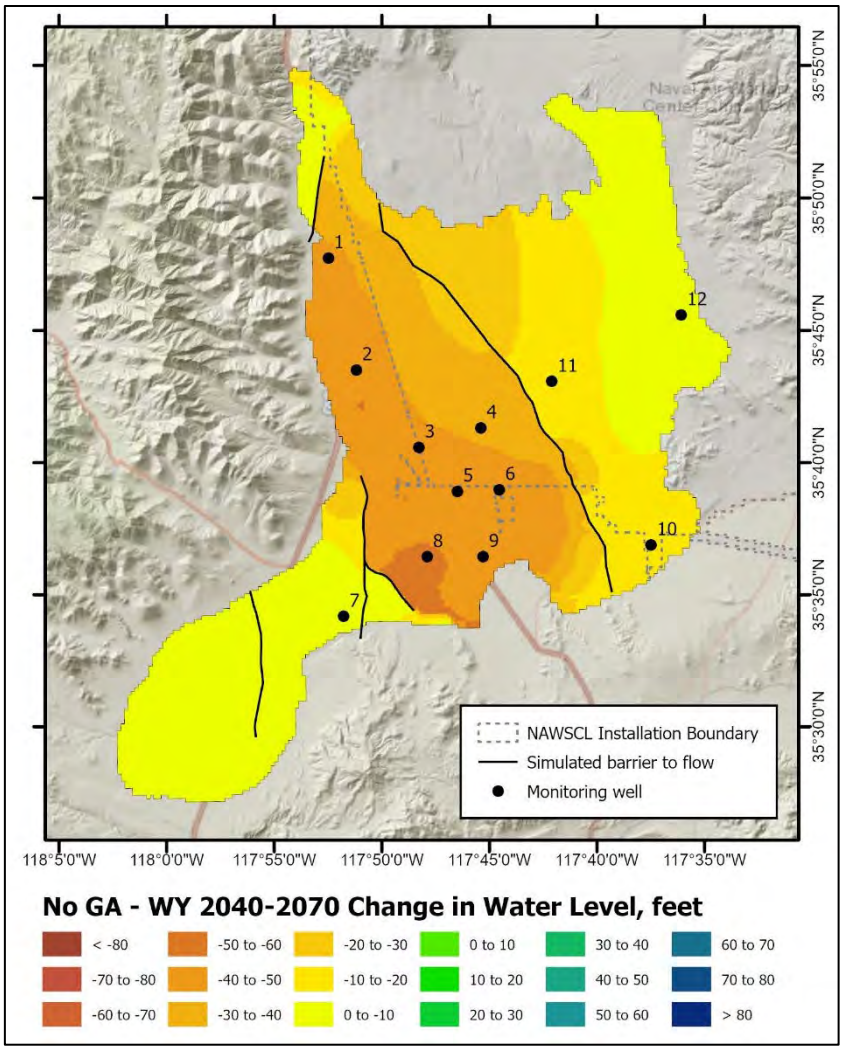






IWV Model Scenario 2 No GA





SCENARIO 2 'NO GA' Change in Groundwater Levels.

Maps of simulated change in water level from WY 2020-2070 (left) and WY 2040-2070 (right). Hydrographs for numbered monitoring wells are presented in IWV Model Results: page 1 of 4: **1**) 25S/38E-03B, **2**) 25S/38E-35B01, **3**) Kerr McGee,
Page 2 of 4: **4**) Sandquist Spa, **5**) MW 32-SM, **6**) USBR-04,
Page 3 of 4: **7**) USBR-01-S, **8**) 27S/39E-08A01, **9**) USBR-03-S
Page 4 of 4: **10**) George Air Corridor, **11**) TTBK-MW05, **12**) TTBK-MW12.

Model Scenario 3 EVT

This model scenario shows conditions of evapotranspiration within the Basin if all groundwater pumping in the Basin were to cease. Groundwater pumping would cease in WY 2024, allowing the IWVGA to understand the extent of evapotranspiration in the Basin and how long it would take to bring the Basin into a steady state with natural hydrogeologic inflows and outflows of recharge, evapotranspiration, and interbasin subsurface flow in the Basin. This model scenario uses the same model code, a 2,006-year time frame, and7,650 AFY average annual recharge. The only changes are to the volume of pumped groundwater.

Scenario 3 ET Study 2020-4025 Annual Water Budget (AFY)

Indian Wells Valley - Total

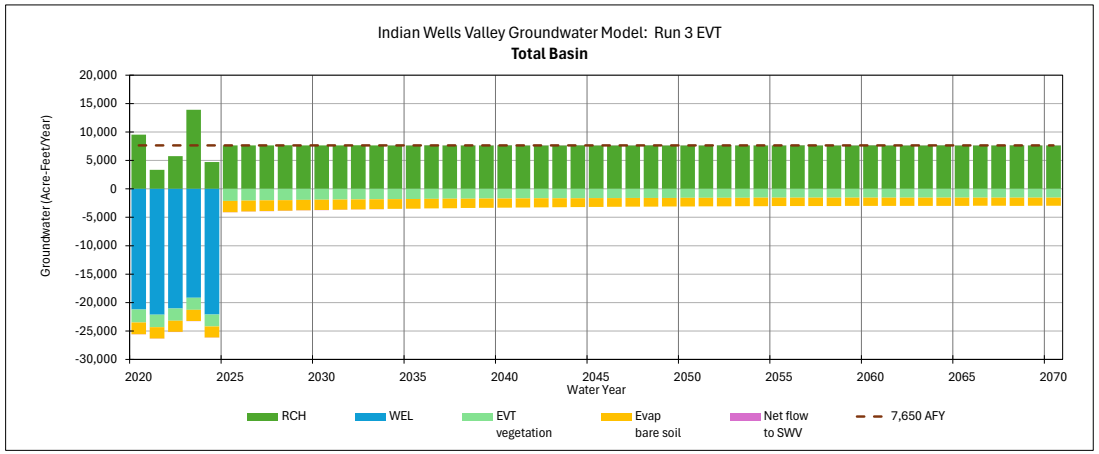
WY Range	Recharge AF/WY	Flow in from SWV AF/WY	Pumping AF/WY	EVT vegetation AF/WY	Evap bare soil AF/WY	Flow to SWV AF/WY	NET Change of GW in Storage AF/WY	Cumulative Change of GW in Storage AF/WY
2020	9,534	0	(21,232)	(2,271)	(2,078)	(11)	(16,059)	(16,059)
2030	7,649	1	-	(1,910)	(1,805)	(2)	3,933	(66,579)
2040	7,670	3	-	(1,689)	(1,621)	(1)	4,362	(24,718)
2050	7,649	4	-	(1,577)	(1,511)	(0)	4,565	20,123
2060	7,670	4	-	(1,540)	(1,465)	(0)	4,669	66,393
2070	7,649	4	-	(1,535)	(1,445)	(0)	4,672	113,120
2020-2070	7,636	3	(2,071)	(1,719)	(1,629)	(2)	2,218	113,120
2041-2070	7,654	4	-	(1,568)	(1,495)	(0)	4,595	137,838

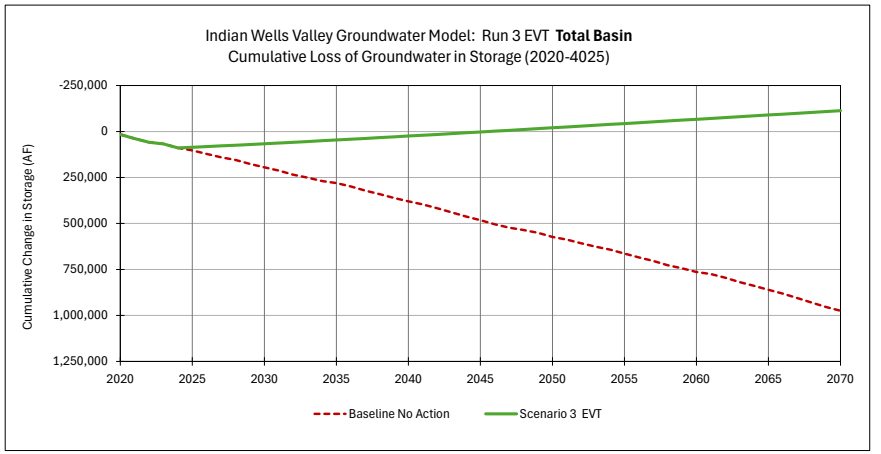
IWV Main Basin

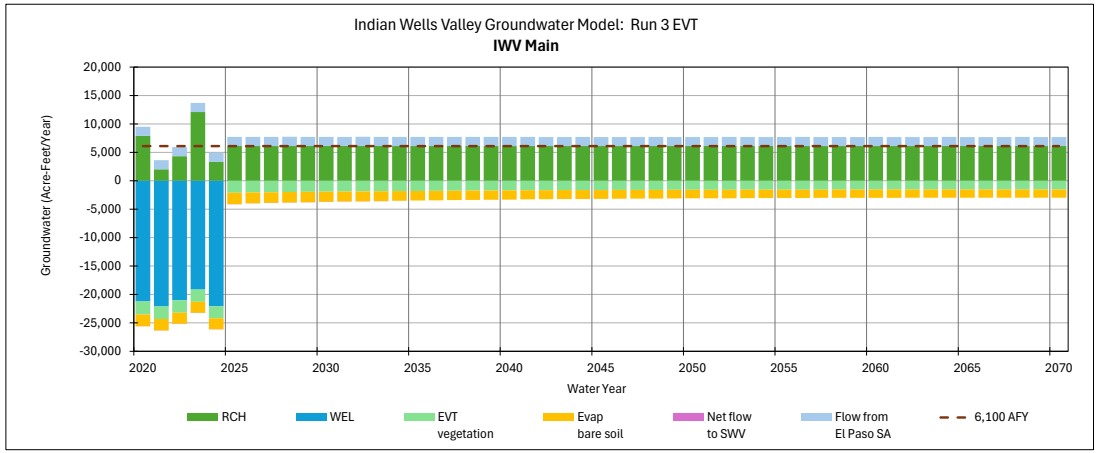
WY Range	Recharge AF/WY	Flow in from SWV AF/WY	Flow in from El Paso SA AF/WY	Pumping AF/WY	EVT vegetation AF/WY	Evap bare soil AF/WY	Flow to SWV AF/WY	Flow out to El Paso SA AF/WY	NET Change of GW in Storage AF/WY	Cumulative Change of GW in Storage AF/WY
2020	7,894	0.12	1,613	(21,231)	(2,271)	(2,078)	(11)	(0.26)	(16,085)	(16,085)
2030	6,102	1	1,608	-	(1,910)	(1,805)	(2)	-	3,993	(65,844)
2040	6,118	3	1,604	-	(1,689)	(1,621)	(1)	-	4,415	(23,423)
2050	6,102	4	1,591	-	(1,577)	(1,511)	(0)	-	4,609	21,893
2060	6,118	4	1,589	-	(1,540)	(1,465)	(0)	(0)	4,706	68,562
2070	6,102	4	1,579	-	(1,535)	(1,445)	(0)	(0)	4,704	115,626
2020-2070	6,088	3	1,597	(2,071)	(1,719)	(1,629)	(2)	(0)	2,267	115,626
2041-2070	6,106	4	1,589	-	(1,568)	(1,495)	(0)	(0)	4,635	139,049

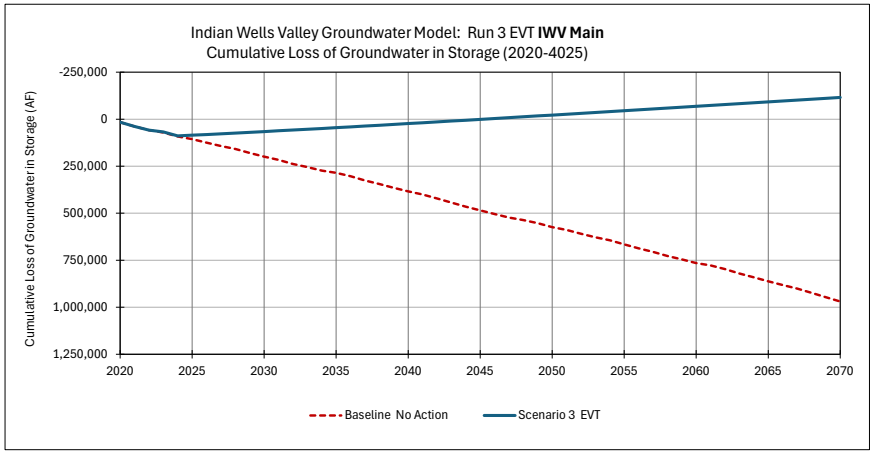
El Paso Subarea

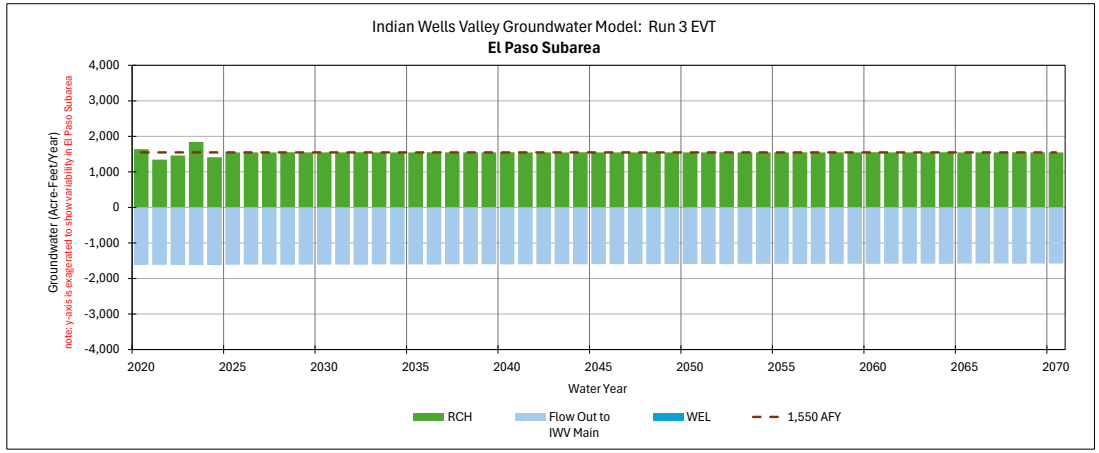
WY Range	Recharge AF/WY	Inflow from IWV Main AF/WY	Pumping AF/WY	Outflow to IWV Main AF/WY	NET Change of GW in Storage AF/WY	Cumulative Change of GW in Storage AF/WY
2020	1,639	0.26	(1.00)	(1,613)	26	26
2030	1,547	-	-	(1,608)	(60)	(735)
2040	1,552	-	-	(1,604)	(52)	(1,295)
2050	1,547	-	-	(1,591)	(44)	(1,770)
2060	1,552	0	-	(1,589)	(37)	(2,169)
2070	1,547	0	-	(1,579)	(31)	(2,506)
2020-2070	1,548	0	(0)	(1,597)	(49)	(2,506)
2041-2070	1,548	0	-	(1,589)	(40)	(1,211)

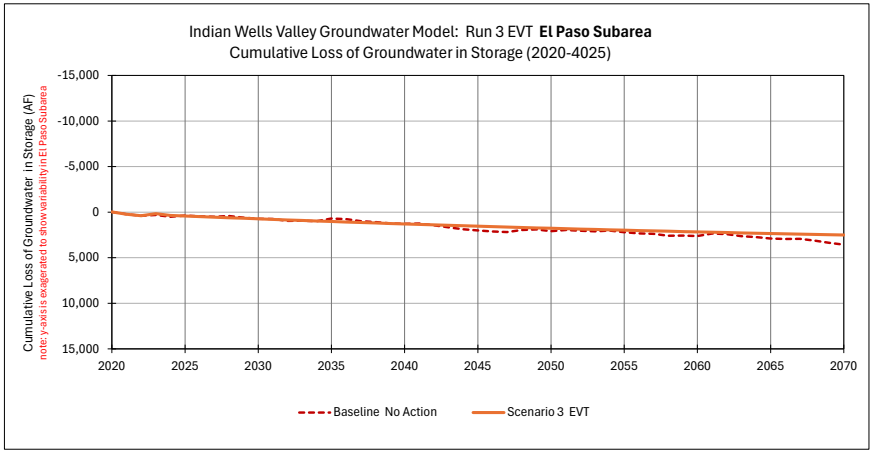




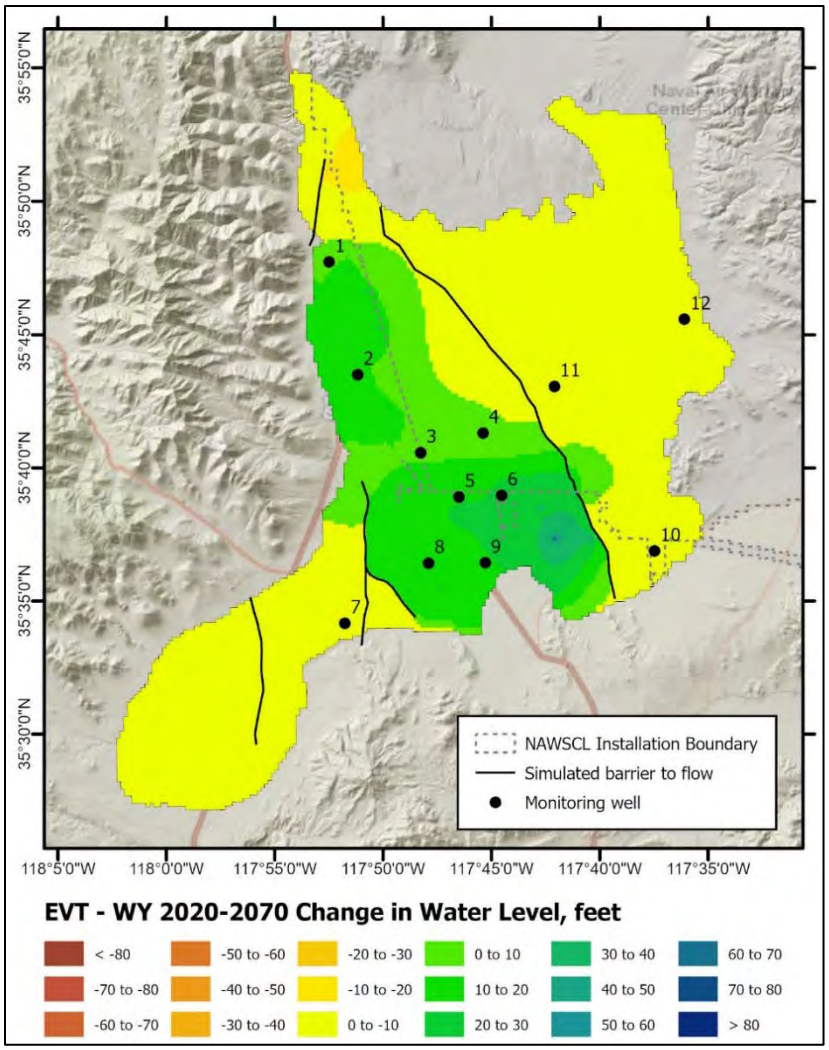


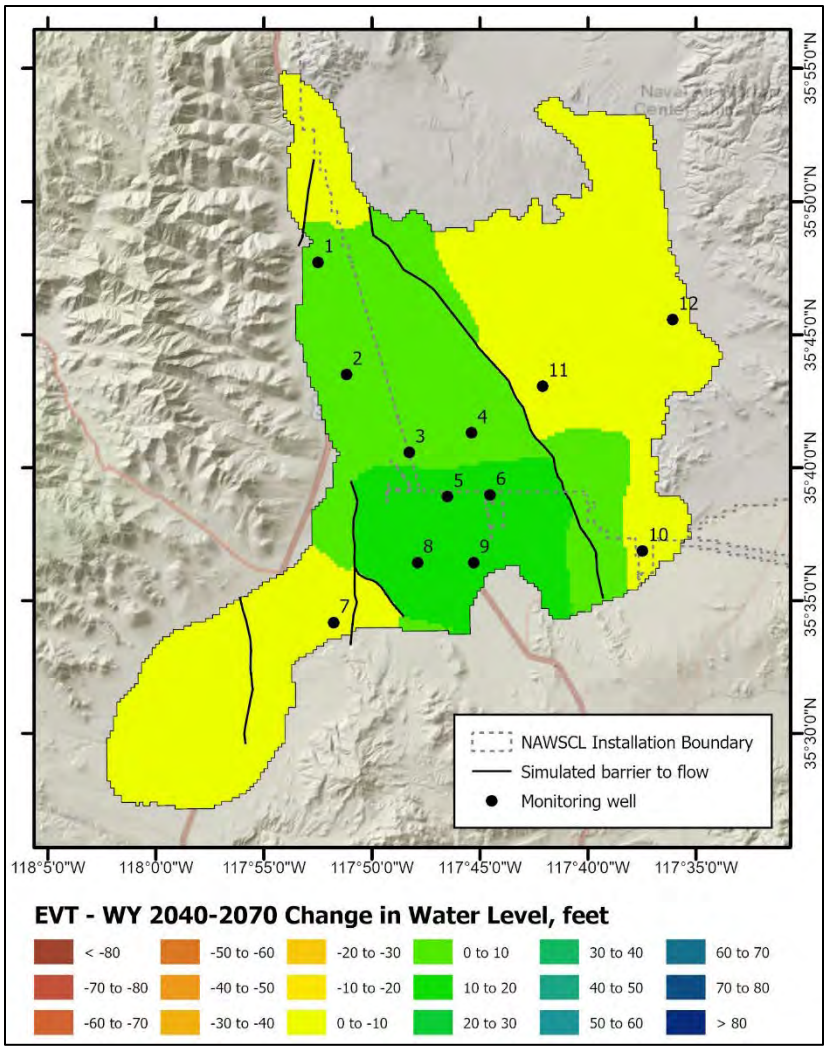






IWV Model Scenario 3 EVT





Scenario 3 EVT Change in Groundwater Levels.

Maps of simulated change in water level from WY 2020-2070 (left) and WY 2070-3020 (right). Hydrographs for numbered monitoring wells are presented in IWV Model Results: page 1 of 4: **1**) 25S/38E-03B, **2**) 25S/38E-35B01, **3**) Kerr McGee,
Page 2 of 4: **4**) Sandquist Spa, **5**) MW 32-SM, **6**) USBR-04,
Page 3 of 4: **7**) USBR-01-S, **8**) 27S/39E-08A01, **9**) USBR-03-S
Page 4 of 4: **10**) George Air Corridor, **11**) TTBK-MW05, **12**) TTBK-MW12.

Model Scenario 4 El Paso Pumping

This model scenario portrays current Basin conditions since the start of GSP implementation and if the Indian Wells Valley Water District's (IWVWD) pumping was relocated to the El Paso Subarea. IWVWD pumping would be relocated to a single well in the El Paso subarea at 726 AFY. This model scenario once again includes currently implemented 2020 GSP projects and managements such as voluntary Basin-wide conservation, the Transient Pool, Shallow Well Mitigation Program, and the Imported Water Project which will allow imported water to be available in 2030. Once imported water is available, total pumping in the Basin will be reduced to the sustainable yield of 7,650 AF. This model scenario uses the same model code, 51-year time frame, and 7,650 AFY average annual recharge from the Model Baseline. The only changes are to the volume of pumped groundwater.

Groundwater Pumping for Model Scenario 4 El Paso Pumping

Pumper	Starting Pumping WY 2024 (AF)	Pumping WY 2030 (AF)	Pumping WY 2040 (AF)	Pumping WY 2070 (AF)	Assumptions
IWVWD	6,095	447	334	0	Pumping reduced to by El Paso pumping and to meet Sustainable Yield in 2030
Navy	2,041	2,041	2,041	2,041	Baseline Pumping
City of Ridgecrest	325	325	325	325	Initial Disclosure Pumping, static
Kern County	22	22	22	22	Baseline Pumping
Searles Valley Minerals	2,544	2,544	2,544	2,544	Baseline Pumping
Mojave Pistachios	3,561	0	0	0	Baseline Pumping until 2027, litigation
Meadowbrook Dairy	4,352	0	0	0	Baseline Pumping until 2027, litigation
Other Large Ag	762	0	0	0	Transient Pool until 2027
Small Ag	281	0	0	0	Transient Pool until 2027
Inyokern CSD	205	218	241	324	Baseline Pumping
Mutuals	414	414	414	414	Baseline Pumping
Domestic	864	913	1,003	1,336	Baseline Pumping
El Paso	726	726	726	643	Pumping reduced to meet Sustainable Yield in 2030
TOTAL PUMPING*	**22,192**	**7,650**	**7,650**	**7,650**	

* Errors in total are due to rounding

Scenario 4 El Paso Pumping 2020-2070 WY Annual Water Budget (AFY)

Indian Wells Valley - Total

WY Range	Recharge AF/WY	Flow in from SWV AF/WY	Pumping AF/WY	EVT vegetation AF/WY	Evap bare soil AF/WY	Flow to SWV AF/WY	NET Change of GW in Storage AF/WY	Cumulative Change of GW in Storage AF/WY
2020	9,534	0	(21,232)	(2,271)	(2,078)	(11)	(16,059)	(16,059)
2030	7,650	1	(7,650)	(1,911)	(1,820)	(5)	(3,735)	(153,456)
2040	7,672	4	(7,650)	(1,661)	(1,611)	(1)	(3,248)	(185,159)
2050	4,715	8	(7,650)	(1,491)	(1,434)	-	(5,852)	(219,647)
2060	7,994	12	(7,650)	(1,415)	(1,372)	-	(2,431)	(243,331)
2070	7,650	17	(7,650)	(1,305)	(1,201)	-	(2,489)	(279,044)
2020-2070	7,650	7	(9,893)	(1,653)	(1,580)	(2)	(5,471)	(279,044)
2041-2070	7,373	12	(7,650)	(1,458)	(1,405)	(0)	(3,129)	(93,885)

IWV Main Basin

WY Range	Recharge AF/WY	Flow in from SWV AF/WY	Flow in from El Paso SA AF/WY	Pumping AF/WY	EVT vegetation AF/WY	Evap bare soil AF/WY	Flow to SWV AF/WY	Flow out to El Paso SA AF/WY	NET Change of GW in Storage AF/WY	Cumulative Change of GW in Storage AF
2020	7,894	0	1,613	(21,231)	(2,271)	(2,078)	(10.93)	(0.26)	(16,085)	(16,085)
2030	6,102	1	1,594	(6,923)	(1,911)	(1,820)	(5.16)	(0.36)	(2,962)	(147,956)
2040	6,120	4	1,540	(6,923)	(1,661)	(1,611)	(0.98)	(0.00)	(2,533)	(172,390)
2050	3,305	8	1,473	(6,923)	(1,491)	(1,434)	-	(0.37)	(5,062)	(199,871)
2060	6,427	12	1,430	(6,923)	(1,415)	(1,372)	-	(0.15)	(1,841)	(217,516)
2070	6,102	17	1,384	(7,005)	(1,305)	(1,201)	-	-	(2,007)	(247,244)
2020-2070	6,102	7	1,507	(9,228)	(1,653)	(1,580)	(2.27)	(0.30)	(4,848)	(247,244)
2041-2070	5,838	10	1,451	(6,931)	(1,458)	(1,405)	(0.06)	(0.28)	(2,495)	(74,854)

El Paso Subarea

WY Range	Recharge AF/WY	Inflow from IWV Main AF/WY	Pumping AF/WY	Outflow to IWV Main AF/WY	NET Change of GW in Storage AF/WY	Cumulative Change of GW in Storage AF
2020	1,639	0.26	(1.00)	(1,613)	26	26
2030	1,548	0.36	(726.95)	(1,594)	(5,500)	(68)
2040	1,552	0.00	(727.06)	(1,540)	(12,770)	(74)
2050	1,410	0.37	(727.18)	(1,473)	(19,776)	(208)
2060	1,567	0.15	(727.31)	(1,430)	(25,815)	(60)
2070	1,548	-	(644.96)	(1,384)	(31,800)	(78)
2020-2070	1,549	0.30	(665.13)	(1,507)	(15,801)	(78)
2041-2070	1,536	0.27	(718.64)	(1,451)	(22,924)	(4)

Scenario 4 El Paso Pumping 2020-2070 CY Annual Water Budget (AFY)

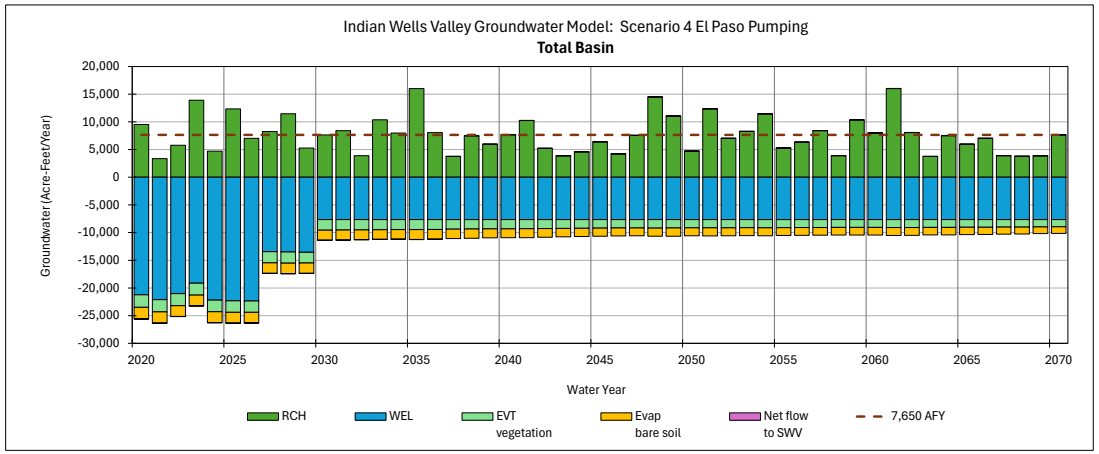
Calander Year

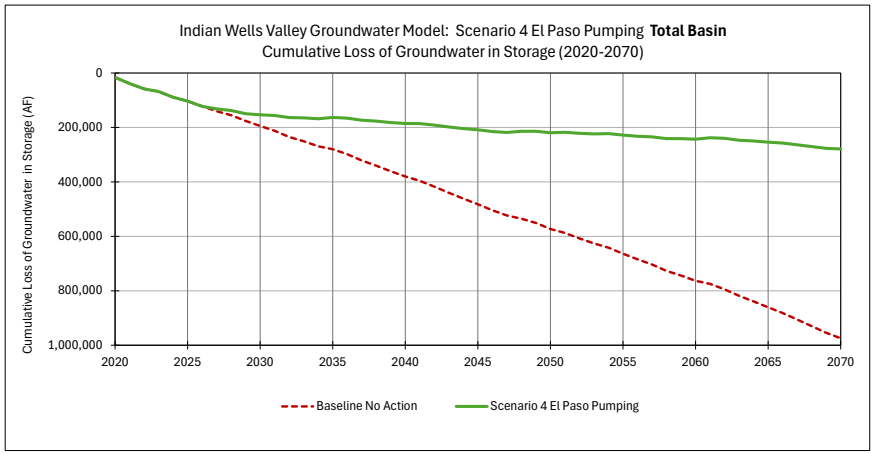
Indian Wells Valley - Total

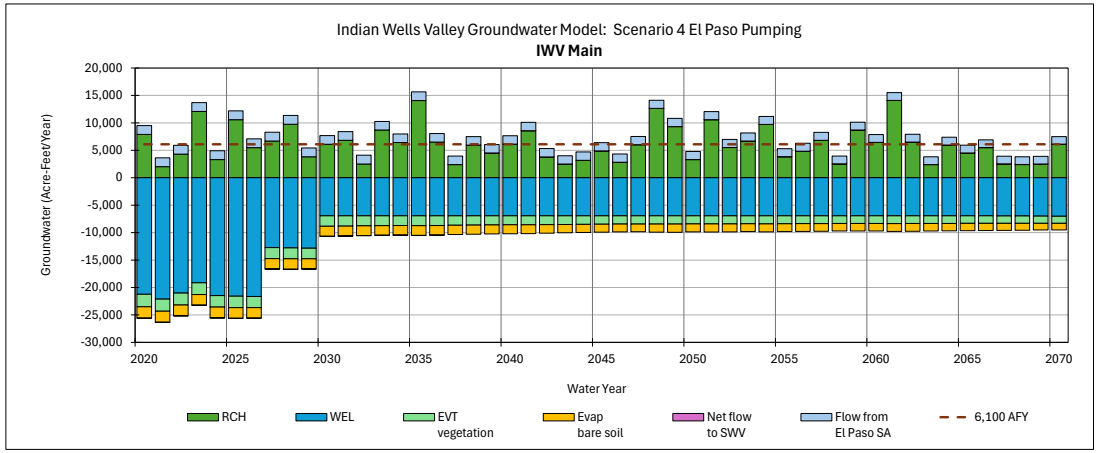
CY Range	Recharge AF/CY	Flow in from SWV AF/CY	Pumping AF/CY	EVT vegetation AF/CY	Evap bare soil AF/CY	Flow to SWV AF/CY	NET Change of GW in Storage AF/CY	Cumulative Change of GW in Storage AF/CY
2020	7,110	0	(21,272)	(2,263)	(2,071)	(11)	(18,506)	(20,018)
2030	6,465	1	(7,650)	(1,904)	(1,814)	(5)	(4,906)	(155,076)
2040	11,289	4	(7,650)	(1,661)	(1,613)	(1)	368	(181,893)
2050	5,025	8	(7,650)	(1,486)	(1,425)	-	(5,528)	(220,696)
2060	11,240	12	(7,650)	(1,416)	(1,376)	-	811	(240,607)
2069	5,022	17	(7,650)	(1,317)	(1,208)	-	(5,135)	(276,729)
2020-2069	7,627	7	(9,895)	(1,656)	(1,584)	(2)	(5,504)	(276,729)
2040-2069	7,374	10	(7,650)	(1,468)	(1,416)	(0)	(3,149)	(94,837)

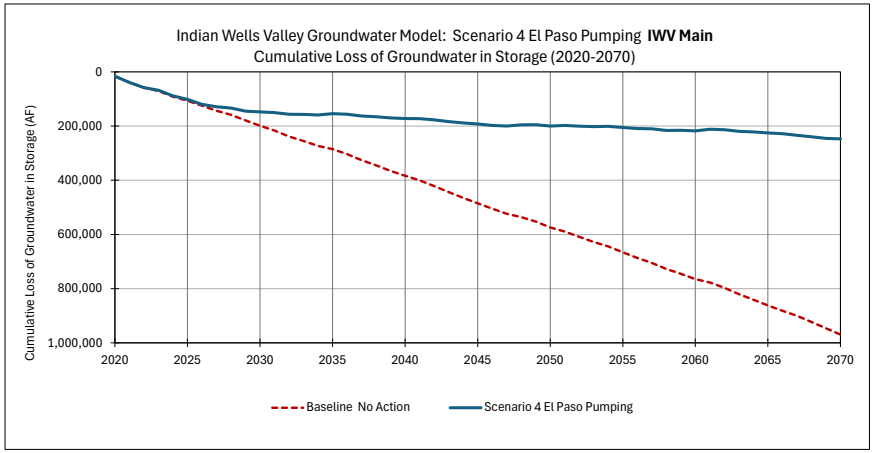
IWV Model is Oct 2019 through Sep 2070

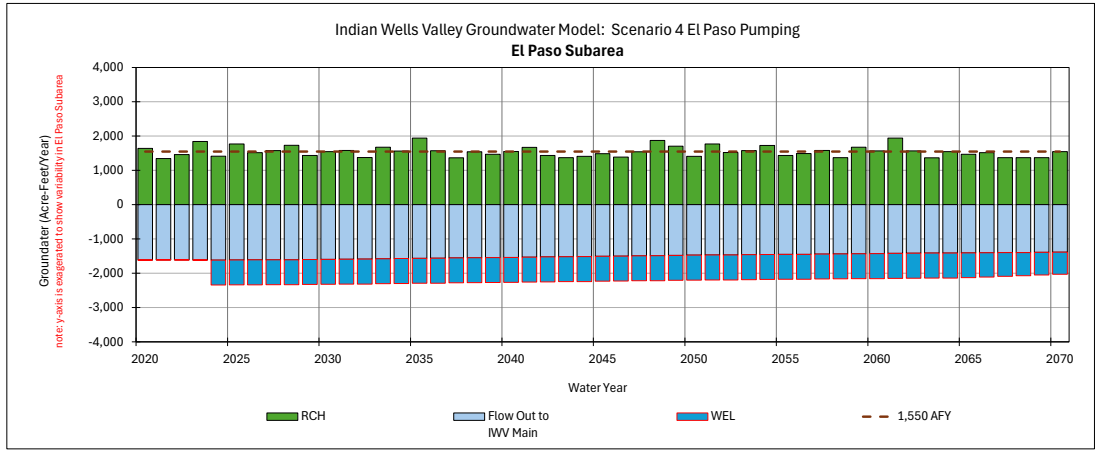
note: partial years for 2019 and 2070 not used in summary table

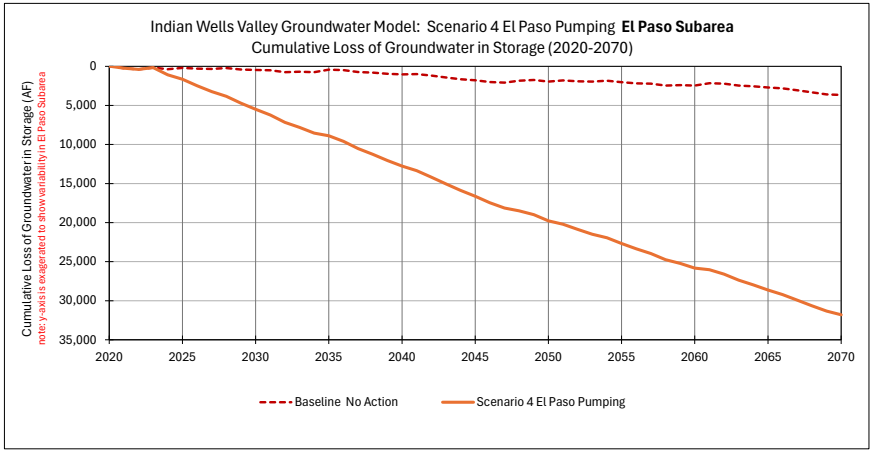




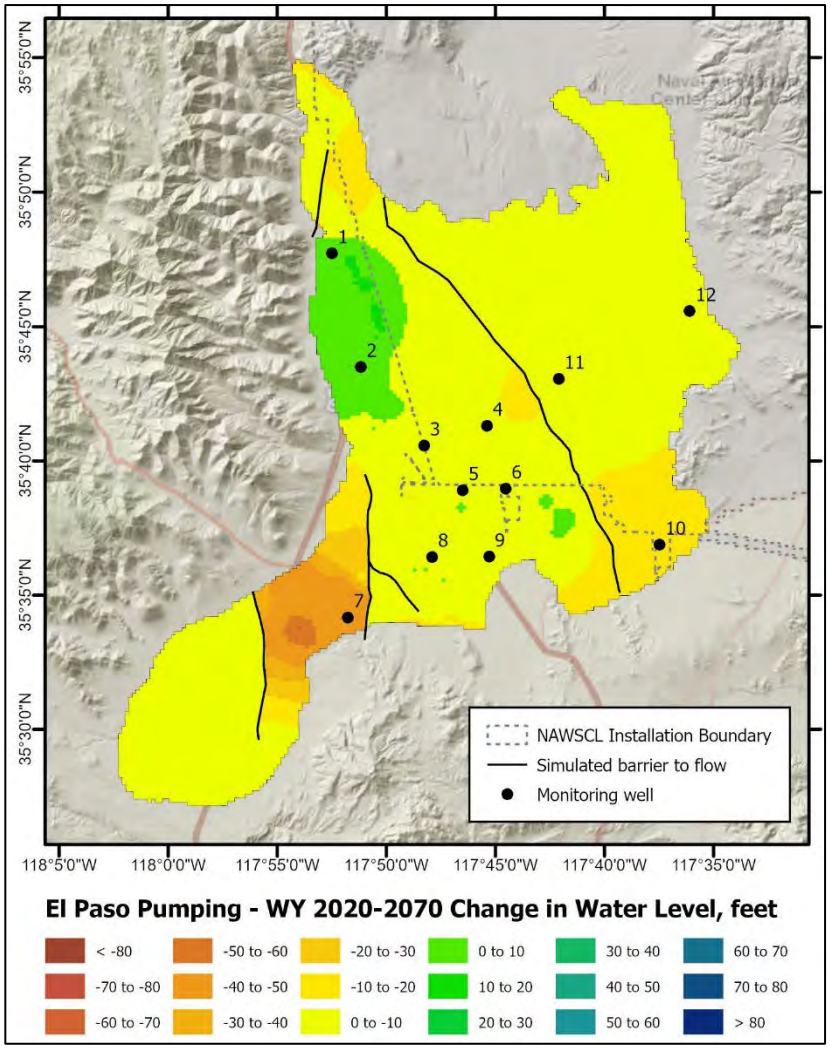


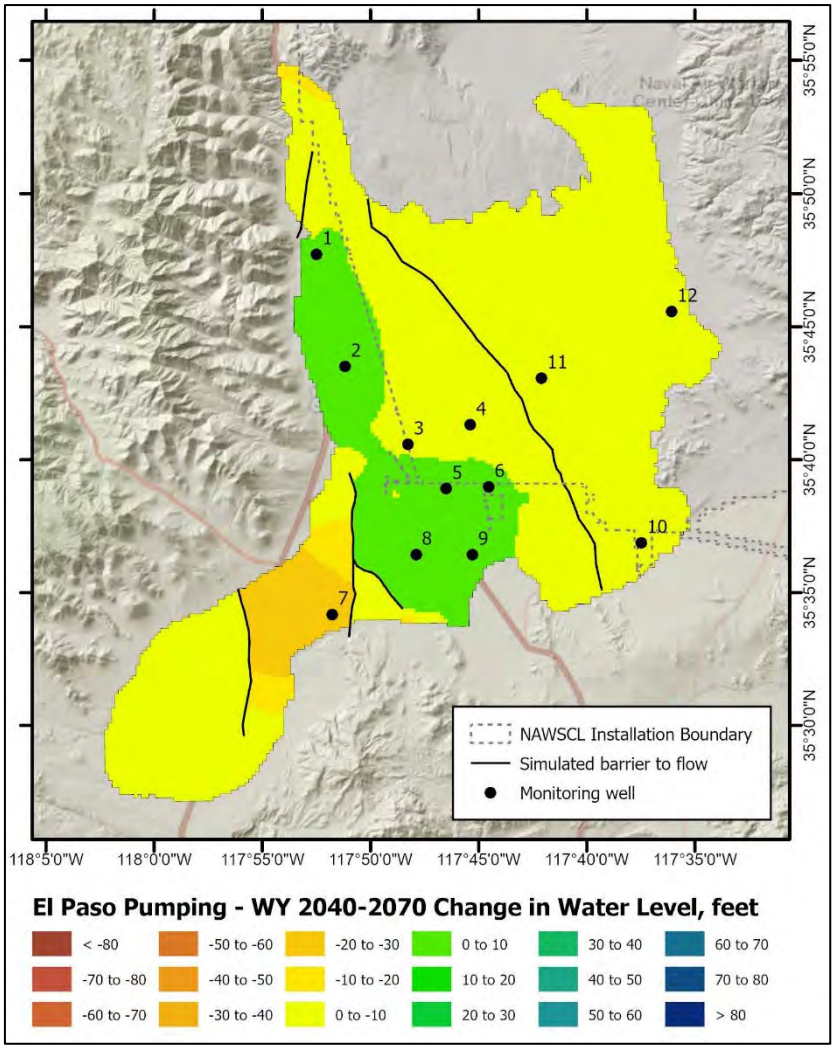






IWV Model Scenario 4 El Paso Pumping





Scenario 4 EL PASO PUMPING Change in Groundwater Levels.

Maps of simulated change in water level from WY 2020-2070 (left) and WY 2040-2070 (right). Hydrographs for numbered monitoring wells are presented in IWV Model Results: page 1 of 4: **1**) 25S/38E-03B, **2**) 25S/38E-35B01, **3**) Kerr McGee,
Page 2 of 4: **4**) Sandquist Spa, **5**) MW 32-SM, **6**) USBR-04,
Page 3 of 4: **7**) USBR-01-S, **8**) 27S/39E-08A01, **9**) USBR-03-S
Page 4 of 4: **10**) George Air Corridor, **11**) TTBK-MW05, **12**) TTBK-MW12.

Hydrographs Comparing Model Results for Key Representative Wells

Hydrographs on the following four pages compare the Baseline and Model Scenario results for the Key Representative Wells in the GSP. The groundwater level change maps included in this attachment show the location of these twelve monitoring wells.

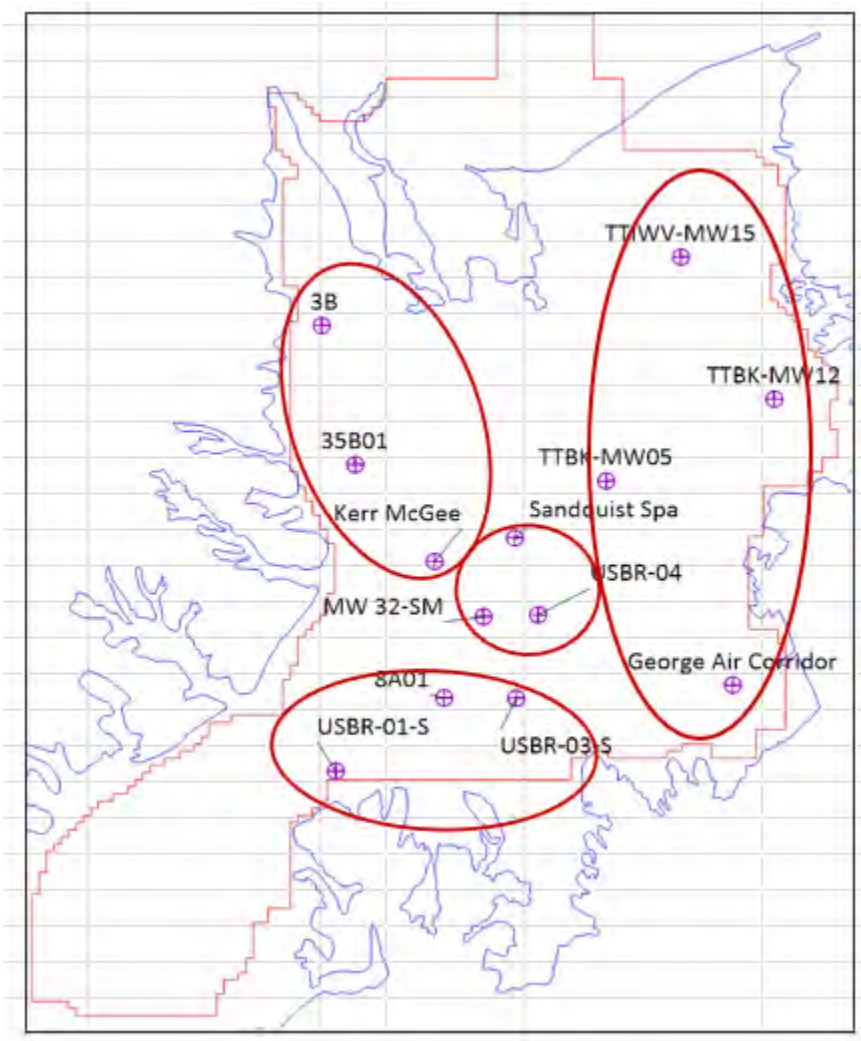
Page 1 of 4: **1**) 25S/38E-03B, **2**) 25S/38E-35B01, **3**) Kerr McGee,

Page 2 of 4: **4**) Sandquist Spa, **5**) MW 32-SM, **6**) USBR-04,

Page 3 of 4: **7**) USBR-01-S, **8**) 27S/39E-08A01, **9**) USBR-03-S,

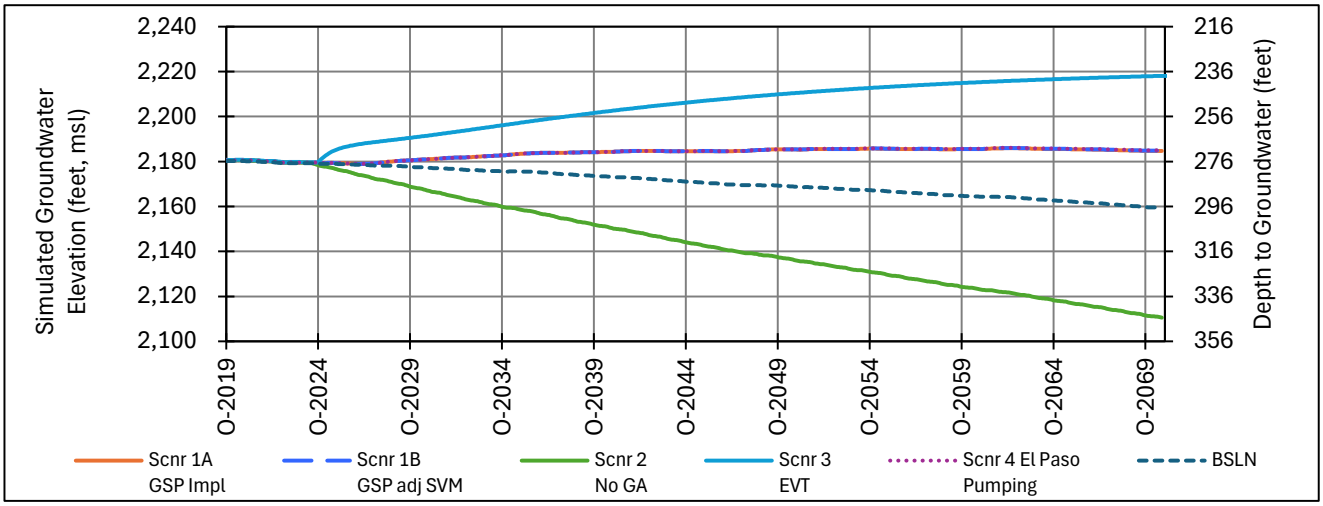
Page 4 of 4: **10**) George Air Corridor, **11**) TTBK-MW12, **12**) TTBK-MW05.

Hydrographs for three GDE wells is shown on the last page of this Attachment.

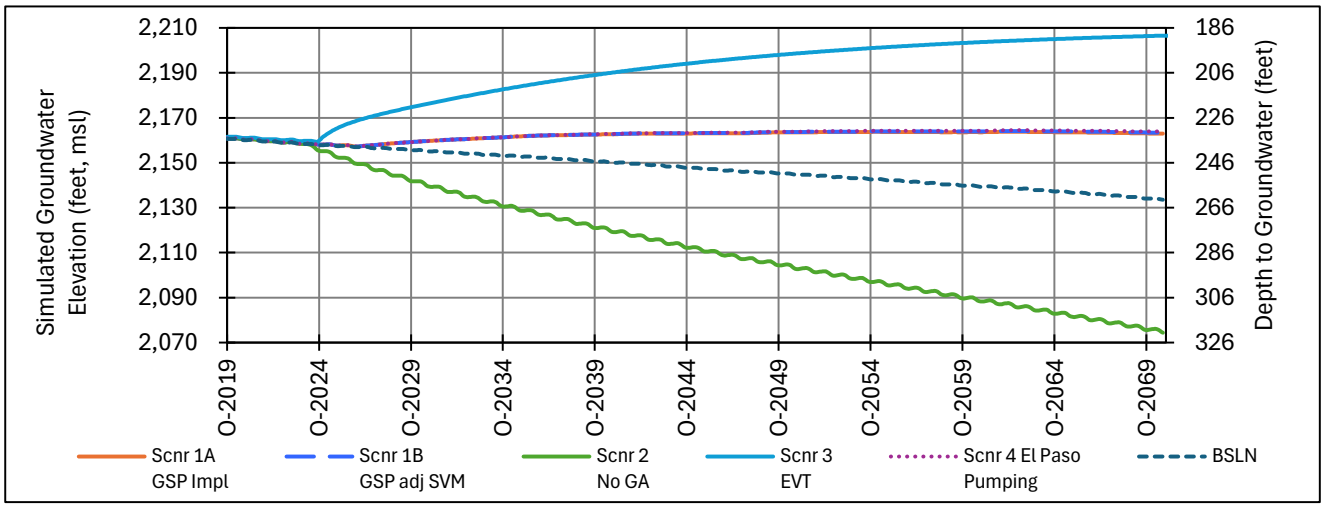


IWV Groundwater Model
Comaprison of Simulated Hydrographs
Baseline, Scenarios 1A, 1B, 2, 3, and 4

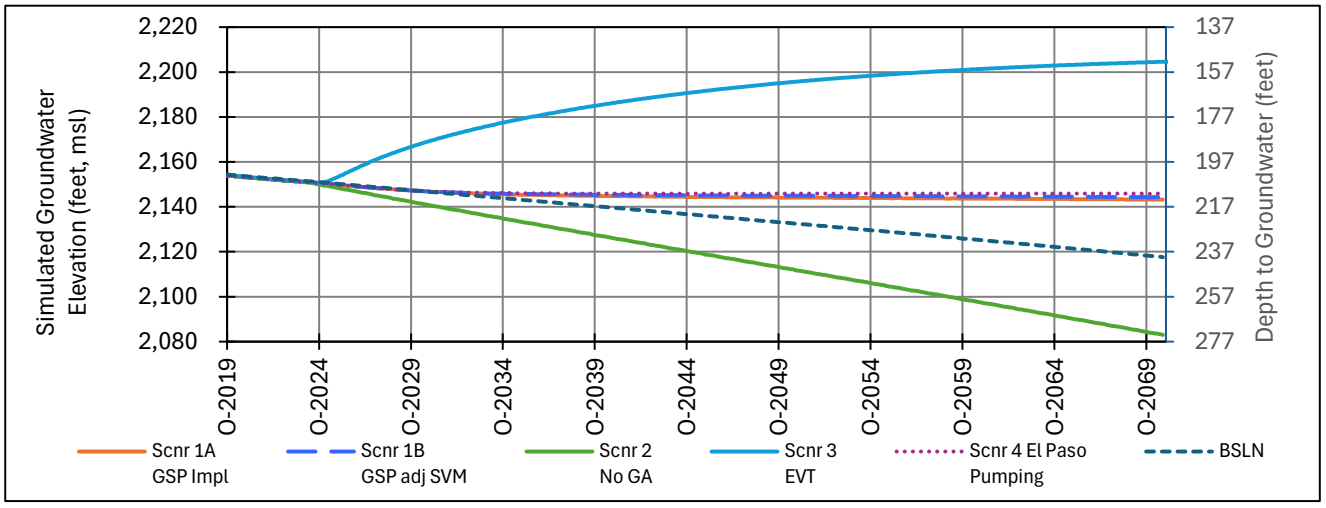
1. 25S/38E-03B Land Elevation: 2456 ft; DBID 207 ; Perforations: 300-360 feet depth



2. 25S/38E-35B01 Land Elevation: 2456 ft; DBID 169 ; Perforations: 200-298 feet depth



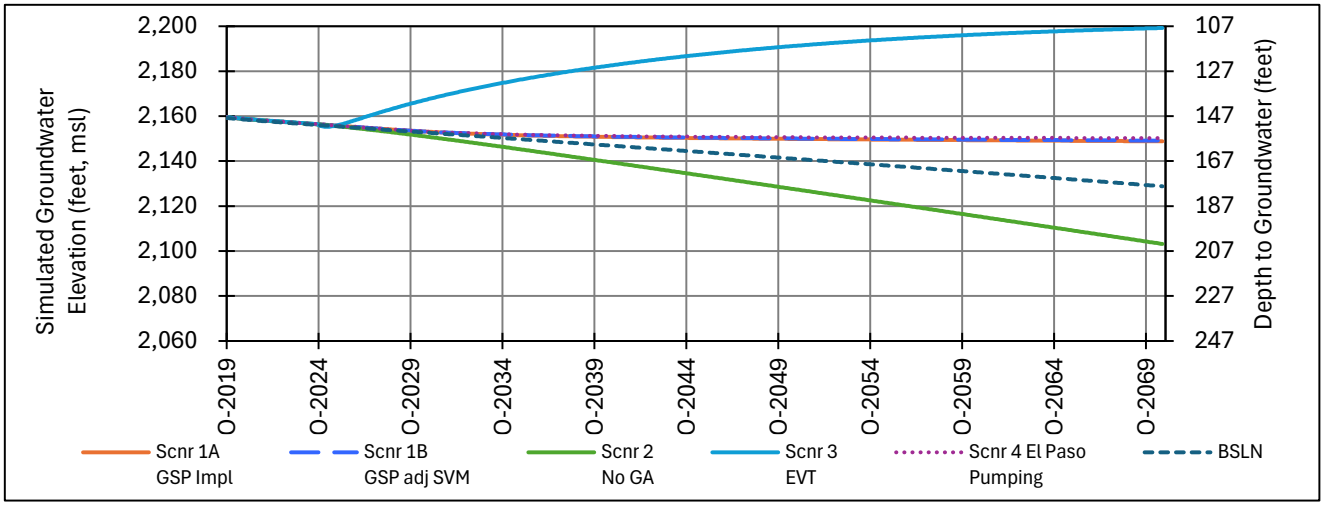
3. Kerr McGee Land Elevation: 2357 ft; DBID 126 ; Perforations: 681-881 feet depth (Kerr McGee)



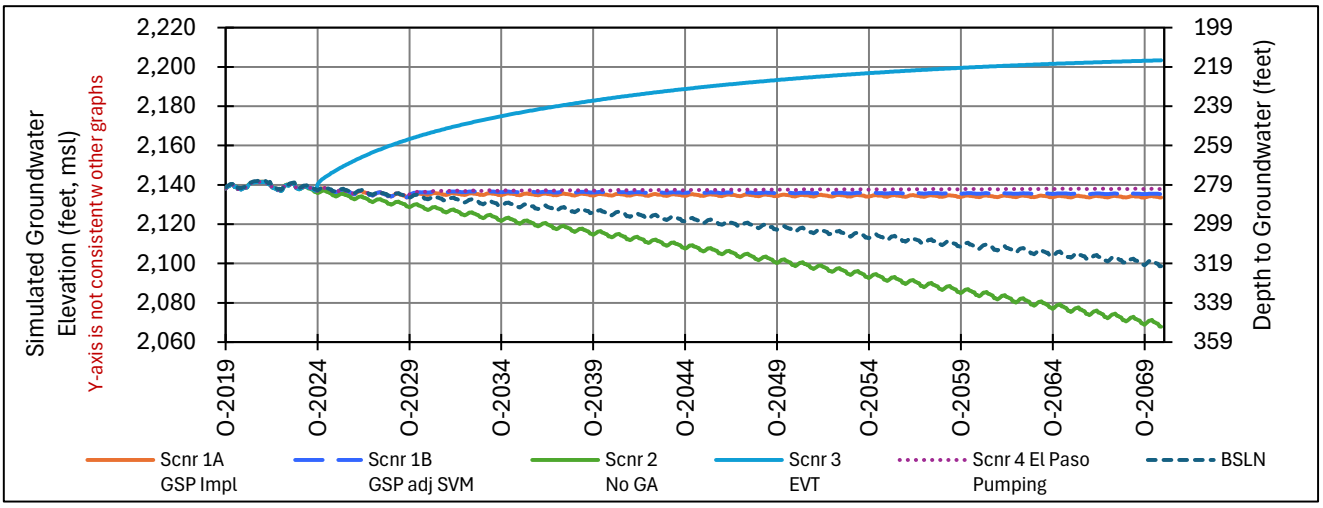
Well location shown on Model Result Map showing Change in Groundwater Levels.

IWV Groundwater Model
Comaprison of Simulated Hydrographs
Baseline, Scenarios 1A, 1B, 2, 3, and 4

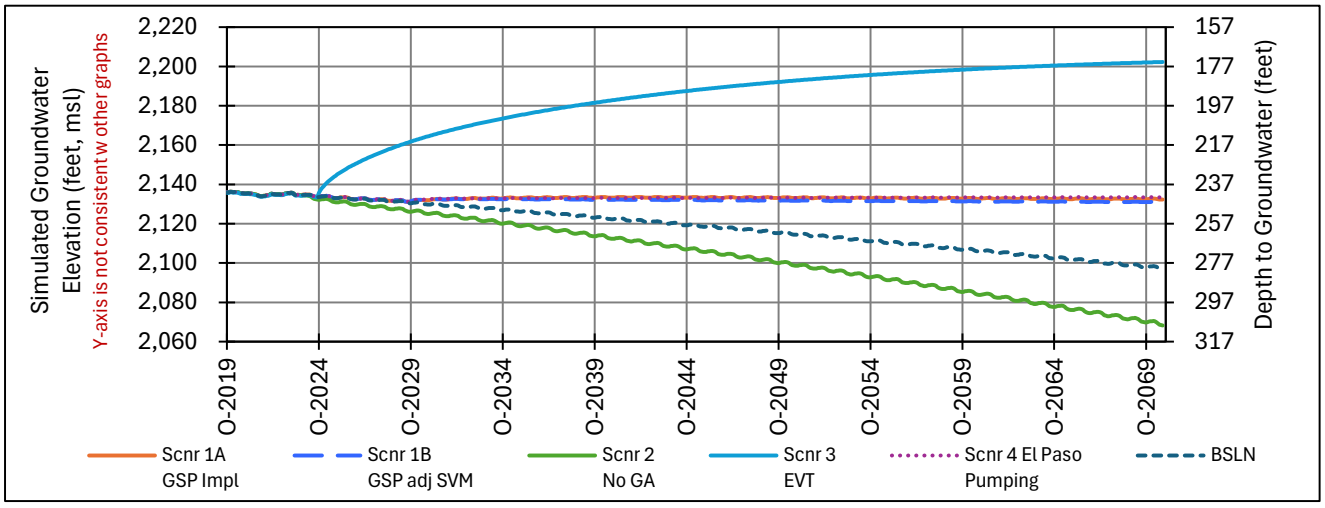
4. Sandquist Spa Land Elevation: 2307 ft; DBID 134 ; Perforations: 135-191 feet depth



5. MW 32-SM Land Elevation: 2419 ft; DBID 84 ; Perforations: 880-900 feet depth



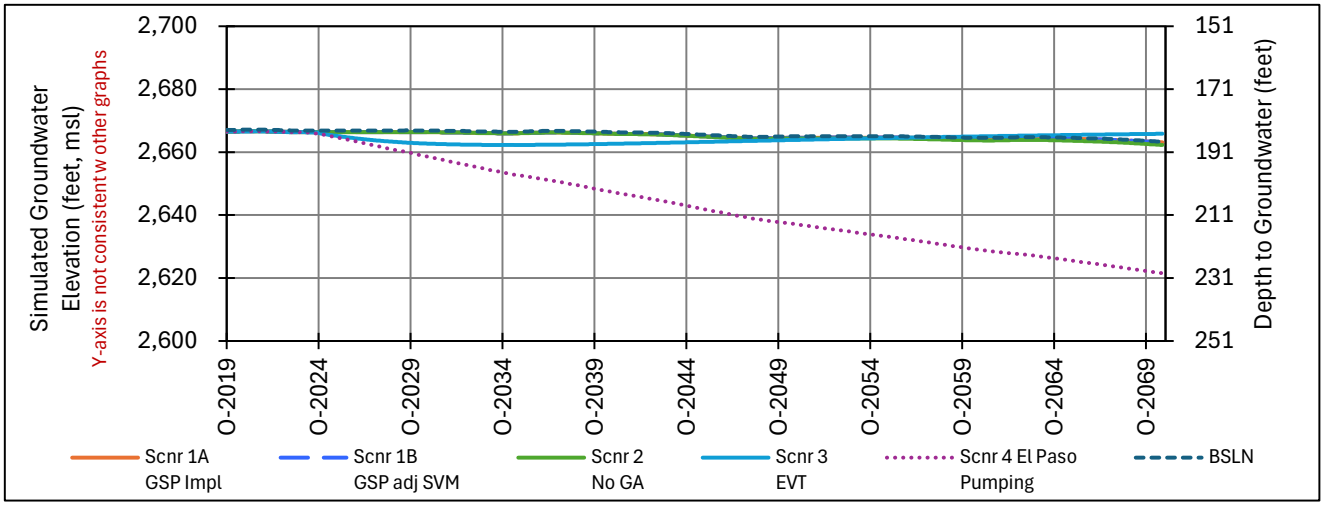
6. USBR-04 Land Elevation: 2377 ft; DBID 88 ; Perforations: 1190-1200 feet depth



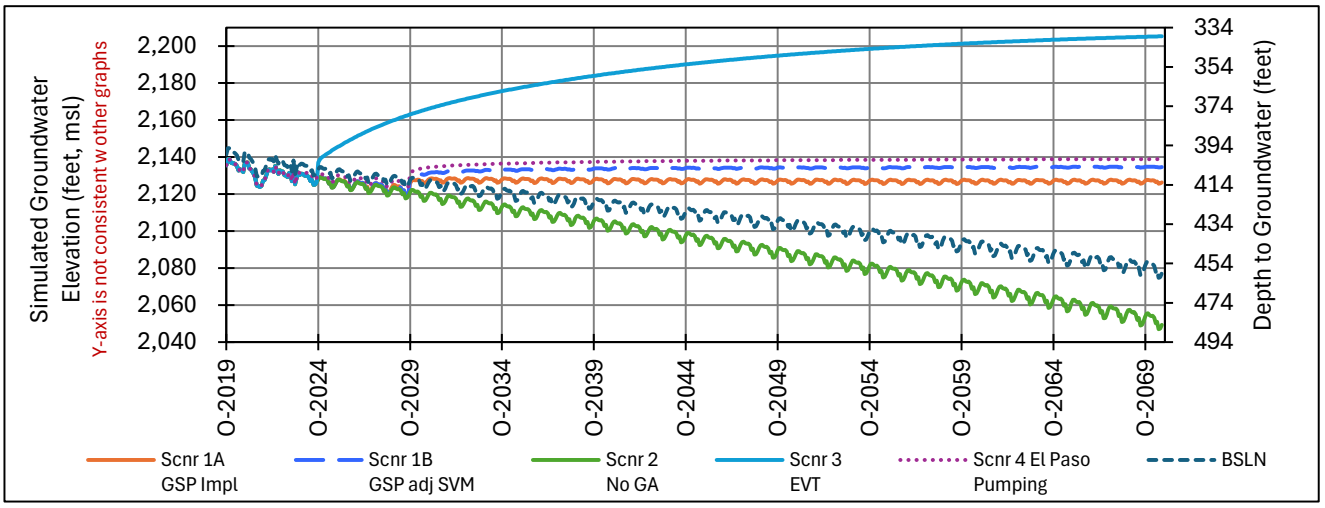
Well location shown on Model Result Map showing Change in Groundwater Levels.

IWV Groundwater Model
Comaprison of Simulated Hydrographs
Baseline, Scenarios 1A, 1B, 2, 3, and 4

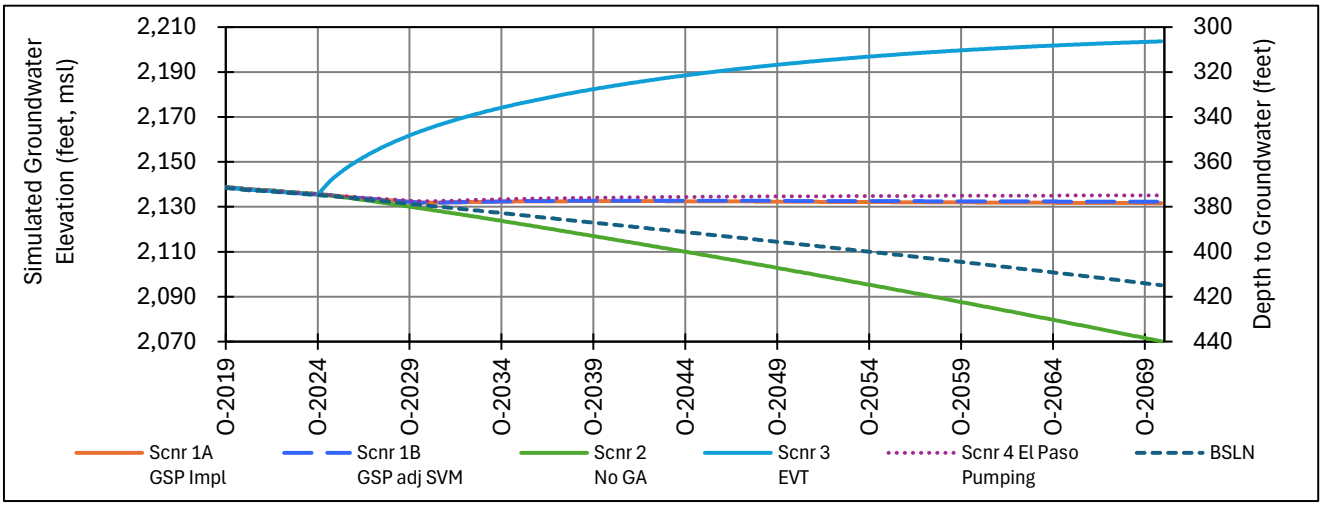
7. USBR-01-S Land Elevation: 2851 ft; DBID 7 ; Perforations: 615-635 feet depth



8. 27S/39E-08A01 Land Elevation: 2534 ft; DBID 235 ; Perforations: 550-865, 895-935 feet depth



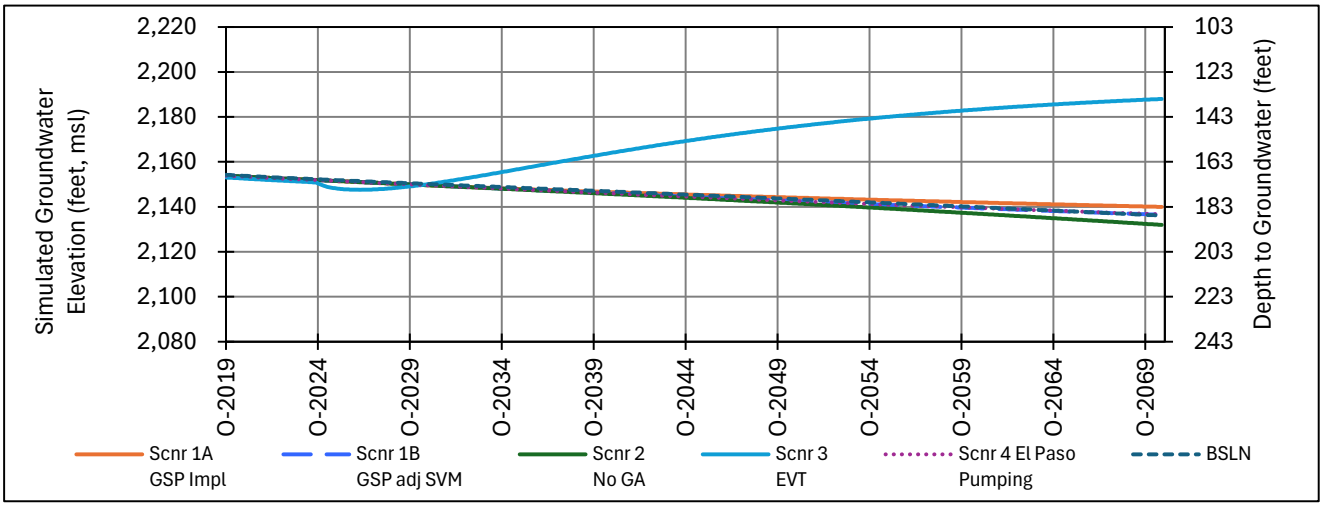
9. USBR-03-S Land Elevation: 2510 ft; DBID 26 ; Perforations: 650-670 feet depth



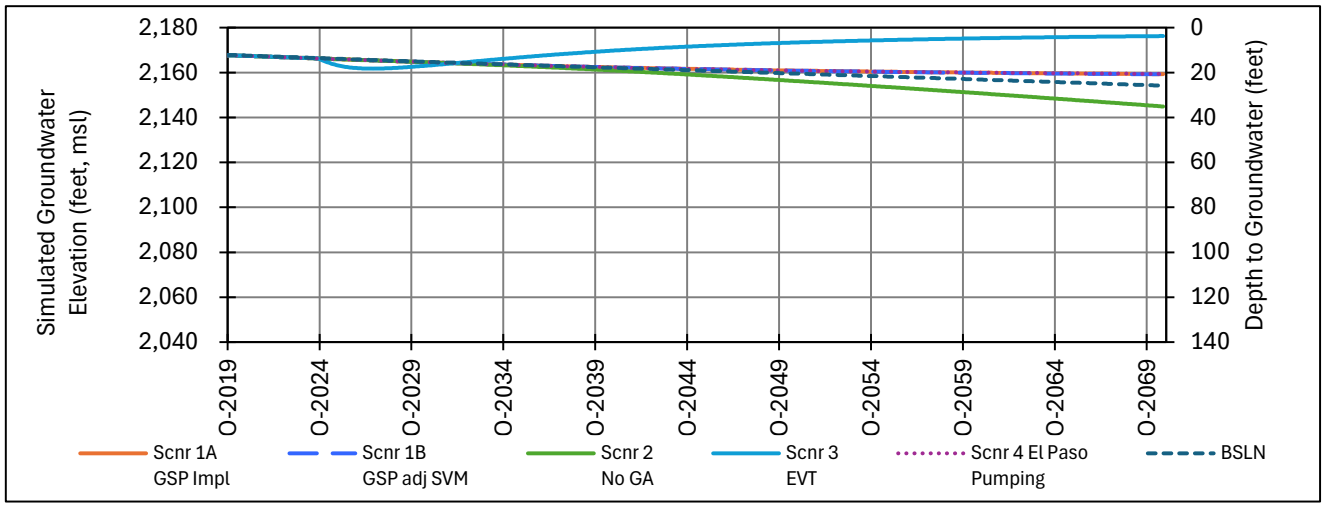
Well location shown on Model Result Map showing Change in Groundwater Levels.

IWV Groundwater Model
Comaprison of Simulated Hydrographs
Baseline, Scenarios 1A, 1B, 2, 3, and 4

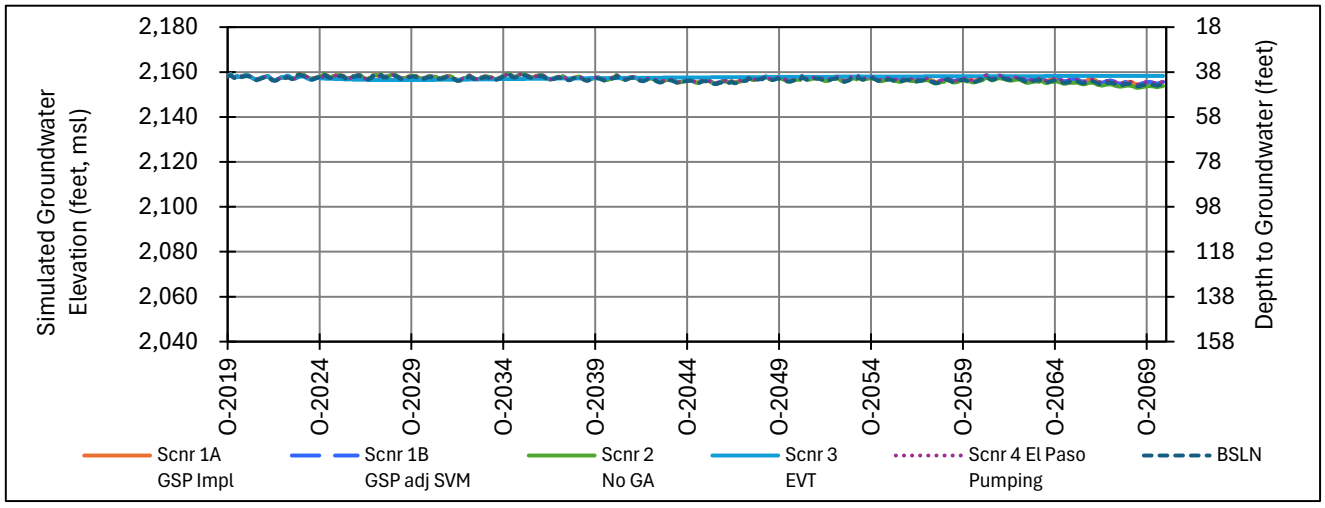
10. George Air Corridor Land Elevation: 2323 ft; DBID 36 ; Perforations: 320-380 feet depth



11. TTBK-MW05 Land Elevation: 2180 ft; DBID ; Perforations: 9-14 feet depth



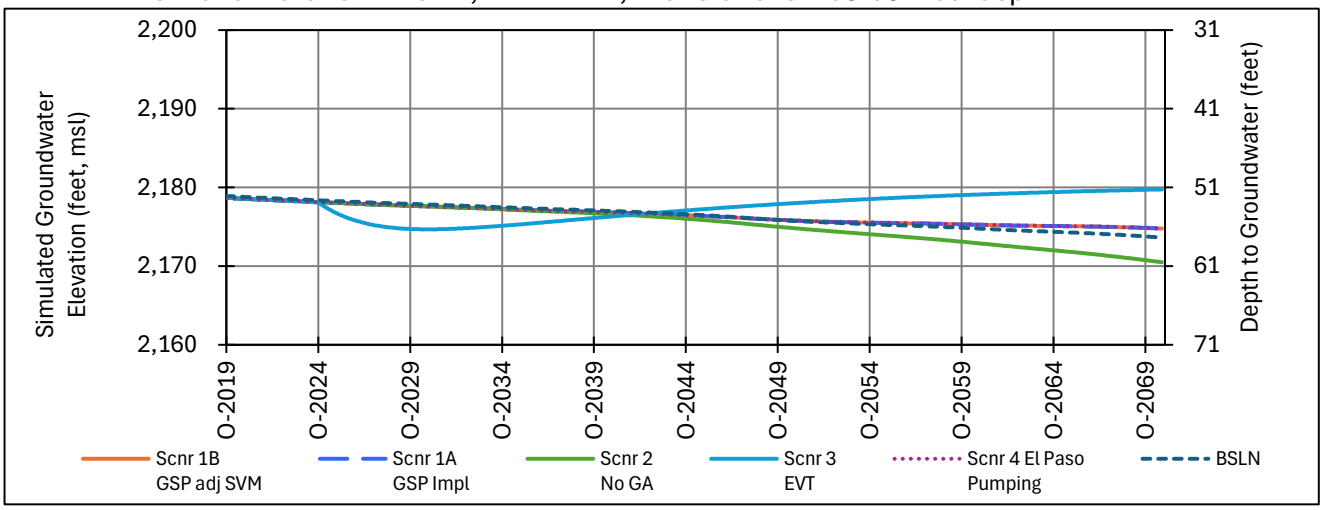
12. TTBK-MW12 Land Elevation: 2198 ft; DBID 211 ; Perforations: 40-50 feet depth



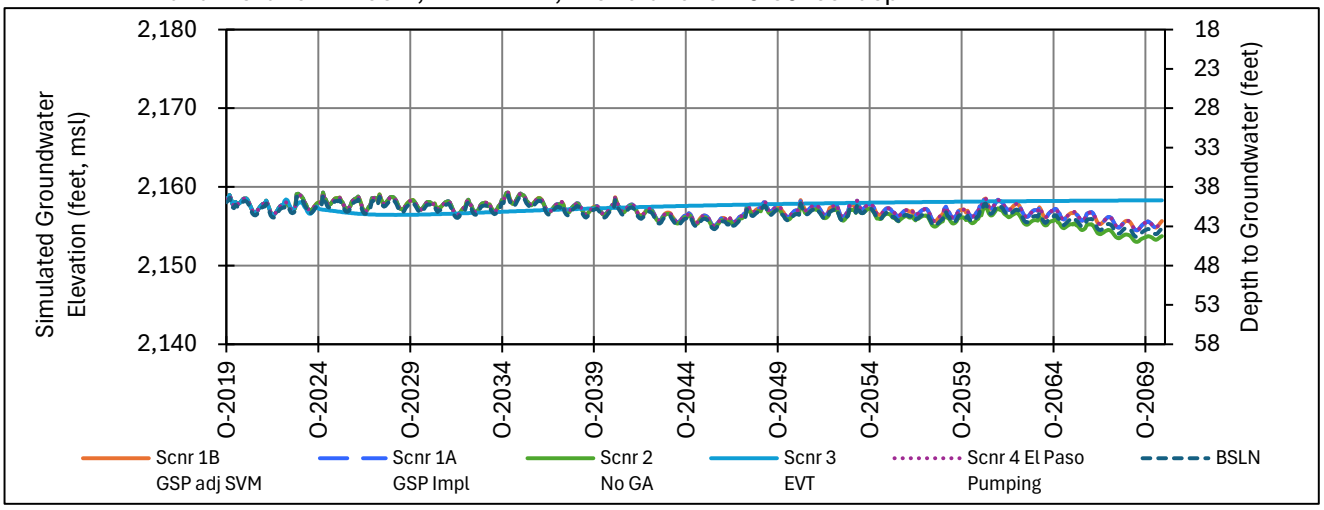
Well location shown on Model Result Map showing Change in Groundwater Levels.

IWV Groundwater Model
Comaprison of Simulated GDE Hydrographs
Baseline, Scenarios 1A, 1B, 2, 3, and 4

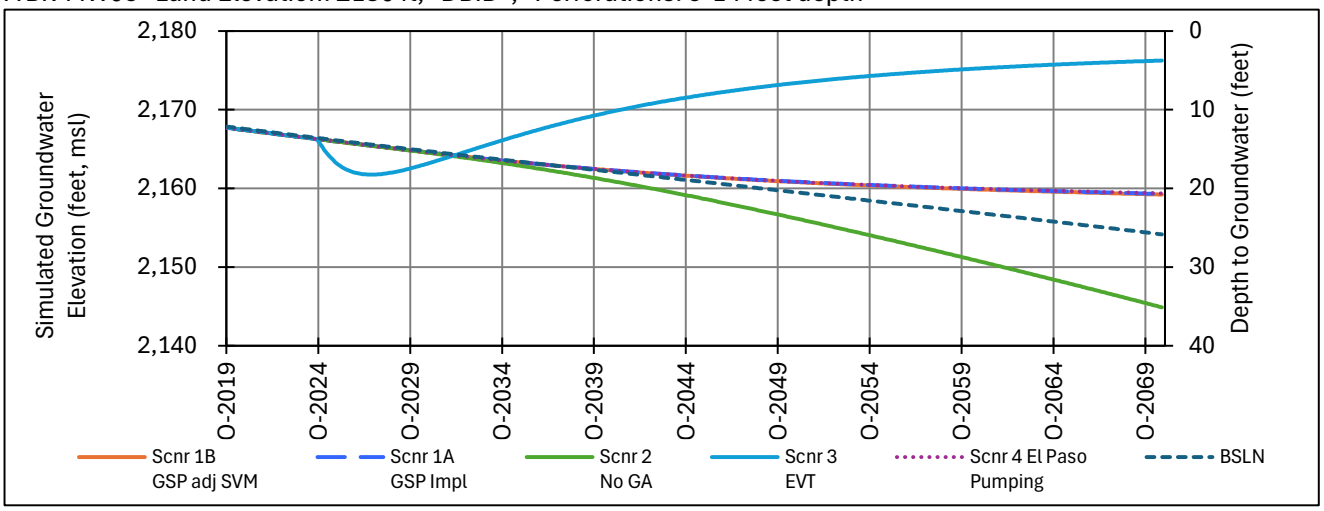
TTIWV-MW15 Land Elevation: 2231 ft; DBID 244 ; Perforations: 280-302 feet depth



TTBK-MW12 Land Elevation: 2198 ft; DBID 211 ; Perforations: 40-50 feet depth



TTBK-MW05 Land Elevation: 2180 ft; DBID ; Perforations: 9-14 feet depth



ATTACHMENT N

IWV Ground Water Production Estimates 1975 - Present

Year	Meadow-brook Farms (e)	Simmons Ranch (f)	China Lake Acres	City of R/C	SVM	IWVWD	Inyokern CSD	NAWS (c)	Neal Ranch	Private Wells	Quist Farms	Orchards (d)	R/C Heights	S. Leroy (a/b)	Annual Totals
1975	1516		400		2781	2983	300	5000	2000				1000		15980
1976	1494		400		2911	3099	300	5000	2000				1000	1600	17804
1977	2702		400		3315	3063	300	5000	2000				1000	1600	19380
1978	3216		400		3081	3357	300	5000	2000				1000	1600	19954
1979	3257		400		3081	3402	300	5154	2000	2100			1000	1600	22294
1980	7515		400		2887	3319	300	4995	2041	2100			1000	1600	26157
1981	10036		400		3065	4223	300	4804	2002	2100			1000	1600	29530
1982	10324		400		2887	3963	300	4450	1478	2100			1000	1600	28502
1983	10087		400		2476	4316	300	4402	1752	2400			1000	1600	28733
1984	10312		400		2307	4940	300	4694	1568	2400			1000	1600	29521
1985	10100		400		2397	4981	300	4002	2450	2500			1000	1600	29730
1986	5389		400		2557	5901	300	4430	2353	2500			1000	1600	26430
1987	4141		Purchased		2560	7426	300	4422	1447	2500			Purchased	Ranch	22796
1988	5255		by		2560	7889	173	3980	1195	2500			by	Closed	23552
1989	7064		IWVWD		2320	8725	175	4205	Purchased	2650		500	IWVWD		25639
1990	6187				2505	8600	170	3667	by	2650		525			24304
1991	6737				2406	7700	150	3364	IWVWD	2650		525			23532
1992	7104				2528	7650	141	3351		2650		550			23974
1993	7701				2607	7800	150	3411		2650		575			24894
1994	7504				2607	8300	146	3684		2650		575			25466
1995	7427				2710	8100	125	3848		2650		595			25455
1996	7807				2620	8504	134	3367		2650		600			25582
1997	7800				2522	8534	139	2983		2650		625			25253
1998	7800				2527	7719	102	3018		2700		640			24506
1999	7800				2537	8242	104	2541		2700		690			24614
2000	7800				2701	8148	111	2690		2800		725			24975
2001	8150				2732	8392	97	2840		2800		750			25761
2002	8460			445	2564	8865	115.6	3138		2800	750	750			27887.6
2003	9420			616	2561	9098	126	3325		2800	750	775			29471
2004	9370			413	2470	8992	118.4	2331		2800	750	800		950	28994.4
2005	9580			366	2504	8545	135	2288		2800	750	825		1025	28818
2006	9460			385	2591.2	8864.4	135	2440		2800	750	840		1050	29315.6
2007	9270			420	2530.4	9198.5	90.7	2533		2800	750	840		1000	29432.6
2008	8957			392	2520.7	8564.8	118	2119		2800	750	900		1200	28321.5
2009	9536			400	2534.5	8398.2	118	1883		2800	750	925		1125	28469.7
2010	9437			339	2586.6	7570	118	1710		2800	750	925		1050	27285.6
2011	9827			370	2457.5	7364.25	118	1734		2800	750	925		1050	27395.75
2012	9876			348	2743	7633.45	117.927	1710		2800	750	1062		800	27840.377
2013	9354	918		423	2706	7531.69	117.68	1538		1100	750	2846			27284.37
2014	7524	1,087		392	2679	7318.7	108	1618		1100	750	4087			26663.7
2015	6517	1,003		427	2518	7050	90.532	1442		1100	750	4387			25284.532
2016	6387	918		373	2377	6411.8	102.335	1595		1100	750	4300			24314.135
2017					2,629	6506.6		1450							
Total	315200	3926	4800	6109	113159	297188.4	7546.174	141156	26286	93250	11250	33062	12000	26850	1081196.9
Avg.	7505	982	400	407	2632	6911	180	3283	1878	2454	750	1181	1000	1343	25743

(a) Spike Leroy ranch started back up in 2004 with approx. 150 acres of alfalfa x 7
(b) 2012 number is an estimate/converted to pistachio 2013
(c) Navy began aggressive water conservation program in 2007

(d) 2013 number based on March 4, 2014 letter to BOS.
2014/2015/2016 data includes 3,700 and 4,000 AF from Mojave Pistacio "based off the UC Davis Pistachio Cost Study plus dust mitigation."
(e) 2005 Brown Road Farming changed to Meadowbrook Farms
(f) Simmons Alfalfa Ranch added March 2014

DRAFT TECHNICAL MEMORANDUM

785 Grand Avenue, Suite 202 • Carlsbad, California • 92008
Phone: (760) 730-0701 FAX: (415) 457-1638 Web site: www.stetsonengineers.com

TO:	IWV TAC	DATE:	October 17, 2019
FROM:	Stetson Engineers, Inc.	JOB NO:	2652-001: 06
RE:	Analysis for Estimating Shallow Well Impact for Historical Conditions and Future Management Scenarios Indian Wells Valley Groundwater Sustainability Plan (GSP)		

Historically, groundwater levels have been declining near pumping centers in the Indian Wells Valley aquifer. Groundwater levels remain stable in other locations within the basin near recharge and discharge zones, as well as in the El Paso area which is separated by a fault from the main Indian Wells Valley aquifer. In areas where groundwater levels have been steadily declining, water levels have dropped enough to impact shallow wells, requiring the well to be deepened, re-drilled, or abandoned as a water source. This technical memorandum summarizes a methodology developed to estimate historical impacts, and potential future impacts, to shallow wells due to changes in groundwater levels from groundwater management within the basin. Shallow wells have also been impacted by changes in water quality, primarily Total Dissolved Solids, which are not addressed in this memorandum.

Limited data are available for knowing the true impact to shallow wells within the basin. For this analysis, assumptions needed to be made regarding the inventory (count and distribution), age and construction details of shallow wells, and the rate of localized groundwater drawdown at the wells. Recent groundwater level contour maps developed by the Kern County Water Agency (KCWA) were used to estimate the historical rate of drawdown within different areas of the basin. Future groundwater level changes were developed using a numerical model to predict changes in groundwater levels under future management alternatives that could cause impacts to shallow wells.

A shallow well is considered impacted when the simulated average static water level (SWL) drops to 5 feet above the well pump which would result in cavitation or air entrainment when the well is pumping. Impact to shallow wells for this analysis was determined based on 1) estimated drill dates and well construction and 2) simulated groundwater level change over time. Analyses of shallow well impacts were completed for 872 wells (832 domestic/private wells, 40 mutual water company wells and community service district wells).

1.0. ESTIMATED SHALLOW WELL INVENTORY

For this analysis, it is estimated that there are approximately 872 shallow wells (Table 1) in Indian Wells Valley that could be affected by declining groundwater levels. This estimate was developed based on the 2014 Todd Engineers' Report[1] estimate of 1,588 private domestic rural residences supplied by on-site wells; and responses to the 2018 Pumping Assessment Survey of mutual water company wells with four or more hookups.

TABLE 1. ESTIMATED SHALLOW WELL INVENTORY

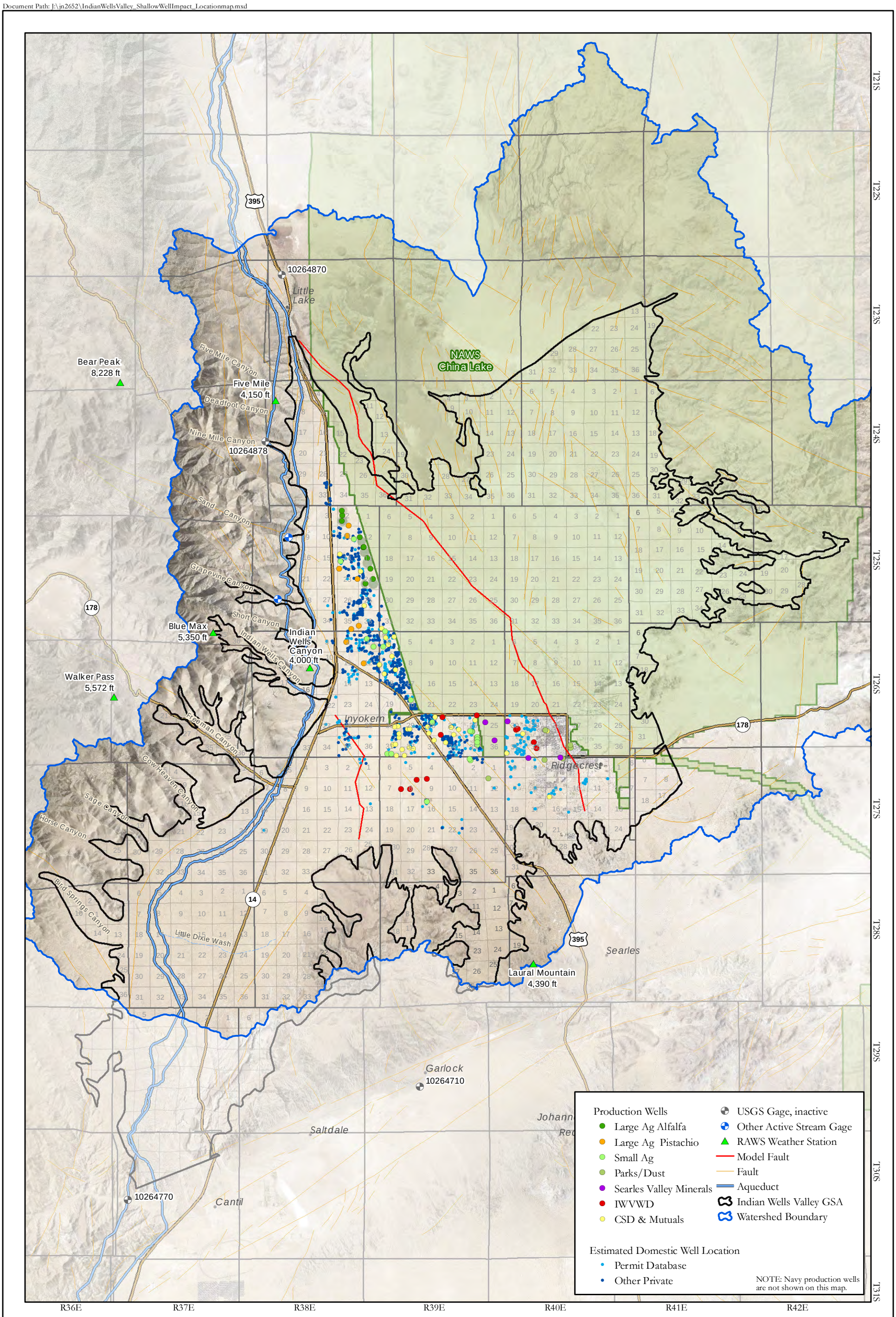
# WELLS	# WATER HOOKUPS	WELL TYPE
2	265	Inyokern Community Service District
38	491	Mutual Water Companies
377	377	Private/Domestic Wells listed in KCHD[a] Well Permit Database
455	455	Other Private Wells estimated from Todd Study[b] total DOM[c]
872	1,588	Estimated Total Number of Shallow Wells

a) KCHD: Kern County Health Department
b) Todd, 2914. *Indian Wells Valley Resource Opportunity Plan; Water Availability and Conservation Report.*
c) DOM: domestic well

Locations for these shallow wells were initially developed using maps provided by earlier reports (Todd, 2014) and modeling studies (DRI, 2016). The exact residences connected to mutual water company and community service districts were not known. Therefore, the assumption was made that residences closest to a water purveyor would use this service, and the recorded number of hook-ups were assigned to each mutual water company well so as not to double account shallow wells within these areas. Figure 1 shows the location of 38 mutual water company wells, 2 community service district wells, 832 private domestic wells, and other larger pumping wells in Indian Wells Valley. The final analysis was completed using aerial photos and GIS to estimate the location for all 872 shallow wells.

[1] Pages 15-16 "Private Domestic" in Todd, 2014. *Indian Wells Valley Resource Opportunity Plan; Water Availability and Conservation Report*. Submitted to Kern County Planning and Community Development Department. January 22, 2014.

Document Path: J:\jn2652\IndianWellsValley_ShallowWellImpact_Locationmap.mxd



STETSON ENGINEERS INC.

SHALLOW WELL IMPACT ANALYSIS
PUMPING WELL LOCATIONS
INDIAN WELLS VALLEY
DRAFT 10/14/2019

0 2 4 Miles

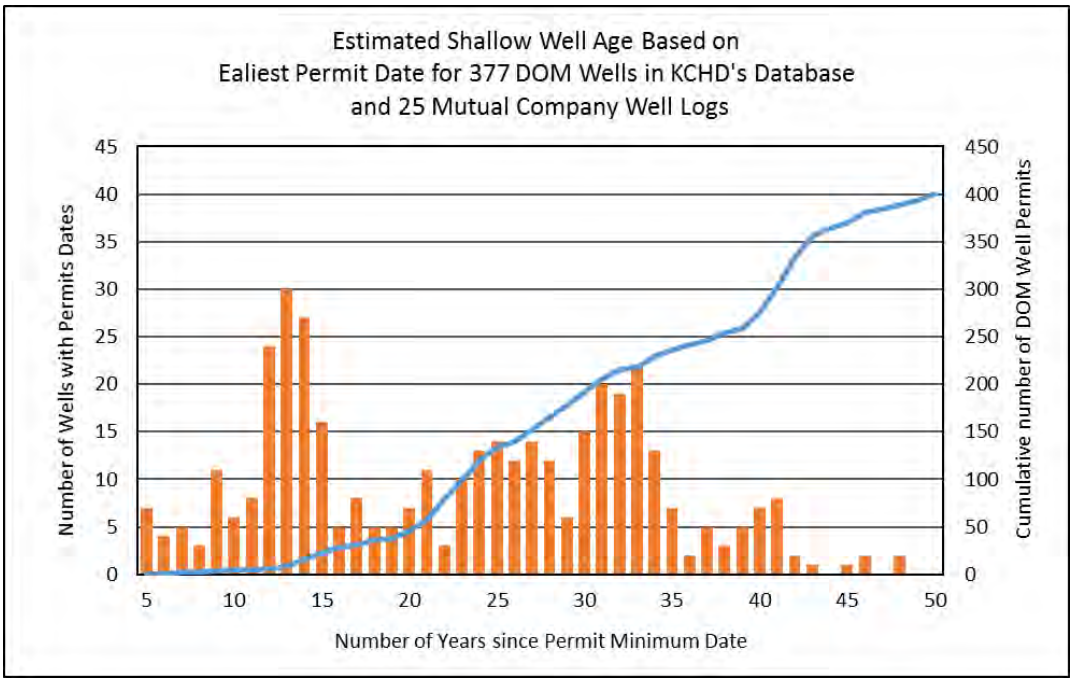
N

FIGURE 1

2.0. ESTIMATED SHALLOW WELL CONSTRUCTION DATE

The Kern County Health Department (KCHD) permit database was used to estimate the year permitted wells were drilled and constructed. Of the 546 permitted wells in the database, there were 377 unique domestic 'shallow' wells with locations inside of Indian Wells Valley. The earliest permit date listed for each well in the KCHD database was used as the year the well was initially constructed. This provided an estimate for the number of years the well would have been influenced by changes in groundwater level. Well logs for 28 mutual water company wells were available from the well registration database. The drilling/construction dates from these well logs were also added into the analysis for a total of 402 estimated drill dates. Figure 2 shows the resulting range of well ages from 5 to 48 years, with the largest number of initial well permits (30) occurring 13 years ago (2006). This database contains the best available data for this initial shallow well impact analysis. More complete data would require a physical survey of the estimated 872 wells.

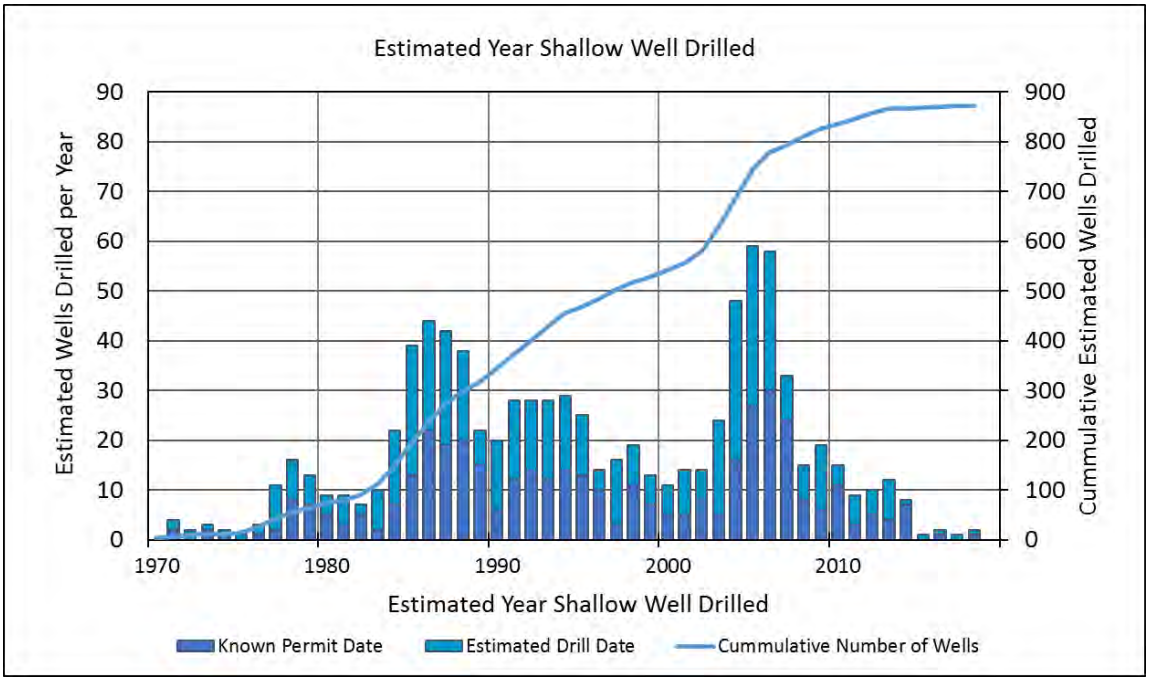
FIGURE 2 ESTIMATED AGE OF 402 SHALLOW WELLS BASED ON EARLIEST PERMIT DATE OR WELL LOG



The remaining 455 domestic/private wells were assigned drill dates using a random number generator to develop a variable drill-date distribution. An assumption was made that the 455 unknown drill dates would have a similar distribution pattern as the 402 'known' well drill dates.

A randomized number was associated with the locations (T/R-S[2]) for the 455 shallow wells without a known drill date within the basin to assign the order that the wells were drilled. The assigned randomized number was sorted and mapped by percentage of wells drilled/year to estimate when each well was drilled. Figure 3 shows the final distribution of the estimated years that the 872 shallow wells were drilled.

FIGURE 3 ESTIMATED DRILL DATE FOR 872 SHALLOW WELLS

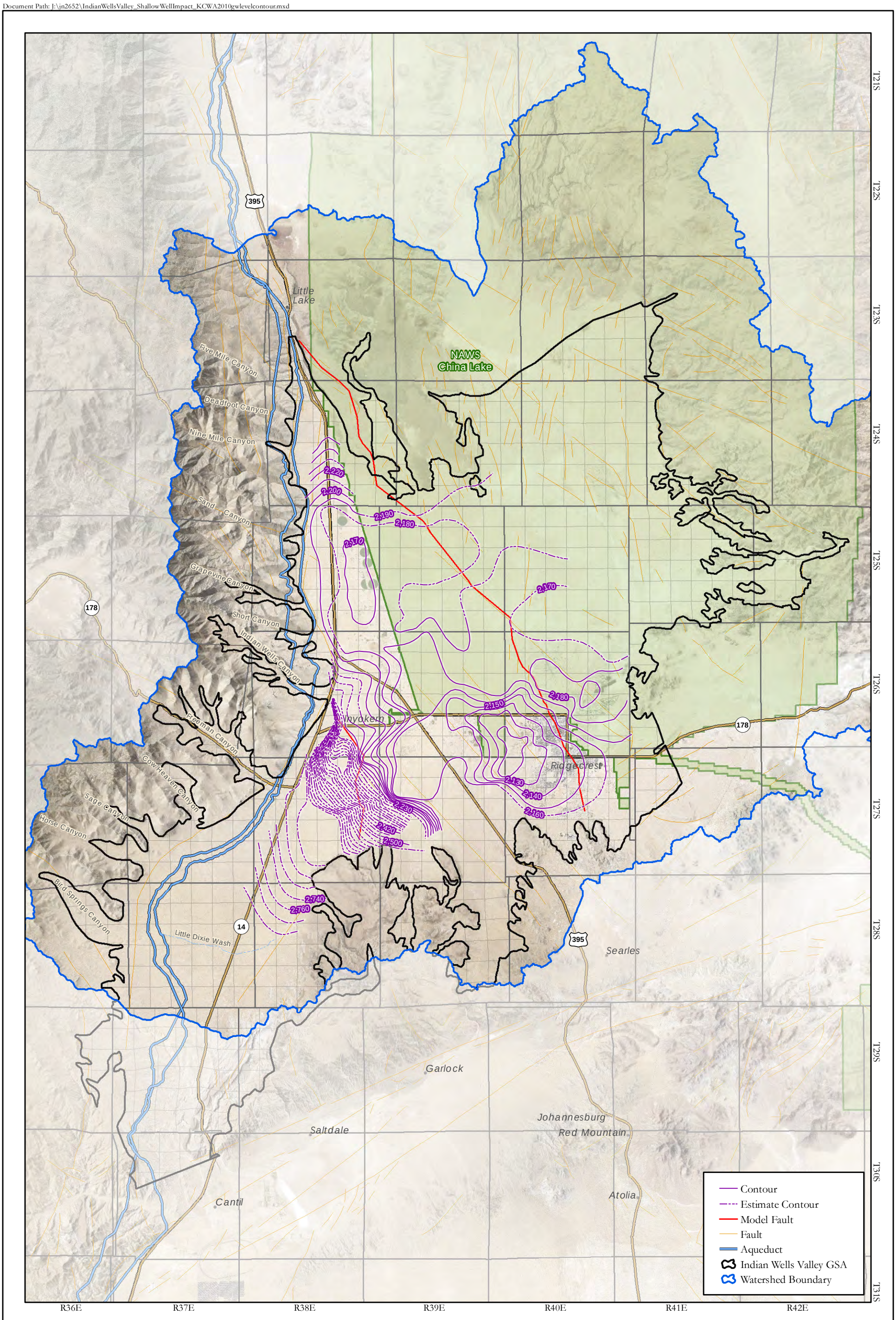


3.0. CHANGES IN DEPTH TO GROUNDWATER (RATE OF DRAWDOWN)

KCWA measures depth to groundwater in the spring and fall each year and develops contour maps showing the water table surface throughout the basin including cones of depression at pumping centers. KCWA's 2010 and 2015[3] groundwater level contours were digitized into GIS files (Figure 4 and Figure 5 respectively), and kriged (a statistical interpolation process) into two surfaces. The average difference of the two groundwater table surfaces was calculated for each 1-square mile section (Section) containing shallow wells. This analysis yielded an average change in groundwater level over 5 years for 428 sections, of which only 76 sections contained shallow wells.

[2] Township/Range-Section public land survey numbering system.
[3] The GIS-digitized contours of KCWA's 2010 and 2015 maps can be viewed on the IWVGSP.com map.

Document Path: J:\jn2652\IndianWellsValley_ShallowWellImpact_KCWA2010gwlevelcontour.mxd



STETSON ENGINEERS INC.

NOTE:
Contours Digitized from KCWA Map
10-foot contour interval; 20-foot contour interval in Southwest/El Paso Areas.

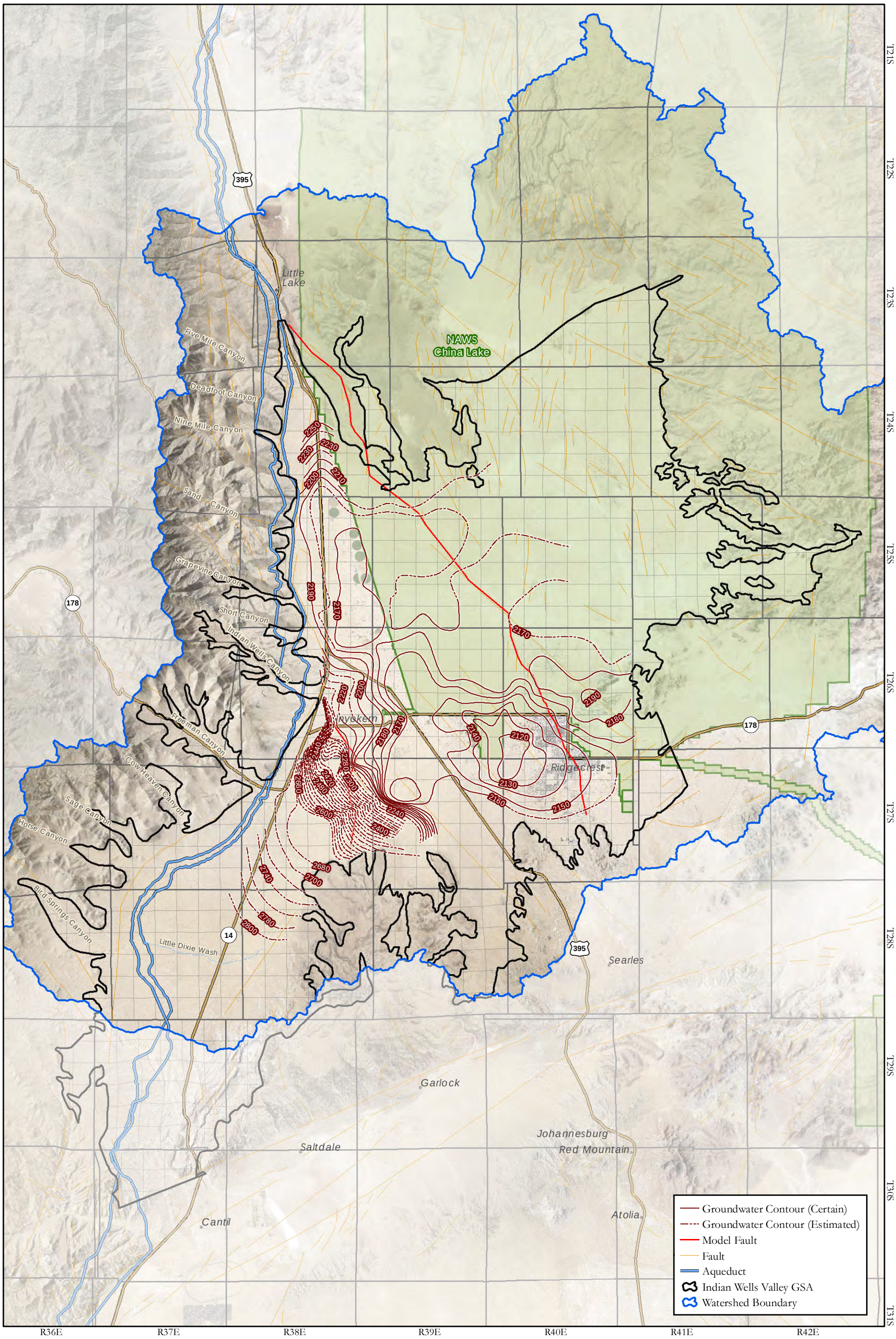
SHALLOW WELL IMPACT ANALYSIS
2010 KCWA GROUNDWATER LEVEL CONTOURS
INDIAN WELLS VALLEY
DRAFT 10/14/2019

0 2 4 Miles

N

FIGURE 4

Document Path: J:\jn2652\IndianWellsValley_ShallowWellImpact_2015gwlevelcontour.mxd



STETSON ENGINEERS INC.

NOTE:
Contours Digitized from KCWA Map
10-foot contour interval; 20-foot contour interval in Southwest/El Paso Areas.

SHALLOW WELL IMPACT ANALYSIS
2015 KCWA GROUNDWATER LEVEL CONTOURS
INDIAN WELLS VALLEY
DRAFT 10/14/2019

0 2 4 Miles

N

FIGURE 5

The resulting averages of drawdown/year/Section between Spring 2010 and Spring 2015 are displayed on Figure 6 ranging from no decline (blue) up to 2.0 to 2.5 feet/year (orange). Groundwater level changes between 2010 and 2015 for Sections with shallow wells are summarized below in Table 2. This analysis resulted in no declines in groundwater levels in 22 (29 %) Sections with wells; and 28 (37%) Sections with shallow wells showing drawdown of less than 0.5 feet/year. The average annual drawdown in 16 Sections in the Indian Wells Valley basin was estimated to be greater than one foot/year. Drawdown analysis for five Sections located north of Pearsonville in the northwest sections of Indian Wells Valley are based on limited data and possibly not representative of what is occurring in this area. However, the other eleven (11) Sections showing steeper rates of groundwater level decline are consistent with measured groundwater levels in these areas.

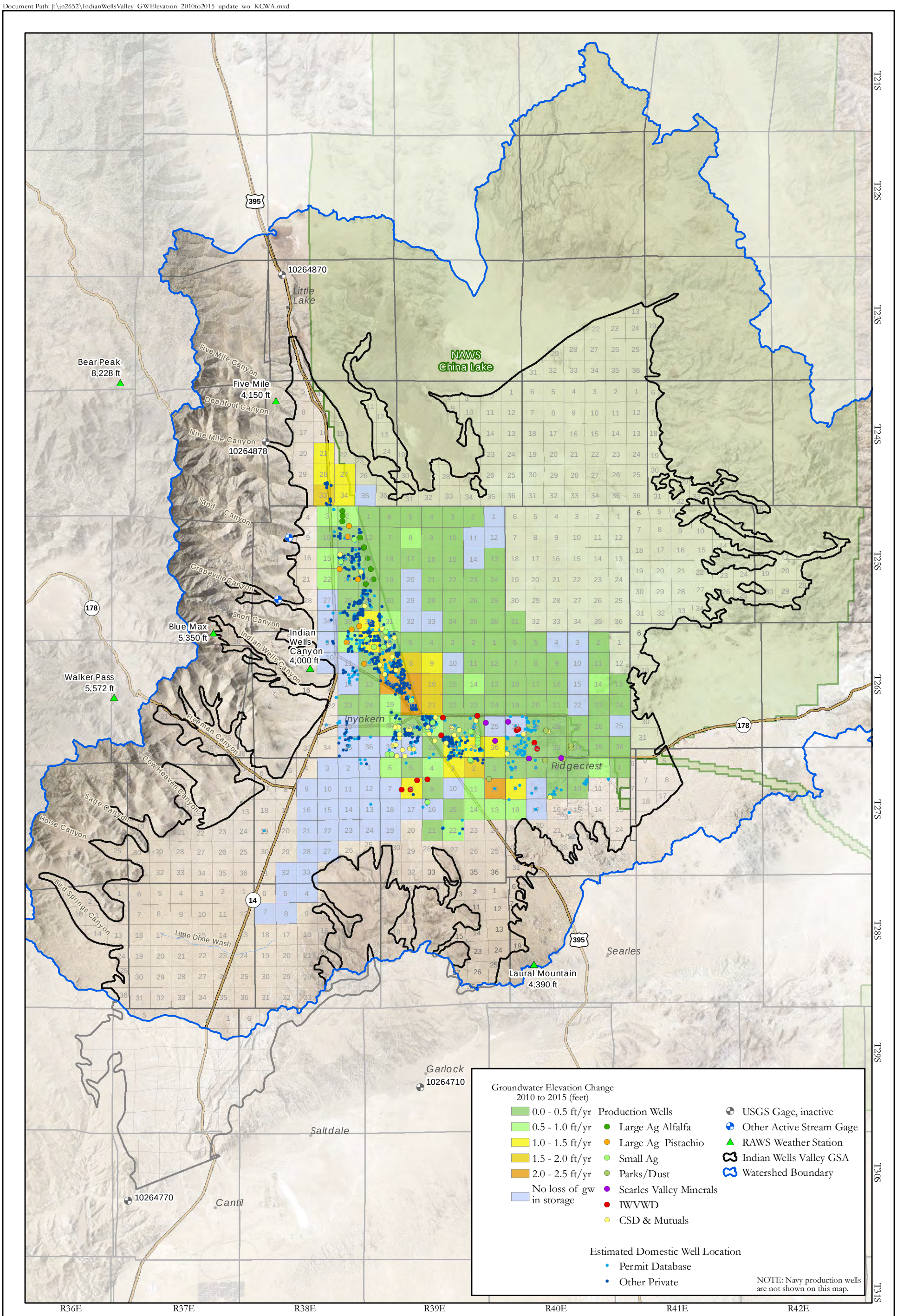
TABLE 2. ESTIMATED AVERAGE DRAWDOWN / YEAR FROM 2010 TO 2015

RANGE IN DRAWDOWN/YEAR	# SECTIONS	# SHALLOW WELLS IN SECTIONS	MAPPED COLOR
No Drawdown	22	108	Blue
> 0.0 to < -0.5	28	333	Darker green
> -0.5 to < -1.0	10	114	Light green
> -1.0 to < -1.5	8	151	Yellow
> -1.5 to < -2.0	4	84	Light orange
> -2.0 to -2.5	4	82	Darker orange
Total:	76	872	

Drawdown based on GIS analysis of KCWA Groundwater Level Contour Maps

The shallow well impact analysis assumed that the recent average rates of drawdown developed for 2010 to 2015 are indicative of the historical average rate of drawdown by Section. Some of this analysis extends the estimated rate of drawdown back in time to estimate historical shallow well impacts. There is both antidotal and reported information of shallow wells in the past that have indicated shallow wells needed to be re-drilled or deepened, but there is no definitive inventory of these impacted wells at this time. A well owner survey would be required to fill in these data gaps.

Document Path: J:\jn2652\IndianWellsValley_GWElevation_2010to2015_update_wo_KCWA.mxd



STETSON ENGINEERS INC.

SHALLOW WELL IMPACT ANALYSIS
INDIAN WELLS VALLEY
DRAFT 10/16/2019

0 2 4 Miles

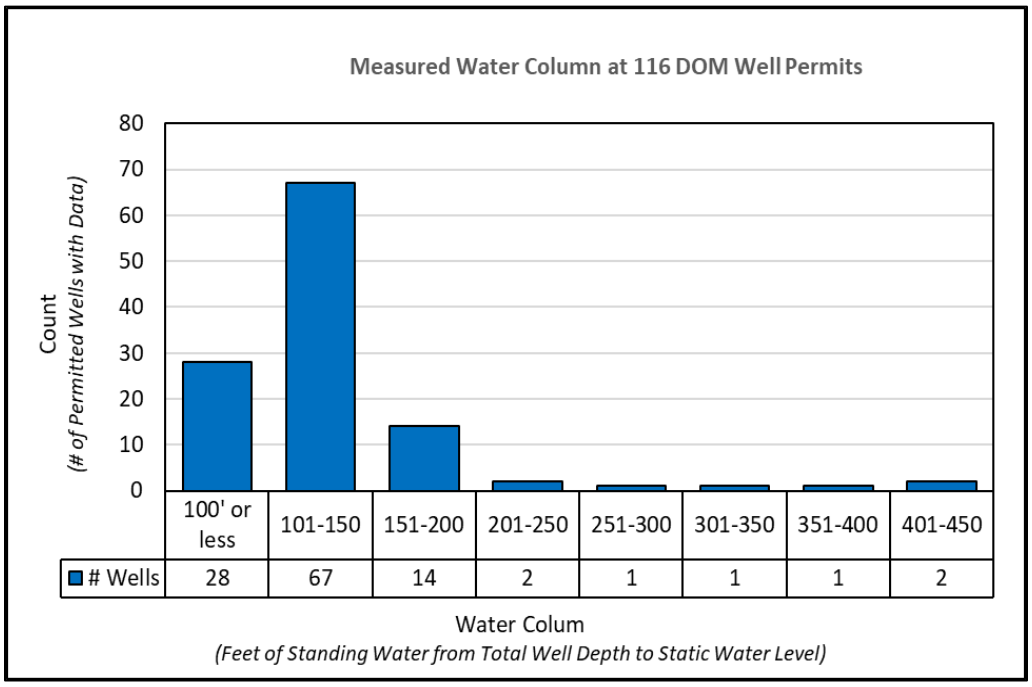
N

4.0. ESTIMATED SHALLOW WELL CONSTRUCTION AND INITIAL USEABLE WATER COLUMN WITHIN A WELL

The useful lifetime of a shallow well before it would be impacted by groundwater level changes is dependent upon the water column within the well above the pump and the rate of drawdown near the well. Estimates of an average water column were developed from the county's permit database and general drilling practices for domestic wells. It was estimated, that at the time of drilling, approximately 70 feet of water column was needed below the pumping water level to the bottom of the well and 48 feet of water column was typical to accommodate changing groundwater levels.

Kern County Health Department's permit database was used to estimate well construction information for 377 private/domestic wells. Each data record included location, owner, and permit date; and sometimes included total depth (TD), static water level (SWL), and well type. The standing water column at the time of well construction was needed to estimate shallow well impacts: (1) the "full" water column from TD to SWL, and (2) the "useable" water column from the pumping water level (PWL) to the SWL. Sufficient data were available for 116 wells with permits that included TD and SWL of the well. For these shallow wells, the full water column ranged from 69 feet to 450 feet with a median of 118 feet. The full water column distribution for available data is shown in Figure 7 bar graph.

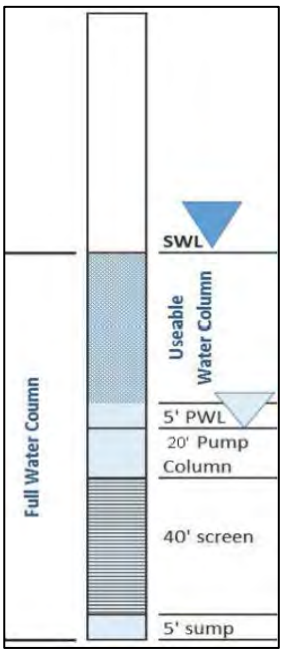
FIGURE 7 MEASURED WATER COLUMN FROM KCHD PERMIT DATABASE



An additional 83 permitted wells had recorded TD, but no SWL. For these wells, an initial water column was estimated by location and drill date. The drawdown calculated in Section 2.0 was used to estimate overall change in groundwater level for the years since the well was drilled. This change was added to the current groundwater level to "back-calculate" the initial SWL.

In areas of the basin where groundwater levels are dropping, the useable water column above the pumping water level establishes how many more years the well can function before having insufficient water column to pump. Screen intervals, pump column depths and other well construction details were not available at this time. The following general assumptions were made with respect to the domestic well construction: drilling past where the groundwater table is encountered to accommodate a sump, perforated casing, and pump column. The total depth of the constructed well can vary based upon the length of screen interval, the type of pump, and how much blank casing is installed to accommodate groundwater level changes (see schematic).

For shallow domestic wells without construction data, it was estimated that at the time of initial construction, the well was drilled to 118 feet below the groundwater table (median of permitted wells with data) and had a useable water column of 48 feet . This would accommodate a 5-foot sump, 40-foot screen interval, 20 feet for the pump column and 5 feet for drawdown in the well while pumping. The life of the well before it would be impacted by groundwater level changes is dependent upon the useable water column and rate of drawdown near the well:



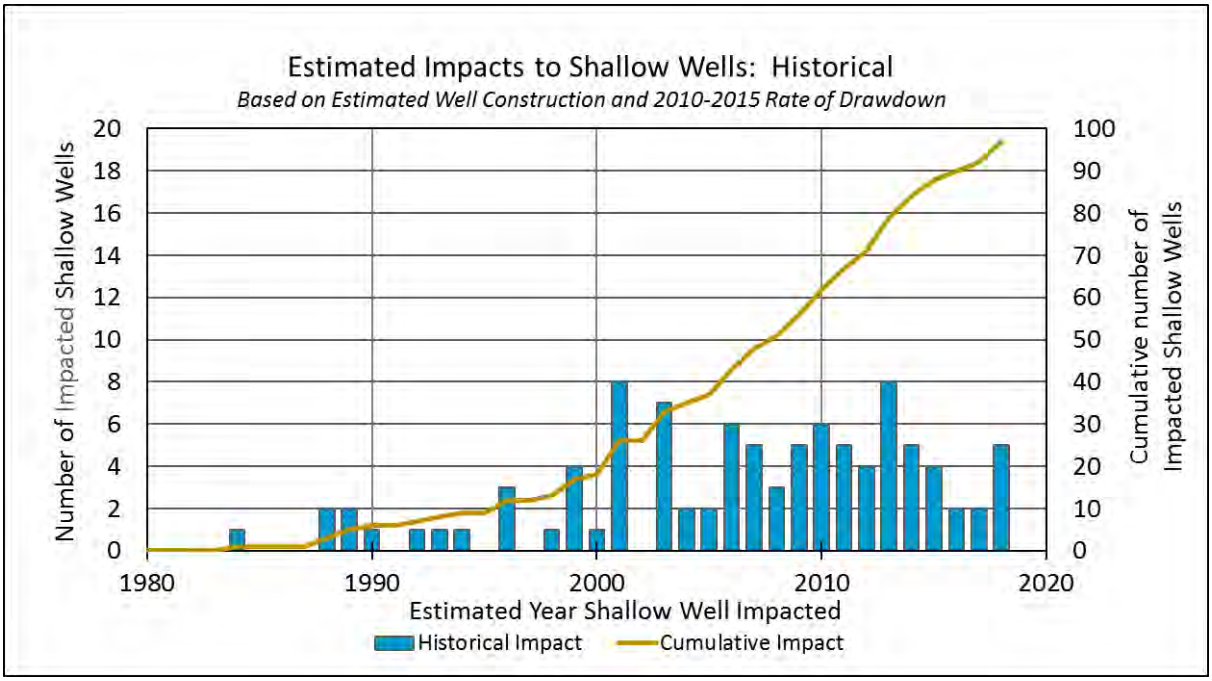
$$\frac{\textit{Useable Water Column (feet)}}{\textit{rate of drawdown per year (feet/year)}} = \textit{\# years left of well operation}$$

5.0. HISTORICAL ESTIMATE OF SHALLOW WELL IMPACT

Historical impacts of changing groundwater levels on shallow wells were assessed using the estimated well construction (Section 4.0), date drilled (Section 2.0), and historical rate of drawdown (Section 3.0). Groundwater level drawdown rates (2010-2015) were used to calculate pre-2019 drawdown. Historical drawdown rates were applied to the number of years since the well was drilled (from drill date to 2019) resulting in the total drawdown since the well was constructed. This drawdown was applied to estimate the usable water column remaining by January 2020. If the well was considered impacted prior to 2019, it was assumed that the well was deepened 40

feet. The graph in Figure 8 shows estimated historical shallow well impacts within Indian Wells Valley, ranging from 0 to 8 wells within any one year. The cumulative number of 97 impacted shallow wells was reached in 2018 using the methodology described above. It is recommended that drilling records be evaluated and outreach to domestic well owners be used to validate this analysis.

FIGURE 8 ESTIMATED HISTORICAL SHALLOW WELL IMPACTS



6.0. METHODOLOGY TO ESTIMATE SHALLOW WELL IMPACT FOR FUTURE CONDITIONS DURING BASELINE (NO ACTION) AND MANAGEMENT ALTERNATIVE 6.2 SCENARIO

The IWV Model groundwater levels are simulated for each active 15.4-acre model cell (820 feet on a side). There are 19,051 active model cells simulated within the model. These model cells overlap with 510 square-mile Sections for this analysis. There are approximately 41.6 model cells per Section (640 acres = 1 square-mile Section). Shallow well locations were estimated to be in 76 of these Sections. The average annual rate of drawdown by Section is applied to estimated depths of shallow wells to evaluate the impact of basin management on shallow wells going dry based on Future Baseline (No Action) and Management Alternatives for the Groundwater Sustainability Plan (GSP).

DRI provided GIS coverages from the IWV Model output files of simulated groundwater levels at the end of five years: 2020, 2025, 2030, 2040, and 2070. These years represent the initial start of the Groundwater Sustainability Plan (2020), the timeframe for different management

actions to be taken (2025, 2030, 2040), and the 50-year planning horizon (2070). It is anticipated that rates of drawdown will vary over time influencing the number of shallow wells impacted based on the aquifer's response to when and where management actions are put into place.

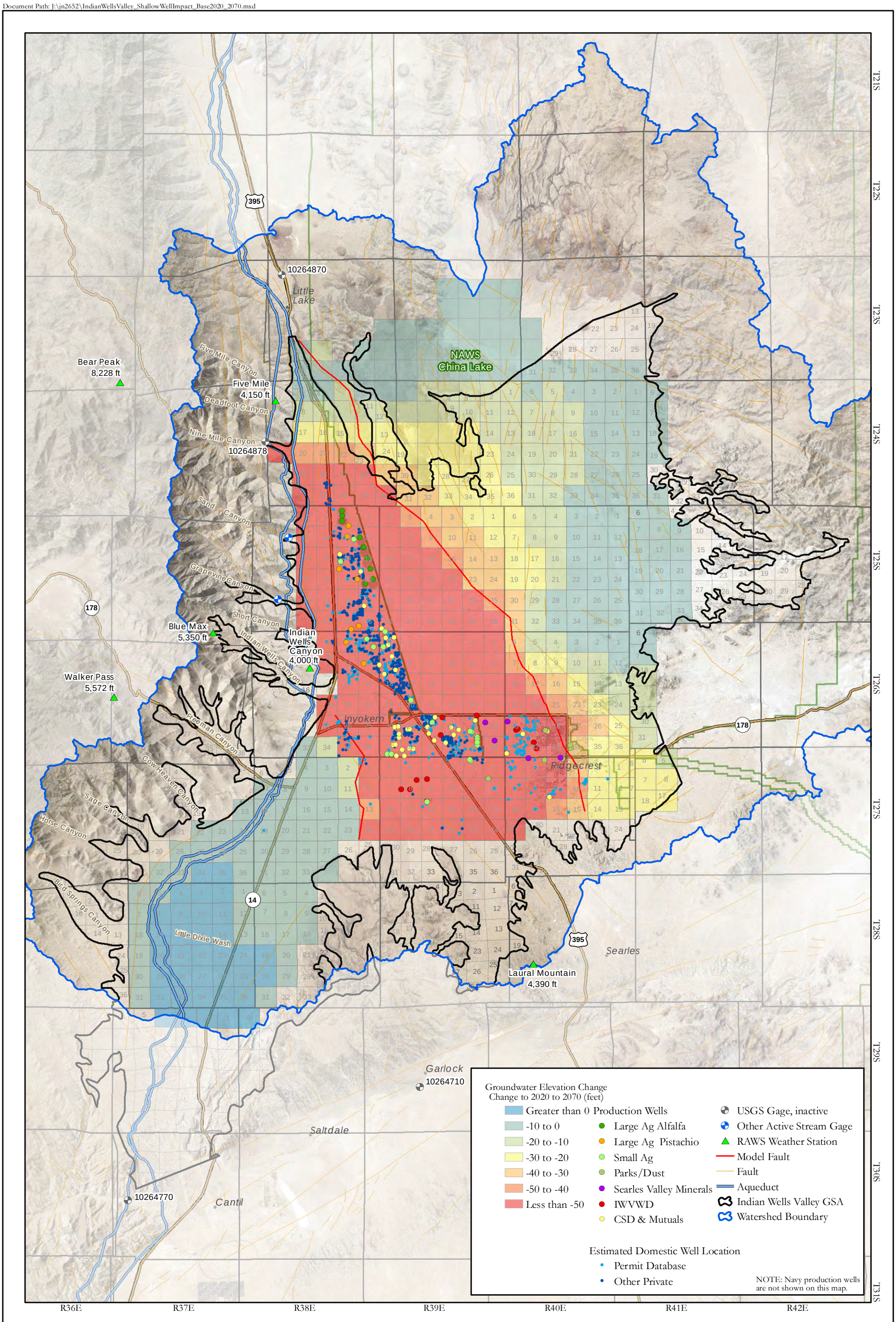
The change in groundwater level for each active model cell was calculated for 2020-25 (5 years), 2025-30 (5 years), 2030-40 (10 years), 2040-70 (30 years), and 2020-70 (50 years) for Baseline and Management Alternatives. Groundwater level changes for each of the 19,051 active model cells were used to calculate average annual drawdown for each of the 510 Sections during the five respective management timeframes.

If a well became impacted after January 2020, it was assumed that drillers would be aware of declining groundwater levels and replace or deepen the well an additional 60 feet from the previous year by the next year. These assumptions were made to determine the future no-action baseline impact and all subsequent management alternatives that were modeled.

7.0. BASELINE (NO ACTION) MANAGEMENT ALTERNATIVE RESULTS

A model run scenario representing "no action" was simulated for the future 50-year baseline condition from 2020 through 2070. This is considered a worst-case scenario where the estimated recent historical pumping of 26,959 acre-feet/year (2010 to 2015 average pumping estimated by IWVGWCG) was projected to increase over time to 38,123 acre-feet/year during the next 50 years (based on input from the major groundwater users in the basin). The shallow well impact analysis results (Figure 9) indicate that most of the 76 Sections with shallow wells will have a drawdown of 1.0 to 1.5 feet/year resulting in a 50-year drawdown of 50 feet or more. The shallow well impact analysis for Baseline conditions estimates that 81 shallow wells would be impacted by 2030, and 231 shallow wells would be impacted by 2040 (Figure 10).

Document Path: J:\jn2652\IndianWellsValley_ShallowWellImpact_Base2020_2070.mxd



STETSON ENGINEERS INC.

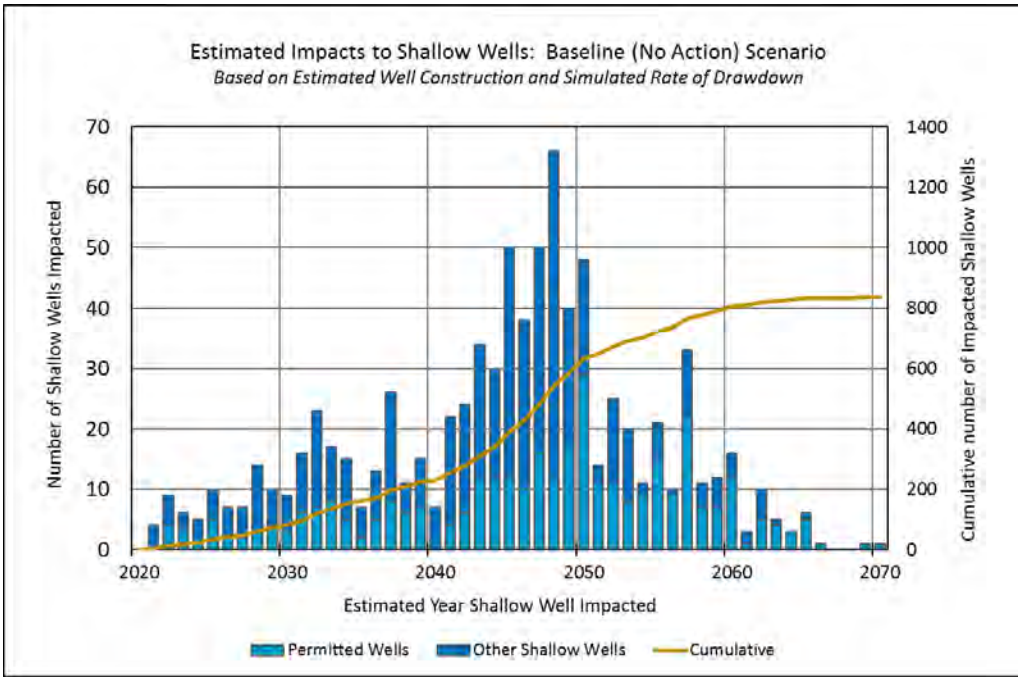
SHALLOW WELL IMPACT ANALYSIS

BASELINE
SIMULATED 50-YEAR DRAWDOWN
INDIAN WELLS VALLEY
DRAFT 3/7/2019

0 2 4 Miles

N

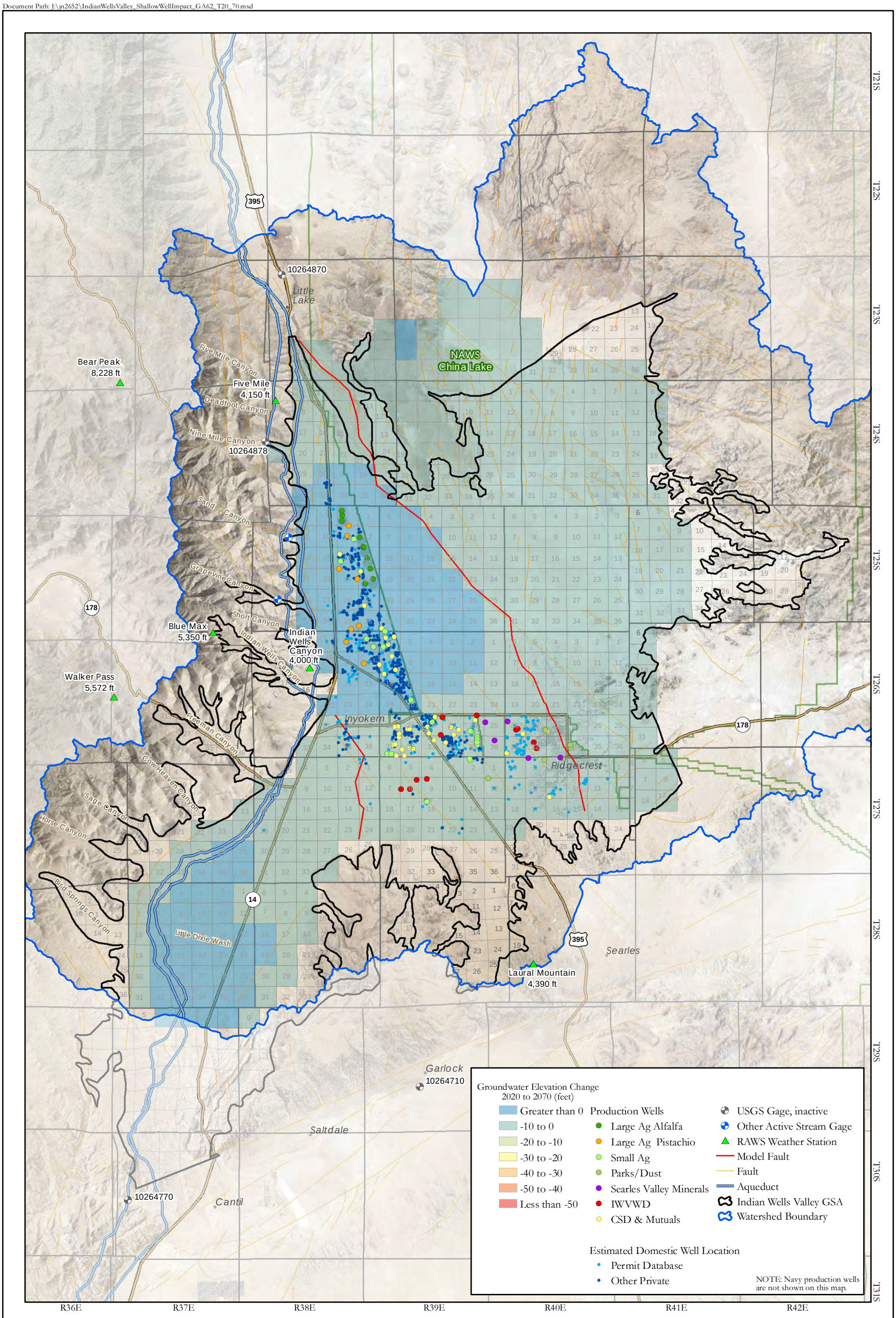
FIGURE 10 ESTIMATED BASELINE (NO ACTION) SHALLOW WELL IMPACTS



8.0. MANAGEMENT SCENARIO 6.2 SHALLOW WELL IMPACT RESULTS

A future 50-year model run representing Management Scenario 6.2 conditions was simulated for 2020 through 2070. This is the GSP scenario developed for the Indian Wells Valley Groundwater Authority with projected pumping at 20,940 acre-feet/year in 2020, 11,150 acre-feet/year in 2030, and 11,252 acre-feet in 2040 and continued with a small population growth consideration through 2070. The shallow well impact analysis results (Figure 11) for Management Scenario 6.2 indicate that most of the 76 Sections with shallow wells will have minimal drawdown resulting in only 22 shallow wells being impacted within the next 50 years. The model simulated drawdowns for Scenario 6.2 conditions estimate 19 shallow wells would be impacted by 2025, and only 3 more wells would be impacted by 2030 (Figure 12).

Document Path: J:\jn2652\IndianWellsValley_ShallowWellImpact_GA62_T20_70.mxd



STETSON ENGINEERS INC.

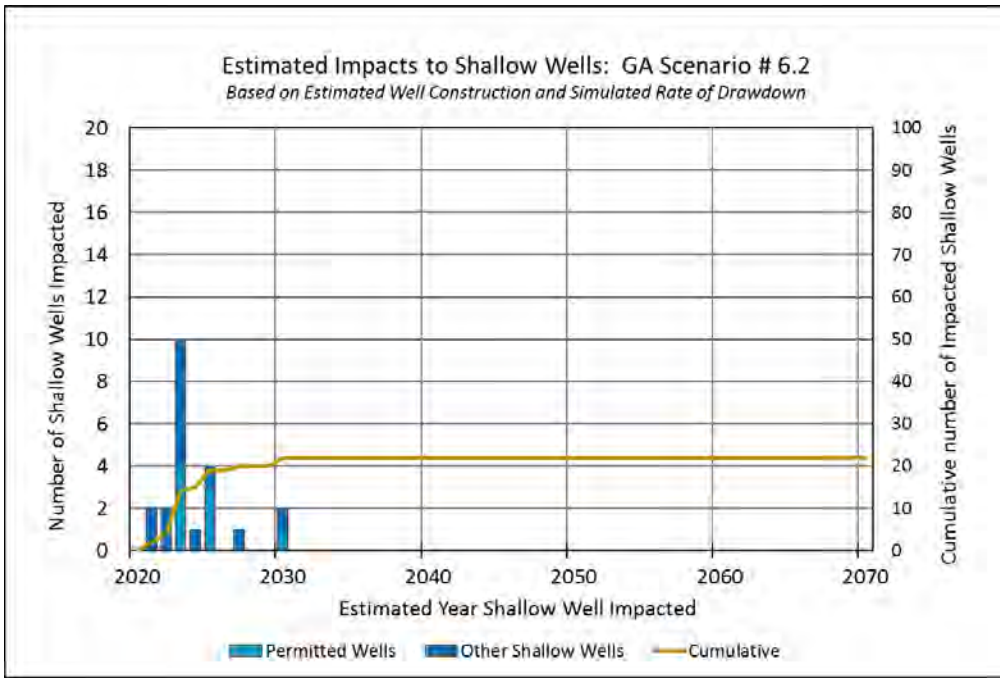
SHALLOW WELL IMPACT ANALYSIS

MANAGEMENT SCENARIO #6.2
SIMULATED 50-YEAR DRAWDOWN
INDIAN WELLS VALLEY
DRAFT 8/5/2019

0 2 4 Miles

N

FIGURE 12 ESTIMATED MANAGEMENT SCENARIO 6.2 SHALLOW WELL IMPACTS



9.0. Recommendations

- Confirm the location of shallow rural domestic and mutual water company wells within the basin.
- Canvas all available resources for well logs (RCD, DWR, County Agencies, Well Owners)
- Develop a comprehensive database of initial well construction data, history of well deepening and/or replacement.

ATTACHMENT O

DRAFT TECHNICAL MEMORANDUM

785 Grand Avenue, Suite 202 • Carlsbad, California • 92008
Phone: (760) 730-0701 FAX: (415) 457-1638 Web site: www.stetsonengineers.com

TO:	IWV TAC	DATE:	October 17, 2019
FROM:	Stetson Engineers, Inc.	JOB NO:	2652-001: 06
RE:	Analysis for Estimating Shallow Well Impact for Historical Conditions and Future Management Scenarios Indian Wells Valley Groundwater Sustainability Plan (GSP)		

Historically, groundwater levels have been declining near pumping centers in the Indian Wells Valley aquifer. Groundwater levels remain stable in other locations within the basin near recharge and discharge zones, as well as in the El Paso area which is separated by a fault from the main Indian Wells Valley aquifer. In areas where groundwater levels have been steadily declining, water levels have dropped enough to impact shallow wells, requiring the well to be deepened, re-drilled, or abandoned as a water source. This technical memorandum summarizes a methodology developed to estimate historical impacts, and potential future impacts, to shallow wells due to changes in groundwater levels from groundwater management within the basin. Shallow wells have also been impacted by changes in water quality, primarily Total Dissolved Solids, which are not addressed in this memorandum.

Limited data are available for knowing the true impact to shallow wells within the basin. For this analysis, assumptions needed to be made regarding the inventory (count and distribution), age and construction details of shallow wells, and the rate of localized groundwater drawdown at the wells. Recent groundwater level contour maps developed by the Kern County Water Agency (KCWA) were used to estimate the historical rate of drawdown within different areas of the basin. Future groundwater level changes were developed using a numerical model to predict changes in groundwater levels under future management alternatives that could cause impacts to shallow wells.

A shallow well is considered impacted when the simulated average static water level (SWL) drops to 5 feet above the well pump which would result in cavitation or air entrainment when the well is pumping. Impact to shallow wells for this analysis was determined based on 1) estimated drill dates and well construction and 2) simulated groundwater level change over time. Analyses of shallow well impacts were completed for 872 wells (832 domestic/private wells, 40 mutual water company wells and community service district wells).

1.0. ESTIMATED SHALLOW WELL INVENTORY

For this analysis, it is estimated that there are approximately 872 shallow wells (Table 1) in Indian Wells Valley that could be affected by declining groundwater levels. This estimate was developed based on the 2014 Todd Engineers' Report[1] estimate of 1,588 private domestic rural residences supplied by on-site wells; and responses to the 2018 Pumping Assessment Survey of mutual water company wells with four or more hookups.

TABLE 1. ESTIMATED SHALLOW WELL INVENTORY

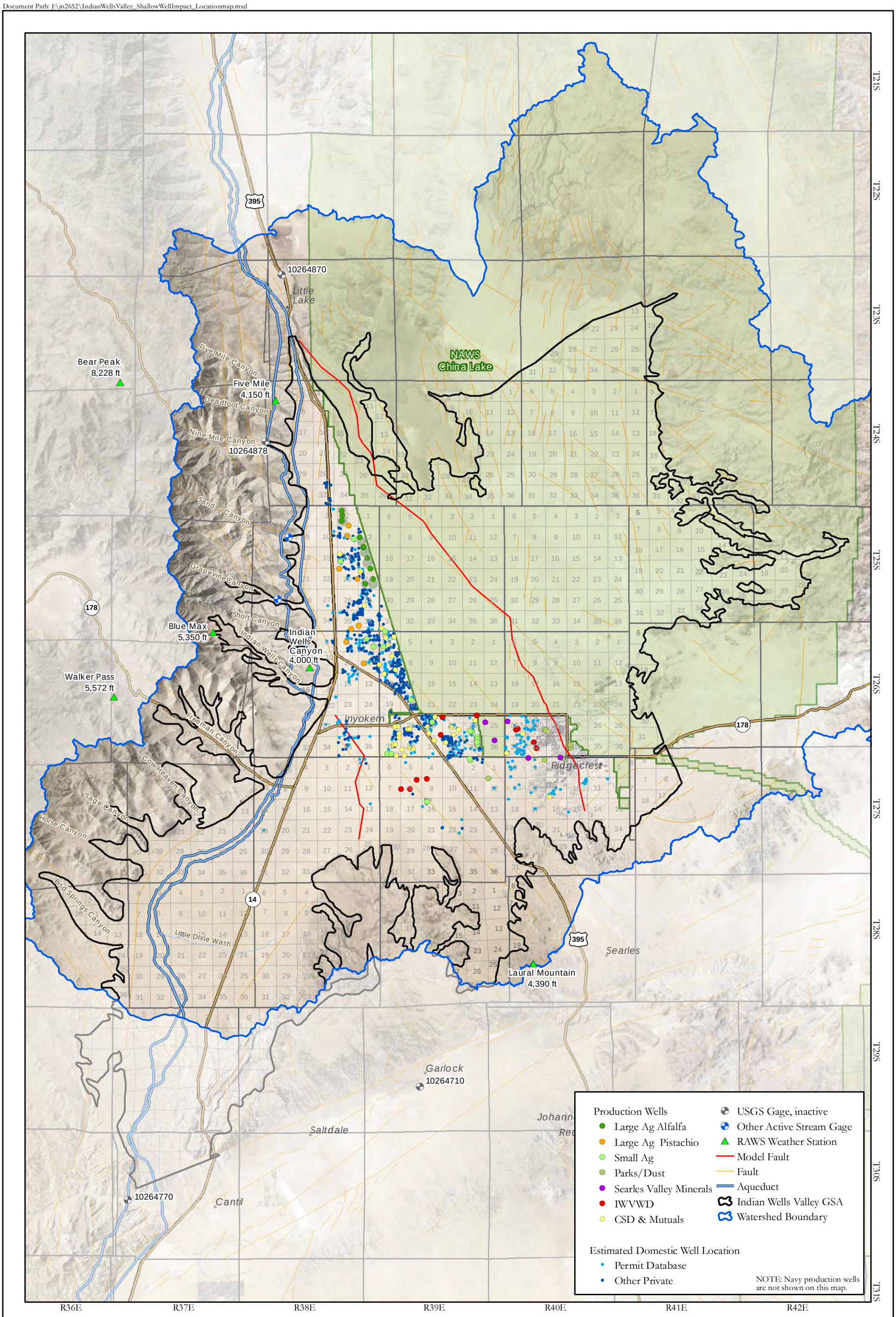
# WELLS	# WATER HOOKUPS	WELL TYPE
2	265	Inyokern Community Service District
38	491	Mutual Water Companies
377	377	Private/Domestic Wells listed in KCHD[a] Well Permit Database
455	455	Other Private Wells estimated from Todd Study[b] total DOM[c]
872	1,588	Estimated Total Number of Shallow Wells

a) KCHD: Kern County Health Department
b) Todd, 2914. *Indian Wells Valley Resource Opportunity Plan; Water Availability and Conservation Report.*
c) DOM: domestic well

Locations for these shallow wells were initially developed using maps provided by earlier reports (Todd, 2014) and modeling studies (DRI, 2016). The exact residences connected to mutual water company and community service districts were not known. Therefore, the assumption was made that residences closest to a water purveyor would use this service, and the recorded number of hook-ups were assigned to each mutual water company well so as not to double account shallow wells within these areas. Figure 1 shows the location of 38 mutual water company wells, 2 community service district wells, 832 private domestic wells, and other larger pumping wells in Indian Wells Valley. The final analysis was completed using aerial photos and GIS to estimate the location for all 872 shallow wells.

[1] Pages 15-16 "Private Domestic" in Todd, 2014. *Indian Wells Valley Resource Opportunity Plan; Water Availability and Conservation Report*. Submitted to Kern County Planning and Community Development Department. January 22, 2014.

Document Path: J:\jn2652\IndianWellsValley_ShallowWellImpact_Locationmap.mxd



STETSON ENGINEERS INC.

SHALLOW WELL IMPACT ANALYSIS
PUMPING WELL LOCATIONS
INDIAN WELLS VALLEY
DRAFT 10/14/2019

0 2 4 Miles

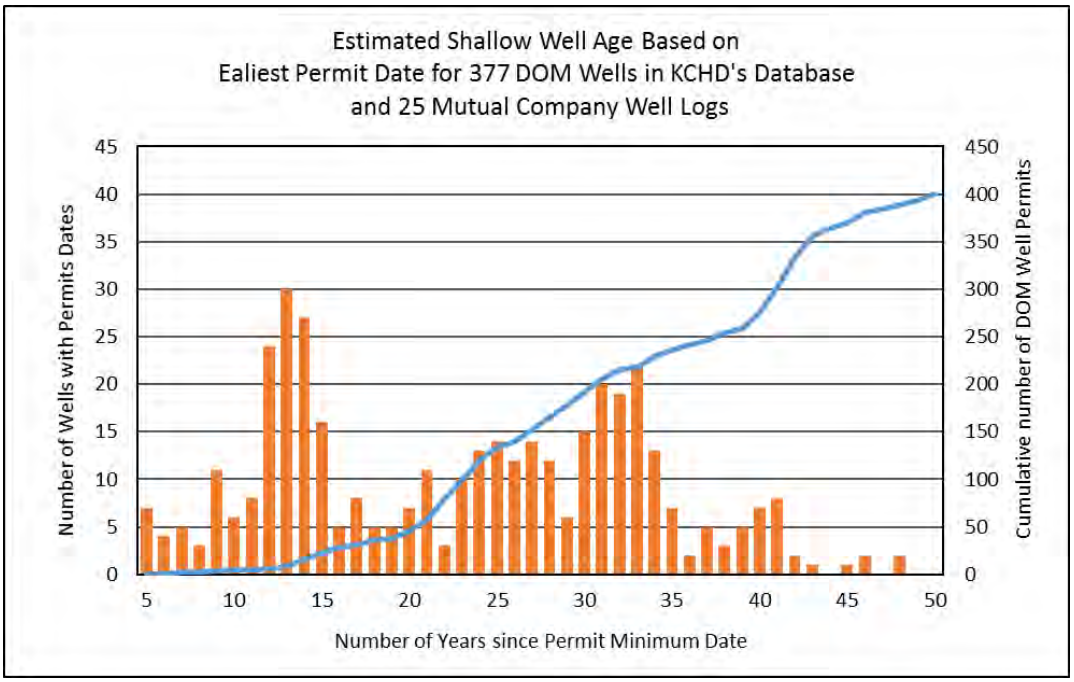
N

FIGURE 1

2.0. ESTIMATED SHALLOW WELL CONSTRUCTION DATE

The Kern County Health Department (KCHD) permit database was used to estimate the year permitted wells were drilled and constructed. Of the 546 permitted wells in the database, there were 377 unique domestic 'shallow' wells with locations inside of Indian Wells Valley. The earliest permit date listed for each well in the KCHD database was used as the year the well was initially constructed. This provided an estimate for the number of years the well would have been influenced by changes in groundwater level. Well logs for 28 mutual water company wells were available from the well registration database. The drilling/construction dates from these well logs were also added into the analysis for a total of 402 estimated drill dates. Figure 2 shows the resulting range of well ages from 5 to 48 years, with the largest number of initial well permits (30) occurring 13 years ago (2006). This database contains the best available data for this initial shallow well impact analysis. More complete data would require a physical survey of the estimated 872 wells.

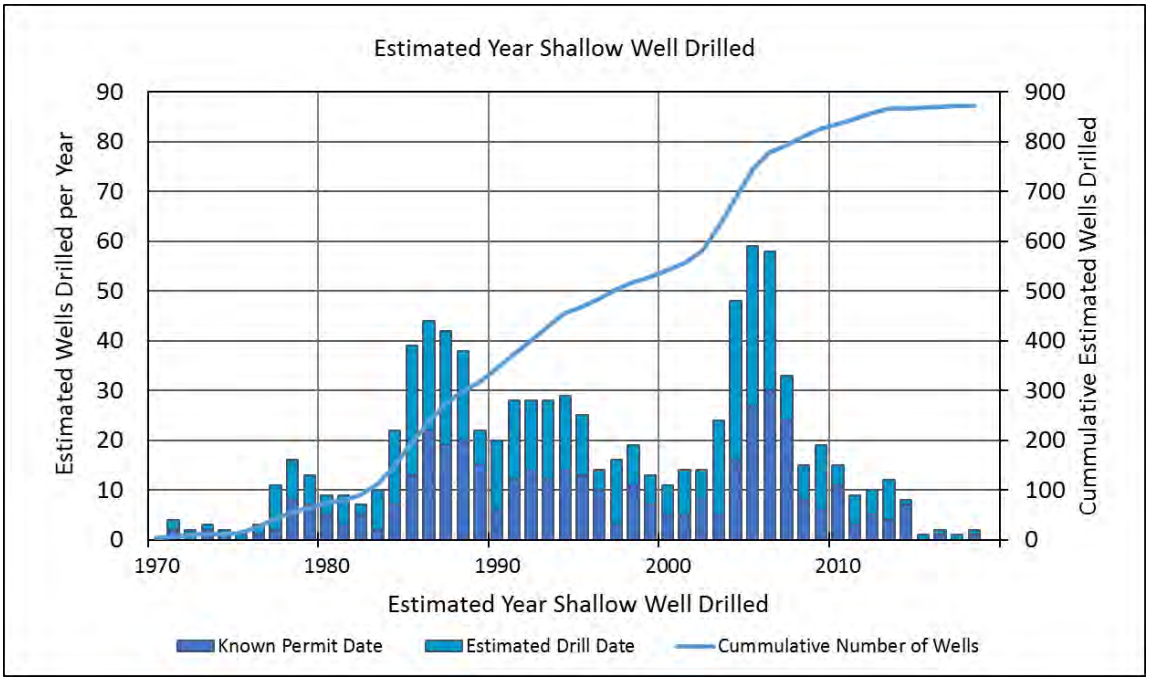
FIGURE 2 ESTIMATED AGE OF 402 SHALLOW WELLS BASED ON EARLIEST PERMIT DATE OR WELL LOG



The remaining 455 domestic/private wells were assigned drill dates using a random number generator to develop a variable drill-date distribution. An assumption was made that the 455 unknown drill dates would have a similar distribution pattern as the 402 'known' well drill dates.

A randomized number was associated with the locations (T/R-S[2]) for the 455 shallow wells without a known drill date within the basin to assign the order that the wells were drilled. The assigned randomized number was sorted and mapped by percentage of wells drilled/year to estimate when each well was drilled. Figure 3 shows the final distribution of the estimated years that the 872 shallow wells were drilled.

FIGURE 3 ESTIMATED DRILL DATE FOR 872 SHALLOW WELLS

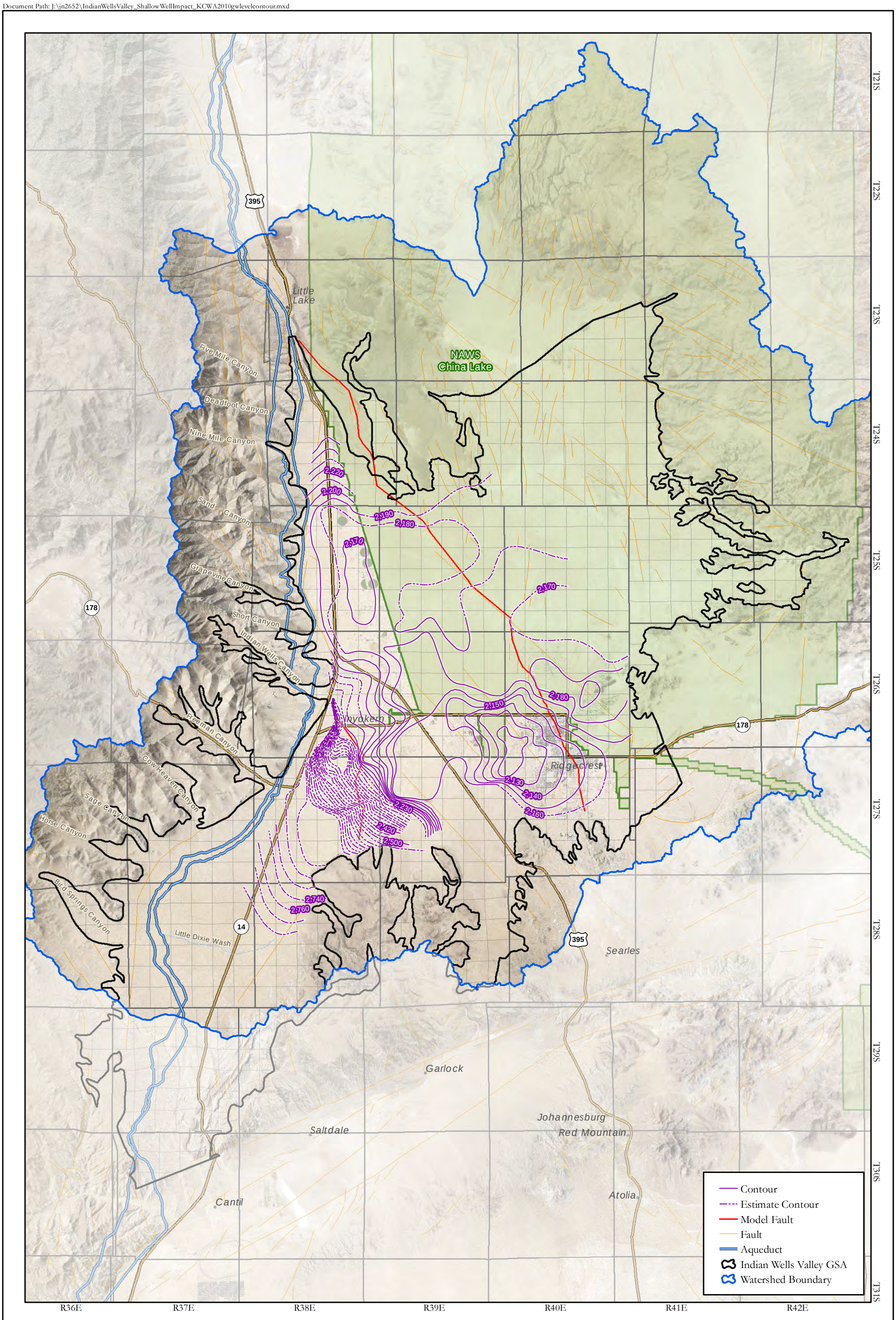


3.0. CHANGES IN DEPTH TO GROUNDWATER (RATE OF DRAWDOWN)

KCWA measures depth to groundwater in the spring and fall each year and develops contour maps showing the water table surface throughout the basin including cones of depression at pumping centers. KCWA's 2010 and 2015[3] groundwater level contours were digitized into GIS files (Figure 4 and Figure 5 respectively), and kriged (a statistical interpolation process) into two surfaces. The average difference of the two groundwater table surfaces was calculated for each 1-square mile section (Section) containing shallow wells. This analysis yielded an average change in groundwater level over 5 years for 428 sections, of which only 76 sections contained shallow wells.

[2] Township/Range-Section public land survey numbering system.
[3] The GIS-digitized contours of KCWA's 2010 and 2015 maps can be viewed on the IWVGSP.com map.

Document Path: J:\jn2652\IndianWellsValley_ShallowWellImpact_KCWA2010gwlevelcontour.mxd



STETSON ENGINEERS INC.

NOTE:
Contours Digitized from KCWA Map
10-foot contour interval; 20-foot contour interval in Southwest/El Paso Areas.

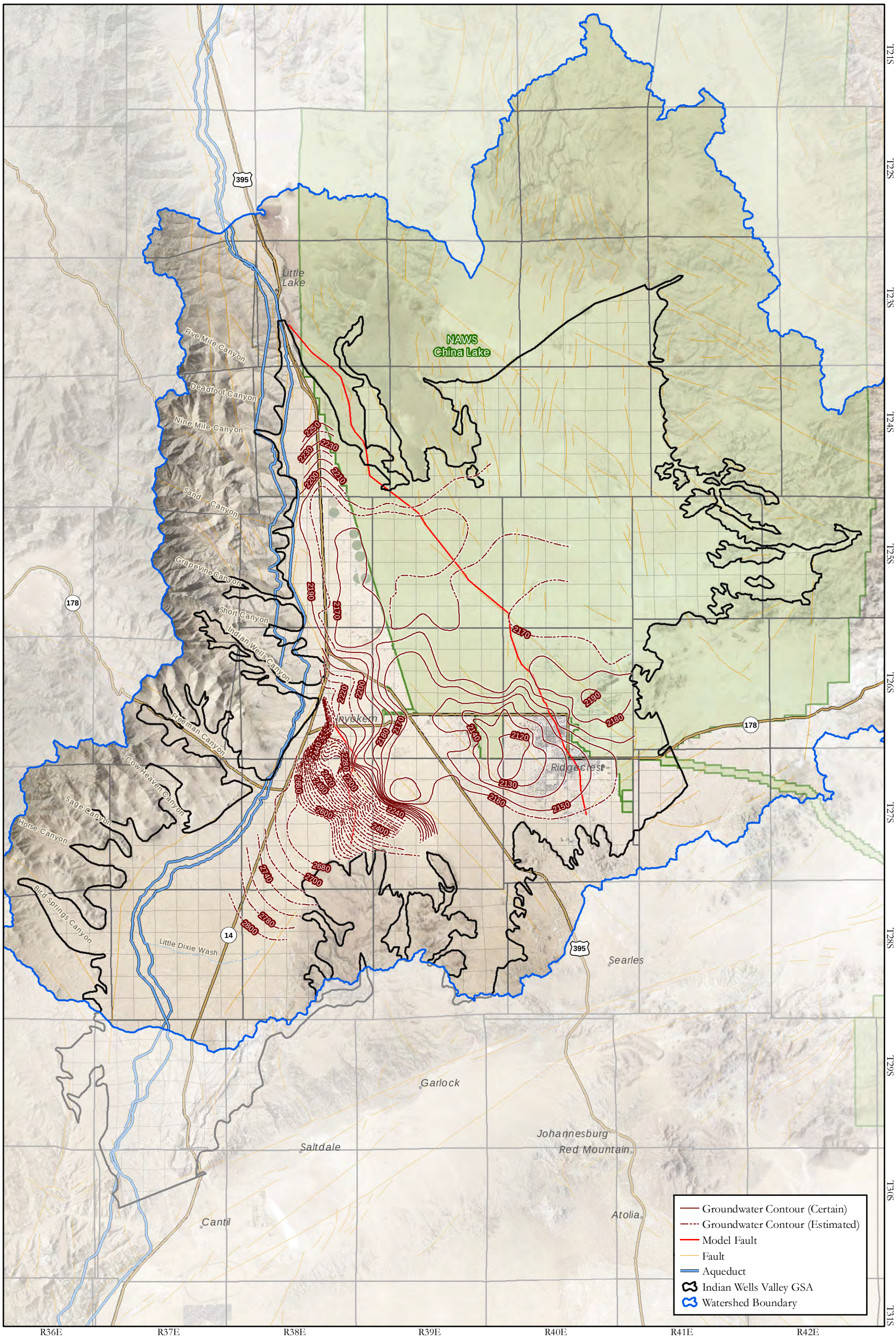
SHALLOW WELL IMPACT ANALYSIS
2010 KCWA GROUNDWATER LEVEL CONTOURS
INDIAN WELLS VALLEY
DRAFT 10/14/2019

0 2 4 Miles

N

FIGURE 4

Document Path: J:\jn2652\IndianWellsValley_ShallowWellImpact_2015gwlevelcontour.mxd



STETSON ENGINEERS INC.

NOTE:
Contours Digitized from KCWA Map
10-foot contour interval; 20-foot contour interval in Southwest/El Paso Areas.

SHALLOW WELL IMPACT ANALYSIS
2015 KCWA GROUNDWATER LEVEL CONTOURS
INDIAN WELLS VALLEY
DRAFT 10/14/2019

0 2 4 Miles

N

FIGURE 5

The resulting averages of drawdown/year/Section between Spring 2010 and Spring 2015 are displayed on Figure 6 ranging from no decline (blue) up to 2.0 to 2.5 feet/year (orange). Groundwater level changes between 2010 and 2015 for Sections with shallow wells are summarized below in Table 2. This analysis resulted in no declines in groundwater levels in 22 (29 %) Sections with wells; and 28 (37%) Sections with shallow wells showing drawdown of less than 0.5 feet/year. The average annual drawdown in 16 Sections in the Indian Wells Valley basin was estimated to be greater than one foot/year. Drawdown analysis for five Sections located north of Pearsonville in the northwest sections of Indian Wells Valley are based on limited data and possibly not representative of what is occurring in this area. However, the other eleven (11) Sections showing steeper rates of groundwater level decline are consistent with measured groundwater levels in these areas.

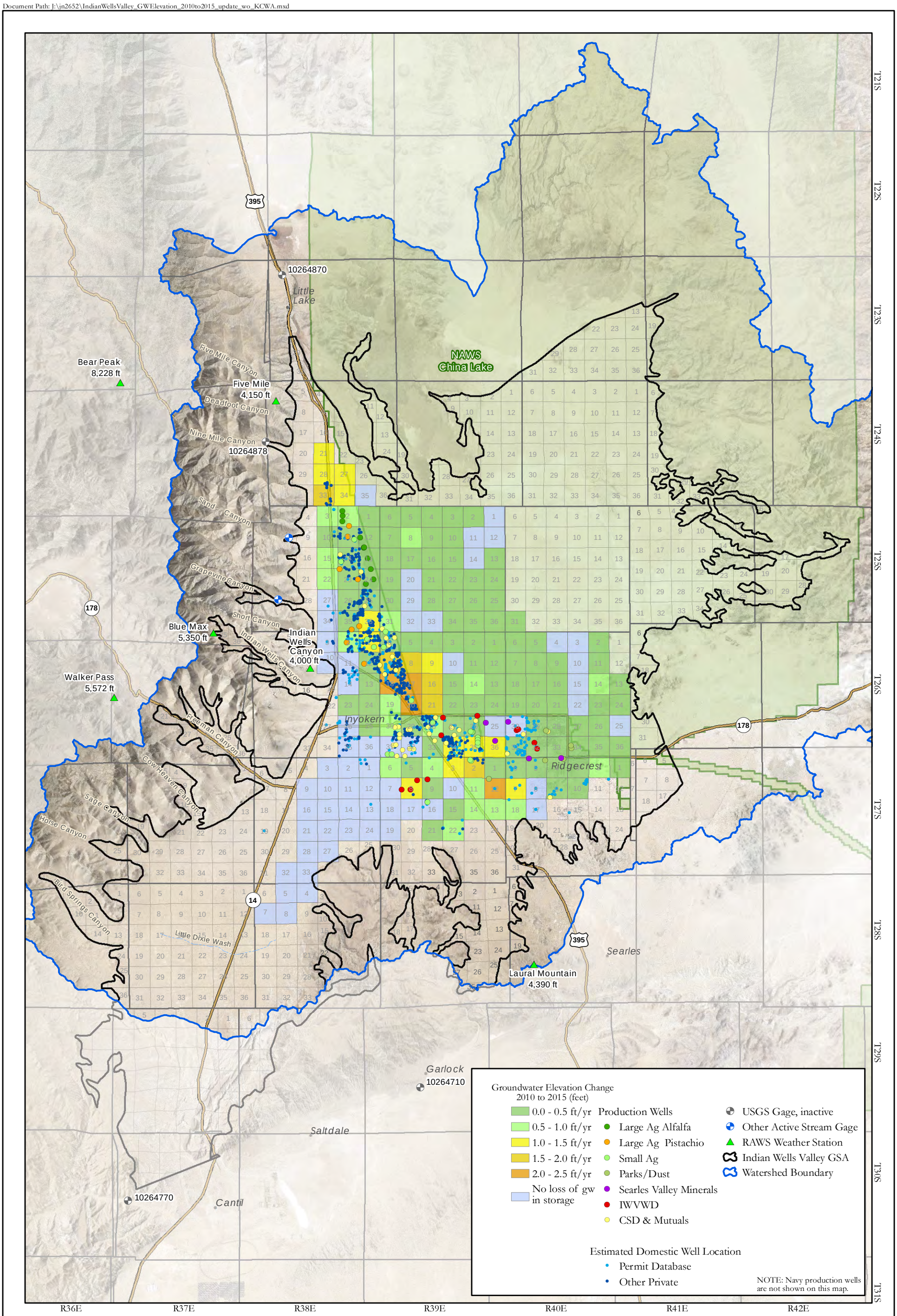
TABLE 2. ESTIMATED AVERAGE DRAWDOWN / YEAR FROM 2010 TO 2015

RANGE IN DRAWDOWN/YEAR	# SECTIONS	# SHALLOW WELLS IN SECTIONS	MAPPED COLOR
No Drawdown	22	108	Blue
> 0.0 to < -0.5	28	333	Darker green
> -0.5 to < -1.0	10	114	Light green
> -1.0 to < -1.5	8	151	Yellow
> -1.5 to < -2.0	4	84	Light orange
> -2.0 to -2.5	4	82	Darker orange
Total:	76	872	

Drawdown based on GIS analysis of KCWA Groundwater Level Contour Maps

The shallow well impact analysis assumed that the recent average rates of drawdown developed for 2010 to 2015 are indicative of the historical average rate of drawdown by Section. Some of this analysis extends the estimated rate of drawdown back in time to estimate historical shallow well impacts. There is both antidotal and reported information of shallow wells in the past that have indicated shallow wells needed to be re-drilled or deepened, but there is no definitive inventory of these impacted wells at this time. A well owner survey would be required to fill in these data gaps.

Document Path: J:\jn2652\IndianWellsValley_GWElevation_2010to2015_update_wo_KCWA.mxd



STETSON ENGINEERS INC.

SHALLOW WELL IMPACT ANALYSIS
INDIAN WELLS VALLEY
DRAFT 10/16/2019

0 2 4 Miles

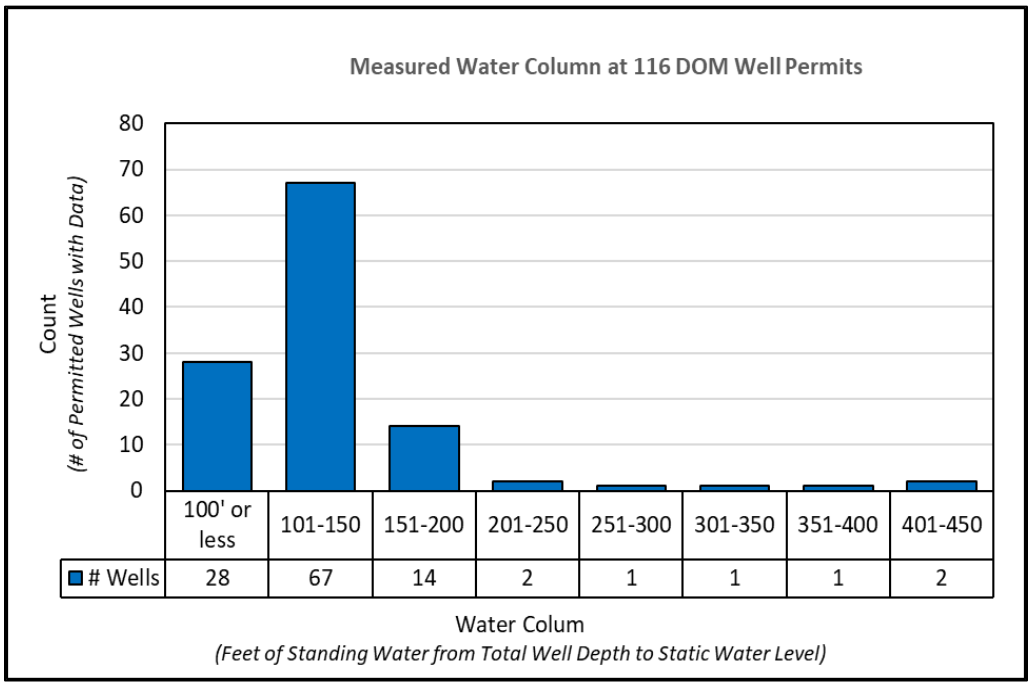
N

4.0. ESTIMATED SHALLOW WELL CONSTRUCTION AND INITIAL USEABLE WATER COLUMN WITHIN A WELL

The useful lifetime of a shallow well before it would be impacted by groundwater level changes is dependent upon the water column within the well above the pump and the rate of drawdown near the well. Estimates of an average water column were developed from the county's permit database and general drilling practices for domestic wells. It was estimated, that at the time of drilling, approximately 70 feet of water column was needed below the pumping water level to the bottom of the well and 48 feet of water column was typical to accommodate changing groundwater levels.

Kern County Health Department's permit database was used to estimate well construction information for 377 private/domestic wells. Each data record included location, owner, and permit date; and sometimes included total depth (TD), static water level (SWL), and well type. The standing water column at the time of well construction was needed to estimate shallow well impacts: (1) the "full" water column from TD to SWL, and (2) the "useable" water column from the pumping water level (PWL) to the SWL. Sufficient data were available for 116 wells with permits that included TD and SWL of the well. For these shallow wells, the full water column ranged from 69 feet to 450 feet with a median of 118 feet. The full water column distribution for available data is shown in Figure 7 bar graph.

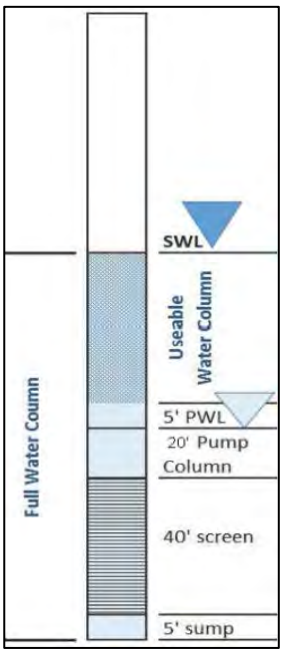
FIGURE 7 MEASURED WATER COLUMN FROM KCHD PERMIT DATABASE



An additional 83 permitted wells had recorded TD, but no SWL. For these wells, an initial water column was estimated by location and drill date. The drawdown calculated in Section 2.0 was used to estimate overall change in groundwater level for the years since the well was drilled. This change was added to the current groundwater level to "back-calculate" the initial SWL.

In areas of the basin where groundwater levels are dropping, the useable water column above the pumping water level establishes how many more years the well can function before having insufficient water column to pump. Screen intervals, pump column depths and other well construction details were not available at this time. The following general assumptions were made with respect to the domestic well construction: drilling past where the groundwater table is encountered to accommodate a sump, perforated casing, and pump column. The total depth of the constructed well can vary based upon the length of screen interval, the type of pump, and how much blank casing is installed to accommodate groundwater level changes (see schematic).

For shallow domestic wells without construction data, it was estimated that at the time of initial construction, the well was drilled to 118 feet below the groundwater table (median of permitted wells with data) and had a useable water column of 48 feet . This would accommodate a 5-foot sump, 40-foot screen interval, 20 feet for the pump column and 5 feet for drawdown in the well while pumping. The life of the well before it would be impacted by groundwater level changes is dependent upon the useable water column and rate of drawdown near the well:



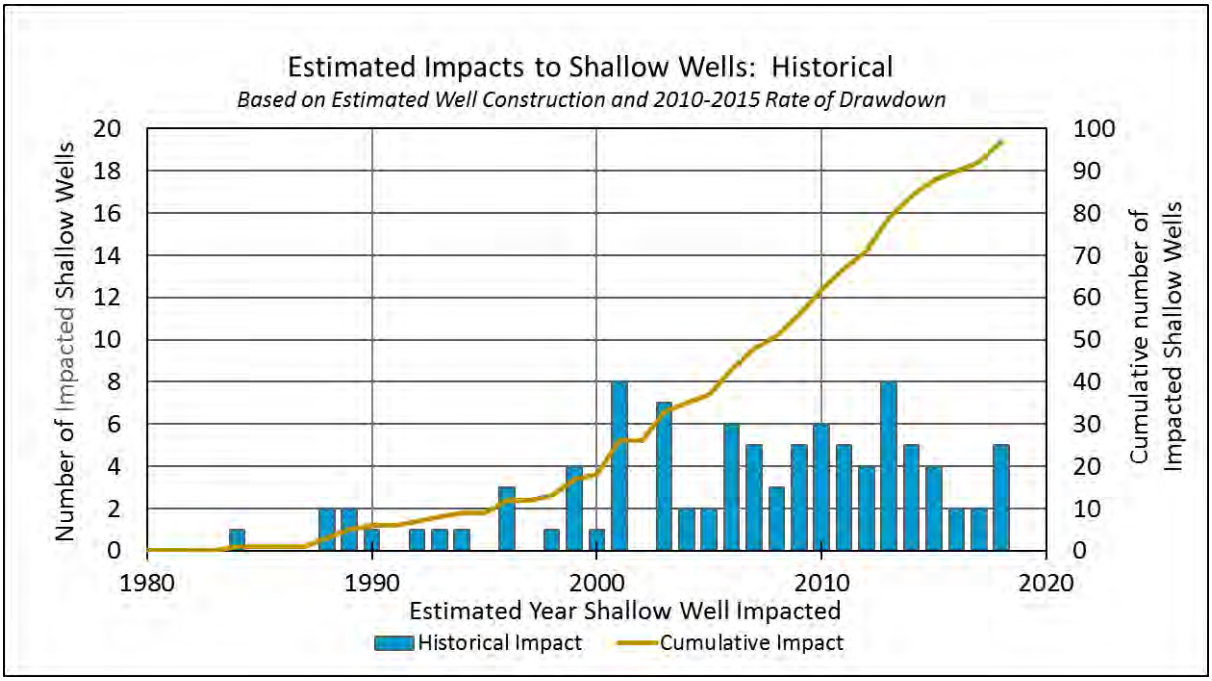
$$\frac{\textit{Useable Water Column (feet)}}{\textit{rate of drawdown per year (feet/year)}} = \textit{\# years left of well operation}$$

5.0. HISTORICAL ESTIMATE OF SHALLOW WELL IMPACT

Historical impacts of changing groundwater levels on shallow wells were assessed using the estimated well construction (Section 4.0), date drilled (Section 2.0), and historical rate of drawdown (Section 3.0). Groundwater level drawdown rates (2010-2015) were used to calculate pre-2019 drawdown. Historical drawdown rates were applied to the number of years since the well was drilled (from drill date to 2019) resulting in the total drawdown since the well was constructed. This drawdown was applied to estimate the usable water column remaining by January 2020. If the well was considered impacted prior to 2019, it was assumed that the well was deepened 40

feet. The graph in Figure 8 shows estimated historical shallow well impacts within Indian Wells Valley, ranging from 0 to 8 wells within any one year. The cumulative number of 97 impacted shallow wells was reached in 2018 using the methodology described above. It is recommended that drilling records be evaluated and outreach to domestic well owners be used to validate this analysis.

FIGURE 8 ESTIMATED HISTORICAL SHALLOW WELL IMPACTS



6.0. METHODOLOGY TO ESTIMATE SHALLOW WELL IMPACT FOR FUTURE CONDITIONS DURING BASELINE (NO ACTION) AND MANAGEMENT ALTERNATIVE 6.2 SCENARIO

The IWV Model groundwater levels are simulated for each active 15.4-acre model cell (820 feet on a side). There are 19,051 active model cells simulated within the model. These model cells overlap with 510 square-mile Sections for this analysis. There are approximately 41.6 model cells per Section (640 acres = 1 square-mile Section). Shallow well locations were estimated to be in 76 of these Sections. The average annual rate of drawdown by Section is applied to estimated depths of shallow wells to evaluate the impact of basin management on shallow wells going dry based on Future Baseline (No Action) and Management Alternatives for the Groundwater Sustainability Plan (GSP).

DRI provided GIS coverages from the IWV Model output files of simulated groundwater levels at the end of five years: 2020, 2025, 2030, 2040, and 2070. These years represent the initial start of the Groundwater Sustainability Plan (2020), the timeframe for different management

actions to be taken (2025, 2030, 2040), and the 50-year planning horizon (2070). It is anticipated that rates of drawdown will vary over time influencing the number of shallow wells impacted based on the aquifer's response to when and where management actions are put into place.

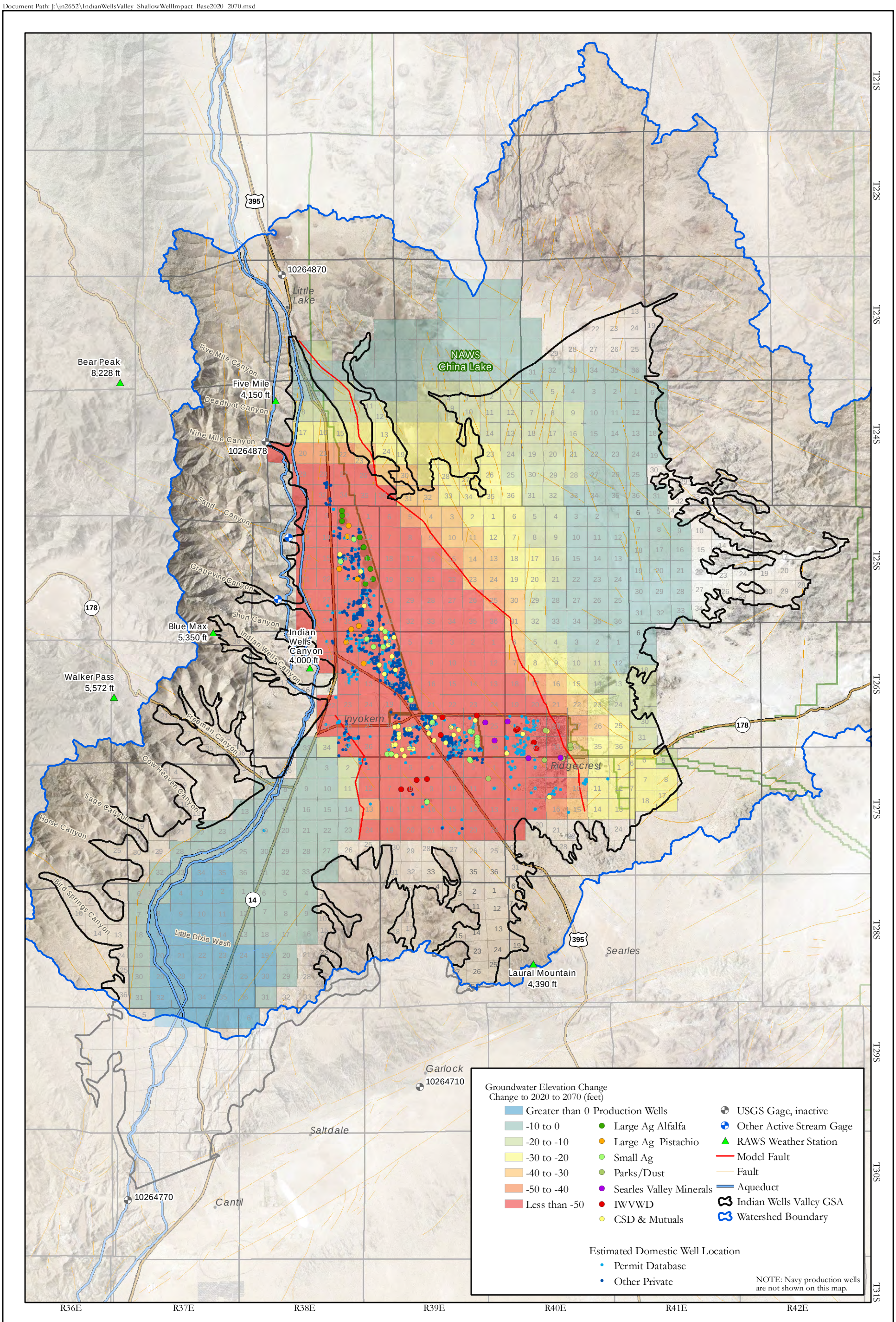
The change in groundwater level for each active model cell was calculated for 2020-25 (5 years), 2025-30 (5 years), 2030-40 (10 years), 2040-70 (30 years), and 2020-70 (50 years) for Baseline and Management Alternatives. Groundwater level changes for each of the 19,051 active model cells were used to calculate average annual drawdown for each of the 510 Sections during the five respective management timeframes.

If a well became impacted after January 2020, it was assumed that drillers would be aware of declining groundwater levels and replace or deepen the well an additional 60 feet from the previous year by the next year. These assumptions were made to determine the future no-action baseline impact and all subsequent management alternatives that were modeled.

7.0. BASELINE (NO ACTION) MANAGEMENT ALTERNATIVE RESULTS

A model run scenario representing "no action" was simulated for the future 50-year baseline condition from 2020 through 2070. This is considered a worst-case scenario where the estimated recent historical pumping of 26,959 acre-feet/year (2010 to 2015 average pumping estimated by IWVGWCG) was projected to increase over time to 38,123 acre-feet/year during the next 50 years (based on input from the major groundwater users in the basin). The shallow well impact analysis results (Figure 9) indicate that most of the 76 Sections with shallow wells will have a drawdown of 1.0 to 1.5 feet/year resulting in a 50-year drawdown of 50 feet or more. The shallow well impact analysis for Baseline conditions estimates that 81 shallow wells would be impacted by 2030, and 231 shallow wells would be impacted by 2040 (Figure 10).

Document Path: J:\jn2652\IndianWellsValley_ShallowWellImpact_Base2020_2070.mxd



STETSON ENGINEERS INC.

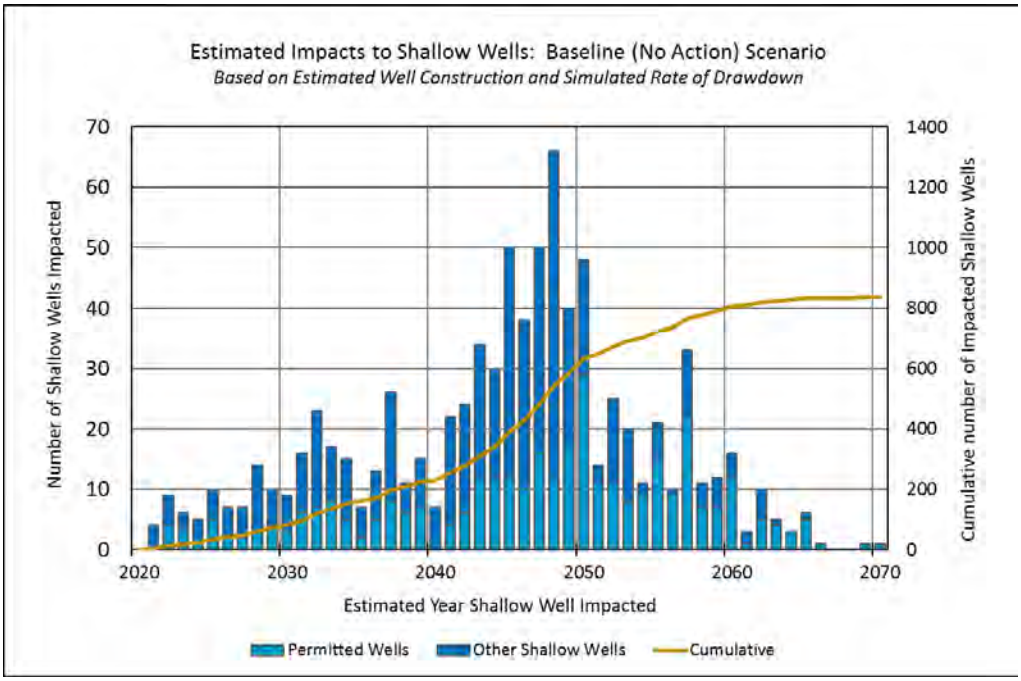
SHALLOW WELL IMPACT ANALYSIS

BASELINE
SIMULATED 50-YEAR DRAWDOWN
INDIAN WELLS VALLEY
DRAFT 3/7/2019

0 2 4 Miles

N

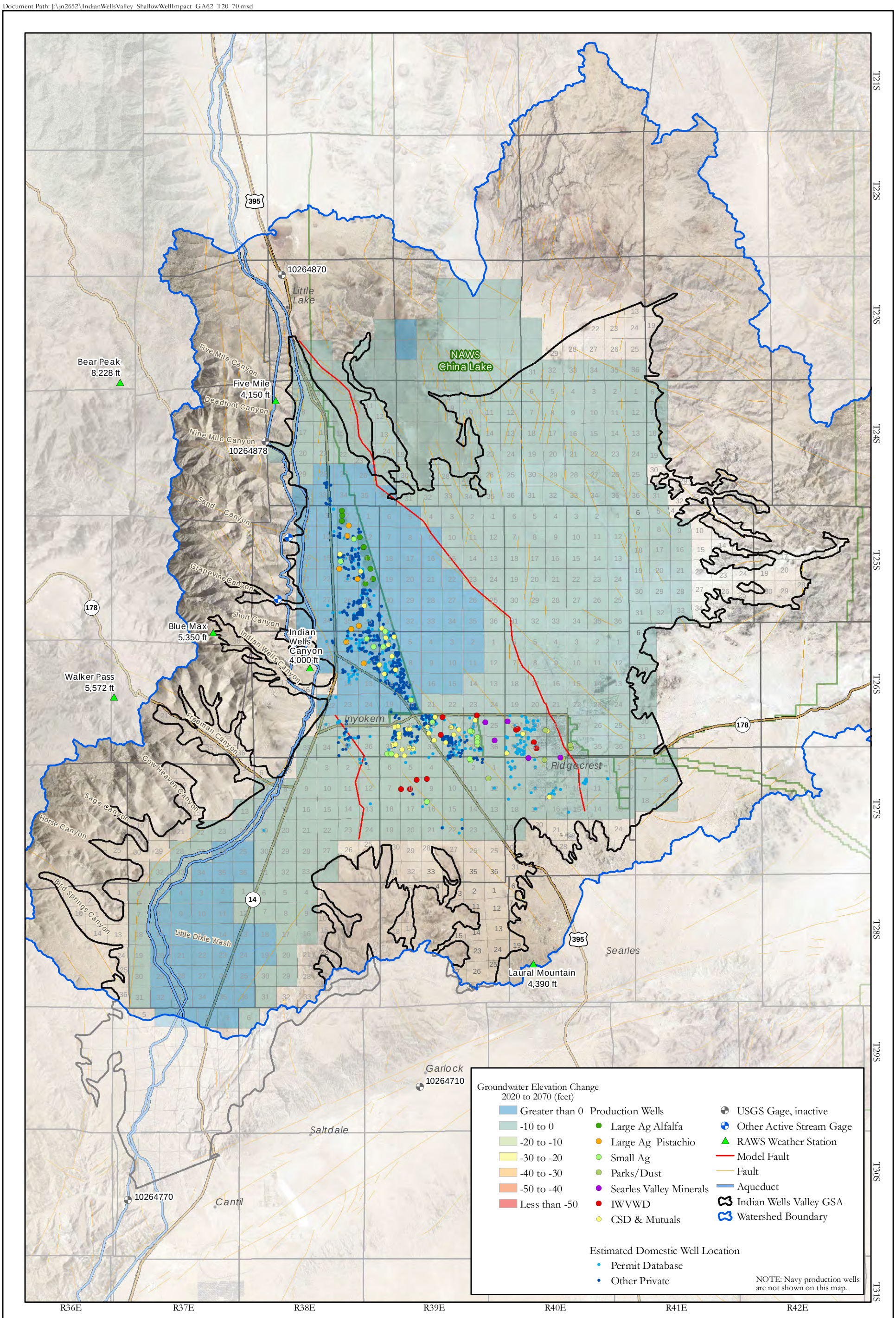
FIGURE 10 ESTIMATED BASELINE (NO ACTION) SHALLOW WELL IMPACTS



8.0. MANAGEMENT SCENARIO 6.2 SHALLOW WELL IMPACT RESULTS

A future 50-year model run representing Management Scenario 6.2 conditions was simulated for 2020 through 2070. This is the GSP scenario developed for the Indian Wells Valley Groundwater Authority with projected pumping at 20,940 acre-feet/year in 2020, 11,150 acre-feet/year in 2030, and 11,252 acre-feet in 2040 and continued with a small population growth consideration through 2070. The shallow well impact analysis results (Figure 11) for Management Scenario 6.2 indicate that most of the 76 Sections with shallow wells will have minimal drawdown resulting in only 22 shallow wells being impacted within the next 50 years. The model simulated drawdowns for Scenario 6.2 conditions estimate 19 shallow wells would be impacted by 2025, and only 3 more wells would be impacted by 2030 (Figure 12).

Document Path: J:\jn2652\IndianWellsValley_ShallowWellImpact_GA62_T20_70.mxd



STETSON ENGINEERS INC.

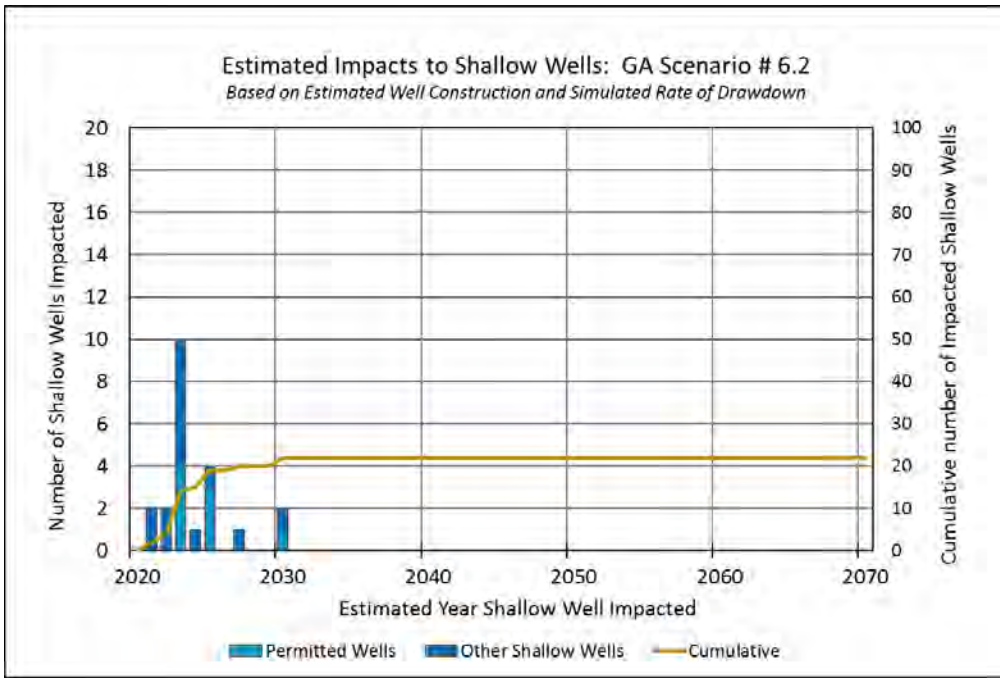
SHALLOW WELL IMPACT ANALYSIS

MANAGEMENT SCENARIO #6.2
SIMULATED 50-YEAR DRAWDOWN
INDIAN WELLS VALLEY
DRAFT 8/5/2019

0 2 4 Miles

N

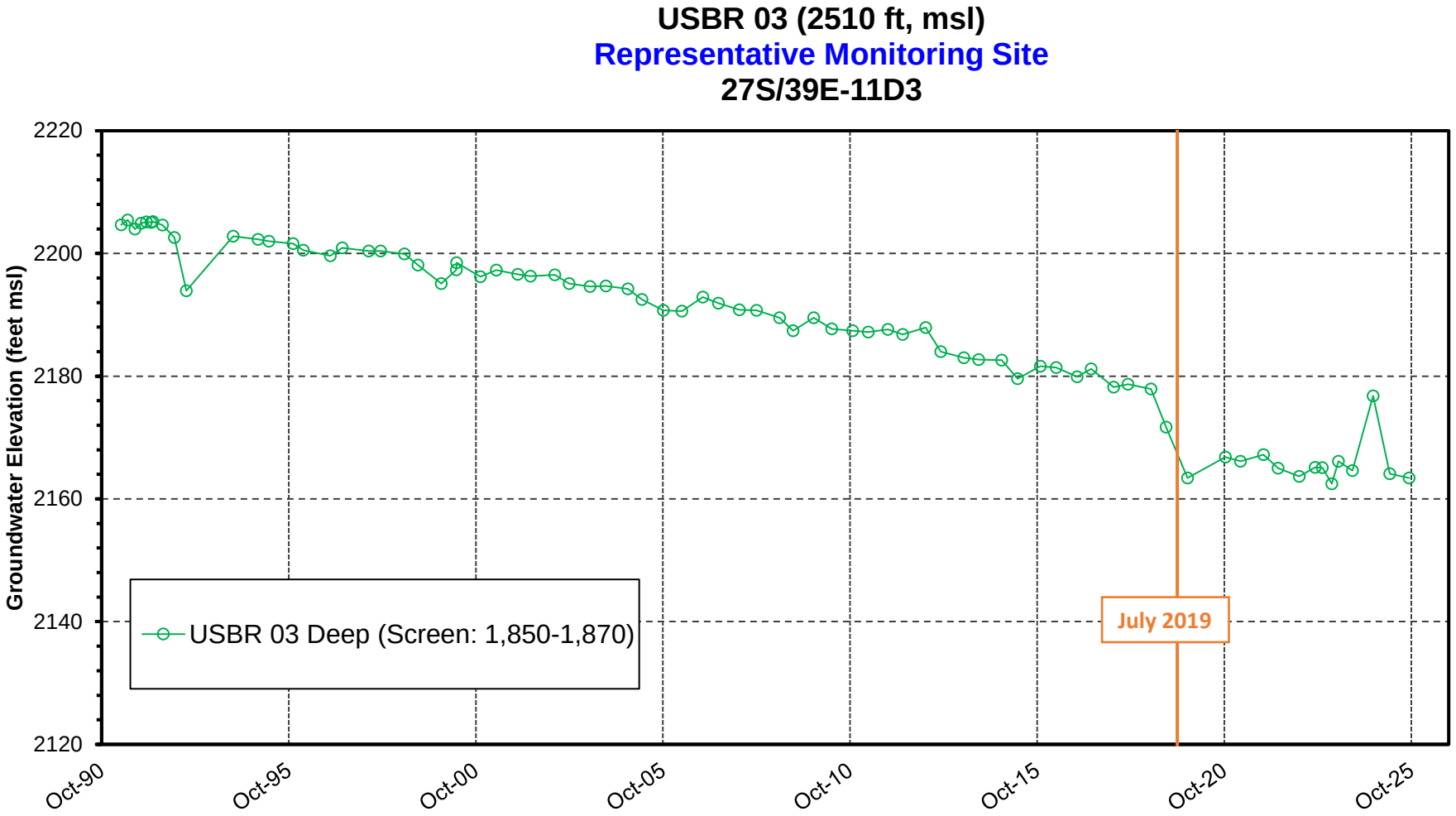
FIGURE 12 ESTIMATED MANAGEMENT SCENARIO 6.2 SHALLOW WELL IMPACTS

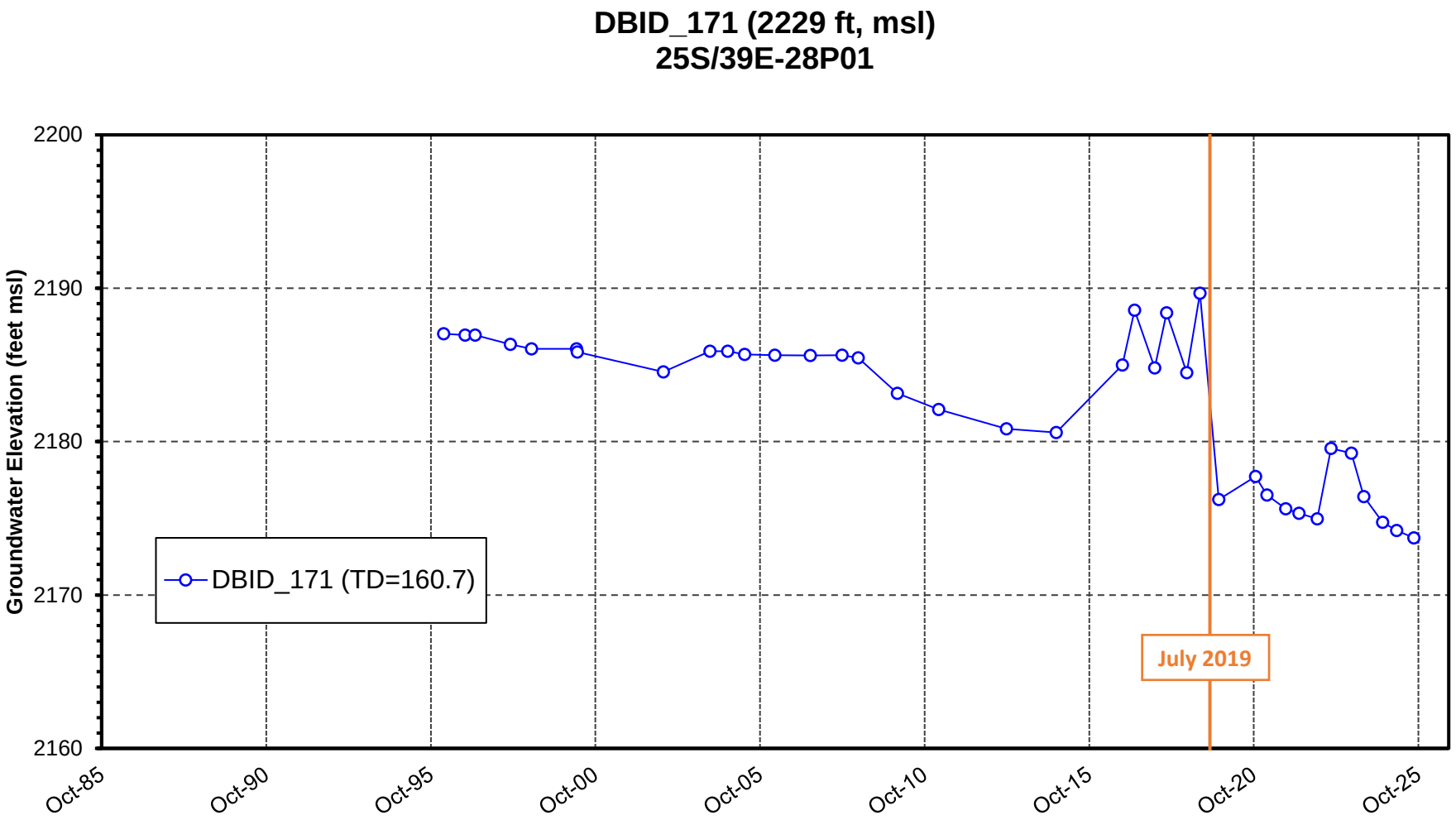


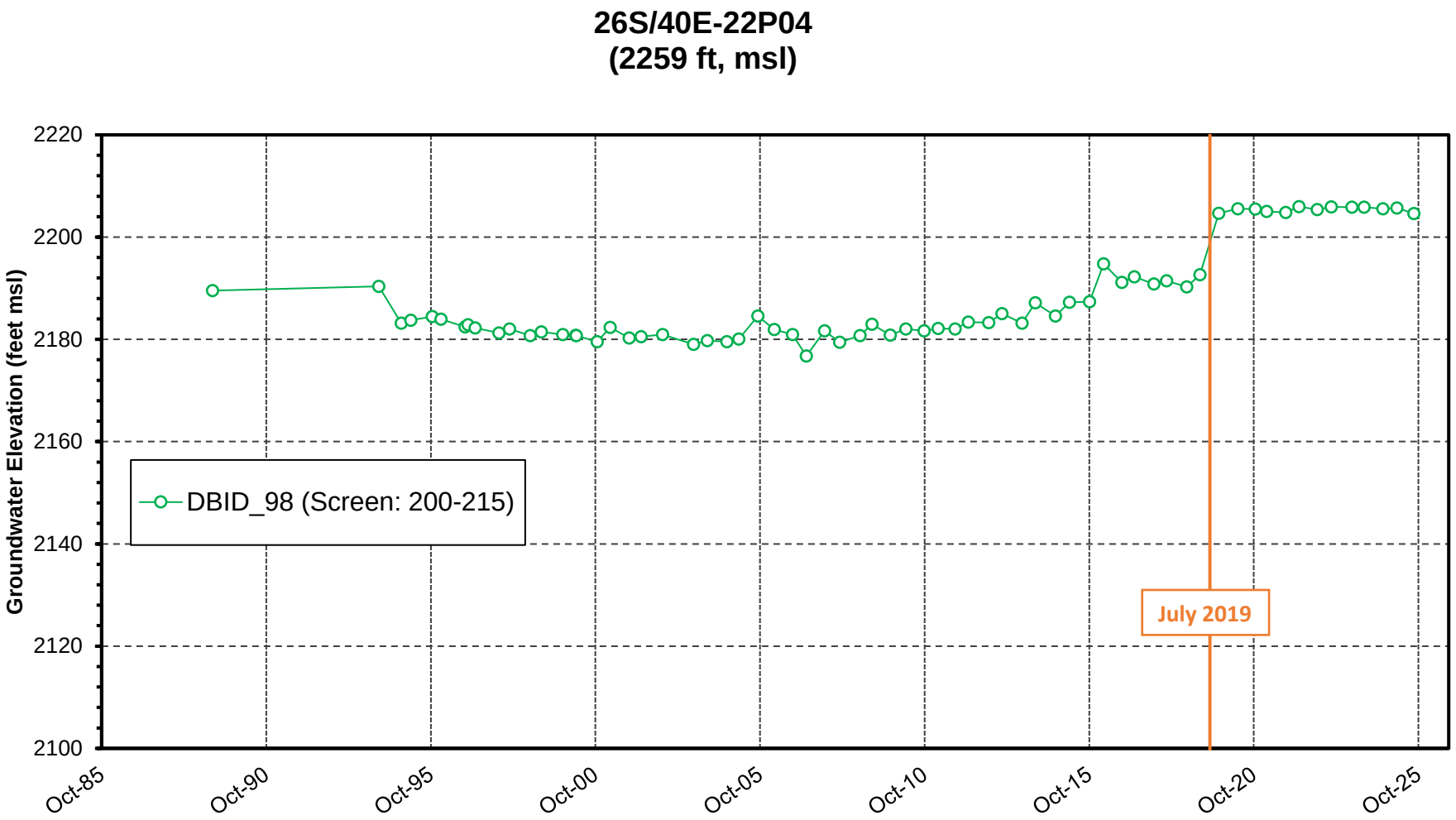
9.0. Recommendations

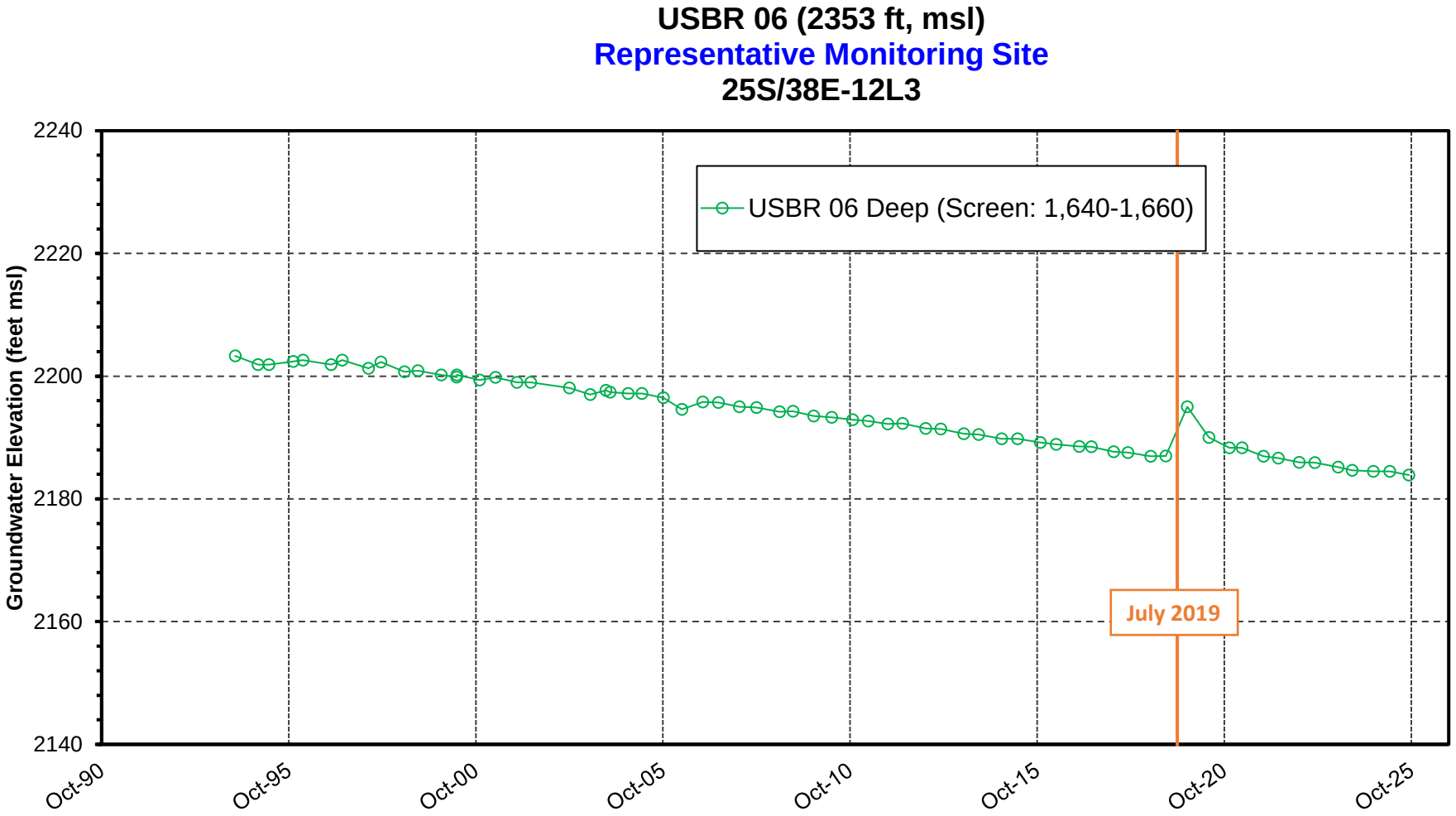
- Confirm the location of shallow rural domestic and mutual water company wells within the basin.
- Canvas all available resources for well logs (RCD, DWR, County Agencies, Well Owners)
- Develop a comprehensive database of initial well construction data, history of well deepening and/or replacement.

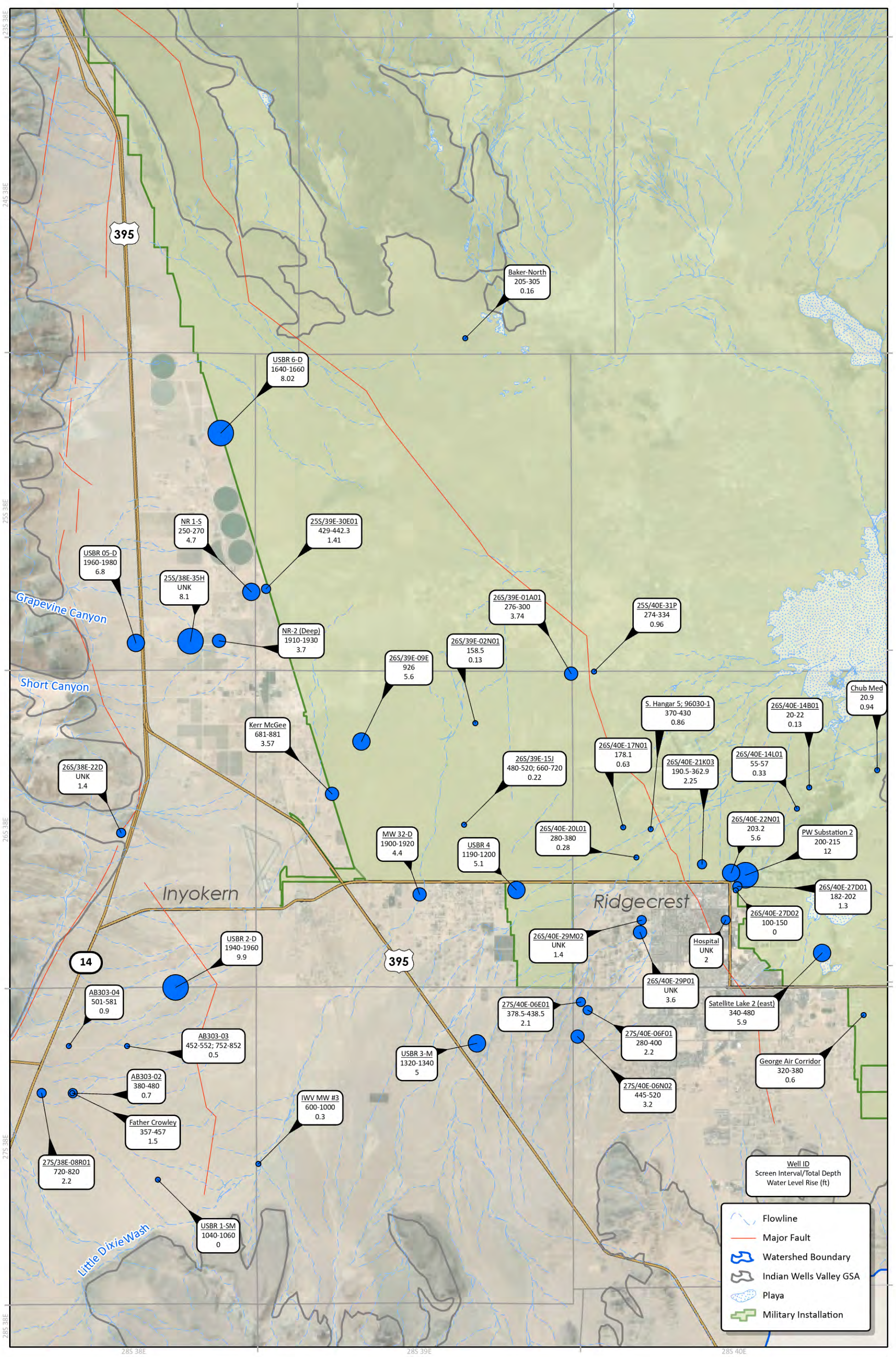
ATTACHMENT P


USBR 03 (2510 ft, msl)
Representative Monitoring Site
27S/39E-11D3
Groundwater Elevation (feet msl)
2220
2200
2180
2160
2140
2120
Oct-90
Oct-95
Oct-00
Oct-05
Oct-10
Oct-15
Oct-20
Oct-25
USBR 03 Deep (Screen: 1,850-1,870)
July 2019


DBID_171 (2229 ft, msl)
25S/39E-28P01
Groundwater Elevation (feet msl)
2200
2190
2180
2170
2160
Oct-85
Oct-90
Oct-95
Oct-00
Oct-05
Oct-10
Oct-15
Oct-20
Oct-25
DBID_171 (TD=160.7)
July 2019


26S/40E-22P04
(2259 ft, msl)
Groundwater Elevation (feet msl)
2220
2200
2180
2160
2140
2120
2100
Oct-85
Oct-90
Oct-95
Oct-00
Oct-05
Oct-10
Oct-15
Oct-20
Oct-25
DBID_98 (Screen: 200-215)
July 2019


USBR 06 (2353 ft, msl)
Representative Monitoring Site
25S/38E-12L3
Groundwater Elevation (feet msl)
2240
2220
2200
2180
2160
2140
USBR 06 Deep (Screen: 1,640-1,660)
July 2019
Oct-90
Oct-95
Oct-00
Oct-05
Oct-10
Oct-15
Oct-20
Oct-25



STETSON ENGINEERS INC.

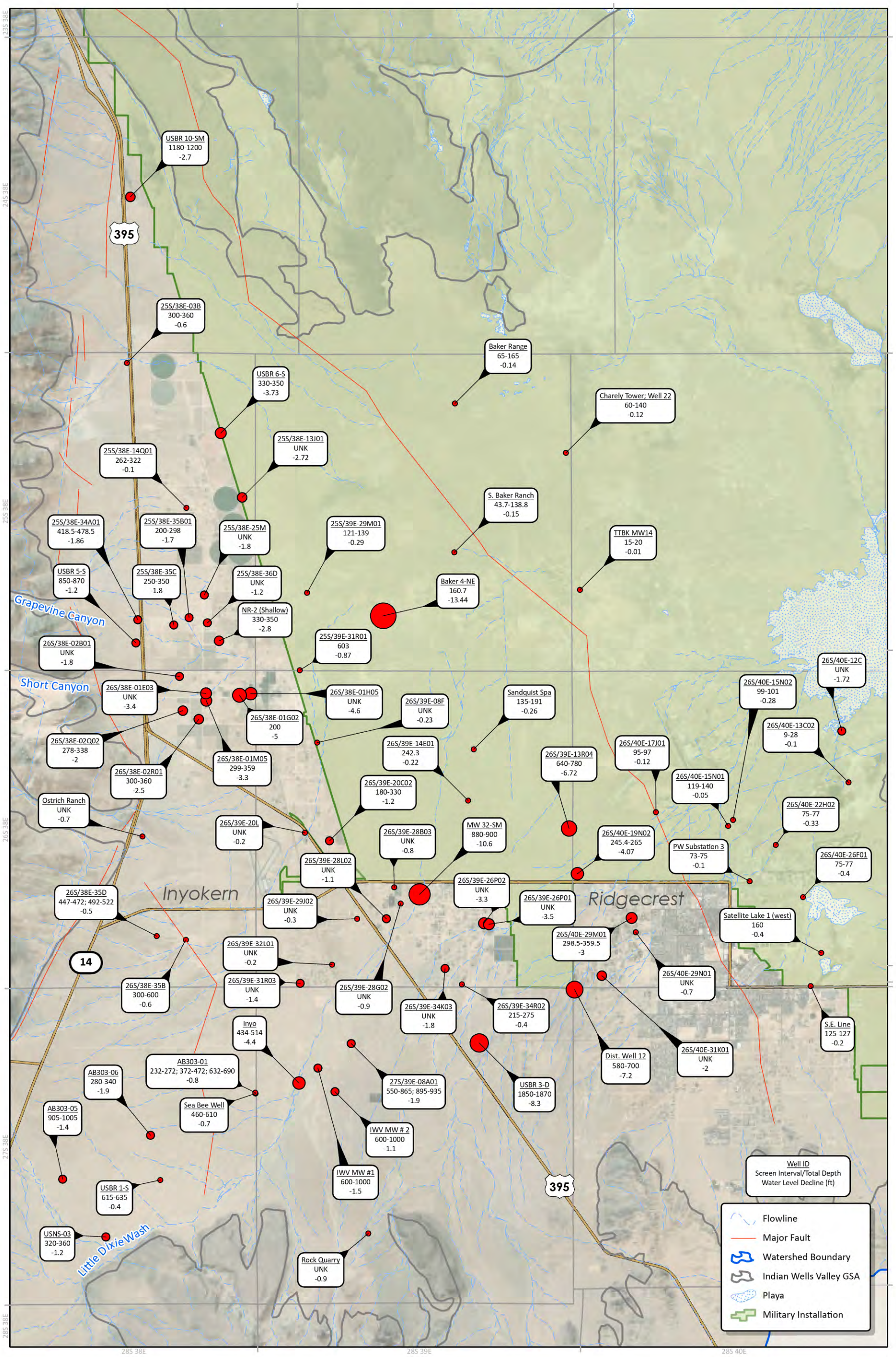
WATER LEVEL RISE BETWEEN MARCH AND OCTOBER 2019

INDIAN WELLS VALLEY, CA

DRAFT
1/23/2024

FIGURE 2

Path: J:\jn2652\IWV GSP 2025.aprx Layout: WL Rise MarOct2019



Path: J:\in2652\IWV GSP 2025.aprx Layout: WL Drop MarOct2019

STETSON ENGINEERS INC.

WATER LEVEL DECLINE BETWEEN MARCH AND OCTOBER 2019

INDIAN WELLS VALLEY, CA

DRAFT
1/23/2024

N

0 1 2
Miles

FIGURE 3

ATTACHMENT Q

Compiled IWV Arsenic Data

Unique Well Name	Alternative Well Name	Sample Date	Arsenic (mg/L)	Analysis Type	Arsenic Reference
24S38E16J02	Sawmill Well #1	6/16/1982	0.011		B
24S38E21A01	USBR-10-S	9/1/1992	0.016		USBR
24S38E21A02	USBR-10-S/M	9/1/1992	0.003		USBR
24S38E21A03	USBR-10-M/D	9/1/1992	0.008		USBR
24S38E21A04	USBR-10-D	9/2/1992	0.010		USBR
24S38E33J02	Pearsonville Well	6/15/1982	0.008		B
24S40E21K01	TTIWV-MW14	2/17/2002	0.056	Est	TTEMI
24S40E21K01	TTIWV-MW14	8/22/2002	0.058		Tri
24S40E36A	TTIWV-MW13	2/16/2002	0.076	Est	TTEMI
24S40E36A	TTIWV-MW13	2/16/2002	0.090	Est	TTEMI
24S40E36A	TTIWV-MW13	12/17/2002	0.085		Tri
25S10E11K01		6/9/1982	0.230		B
25S38E12L01	USBR-06-S	1/10/1992	0.195		USBR
25S38E12L02	USBR-06-M	1/10/1992	0.135		USBR
25S38E12L03	USBR-06-D	1/10/1992	0.075		USBR
25S38E13L01		6/15/1982	0.002		B
25S38E25J01	NR1-S (Neal Ranch-1-S)	2/2/1991	0.010		USBR
25S38E25J02	NR1-M (Neal Ranch-1-M)	2/26/1991	0.028		USBR
25S38E25J03	NR1-D (Neal Ranch-1-D)	2/26/1991	0.130		USBR
25S38E34G02	USBR-05-M	1/6/1992	0.080		USBR
25S38E34G03	USBR-05-D	1/6/1992	0.025		USBR
25S38E36G01	NR2-S (Neal Ranch-2-S)	2/26/1991	0.010		USBR
25S38E36G02	NR2-M (Neal Ranch-2-M)	2/26/1991	0.012		USBR
25S38E36G03	NR2-D (Neal Ranch-2-D)	2/26/1991	0.460		USBR
25S40E08A01	USGS-354658117411201	5/16/1979	0.150		B
25S40E08A01	USGS-354658117411201	5/20/1980	0.170		B
25S40E08A01	USGS-354658117411201	6/9/1982	0.170		B
25S40E14H01	TTIWV-MW12	2/16/2002	0.099	Est	TTEMI
25S40E14H01	TTIWV-MW12	2/16/2002	0.104	Est	TTEMI
25S40E14H01	TTIWV-MW12	2/16/2002	0.135	Est	TTEMI
25S40E14H01	TTIWV-MW12	2/16/2002	0.127	Est	TTEMI
25S40E14H01	TTIWV-MW12	8/23/2002	0.126		Tri
25S40E18R01	TTBK-MW12	5/16/1979	0.220		B
25S40E18R01	TTBK-MW12	5/20/1980	0.088		B
25S40E18R01	TTBK-MW12	6/9/1982	0.054		B
25S40E18R01	TTBK-MW12	11/5/1989	0.027		Tri
25S40E20F01	USGS-354450117415301	5/16/1979	0.044		B
25S40E20F01	USGS-354450117415301	5/20/1980	0.079		B
25S40E20F01	USGS-354450117415301	6/9/1982	0.042		B
25S40E30E01	TTBK-MW14	5/11/1999	0.042		Tri
25S40E33L01	USGS-354258117403901	5/21/1980	2.000		B
25S40E33L01	USGS-354258117403901	6/9/1982	2.900		B

Compiled IWV Arsenic Data

Unique Well Name	Alternative Well Name	Sample Date	Arsenic (mg/L)	Analysis Type	Arsenic Reference
25S40E33L02	USGS-354258117403902	5/31/1979	0.002		B
25S40E33L02	USGS-354258117403902	5/22/1980	0.003		B
25S40E33L02	USGS-354258117403902	6/9/1982	0.007		B
25S40E35D01	TTBK-MW13	2/16/2002	0.500	Est	TTEMI
25S40E35D01	TTBK-MW13	2/16/2002	0.052	Est	TTEMI
25S40E35D01	TTBK-MW13	2/16/2002	0.500	Est	Tri
26S38E35B01		6/15/1982	0.005		B
26S39E26A01	USBR-04	10/30/1990	0.015		USBR
26S39E26A02-D	TTIWV-MW01 (D)	2/17/2002	0.015	Est	TTEMI
26S39E26A02-D	TTIWV-MW01 (D)	2/17/2002	0.005	ND	TTEMI
26S39E26A02-I	TTIWV-MW01 (I)	2/17/2002	0.005	ND	TTEMI
26S39E27D01	MW 32-S	10/17/1991	0.026		USBR
26S39E27D02	MW 32-S/M	10/18/1991	0.036		USBR
26S39E27D03	MW 32-M/D	10/21/1991	0.010		USBR
26S39E27D04	MW 32-D	10/21/1991	0.061		USBR
26S40E01A02		6/9/1982	0.640		B
26S40E01J01	USGS-354155117370201	5/16/1979	0.028		B
26S40E01J01	USGS-354155117370201	5/21/1980	0.180		B
26S40E01J01	USGS-354155117370201	6/10/1982	0.180		B
26S40E01Q01		5/16/1979	0.005		B
26S40E01Q01		5/20/1980	0.001		B
26S40E01Q02		5/15/1979	0.009		B
26S40E01Q02		5/20/1980	0.008		B
26S40E01Q02		6/11/1982	0.020		B
26S40E06D02		6/18/1996	0.050		H96
26S40E10F01	USGS-354125117393701	6/5/1979	0.009		B
26S40E10F01	USGS-354125117393701	5/20/1980	0.008		B
26S40E10F01	USGS-354125117393701	6/9/1982	0.003		B
26S40E11J01	USGS-354108117380801	5/28/1980	0.029		B
26S40E12A01		6/29/1978	0.016		B
26S40E12A01		5/17/1979	0.001		B
26S40E12A01		5/21/1980	0.001		B
26S40E12D01		5/24/1996	1.100		H96
26S40E12G01		6/29/1978	0.004		B
26S40E12G01		5/27/1980	0.001		B
26S40E12G01		6/11/1982	0.020		B
26S40E12Q01	USGS-354101117372201	6/29/1978	0.004		B
26S40E12Q01	USGS-354101117372201	5/15/1979	0.005		B
26S40E12Q01	USGS-354101117372201	5/27/1980	0.018		B
26S40E12R01		6/29/1978	0.003		B
26S40E12R01		6/6/1979	0.002		B
26S40E12R01		5/27/1980	0.002		B

Compiled IWV Arsenic Data

Unique Well Name	Alternative Well Name	Sample Date	Arsenic (mg/L)	Analysis Type	Arsenic Reference
26S40E13C01	USGS-354037117373201	6/29/1978	0.003		B
26S40E13C01	USGS-354037117373201	6/6/1979	0.002		B
26S40E13C01	USGS-354037117373201	5/21/1980	0.002		B
26S40E13C01	USGS-354037117373201	6/11/1982	0.001		B
26S40E13M01	USGS-354010117375601	5/21/1980	0.001		B
26S40E14B01	USGS-354039117382801	5/15/1979	0.230		B
26S40E14B01	USGS-354039117382801	5/20/1980	0.310		B
26S40E14B01	USGS-354039117382801	6/9/1982	0.230		B
26S40E14B01	USGS-354039117382801	5/24/1996	1.200		H96
26S40E14L01	USGS-354020117384201	5/15/1979	0.011		B
26S40E14L01	USGS-354020117384201	5/20/1980	0.042		B
26S40E15E01	USGS-354036117400701	5/31/1979	0.013		B
26S40E15E01	USGS-354036117400701	5/22/1980	0.018		B
26S40E15E02	USGS-354033117400601	6/10/1982	0.014		B
26S40E15N01	USGS-354002117400601	5/31/1979	0.006		B
26S40E15N01	USGS-354002117400601	5/22/1980	0.033		B
26S40E15N01	USGS-354002117400601	5/22/1980	0.008		B
26S40E15N02	USGS-354011117400001	6/14/1982	0.006		B
26S40E16K	TTIWV-MW06	2/17/2002	0.062	Est	TTEMI
26S40E16K	TTIWV-MW06	2/17/2002	0.036	Est	TTEMI
26S40E19N	TTIWV-MW02 (s)	2/18/2002	0.011	Est	TTEMI
26S40E19N	TTIWV-MW02 (S)	8/22/2002	0.012		Tri
26S40E20A	TTBK-MW04	11/6/1998	0.006	Est	Tri
26S40E22H01	USGS-353942117390801	5/15/1979	0.910		B
26S40E22H01	USGS-353942117390801	5/20/1980	0.990		B
26S40E22H01	USGS-353942117390801	6/8/1982	0.880		B
26S40E22H01	USGS-353942117390801	5/24/1996	0.050		H96
26S40E22H02	USGS-353942117390802	5/15/1979	0.019		B
26S40E22H02	USGS-353942117390802	5/20/1980	0.094		B
26S40E22H02	USGS-353942117390802	6/8/1982	0.100		B
26S40E22H03	USGS-353942117390803	5/15/1979	0.091		B
26S40E22H03	USGS-353942117390803	5/20/1980	0.190		B
26S40E22H03	USGS-353942117390803	6/8/1982	0.130		B
26S40E22N01	USGS-353913117400601	5/31/1979	0.170		B
26S40E22N01	USGS-353913117400601	5/23/1980	0.250		B
26S40E22P01	USGS-353908117395201	5/17/1979	0.008		B
26S40E22P01	USGS-353908117395201	5/28/1980	0.013		B
26S40E22P02	USGS-353908117394001	5/29/1996	0.030		H96
26S40E23A01	USGS-353948117381001	5/17/1979	0.081		B
26S40E23A01	USGS-353948117381001	5/21/1980	0.084		B
26S40E23A01	USGS-353948117381001	6/10/1982	0.080		B
26S40E23A02	USGS-353948117381002	5/17/1979	0.016		B

Compiled IWV Arsenic Data

Unique Well Name	Alternative Well Name	Sample Date	Arsenic (mg/L)	Analysis Type	Arsenic Reference
26S40E23A02	USGS-353948117381002	5/21/1980	0.019		B
26S40E23A02	USGS-353948117381002	6/10/1982	0.006		B
26S40E23G01	USGS-353942117383101	5/29/1996	1.400		H96
26S40E24C01	USGS-353953117373701	5/21/1980	0.004		B
26S40E24C01	USGS-353953117373701	6/10/1982	0.036		B
26S40E25C	TT64-MW01	6/7/2002	0.540		Tri
26S40E26F01		6/14/1982	0.013		B
26S40E26N02	TTBK-MW02	2/18/2002	0.005	Est	TTEMI
26S40E26N02	TTBK-MW02	8/24/2002	0.014		Tri
26S40E26N02	TTBK-MW02	2/18/2020	0.009	Est	TTEMI
26S40E28J01	USGS-353828117401301	6/29/1978	0.001		B
26S40E28J01	USGS-353828117401301	6/1/1979	0.001		B
26S40E28J01	USGS-353828117401301	5/27/1980	0.008		B
26S40E35H02		8/5/1996	0.040		H96
26S40E36A01	USGS-353801117370701	6/29/1978	0.024		B
26S40E36A01	USGS-353801117370701	6/6/1979	0.013		B
26S40E36A01	USGS-353801117370701	5/27/1980	0.013		B
26S40E36A01	USGS-353801117370701	6/14/1982	0.034		B
26S41E06P01	TTIWV-MW09	2/16/2002	0.022	Est	TTEMI
26S41E06P01	TTIWV-MW09	5/28/2002	0.035	St. Add	Tri
26S41E06P01	TTIWV-MW09	5/28/2002	0.031	St. Add	Tri
26S41E07D01		6/29/1978	0.008		B
26S41E07D01		5/17/1979	0.001		B
26S41E07D01		5/21/1980	0.003		B
26S41E07E01		6/29/1978	0.022		B
26S41E07E01		5/17/1979	0.016		B
26S41E07E01		5/20/1980	0.017		B
26S41E07E01		6/10/1982	0.008		B
26S41E07G01		6/29/1978	0.018		B
26S41E07G01		5/17/1979	0.018		B
27S38E02C02	USBR-02-M	10/30/1990	0.017		USBR
27S38E02C03	USBR-02-D	10/30/1990	0.014		USBR
27S38E23F01	USBR-01-S	3/2/1991	0.010		USBR
27S38E23F02	USBR-01-S/M	3/18/1991	0.010		USBR
27S38E23F03	USBR-01-M/D	3/18/1991	0.010		USBR
27S38E23F04	USBR-01-D	3/18/1991	0.010		USBR
27S39E11D01	USBR-03-S	3/18/1991	0.010		USBR
27S39E11D02	USBR-03-M	3/18/1991	0.010		USBR
27S39E11D03	USBR-03-D	3/18/1991	0.010		USBR
27S40E01G01		5/29/1996	0.090		H96
27S40E02J01	DMP Cemetery	6/28/1978	0.026		B
27S40E02J01	DMP Cemetery	6/1/1979	0.024		B

Compiled IWV Arsenic Data

Unique Well Name	Alternative Well Name	Sample Date	Arsenic (mg/L)	Analysis Type	Arsenic Reference
27S40E02J01	DMP Cemetery	5/23/1980	0.038		B
27S40E03R01	USGS-353630117390901	6/29/1978	0.026		B
27S40E03R01	USGS-353630117390901	6/6/1979	0.013		B
27S40E03R01	USGS-353630117390901	5/27/1980	0.025		B
27S40E03R01	USGS-353630117390901	6/15/1982	0.012		B
27S40E10R01	USGS-353540117390601	6/28/1978	0.003		B
27S40E10R01	USGS-353540117390601	5/28/1980	0.001		B
ITC02-MW21	ITC02-MW21	5/11/1999	0.006	Est	Tri
JMM12-MW08	JMM12-MW08	2/19/2002	0.022	Est	TTEMI
JMM12-MW08	JMM12-MW08	2/19/2002	0.025	Est	TTEMI
MK12-MW12	MK12-MW12	11/12/1999	0.011		Tri
MK12-MW16	MK12-MW16	11/14/1999	0.012		Tri
MK29-MW13	MK29-MW13	2/15/2002	0.028	Est	TTEMI
MK29-MW13	MK29-MW13	2/15/2002	0.025	Est	TTEMI
MK29-MW13	MK29-MW13	6/6/2002	0.047	St. Add	Tri
MK69-MW01	MK69-MW01	11/15/1999	0.087		Tri
MK69-MW01	MK69-MW01	2/18/2002	0.053		TTEMI
MK69-MW01	MK69-MW01	2/18/2002	0.055		TTEMI
MK69-MW02	MK69-MW02	2/18/2002	0.041		TTEMI
MK69-MW02	MK69-MW02	2/18/2002	0.029		TTEMI
MKFL-MW01	MKFL-MW01	2/20/2002	0.058		TTEMI
MKFL-MW01	MKFL-MW01	2/20/2002	0.075	St. Add	TTEMI
MKFL-MW01	MKFL-MW01	4/1/2005	0.348		Tri
MKFL-MW02	MKFL-MW02	2/20/2002	0.023	Est	TTEMI
MKFL-MW02	MKFL-MW02	2/20/2002	0.020	Est	TTEMI
RLS12-MW04	RLS12-MW04	2/19/2002	0.012	Est	TTEMI
RLS12-MW04	RLS12-MW04	2/19/2002	0.015	Est	TTEMI
RLS13-MW05	RLS13-MW05	2/28/1999	0.146		Tri
RLS15-MW03	RLS15-MW03	4/15/1999	0.170		Tri
RLS22-MW08	RLS22-MW08	5/13/1996	0.156		Tri
RLS29-MW01	RLS29-MW01	2/21/1992	0.076		Tri
RLS29-MW01	RLS29-MW01	2/16/2002	0.065	Est	TTEMI
RLS29-MW01	RLS29-MW01	2/16/2002	0.043	Est	TTEMI
RLS43-MW06	RLS43-MW06	4/14/2000	0.343		Tri
TT37-MW01	TT37-MW01	7/11/2001	0.111		Tri
TT37-MW02	TT37-MW02	7/10/2001	0.186		Tri
TT37-MW03	TT37-MW03	7/11/2001	0.173		Tri
TTBK-MW03	TTBK-MW03	8/6/1999	0.074		Tri
TTBK-MW06	TTBK-MW06	2/11/1999	0.002	Est	Tri
TTBK-MW08	TTBK-MW08	2/10/1999	0.017		Tri
TTBK-MW09	TTBK-MW09	5/13/1999	0.089	Est	Tri
TTBK-MW10	TTBK-MW10	8/4/1999	0.024		Tri

Compiled IWV Arsenic Data

Unique Well Name	Alternative Well Name	Sample Date	Arsenic (mg/L)	Analysis Type	Arsenic Reference
TTIWV-MW02-D	TTIWV-MW02 (D)	2/18/2002	0.013	Est	TTEMI
TTIWV-MW02-D	TTIWV-MW02 (D)	2/18/2002	0.018	Est	TTEMI
TTIWV-MW02-I	TTIWV-MW02 (I)	2/18/2002	0.007	Est	TTEMI
TTIWV-MW02-I	TTIWV-MW02 (I)	2/18/2002	0.011	Est	TTEMI
TTIWV-MW04	TTIWV-MW04	2/20/2002	0.035		TTEMI
TTIWV-MW04	TTIWV-MW04	2/20/2002	0.037		TTEMI
TTIWV-MW07	TTIWV-MW07	2/21/2002	0.028		TTEMI
TTIWV-MW07	TTIWV-MW07	2/21/2002	0.031		TTEMI
TTIWV-MW08	TTIWV-MW08	2/18/2002	0.007	Est	TTEMI
TTIWV-MW08	TTIWV-MW08	2/18/2002	0.008	Est	TTEMI
TTIWV-MW10	TTIWV-MW10	2/16/2002	0.022	Est	TTEMI
TTIWV-MW10	TTIWV-MW10	2/16/2002	0.014	Est	TTEMI
TTIWV-MW15	TTIWV-MW15	2/17/2002	0.022	Est	TTEMI
TTIWV-MW16	TTIWV-MW16	2/16/2002	0.010	Est	TTEMI
TTIWV-MW16	TTIWV-MW16	2/16/2002	0.008	Est	TTEMI
	RLS15-MW01	4/13/1999	0.360		Tri
	RLS15-MW02	4/13/1999	0.193		Tri
	VSI15-MW04	4/14/1999	0.058		Tri
	VSI15-MW03	4/15/1999	0.204		Tri
	RLS15-MW04	4/16/1999	0.286		Tri
	VSI15-MW01	4/16/1999	0.221		Tri
	VSI15-MW02	4/16/1999	0.214		Tri
	TTBK-MW11	5/19/1999	0.066		Tri
	RLS03-MW02	5/27/1999	0.018		Tri
	RLS03-MW03	5/27/1999	0.015		Tri
	RLS16-MW01	6/26/1999	0.184		Tri
	RLS17-MW01	6/26/1999	0.196		Tri
	TTBK-MW01	8/5/1999	0.056		Tri
	TTBK-MW05	8/5/1999	0.031		Tri
	TTBK-MW07	8/5/1999	0.004	ND	Tri
	RLS22-MW01	11/12/1999	0.174		Tri

ATTACHMENT R

Groundwater Sustainability Plan: Land subsidence conditions

Steven N. Bacon, P.G., C.E.G., Desert Research Institute, Reno, Nevada
Jenny Chapman, Desert Research Institute, Las Vegas, Nevada

I. Subsidence Environment

I.1 Aquifer materials and conditions in IWV

The Indian Wells Valley (IWV) groundwater basin includes up to about 610 m of water-bearing valley fill originating primarily from the Sierra Nevada Mountains. The valley fill consists of interbedded clay, silt, sand, and gravel deposited in alluvial, fluvial, and lacustrine environments typical for basins in the "Basin and Range Province" of the western United States (Fig. 1). Four general hydrogeologic units have been identified in the IWV groundwater basin, corresponding to unconsolidated sediment deposited in alluvial, lacustrine, playa, and sand dune environments, and these are underlain and bounded by consolidated and indurated basement rock (e.g., Kunkel and Chase, 1969, McGraw et al., 2016). The unconsolidated hydrogeologic units have variable degrees of permeability and are distributed across the valley based on their depositional environments. The distribution and depths of the hydrogeologic units are also structurally controlled by faults. The characteristics of the four hydrogeologic units in the IWV groundwater basin are summarized below from previous studies (e.g., Kunkel and Chase, 1969; Berenbrock and Martin, 1991; McGraw et al., 2016):

- The "alluvial hydrogeologic unit" (i.e., coarse-grained sediment) consists of interbedded, moderately to well-sorted gravel, sand, silt, and clay of Pleistocene and Holocene age having relatively high permeability. The percentage of interbedded silt and clay layers increase towards the depocenter of China Lake playa and commonly form thin and discontinuous aquitards of reduced relative permeability. These sediments include both older and younger alluvium, alluvial fan, and stream terrace deposits, plus elevated pediments (i.e., eroded bedrock). Alluvium extends across the IWV groundwater basin and is thickest along the westerly and southerly edges of the IWV groundwater basin along the range-front of the Sierra Nevada and low relief hills, respectively.

- The “lacustrine hydrogeologic unit” (i.e., fine-grained sediment) includes relatively thick deposits of silt and silty clay of Pleistocene age that have low permeability. The lacustrine unit is underlain by alluvium and is interbedded with deeper alluvium in the central portion of the basin. The extent of the clayey lacustrine unit coincides with the depocenter of China Lake basin and past water levels of China Lake and high stands of coalesced China-Searles Lake during the Pleistocene (Fig. 2).

- The “playa hydrogeologic unit” (i.e., fine-grained sediment) consists of low permeability silt and clay deposits with minor thin sand lenses of Holocene age.

- The “sand dune hydrogeologic unit” (i.e., coarse-grained sediment) is composed of surficial windblown sand deposits and/or fan delta deposits of Holocene to late Pleistocene age. This unit is typically less than about 30 m thick and occurs above the water table, thereby being unsaturated.

Cross sections developed by Kunkel and Chase (1969) across the IWV groundwater basin show the distribution and thickness of highly permeable alluvial gravel and interbedded alluvial (clay to gravel) hydrogeologic units at, and near, the land surface along the westerly and southerly margins of the IWV groundwater basin, as well as the extent and thickness of low-permeability lacustrine and playa hydrogeologic units near the center of the valley (Fig. 3). In addition, the westerly and southerly lateral margins of the lacustrine hydrogeologic unit are either in fault contact (Transects B-B’ and C-C’; Figs. 2 and 3) or form a facies sequence (i.e., interfinger relation) between overlapping and wedged shaped alluvial and lacustrine layers associated with Pleistocene paleolake fluctuations (Transect A-A’; Figs. 2 and 3).

I.2 Susceptibility of aquifer materials to subsidence

The weight of materials overlying an aquifer (e.g., sediment, water, vegetation, and structures on the land surface) is supported within an aquifer system by both the water in the pore spaces and by the clay, silt, sand, and gravel that form the granular mineral skeleton of the aquifer. When pumping lowers groundwater levels and thus fluid pressure in the pores (i.e., pore pressure), the weight of overlying materials must be increasingly supported by the mineral skeleton of the aquifer. Consequently, the increased pressure or stress on the mineral grains (i.e.,

effective stress) is equal to the support lost by decreased pore pressure. Increased effective stress may cause some compression of the aquifer system skeleton and, if the stresses are large enough, then some compaction of the aquifer system may occur. The cumulative result of the aquifer response to compaction over the full thickness of the aquifer system is expressed as subsidence at the land surface (e.g., Galloway et al., 1999; Borchers and Carpenter, 2014; Faunt et al., 2015) (Fig. 4). Aquifer-system deformation can range from fully reversible (elastic) to largely permanent (inelastic). Elastic deformation occurs when sediments compress as pore pressure decreases, and expand equally as pore pressure increases. The consequent cycles of subsidence and rebound of the land surface commonly occur seasonally, coincident with cyclic groundwater discharge and recharge. The compressibility of clayey aquitards typically is several times larger than that of coarser-grained aquifers.

Elastic deformation does not permanently alter the water storage properties of an aquifer, that is, the same volume of water can be stored in an aquifer after many cycles of solely elastic compression and expansion. If water-levels decline over large areas, broad and shallow (about 8 cm-deep) subsidence bowls commonly form at the land surface, but then soon disappear when water-levels recover and land surface rebounds. The rebound occurs because the aquifer system has not been permanently reconfigured into a denser, more closely packed arrangement (e.g., Borchers and Carpenter, 2014).

In contrast, permanent compaction results when the sediments are compressed inelastically beyond their previous maximum effective stress (pre-consolidation stress). Pre-consolidation stress is the effective stress threshold at which inelastic compaction begins, and generally is exceeded when groundwater levels decline past historical low levels. At these stress ranges, the materials compress inelastically, and the inelastic compaction and consequent land subsidence are largely permanent and irreversible. Because silt- and clay-rich sediment are often highly compressible and subject to rearrangement of grains, depressurization results in more compaction and land subsidence in fine-grained deposits than depressurization of less compressible, coarser-grained deposits of sand and gravel (Galloway et al., 1999; Borchers and Carpenter, 2014; Faunt et al., 2015).

The hydrogeologic units in the IWV groundwater basin have variable degrees of susceptibility to compaction. The inelastic compaction of the coarse-grained alluvial hydrogeologic units generally is negligible unless very large decreases in pore pressure increase effective stress to levels that fracture mineral grains (such as what occurs in oil and gas fields;

e.g., Galloway et al., 1999), which is unlikely to occur in the IWV groundwater basin. In contrast, the fine-grained lacustrine and playa hydrogeologic units, as well as the fine-grained aquitard interbeds in the alluvial hydrogeologic units, are prone to inelastic compaction. As a result, the land surface in areas underlain by the extensive fine-grained hydrogeologic units have high to very high susceptibility to land subsidence when the groundwater table is lowered below historically low levels (e.g., Fig. 4). Furthermore, the relative magnitude of potential land subsidence across the IWV groundwater basin is not expected to be uniform because of the heterogeneous nature of the alluvial hydrogeologic unit, overlapping lateral margins between the alluvial and lacustrine hydrogeologic units, and abrupt fault contacts. As a result, there is also high to very high susceptibility to differential land subsidence (i.e., subsidence occurring at different rates) across the valley.

I.3 Tectonic setting and implications for subsidence

The IWV groundwater basin is located within a tectonically active area of California referred to as the northern Eastern California shear zone or southern Walker Lane (e.g., Dokka and Travis, 1990; Monastero et al., 2002; Wesnousky, 2005). The valley floor of IWV is cross-cut by a northerly trending mosaic of fault segments with a wide-range of fault activity that merge towards the north with the Sierra Nevada frontal fault system and Coso volcanic center (e.g., Hauksson et al., 1995) (Fig. 5). The active faults in the valley include the Little Lake fault zone (LLFZ) and Airport Lake fault zone (ALFZ) (Bryant and Hart, 2007). The LLFZ is considered the principal fault system in the IWV and is characterized as an oblique, right-lateral (horizontal) fault with down-to-the-east normal (vertical) displacement, whereas the ALFZ is an oblique, right-lateral fault with down-to-the-west normal displacement that bifurcates from LLFZ in the north-central part of the IWV (Zellmer and Roquemore, 1997) (Fig. 5). Both fault zones are expressed at the surface as a distributed zone of short, en echelon scarps that have experienced two historical ground-rupturing earthquakes, the first in 1982 and the second in 1995 (Fig. 5). Although the surface rupture traces were relatively short (about 2 to 3 kilometers (km)) showing little displacement, they were associated with earthquakes with magnitudes (M) of up to M 4.9 and 5.4, respectively (Hauksson et al., 1995). Recently, significant ground rupture events on July 4 and 5, 2019 occurred during the M6.4 and M7.1 Searles Valley and Ridgecrest earthquakes, respectively. The main M7.1 earthquake rupture occurred in the eastern sector of China Lake basin and defined a broad zone of distributive faulting associated with the LLFZ and

ALFZ system (Fig. 5). In addition to the active LLFZ and ALFZ, a northerly trending series of unnamed fault segments that cross the eastern margin of El Paso Valley within the southwestern sector of the groundwater basin are mapped having an activity of less than 15,000 years (USGS, 2016) (Fig. 5). The zone of unnamed faults are informally referred to as the El Paso fault (EPF). The surface expression of the EPF appears as a well-defined fault lineament with vertical east-side-down separation that displaces a broad and relatively older alluvial fan associated with the axial drainage of El Paso Valley. All of these faults collectively control groundwater levels in the IWV groundwater basin by acting as groundwater barriers (Garner et al., 2017).

In general, land subsidence primarily, can occur as a result of groundwater extraction, but can also result from collapse of underground cavities, tectonic activity, natural consolidation of sediment, oxidation and compaction of organic deposits, hydrocompaction of moisture deficient soil and sediments, development of geothermal energy, and extraction of hydrocarbons (Borchers and Carpenter, 2014). The IWV is located in a tectonically and volcanically active area of California. Consequently, it is prudent to consider the tectonic effects on the land surface elevation in subsiding areas when evaluating subsidence in alluvial basins related to groundwater production. In contrast to other groundwater basins in the Mojave Desert that have a relationship between groundwater production and land subsidence (e.g., Motts et al., 1969; Galloway et al., 1999; Stamos et al., 2001, 2007; Sneed et al., 2003; Solt et al., 2014), the IWV groundwater basin is crossed by the active LLFZ and ALFZ and has experienced historical ground rupturing earthquakes (e.g., 1982, 1995, 2019) and continuous seismic activity. As a result, the hydrogeologic setting of the IWV groundwater basin is relatively more complex than most other groundwater basins in the western U.S. (e.g., Motts et al., 1969), and interpretation of observed land subsidence across the groundwater basin needs to be made in the context of a seismically active basin to differentiate between land subsidence from groundwater production and from tectonic activity.

II. Historical Observations of Subsidence

II.1 Public observations of valley subsidence

Historical information from anecdotal reports has been used in California to provide estimates of the location and magnitude of land subsidence due to groundwater extraction prior to extensive land-subsidence monitoring (e.g., Borchers and Carpenter, 2014). Isolated areas of land subsidence associated with early agricultural groundwater pumping were observed through

the 1970s in the greater Ridgecrest area. Two specific areas of land subsidence were observed centered at the old Bowman Ranch (near presented day Walmart) and in the vicinity of North Brown Road between Leliter and Neal Ranch Roads. These isolated areas of subsidence are reported to be evident today in the form of about 0.5 mi diameter depressions that are nearly 15 ft below the surrounding ground level (these depressions require greater vertical resolution than current 2-meter digital elevation models to observe). Additional evidence for the magnitude of subsidence in the two areas is from several groundwater pump wells that showed well-head protrusion (Don Decker, 2019, personal commun.). The isolated areas of subsidence coincide with an extensive organic-rich clay that is about 1600 ft thick and located west of the LLFZ (Don Decker, 2019, personal commun.). The organic-rich clay unit was commonly observed during well construction in the area, however, the clay unit was not included in the Kunkel and Chase (1969) hydrogeologic cross sections of the IWV groundwater basin. These anecdotal accounts of subsidence associated with groundwater pumping demonstrate that land subsidence from groundwater extraction has historically occurred in the IWV groundwater basin.

II.2 Level-line surveys showing tectonic ground deformation

In some seismically active areas, ground deformation is commonly associated with discrete movements on faults during coseismic slip (i.e., slip during earthquake) or interseismic creep (i.e., slip during no earthquakes). The area of IWV that the LLFZ and APFZ cross is actively deforming based on historical surface rupturing events, as well as from land-based geodetic data from repeat, high-resolution level-line surveys of the 6.55-km (4.07-miles (mi)) long Supersonic Naval Ordnance Research Track (SNORT) alignment within Naval Air Weapons Station China Lake (NAWSCL) (Zellmer and Roquemore, 1997) (Fig. 5). The style and magnitude of historical surface deformation of the SNORT alignment reflects complex fault geometry between the LLFZ and ALFZ, and an underlying shallow (about 3-km deep) magma body. The intersection of the LLFZ and ALFZ occurs about 2.1 km (1.3 mi) east of the northern end (muzzle end) of SNORT. Here, the LLFZ exhibits a large left-step and forms a localized graben (pull-apart basin) that distributes strain in a northwest-southeast direction, whereas the western ALFZ bifurcates to the north and transfers strain along the eastern margin of the graben (Fig. 5). The dominant style of coseismic deformation within the left-step during surface rupturing events is permanent surface subsidence, whereas interseismic deformation is reflected by cyclic strain accumulation in the form of uplift (Zellmer and Roquemore, 1997).

Active ground deformation attributed to cyclic strain accumulation up to about 50 millimeters (mm) of uplift (positive values) and up to about 40 mm of subsidence (negative values) near the LLFZ is shown by geodetic level-line surveys of the SNORT alignment from five survey intervals between 1952 and 1986 (Zellmer and Roquemore, 1997) (Fig. 6). The elevation differences between the surveys were computed as relative elevation changes along the track based on a fixed elevation of the initial survey's base station at the south end of SNORT (monument SF-0). This procedure removes the complications resulting from local and regional elevation changes, as well as possible surveying errors in determining absolute elevations of SF-0 over the period of record (Zellmer and Roquemore, 1997). The use of relative elevation survey data also resolves only ground deformation associated with tectonic deformation. The data demonstrates that the intervals of time with no seismic activity (i.e., interseismic periods) are predominantly characterized by uplift of the northern half of the alignment closest to the LLFZ, whereas the intervals of time between surveys that had seismic activity (i.e., coseismic periods) are mostly characterized by subsidence in the same general area (Zellmer and Roquemore, 1997) (Fig. 6). The observed ground deformations that occurred between the 1957 and 1977 surveys and the 1978 and 1984 surveys resulted from mostly tectonic stress buildup and subsequent release associated with approximately M5 earthquakes near SNORT in 1961 and 1982 (Fig. 6).

Evaluation of SNORT survey data for the period 1986–2000 was performed in this study to extend the period of record by 14 years. High-resolution, differential global positioning system (GPS) data acquired in 4 October to 6 November, 2000 by NAWSCL was compared with SNORT survey data collected in 1986 using the same methods of Zellmer and Roquemore (1997). To resolve the data to be fixed to the SNORT base station (SF-0), an offset of +33.7 mm was applied. This offset, and perhaps other offsets previously used by Zellmer and Roquemore (1997), could be a signal of land subsidence associated groundwater-related compaction of aquifer materials or errors between individual survey methods that included ground-based geodetic techniques and more recently GPS. Comparison of the relative elevation changes for the 1986–2000 dataset, however, shows similar trends with previous survey intervals where there was a large tectonic stress buildup during the period 1984–1986 and subsequent release associated with the 1995 M5.4 Ridgecrest earthquake sequence that was centered within the ALFZ northeast of SNORT in China Lake basin (Fig. 7).

II.3 InSAR data showing ground deformation from seismicity and groundwater production

Ground deformation at a valley-wide scale within the IWV groundwater basin has been previously characterized for the periods 1992–2000 and 2005–2010 using satellite-based Interferometric Synthetic Aperture Radar (InSAR) techniques (Peltzer et al., 2001; Katzenstein, 2013; 2015). The InSAR data analyzed between 1992 and 2000 shows three discrete areas of subsidence that correspond with the locations of seismic activity and mapped faults, geothermal production, and fine-grained aquifer materials (Fig. 7). Two of the three areas of subsidence in the IWV groundwater basin include a locus of subsidence within the depocenter of China Lake basin referred to as the northern subsidence area (SB N) and a locus of subsidence in the greater Ridgecrest area referred to as the southern subsidence area (SB S) (Fig. 7). In addition, the third locus of subsidence overlaps with the northern groundwater model domain boundary in the vicinity of the Coso geothermal field (COSO; Fig. 7). The extent of subsidence in the northern subsidence area and Coso geothermal field was previously identified by Peltzer et al. (2001) to correspond with the epicenters of the M5.4 Ridgecrest earthquake sequence beginning on 17 August 1995 and with the Coso volcanic center, respectively (e.g., Hauksson et al., 1995). The northern subsidence area shows the greatest amount of surface change during the period 1992–2000 with up to 35 to 38 mm of subsidence (Fig. 7). The extent of subsidence in the southern subsidence area near Ridgecrest was identified by Katzenstein (2015) to have up to 20 to 25 mm of subsidence that appeared to be associated with the surface trace of the LLFZ and ALFZ, and bounded by northwesterly striking bedrock faults (Fig. 7).

The InSAR data evaluated from 2005 to 2010 shows an example of 5 years of surface change during a period with no significant seismic activity. The area of the Coso geothermal field had the greatest amount of surface change during the period 2005–2010 with up to about 20 to 24 mm of subsidence (Coso; Fig. 8). The northern subsidence area (SB N) during this period shows mostly negligible to slightly positive surface change within the area of the 1995 Ridgecrest earthquake sequence. The southern subsidence area (SB S), however, exhibited continued subsidence of up to 10 to 15 mm that was narrowly distributed along the southern LLFZ and bounded by bedrock faults similar to the earlier period (Fig. 8).

The broad distribution of surface change from the InSAR analysis appears to show cyclic strain accumulation within the IWV groundwater basin similar to the geodetic survey data measured along the SNORT alignment in areas proximal to faults and earthquake epicenters.

During the period 1992–2000, the area where the ALFZ bifurcates from the LLFZ near the northern end of the SNORT alignment shows mostly negative surface change (subsidence), indicating the occurrence of a tectonic stress drop in this area during the 1995 Ridgecrest earthquake sequence (Fig. 7). The same area during the period 2005–2010, however, shows relatively less negative surface change, indicating tectonic stress buildup during 15 years after the earthquake sequence (Fig. 8). In contrast, the southern subsidence area (SB S) during the period 2005–2010 shows continued subsidence that is more narrowly distributed than during the 1992–2000 period with the Ridgecrest earthquake (Figs. 7 and 8). This indicates processes not entirely associated with tectonic cyclic strain accumulation.

An evaluation of how surface change is distributed along a about 6.55-km transect was performed by intersecting the InSAR data for the periods 1992–2000 and 2005–2010 with the location of monuments along the SNORT alignment to better understand cyclic strain accumulation associated with faults in the IWV. The georeferenced points of each SNORT monument along the alignment were intersected with the InSAR raster datasets using ArcGIS to determine the magnitude of surface change during the two periods at monument sites. Direct analysis between the SNORT level-line surveys and InSAR data cannot be made because the SNORT data are processed as relative elevation changes to identify only tectonic deformation. The absolute elevations of the base station F0 reported in the 1986 and 2000 surveys, however, were used to measure surface change for the period 1986–2000 to compare with InSAR measurements. The results of the analysis show subsidence of up to 10 and 11 mm during the 1992–2000 and 2005–2010 periods, respectively. This resulted in up to 20.5 mm of cumulative subsidence along the SNORT alignment from 1992 to 2010, which is considered a minimum because a 5-year gap was not analyzed between 2000 and 2005 (Fig. 9A). In addition, the absolute elevation difference of the SNORT base station F0 shows that 8.8 mm of subsidence occurred between 1986 and 2000 at the south end of the alignment, which is similar to the 10 mm estimate from InSAR for the period 1992–2000. (Fig. 9A) The 8.8 and 10 mm subsidence values are likely within the uncertainties of the ground- and satellite-based survey methods, respectively, thereby providing confidence in both types of measurements.

Estimates of the rate of subsidence during the two periods from the InSAR data and the absolute elevations of the SNORT base station F0 during 1986–2000 were also made to characterize land subsidence in the area. The rate of subsidence along the SNORT alignment has increased over the period between 1986 and 2010. Rates of subsidence during the 2005–2010

period range from up to 2.2 mm/yr in the south end to 1.3 mm/yr at the north end of the alignment (Fig. 9B). Furthermore, the effects of cyclic strain release reflected by subsidence during 1992–2000 and accumulation in the form of rebound during 2005–2010 following the 1995 Ridgecrest earthquake sequence is also evident in the InSAR data. This supports the Zellmer and Roquemore (1997) model of tectonic deformation associated with the LLFZ at the northern end of the SNORT alignment from repeat, high-resolution level-line surveys (Fig. 9).

II.4 Spatiotemporal correspondence between simulated groundwater-level and InSAR land-surface changes

An evaluation of groundwater drawdown and InSAR datasets was performed in this study to characterize potential spatiotemporal correspondence between groundwater level and land surface changes across the IWV groundwater basin. Simulation of drawdown from the IWV groundwater model (McGraw et al., 2016; Garner et al., 2017) were compared to InSAR datasets (Katzenstein, 2015) for the periods 1992–2000 and 2005–2010. The evaluation also included the location of faults used in the groundwater model and the extent of the clay-rich lacustrine/playa unit, along with the location of wells with greater than 900 acre-feet of production during each period noted above (Figs. 10 and 11). Collectively, all the data were used to examine potential explanations for non-tectonic subsidence in IWV.

Simulated drawdown during the period 1992–2000 shows three primary cones of depression with 5 to 10 ft of groundwater lowering. The southern cones of depression coalesce in areas of the LLFZ and southern subsidence area (Fig. 10). The effects of ground rupture and seismicity from the 1995 Ridgecrest earthquake is widely distributed in the northern subsidence area with corresponding simulated drawdown of less than 1 ft. The southern subsidence area, however, shows 10 to 25 mm of subsidence in areas with about 5 to 8 ft of drawdown (Fig. 10). In addition, the distribution of subsidence of 0.5 to 1.0 mm closely corresponds with the southwestern cone of depression with up to 10 ft of simulated drawdown (Fig. 10).

Simulated drawdown during the period 2005–2010 was relatively less in the southern subsidence area compared to the earlier period, and the distribution of subsidence of 10 to 15 mm is narrow (Fig. 11). Simulated drawdown during this period shows 3 to 8 ft of groundwater lowering at two well-defined cones of depression and two areas with poorly defined areas of drawdown. Three of the four drawdown features are located outside the southern subsidence area (Fig. 11).

Simulated drawdown for the entire period 1992–2010 displays two primary cones of depression with 18–28 ft of groundwater lowering in areas northwest and southwest of the southern subsidence area (Fig. 12). The area of the Coso geothermal field along the northern groundwater model domain boundary had the greatest amount of surface change during the period 1992–2010 with up to 40 to 46 mm of subsidence. The southern subsidence area had the second highest cumulative amount of surface change measured in IWV between 1992 and 2010 with up to 35–40 mm of subsidence that corresponded with 10–18 ft of simulated drawdown (Fig. 12). The magnitude of subsidence measured in the northern subsidence area is attributed to the 1995 Ridgecrest earthquake sequence with corresponding simulated drawdown of less than two ft. The magnitude and extent of measured subsidence on the northeastern boundary of the southern subsidence area appears to be controlled by the southern margin of the clay-rich unit and location of the LLFZ. In addition, the southwestern boundary of the southern subsidence area appears to parallel nearby bedrock faults and the distribution of densely placed wells with variable production volumes of 4,000 to 20,000 acre-feet during the period 1992–2010 (Figs. 7 and 12).

Georeferenced points of production wells were intersected with the InSAR raster datasets using ArcGIS to determine the magnitude of potential surface changes in areas of drawdown from groundwater production. Plots were constructed that show the elevation of simulated drawdowns on the primary y-axis and surface change on the secondary y-axis versus the year during the period of the model simulation from 1920 to 2017. The InSAR surface change values for the periods 1992–2000 and 2005–2010 are plotted on the x-axis as the midpoint for each time interval (e.g., 1996 and 2007.5, respectively). There is apparent temporal correspondence between the magnitude of simulated drawdown and land-surface changes at the well sites. A subset of three wells (Wells 8, 18, and 26) were used to show relations between drawdown and land surface change in different hydrogeologic settings relative to the southern subsidence area (Fig. 12). The wells have been categorized into sites that are: (1) proximal to faults within the southern subsidence area (Fig. 13); (2) in areas with greater than 20,000 acre-feet of groundwater pumping (Fig. 14); and (3) in areas with agriculture along the Sierra Nevada range front (Fig. 15).

Well 26 is situated on the boundary of the southern subsidence area within distal alluvial fans and playa margins (Fig. 12). Areas of the well 26 site have had up to about 58 ft of groundwater lowering over the past about 100 years (Fig. 13). In addition, there has been up to

about 12 ft of simulated drawdown and 19.0 mm of total subsidence at the well site during the period 1992–2010 (Fig. 13). The rate of subsidence at the well 26 site during this period is 1.1 mm/yr. This subsidence rate corresponds to variable rates of groundwater lowering ranging from about 80 mm/yr between 1992 and 2010 to about 396 mm/yr between 2000 and 2007.5 (Fig. 13).

Well 18 is situated outside of the western boundary of the southern subsidence area and is the site of greater than 20,000 acre-feet of groundwater production during the period 1992–2010 (Fig. 12). The well 18 site is also adjacent to other wells that produced groundwater greater than 4,000 and up to 20,000 acre-feet on medial to distal alluvial fans. Areas of the well 18 site have had up to about 70 ft of groundwater lowering over the past about 100 years. In addition, there has been up to about 18 ft of simulated drawdown and 16.1 mm of total subsidence at the well site during the period 1992–2010 (Fig. 14). The rate of subsidence at the well 18 site during this period is 0.9 mm/yr. The subsidence rate corresponds to a nearly constant rate of groundwater lowering of about 300 mm/yr between 1992 and 2010 (Fig. 14).

Well 8 is situated outside of the southern subsidence area and is the site of groundwater production of greater than 10,000 acre-feet during the period 1992–2010 (Fig. 12). The well 8 site is also adjacent to numerous wells that produced groundwater greater than 10,000 acre-feet in agricultural areas on medial to distal alluvial fans along the Sierra Nevada range front. Areas of the well 8 site have had up to about 68 ft of groundwater lowering over the past 100 years with most production beginning in the mid-1970s (Fig. 15). In addition, there has been up to about 19 ft of simulated drawdown and 5.0 mm of total subsidence at the well site during the period 1992–2010 (Fig. 15). The rate of subsidence at the well 8 site during this period is 0.3 mm/yr. The subsidence rate corresponds to a nearly constant rate of groundwater lowering of about 322 mm/yr between 1992 and 2010 (Fig. 15).

II.5 Subsidence modeling with MODFLOW

Potential subsidence in the IWV groundwater basin were previously estimated using the IWV groundwater model of McGraw et al., (2016). Simulations of subsidence were made with the Subsidence and Aquifer-System Compaction Package for Water-Table Aquifers in the USGS MODFLOW groundwater program. The results of the simulations were compared to the distribution of InSAR surface change of Katzenstein (2015). Comparisons between the two datasets yielded moderate to poor spatiotemporal correspondence because the MODFLOW simulations showed greater areas of subsidence than the measured amounts in the area west of

the southern subsidence area. McGraw et al. (2016) attribute the disparity to large uncertainty in parameterization of the subsurface properties. Specifically, the location and compressibility of the fine-grained interbeds within the alluvial hydrogeologic unit are largely unknown. Therefore, the distribution of specific yield in the upper aquifer layer in the MODFLOW groundwater model was used as a general indicator of compressibility for the calibration process. Furthermore, during this initial stage of the development of the IWV groundwater model, faults were not included in the model. The newer version of the IWV groundwater model (Garner et al., 2017) now includes faults, which may produce different results if subsidence modeling was to be performed again.

III. Assessment of Subsidence in Indian Wells Valley

III.1 Summary of rate, extent, and likely cause of historically observed subsidence

The hydrogeologic information, high-resolution level-line surveys of the SNORT alignment, InSAR remote sensing data, and simulated drawdown are integrated to assess subsidence in the IWV groundwater basin. Previous studies of the hydrogeology of IWV describe extensive fine-grained sediment in the central part of the valley in fault contact with the active Little Lake fault zone (LLFZ) and other bedrock faults, whereas discontinuous, interbedded fine-grained layers are present within alluvial sediment west of the LLFZ. These fine-grained layers have high to very high susceptibility to compaction when groundwater levels are lowered below historical levels. Ground- and satellite-based techniques have previously been used to measure land surface change across IWV. Site-specific, ground-based level-line surveys along the SNORT alignment at NAWSCL show active tectonic ground deformation in areas nearest to the LLFZ from cyclic strain accumulation of as much as about 50 mm of uplift and about 40 mm of subsidence between 1952 and 2000.

IWV-wide surface changes have also been documented based on remote sensing techniques for the periods 1992–2000 and 2005–2010. The InSAR analysis showed up to –38 and +64 mm of surface change between 1992 and 2000, as well as up to –24 to +19 mm between 2005 and 2010. The InSAR analysis measured two loci of subsidence near Ridgecrest, a northern subsidence area associated with the 1995 Ridgecrest earthquake sequence and a southern subsidence area in the vicinity of the southern LLFZ, bedrock faults, and production wells. The southern subsidence area during the 1992–2000 period had up to 25 mm of subsidence with a corresponding rate of 3.1 mm/yr. The same general area during the 2005–2010 period had up to

15 mm of subsidence with a corresponding rate of 3.0 mm/yr. The different periods of InSAR measurement yielded similar subsidence rates in the southern subsidence area even with the occurrence of the 1995 Ridgecrest earthquake sequence during the earlier period and relatively less groundwater drawdown during the latter period. The southern subsidence area also had the highest total amount of surface change compared to areas affected by the 1995 Ridgecrest earthquake sequence with up to 35 to 40 mm of subsidence that corresponded with 10 to 18 ft of simulated groundwater drawdown during the 1992–2010 period. The subsidence rate of the southern subsidence area over the entire 18-year period is up to 2.2 mm/yr.

The spatiotemporal distribution of the InSAR surface change was previously interpreted by Katzenstein (2013; 2015) to be controlled by the location of faults and historical seismicity, plus groundwater production. Additional analysis of the InSAR dataset with other information also indicates the southern subsidence area is geologically controlled by bounding conditions that include the southern margin of a clay-rich hydrogeologic unit and southern LLFZ on the northeast and a linear field of production wells and bedrock faults on the southeast.

Analysis of InSAR data along the SNORT alignment confirmed cyclic strain accumulation from tectonic processes, but showed the SNORT alignment has also been affected by non-tectonic subsidence. Measurements indicate that the magnitude and rates of subsidence in areas of SNORT have increased over the period between 1986 and 2010 with the largest values along the southern end of the alignment. InSAR measurements along the southern alignment show up to 20.5 mm of cumulative subsidence between 1992 and 2010. In addition, subsidence rates increased from up to 2.2 mm/yr in the south end to 1.3 mm/yr at the north end of the alignment during the 2005–2010 period. The south to north decreasing gradient of subsidence coincides with the northwest margin of the southern subsidence area and a northward migrating cone of depression from production wells west and south of SNORT from simulations of drawdown from the IWV groundwater model (e.g., McGraw et al., 2016; Garner et al., 2017).

The southern locus of subsidence is primarily in an area with no production wells in the immediate vicinity. Most of the production wells in IWV are located outside the area with the highest subsidence. It is likely that the locus of subsidence has developed from compaction of the thickly interbedded fine-grained lacustrine hydrologic units between coarse-grained alluvial units. Furthermore, the spatial configuration of the subsidence area also appears to be structurally controlled by two northwest-striking bedrock faults that are bisected by the active LLFZ. The structural configuration of these faults control the local flow paths by producing groundwater

barriers based on simulations of groundwater drawdown. Given these factors, the southern subsidence area appears to be associated with differential compaction of a laterally extensive and fault bounded interbedded clay-rich hydrogeologic unit experiencing drawdown from groundwater production areas to the west. In addition, historical seismicity and moderate M5 earthquakes could have also produced some of the measured subsidence in IWV by producing soft-sediment deformation and compaction of previously dewatered fine-grained aquifer materials. Continued subsidence in the southern subsidence area during the period 2005–2010 at a similar subsidence rate of ~3 mm/yr compared to the earlier period that included the 1995 Ridgecrest earthquake implies processes not entirely associated with tectonic ground deformation.

III.2 Risk of groundwater withdrawal-related subsidence in Indian Wells Valley

Sustained groundwater production in current areas will continue to lower water levels. The greater Ridgecrest area, especially in the vicinity of the southern subsidence area, have high to very high susceptibility to land subsidence because of the hydrogeologic and tectonic setting of IWV. With continued groundwater withdrawal, the spatial extent of aquifer materials that are prone to compaction will increase. This in turn will increase the risk of environmental consequences from significant or unreasonable land subsidence caused by compaction of aquifer systems. Some of the more costly consequences include damage to engineered structures, such as buildings, bridges, roadways, runways, sewerages, and well casings (Hoffman et al., 2003; Borchers and Carpenter, 2014). The magnitude of "significant or unreasonable" land subsidence depends on the engineered structure of concern. The above examples have a wide-range of allowable tolerances of vertical and horizontal displacements. It's only when the allowable tolerances are exceeded that the risk of damage increases.

The magnitude of land subsidence during the period 1992–2010 ranged from 0 to 0.5 to 35 to 40 mm in the vicinity of production wells and simulated cones of depression in the greater Ridgecrest area. The magnitudes of land subsidence during the 18-year period corresponded to subsidence rates of up to 2.2 mm/yr. In comparison to other areas in California, such as the San Joaquin Valley that had subsidence rates in excess of about 300 mm/yr (1 ft/yr) related to groundwater extraction (e.g., Borchers and Carpenter, 2014), the magnitude of subsidence and associated rates measured in IWV is relatively small.

III.3 Land subsidence monitoring in Indian Wells Valley

Land subsidence monitoring in groundwater basins of the Mojave Desert is commonly used to determine the location, extent, and magnitude of vertical land surface changes associated with groundwater extraction for domestic, agricultural, and municipal water supplies. Common land monitoring techniques include ground-based level-line surveys and space-based GPS and InSAR measurements (e.g., Sneed et al., 2003). In addition, subsurface methods including borehole extensometers are commonly used to directly quantity aquifer compaction by measuring the continuous change in vertical distance between the land surface and a subsurface reference point in the borehole (e.g., Borchers and Carpenter, 2014). The methods previously used in IWV to monitor potential land surface changes associated with groundwater extraction included level-line surveys at the SNORT alignment and InSAR surveys during 1992–2000 and 2005–2010. Possible future monitoring approaches could also include additional SNORT and InSAR surveys, as well as developing a GPS monitoring network that is integrated with established survey benchmarks and continuous GPS stations. The surveying effort can be made in coordination with NAWSCL since there is a long history of repeat measurements of numerous survey bench marks on base.

Nearly 10 years have passed since the last analysis of SNORT and InSAR survey data. Since this time, there has been continued groundwater extraction and the occurrences of the July 2019 M6.4 and M7.1 Searles Valley and Ridgecrest earthquakes that produced large surface ruptures and severe seismic shaking in the IWV groundwater basin. Additional land surface monitoring in areas of the southern subsidence area and production wells in lieu of continued groundwater lowering and recent seismic activity since 2010 will provide additional data to better understand the land subsidence potential in the greater Ridgecrest area associated with either tectonic or non-tectonic process, which in turn can be used to assist in making informed decisions of the water resources of the IWV groundwater basin. The California DWR in cooperation with NASA have recently published InSAR analyses between 6/13/2015 and 3/1/2018 - 6/1/2018 for high-use and populated groundwater basins across California, including the IWV groundwater basin. The InSAR analysis shows the total vertical displacement across the IWV groundwater basin ranged from -0.25 to 0.25 feet during this period. The DWR InSAR analysis, however, is processed at 100 m resolution, compared to the 50 m resolution InSAR survey data used between 1992–2000 and 2005–2010 in this study; and the DWR categories of total vertical displacement are categorized at 0.25 feet intervals. As a result, the DWR analysis is

too coarse of resolution to identify the spatiotemporal changes of land subsidence associated with either tectonic or non-tectonic processes. The DWR analysis does demonstrate that the magnitude of subsidence across the groundwater basin between 6/13/2015 and 3/1/2018 - 6/1/2018 has been no more than -0.25 feet.

References

Borchers, J. W., and Carpenter, M. (2014). Land subsidence from groundwater use in California, Full Report of Findings, report, California Water Foundation, 151 pp.

Bryant, W.A., and Hart, E.W. (2007). Fault rupture hazard zones in California: Alquist-Priolo earthquake fault zoning act with index to earthquake fault zones maps. California Geological Survey Special Publication 42, 42 p.

Bullard, T.F., Bacon, S.N., Adams, K.D., and Decker, D.L., 2018. Phase II: Geomorphic map of China Lake basin below 700 m in support of cultural resource management at NAWS China Lake. Final report prepared for Naval Air Warfare Center, Weapons Division by Naval Earth Sciences and Engineering Program, Desert Research Institute. Dated October 12, 2018, 31 p. plus appendices.

Danskin, W.R. (1998). Evaluation of the hydrologic system and selected water-management alternatives in the Owens Valley, California: U.S. Geological Survey Water-Supply Paper 2370-H, 175 p.

Dokka, R.K., and Travis, C.J. (1990). The role of the Eastern California shear zone in accommodating Pacific–North American plate motion. Geophysical Research Letters 17, 1323–1326.

dePolo, C.M., Clark, D.G., Slemmons, D.B., and Ramelli, A.R. (1991). Historic surface faulting in the Basin and Range Province, western North America: Implications for fault segmentation. Journal of Structural Geology 13, 123–136

Faunt, C.C., Sneed, M., Traum, J., and Brandt, J.T. (2015). Water availability and land subsidence in the Central Valley, California, USA. Hydrogeology Journal, DOI 10.1007/s10040-015-1339-x.

Galloway D.L., Jones D.R., and Ingebritsen S.E. (1999). Land subsidence in the United States. U.S. Geological Survey Circular 1182, 175 pp.

Garner, C., Bacon, S., Pohll, G., and Chapman, J. (2017). RE: Indian Wells Valley Groundwater Model Update. Technical Memorandum to Stetson Engineers from Desert Research Institute dated November 17, 2017, p. 28, plus figures and appendices.

Hauksson, E., Hutton, K., Kanamori, H., Jones, L., Mori, J., Hough, S., and Roquemore, G. (1995). Preliminary report on the 1995 Ridgecrest earthquake sequence in eastern California. Seismological Research Letters 66, 54–60.

Hoffmann, J., Galloway, D.L., and Zebker, H.A. (2003). Inverse modeling of interbed storage parameters using land subsidence observations, Antelope Valley, California. Water Resources Research 39, 1–13.

Katzenstein, K. (2013). Evaluation potential land subsidence induced by ground water withdrawal from the Indian Wells Valley, CA using InSAR. Geological Society of America Abstracts with Programs. Vol. 45, No. 7, p.775.

Katzenstein, K. (2015). InSAR analysis of aquifer-system response to pumping in the Indian Wells Valley, Kern County, California. Final Technical Report prepared for Desert Research Institute. January 21, 2015. 23 p.

McGraw, D., R. Carroll, G. Pohll, J. Chapman, S. Bacon, and R. Jasoni, 2016. Groundwater Resource Sustainability: Modeling Evaluation for the Naval Air Weapons Station, China Lake, California, Prepared by Desert Research Institute for the Naval Air Warfare Center Weapons Division, China Lake, CA, NAWCWD TP 8811.

Monastero, F.C., Walker, J.D., Katzenstein, A.M., and Sabin, A.E., 2002. Neogene Evolution of the Indian Wells Valley, East-Central California, In:Glazner, A.F., Walker, J.D., and Bartley, J.M., (eds.), Geologic Evolution of the Mojave Desert and Southwestern Basin and Range, Boulder, Colorado, Geological Society of America Memoir 195, p. 199–228.

Motts, W.S., ed., (1969). Geology and hydrology of selected playas in Western United States: Amherst, University of Massachusetts, 305 p.

Peltzer, G., Crampé, F., Hensley, S., and Rosen, P. (2001). Transient strain accumulation and fault interaction in the eastern California shear zone. Geology 29, 975–978.

Sneed, M. and Galloway, D.L. (2000). Aquifer-system compaction and land subsidence: measurements, analyses, and simulations—the Holly site, Edwards Air Force Base, Antelope Valley, California. U.S. Geological Survey Water-Resources Investigations Report 00-4015, p. 91–97.

Sneed, Michelle, Ikehara, M.E., Stork, S.V., Amelung, Falk, and Galloway, D.L. (2003). Detection and measurement of land subsidence using interferometric synthetic aperture radar and global positioning system, San Bernardino County, Mojave Desert, California: U.S. Geological Survey Water-Resources Investigations Report 03-4015, 60 p.

Solt, M., and Sneed, M. (2014). Subsidence (2004–2009) in and near lakebeds of the Mojave River and Morongo groundwater basins, southwest Mojave Desert, California: U.S. Geological Survey Scientific Investigations Report 2014-5011, unpaginated, http:// dx.doi.org/10.3133/sir20145011.

Stamos, C.L., Glockhoff, C.S., McPherson, K.R., and Julich, R.J. (2007), Water-level and land-subsidence studies in the Mojave River and Morongo groundwater basins: U.S. Geological Survey Scientific Investigations Report 2007-5097, unpaginated, http://pubs.usgs.gov/ sir/2007/5097/.

Stamos, C.L., Martin, Peter, Nishikawa, Tracy, and Cox, B.F. (2001). Simulation of ground-water flow in the Mojave River Basin, California (ver. 3, September 2001): U.S. Geological Survey Water- Resources Investigations Report 2001-4002, 137 p.

USGS [U.S. Geological Survey and California Geological Survey] (2006). Quaternary fault and fold database for the United States, accessed April 14, 2009, from USGS web site: http//earthquake.usgs.gov/hazards/qfaults/.

Wesnousky, S.G. (2005). Active faulting in the Walker Lane. Tectonics, 24, TC3009, doi: 10.1029/2004TC001645.

Zellmer, J.T., and Roquemore, G.R. (1997). Tectonic deformation of a Supersonic Naval Ordnance Research Track, Indian Wells Valley, California. Environmental and Engineering Geoscience 3, 205–215.

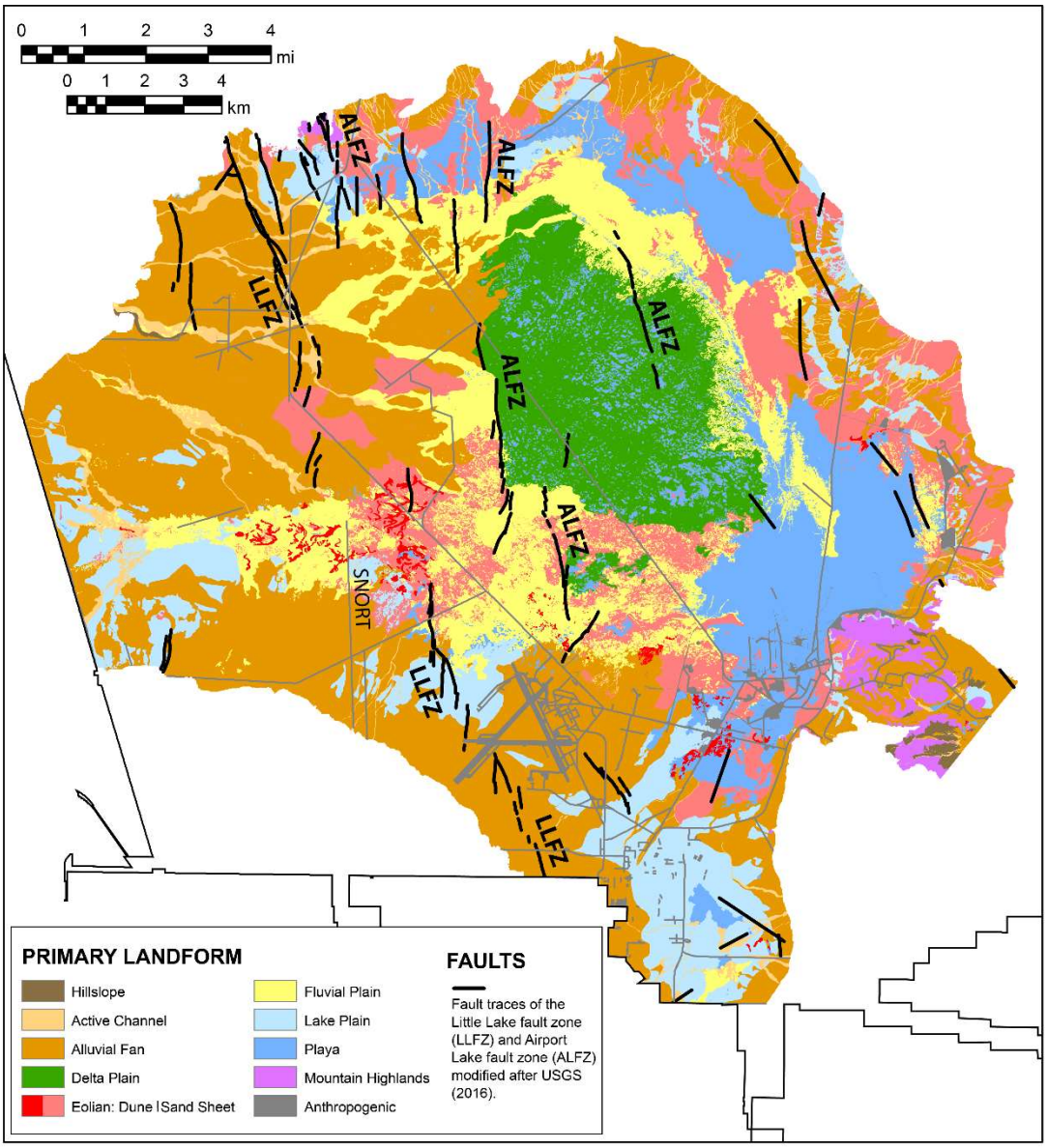


Figure 1. Geomorphic map of China Lake basin below ~2300 ft (700 m) elevation contour showing the distribution of primary landform types and major fault zones in the vicinity of the depocenter of Indian Wells Valley. LLFZ – Little Lake fault zone; ALFZ – Airport Lake fault zone. (from Bullard et al., 2018).

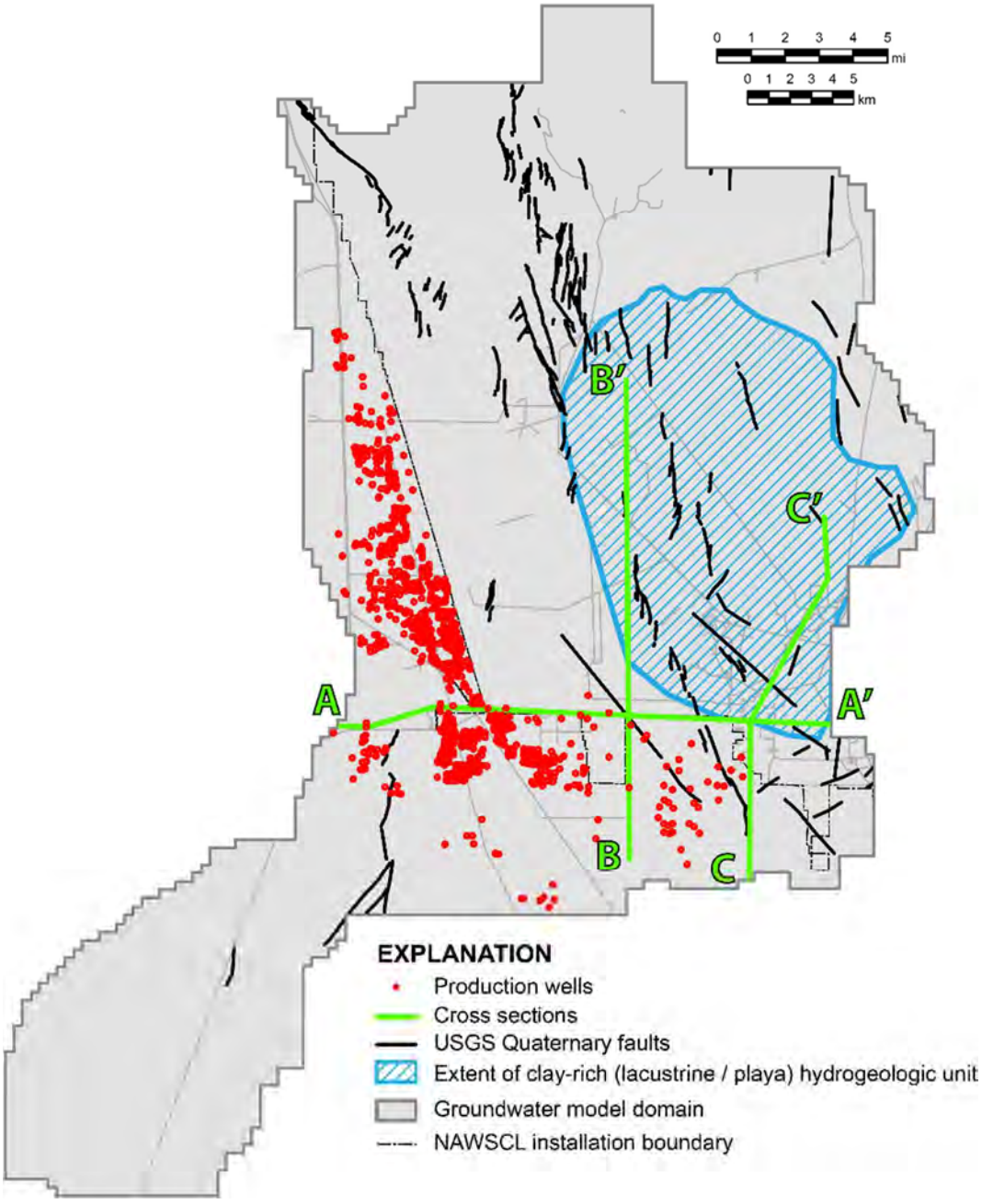


Figure 2. Spatial extent of fine-grained lacustrine and playa hydrogeologic units in Indian Wells Valley. Transects A-A', B-B', and C-C' of hydrogeologic cross sections in Figure 3 are shown. Adapted from Kunkel and Chase (1969) and McGraw et al. (2016).

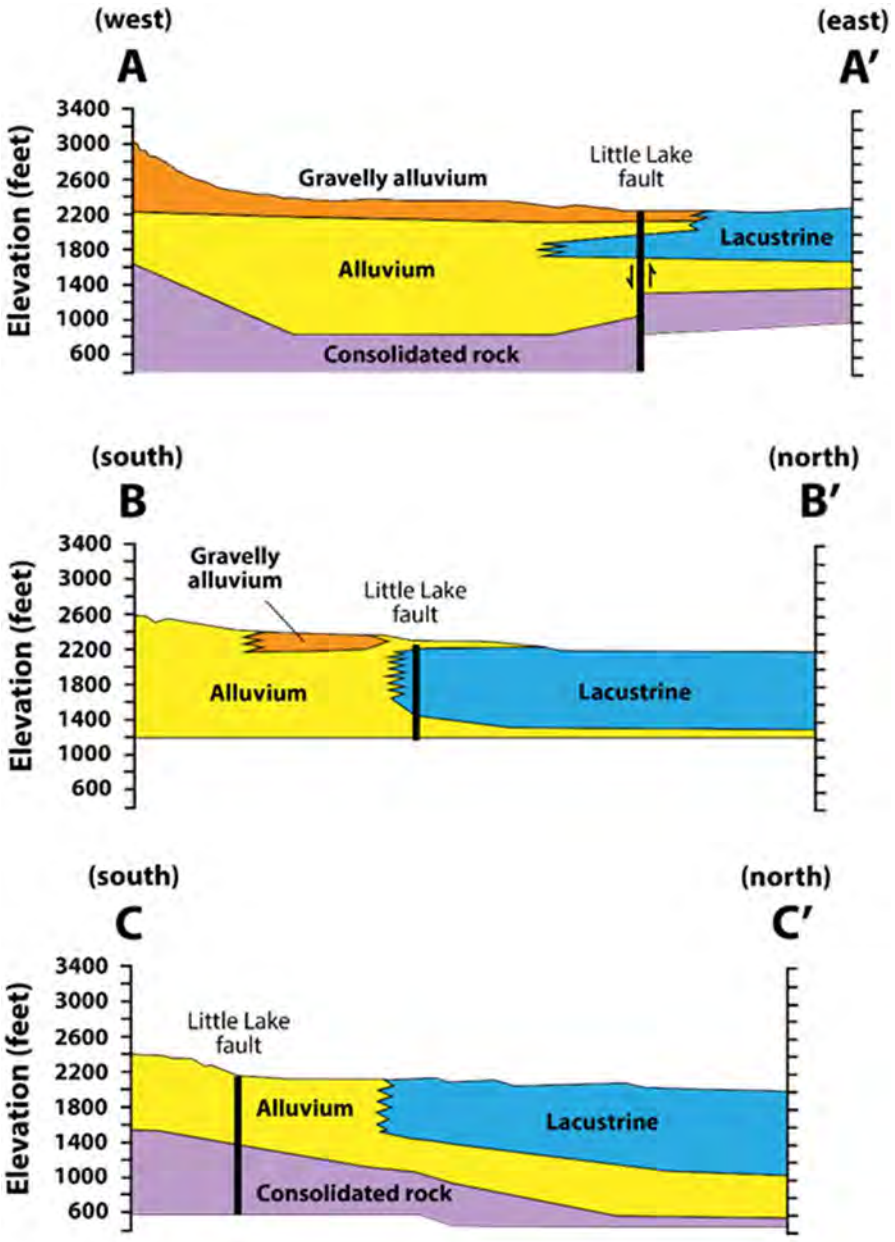


Figure 3. Cross sections of the primary hydrogeologic units in the IWV groundwater basin showing the distribution and depth of coarse-grained (gravel and alluvium) and fine-grained (lacustrine) deposits, as well as consolidated basement rocks. Also shown are the general locations of the active Little Lake fault (LLF). Modified after Kunkel and Chase (1969) and McGraw et al. (2016).

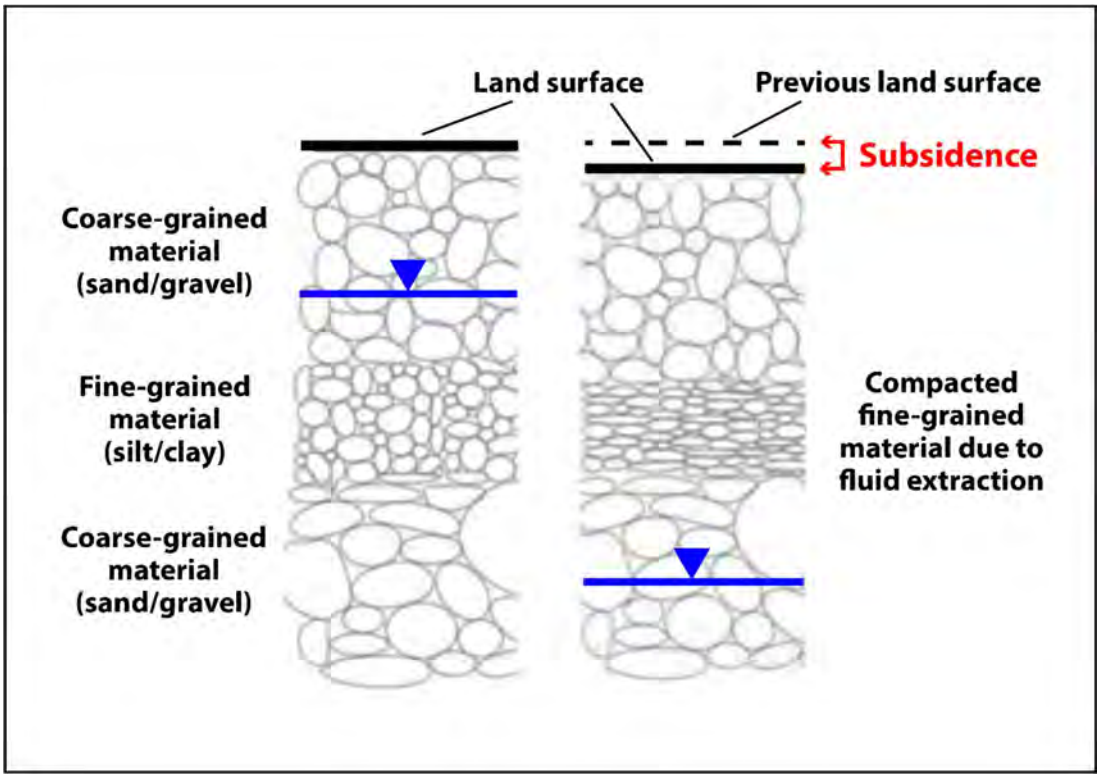


Figure 4. Conceptual model of land subsidence due to compaction of an interbedded fine-grained layer after fluid extraction from groundwater drawdown. (adapted from Sneed and Galloway, 2000; Borchers and Carpenter, 2014)

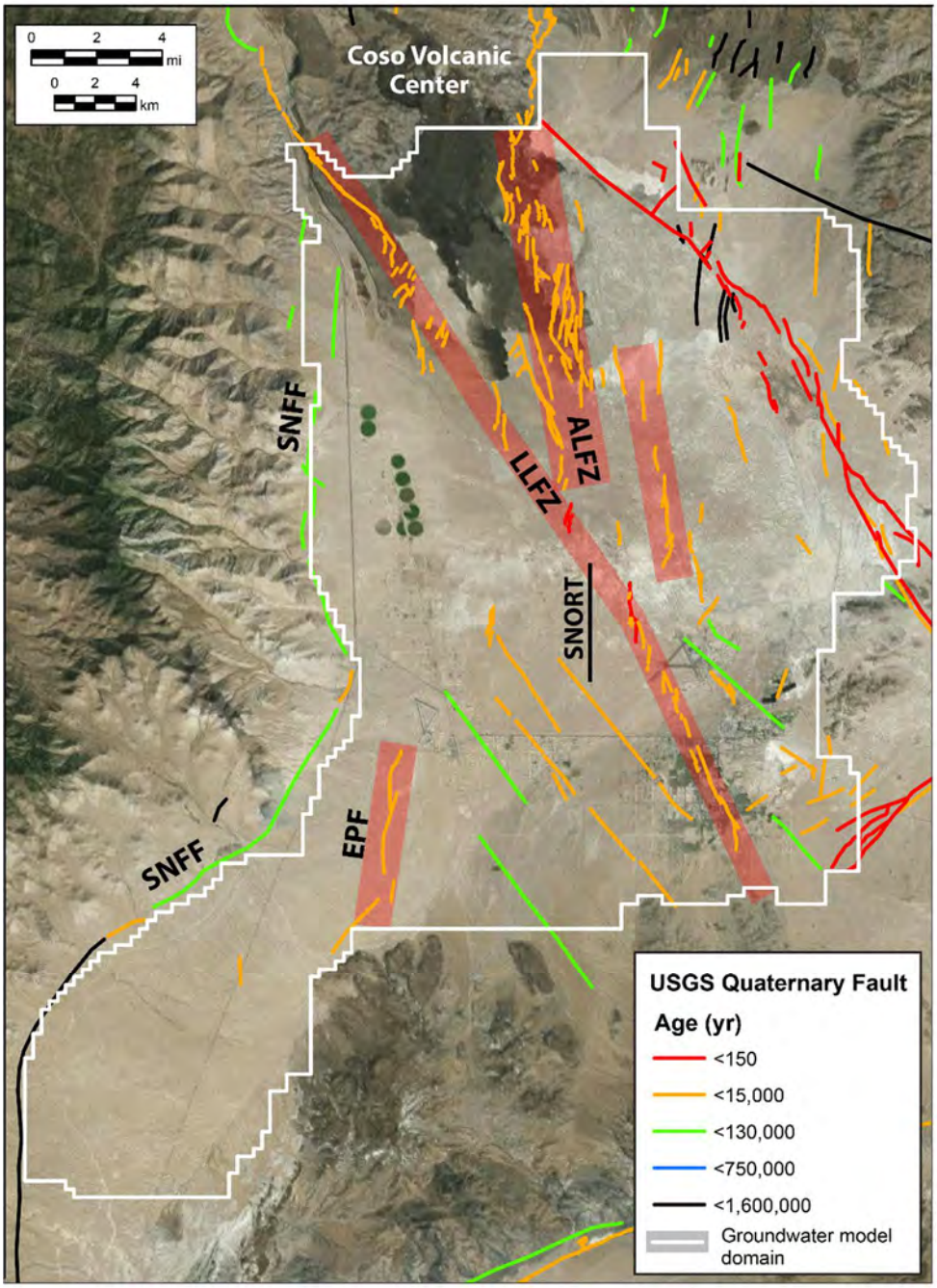


Figure 5. Map of the Indian Wells Valley groundwater model domain showing the location of the Supersonic Naval Ordnance Research Track (SNORT) alignment and faults of USGS (2016). The active Little Lake and Airport Lake fault zones (LLFZ and ALFZ, respectively), a well-defined series of faults informally referred to as the El Paso fault (EPF) are shown with red boxes. The Sierra Nevada Frontal fault (SNFF) system and the Coso Volcanic center are also

shown. The July 4 and 5, 2019 fault ruptures associated with the M6.4 Searles Valley and M7.1 Ridgecrest earthquakes, respectively, are shown as red faults, but without red boxes.

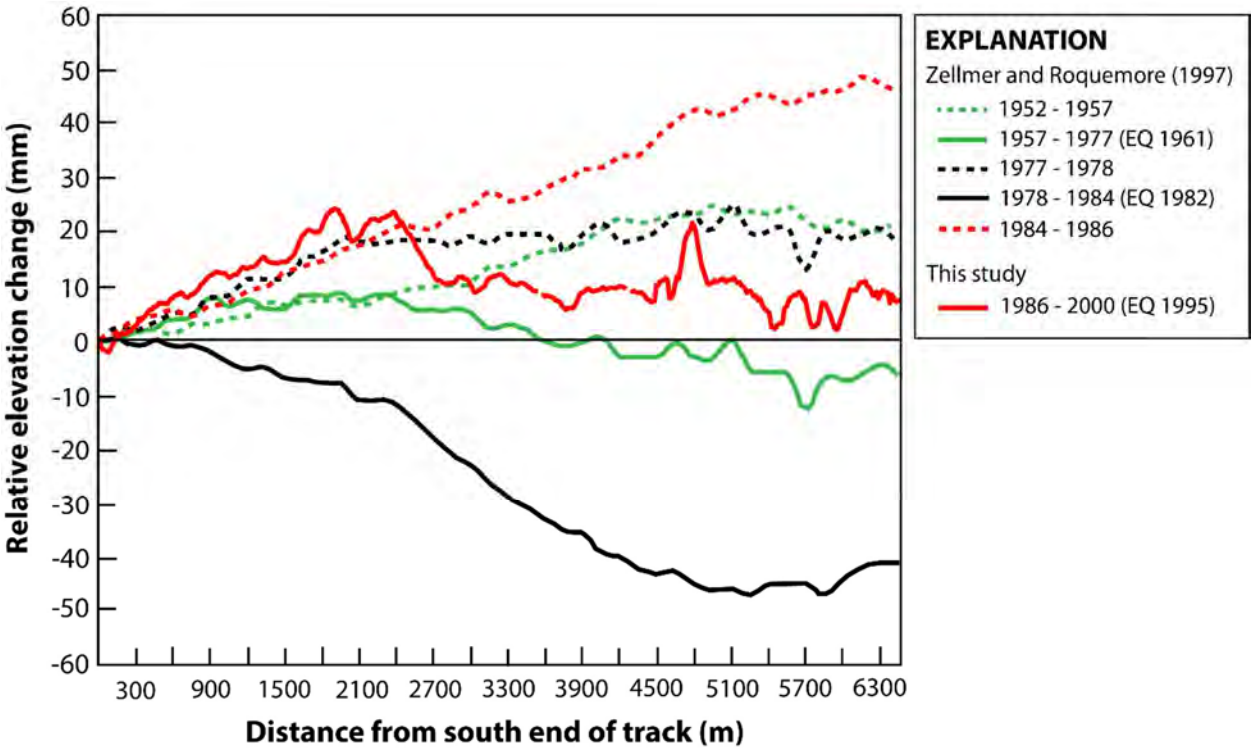


Figure 6. Plots of relative elevation change in the vertical directions of the SNORT alignment for the periods 1952–1957, 1957–1977, 1977–1978, 1978–1984, and 1984–1986 (Zellmer and Roquemore, 1997). The period 1986–2000 is from processing of SNORT GPS data of this study. Survey stations are spaced 15.2 m apart along the south to north oriented alignment. Positive values indicate an increase in relative elevation and negative values a decrease with respect to the zero-base station. Survey data reflect vertical and horizontal cyclic-strain accumulation along the LLFZ from stress build up (uplift) during periods with no seismic activity and a stress drop (subsidence) after notable nearby ~M5 earthquakes (EQ) in 1961, 1982, and 1995.

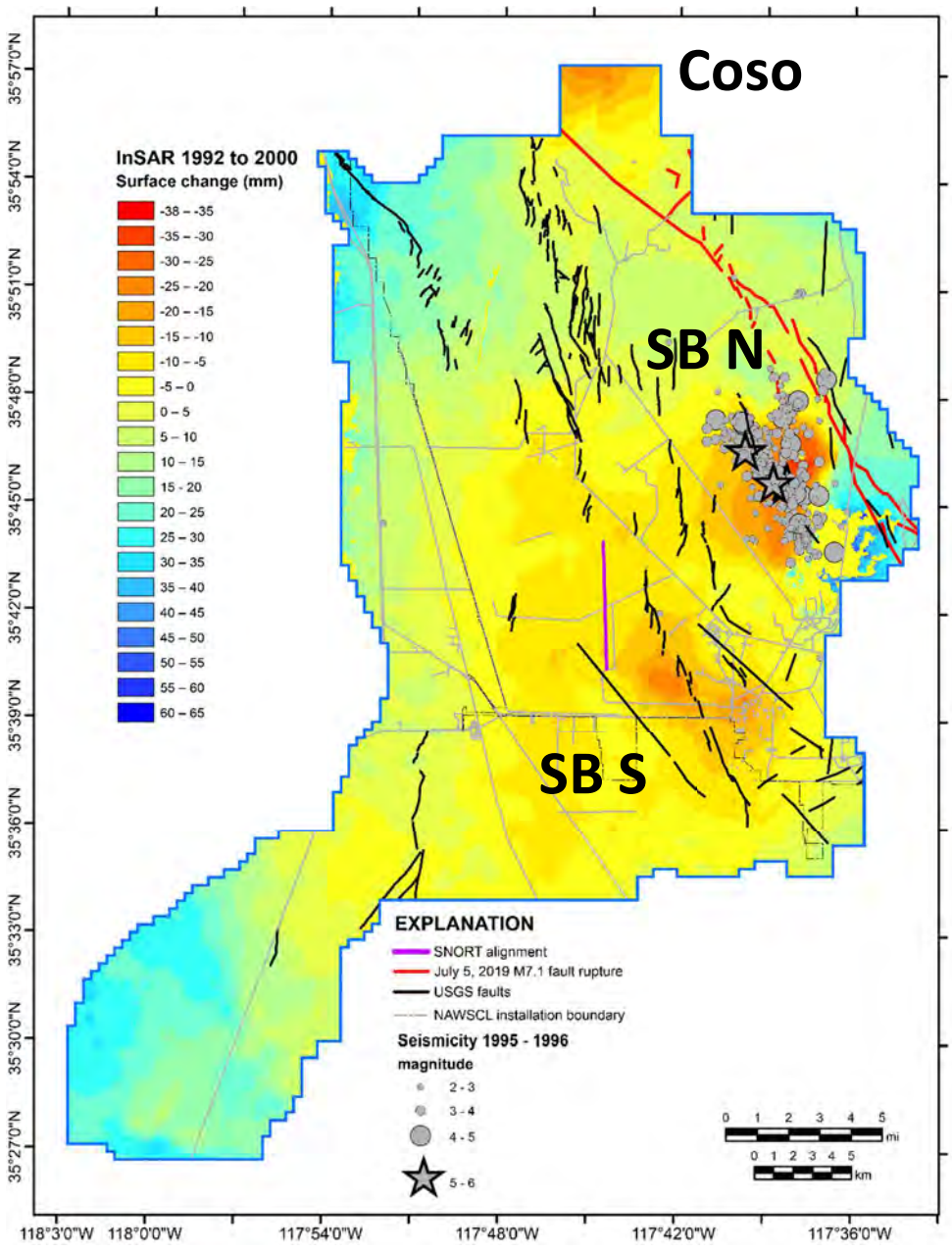


Figure 7. Map showing 8 years of surface change within the Indian Wells Valley (IWV) groundwater model domain from Interferometric Synthetic Aperture Radar (InSAR) data between 1992 and 2000 (Katzenstein, 2015). The location of faults from USGS (2016), the epicenters of the 1995 M5.4 Ridgecrest earthquake sequence, and SNORT alignment near the Little Lake fault zone are also shown. The SB N and SB S delineate the northern and southern subsidence areas, respectively; and Coso is a subsidence area related to the Coso geothermal field.

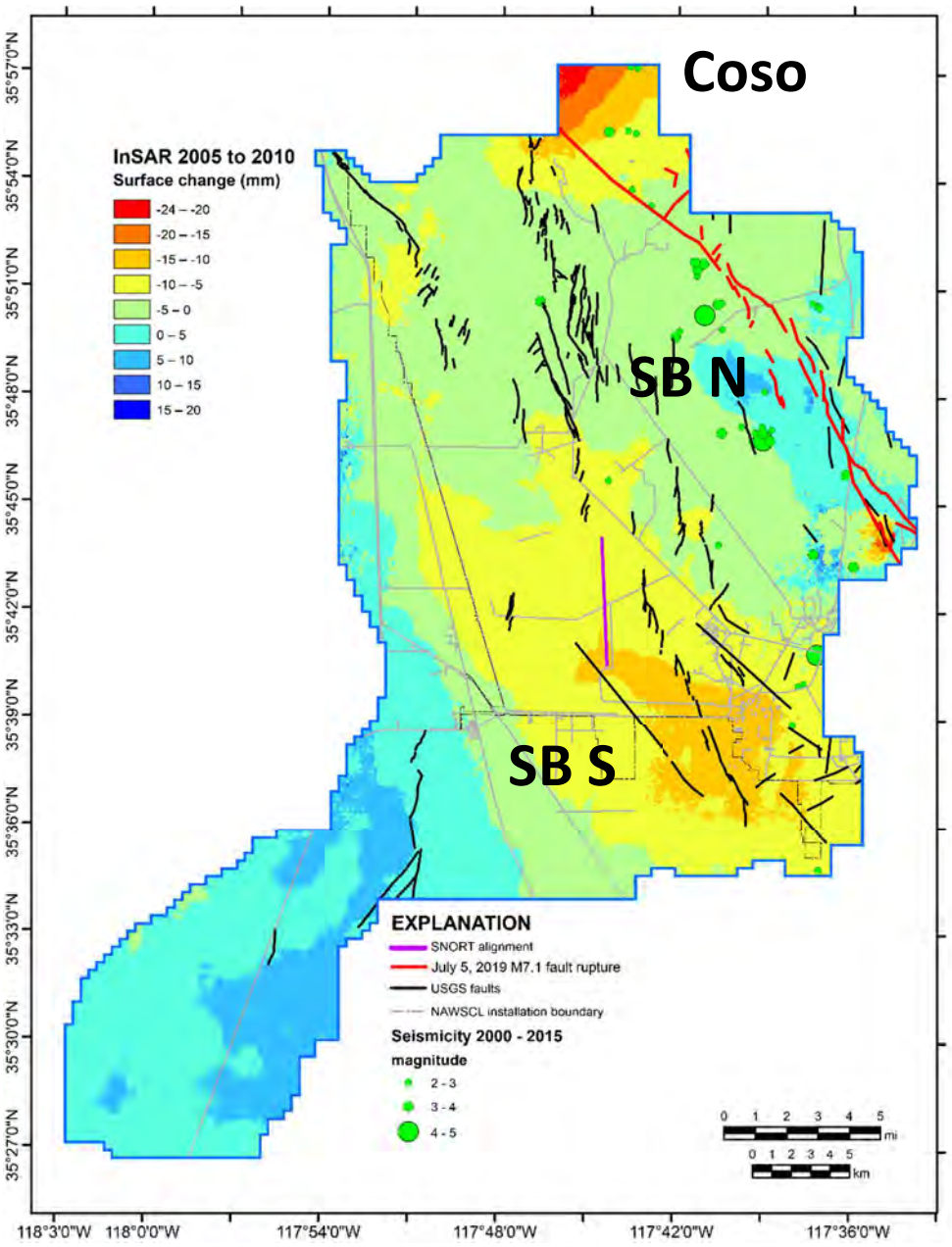


Figure 8. Map showing 5 years of surface change within the Indian Wells Valley (IWV) groundwater model domain from Interferometric Synthetic Aperture Radar (InSAR) data between 2005 and 2010 processed by Katzenstein (2015). The location of faults from USGS (2016), seismicity from 2000–2015, and SNORT alignment near the LLFZ is shown. The SB N and SB S delineate the northern and southern subsidence areas, respectively; and Coso is a subsidence area related to the Coso geothermal field.

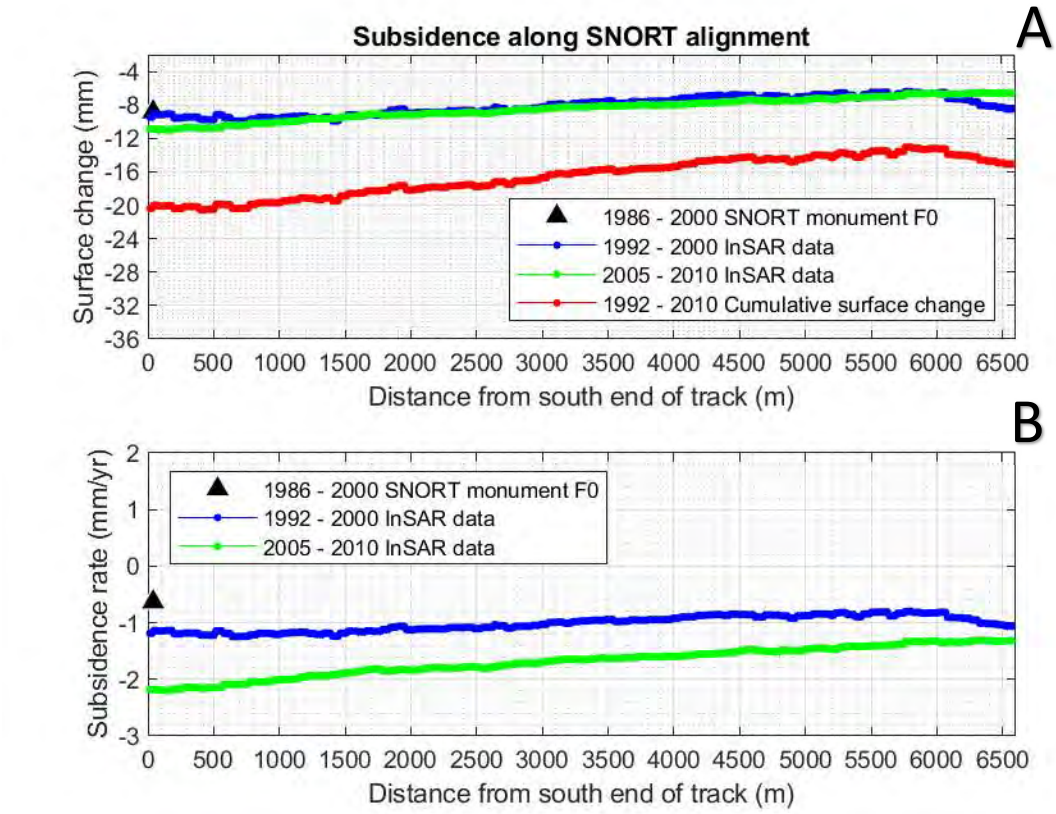


Figure 9. Plots showing discrete and cumulative subsidence (A) and subsidence rate (B) along the SNORT alignment from Interferometric Synthetic Aperture Radar (InSAR) data for the periods 1992–2000, 2005–2010, and 1992–2010. The amount of subsidence and rate of the SNORT base station (monument F0) from the difference of reported absolute elevations for the period 1986–2000 are also shown.

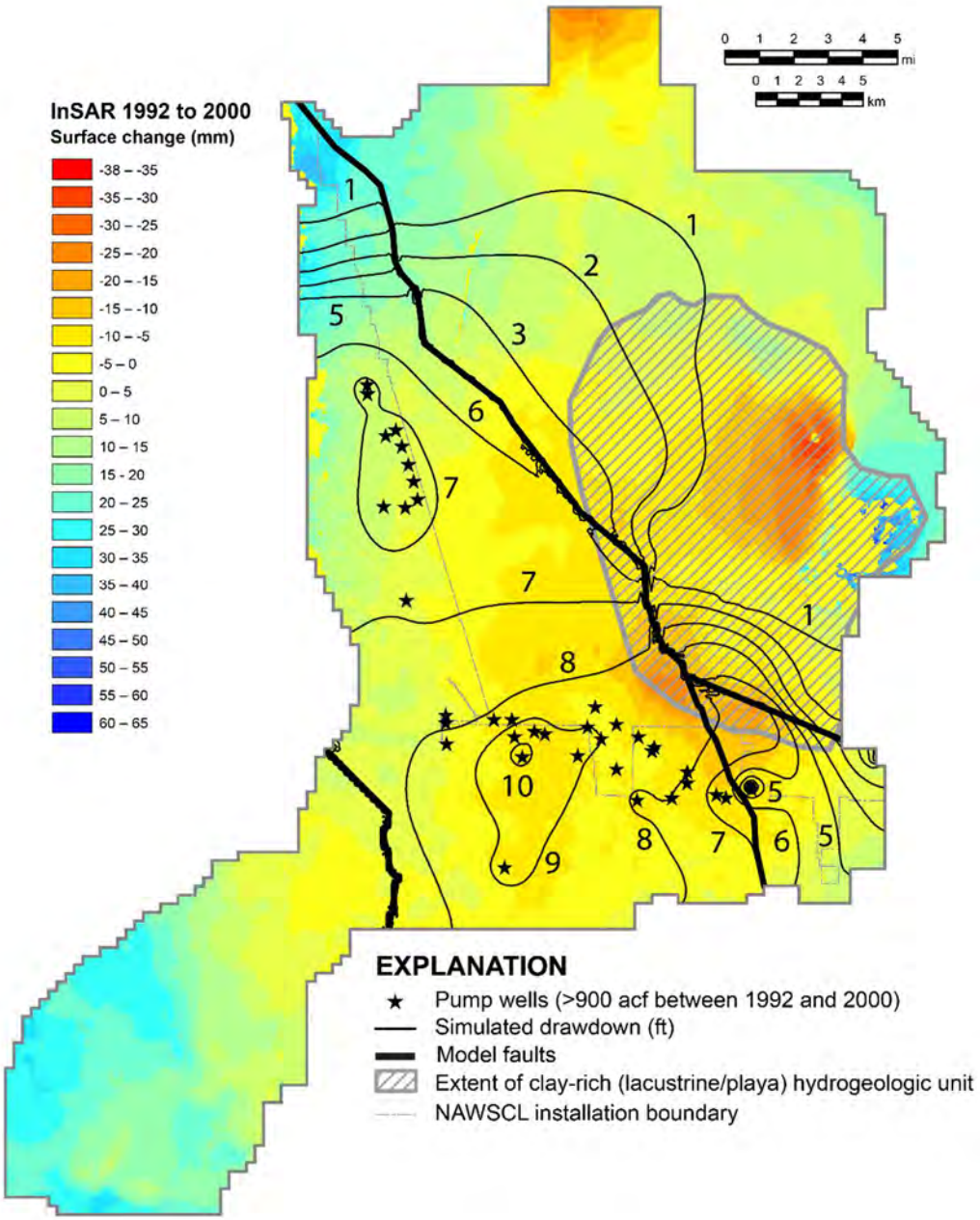


Figure 10. Map showing 8 years of surface change within the Indian Wells Valley (IWV) groundwater model domain from Interferometric Synthetic Aperture Radar (InSAR) data between 1992 and 2000 (Katzenstein, 2015). The location of modeled faults, simulated drawdown from the IWV groundwater model, and the extent of a clay-rich hydrogeologic unit

are shown. The distribution of wells with greater than 900 acre-feet of groundwater extraction during the period are also shown.

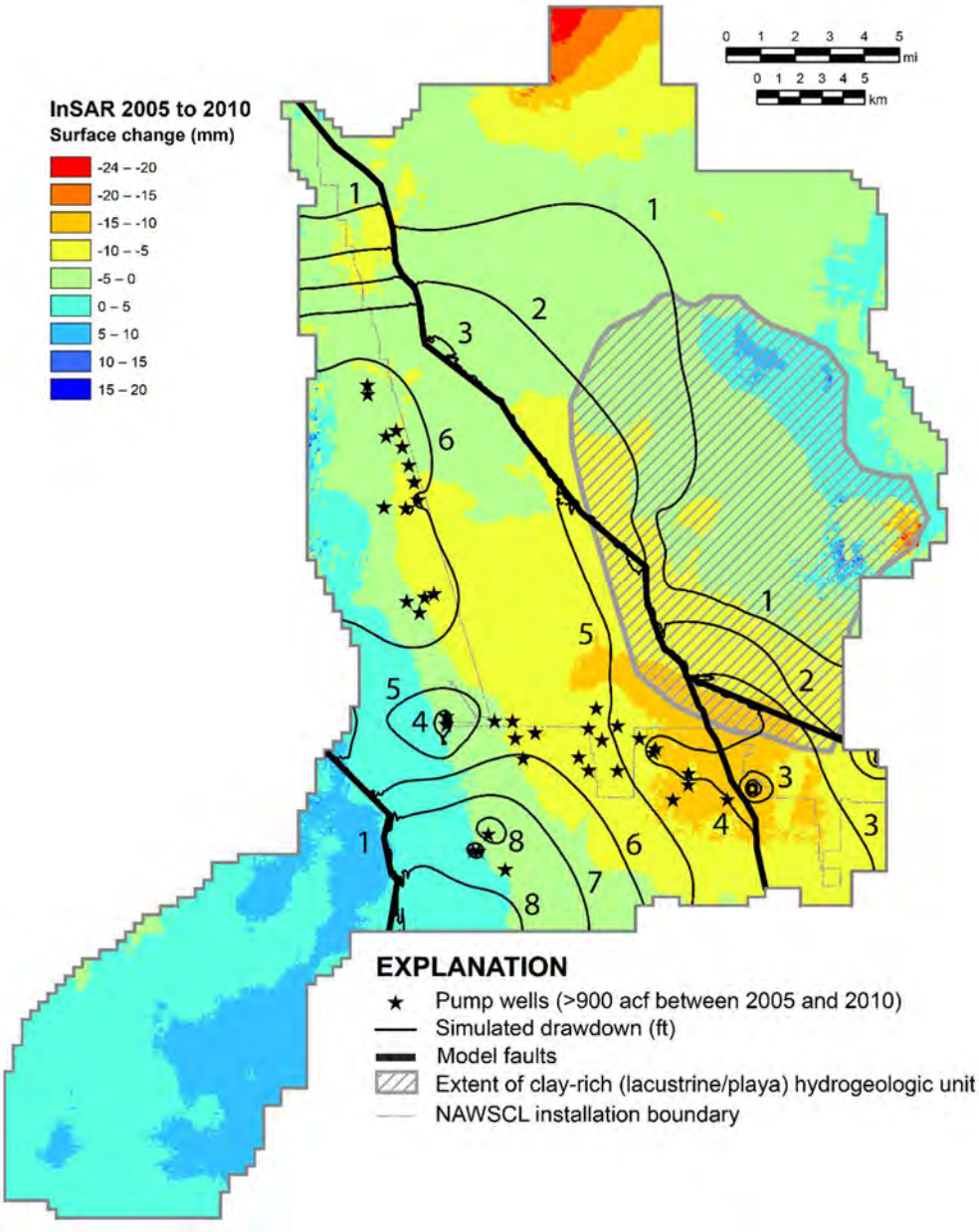


Figure 11. Map showing 5 years of surface change within the Indian Wells Valley (IWV) groundwater model domain from Interferometric Synthetic Aperture Radar (InSAR) data

between 2005 and 2010 (Katzenstein, 2015). The location of modeled faults, simulated drawdown from the IWV groundwater model, and the extent of a clay-rich hydrogeologic unit are shown. The distribution of wells with greater than 900 acre-feet of groundwater extraction during the period are also shown.

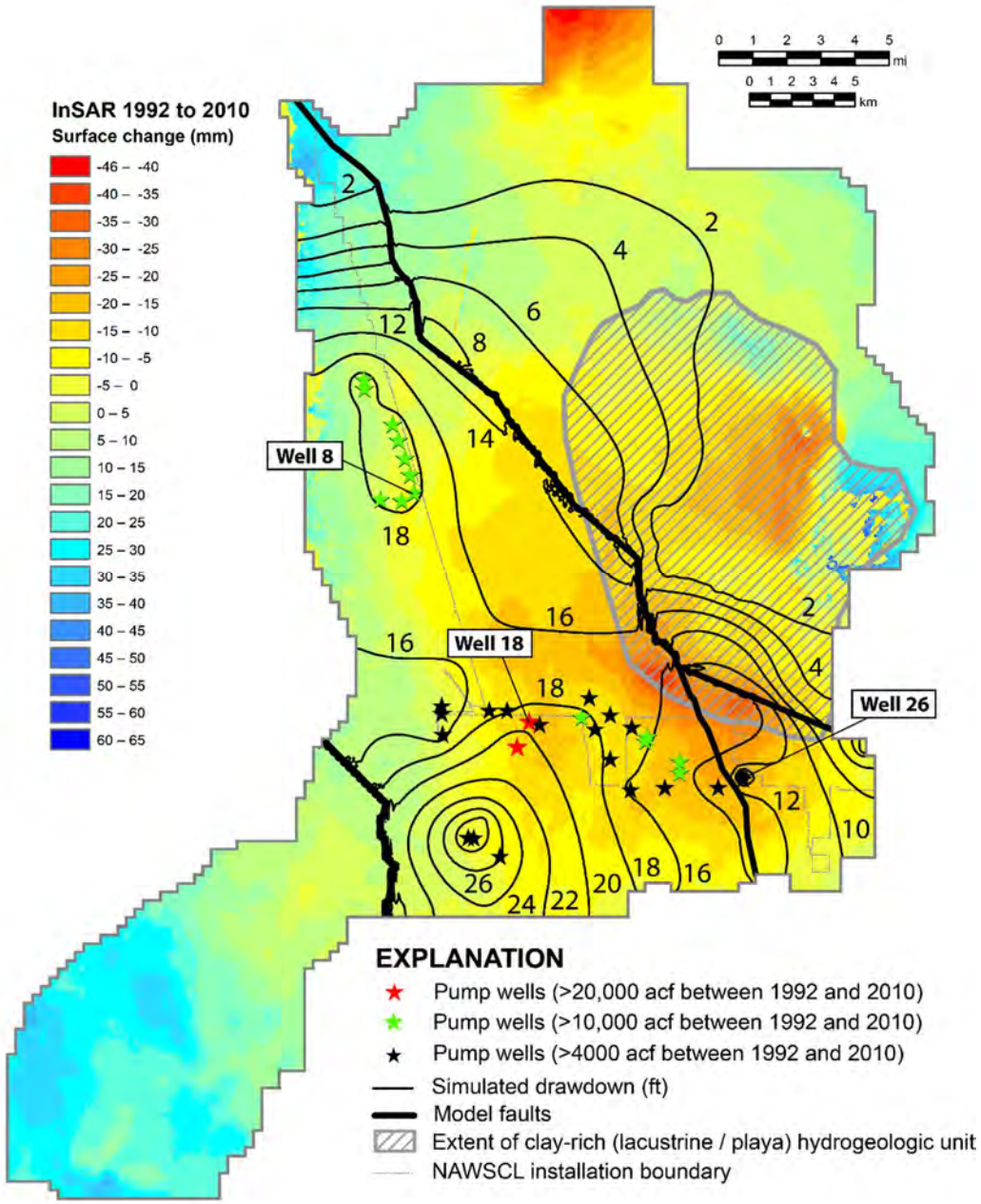


Figure 12. Map showing 18 years of surface change within the Indian Wells Valley (IWV) groundwater model domain from Interferometric Synthetic Aperture Radar (InSAR) data between 1992 and 2010 (Katzenstein, 2015). The location of modeled faults, simulated drawdown from the IWV groundwater model, and the extent of a clay-rich hydrogeologic unit

are shown. The distribution of wells with greater than 4000, 10,000, and 20,000 acre-feet of groundwater extraction during the period are also shown. The location of wells (8, 18, and 26) referred to in text are shown.

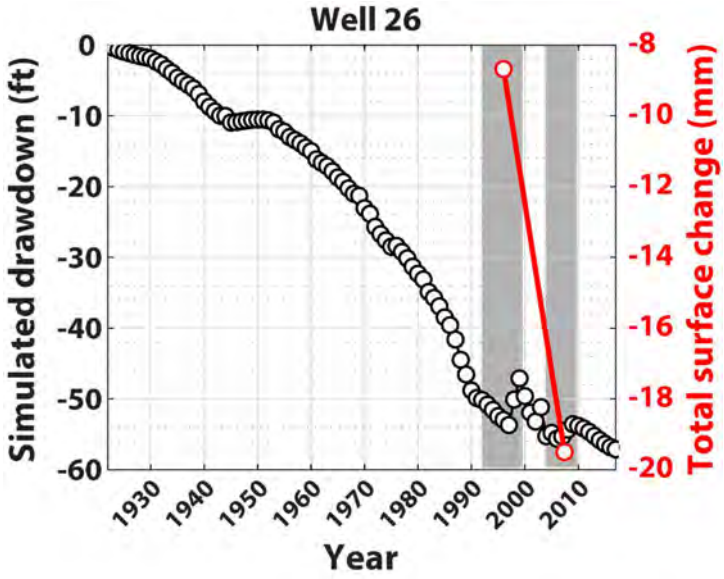


Figure 13. Plots showing temporal correspondence between simulated drawdown from the IWV groundwater model and land surface changes at well site 26 in areas of the southern subsidence area on distal alluvial fans and playa margins. Total surface change measured by Interferometric Synthetic Aperture Radar (InSAR) at the well site between the periods 1992–2000 (midpoint 1996) and 2005–2010 (midpoint 2007.5) are also shown. Well location and corresponding InSAR surface change value are on Figure 12.

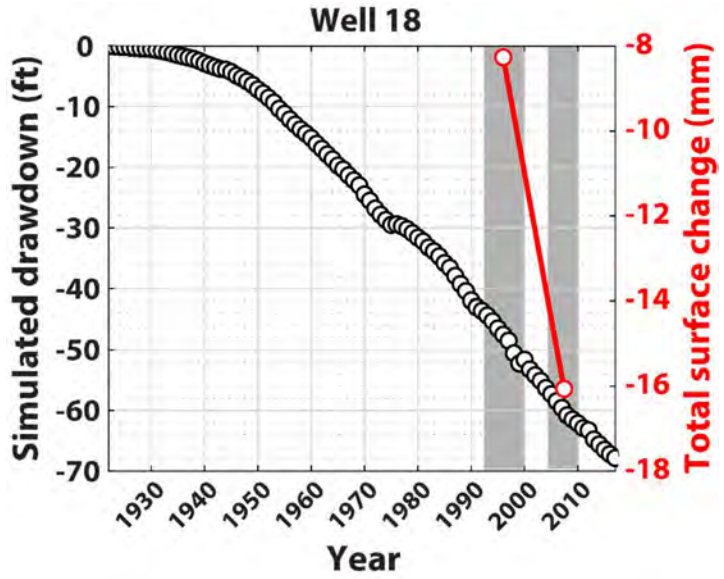


Figure 14. Plots showing temporal correspondence between simulated drawdown from the IWV groundwater model and land surface changes at well site 18 in areas of groundwater extraction of greater than 20,000 acre-feet on medial to distal alluvial fans during the period 1992–2010. Total surface change measured by Interferometric Synthetic Aperture Radar (InSAR) at the well site between the periods 1992–2000 (midpoint 1996) and 2005–2010 (midpoint 2007.5) are also shown. Well location and corresponding InSAR surface change value are on Figure 12.

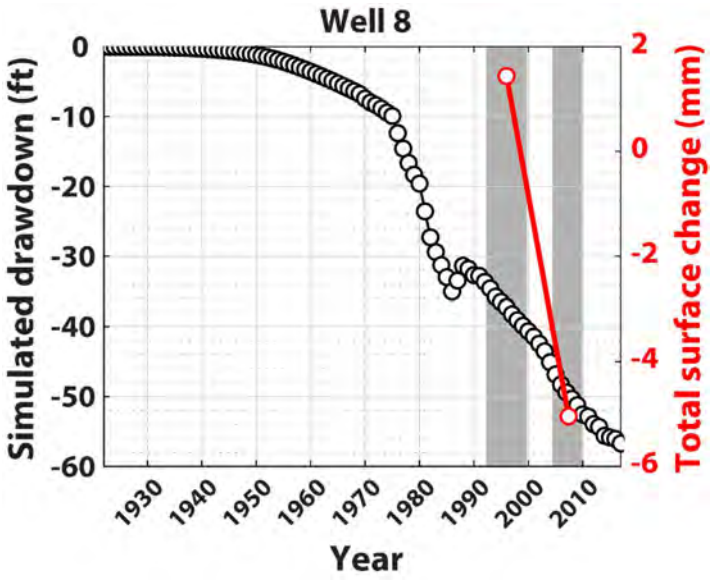
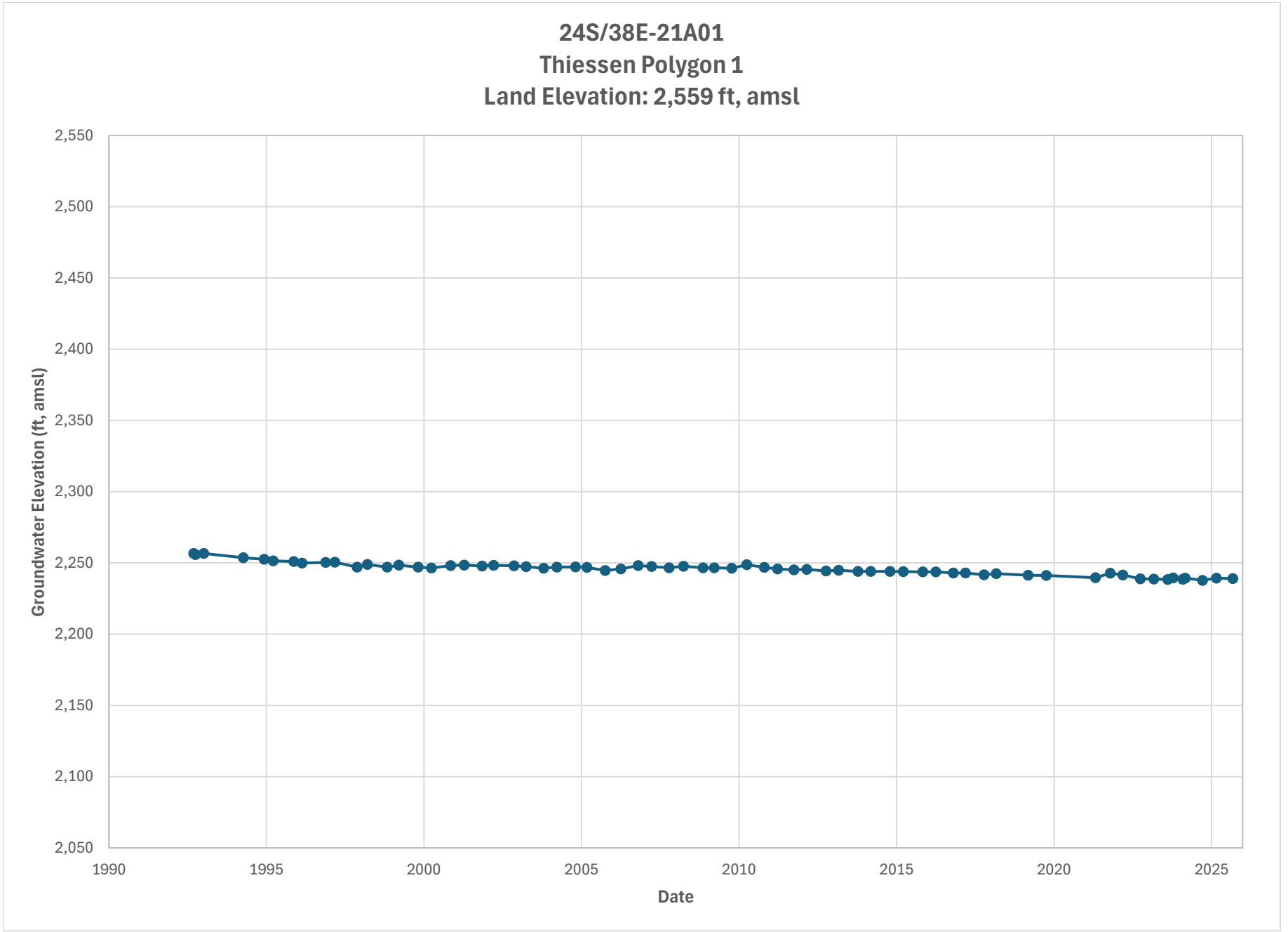
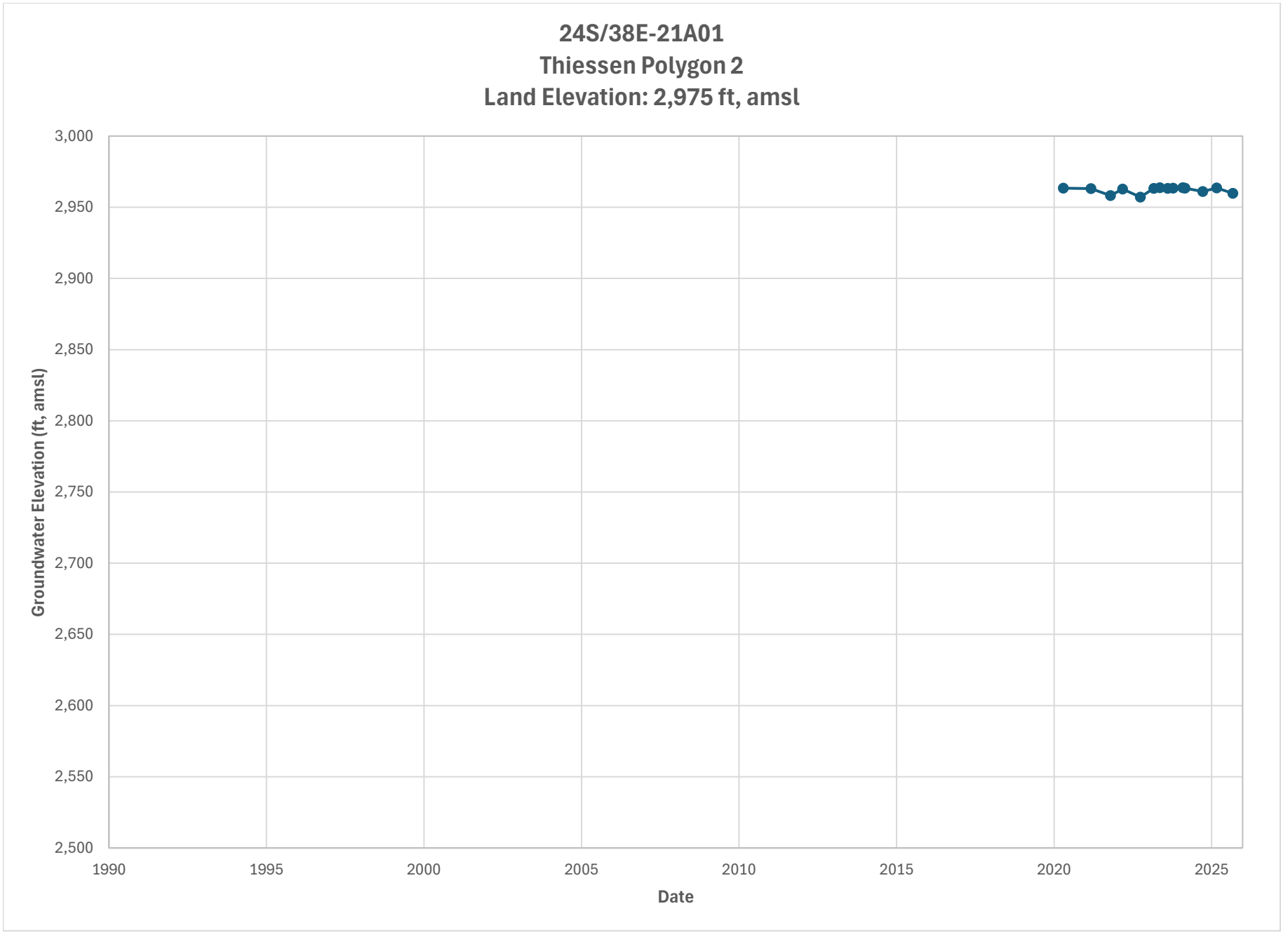
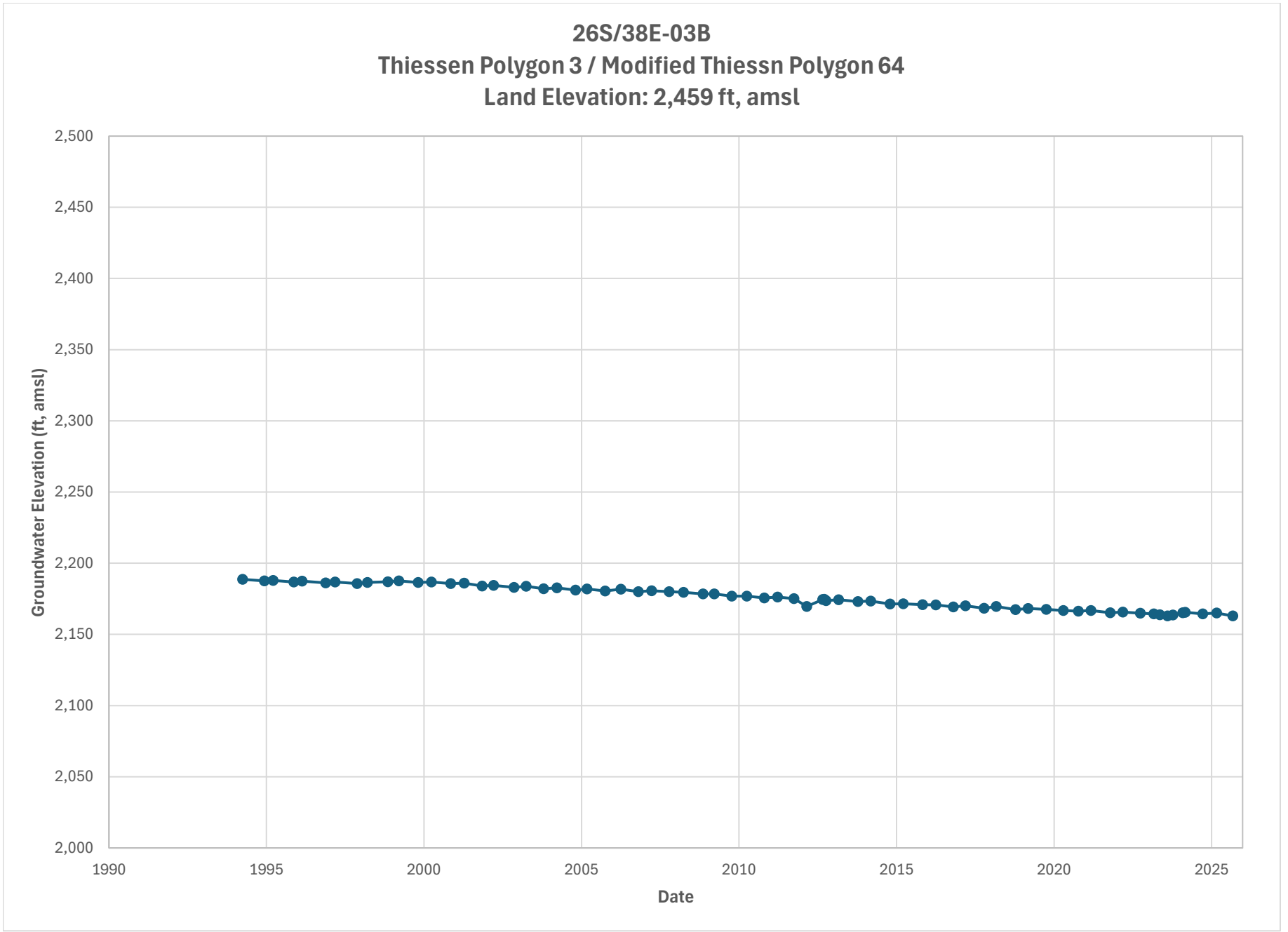


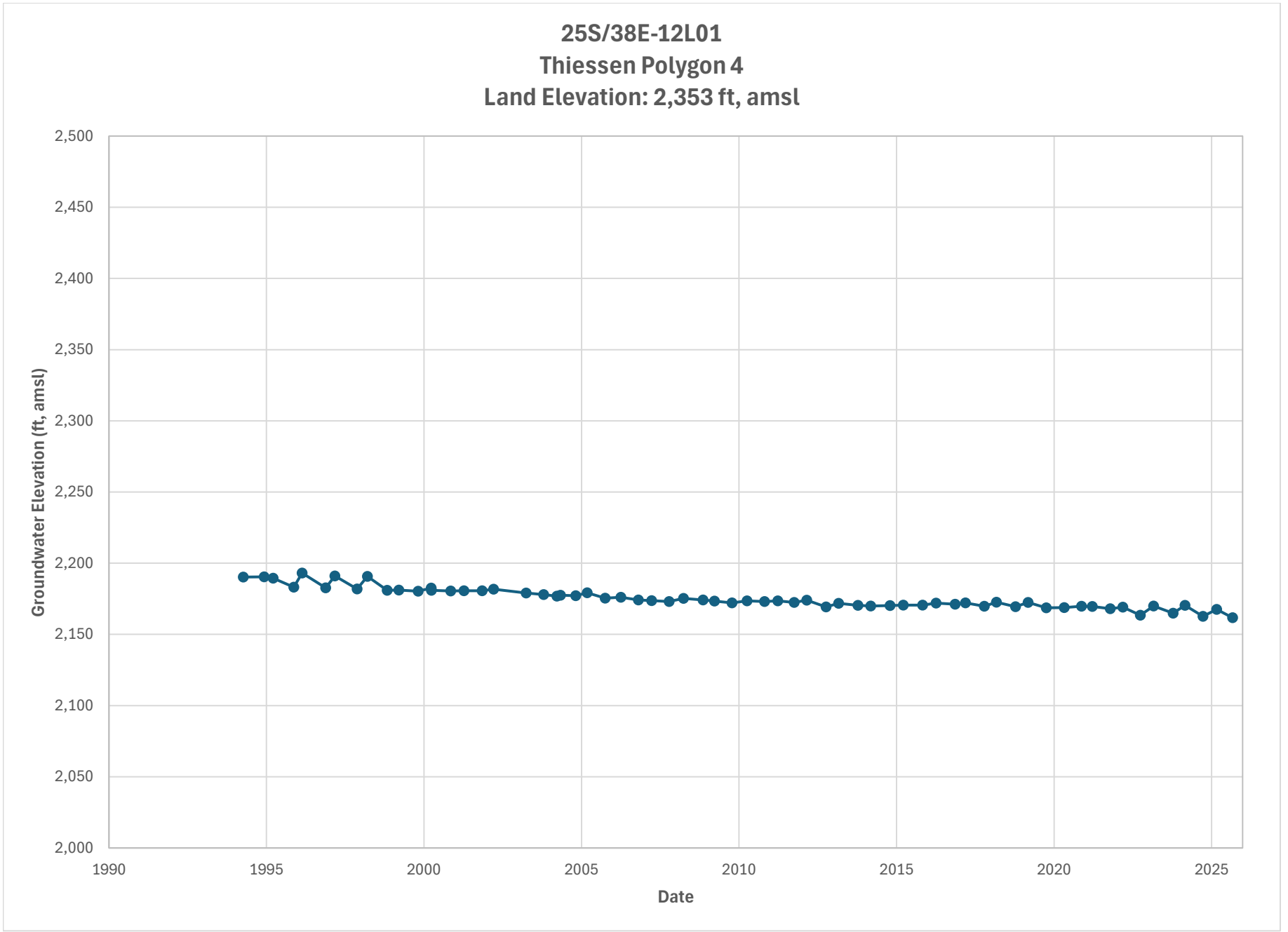
Figure 15. Plots showing temporal correspondence between simulated drawdown from the IWV groundwater model and land surface changes at well site 8 in areas of agricultural fields on medial to distal alluvial fans. Total surface change measured by Interferometric Synthetic Aperture Radar (InSAR) at the well site between the periods 1992–2000 (midpoint 1996) and 2005–2010 (midpoint 2007.5) are also shown. Well location and corresponding InSAR surface change value are on Figure 12.

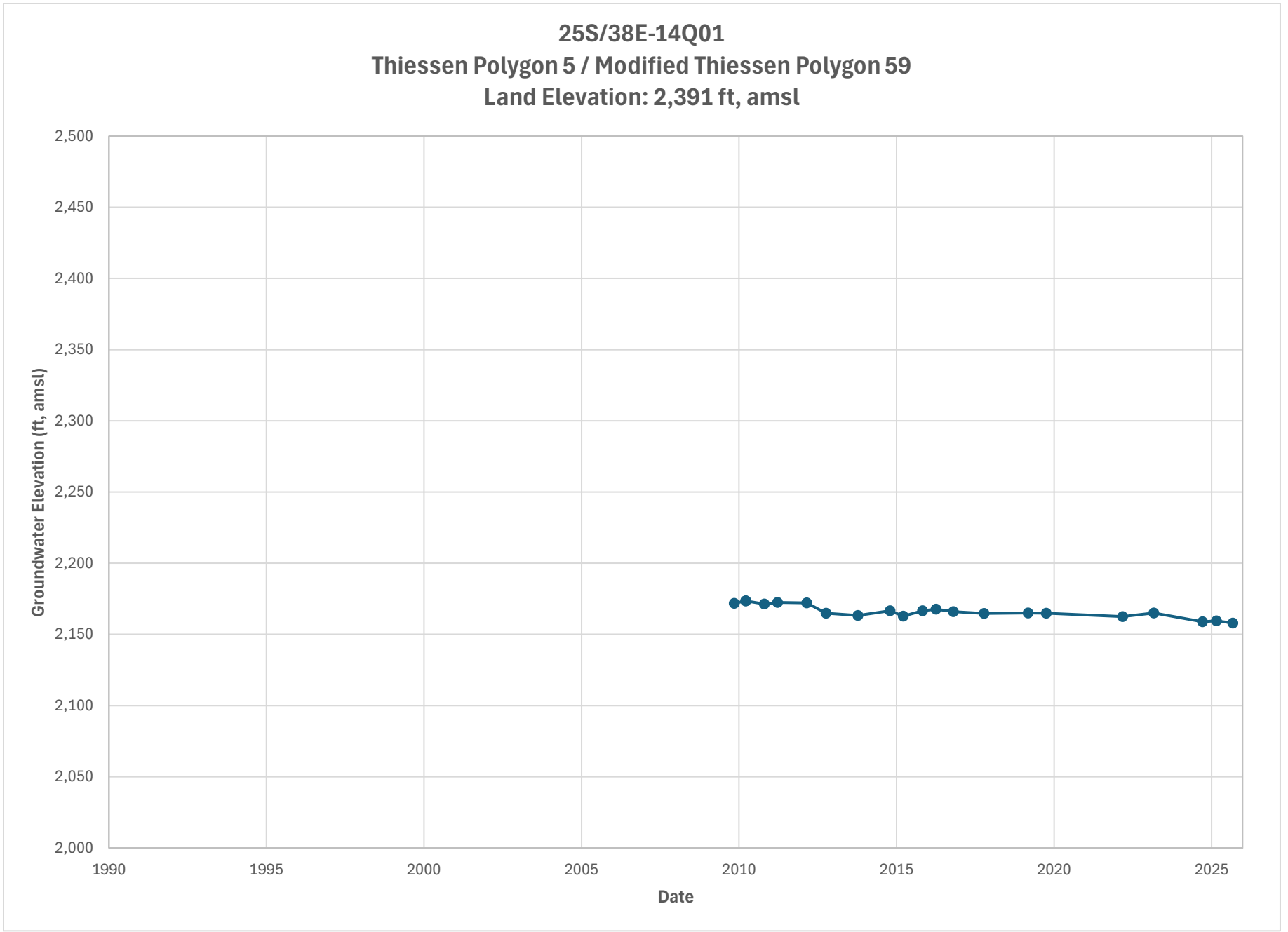
ATTACHMENT S

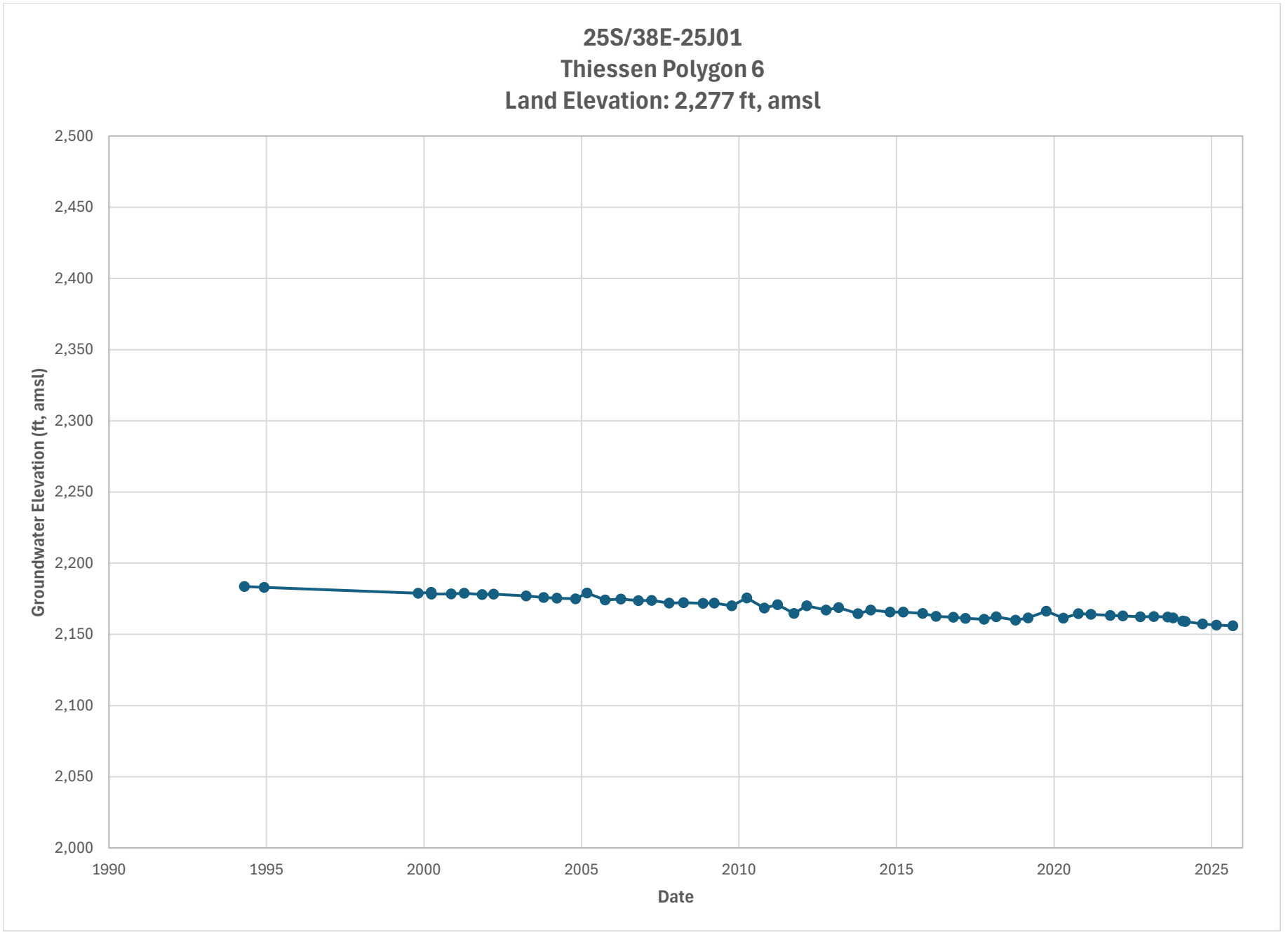

24S/38E-21A01
Thiessen Polygon 1
Land Elevation: 2,559 ft, amsl
Groundwater Elevation (ft, amsl)
2,550
2,500
2,450
2,400
2,350
2,300
2,250
2,200
2,150
2,100
2,050
1990
1995
2000
2005
2010
2015
2020
2025
Date

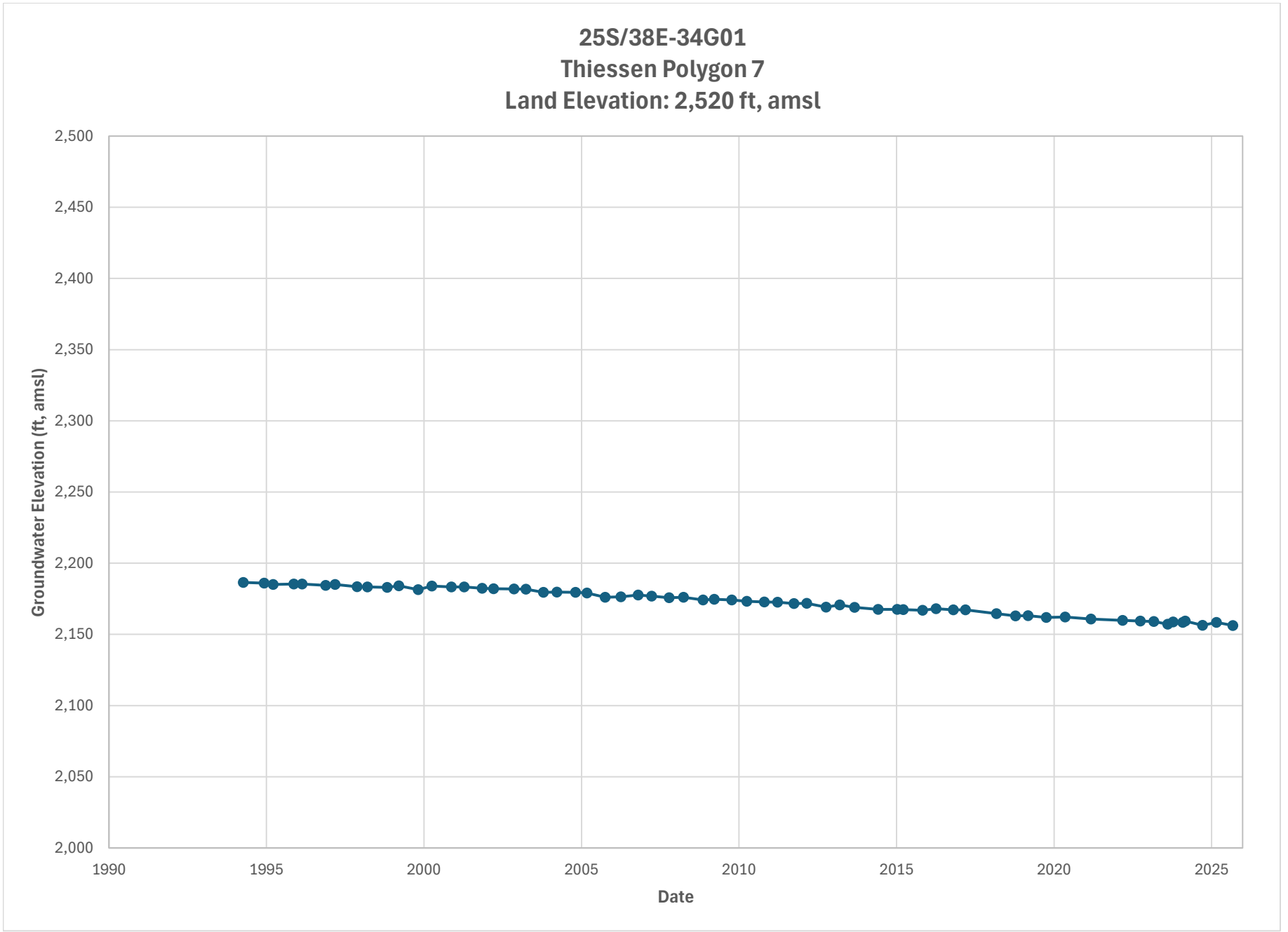

24S/38E-21A01
Thiessen Polygon 2
Land Elevation: 2,975 ft, amsl
Groundwater Elevation (ft, amsl)
3,000
2,950
2,900
2,850
2,800
2,750
2,700
2,650
2,600
2,550
2,500
1990
1995
2000
2005
2010
2015
2020
2025
Date

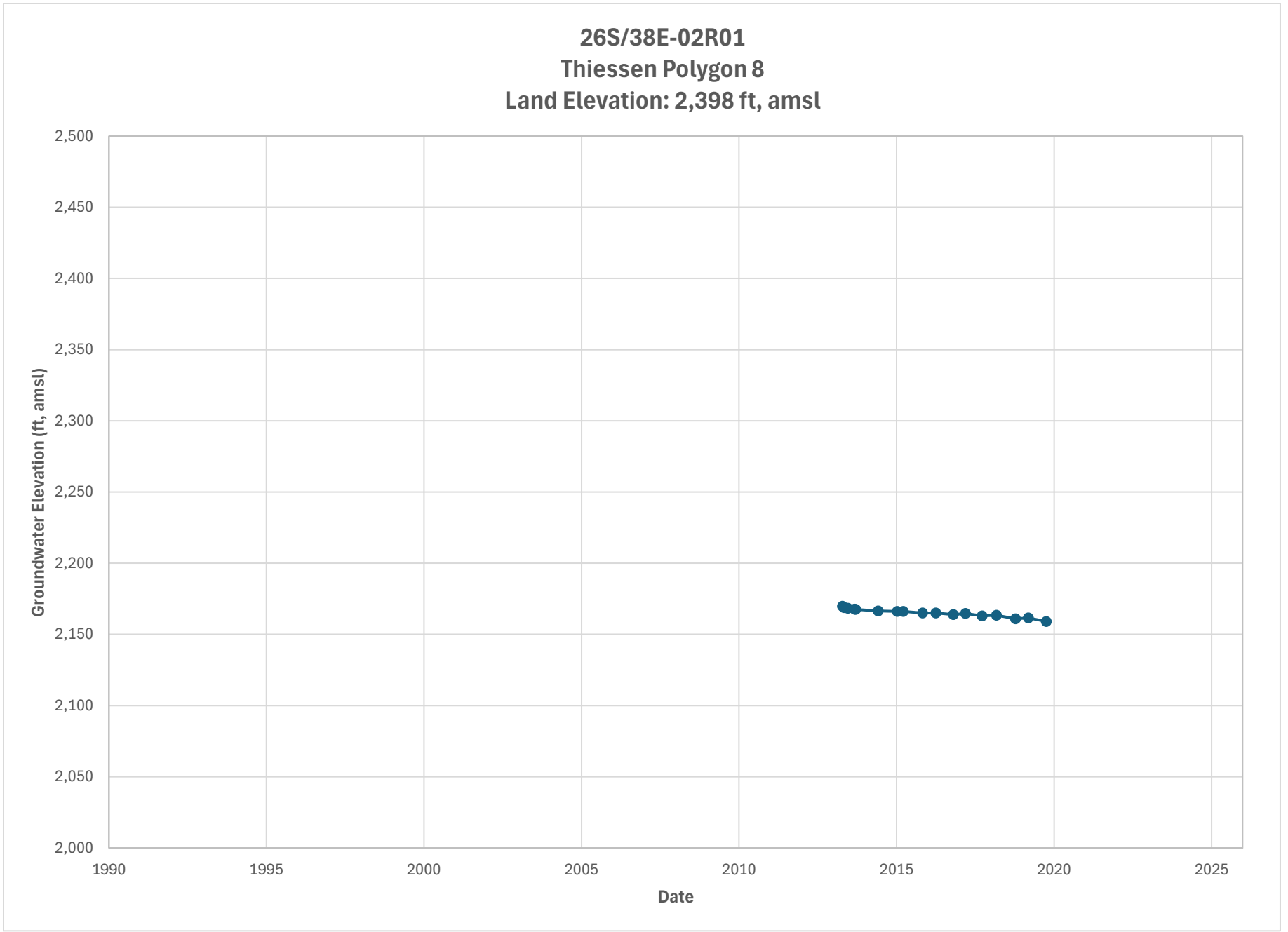

26S/38E-03B
Thiessen Polygon 3 / Modified Thiessn Polygon 64
Land Elevation: 2,459 ft, amsl
Groundwater Elevation (ft, amsl)
2,500
2,450
2,400
2,350
2,300
2,250
2,200
2,150
2,100
2,050
2,000
1990
1995
2000
2005
2010
2015
2020
2025
Date

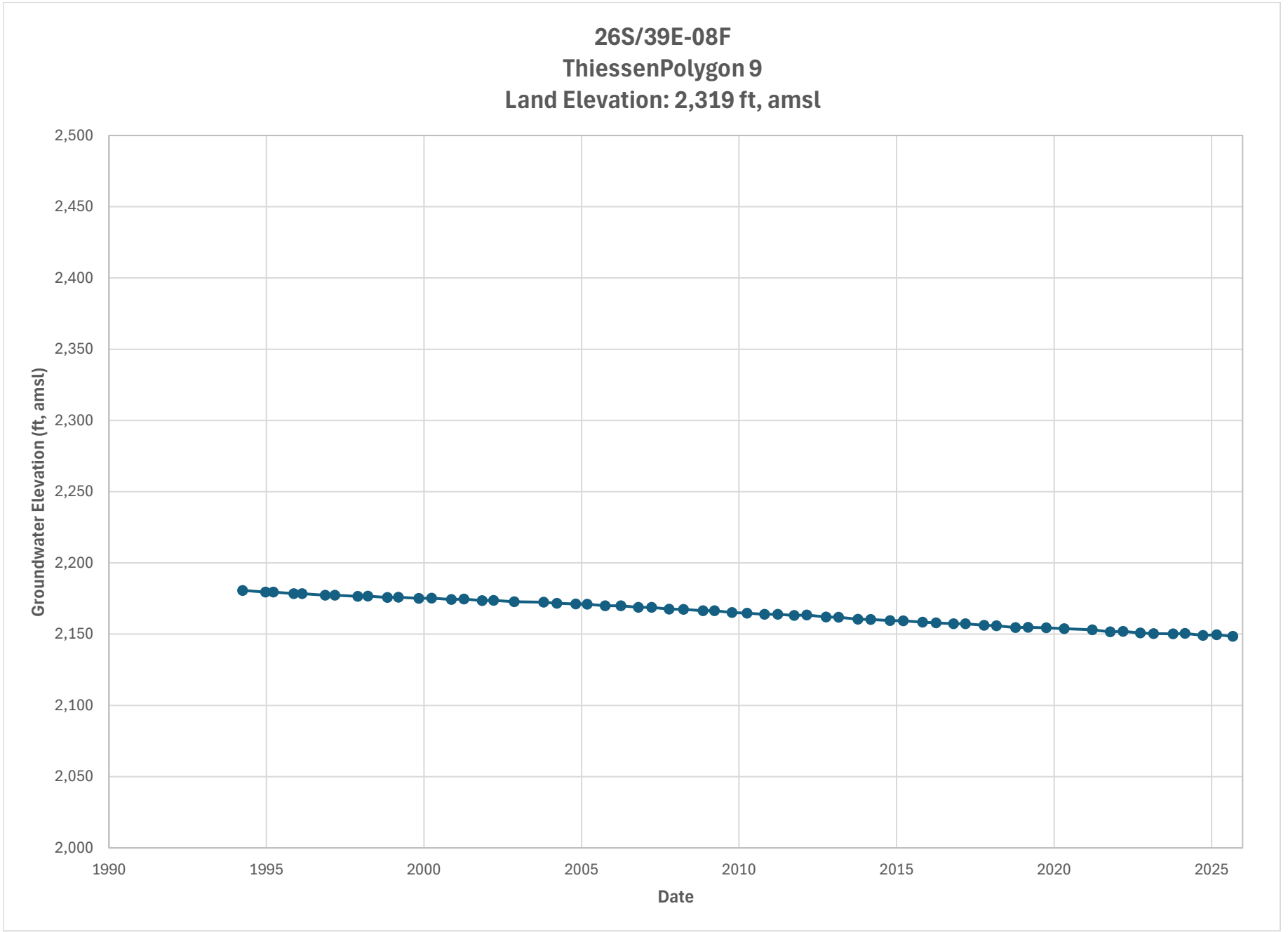

25S/38E-12L01
Thiessen Polygon 4
Land Elevation: 2,353 ft, amsl
Groundwater Elevation (ft, amsl)
2,500
2,450
2,400
2,350
2,300
2,250
2,200
2,150
2,100
2,050
2,000
1990
1995
2000
2005
2010
2015
2020
2025
Date

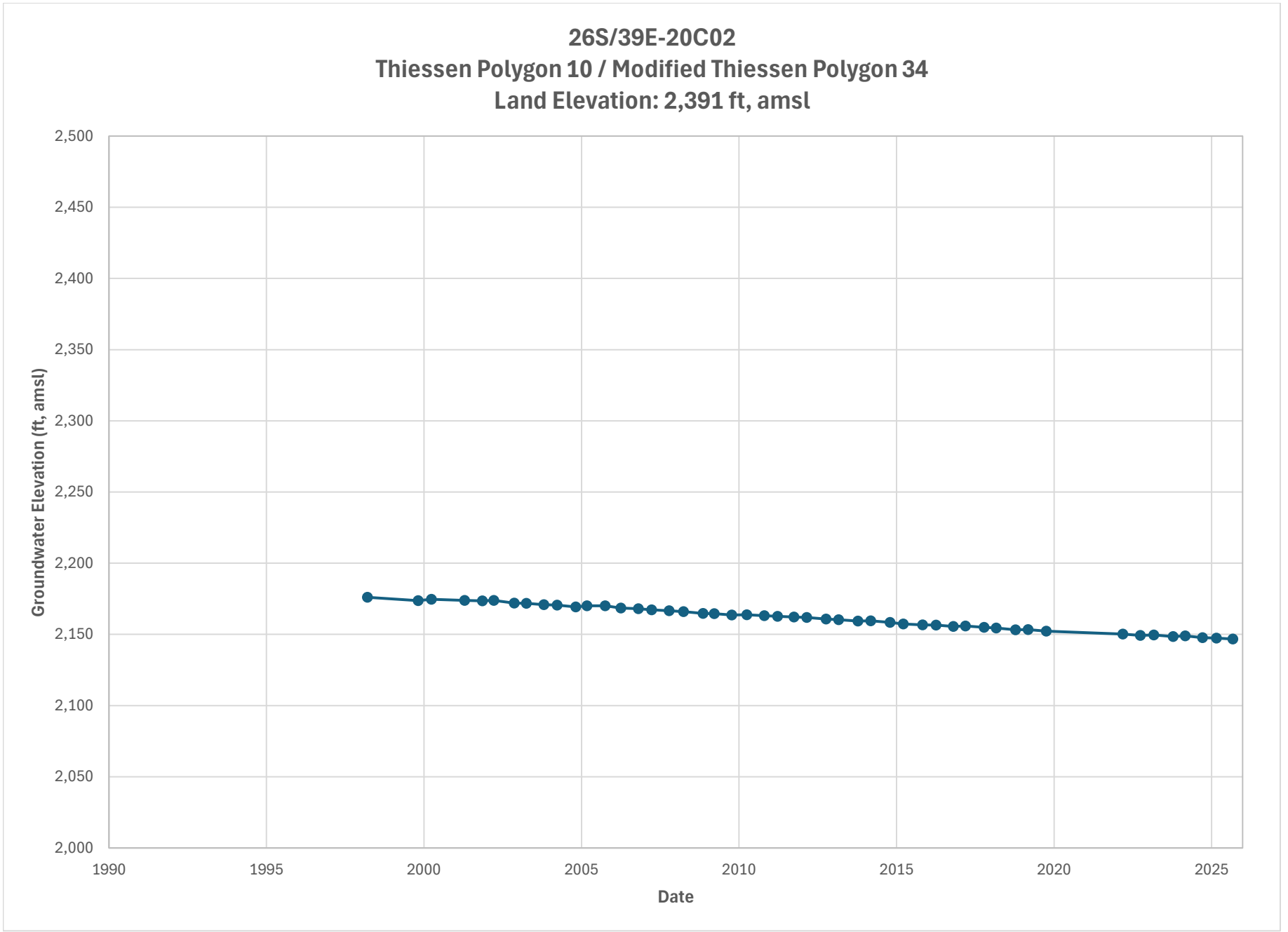

25S/38E-14Q01
Thiessen Polygon 5 / Modified Thiessen Polygon 59
Land Elevation: 2,391 ft, amsl
Groundwater Elevation (ft, amsl)
2,500
2,450
2,400
2,350
2,300
2,250
2,200
2,150
2,100
2,050
2,000
1990
1995
2000
2005
2010
2015
2020
2025
Date

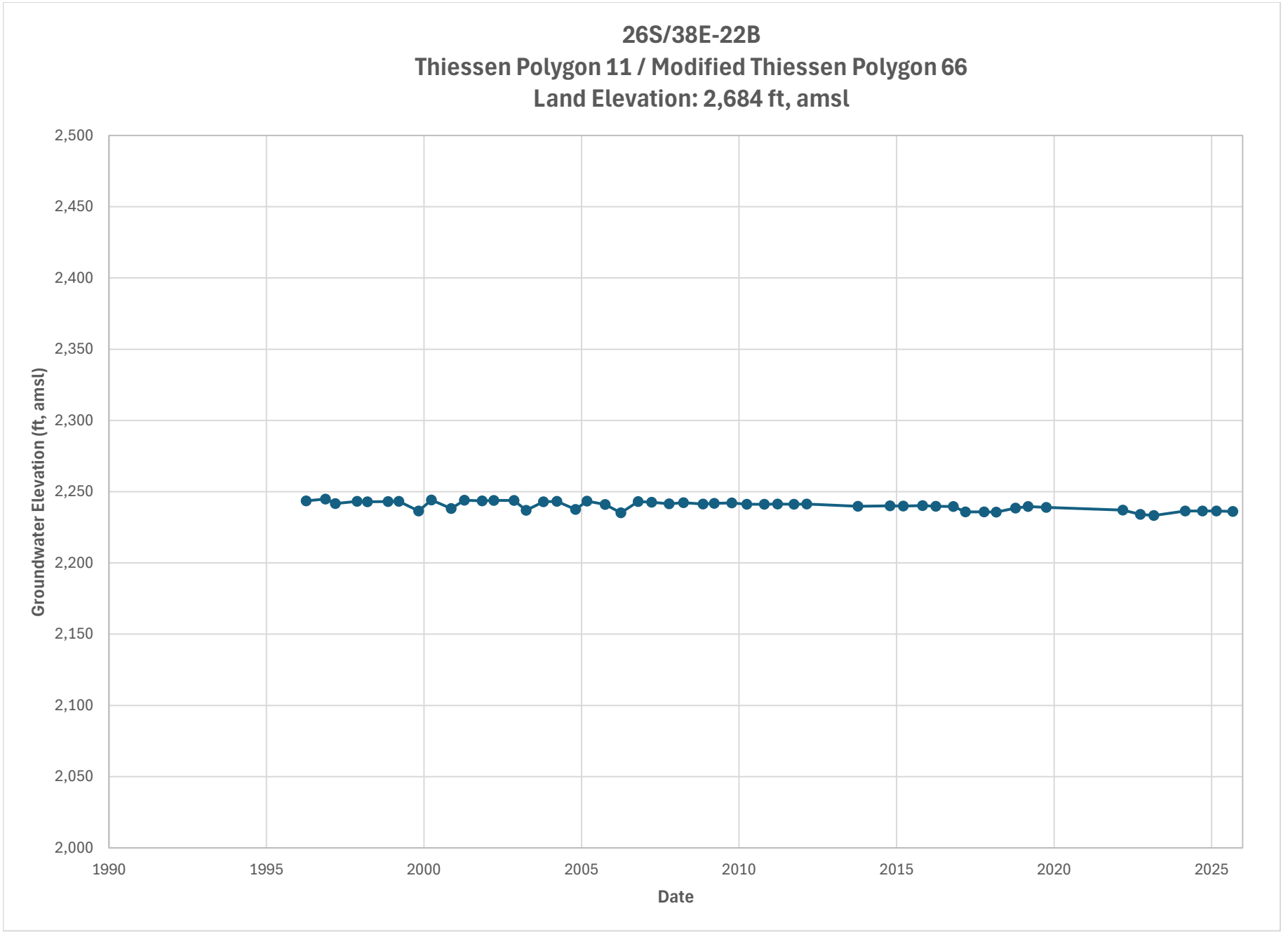

25S/38E-25J01
Thiessen Polygon 6
Land Elevation: 2,277 ft, amsl
Groundwater Elevation (ft, amsl)
2,500
2,450
2,400
2,350
2,300
2,250
2,200
2,150
2,100
2,050
2,000
1990
1995
2000
2005
2010
2015
2020
2025
Date

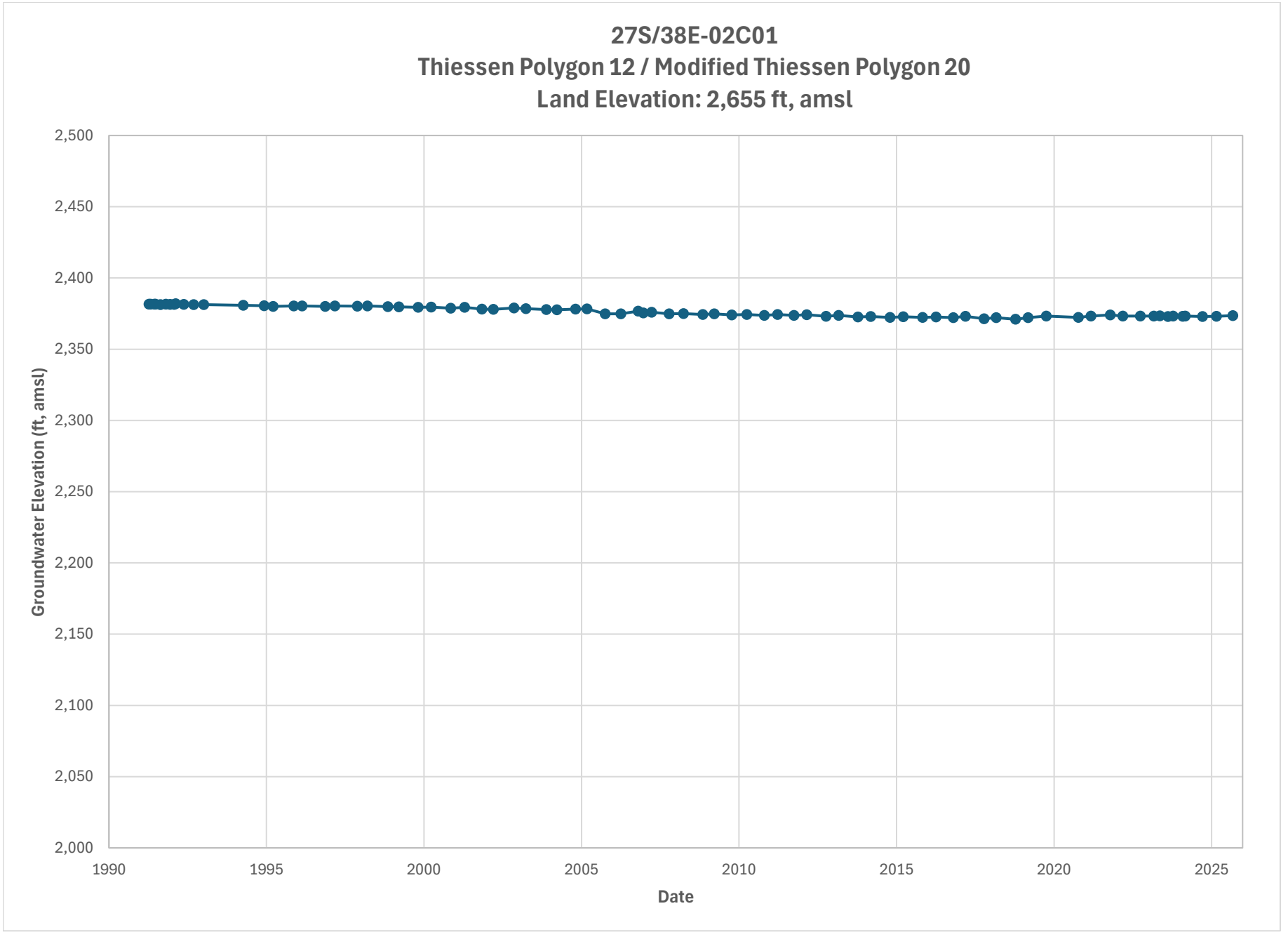

25S/38E-34G01
Thiessen Polygon 7
Land Elevation: 2,520 ft, amsl
Groundwater Elevation (ft, amsl)
2,500
2,450
2,400
2,350
2,300
2,250
2,200
2,150
2,100
2,050
2,000
1990
1995
2000
2005
2010
2015
2020
2025
Date

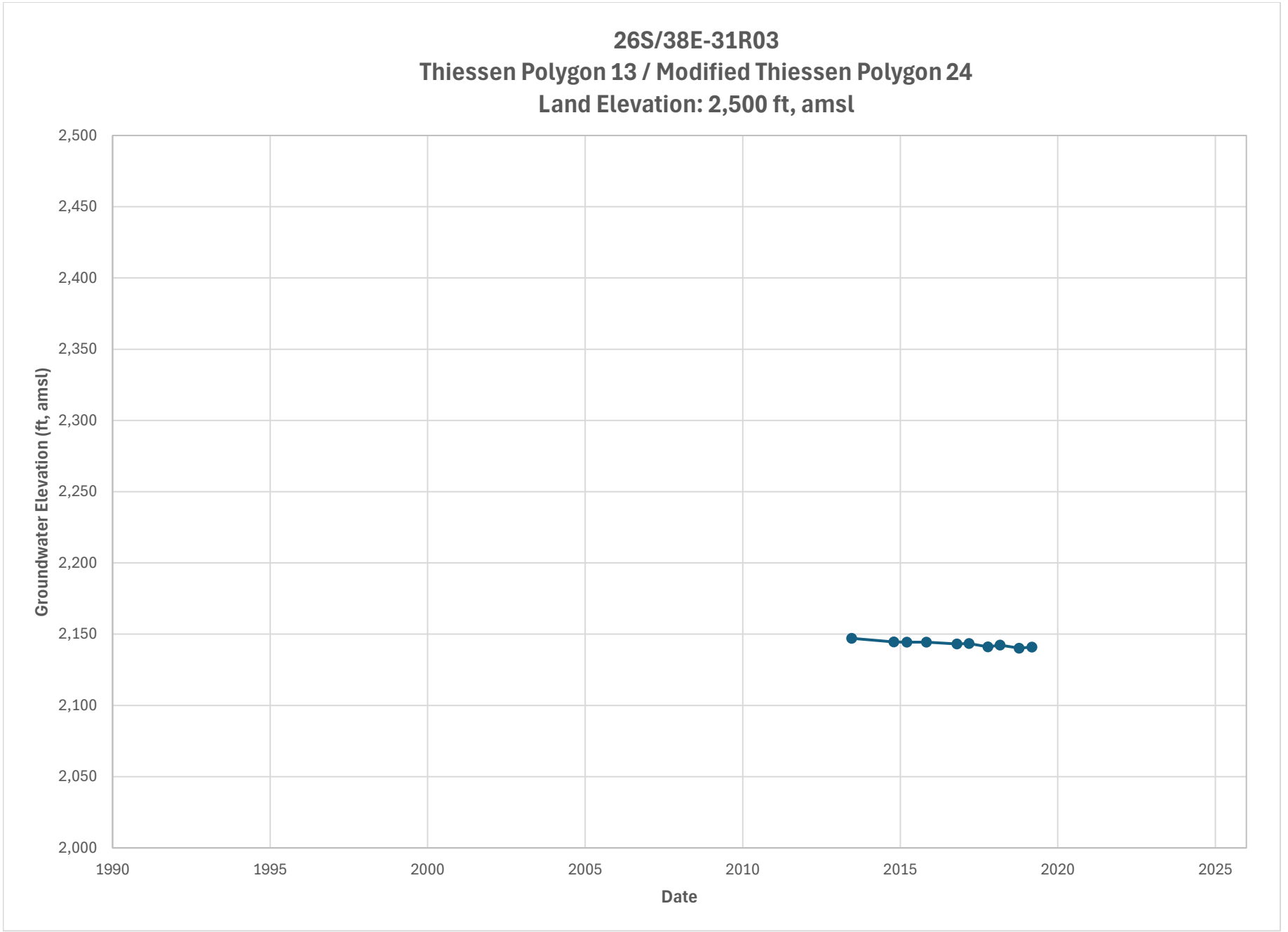

26S/38E-02R01
Thiessen Polygon 8
Land Elevation: 2,398 ft, amsl
Groundwater Elevation (ft, amsl)
2,500
2,450
2,400
2,350
2,300
2,250
2,200
2,150
2,100
2,050
2,000
1990
1995
2000
2005
2010
2015
2020
2025
Date

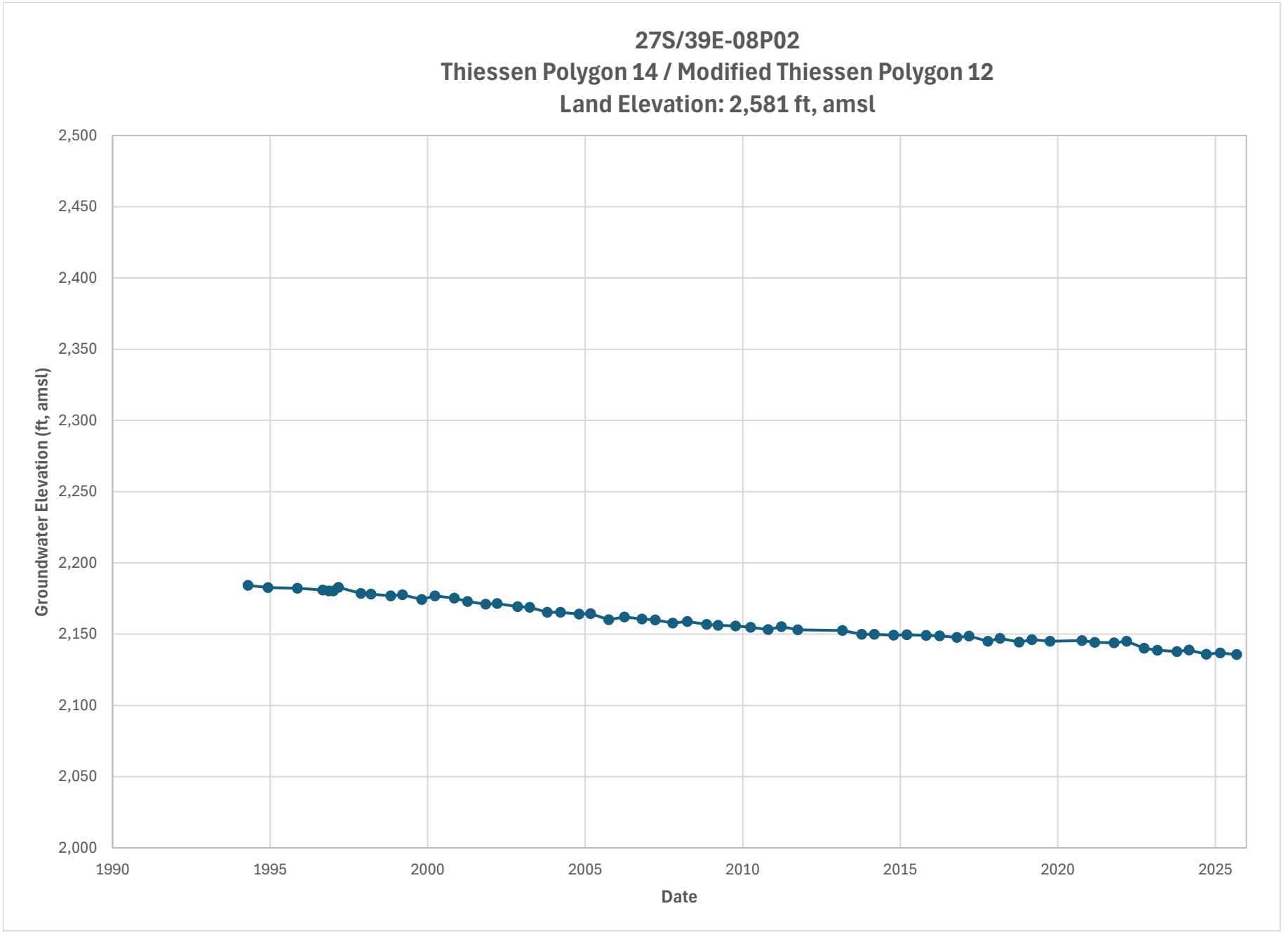

26S/39E-08F
ThiessenPolygon 9
Land Elevation: 2,319 ft, amsl
Groundwater Elevation (ft, amsl)
2,500
2,450
2,400
2,350
2,300
2,250
2,200
2,150
2,100
2,050
2,000
1990
1995
2000
2005
2010
2015
2020
2025
Date

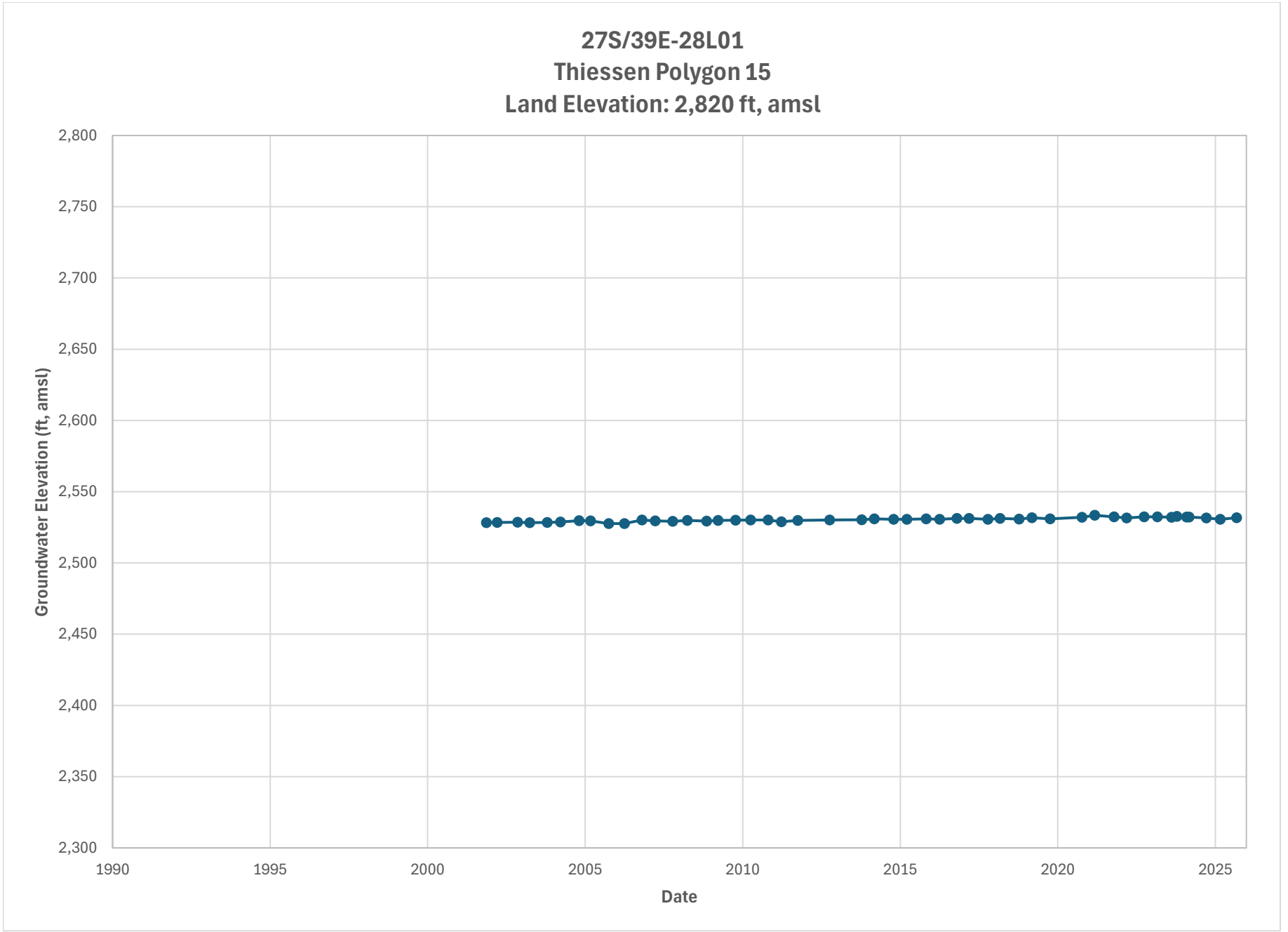

26S/39E-20C02
Thiessen Polygon 10 / Modified Thiessen Polygon 34
Land Elevation: 2,391 ft, amsl
Groundwater Elevation (ft, amsl)
2,500
2,450
2,400
2,350
2,300
2,250
2,200
2,150
2,100
2,050
2,000
1990
1995
2000
2005
2010
2015
2020
2025
Date

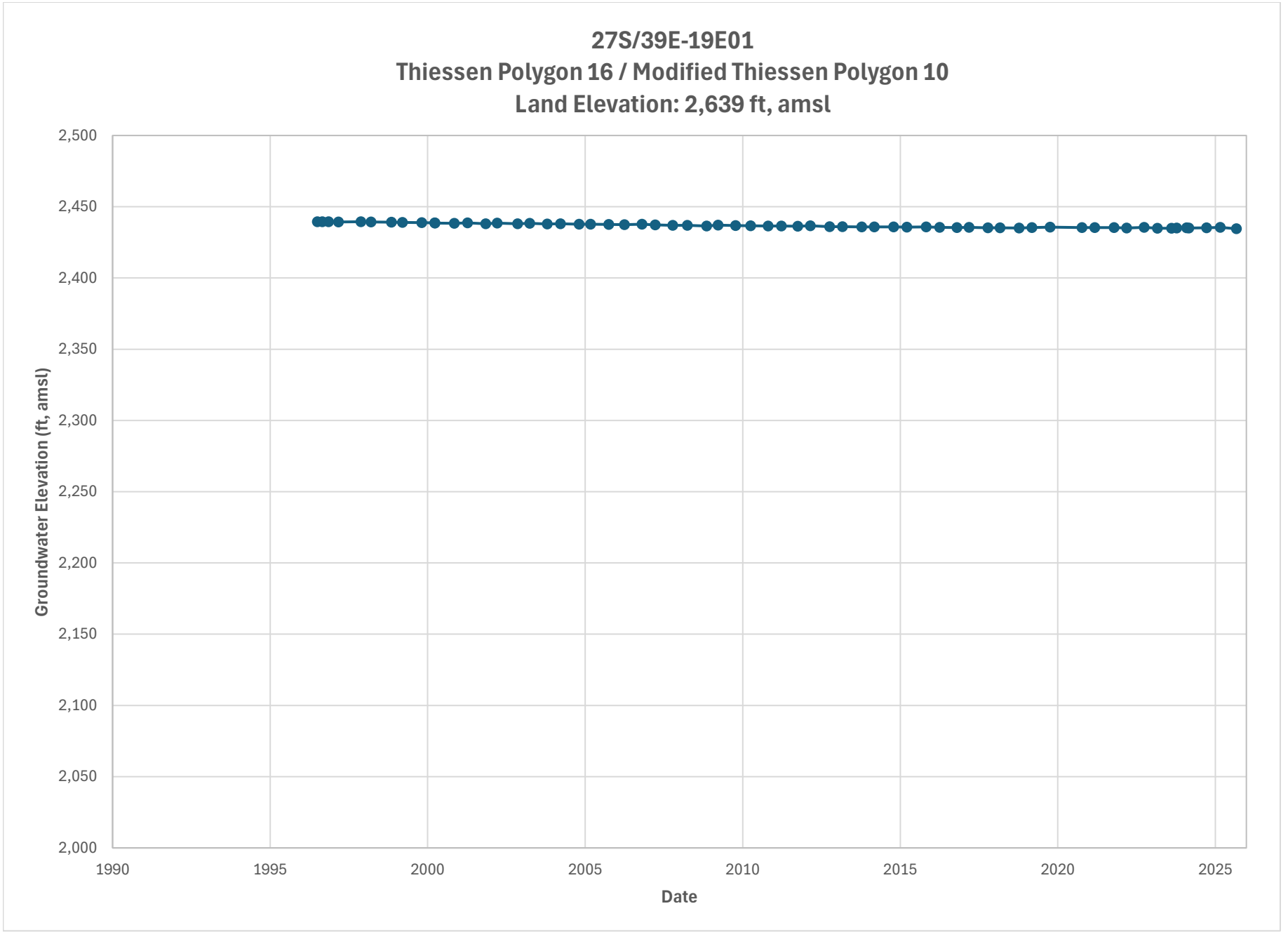

26S/38E-22B
Thiessen Polygon 11 / Modified Thiessen Polygon 66
Land Elevation: 2,684 ft, amsl
Groundwater Elevation (ft, amsl)
2,500
2,450
2,400
2,350
2,300
2,250
2,200
2,150
2,100
2,050
2,000
1990
1995
2000
2005
2010
2015
2020
2025
Date

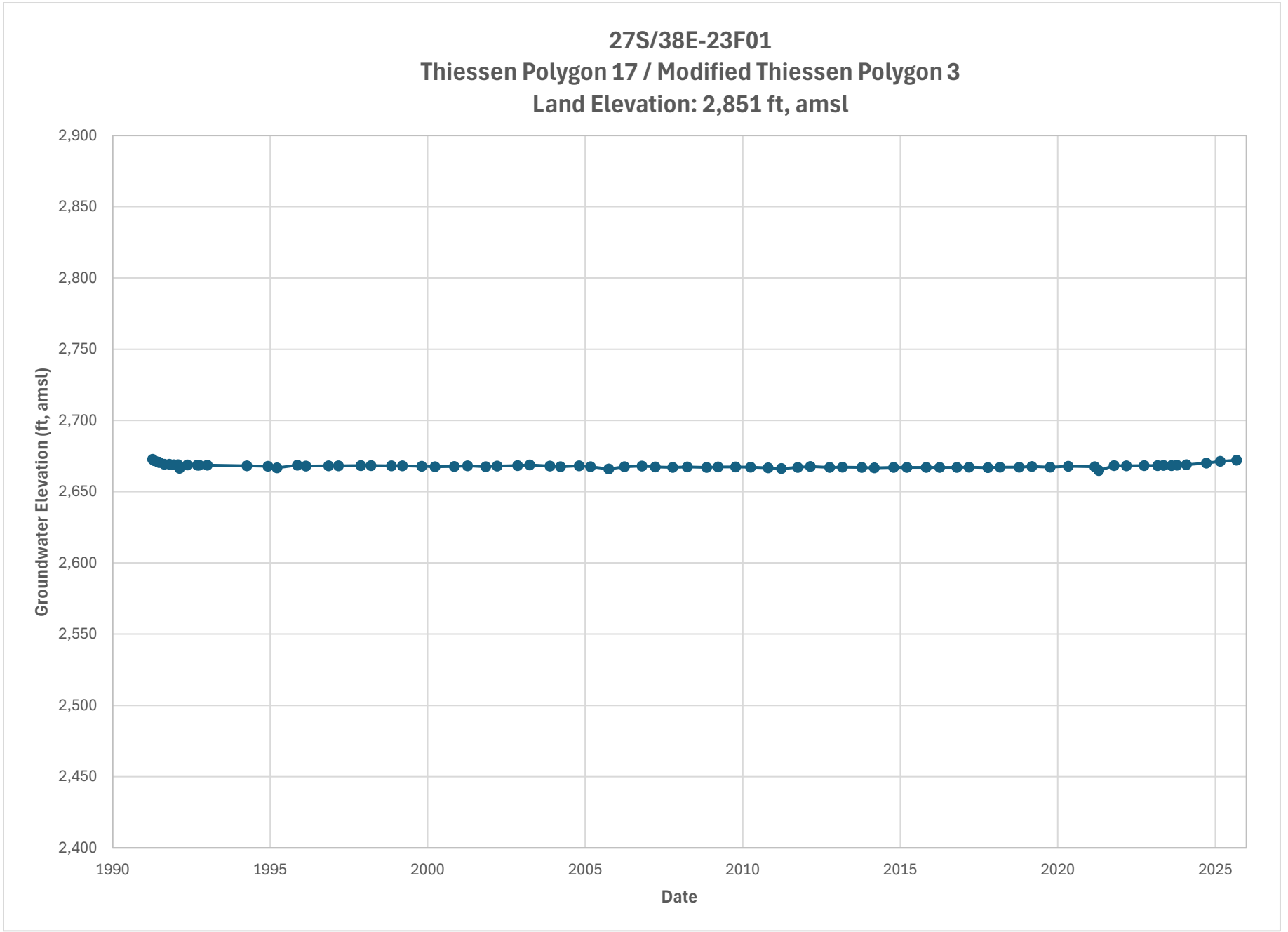

27S/38E-02C01
Thiessen Polygon 12 / Modified Thiessen Polygon 20
Land Elevation: 2,655 ft, amsl
Groundwater Elevation (ft, amsl)
2,500
2,450
2,400
2,350
2,300
2,250
2,200
2,150
2,100
2,050
2,000
1990
1995
2000
2005
2010
2015
2020
2025
Date

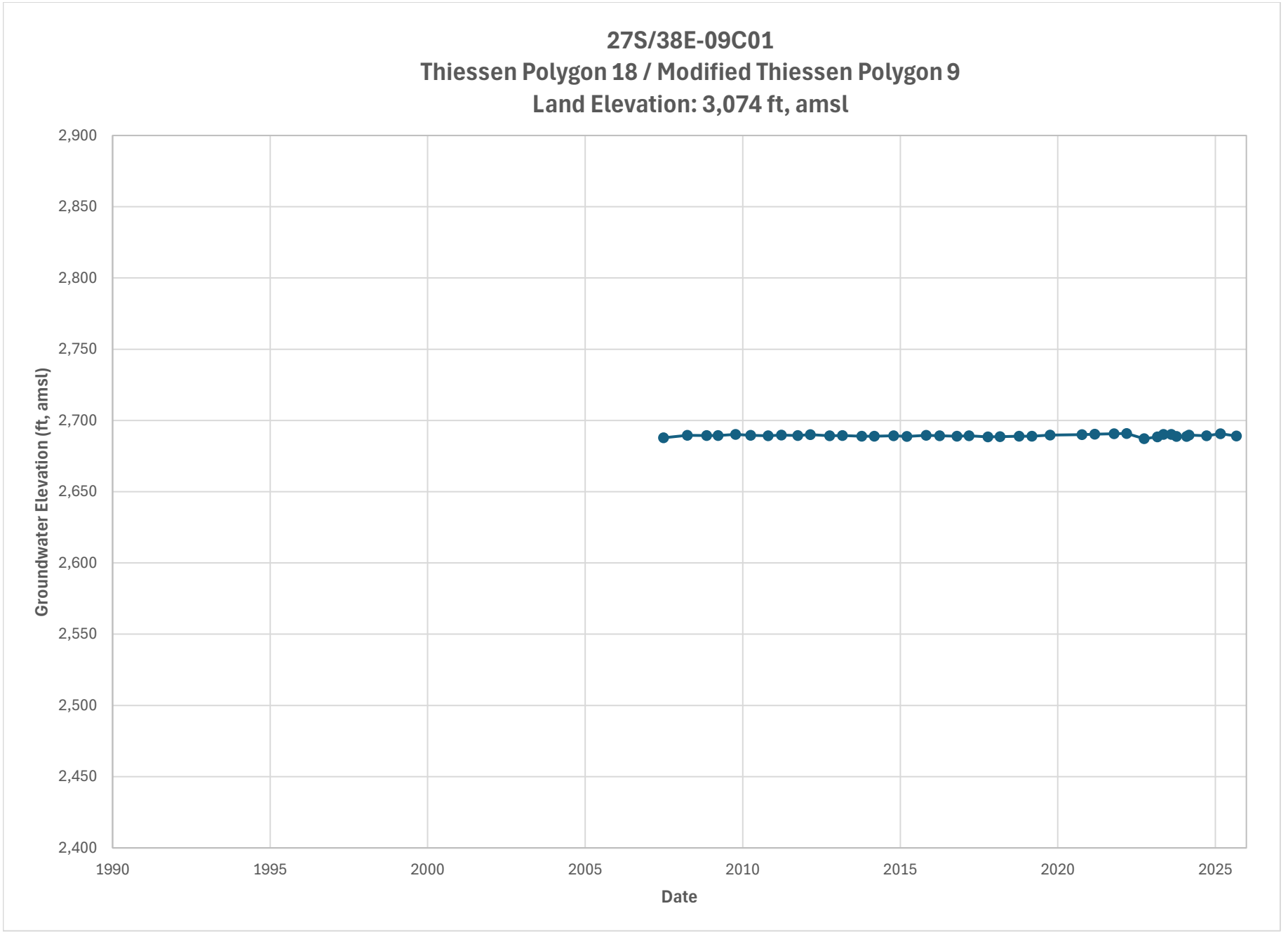

26S/38E-31R03
Thiessen Polygon 13 / Modified Thiessen Polygon 24
Land Elevation: 2,500 ft, amsl
Groundwater Elevation (ft, amsl)
2,500
2,450
2,400
2,350
2,300
2,250
2,200
2,150
2,100
2,050
2,000
1990
1995
2000
2005
2010
2015
2020
2025
Date

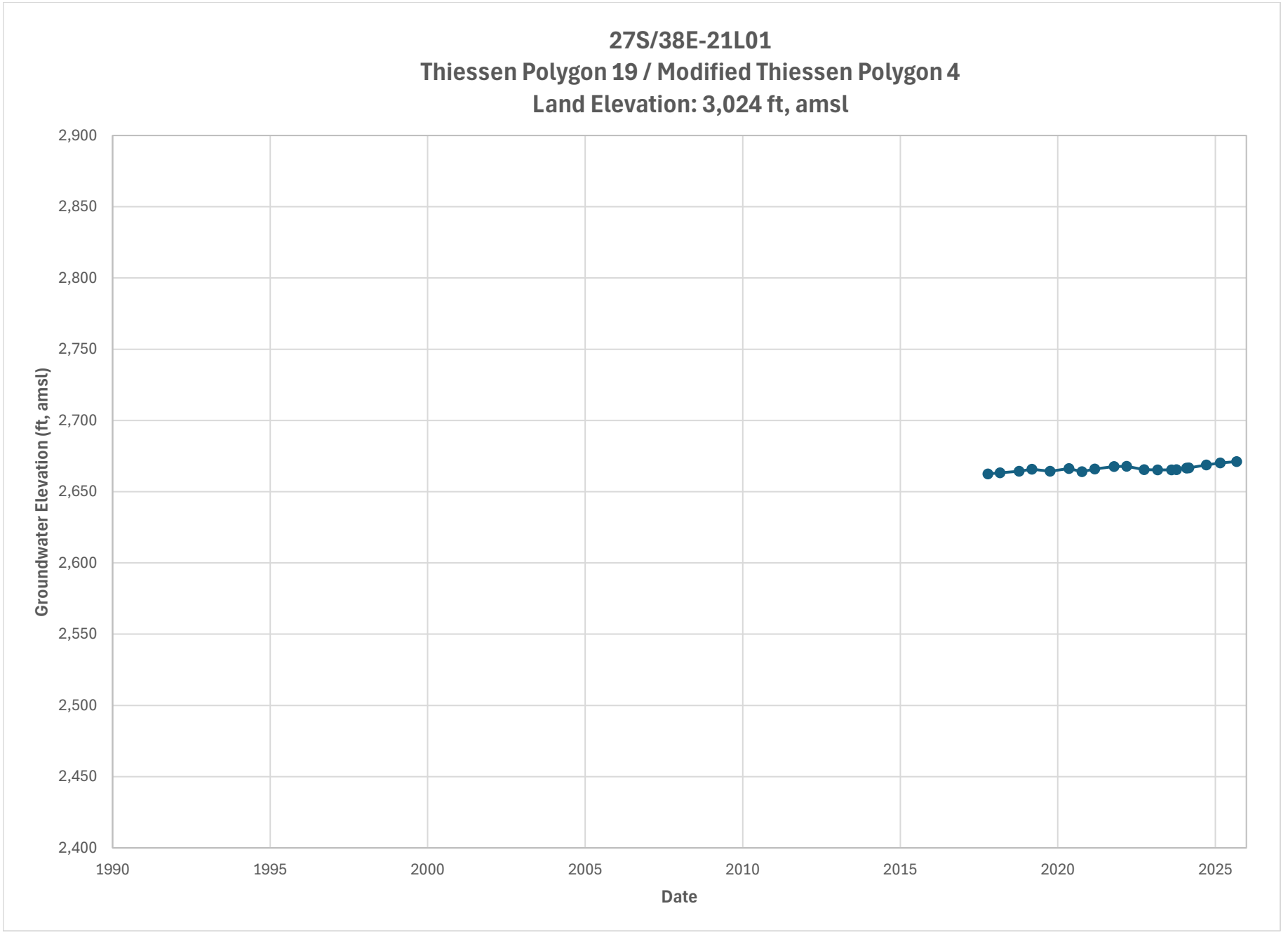

27S/39E-08P02
Thiessen Polygon 14 / Modified Thiessen Polygon 12
Land Elevation: 2,581 ft, amsl
Groundwater Elevation (ft, amsl)
2,500
2,450
2,400
2,350
2,300
2,250
2,200
2,150
2,100
2,050
2,000
1990
1995
2000
2005
2010
2015
2020
2025
Date

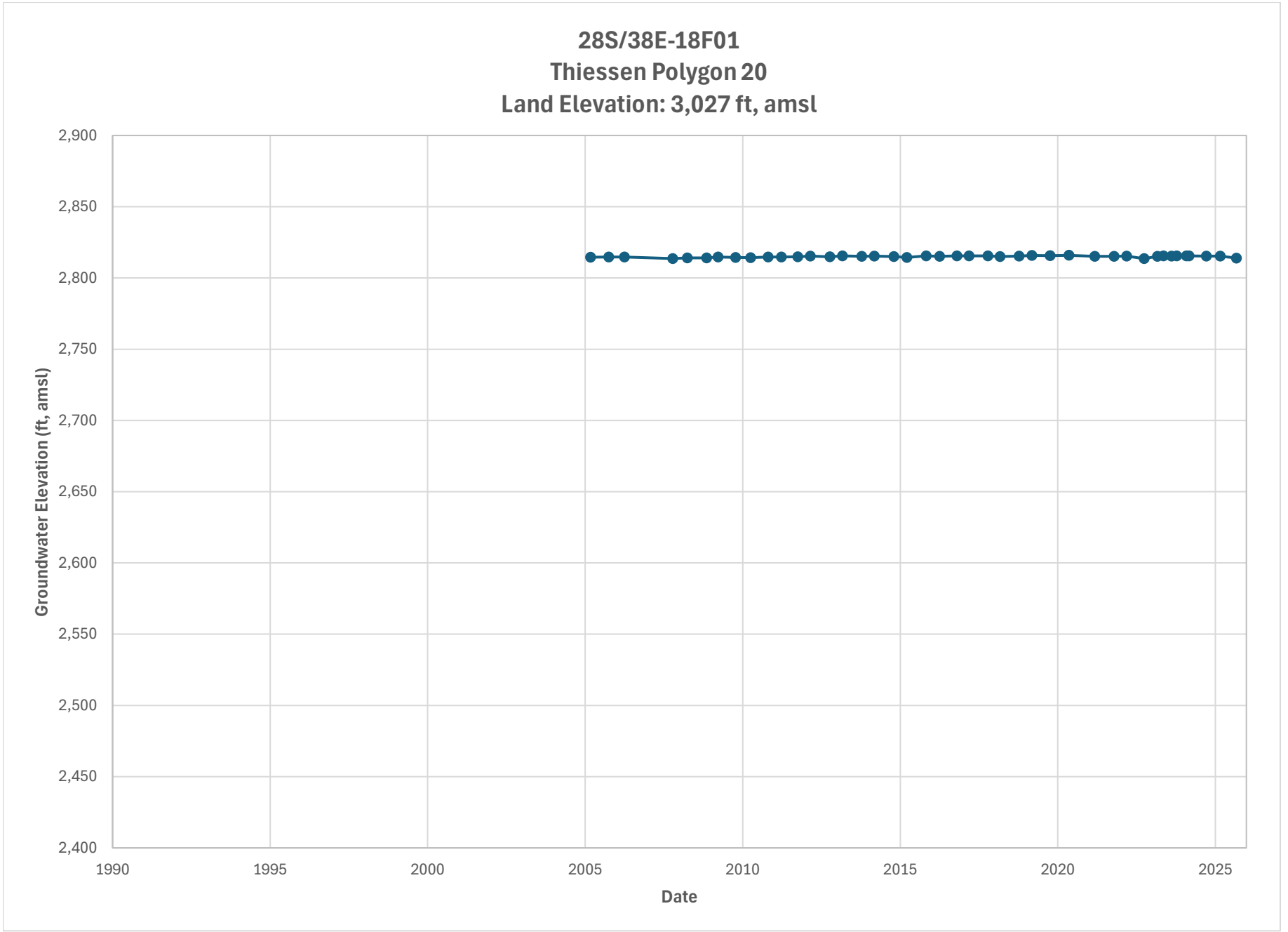

27S/39E-28L01
Thiessen Polygon 15
Land Elevation: 2,820 ft, amsl
Groundwater Elevation (ft, amsl)
2,800
2,750
2,700
2,650
2,600
2,550
2,500
2,450
2,400
2,350
2,300
1990
1995
2000
2005
2010
2015
2020
2025
Date

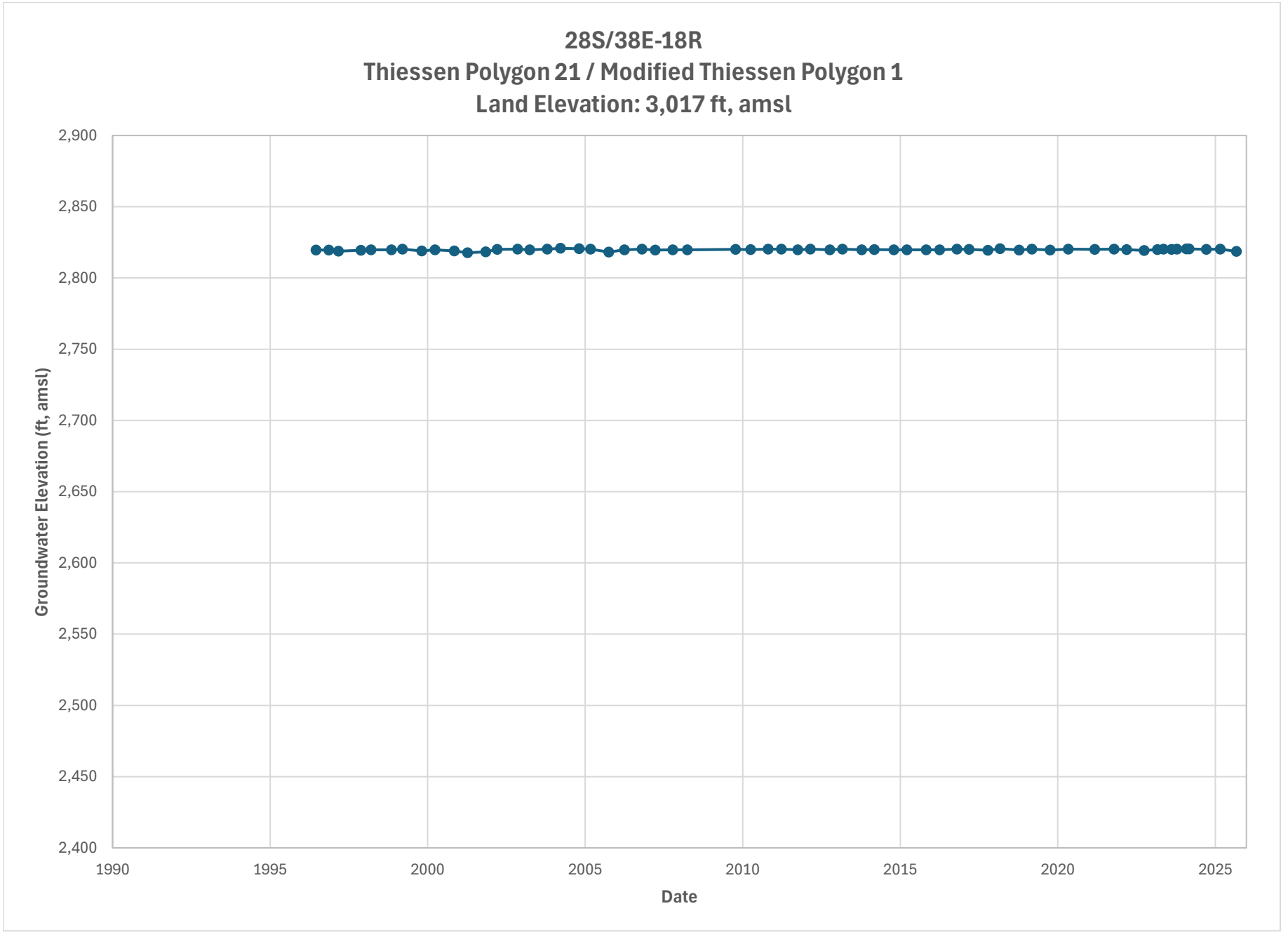

27S/39E-19E01
Thiessen Polygon 16 / Modified Thiessen Polygon 10
Land Elevation: 2,639 ft, amsl
Groundwater Elevation (ft, amsl)
2,500
2,450
2,400
2,350
2,300
2,250
2,200
2,150
2,100
2,050
2,000
1990
1995
2000
2005
2010
2015
2020
2025
Date

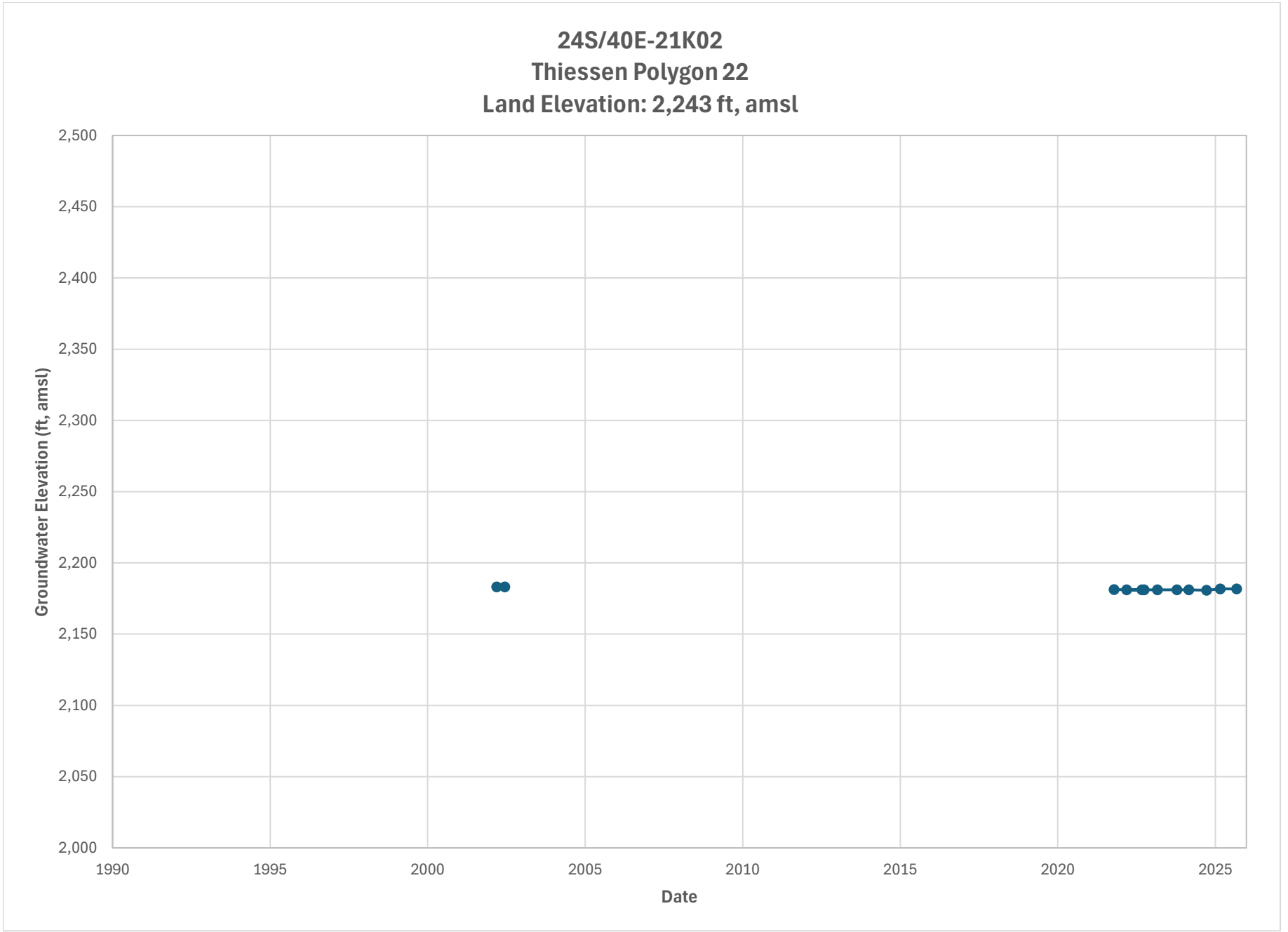

27S/38E-23F01
Thiessen Polygon 17 / Modified Thiessen Polygon 3
Land Elevation: 2,851 ft, amsl
Groundwater Elevation (ft, amsl)
2,900
2,850
2,800
2,750
2,700
2,650
2,600
2,550
2,500
2,450
2,400
1990
1995
2000
2005
2010
2015
2020
2025
Date

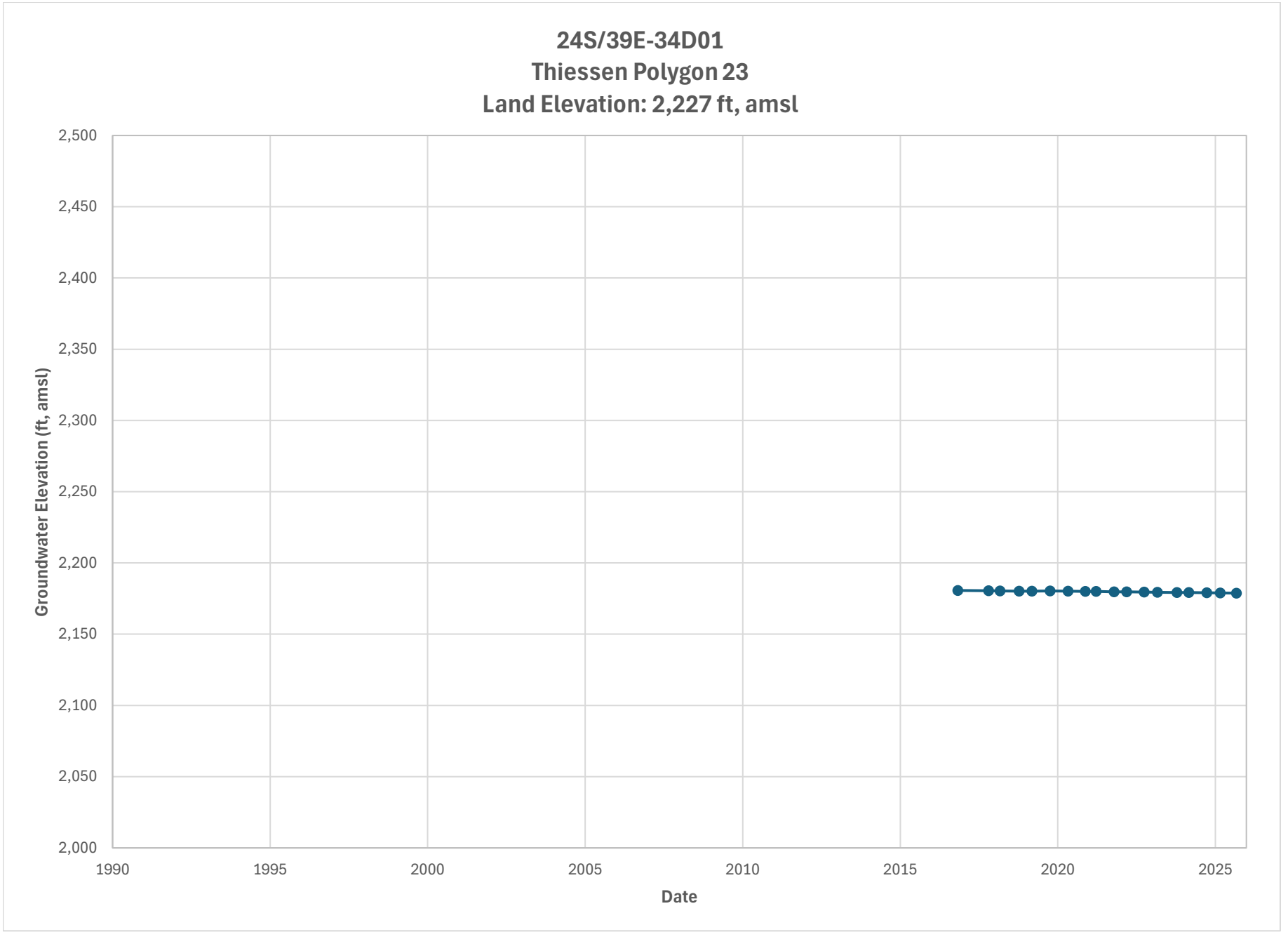

27S/38E-09C01
Thiessen Polygon 18 / Modified Thiessen Polygon 9
Land Elevation: 3,074 ft, amsl
Groundwater Elevation (ft, amsl)
2,900
2,850
2,800
2,750
2,700
2,650
2,600
2,550
2,500
2,450
2,400
1990
1995
2000
2005
2010
2015
2020
2025
Date

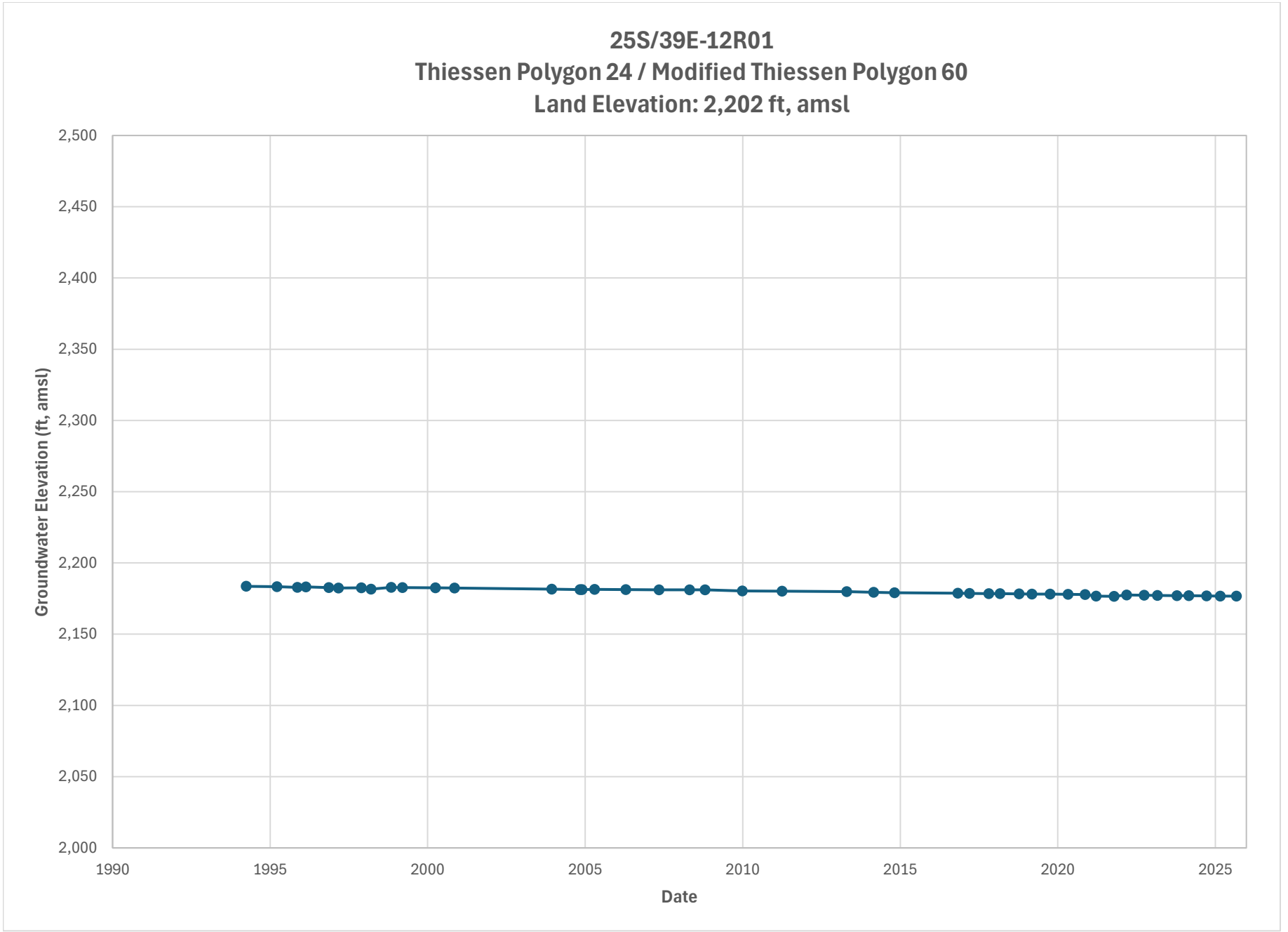

27S/38E-21L01
Thiessen Polygon 19 / Modified Thiessen Polygon 4
Land Elevation: 3,024 ft, amsl
Groundwater Elevation (ft, amsl)
2,900
2,850
2,800
2,750
2,700
2,650
2,600
2,550
2,500
2,450
2,400
1990
1995
2000
2005
2010
2015
2020
2025
Date

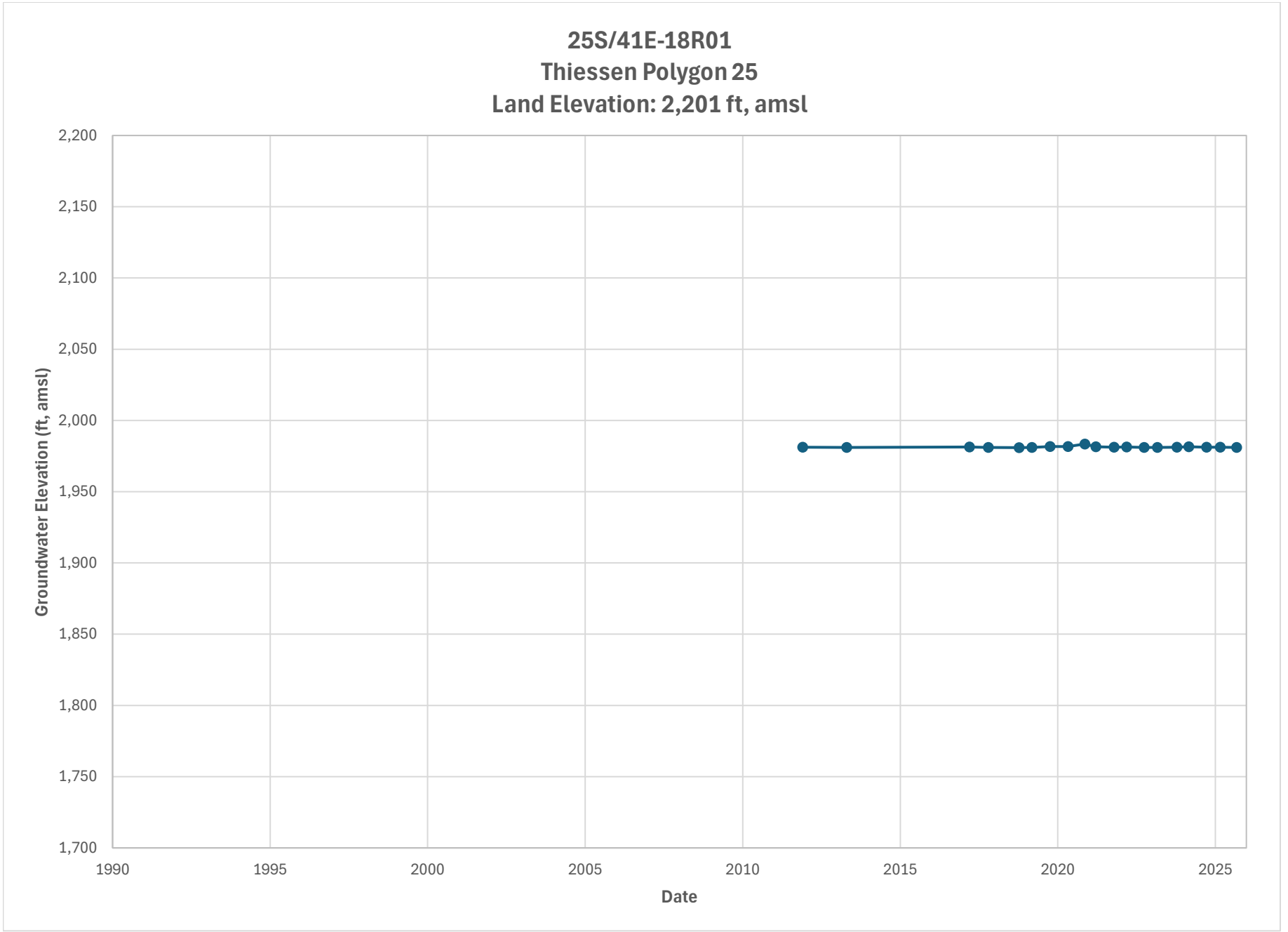

28S/38E-18F01
Thiessen Polygon 20
Land Elevation: 3,027 ft, amsl
Groundwater Elevation (ft, amsl)
2,900
2,850
2,800
2,750
2,700
2,650
2,600
2,550
2,500
2,450
2,400
1990
1995
2000
2005
2010
2015
2020
2025
Date

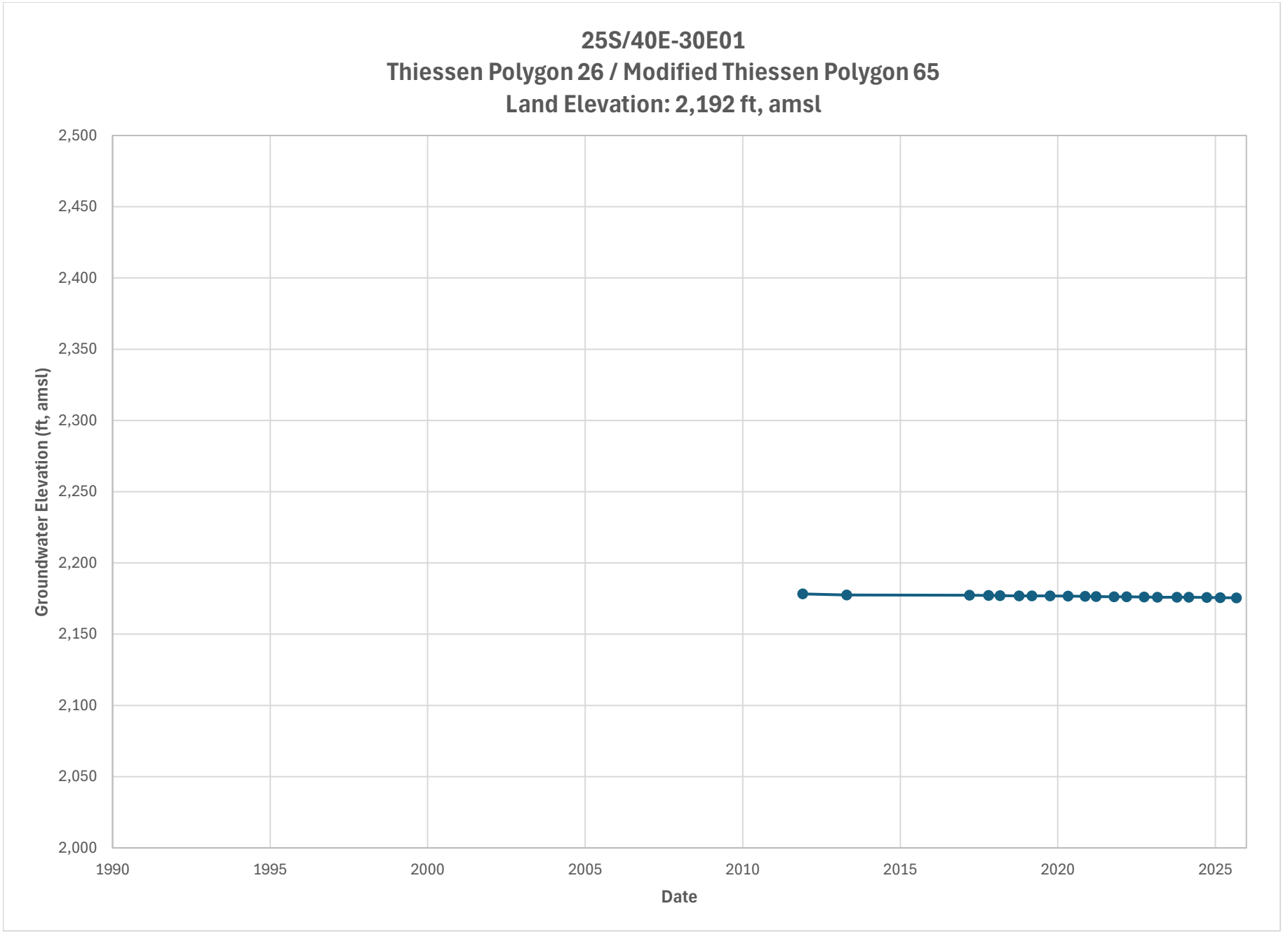

28S/38E-18R
Thiessen Polygon 21 / Modified Thiessen Polygon 1
Land Elevation: 3,017 ft, amsl
Groundwater Elevation (ft, amsl)
2,900
2,850
2,800
2,750
2,700
2,650
2,600
2,550
2,500
2,450
2,400
1990
1995
2000
2005
2010
2015
2020
2025
Date

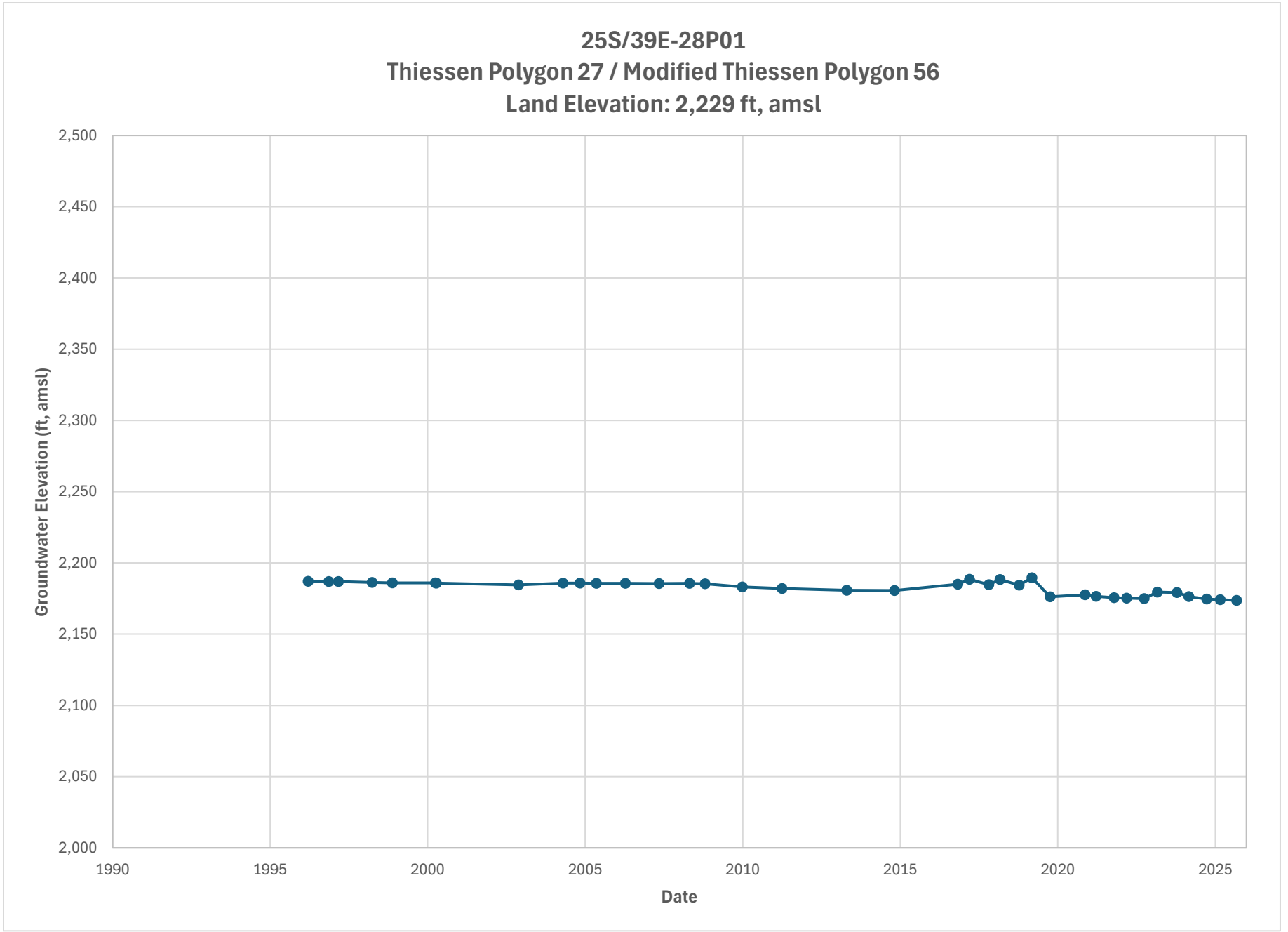

24S/40E-21K02
Thiessen Polygon 22
Land Elevation: 2,243 ft, amsl
Groundwater Elevation (ft, amsl)
2,500
2,450
2,400
2,350
2,300
2,250
2,200
2,150
2,100
2,050
2,000
1990
1995
2000
2005
2010
2015
2020
2025
Date

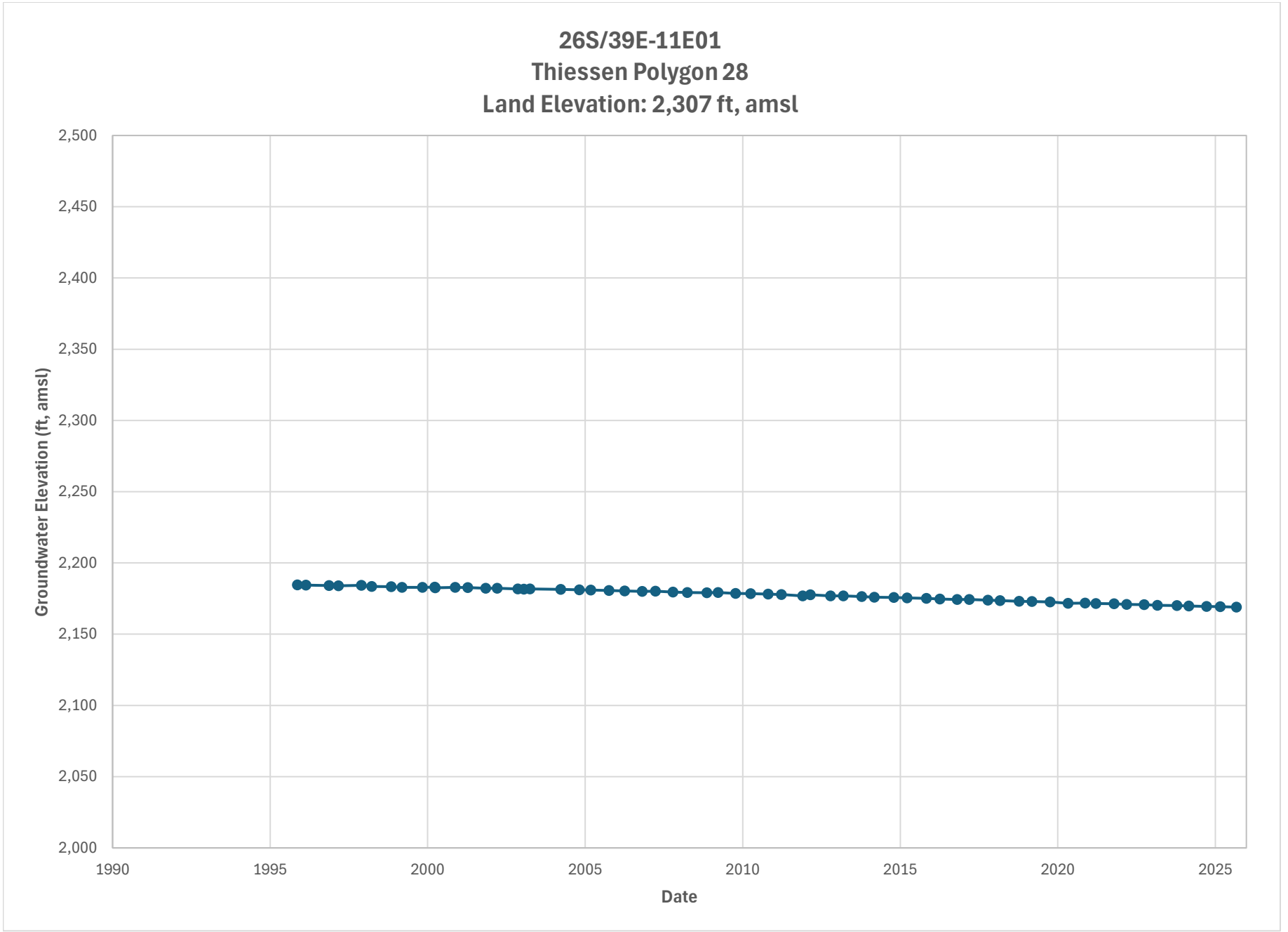

24S/39E-34D01
Thiessen Polygon 23
Land Elevation: 2,227 ft, amsl
Groundwater Elevation (ft, amsl)
2,500
2,450
2,400
2,350
2,300
2,250
2,200
2,150
2,100
2,050
2,000
1990
1995
2000
2005
2010
2015
2020
2025
Date

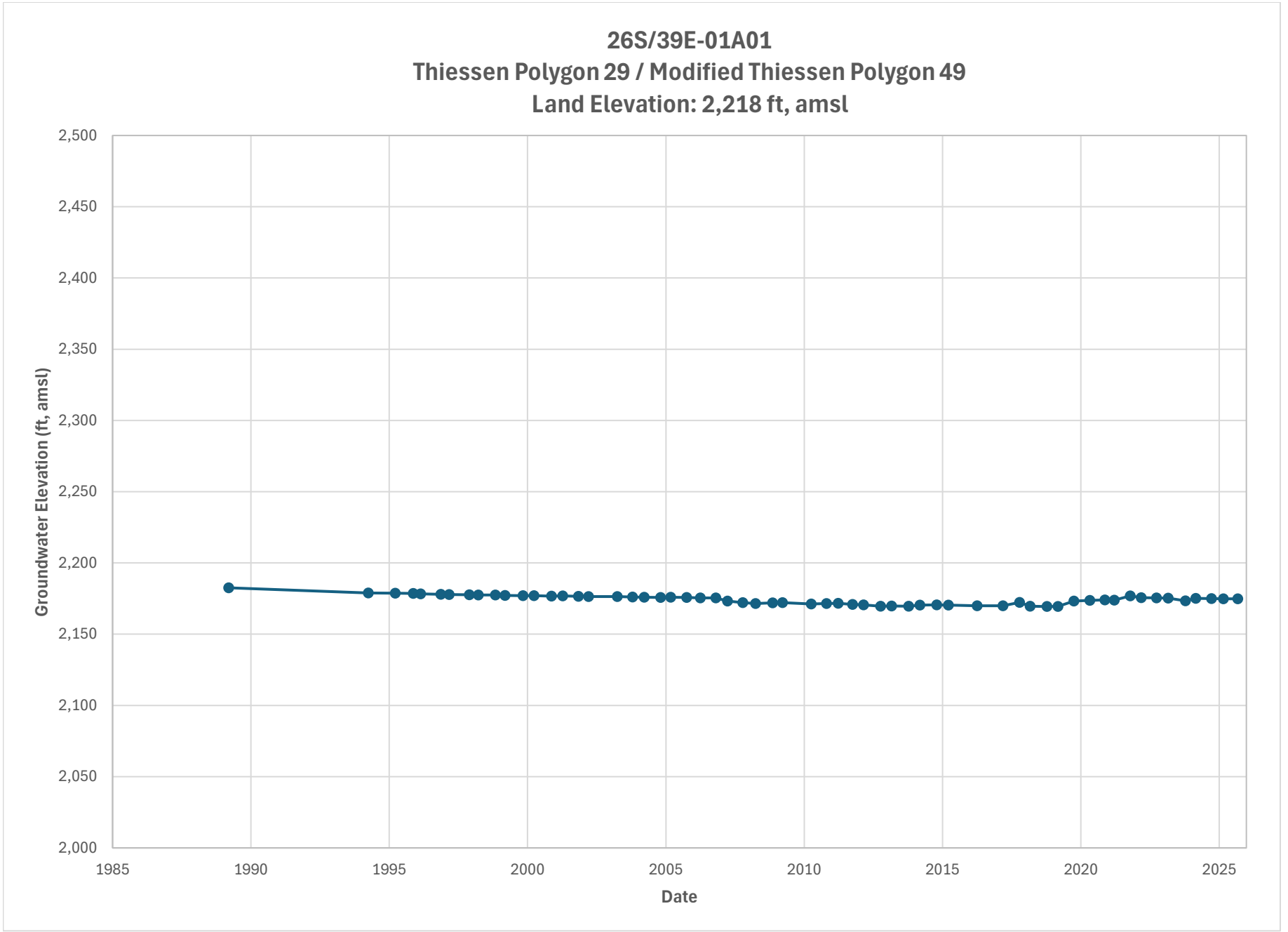

25S/39E-12R01
Thiessen Polygon 24 / Modified Thiessen Polygon 60
Land Elevation: 2,202 ft, amsl
Groundwater Elevation (ft, amsl)
2,500
2,450
2,400
2,350
2,300
2,250
2,200
2,150
2,100
2,050
2,000
1990
1995
2000
2005
2010
2015
2020
2025
Date

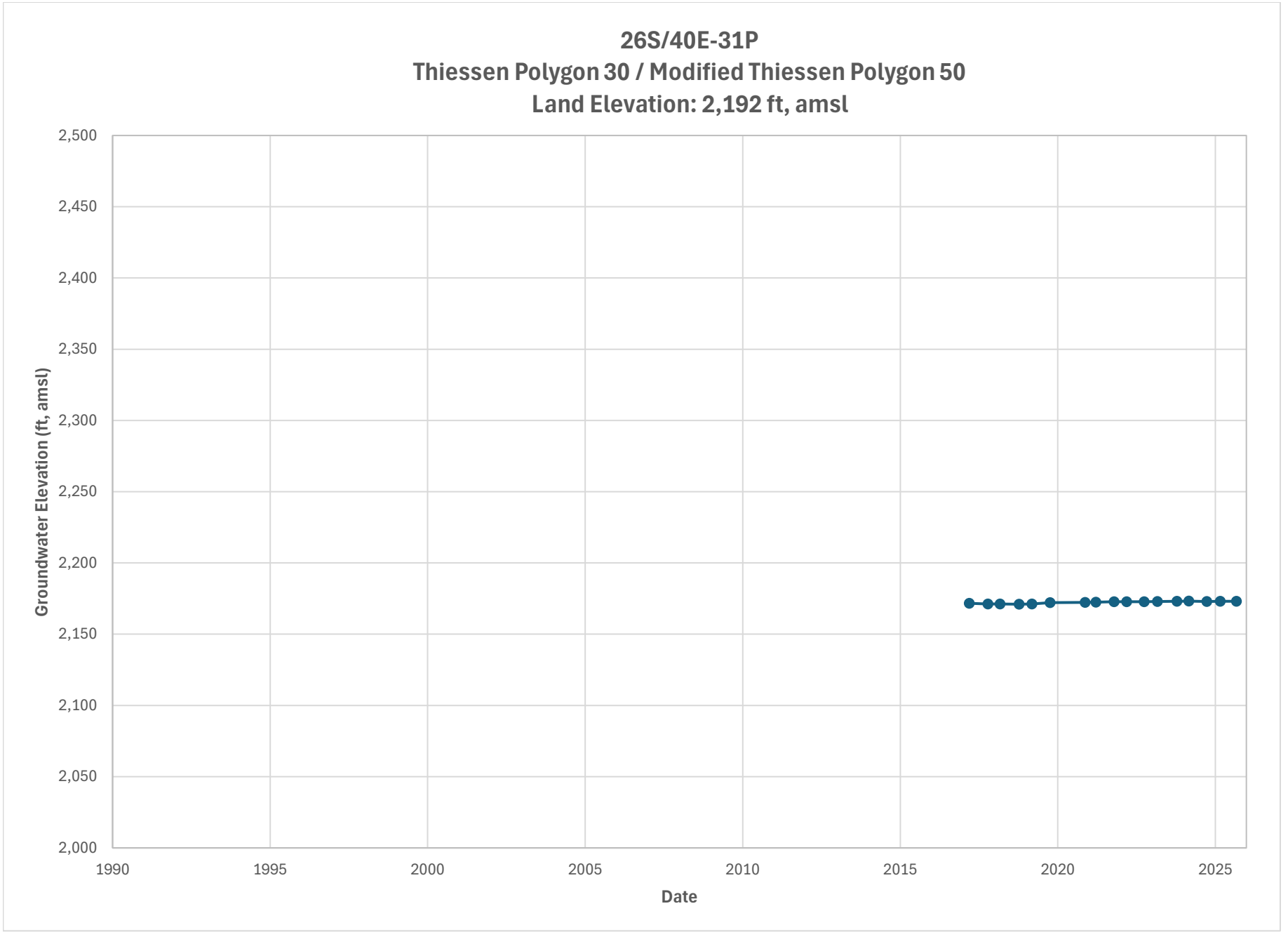

25S/41E-18R01
Thiessen Polygon 25
Land Elevation: 2,201 ft, amsl
Groundwater Elevation (ft, amsl)
2,200
2,150
2,100
2,050
2,000
1,950
1,900
1,850
1,800
1,750
1,700
1990
1995
2000
2005
2010
2015
2020
2025
Date

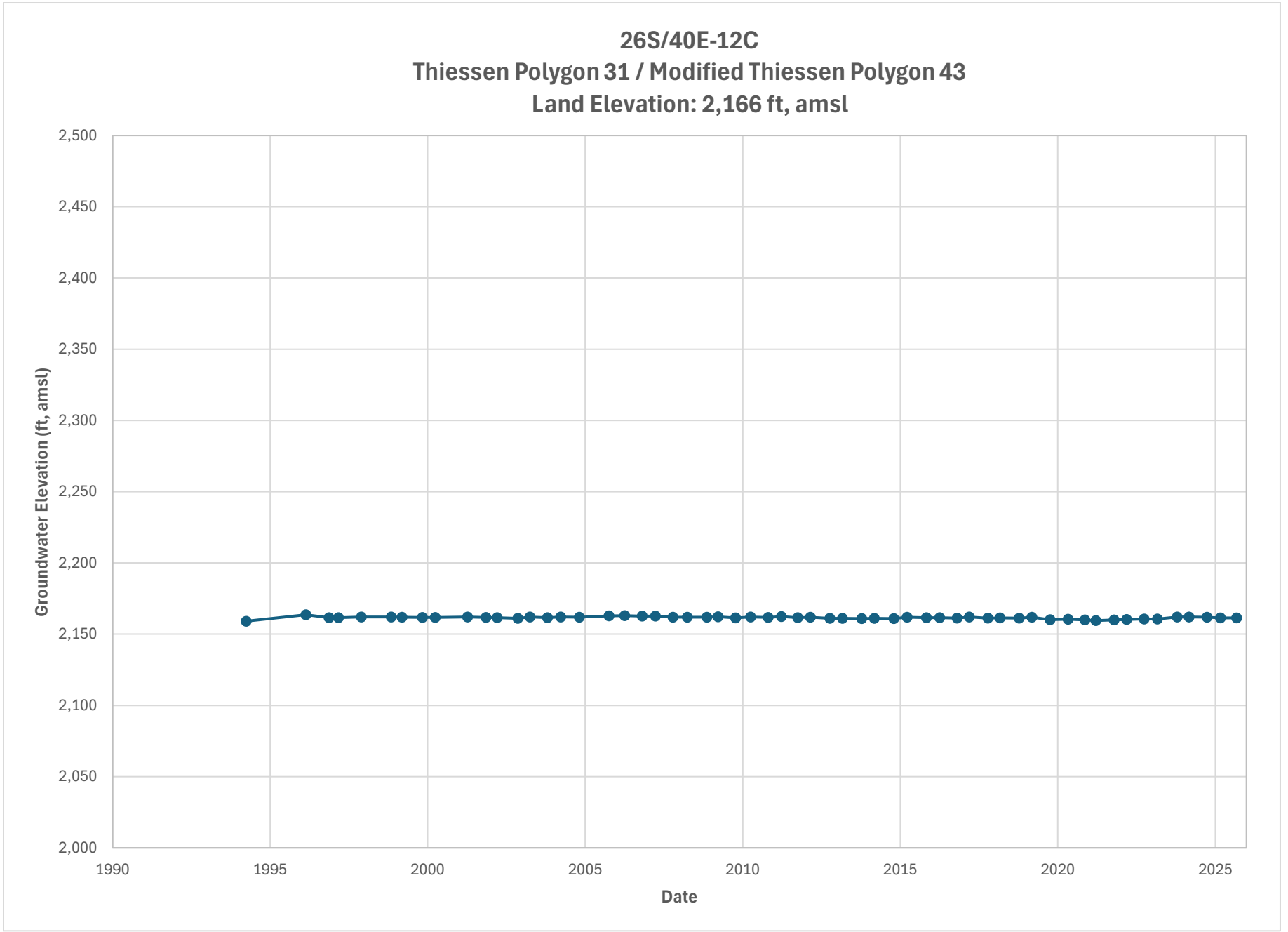

25S/40E-30E01
Thiessen Polygon 26 / Modified Thiessen Polygon 65
Land Elevation: 2,192 ft, amsl
Groundwater Elevation (ft, amsl)
2,500
2,450
2,400
2,350
2,300
2,250
2,200
2,150
2,100
2,050
2,000
1990
1995
2000
2005
2010
2015
2020
2025
Date

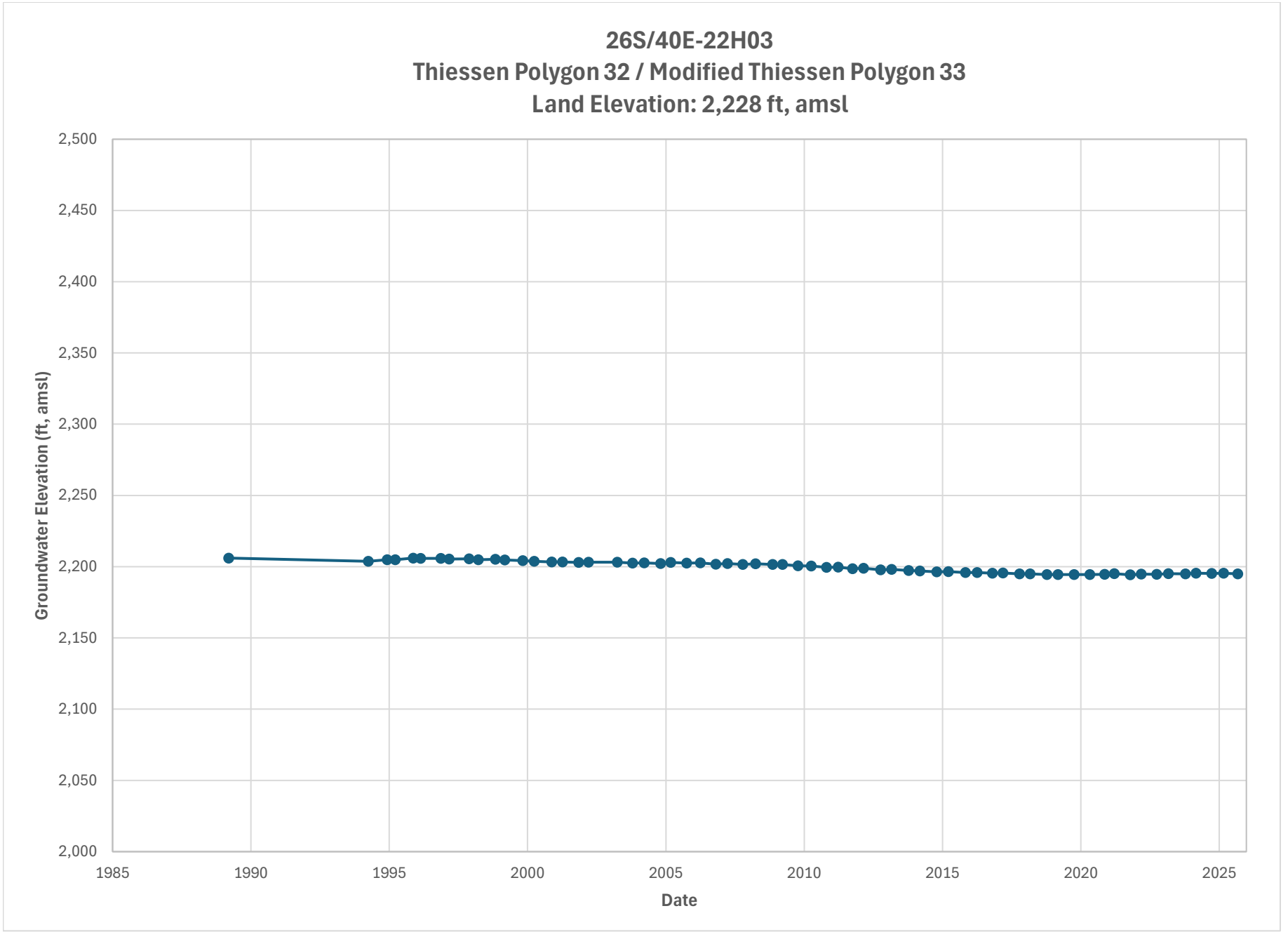

25S/39E-28P01
Thiessen Polygon 27 / Modified Thiessen Polygon 56
Land Elevation: 2,229 ft, amsl
Groundwater Elevation (ft, amsl)
2,500
2,450
2,400
2,350
2,300
2,250
2,200
2,150
2,100
2,050
2,000
1990
1995
2000
2005
2010
2015
2020
2025
Date

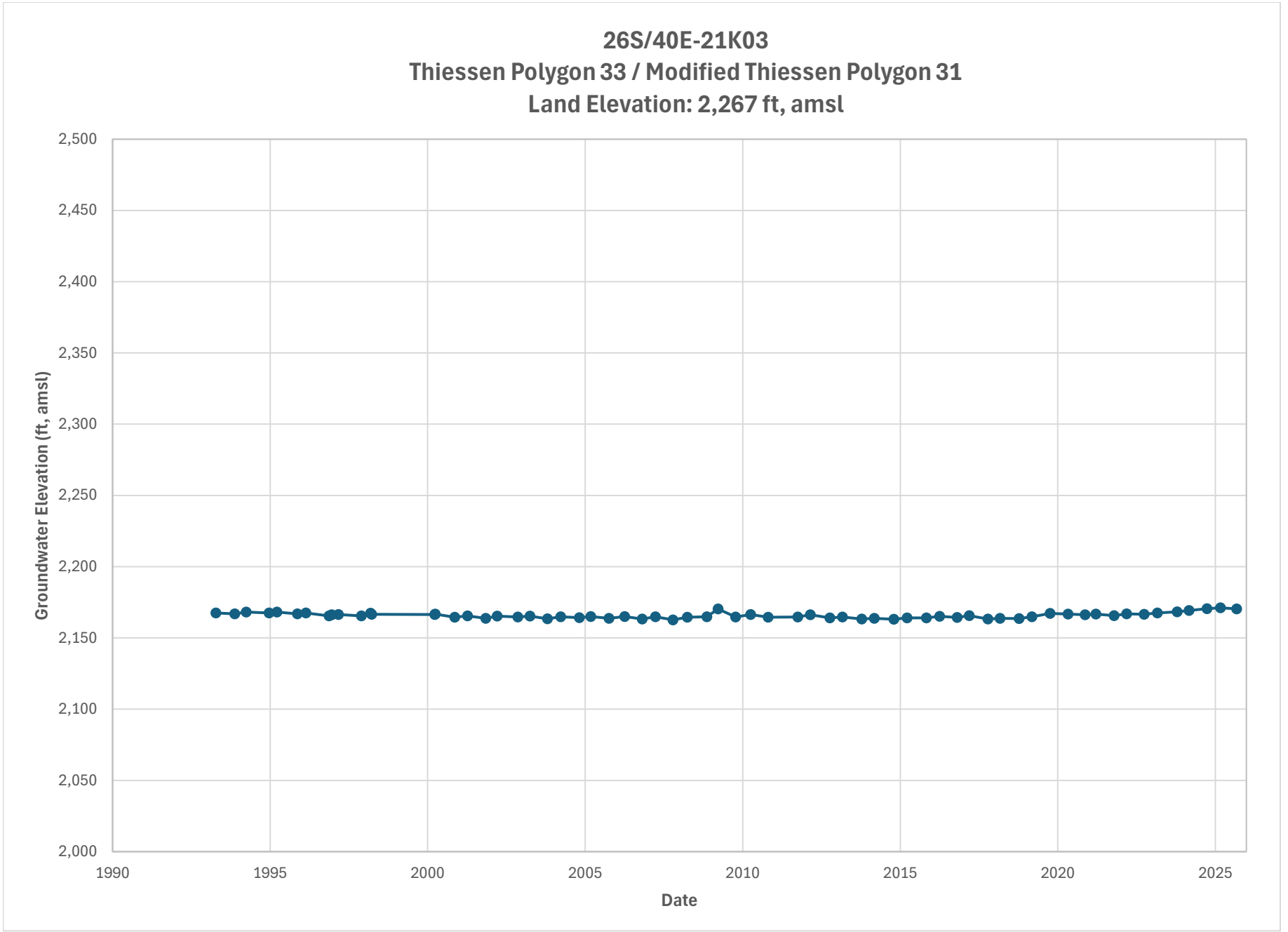

26S/39E-11E01
Thiessen Polygon 28
Land Elevation: 2,307 ft, amsl
Groundwater Elevation (ft, amsl)
2,500
2,450
2,400
2,350
2,300
2,250
2,200
2,150
2,100
2,050
2,000
1990
1995
2000
2005
2010
2015
2020
2025
Date

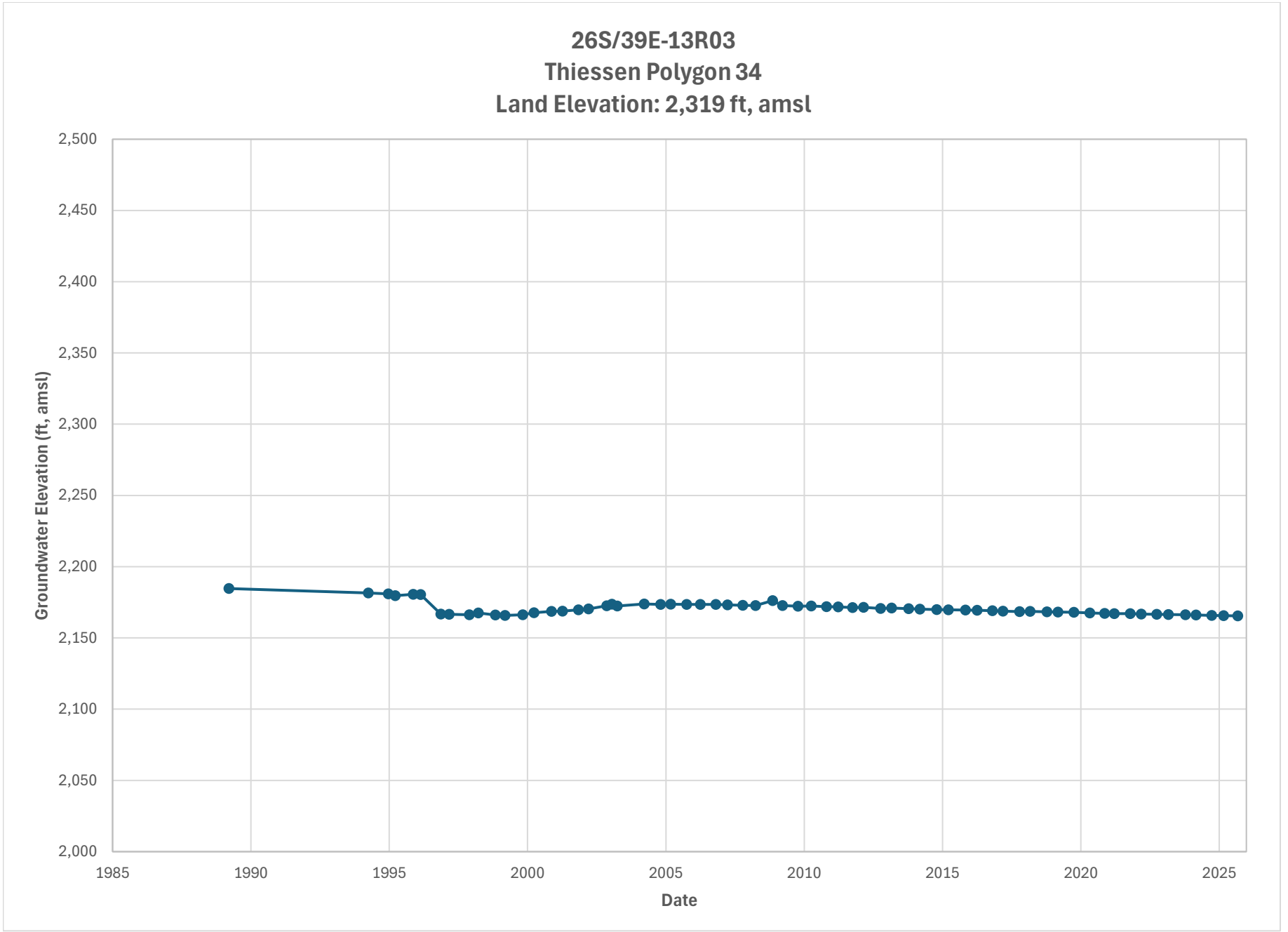

26S/39E-01A01
Thiessen Polygon 29 / Modified Thiessen Polygon 49
Land Elevation: 2,218 ft, amsl
Groundwater Elevation (ft, amsl)
2,500
2,450
2,400
2,350
2,300
2,250
2,200
2,150
2,100
2,050
2,000
1985
1990
1995
2000
2005
2010
2015
2020
2025
Date

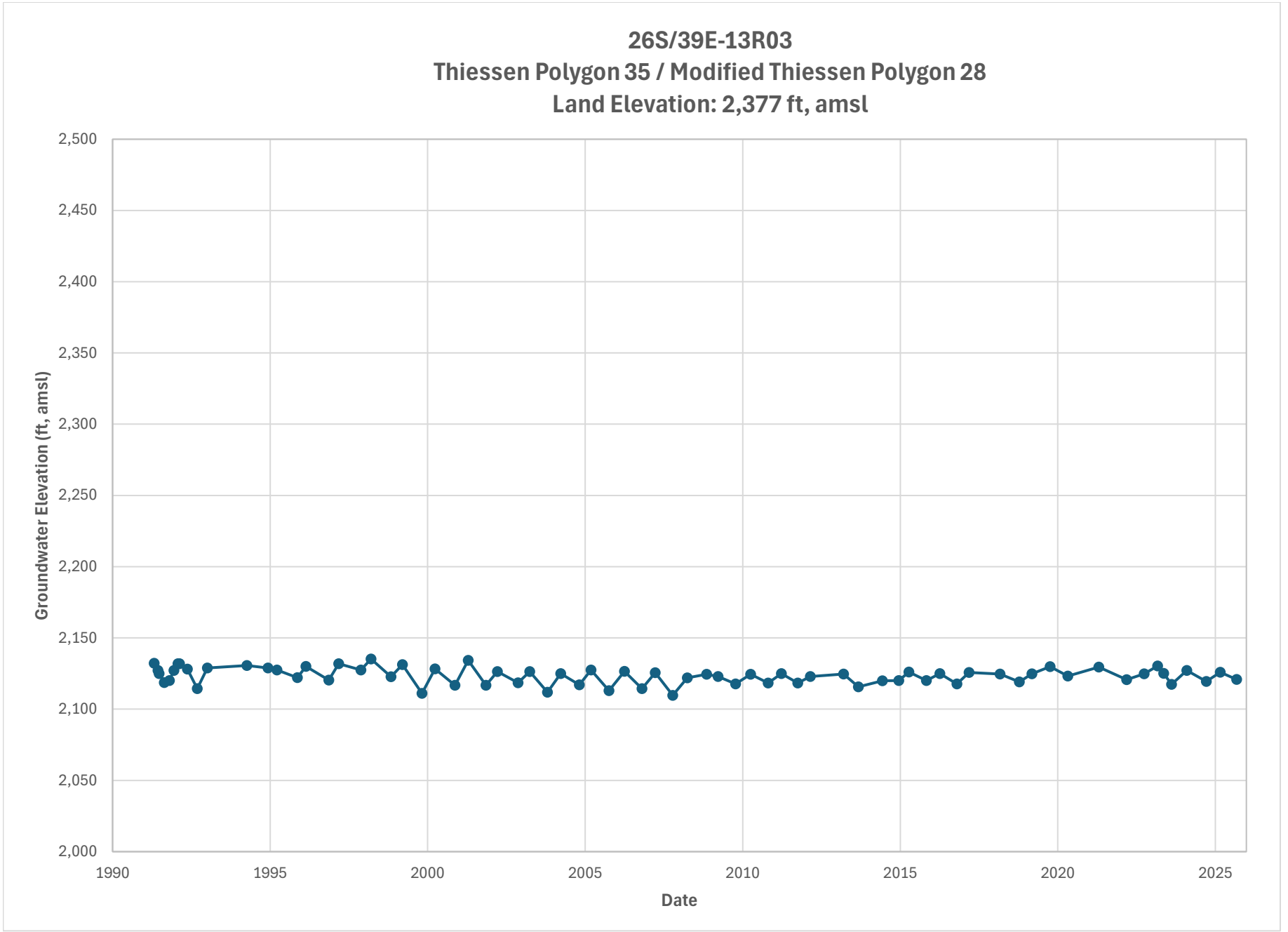

26S/40E-31P
Thiessen Polygon 30 / Modified Thiessen Polygon 50
Land Elevation: 2,192 ft, amsl
Groundwater Elevation (ft, amsl)
2,500
2,450
2,400
2,350
2,300
2,250
2,200
2,150
2,100
2,050
2,000
1990
1995
2000
2005
2010
2015
2020
2025
Date

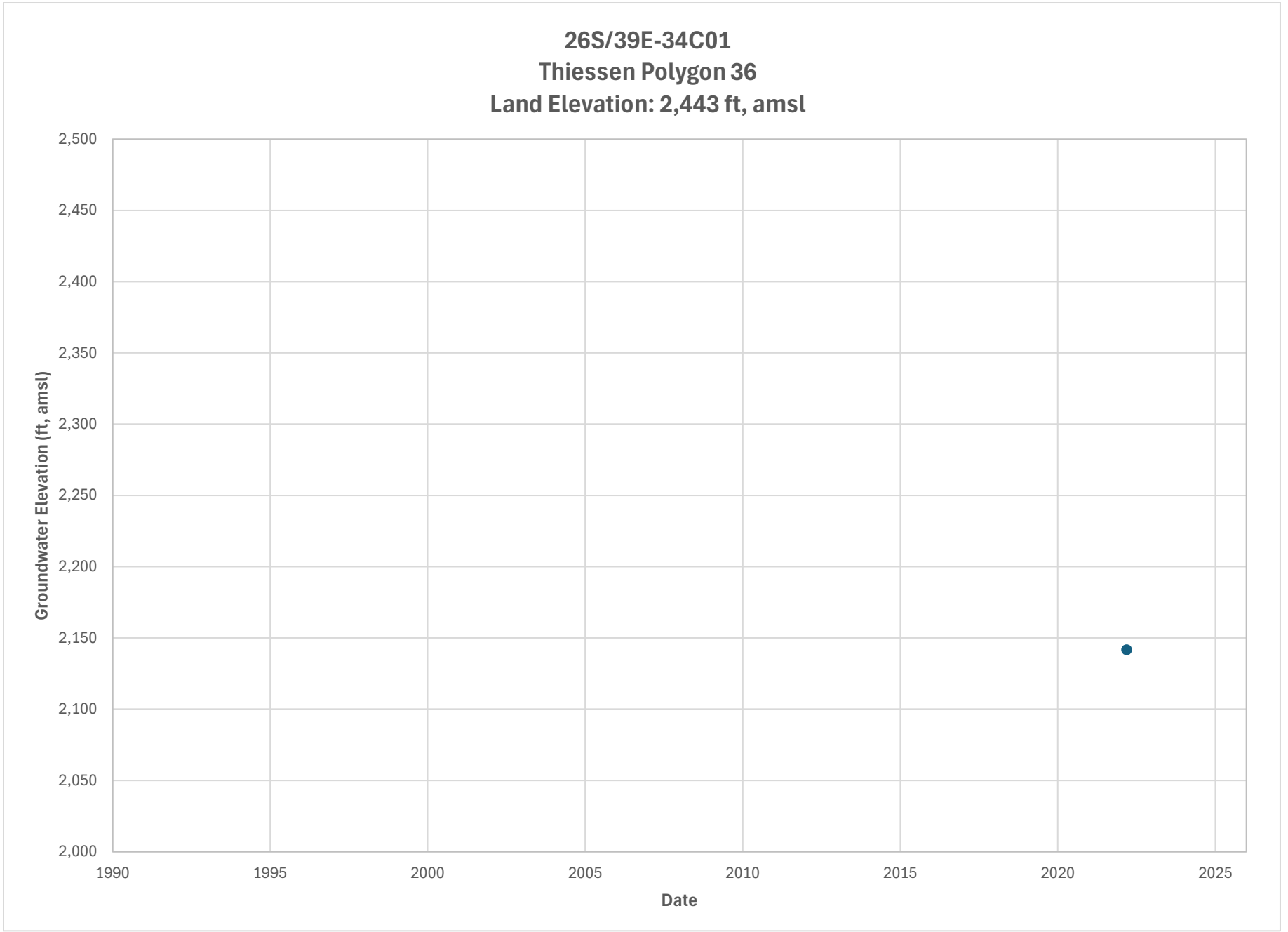

26S/40E-12C
Thiessen Polygon 31 / Modified Thiessen Polygon 43
Land Elevation: 2,166 ft, amsl
Groundwater Elevation (ft, amsl)
2,500
2,450
2,400
2,350
2,300
2,250
2,200
2,150
2,100
2,050
2,000
1990
1995
2000
2005
2010
2015
2020
2025
Date

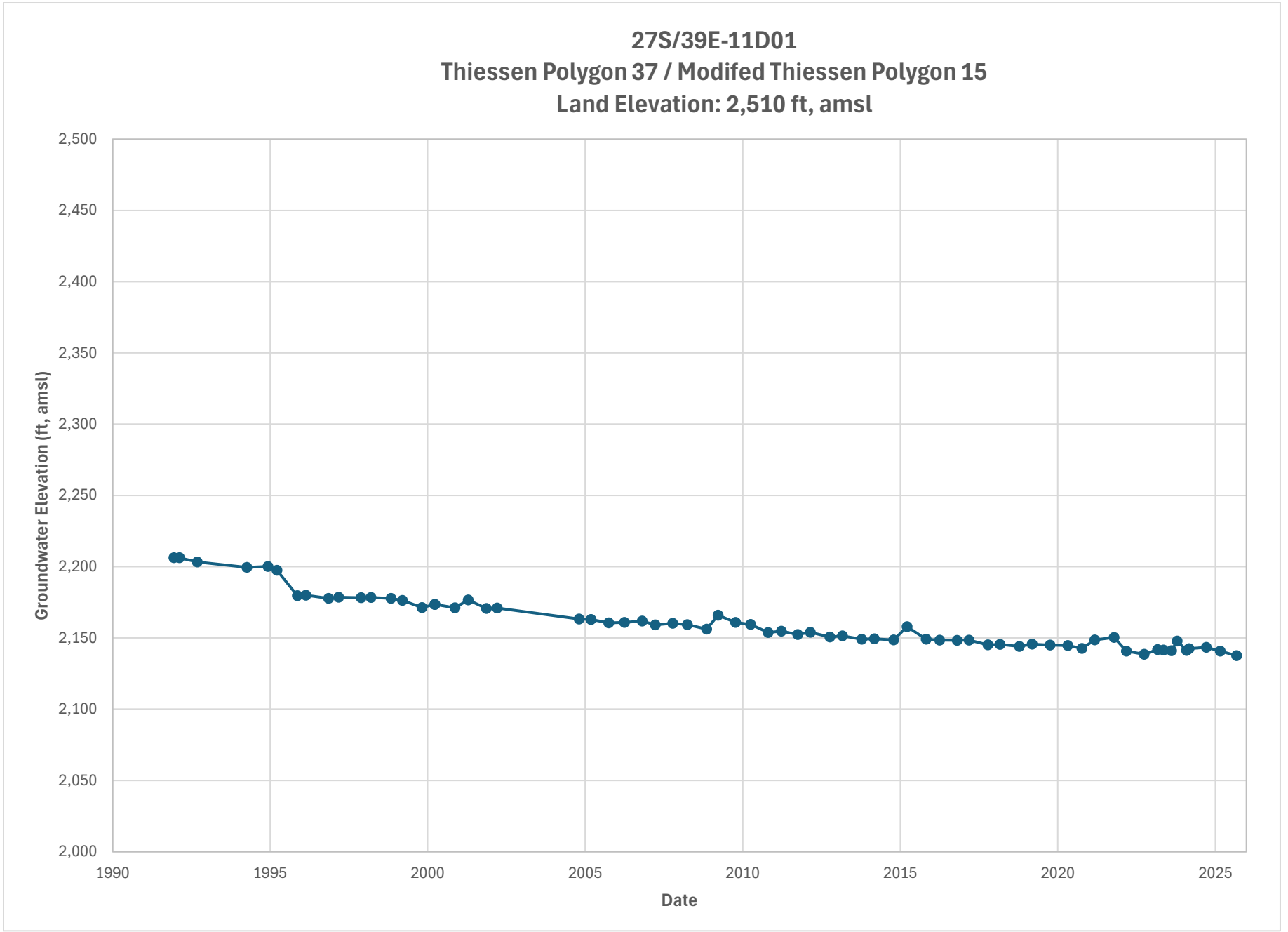

26S/40E-22H03
Thiessen Polygon 32 / Modified Thiessen Polygon 33
Land Elevation: 2,228 ft, amsl
Groundwater Elevation (ft, amsl)
2,500
2,450
2,400
2,350
2,300
2,250
2,200
2,150
2,100
2,050
2,000
1985
1990
1995
2000
2005
2010
2015
2020
2025
Date

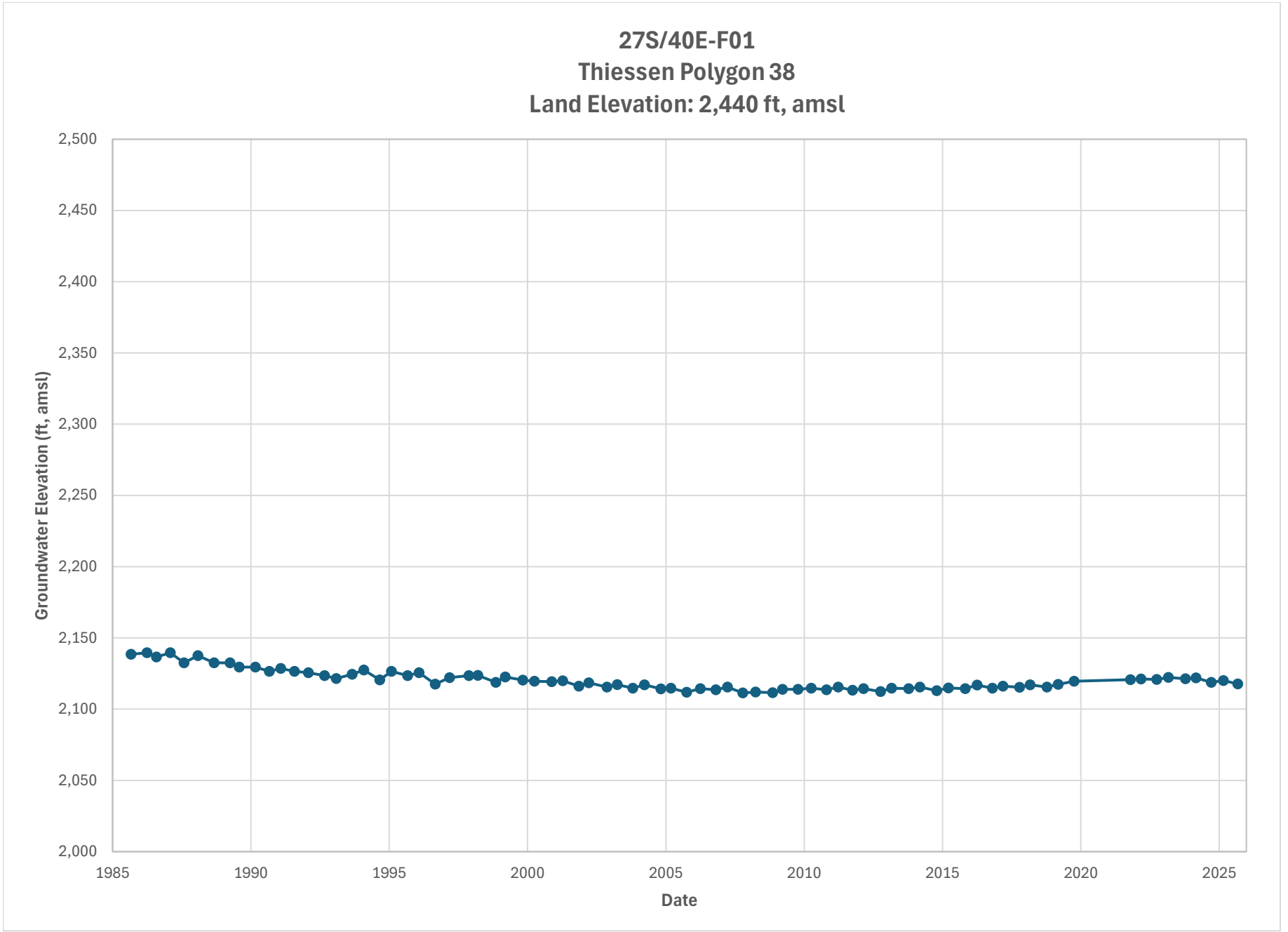

26S/40E-21K03
Thiessen Polygon 33 / Modified Thiessen Polygon 31
Land Elevation: 2,267 ft, amsl
Groundwater Elevation (ft, amsl)
2,500
2,450
2,400
2,350
2,300
2,250
2,200
2,150
2,100
2,050
2,000
1990
1995
2000
2005
2010
2015
2020
2025
Date

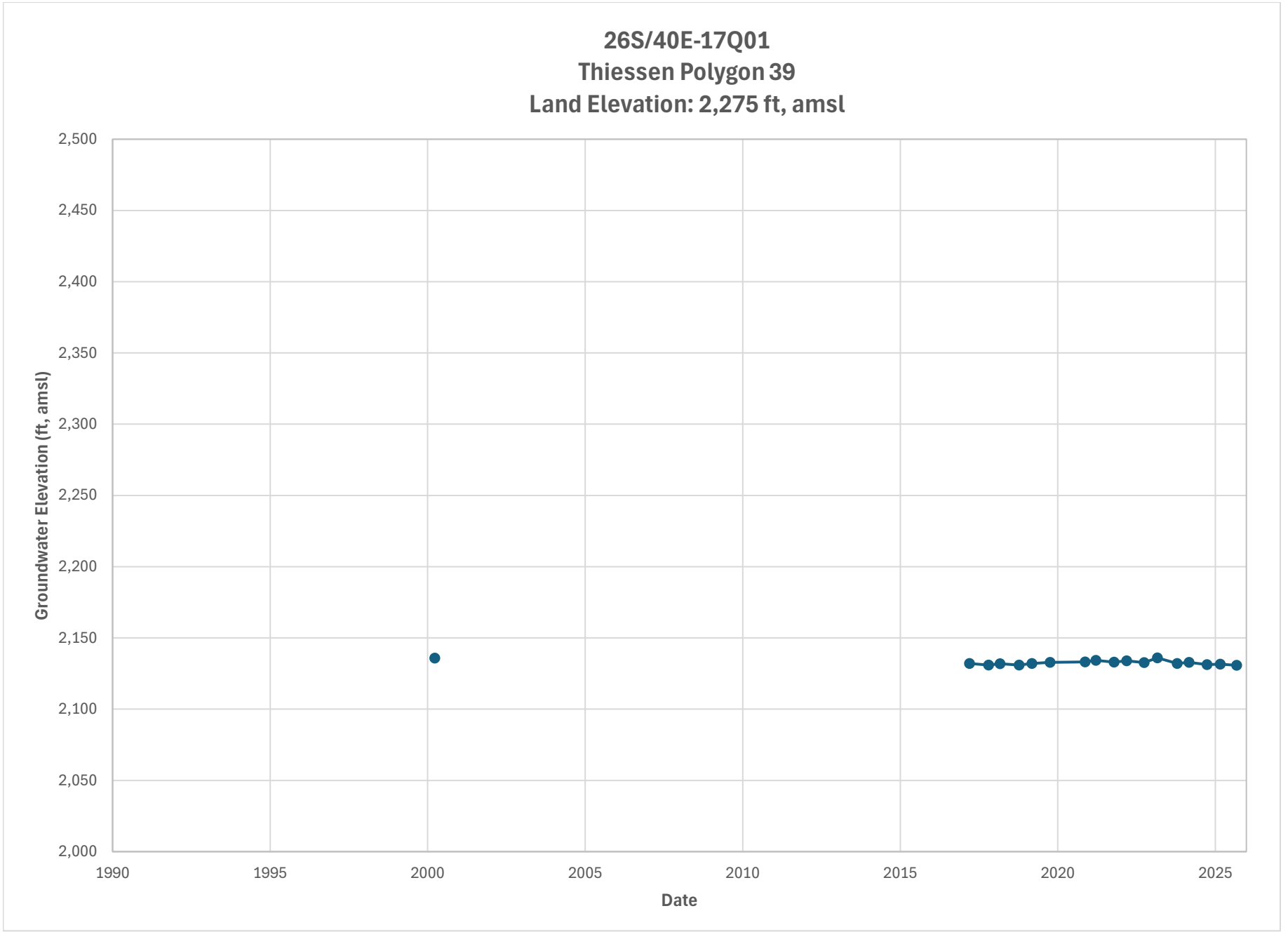

26S/39E-13R03
Thiessen Polygon 34
Land Elevation: 2,319 ft, amsl
Groundwater Elevation (ft, amsl)
2,500
2,450
2,400
2,350
2,300
2,250
2,200
2,150
2,100
2,050
2,000
1985
1990
1995
2000
2005
2010
2015
2020
2025
Date

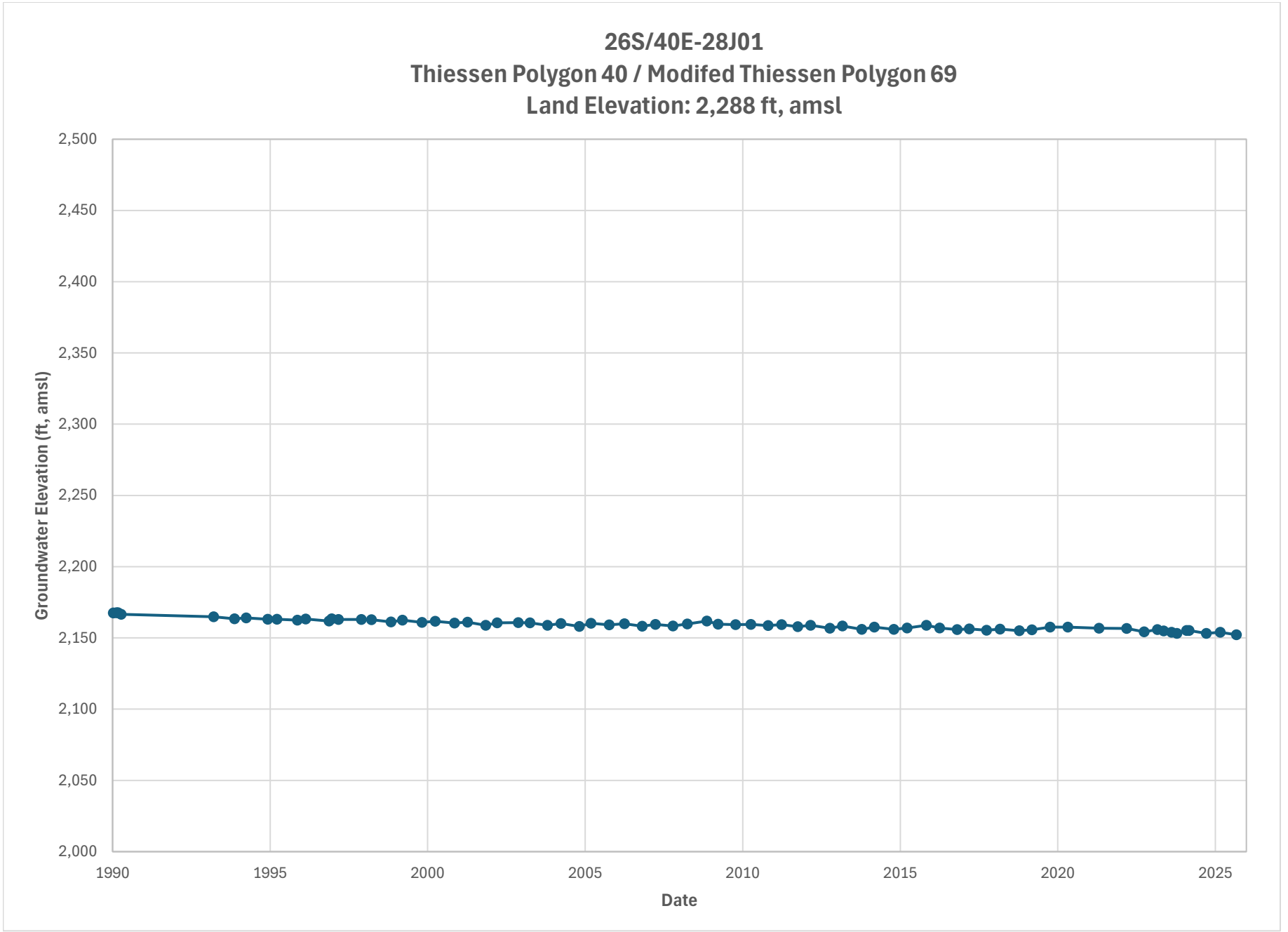

26S/39E-13R03
Thiessen Polygon 35 / Modified Thiessen Polygon 28
Land Elevation: 2,377 ft, amsl
Groundwater Elevation (ft, amsl)
2,500
2,450
2,400
2,350
2,300
2,250
2,200
2,150
2,100
2,050
2,000
1990
1995
2000
2005
2010
2015
2020
2025
Date

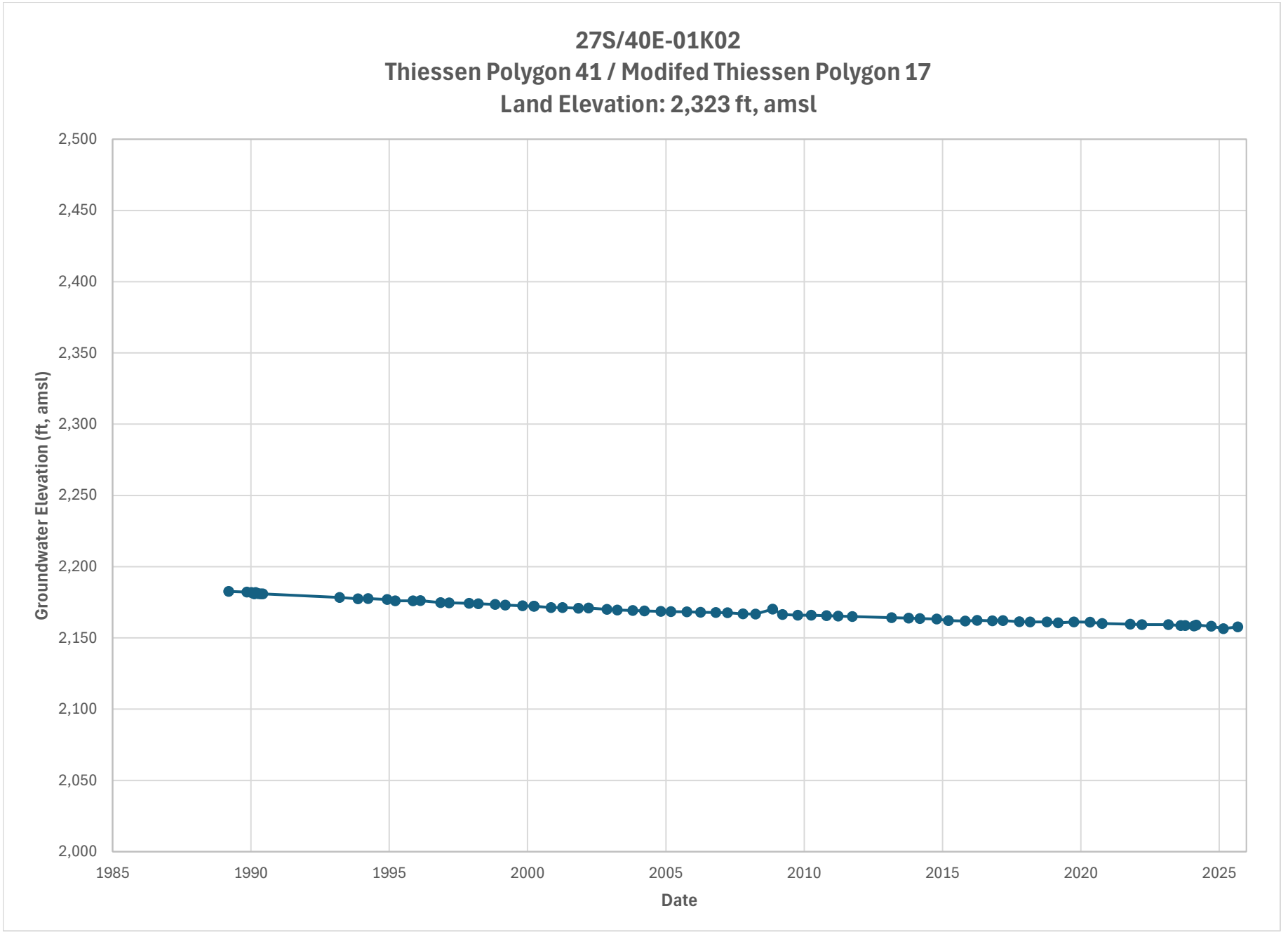

26S/39E-34C01
Thiessen Polygon 36
Land Elevation: 2,443 ft, amsl
Groundwater Elevation (ft, amsl)
2,500
2,450
2,400
2,350
2,300
2,250
2,200
2,150
2,100
2,050
2,000
1990
1995
2000
2005
2010
2015
2020
2025
Date

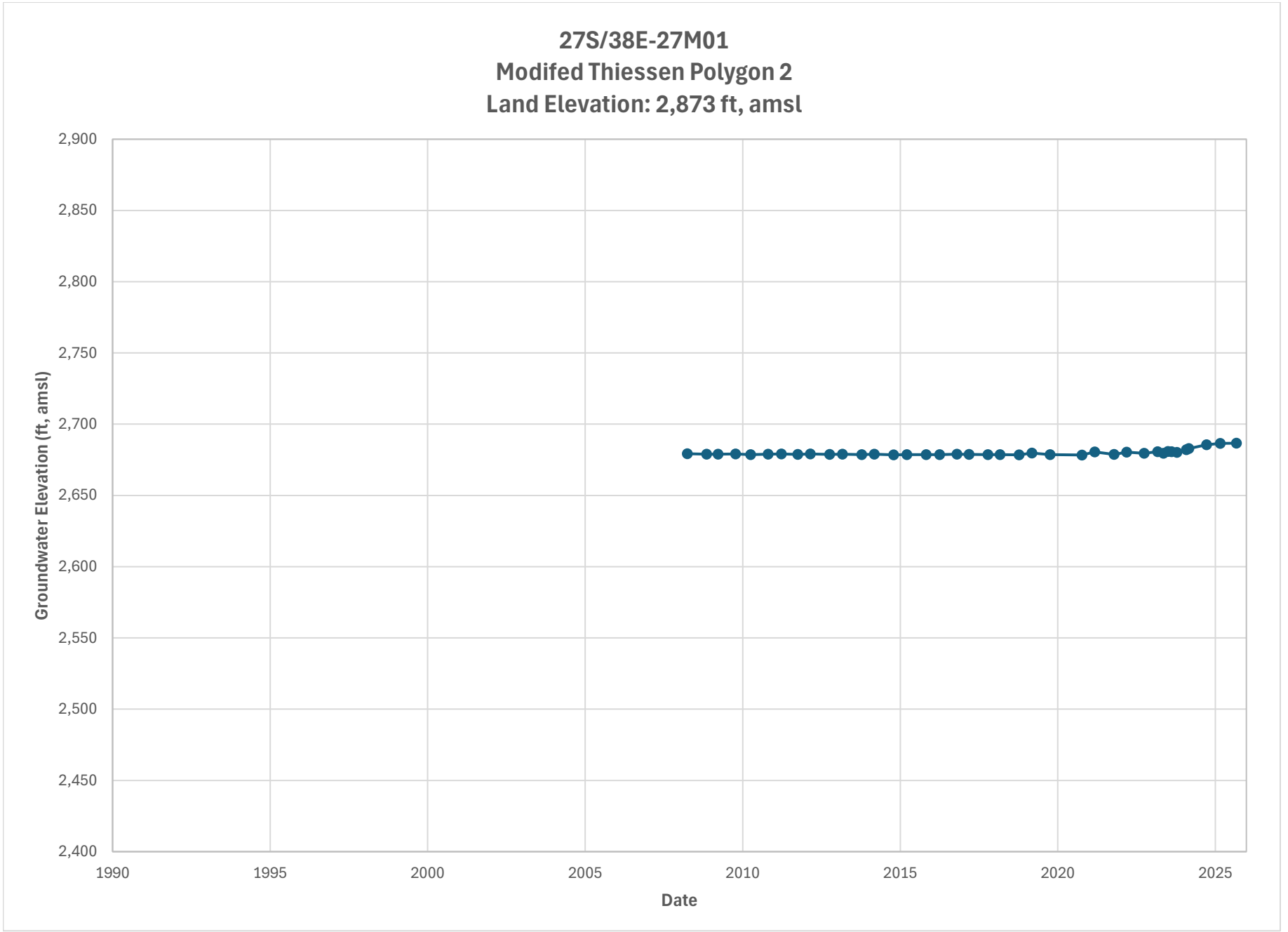

27S/39E-11D01
Thiessen Polygon 37 / Modifed Thiessen Polygon 15
Land Elevation: 2,510 ft, amsl
Groundwater Elevation (ft, amsl)
2,500
2,450
2,400
2,350
2,300
2,250
2,200
2,150
2,100
2,050
2,000
1990
1995
2000
2005
2010
2015
2020
2025
Date

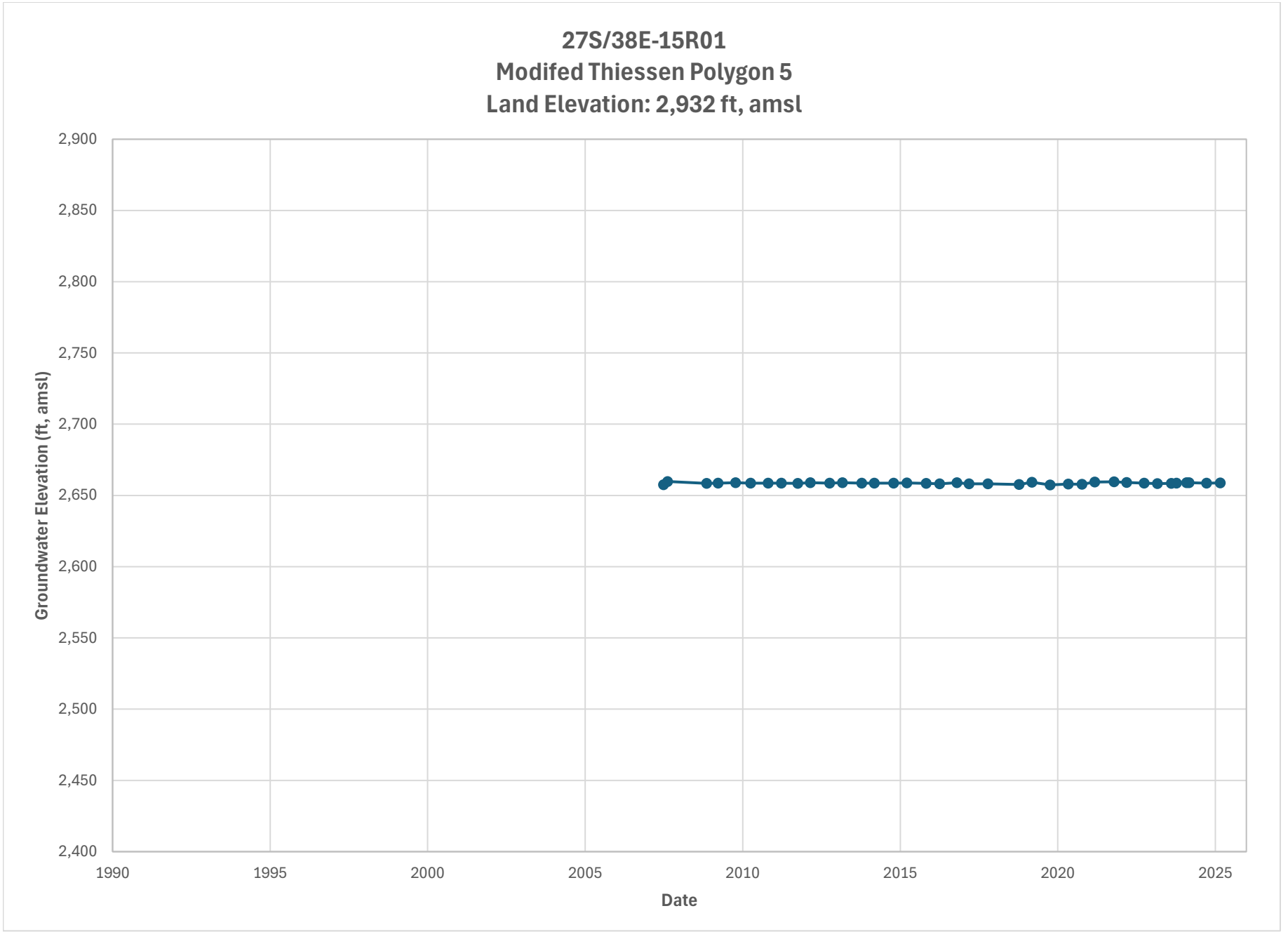

27S/40E-F01
Thiessen Polygon 38
Land Elevation: 2,440 ft, amsl
Groundwater Elevation (ft, amsl)
2,500
2,450
2,400
2,350
2,300
2,250
2,200
2,150
2,100
2,050
2,000
1985
1990
1995
2000
2005
2010
2015
2020
2025
Date

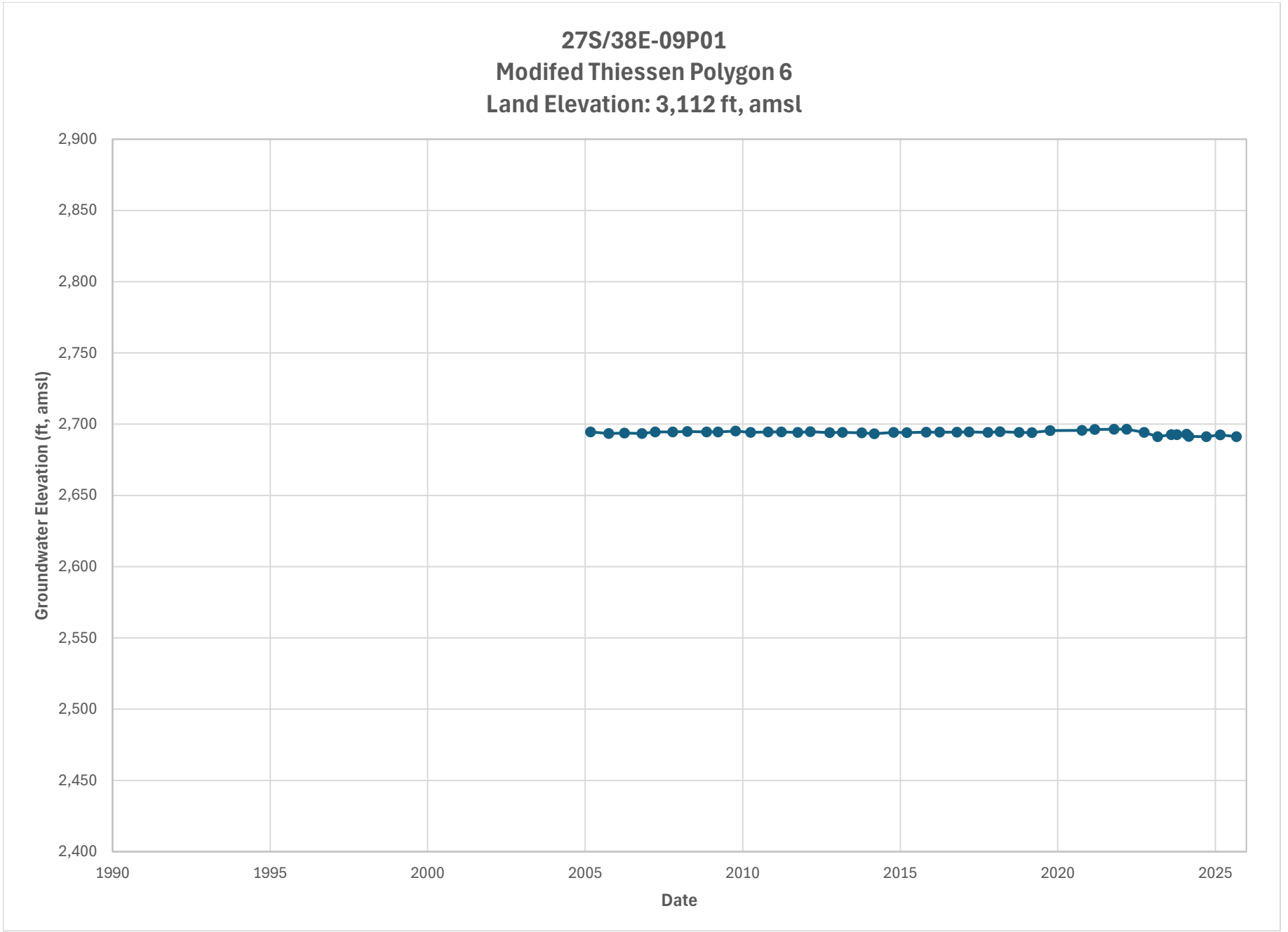

26S/40E-17Q01
Thiessen Polygon 39
Land Elevation: 2,275 ft, amsl
Groundwater Elevation (ft, amsl)
2,500
2,450
2,400
2,350
2,300
2,250
2,200
2,150
2,100
2,050
2,000
1990
1995
2000
2005
2010
2015
2020
2025
Date

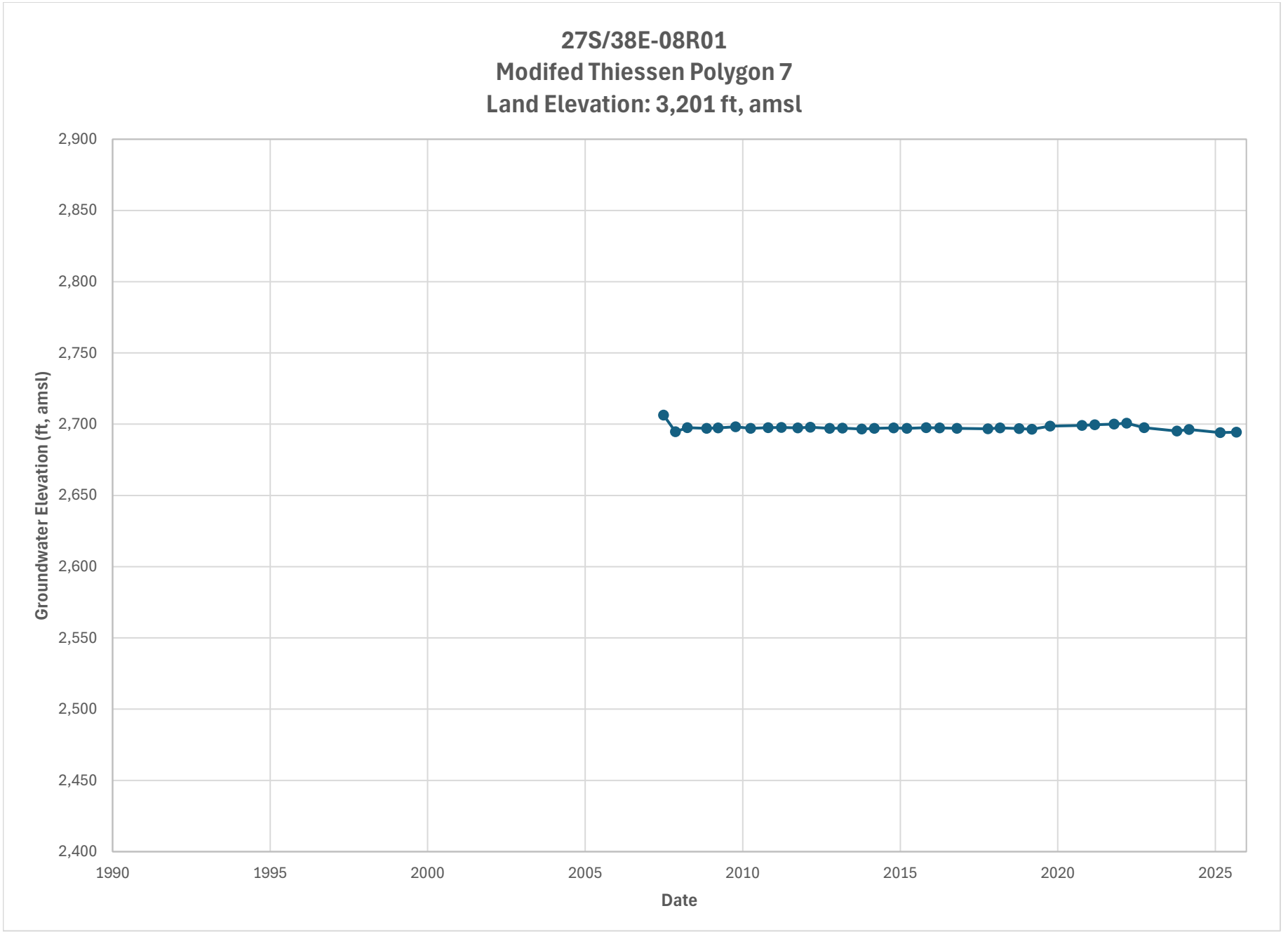

26S/40E-28J01
Thiessen Polygon 40 / Modifed Thiessen Polygon 69
Land Elevation: 2,288 ft, amsl
Groundwater Elevation (ft, amsl)
2,500
2,450
2,400
2,350
2,300
2,250
2,200
2,150
2,100
2,050
2,000
1990
1995
2000
2005
2010
2015
2020
2025
Date

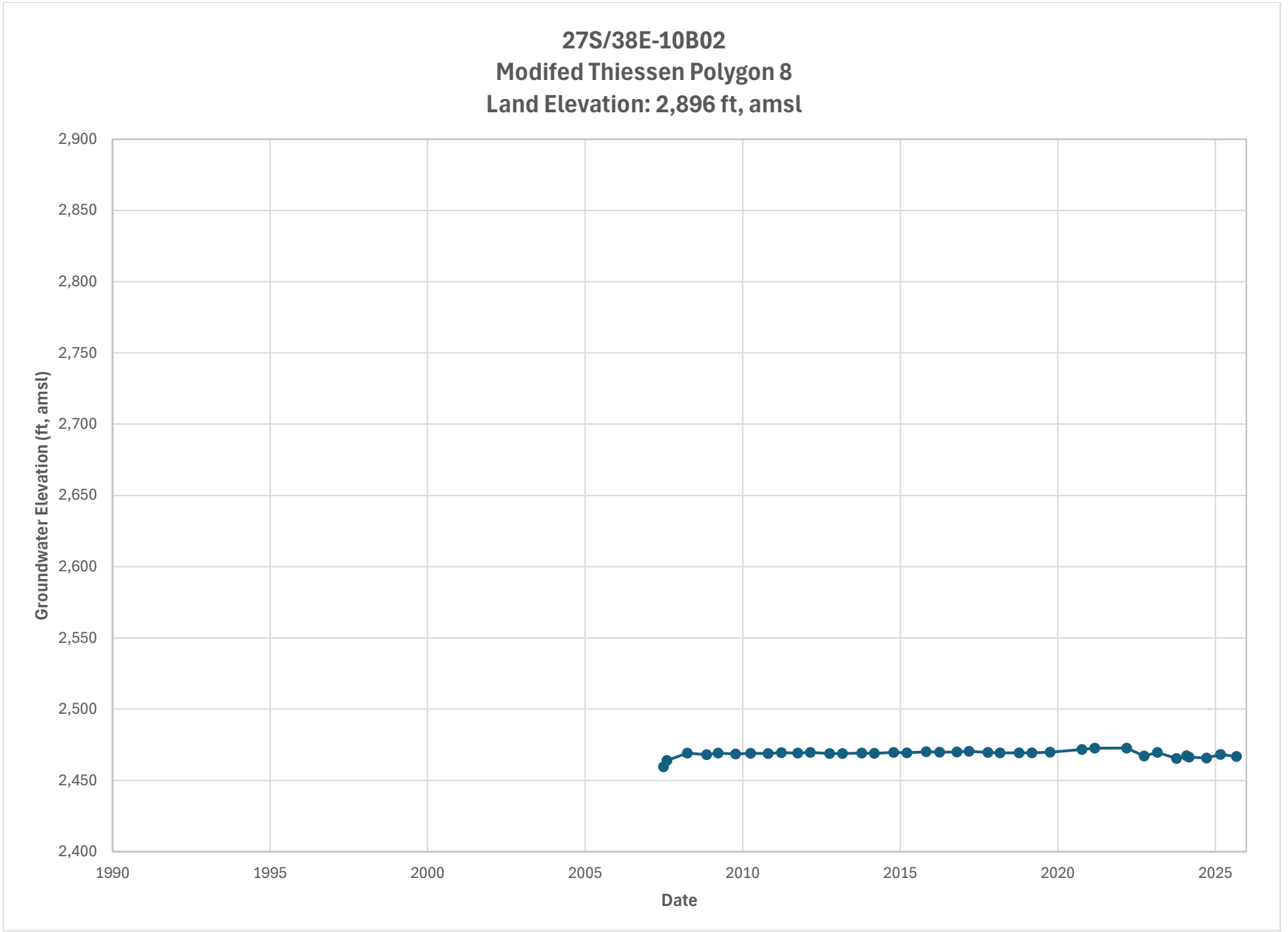

27S/40E-01K02
Thiessen Polygon 41 / Modifed Thiessen Polygon 17
Land Elevation: 2,323 ft, amsl
Groundwater Elevation (ft, amsl)
2,500
2,450
2,400
2,350
2,300
2,250
2,200
2,150
2,100
2,050
2,000
1985
1990
1995
2000
2005
2010
2015
2020
2025
Date

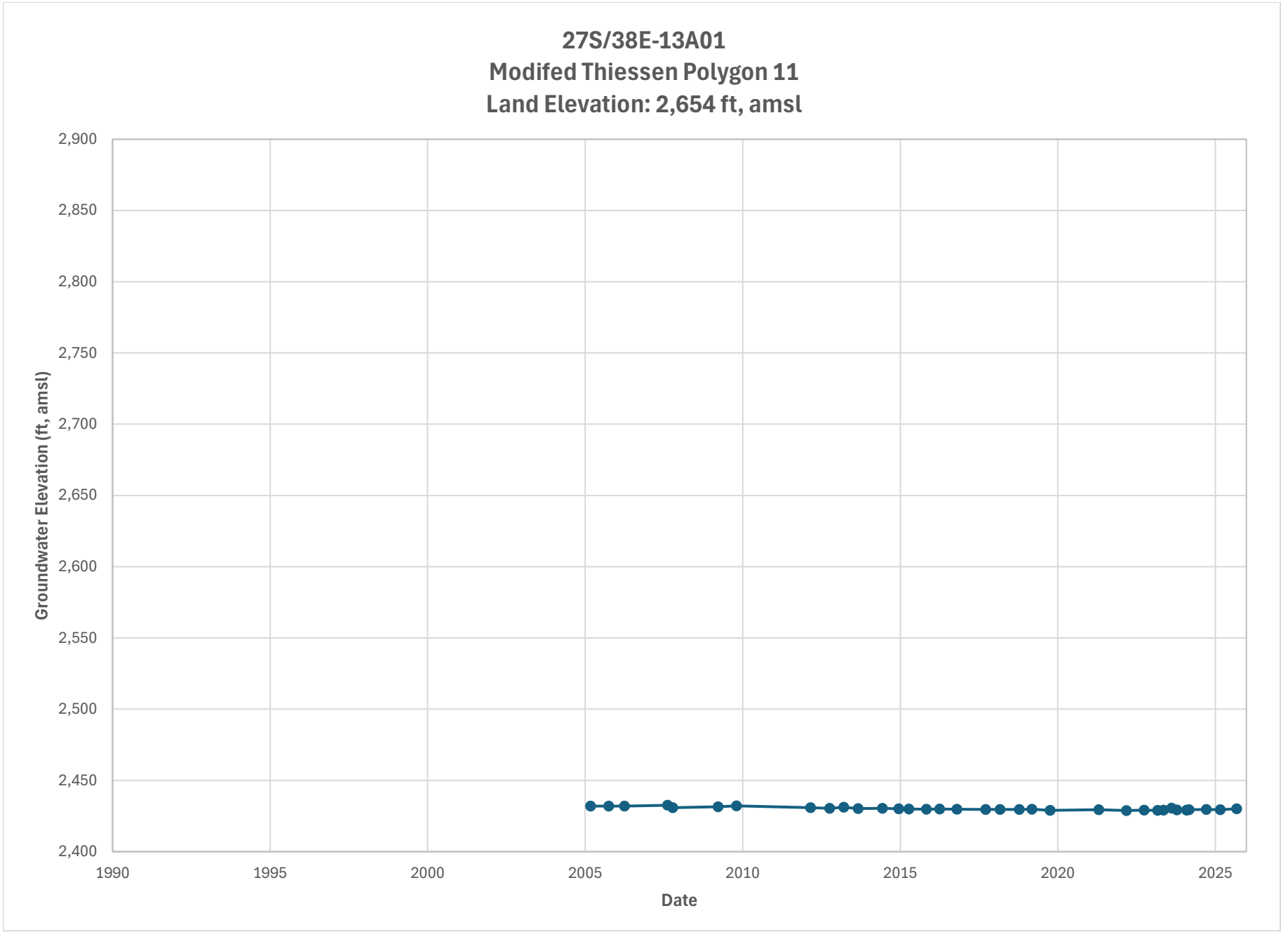

27S/38E-27M01
Modifed Thiessen Polygon 2
Land Elevation: 2,873 ft, amsl
Groundwater Elevation (ft, amsl)
2,900
2,850
2,800
2,750
2,700
2,650
2,600
2,550
2,500
2,450
2,400
1990
1995
2000
2005
2010
2015
2020
2025
Date

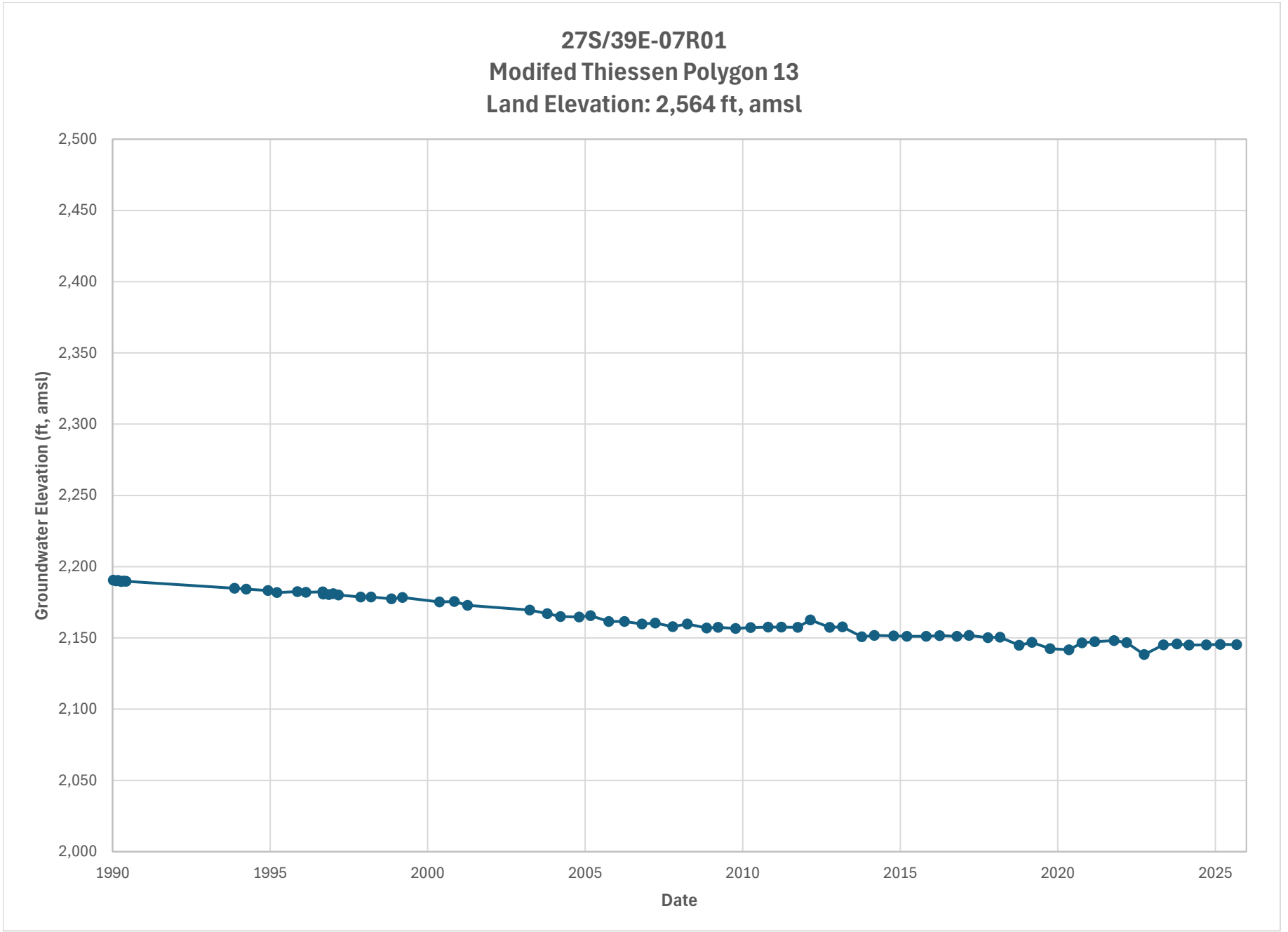

27S/38E-15R01
Modifed Thiessen Polygon 5
Land Elevation: 2,932 ft, amsl
Groundwater Elevation (ft, amsl)
2,900
2,850
2,800
2,750
2,700
2,650
2,600
2,550
2,500
2,450
2,400
1990
1995
2000
2005
2010
2015
2020
2025
Date

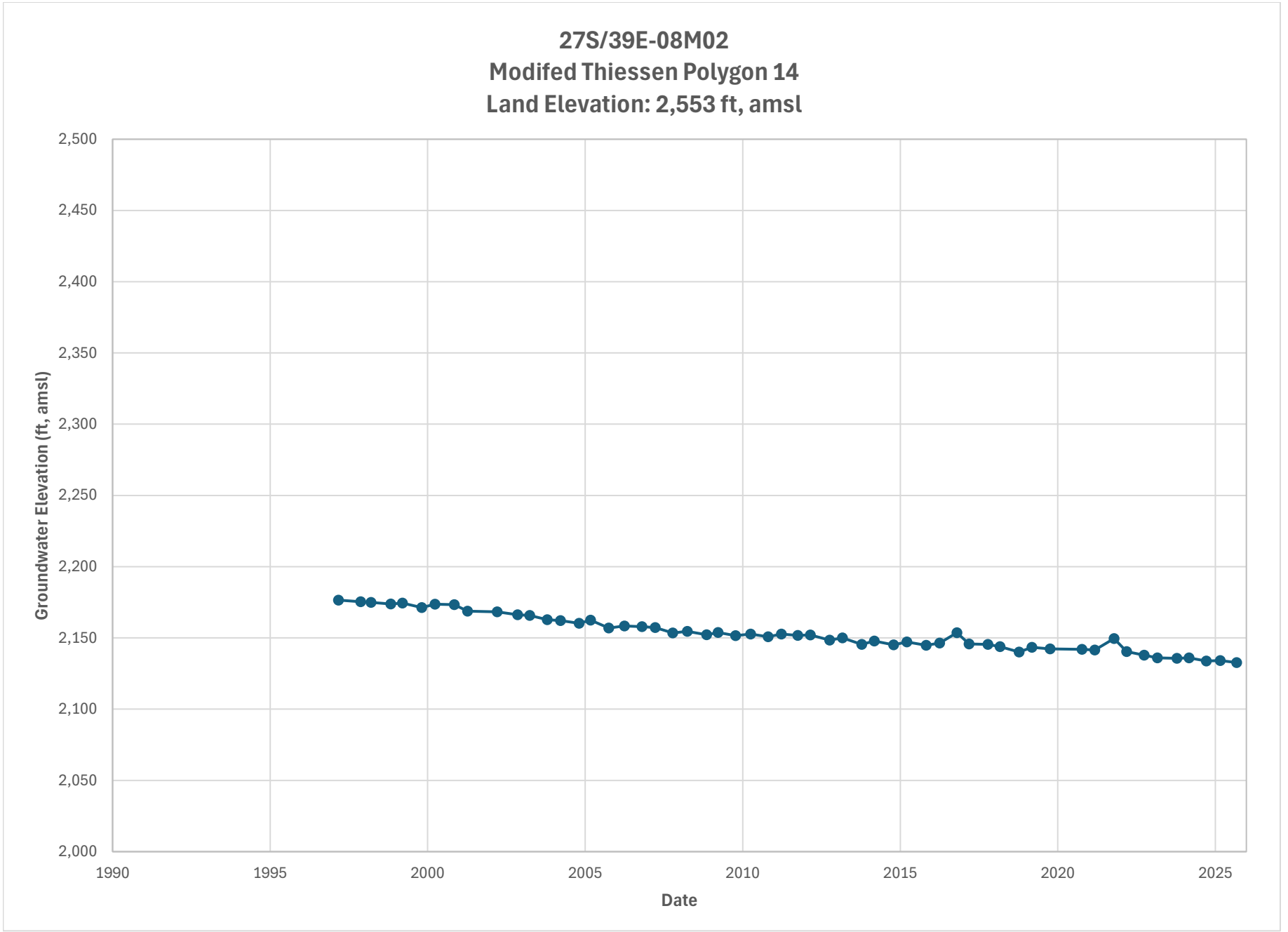

27S/38E-09P01
Modifed Thiessen Polygon 6
Land Elevation: 3,112 ft, amsl
Groundwater Elevation (ft, amsl)
2,900
2,850
2,800
2,750
2,700
2,650
2,600
2,550
2,500
2,450
2,400
1990
1995
2000
2005
2010
2015
2020
2025
Date

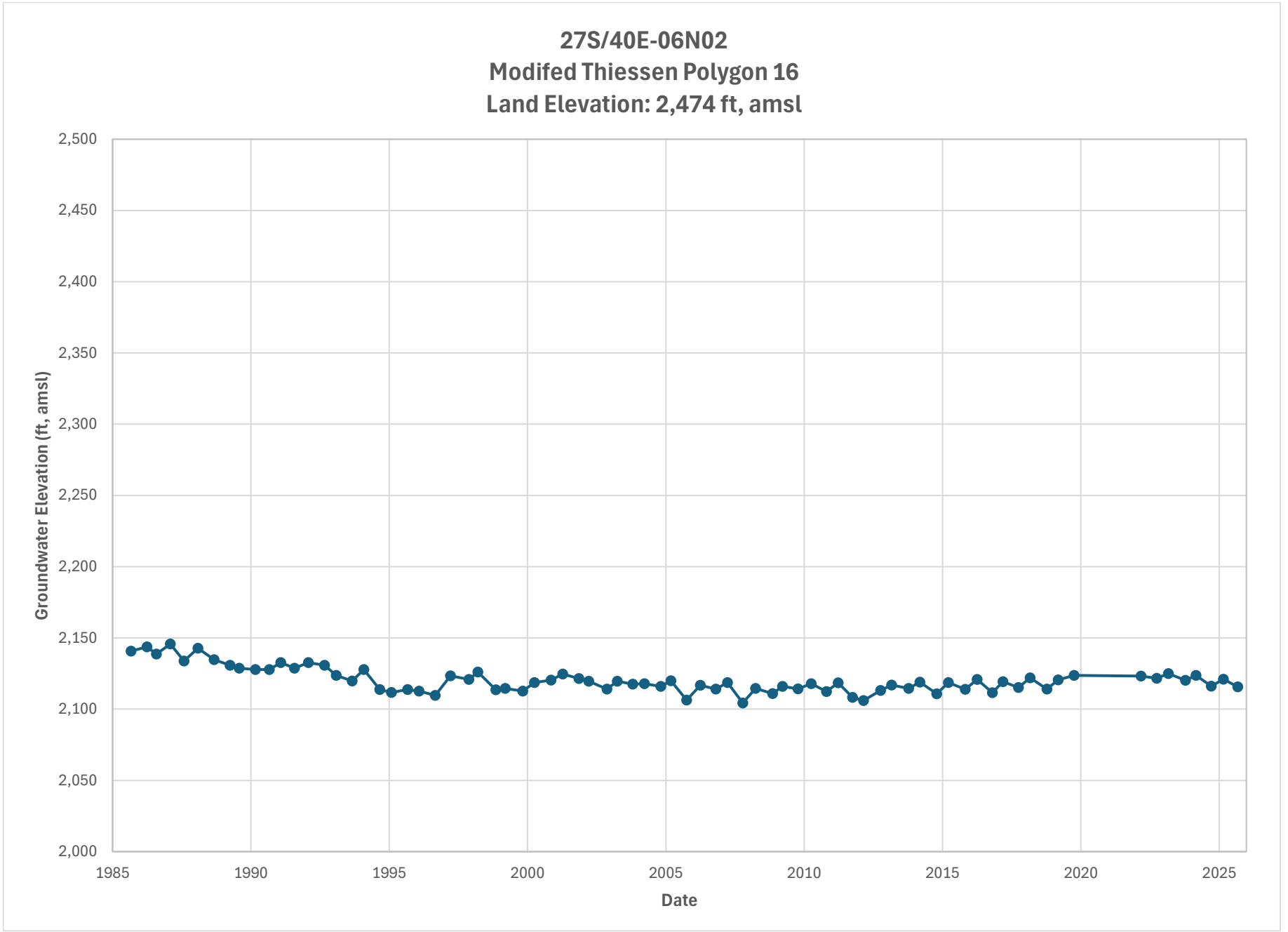

27S/38E-08R01
Modifed Thiessen Polygon 7
Land Elevation: 3,201 ft, amsl
Groundwater Elevation (ft, amsl)
2,900
2,850
2,800
2,750
2,700
2,650
2,600
2,550
2,500
2,450
2,400
1990
1995
2000
2005
2010
2015
2020
2025
Date

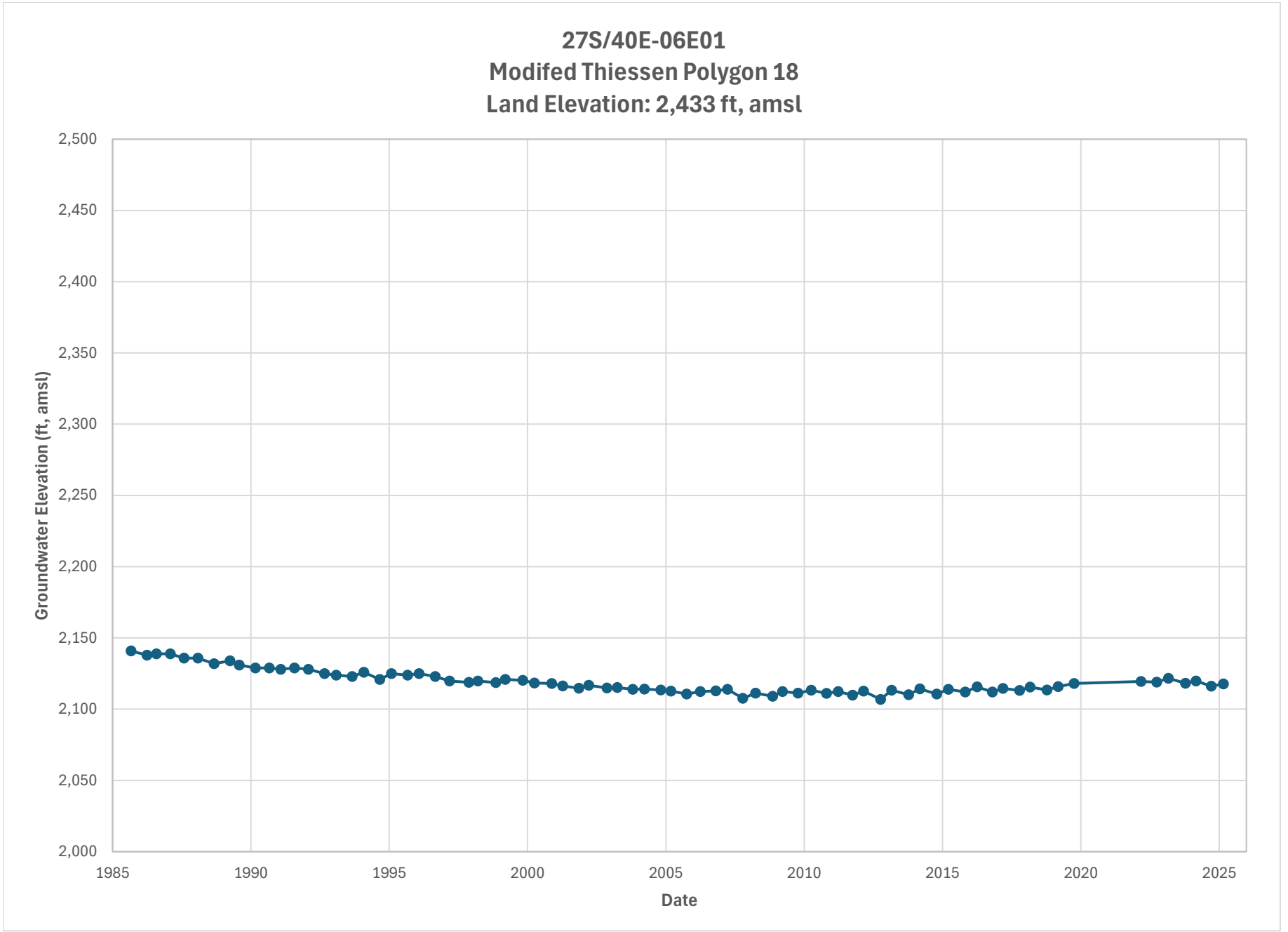

27S/38E-10B02
Modifed Thiessen Polygon 8
Land Elevation: 2,896 ft, amsl
Groundwater Elevation (ft, amsl)
2,900
2,850
2,800
2,750
2,700
2,650
2,600
2,550
2,500
2,450
2,400
1990
1995
2000
2005
2010
2015
2020
2025
Date

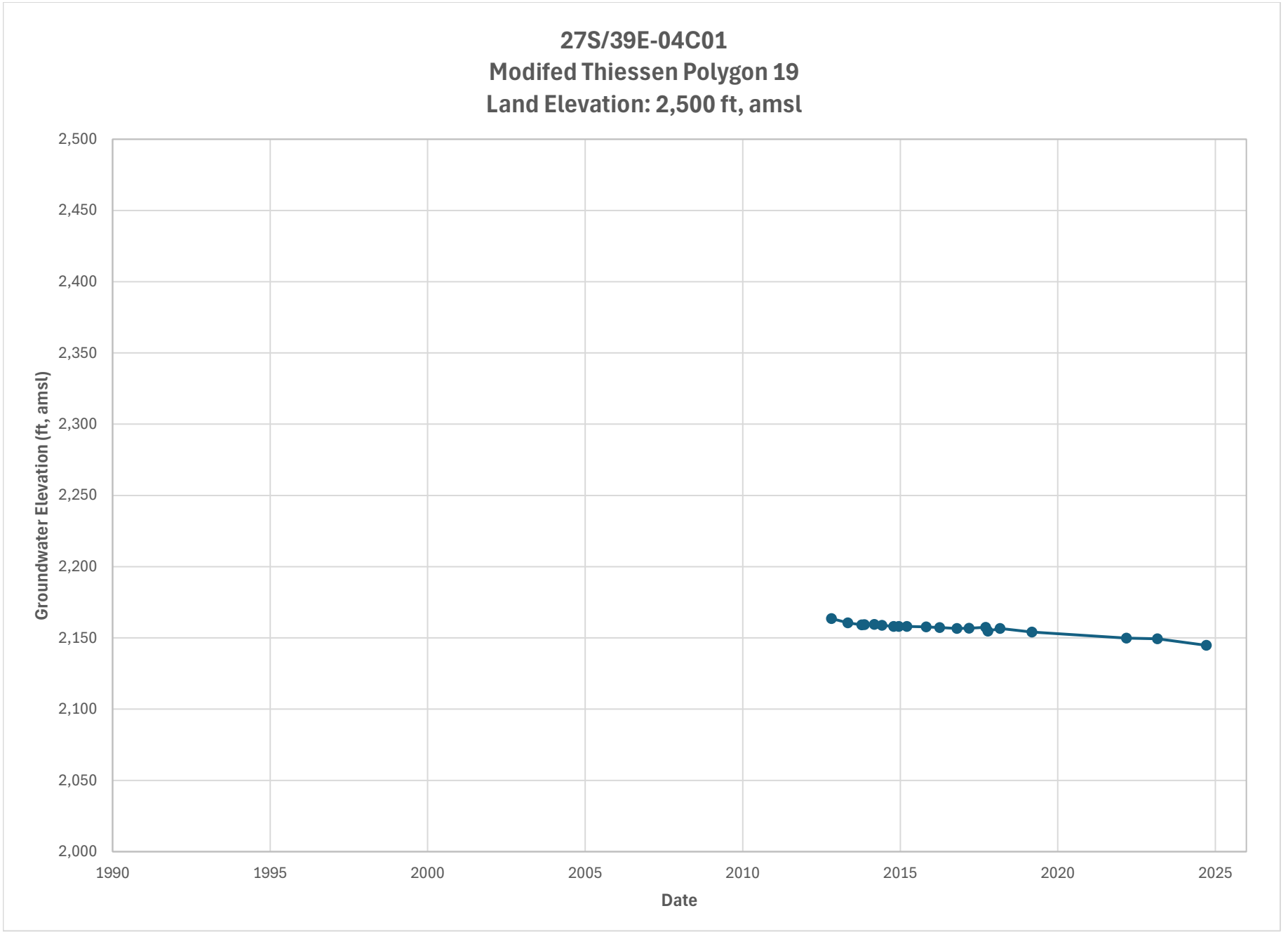

27S/38E-13A01
Modifed Thiessen Polygon 11
Land Elevation: 2,654 ft, amsl
Groundwater Elevation (ft, amsl)
2,900
2,850
2,800
2,750
2,700
2,650
2,600
2,550
2,500
2,450
2,400
1990
1995
2000
2005
2010
2015
2020
2025
Date

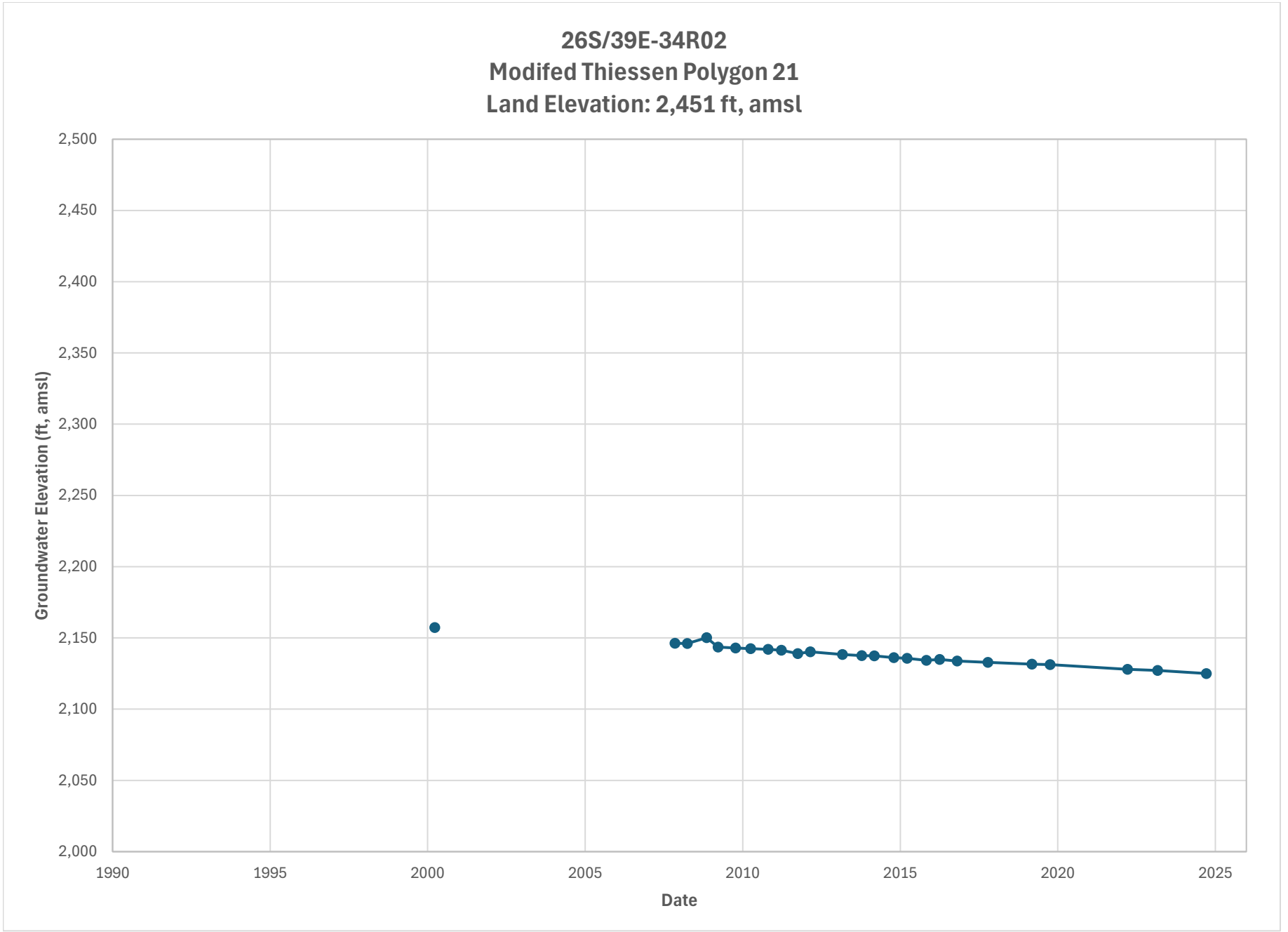

27S/39E-07R01
Modifed Thiessen Polygon 13
Land Elevation: 2,564 ft, amsl
Groundwater Elevation (ft, amsl)
2,500
2,450
2,400
2,350
2,300
2,250
2,200
2,150
2,100
2,050
2,000
1990
1995
2000
2005
2010
2015
2020
2025
Date

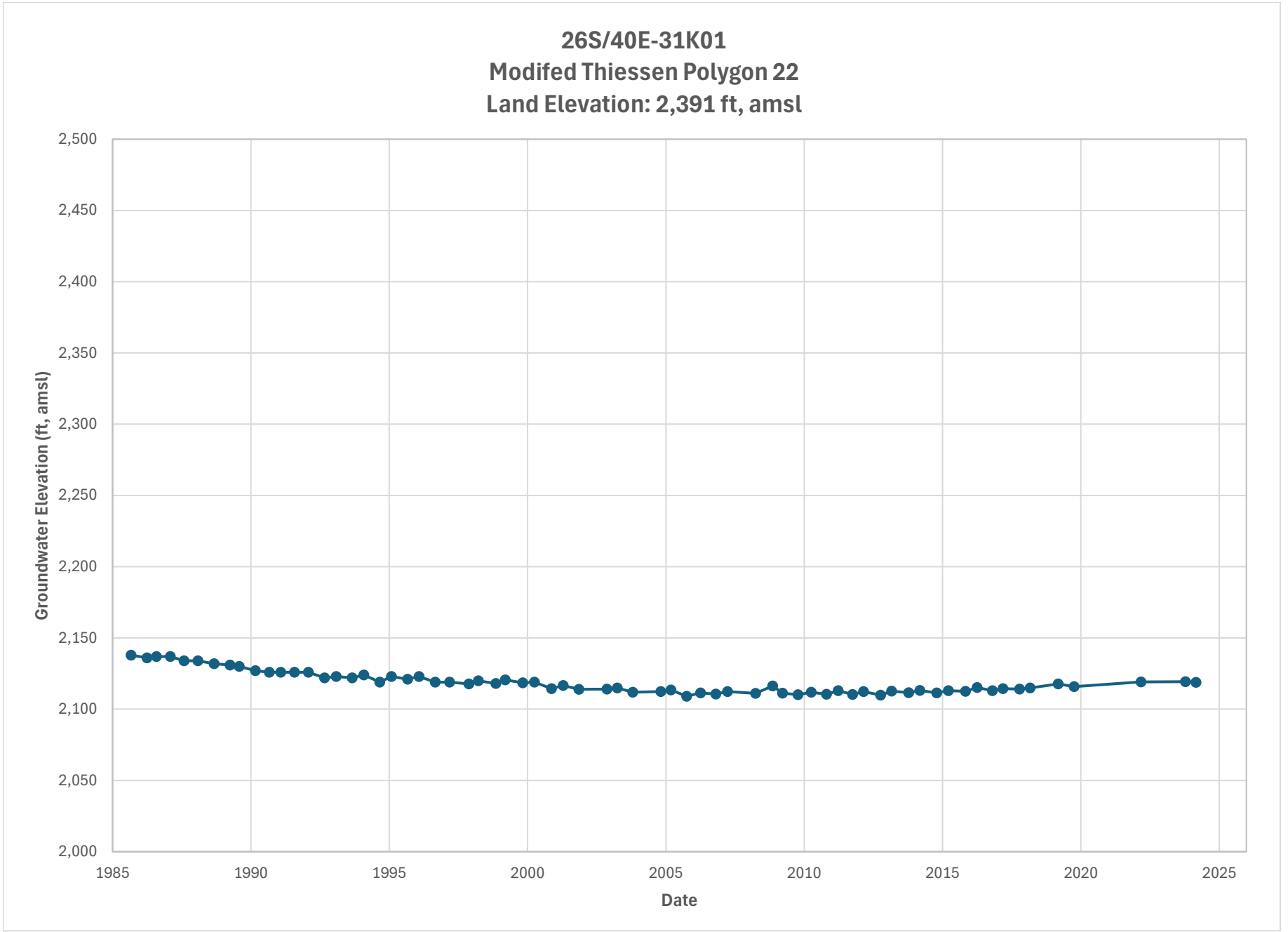

27S/39E-08M02
Modifed Thiessen Polygon 14
Land Elevation: 2,553 ft, amsl
Groundwater Elevation (ft, amsl)
2,500
2,450
2,400
2,350
2,300
2,250
2,200
2,150
2,100
2,050
2,000
1990
1995
2000
2005
2010
2015
2020
2025
Date

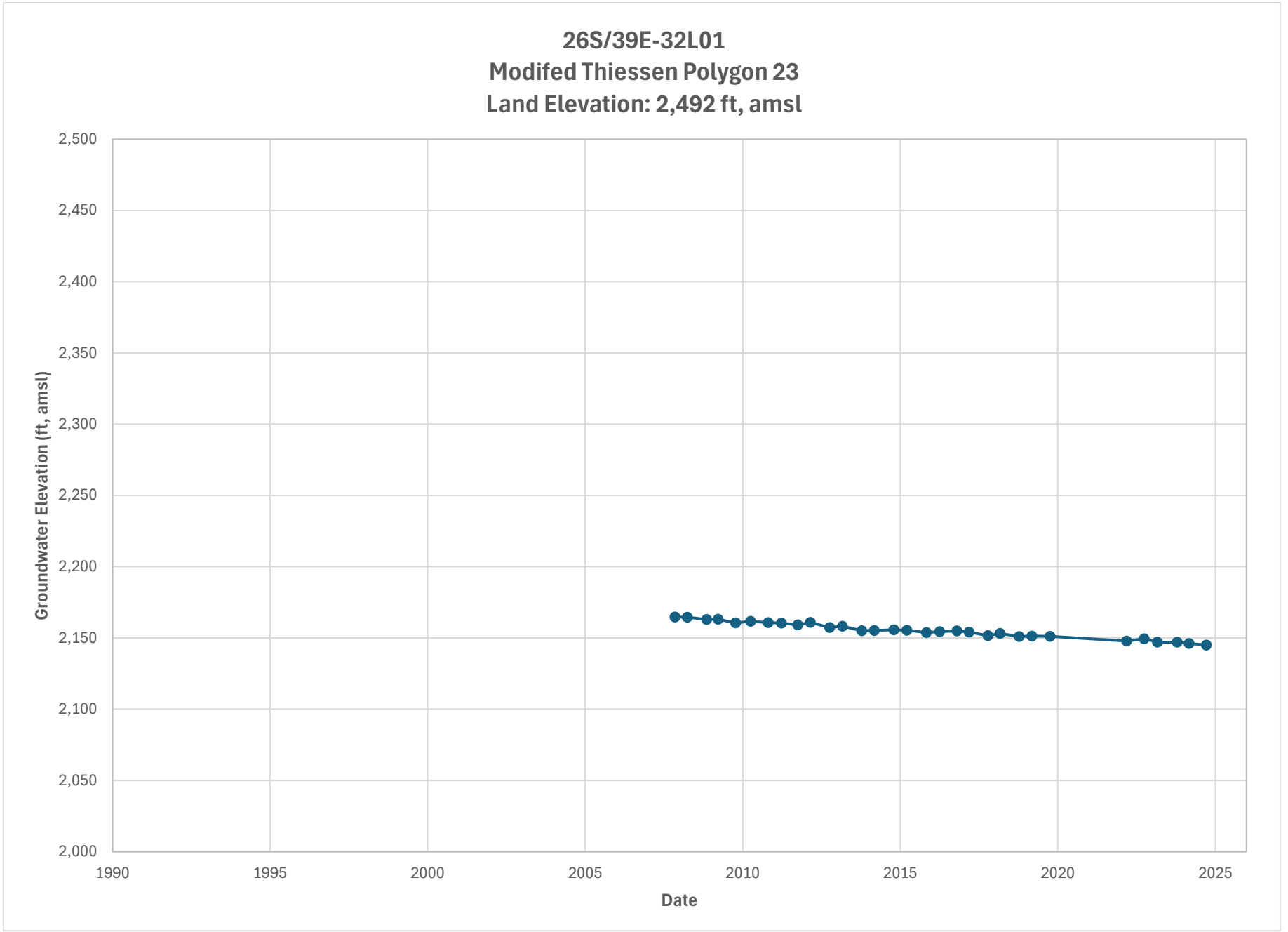

27S/40E-06N02
Modifed Thiessen Polygon 16
Land Elevation: 2,474 ft, amsl
Groundwater Elevation (ft, amsl)
2,500
2,450
2,400
2,350
2,300
2,250
2,200
2,150
2,100
2,050
2,000
1985
1990
1995
2000
2005
2010
2015
2020
2025
Date

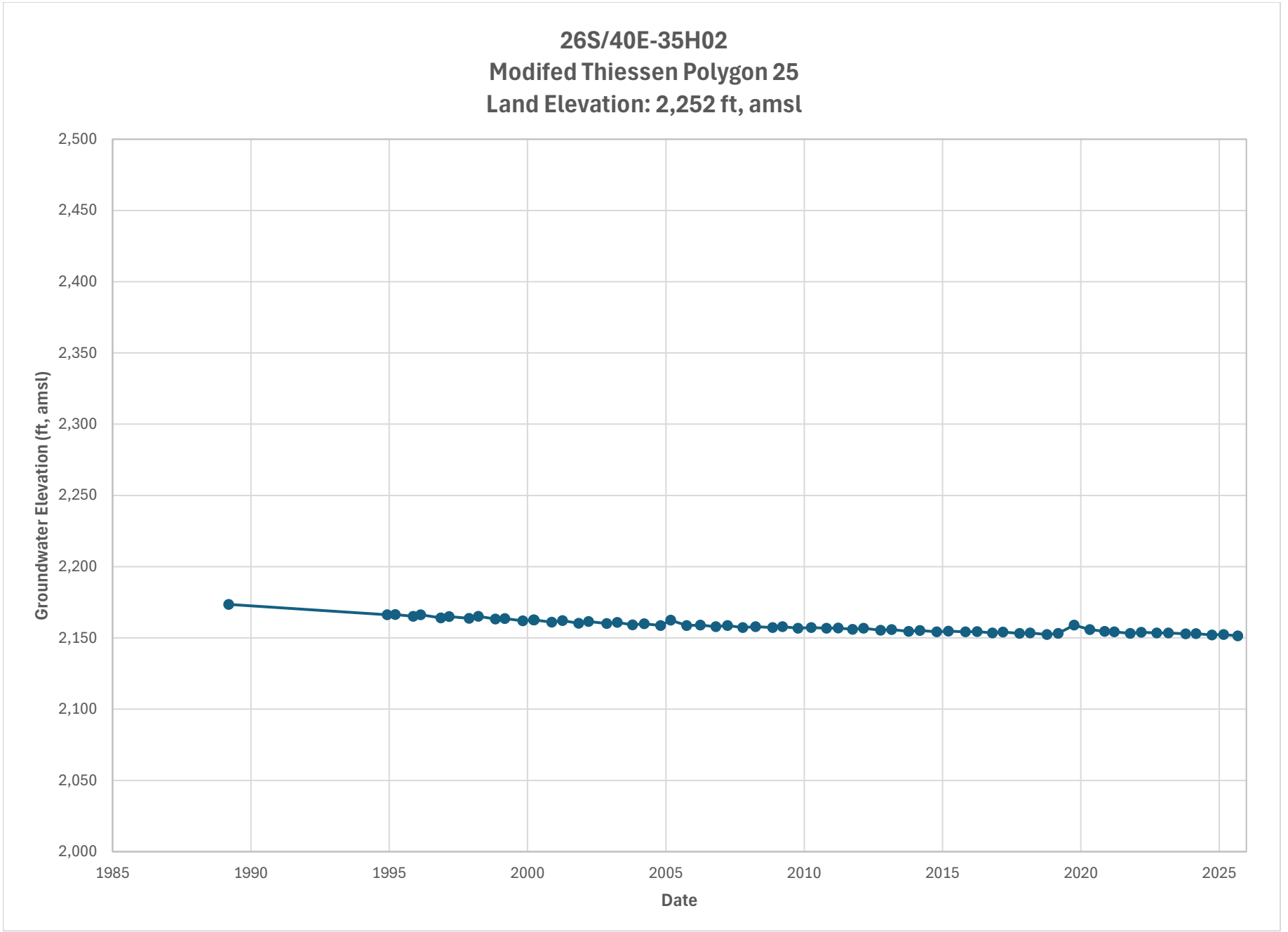

27S/40E-06E01
Modifed Thiessen Polygon 18
Land Elevation: 2,433 ft, amsl
Groundwater Elevation (ft, amsl)
2,500
2,450
2,400
2,350
2,300
2,250
2,200
2,150
2,100
2,050
2,000
1985
1990
1995
2000
2005
2010
2015
2020
2025
Date

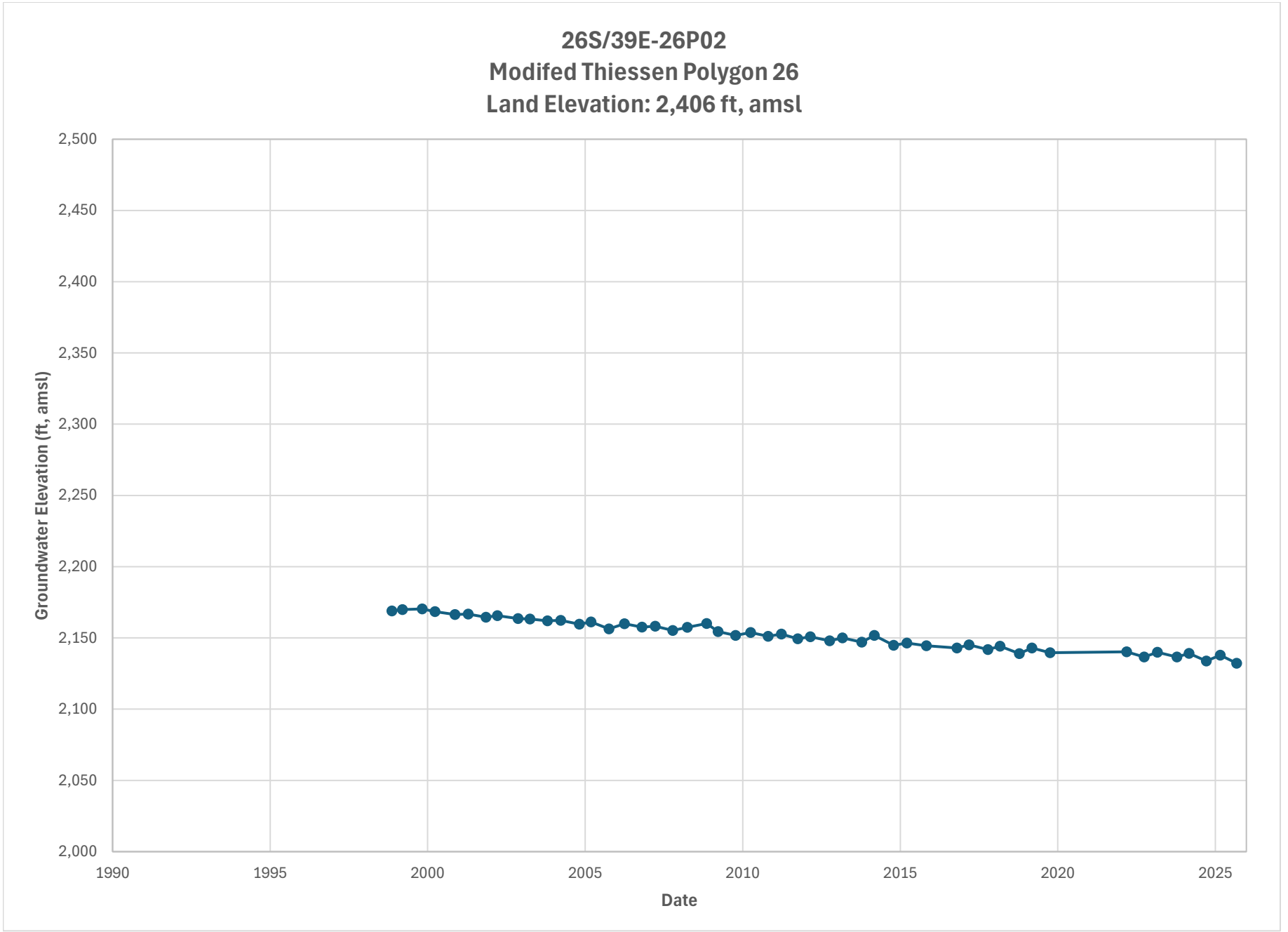

27S/39E-04C01
Modifed Thiessen Polygon 19
Land Elevation: 2,500 ft, amsl
Groundwater Elevation (ft, amsl)
2,500
2,450
2,400
2,350
2,300
2,250
2,200
2,150
2,100
2,050
2,000
1990
1995
2000
2005
2010
2015
2020
2025
Date

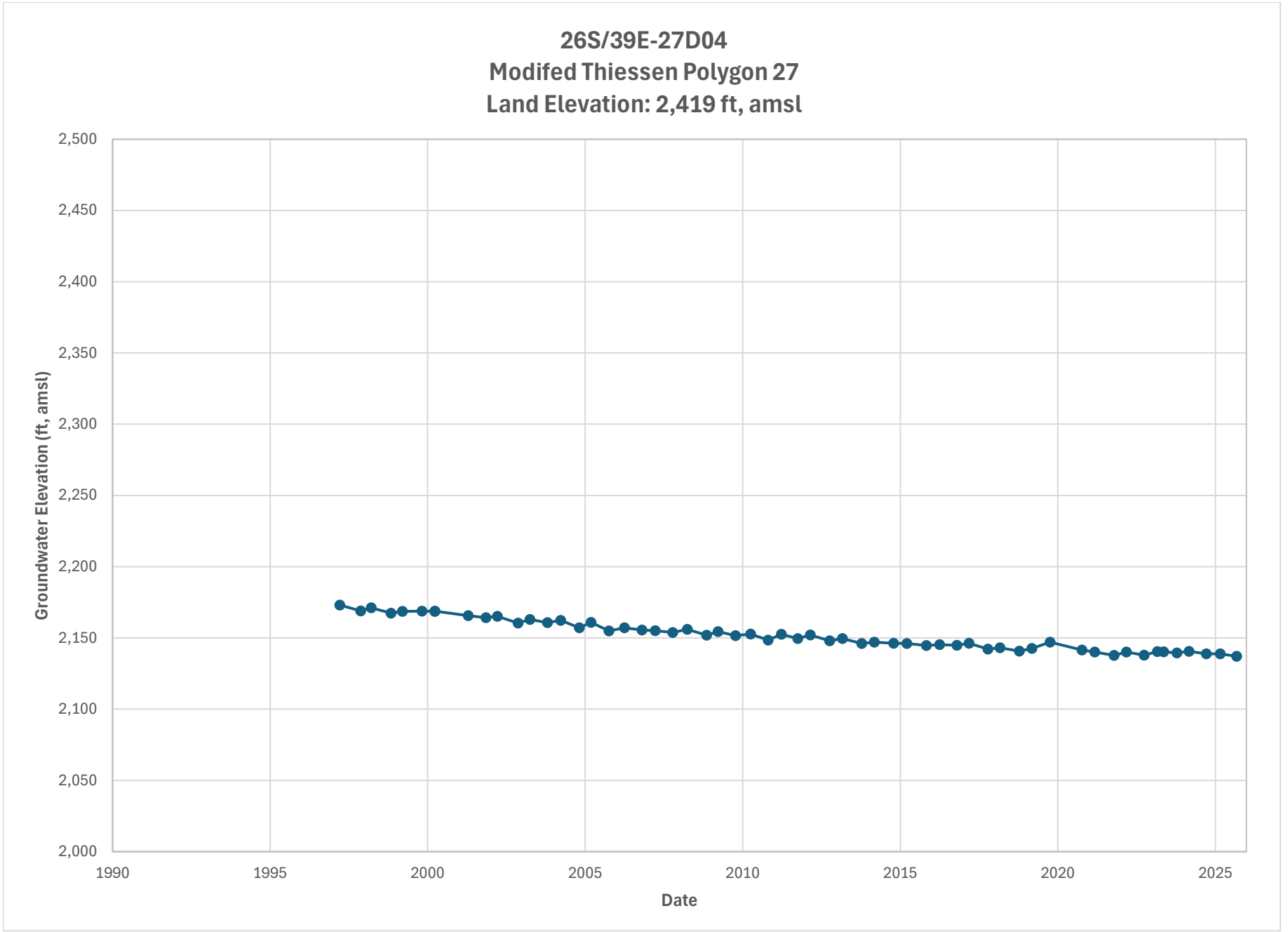

26S/39E-34R02
Modifed Thiessen Polygon 21
Land Elevation: 2,451 ft, amsl
Groundwater Elevation (ft, amsl)
2,500
2,450
2,400
2,350
2,300
2,250
2,200
2,150
2,100
2,050
2,000
1990
1995
2000
2005
2010
2015
2020
2025
Date

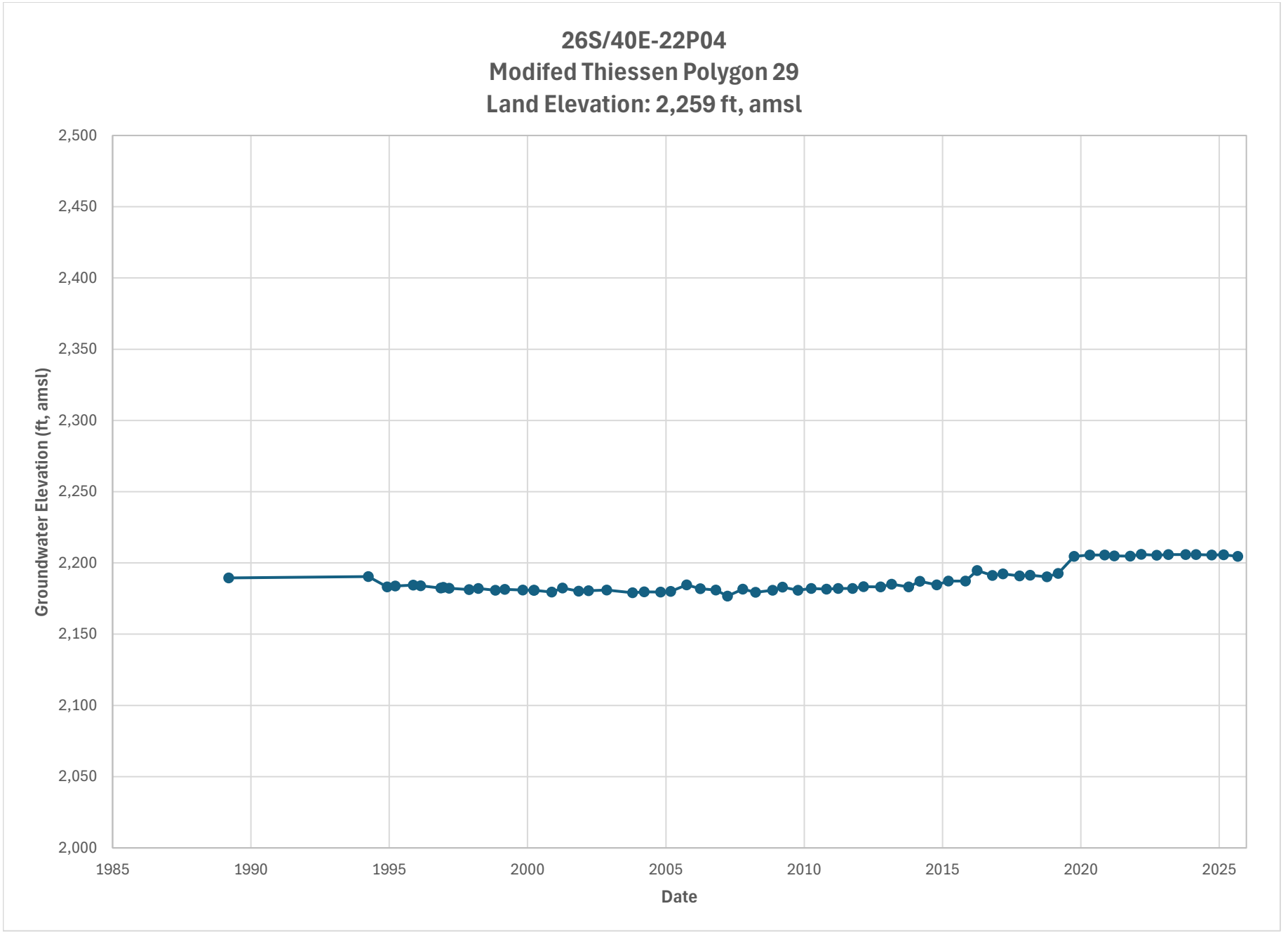

26S/40E-31K01
Modifed Thiessen Polygon 22
Land Elevation: 2,391 ft, amsl
Groundwater Elevation (ft, amsl)
2,500
2,450
2,400
2,350
2,300
2,250
2,200
2,150
2,100
2,050
2,000
1985
1990
1995
2000
2005
2010
2015
2020
2025
Date

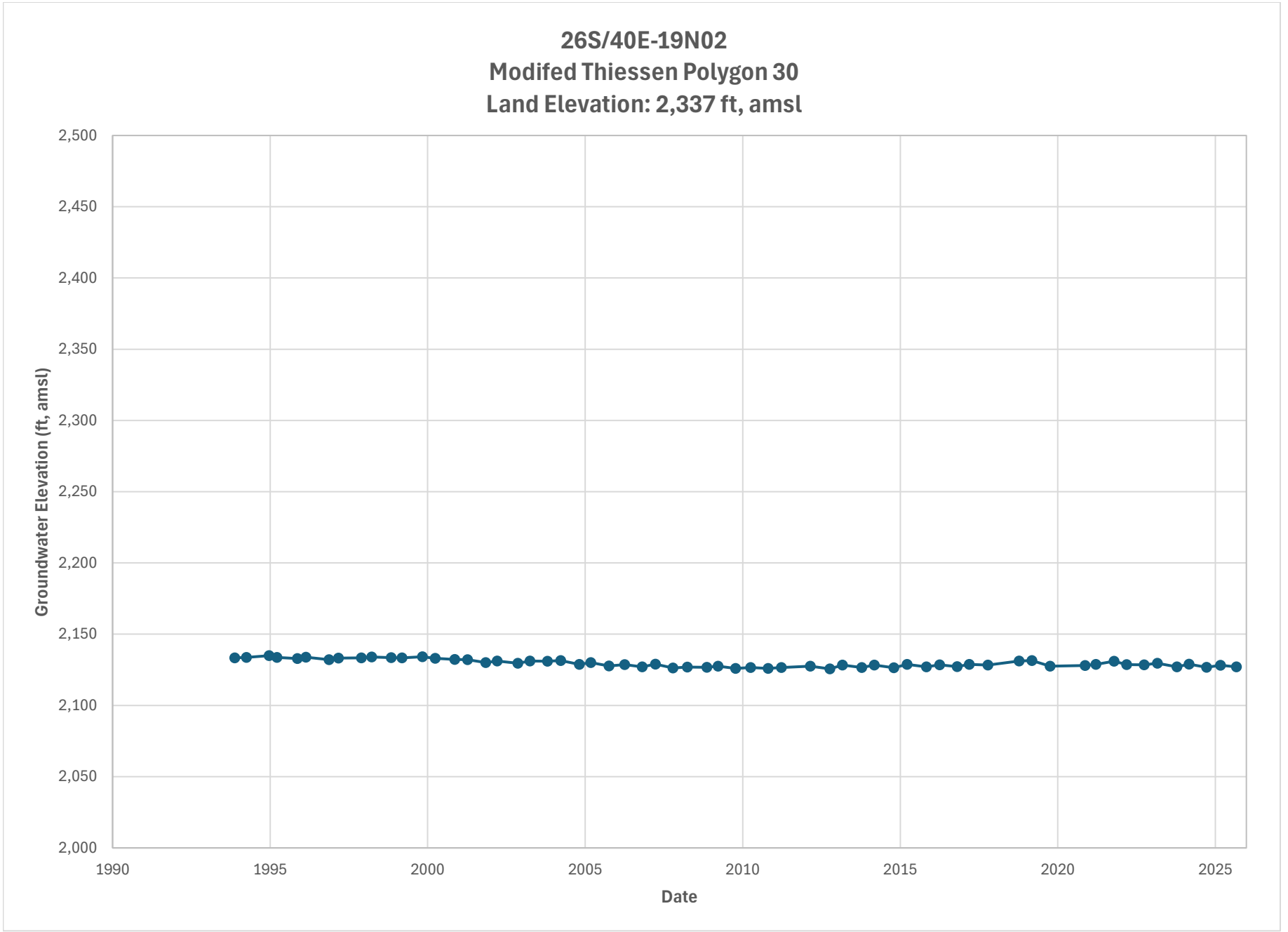

26S/39E-32L01
Modifed Thiessen Polygon 23
Land Elevation: 2,492 ft, amsl
Groundwater Elevation (ft, amsl)
2,500
2,450
2,400
2,350
2,300
2,250
2,200
2,150
2,100
2,050
2,000
1990
1995
2000
2005
2010
2015
2020
2025
Date

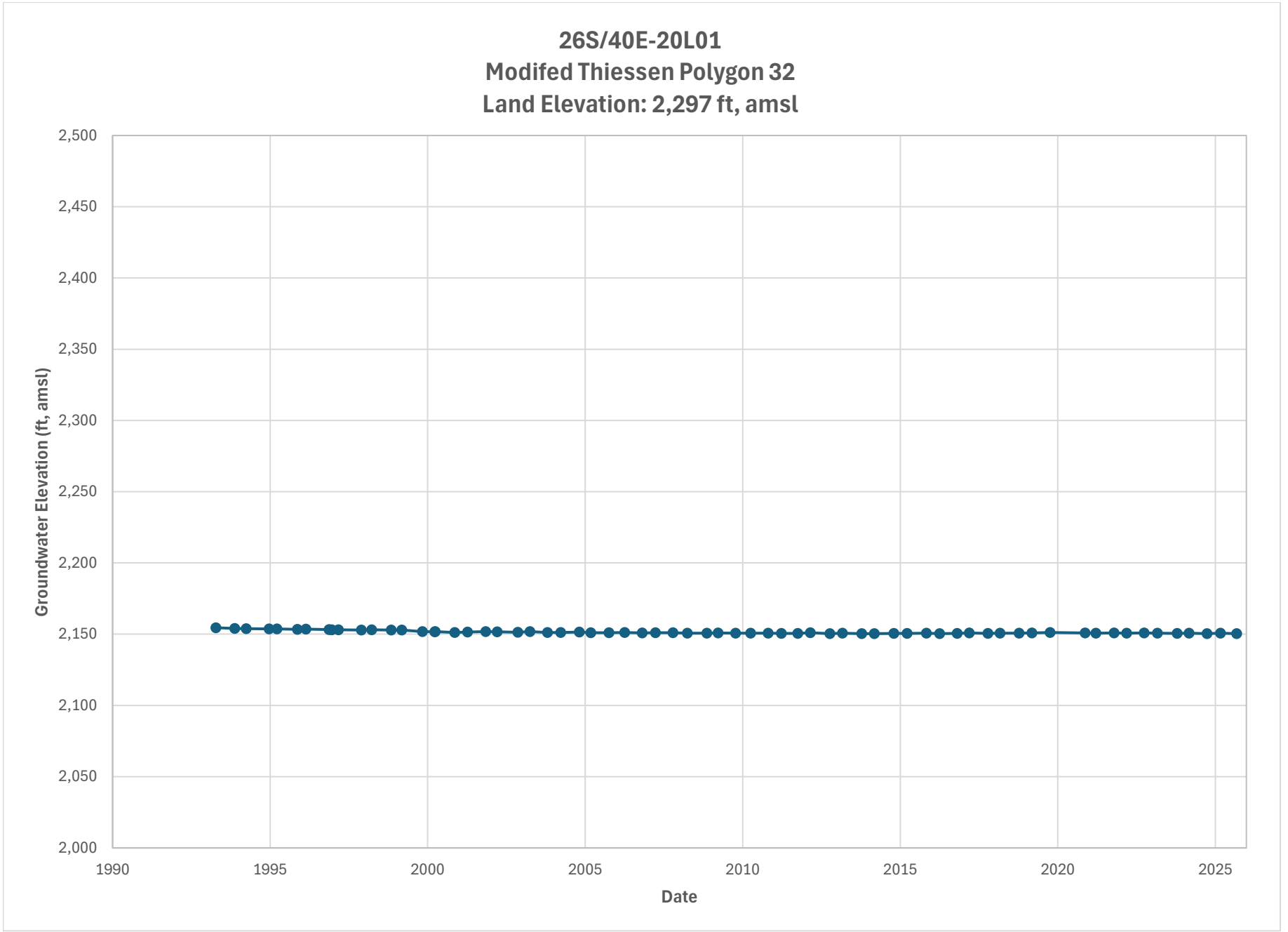

26S/40E-35H02
Modifed Thiessen Polygon 25
Land Elevation: 2,252 ft, amsl
Groundwater Elevation (ft, amsl)
2,500
2,450
2,400
2,350
2,300
2,250
2,200
2,150
2,100
2,050
2,000
1985
1990
1995
2000
2005
2010
2015
2020
2025
Date

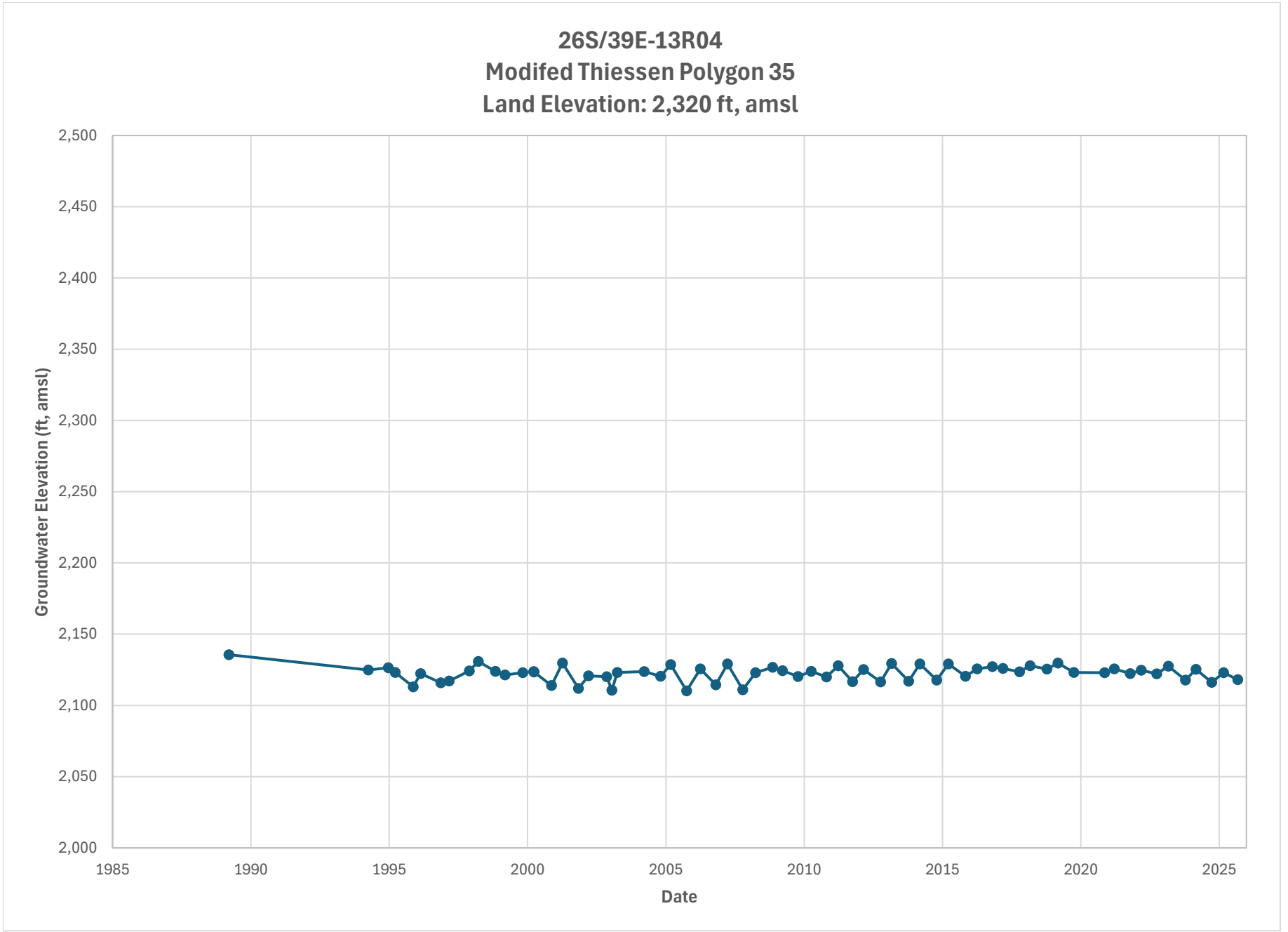

26S/39E-26P02
Modifed Thiessen Polygon 26
Land Elevation: 2,406 ft, amsl
Groundwater Elevation (ft, amsl)
2,500
2,450
2,400
2,350
2,300
2,250
2,200
2,150
2,100
2,050
2,000
1990
1995
2000
2005
2010
2015
2020
2025
Date

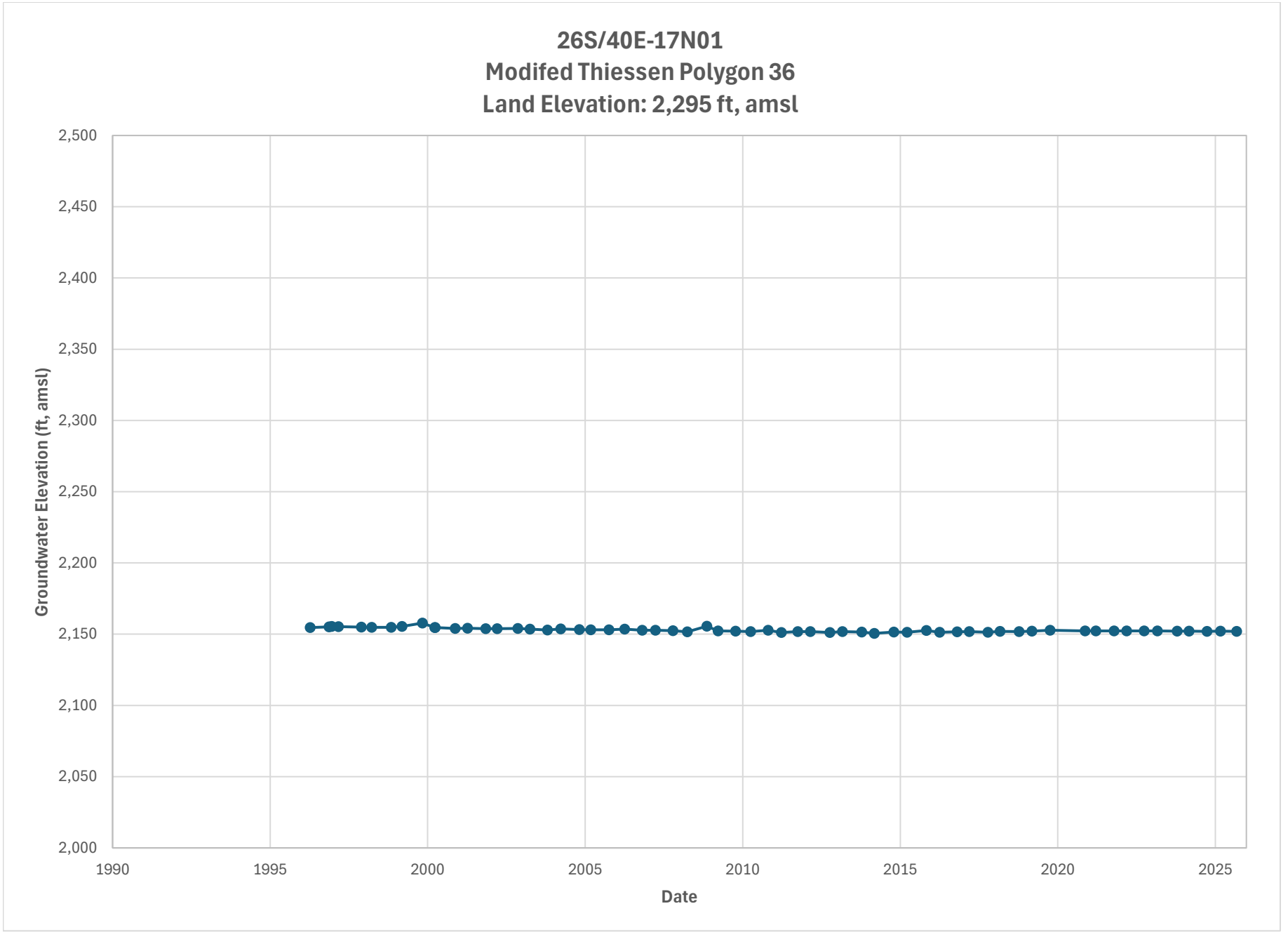

26S/39E-27D04
Modifed Thiessen Polygon 27
Land Elevation: 2,419 ft, amsl
Groundwater Elevation (ft, amsl)
2,500
2,450
2,400
2,350
2,300
2,250
2,200
2,150
2,100
2,050
2,000
1990
1995
2000
2005
2010
2015
2020
2025
Date

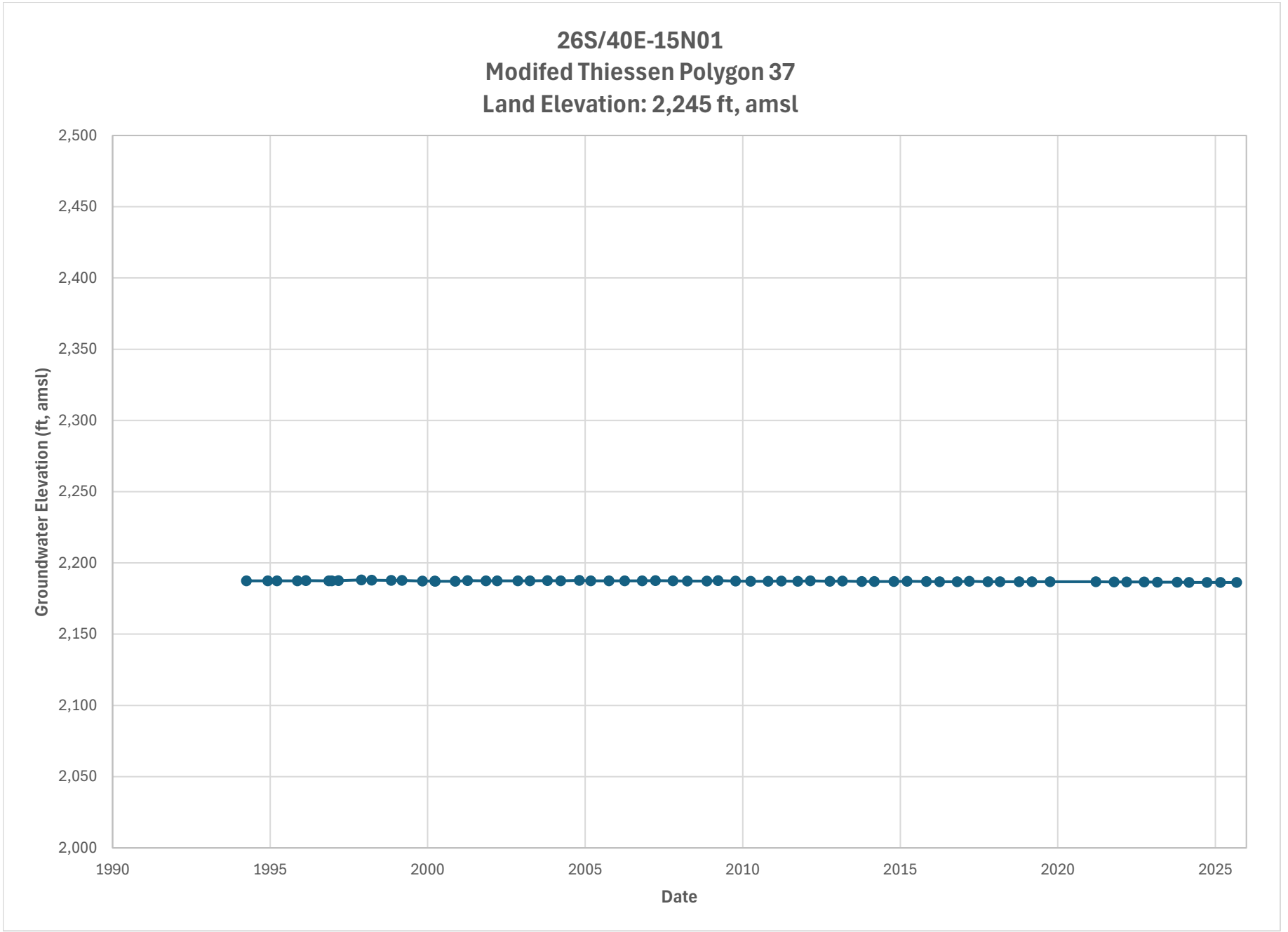

26S/40E-22P04
Modifed Thiessen Polygon 29
Land Elevation: 2,259 ft, amsl
Groundwater Elevation (ft, amsl)
2,500
2,450
2,400
2,350
2,300
2,250
2,200
2,150
2,100
2,050
2,000
1985
1990
1995
2000
2005
2010
2015
2020
2025
Date

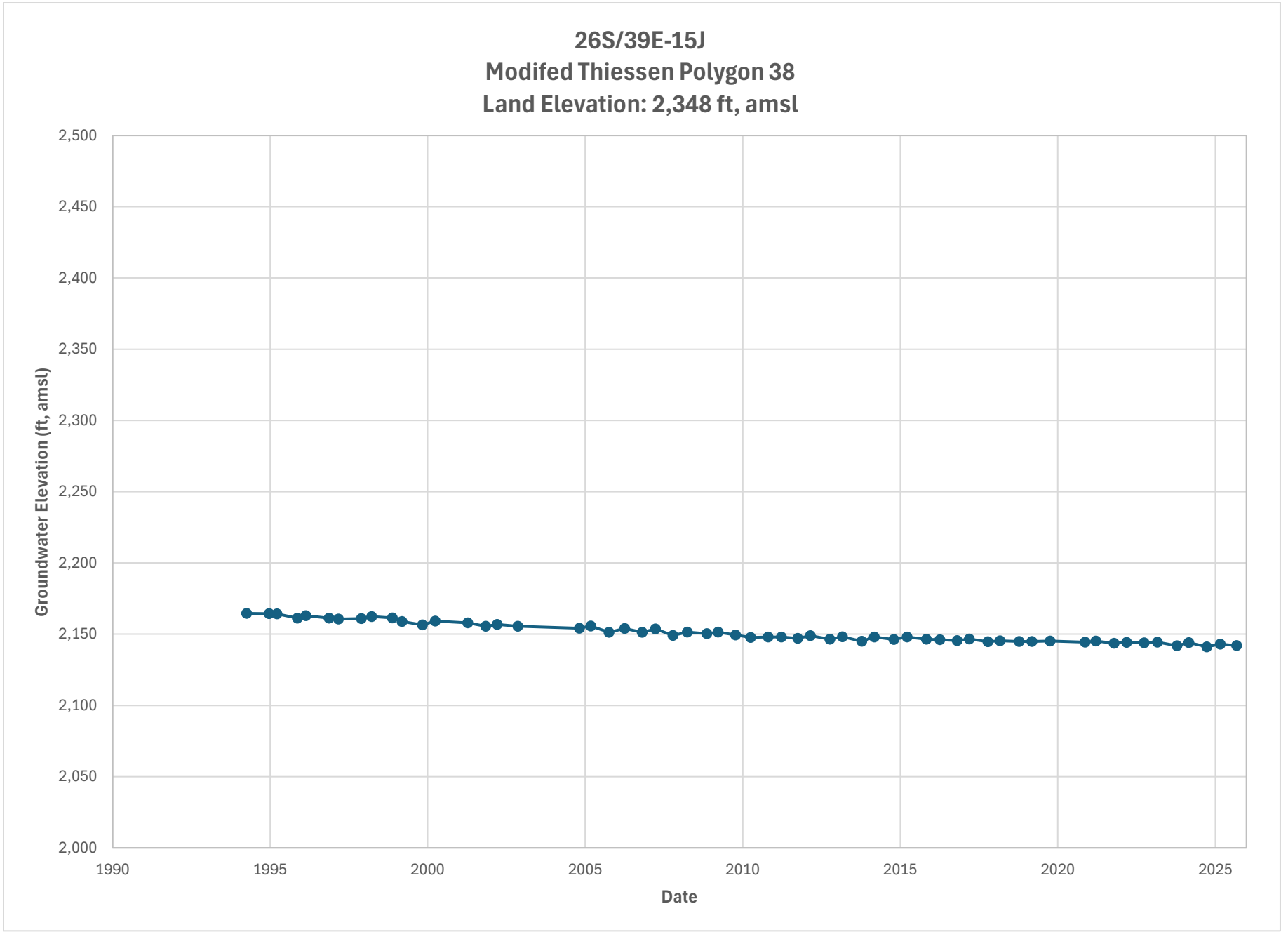

26S/40E-19N02
Modifed Thiessen Polygon 30
Land Elevation: 2,337 ft, amsl
Groundwater Elevation (ft, amsl)
2,500
2,450
2,400
2,350
2,300
2,250
2,200
2,150
2,100
2,050
2,000
1990
1995
2000
2005
2010
2015
2020
2025
Date

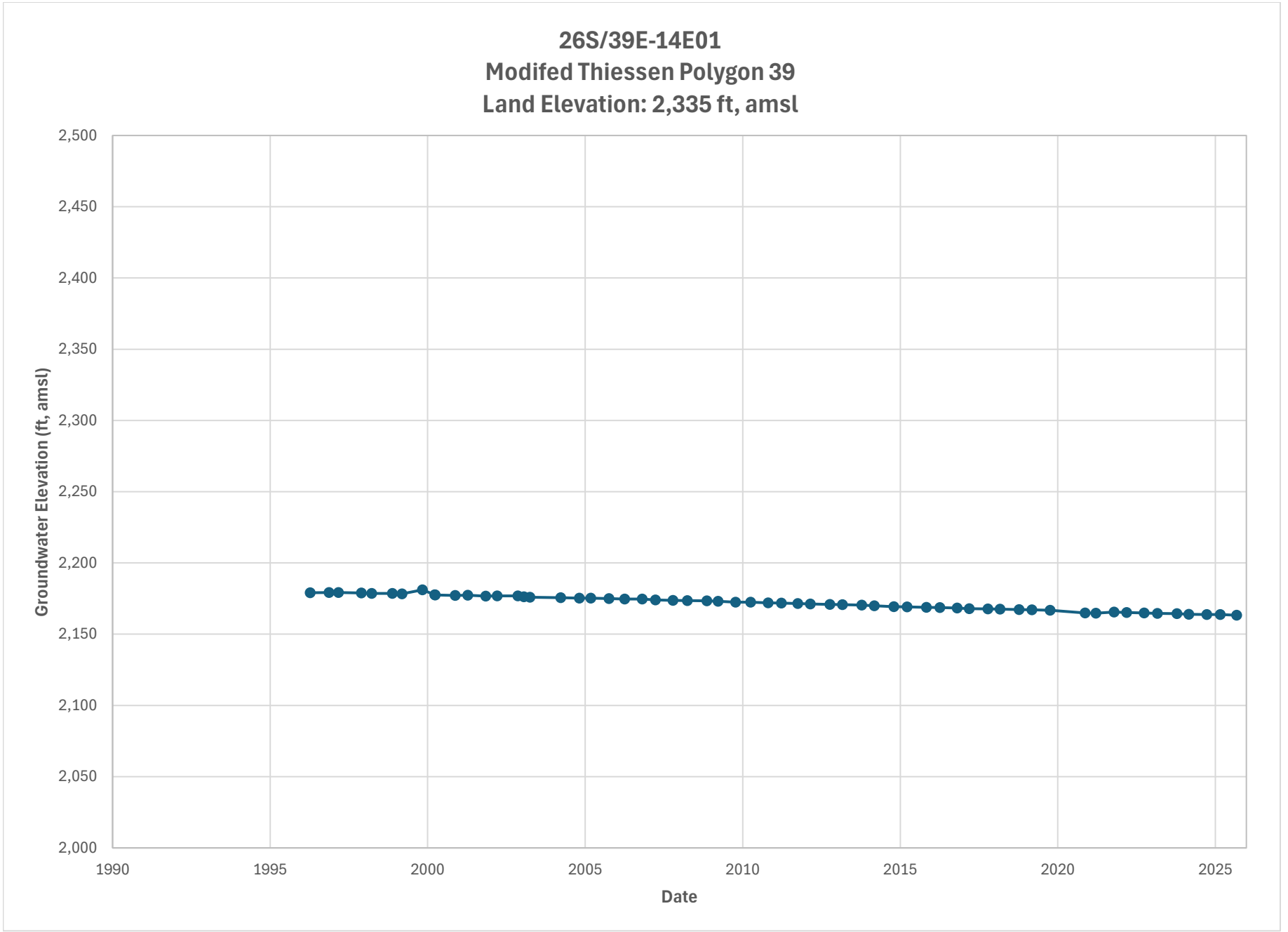

26S/40E-20L01
Modifed Thiessen Polygon 32
Land Elevation: 2,297 ft, amsl
Groundwater Elevation (ft, amsl)
2,500
2,450
2,400
2,350
2,300
2,250
2,200
2,150
2,100
2,050
2,000
1990
1995
2000
2005
2010
2015
2020
2025
Date

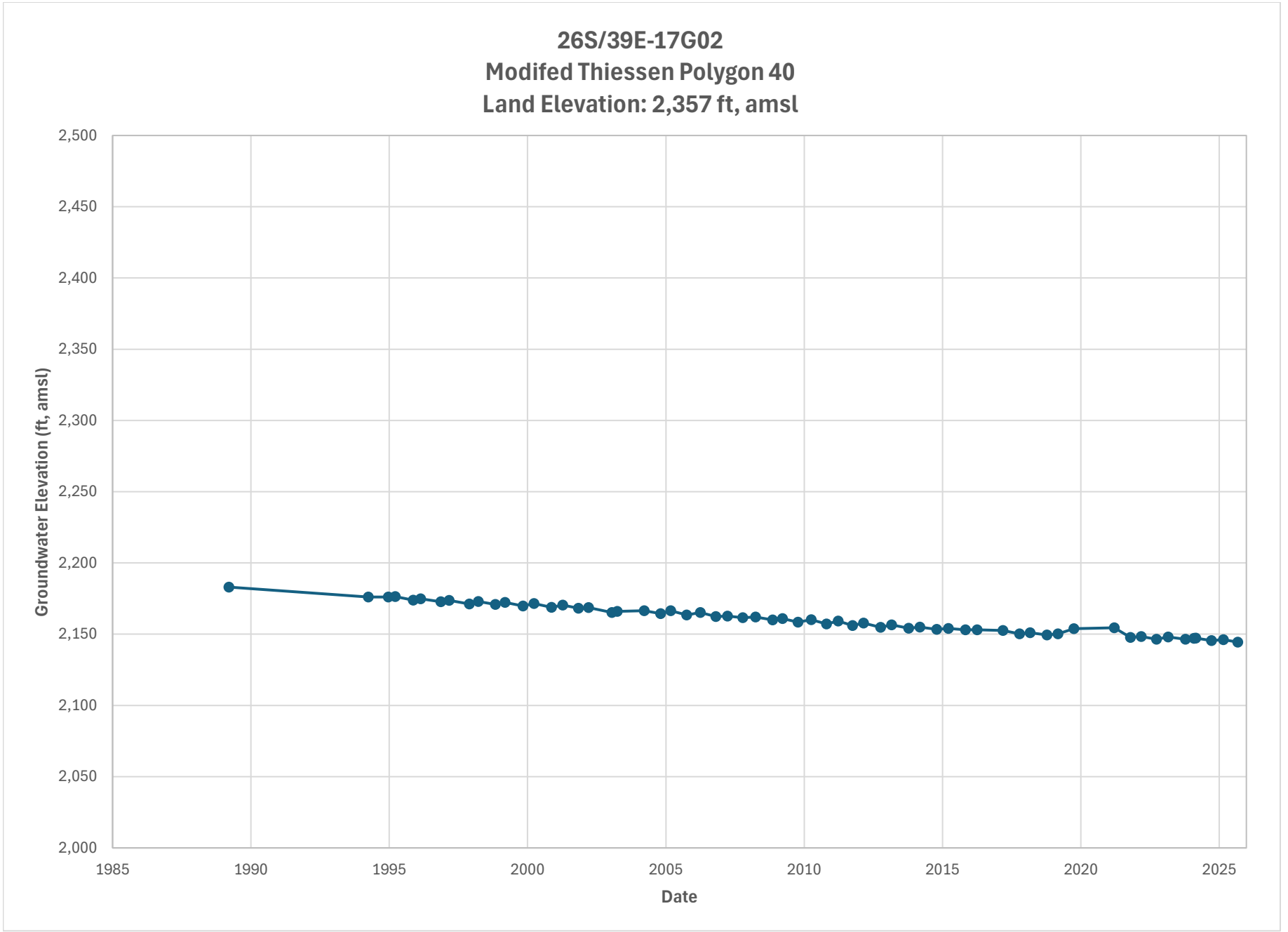

26S/39E-13R04
Modifed Thiessen Polygon 35
Land Elevation: 2,320 ft, amsl
Groundwater Elevation (ft, amsl)
2,500
2,450
2,400
2,350
2,300
2,250
2,200
2,150
2,100
2,050
2,000
1985
1990
1995
2000
2005
2010
2015
2020
2025
Date

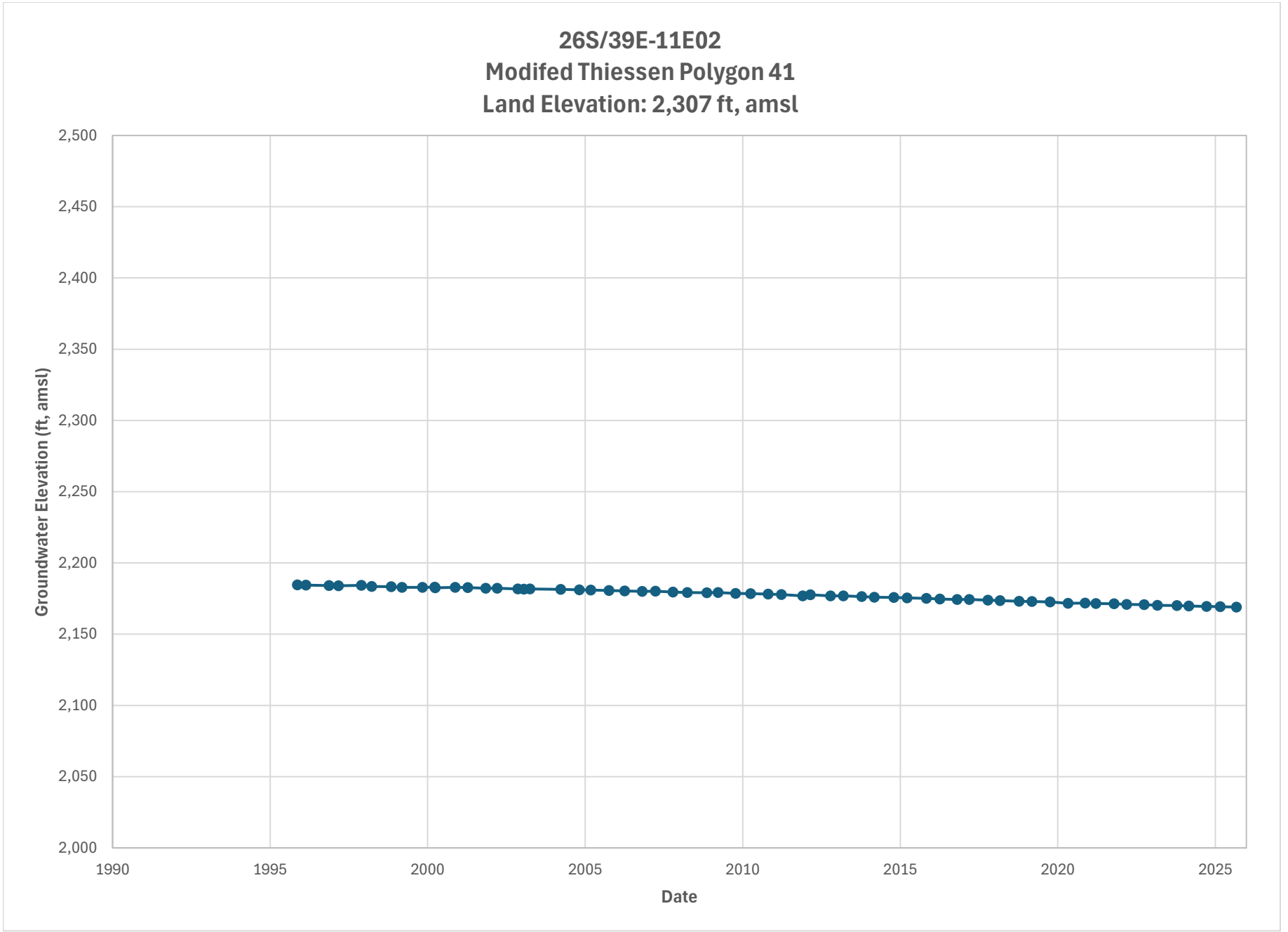

26S/40E-17N01
Modifed Thiessen Polygon 36
Land Elevation: 2,295 ft, amsl
Groundwater Elevation (ft, amsl)
2,500
2,450
2,400
2,350
2,300
2,250
2,200
2,150
2,100
2,050
2,000
1990
1995
2000
2005
2010
2015
2020
2025
Date

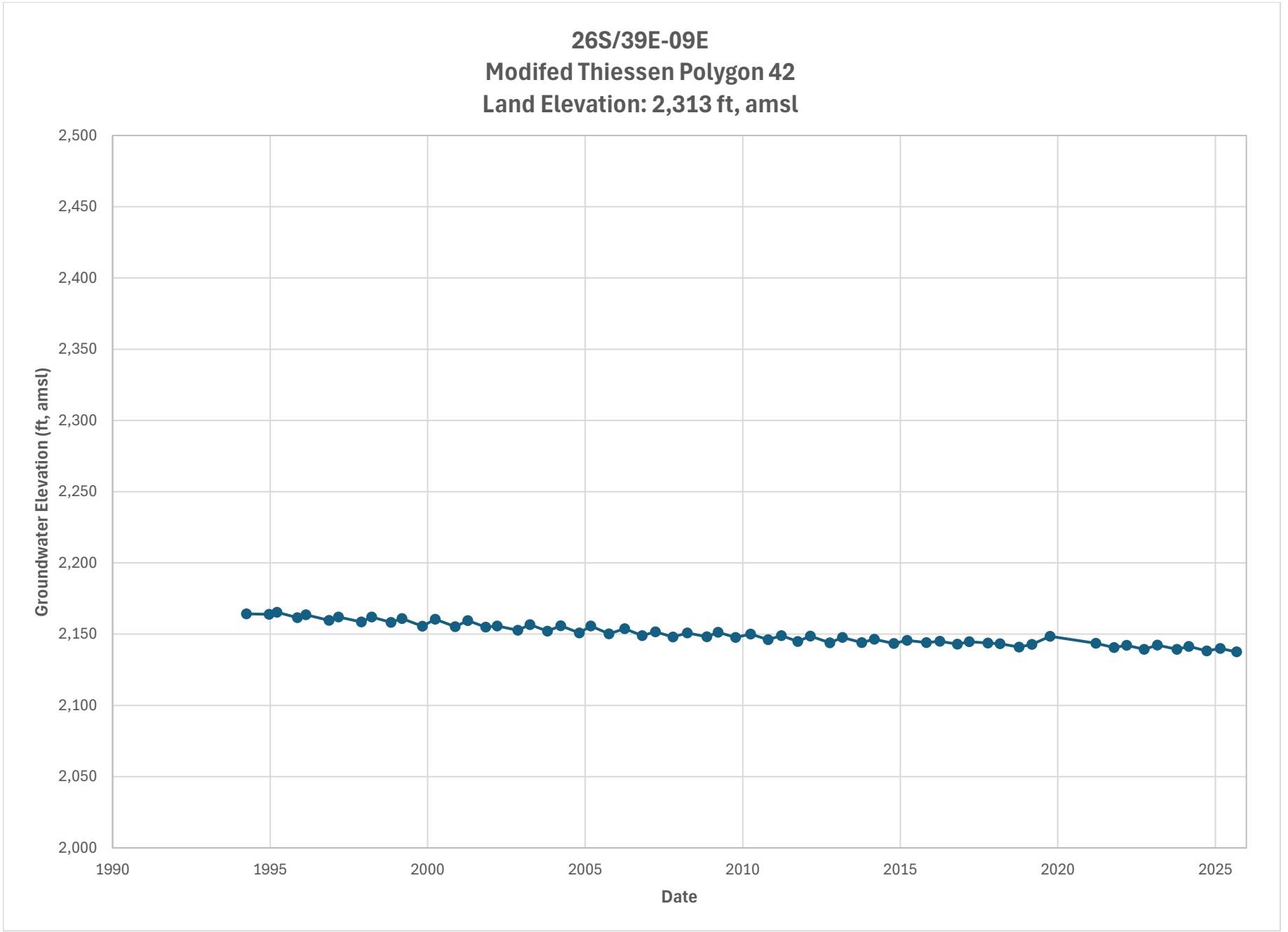

26S/40E-15N01
Modifed Thiessen Polygon 37
Land Elevation: 2,245 ft, amsl
Groundwater Elevation (ft, amsl)
2,500
2,450
2,400
2,350
2,300
2,250
2,200
2,150
2,100
2,050
2,000
1990
1995
2000
2005
2010
2015
2020
2025
Date

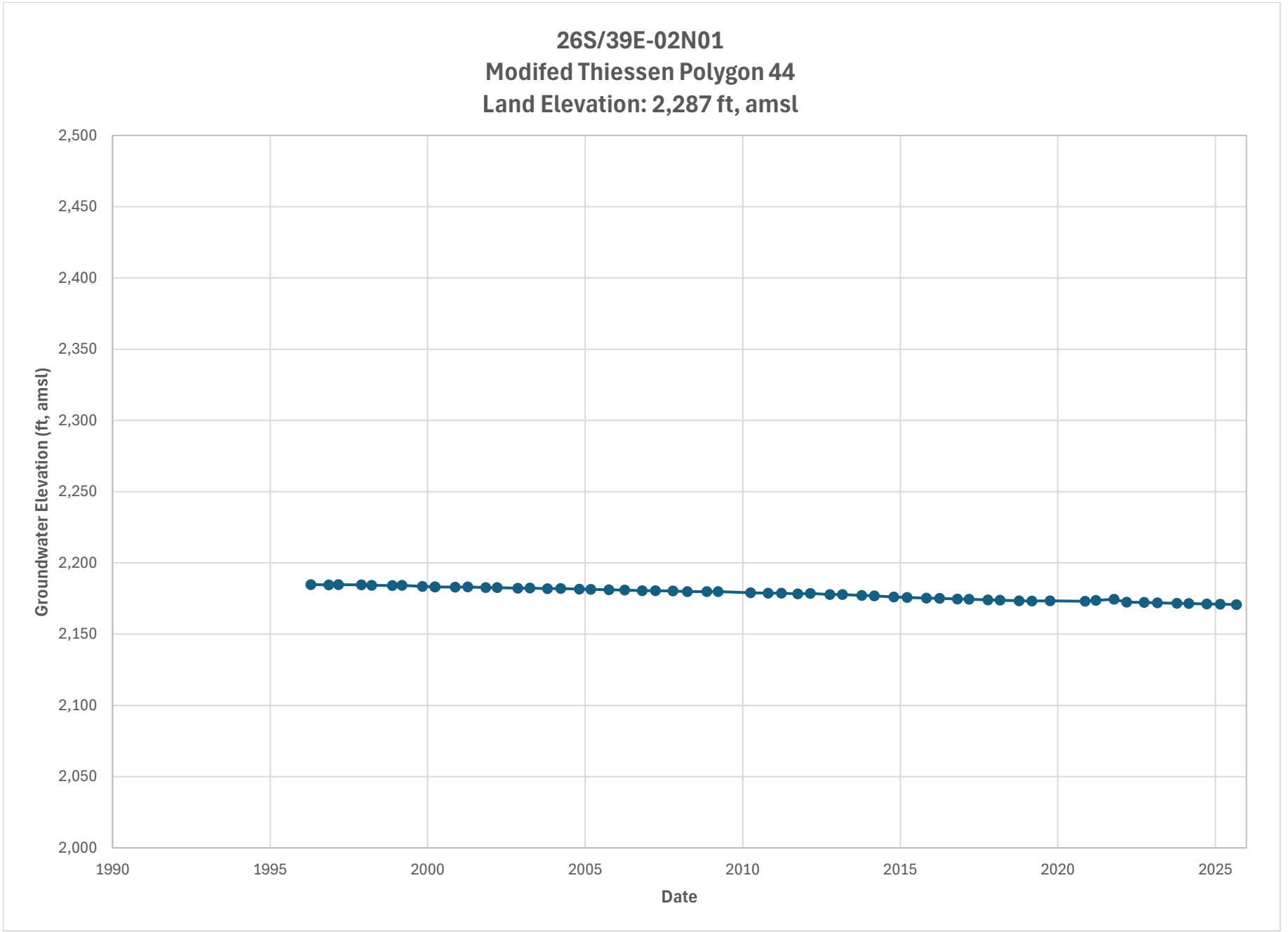

26S/39E-15J
Modifed Thiessen Polygon 38
Land Elevation: 2,348 ft, amsl
Groundwater Elevation (ft, amsl)
2,500
2,450
2,400
2,350
2,300
2,250
2,200
2,150
2,100
2,050
2,000
1990
1995
2000
2005
2010
2015
2020
2025
Date

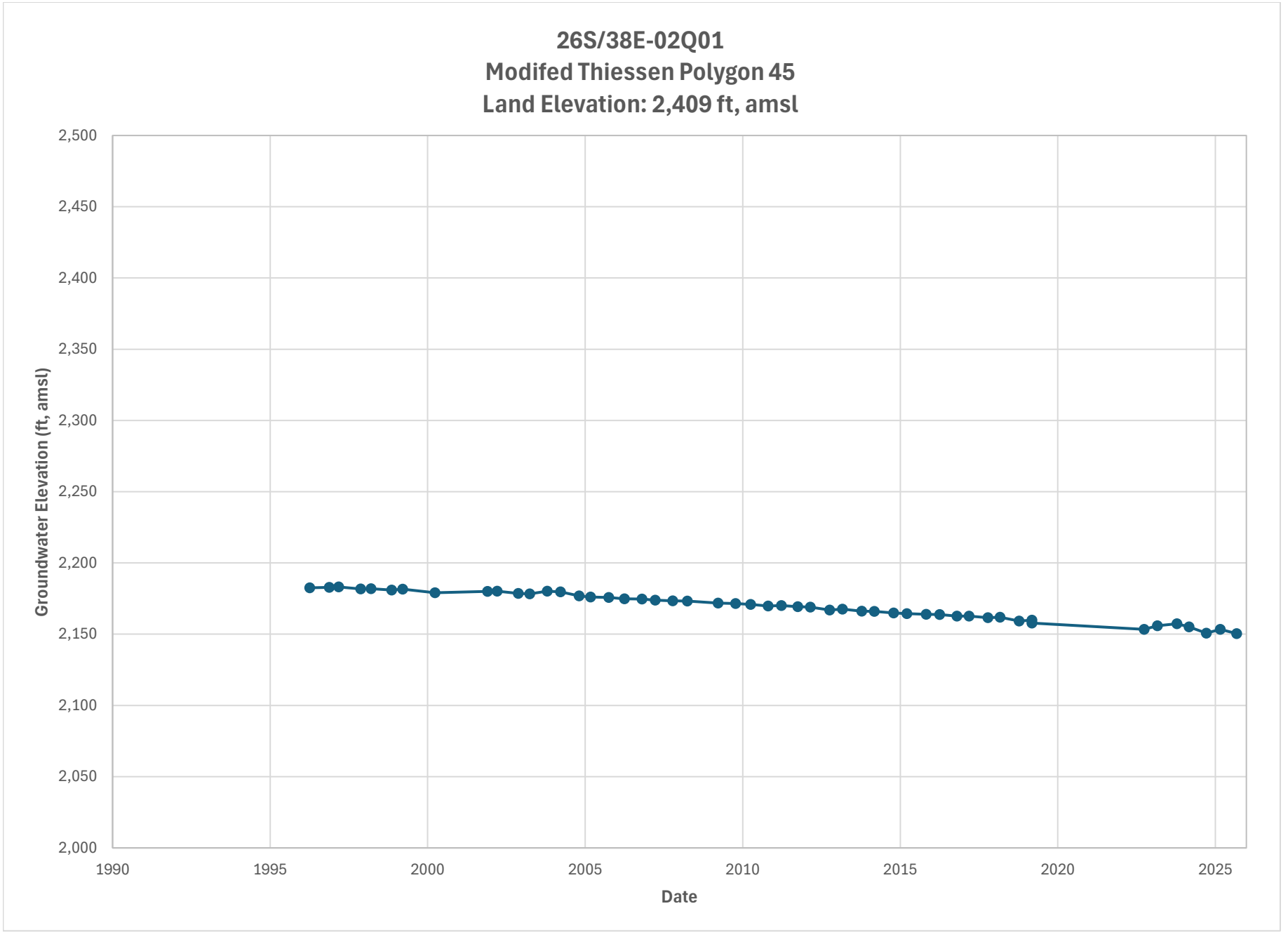

26S/39E-14E01
Modifed Thiessen Polygon 39
Land Elevation: 2,335 ft, amsl
Groundwater Elevation (ft, amsl)
2,500
2,450
2,400
2,350
2,300
2,250
2,200
2,150
2,100
2,050
2,000
1990
1995
2000
2005
2010
2015
2020
2025
Date

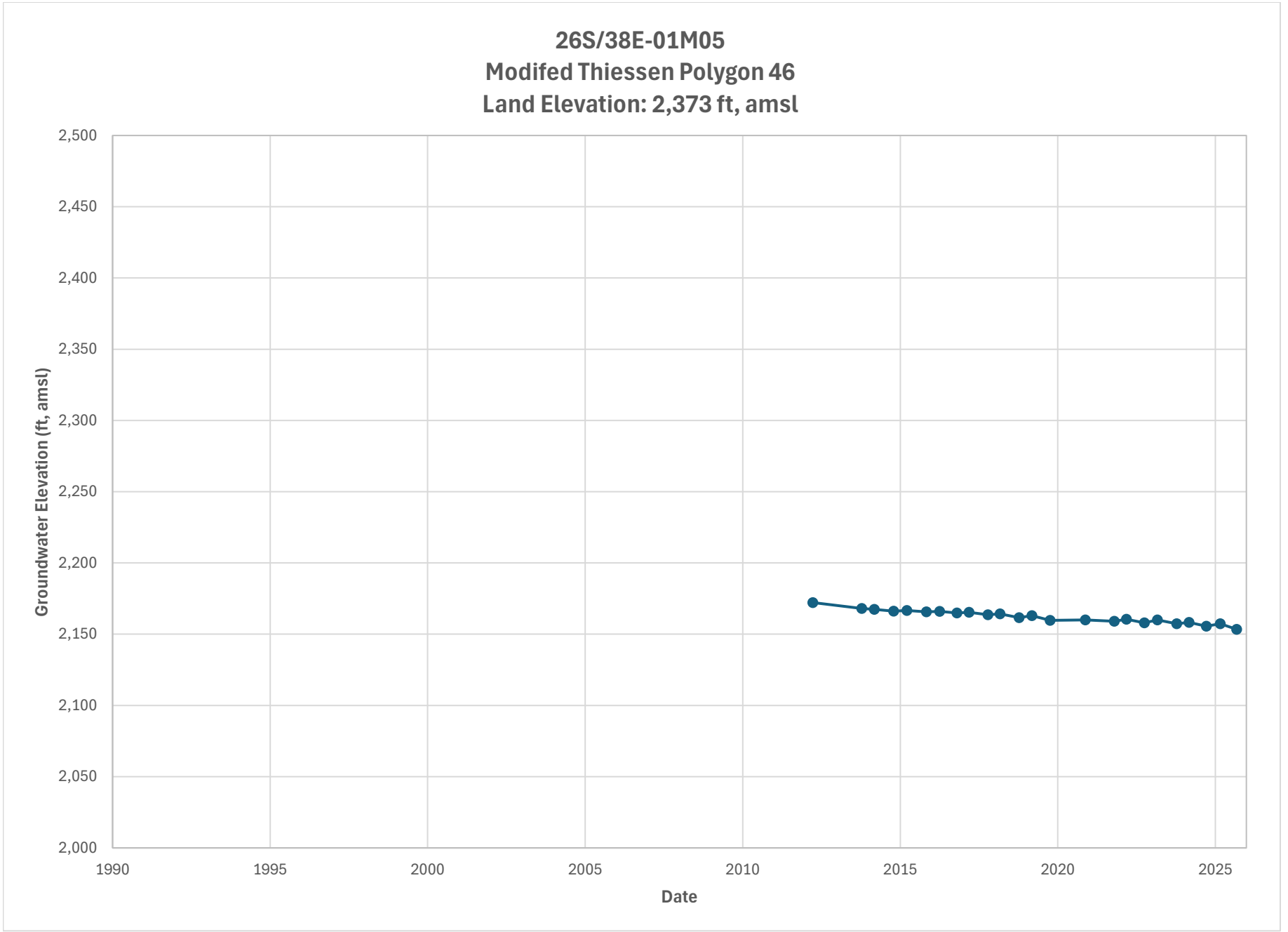

26S/39E-17G02
Modifed Thiessen Polygon 40
Land Elevation: 2,357 ft, amsl
Groundwater Elevation (ft, amsl)
2,500
2,450
2,400
2,350
2,300
2,250
2,200
2,150
2,100
2,050
2,000
1985
1990
1995
2000
2005
2010
2015
2020
2025
Date

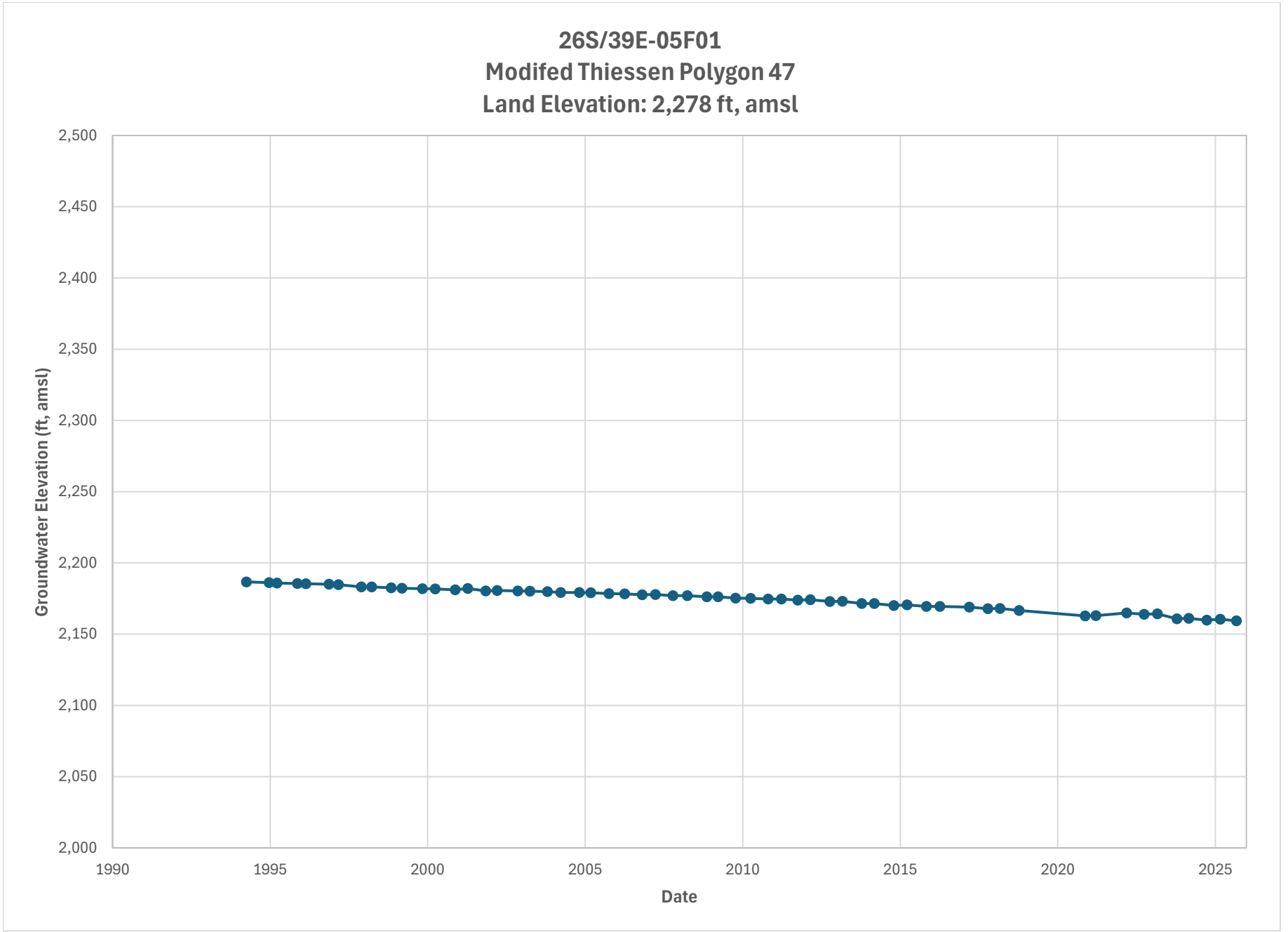

26S/39E-11E02
Modifed Thiessen Polygon 41
Land Elevation: 2,307 ft, amsl
Groundwater Elevation (ft, amsl)
2,500
2,450
2,400
2,350
2,300
2,250
2,200
2,150
2,100
2,050
2,000
1990
1995
2000
2005
2010
2015
2020
2025
Date

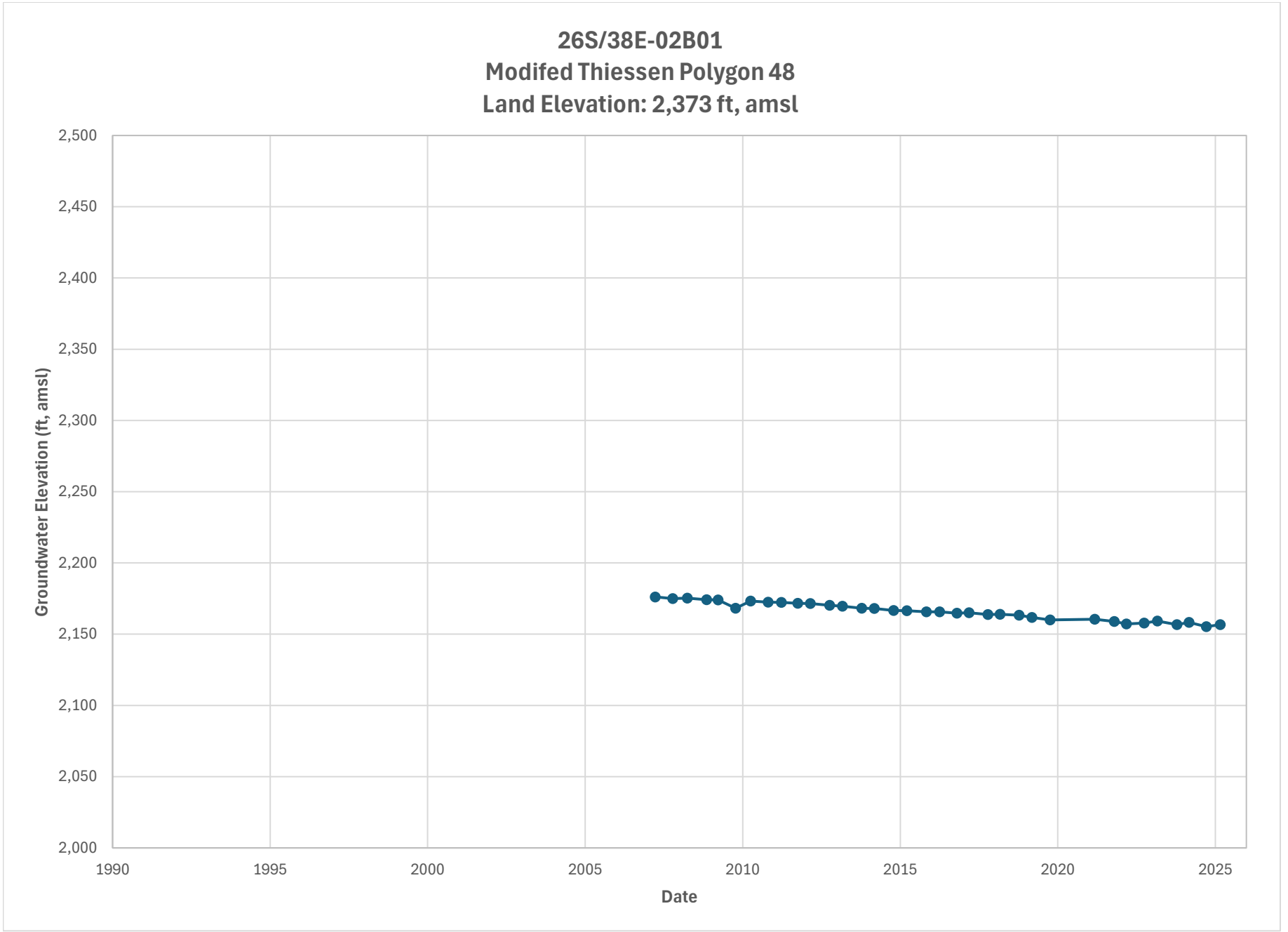

26S/39E-09E
Modifed Thiessen Polygon 42
Land Elevation: 2,313 ft, amsl
Groundwater Elevation (ft, amsl)
2,500
2,450
2,400
2,350
2,300
2,250
2,200
2,150
2,100
2,050
2,000
1990
1995
2000
2005
2010
2015
2020
2025
Date

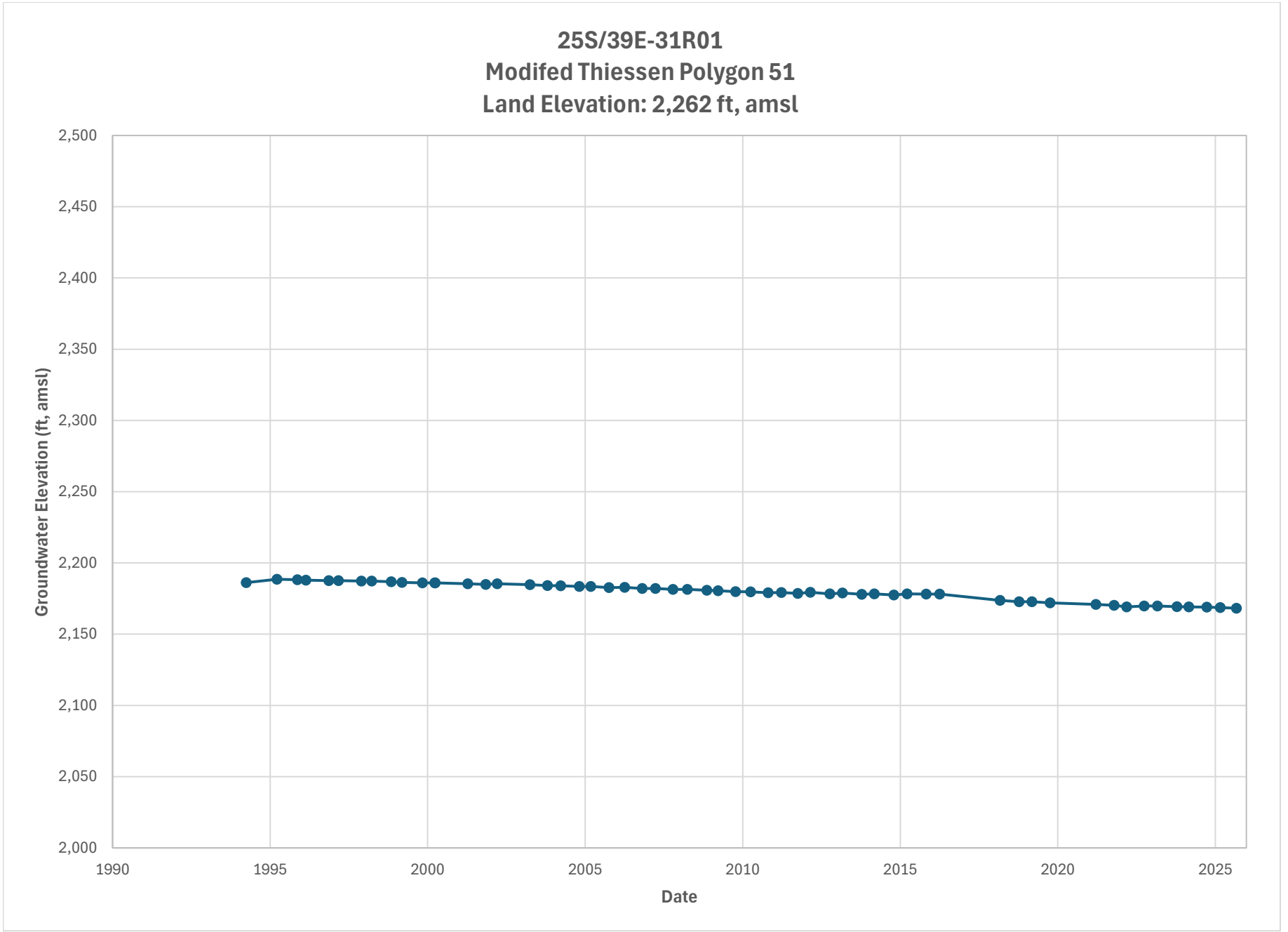

26S/39E-02N01
Modifed Thiessen Polygon 44
Land Elevation: 2,287 ft, amsl
Groundwater Elevation (ft, amsl)
2,500
2,450
2,400
2,350
2,300
2,250
2,200
2,150
2,100
2,050
2,000
1990
1995
2000
2005
2010
2015
2020
2025
Date

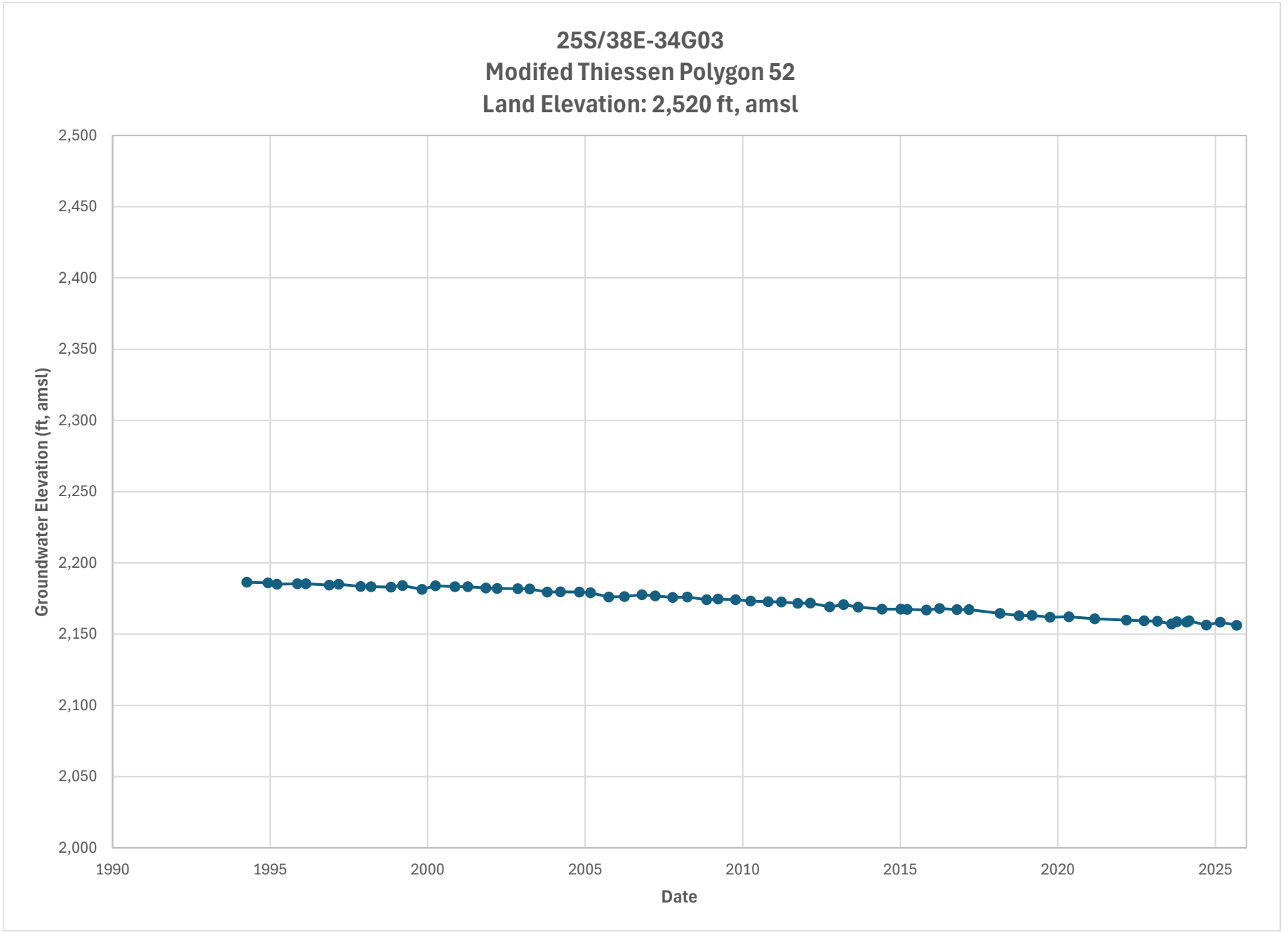

26S/38E-02Q01
Modifed Thiessen Polygon 45
Land Elevation: 2,409 ft, amsl
Groundwater Elevation (ft, amsl)
2,500
2,450
2,400
2,350
2,300
2,250
2,200
2,150
2,100
2,050
2,000
1990
1995
2000
2005
2010
2015
2020
2025
Date

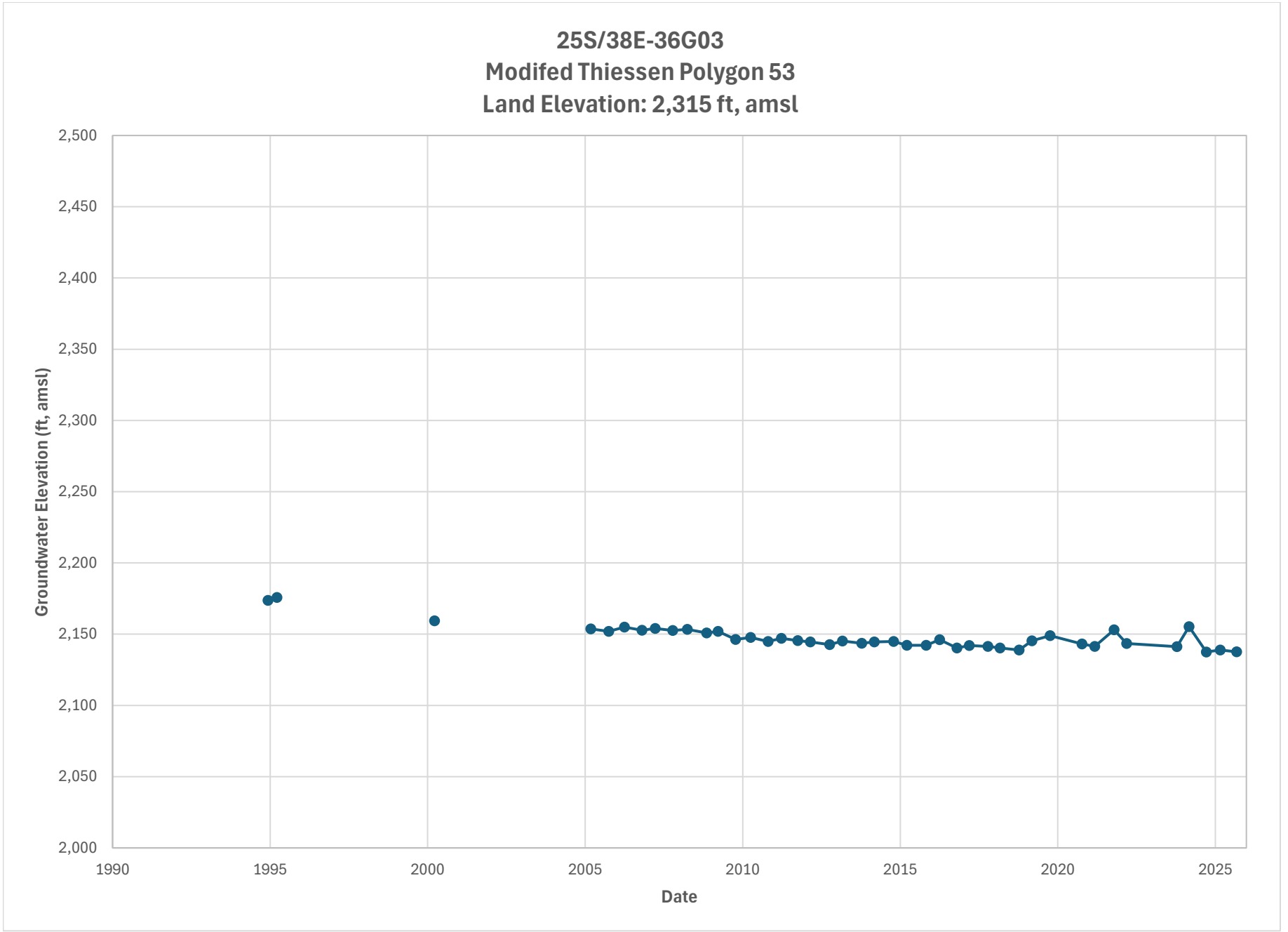

26S/38E-01M05
Modifed Thiessen Polygon 46
Land Elevation: 2,373 ft, amsl
Groundwater Elevation (ft, amsl)
2,500
2,450
2,400
2,350
2,300
2,250
2,200
2,150
2,100
2,050
2,000
1990
1995
2000
2005
2010
2015
2020
2025
Date

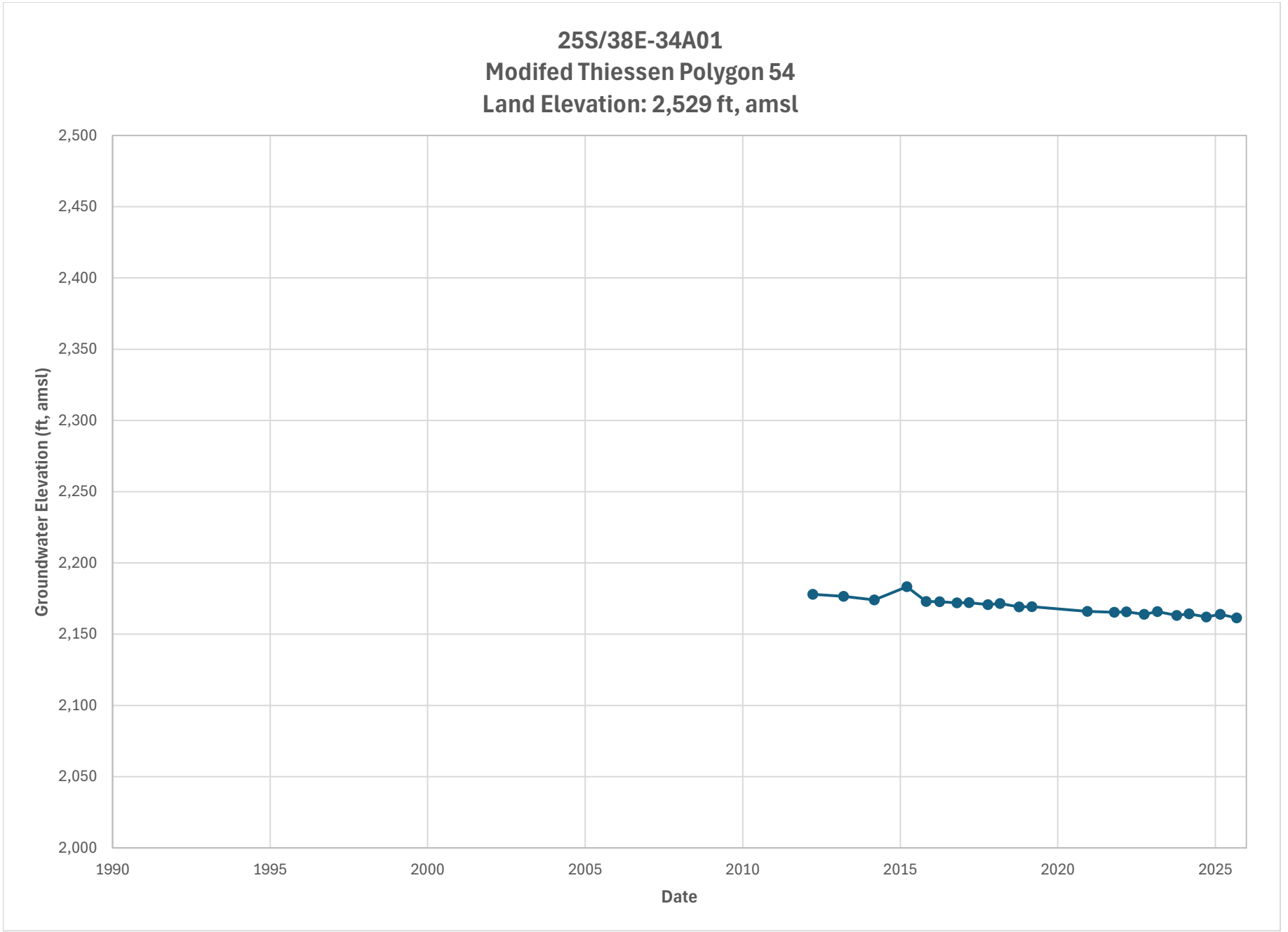

26S/39E-05F01
Modifed Thiessen Polygon 47
Land Elevation: 2,278 ft, amsl
Groundwater Elevation (ft, amsl)
2,500
2,450
2,400
2,350
2,300
2,250
2,200
2,150
2,100
2,050
2,000
1990
1995
2000
2005
2010
2015
2020
2025
Date

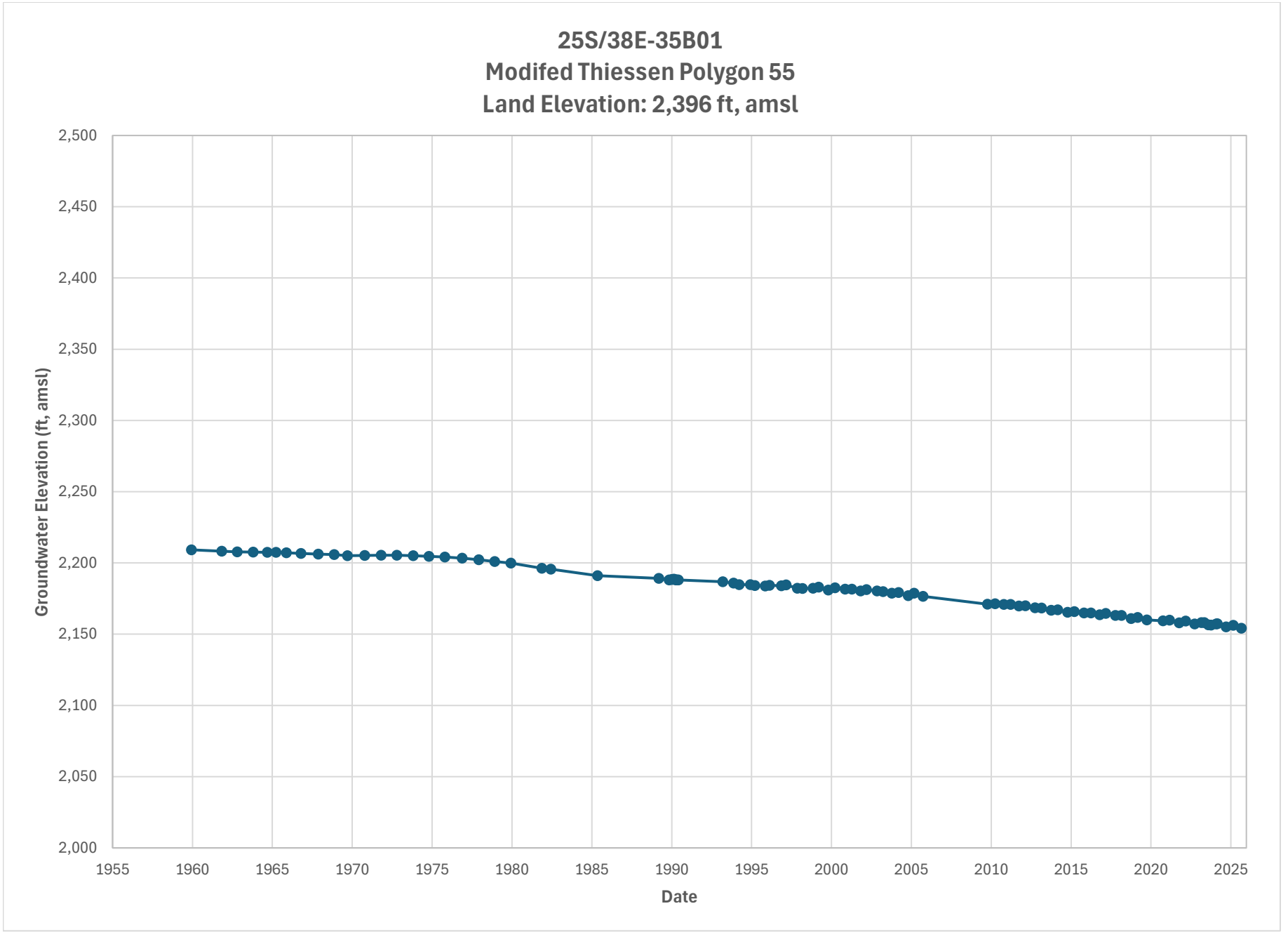

26S/38E-02B01
Modifed Thiessen Polygon 48
Land Elevation: 2,373 ft, amsl
Groundwater Elevation (ft, amsl)
2,500
2,450
2,400
2,350
2,300
2,250
2,200
2,150
2,100
2,050
2,000
1990
1995
2000
2005
2010
2015
2020
2025
Date

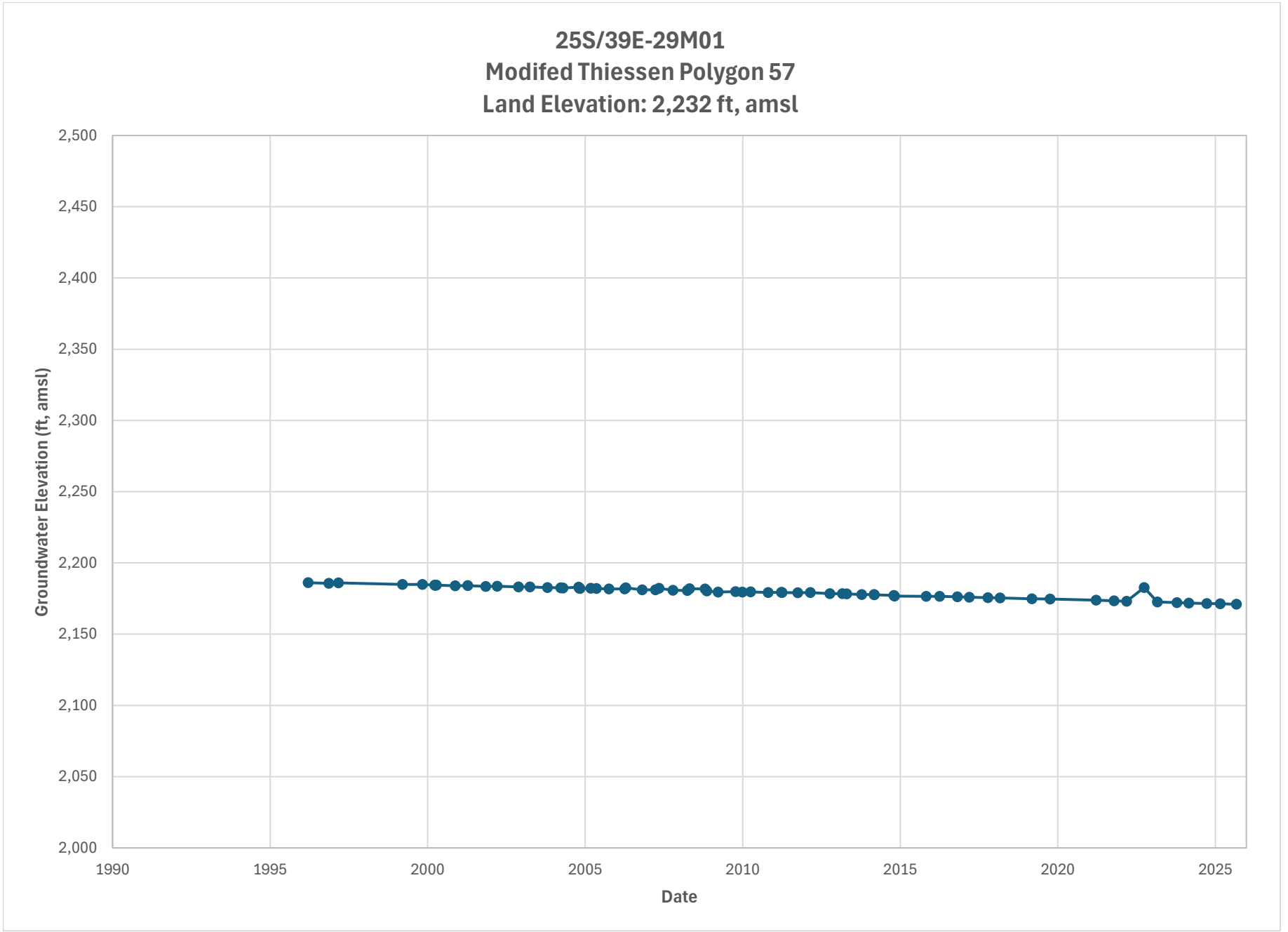

25S/39E-31R01
Modifed Thiessen Polygon 51
Land Elevation: 2,262 ft, amsl
Groundwater Elevation (ft, amsl)
2,500
2,450
2,400
2,350
2,300
2,250
2,200
2,150
2,100
2,050
2,000
1990
1995
2000
2005
2010
2015
2020
2025
Date

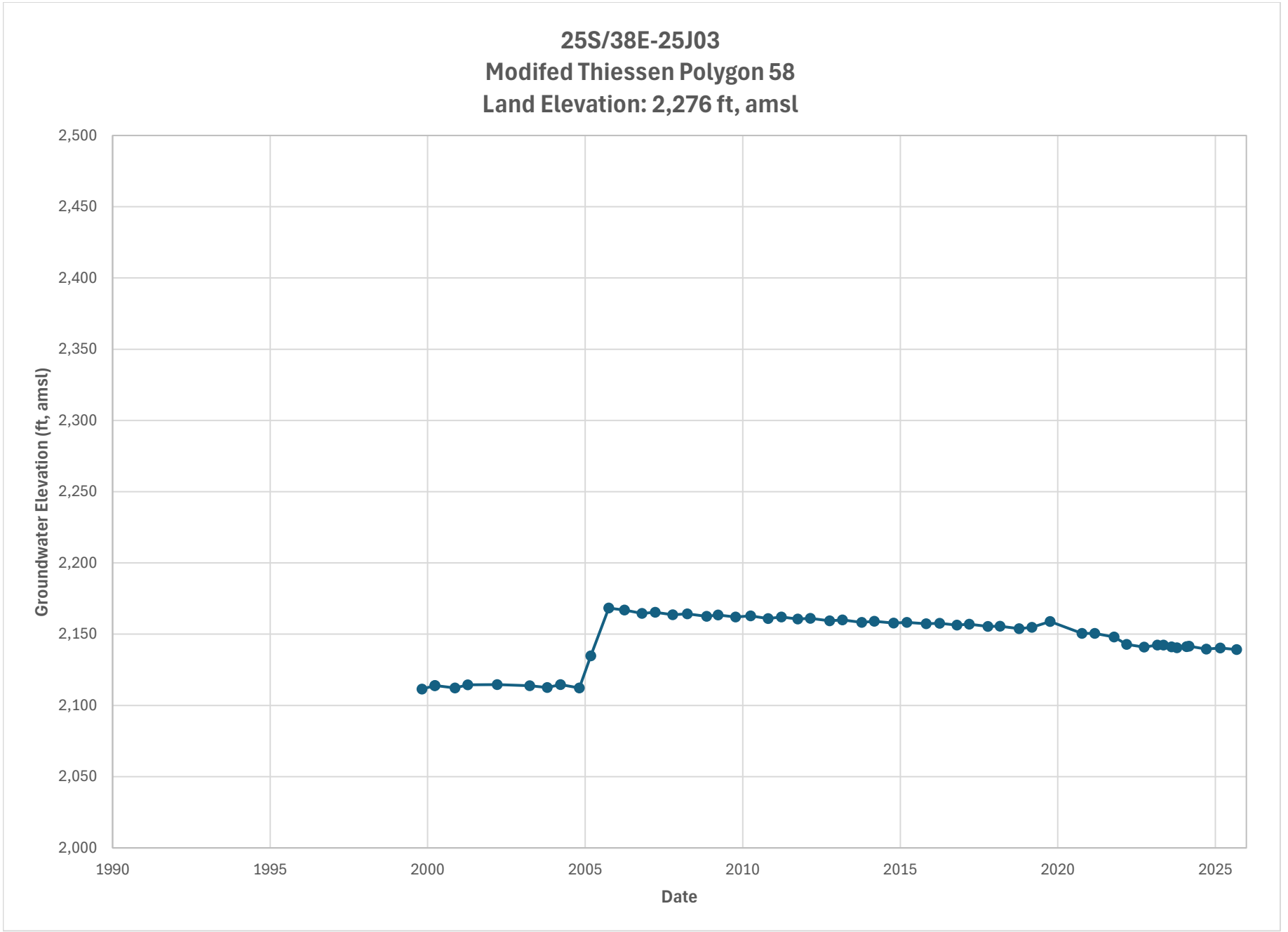

25S/38E-34G03
Modifed Thiessen Polygon 52
Land Elevation: 2,520 ft, amsl
Groundwater Elevation (ft, amsl)
2,500
2,450
2,400
2,350
2,300
2,250
2,200
2,150
2,100
2,050
2,000
1990
1995
2000
2005
2010
2015
2020
2025
Date

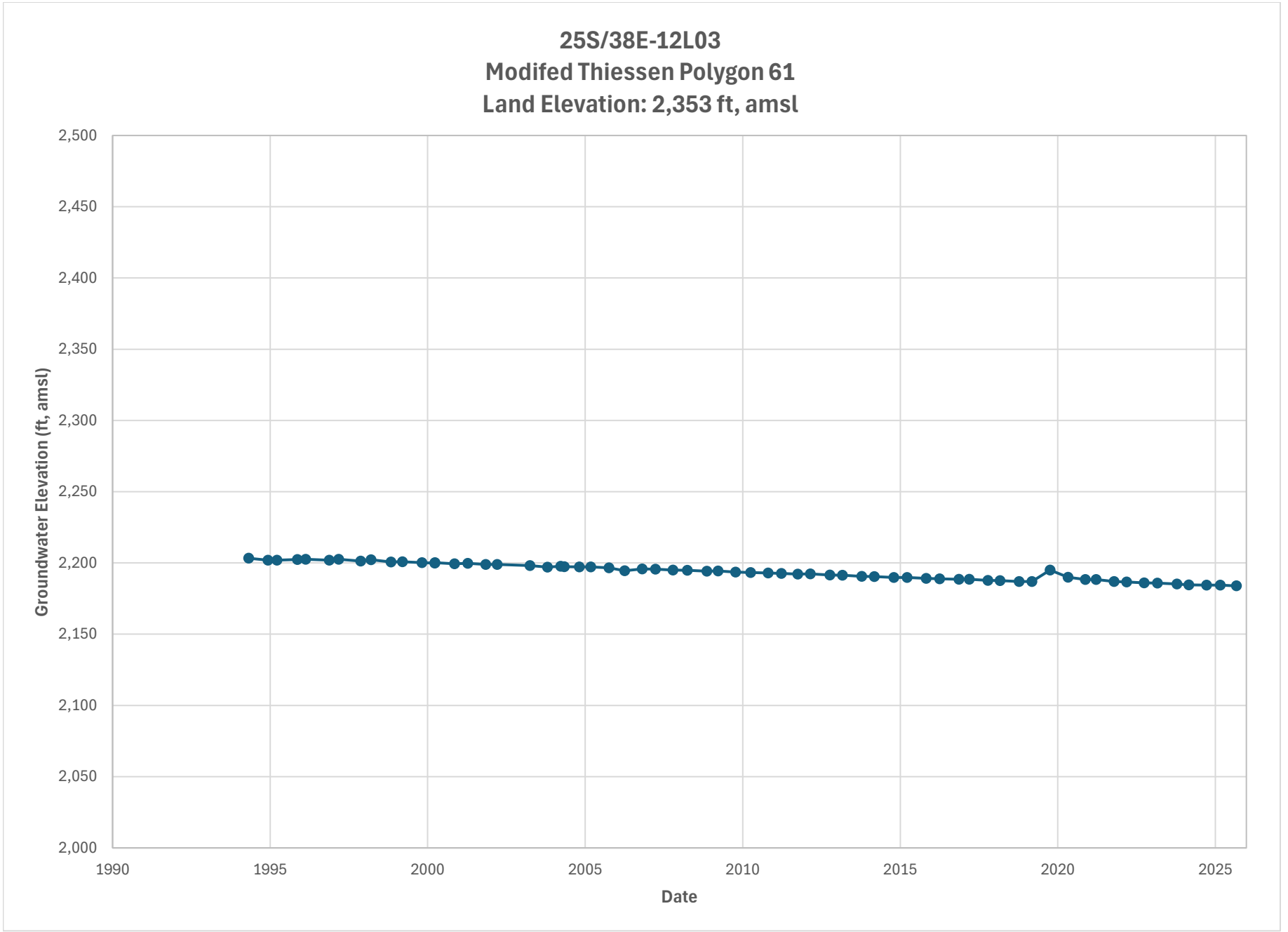

25S/38E-36G03
Modifed Thiessen Polygon 53
Land Elevation: 2,315 ft, amsl
Groundwater Elevation (ft, amsl)
2,500
2,450
2,400
2,350
2,300
2,250
2,200
2,150
2,100
2,050
2,000
1990
1995
2000
2005
2010
2015
2020
2025
Date

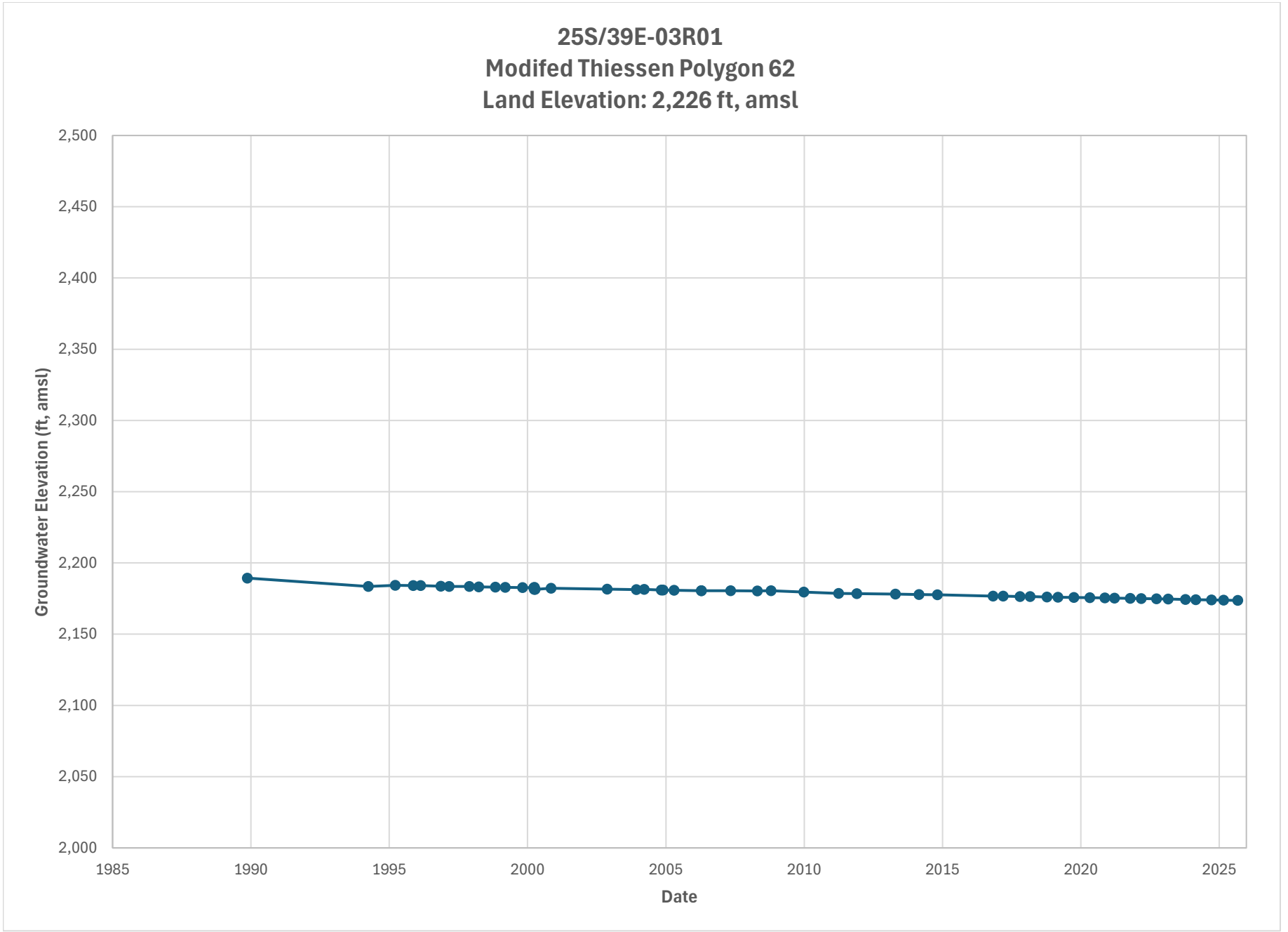

25S/38E-34A01
Modifed Thiessen Polygon 54
Land Elevation: 2,529 ft, amsl
Groundwater Elevation (ft, amsl)
2,500
2,450
2,400
2,350
2,300
2,250
2,200
2,150
2,100
2,050
2,000
1990
1995
2000
2005
2010
2015
2020
2025
Date

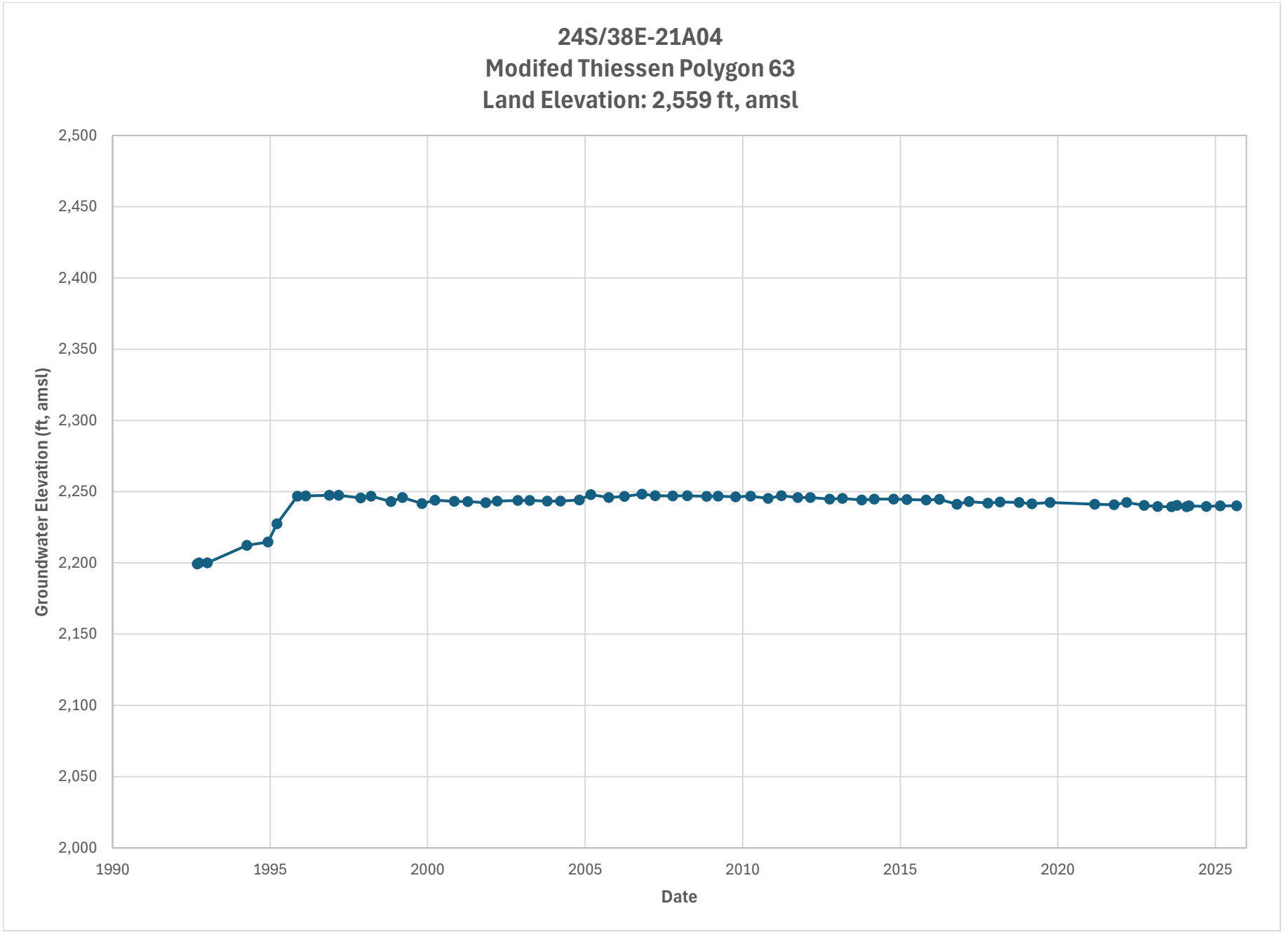

25S/38E-35B01
Modifed Thiessen Polygon 55
Land Elevation: 2,396 ft, amsl
Groundwater Elevation (ft, amsl)
2,500
2,450
2,400
2,350
2,300
2,250
2,200
2,150
2,100
2,050
2,000
1955
1960
1965
1970
1975
1980
1985
1990
1995
2000
2005
2010
2015
2020
2025
Date

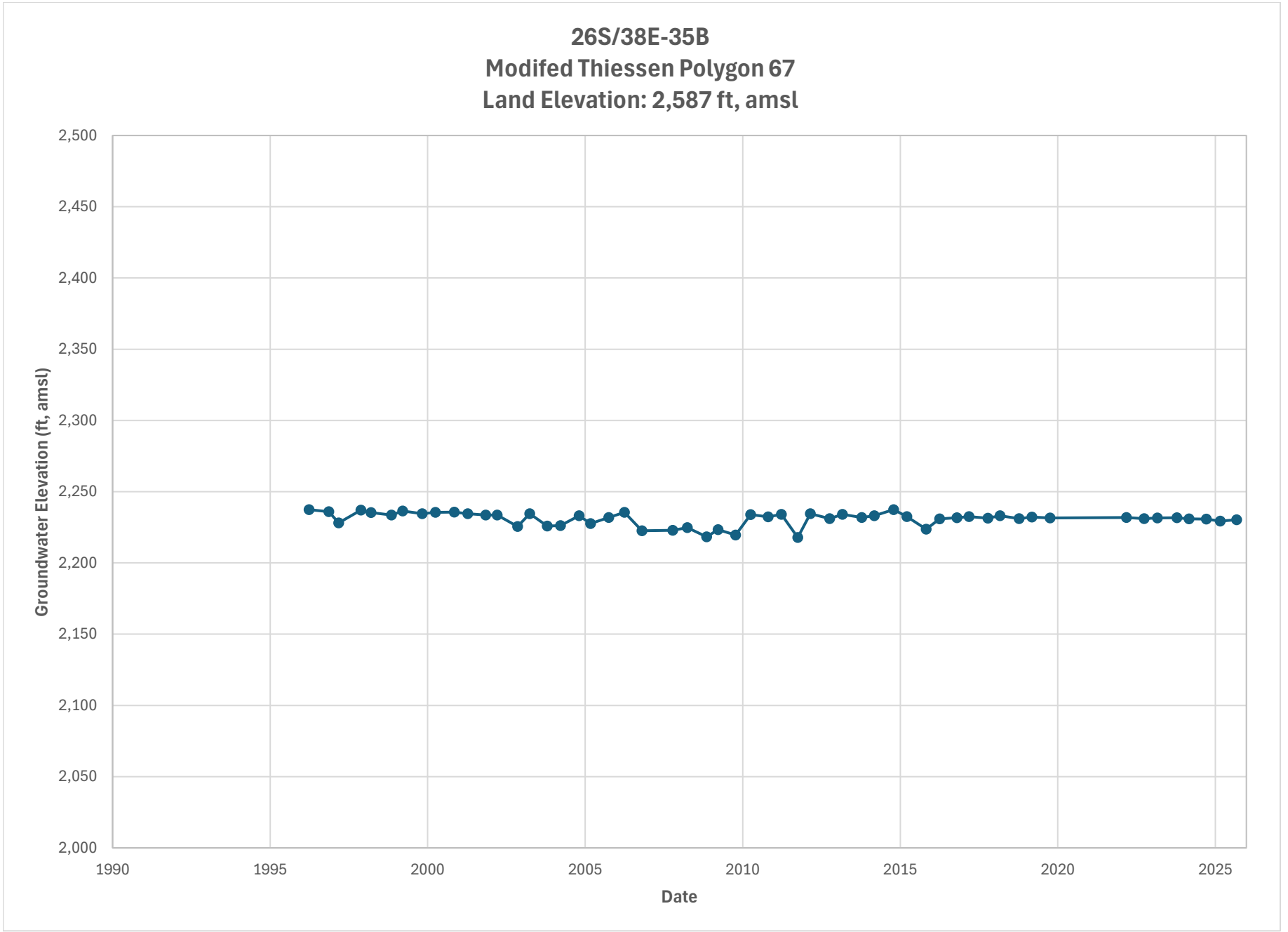

25S/39E-29M01
Modifed Thiessen Polygon 57
Land Elevation: 2,232 ft, amsl
Groundwater Elevation (ft, amsl)
2,500
2,450
2,400
2,350
2,300
2,250
2,200
2,150
2,100
2,050
2,000
1990
1995
2000
2005
2010
2015
2020
2025
Date

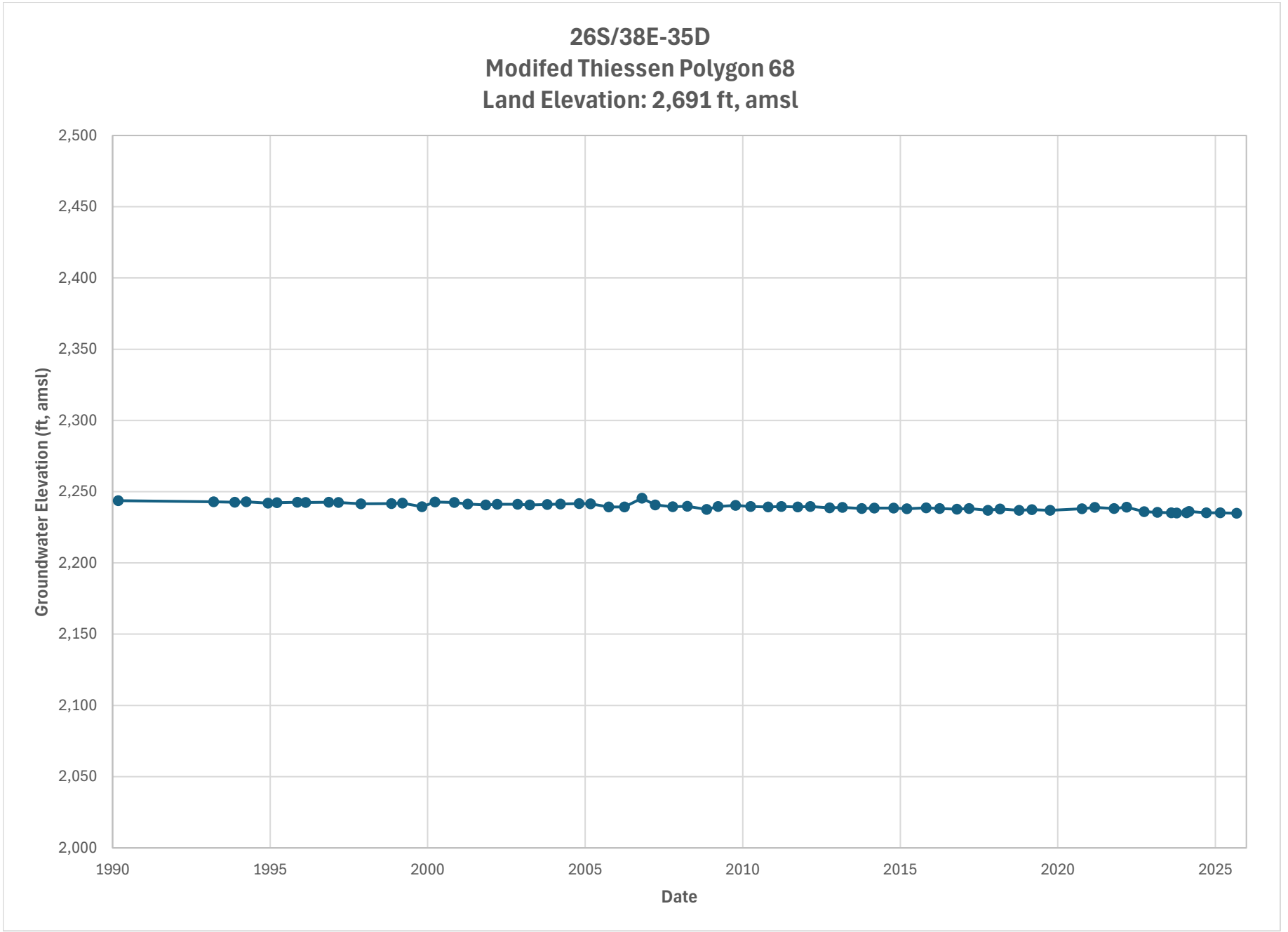

25S/38E-25J03
Modifed Thiessen Polygon 58
Land Elevation: 2,276 ft, amsl
Groundwater Elevation (ft, amsl)
2,500
2,450
2,400
2,350
2,300
2,250
2,200
2,150
2,100
2,050
2,000
1990
1995
2000
2005
2010
2015
2020
2025
Date

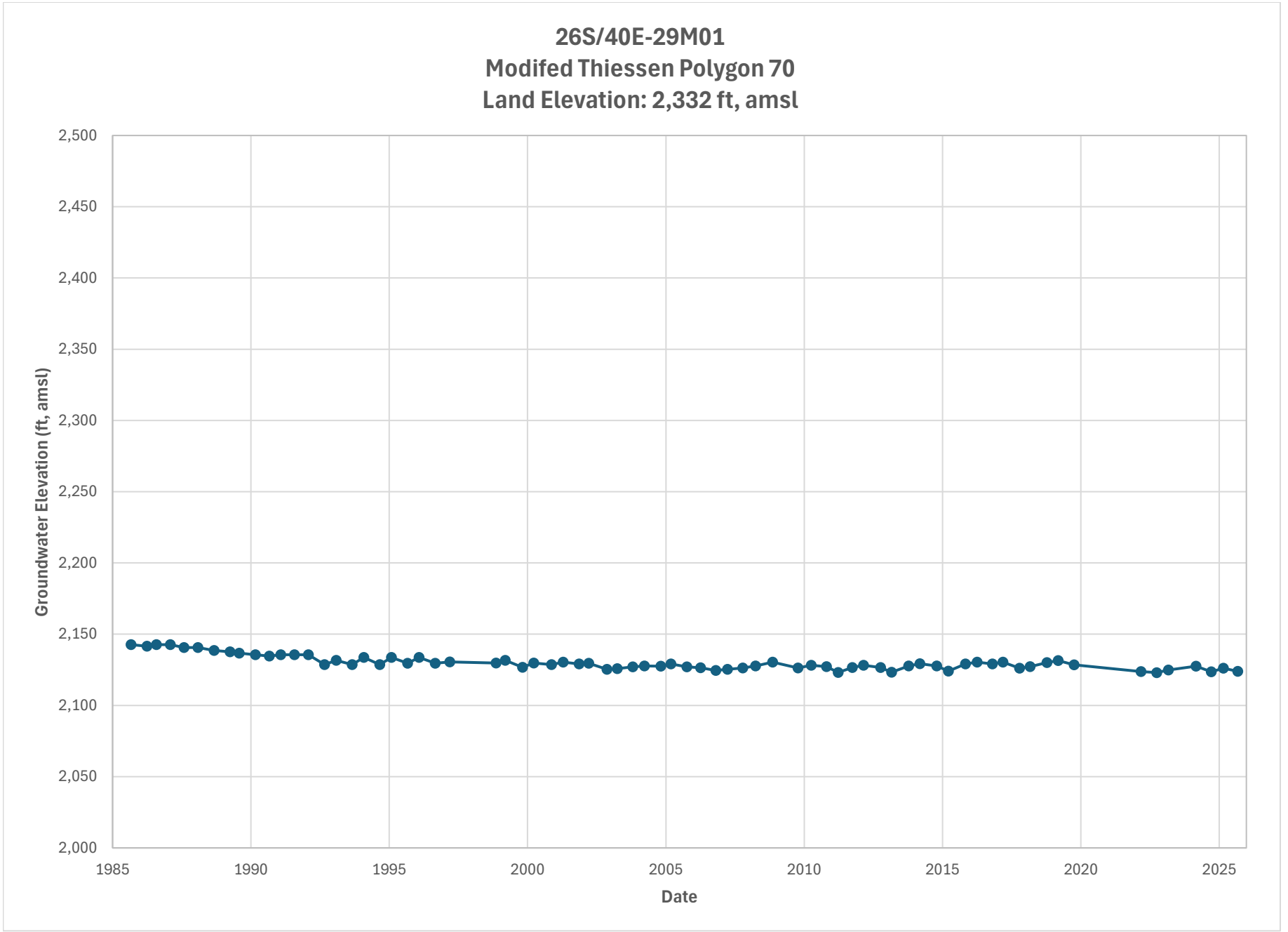

25S/38E-12L03
Modifed Thiessen Polygon 61
Land Elevation: 2,353 ft, amsl
Groundwater Elevation (ft, amsl)
2,500
2,450
2,400
2,350
2,300
2,250
2,200
2,150
2,100
2,050
2,000
1990
1995
2000
2005
2010
2015
2020
2025
Date

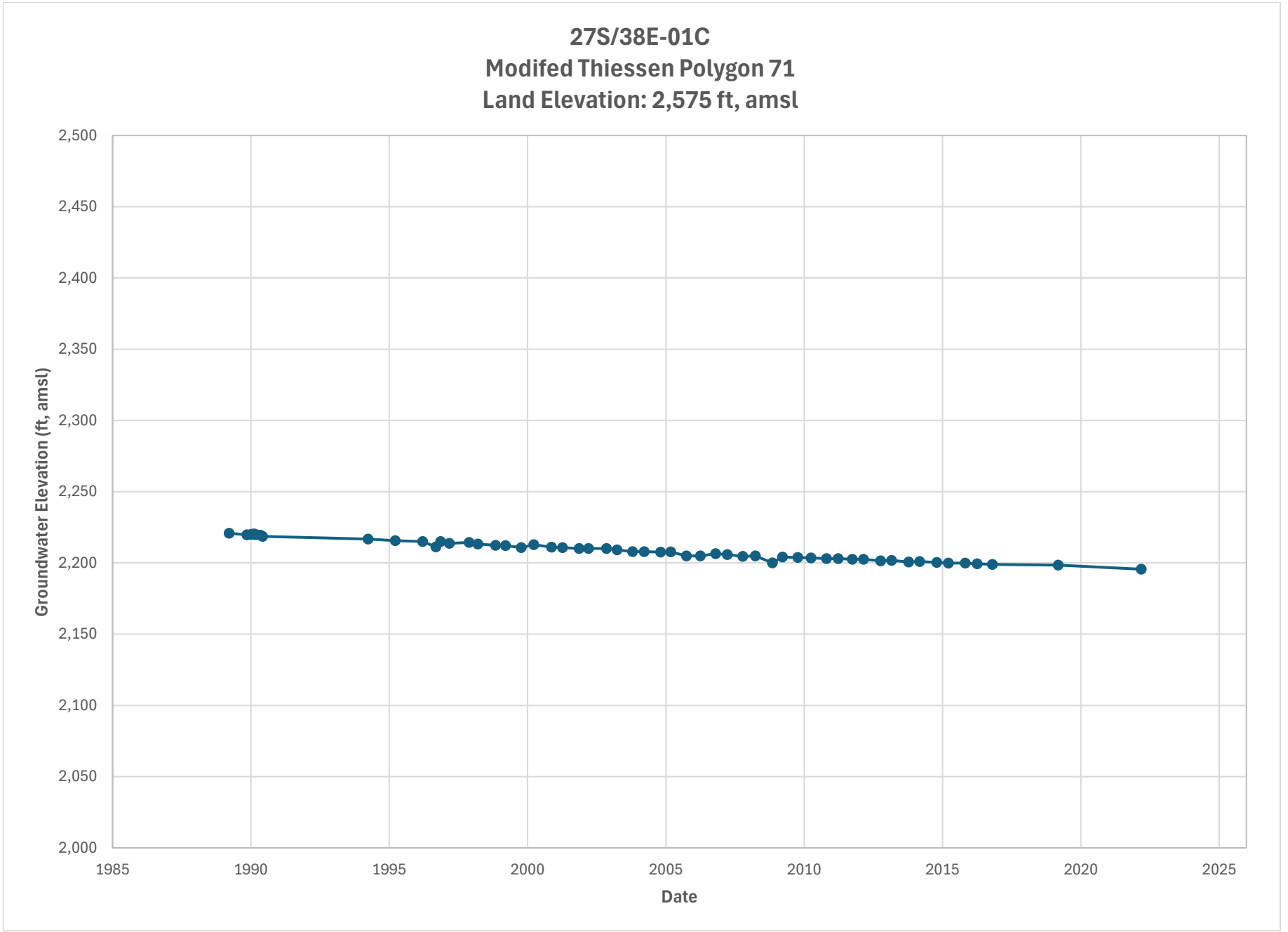

25S/39E-03R01
Modifed Thiessen Polygon 62
Land Elevation: 2,226 ft, amsl
Groundwater Elevation (ft, amsl)
2,500
2,450
2,400
2,350
2,300
2,250
2,200
2,150
2,100
2,050
2,000
1985
1990
1995
2000
2005
2010
2015
2020
2025
Date

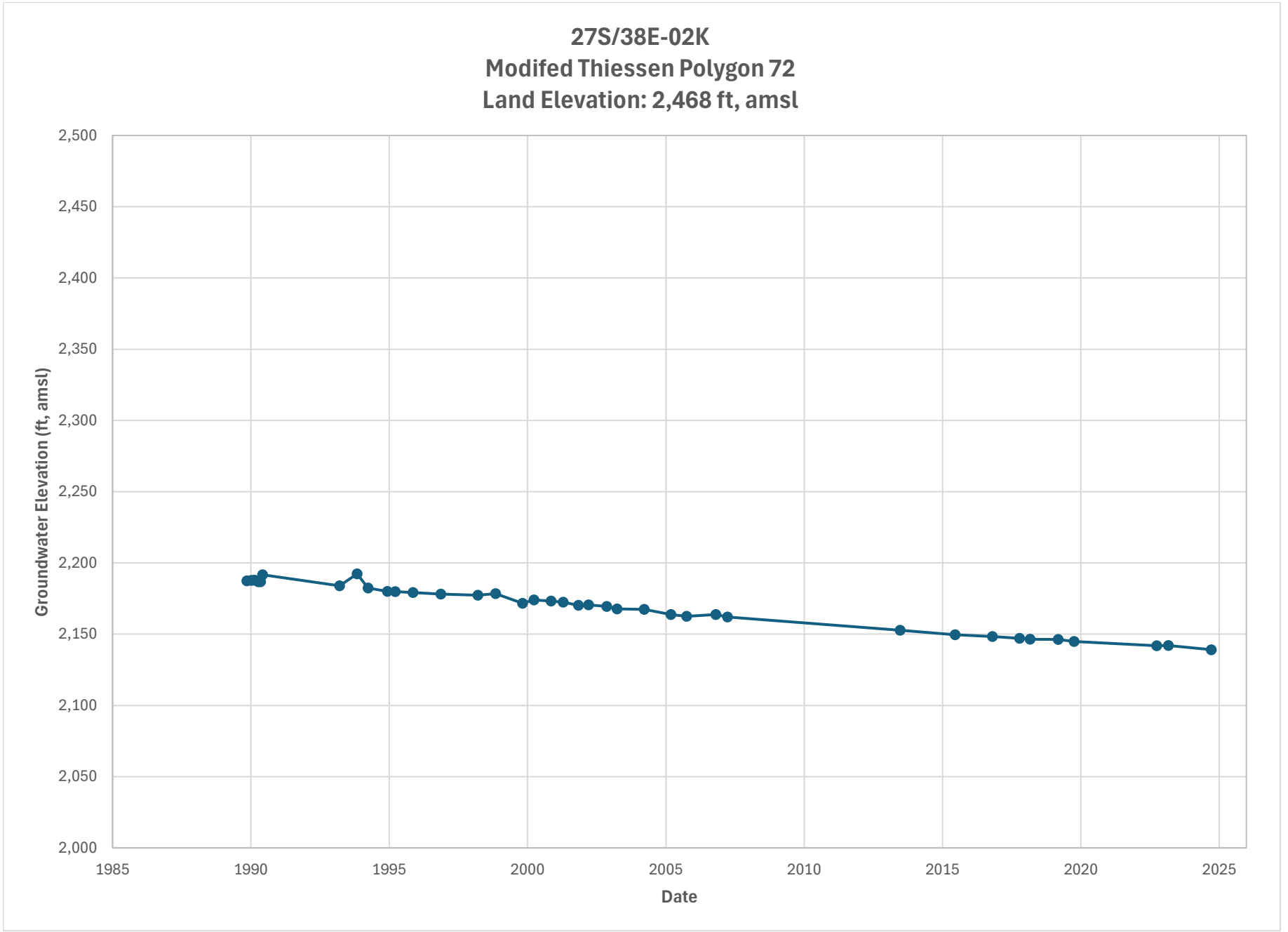

24S/38E-21A04
Modifed Thiessen Polygon 63
Land Elevation: 2,559 ft, amsl
Groundwater Elevation (ft, amsl)
2,500
2,450
2,400
2,350
2,300
2,250
2,200
2,150
2,100
2,050
2,000
1990
1995
2000
2005
2010
2015
2020
2025
Date

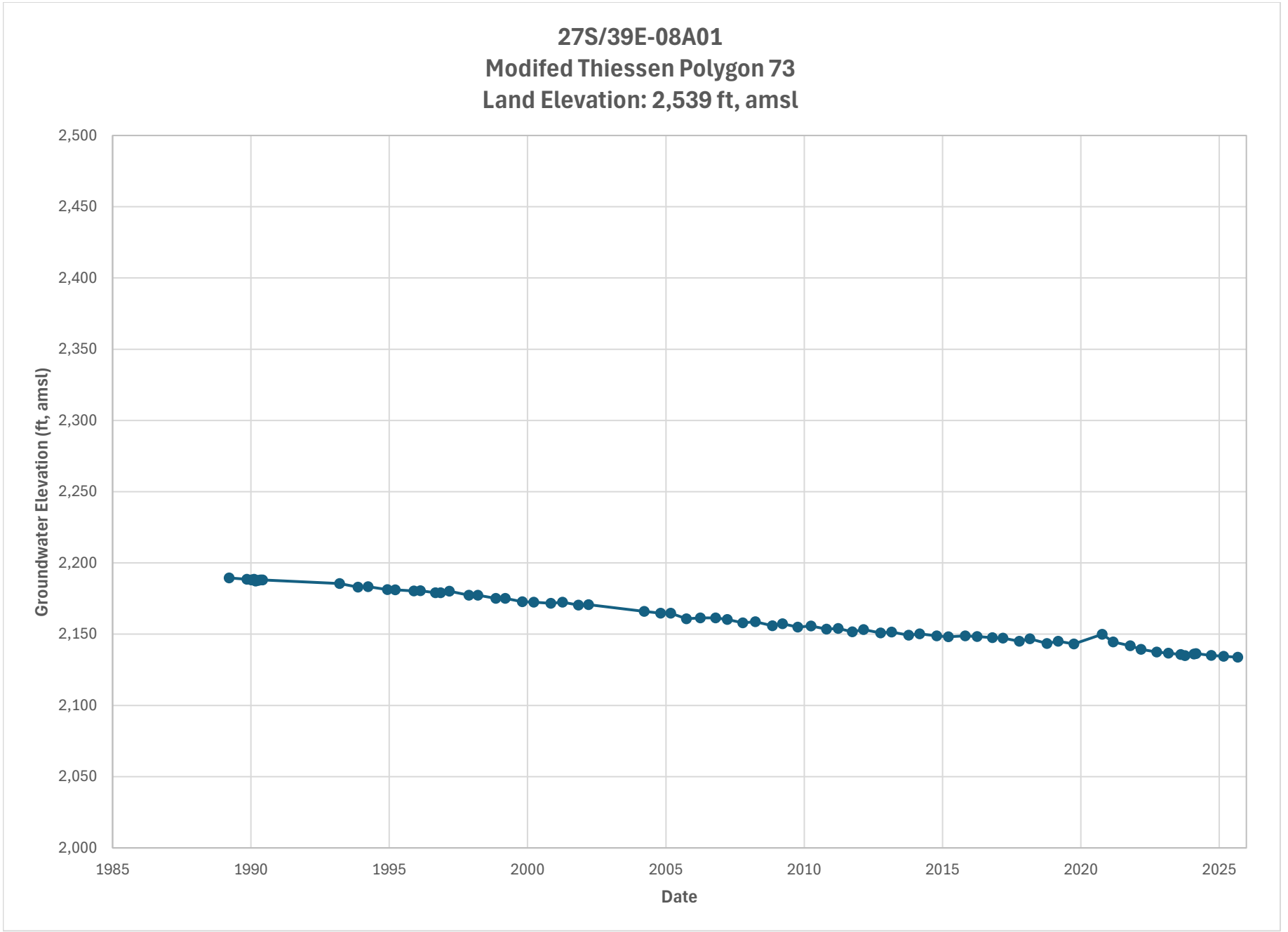

26S/38E-35B
Modifed Thiessen Polygon 67
Land Elevation: 2,587 ft, amsl
Groundwater Elevation (ft, amsl)
2,500
2,450
2,400
2,350
2,300
2,250
2,200
2,150
2,100
2,050
2,000
1990
1995
2000
2005
2010
2015
2020
2025
Date

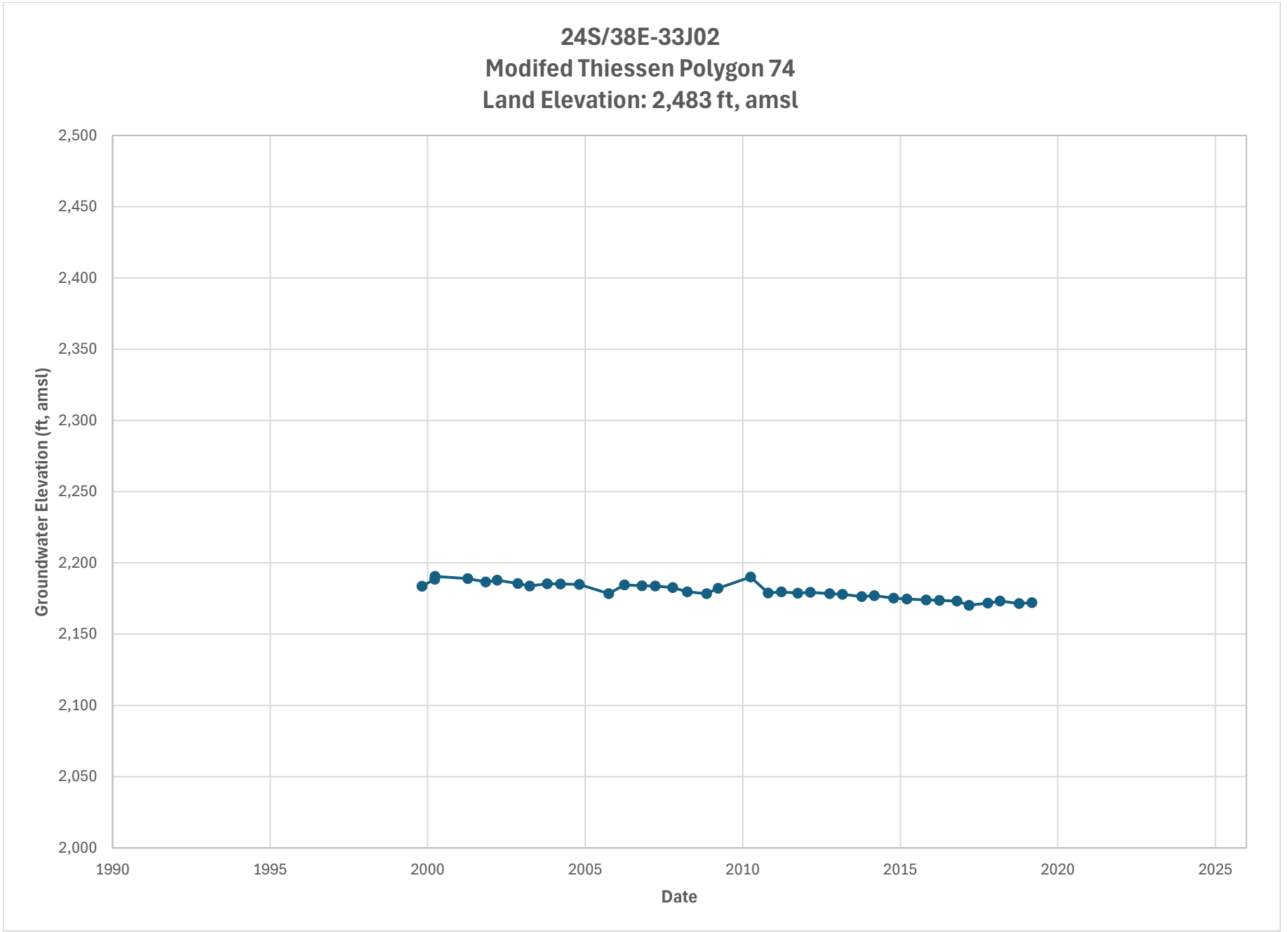

26S/38E-35D
Modifed Thiessen Polygon 68
Land Elevation: 2,691 ft, amsl
Groundwater Elevation (ft, amsl)
2,500
2,450
2,400
2,350
2,300
2,250
2,200
2,150
2,100
2,050
2,000
1990
1995
2000
2005
2010
2015
2020
2025
Date

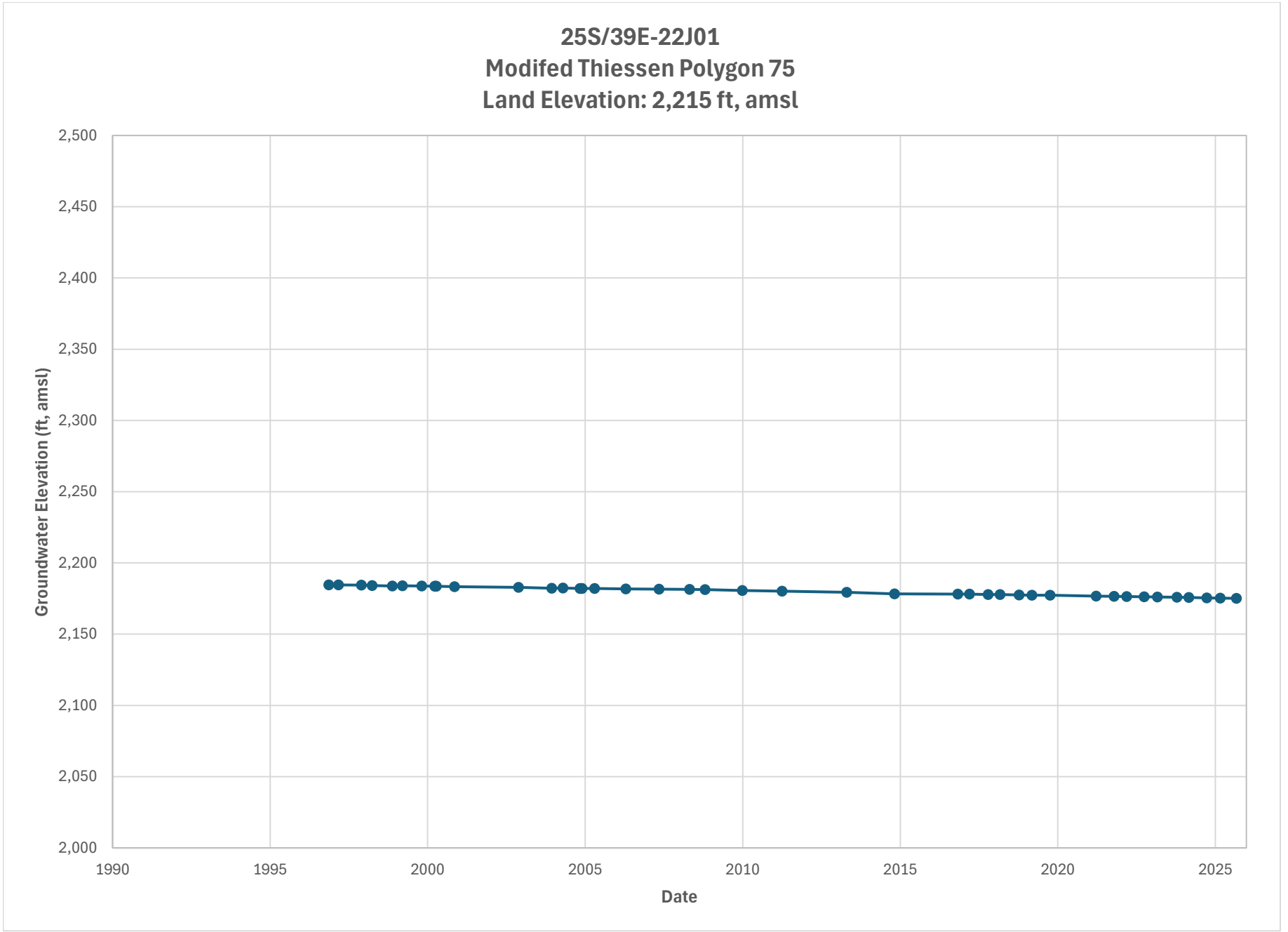

26S/40E-29M01
Modifed Thiessen Polygon 70
Land Elevation: 2,332 ft, amsl
Groundwater Elevation (ft, amsl)
2,500
2,450
2,400
2,350
2,300
2,250
2,200
2,150
2,100
2,050
2,000
1985
1990
1995
2000
2005
2010
2015
2020
2025
Date

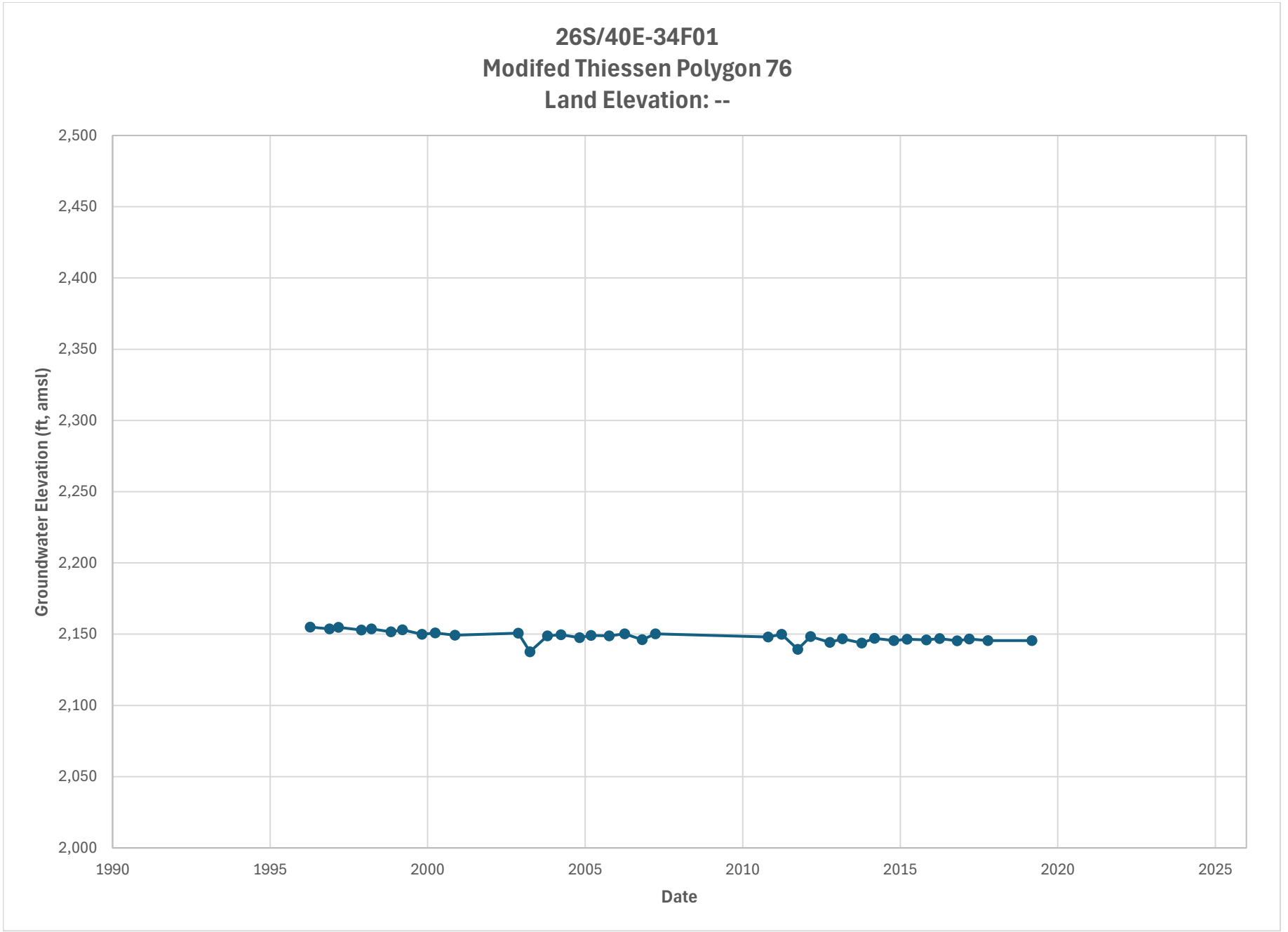

27S/38E-01C
Modifed Thiessen Polygon 71
Land Elevation: 2,575 ft, amsl
Groundwater Elevation (ft, amsl)
2,500
2,450
2,400
2,350
2,300
2,250
2,200
2,150
2,100
2,050
2,000
1985
1990
1995
2000
2005
2010
2015
2020
2025
Date

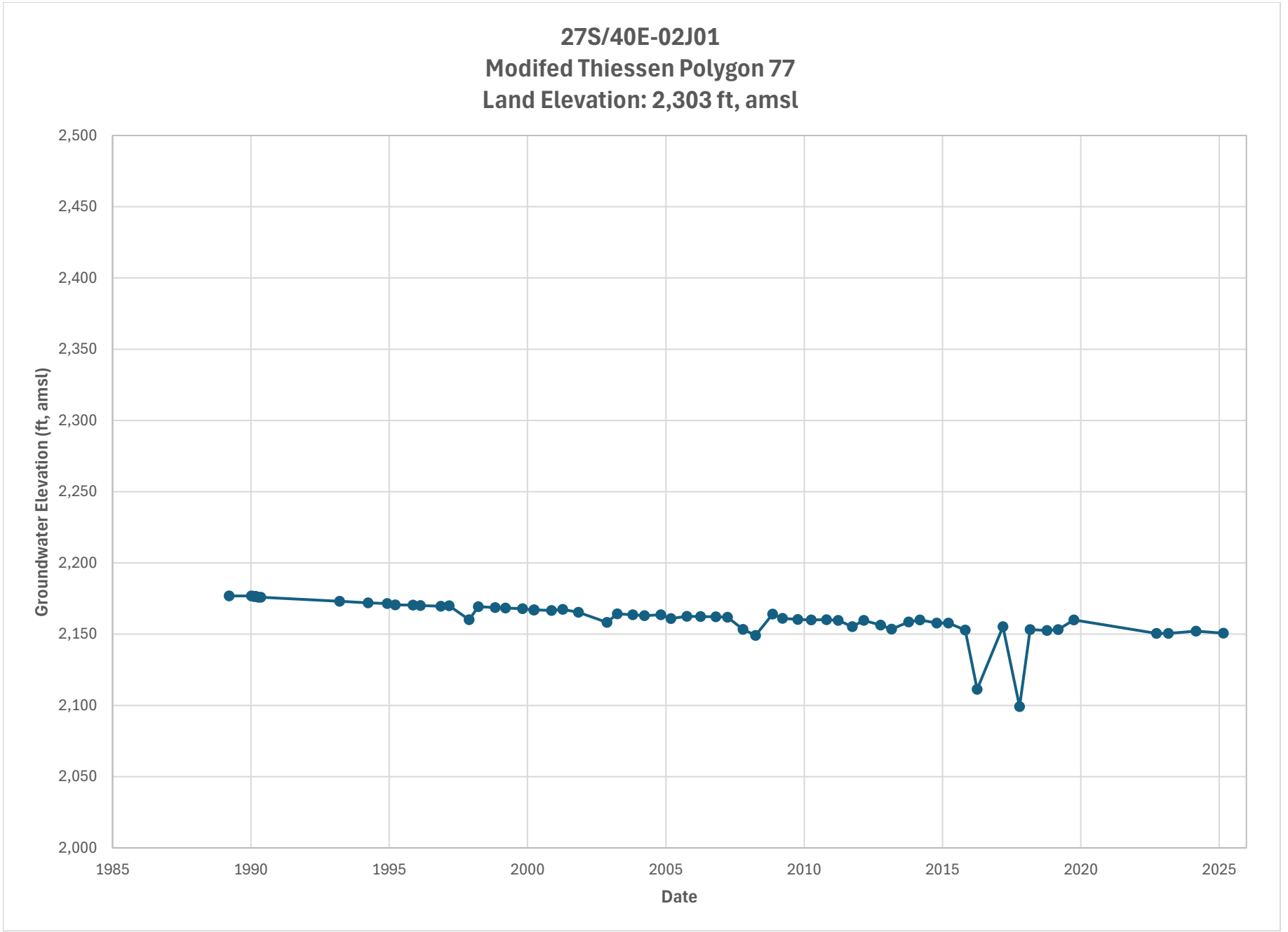

27S/38E-02K
Modifed Thiessen Polygon 72
Land Elevation: 2,468 ft, amsl
Groundwater Elevation (ft, amsl)
2,500
2,450
2,400
2,350
2,300
2,250
2,200
2,150
2,100
2,050
2,000
1985
1990
1995
2000
2005
2010
2015
2020
2025
Date


27S/39E-08A01
Modifed Thiessen Polygon 73
Land Elevation: 2,539 ft, amsl
Groundwater Elevation (ft, amsl)
2,500
2,450
2,400
2,350
2,300
2,250
2,200
2,150
2,100
2,050
2,000
1985
1990
1995
2000
2005
2010
2015
2020
2025
Date


24S/38E-33J02
Modifed Thiessen Polygon 74
Land Elevation: 2,483 ft, amsl
Groundwater Elevation (ft, amsl)
2,500
2,450
2,400
2,350
2,300
2,250
2,200
2,150
2,100
2,050
2,000
1990
1995
2000
2005
2010
2015
2020
2025
Date


25S/39E-22J01
Modifed Thiessen Polygon 75
Land Elevation: 2,215 ft, amsl
Groundwater Elevation (ft, amsl)
2,500
2,450
2,400
2,350
2,300
2,250
2,200
2,150
2,100
2,050
2,000
1990
1995
2000
2005
2010
2015
2020
2025
Date


26S/40E-34F01
Modifed Thiessen Polygon 76
Land Elevation: --
Groundwater Elevation (ft, amsl)
2,500
2,450
2,400
2,350
2,300
2,250
2,200
2,150
2,100
2,050
2,000
1990
1995
2000
2005
2010
2015
2020
2025
Date


27S/40E-02J01
Modifed Thiessen Polygon 77
Land Elevation: 2,303 ft, amsl
Groundwater Elevation (ft, amsl)
2,500
2,450
2,400
2,350
2,300
2,250
2,200
2,150
2,100
2,050
2,000
1985
1990
1995
2000
2005
2010
2015
2020
2025
Date

ATTACHMENT T

DRAFT MEMORANDUM

2171 E. Francisco Blvd., Suite K • San Rafael, California • 94901
TEL: (415) 457-0701 FAX: (415) 457-1638 e-mail: mollyp@stetsonengineers.com

TO: Greg Pohll, Desert Research Institute DATE: December 12, 2018

FROM: Stetson Engineers JOB NO: 2652

RE: Notes on Determination of Balanced Hydrologic Period and Model Recharge Distribution

Below is a preliminary description of the methods Stetson used to develop a balanced hydrologic period and mountain-front recharge distribution for the Indian Wells Valley Groundwater Model.

- Precipitation data in and near the model area were obtained from NOAA cooperative stations and RAWS stations (source: WRCC). Streamflow data in the basin are limited, so precipitation was considered the better option for assessing long-term hydrologic trends.
- Long-term records were available for two cooperative stations, Haiwee and China Lake NAF.
- Haiwee and China Lake NAF monthly records were filled and QC'd using data from nearby stations; spatial data from the OSU PRISM raster data set was used to adjust data linearly from one station to another.
- Cumulative departure from mean curves were prepared for Haiwee and China Lake NAF. Balanced hydrologic periods were examined, with more emphasis on the Haiwee station due to its location within the recharge area. See Figure 1 for graph.
- When examining the hydrologic trends, a more recent balanced period was selected to take advantage of recent precipitation data available at stations within the recharge zones. Earlier periods were examined (for example, 1929-1979), but precipitation data would have been limited to only one station within the recharge zones.
- A 26-year period from 1990-2015 was selected as a balanced hydrologic period, to be repeated to complete the 51-year future modeling period of 2020-2070. The 51-year future period will use hydrology from 1990-2015, then 1990-2014. In addition to the Haiwee station, which is located in the Rose Valley recharge zone, precipitation data is available at the Laural Mountain station (near El Paso recharge zone) and the Indian Wells Canyon station (within the Sierra Nevada N recharge zone). All other stations examined were located west of the basin's watershed (Walker Pass, Bear Peak) or on the valley floor (Inyokern, China Lake NAF) and are not the most appropriate for assessing trends in the mountain-front recharge zones. See map of precipitation stations in Figure 2. See Figure 3 for data availability at the precipitation stations.
- Annual exceedance curves were prepared for the 26-year period from 1990-2015 for the precipitation stations in the recharge zones. Missing data at the Laural Mountain and Indian Wells Canyon stations were filled linearly using data from another station and the linear ratio of average annual precipitation at the two stations (source: OSU PRISM raster data set). See Figure 3 for exceedance curves.
- A precipitation index was computed for the three stations within the recharge zones: Haiwee, Indian Wells Canyon, and Laural Mountain. The index is the average annual of the precipitation

values at the three stations. The index was computed monthly for the period 1990-2015. The annual exceedance curve for the precipitation index is plotted in Figure 4 (dashed blue line).

- The precipitation index was used to scale the average annual recharge for the groundwater model (7,650 AFY) using a linear relationship between the precipitation index and recharge. See values in Table 1. The driest year on record (1.1 inches of rain) was assumed to have zero recharge. Annual values are plotted in Figure 5. The distribution of recharge within the individual zones was not adjusted for this analysis. The zonal distribution is assumed to be fixed for each year, following the average annual values prepared by DRI:

Zone:	Argus and Coso	El Paso	Sierra Nevada S	Sierra Nevada N	Rose Valley	Total
Annual Recharge (afy):	1,600	50	1,500	2,100	2400	7,650
Percent:	21%	1%	20%	27%	31%	100%

- The annual recharge volumes in Table 1 were distributed to monthly volumes using the monthly precipitation index, i.e. monthly recharge volume was computed by multiplying the annual precipitation volume by the ratio of the monthly precipitation index to the annual precipitation index for that calendar year.
- Each monthly recharge volume was then computed as a percentage of the model average monthly recharge, which is 638 AFM (7,650 AFY divided by 12). The time series gives each monthly recharge volume as a percent of the average monthly model recharge. See attached spreadsheet.

Sources/References:

California RAWS data: https://raws.dri.edu/scaF.html

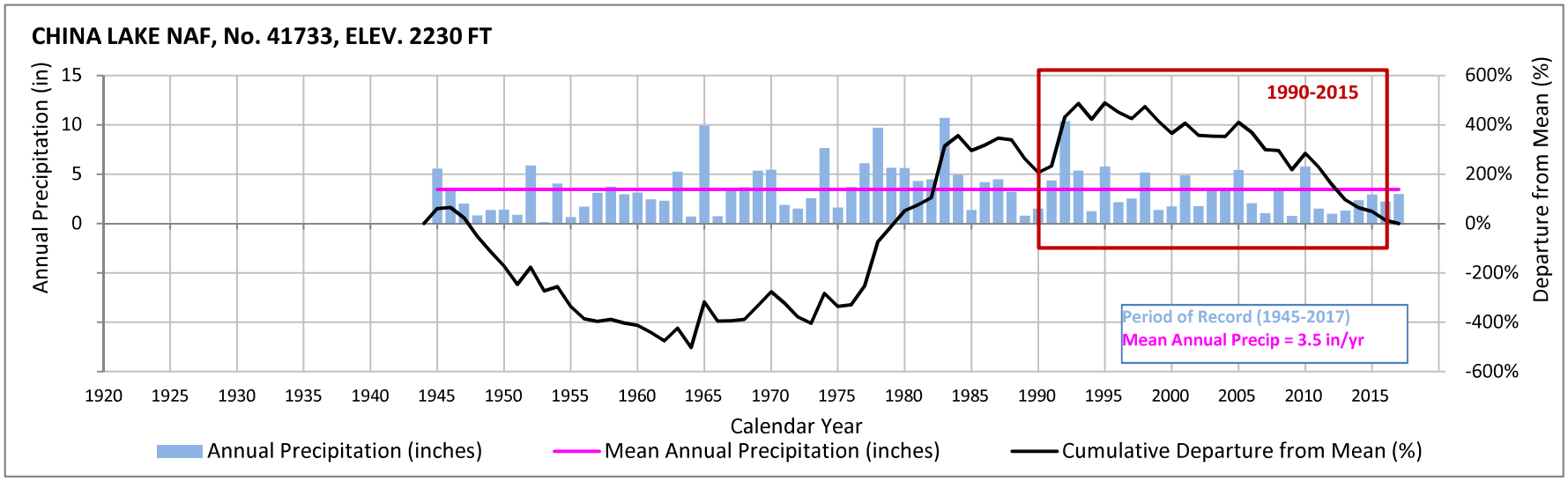
California Cooperative weather station data: https://wrcc.dri.edu/summary/Climsmsca.html

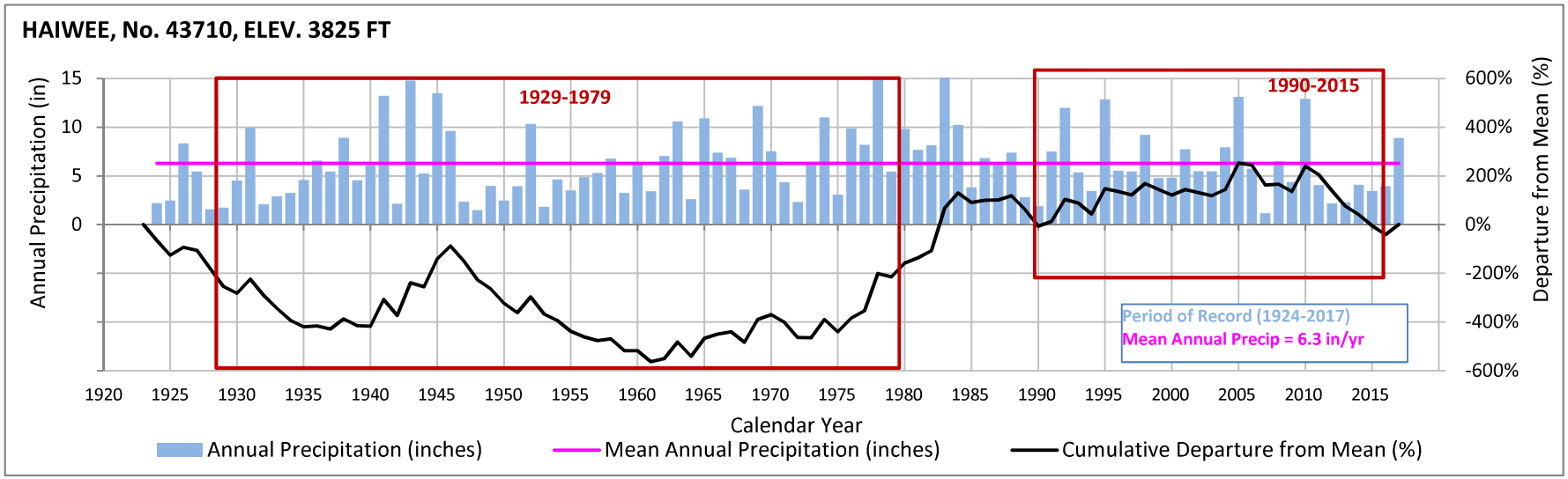
OSU PRISM Climate Normals for 1981-2010 (800-meter spatial raster for annual precipitation): http://prism.oregonstate.edu/normals/

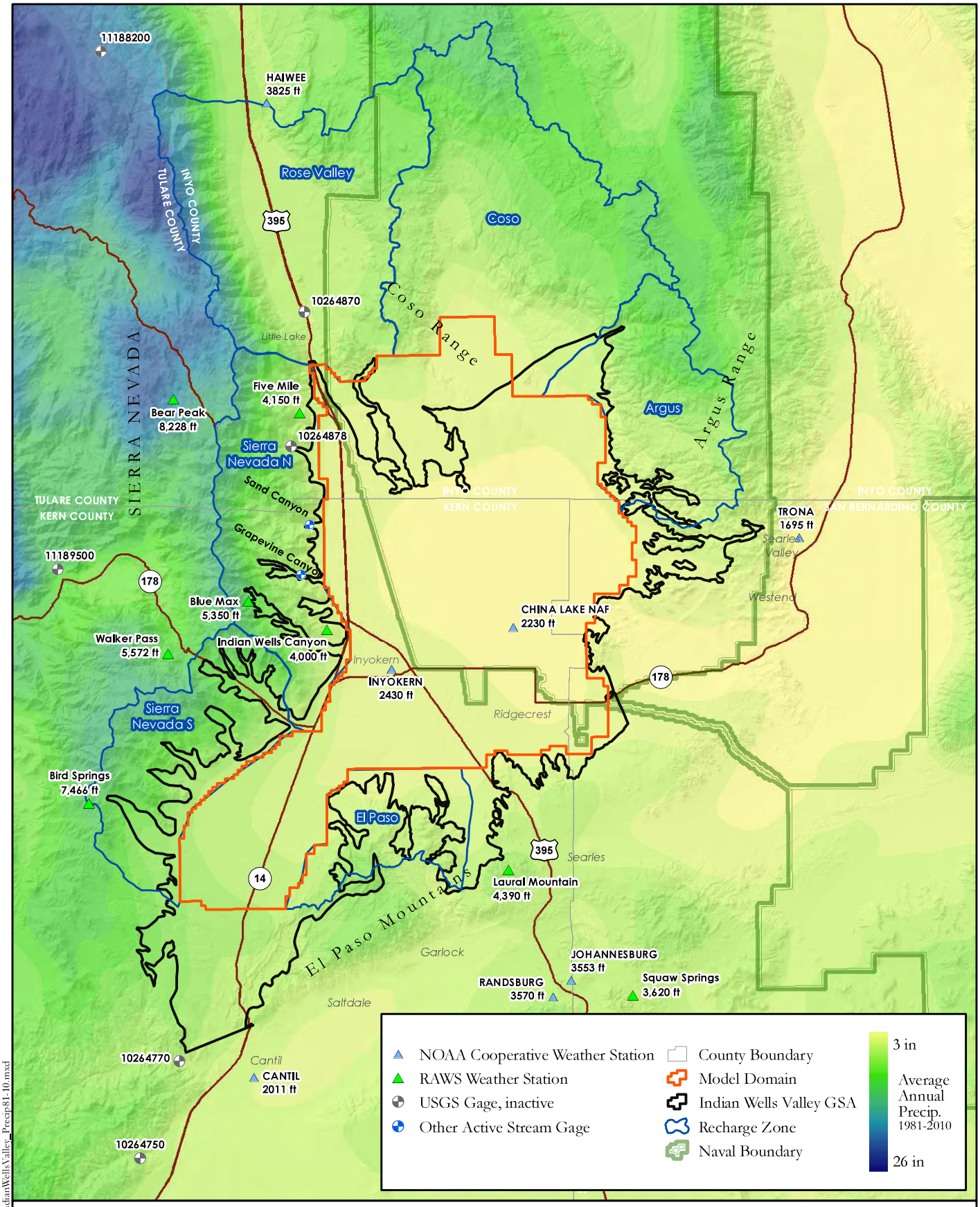
TABLE 1. ANNUAL RECHARGE VOLUMES SCALED LINEARLY FROM PRECIPITATION INDEX.

Future Year	Hydrology Year	Precipitation Index (in/yr)	Annual Model Recharge (ac-ft)
2020	1990	2.2	1,660
2021	1991	7.6	9,710
2022	1992	14.5	19,900
2023	1993	7.0	8,740
2024	1994	3.0	2,840
2025	1995	11.9	16,040
2026	1996	6.7	8,350
2027	1997	5.4	6,450
2028	1998	8.7	11,290
2029	1999	3.1	3,010
2030	2000	4.5	5,110
2031	2001	8.3	10,750
2032	2002	4.9	5,630
2033	2003	5.5	6,570
2034	2004	10.0	13,240
2035	2005	12.0	16,100
2036	2006	5.7	6,840
2037	2007	1.1	0
2038	2008	7.2	9,050
2039	2009	3.4	3,360
2040	2010	11.4	15,340
2041	2011	3.6	3,730
2042	2012	2.5	2,160
2043	2013	2.1	1,540
2044	2014	3.9	4,090
2045	2015	6.1	7,430
2046	1990	2.2	1,660
2047	1991	7.6	9,710
2048	1992	14.5	19,900
2049	1993	7.0	8,740
2050	1994	3.0	2,840
2051	1995	11.9	16,040
2052	1996	6.7	8,350
2053	1997	5.4	6,450
2054	1998	8.7	11,290
2055	1999	3.1	3,010
2056	2000	4.5	5,110
2057	2001	8.3	10,750
2058	2002	4.9	5,630
2059	2003	5.5	6,570
2060	2004	10.0	13,240
2061	2005	12.0	16,100
2062	2006	5.7	6,840
2063	2007	1.1	0
2064	2008	7.2	9,050
2065	2009	3.4	3,360
2066	2010	11.4	15,340
2067	2011	3.6	3,730
2068	2012	2.5	2,160
2069	2013	2.1	1,540
2070	2014	3.9	4,090

Annual Precipitation and Cumulative Departure from Mean at Stations near Indian Wells Valley







DRAFT

AVERAGE ANNUAL PRECIPITATION (1981 – 2010)
INDIAN WELLS VALLEY

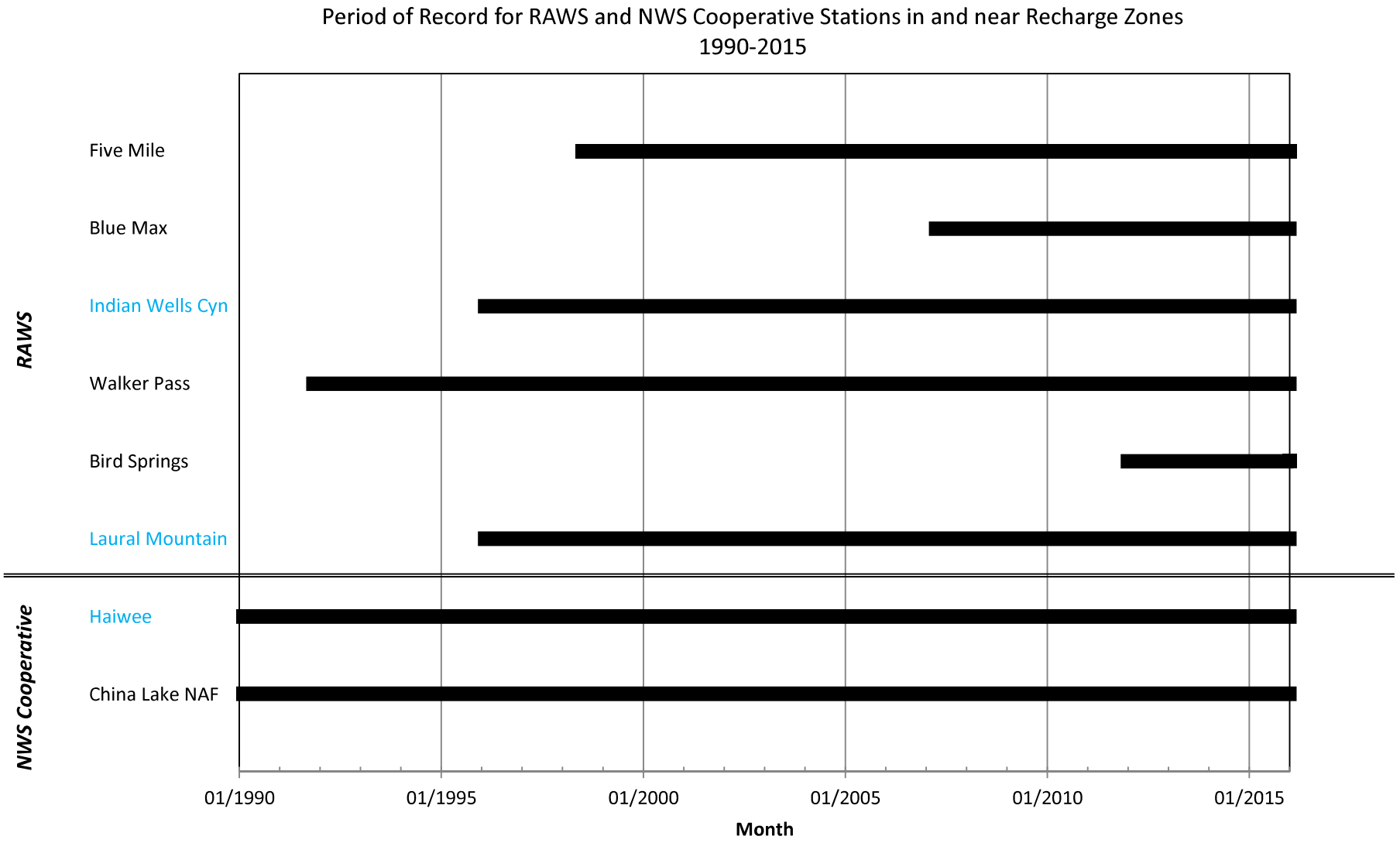
OREGON STATE PRISM CLIMATE GROUP, CLIMATE NORMALS FOR 1981-2010

STETSON ENGINEERS INC.

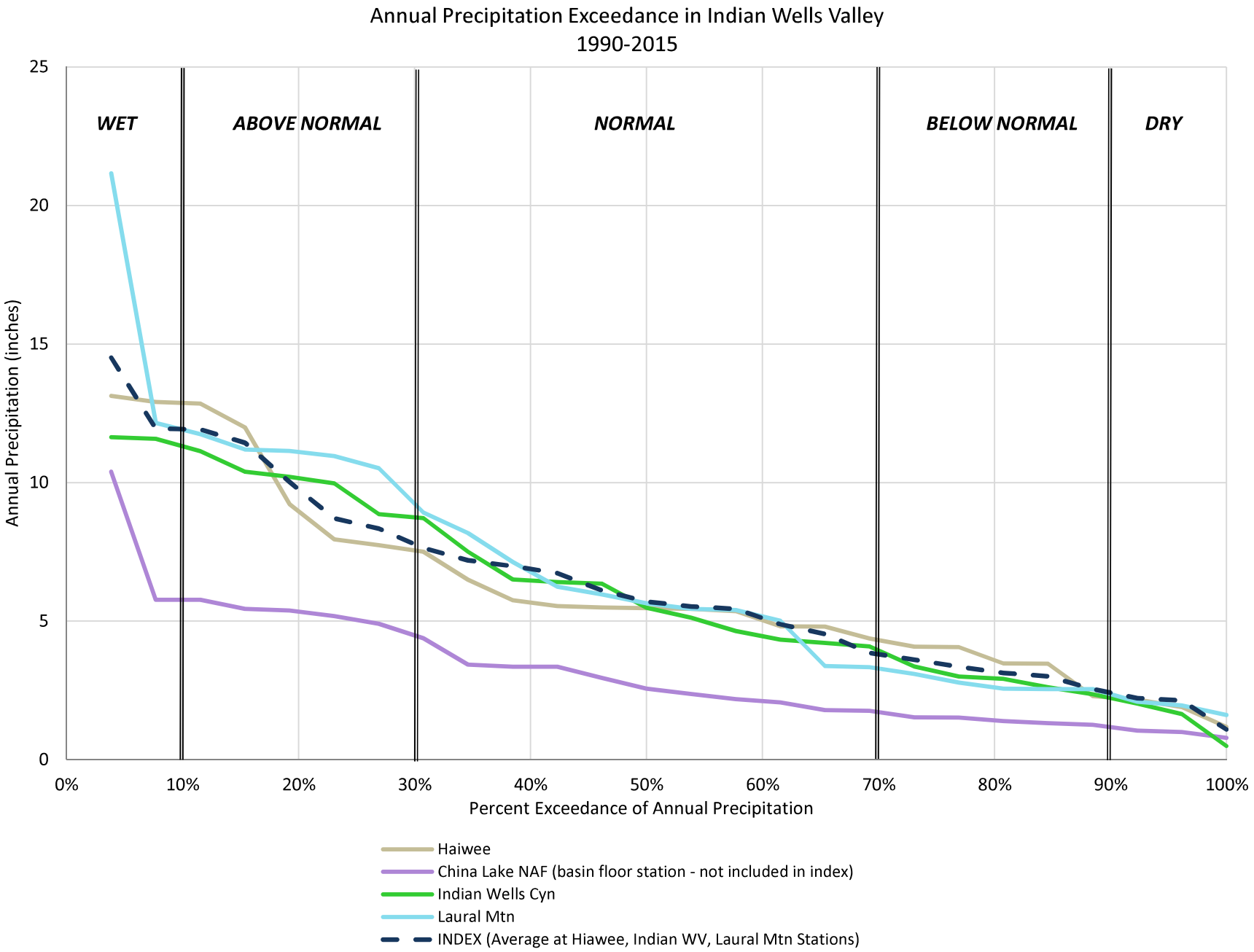
N

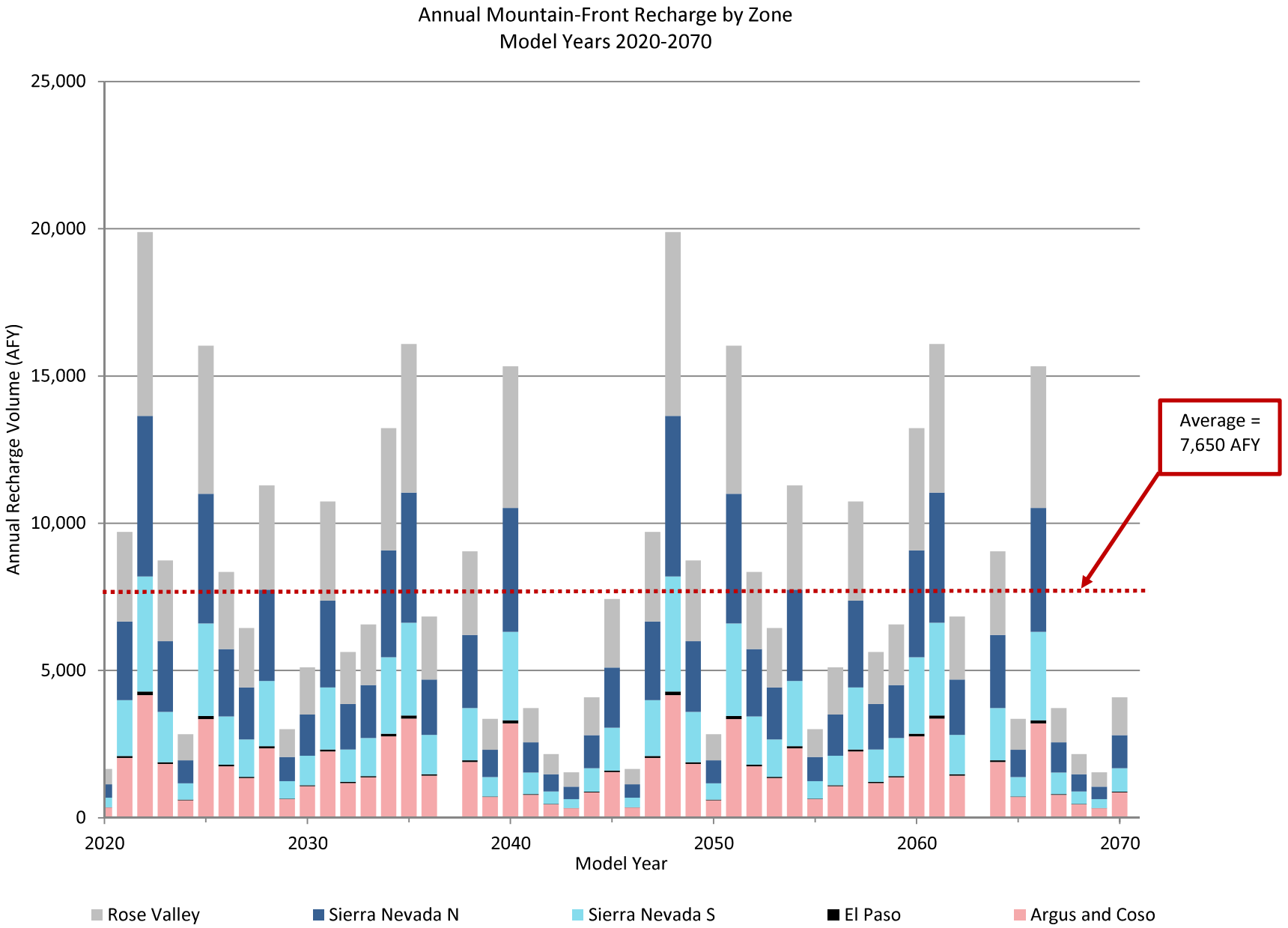
0 4 8 Miles

Document Path: J:\jn2652\IndianWellsValley_Precip81-10.mxd



Notes:
Haiwee and China Lake NAF are NWS cooperative stations with records dating back to 1924 and 1945, respectively. All others are RAWS stations.
Stations in blue are included in the hydrologic index for allocating annual recharge.


Annual Precipitation Exceedance in Indian Wells Valley
1990-2015
WET
ABOVE NORMAL
NORMAL
BELOW NORMAL
DRY
Annual Precipitation (inches)
25
20
15
10
5
0
0%
10%
20%
30%
40%
50%
60%
70%
80%
90%
100%
Percent Exceedance of Annual Precipitation
Haiwee
China Lake NAF (basin floor station - not included in index)
Indian Wells Cyn
Laural Mtn
INDEX (Average at Hiawee, Indian WV, Laural Mtn Stations)


Annual Mountain-Front Recharge by Zone
Model Years 2020-2070
Annual Recharge Volume (AFY)
25,000
20,000
15,000
10,000
5,000
0
2020
2030
2040
2050
2060
2070
Model Year
Average = 7,650 AFY
Rose Valley
Sierra Nevada N
Sierra Nevada S
El Paso
Argus and Coso